Introduction to Autogyros, Helicopters, and Other V/STOL Aircraft

Volume III: Other V/STOL Aircraft

Edited by
Catherine Dow, Dow Technical Services

Cover Design by
Susan O

Cover Photo
The Transcendental Model 1-G, the world's first successful tiltrotor, made its initial untethered hovering flight on July 6, 1954.

The first step towards the Model 1-G was taken when Mario A. Guerrieri and Robert L. Lichten left the Kellett Autogyro Company and started up the Transcendental Aircraft Corporation in October 1946. The company had its office in Glen Riddle, Pennsylvania. After completing preliminary design in early 1948, Lichten left to join Bell Aircraft Corporation. Guerrieri continued (nearly alone) with development of the Model 1, which was completed in September 1950. However, the Model 1 was destroyed by ground resonance in November 1950. On January 1, 1951, William E. Cobey joined the organization as Chief Engineer. Together, Guerrieri and Cobey carried on with development of the Model 1, renamed the Model 1-G. In September of 1952, Guerrieri sold his share of Transcendental to Cobey and left to take a position at Hiller Helicopters. Cobey, as president of Transcendental, continued development of the Model 1-G. Then, on July 20, 1955, while in high-speed forward flight with conversion virtually completed, the friction lock on the collective pitch stick slipped, causing the aircraft to enter a steep dive very abruptly. Although the pilot was able to initiate recovery, insufficient altitude was available for complete recovery, and the landing gear struck the Delaware River, flipping the aircraft onto its back. At the time of this accident, during which the aircraft suffered major damage, it had accumulated 23 airborne hours in over 100 individual flights.

NASA/SP–2015-215959 Vol III

Introduction to Autogyros, Helicopters, and Other V/STOL Aircraft

Volume III: Other V/STOL Aircraft

Franklin D. Harris

Piedmont, Oklahoma

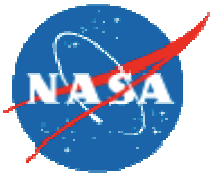

National Aeronautics and
Space Administration

Ames Research Center
Moffett Field, California 94035-1000

November 2015

Prepared for Monterey Technologies, Inc.
under NASA Contract NNA13AA84B
Subcontract Task Order No. NNA14AA34T
ISBN: 978-0-692-56830-9

Available from:

NASA Scientific and Technical Information Program
Mail Stop 148
NASA Langley Research Center
Hampton, VA 23681-2199
(757) 864-9658

DEDICATION

To my mentors,

Joe Mallen, Steppy Stepniewski, Gordon Fries, Phil Sheridan, Bob Lowey, Ken Grina, Lee Douglas, George Schairer, Jan Drees, Bob Lynn, Chuck Rudning, Webb Joiner, Jack Horner, Jim Atkins, Dick Carlson, and Bud Forster.

These men taught me to be a good, thorough, and honest engineer. They raised my technical standards to a level I would never have reached on my own. They showed me examples of excellent management styles and encouraged my search for my own style. And they did all that without snuffing out my maverick tendencies. Unfortunately, they couldn't do much to curb my opinionated, outspoken, blunt, and occasionally very demanding, personality.

I was the "project engineer" on Vertol's first powered force model test. The test ended halfway through the first forward-flight run. The rest of the blade was embedded in the tunnel wall. (University of Maryland Wind Tunnel test number 398, 1962. Repaired and successfully retested, UMWT test number 413.)

TABLE OF CONTENTS

PREFACE

This last volume could easily be subtitled, *Having Our Cake and Eating It Too*. I write this because ever since the convincing demonstrations of the autogyro, the helicopter, and the airplane,* the aviation industry has continually focused on two fundamental objectives. These two objectives have been to:

1. Offer fixed-wing machines that carry more, go faster, fly higher, *and yet still take off and land within rationally sized airports*. This aviation branch has pursued its objective with metal monoplanes, retractable landing gears, variable-pitch propellers, swept wings, gas turbine engines, and of course, high-wing-lift devices such as the Fowler flap.
2. Offer rotary wing machines that carry more, go faster, fly higher, *and yet still take off and land vertically (VTOL)*. This side of the aviation industry has pursued its objective with successive improvements to the helicopter (including the use of gas turbine engines) and with a decades-long search for airplane-like speeds. Today, the tiltrotor configuration has emerged as the first positive rotorcraft step toward a VTOL machine having a significantly higher operational speed increment than the helicopter.

It is with these two fundamental objectives in mind that I thought you would like to know a little about rotary wing performance at high speed and fixed-wing performance at low speed. Thus, Chapters 2 and 3 provide at least an introduction to these subjects, and they constitute the bulk of this volume.

In Chapter 2 you will read about how the rotorcraft industry has dealt with rotor behavior at high advance ratios. These advocates view advance ratios typical of today's helicopters as the lower bound of "high." On the upper end, they have restricted their thinking to advance ratios less than 1.0. My view is that high advance ratio extends up to forward speeds divided by tip speeds more like 2.0, and I have provided rotor performance test data showing that rotor-alone lift-to-drag ratios above 10 can be achieved. Of course, the tiltrotor type of rotorcraft—specifically the U.S. Marine Corps/Bell Boeing V-22 now in service—has established one way of *having our cake and eating too*. Therefore, you may reasonably ask if the edgewise flying rotor, with the limitations I have suggested, is worth pursuing. I have no answer to that question.

In Chapter 3 you will see that STOL performance at low speed was thoroughly studied, both with propeller-driven aircraft and then with turbojet-engine-driven aircraft. The fixed-wing advocates of STOL got a big boost when the turboshaft engine was coupled to a ducted fan (they call this power plant a bypass engine). Using relatively lower temperature,

* I suggest that Wilber and Orville Wright accomplished this in 1908. After rather secretive development from 1903 to 1907, Wilber gave widely attended demonstrations in Europe, and Orville fulfilled the brothers' U.S. Army contract at Ft. Myer, Virginia. In 1925, Juan de la Cierva demonstrated his C-4 Autogyro to the Royal Aeronautical Society in England, and then Henrich Focke's helicopter was flown before thousands inside the Deutschland Halle sports stadium in Berlin in 1936.

high-volume airstreams from the ducted fan to blow over deflected flaps, they jumped maximum lift coefficients from 3 up to 6, 7, and even 8. This led STOL advocates to develop what they called "powered lift." By the early 1970s, powered lift STOL technology was so well developed that the U.S. Air Force created a competition for an Advanced Medium STOL Transport (AMST). The Air Force ultimately chose Boeing to build a YC-15 and McDonnell Douglas to build a YC-14. The competition was fierce right up to the end when the Air Force changed their mind. They decided that a tactical machine was not what they wanted; they wanted a strategic aircraft instead, and this led to the McDonnell Douglas C-17, which is now in service. And so a STOL aircraft comparable to the U.S. Marines/Bell Boeing V-22 has yet to be seen in either military or commercial service.

Chapter 4 summarizes my examination of 100 V/STOL aircraft split nearly equally between rotorcraft types that can hover and go fast, and fixed-wing types that can go fast and land slow. My selection is hardly complete, but I have gathered enough data about each aircraft to convey the progress made by the aviation industry since the 1920s. This data may be of use in the future. From this data, I selected 16 concrete examples of V/STOL aircraft that are representative of what has been accomplished over nine decades.

Let me add that what interested me most in my literature search and compiling of this volume was the continual rejection of V/STOL by the commercial side of the business. This rejection by airlines and government regulatory bodies—despite aircraft having demonstrated quite adequate technology—appears to be simply because a pressing need has yet to come upon us. In short, I found no clamoring by the traveling public for short-haul service. The traveling public appear satisfied with their cars, some buses, and a few trains. Over the decades, rotorcraft and fixed-wing STOL advocates alike have offered any number of solutions to congestion and no one has taken them up on them—regardless of the cost of a ticket. I imagine this situation will change sometime in the future, in which case this concluding volume may be of some use.

In closing, Winston Churchill famously said:

> "Writing a book is an adventure. To begin with it is a toy and an amusement. Then it becomes a mistress, then it becomes a master, then it becomes a tyrant. The last phase is that just as you are about to be reconciled to your servitude, you kill the monster and fling him to the public."

He's right about servitude. So I particularly want to thank my wife, Sue, for putting up with this three-volume tyrant who has occupied our house and made constant demands.

ACKNOWLEDGMENTS

I could never have written this three-volume book without the contributions of many, many, many people. So, let me first acknowledge the authors of the nearly 1,600 references I have used in compiling these three volumes. These references were contributed by over 3,000 people, mostly engineers. As to this Volume III, you will find a listing of just over 250 individuals (beginning on page 783) whose contributions particularly influenced what you will read in just this last volume alone. Thankfully, I have been able to express my appreciation to many of these men and women directly.

You should know that my e-mail contact list contains 256 people directly related to this book. I owe these men and women big time.

Of course, there are several people that I must acknowledge who have given me enormous encouragement and unwavering support throughout the writing process. First of all, Bill Warmbrodt at NASA Ames and Berry Lankinsmith at AFDD have been steady supporters of my efforts; not just this last year and a half devoted to Volume III, but for the 7 years it has taken to compile all three volumes. Secondly, Wayne Johnson, Mike Scully, and Bob Ormiston have each helped get me back on track when I was clearly far off the mark with my words, or my facts, or my figures, or my tables, or all four at the same time.

Finding long-lost references is no easy task, and I am deeply indebted to Kathy Ponce, the librarian at NASA Ames. Kathy recovered many references that add depth to several discussions you will read. I thank her very, very much.

Cathy Dow has been my constant editorial rock, advisor, encourager—you name it—in writing all three volumes. I cannot tell you how many times she said, “Don’t worry about that, I can fix that easily.” Or, even more importantly to you, she would say, “It would read better if you said this...” and then she would quietly add, “if it’s still technically correct.” It is quite impossible for me to express to her all my appreciation—and all my admiration of her skill.

With her New England reserve, my wife said this book would be finished “eventually.” Well Sue, this third and last volume is finished, and it is October 28, 2015.

1 INTRODUCTION

The period from Cierva's demonstration of his C.6A Autogiro in Farnborough, England, in October 1925, up to when Pan American World Airways ushered in jet age service to Europe with a Boeing 707-120 on October 26, 1958, was one of enormous progress in the aviation world. This progress was made primarily in the fixed-wing world as references [1-3] clearly relate. This 33-year period saw the conventional takeoff and landing (CTOL) machine achieve increases in cruise speed, range, cruise altitude, and number of passengers carried. These improvements were not, however, accompanied by reductions in takeoff and landing space required. In fact, just the opposite occurred. And with the arrival of the autogyro, and then the helicopter, fixed-wing advocates were presented with a clear challenge to fix the airplane's major shortcomings—stalling and loss of control at low speed.

I do not think airplane advocates felt particularly threatened by autogyros in the late 1920s because it quickly became apparent that the cruise performance of these short takeoff and landing (STOL) aircraft would never become competitive. Even the vertical takeoff and landing (VTOL) capability offered by the helicopter was relegated to a niche market. Fixed-wing advocates felt (and still feel, in my opinion) that helicopters would never take much of the traveling public's business away from their major civil airlines—or trains, buses, cars, or ships for that matter.

Understanding the fundamental performance problem of the CTOL is a prerequisite to learning about VTOLs and STOLs. Therefore, let me use this introduction to set the stage for an in-depth discussion of vertical and short takeoff and landing (V/STOL) aircraft.

1.1 THE AIRPLANE

The issues of airplane stability, control, and performance at low speed have been serious ones for fixed-wing advocates. The public's perception of airplane safety was quite unsatisfactory until the late 1940s. You read about this safety situation, and the attack on the growing number of fixed-wing-aircraft accidents, in Volume II, Chapter 2.10. What you may not know is that a safe aircraft competition was held in the late 1920s. This competition was sponsored by Daniel Guggenheim and his son Harry (an aviator), major figures who promoted aeronautics in the United States through the Daniel Guggenheim Fund.[1] As the final report [5] about the competition relates, they announced on April 20, 1927:

> "A Safe Aircraft Competition. The object of this competition was to achieve a real advance in the safety of flying through improvement in the aerodynamic characteristics of heavier-than-air [machines], without sacrificing the good, practical qualities of the present day aircraft.
>
> As an incentive to the development and construction of an aircraft having characteristics which would fulfill the conditions laid down by the Rules for the Daniel Guggenheim Safe Aircraft Competition, the Fund offered a First Prize of $100,000 and five 'Safety Prizes' of $10,000 each.
>
> Applications for entry in the Competition were invited on and after September 1, 1927, up to October 31, 1929, as a final date."

To *just qualify* for the competition, any aircraft entered had to meet minimum rules, which, with respect to general performance, were stated as:

> "3. Performance
>
> When carrying full load the aircraft shall satisfy the following minimum requirements in regard to performance:
>
> Maximum Speed (corrected to standard air at sea level)—110 m.p.h.
> Rate of Climb (at 1000 ft.)—400 ft. per min.
>
> 4. Useful Load
>
> The aircraft shall carry 5 lbs. of useful load per h.p. 'Useful load' shall include the following items:
>
> Pilot
> Observer
> Fuel
> Oil
>
> Any special instruments or equipment fitted by the Fund for the purpose of the Competition.

[1] A portion of Daniel Guggenheim's fortune was used to create the School of Aeronautics (a part of the College of Engineering) at New York University in 1926. Daniel's son Harry championed the creation. This was the first university aeronautical program in the United States. The professor was Alexander Klemin, who we honor in the American Helicopter Society with an annual award to a very deserving individual. The school's 30th anniversary was celebrated in 1956 with a small, beautiful pamphlet [4] that recounts the school's history and honors Klemin for his enormous effort in making the school so successful. Many of our rotary wing pioneers graduated from the School of Aeronautics and were taught by Klemin (May 15, 1888–March 13, 1950). Wayne Wiesner, a graduate of the school, gave me his copy of the pamphlet shortly before he died.

5. Fuel and Oil

The aircraft shall provide tank capacity for fuel and oil for 3 hours at full throttle at the normal r.p.m.

6. Instruments

The aircraft shall be provided with all necessary power plant instruments required by the engine installation, and the following flying instruments:

Altimeter
Air Speed Indicator

7. Accommodations

Adequate accommodations and dual control for pilot and observer. For every 10 lbs. of useful load carried in addition to the items specified under (4) above, there shall be at least one cubic foot of cabin or cargo space."

Any aircraft that satisfied the qualification requirements was then permitted to do "Safety Tests and Demonstrations." I have include (a) the complete description of the nine tests/demonstrations, (b) the basis for the award of prizes, and (c) other more general conditions in Appendix A of this volume. In summary, the nine tests were:

1. Speed Tests—controlled flight at minimum speeds not in excess of 35 mph.
2. Test of Landing Run—power-off landing and come to rest within a distance of 100 feet from touchdown. Safe, controlled braking allowed. No trick flying allowed.
3. Test of Landing in Confined Space—glide over a 35-foot-high obstruction and, after touchdown, come to a rest within a distance of 300 feet from the base of the obstruction.
4. Test of Takeoff—wheels off the ground in less than 300 feet. Clear a 35-foot obstacle before 500 feet. Trick flying not permitted.
5. Test of Gliding Angle—a power-off "flat glide" angle no greater than 8 degrees. A "steepest glide," power off, of at least 16 degrees with airspeed less than 45 mph.
6. Test of Stability in Normal Flight—remain in stable flight for at least 5 minutes with hands (and feet) off all controls for any airspeed between 45 mph and 100 mph, even in gusty air.
7. Test of Ability to Recover From Abnormal Conditions—benign behavior following loss of power even in dive at an airspeed up to 120 percent of maximum level flight speed.
8. Test of Controllability—in both calm and gusty air, demonstrate effectiveness of each and all controls throughout the flight envelope.
9. Tests of Maneuverability in Restricted Territory and on the Ground—given a 500-foot-by-500-foot square plot surrounded by an obstruction 25 feet high along its entire boundary, land and take off.

There was real interest in this competition as evidenced by the 27 aircraft manufacturing companies that entered.[2] However, as you might expect, only 15 airplanes (Table 1-1) appeared at Mitchel Field[3] where the tests were conducted. The tests were finally completed on January 1, 1930, and the Curtiss Aeroplane and Motor Company collected the $100,000 first prize with its Curtiss Tanager, shown here in Fig. 1-1. In 2012 dollars, $100,000 becomes about $1.4 million according to the U.S. Bureau of Labor Statistics.

Fig. 1-1. The Glenn Curtiss Tanager was the outright winner of the Guggenheim Safe Aircraft Competition. It featured manually controlled flaps, floating ailerons, long-stroke rugged landing gear, and independently operated brakes.

[2] Both the Cierva Autogiro Company and the Pitcairn-Cierva Autogiro Company of America signed up but, as Peter Brooks notes on page 91 of his superb book about autogyros [6], "the C.18 machine's high vibration and poor performance" caused the Cierva and Pitcairn teams to withdraw.

[3] Located on the Hempstead Plains of Long Island, New York.

Table 1-1. Only the Glenn Curtiss Tanager and the Handley-Page Entries Were Clearly in the Running Out of 27 Initial Contestants Who Entered and the 15 Who Actually Showed Up

	Maximum speed (m.p.h.)	Rate of climb at 5000' (ft/min)	Minimum horizontal speed (m.p.h.)	Minimum gliding speed (m.p.h.)	Landing run (feet)	Landing over obstruction (feet)	Take off run (feet)	Take off over obstacle (feet)	Planform glide (degrees)	Steepest glide (degrees)	Empty weight (lbs.)	Useful load (lbs.)	Full load weight (lbs.)	Rated horsepower	Wing loading (lbs. per sq. ft.)	Power loading (lbs. per h.p.)
1. Alfaro	108.6										1,800	550	1,650	110	9.7	15.0
2. Bourdon	103.3										1,179	486	1,665	90	7.1	18.5
3. Brunner Winkle	106.0										1,205	451	1,656	90	6.5	18.4
4. Burnelli	Appeared at		Field but	withdrew												
5. Command-Aire	114.8	900	46.0								1,482	851	2,333	170	9.5	13.7
6. Cunningham-Hall	94.2		44.0	41.0							1,301	470	1,771	90	8.7	19.7
7. Curtiss	111.6	700	30.6	37.1	90	295	295	500	6	13.2	1,979	880	2,859	170	8.6	16.3
8. Fleet	108.6	610									1,400	500	1,400	90	8.1	17.3
9. Ford-Leigh	102.4										1,550	575	2,125	115	7.3	18.5
10. Gates	Appeared at		Field but	withdrew												
11. Handley-Page	112.4	750	33.4	39.7	82	320	290	440	7.2	12.8	1,378	778	2,156	155.6	7.4	11.9
12. McDonnell	Airplane crashed in demonstration flight															
11. Moth	Appeared at		Field but	withdrew												
14. Schroeder-Wentworth	Airplane crashed in preliminary flight															
15. Taylor	108.5		45.5	50.4							1,197	470	1,667	90	9.5	18.5

The reason I have brought this Safe Aircraft Competition to your attention is because it demonstrated the very practical benefit of flaps (and later, slots and slats) and their ability to reduce landing speeds to values that pilots could handle given the size of "airports" then in use. In fact, in early airplane designing during and after World War I, a rather interesting rule of thumb was often quoted. The rule was that the ratio of maximum speed to minimum speed was about 3. When landing speeds approached, and then began to exceed, 50 miles per hour, many pilots were very reticent to fly the new, "hot," larger machines. Of course, the design objective was always faster, higher, and farther, which just meant higher landing speeds, longer runways, and bigger airports. By the early 1930s, speeds were exceeding 200 miles per hour and, even with flaps, landing speeds were over 60 miles per hour.

An interesting example of the importance and application of flaps and other high-lift devices to CTOL aircraft is illustrated in Fig. 1-2. Here you see the trend in landing speed versus maximum speed for about 800 airplanes certificated by the Civil Aeronautics Authority (CAA) and the Federal Aviation Administration (FAA) from 1926 up to the end of 1946. You can see that without flaps the landing speed was, in fact, increasing as maximum speed increased, roughly as $V_{land} = V_{max}/3$. Had fixed-wing advocates not accepted the increase in complexity, weight, and cost associated with high-lift devices, 10,000-foot runways would probably not be long enough, even today!

The scatter that you see in Fig. 1-2 is due, of course, to variations in aircraft type (i.e., monoplanes, biplanes, and seaplanes) and basic design parameters (i.e., gross weight, wing area, wingspan, aircraft drag, installed power, etc.). Still in all, the difference between CTOL aircraft with and without high-lift devices is quite clear.

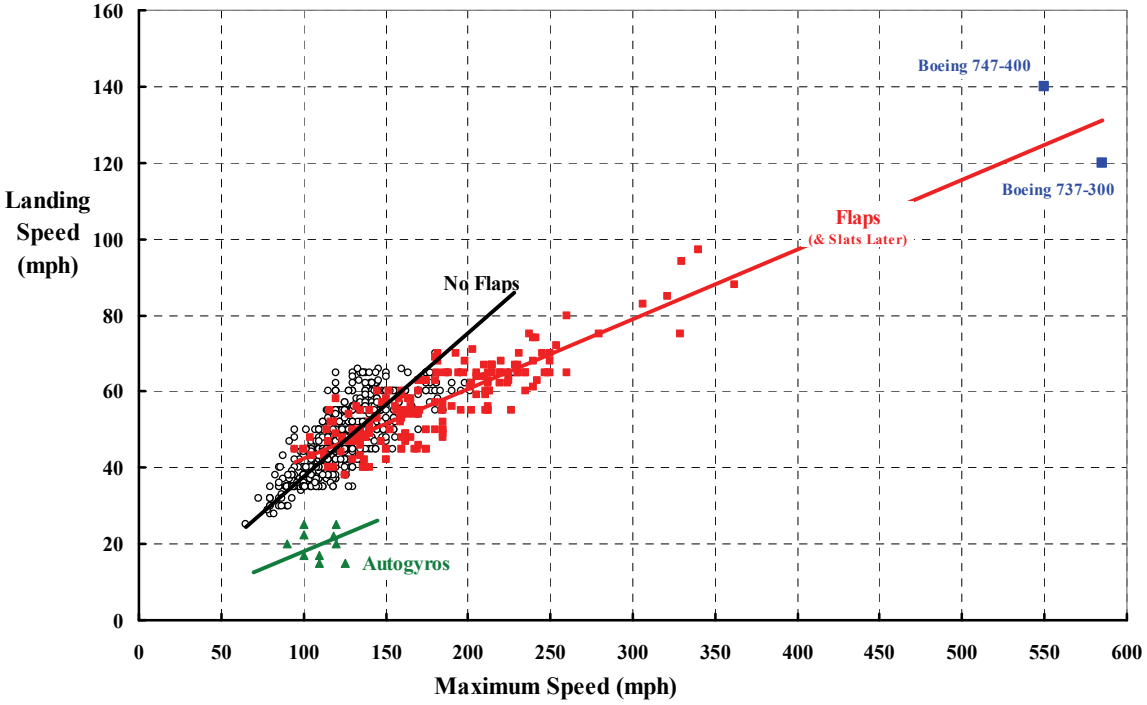

Fig. 1-2. High landing speeds have only been accommodated with 5,000- to 10,000-foot runways.

The data for Fig. 1-2 came from a very unique source that you should be aware of. Joseph P. Juptner (Dec. 3, 1913 to Jan. 3, 2000) compiled a 9-volume set of over 800 civil aviation aircraft [7]. He organized the volumes by CAA Aircraft Type Certificate Number. Using a lifetime of collected historical data, books, magazines, and photos, he gave us a story of aviation (in the United States from 1927 to 1957) that is absolutely unmatched. Because the story of each aircraft is intertwined with the airplane companies that grew—and the many that failed—I think even the casual reader will find each volume a treasure. To whet your appetite, I have included the forward of each volume in Appendix B.

The fact that landing speed is related to maximum speed in a linear manner is quite easy to understand given some simple thinking and the most basic experimental data. Consider, if you will, the fundamental wing lift coefficient (C_L) defined as

$$(1.1) \quad C_L = \frac{L}{qS_w} = \frac{L}{\left(\frac{1}{2}\rho V_{FP}^2\right)S_W},$$

where (L) is wing lift in pounds, (q) is dynamic pressure in pounds per square foot, (ρ) is the density of air being 0.002378 slugs per cubic foot at sea level on a standard day, and (V_{FP}) is the aircraft's speed along the flightpath in feet per second. A constant (L/S_W) for a given airplane flying at a given gross weight (W) and having a given wing area (S_W) means that $C_L\ q = L/S_W$ and, therefore, it follows that at all airspeeds and altitudes (i.e., densities) you have the following relationship

$$(1.2) \quad \left(C_L q\right)_{\substack{\text{landing}\\\text{speed}}} = \frac{L}{S_w} = \left(C_L q\right)_{\substack{\text{max}\\\text{speed}}},$$

which, with a little algebra, becomes

$$(1.3) \quad \frac{V_{landing}}{V_{max}} = \left(\frac{\rho_{\text{at max speed}}}{\rho_{\text{at landing}}}\right)^{1/2}\left(\frac{C_{L\,\text{at max speed}}}{C_{L\text{ at landing}}}\right)^{1/2}.$$

Broadly speaking, airplanes have a maximum lift coefficient that is associated with stalling of the wing. This coefficient is frequently written as C_{Lmax} or sometimes as C_{Lstall}. When a pilot forces his airplane to fly at slower and slower speeds, wing stalling will occur at some speed denoted here as V_{stall}, and the pilot must be ready for his airplane's nose to drop toward a dive, followed by the beginnings of a spin. The general advice to pilots is to approach landing at a speed no slower than 1.25 to 1.3 times V_{stall}. As the airplane gets very close to the runway surface, the pilot can reduce speed below the approach speed, fly just above the ground while slowing down and, with practice, lightly touch down just before stalling occurs. At the other extreme, airplanes are designed for high-speed cruising flight at the lift coefficient where the best lift-to-drag ratio occurs. This lift coefficient for $(L/D)_{max}$ is considerably lower than the lift coefficient for landing. Furthermore, the lift coefficient for maximum speed is again lower than the lift coefficient at which maximum L/D is obtained. In short, the ratio of $C_{L\text{ at max speed}}$ to $C_{L\text{ at landing}}$ as used in Eq. (1.3) is considerably less than 1.0.

The square root of the ratio of densities is 0.9282 at 5,000 feet on a standard day and decreases to 0.5565 at 35,000 feet. Juptner was only able to quote altitude at which maximum speed was obtained for a few points shown on Fig. 1-2. However, judging from the maximum altitude most of the early aircraft were capable of, I would say a square root of 0.93 is reasonable. Of course, the two Boeing aircraft are associated with 35,000 feet.

There are literally thousands of reports offering experimental data on the aerodynamic behavior of lifting wings and providing values of lift coefficients suitable to Eq. (1.3), but let me suggest starting with Ludwig Prandtl's fundamentals from the mid-1910s, which were reported in NACA Report No. 116 [8]. Prandtl discovered the now classical relationship between wing lift and drag, which we write in modern notation as

$$(1.4) \qquad C_D = \frac{D}{q S_W} = C_{Do} + \frac{C_L^2}{\pi AR}.$$

Here Prandtl used (C_{Do}) as the profile drag coefficient, aspect ratio (AR) as wingspan (b) divided by wing chord (c) for the rectangular wing, and defined wing lift coefficient (C_L) in accordance with Eq. (1.1).

Prandtl supported his theoretical work with experimental lift-drag polars for rectangular wings having aspect ratios from 7 down to 1, which is a square wing. His results are reproduced here (to the best of my ability) as Fig. 1-3. To give more weight to the validity of Prandtl's theory, I have replotted his experimental results in Fig. 1-4.

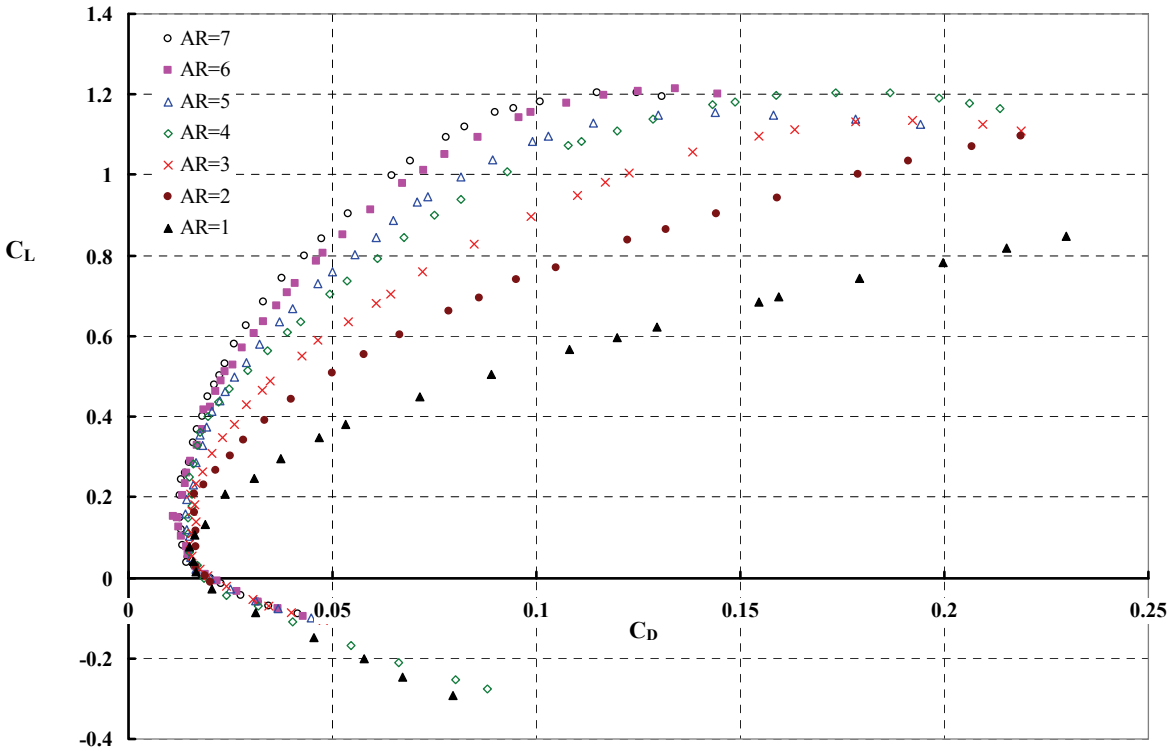

Fig. 1-3. Prandtl's experimental data for rectangular wing lift and drag [8].

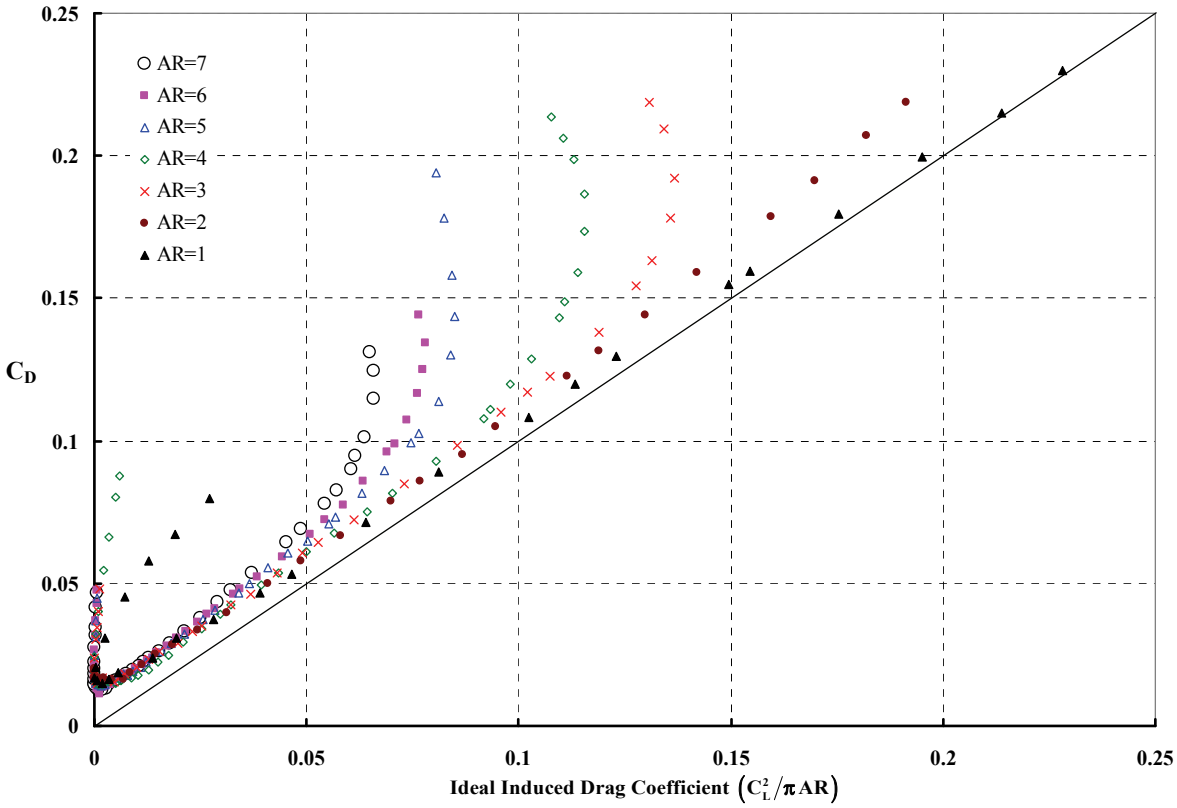

Fig. 1-4. Prandtl's theory is clearly supported by experimental data as you see here.

Prandtl defined the ideal-induced-drag coefficient as

$$(1.5) \qquad C_{D_{ideal}} = \frac{D_{induced}}{q S_W} = \frac{C_L^2}{\pi AR}.$$

It is rather natural to plot experimental wing drag versus Prandtl's ideal induced drag as I have done in Fig. 1-4. Now you see that Prandtl's drag measurements—primarily at induced drag coefficients below 0.05—have collapsed the data at several aspect ratios from Fig. 1-3 to one line. For Prandtl's wings (which had a cambered airfoil), a reasonable approximation is simply

$$(1.6) \qquad C_D = \frac{D}{q S_W} = 0.0106 + 1.0443 \frac{C_L^2}{\pi AR}.$$

One thing that has always fascinated me is to see experimental data for low-aspect-ratio wings give the appearance of being immune to stalling when the results are presented in the format of Fig. 1-4. Of course, as Fig. 1-3 shows, low-aspect-ratio wings actually have very high drag when compared to high-aspect-ratio wings at the same lift coefficient.

It might surprise you to know that wing aspect ratio is not a major parameter in actual pounds of drag. Aspect ratio only appears in the coefficient form of drag versus lift. You see

this immediately by dimensionalizing Eq. (1.4). That is, if you multiply Eq. (1.4) through by qS_W, and remember that AR equals b/c for a rectangular wing, you arrive at

$$(1.7) \quad D = qS_W C_{Do} + \frac{1}{\pi q}\left(\frac{L}{b}\right)^2,$$

and this result shows that induced drag in pounds is a function of what we call span loading (i.e., L/b). Many aerodynamicists, myself included, prefer to work in terms of drag divided by dynamic pressure (D/q) in square feet, where you have

$$(1.8) \quad \frac{D}{q} = S_W C_{Do} + \frac{1}{\pi}\left(\frac{L}{qb}\right)^2.$$

Another fundamental that Prandtl gave us with Eq. (1.4) is the fact that every practical wing has a maximum lift-to-drag ratio (L/D), Fig. 1-5, or C_L/C_D if you prefer. Simple calculus shows you that a wing achieves a maximum L/D when the lift coefficient is

$$(1.9) \quad C_L \text{ for maximum } L/D = \sqrt{\pi C_{Do} AR}$$

and, therefore, the maximum lift-to-drag ratio is calculated as

$$(1.10) \quad \text{Maximum}\frac{L}{D} = \frac{1}{2}\sqrt{\frac{\pi AR}{C_{Do}}}.$$

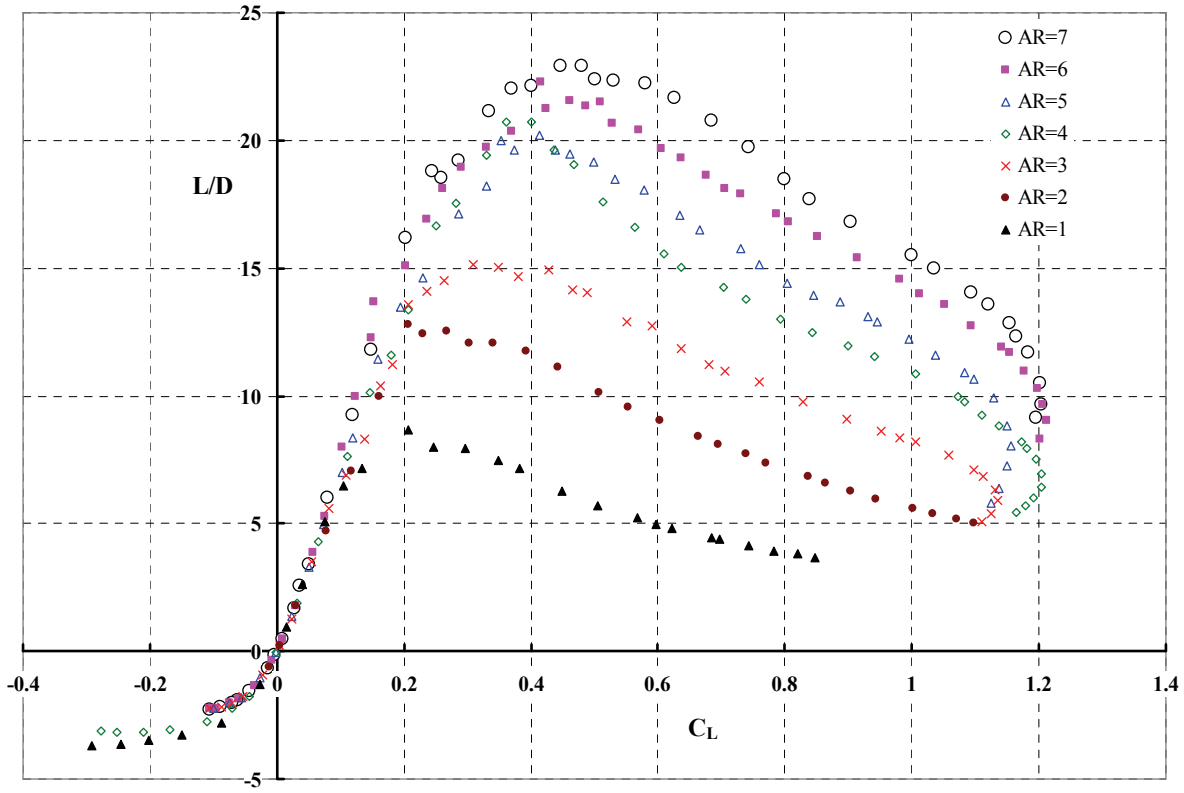

Fig. 1-5. Maximum L/D occurs at lift coefficients well before stall (i.e., $C_{L\,max}$).

This discussion giving you some background about conventional takeoff and landing (CTOL) airplanes would be incomplete without extending Prandtl's wing theory contribution to a complete airplane. The example I have selected comes from the National Advisory Committee for Aeronautics (N.A.C.A.), specifically from the Langley Memorial Aeronautical Laboratory located near Newport News, Virginia. In 1936, researchers tested a Fairchild Model 22 C7A, powered by a 95-horsepower engine with a modified wing, in the Langley 30- by 60-foot full-scale wind tunnel and in flight. They were investigating the change in performance and handling qualities that came with a Fowler flap.[4] Their Langley report came out in August of 1936 [9]. The commercial Fairchild 22 C7, Fig. 1-6, was not sold with flaps. The Langley engineers built a test wing that had the Fowler flap system, which is shown in cross section in Fig. 1-7. The flap span was 22 feet, and it had a chord of 1.29 feet. The wingspan was 31 feet—a reduction from the commercial model—and the wing area, with flaps not deployed, was 132 square feet.

Fig. 1-6. The Fairchild 22 C7 had a 75-hp engine. The wingspan was 32.83 feet with a 66-inch chord and an area of 170 square feet. The weight empty was 870 pounds, and the gross weight was 1,400 pounds. It sold for $2,675 at the factory [10].

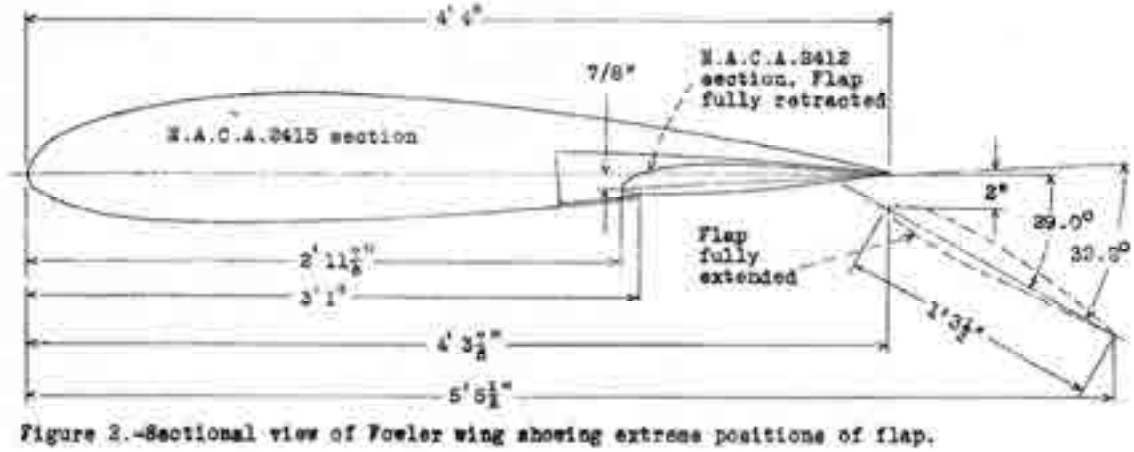

Figure 2.-Sectional view of Fowler wing showing extreme positions of flap.

Fig. 1-7. N.A.C.A. Fowler flap configuration used in Langley testing [9].

[4] Harlan D. Fowler (June 18, 1895–April 27, 1982). His papers can be found in the Special Collections and Archives at San Jose State University in File Identification MSS-1995-04.

The Langley engineers showed just how practical their experiments could be by selecting the Fairchild 22 as the test aircraft. When you look at this "parasol" monoplane, you can see that changing to any kind of wing was extremely easy from a structural point of view. After all, the wing was attached by a simple arrangement of struts. The aircraft became nothing more than a flying wind tunnel to study wings. This is very clever thinking in my mind. The Langley Fairchild 22 with the Fowler flap test wing is shown in Fig. 1-8. Because of reflected sunlight, the wing appears tapered. It was, in fact, rectangular.

The summary to the test report [9] is quite interesting. The authors, Dearborn and Soulé, stated:

> "Full-scale wind-tunnel and flight tests were made of a Fairchild 22 airplane equipped with a Fowler flap to determine the effect of the flap on the performance and control characteristics of the airplane. In the wind-tunnel tests of the airplane with the horizontal tail surfaces removed, the flap was found to increase the maximum lift coefficient from 1.27 to 2.41. In the flight tests, the flap was found to decrease the minimum speed from 58.8 to 44.4 miles per hour. The required take-off run to attain an altitude of 50 feet was reduced from 935 feet to 700 feet by the use of the flap, the minimum distance being obtained with five-sixths full deflection. The landing run from a height of 50 feet was reduced one-third. The longitudinal and directional control was adversely affected by the flap, indicating that the design of the tail surfaces is more critical with a flapped than a plain wing."

The classical aerodynamic characteristics of the Langley Fairchild 22 with flap retracted and at flap angles of 7.0, 18.0, 24.5, and fully extended and fully deflected to 32.2 degrees, is shown in the following figures. The coefficients are based on a wing area of 132 square feet even though the flap increases the actual area as it deflects as Fig. 1-7 shows. The progression is that the "chord" grows as follows: 0 deg (c_0 = 4 ft 4 in.), 7 deg (c = 1.1 c_0), 18 deg (c = 1.19 c_0), 24.5 deg (c = 1.226 c_0), and 32.2 deg (c = 1.26 c_0).

Fig. 1-8. The Langley modified Fairchild 22 had a 95-hp engine at 2,100 rpm. The wingspan was 31 feet with a chord of 4 feet 4 inches and an area of 132 square feet. The aspect ratio was 7.27, and the airfoil was a NACA 2415. The testing was conducted at a weight of 1,574 to 1,600 pounds (photo courtesy of Langley Memorial Aeronautical Laboratory).

The wind-tunnel-measured drag polar (i.e., C_L versus C_D) for the Langley Fairchild 22 is summarized in Fig. 1-9 and enlarged in Fig. 1-10, but with a reversal of axes (i.e., C_D versus C_L). A number of important facts can be obtained from these two graphs. First, from Fig. 1-9, progressively deflecting and extending the flap does raise the maximum lift coefficient. It also raises the aircraft drag, which can be very helpful in the approach to landing and to the final flare and touchdown. Second, the aircraft, like most airplanes, has a drag polar that is not symmetrical around $C_L = 0$. This is a measure of the overall aircraft camber. Because of this cambered aircraft geometry and the resultant airflow, the drag polar is not as simple as Prandtl's data for a cambered wing showed. You see this fact in Fig. 1-10. To quantify this point, I have curve fit[5] the five polars in the region below stall with a second-order polynomial as

$$C_D = C_{Do} + \delta_1 C_L + k C_L^2 \tag{1.11}$$

and included the constants (C_{Do}, δ_1, and k) for each flap deflection where test data was obtained.

It is worth noting that the lift coefficient for maximum L/D and the actual maximum L/D now become

$$C_{L\,for\,max\,L/D} = \sqrt{\frac{C_{Do}}{k}} \quad \text{and} \quad \left(\frac{L}{D}\right)_{max} = \frac{1}{2\sqrt{kC_{Do}} + \delta_1}. \tag{1.12}$$

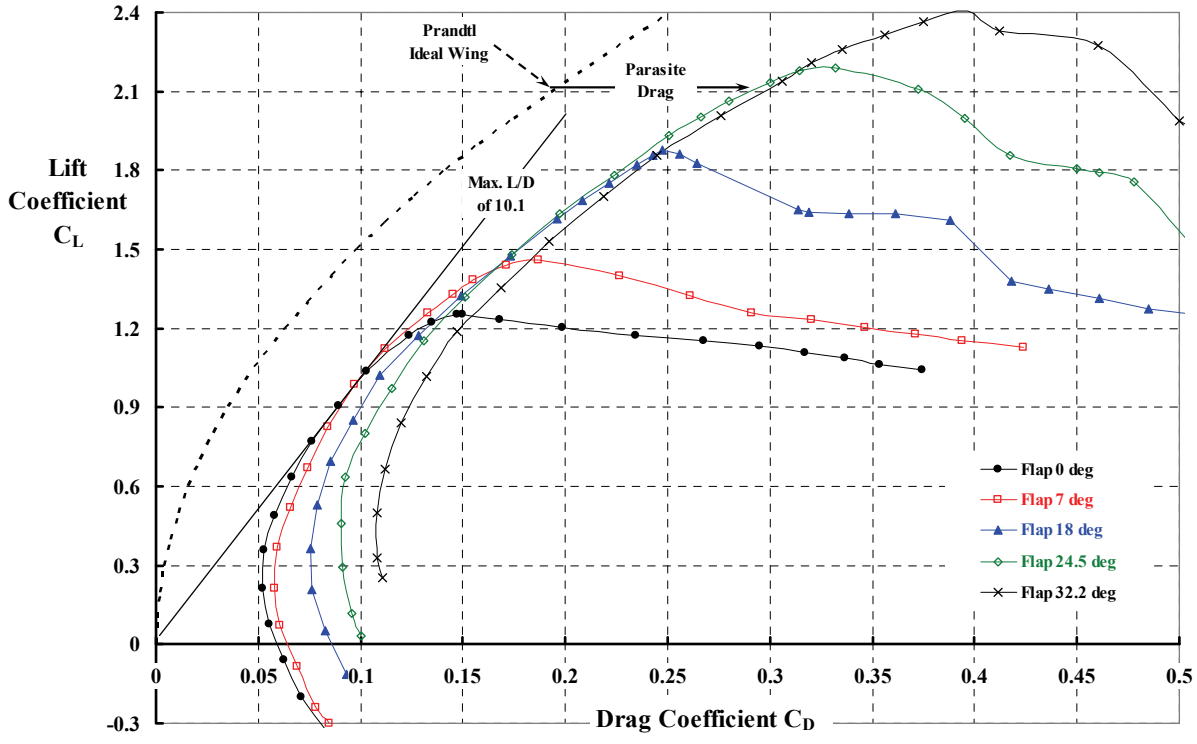

Fig. 1-9. Drag polars for the Langley Fairchild 22 [9].

[5] I used the Microsoft® Excel® trendline tool assuming a polynomial.

Keep in mind that the constant (k) in Eq. (1.11) includes Prandtl's $1/\pi AR$ that accounts for ideal induced drag. Thus, for the wing with the flap fully retracted (i.e., a plain wing of aspect ratio 7.27), the Langley Fairchild 22 had a drag polar described by

(1.13) $$C_D = 0.05808 - 0.04479C_L + 0.08836C_L^2$$

and k = 0.08836. Now, $1/\pi AR = 0.04378$, and if you say that $k = \delta_2 + 1/\pi AR$, it follows that δ_2 equals 0.04458. Therefore an aircraft's drag polar can be approximated as

(1.14) $$C_D = C_{Do} + \delta_1 C_L + \delta_2 C_L^2 + \frac{C_L^2}{\pi AR} = C_{Dparasite} + \frac{C_L^2}{\pi AR}$$

where the parasite drag is defined as $C_{Dparasite} = C_{Do} + \delta_1 C_L + \delta_2 C_L^2$.

The major point of this opening discussion of CTOL aircraft and the importance of Eq. (1.3), repeated here for convenience,

(1.3) $$\frac{V_{landing}}{V_{max}} = \left(\frac{\rho_{at\ max\ speed}}{\rho_{at\ landing}}\right)^{1/2} \left(\frac{C_{L\ at\ max\ speed}}{C_{L\ at\ landing}}\right)^{1/2},$$

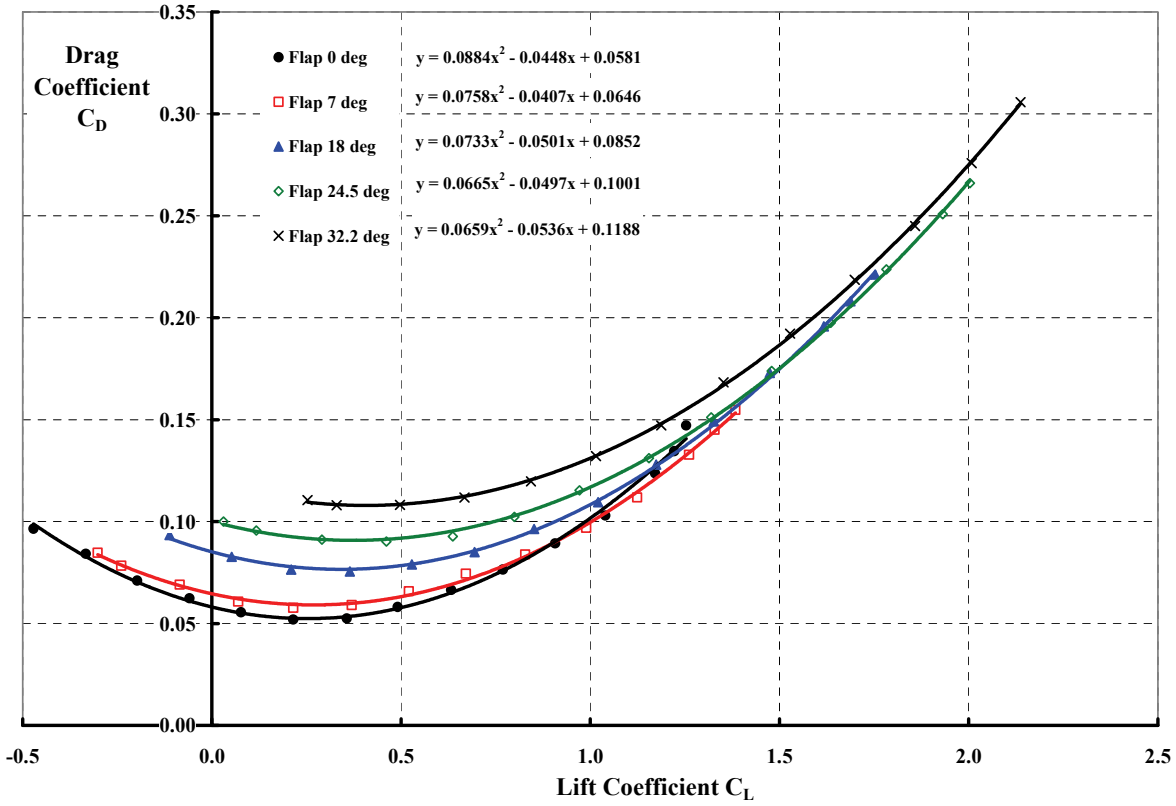

Fig. 1-10. Below stall, a drag polar can be approximated with a second-order polynomial [9].

is that flaps reduce the ratio of $C_{L\ at\ max.\ speed}$ to $C_{L\ at\ landing}$. You see this for the Langley Fairchild 22 in Fig. 1-11. I have set the $C_{L\ at\ max.\ speed}$ at 0.9 based on Fig. 1-9. The $C_{L\ at\ landing}$ can be taken as $C_{L\ max.}$, which increases with Fowler flap deflection. If you now say that landing occurs at sea level, then $\rho_{\ at\ landing}$ is 0.002378 slugs per cubic foot. The only other variable is $\rho_{\ at\ max.\ speed}$, and this says *obtain maximum speed at as high an altitude as practical because density goes down with altitude*.

There is an important additional message here. Advocates of CTOL aircraft learned that their aircraft—designed first for maximum speed at high altitude—could have its landing speed further reduced by increasing the wing area (S_W) for landing. I have not included that variable in the preceding discussion, but many flap and slot/slat high-lift systems do just that. This fact leads you to the subject of short takeoff and landing (STOL) aircraft, which I will discuss later in this volume.

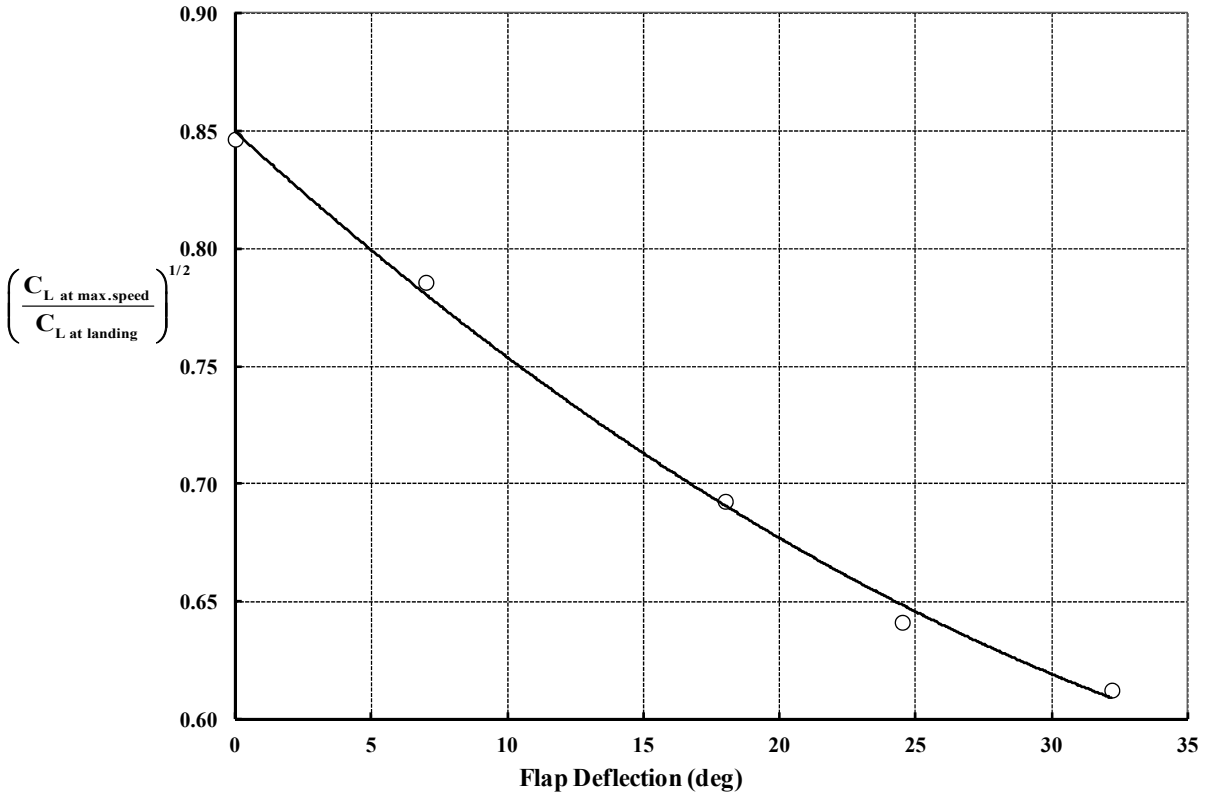

Fig. 1-11. Flaps, slats, and slots allow a wing to have two configurations—one configuration optimized for efficient cruise and the other for slow-speed landing.

1.2 GROWTH OF CTOLS, HELICOPTERS, AND OTHER V/STOL AIRCRAFT

There are three concluding points to this introduction that I want you to appreciate. The first point has to do with how slowly the helicopter (VTOL) side of the aviation industry developed in comparison to the progress made with CTOL aircraft. To make this point, I have used the growing number of Aircraft Type Certificates issued by the CAA and the FAA since 1926.[6] For the 800 CTOL aircraft, I have used data from Juptner's 9 books [7]. For the helicopter count, I have gone to the FAA website and downloaded every Helicopter Type Certificate Data Sheet I could find (there may be more). You see the comparison in Fig. 1-12. To make the comparison crystal clear, I have indexed the date as years after the first Type Certificate was issued.

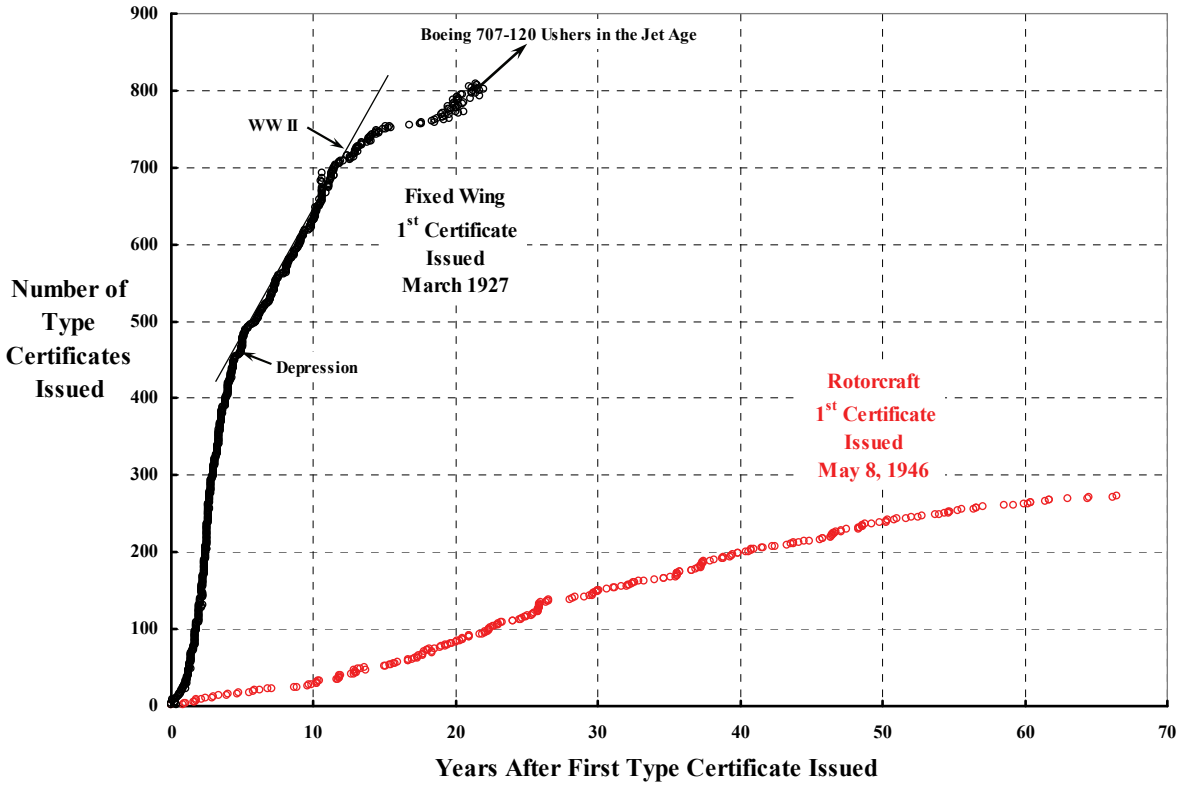

Fig. 1-12. Compared to CTOL aircraft, helicopters have been very slow taking their place in the civil aviation world.

[6] The Air Commerce Act of 1926 created the father of aviation regulation, the Civil Aeronautics Authority (CAA). Legislation gave the CAA power to regulate airline fares, approve routes, and oversee safety. The safety arm of the CAA, the Civil Aeronautics Board (CAB), was established in 1940; the CAA issued pilot and aircraft certifications and handled safety enforcement, and the CAB became responsible for safety regulations and accident investigations. The Federal Aviation Act of 1958 recombined the CAA and CAB into the Federal Aviation Administration (its name was formalized in 1967), which became a part of the newly created U.S. Department of Transportation. The National Transportation Safety Board (NTSB) was made independent of the FAA in 1967.

It is very interesting to me to see just what impact the economic crash of October 1929 (i.e., the Great Depression) had on the aviation world as viewed in Fig. 1-12. Juptner devotes the forewords of several volumes (see Appendix B) to how the fixed-wing manufacturers dealt with the economic circumstances. Furthermore, when World War II loomed on the horizon, manufacturers seemed to have rushed certification of many new models. Then when the industry buildup for WWII really began, all attention was devoted to converting civil aircraft to military use, and the development of fighters and bombers. With the end of WWII, industry turned back to commercial aviation, and then, as you know, jet engines and swept wings arrived.

What is so painfully obvious about Fig. 1-12 is that there is not one V/STOL—other than helicopters—that appears on the FAA list of certificated rotorcraft. Well, that is not quite right. There are a few autogyros (STOLs in my mind) and a few other fixed-wing STOLs to be considered, but too few to single out at this point in this volume. That is not to say that both fixed-wing and rotary wing sides of the aircraft industry were not doing V/STOL in-house homework. There were literally hundreds, if not thousands, of paper studies. However, and even more importantly, all three military branches in several countries began to take a very serious look at V/STOLs—so serious, in fact, that many experimental and development programs were funded.

My second point helps you appreciate the search for a useful V/STOL aircraft just by counting the sheer number of configurations that reached some level of flight status. By my count shown in Fig. 1-13, all the paper studies led to 100 V/STOL aircraft that have become

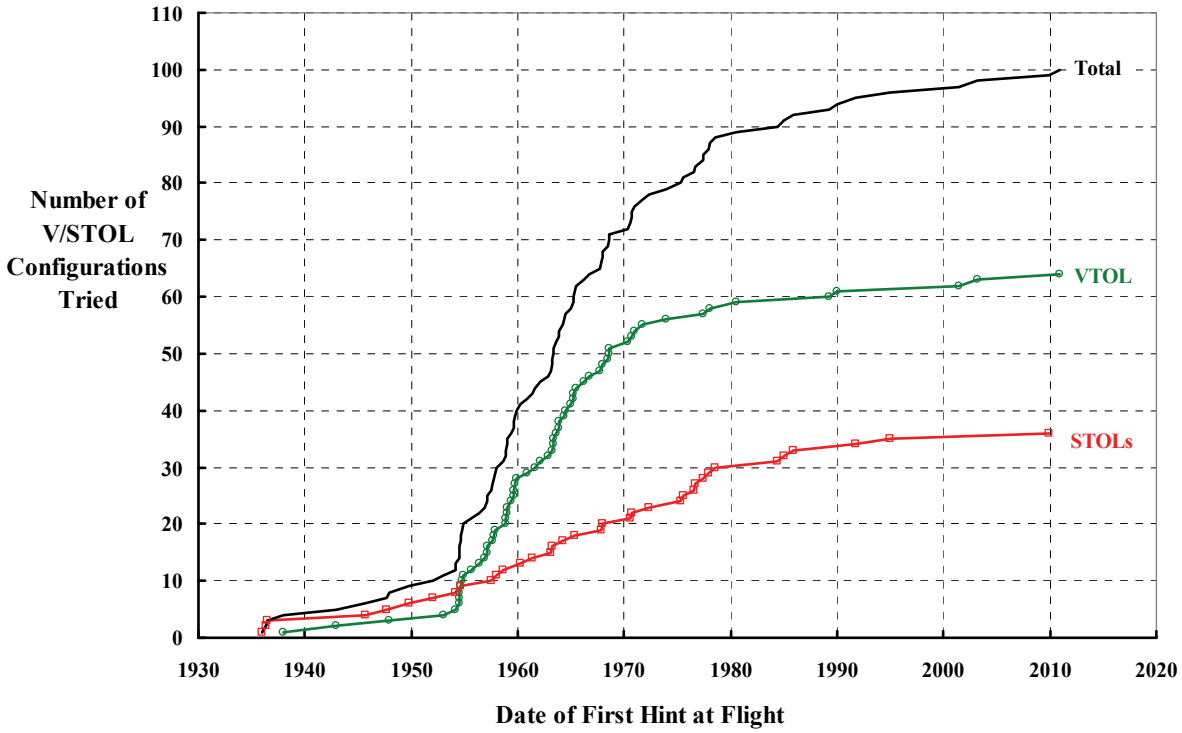

Fig. 1-13. The number of V/STOL aircraft that have demonstrated at least a hint of flight worthiness. The real weeding-out process took less than 25 years.

technologically and historically significant. Of these 100, only 64 are VTOL machines, and out of the 64, only 2 have gone into production. Of the 36 STOLs, only a very few reached production status and, as I have said, only a few STOLs have obtained an FAA Type Certificate. *As of December 2015, no VTOL has received an FAA Type Certificate*

This raises my last point, which is how I have kept track of VTOLs, STOLs, and CTOLs in this volume. The way I think about the three classifications (Fig. 1-14) is this:

1. A VTOL aircraft can take off and land vertically at a quite respectable operational weight, which includes operationally useful payload and fuel. At an overload weight, it can also take off and land over a 50-foot obstacle in 1,000 feet or less, which is the demarcation used by the U.S. Air Force for a short takeoff and landing aircraft [11] (i.e., a STOL[7] aircraft). Furthermore, most VTOL aircraft can operate as CTOL machines.
2. A STOL aircraft *cannot* take off and land vertically, but it meets the U.S. Air Force 1,000-foot criteria. While a STOL aircraft may have the power to perform as a VTOL, it does not have an adequate flight control system for flight at zero, or even very low, speeds.
3. A CTOL aircraft cannot take off and land vertically and, because of an inadequate flight control system, has only a bare minimum of STOL capability and no VTOL capability.

You might note that by applying the U.S. Air Force criteria for STOL, I have immediately included virtually every light airplane and glider ever made, whether it had flaps and other high-lift devices or not. This is *not my intent at all* for the purposes of this V/STOL volume as you will see from the examples of STOL aircraft I have selected. At the other extreme are airplanes that operate off of a Navy carrier deck. I suppose these are the ultimate STOLs. But my emphasis in this Volume III is on aircraft suited to civil aviation and particularly passenger- carrying V/STOL aircraft, which I think of as transports. For the 10- to 120-passenger V/STOL machine that will become FAA certificated, it is hard for me to accept STOL landing or takeoff accelerations greater than 0.2 times 1 unit of gravity (g = 32.17-feet-per-second squared), which means about 6-feet-per-second squared. With this criteria, you can imagine a STOL landing over a 50-foot obstacle with a deceleration of 6-feet-per-second squared. Basic F = ma physics says that

$$V_{landing} = \sqrt{2aS}, \quad (1.15)$$

where deceleration (a) equals 6 ft/sec^2 in my view and, say, landing distance from the obstacle (S) equals 1,000 feet. Then the landing speed at the obstacle can be no greater than 110 feet per second, which is 75 miles per hour or, if you prefer, 65 knots. If you extend the runway length to 2,000 feet, the landing speed at the obstacle becomes 105 miles per hour or 92 knots. At 5,000 feet, you compute 167 miles per hour or 145 knots, and in the extreme of a 10,000-foot runway, you get 236 miles per hour or 205 knots.

[7] The U.S. Air Force later amended its position by extending the distance to 1,500 feet [12].

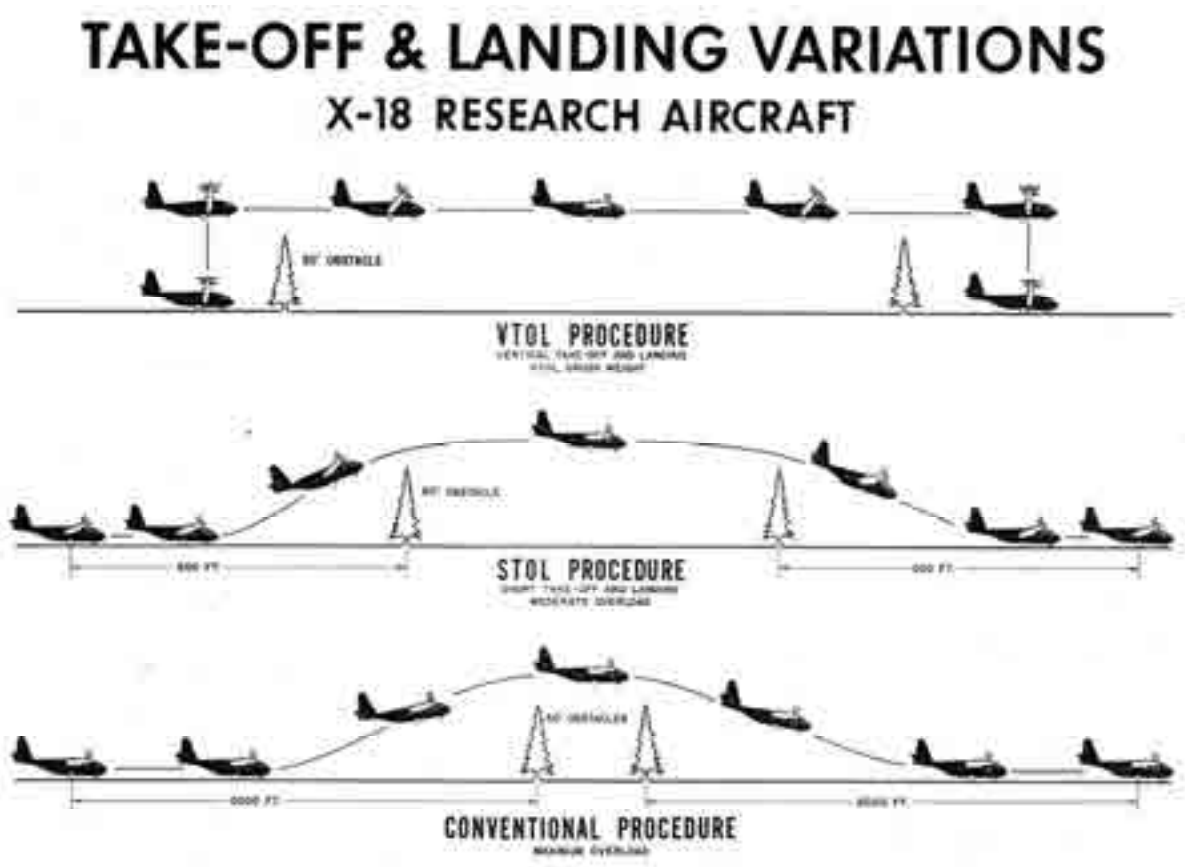

Fig. 1-14. Most VTOLs can improve their takeoff and landing performance as STOLs and even as CTOLs [13].

In late September of 1969, George Schairer, Vice President of Research and Development for the Boeing Company, provided a more practical view[8] of landing distance as related to approach speed than what Eq. (1.15) offers [14]. Mr. Schairer noted, with my additions in brackets, "I can assure you that I started my career designing helicopters 35 years ago and have had many years of experience with propellers [B-17, B-29], jets [B-47, B-52, Dash 80, 707, etc.], and fans. I will try to be impartial." Based on his decades of experience, he offered the statement that

$$S = 600 + 0.255V_{kts}^2 \tag{1.16}$$

where the all-weather, safe landing field length (S) in feet was for sea level on a standard day, and the approach speed (V) was in knots. He included several very important comments about operational considerations that 35 years of experience had taught him. He wrote:

"TAKEOFF AND LANDING DISTANCE

Takeoff and landing performance as presented in V/STOL literature has been computed to widely different standards and direct comparisons are seldom possible. In this

[8] This view was presented in his speech given at the U.S. Air Force–sponsored V/STOL Technology and Planning Conference held in Las Vegas, Nevada—then the V/STOL technology capital of the world!

paper I will attempt to make comparisons using field size and the ability to hover as primary definitions. Takeoff field length means to me the size field from which an aircraft can take off under all weather conditions at the stated temperature and altitude. This field length permits aborting the takeoff, following an engine failure, to land back into the same takeoff field, or alternatively, the aircraft must be able to complete the takeoff without aborting. The field size definition is the size field which an operator would find acceptable for day-in and day-out continued operation at the stated altitude and temperature. Similarly, my definition of landing field length is the size field into which, for the stated altitude and temperature, and under instrument weather conditions, landing operations can be safely completed and with engine failures anticipated at any time during the landing operation. Thus, field length represents the size field into and from which the aircraft can be routinely operated and not the performance which can be demonstrated under flight test and stunt operations.

In addition to the field length and engine-out definitions given above, I define VTOL aircraft as those aircraft which are able to hover in and out of ground effect at takeoff gross weight with all engines operating. I define STOL aircraft as those aircraft which operate into and out of small fields but which are unable to hover in or out of ground effect.

LANDING FIELD LENGTH

Although there are many factors affecting the choice of a safe landing field length, experience has shown that approach speed dominates any comparison. Figure 1 [see Fig. 1-15] is a plot of landing field length versus approach speed. The data at higher approach speeds are taken directly from aircraft which are approved under civil air regulations to operate in these length fields. They permit wet weather landings under instrument conditions of aircraft equipped with good brakes and aerodynamic braking devices such as reverse thrust, but operating into slippery landing fields. These aircraft have provisions, through redundancy, for a degree of failure of the braking devices. The approach speed is one which can be used under most circumstances of gusts and winds and provides for adequate margin from stall. There have been very few commercial landing accidents due to lack of adequate field length, but most commercial operations are conducted from landing fields substantially longer than that which is permitted, as shown on figure 1.

Aircraft with hovering capability can complete their approaches and slow to a hover before landing. They require a cleared area for a safe landing but only a pad for touchdown. Slow flying aircraft will need both clearance during approach and a reasonable length of runway.

Quite arbitrarily I have chosen 600 feet as the minimum length of field into which most operators would care to conduct day-in and day-out all weather VTOL landing operations. The landing field sizes shown provide for being in error by a reasonable amount when flying down a landing approach aid and for reasonable alertness in the application of deceleration devices following landing. Developments are possible which will permit bettering this relationship shown in Figure 1, but I doubt that they will come soon, and suggest that the required landing field size for safe operation of V/STOL aircraft is well represented by Figure 1. If operations are desired into small fields, low approach speeds are absolutely necessary. I do not believe that safe operations, all weather or otherwise, can be conducted by approaching at 100 knots and using 1 G deceleration devices to permit operation into fields like 1500 feet long."

You might note in passing that the Super Sonic Transport (SST), the Concorde, had a maximum speed of 1,350 knots and was certificated to a minimum control speed—during approach to landing, with the critical engine inoperative—of 150 knots [15], which is 172.5 miles per hour. It was said that the Concord could land anywhere a Boeing 747 could land.

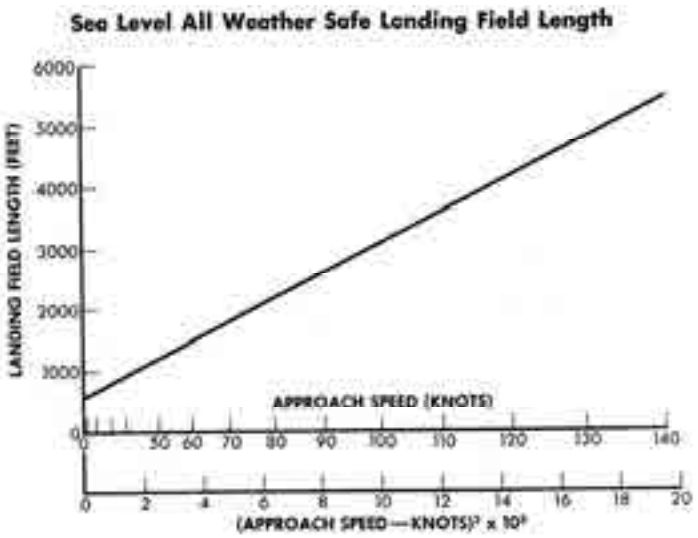

Fig. 1-15. Boeing's Vice President of R&D, George Schairer, presented this view on aircraft landing field lengths in September 1969 [14].

From Mr. Schairer's experience, the safe landing field length for the Concorde would be no less than 6,400 feet.

It is fascinating to me to reread Mr. Schairer's views [16] from 1961.[9] This vintage 50-page paper includes 5 pages of references that he used to examine data for a number of configurations in the most fundamental aerodynamic way I am aware of. It includes no direct discussion of the tiltrotor. I believe he felt that the tiltwing was the more promising VTOL configuration. His final summary is quite brief—all he said was:

> "In final summary, the author finds that the technology of vertical lift aircraft is reasonably well developed in the case of the helicopter but hardly explored for other arrangements. Much progress is possible in the helicopter and very great improvements can be expected in other vertical take-off schemes. The application of the design methods used for large fixed-wing aircraft is likely to result in a marked rate of improvement in V/STOL aircraft."

To refer to V/STOL aircraft as "vertical take-off schemes" seems, to me, an indication of just how unsatisfied with industry progress Mr. Schairer and many, many other V/STOL advocates were in 1961.

---

[9] I applied to Piasecki Helicopter Corp. for a job in late 1955. But in March of 1955, Frank Piasecki was forced out by Laurence Rockefeller and Felix DuPont, and my job offer came from the Vertol Aircraft Corp. I went to work at Vertol in June of 1956. On March 31, 1960, we became the Vertol Division of the Boeing Company. The Boeing guys came in to manage us. The first thing they did—that affected me—was to take the coffee machines out. Later we became the Boeing Vertol Company, and we moved from Morton, Pennsylvania, to brand new offices in Ridley Park, Pennsylvania. The name was changed to the Boeing Helicopter Division in 1987, but I had moved to Bell Helicopter Textron in July of 1977. As a part of my apprenticeship, it was my privilege to discuss, and rarely debate, many helicopter and V/STOL thoughts with Mr. Schairer. In truth, I was in awe of Mr. Schairer, who had (I felt then and still feel) more in-depth knowledge of ALL aviation fundamentals then any leader I have encountered in my career. I contributed in a minor way, along with several others, to three papers [14, 16, 17] that Mr. Schairer wrote, and he signed copies of the papers, which I cherish. In 1991, Mr. Schairer wrote me a letter in which he said, "Take a good look at tiltwings with rotors instead of propellers. They may be much simpler." He retired from Boeing in 1978 and died in late October 2004.

1.3 CATEGORIZING V/STOLS

The successful application of gas turbine engine technology shortly after World War II let the decades-long imagination of V/STOL advocates soar. You get a sense of this pent-up imagination by reading volume 13 of Gene Liberatore's *Rotary Wing Aircraft Handbooks and History* [18]. He prepared this 18-volume series for the U.S. Air Force Wright Air Development Center, located on the Wright-Patterson Air Force Base in Ohio. At that time (1954), VTOL aircraft were quite frequently referred to as convertiplanes. Volume 13 opens with an organization table showing what could be done with rotary wing aircraft. I have included his table here as Fig. 1-16, and the sketches he drew are in Appendix C. When you look at Gene's sketches in Appendix C, I think you will conclude that he emphasized what we have categorized today as compound helicopters. Note that he shows most concepts first in a vertical takeoff configuration and secondly in the forward-flight configuration.

The rest of Liberatore's volume 13 is devoted to some 70 different "convertiplanes" and includes historical summaries with some technical data. He reaches back to 1904 and concludes in the 1940s. If your criteria were more generous than just some hint of flying—which was the basis of Fig. 1-13—then you could probably add 100 to 150 more "V/STOLs" to the list. For one example, Mr. Luther C. Crowell of West Dennis, Massachusetts, got a patent [19] on June 3, 1862, for a configuration that could be flight adjusted to be a compound, an airplane, a tiltrotor, or many combinations thereof. The patent allowed for folding wings (to avoid download in hover), and the wings could tilt independent of the tiltable rotors! As a second example, Liberatore might have included the famous Danish aviation engineer Jacob Ellehammer's coaxial fan-in-wing model from the 1930s [20], which you see here as Fig. 1-17.

When military interest became serious, there was real money infused into the search for both tactical and logistic aircraft (i.e., fighters and transports). V/STOL advocates at the McDonnell Aircraft Corporation composed what was called a wheel so their aviation industry activity could be summarized at a glance. I believe the first version came out in 1963. This first version accounted for 76 aircraft in various stages of thinking or doing. By 1967 the V/STOL waterfront was becoming clearer, and the first McDonnell V/STOL wheel was cleaned up with a revision published in September of that year and shown here in Fig. 1-18. You read this wheel from the innermost ring outward. Thus, the top level of categorization consists of just five approaches to V/STOL:

1. Same propulsion system for hover and forward flight.
2. Augmented power plant for hover.
3. Combined power plant for hover.
4. Separate power plant for hover.
5. And, of course, the proverbial catchall for some fixed-wing advocates, special types and helicopters.

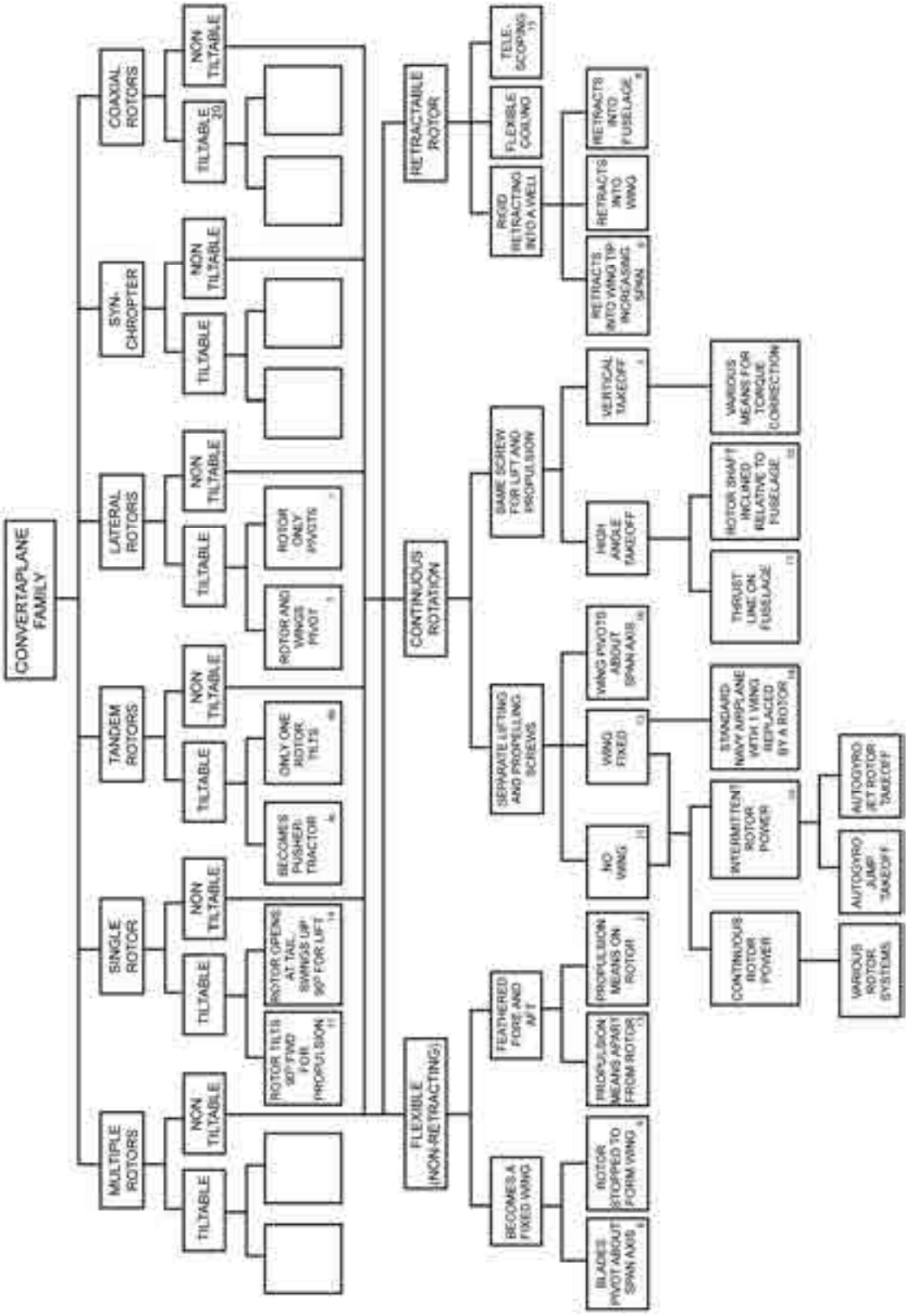

Fig. 1-16. Liberatore's categorizing of VTOLs in 1954 [21].

Fig. 1-17. Jacob Ellehammer believed that "an aircraft should have the maximum cruising speed and require a minimum of runway." A venetian blind was to unroll over the fans (top and bottom) in forward flight [20].

In 1988 Bernard (Bernie) Lindenbaum, with the benefit of several decades of hindsight, constructed a different V/STOL categorizing chart. Bernie wrote an extremely valuable report [22] for the U.S. Air Force Flight Dynamics Laboratory. You can see from Fig. 1-19 and Fig. 1-20 that Bernie used disc loading (the ratio of weight to disc area) as the primary sorting parameter, and worked his way from rockets and turbojets/turbofans (Fig. 1-19) down to propellers and finally rotors (Fig. 1-20). In his foreword to the first volume, he wrote:

> "To date only the first volume has been completed and published. It contains, in addition to the Introduction and Background section, sections covering: Rocket Based Vehicles, Turbojet/Turbofan-Powered Vehicles of the wingless type, and Turbojet/Turbofan-Powered Aircraft of the Vertical Attitude Take Off and Landing type. Other volumes, yet to be written, are intended to cover all of the other forms of turbojet/turbofan V/STOL aircraft, aircraft which use propellers, and those which use helicopter type rotors."

There were to be five volumes in toto, but I do not think he was able to finish them before he died in late September of 2002. The depth of detail Bernie was able to go into from his massive collection is just mind-boggling. Today, thanks to his son Stephen, Bernie's papers are in the library at Wright State University in Dayton, Ohio. (This collection is a gold mine that I hope will be tackled and published for all to read.)

The V/STOL wheel that we know today (Fig. 1-21) began with Harold (Hal) Andrews' efforts in the mid-1990s. At that time the U.S. Air Force, Navy, and Marines began a very serious effort to develop a fighter that could at least supplement, if not replace, the Harrier. It is now called the Joint Strike Fighter (JSF) program. Hal went to work to update the V/STOL wheel [23]. He limited the aircraft to be included to "only those VSTOLs that had reached the stage of getting off the ground." We owe a great deal of thanks to Mike Hirschberg for the beautiful artwork that first appeared in the March/April 1997 issue of *Vertiflite* [23], the American Helicopter Society's (AHS's) quarterly magazine. Mike was an engineer at the

ANSER Corporation at that time. Later, Mike changed hats and became Director of the AHS when Rhett Flater retired. Mike has not, however, lost his interest in V/STOL history, which we can also appreciate.

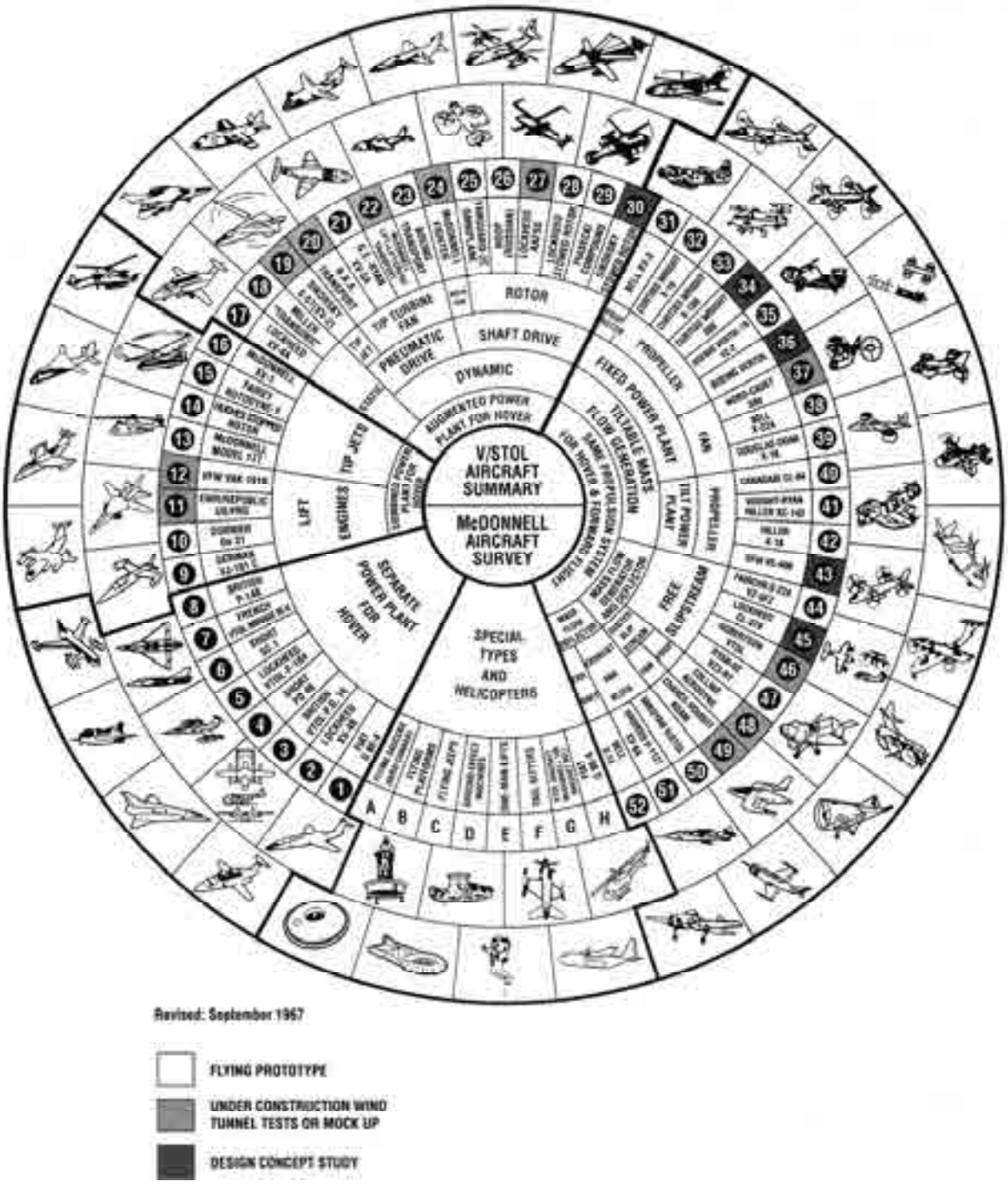

Fig. 1-18. By 1967 the aviation industry had a much clearer view of potentially worthwhile V/STOL configurations.

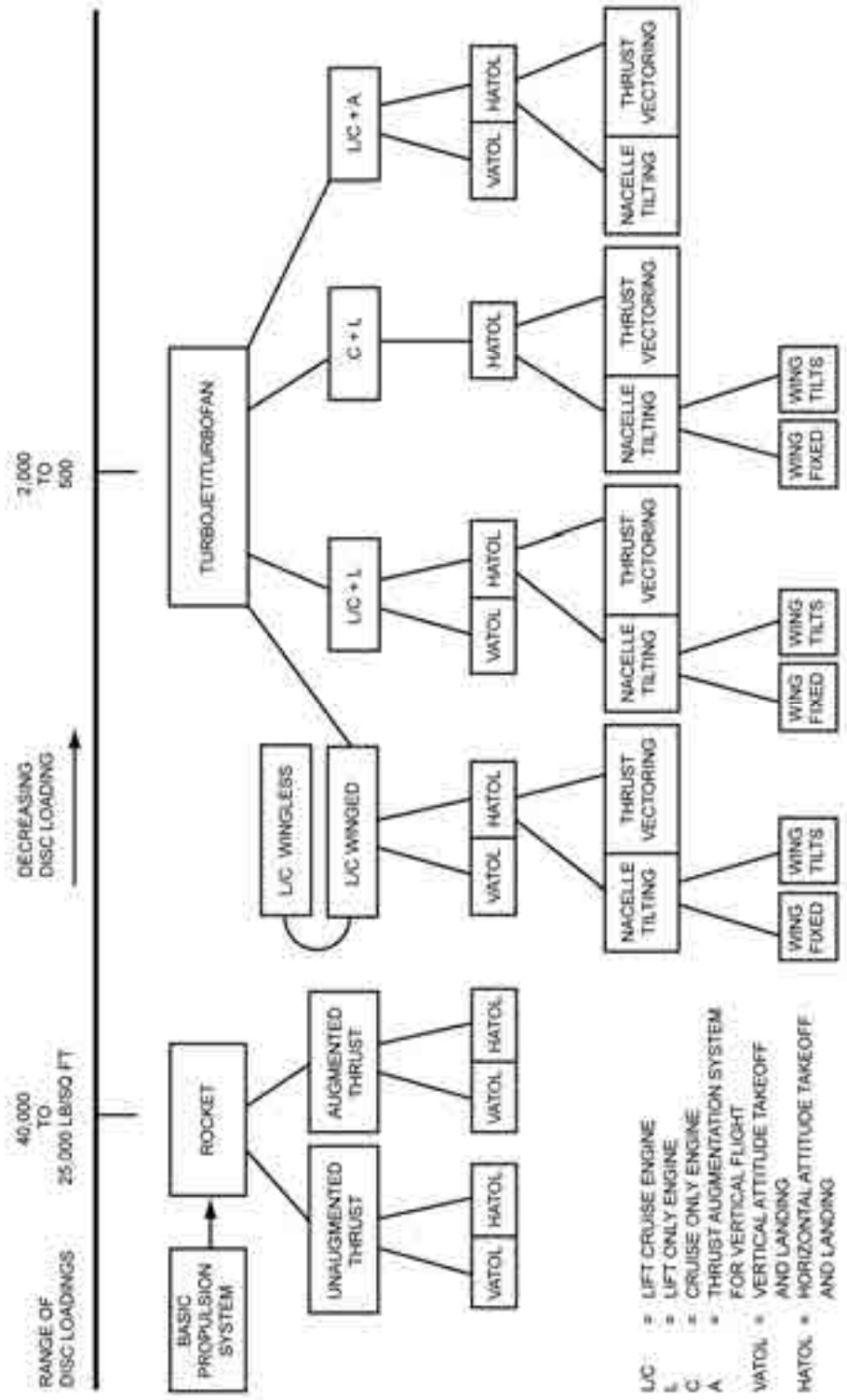

Fig. 1-19. Bernie Lindenbaum's 1988 view of all the possible configurations for V/STOL (part 1) [22].

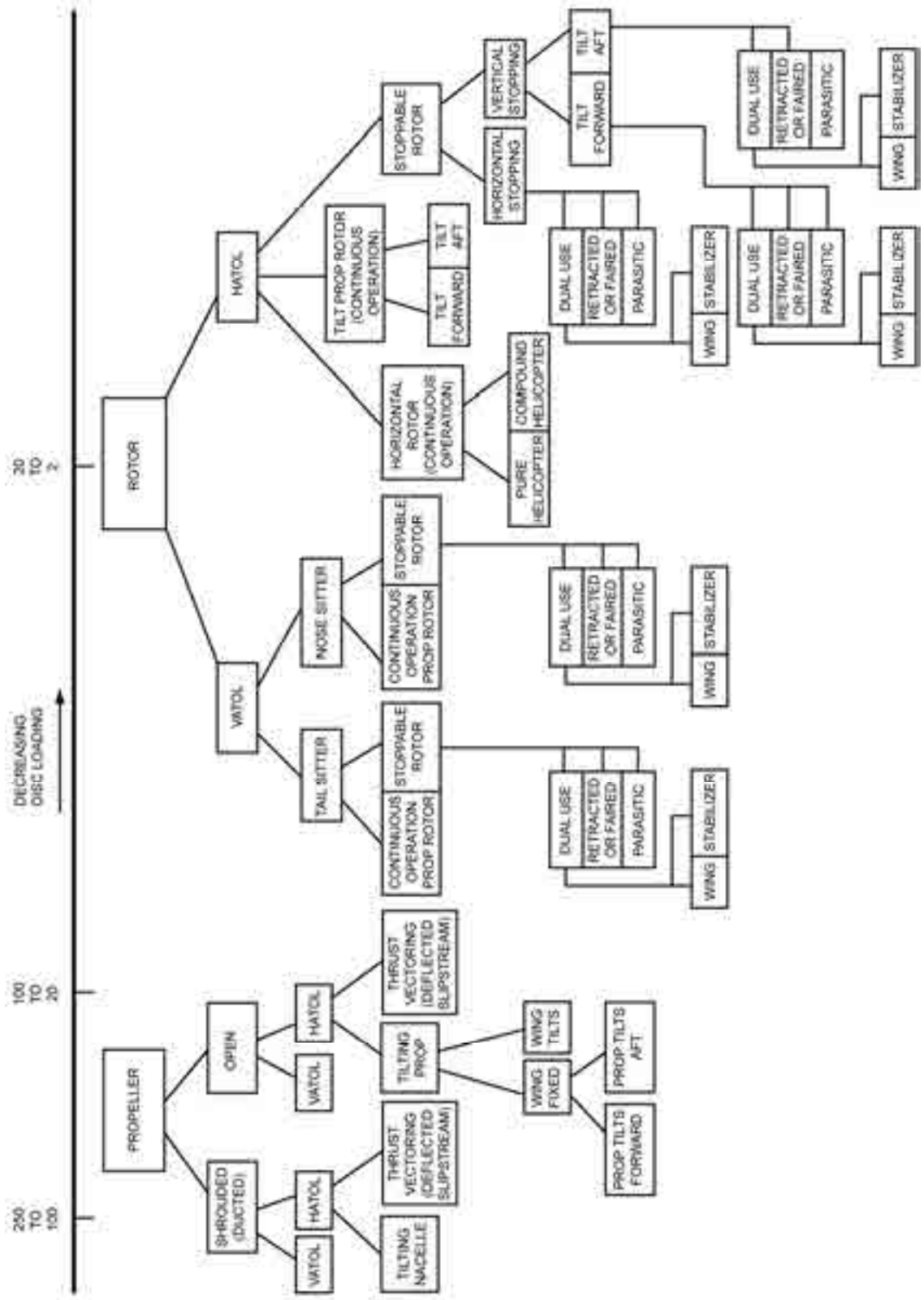

Fig. 1-20. Bernie Lindenbaum's 1988 view of all the possible configurations for V/STOL (part 2) [22].

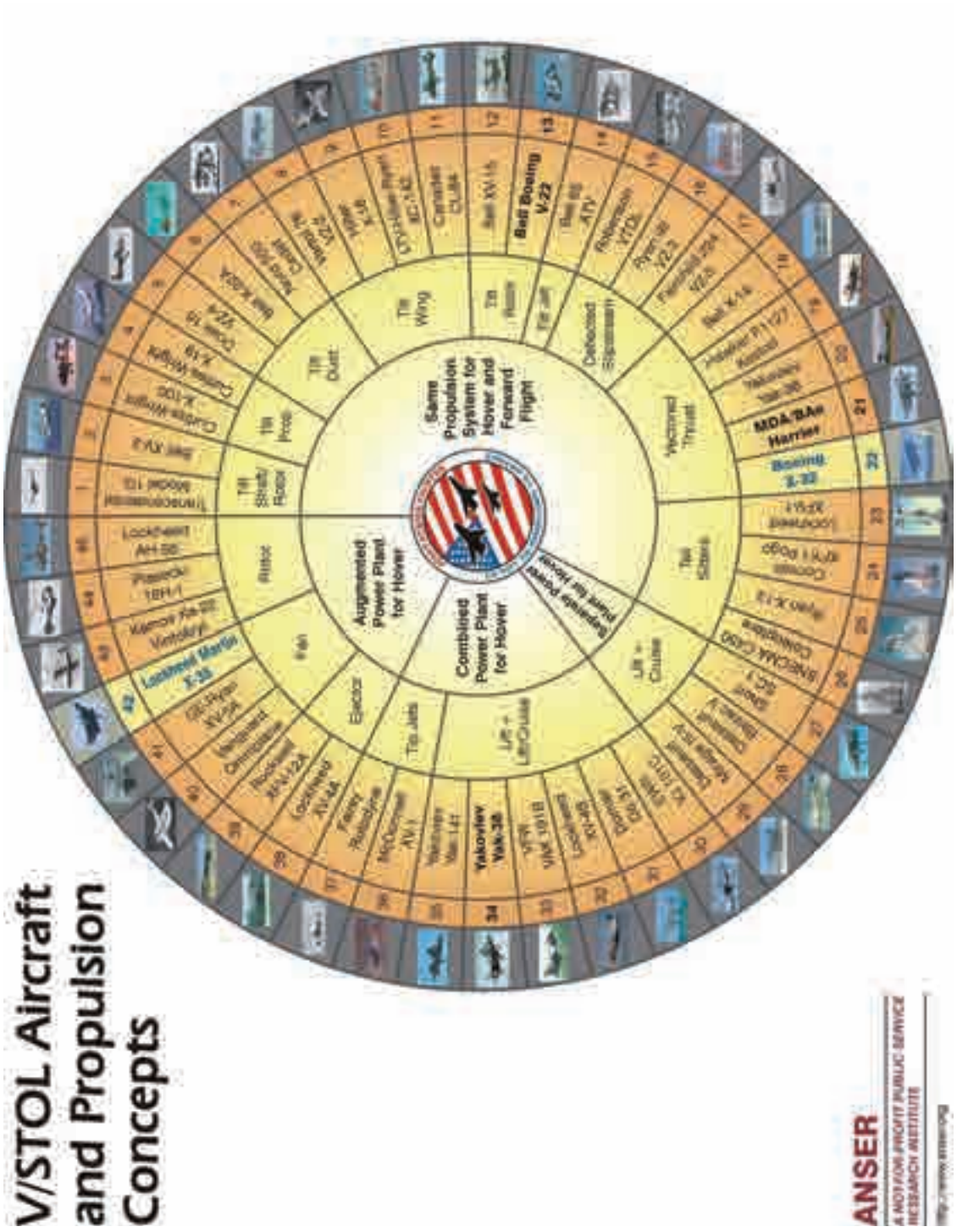

Fig. 1-21. Hal Andrews updated the McDonnell wheel to help the Joint Strike Fighter (JSF) program survey the state of the art for V/STOLs. Mike Hirschberg, then at ANSER Corporation, turned Hal's careful selection into an absolute work of art in 1997 [23].

The one thing that stands out above all else in the categorizing of V/STOL aircraft that you have just read is this: *The engines (power plants, if you prefer) are all important to V/STOL.* Because of this indisputable fact, I group V/STOLs by engine type (and there are really only two available types): (1) piston engines and (2) gas turbine engines. It is true, of course, that subsets of the two engine types are available. For instance, a piston engine can be turbocharged or not. The gas turbine has three popular subsets: (1) turboshaft (which includes turboprop in my mind), (2) turbojet, and (3) turbofan.[10] To me, that is it—at least in this year of 2014. All the aircraft that have come and gone fall into piston or gas turbine boxes, ***but*** several gas-turbine-powered V/STOL aircraft use a combination of turboshaft (or turboprop) and turbojet (or turbofan) engines. Because there are several helicopter rotors that are rotor-blade tip driven rather than shaft driven, you can have a category of tip driven for hover and piston or gas turbine for forward flight. You can see right away how difficult it can be to categorize V/STOL aircraft on a wheel or in an organization chart format.

After putting a configuration into the piston or gas turbine column in my mind, the most logical subsets appear (in hindsight) to be transports (commercial and military) and fighters (just military); then below that you have VTOL and STOL. In Fig. 1-22 you see 100 aircraft that I have selected for further study in this volume.

It is now November of 2014 and, from the efforts of so many over 75 years, the V/STOLs that are currently in production number just three by my count. They are:

1. The Bell/Boeing V-22 (Fig. 1-23), a VTOL transport powered with gas turbines.
2 The Boeing C-17A (Fig. 1-24), a STOL transport powered with gas turbines.
3. The McDonnell/British Aerospace Harrier (Fig. 1-25), a VTOL fighter powered with a gas turbine.

Now stop for a moment and take a close look at each of these aircraft. Imagine a commercial airliner derivative carrying ticket-paying passengers rather than transporting military troops or cargo. When I look, I do not see a sleek fuselage like, oh say, a Boeing 737 that Southwest operates. Furthermore, I cannot imagine approaching a Southwest executive with some warmed-over artist's rendition of any one of these aircraft in airliner colors. I suppose you could take the Harrier and convert it to a corporate jet capable of carrying 3 or maybe 4 passengers in rather cramped quarters. You might even add some windows. The C-17A's fuselage probably could be converted to an upper- and lower-deck seating arrangement since its basic fuselage is a tube, 15 feet in diameter and 70 feet long. The V-22's fuselage looks to be one-third rear ramp, and it only seats 24 troops. In short, modern day fuselages for the military just never appear adaptable to commercial airliners. This is a direct contrast to the situation just prior to WWII when Douglas and Lockheed airliners were pressed into quite satisfactory service for the military, who could then concentrate on designing and building just bombers and fighters.

[10] I really think a turbofan engine is just a turboshaft engine driving a ducted fan, and a turboprop engine is really a turboshaft engine with a gearbox to reduce RPM down to what propellers need.

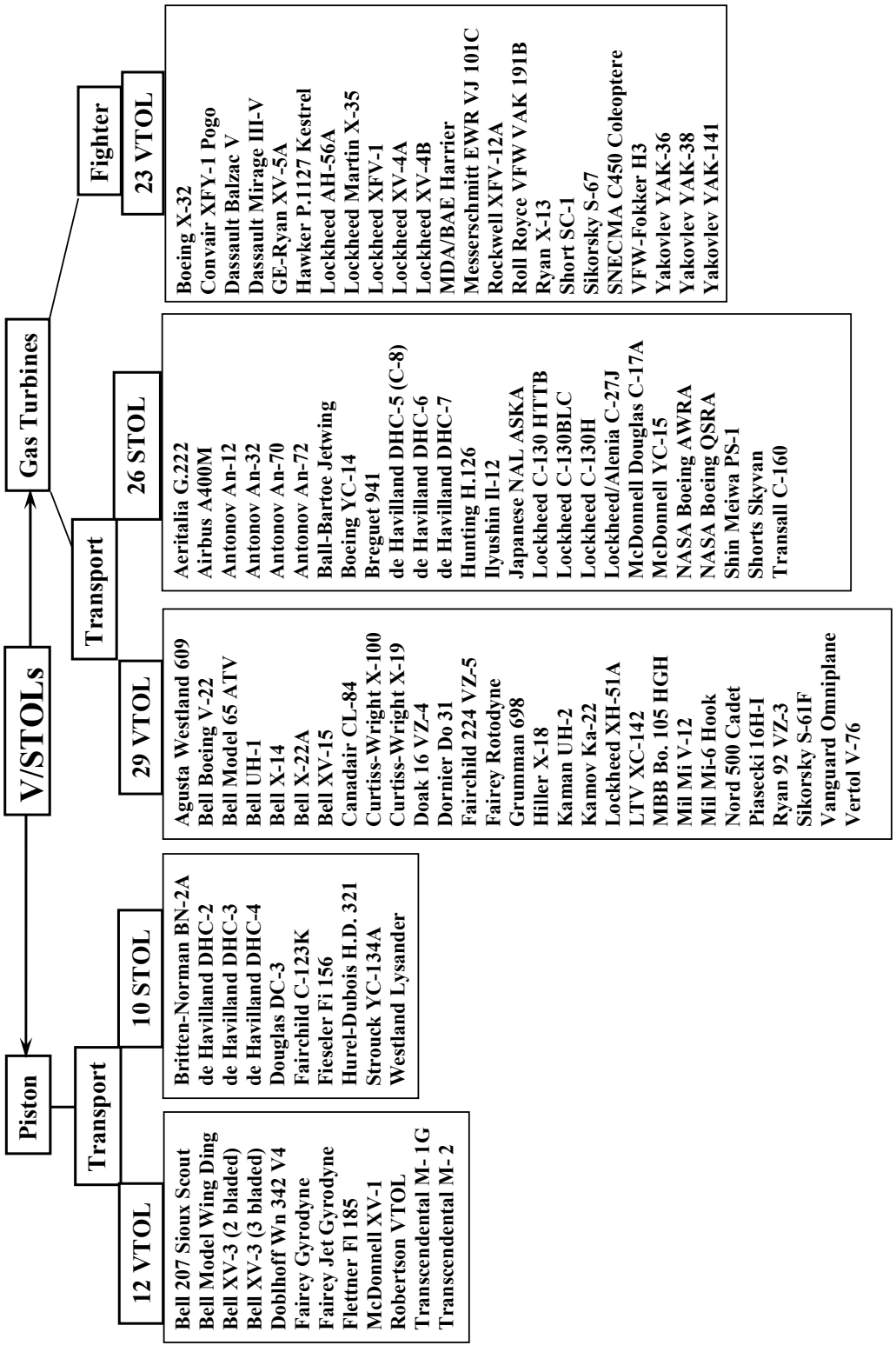

Fig. 1-22. Harris' categorizing of V/STOLs.

Fig. 1-23. The Bell/Boeing V-22, a VTOL transport powered with gas turbines. A collage showing the aircraft in hover, in transition with the rotors partially tilted, and in cruise flight.

Fig. 1-24. The Boeing C-17A, a STOL transport powered with gas turbines. Jet engine exhaust increases lift from the flaps.

Fig. 1-25. The McDonnell/British Aerospace Harrier, a VTOL fighter powered with a gas turbine. To hover, the single engine directs all of its jet thrust downward.

The three V/STOLs that emerged from the 75-year weeding-out process have four things in common. First, they all use a wing for forward flight. Second, they all use gas turbines. Third, the same power plant system is used for takeoff and landing, and for forward flight. Configurations that succeeded experimentally with multiple engines—one set for hover and another for forward flight—proved unacceptable. Spin-offs of helicopter rotors using tip drive (rather than shaft drive) plus another power plant for forward flight were equally unacceptable. Fourth, the 75 years of research and experimentation established that V/STOLs having two separate lifting surfaces (such as a rotor for hovering, and a wing and propeller for forward flight) have also just not been in the cards.

One thing you should keep in mind is that the three V/STOLs that reached production achieved this milestone because the need (military or civil) coincided with available, low-risk technology, and both coincided with development money—and then production money—being available. But most important, in my mind, is that each of the three V/STOLs had champions who stayed the course.

Should you find yourself exploring the pros and cons of V/STOLs other than the ones I have listed in Fig. 1-22, let me suggest a path that I have found quite helpful. I find it rather easy to sort out the configurations themselves based solely on the fundamental force equations that follow from F = ma. That is, the sum of vertical forces in the lift (L) direction (Z), and the sum of the propulsive forces (PF) in the horizontal direction (X), must always equal mass times acceleration in that direction. This must be true whether the aircraft is in hover or forward flight or anywhere in between. Following this logic, I suggest that

$$\sum F_Z = ma_Z = L_{Wings} + L_{Rotors} + L_{Props} + L_{Ducted\ Fans} + L_{Pistons} + L_{Turboshafts} + L_{Turbojets} + L_{Turbofans} + etc. - W_{Aircraft} \quad (1.17)$$

and

$$\sum F_X = ma_X = PF_{Wings} + PF_{Rotors} + PF_{Props} + PF_{Ducted\ Fans} + PF_{Pistons} + PF_{Turboshafts} + PF_{Turbojets} + PF_{Turbofans} + etc. - D_{Aircraft} \quad (1.18)$$

From these two equations you can imagine all of the V/STOLs I have listed in Fig. 1-22. Frankly, if you think about it, there is the possibility that an 8-by-8 matrix can exist from Eqs. (1.17) and (1.18). Thus, one very complicated V/STOL configuration could have 64 components in some unbelievable combination. More rationally, for example, a tiltrotor (Fig. 1-23) uses the same thrusting unit for lift in hover and propulsion in forward flight, and uses a wing for lift in forward flight.

A bird is the most fundamental "V/STOL aircraft" you might consider. A bird uses just one "device," a wing, to both lift and propel itself. A helicopter is close to a bird because its rotary wings both lift and propel. Experiments have been conducted where a wing has been added to a helicopter to augment rotor lift. Other experimental helicopter configurations have been tested where an additional propulsive force device has been added to obtain high speed. In my opinion, a compound helicopter is nothing more than a CTOL with the addition of a rotor. A CTOL fixed-wing aircraft uses a wing plus a propeller (or rotor, or ducted fan) driven by a piston or turboshaft engine. Alternately, you could have a CTOL with a wing plus a turbojet or turbofan. It is just a matter of carefully booking the aircraft's components. It seems to me that there really is very little need to create a name for each configuration that can be constructed from Eqs. (1.17) and (1.18), although we do have a tendency to do just that.

1.4 POPULAR REFERENCES

In contrast to popular books about airplanes and helicopters, which are quite numerous, authoritative books about V/STOLs are few and far between. However, in conjunction with this volume, I think you will find the following books and documents of considerable value:

1. *Vertical Takeoff & Landing Aircraft* by John P. Campbell [24] (1962). John and many other key researchers at NASA Langley completed research on virtually every aerodynamic aspect of most configurations engineers were proposing. The sketches of VTOL configurations (Fig. 1-26) John included on the book's flyleaf are particularly clear. The key problems of many machines, and solutions that were found, are covered in simple language and without introducing a raft of equations.
2. *VTOL Military Research Aircraft* by Mike Rogers [25] (1989). You are updated to 1989 with this compilation of program aspects and operational facts in the most comprehensive study of virtually every VTOL (and a few STOLs) you can name (Fig. 1-27). Rogers pays particular attention to flight control systems and handling qualities.

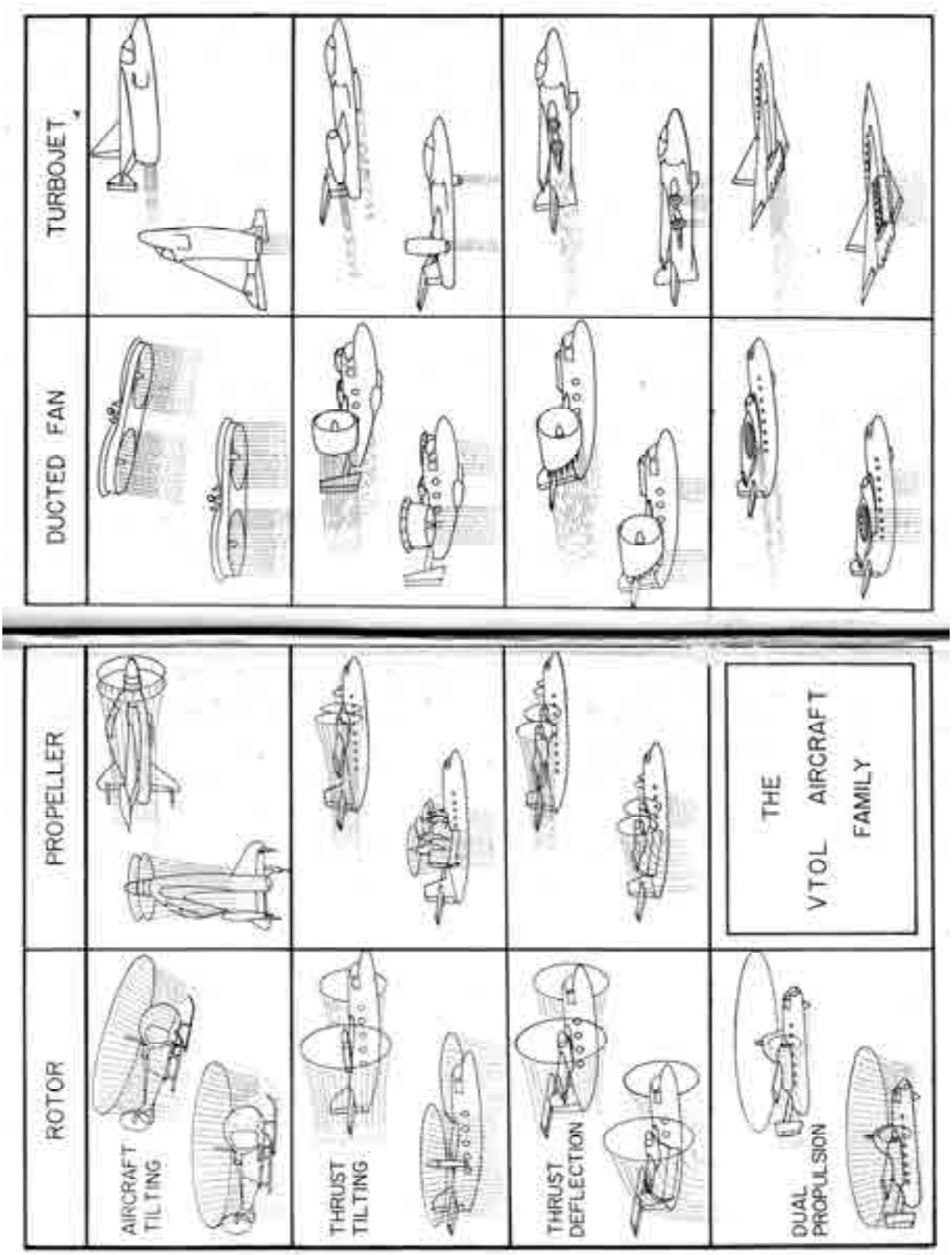

Fig. 1-26. Campbell's categorization of VTOLs in 1962 [24].

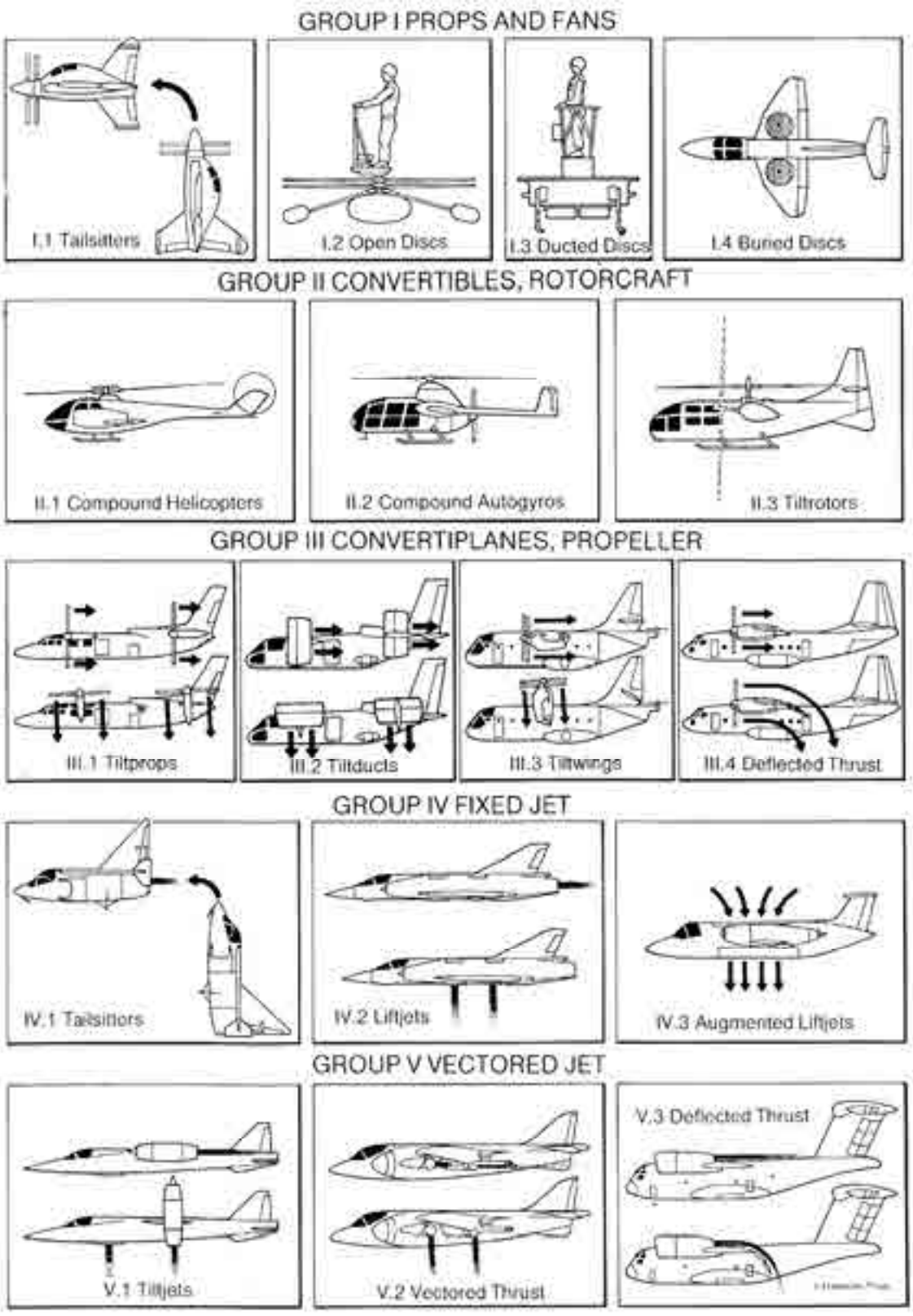

Fig. 1-27. Rogers' categorization of VTOLs and STOLs in 1989 [25].

You will quickly see that each machine was initially very deficient in flying qualities—in fact, dangerously so in several cases. The photos and numerical data Rogers includes are as comprehensive as any you will find in just one book.

3. *STOL Progenitors: The Technology Path to a Large STOL Aircraft and the C-17A* by Bill Norton [26] (2002). Published by the AIAA as one of its case studies, this book acquaints you with *real* STOL aircraft and shows you how the U.S. Air Force and the fixed-wing side of the house slowly and surely evolved CTOL aircraft into STOLs *without giving up an arm and a leg on cruise speed*. In short, it is a story of how to have your cake and eat it too. The comparison of takeoff and landing distances for 25 aircraft (Fig. 1-28) cannot be found anywhere else. Bill Norton got an aeronautical degree from Cal Poly, San Luis Obispo, California, and the Air Force Institute of Technology in Dayton, Ohio. He was able to draw on his 20 years as an Air Force officer with considerable flight test engineering experience, which makes his book all the more valuable.

Aircraft	GTOW, lb	Typical takeoff distance, ft	Typical landing distance, ft	Comments
C-17A	585,000	3000	3000	160,000-lb payload
Il-12	418,880	2790	1475	payload weight unknown
An-70	286,600	(2960)	(7716)	estimated performance
A400M	(256,840)	(4750)	(1805)	projected, over 50-ft obstacle
YC-14	225,000	1470	1500	semiprepared field
YC-15	216,680	2120	2175	semiprepared field
C-130H	175,000	5160	2400	over 50-ft obstacle
An-12	134,480	2300	1640	
HTTB	130,073	1509	1198	
C-130 BLC	105,000	800	650	
Transall C-160F	112,435	2950	2750	over 50-ft obstacle
Shin Meiwa PS-1	94,800	600	260	over 50-ft obstacle, flying boat
ASKA	85,320	1932	1624	over 35-ft obstacle
C-27J	70,044	1353	1287	
An-72	72,750	1542	1525	
G.222	61,730	2172	1788	
C-123K	60,000	1900	2360	
An-32	59,525	1676	1542	
Breguet 941	58,422	1050	820	over 35–50-ft obstacle
QSRA	50,000	1325	1425	
AWRA	45,000	965	<1000	over 35–50-ft obstacle
XC-142	43,700	≈500	≈500	STOL operations
C-8	41,000	1250	1135	over 50-ft obstacle
C-7A	28,500	1185	1235	
AT[3]	11,500	900	900	maximum weight flown

Fig. 1-28. Norton's summary comparison of demonstrated takeoff and landing performance of several real STOLs [26].

4. *Aerodynamics of V/STOL Flight* by Barnes McCormick [27] (1967). This is the only book I know of that provides a comprehensive education in V/STOL aerodynamics at the textbook level, and we are lucky to have it. Barney's textbook includes both theoretical and applied aerodynamics, and gives you an understanding of the basic physics that control V/STOL configuration possibilities. His discussion of how flaps (Fig. 1-29) improve wing maximum lift, and how that lift can be raised even higher with propeller slipstream or jet engine exhaust, is particularly helpful in calculating STOL performance.
5. *Experimental V/STOL Aircraft Lessons Learned* by the Dayton Chapter of the American Helicopter Society [28] (1990). Just the table of contents of this group of papers should bring you to attention. In mid-September of 1990, an Aircraft Design, Systems, and Operations Conference was held in Dayton, Ohio. The AHS Dayton Chapter contributed the Lessons Learned session. The foreword to the collection of 12 papers states:

> "The papers were selected to provide a good representation of projects which were successful (XV-3 & XV-15, XC-142, CL-84, X-22, X-13, P.1127, and XV-5A), and unsuccessful (X-18, X-19, X-wing, Avrocar, XFV-12A). Insofar as possible, individuals who were directly involved in these projects authored and presented the papers. Consequently, this compilation of lessons learned may never again be duplicated and is, therefore, historically significant."

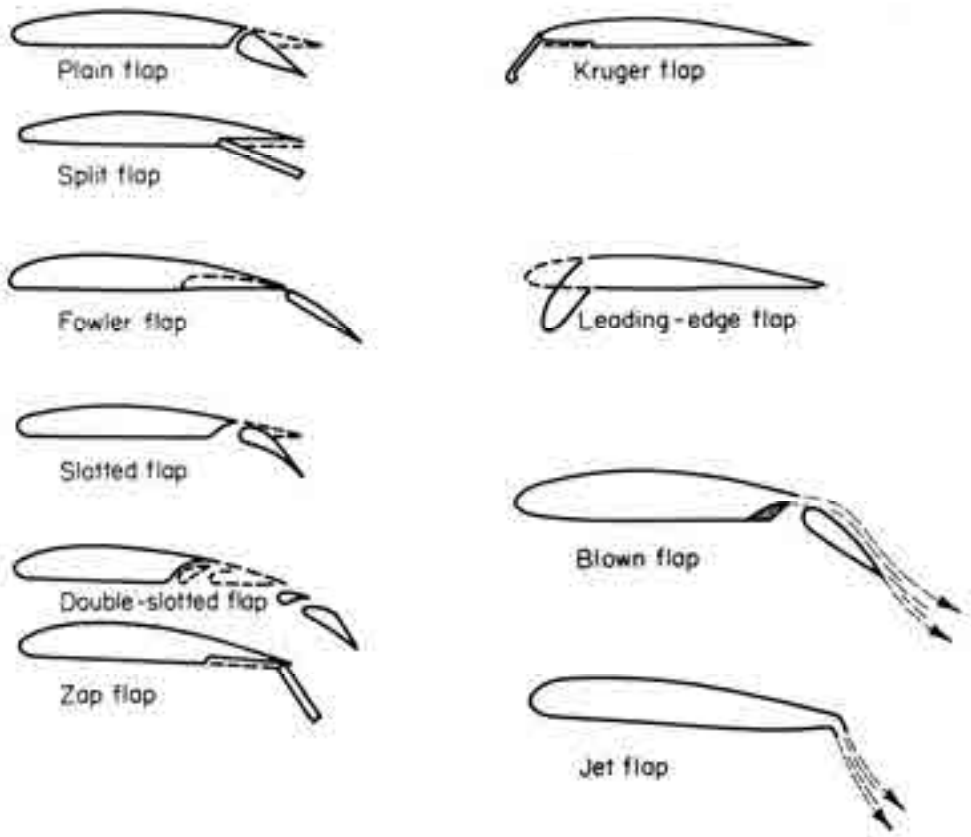

Fig. 1-29. McCormick's collection of flap sketches includes blown and jet types that many group in a class called powered lift [27].

A panel discussion followed the presentation of the 12 papers, and reference [28] includes a summary of the panel's views, which I have included here:

"Summary of Panel Discussion

A panel discussion followed the twelve presentations on specific V/STOL aircraft development projects. The purpose of the panel discussion was to contrast and compare the lessons learned from the specific development projects and to provide guidance for future V/STOL development projects. The format included time for each panelist to make an opening statement followed by questions submitted from the audience. The panel was moderated by Dr. David Quam of Aerial Mobility, Inc., and the panelists were Harold Andrews, U.S. Navy, Leo Celniker, Lockheed (retired), Charles Crawford, Georgia Tech Research Institute, William Lamar, U.S. Air Force (retired), and William Thurman, Boeing Helicopters. Seven major points were brought out in this discussion. Most of these points were mentioned by several panelists, and were often amplified by other panelists and speakers. These seven major points are:

1. Historically, an extraordinary persistence has been necessary for operational V/STOL aircraft to become a reality (the Harrier, and potentially the Osprey).

The more complex the development program the higher the priority it must have to be successfully completed within the funding limit and time frame of a single government agency. V/STOL programs have not been accorded that priority. Consequently, in the cases of the Harrier and the Osprey, the manufacturers had to find additional agencies for monetary support (sometimes with additional applications) to continue the development process. It appears such persistence cannot happen within a government agency because of turnovers in administration and the accompanying loss of 'corporate memory.' Thus, a potential V/STOL manufacturer must have an extremely strong commitment to finding ways to continue a project to completion.

2. It must be emphasized that V/STOL aircraft provide considerably increased capability (and survivability) for the price.

Decision makers are apparently not convinced of the overall cost effectiveness of V/STOL aircraft for many missions. The 'selling' of V/STOL aircraft must address several issues. These issues include operational capabilities and restraints, the ground-based infrastructure required, and the political environment. In the current situation of tighter defense budgets, less prototyping, and more emphasis on operational capabilities, the 'people issues' must be directly addressed. In order for decision makers to embrace new technology, the perceived advantages must outweigh both the risks and the background with conventional aircraft manufacturers. The engineer/developer must work with the decision makers to find out and allay these fears and threats. This requires diplomacy and persistence, because people's fears and misgivings are generally personal and difficult to surface.

On the other hand, the decision maker must make 'learned decisions,' by weighing all possibilities early in a program to avoid unnecessary effort and expense. He must trust his technical experts, to decide if the new technology is feasible, and then develop the support necessary to see the program to completion.

3. A development program should be technically well-founded. For new technology, whose behavior is not well-known for the particular application, sufficient research should be conducted before design layout. The developing organization needs to have the capability to solve any problems encountered, or have access to such capability. Otherwise the program will suffer the fate of being perceived as a failure, and the whole V/STOL industry gets a 'black eye.'

4. A development program should be 'lean and mean,' using only the resources necessary to accomplish the program. Innovation should be encouraged, rather than constraining the contractor by over-specifying the requirement. However, sufficient attention should be given to detail to deal with possible problems. Success is more likely when the contract monitor works with the manufacturer from the outset as a team member to help solve problems, rather than as an adversary.

5. Several factors should be considered at the design stage for any V/STOL aircraft. In addition to the usual factors of weight, thrust, and performance, these factors should be addressed:

a. STOL performance
b. Re-ingestion
c. Blowing debris
d. Adequate control power (especially in ground effect)
e. Interior and exterior noise (and fatigue)

Solutions for possible problems should be proposed at the design stage to ensure success.

6. Sufficient ground testing should be included in the development program to verify installed thrust and other appropriate parameters wherever previous data or analysis is insufficient.

7. Several elements of new technology developed for conventional aircraft should result in a greater improvement for V/STOL aircraft. These elements are:

a. Integrated flight/fire/propulsion controls
b. Failure management in conjunction with redundant systems
c. The wide use of simulation for cockpit development to reduce pilot workload and also for training
d. Damage tolerant structures
e. Lightweight, composite structures
f. Computational Fluid Dynamics
g. LO (Low Observables)"

In my experience, the panel's first point says it all.

There are, of course, many other general references for you to peruse. I would suggest starting with the American Helicopter Society (www.vstol.org) and devouring everything that Mike Hirschberg has published. Mike includes marvelous photos with his many papers and presentations. Then there are several general references from the V/STOL experimental era that should provide you more in-depth information [29-72].

1.5 CONCLUDING REMARKS

After 75 years of searching and weeding out, the first round of V/STOL development is over and immediate military needs have been satisfied. The militaries of several nations have both the transports and fighters that they say they need. Furthermore, the second generation of V/STOL development has begun with a fighter to replace the Harrier. This aircraft is called the Joint Strike Fighter, shown in Fig. 1-30.

The task now is to satisfy the commercial side of the industry. However, this aviation group has not said that it needs V/STOL nor has it said if it would ever even consider introducing V/STOL machines into the world's transportation system.

The following chapters of this volume are aimed at keeping V/STOL history and technology handy so that future V/STOL advocates will be ready to respond to the civil aviation world when the need does arise.

Fig. 1-30. The Joint Strike Fighter, the F-35, is a slightly compromised V/STOL called a STOVL, which stands for Short Takeoff and Vertical Landing. The approach defines the mission takeoff gross weight based on a STOL takeoff rather than a vertical takeoff. After fuel is burned off, a vertical landing and takeoff is easily accomplished.

2 ROTARY WING PERFORMANCE AT HIGH SPEED

The number of practical limitations to CTOL, STOL, and VTOL aircraft are so numerous that they are, in my opinion, beyond the scope of this book. You only need to think about how to get more productivity from a gallon of gas and you have opened Pandora's box. The limitations on reducing weight empty are partly due to design ingenuity and partly due to material properties such as strength-to-weight ratio. Flight envelopes are frequently limited by aeroelastic instabilities such as flutter and by unsatisfactory flying qualities, and each aircraft class suffers from an insatiable appetite for more efficient installed power to go faster, reach higher cruise altitudes, and go farther with greater payload.

But within a very long list of practical issues lie just a few, very fundamental aerodynamic limitations. You might suggest that airfoil and wing stalling are so fundamental that they should be on top of any list, but suppose the limitation still existed even if the airfoil or wing was assumed to never stall. In other words, suppose that the lift and angle-of-attack equation was $C_L = 2\pi\alpha$ for all angles of attack between –90 and +90 degrees. Or take another example—suppose that compressibility did not increase drag. Suppose the Prandtl-Glauert Mach number correction to incompressible lift-curve slope (i.e., $a = 2\pi$), classically written as $a_{comp.} = 2\pi/\sqrt{1-M^2}$, disappeared, and an aerodynamic limitation to wing behavior still existed. For that matter, suppose that airfoils and wings (both fixed and rotary classes) had zero skin friction *and* zero profile drag, and limitations still existed.

That is what I mean when I say fundamental aerodynamic limitations. Edgewise flying rotors and fixed wings each have such limitations on their aerodynamic behavior, and the limitations are there assuming only that $C_L = 2\pi\alpha$—or more fundamentally, $L = \rho V\Gamma$. The purpose of this chapter is to bring your attention to limitations that affect edgewise flying rotors (e.g., helicopter rotors) at high speed. Chapter 3 deals with limitations that affect wings at slow speed.

2.1 ROTOR PROPULSIVE FORCE AND LIFT LIMITATIONS AT HIGH SPEED

The conventional helicopter is very unique in that it uses the same device to both lift and propel. In that regard, it is a direct parallel to a bird. A bird, of course, uses a single surface, a wing, to both lift and propel. In contrast, an airplane uses a wing to lift and a propeller or jet engine to propel. Unfortunately, the conventional, nearly edgewise flying rotor is unable to propel when the operating advance ratio is approximately 1.0. You will remember from early discussions about autogyros in Volume I that a rotor's advance ratio is a nondimensional form of speed. That is, advance ratio (μ) is defined as

$$\mu_{hp} = \frac{V_{FP}\cos\alpha_{hp}}{V_t}. \tag{2.1}$$

When this speed-ratio parameter is 1.0, the conventional helicopter rotor ceases to have any ability to propel. The rotor can still do quite useful lifting, but forward tilting of the tip path

plane (α_{tpp}) will produce no propulsive force. The tip path plane, you will recall, is defined geometrically in Fig. 2-1.

Volume I: Overview and Autogyros gave you basic information about how the tip path plane is controlled by the pilot. This primary angle (α_{tpp}) is determined by the angle of attack of the shaft (i.e., the aircraft fuselage angle of attack) and the longitudinal flapping (a_{1S}) as Fig. 2-1 shows. In turn, the longitudinal flapping is controlled with longitudinal cyclic (B_{1C}) input, which comes from the pilot through the aircraft control system hardware. Thus, control of the tip path plane controls trim of an autogyro (and a helicopter). You also learned that the pilot controls the rotor thrust with his collective stick, which provides the same collective pitch (θ_0) to all blades. These two ingredients of controlling rotor thrust and feathering in the tip path plane are, in their simplest form and for advance ratios up to 1.0, written as

$$(2.2)\quad \frac{2C_T}{\sigma a} = \lambda_{tpp}\left[\frac{1}{2}+\frac{1}{4}\mu^2\right] + \theta_0\left[\frac{1}{3}+\frac{1}{2}\mu^2-\frac{4}{9\pi}\mu^3\right] + \theta_t\left[\frac{1}{4}+\frac{1}{4}\mu^2-\frac{1}{32}\mu^4\right] - \left(B_{1C}+a_{1S}\right)\left[\frac{1}{2}+\frac{1}{8}\mu^3\right]$$

and

$$(2.3)\quad \left(B_{1C}+a_{1S}\right) = \frac{2\lambda_{tpp}\left[\mu-\frac{1}{4}\mu^3\right]+\frac{8}{3}\theta_0\left[\mu+\frac{4}{15\pi}\mu^4\right]+2\theta_t\left[\mu+\frac{1}{24}\mu^5\right]}{\left[1+\frac{3}{2}\mu^2-\frac{3}{2}\mu^4\right]} \quad \left[\begin{array}{l}\text{For rolling}\\ \text{moment}=0\end{array}\right]$$

where the collective pitch is denoted as (θ_0) and longitudinal cyclic is denoted as (B_{1C}). Keep in mind that the tip-path-plane inflow ratio (λ_{tpp}) is calculated as

$$(2.4)\quad \lambda_{tpp} = \frac{V_{FP}\sin\alpha_{tpp} - v}{V_t},$$

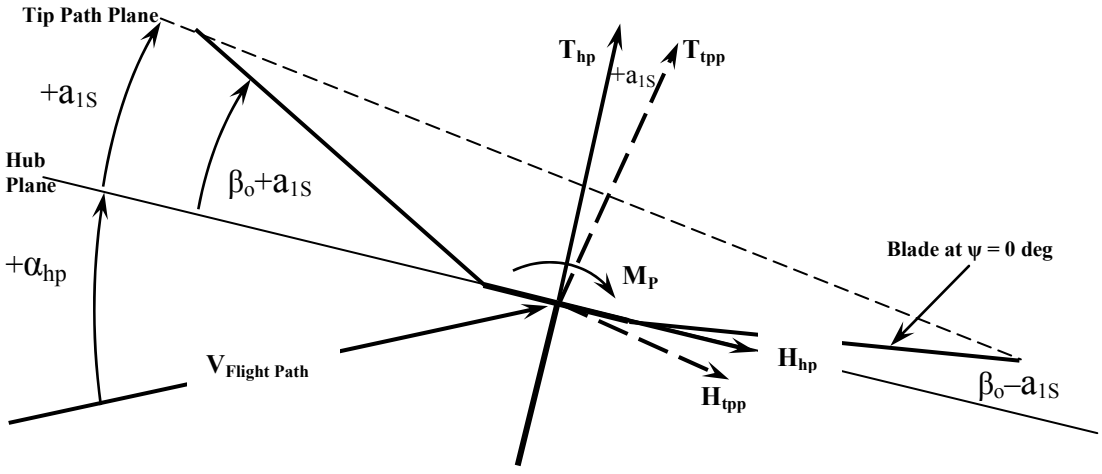

Fig. 2-1. The tip-path-plane angle of attack is the sum of the hub-plane angle of attack and the first harmonic longitudinal flapping, or $\alpha_{tpp} = \alpha_{hp} + a_{1S}$.

and remember that $\alpha_{tpp} = \alpha_{hp} + a_{1S}$. It only takes a little algebra to show that, to a first approximation, the rotor-thrust coefficient behaves as

$$(2.5) \quad \frac{C_T}{\sigma} = \frac{a}{2}\left[T_1\alpha_{tpp} + T_2\theta_0\right] = \frac{\partial C_T/\sigma}{\partial \alpha_{tpp}}\alpha_{tpp} + \frac{\partial C_T/\sigma}{\partial \theta_0}\theta_0 ,$$

and the feathering in the tip-path-plane coordinate system is

$$(2.6) \quad \left(B_{1C} + a_{1S}\right) = \frac{\partial\left(B_{1C} + a_{1S}\right)}{\partial \alpha_{tpp}}\alpha_{tpp} + \frac{\partial\left(B_{1C} + a_{1S}\right)}{\partial \theta_0}\theta_0$$

for the conventional helicopter with an articulated rotor system. Here, the partial derivatives depend primarily on advance ratio and secondarily on the airfoil lift-curve slope (a).

You can immediately see the propulsive force (X) problem that Eq. (2.5) creates by approximating the propulsive force coefficient as

$$(2.7) \quad \frac{C_X}{\sigma} \approx -\alpha_{tpp}\frac{C_T}{\sigma} = -\alpha_{tpp}\left[\frac{\partial C_T/\sigma}{\partial \alpha_{tpp}}\alpha_{tpp} + \frac{\partial C_T/\sigma}{\partial \theta_0}\theta_0\right] \quad \text{Assumes airfoil } C_d = 0 ,$$

where the propulsive force component of thrust acts like a propeller in overcoming aircraft drag. Of course, I have made a number of small angle assumptions along the way. But now suppose that the collective pitch (θ_0) is zero, and the rotor is flown at a positive tip-path-plane angle of attack. Then the rotor will act like a wing and have a negative propulsive force coefficient, which you and I would call drag, and the aircraft (say an autogyro) will need a propeller to pull the rotary wing along or the aircraft will start to descend.

Now suppose the tip path plane is tilted forward with a negative angle of attack (the symbol α_{tpp}). The rotor will have a negative lift (because I chose to start the discussion with $\theta_0 = 0$), and the rotor will have a negative propulsive force. To get positive thrust and, therefore, a useable propulsive force, the collective pitch must be increased from zero. This will happen in the helicopter world because the partial derivative of thrust with collective pitch is quite large and *positive* at all *helicopter* advance ratios. But imagine you are designing a high-speed helicopter having a tip speed of, say, 600 feet per second, and you want to achieve a maximum speed of 600 feet per second. This is a speed of about 500 knots and competitive with a swept wing, turbojet- (or turbofan-) powered commercial transport. Yes, practically, compressibility is a real stumbling block, but remember, I assumed airfoils with zero friction drag and said that compressibility did not exist. While it is possible to tilt the rotor tip path plane forward at an advance ratio of 1.0 using longitudinal cyclic (B_{1C}), if thrust cannot be obtained with collective pitch then we have reached a fundamental roadblock.

In 1987, I offered an explanation to what could be termed a "control reversal" [73]. Using a simple sketch, I wrote:

> "The simple physics of how the reverse flow region creates this unique, conventional rotor-thrust characteristic is quite easy to see. Sketch A below shows the velocity diagrams at blade azimuths of 0° and 270° for an advance ratio equal to 1.0. Both regions have exactly the same velocity distributions. Unfortunately, the reverse flow region has the velocity approaching the trailing edge of the airfoil.

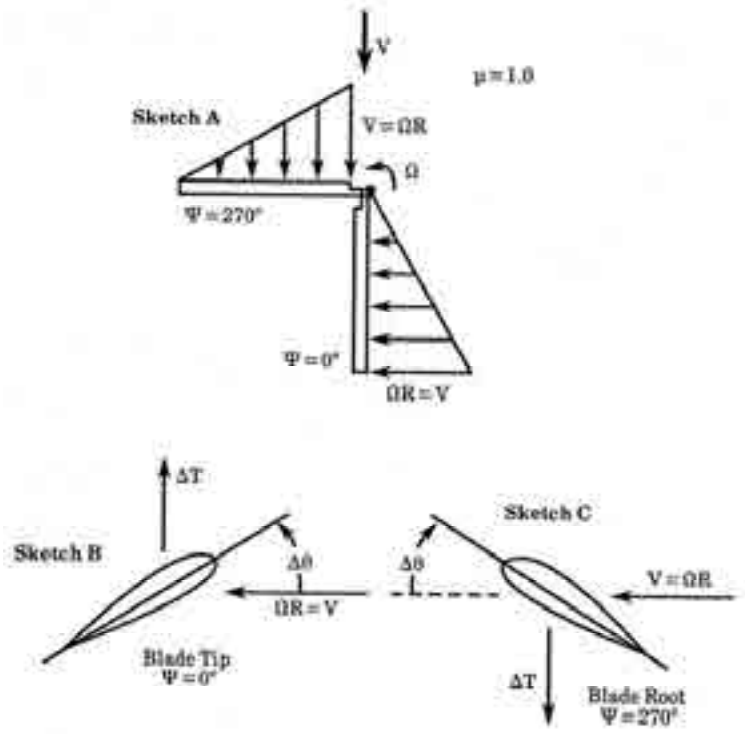

First, consider the 0° azimuth position and the blade element velocity and angle-of-attack diagram shown above in Sketch B. The flow approaches the airfoil leading edge. The blade element is at a positive angle of attack, and an increase in collective pitch increases the thrust at the 0° azimuth position. Now, consider the root of the blade in the azimuth position of 270° as shown by Sketch C. A positive increase in collective pitch will provide a thrust download. At an advance ratio of 1.0, these thrust increments at these two azimuth positions approximately cancel for a positive increase in collective pitch. For a rotor in both rolling and pitching equilibrium (such as teetering or flapping or articulated rotor system, or even a propeller with correct cyclic inputs) the azimuth positions of 90° and 180° have about the same symmetry. Thus, the net effect of a positive change in collective pitch is no change in thrust. From this discussion, it is clear that the primary culprit in this unusual conventional rotor characteristic at advance ratios approaching 1.0 is simply the reverse flow region, the velocity orientation in this region, and the ability of airfoils to produce lift proportional to angle of attack in this environment. The accomplice is the statement that the rotor is in at least roll equilibrium."

The preceding quote from reference [73] was accompanied by several figures that showed how the partial derivatives in Eqs. (2.5) and (2.6) varied with advance ratio using data from eight separate experiments. During my association with the Aeromechanics Branch of NASA and the U.S. Army Aeroflightdynamics Directorate (AFDD), both located at Ames Research Center, I was fortunate to be able to revisit this fundamental limit in two additional reports [74, 75]. Now, this volume provides an opportunity to extend the experimental behavior of rotors to an advance ratio of 2.4, based in part on data from two rotor systems as reported in references [74-79].

Now take a look at Fig. 2-2, Fig. 2-3, Fig. 2-4, and Fig. 2-5 on the following pages. These four figures illustrate the trends of the four partial derivatives with advance ratio that Eqs. (2.5) and (2.6) called to your attention. Unfortunately, the trend of $\partial C_T/\sigma/\partial \theta_0$ goes to zero when advance ratio lies in the range of 0.8 to 1.0. That is the end of the conventional rotor's ability to propel. Fortunately for the compound helicopter, the conventional articulated rotor's ability to lift appears to have no obvious fundamental limitation. You can see this from Fig. 2-3 where the rotor lift-curve slope, $\partial C_T/\sigma/\partial \alpha_{tpp}$, is positive at least up to advance ratios of about 2.0. Keep in mind, however, that you would now be getting close to potential instabilities in flapping [76]. Furthermore, in my experience, blade tracking is a common problem with lifting rotors at high advance ratios because manufactured blades (whether model or full scale) for a given rotor system are definitely not "identical."

Table 2-1 will help you identify the rotors included on Fig. 2-2, Fig. 2-3, Fig. 2-4, and Fig. 2-5.

Table 2-1. Ten Examples of High-Advance-Ratio Experimental Data

Parameter	**Units**	**A**	**B**	**C**	**D**	**E**	**F**	**G**	**H**	**I**	**J**
Reference		[80]	[80]	[81, 82]	[80]	[81, 82]	[80]	[80]	[83, 84]	[74, 76]	[75, 77-79]
Hub	–	Teeter	Teeter	Teeter	Teeter	Teeter	Articulate	Articulate	Teeter	Articulate	Articulate
Blade no.	–	2	2	2	2	2	4	4	2	4	4
Diameter	ft	48.00	48.00	44.00	34.00	34.00	56.00	56.00	15.25	2.22	8.06
Chord	ft	1.75	1.75	1.75	1.75	1.75	1.337	1.337	1.16	0.167	0.417
Cutout	ft	2.04	2.04	2.04	2.04	2.04	4.48	4.48	1.25	0.165	0.9269
Twist	deg	–10.9	–10.9	–1.8	–7.7	–1.4	–8	0	0	0	0
Solidity	–	0.0464	0.0464	0.0506	0.0656	0.0656	0.062	0.062	0.09685	0.165	0.133
Flap hinge	ft	0	0	0	0	0	1.0	1.0	0	0.069	0.261
Flap inertia	ft-lb-sec^2	2,458	2,289	1,995	1,584	1,362	1,264	1,264	–	variable	2,972 lb/in^2
Delta 3	deg	0	0	0	0	0	0	0	0	0	26.5
Airfoil		0012	0012 to .8R Linear taper to 21006 at tip	0012 to .8R Linear taper to 21006 at tip	0012	0012	0012	0012	0012	0012	
Torsional lock number	$\frac{\rho c^2 V_t^2}{GJ}$	6.05	6.66	–	1.01	0.46	6.88	1.39	–	–	–
at RPM	rpm	324	324	–	269	182	222	100	–	–	–

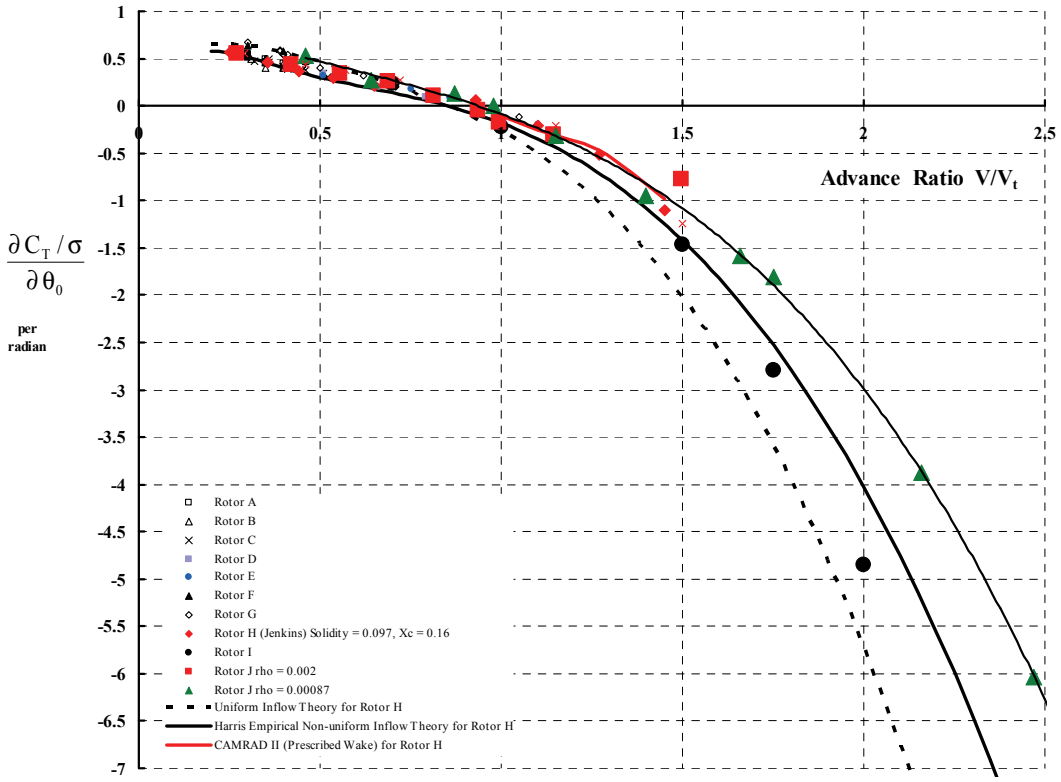

Fig. 2-2. The change in thrust with collective pitch.

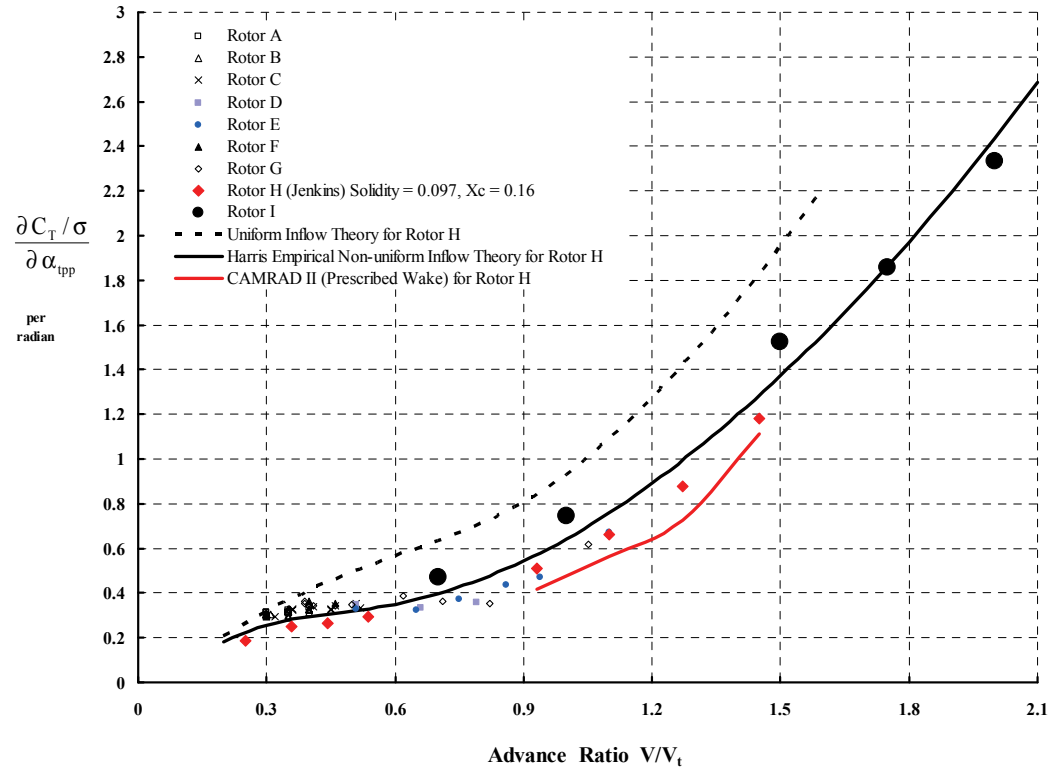

Fig. 2-3. The change in thrust with tip-path-plane angle of attack.

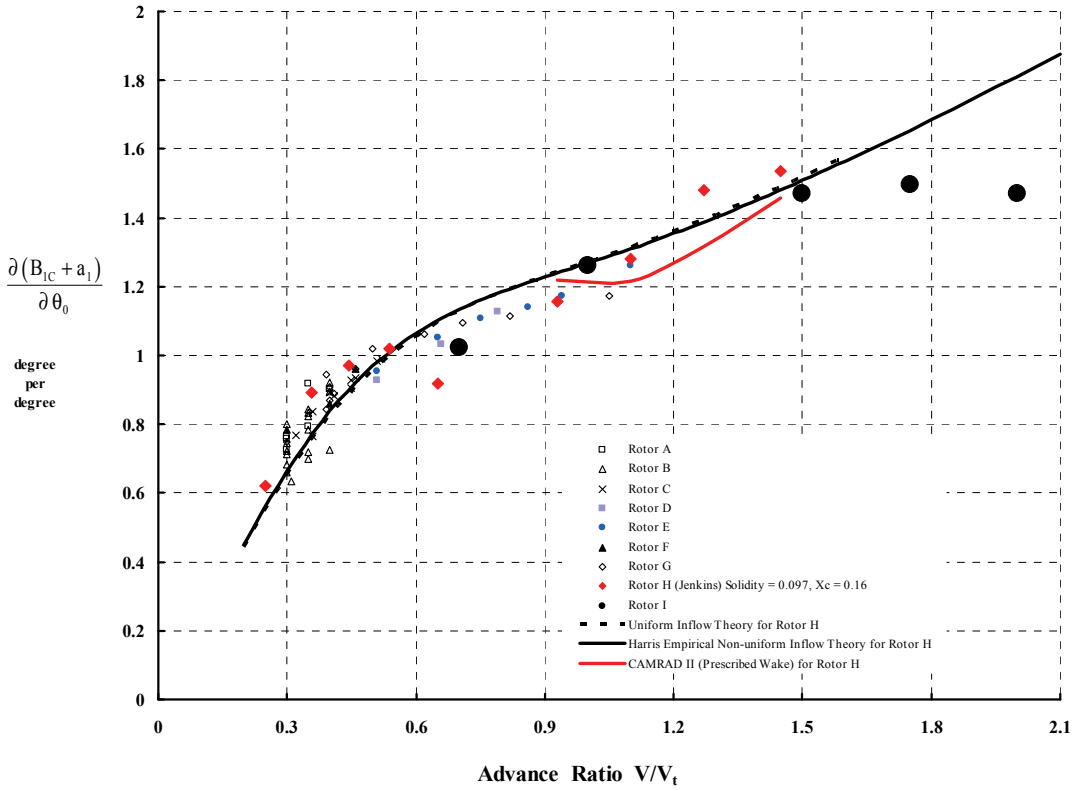

Fig. 2-4. The change in feathering with collective pitch.

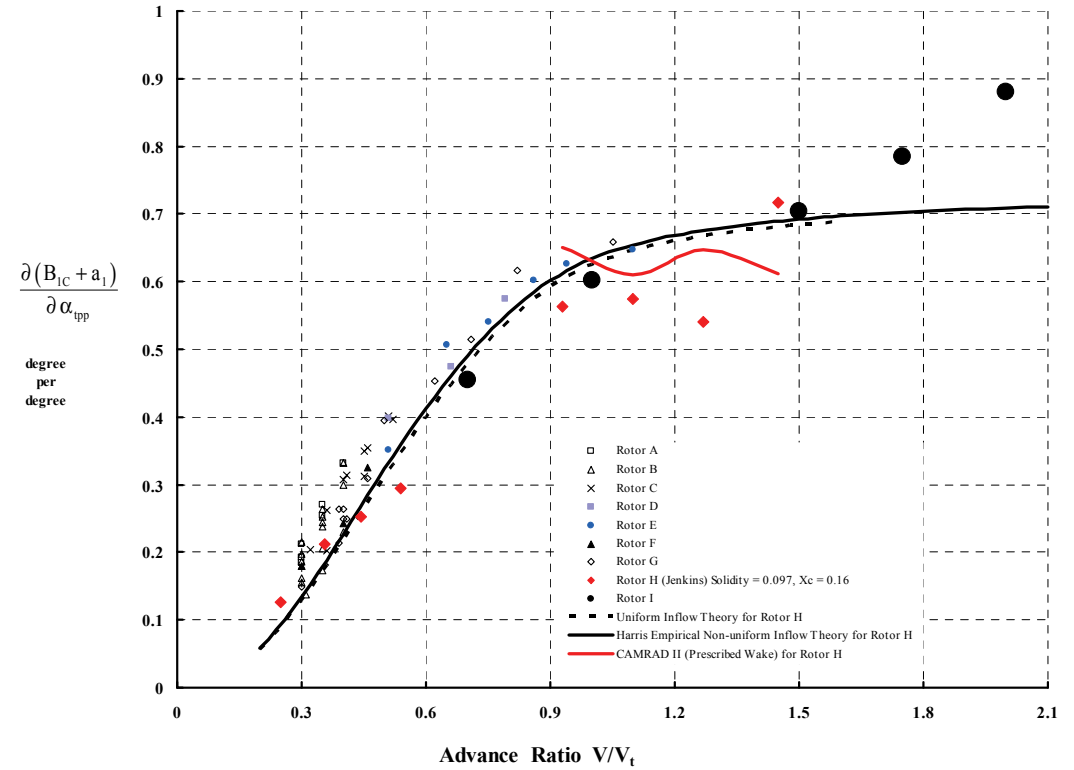

Fig. 2-5. The change in feathering with tip-path-plane angle of attack.

2.2 SOME KEY STEPS

To say that Eq. (2.5), in some form, is a rotary wing classic is a real understatement. However, as memories of autogyro technology faded with the all-out attack on helicopter development, rotary wing engineers lost track of rotor thrust and flapping behavior at high advance ratio. After all, all the helicopters we have been developing since 1938 rarely operate at advance ratios even up to 0.4. It was not until the beginning of the V/STOL era (say 1950) that questions about rotor operation at high advance ratio ($\mu = 0.5$ to 2.5) started being asked. The questions arose when compound helicopters were being seriously considered as a way to, perhaps, double the cruise speed of conventional helicopters.

The problem of slowing down rotor tip speed and shifting rotor lift to a wing (plus shifting rotor propulsive force onto a propeller or some other propulsive device) meant that maximum advance ratio might be increased well beyond anything that autogyros had been operating at. And rotorcraft aerodynamicists and dynamists of all ages were completely in the dark, to put it mildly. At the start of the 1950s, this engineering group was just beginning to experimentally examine rotors at moderately high advance ratios approaching 1.0 as associated with the McDonnell XV-1 (Fig. 2-6) and the Fairey Rotodyne (Fig. 2-7). The problem at that time was rotor-blade flapping stability and the concern that blade flapping would go unstable at some "high" advance ratio [85, 86]. The conventional rotor system *does* have a "critical advance ratio" where blade flapping instability occurs [74]. However, this advance ratio is in the range of $\mu = 2.0$, well beyond the fundamental propulsive force limit around $\mu = 1.0$ that I am discussing. Kurt Hohenemser, then at McDonnell Aircraft in St. Louis working to develop the XV-1, was, I think, the first to tackle technology for the unloaded rotor at high advance ratio [87-90]. There are many, many more contributions Kurt made during his career, which you will find if you do a complete literature search.

It was, in my opinion, aerodynamic engineers at Sikorsky and United Aircraft Corporation Research Laboratories in Hartford, Connecticut, who did the second exploration of conventional articulated (including teetering) rotor thrust and flapping behavior up to very high advance ratios. At the 19th AHS Forum held in May of 1963, Dave Jenny and Peter Arcidiacono of Sikorsky,[11] and Art Smith at United Technology Research Labs presented a paper [76] discussing about 5 years worth of their theoretical and supporting experimental [74] work.[12] The experimental work has not been distributed much beyond Sikorsky,[13] which is, today, a real tragedy because of its groundbreaking results. However, Dave and Pete did highlight the key points in their published paper. They wrote:

> "1. In the absence of blade stall, the flapping motions at high advance ratios (above 1.0) for both articulated and teetering rotors having rigid blades can be determined with sufficient accuracy for preliminary design purposes by the linearized analysis presented herein.

[11] In every rotorcraft company, there have always been engineers who just stand head and shoulders above the rest of us. For my money, Kurt, Dave, and Pete easily fall in this group of immensely talented people. Talking with them at technical meetings was the greatest of pleasures for me and *always* a terrific learning experience.

[12] Boeing Vertol was much more interested in the tiltwing approach (i.e., the Model 76 or VZ-2) at the time, and Bell Helicopter Textron was developing the tiltrotor (i.e., XV-3).

[13] I got a nearly complete copy (printed from microfiche) directly from then Sikorsky President Dean Borgman.

Fig. 2-6. The XV-1 was designed and tested by Fred Doblhoff and Kurt Hohenemser. It first lifted off in February 1954, and the "official" first flight was in July of 1954.

Fig. 2-7. The Rotodyne first flew on November 6, 1957. On January 5, 1959, it raised the world speed record to 167 knots [70].

2. The flapping motion of both the articulated and teetering rotors becomes increasingly sensitive to control changes as advance ratio is increased. Introduction of pitch-flap coupling reduces the flapping sensitivity.

3. Instability of the flapping motion of an articulated rotor having rigid blades and no pitch-flap coupling is predicted at advance ratios above approximately 1.8 to 2.2 for rotor Lock numbers of 10 to 5, respectively. A necessary condition for the presence of this instability appears to be the existence of second harmonic flapping.

4. The sensitivity of rotor thrust to disturbances as predicted by the linear theory is approximately 25% higher than that measured experimentally or predicted by a more exact nonlinear analysis, which includes the effects of blade stall and of large inflow angles.

5. The profile drag of a fully unloaded rotor is predicted to be between 10% and 20% of the total drag of the aircraft depending on the advance ratio at which the rotor is operated and the overall drag level of the aircraft."

Dave and Pete's study illuminated the positive influence of high-inertia blades in delaying flapping instability and reducing excessive sensitivity to control inputs and gusts. While that was the basic intent of the experiment, what is significant to my discussion here is the lift capability of the conventional rotor that was demonstrated in the experiment [74]. This capability is shown in Fig. 2-8. The blade loading coefficient (i.e., C_T/σ) was limited more by blade tracking problems and test stand limitations. The blade loading coefficient versus rotor angle of attack (at fixed collective pitch) were quite linear at all advance ratios. This suggests that with some minor test stand modifications, higher C_T/σ's could have been obtained. While the conventional helicopter rotor might not be able to propel, this early evidence says the rotor could most assuredly lift at all high advance ratios.

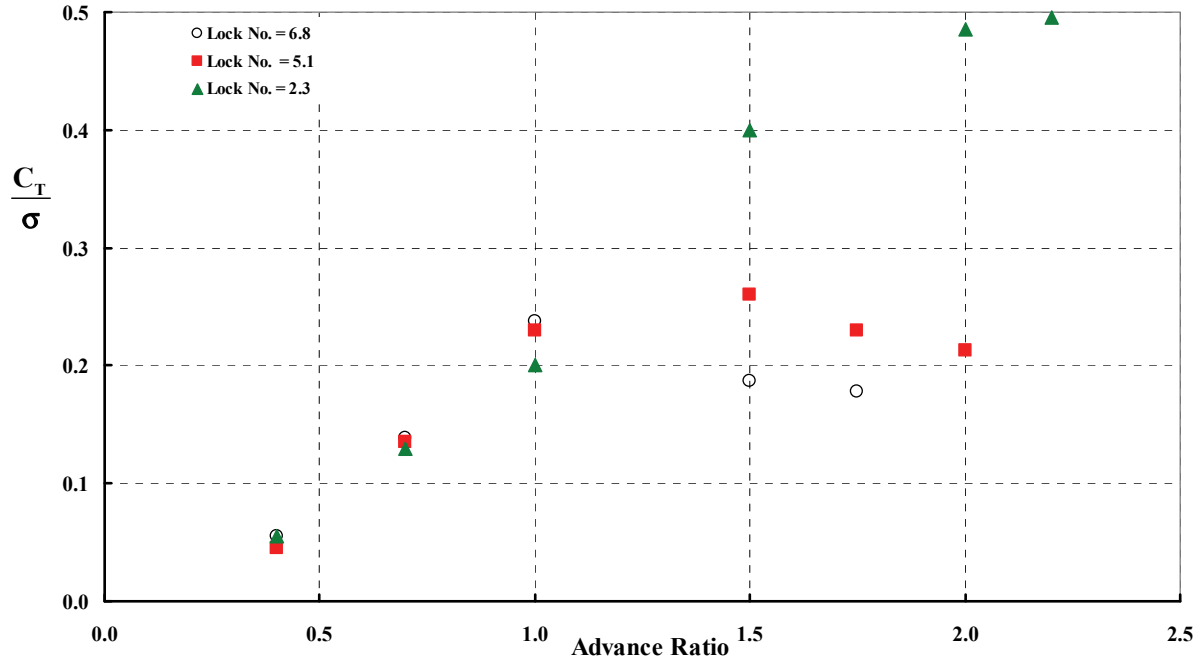

Fig. 2-8. A 1959 experiment showed that a conventional, articulated model rotor appeared to have no limit to lift capability at high advance ratio *provided* it did not have to propel [74]. Points shown are where testing was stopped because required data was obtained, not because maximum lift had been reached.

Then Larry Jenkins at NASA Langley[14] completed an eye-opening experiment with a 15-foot, two-bladed teetering rotor tested in the Langley 30- by 60-foot full-scale wind tunnel. With the publishing of his findings [83] in February of 1965, I, for one, saw how incomplete my apprenticeship really was. In his report, Larry stated:

> "The experimental data obtained from wind-tunnel tests of a teetering-type rotor operating at tip-speed ratios from 0.65 to 1.45 are presented in figure 4. These data are presented for shaft angles of attack of 0.5° and 5.5° with the tip-path plane of the rotor trimmed normal to the shaft. This presentation highlights a trend in the rotor-thrust variation which is not believed to have been previously reported; that is, the slope of the variation of rotor thrust with collective pitch becomes increasingly negative with increasing tip-speed ratio for tip-speed ratios greater than 1.00. As shown in reference 3, for the same rotor, the variation of thrust with collective pitch has a positive slope for tip-speed ratios to 0.54 for the tip-path-plane angles from -9.5° to 10.50. This same positive slope is evident in the present test for tip-speed ratios below 0.94.

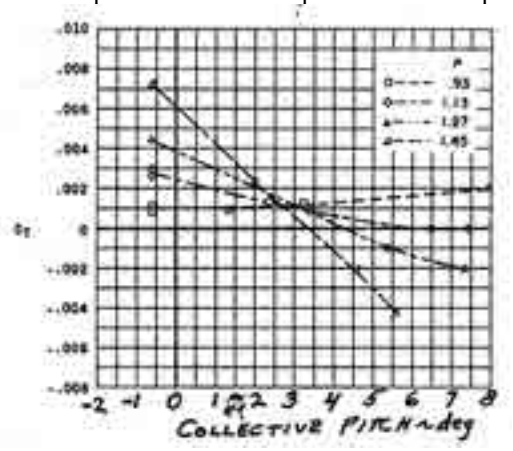

Harris Note: Tip path plane constant at 0.5 deg nose up [83].

> The trends shown by these results suggest that at a tip-speed ratio of approximately 1.00 the variation of thrust with collective pitch is zero for a constant rotor-disk attitude. In other words, increasing collective pitch and retrimming the rotor tip-path plane to its original attitude with cyclic control produces no change in rotor thrust at a tip-speed ratio of 1.00. At higher tip-speed ratios, this same procedure produces a loss in thrust and is, in effect, a control reversal in the sense that the combination of collective and cyclic pitch inputs which produces a positive thrust increment at conventional tip-speed ratios now produces a negative thrust increment.
>
> This reversal could be quite disconcerting to a pilot of a compound helicopter with manual control of the rotor because a reduction in collective pitch and longitudinal cyclic control is required in order to increase rotor thrust and simultaneously to maintain a relatively constant rotor attitude. Constant rotor attitude is desired at high tip-speed ratios in order to maintain a safe rotor-fuselage clearance during maneuvers or gusts. If the rotor is controlled automatically rather than manually, specific consideration of the problem of rotor-thrust reversal will be required during the design stage to ensure acceptable operation over the entire speed range."

Larry Jenkins was the first to clearly identify a control reversal (i.e., $\partial C_T/\sigma/\partial \theta_0$ goes negative in Eq. (2.5)) for conventional rotors operating near an advance ratio of 1.0.

[14] Larry worked with George Sweet and others at Langley to gather and report on blade stall [84] and rotor behavior at low advance ratio [91]. Larry later came to Bell to become Director of Technology. It was my great pleasure to work with him until I retired in January of 1992.

2.3 THE SEGMENTED ROTOR

A particularly interesting approach to overcoming the propulsive force degradation of the conventional rotor due to the extent of the reverse flow region at high advance ratio was mounted during the V/STOL era. The approach was based on segmenting the rotor blade into two separately controllable segments. This approach was moderately successful, aerodynamically speaking, from a theory point of view, but many rotor blade design engineers were, in a word, appalled. I wonder if fixed-wing designers felt the same way about flaps.

The initial feasibility study of how to add a generalized pitch control (to what was then the HC-1B, the forerunner of the CH-47 Chinook) was reported by interoffice memo on December 4, 1962.[15] This effort at the Vertol Division of Boeing was conceived by Leo Kingston and Maurice Young, and the preliminary design work was done by Adrian Kisovec. The idea was to have the blade segment from the root to the 50-percent radius station be controlled separately from the outboard portion of the blade. The outboard segment remained under the helicopter's conventional swashplate control. The summary report of the initial preliminary design [92], distributed August 23, 1963, included several photographs of the twistable segment, one of which is shown here as Fig. 2-9. Two different approaches to finishing the segment's airfoil surface were considered as you can see from Fig. 2-10. One approach was an elastic membrane, the other an elastomeric filling. With that encouragement, upper management agreed to build and wind tunnel test a model so that some level of aerodynamic performance assurance—beyond theory—could be established before going further.

As it turned out, the independently movable inboard segment was *non-twisting* for the 8-foot-diameter model (Fig. 2-11). This concept-proving model was designed and built by Mike Drozda[16] (chief of models at Vertol for many years) and his small group, and then tested at the Glenn L. Martin 8- by 10-foot wind tunnel at the University of Maryland. Results were reported by Harris [93] in April of 1965, and more formally by Don Ekquist [94] in October 1965. The movable segment was controlled by a pitch link driven at its bottom end by a cam. Two different cam (i.e., feathering) schedules were selected for test, which you see in Fig. 2-12.

As Don reported [94], all testing was done at a tunnel-speed-to-tip-speed ratio of 0.6 and an advancing tip Mach Number of 0.36. This is approximately a tip speed of 250 feet per second and a tunnel speed of 150 feet per second. Don noted further that "shaft angle sweeps were made at constant collective and [constant] cyclic pitch [of the outboard segment], data being recorded at incremental shaft positions."

---

[15] IOM 8-7075-2-238. Subject: Feasibility Study of Generalized Pitch Control on HC-1B Helicopter (author's library).

[16] Mike Drozda taught me all I know about designing and making models. He was my right-hand man for model design during my tenure as manager of Boeing's V/STOL wind tunnel, and he was a very good friend.

Fig. 2-9. The inboard segment of the twistable, segmented rotor concept as visualized in August of 1963 [92].

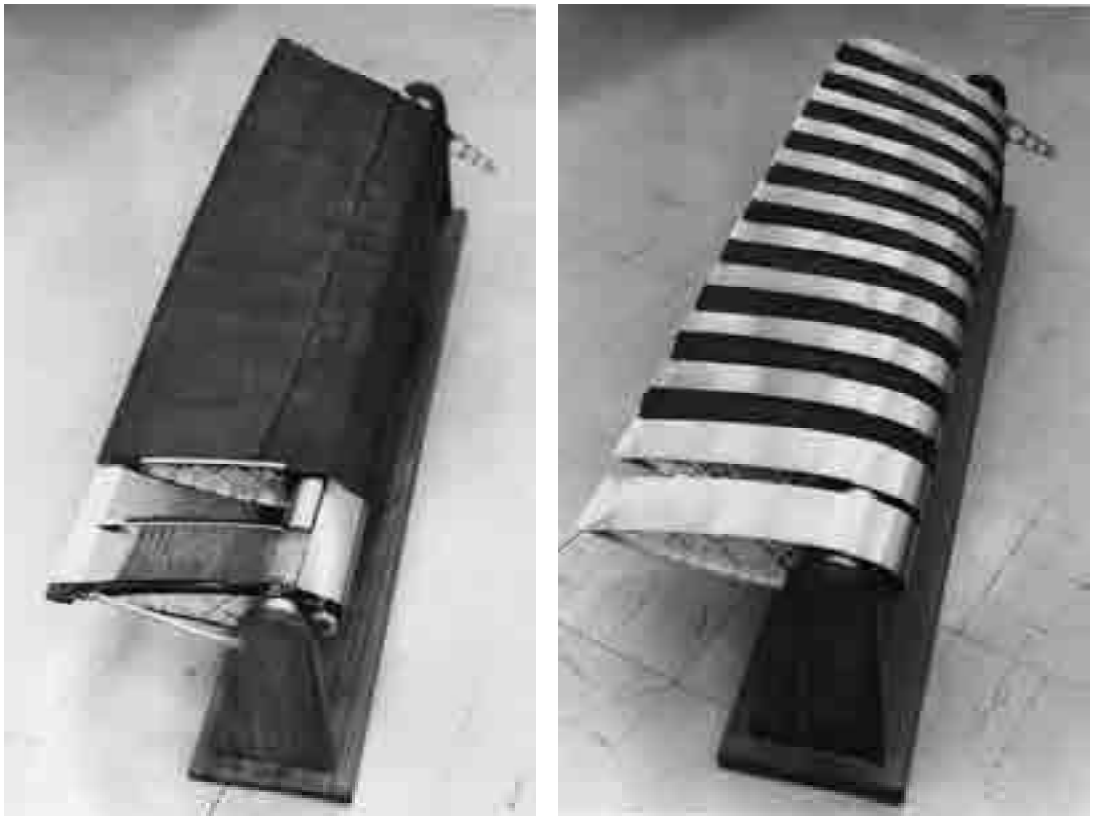

Fig. 2-10. Two approaches to completing the airfoil shape of the twistable segment [92].

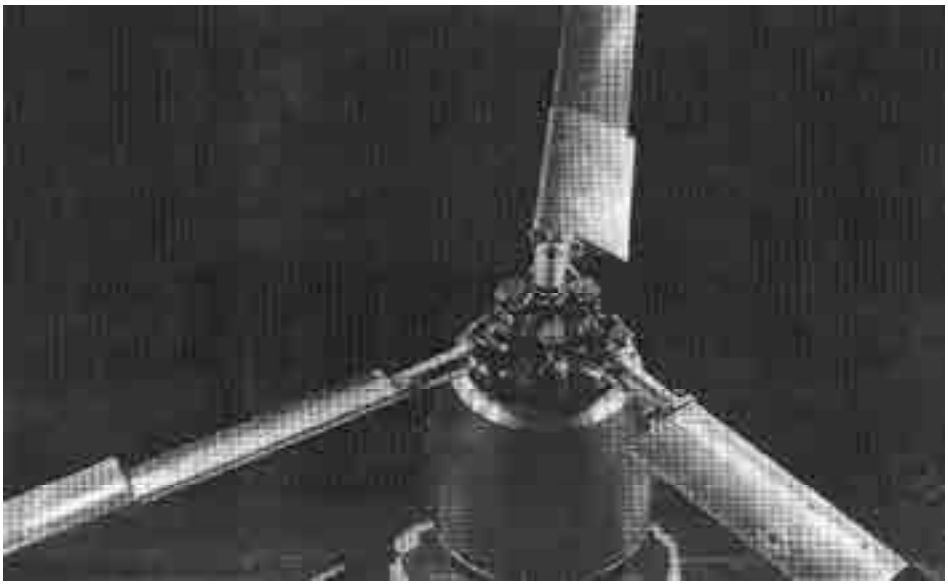

Fig. 2-11. The inboard segment of the 8-foot-diameter rotor blade was *non-twisting*. The rotor blades were untwisted, and the solidity was 0.119.

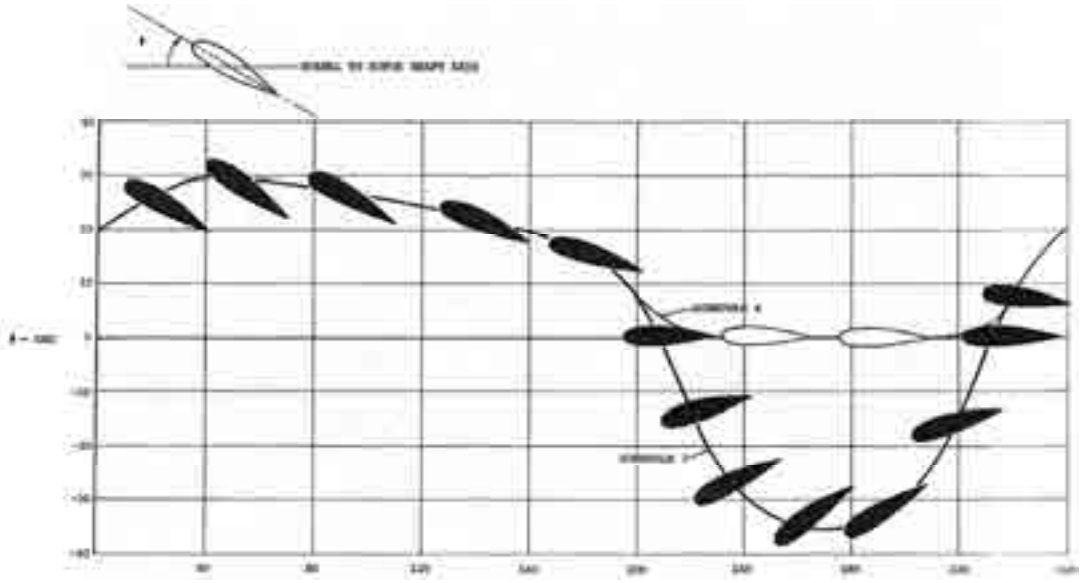

Fig. 2-12. The inboard segment was tested with two different feathering schedules [94].

The lift-propulsive-force comparison between the conventional and the segmented rotor configurations is shown in Fig. 2-13. Clearly, segmentation can extend the propulsive-force-producing capability of "conventional" rotors. However, the complexity was judged as just too much, and Vertol decided against pursuing the concept. Much later (in 2001) the benefits of the concept were re-examined in a paper by Tom Zientek [95]. He explored inboard segment feathering at two- and three-per-revolution and showed "significantly increased lifting capability of rotors in high-speed edgewise flight."

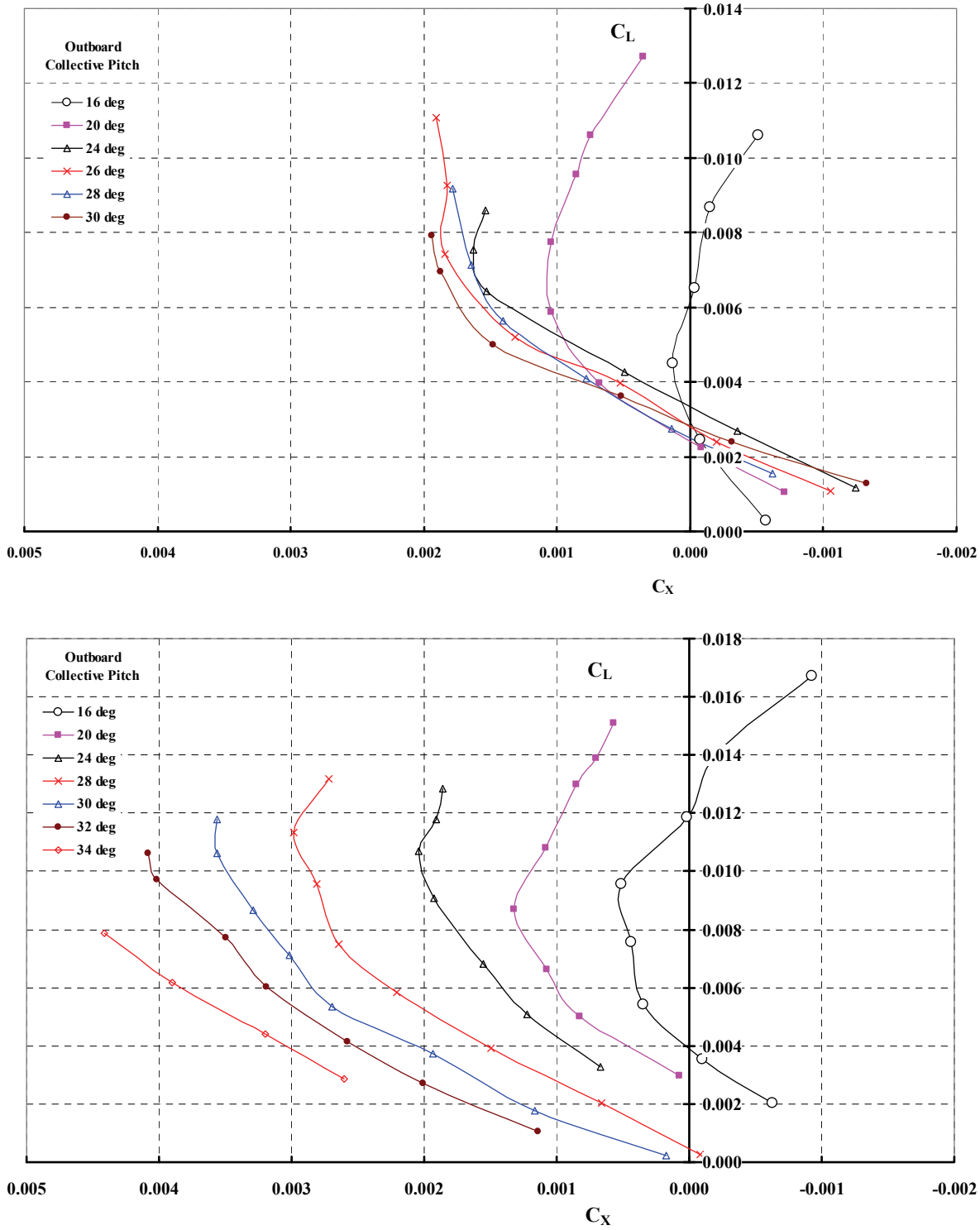

Fig. 2-13. The inboard segment locked to the outboard segment simulated the conventional rotor (upper figure). The lower figure shows the expanded envelope using Schedule 3 shown in Fig. 2-12. The ratio of flightpath speed to tip speed was 0.6 [94].

2.4 THE REVERSE VELOCITY ROTOR

More experimental data became available in the 1970s when the Fairchild Republic Company and Boeing Vertol started to investigate a Reverse Velocity Rotor (RVR) [75, 77-79]. The concept was to add second harmonic feathering to the conventional rotor to increase lift at advance ratios from about 0.3 on up to somewhat above 2.0. The focus of the model rotor experiments was on the lifting capability, not on propulsive force capability. The approach was, in my opinion, rather promising for a compound helicopter because of the possibility of unloading the propulsive force requirement onto a propeller (or even a ducted fan, or turbojet, or turbo fan) and *not* add a wing. On the negative side, control loads were more than twice those of a conventional rotor. Nobody in a position to be a real champion came forth, and the concept never made it to flight testing.

The 8-foot, four-bladed RVR was tested in the NASA Ames 12-foot pressure wind tunnel,[17] first as a conventional rotor [75] in June and July of 1972. The two-per-revolution feathering control system was activated for the second tunnel entry, which extended from late February to early April of 1974 [77]. This model rotor accumulated data for advance ratios from 0.3 to 2.46 at tunnel speeds up to 350 knots. The two reports included *tabulated data* for rotor forces, moments, flapping, shaft angle of attack, control positions, etc., which saved the results "forever"! Now that is an example of foresight.

The fact that the RVR data from the 1972 test gave another example of the derivative $\partial C_T/\sigma/\partial\theta_0$ going to zero around an advance ratio of 1.0 is, of course, noteworthy. However, the apparent stall-free lifting capability of the articulated rotor, *even with the higher harmonic feathering turned off,* should be of fundamental interest. You see the maximum levels of C_T/σ (i.e., the rotor-system blade loading coefficient) reached as a function of advance ratio in Fig. 2-14. The C_T/σ for the best ratio of lift (L) to effective drag (D_E) is considerably below the thrust levels this rotor demonstrated. The effective drag as used in Fig. 2-15 is defined as

$$D_E = \frac{P_{total} - XV_{FP}}{V_{FP}} = \frac{P_{induced} + P_{profile}}{V_{FP}} \tag{2.8}$$

and gives a measure of rotary wing performance in terms that most aircraft engineers immediately understand and appreciate. Because this rotary wing parameter, effective drag, is frequently misunderstood, I will discussed it in more detail shortly.

The 1972 RVR test also provided some evidence that the rotor-blades-alone performance was considerably better than what many of us thought possible based on our helicopter experience. Of course, in 1965 Larry Jenkins had reported [83] blade loading coefficients well above $C_T/\sigma = 0.1$ at advance ratios above 1.0. He also obtained maximum

[17] It is a sad thing to report that the Ames 12-foot pressure wind tunnel is now mothballed for lack of use—or to save money. There sits the capability to test at altitude *and* high speed. So much for short-sighted, penny-wise, pound-foolish bureaucrats and, perhaps, a lack of awareness by the rotorcraft industry.

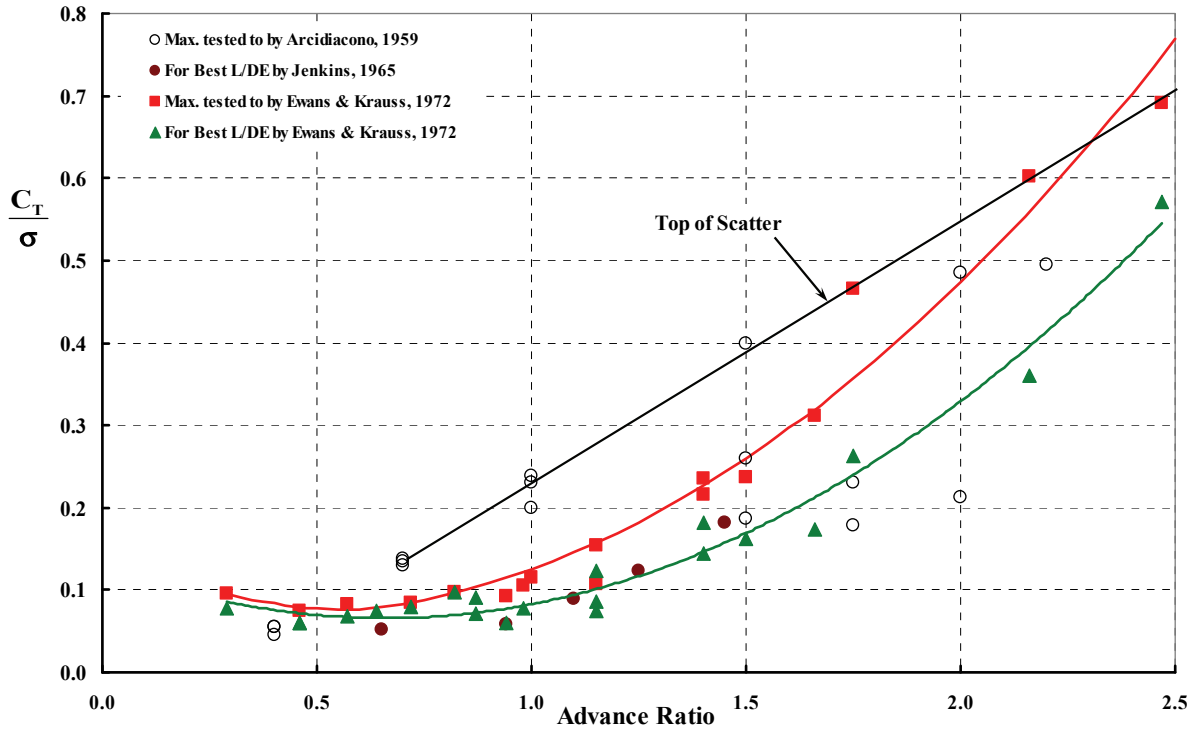

Fig. 2-14. The 8-foot-diameter RVR in conventional mode began to experimentally confirm the very high lift as a function of high advance ratio [75].

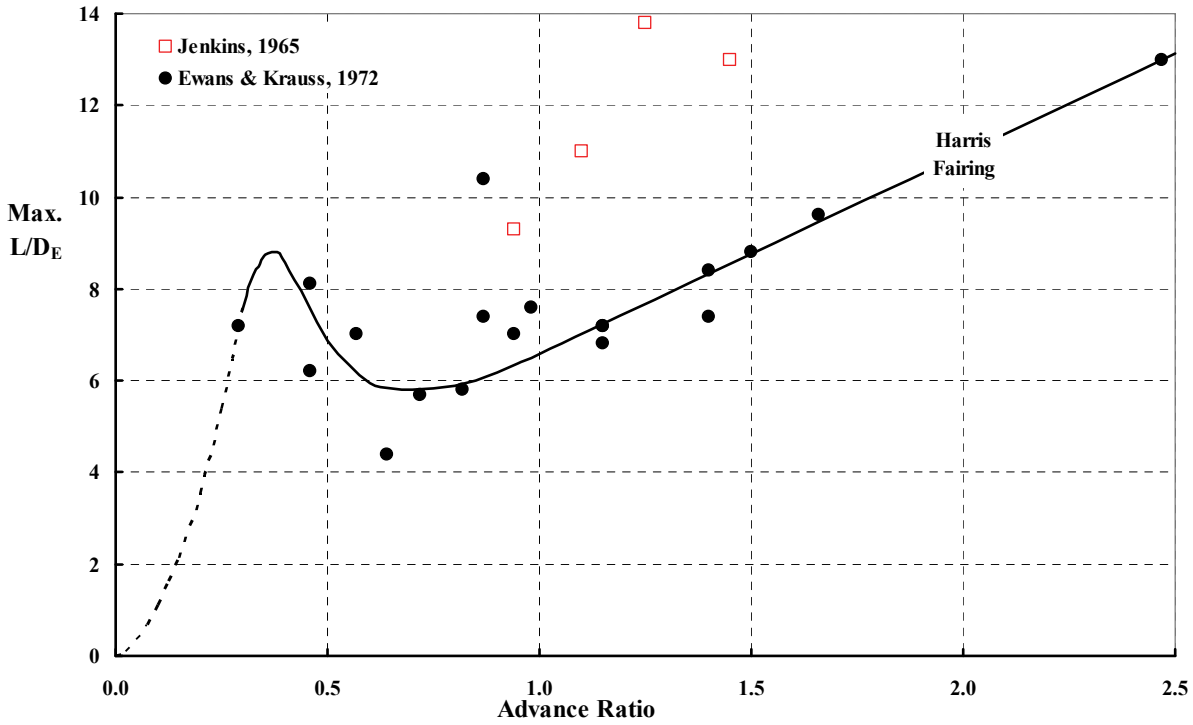

Fig. 2-15. As a conventional rotor, the RVR demonstrated a potential for fixed-wing-like maximum lift-to-drag ratios [75].

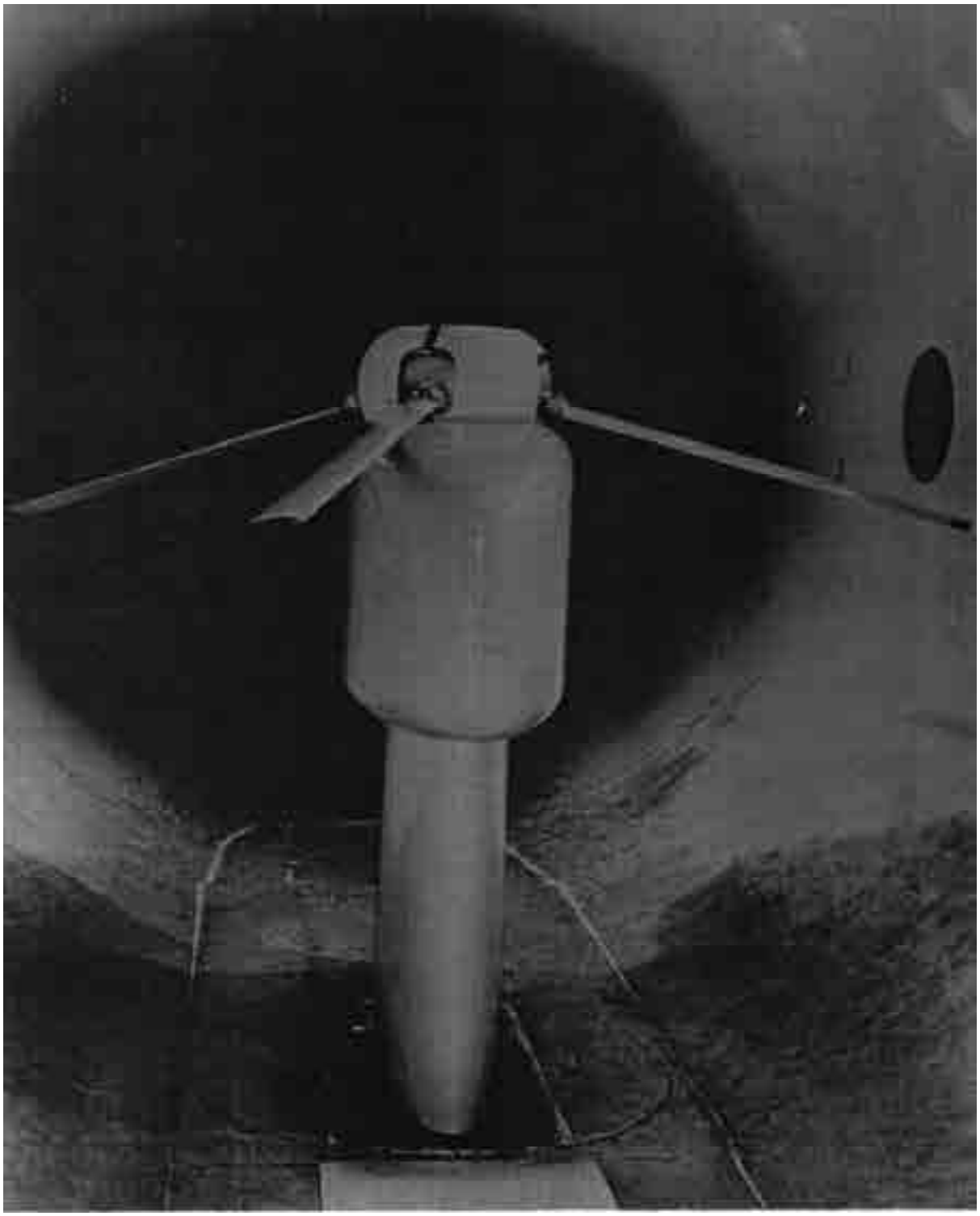

Fig. 2-16. The Fairchild 8-foot-diameter RVR as installed in the NASA Ames 12-foot pressure wind tunnel [77]. The rotor solidity was 0.1333.

L/D_E in the range of 9 to 14. Larry's data are included in Fig. 2-14 and Fig. 2-15 for the sake of completeness. These data from 1965 certainly added to a renewed interest in compound helicopters.

It was, however, with the data from the second entry of the RVR (now with higher harmonic feathering operating) in the NASA Ames 12-foot pressure wind tunnel, Fig. 2-16, that I, for one, really sat up and took notice. Just one set of results published in Ewans, McHugh, Seagrist, and Taylor's report [77] is sufficient for you to appreciate the potential this lifting rotor technology might have. The drag polar (i.e., lift versus effective drag) data is shown here in Fig. 2-17. The tunnel airspeed was 515 feet per second (about 300 knots), and the rotor tip speed was 365 feet per second. This is an advance ratio of 1.4 and an advancing tip Mach Number ($M_{1,90}$) of just under 0.78. The tunnel air density was reduced to 0.001168 slugs per cubic foot, which corresponds to about 16,900 feet altitude. The wind tunnel air temperature was 91 ^{o}F giving a speed of sound of 1,150 feet per second.

There is a major point in Fig. 2-17 that I hope you will not overlook. The RVR model—as a rotor system that includes the hub—has a maximum lift-to-effective-drag ratio of 2.2 because the hub drag is so large in relation to the blades-alone minimum drag. Of course, if you choose to include the hub drag as part of the airframe drag, then the blades-alone

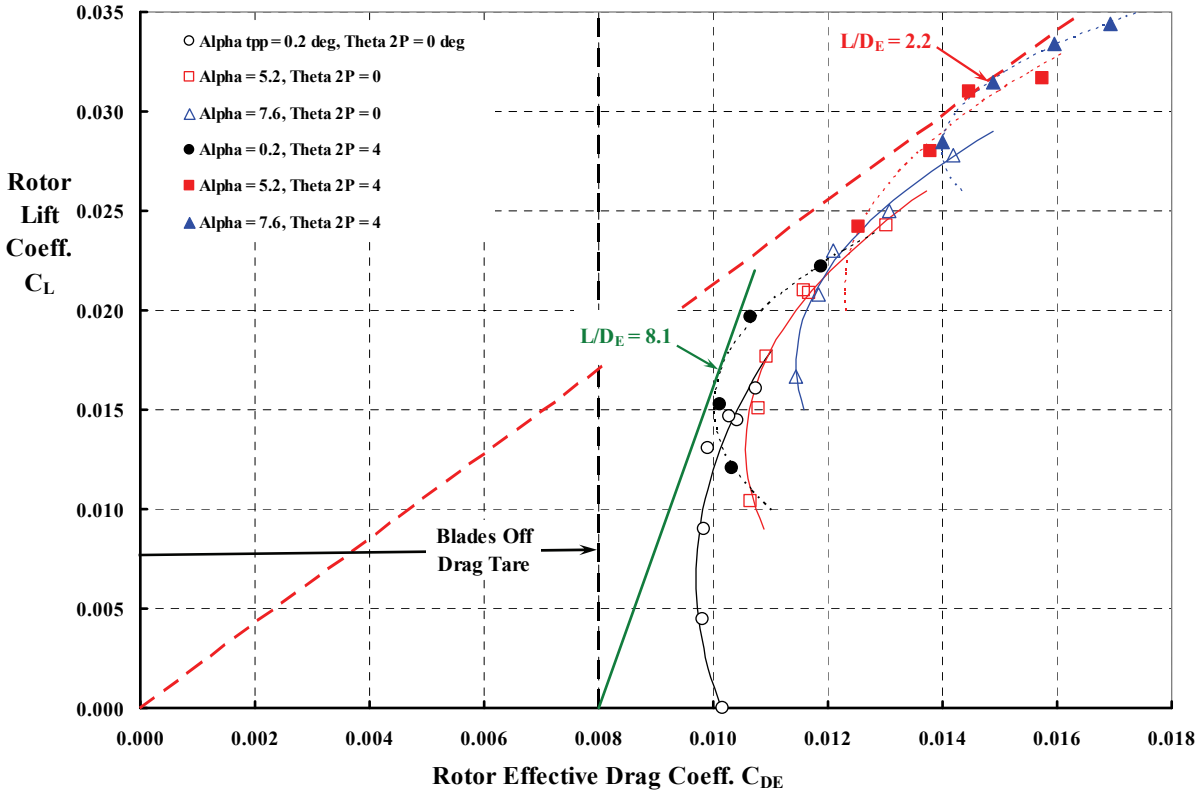

Fig. 2-17. The 8-foot-diameter RVR with 4 degrees of two-per-revolution feathering input demonstrated a maximum L/D_E of 8.1 at 300 knots, a V_{FP}/V_t of 1.4 [77].

maximum L/D_E is 8.1, which is on par with the maximum L/D_E recorded in the helicopter advance ratio region shown in Fig. 2-15. It is more than just interesting that Kurt Hohenemser, the chief engineer of the McDonnell XV-1 compound helicopter, made the statement in 1949 [88] that "actually, in a compound aircraft, the drag of pylon and hub is of more importance than the drag of the rotating blades." This is particularly true for the model RVR pictured in Fig. 2-16 because the "hub fairing" is overly large to house a portion of the higher harmonic (i.e., two-per-rev) feathering controls.

The two-per-revolution blade feathering motion used during this experiment appears in the feathering equation as

$$\theta_{x,\psi} = \theta_0 + x\theta_t - B_{1C}\sin\psi - A_{1C}\cos\psi + \theta_{2\psi}\cos(2\psi), \quad (2.9)$$

where the radial station is defined as (x = r/R), the blade root collective pitch is (θ_0), the total linear twist between blade root and blade tip is (θ_t), and (B_{1C} and A_{1C}) are the conventional once-per-revolution feathering motions introduced at the blade's root end by a swashplate. The data shown here in Fig. 2-17 is for 0 and +4 degrees of $\theta_{2\psi}$. You have probably already concluded that a conventional rotor system is modeled when $\theta_{2\psi}$ = 0 degrees. The *increment* in feathering, due to a positive value of $\theta_{2\psi}$ as the blade completes a revolution, is illustrated by the sketch. Note that in the reverse flow region around 270-degrees azimuth, the blade's trailing edge is raised so that a positive lift is obtained. The Fairchild design rounded the blade's airfoil trailing edge in the expectation that this would improve airfoil performance over that of a typically sharply pointed, trailing edge when the airfoil was "flying backwards."

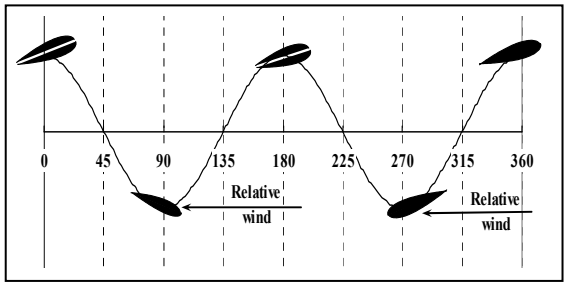

The second fact you should be aware of is that at advance ratios well above 1.0, control of the rotor's thrust and tip path plane relative to the shaft hub plane is amazingly linear with the parameters associated with Eq. (2.9)—even up to extraordinary C_T/σ's far exceeding those levels associated with helicopter retreating blade stall. To illustrate this point, you need only look at Fig. 2-18 and Fig. 2-19. Here, I have used the Microsoft® Excel® linear regression analysis tool to evaluate data from reference [77], Run 119, which led to Fig. 2-17.

While there is little evidence of blade stall in the fundamental trim parameters of thrust and flapping, the lift-drag polar of the model RVR shown in Fig. 2-17 is hardly encouraging. However, a conceptual design study of two compound helicopter configurations applying the rotor system was reported in 2002 by members of Sikorsky's Advanced Vehicle Concepts Group [79]. Their 80-passenger concepts (Fig. 2-20) suggested that cruise speeds from 310 to 340 knots would be a reasonable objective. However, the ratio of weight empty to takeoff gross weight would be on the order of 0.65, which would detract from the concept. Both designs envisioned installed engines rated at 23,000 to 26,000 horsepower at sea level. Most of this power would drive a 6- to 9-foot-diameter "ducted propfan" at the 10,000- to 20,000-foot cruise altitude. No champion of the concepts has stepped forward in the decade since this work by Sikorsky engineers was presented.

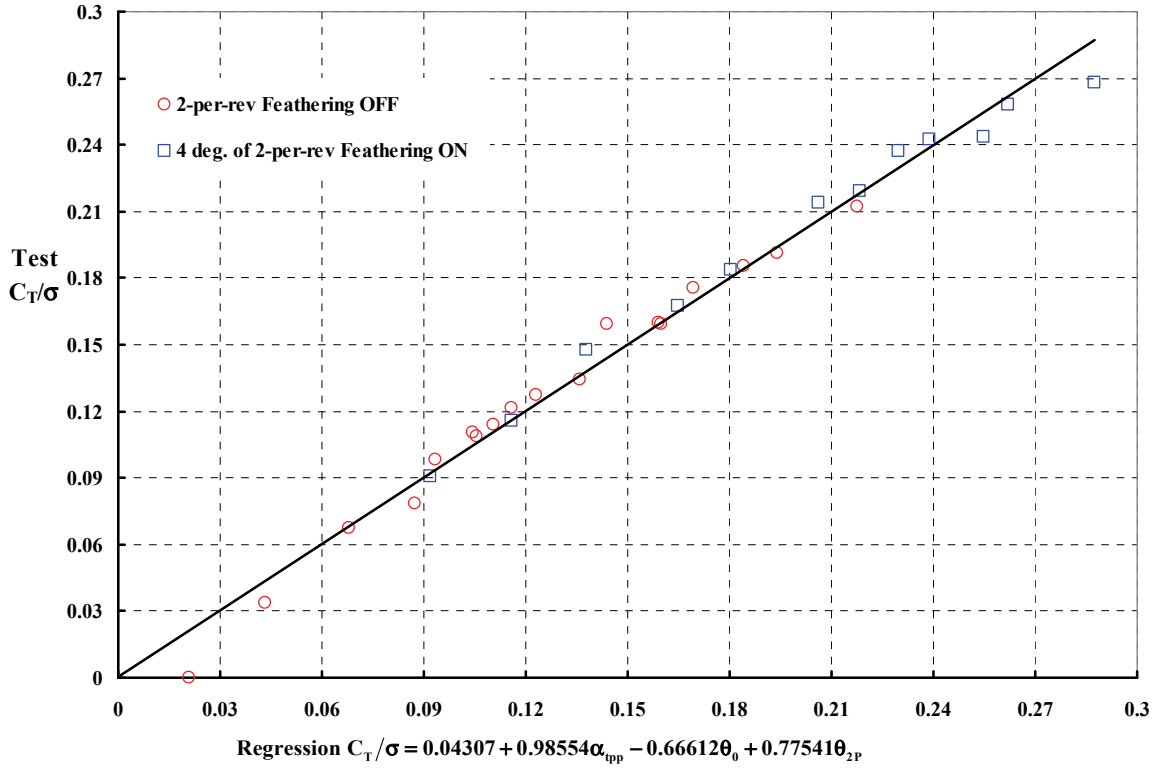

Fig. 2-18. The RVR demonstrated a quite useable lift coefficient at a V_{FP}/V_t of 1.4 [77].

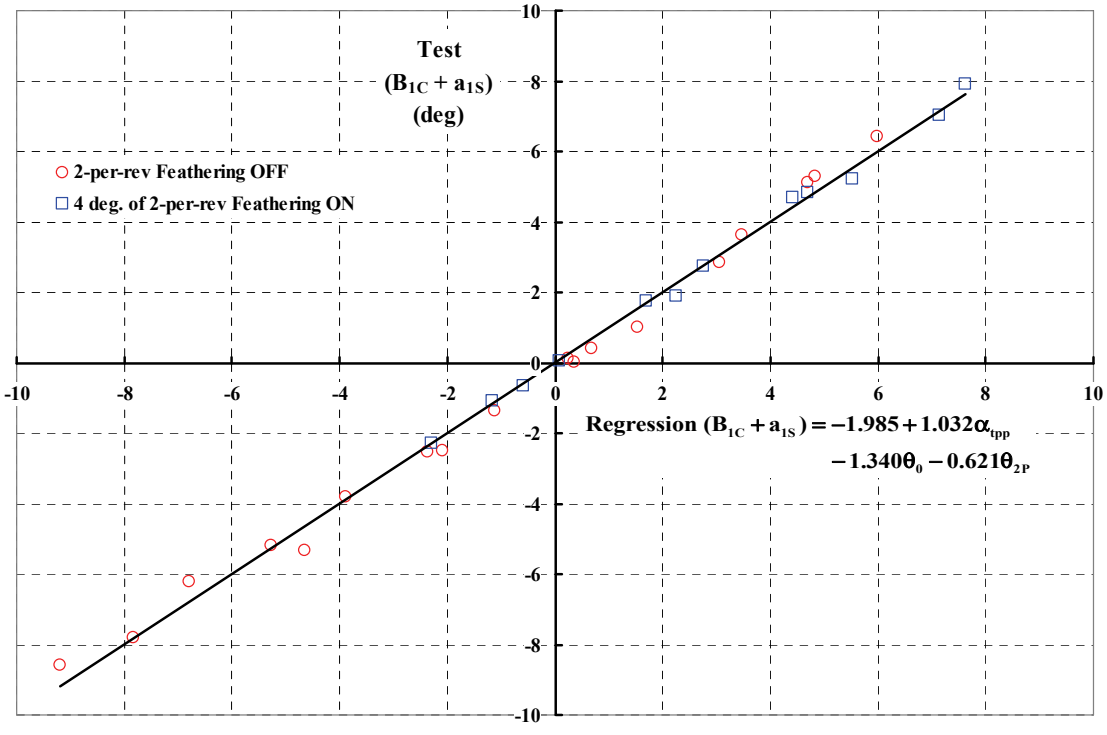

Fig. 2-19. The RVR remained quite controllable at a V_{FP}/V_t of 1.4 [77].

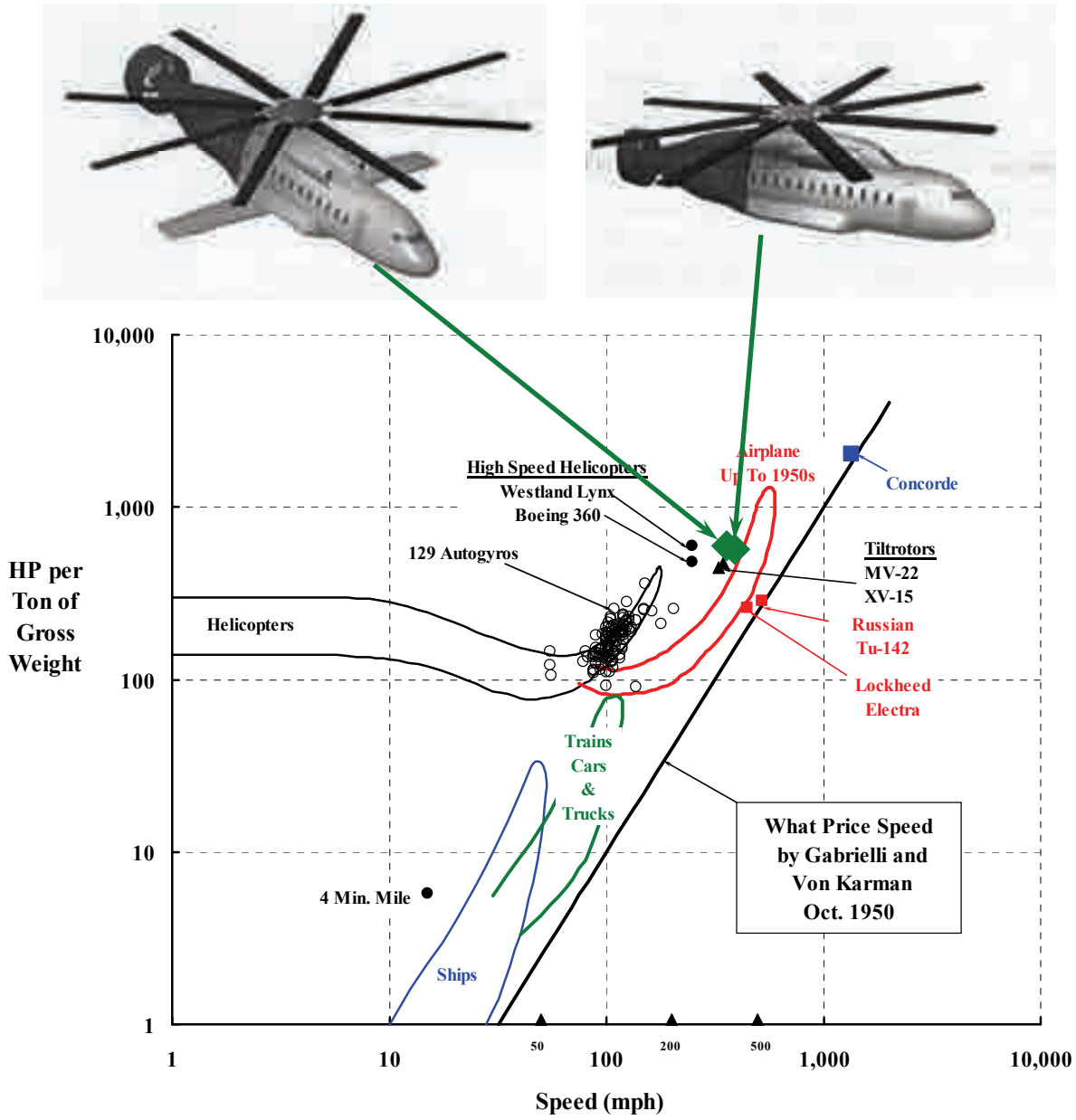

Fig. 2-20. In November of 2002, Sikorsky engineers took another look at what the RVR system had to offer [79].

2.5 FRANK MCHUGH'S ROTOR LIMITATION STUDY

Frank McHugh was the leader of the advanced rotor system technology program at Boeing Vertol throughout the 1970s. He was also a major contributor to the Reverse Velocity Rotor (RVR) investigation [77]. In May of 1975 he presented a paper [96] at the AHS Forum that provided a very concise snapshot of the performance of a "6-foot-diameter, Mach scaled, dynamically similar model of a CH-47B." In a 1974 preliminary test of this rotor,[18] he reported the performance data shown here in Fig. 2-21. This preliminary test raised clear questions about the performance limitations of a conventional rotor. Frank summed up the situation in his paper by asking, "Can the 200- to 300-knot conventional helicopter be practically achieved without recourse to auxiliary propulsion and auxiliary lift?"

At that point Frank had a rugged 1/10-scale model of a CH-47B rotor system, a powerful rotor test stand, and a wind tunnel—in short, the basic tools—to expand the test envelope beyond his preliminary test. He found a kindred spirit in Larry Jenkins at NASA Langley, and a NASA contract (NAS 1-14317) allowed a follow-on test to be completed. This was Boeing VSTOL Wind Tunnel Test No. 193 conducted in November 1976. There were two phases to the test because a swashplate bearing burned up, which caused a loss of blades. Phase I stopped after 54 runs. Test stand repairs were made, *including a new set of blades*, and runs 219 to 274 completed Phase II. In October of 1977, Frank and his coauthors (Ross Clark and Mary Soloman) delivered a massive three-volume report [97-99] about the test, which NASA published as NASA CR 145217-1 (210 pages), -2 (607 pages), and -3 (360 pages). The second and third volumes contain graphs of most of the key data from runs 21 to 54 (original blades), 55 to 57 (low-torsional-stiffness blades), and 219 to 274 (replacement blades).

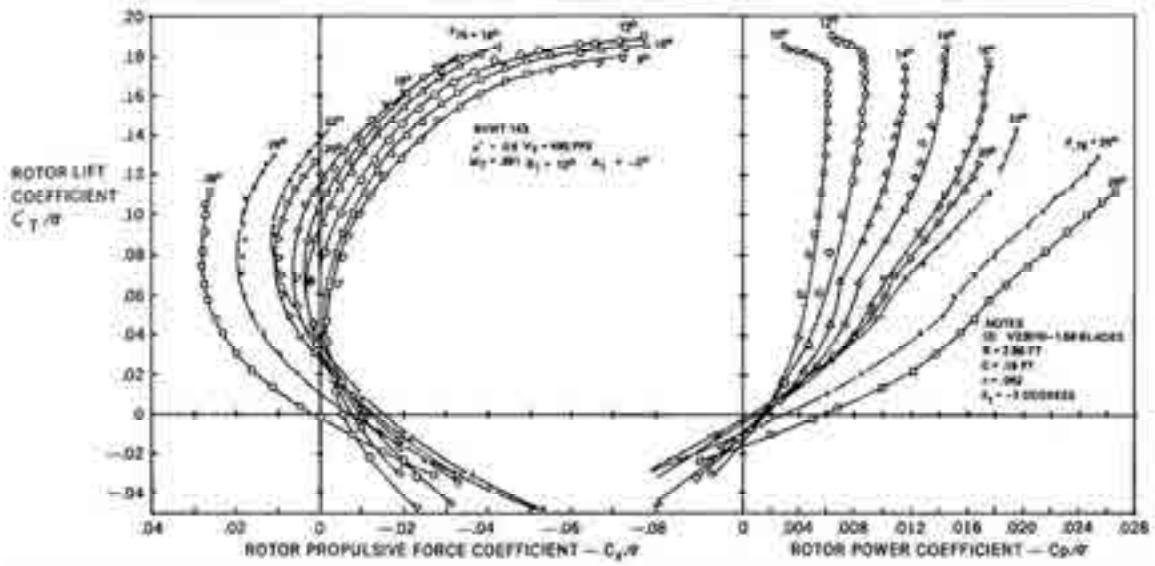

Fig. 2-21. McHugh's performance data for a model CH-47B forward rotor at a forward speed of 250 knots and a tip speed of 486 feet per second, a V_{FP}/V_t of 0.6 [96].

[18] I got to see the beginnings of Frank's preliminary test as my tenure as Manager of Boeing Vertol's V/STOL Wind Tunnel Complex drew to a close. In January of 1974 "they" sent me over to be Director of R&D, and I had to expand my interests.

Frank's approach to the test procedure for the nearly 115-run experiment was quite different from the earlier test results you saw graphed in Fig. 2-21. Rather than "map out" the lift, propulsive force, and power performance using a "fix the collective and do a shaft angle sweep," Frank chose to fly the model rotor much like a pilot would collect data in flight test. I believe he was the first one to choose this less traditional test procedure, and the logic behind his test procedure deserves more discussion.

When you think about it, the domain to be studied centers around a helicopter trimmed to fly at some given speed. So follow this philosophical thought using Fig. 2-22 as your focal point. First, select the coordinate system as a rotor lift coefficient (maybe divided by rotor solidity) versus a rotor propulsive force coefficient (maybe divided by solidity). That is, following the nomenclature Frank, Ross, and Mary used in their reports [97-99], you have:

$$(2.10)\quad \frac{C_T'}{\sigma}=\frac{L}{\rho\left(\pi R^2\right)V_t^2\sigma}\quad\text{and}\quad\frac{C_X}{\sigma}=\frac{X}{\rho\left(\pi R^2\right)V_t^2\sigma}\quad\text{and}\quad\frac{C_P}{\sigma}=\frac{P}{\rho\left(\pi R^2\right)V_t^3\sigma}.$$

Second, define the aircraft and its trim point for the given speed. At that time they were, for all intents and purposes, modeling the forward rotor of the tandem rotor CH-47B. This Boeing Vertol helicopter was in service at a normal gross weight of 33,000 pounds and had a frequently quoted parasite drag area ($X/q = f_e$) of about 47 square feet. The 60-foot-diameter rotor had three blades, each with a chord of 25.5 inches, which makes the solidity 0.067. The normal tip speed was 720 feet per second. The maximum cruise speed has been stated as 154 knots, but this is not the normal speed for best range. It was decided that a parasite drag area to be overcome by *one* rotor of a low-drag *advanced* CH-47B would be an X/q of about 12 square feet. They chose to nondimensionalize the 12-square-foot drag area using a variation on a George Schairer propulsive force coefficient. That is, they set $X/qD^2\sigma$ to 0.05 as the baseline propulsive force trim, which is, approximately, independent of advance ratio. Keep in mind that a conversion from an X/q baseline means that the rotor's propulsive force coefficient is dependent on advance ratio. That is to say,

$$(2.11)\quad \frac{C_X}{\sigma}=\frac{2}{\pi}\left(\frac{V}{V_t}\right)^2\left(\frac{X}{qD^2\sigma}\right)=0.03183\left(\frac{V}{V_t}\right)^2\quad\text{for}\quad\frac{X}{qD^2\sigma}=0.05.$$

For a nominal-trim rotor lift coefficient, they envisioned an advance CH-47B that would operate at a C_T'/σ of 0.08. For their summary example, they used a forward-speed-to-tip-speed ratio of 0.53. This baseline trim point is about where the red and green arrows cross in Fig. 2-22.

Now you can see in Fig. 2-22 that from this trim point the rotor lift limits can be explored by increasing rotor lift at constant propulsive force. This is similar to collecting flight test data at several gross weights. Rotor propulsive force limits can be searched for by tilting the tip path plane nose-down (and increasing collective pitch) while holding lift constant. This is equivalent to increasing the helicopter's parasite drag, which happens when landing gear is lowered for landing or carrying external stores on some mission. Frank decided that the primary starting point for the V_{FP}/V_t range would be 0.4 and extend to at least

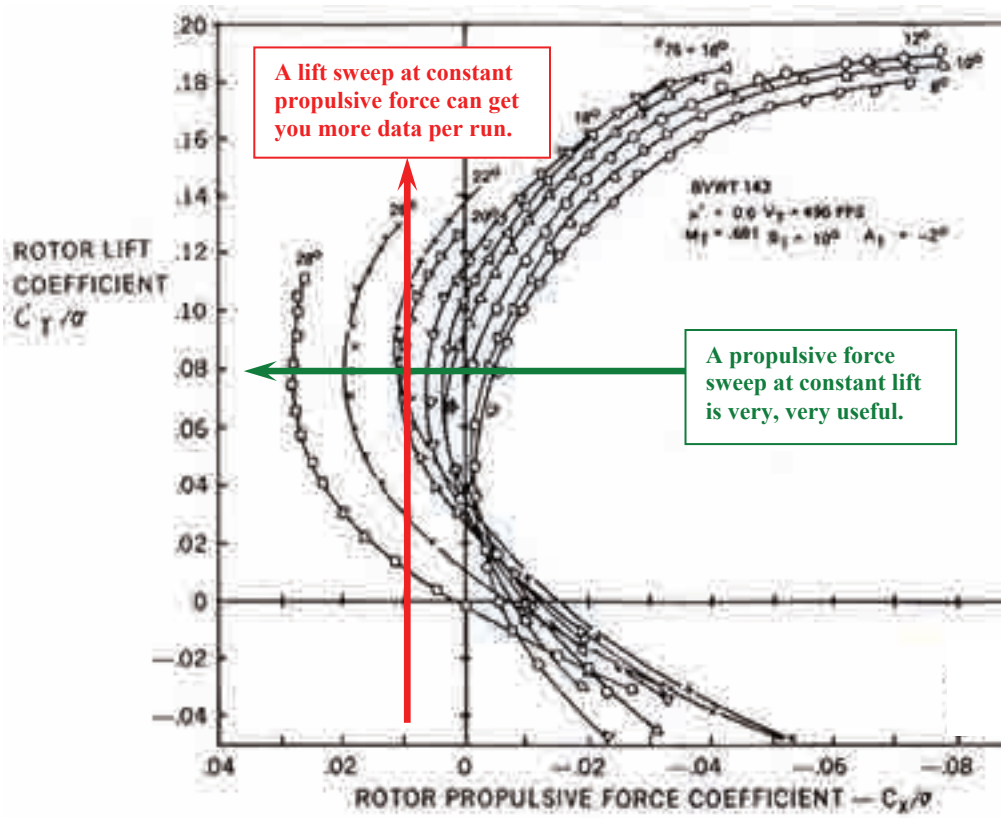

Fig. 2-22. You can answer many performance questions without filling out a full matrix of shaft angles and collective pitches.

0.6, which was obtained in the preliminary test in 1974. Because the nominal tip speed of the 1/10-scale model was 620 feet per second, the Boeing V/STOL tunnel was operated at 215 to about 307 knots. The model radius was 2.9583 feet, the chord was 0.1913 feet, and the solidity with three blades was 0.06175, as you will see on page 32 of reference [97], the data analysis volume.

When you look at the experiment's run log beginning on page 51 of the data analysis volume [97], you will see that after some check-out and hover testing, runs 25 through 54 were primarily devoted to finding lift limits at $X/qD^2\sigma$ ranging from 0.025 up to 0.2. Only about 30 runs were used to find the aerodynamic lift limits. It was from this primary data set of runs with the original blades that Frank obtained his now classic graph. The original graph, which you will find on page 68 of his data analysis volume, is included here as Fig. 2-23. There are any number of papers and reports that have included some version of Frank McHugh's original graph—a few, I might add, with several degrees of poetic license taken in the reproduction. Note on Fig. 2-23 that while the abscissa is labeled advance ratio, the correct label is simply $\mu' = V_{FP}/V_t$. This is an important point because some key data was gathered at tip path planes approaching −45 degrees forward tilt. And as you know, strictly speaking, advance ratio is defined in the tip-path-plane coordinate system as

$$(2.12)\quad \mu_{tpp} = \frac{V_{FP}\cos\alpha_{tpp}}{V_t}.$$

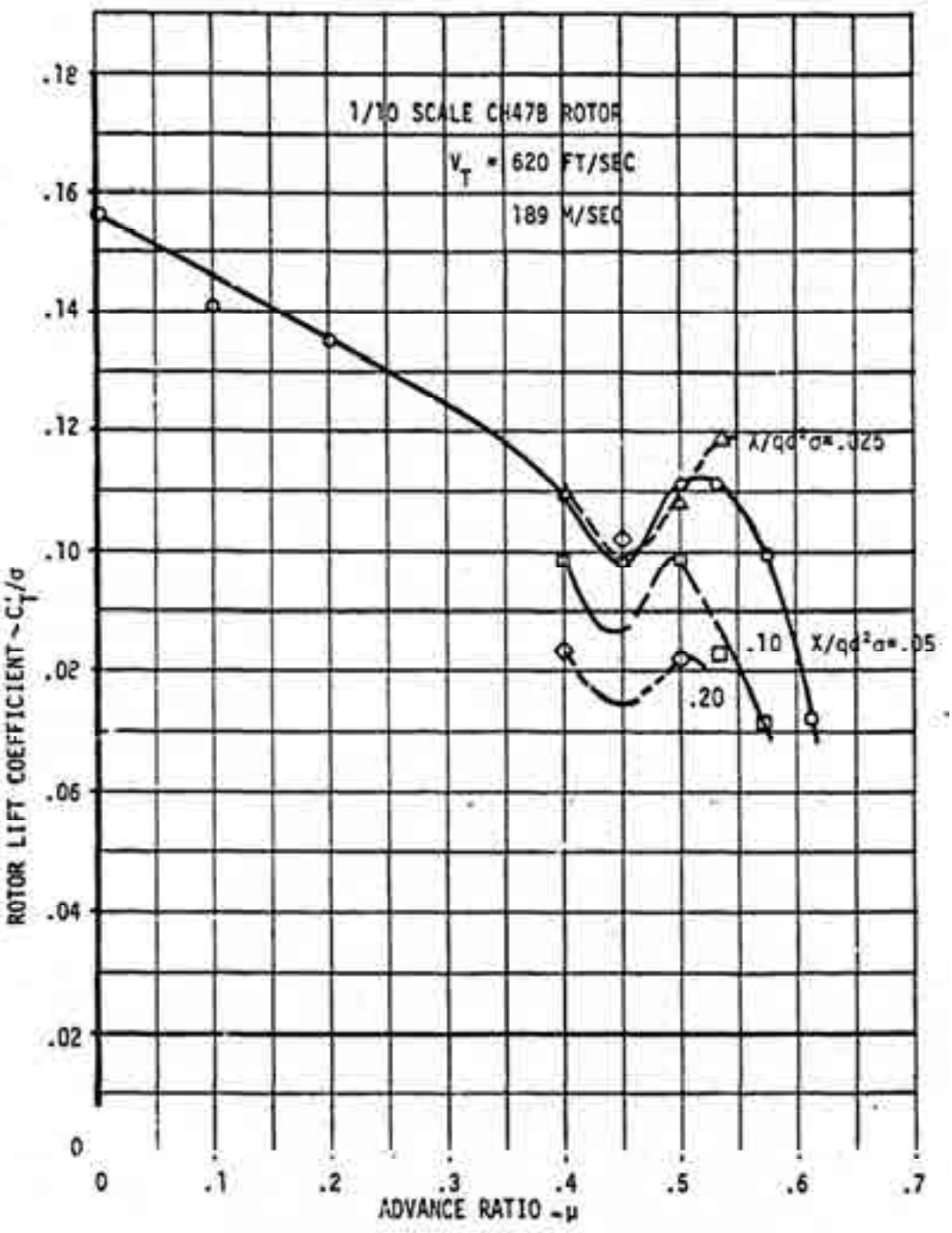

FIGURE 6.1.6 EFFECT OF PROPULSIVE FORCE REQUIREMENTS ON MAXIMUM LIFT LIMIT

Fig. 2-23. Frank McHugh's classic 1977 maximum-lift data from a 1/10-scale-model test of a CH-47B forward rotor at near full-scale tip speed. The abscissa is labeled advance ratio, but it is actually just V_{FP}/V_t [97].

How Frank defined and found the limit lift at each V_{FP}/V_t was explained with a figure (reproduced here, with some of my additions, as Fig. 2-24) about which he wrote in the data analysis summary on page 3 of reference [97]:

> "A sweep in rotor lift was made at a fixed rotor propulsive force coefficient ($X/qd^2\sigma$), increasing the lift until a limit defined by aerodynamic capability, blade loads or control capability was reached. Since collective pitch defined the rotor lift, this variation was used to establish any aerodynamic limitation on lift. Figure 1.2 [reproduced here as Fig. 2-24] presents a typical variation of rotor lift coefficient C_T'/σ with collective pitch (0.758) at an advance ratio ($\mu' = V/V_t$) of 0.53 for three levels of propulsive force coefficient ($X/qd^2\sigma$) of 0.025, 0.05 and 0.10. At the lower level of rotor lift, the sensitivity to collective is very high but as C_T'/σ becomes greater than 0.08 the sensitivity gradually decreases to a point where further increases in collective pitch produce either no change or a decrease in rotor lift coefficient. This indicates the lift is limited by the aerodynamic capability of this model rotor system. The most critical load monitored during the test was alternating blade root torsion because it was the primary indicator of blade stall and had the smallest margin with the anticipated loads. Maximum measured torsion loads never exceeded 60 percent of the allowable, so loads were never the cause for limiting testing. There were only a few cases where longitudinal or lateral cyclic capability limited the testing and not the aerodynamic capability."

Fig. 2-24 illustrates Frank's "rotor lift sweep" for a tip speed of 620 feet per second and a tunnel speed of 329 feet per second (i.e., $V_{FP}/V_t = 0.53$). You see my additions for a stall flutter onset boundary and my choice for collective pitches where maximum rotor lift is reached. The flutter onset lift was indicated by a sharp increase in alternating torsion loads as

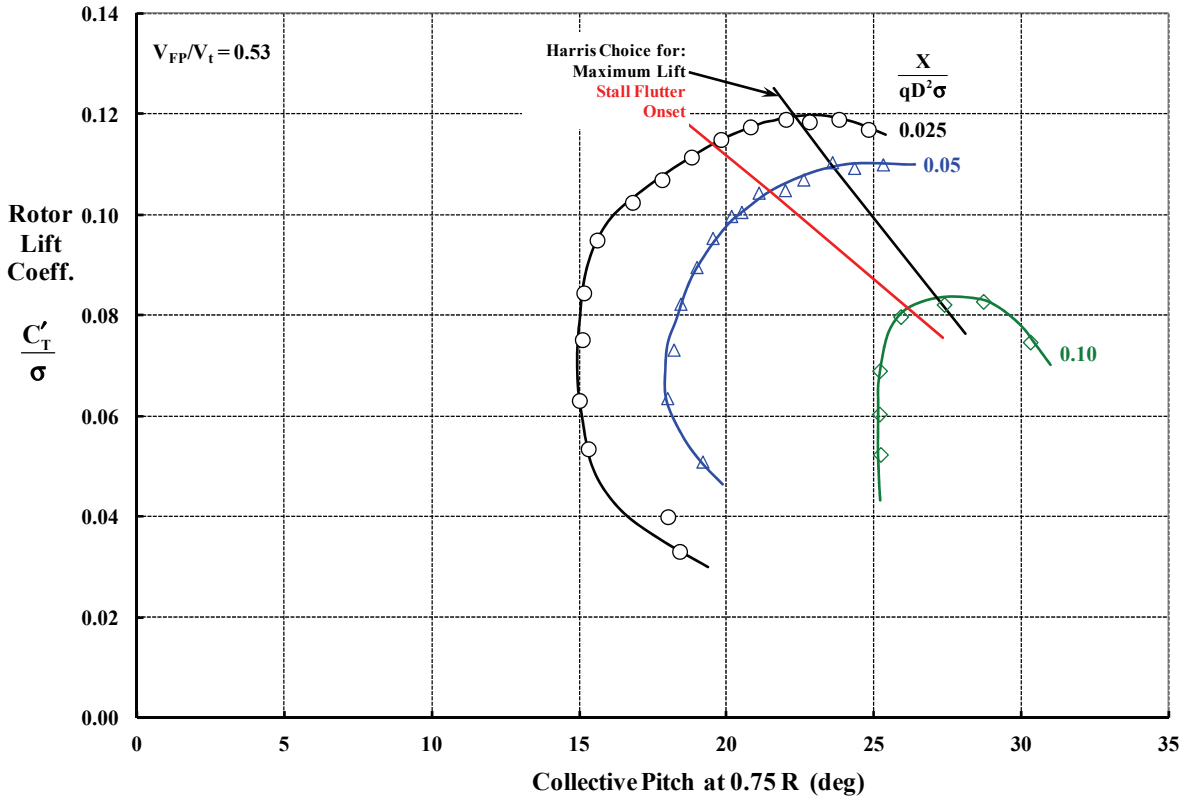

Fig. 2-24. Frank McHugh's maximum lift levels were generally clearly defined [97].

measured at the blade root and two outboard radius stations. Fig. 2-25 shows the accompanying power required to obtain the lifts and propulsive force levels shown in Fig. 2-24. Marc Sheffler compared the then-current theory to McHugh's stall boundary in a 1979 report [100].[19]

What you cannot fully appreciate from these levels of power required curves is just how much more power these curves imply relative to power required to hover. To make sure that this situation was quite clear, Frank gathered data in forward flight by "flying" the model CH-47B rotor as if it was trimmed at a rotor lift coefficient of C_T'/σ equal to 0.08 and at three levels of the parasite drag coefficient ($X/qD^2\sigma$). His results are included in volume 1 of reference [97], page 25, and I have reproduced the original graph here as Fig. 2-26.

What struck me most about Fig. 2-26 when I first saw it was this: *It takes about twice the hover power for the model rotor to just overcome its own drag* (i.e., $X/qD^2\sigma = 0$) *at a 0.53 ratio of tunnel speed to tip speed and a* C_T'/σ *of 0.08*. While it is true that a rotor can both lift and propel at V_{FP}/V_t ratios at least up to 0.6, the power required is so large that the pure helicopter with a conventional rotor(s) begins to seem very, very expensive.

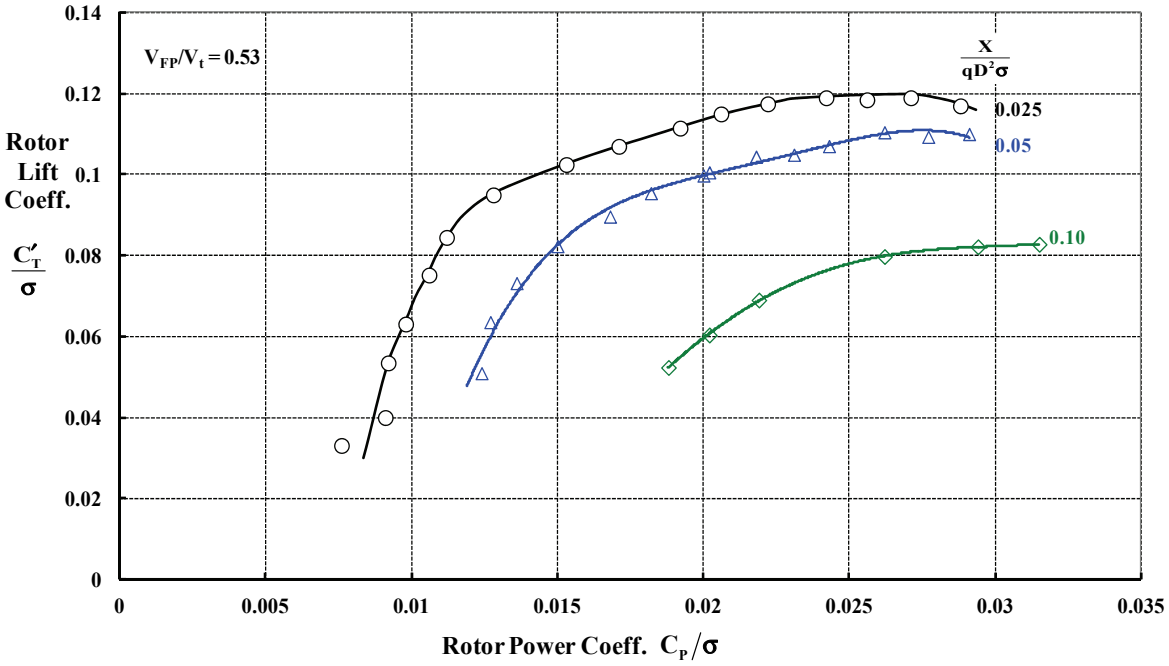

Fig. 2-25. Frank McHugh's example of power required increases during a rotor lift sweep at three constant-propulsive-force levels (for a tunnel speed of 286 knots and a tip speed of 620 feet per second) [97].

[19] It took 25 years before another person made use of McHugh's work. In early 2003, Hyeonsoo Yeo (a member of AFDD at Ames Research Center) compared McHugh's experimental lift-limit-boundary data to theoretical calculations using several different airfoil stall models. His paper [101] stands out because he shows that "modern" theory and test are quite close. Both Marc's and Dr. Yeo's papers are most certainly worth your reading time.

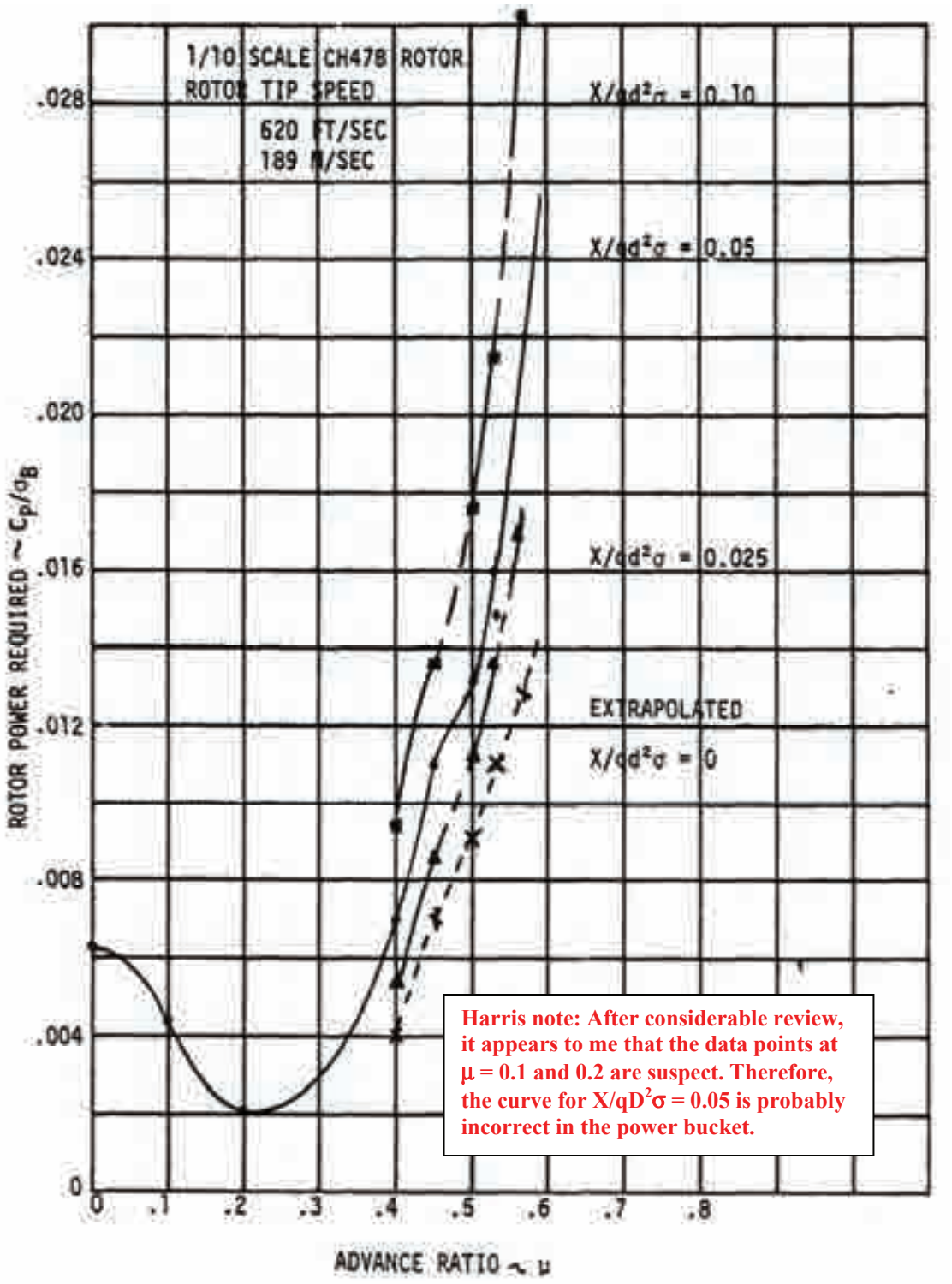

Fig. 2-26. Frank McHugh's power-required-versus-speed data at a constant rotor lift coefficient of $C_T'/\sigma = 0.08$. The model CH-47B requires considerable power to just overcome its own drag [97]. Blade instrumentation raised the average airfoil minimum drag coefficient to 0.013 based on hover-thrust-versus-power data.

2.6 THE HELICOPTER ROTOR'S PRACTICAL PERFORMANCE PROBLEMS

The power required curves you see in Frank McHugh's summary graph, Fig. 2-26, show that the edgewise flying conventional rotor absorbs a great deal of power in just overcoming its own drag, never mind the parasite drag of the helicopter it is attached to. This seems to me to be a practical—if not even fundamental—limitation. Therefore, it is worth a moment to see if the situation can be explained with the simplest of theory.

Simple thinking says that the rotor's total power required contains (1) power for lifting, (2) power to overcome the profile drag of the blades, and (3) power to overcome the parasite drag of the rest of the helicopter. You learned about this in Volumes I and II. So let me start with power required calculated by the energy method (Vol. I, Eq. 2.60) restated as

$$(2.13)\quad P_{req'd} = P_{induced} + P_{profile} + X V_{FP}\,.$$

You learned that induced power created by the requirement to lift is calculated, following Glauert's ideal assumption, as

$$(2.14)\quad \text{Ideal } P_{induced} = Lv \quad \text{where } v = \frac{L}{2\rho\left(\pi R^2\right)\sqrt{\left(V_{FP}\sin\alpha_{tpp} - v\right)^2 + \left(V_{FP}\cos\alpha_{tpp}\right)^2}}\,,$$

and that Glauert's ideal induced velocity (v) is a root of a quartic equation. You will also remember from Volume I, Fig. 2-100, page 215, that the edgewise flying rotor solution of the quartic has the result of

$$(2.15)\quad \text{Ideal } P_{induced} = Lv \quad \text{where } v = v_h\left[\sqrt{\left(\frac{V^2}{2v_h^2}\right)^2 + 1} - \frac{V^2}{2v_h^2}\right]^{1/2} \quad \text{for } \alpha_{tpp} \approx 0 \text{ deg}$$

where the ideal induced velocity in hover (v_h) is defined as $v_h = \sqrt{T/2\rho A}$.

However, you also received the first indication from Kenneth and Steven Hall [102] that Glauert's ideal equation was significantly in error as discussed in my Closing Remarks of the Forward-Flight Performance discussion (Volume II, section 2.4.5, pages 265 and 266). I have used the Hall brothers' computations to create a correction factor (K_{Hall}) to Glauert's ideal induced power such that

$$(2.16)\quad P_{induced} = K_{Hall}\left(Lv_h\right)\left\{\left[\sqrt{\left(\frac{V^2}{2v_h^2}\right)^2 + 1} - \frac{V^2}{2v_h^2}\right]\right\}^{1/2} \quad \text{where } v_h = \sqrt{\frac{T}{2\rho A}}\,.$$

The Hall correction factor for two-, three-, and four-bladed conventional helicopter rotors (operating at a tip-path-plane angle of attack of –5 degrees) is shown in Fig. 2-27. No doubt there will be significant follow-on studies to what the Hall brothers have started, but for this discussion I believe that their results are close enough to the induced power required by an ideal, loaded articulated rotor. Keep in mind that induced power *does not*—to the first approximation—depend on solidity. This is in contrast to profile power, which *does* depend on solidity.

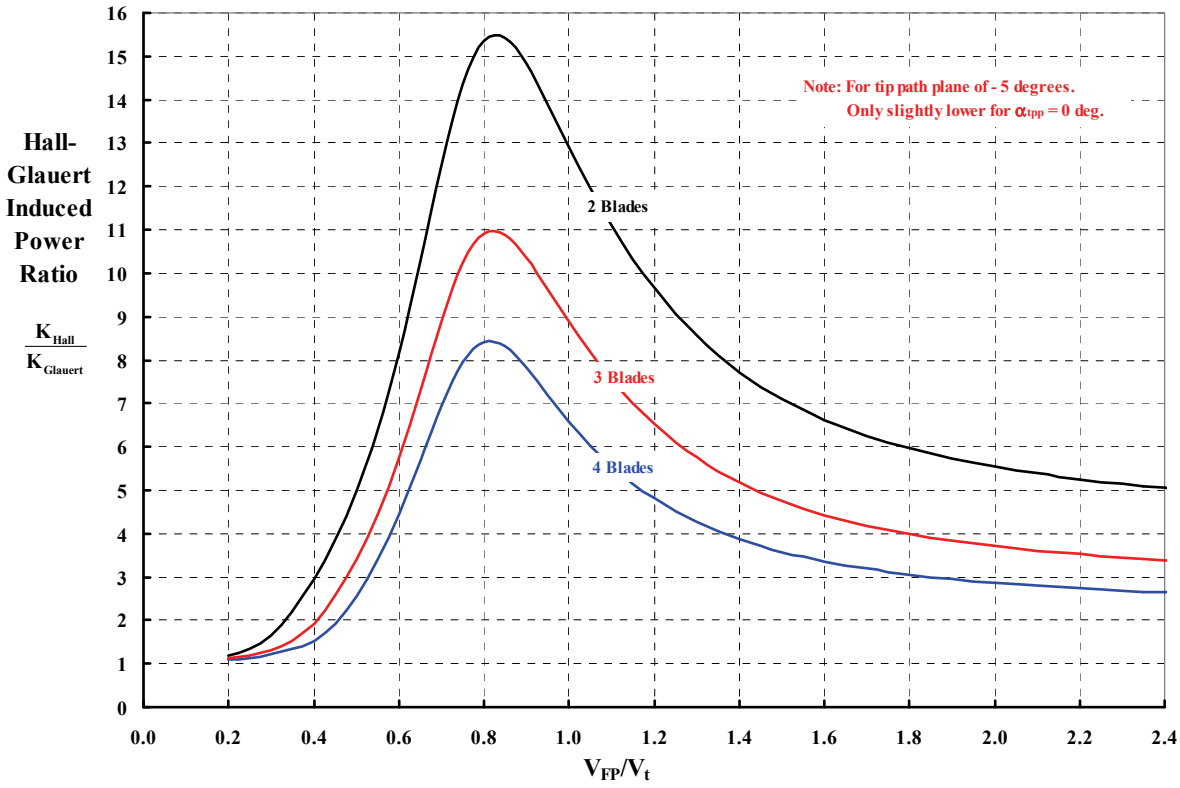

Fig. 2-27. The Hall correction factor to Glauert's ideal induced power theory for two-, three-, and four-bladed rotors [102].

Next, consider the minimum profile power ($P_{profile}$) that a rotor in any flight condition, edgewise or otherwise, requires. You learned from Appendix J in Volume I that this power is calculated as

$$P_{profile} = \left(\rho A V_t^3\right)\frac{\sigma C_{do}}{8} P_{(\mu,\lambda)}, \tag{2.17}$$

where the parameter $P_{(\mu,\lambda)}$ was given as

$$P_{(\mu,\lambda)} = \sqrt{1+JJ}\left[1+\frac{5}{2}JJ+\frac{3}{8}\mu^2\frac{4+7JJ+4JJ^2}{(1+JJ)^2}-\frac{9}{16}\frac{\mu^4}{(1+JJ)}\right] + \left(\frac{3}{2}\lambda^4+\frac{3}{2}\lambda^2\mu^2+\frac{9}{16}\mu^4\right)\ln\left(\frac{1+\sqrt{1+JJ}}{\sqrt{JJ}}\right), \tag{2.18}$$

and where $JJ = \mu^2 + \lambda^2 = (V_{FP}/V_t)^2$. Note immediately that profile power *does* depend on solidity. More precisely, the product of disc area (A) and solidity (σ) is the total area of all blades. That is, $A\sigma = bcR$, at least for a rectangular blade of chord (c) and including all blades (b). Values of $P_{(\mu,\lambda)}$ for several values of V_{FP}/V_t at λ equal to zero are:

V_{FP}/V_t	0.0	0.1	0.2	0.3	0.4	0.5	0.6	0.7	0.8	0.9	1.0
$P_{(\mu,\lambda)}$	1.0	1.048	1.215	1.553	2.125	3.000	4.250	5.948	8.168	10.985	14.473

Finally, as you study Eq. (2.13), you see that total power required varies linearly with the product of the useable rotor propulsive force (X) and the flightpath velocity (V_{FP}). This product could be labeled ($P_{propulsion}$). Frank McHugh's multi-volume test report [97-99] experimentally examines this linear dependency statement in appendix B of his second volume [98]. Fig. 2-28 shows that the energy approach to power required is very useful. What is fascinating to me is that providing a useable propulsive force can, depending on the ratio of forward speed to tip speed, significantly drive up the sum of induced and profile power. You see this from Fig. 2-28 because the slopes of the plotted lines are not 1.0.[20] This raises the logical question of the propulsive efficiency of the nearly edgewise flying rotor and, perhaps more importantly, how to think about and include propulsive efficiency.

Efficiency is frequently formed as the ratio of ideal to actual. Therefore, it seems reasonable to take for ideal the sum of ideal induced power plus ideal propulsive power. For ideal induced power, I suggest that Glauert's approximation for V_{FP}/V_t greater than, say, 0.2 will do for this discussion. Therefore, the ratio of ideal power to actual power given by Eq. (2.13) can be stated as

$$(2.19)\quad \text{Total Rotor Efficiency} = \frac{\text{Ideal } P_{induced} + XV_{FP}}{P_{induced} + P_{profile} + XV_{FP}} \quad \text{for } V_{FP}/V_t \geq 0.2 \text{ and } \alpha_{tpp} < \pm 5\,\text{deg}.$$

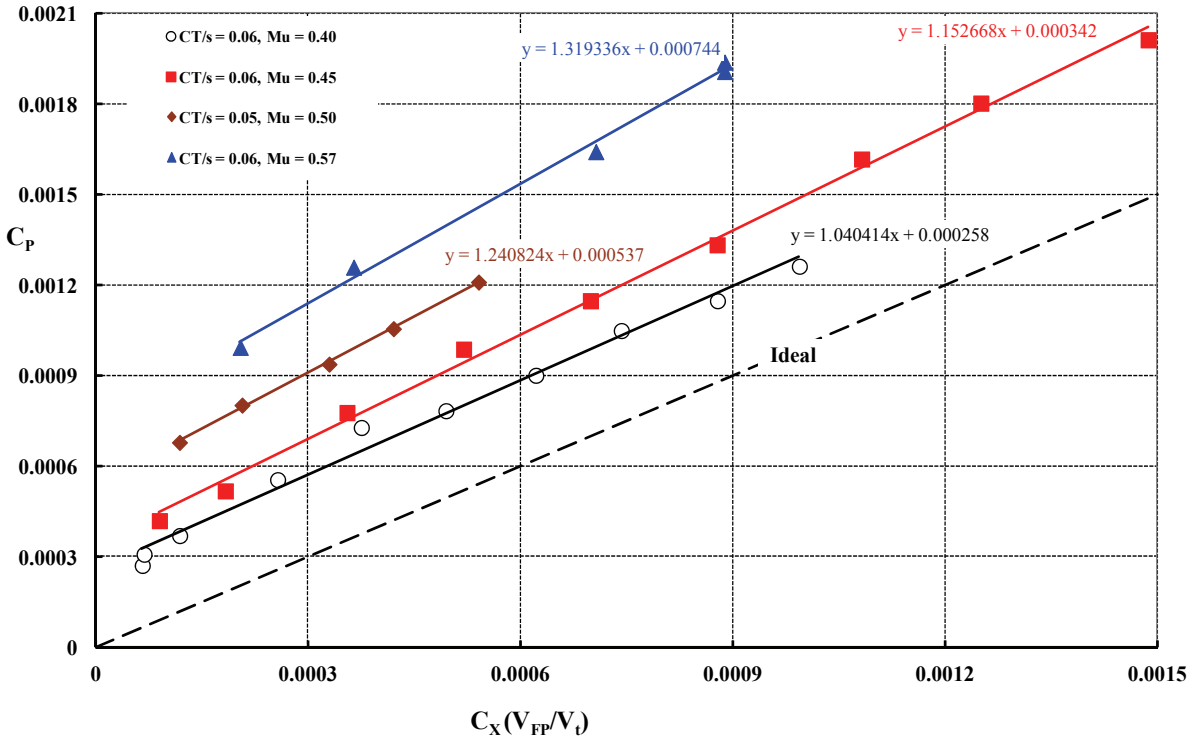

Fig. 2-28. Power varies linearly with propulsive force at constant rotor lift.

[20] The lines on Fig. 2-28 were obtained using the Microsoft® Excel® trendline tool and represent a linear regression analysis.

Now you can immediately see a bookkeeping problem arise when the propulsive power (XV_{FP}) equals zero. The total rotor efficiency parameter I have defined will be considerably less than 1.0, simply because of the actual profile power ($P_{profile}$), even if the rotor is not doing any useful propulsion. So, after giving some thought to Eq. (2.19), I suggest that all of the actual power required—over and above the actual power required at zero propulsive force—is under discussion. In effect, the lines on Fig. 2-28 give the quantitative insight into propulsive efficiency. The measure of propulsive efficiency is nothing more than the inverse of the slope of a line on Fig. 2-28 and, therefore, the total power required can be computed as

$$\text{(2.20)}\quad \text{Actual } P_{req'd} = \left(\text{Actual } P_{req'd} \text{ at } X = 0\right) + \frac{XV_{FP}}{\eta_P}.$$

The data says to me that creating a propulsive force drives up both induced and profile power required. Without careful theoretical study, I know of no way to apportion the increase.

Frank McHugh's groundbreaking experiment provides (in my mind) only a meager amount of data[21] to construct the trend I have speculated about in Fig. 2-29. Below a forward-speed-to-tip-speed ratio of 0.4, it appears the conventional rotor can provide propulsive force at virtually 100 percent efficiency. That is, at relatively low speeds (say up to V_{FP}/V_t of 0.4), the conventional rotor (1) can be tilted forward, (2) will produce useable propulsive force (X) approximately as $-T\alpha_{tpp}$, and (3) requires little, if any, increase in power required (over and above XV_{FP}). I have projected the trend to a zero efficiency at a V_{FP}-to-V_t ratio of 0.9 based on the discussion leading up to Fig. 2-2. It is doubtful that this one speculation is good for all advancing tip Mach numbers, lift coefficients, or even for all conventional helicopter rotors. However, because conventional propellers, which do not provide significant lift, have propulsive efficiencies above 0.8, it appears that conventional helicopter rotors such as the CH-47B's are a poor choice for propulsion if the objective forward-speed-to-tip-speed ratio is greater than 0.45 to 0.50.

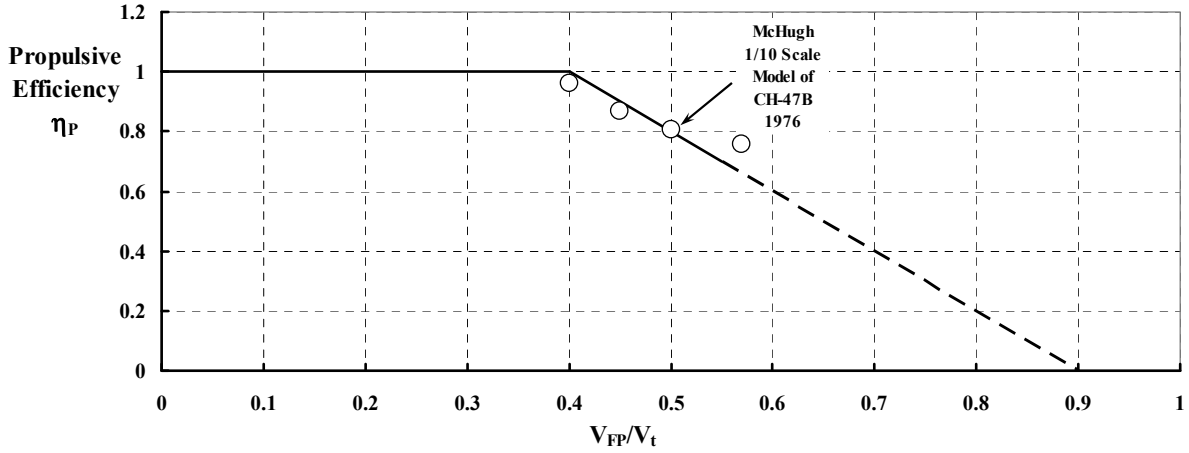

Fig. 2-29. A speculation about the propulsive efficiency of conventional helicopter rotors.

[21] For example, it would be quite helpful if the propulsive force sweep at constant lift began around autorotation (i.e., CP = 0) and extended even further into the positive propulsive force region. Furthermore, propulsive force sweeps at many more lift coefficients would be especially valuable.

The practical problem faced by the conventional helicopter rotor is simply the quite excessive power required to overcome its own drag. To see this more clearly, the several equations given previously can be collected and power can be converted to standard rotor coefficient form, which is based on $\rho A V_t^2$ for McHugh's lift coefficient (C_T') and $\rho A V_t^3$ for a power coefficient (C_P). It is helpful to remember that $v_h = \sqrt{T/2\rho A}$ so that $v_h = V_t\sqrt{C_T'/2}$ when using McHugh's notation that C_T' refers to rotor lift nondimensionalized by $\rho A V_t^2$. Thus, the power required as given by Eq. (2.13) becomes, in coefficient form,

$$P_{req'd} = P_{induced} + P_{profile} + XV_{FP}$$

$$(2.21)\quad C_{P-req'd} = K_{Hall}\left(\frac{C_T}{\sqrt{2}}\right)\left(\frac{V_{FP}}{V_t}\right)\left\{\sqrt{1+\left[\frac{C_T^2}{\left(V_{FP}/V_t\right)^4}\right]}-1\right\}^{1/2} + \frac{\sigma C_{do}}{8}P_{(\mu,\lambda)} + C_X\left(\frac{V_{FP}}{V_t}\right).$$

Some simplification occurs if $C_T^2/\left(V_{FP}/V_t\right)^4$ is small compared to 1.0 (usually for V_{FP}/V_t greater than 0.2) *and* the tip-path-plane angle of attack is in the range of ±5 degrees, which is one way of referring to the conventional helicopter's edgewise flying rotor. Under those constraints, Eq. (2.21) reduces to

$$(2.22)\quad C_{P-req'd} = K_{Hall}\frac{\left(C_T'\right)^2}{2\left(V_{FP}/V_t\right)} + \frac{\sigma C_{do}}{8}P_{(\mu,\lambda)} + C_X\left(V_{FP}/V_t\right).$$

At the other extreme, as $\left(V_{FP}/V_t\right)$ goes to zero, you have the rotor in hover, in which case you will see that Eq. (2.21) reduces to

$$(2.23)\quad \text{Hover } C_{P-req'd} = \frac{\sqrt{2}\left(C_T'\right)^{3/2}}{2} + \frac{\sigma C_{do}}{8},$$

and you have Glauert's ideal induced power plus the first approximation of profile power.

Now let me draw your attention back to Fig. 2-26 and specifically to the power-required-versus-speed curve where $X/qD^2\sigma$ equals zero, which Frank obtained by slight extrapolations. The primary objective is to see how close Eq. (2.21) comes to this case where the rotor is just overcoming its own drag. Because the useable propulsive force (C_X) is zero, the secondary objective is to see how the proportions of the two remaining components—induced power and profile power—contribute to the total power required. I will refrain from dividing the coefficients by solidity (which is a too common practice) because induced power does not depend on solidity but profile power does.[22] The rotor solidity of the model CH-47B was taken as 0.06175 in Frank McHugh's model experiments. This is based on a model rotor radius (R) of 2.9583 feet, a blade chord (c) of 0.1913 feet, and three blades.

[22] While many of the graphs and some equations show coefficients divided by solidity, I really believe that that notation can imply that the data is good for rotors of any solidity. This is most certainly not true for power. An exception might be made for a rotor thrust coefficient in some cases, but it still is a very questionable practice in my opinion.

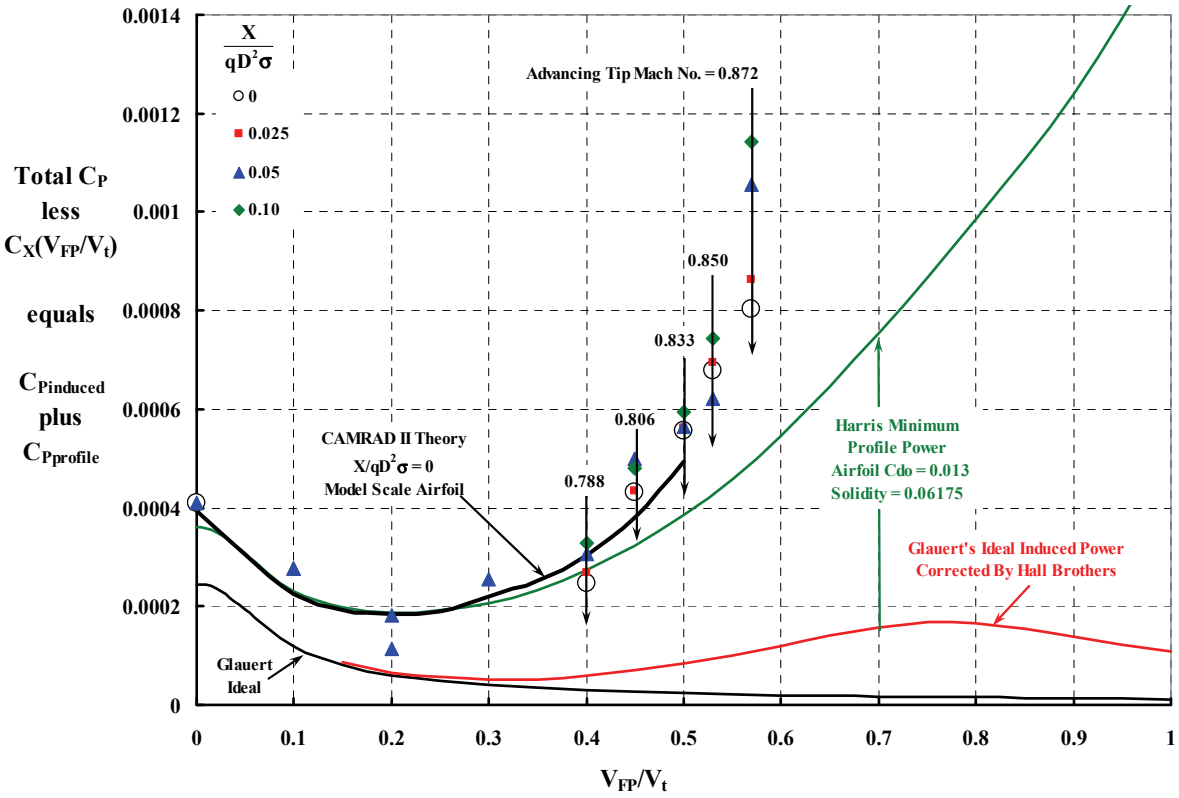

Fig. 2-30. The conventional helicopter rotor has a very big minimum profile power problem plus a serious ideal induced power problem above forward-speed-to-tip-speed ratios of 0.4 to 0.5. Data for a lift-coefficient-to-solidity ratio of 0.08 with original blades [97].

You can see from Fig. 2-30 that my ideal rotor, defined by Eq. (2.21) and using a solidity of 0.06175 and an average blade airfoil drag coefficient of 0.013, captures the power required problem of this conventional model rotor reasonably well up to a flight-speed-to-tip-speed ratio of 0.4. Beyond that, all types of nonlinear airfoil and rotor characteristics creep into the problem. Understanding and building prediction tools to reflect the differences between the ideal theory and actual test results has occupied rotor aerodynamic careers (mine included) for decades. Fortunately, progress has been made. Fig. 2-30 includes just one example, described below.

To illustrate an example of modern prediction capability, I prevailed on Hyeonsoo Yeo (a leader at AFDD at Ames Research Center) in January of 2013 to make a calculation using Wayne Johnson's CAMRAD II analysis [103]. This analysis includes most of the airfoil and rotor nonlinearities such as Mach number, unsteady aero, free wake, blade elastic deformations, etc. Furthermore, Dr. Yeo had available airfoil data at model scale [101], which is a big step forward in accounting for Reynolds number. The calculation was made for the McHugh CH-47B model rotor "flying" at sea level standard day with a tip speed of 620 feet per second. The rotor had a solidity of 0.06175 and was trimmed to a lift-coefficient-to-solidity ratio of 0.08 and zero usable propulsive force, which is to say $C_T'/\sigma = 0.08$ and $X/qD^2\sigma = 0$.

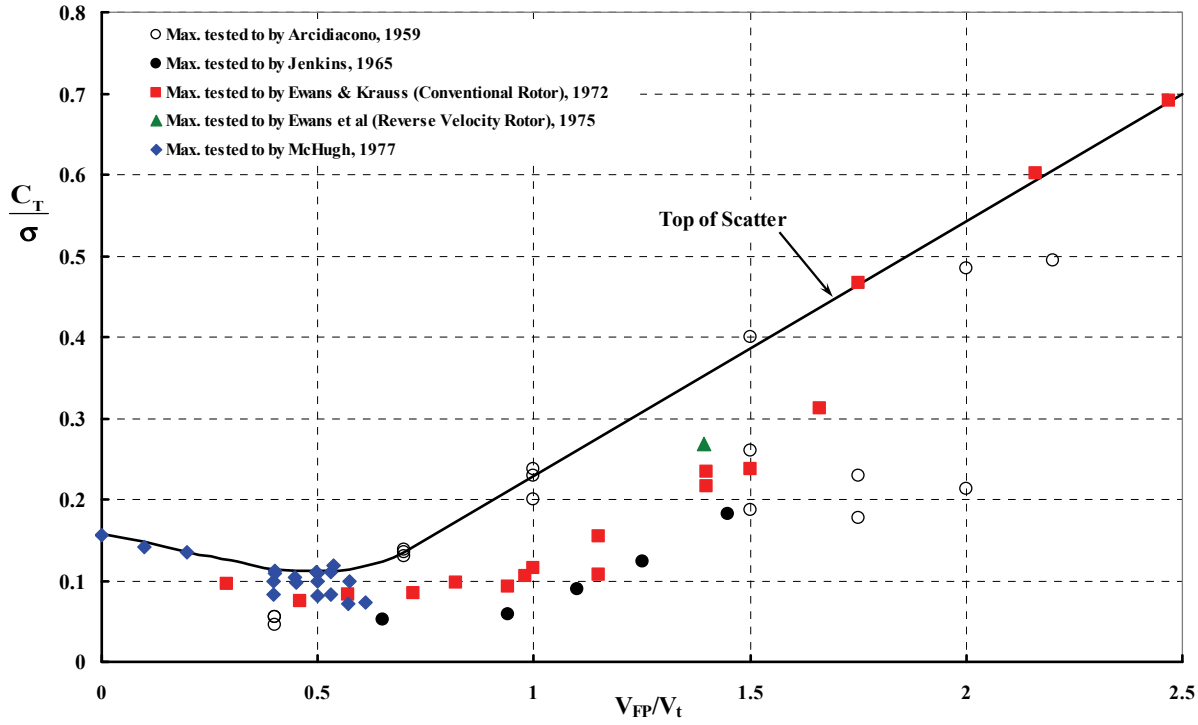

Fig. 2-31. The 8-foot-diameter RVR in conventional mode began to experimentally confirm very high lift at high advance ratios [75].

It is important to remember that the conventional helicopter rotor has a significant lifting capability that is not so obviously limited, which is in contrast to its fundamentally limited propulsive-force capability. You can appreciate this fact from Fig. 2-31, where I have complied the small amount of experimental data that is available.

2.7 THE EDGEWISE FLYING ROTOR'S LIFT-TO-DRAG-RATIO PROBLEMS

These examples of rotor configuration technology raise two very interesting questions. First, just what is the ratio of maximum lift to effective drag for an edgewise flying rotor and second, at what lift does the maximum L/D_E occur? To begin to answer these questions requires that you first understand, appreciate, and correctly use the rotary wing effective drag parameter, D_E. The place to start to understand this rotary wing parameter is with the minimum airplane, which consists of a wing and a propeller.

You no doubt have encountered the classical, fixed-wing parameter called the lift-to-drag ratio, which is classically written simply as L/D. You were reminded about the aerodynamic lift and drag properties of a fixed wing in Fig. 1-3 and Fig. 1-4, which led to the wing's L/D as arrived at in Fig. 1-4. I would also remind you that it takes a fixed wing *and* a propeller (plus an engine) to equal the edgewise flying rotor (plus an engine). This is because, as used by a helicopter, a rotary wing combines both lifting and propelling functions in one device—a rotor. The only comparable human-designed machine—that I know of—that combines both lift and propelling requirements in one is the ornithopter. I might add that the

only successful ornithopter I have seen demonstrated and reported on [104] was at the American Helicopter Society Future Vertical Lift Aircraft Design Conference in January 2012. This radio-controlled electric-motor-powered replica of a hummingbird, Fig. 2-32, took off and landed in the palm of Matt Keennon's hand. He had it flying all around the conference room, which was filled with some 100 seated rotorcraft engineers. It was an absolutely fantastic flight demonstration. The 19-gram-gross-weight, 16.5-centimeter-wingspan configuration had a maximum thrust-to-shaft-power ratio of about 8.9 grams per watt in hover, which is 14.6 pounds per horsepower. The maximum demonstrated speed was about 12 meters per second with a power required of 1.9 watts from the motor output shaft, but the cruise speed was more like 6.7 meters per second, which is approximately 15 miles per hour. The endurance, as quoted in the paper, was 4 minutes.

For the discussion here, I would say a flying wing such as Jack Northrop's XB-35 (Fig. 2-33) is a more comparable aircraft from which to understand the edgewise flying rotor because you have the minimum basic airplane ingredients—a wing and propeller(s). The trim in steady, level flight of the wing with a propeller requires that wing lift (L) equals aircraft weight (W) and that wing drag (D_W) be balanced by propeller thrust (T_P). The basic performance equation was describe in Eq. (1.7) and is repeated here as

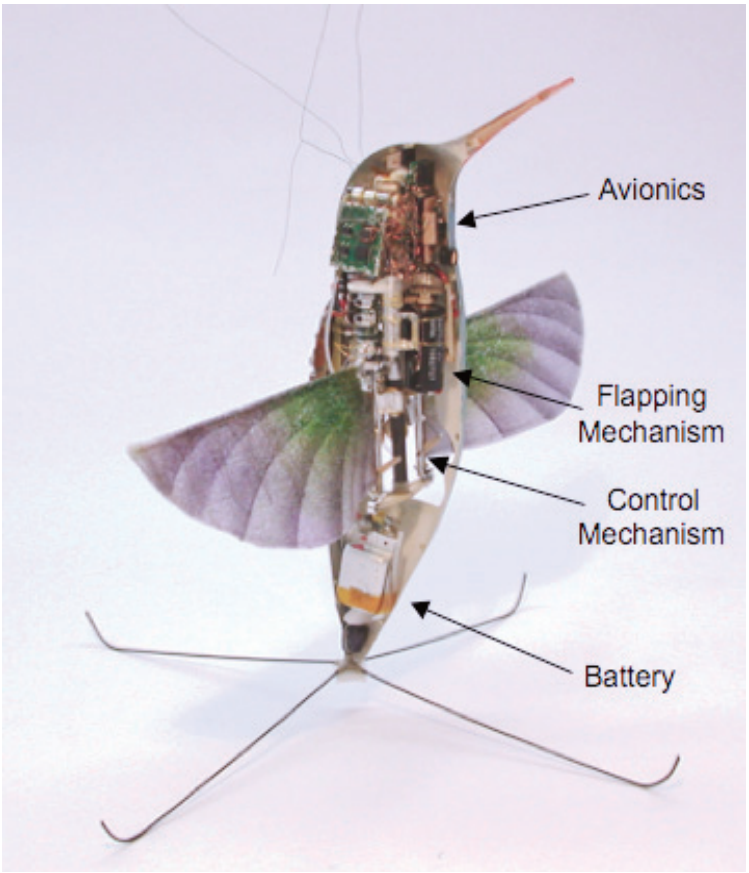

Fig. 2-32. I saw the final Nano Hummingbird prototype, created by AeroVironment, Inc., [104] flown all around a large conference room in January 2012. It was fantastic.

Fig. 2-33. Jack Northrop's XB-35 had a wingspan of 172 feet and a wing area of 4,000 square feet, which is an aspect ratio of 7.4. Four Pratt & Whitney R-4360 engines provided a total of 12,000 horsepower. The propellers were 15 feet, 1 inch in diameter and gave the 206,000-pound-gross-weight aircraft a maximum speed of about 340 knots (391 mph).

$$T_P = D_{wing} = qS_W C_{Do} + \frac{1}{\pi q}\left(\frac{W}{b}\right)^2 . \tag{2.24}$$

In explaining the equivalent drag (D_E) for an edgewise flying rotor it is very helpful to deal in power units of foot-pounds per second. (The rotorcraft engineer uses the E in D_E to define the rotor equivalent to a wing *and* a propeller because a rotor can perform both functions.) So, let me multiply Eq. (2.24) through by flightpath velocity (V_{FP}), which yields

$$T_P V_{FP} = D_{wing} V_{FP} = \underset{\substack{\uparrow \\ \text{Profile Power}}}{qS_W C_{Do} V_{FP}} + \underset{\substack{\uparrow \\ \text{Ideal Induced Power}}}{\frac{1}{\pi q}\left(\frac{W}{b}\right)^2 V_{FP}} \tag{2.25}$$

and then designate profile power and induced power as shown in Eq. (2.25). This step quantifies the wing and propeller power required performance *if* the propeller is 100 percent efficient (i.e., $\eta_P = 1$) because the engine power required is calculated as

$$\text{Engine SHP}_{req'd} = \frac{T_P V_{FP}}{550\eta_P} . \tag{2.26}$$

Of course, if the engine is turned off, the flying wing will have to glide with some rate of descent (R/D) following the glide slope (γ) that you see sketched here. In this circumstance, energy per unit time associated with propeller thrust times flightpath velocity is replaced by a vertical velocity (V_Z) times weight (W).

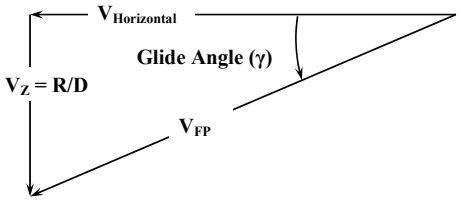

For an edgewise flying rotor and a flying wing to be comparable, you must (I think) include the propeller efficiency and, therefore, the wing's classical L/D must be contaminated with propeller efficiency. I suggest that the contaminated wing and propeller lift-to-drag ratio use an equivalent drag denoted as D_E and that this equivalent drag be derived from the total energy per unit time to overcome drag. On this basis, you have

$$(2.27)\quad \text{Fixed Wing } D_E = \frac{550\left(\text{Engine SHP}_{\text{req'd}}\right)}{V_{FP}} = \frac{T_P V_{FP}}{\eta_P V_{FP}} = \frac{qS_W C_{Do} + \frac{1}{\pi q}\left(\frac{W}{b}\right)^2}{\eta_P}.$$

Now consider the edgewise flying rotor. This flying "rotary" wing can both propel and lift so "propeller" efficiency is *embedded* in its energy per unit time (i.e., its power required) theory. Classically, the power required of the edgewise flying rotor is written as

$$(2.28)\quad P_{\text{req'd}} = \left(P_{\text{induced}} + P_{\text{profile}}\right)_{\text{rotary wing}} + V_{FP} D_{\text{everything else}}.$$

The induced power ($P_{induced}$) and profile power ($P_{profile}$) terms occupy the same character as those for my flying wing example in Eq. (2.25). The wrinkle is that the engine must supply power to the rotor for the usable propulsive force (X) required to overcome the drag of everything else. This additional power is calculated as ($V_{FP}X = V_{FP}D_{everything\ else}$), which is an ideal value. And if, in providing propulsion, the induced and profile power of the edgewise flying rotor are increased, a helicopter chief engineer might simply say, "So be it. Charge it off to some sort of propulsive efficiency and let's get on with installing a slightly bigger engine."

Fortunately, there is one approach that the aerodynamicist can take in making an edgewise flying rotary wing comparable to a fixed wing plus propeller. The approach to getting the equivalent drag of a rotary wing is to simply subtract the ideal power for propulsion from the total power required, and then divide by the flightpath velocity. That is

$$(2.29)\quad \text{Rotary Wing } D_E = \frac{P_{\text{req'd}} - V_{FP} D_{\text{everything else}}}{V_{FP}} = \frac{\left(P_{\text{induced}} + P_{\text{profile}}\right)_{\text{rotary wing}}}{V_{FP}}.$$

You will see, over and over again in isolated rotor tests conducted in wind tunnels, that D_E is obtained from test data by measuring the rotor shaft torque (Q_{shaft} in foot-pounds) with strain gauges and then multiplying shaft torque by the rotor speed (Ω in radians per second) to obtain power required ($P_{req'd}$). During a wind tunnel test, a balance measures the

wind axis lift force (L) and propulsive force (X), so it is a simple matter to obtain the power required for propulsion because the propulsive force equals the drag of everything else. The "standard" practice has been to say that

$$(2.30)\quad D_E = \left[\frac{P_{req'd} - V_{FP}X}{V_{FP}}\right]_{\text{From Test}} .$$

Because today most rotary wing theories are quite capable of calculating both induced and profile powers individually, computer output data shows the effective drag as

$$(2.31)\quad D_E = \left[\frac{\left(P_{induced} + P_{profile}\right)_{\text{rotary wing}}}{V_{FP}}\right]_{\text{From Theory}}$$

Note: Must have a propulsive force associated with it.

Having absorbed the preceding essentials, you are now in a position to consider two edgewise flying rotor cases of particular interest—at least as I see them. Suppose that the rotary wing is used on a helicopter where the parasite drag is zero. That is, X equals zero, and the rotor is just overcoming its own drag. Then power required equals the sum of induced and profile power, and all shaft torque (Q_{shaft}) times rotor speed (Ω), whether measured or calculated, equals $D_E V_{FP}$. Now consider a second case where the edgewise flying rotor is flying with zero shaft torque, in which case you have

$$(2.32)\quad P_{req'd} = Q_{shaft}\Omega = 0 = \left(P_{induced} + P_{profile}\right)_{\text{rotary wing}} + V_{FP}X ,$$

from which it follows that

$$(2.33)\quad -X = D_E = \frac{\left(P_{induced} + P_{profile}\right)_{\text{rotary wing}}}{V_{FP}} .$$

It also follows that X becomes drag (measured by a wind tunnel balance directly), and you can safely state that $D_E = -X$ when $Q = 0$. Keep in mind that the propulsive force of the rotor is negative in this case, so the effective drag is always positive. In this Q_{shaft} equals zero case, the edgewise rotor acts just like a fixed wing, and only three ways exist for equilibrium flight. The rotor must (1) be held tightly by the wind tunnel balance (which requires no energy), or (2) the rotor must be in gliding flight (which is what a helicopter is in autorotation after an engine failure), or (3) the rotor must be towed or pushed along by a propeller or some other auxiliary propulsion device.

The only remaining question arises when the edgewise rotor is flying between the cases of zero shaft torque (i.e., $Q_{shaft} = 0$) and zero useable propulsive force (i.e., $X = 0$). To understand this gray area, you only need to turn to Eq. (2.28) and write a total-energy-per-unit-time equation for the equilibrium state as

$$(2.34)\quad P_{req'd} = Q_{shaft}\Omega = \left(P_{induced} + P_{profile}\right)_{\text{rotary wing}} + V_{FP}X - T_P V_{FP} - V_Z W .$$

Now you see that any energy-per-unit-time shortfall that occurs because of insufficient propeller thrust (T_P) or a lack of a descent velocity (V_Z) will create a need for rotor shaft torque (Q_{shaft}).

Finally, consider an edgewise "flying" rotor being towed along by a propeller in steady, level flight. In this case Eq. (2.34) can be solved for the propeller thrust required to have energy balance, and you have

$$(2.35)\quad T_P = \frac{\left(P_{induced} + P_{profile}\right)_{rotary\ wing} + V_{FP}X - Q_{shaft}\Omega}{V_{FP}}.$$

Equation (2.35) takes you into the world of compound helicopters, and you will find this configuration discussed more fully in Appendix D.

Now let me complete the discussion of rotor L/D_E by showing you *my ideal* equation for this performance parameter, which, in rotor coefficient form using Eq. (2.22) as the basis, is

$$(2.36)\quad \text{Ideal}\ \frac{L}{D_E} = \frac{C_L\left(V_{FP}/V_t\right)}{C_{P-req'd} - C_X\left(V_{FP}/V_t\right)} = \frac{C_L\left(V_{FP}/V_t\right)}{K_{Hall}\dfrac{\left(C_L\right)^2}{2\left(V_{FP}/V_t\right)} + \dfrac{\sigma C_{do}}{8}P_{(\mu,\lambda)}} \quad \text{for}\ \frac{V_{FP}}{V_t} > 0.15,\ \alpha_{tpp} < \pm 5\,\text{deg}.$$

Note that while I have restricted my ideal L/D_E equation to ratios of flightpath speed to tip speed above 0.15, and tip-path-plane angle of attack to less than 5 degrees, it is of considerable value for both helicopters and compound helicopters.

The ratio of lift to effective drag is, of course, the parameter to maximize, so with a little mathematics you have two very simple relationships:

$$(2.37)\quad \left(\frac{L}{D_E}\right)_{max} = \frac{2\left(V_{FP}/V_t\right)^{3/2}}{\sqrt{K_{Hall}\sigma C_{do}P_{(\mu,\lambda)}}} \quad \text{at} \quad C_L = \frac{1}{2}\sqrt{\frac{\sigma C_{do}P_{(\mu,\lambda)}\left(V_{FP}/V_t\right)}{K_{Hall}}}.$$

It only remains to make an educated guess about some rotor parameters to create the ideal performance capability of an edgewise flying rotor for any V_{FP}/V_t. Suppose for an example of ideal theory versus actual experimental results, you choose the Sikorsky S-76 main rotor as representative of an edgewise flying rotor. A main rotor from this commercially successful helicopter has been tested in the full-scale 40- by 80-foot wind tunnel at NASA Ames Research Center. The production blade uses a "swept-tapered tip," and this is one of four tip geometries tested at full scale. You will find the experimental results reported in reference [105]. The S-76 has a four-bladed, 44-foot-diameter rotor. Its solidity (σ) is 0.07476, and it normally has a tip speed of 675 feet per second. You see the ideal-theory-versus-test comparison in Fig. 2-34.

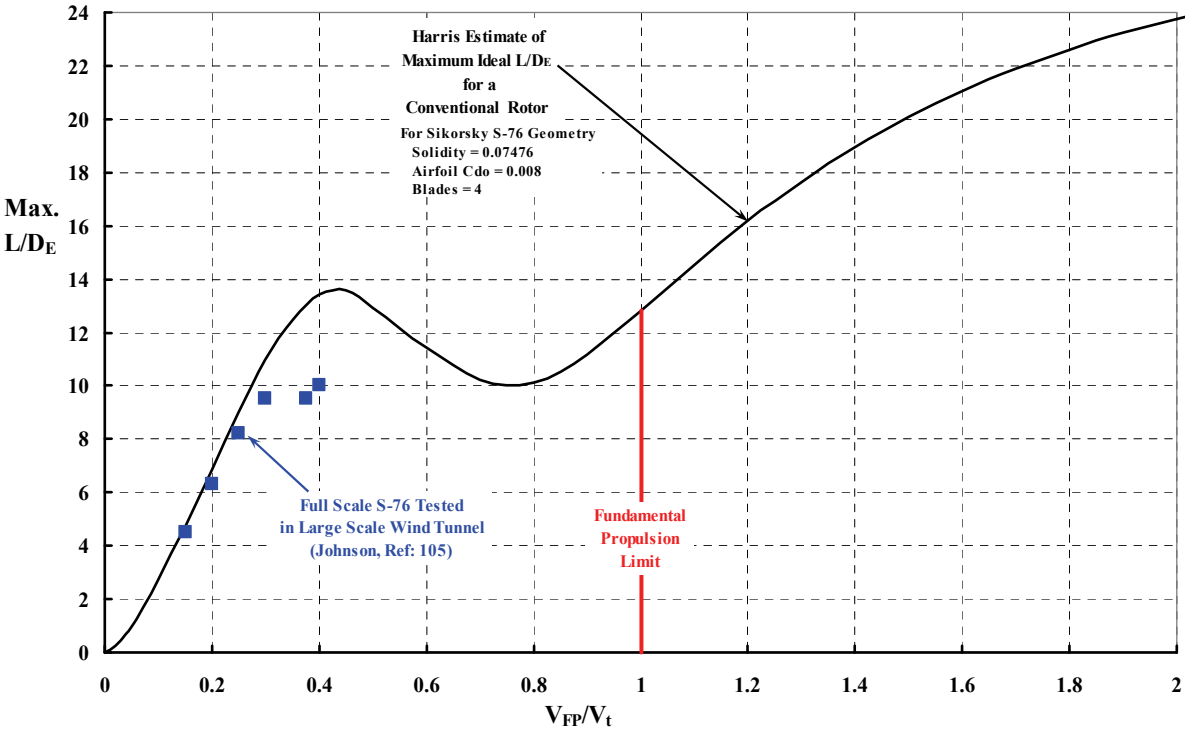

Fig. 2-34. Harris' view of the ideal performance capability of the conventional edgewise flying rotor expressed in L/D_E form.

As with most full-scale helicopter rotor tests in large wind tunnels, experimental data, such as those shown in Fig. 2-34 for the propelling rotor, are rarely acquired in the V_{FP}/V_t region beyond 0.4 or 0.5, on up to 1.0. Also, you will recall that a fundamental propulsive force limit, shown as the vertical red line on Fig. 2-34, was postulated with Eq. (2.7) on page 43.

What immediately jumps out at me in Fig. 2-34 is that my ideal theory shows that the conventional rotor reaches its first maximum L/D_E right around a V_{FP}/V_t of 0.4. Higher than that speed ratio, the ideal theory says that conventional rotors as used on helicopters can expect a substantial loss in performance. The maximum ideal L/D_E is not obtained again until the speed ratio is greater than 1.0. Beyond V_{FP}/V_t of 1.0, the rotor begins to approach a slowed and nearly stopped rotating condition, which you might think of as some sort of wing—depending on what azimuth position the stopped blades ultimately take.[23]

The behavior of maximum ideal L/D_E with speed ratio seems to naturally divide the edgewise flying rotor into two distinct regions. The first region is from $V_{FP}/V_t = 0$ up to 1.0 where the rotor finds it increasingly difficult, or even impossible, to overcome its own drag. The second region is from $V_{FP}/V_t = 1.0$ on up to where the rotor rotational speed approaches zero. These are the two regions I will discuss next.

[23] You will find data from a rotor starting and stopping experiment in reference [106].

2.7.1 The Rotor's L/D_E Problem in Overcoming Its Own Drag

Fig. 2-34 suggests a considerable lack of experimental data in the low-speed-ratio region (i.e., $V_{FP}/V_t = 0.2$ to 1.0) where the helicopter rotor is expected to propel the machine. To allay your concern about a lack of data, let me show you a reasonable amount of experimental data that demonstrates how the maximum L/D_E of the edgewise flying rotor decreases as the fundamental propulsive force limit is approached. I turned to Wayne Johnson and asked him to make computations with his CAMRAD II theory in the low-speed-ratio region below a V_{FP}/V_t of 1.0. His computations shed light on the ability of the conventional rotor to propel at a V_{FP}/V_t beyond 0.5. The specific question raised required calculating the maximum L/D_E of an S-76 rotor with the useable propulsive force (X) equal to zero. The only conditions set were that (1) the computations be made assuming no influence of compressibility, (2) known incompressible airfoil properties reflecting stall be used [i.e., $C_{do} = f(\alpha_{BE})$], and (3) full nonuniform induced velocity created by the rotor's free wake structure be included. The results of this homework are included here as Fig. 2-35.

It is immediately clear from Fig. 2-35 that today's edgewise flying rotors struggle to propel themselves—much less provide a force to overcome the drag of the rest of the helicopter—when the speed ratio exceeds 0.45. Certainly, the maximum L/D_E drops to impractically low values beyond a speed ratio of 0.5. Because rotor-shaft power required can be quickly estimated from $P_{req'd} = \frac{W}{L/D_E} V_{FP} + XV_{FP}$, you can immediately appreciate what a

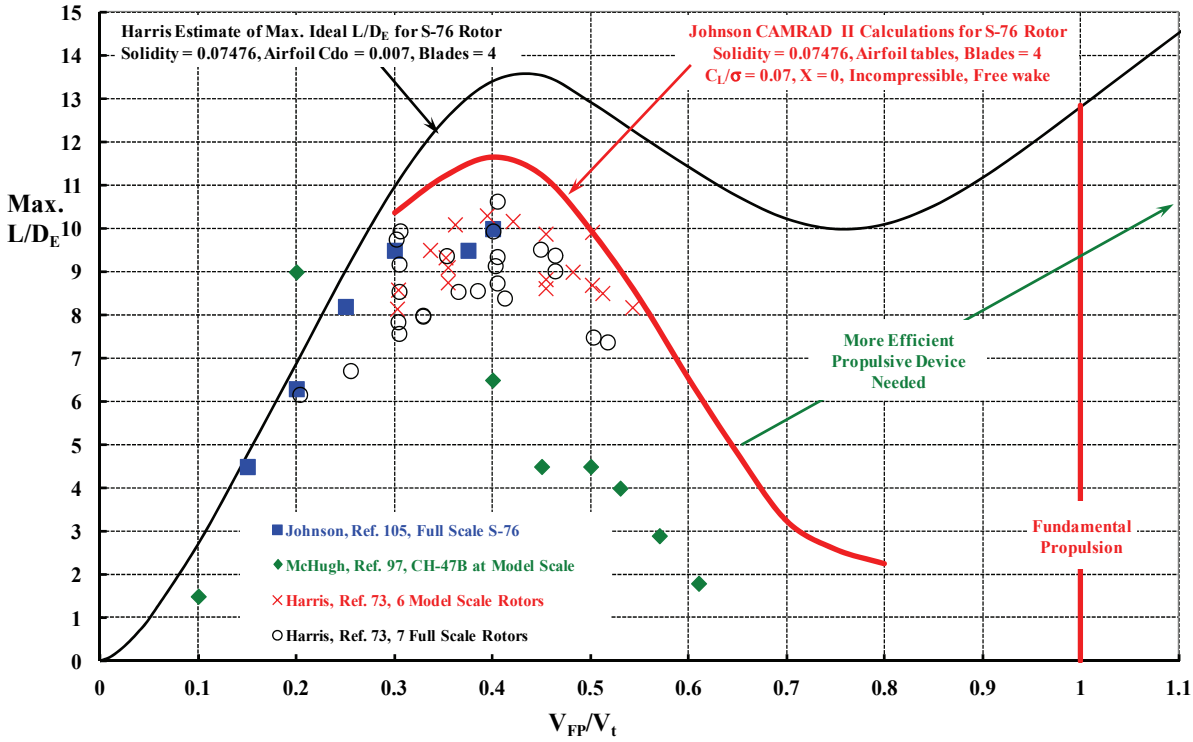

Fig. 2-35. The conventional helicopter rotor has a poor L/D_E above a V_{FP}/V_t of 0.5 when asked to overcome its own drag.

drop in maximum L/D_E from 10 to 12, down to values like 5 to 6, means in helicopter design. In my experience, getting the conventional rotor to even overcome its own drag meant installing three engines instead of two. Such skyrocketing levels of power required, implied by Fig. 2-35 and made just as clear with Fig. 2-30 as you saw earlier, have stymied the rotorcraft industry for decades.

The reason the accumulated experimental data diverges from ideal theory as the speed ratio increases beyond a value of, say, 0.45 is simply that the edgewise flying rotor is a reasonably adequate lifting device (particularly in hover) but a lousy—there is no other word for it—propeller.[24]

Such a strong feeling about the edgewise flying rotor deserves some technical explanation as to what the cause of its propeller *inefficiency* is. The cause does not lie with just excessive profile power alone as has been the view of many for several decades. This group has determined that having to use real airfoils (distributed along the rotor blade in some fashion, and all having unfavorable stall and compressibility aerodynamic properties) is a severe constraint to obtaining advanced helicopter high-speed performance. This point of view was built on the assumption that Glauert's theory for induced power was close enough.

In fact, Glauert's theory has been steering us wrong in charging virtually all of the adverse L/D_E trend to profile power. The inclusion of a correct theory (based on "free wake" behavior) for the calculation of induced power has shown that it is a very large player in the adverse L/D_E trend when advanced theories such as CAMRAD II are used (Fig. 2-35). Let me illustrate this point using the correction to Glauert's induced power theory with the constant I referred to earlier as K_{Hall} (Fig. 2-27) compared to a constant that I will call K_{CAMRAD}. Keep in mind that $K_{Glauert}$ is 1.0. Johnson conveniently provides an output data line in CAMRAD II labeled "kappa_ind = P_{ind}/P_m," which is the ratio of induced power calculated with a free wake to induced power calculated by Glauert's momentum theory. I chose here to relabel Wayne's information as K_{CAMRAD}. You can see from Fig. 2-36 that even the ideal-induced-power correction factor (K_{Hall}) for four blades leads to a rotary wing with very poor performance when compared to a fixed wing (i.e., $K_{Glauert} = 1$). The message is quite clear: the ideal rotor-induced power stated by Glauert may be small at high-speed ratios, but when you start increasing its value by 10 to 30, conventional rotor-induced power is not something you can ignore in your power required or L/D_E calculations—at least at "high speed."

Now consider the profile power contribution to the ideal rotor maximum L/D_E. I chose an airfoil drag coefficient of C_{do} equal to 0.007 for the estimate of this ideal case. This is an average drag coefficient of all blade elements of all blades. The CAMRAD II calculation does not use an average airfoil drag coefficient, so the result you see in Fig. 2-37 is a direct comparison of profile power coefficients divided by solidity. It is, of course, quite easy to create an average airfoil coefficient from the CAMRAD II calculation by saying

[24] This statement *does not* apply when a rotor is operated in axial flight like a true propeller, as you will learn later.

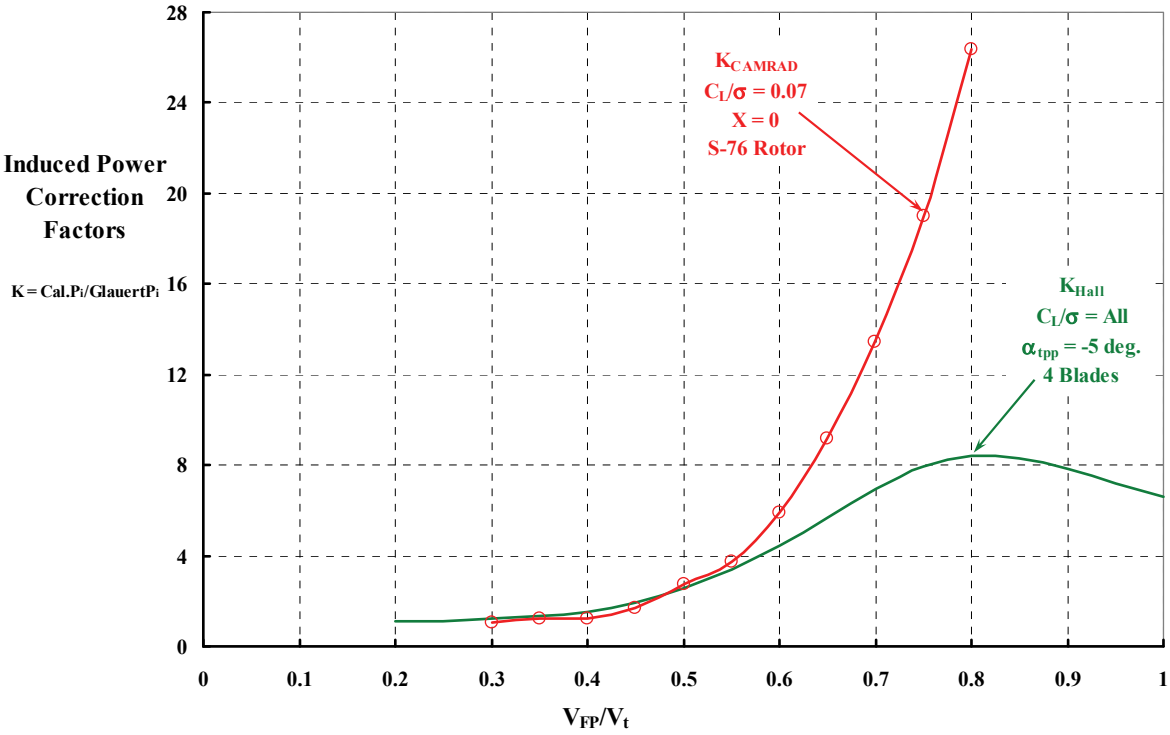

Fig. 2-36. The induced power of a conventional rotor can be many times that predicted by Glauert's theory.

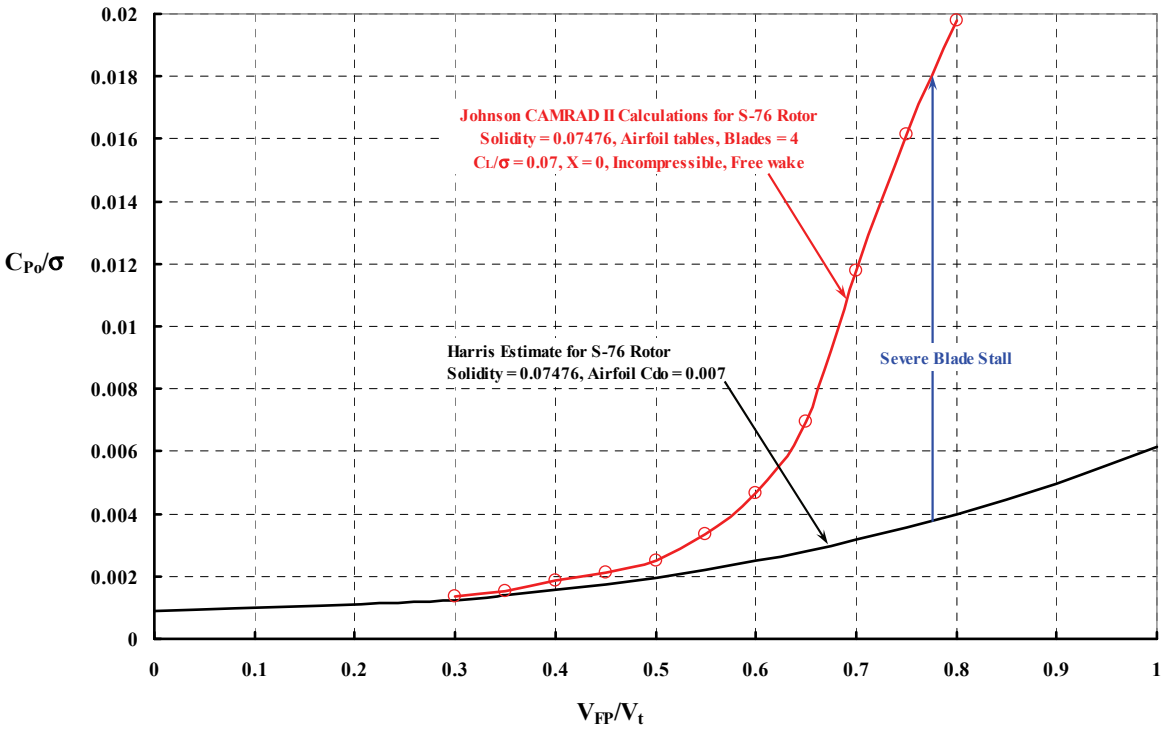

Fig. 2-37. Severe blade stall is encountered when the conventional rotor tries to overcome its own drag at speed ratios beyond 0.5.

$$(2.38)\quad \text{Average } C_{do} = \frac{8\left(C_{Po}/\sigma\right)_{CAMRAD}}{P_{(\mu,\lambda)}}.$$

This average C_{do} based on CAMRAD II output is very useful in apportioning the induced and profile contributions to the adverse maximum L/D_E trend. Let me illustrate this point.

Suppose you start with the ideal case and substitute K_{CAMRAD} for K_{HALL} in Eq. (2.37), but keep the average C_{do} at 0.007. That is,

$$(2.39)\quad \left(\frac{L}{D_E}\right)_{max} = \frac{2\left(V_{FP}/V_t\right)^{3/2}}{\sqrt{K_{CAMRAD}\sigma\left(C_{do}=0.007\right)P_{(\mu,\lambda)}}}.$$

For the next step, change my chosen C_{do} of 0.007 to CAMRAD's average C_{do} according to Eq. (2.38). Now you are in a position to display the steps as they appear in Fig. 2-38. Apportioning induced and profile powers as shown in Fig. 2-38 is, of course, somewhat dependent on the order the input changes are made. However, I think the basic point is clear: The conventional edgewise flying rotor can overcome its own drag at speed ratios (V_{FP}/V_t) above 0.5 and even up to a speed ratio of 0.8. However, its propulsive efficiency is so poor, and maximum L/D_E becomes so low, that a practical, pure helicopter—in my mind—ceases to exist if the design objective requires a speed ratio beyond 0.5. Aerodynamically speaking, this becomes a serious misuse of installed power.

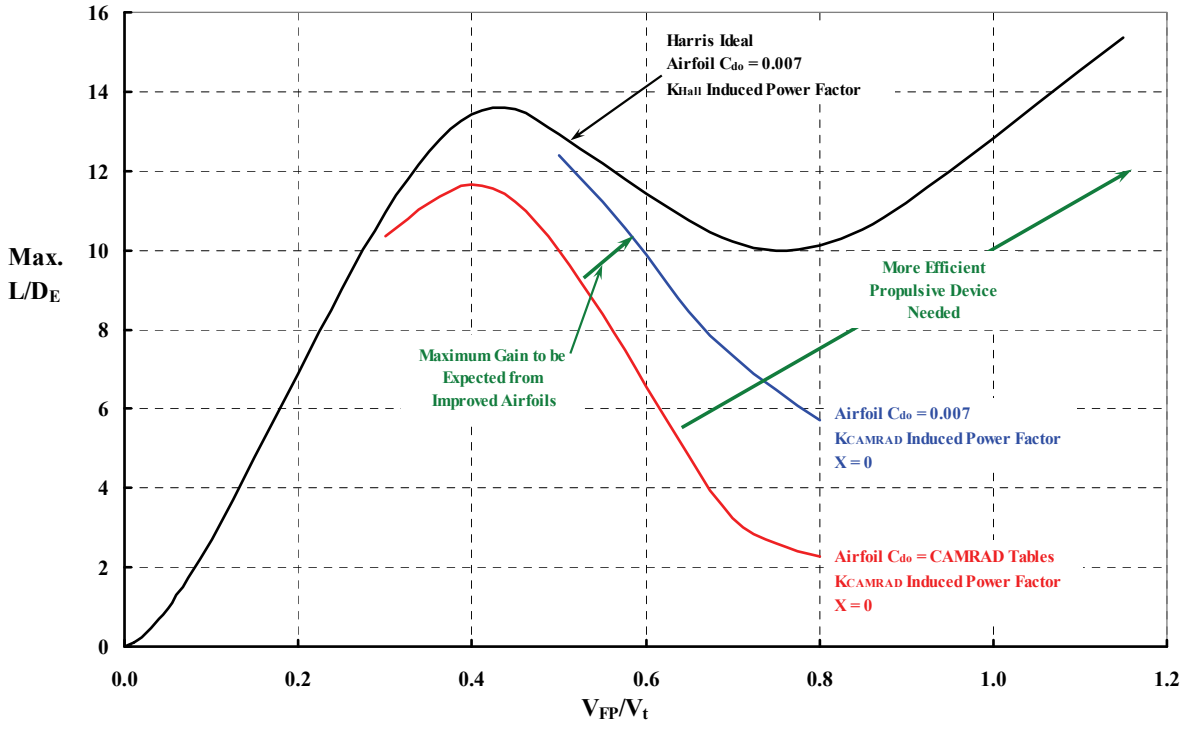

Fig. 2-38. The edgewise flying rotor has very poor performance if asked to propel at speed ratios (V_{FP}/V_t) above 0.5.

2.7.2 The Rotor's L/D_E Capability in Autorotation

The practical usefulness of the edgewise flying rotor as a combined wing and propeller is over at speed ratios (V_{FP}/V_t) above 0.5. However, this does not mean that the rotor's usefulness as a rotating wing is over. There is sufficient experimental data to suggest that, given some other, more efficient propulsive device to tow it along, the rotor can provide more than enough lift for many machines. You saw this fact emerging in Fig. 2-14. The only sticking point deals with the lifting rotor's performance as measured, say, with maximum L/D_E. This raises the question of rotor performance at or near autorotation where the shaft torque is zero and the effective drag (D_E) is calculated as

$$-X = D_E = \frac{\left(P_{induced} + P_{profile}\right)_{rotary\ wing}}{V_{FP}}, \tag{2.40}$$

and the ideal, maximum L/D_E is, to repeat, given by

$$\left(\frac{L}{D_E}\right)_{max} = \frac{2\left(V_{FP}/V_t\right)^{3/2}}{\sqrt{K_{Hall}\sigma C_{do} P_{(\mu,\lambda)}}} \quad \text{at} \quad C_L = \frac{1}{2}\sqrt{\frac{\sigma C_{do} P_{(\mu,\lambda)}\left(V_{FP}/V_t\right)}{K_{Hall}}}. \tag{2.41}$$

(Do not forget that the efficiency of the propulsive device is not included here, so the total system power required is not yet apparent.) As you can appreciate, the following discussion might well have been included in *Volume I: Overview and Autogryos*, because the principles you have just read about are directly aimed at reinventing the autogyro—in some form.

You will recall from Volume I that John Wheatley tested a full-scale PCA-2 rotor in the NACA Langley 30- by 60-foot wind tunnel in 1934. His report [107] provided the early rotorcraft industry with an experimental performance rock on which to base the autogyro's capability. Questions about the performance of the edgewise flying rotor in autorotation were not seriously raised again until the late 1940s. It was Kurt Hohenemser, then working on developing the XV-1 (Fig. 2-6) at the McDonnell Aircraft Corporation in St. Louis, Missouri, who began the modern investigations. His first experiments were conducted with a 7.58-foot-diameter, two-bladed rotor having a solidity of 0.087. The "seesaw" (i.e., teetering hub) model rotor was tested in the University of Washington wind tunnel in two phases. The first phase, an exploratory phase to see the lay of the land, happened in July 1949. After some key modifications to the rotor hub and control system were made, a second wind tunnel phase was conducted in October 1949. The experiments were funded by the Office of Naval Research, and the final report [89] was classified confidential when it was published January 22, 1951.[25] The rather short introduction contained in this historically significant report, authored by Bob Head and Kurt Hohenemser, is worth reading in its entirety.

[25] I knew this report existed because of conversations with Bob Head during the preparation of reference [108] and because Ray Prouty told me he helped perform two later tests as a graduate student at the University of Washington in Seattle. Finding a copy of the report was not so easy. Finally, I called Dave Peters, a student at Washington University in St. Louis and later an officemate of Kurt's after Kurt left McDonnell. Dave used his pipeline into the McDonnell (now Boeing) library and, with the wonderful help of Mary Marr and Brittany Mudd, got a copy of this report out into the open—and street legal (see DTIC 0109764).

"2.0 INTRODUCTION

Early in 1949 a contract was entered into by the Office of Naval Research and McDonnell Aircraft Corporation for research into the problem of the rotor-fixed wing aircraft configuration. It was held that in order to accomplish high level flight speeds of the order of 300 to 400 miles per hour, it would be necessary to have the rotor operate at tip-speed ratios very much higher than are conventionally used in helicopters and autogyros.

Consequently, the test program reported herewith was undertaken. The rotor model used was a two-bladed, see-saw type of rotor which was built from a salvaged rotor of the XH-20, 'Little Henry,' helicopter. The diameter of [this] rotor was reduced and a special hub mounting was devised for mounting the rotor in the twelve foot UWAL wind tunnel at the University of Washington, Seattle, Washington. The prototype rotor was postulated as a pressure-jet type of rotor having burners at the blade tips. To simulate the drag of such tip-burners, small spheres of various sizes were attached to the tips of the model blades.

The first series of tests with this rotor during July 1949 clearly demonstrated the possibility of using a rotor at very high advance ratios where the efficiency of the rotor is considerably improved over the low advance ratio operation. However, it also became clear that the rotor was quite sensitive to small changes in rotor attitude.[26]

After this first series of tests, this model was modified to eliminate most of the drag of the blade hub fittings which proved objectionable in the previous tests. This entailed reducing the diameter of the rotor slightly and constructing a lens-shaped fairing for the rotor hub. Further, a device was designed for automatic control of the rotor attitude which was to govern the speed of the rotor.

The second series of tests was then conducted in the UWAL wind tunnel during October 1949. These tests covered the high range of tip-speed ratios ($\mu = 0.5$ to $\mu = 2.5$) and a large range of blade pitch angles ($\theta = -4.5^o$ up to $\theta = +3.0^o$) for autorotation and for both accelerating and decelerating torques applied to the rotor. The aerodynamic characteristics of the rotor as determined by test were in reasonable agreement with the characteristics as determined theoretically in Reference 1 [Head, R.E. MAC Report No. 1686].

The governor, while capable of stabilizing the rotor for small attitude changes, would require major modifications in order to correct larger attitude changes."

Kurt Hohenemser and Bob Head's tests in 1949 provide the first data on which really high advance ratio performance of an edgewise flying rotor can be based. You see this data, along with John Wheatley's rotor-alone data, in Fig. 2-39.

Chronologically, I would suggest that Larry Jenkins' experiment was the next key step. Data from Larry's 1965 report [83] is shown with the blue squares on Fig. 2-39. Data from other tests obtained in the 1960s, as identified by Table 2-1 and compiled in references [73, 109, 110], are shown with the light gray symbols on Fig. 2-39.

The next high-advance-ratio data was obtained by Ewan [75] as part of the Reverse Velocity Rotor (RVR) conceptual studies in the 1970s.

[26] Kurt ultimately found a much better "rotor attitude control," which turned out to be a delta-three angle of 62.2 degrees (i.e., pitch down 2.2 degrees for 1-degree flap up). You can read about both the theory behind his concept, and the aircraft (the XV-1) on which he successfully applied the theory, in reference [108].

Another contribution of experimental data dealing with the autorotating rotor came in 2010 [111]. These results are shown with black circles in Fig. 2-39. Todd Quackenbush, a leader at Continuum Dynamics, Inc. located in Princeton, New Jersey, got some cohorts (Dan Wachspress and Bob McKillip, to name a few) together and, with a contract from NASA Ames Research Center, tested a 52-inch-diameter, three-bladed "seesaw" rotor in the Glenn L. Martin wind tunnel at the University of Maryland. There are so many similarities between Todd's 2008–2010 test experiences and Kurt Hohenemser's test experiences in 1949 that it is absolutely fascinating. Both ran into, and needed to solve, the problem of excessive rotor sensitivity to shaft angle of attack. Both encountered worrisome blade flapping behavior. Both had to deal with significant hub drag, which made getting an accurate measurement of blades-alone drag difficult. Both had some difficulty in controlling rotor speed. The list of similarities is just uncanny. One suggestion I might make is that using Kurt's unusually large amount of delta-three (δ-3), which is feathering coupled to flapping as discussed in Volume I, is an extremely satisfactory way to remedy a number of problems that come up in the "very high advance ratio" region.

You will see in Fig. 2-39 that the available data for maximum L/D_E seems to collect along straight lines for each rotor data set. That is my interpretation, and I have chosen to emanate the lines from John Wheatley's 1934 isolated PCA-2 rotor test. You might immediately say that there seems to be a varying degree of scatter in the data. I would agree and further note that I cannot readily explain the differences between the five examples you

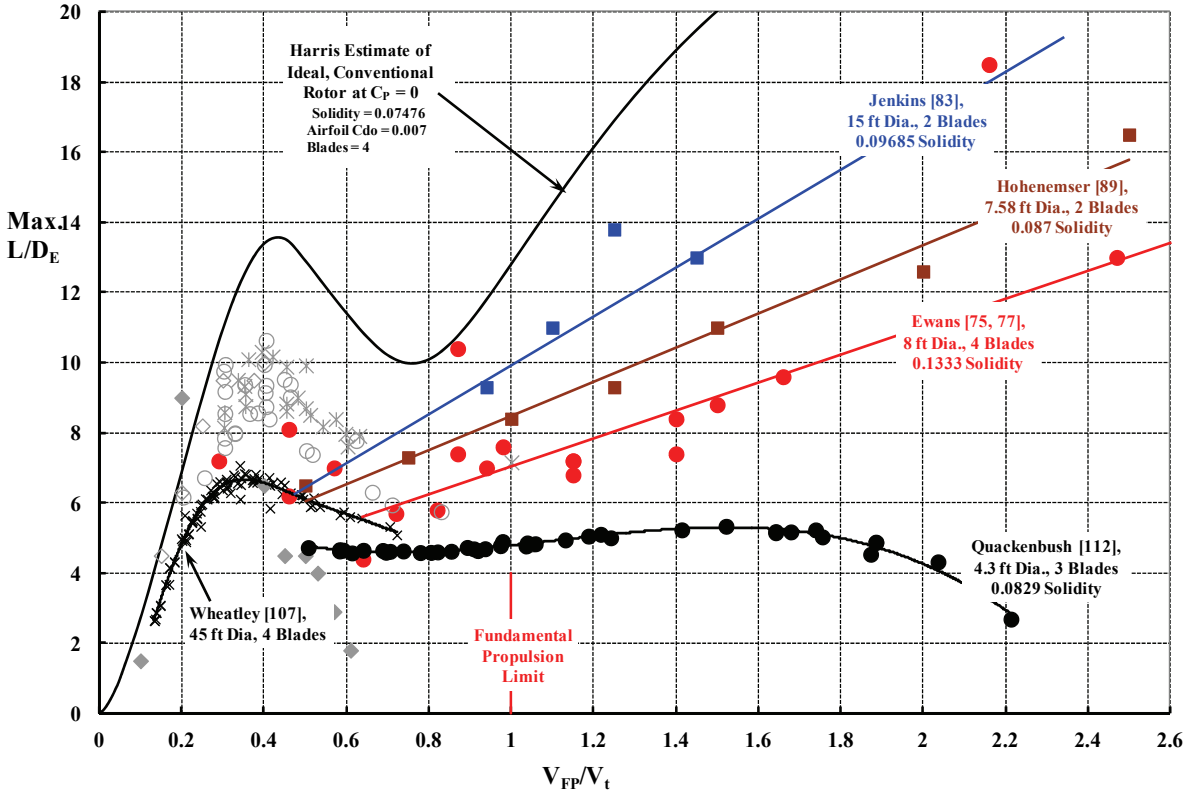

Fig. 2-39. The conventional, articulated rotor recovers its L/D_E performance when the speed ratio of $V_{FP}/V_t = 1.5$ is reached.

have before you. However, other than the Wheatley PCA-2 rotor test, the four other experiments were small-scale models and exploratory in nature and, therefore, I am inclined to wait for results from a few definitive full-scale rotor tests.[27]

The important corollary data to maximum L/D_E is the rotor lift coefficient (C_L) at which the maximum L/D_E is obtained. Let me use results from Kurt Hohenemser's 1949 experiment to illustrate the behavior of the rotor-lift-to-effective-drag ratio versus rotor lift coefficient at three of the flightpath-to-tip-speed ratios (V_{FP}/V_t) Kurt tested at. As you can see from Fig. 2-40, the C_L at which maximum L/D_E is obtained is not a precisely defined point. In fact, a rather wide range in lift coefficient is available for a speed ratio objective. The secondary abscissa shows that the rotor blade loading coefficient (C_L/σ) is at levels far beyond helicopter operating levels today.

The data provided by Kurt can now be used to update an earlier chart, Fig. 2-14, for blade loading coefficients as a function of speed ratio, which you now see as Fig. 2-41.

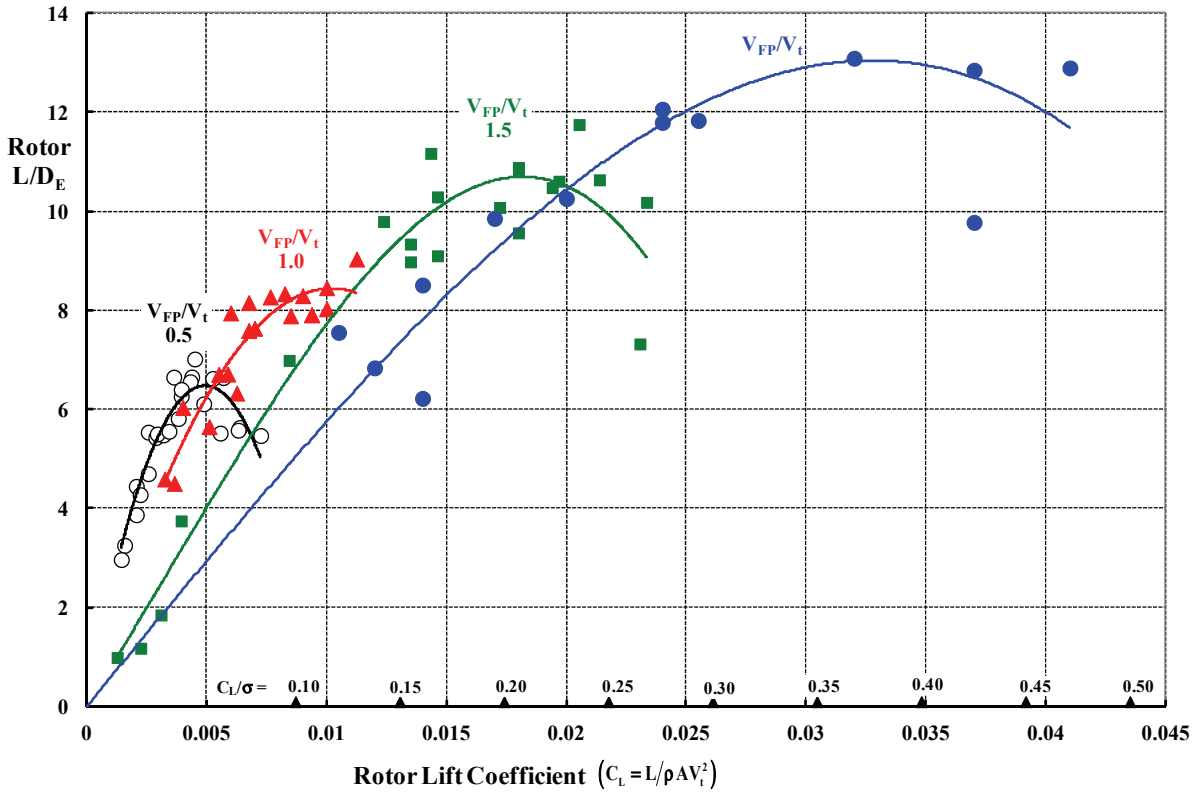

Fig. 2-40. Maximum L/D_E occurs at quite high lift coefficients (C_L) as the speed ratio of the edgewise flying rotor is increased. Kurt Hohenemser found this out at the start of the XV-1 development in 1949, with a two-bladed, 8-foot-diameter rotor with a solidity of 0.087.

[27] You might start by buying a tail rotor system for the Mi-26 from the Mil company in Russia. This is a five-bladed, 25-foot-diameter articulated rotor with, I believe, more than sufficient strength for testing at high speed. It could easily be tested in any of the world's full-scale wind tunnels.

What I find so interesting about the results in Fig. 2-41 is that for speed ratios around 1.0 and above, the data trends are approximately of the form

$$(2.42)\quad C_L/\sigma \text{ for} \left(\frac{L}{D_E}\right)_{Max.} \approx \text{constant}\left(\frac{V_{FP}}{V_t}\right)^2,$$

and you can easily see that a constant equal to 0.1 is a quite adequate representation. Accepting this observation, it follows that the high L/D_E edgewise flying rotor operating at or near autorotation must generally have lift-to-*blade-area* ratios on the order of

$$(2.43)\quad \left(C_L/\sigma\right)_{Max.\,L/D_E} = \frac{L}{\rho A V_t^2 \sigma} = \text{constant}\left(\frac{V_{FP}}{V_t}\right)^2,$$

and because disc area (A) times solidity (σ) equals total blade area (bcR) for rectangular blades, you simply have a wing-type lift coefficient. That is,

$$(2.44)\quad \frac{L}{\rho A V_{FP}^2 \sigma} = \frac{L}{\rho V_{FP}^2 (bcR)} = \text{constant}\,(\text{say } 0.1).$$

It would be nice to report that today's rotor theories are quite capable of predicting the experimental performance characteristics you see in Fig. 2-39, Fig. 2-40, and Fig. 2-41. Unfortunately, this is not the case. Considerable success up to an advance ratio of 0.5 has been demonstrated [109], but only minor work [112] has been done in theory development and validation in the high-advance-ratio regime explored by Kurt Hohenemser in 1949 and then again by Todd Quackenbush in 2010.

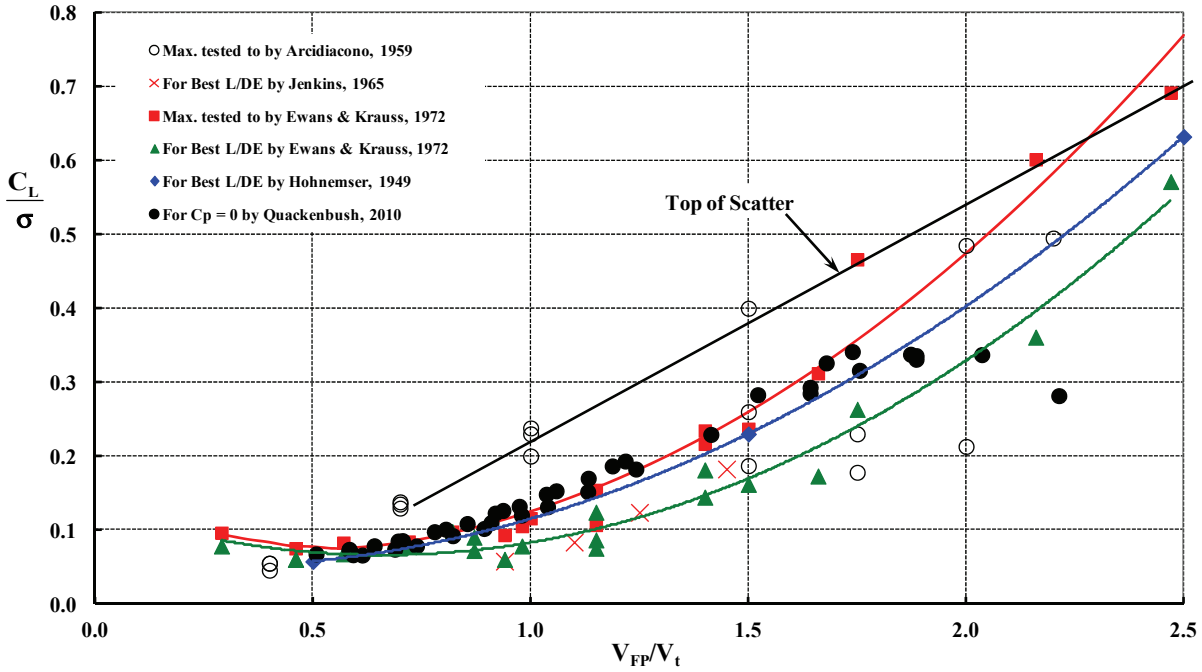

Fig. 2-41. Harris' summary "design chart" for the blade loading coefficient at which maximum L/D_E can be obtained (for articulated rotor hubs only).

2.8 KURT HOHENEMSER'S 1949 DISCOVERIES

Kurt Hohenemser and Fred Doblhoff's XV-1 technology demonstrator efforts came to an end after final testing in late 1957 when the U.S. Office of Naval Research offered no follow-on contract.[28] Because the program was classified confidential, many invaluable reports disappeared into the files at McDonnell Aircraft Corporation. The odds are very good, however, that much of this work exists on microfiche in the Defense Technical Information Center (DTIC) files. That is how I tracked down Kurt's reported results from his first wind tunnel tests in 1949 at the University of Washington (see footnote 26 on page 87). This McDonnell Report No. 1975 was volume IX of a group titled *Detailed Final Report of Research on High Speed Rotary–Fixed Wing Aircraft*, so you can easily imagine what the rotorcraft industry has been missing for some six decades [113].

McDonnell Report No. 1975, prepared by Bob Head and Kurt Hohenemser, is 358 pages long—cover to cover. The text and figures are contained in the first 40 pages. Then, from page 41 to the end, you have page after page of graphs divided into three batches. Kurt tested the model rotor first without simulating the drag of the tip drive units (pages 41 to 84).[29] Despite the poor quality of the reproduction, I was able to read the data (slowly and accurately enough for this discussion) from the graphs.

In Kurt's report you will note his first impressions about trimming the model and controlling rotor speed. For example, he wrote in his introduction that "it also became clear that the rotor was quite sensitive to small changes in rotor attitude" at high advance ratios. Later, in the body of his report, he expanded this point in paragraph 3.5.5.1 saying that

> "figure 11 shows the thrust coefficient, C_T, against α for zero tip drag and for a blade pitch angle of $\theta = -1.5°$. The slope of the C_T versus α curves become very steep at higher advance ratios, μ. The blade loading, (C_T/σ), reach[es] extraordinarily high values at high advance ratios. (C_T/σ) values up to 0.35 were measured. The autorotation curve indicates clearly the instability at higher advance ratios. Above $\mu = 1.25$ this curve is nearly vertical and small changes in α [shaft] have a very large effect on the equilibrium advance ratio, μ; that is, on the equilibrium RPM. Below $\alpha = 4^o$ no autorotation is possible."

You see Kurt's figure 11 reconstructed here as Fig. 2-42. Kurt's model had no cyclic pitch and, therefore, an aft tilt of the rotor shaft (say while holding collective pitch constant) was accompanied by significant longitudinal flapping. You see this growth in flapping sensitivity with increasing advance ratio in Fig. 2-43. Because the tip-path-plane angle of attack equals the sum of shaft angle of attack and longitudinal flapping (i.e., $\alpha_{hp} + a_{1S}$), the rotor lift-curve slope grows rapidly. This leads to a nearly uncontrollable problem in rotor trimming. Several experiments [74, 89, 111] show that a human—be it in a wind tunnel situation or a pilot in flight test—is much too slow in dealing with this very undesirable rotor behavior.

---

[28] You know, of course, that the Bell XV-3 tiltrotor program was continued with U.S. Air Force support. You might not know that the Sikorsky XV-2 program for development of a stopped and stowed, single-blade rotor configuration did not go beyond a paper study supported by model experiments. Thus, the 1949–1952 period saw the first competition between a compound helicopter and a tiltrotor.

[29] He simulated the tip drive by adding spheres at the model blade tips—small ones first and larger ones second.

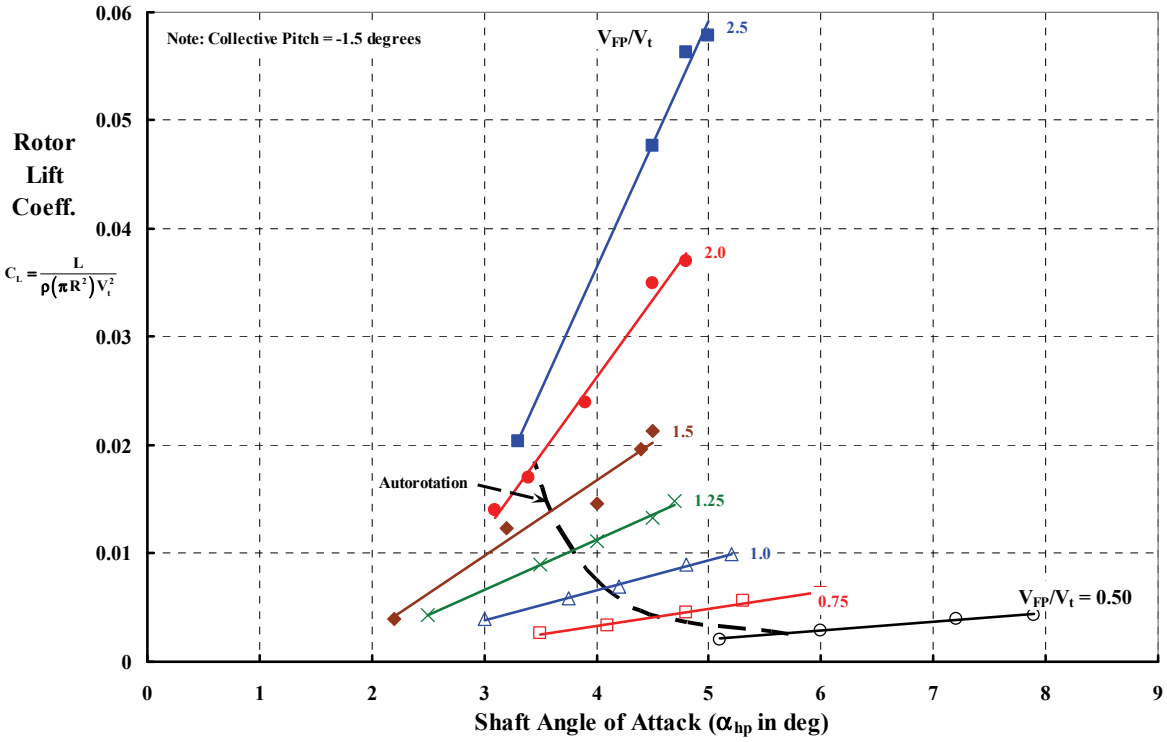

Fig. 2-42. The articulated rotor lift-curve slope becomes very large at high-speed ratios. Autorotation at $V_{FP}/V_t = 2.5$ and $\theta = -1.5$ degrees was not possible in Kurt's 1949 model test.

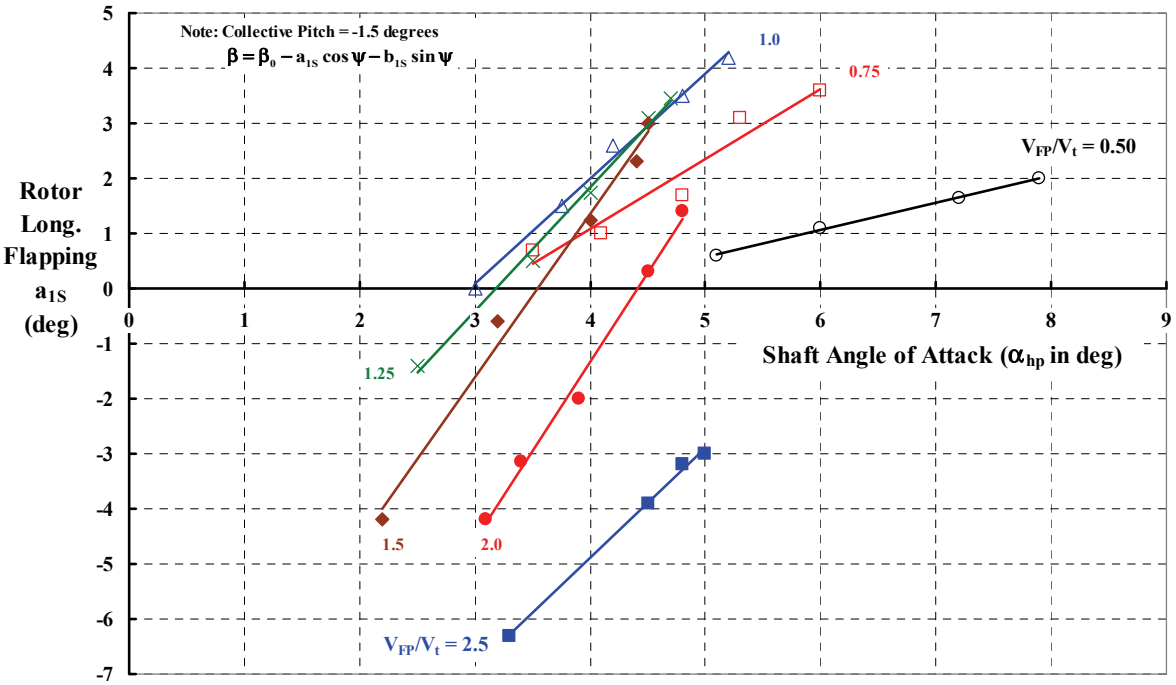

Fig. 2-43. Longitudinal flapping response to shaft tilt can be a problem in itself as Kurt Hohenemser found out in 1949.

Now let me reinforce this introductory point dealing with Eqs. (2.5) and (2.6). The rotor lift—thrust if you prefer, because the shaft angle of attack (α_{hp}) is a small angle for an edgewise flying rotor—depends on an angle of attack and a collective pitch. You saw the dependency with Fig. 2-2 through Fig. 2-5. However, the sensitivities of thrust to angle of attack and to collective pitch depend on whether you are working in the tip-path-plane axis system or the shaft axis system. Let me emphasize this point using Hohenemser's 1949 model test data.

The data shown in Fig. 2-42 and Fig. 2-43 single out teetering rotor behavior at one collective pitch (θ), namely $\theta = -1.5$ degrees, as the shaft axis is inclined to the wind tunnel free stream by the hub plane angle (α_{hp}).[30] Because the rotor lift and longitudinal flapping (a_{1S}) behavior is, perhaps surprisingly, linear, I used a simple linear regression analysis to reduce Kurt's lift and longitudinal flapping data for all collective pitches and shaft angles to individual "curve fit" equations. For a speed ratio of 1.5, I obtained

$$C_L/\sigma = 4.71\alpha_{hp} + 5.11\theta \tag{2.45}$$

with angles in radians. For longitudinal flapping you have

$$a_{1S} = 3.00\alpha_{hp} + 5.00\theta\,, \tag{2.46}$$

and angles can all be in radians or degrees.

Now notice in Eq. (2.45) that the change of thrust with collective pitch, $d(C_L/\sigma)/d\theta$, is +5.11 per radian for this speed ratio of 1.5. However, if you turn back to Fig. 2-2, you will read that the same derivative is on the order of –0.75 to –1.5 per radian. It is the choice of the axis system that causes this apparent difference.[31] A little algebra shows you one way of converting from one axis system to the other. Recall that the tip-path-plane angle of attack is found from the hub-plane angle of attack as

$$\alpha_{tpp} = \alpha_{hp} + a_{1S} \quad \text{or} \quad \alpha_{hp} = \alpha_{tpp} - a_{1S}\,. \tag{2.47}$$

With this fundamental first-order relationship, you can write the longitudinal flapping equation as

$$a_{1S} = \frac{da_{1S}}{d\alpha_{hp}}\left(\alpha_{tpp} - a_{1S}\right) + \frac{da_{1S}}{d\theta}\theta \tag{2.48}$$

and then solve for the flapping, which gives you

[30] Keep in mind that the hub plane is normal to the shaft and that it is very common for engineers to use the terms interchangeably. That is, α_S means the same as α_{hp}.

[31] I believe that rotors must be studied in both axis systems. Rotor flapping relative to the shaft is very important in the geometric layout of a blade's position relative to the airframe, which brings preliminary and detailed design reality to the problem. On the other hand, working in the tip-path-plane axis system can give you a broader outlook during conceptual design.

$$(2.49)\quad a_{1S} = \left[\frac{da_{1S}/d\alpha_{hp}}{1+da_{1S}/d\alpha_{hp}} = \frac{da_{1S}}{d\alpha_{tpp}}\right]_{tpp}\alpha_{tpp} + \left[\frac{(da_{1S}/d\theta)_{hp}}{1+da_{1S}/d\alpha_{hp}} = \left(\frac{da_{1S}}{d\theta}\right)_{tpp}\right]_{tpp}\theta .$$

You can see from Fig. 2-43 that $da_{1S}/d\alpha_{hp}$ is positive so that flapping sensitivity appears to be reduced when you work in the tip-path-plane axis system. However, you must keep in mind another fundamental for an articulated or teetering hub, which is that flapping (a_{1S}) and feathering (B_{1C}) are—to the first order—interchangeable. That is why you encountered Eq. (2.6) early in this chapter. This equation, to repeat, stated that

$$(2.6)\quad (B_{1C} + a_{1S}) = \frac{\partial(B_{1C}+a_{1S})}{\partial\alpha_{tpp}}\alpha_{tpp} + \frac{\partial(B_{1C}+a_{1S})}{\partial\theta_0}\theta_0 .$$

The reason the change of rotor lift with collective pitch, $d(C_L/\sigma)/d\theta$, *might* change from positive to negative in value now becomes clear by writing

$$(2.50)\quad C_L/\sigma = \frac{d(C_L/\sigma)}{d\alpha_{hp}}(\alpha_{tpp} - a_{1S}) + \frac{d(C_L/\sigma)}{d\theta}\theta .$$

When you substitute the flapping equation, Eq. (2.49), in the lift equation, Eq. (2.50), and simplify the result you will see that

$$(2.51)\quad C_L/\sigma = \left[\frac{d(C_L/\sigma)}{d\alpha_{hp}}\left(\frac{1}{1+da_{1S}/d\alpha_{hp}}\right)\right]\alpha_{tpp} + \left\{\left[\frac{d(C_L/\sigma)}{d\theta}\right]_{hp} - \left[\frac{d(C_L/\sigma)}{d\alpha_{hp}}\right]_{hp}\left[\frac{(da_{1S}/d\theta)_{hp}}{1+da_{1S}/d\alpha_{hp}}\right]\right\}\theta .$$

Admittedly, this result is a little messy, but such is the life of engineers who delve into rotor characteristics in any detail.

Kurt Hohenemser's McDonnell Report No. 1975 provided the rotor trim and lift derivatives from which I could do several regression analyses. My results are summarized here in Table 2-2 and Table 2-3.

Table 2-2. Longitudinal Flapping Derivatives for Kurt's Two-Bladed, Teetering Rotor

	Hub-Plane Axis System				Tip-Path-Plane Axis System			
V_{FP}/V_t	$\frac{da_{1S}}{d\alpha_{hp}}$	$\frac{da_{1S}}{d\theta}$	Constant	R^2	$\frac{da_{1S}}{d\alpha_{tpp}}$	$\frac{da_{1S}}{d\theta}$	Constant	R^2
0.50	0.690	1.699	–0.727	0.989	0.419	1.005	–0.523	0.996
0.75	1.263	2.541	–0.343	0.969	0.578	1.120	–0.294	0.994
1.00	1.755	3.175	–0.514	0.960	0.674	1.130	–0.473	0.995
1.25	2.204	4.064	–1.014	0.993	0.694	1.263	–0.356	0.999
1.50	2.996	4.998	–3.295	0.993	0.697	1.438	–0.406	0.995
2.00	3.186	6.026	–5.028	0.998	0.774	1.637	–1.377	0.979
2.50	1.963	6.199	–3.555	0.998	0.899	0.929	–1.153	0.950

Table 2-3. Lift Derivatives for Kurt's Two-Bladed, Teetering Rotor (angles in radians)

	Hub-Plane Axis System				Tip-Path-Plane Axis System			
V_{FP}/V_t	$\frac{d(C_L/\sigma)}{d\alpha_{hp}}$	$\frac{d(C_L/\sigma)}{d\theta}$	Constant	R^2	$\frac{d(C_L/\sigma)}{d\alpha_{tpp}}$	$\frac{d(C_L/\sigma)}{d\theta}$	Constant	R^2
0.50	0.542	0.870	–0.00256	0.995	0.317	0.326	0.00208	0.993
0.75	1.032	1.311	–0.00117	0.986	0.441	0.154	0.00345	0.968
1.00	1.782	1.935	–0.00006	0.993	0.690	–0.149	–0.00005	0.960
1.25	2.998	3.190	0.00346	0.985	0.920	–0.599	0.02165	0.974
1.50	4.709	5.108	–0.00259	0.980	1.163	–0.761	0.06658	0.972
2.00	9.201	11.129	–0.04517	0.992	2.280	–2.093	0.14115	0.994
2.50	14.991	19.628	–0.11749	0.996	5.019	–11.662	0.19855	0.993

Both of the preceding tables show that the regression analyses found that the "curve fitting" is quite accurate (i.e., $R^2 > 0.95$), but the analyses detected a constant that said the experimental results had an overall zero shift. Kurt's 8-foot-diameter rotor used untwisted blades, and theoretically the "constant" should be zero. That is, if the angle of attack is zero and the collective pitch is zero, then the rotor should not be flapping and the lift should be zero. All the experimental data I am acquainted with has presented difficulties of this sort.[32] Most often, the elastic deflections in blade torsion are the cause. You will remember from Volume I that Cierva had considerable problems with blade torsion on his C.30 autogyro.

This brings to an end the discussion about edgewise flying rotors and some of the aerodynamic limitations the rotorcraft industry has uncovered and experimentally confirmed.

Now let me turn to the actual progress demonstrated by full-scale rotary wing aircraft from the 1960s to today.

2.9 COMPOUNDS AND THE LOCKHEED AH-56

Dissatisfaction with the top-speed performance of the "pure" helicopter was prevalent from the 1950s through the 1970s. Very few leaders saw practical demonstrations of high-speed edgewise flying rotors despite a short-term burst of enthusiasm that came with the McDonnell XV-1 (Fig. 2-6) and the Fairey Rotodyne (Fig. 2-7) in the 1950s. A superb article [114] about this "quest for speed" by Raymond Robb was published in the American Helicopter Society's *Vertiflite* magazine in the summer 2006 edition. This article gives you an overview of what Robb called "hybrid helicopters," and it is well worth your reading time.

In the early 1960s, TRECOM[33] initiated a multi-contract effort with four companies to add auxiliary propulsion and wings to conventional helicopters, and explore rotor behavior at high advance ratios. This major research initiative was commonly referred to at Bell

[32] I always end up wondering if Newton's equation should really be written as $F = k_1 (ma) + k_2$.

[33] Transportation Research and Engineering Command located at Ft. Eustis, Virginia, and now known as the U.S. Army Aviation Research and Development Command (USAAVRADCOM). I knew them best when they were U.S. Army Aviation Material Laboratories (USAAVLABS) on March 1, 1965.

Helicopter Textron as the High Performance Helicopter (HPH) Program. The U.S. Government-funded research (with several of the aircraft shown in the collage in Fig. 2-44) was summarized from a technical point of view by John White and Duane Simon in August 1992 [115].[34]

The focus on speed and the fruits of all the compound helicopter research were brought to bear when the U.S. Army began a search for a new attack helicopter to replace the Vietnam-era Huey Cobra supplied by Bell Helicopter. A competition for a machine able to dash at 220 knots and cruise at 195 knots, while retaining the capability to hover at 6,000 feet on a 95 ^{o}F day, was ultimately won by Lockheed with its AH-56—the Cheyenne. This fully compounded helicopter was designed by a company well versed in obtaining efficient high speed with fixed-wing aircraft as you might guess from Fig. 2-45 and Fig. 2-46. The contractual efforts began in March of 1966 with the expectation that 10 prototypes, designated as the AH-56A, would be built and tested, and the Army would be operating them before 1972. Things did not go as planned, and the program was canceled by the Secretary of the Army on August 9, 1972. The more complete story, with all its ups and downs, is told by Landis and Jenkins [116].

Fig. 2-44. Some past high-speed rotary wing aircraft (1950s through 1970s). Top row—Fairey Rotodyne, McDonnell XV-1, and Lockheed XH-51; center row—Sikorsky NH-3, Bell 533, and Sikorsky S-67; bottom row—Lockheed AH-56, Sikorsky S-69 Advancing Blade Concept, and Sikorsky/NASA/DARPA Rotor Systems Research Aircraft (RSRA) with a prototype x-wing installed (photos courtesy of Todd Quackenbush).

[34] This very valuable document was prepared under a contract between CAPCON, Ltd. and Boeing Vertol. My copy came when I helped Wayne Wiesner distribute his library somewhat before he died. Because of its value, I made a PDF of my copy and sent the file to Wayne Johnson at NASA Ames and Mike Hirschberg at the AHS.

Fig. 2-45. The Lockheed AH-56 had a tail rotor for hover, and a pusher propeller and wing for forward flight.

Fig. 2-46. The AH-56 rotor reached an advance ratio slightly over 0.52 at a flight speed of 204 knots.

The performance that several of these compound helicopters demonstrated *before* 1970 is noteworthy as a prelude to more recent accomplishments. A simple, tabulated summary, guided by data from John White and Duane Simon's report [115], is provided here in Table 2-4. You might also find the graphical summary shown in Fig. 2-47 equally interesting.

Table 2-4. U.S. Army Funding of High-Speed Helicopter Research Led to Greater Understanding of the Potential Offered by Auxiliary Propulsion and Lift; These Compound Helicopter Programs Laid the Foundation for the AH-56A

Rotorcraft	Reference Label, Figures, Pages	Max True Airspeed (knot/mph)	Engine SHP	Jet Engine Thrust (lb)	Gross Weight (lb)	Equivalent SHP*	ESHP Per Ton of GW
Bell YH-40/ YUH-1B Phase 1	[117] Fig 18, pg. 58	157/181	1,065	na	6,480	1,065	329
Bell YH-40/ YUH-1B Phase 2	[118] Text pg. 14	186/214	na	na	9,200	1,860	404
Bell YH-40/ YUH-1B	[119] Fig. 6, pg. 33	217/250	na	na	9,800	2,700	551
Bell YH-40/ YUH-1B	[120] Fig. 9, pg. 20	274/315	300	3,200	9,540	3,000	629
Kaman UH-2	[121] Table 1, pg. 33, Flt. 83, Rec. 6; see also [122-124]	188/216	946	2,574	9,200	2,436	530
Lockheed XH-51A	[125] Table 11, pg. 114	210/242	165	1,400	4,800	1,070	446
Lockheed XH-51A	[126] Table 1, pg. 4, Fig. 5, pg. 15	236/271	245	1,595	4,500	1,675	744
Lockheed XH-51A	[127] Fig. 65, pg. 115	240/276	250	1,880	5,875	2,000	681
Lockheed XH-51A	[128] Fig. 3, pg. 7; see also [129-132]	263/303	250	1,880	4,500	2,000	889
Sikorsky NH-3A/ S-61F	[133] Text pg. 12, Fig. 7c & d, pg. 54/55	211/243	1,668	5,485	19,000	5,227	550
Piasecki 16H-1A	[134] Fig. 32, pg. 87	163/188	1,240	na	6,700	1,240	370
Sikorsky ABC (Helicopter)	[135] Text pg. 24, Fig. 64, pg. 132	156/180	1,800	na	11,000	1,800	327
Sikorsky ABC (Compound)	[135] Text pg. 24, Fig. 135, pg. 210; see also [136-138]	238/274	1,726	6,600	13,300	4,000	602
Sikorsky S-67 Blackhawk	[139] Fig. B, pg. 8	183/211	2,800	na	18,700	2,800	299
Lockheed AH-56A (AMCS)	[140] Fig. 2-11, pg. 2-31; see also [141, 142]	221/254	4,600	na	18,300	4,600	503

* $\text{Equivalent SHP} = \text{Engine SHP} + \text{Jet Thrust in lbs}\left(\frac{V_{kts}}{325}\right)$.

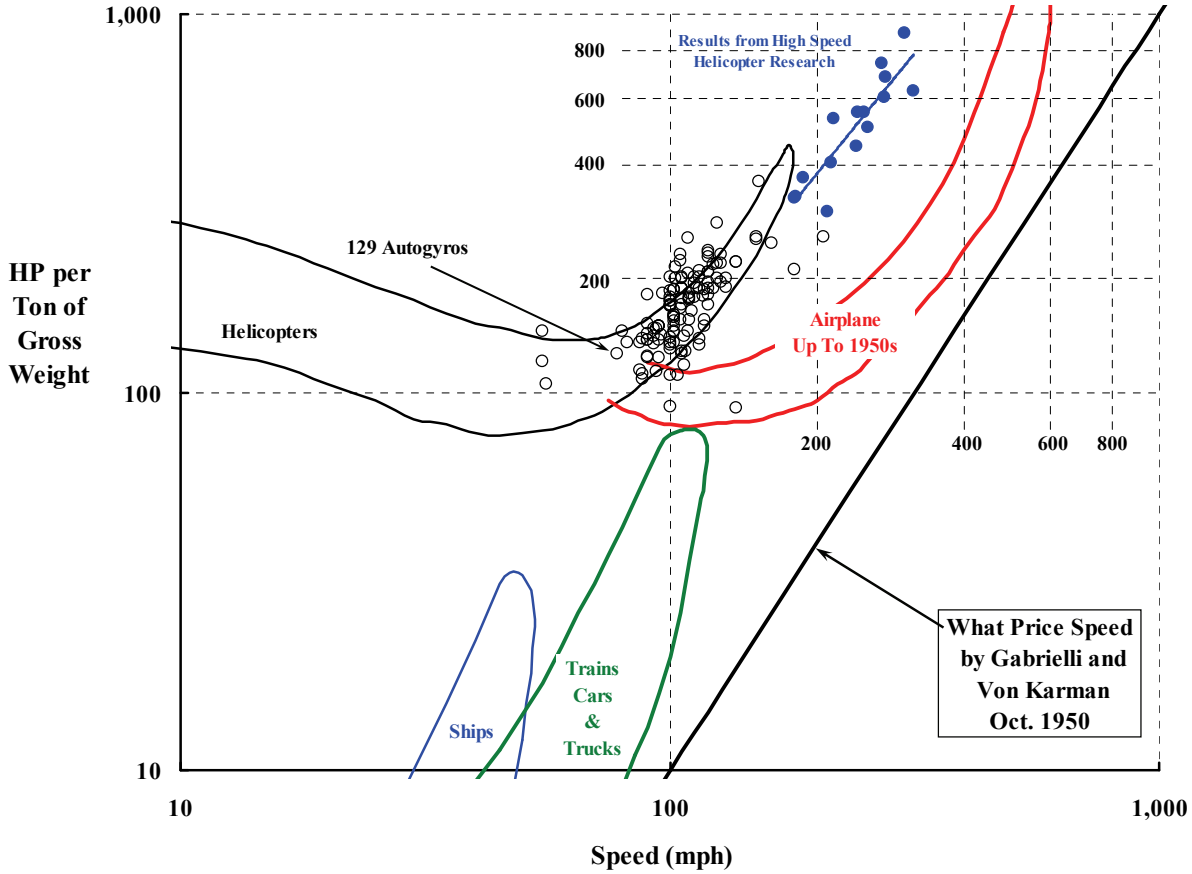

Fig. 2-47. Compound helicopter research in the 1960s and 1970s did not lead to a production aircraft, although the Lockheed AH-56 came close.

2.10 FIVE RECENT TECHNOLOGY DEMONSTRATORS

The Bell XV-15 tiltrotor achieved 301 knots true airspeed in June of 1980, and then the Westland G-Lynx set the world speed record at 216 knots true airspeed in August of 1986. I think these two milestones reawakened the rotorcraft industry's thoughts about what efficient high-speed potentials still remained to be explored. Clearly, the potential of the edgewise flying rotor had not been reached. The "standard" approach of installing only sufficient power to meet hovering requirements, and taking whatever falls out for forward-flight performance, was rather shortsighted for advanced helicopters. More creative thinking produced three other technology demonstrators during the following 50 years. Ways to get around several limitations inherent in edgewise flying rotors were demonstrated in flight, and the foundation for rotors acting as propellers was more clearly established. One major difference between the edgewise flying and propeller-like devices—beyond the limitations you have already read about—has to do with rotor/propeller tip Mach number. The helicopter engineer thinks in terms of an advancing tip Mach number ($M_{1,90}$); the propeller engineer thinks in terms of a helical tip Mach number ($M_{helical}$). It is simply

$$M_{1,90} = \frac{V_{FP} + V_t}{a_s} \quad \text{versus} \quad M_{helical} = \frac{\sqrt{V_{FP}^2 + V_t^2}}{a_s},$$

and the advantage goes to the propeller as Table 2-5 and Fig. 2-48 show. This fundamental aerodynamic performance characteristic relegates the conventional rotor to a relatively small region in the classical forward-speed-to-advance-ratio envelope. To make this point clearer, in Fig. 2-48 I have included the five highest-speed "rotorcraft" experimental results since the 1980s. Rotorcraft is in quotes here because only two (Fig. 2-49 and Fig. 2-50) of the four are pure helicopters, the third has auxiliary propulsion (Fig. 2-51), the fourth is a fully compounded helicopter (Fig. 2-52), and the fifth (Fig. 2-53) is a tiltrotor, which I think of more as a turboprop airplane with VTOL capability.

Table 2-5. Five High-Speed Technology Demonstrators

Reference	Perry [143]	Mecklin [144]	Walsh [145]	Harris' Estimate	Maisel [37]
Company	Westland	Boeing	Sikorsky	Eurocopter	Bell
Aircraft	G-Lynx	Model 360	X2 TD	X^3	XV-15
True airspeed (kts)	216.3	214	250^+	232	301
Date	Aug. 11, 1986	Oct. 23, 1989	Sept. 15, 2010	May 12, 2012	June 17, 1980
Advance ratio	0.50	0.517	0.768	0.688	0.752

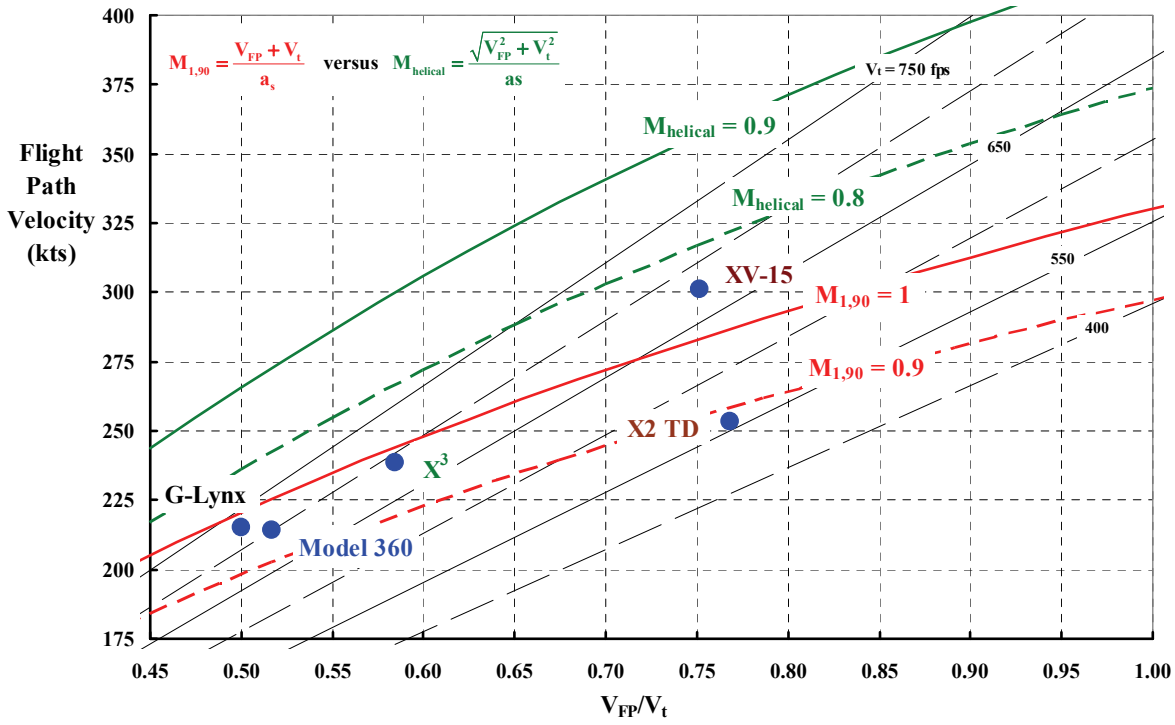

Fig. 2-48. Flightpath speed versus speed ratio domain shows the accomplishments of five companies with their technology demonstrators.

Fig. 2-49. The Westland Helicopter Limited G-Lynx set the current world speed record of 216.3 knots on August 11, 1986. The blade tips had a very tailored planform, commonly known as the British Experimental Rotor Programme (BERP) tip [143, 146].

Fig. 2-50. Boeing Vertol Model 360 [144, 147-158] (photo courtesy of Ron Mecklin).

Fig. 2-51. The Sikorsky X2 Technology Demonstrator [145, 159-162].

Fig. 2-52. The Eurocopter X^3 [163].

Fig. 2-53. The Bell XV-15.

These five most recent rotorcraft technology demonstrators deserve a little more background than what you have with Table 2-5 and Fig. 2-48. Therefore, let me begin with the current world record holder.

Westland Helicopter Limited set the current helicopter world speed record at 216.3 knots true airspeed on August 11, 1986[35] with its G-Lynx, Fig. 2-49. The story [143] is well told by John Perry who was then Chief of Aerodynamics at Westland. His conclusions about helicopter high speed, which I wholeheartedly endorse, were very well stated in his presentation at the 43rd Annual Forum of the American Helicopter Society in May of 1987:

> "The World Speed Record flying has demonstrated the capability of the BERP [British Experimental Rotor Programme] rotor to provide high speed performance for a modest blade area. The aircraft was able to achieve 216.3 knots utilising engine maximum contingency ratings and water methanol injection. The aircraft was smooth with low levels of main rotor induced vibration throughout its speed range notwithstanding the high control power of its rotor head. These characteristics were achieved with the aid of a powerful rotor dynamic aeroelastic and performance analyses. The performance and rotor load measurements produced by the speed record flying agreed very well with analytical predictions, and this was especially satisfying given the extremes in advance ratio and Mach number covered. The design of rotors for high speed helicopter applications therefore may be carried out with confidence.

[35] This replaced the helicopter absolute world speed record over a 15/25-km course set with the Mil A-10 at 199.13 knots on September 21, 1978. The Mil A-10 led to the Mil Mi-24, the Russian Hind attack helicopter.

> *High speed flight requires high installed power levels. A helicopter whose engines are sized for high speed conditions will have outstanding single engine performance at low speeds and a significantly enhanced level of safety when operating from restricted sites in built-up areas. If the power of the engines can be applied directly to produce propulsive force in forward flight, transmissions of conventional size can continue to be used [in] minimizing the weight penalty due to high installed power levels* [my italics].
>
> G-LYNX has demonstrated that a conventionally configured helicopter could possess a high dash speed utilising simple variable area nozzles, and the level of power installed gave it outstanding climb and sustained manoeuvre capability. The aircraft could also sustain an indicated airspeed of 200 knots in level flight without exceeding the dry maximum continuous rating of either its engines or the twin continuous torque limit of its transmission."

Much has been made of how Westland used the residual jet exhaust of the turboshaft engine (never mind the water methanol injection) to provide auxiliary propulsion and that this should really disqualify the machine as a "pure" helicopter. I do not share this view because *all* helicopter turboshaft engines have some residual jet thrust that *does* contribute to a positive propulsive force. It is just that most helicopter engineers, thinking that the jet thrust is small and therefore negligible, ignore this fact of life when quoting performance. In Westland's case, a very smart approach to using engine jet thrust was employed and I, for one, applaud the Westland engineers.

The much more interesting aspect of the G-Lynx was the BERP rotor blade tip shown here in Fig. 2-54, which John included in his paper. About 4 years after the fact, this blade tip configuration was independently examined with both test data and theory [146]. This evaluation confirmed the benefits of the BERP tip and suggested that even more benefits could be obtained.

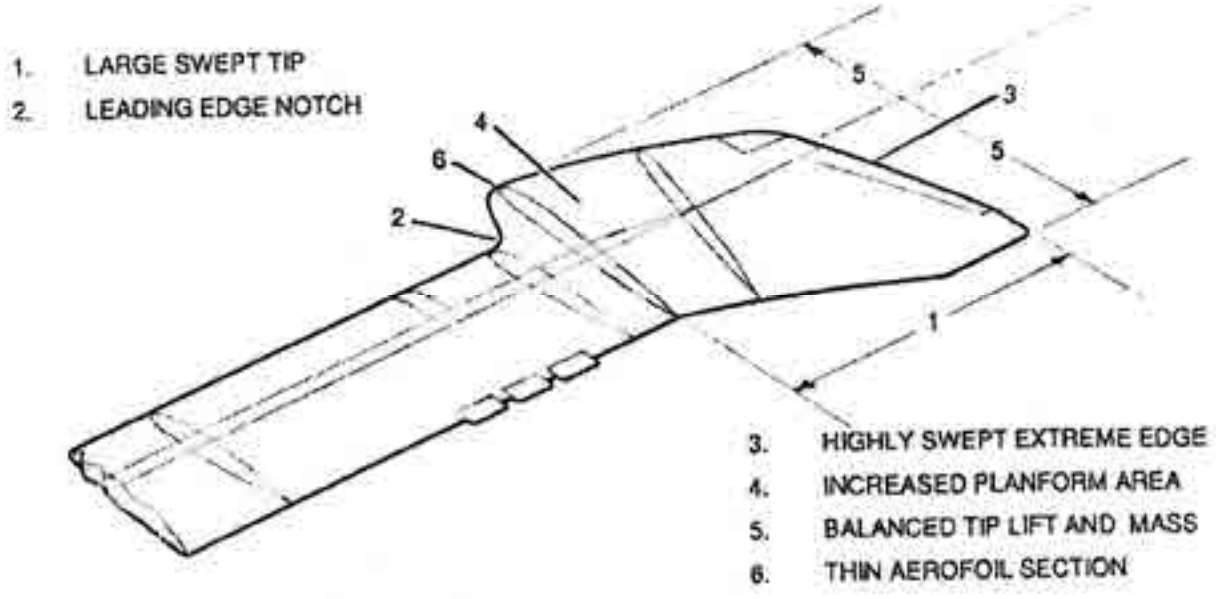

Fig. 2-54. The BERP tip geometry is, so far, the most creative tip shape the rotorcraft industry has come up with [143, 146].

Now turn your attention to the Boeing Vertol Model 360, Fig. 2-50.

The Model 360 was designed from inception with a 200-plus-knot cruise speed in mind, but the more important aspect of the helicopter was the nearly all-composite construction. When it first took off on June 10, 1987, it was the world's largest all-composite helicopter to fly. (The same thing might be said about the Boeing 787 airplane.) Overall, the Model 360 was a very much improved copy of the venerable U.S. Marine CH-46, with the power and drivetrain replaced with components from the larger U.S. Army CH-47 Chinook. The business idea was to compete with the Bell Helicopter Textron tiltrotor aircraft to become the Marine's replacement for the "metal" CH-46. Ken Grina, who became Vice President of Research and Engineering in 1979, was the directing genius behind the Model 360. He put together a small "Skunk Works-like" four-man team with Bob Wiesner as project engineer. A September 1987 *Vertiflite* article written by Ken [148] was prefaced with:

> "Editor's note: Boeing Helicopter's Model 360 made its first flight on June 10, 1987, becoming the largest composite aircraft in existence. The aircraft was the result of a rigorous development program led by Ken Grina, Boeing Helicopter vice president of research and engineering. Grina started at Boeing in 1947 after he graduated from the University of Minnesota with a degree in aeronautical engineering, and gradually rose through the ranks until he reached his current position in 1979. His specialty is structures and he played an important role in Boeing developing the first composite rotor blades in the United States.[36]
>
> The Model 360 was affectionately nick-named 'Grina's bootleg helicopter' in reference to his ability to surmount almost any obstacle that presented itself, and his genius in utilizing parts and ideas from other Boeing programs to reduce the cost and speed along the development of the Model 360. 'We may never see another program like this again,' Grina said.
>
> The Model 360 was also Grina's last program at Boeing. He retired on October 31, 1987, leaving behind a lengthy and distinguished career that included the honor of the American Helicopter Society's Klemin award and the 1993 Alexander A. Nikolsky Lecture [149]. Grina said he plans to devote himself to traveling with his wife Nellavon and working on his home in suburban Philadelphia. He has designed several additions to the house, including a gym, and will be busy working on their completion. We have no doubt that he will utilize the latest technology and composite materials."

An article in *Rotor & Wing* magazine written by Dave Harvey [150] said that the Model 360 program was "something you can afford to do with $100 million of your own money and $25 million kicked in by various suppliers."

Ken gave the most comprehensive details about the Model 360 in a paper [147] he presented on February 13, 1989, at Israel's 30th Annual Conference on Aviation and

---

[36] As director of R&D, I reported to Ken and can tell you firsthand that he was a very "can do" engineer. He did not brook much "can't do" and absolutely no "won't do." Ken revised my approach to the bearingless main rotor hub design using an Erector Set configuration, which was a much smarter way to go considering the explorative nature of the program. I never forgot that lesson. You should also know that it was Pete Dixon who detail designed, fabricated, and, along with Bill Walls, got the Boeing BMR into flight test [123-125] after I moved to Bell in June of 1977. Another lesson Ken taught me was the value of turning an idea into hardware and test results *before* the vision clouds or disappears. Finally, I took his downsizing a CH-47 into a CH-46 composite look-alike really to heart. If you study the Bell OH-58D closely [164], you will see that it is really a Bell Model 206B fuselage with Model 206L engine and drivetrain components.

Astronautics. He was a consultant at that time and championed composite materials. In earlier papers he acknowledged (with considerable pride, which does not come through in the papers) the payoff on money spent during years of rotor system research that went into the Model 360. In this regard, I suggest you read Tony McVeigh and Frank McHugh's paper [154] and a later paper by Leo Dadone, Seth Dawson, Bob Boxwell, and Don Ekquist [158] where a model of the 360 rotor was tested in the Deutsch-Niederländischer Windkanal (DNW). These reports, along with Larry Hartman, Ron Mecklin, and Bob Wiesner's paper [153], and the paper on the Model 360's weights by Jack Wisniewski [155], offer the most important aspects of the program and configuration details I have been able to obtain. From a rotor technology point of view, the blade geometry of the model as tested in the DNW (Table 2-6) and the all-composite hub design (Fig. 2-55 and Fig. 2-56) may be of particular interest to you.

Table 2-6. The Full-Scale Model 360 Rotor Characteristics Compared to the 1/5-Scale Model Tested in the DNW [158] (both were tested at a tip speed of 700 feet per second)

Parameter	Units	Full Scale	DNW Model
Blade Geometry			
Radius	in.	298.2	60.619
Basic chord	in.	26.0	5.285
Number of blades	na	4	4
Tip taper, c(tip)/c(basic)	na	0.3206	0,3206
Tapered section start, r/R	na	0.9	0.9
Thrust weighted solidity	na	0.10053	0.10053
Root cutout, r/R	na	0.268	0.268
Airfoils			
Tip (r/R = 1.0)		VR-15	VR-15
r/R 0.268 to 0.85		VR-12	VR-12
Hinge Geometry			
Horizontal pin offset	in.	10.68	1.734
Vertical pin offset	in.	38.75	5.46
Hub offset	in.	2.14	0.435
Pitch axis, x/c	na	0.202	0.202
Other Properties			
Weight to vertical pin	lb	181.9	1.57
Weight moment to vertical pin	in-lb	20,670	34.71
Weight moment to horizontal pin	in-lb	27,391	52.75
Moment of inertia about horizontal pin	lb-in^2	4,910,000	1,777
Centrifugal force to horizontal pin	lb	56,970	2,437
Nominal Frequencies on a Per-Rev Basis			
1st flap	na	2.607	2.626
2nd flap	na	4.64	4.679
3rd flap	na	7.45	7.518
1st chord	na	7.37	7.80
1st torsion	na	5.49	5.25

I cannot conclude this short discussion about the Boeing Model 360 without touching on its performance and specifically the power required versus speed measured early in the program on Flight X-78 [153]. This is quite relevant to the near record breaking performance during Flight X-255 on October 23, 1989, when 215 knots was achieved in level flight and 223 knots was achieved in a 300-foot-per-minute descent [152]. The test results for Flight X-78 were published [153] in a nondimensional form as the ratio of power required in forward flight to power required in hover. You will find this power required ratio plotted versus flightpath speed, divided by the square root of ambient air temperature, and divided by the temperature on a standard day (i.e., $\sqrt{\theta}$), as figure 11 in reference [153].[37] Just for the fun of it, I decided to reconstruct the power required curve assuming (as Ron Mecklin and I talked about in January 2013) that he and Frank Duke were on the transmission limit of 7,000 horsepower at 215 knots, and it was a near standard day with the ambient temperature about 59 ^{o}F at an altitude of 2,500 feet. Ron sent me his paper that he gave to the Society of Experimental Test Pilots [144], which gives the nominal gross weight as 30,000 pounds and a rotor speed of 269 rpm. You see the results of my effort in Fig. 2-57. One important performance aspect you might note from my reconstruction of the Model 360 power required curve is that the speed for maximum L/D (WV/P) is around 125 knots while the speed for maximum continuous cruising is certainly in the range of 215 knots.

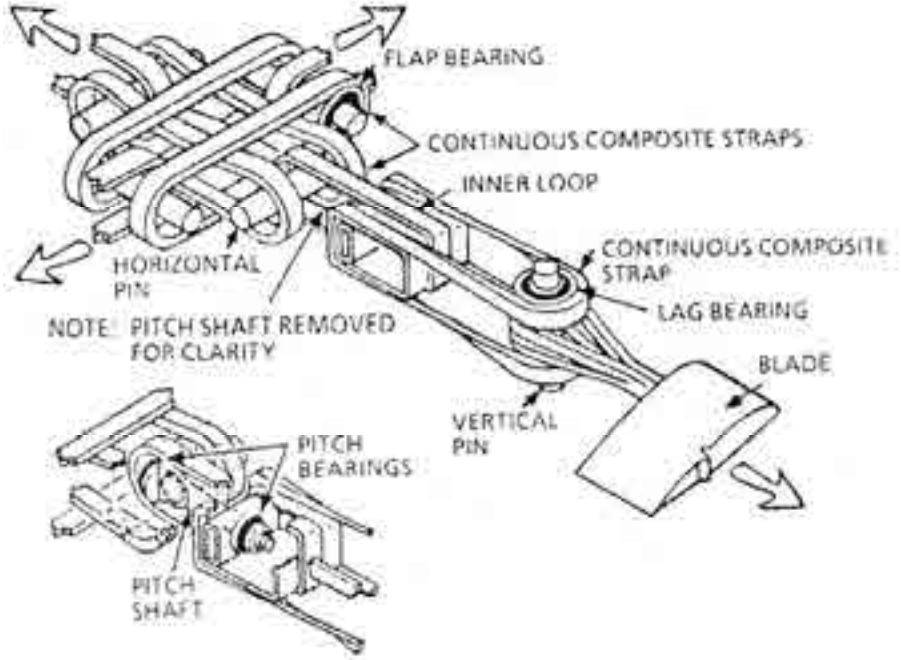

Fig. 2-55. The Model 360 hub used all-composite straps and elastomeric bearings—a major improvement over a CH-46 (or CH-47) hub with respect to reliability, maintainability, parts' life, manufacturing cost, and of course, weight reduction [147].

[37] Twice I asked Bob Wiesner, the Model 360 project engineer, for the flight test data in "raw" form and twice he punted. The first time he was still immersed in Boeing and, because of the competitive environment at that time, Boeing put the clamps on releasing the data, which was somewhat understandable. The second time, January 2013, he was long retired and could not remember where the data was, which was completely understandable. Of course, the real problem is that I have tackled this three-volume book a decade too late.

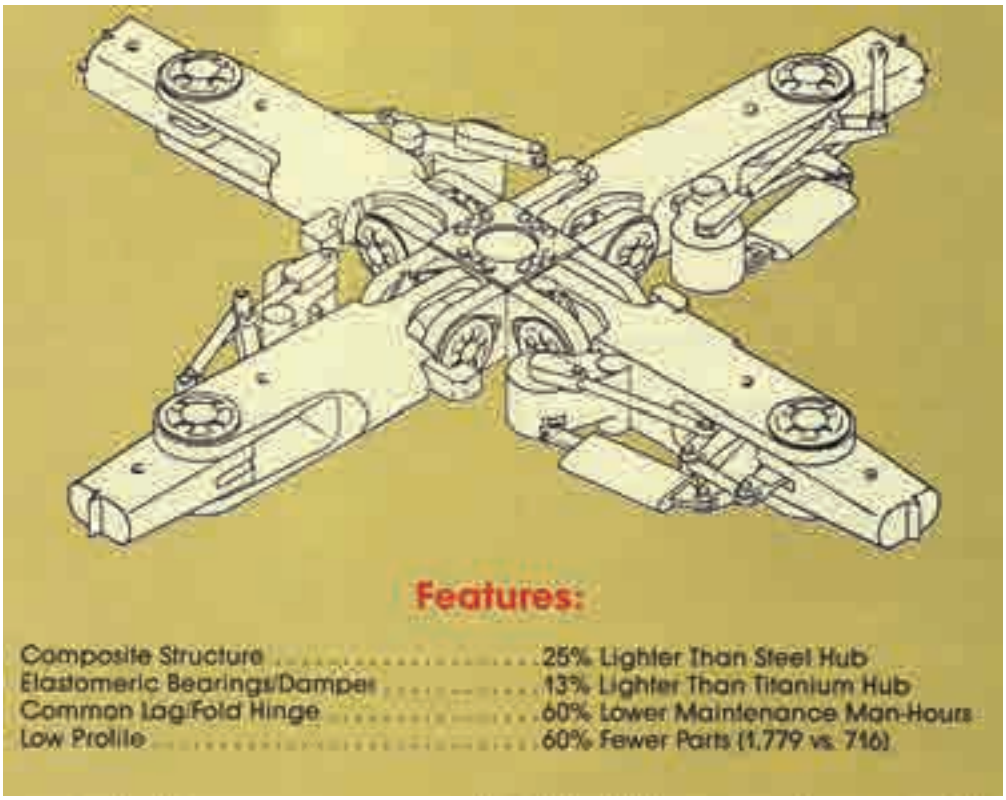

Fig. 2-56. The Model 360 hubs were, in my opinion, better than our "modern day" bearingless hubs [150].

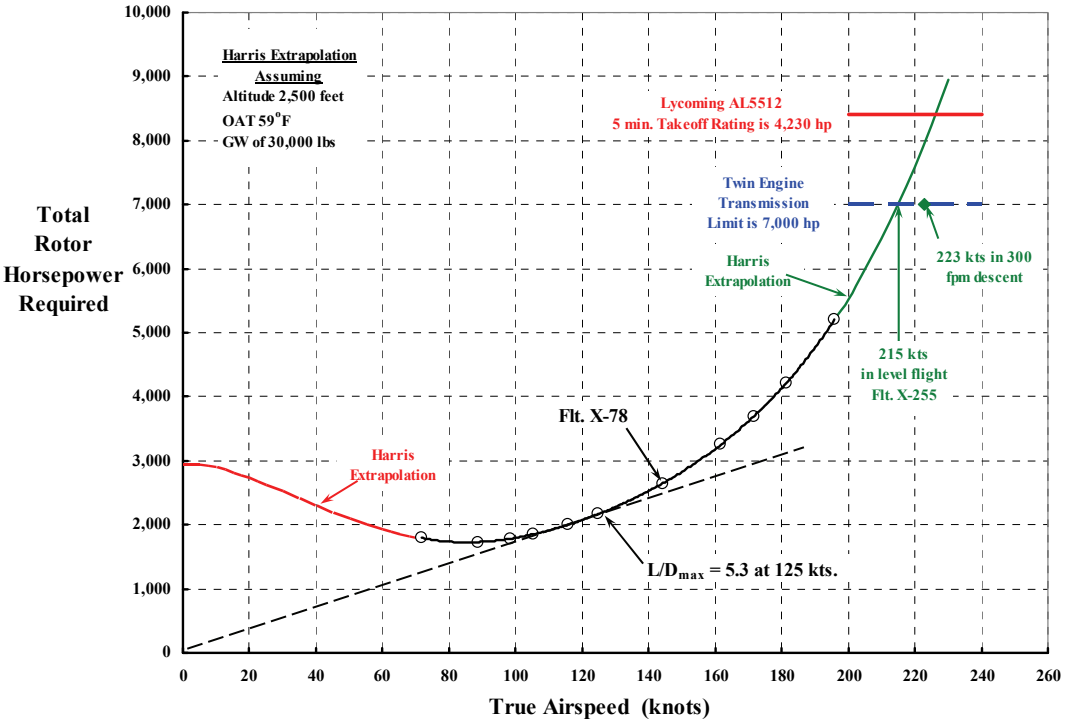

Fig. 2-57. Harris' summary of the high-speed performance of the Boeing Model 360.

Subsequent to the high-speed flight, "a crack was discovered in the rear rotor hub and the Model 360 was grounded" for repairs [165]. Later, an article in the July issue of *Flight International* [166] appeared that quoted Frank Duke (then Program Director and test pilot) saying, "We think we have good potential for the world speed record." After acknowledging the grounding problem, Frank went on to say:

> "The single Model 360 built started flying again earlier this year after several months of ground work, partly to cure a rotor-hub delamination problem at high speed. The rotor hub has two significant composite components which are joined with adhesive. Due to the torsional requirements that we imposed on the hub at very high speeds, some of the layers started to delaminate and we got a minute, but significant, relative movement between the two [components] at more than 200 kts. Boeing is to begin first demonstration of the aircraft outside the company during the next few weeks. We will be demonstrating it to those people who will be considering what is next for a medium-lift helicopter. We have [also] invited those individuals from the U.S. Army who will be involved in determining what will follow the CH-47D and MH-47E."

As you know, things did not go Boeing's way. The U.S. Marines chose to develop the then–Bell Boeing V-22, and the U.S. Army showed little interest in applying Model 360 technology to the CH-47 series.

Let me leave you with one quote from Ken Grina's Alexander A. Nikolsky Lecture [149] that I think reflects Ken's true character. In the last paragraph of the article he said, "Perhaps the greatest benefit of all is that we've now produced a cadre of composite engineers, people working not just in structures but in dynamics as well." A lot of that talented "cadre" that Ken taught went to work on the V-22.

Now consider the Sikorsky X2 Technology Demonstrator, Fig. 2-51. This is another example of a small, company-funded team[38] (led by Steve Weiner, Director of Engineering Sciences) successfully building on a good idea (the Sikorsky XH-59A or, if you prefer, the ABC). Steve and his team used advanced technology to create a modern and, in my opinion, exceptional machine, with little money and in the blink of an eye—at least when compared to most Department of Defense funded programs. By the time the rotorcraft industry became fully aware of Sikorsky's program, the X2 TD had reached 250-plus knots in level flight.

Dave Walsh and his coauthors reported on the X2 TD's unofficial breaking of the Westland G-Lynx world record at the 67th Annual Forum of the AHS on May 4, 2011. Their paper recounted the high-speed flight with these words:

---

[38] This program, initiated during Stephen Finger's presidency at Sikorsky, had the wholehearted support of Jeff Pino when he became President of Sikorsky on March 8, 2006. I got to know Jeff when he was Captain Pino and assigned to flight testing the OH-58D. He later joined Bell Helicopter Textron and, under Jack Floyd's program management mentorship, grew rapidly during the LHX program. When the Bell-McDonnell "Super Team" lost the competitive bid to Boeing-Sikorsky's "First Team," Jeff rose quickly at Bell in the marketing department. Then, in January 2002, Dean Borgman hired Jeff away from Bell. (Dean took great pride in telling me of this robbery.) When a small team has the kind of support that a man with Jeff Pino's leadership qualities can bring to an idea, they can do really wonderful things. Jeff retired in June 2012. You might think that Kelly Johnson's Lockheed Skunk Works [167] was the only example of U.S. technology demonstrator talent, but for my money, nothing could be further from the truth.

> "With the FBW/SAS [fly-by-wire/stability augmentation system] optimized and overall vibration in the cockpit, on the engine, and at equipment locations at satisfactory levels, it was time to continue the envelope expansion toward the goal of 250 KTAS [true airspeed in knots]. Flight 17 was conducted in the early morning of September 15, 2010. The takeoff was the most aggressive to date with the pilot accelerating to 150 knots in a level attitude before rotating into a cruise climb at 140 knots and 800 fpm. Level off was at [approximately] 7000 ft. density altitude. Prop pitch was increased to trim the aircraft at 200 knots, 220 knots, and 230 knots. The prop pitch was then increased a few degrees while the collective was lowered to [approximately] 10% above the flat pitch setting. The aircraft trimmed at 253 KTAS in level flight. The chase aircraft showed a true airspeed of 255 knots. After taking data at 250+ knots the pitch attitude was lowered by 3 to 4 degrees, with the same prop and collective settings, and the aircraft entered an 800 fpm descent. Speed increased to 263 KTAS. After recovery from the dive, the aircraft was slowed to a very comfortable 200 knots. A three perpendicular-leg GPS airspeed calibration was completed at 200 knots. The aircraft returned to base for an uneventful landing."

You will find considerable details about the Sikorsky X2 TD in Walsh and his coauthors' paper [145], including the power-required-versus-speed data, a copy of which I have included here as Fig. 2-58. From this data you can immediately see that by 175 knots virtually all of the engine power was going to the six-bladed, 6.66-foot-diameter propeller (called a propulsor by Sikorsky). The power going up the rotor shaft is simply ensuring that rotor speed is controlled.

As I did for the Boeing Model 360, I have added a light, dashed blue line that becomes tangent to the total power required curve at about 160 to 165 knots. This suggests that the speed for maximum L/D of the X2 TD is about 40 knots faster than the Model 360. Evidently, the X2 TD could continuously cruise at 260 to 265 knots considering the maximum continuous power available line (labeled MCP) that you see on Fig. 2-58.

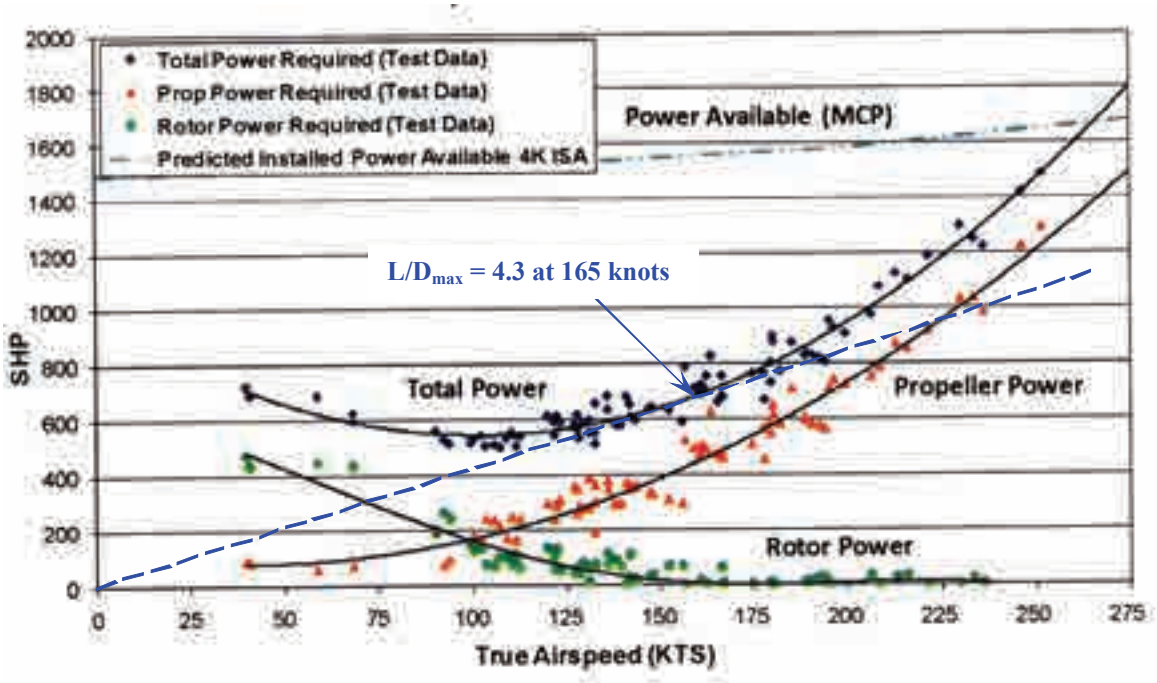

Fig. 2-58. The Sikorsky X2 TD could have easily cruised continuously at 260 to 265 knots (if not faster), which is one indication of the streamline shape shown in Fig. 2-51 [145].

Reaching a speed of over 250 knots is, of course, a tremendous accomplishment for an edgewise flying rotor system. Certainly, Sikorsky being awarded the Collier Trophy for the program on May 5, 2011, was a well-deserved honor. However, the program accomplished considerably more technically than you may be aware of. Let me point out just three technology facets that I believe to be extremely important.

To begin with, the X2 TD high-speed flight envelope expansion *was not* accompanied by the severe vibration that hampered the earlier XH-59A envelope expansion. You can appreciate this from just a comparison of vertical vibration at the pilot's station, which Walsh included in his paper [160] and I have reproduced here as Fig. 2-59. This vibration reduction was obtained using the Sikorsky-developed Active Vibration Control System that was incorporated into the Sikorsky S-92A and UH-60M, as you learned in the discussion of vibration in Volume II, Chapter 2.6. This vibration solution was discussed by Bob Blackwell and Tom Millott in their paper presented at the 64th Annual Forum of the AHS [161]. Two paragraphs they wrote that I found very interesting stated:

> "Experience on the XH-59A showed that adequate control of the N/rev vibration may be an absolute requirement to achieve high speed flight. An active vibration control (AVC) approach was selected due to both its weight efficiency as well as its ability to track changes in rotor speed without performance degradation. Other vibration control approaches such as hub-mounted vibration absorbers and higher harmonic control (Ref. 9) were briefly considered. A hub-mounted vibration absorber, such as the bifilar used on many Sikorsky helicopter models, was rejected due to the drag penalty it would introduce at high airspeeds. Higher-harmonic control was considered too complex and offered too many design challenges to be an appropriate choice for a rapid prototype development program such as the X2 Technology™ Demonstrator.

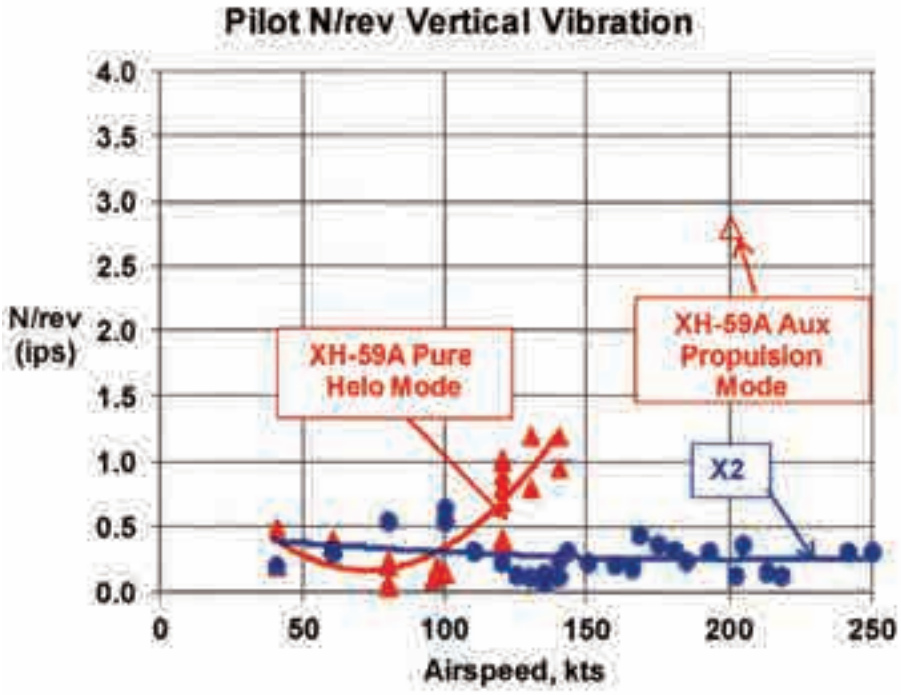

Fig. 2-59. The X2's low vibration level was achieved with an anti-vibration device Sikorsky developed and applied to its S-92A and UH-60M helicopters [160].

> The AVC system incorporated into the demonstrator is based upon the existing off-the-shelf system currently utilized on the S-92ATM (Ref. 10) and the UH-60M BLACK HAWK (Ref. 11) production helicopters. AVC achieves this attenuation by applying 4/rev vibratory forces to the airframe to counteract those produced by the rotor system. AVC implements a closed-loop feedback control algorithm utilizing accelerometers as the feedback sensors and airframe-mounted force generators (FGs) as actuators. A tachometer (Nr) sensor is used to provide a reference signal to allow AVC to swiftly and accurately track changes in rotor speed. An architecture block diagram of the AVC system is shown in Figure 16 (AVC components shown in light green)."

Even as I write this in 2013, there still appears to be no amount of fuselage and/or rotor system tuning that can produce the "jet smooth" vibration characteristics that the rotorcraft industry needs for its future products. It almost seems that licking vibration at the source—as so many rotorcraft engineers have hoped for—is a lost cause. This suggests that a weight allowance for vibration reduction must always be included on all future rotorcraft weight empty statements.

The second facet of immediate interest to me is the similarity between the X2 TD blade and Cierva's early blade designs, which you see in Fig. 2-60. Of course, rotary wing aerodynamicists may be more interested in the blade geometry contrast between the XH-59A and the X2 TD. Ashish Bagai shared the background about the main rotor blade in his presentation at the 64th Annual Forum of the AHS [159]. The very tailored geometry of the X2 TD is shown here in Fig. 2-61. You might note that a thinning of the airfoil (i.e., the airfoil-thickness-to-chord ratio) outboard of the 0.6-radius station was not selected even though advancing tip Mach numbers approaching 0.9 were anticipated. Ashish noted that the tip region uses supercritical airfoils, which minimize compressibility problems.

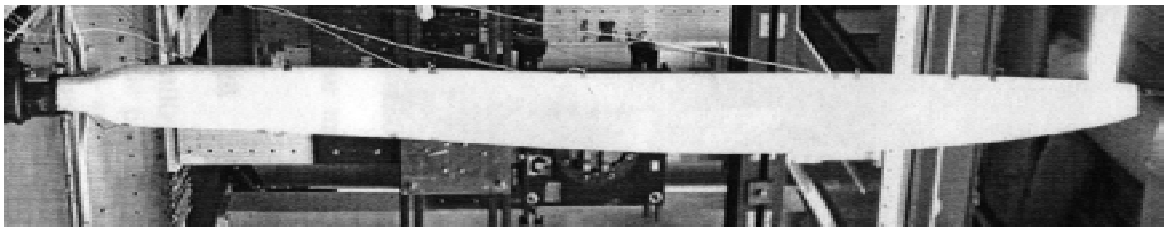

Sikorsky X2 TD in the first decade of the 2000s.

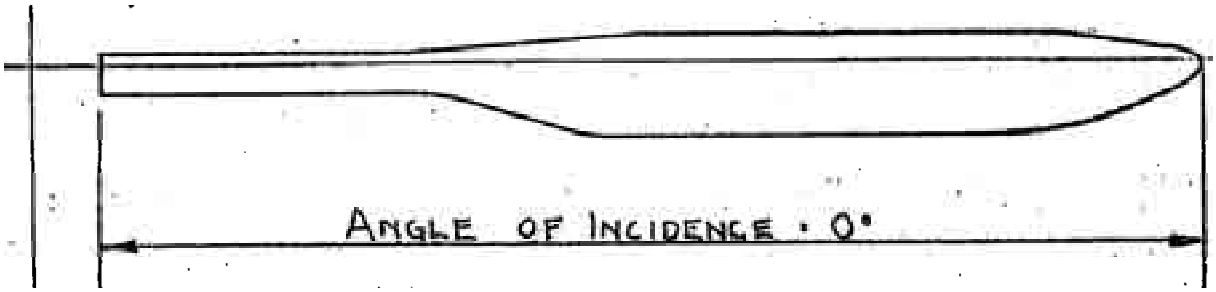

Cierva rotor blades (see Volume I, Fig. 2-66 on page 142).

Fig. 2-60. What an extraordinary design similarity between the Sikorsky X2 TD blade [160] and Cierva's early autogiro blades.

The third facet of interest deals with how drag could be minimized in the hubs, and in the region between the upper and lower rotors of this coaxial machine. The problem was tackled with computational fluid dynamics and some wind tunnel testing as Brian Wake and his coauthors explained in their paper presented at the 65th Annual Forum of the AHS [162].

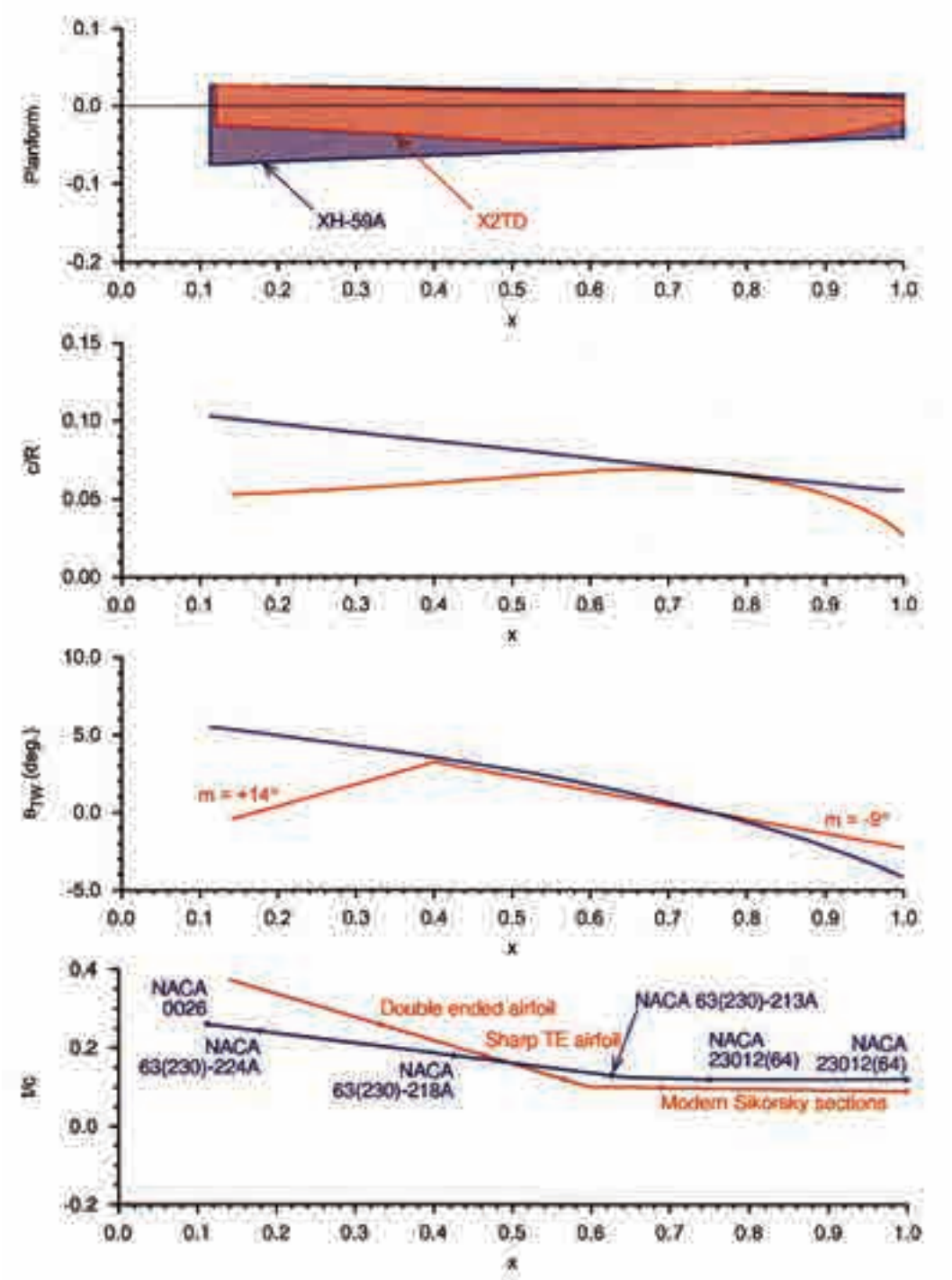

Fig. 2-61. The X2 TD blade design benefited from advanced technology [159].

The fourth technology demonstrator that you should know about is the Eurocopter X^3, which you saw in Fig. 2-52. The first flight of this fully compounded helicopter was made on September 6, 2010. Only 8 months passed before the aircraft demonstrated 232 knots on May 12, 2011. Very little technical data has been released by Eurocopter about its X^3 (or X cubed as it is called by some). However, a somewhat background-oriented presentation [163] of the program was given at the AHS Future Vertical Lift Aircraft Design Conference held in January of 2012. The configuration overview was discussed with one chart, which I have reproduce here as Fig. 2-62. Eurocopter's ability to put together a small team of experts that gathered off-the-shelf components to get the concept flying in a short time is, in my opinion, another example showing that Kelly Johnson's "skunk-works" approach is alive and well. Then, in July of 2012, *Aviation Week* published an article by Douglas Nelms where he related his experiences flying the aircraft [168]. The pilot-oriented discussion was, as always, very valuable. Toward the end of the article Nelms wrote:

> "When we were clear of the controlled area, Jammayrac [the company pilot] pushed the TLC forward and put us in a 3,000 ft./min. climb at 118 kt. at 20% torque, climbing to 7,000 ft. The X3 literally pushes you back in the seat as though it is a corporate jet on climb-out. Performance limits for climbs are up to 5,500 ft./min. with a climb slope of 40 deg.
>
> As mentioned, the dissymmetry in blade speeds causes increasing vibration. Traditionally these are controlled through use of either passive dampeners or active devices that sense and counter the vibration frequencies. No anti-vibration systems are installed on the X3, and test pilots who have flown the aircraft at speeds in excess of 232 kt. say that neither vibration nor stability appear to be a problem and that the aircraft can be flown hands-off without either anti-vibration or stability-augmentation systems installed.
>
> It is still too early to determine whether such systems will be needed in a production aircraft, but Eurocopter says the X3 'has validated the H3 concept beyond expectations, [and] even at 232 kt. is behaving like a flying carpet without autopilot or stabilization systems, and can be flown hands-off.' We took the X3 up to 220 kt., where I found the aircraft can indeed be flown hands-off with good stability, but with a noticeable amount of vibration.
>
> As for stability, I was able to put the aircraft into a series of turns increasing to 60 deg. of bank, with feet off the pedals and collective lever down, maintaining both altitude and airspeed—more or less. In unfamiliar helicopters I tend to lose a couple hundred feet of altitude while losing or gaining 10–20 kt. in sharp turns, but in the X3 the loss or gain was about half that, or less. Turn-speed limitations are 45 deg. at 220 kt. and 60 deg. at 210 kt.
>
> The aircraft does have a four-axis autopilot, taken from the EC155. At one point while I had the aircraft in straight and level flight, Jammayrac turned off the autopilot. The cyclic got just 'squirrelly' enough to notice it, but not so much that it would present a problem."

When you think about the article Nelms wrote in toto, it is a very good first impression for any technology demonstrator.

The fifth rotorcraft technology demonstrator is one that showed enough promise that its configuration was adopted for production. This was the Bell XV-15 tiltrotor (Fig. 2-53), and it was scaled-up for the U.S. Marines to become the V-22 Osprey (Fig. 2-63). The most authoritative story of the XV-15 [37] was pulled together by three men: Marty Maisel, Demo Giulianetti, and Dan Dugan, all from NASA Ames Research Center. When you add in the familiarization manual [169] Marty wrote, you have a very good understanding of the XV-15.

Fig. 2-62. The Eurocopter X^3 was unveiled for first flight on September 6, 2010 [163].

Fig. 2-63. The Bell/Boeing V-22 Osprey: a collage showing the aircraft in hover, then in transition with the rotors partially tilted, and finally in cruise flight.

Flight envelope expansion is a major step in the life of a technology demonstrator program. In the XV-15 program, the envelope was expanded beyond the low-altitude hover and conversion maneuver to altitudes of 25,000 feet density and speeds to 300-plus knots. You see the XV-15 envelope in Fig. 2-64 where test conditions flown are gathered up on a graph of density altitude versus, in this case, true airspeed in knots. What is immediately apparent from this presentation is that the XV-15 could be put into a slight dive, and then speeds up to 335 knots could be reached and data could be taken. Note that in steady, level flight at 16,000-foot density altitude, the XV-15 had a high-speed cruise capability of 300-plus knots. This speed was limited by the transmission torque, and this limit coincides with the normal rated power of the two Lycoming T-53 engines. Because the transmission was designed for 3,000-hour life [169], the XV-15 could, in fact, cruise at 300 knots and 16,000 feet for virtually all of the 3,000-hour transmission life. If you think about a commercial business application where 1,000-rotor-turning hours per year would not be unreasonable, the XV-15, as a technology demonstrator, would need major inspections once every 3 years. As it turned out, the XV-15 aircraft became a very impressive tool for the Bell marketing department until it was retired in 1999 after accumulating 2,000 flight hours.

Perhaps the most positive aspect of the XV-15 commented on by many of the guest pilots was how "easy it was to convert from helicopter to airplane flight and back again" (Fig. 2-65). This is in stark contrast to most of the early "convertiplanes," which could lose

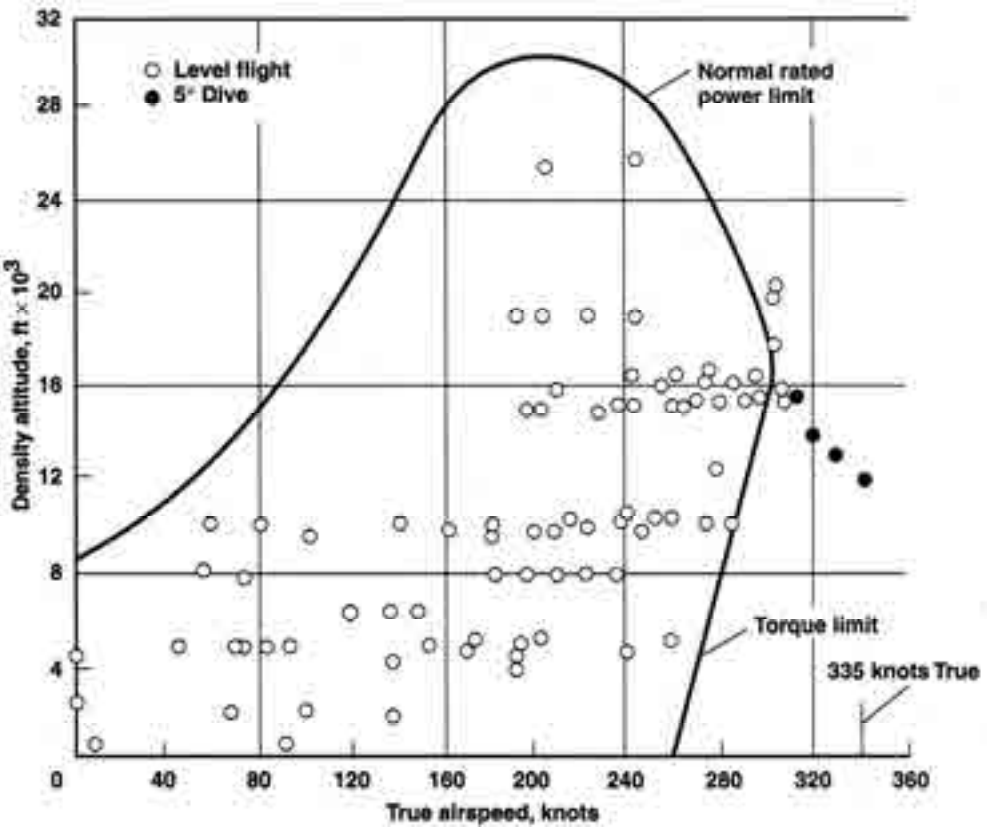

Fig. 2-64. The flight envelope of the XV-15 cleared the aircraft to 335 knots in a slight dive. The flight at 25,000 feet was an unofficial world record [37].

500 feet in altitude during the conversion maneuver. Many VTOL aircraft had conversion "corridors" that were quite restrictive and demanded considerable pilot attention [25]. Maisel's history of the XV-15 [37] describes the aircraft's flight control system in considerable detail. He writes:

> "The flight controls in the hover and helicopter modes resemble those of a lateral-tandem rotor helicopter. While the fixed-wing control surfaces remain active at all times, the primary low speed control forces and moments are provided by proprotor collective- and cyclic-blade angle (pitch) changes. Differential collective pitch produces aircraft roll and differential cyclic pitch results in yaw motions. The proprotor rpm is regulated by automatic control of the collective pitch. To reduce the hover performance loss resulting from the proprotor's wake impinging on the surface of the wing, the inboard flaps can be lowered to preset deflection positions. The outboard wing control surfaces are also deflected down when the flaps are deployed, but to a displacement less than two-thirds of the flap position. The outboard wing control surfaces serve as ailerons in high speed flight and are referred to as 'flaperons.'
>
> During conversion from helicopter flight to airplane mode flight, the helicopter-type control inputs to the proprotor are mechanically phased out, and the conventional airplane control surfaces provide all flight path-control forces and moments. By the time the nacelles are in the airplane position, the collective lever inputs to the proprotor are nulled, and the total control of the collective pitch is transferred to the automatic rpm governor."

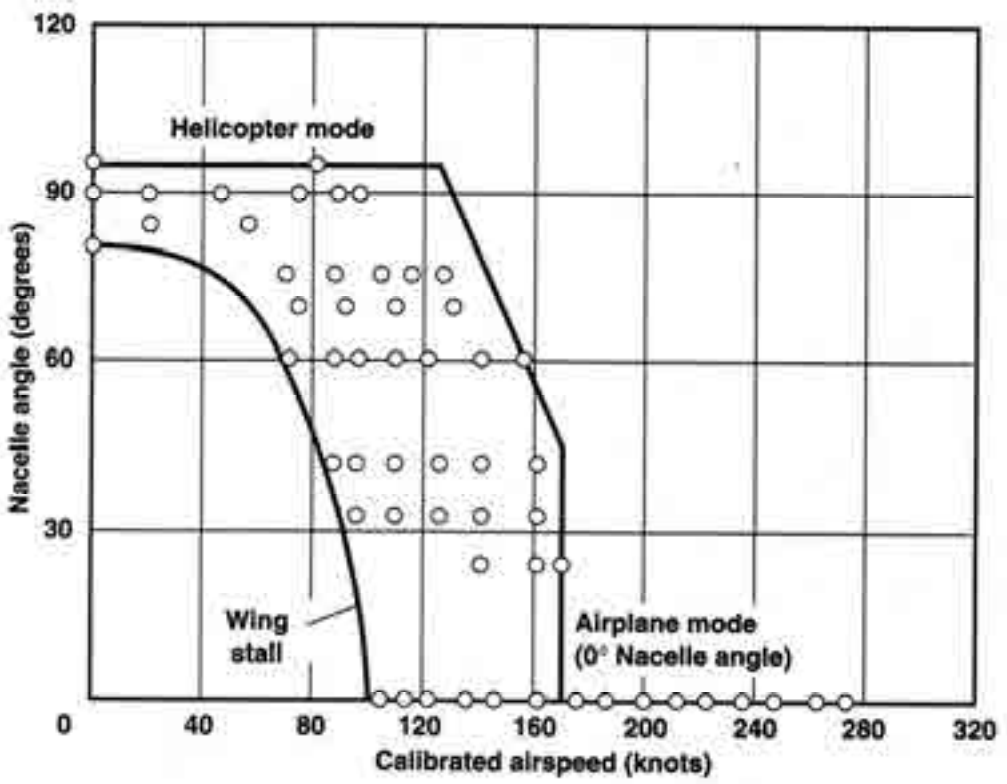

Fig. 2-65. The XV-15 had a very wide conversion "corridor," and the flight controls were mechanically phased from helicopter to airplane flight without requiring pilot assistance [37].

The actual power required during the conversion was, I found, a particularly interesting aerodynamic performance aspect of the XV-15. The rotor-shaft power required versus airspeed at several fixed nacelle positions available during the conversion maneuver is shown in Fig. 2-66. The propulsion units, located at each wingtip, are tilted as the preceding figure of the V-22 illustrates. What begins as an edgewise flying rotor in hover, and at relatively slow-speed flight (i.e., nacelle angle of +90 degrees) becomes, by 140 knots, a rotor whose tip-path-plane angle of attack (α_{tpp}) is –90 degrees, which corresponds to a nacelle angle of 0 degrees. For all intents and purposes, the rotor has now become a large-diameter propeller. By 140 knots the wing is able to provide all of the lift required by the 13,000-pound aircraft, and the machine has become a turboprop airplane.

You will note on Fig. 2-66 that the power being displayed is the total power required from the two XV-15 turboshaft engines. That is, the power is the total power delivered to the rotor shafts, which are frequently referred to as rotor masts. Power required by the accessories (SHP_{acc}) and loss of power to transmission inefficiency (η_{tran}) are not included. One simple way to convert from rotor power required ($RHP_{req'd}$) to total twin-engine power required ($SHP_{req'd}$) is to assume that

$$\text{(2.52)}\quad \text{Twin Engine } SHP_{req'd} = \frac{\text{Left } RHP_{req'd} + \text{Right } RHP_{req'd}}{\eta_{tran}} + SHP_{acc}$$

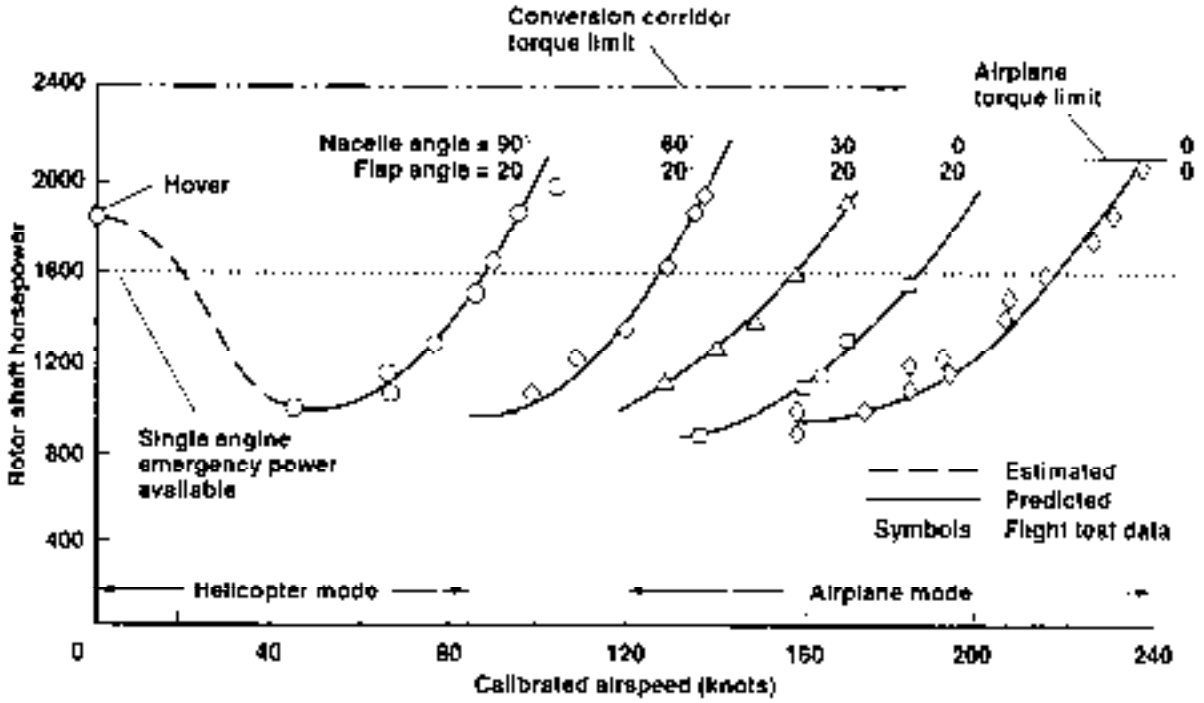

Fig. 2-66. The speed capability of the XV-15 rapidly increases as the propulsion units are tilted forward. All edgewise flying rotor limitations disappear by the time the aircraft has completed its transition to the airplane mode. Conversion is accomplished at 589 rpm; then the rotors are slowed to 517 rpm for the airplane mode [37].

where, for the XV-15, you might assume 20 horsepower for accessories and a very low transmission efficiency of 0.91. (The transmission efficiency was poor because of extra gearboxes needed to accommodate the two modified Lycoming T53-L-13B engines, a change from P&W PT6 engines that was made early in the design process).

A second point to note on Fig. 2-66 is that the forward airspeed axis is labeled calibrated airspeed in knots. *This is not true airspeed*. The pilot's indication of airspeed on the XV-15 came from pitot and static pressure ports on the tip of the flight-test nose boom. As you may know, pressures from the two ports get connected to an airspeed dial by tubes, and the dial is calibrated in airspeed units. Generally the laboratory calibration of the airspeed device, and the actual reading one gets with the device installed on the aircraft, differ slightly. This situation frequently leads to what is called the indicated airspeed, which gets corrected for the error created by flow about the aircraft. Frequently, the aircraft can be flown parallel to some machine (sometimes just a car) so comparative speeds can be obtained. A minor correction to the indicated speed can be applied, and then you have calibrated airspeed. Thus, Fig. 2-66 is showing you rather accurate airspeeds, but stop and think for a moment. The airspeed indicator depends on the air density. If, for example, the aircraft was flying along parallel to a car, but at such an altitude where the air density was nil, the pilot would say his airspeed is zero—yet the pilot and the car are travelling at the same speed. To get the true airspeed, you must turn to this equation

$$V_{true} = \frac{V_{calibrated}}{\sqrt{\sigma}} \tag{2.53}$$

where the density ratio (σ) is the ratio of the air density at which you are recording data to the density of air at sea level on a standard day (i.e., 0.002378 slugs per cubic foot).

The example of power required during conversion provided in Fig. 2-66 is for the XV-15 at 13,000 pounds gross weight with the rotors turning at 740-feet-per-second tip speed, and at a density altitude of approximately 2,000 feet. This means that the true airspeed is about 3 percent higher than the calibrated airspeed because the density ratio is 0.9427.

Now let me discuss the performance of the XV-15 in the airplane mode. To me, the XV-15 is *nearly* a conventional turboprop airplane at the end of conversion. I say nearly because virtually all propeller-driven airplanes have a limit to propeller diameter because of ground clearance restrictions. Even one of the largest propeller-driven airplanes, the Russian Tupolev TU-95 weighing over 370,000 pounds at takeoff, was constrained to four, 18.3-foot-diameter counter-rotating propellers. The installed power of each Kuznetsov NK-12M turbine engine was 14,785 horsepower, which gives a ratio of engine shaft horsepower to ton of gross weight equal to 320. This turboprop strategic bomber could do Mach 0.83 (about 500 knots), which made it quite competitive with the turbojet-powered Boeing B-52 during the Cold War era.[39]

[39] Mike Scully, emeritus engineer at the U.S. Army Aviation and Missile Research, Development, and Engineering Command (AMRDEC), Research, Development, and Engineering Command (RDECOM) at NASA Ames Research Center when he retired in January 2013, shared his assessment of this TU-95 with me [170].

Of course, one item of immediate interest about a turboprop aircraft is the propulsive efficiency of the propeller(s). The XV-15 development program benefited in this regard because a full-scale test of a "proprotor," as many began calling it, was completed in November 1970 (Fig. 2-67). The test report [171] provides performance data at tunnel speeds from hover to over 185 knots. (Early tests were made with the propeller mounted on a cantilever wing to examine the dynamic stability of the configuration.)

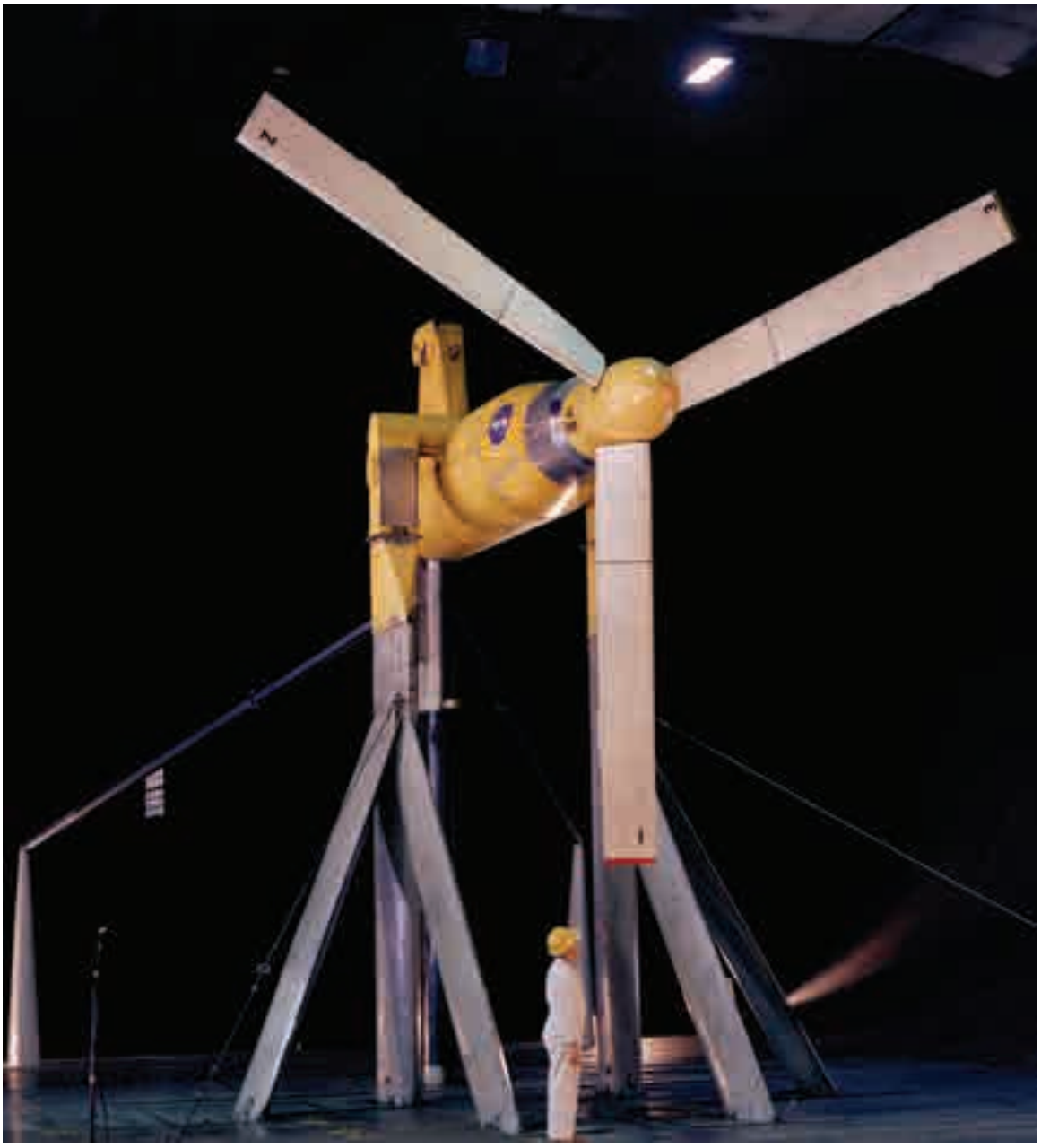

Fig. 2-67. A single XV-15 25-foot-diameter propeller was tested in the 40- by 80-foot wind tunnel at NASA Ames Research Center. Data was obtained in hover at several nacelle tilt angles, and 56 data points were obtained in airplane mode (photo courtesy of Bill Warmbrodt).

The classical study of propeller performance emphasizes the device's propulsive efficiency expressed as

$$\eta_P = \frac{T_P V_{FP}}{P_{actual}}. \tag{2.54}$$

I am not a fan of this generic parameter as you know from reading the discussion in Volume II, pages 219 through 226. So let me start with some fundamentals and then show you results using XV-15 propeller data reported in reference [171]. From the energy approach, you have

$$\begin{aligned} P_{req'd} &= P_{induced} + P_{profile} + P_{propulsion} \\ &= T_P v_{Glauert} \\ &\quad + \rho\left(\pi R^2\right) V_t^3 \left(\frac{\sigma C_{d-average}}{8}\right)\left\{1 + 3\left(\frac{V_{FP}}{V_t}\right)^2 + \left[\frac{9}{8} + \frac{3}{2}\ln\left(\frac{2}{V_{FP}/V_t}\right)\right]\left(\frac{V_{FP}}{V_t}\right)^4\right\} \\ &\quad + T_P V_{FP} \end{aligned} \tag{2.55}$$

where Glauert's ideal induced velocity for a propeller, based on momentum theory, is

$$v_{Glauert} = \frac{1}{2}\left(T_P V_{FP}\right)\left[\sqrt{1 + \frac{4}{\pi}\frac{T_P}{q D^2}} - 1\right]. \tag{2.56}$$

Now these fundamental equations are classically put in coefficient form by two different aerodynamic groups. Rotorcraft engineers would change to coefficient form by dividing through by $\rho\left(\pi R^2\right) V_t^3$, which is what you see as Eq. 2.185 on page 225 of Volume II. Fixed-wing propeller engineers would divided through by $\rho n^2 D^5$. If you refer to Table 2-15 on page 229 of Volume II, you will see how rotor and propeller nomenclature differ in more detail. I propose a third way to nondimensionalize Eqs. (2.55) and (2.56), which is to divide through by $\left(\frac{1}{2}\rho V_{FP}^2\right) V_{FP} D^2$, or simply $q V_{FP} D^2$.[40] This method retains some sense of the propeller's geometry (i.e., diameter or D), dynamic pressure (q), and propeller thrust (T_P), all of which can be easily understood by both engineering groups. Furthermore, the propulsive force coefficient is clearly identified as (T_P/qD^2)—the major variable. With this in mind, I suggest that the examination of the XV-15's isolated propeller performance be studied using

$$\begin{aligned} \frac{P_{req'd}}{q V_{FP} D^2} &= \frac{1}{2}\left(\frac{T_P}{qD^2}\right)\left[\sqrt{1 + \frac{4}{\pi}\left(\frac{T_P}{q D^2}\right)} - 1\right] \\ &\quad + \frac{\pi}{16}\left(\sigma C_{d-average}\right)\left\{\frac{1}{\left(V_{FP}/V_t\right)^3} + \frac{3}{\left(V_{FP}/V_t\right)} + \left(\frac{V_{FP}}{V_t}\right)\left[\frac{9}{8} + \frac{3}{2}\ln\left(\frac{2}{V_{FP}/V_t}\right)\right]\right\}. \\ &\quad + \left(\frac{T_P}{qD^2}\right) \end{aligned} \tag{2.57}$$

[40] George Schairer, Boeing's Vice President of Research and Development, taught me this in 1961 [16]. It has been invaluable to me for over five decades.

The only other thing required in talking to the two engineering groups is that rotorcraft engineers use solidity ($\sigma = bc/\pi R$) instead of Activity Factor ($AF = 100{,}000\pi\,\sigma/128B$), which Barney McCormick addresses [27]. Of course, the number of blades is (b) in the rotorcraft world and (B) in the propeller world, and rotorcraft engineers use the propeller advance ratio ($\mu = V_{FP}/V_t$) instead of ($J = V_{FP}/nD$).

With this background, turn your attention to Fig. 2-68. The propeller performance of the XV-15 can be estimated with relatively simple theory because it is a lightly loaded propeller. Additionally, the helical Mach number, given as

$$(2.58)\quad M_{helical} = \frac{\sqrt{V_{FP}^2 + V_t^2}}{a_s} = \frac{\sqrt{\left(V_{FP}/\sqrt{\theta}\right)^2 + \left(V_t^2/\sqrt{\theta}\right)^2}}{1{,}116},$$

is quite modest. In fact, no data point reported in reference [171] and shown in Fig. 2-68 is greater than 0.73, which is still an incompressible operating condition for this discussion.

Before introducing the drag of the aircraft, which determines the propeller thrust (T_P) required, let me take a moment to address propeller efficiency. You noted earlier that

$$(2.59)\quad \eta_P = \frac{T_P V_{FP}}{P_{actual}},$$

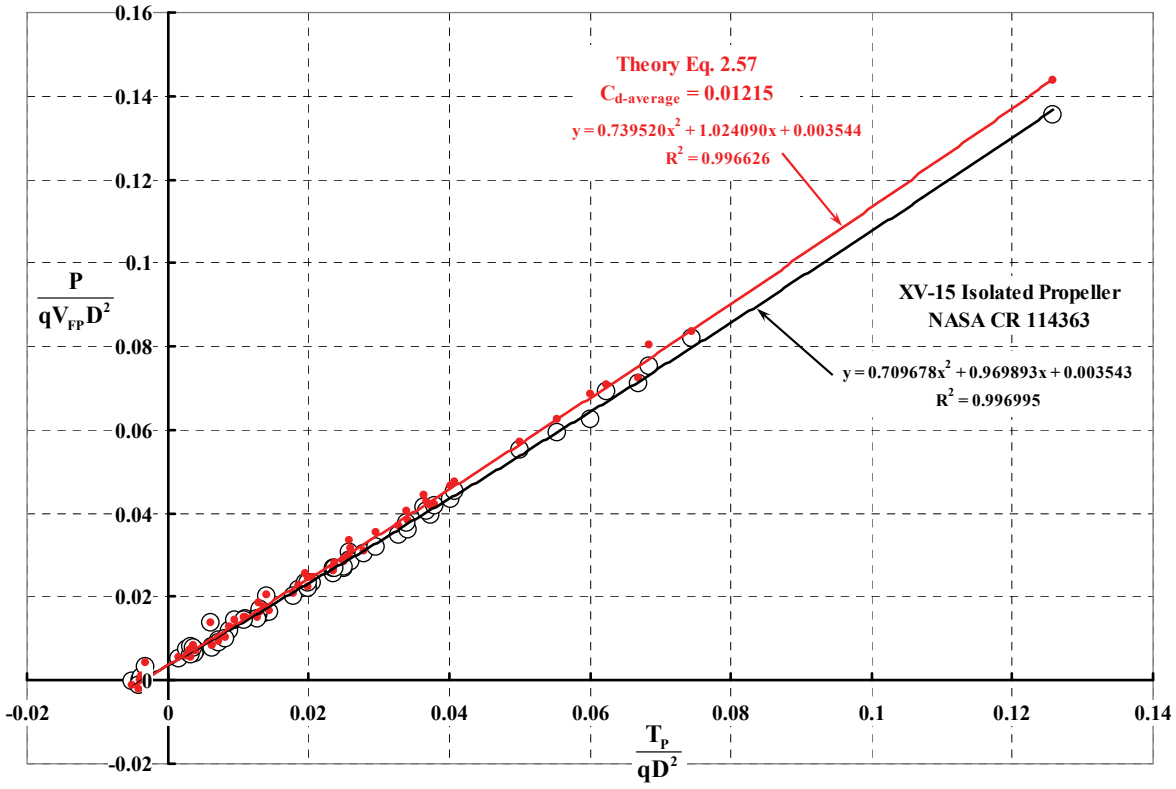

Fig. 2-68. XV-15 propeller performance can be estimated with simple theory.

which immediately says that propeller efficiency depends on the propulsive force coefficient (T_P/qD^2) and the speed ratio (V_{FP}/V_t). Therefore, a family of lines can be constructed as efficiency versus the speed ratio for constant values of the propulsive force coefficient. You see this "design" chart—using the XV-15 propeller as representative—here as Fig. 2-69, which shows you that there is a point of diminishing returns for each propulsive force constant. More importantly, a propeller, like the lightly loaded XV-15 with a solidity of 0.089, benefits enormously by operating at as high a speed ratio as practical design and fabrication will allow. Certainly, weight and cost are factors of particular importance, but the primary emphasis from an aerodynamic performance point of view must start with high propulsive efficiency as Fig. 2-69 shows.

The next step in examining the performance of the XV-15 is to account for aircraft drag ($D_{A/C}$). Aircraft drag is balanced by the thrust of two propellers, and classical airplane theory shows that

$$\text{(2.60)}\quad \text{Left } T_P + \text{Right } T_P = D_{A/C} = qS_{wing}C_{Do} + \frac{1}{\pi q}\left(\frac{W}{b_{wing}}\right)^2 .$$

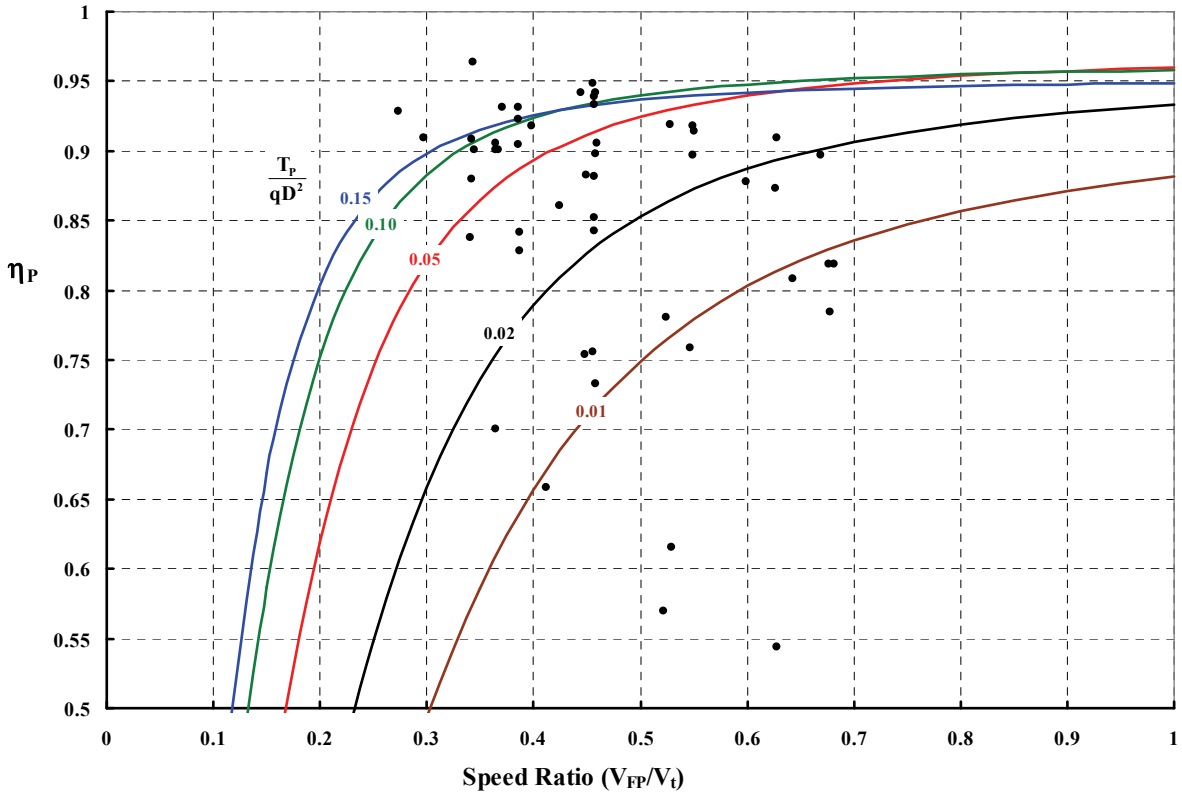

Fig. 2-69. The XV-15 propellers were slowed down to 517 rpm (V_t = 676 ft/sec) for the airplane mode; hover and conversion were accomplished at 589 rpm (V_t = 770 ft/sec). XV-15 experimental data from Fig. 2-68 shown as solid black circles.

You can assume that for trimmed, steady level flight, the left and right propellers are providing equal thrust. And you can also divide through by dynamic pressure (q) and the propeller-diameter squared to get the propulsive force coefficient (T_P/qD^2) of one propeller. This step shows that

$$(2.61)\quad \text{One Propeller's } \frac{T_P}{qD^2} = \frac{1}{2D^2}\left[S_{wing}C_{Do} + \frac{1}{\pi}\left(\frac{W}{qb_{wing}}\right)^2\right].$$

Once the propulsive force coefficient of one propeller is obtained, you only have to use Eq. (2.57) to find the power required of one propeller and then double it to find the total propeller power required for the XV-15. Of course, this is not the total engine(s) horsepower required because the transmission efficiency and accessory power are yet to be included.

The power required data for the XV-15 was reported in reference [172], and the tabulated experimental data offers some results of applying Eq. (2.61) coupled with Eq. (2.57). Fig. 2-70 shows you experimental twin proprotor power required graphed versus simple theory. You can see that rather simple theory captures this turboprop performance quite adequately—at least from the practicing engineer's point of view. The parameters I used in making the theory calculation are listed on Fig. 2-70.

Once an aircraft design is "frozen," there is a surprisingly simple way of calculating total propeller power required for a wide range of altitudes, speeds, and weights. If you accept

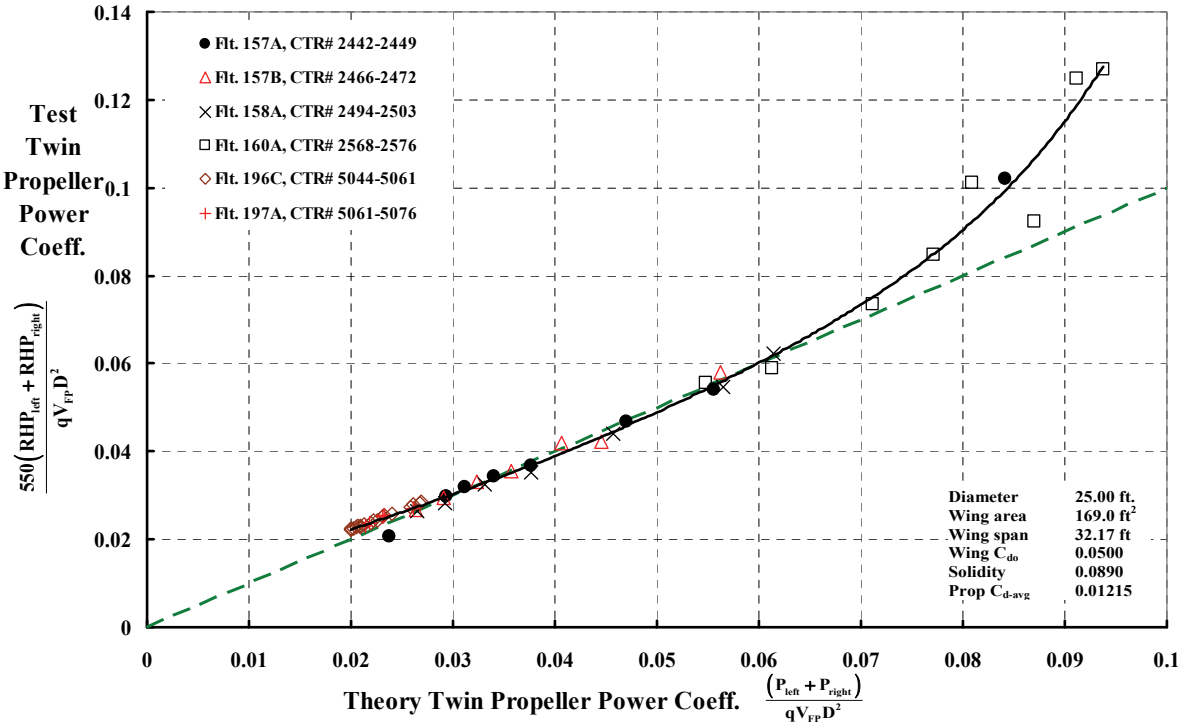

Fig. 2-70. Basic aerodynamic theory can give a rather accurate estimate of performance if separated flow (i.e., stall) and compressibility are not considerations.

that the XV-15 is "frozen" and that *its propeller RPM is constant in the airplane mode*, then flight-test performance data can be used to create a composite aircraft drag plus propeller losses. In essence, the propeller-induced and profile-power losses can simply be folded into a drag polar for the aircraft. That is, you can define a composite drag coefficient as

$$\text{(2.62)}\quad \text{Composite } C_D = \frac{550\left(RHP_{left} + RHP_{right}\right)}{qV_{FP}S_{wing}}$$

and, because the propellers contribute little lift in the airplane mode, a classical fixed-wing lift coefficient based on gross weight is quite satisfactory. You can see from Fig. 2-71 that an approximation of this sort can be very useful, if for no other reason than for interpolation. Of course, you could use the approach to make a first estimate of performance of a scaled-up XV-15 where geometry is scaled proportional to wing area. The scaled-up aircraft must have the same tip speed (i.e., 676 ft/sec) and the same solidity (i.e., $\sigma = 0.089$).

The last point about the XV-15 to be examined is the 300-knot true airspeed reached as part of the envelope expansion [173]. You probably noted this corner of the envelope from Fig. 2-64. Flight 197A (counter numbers 5061–5076) offers a few points to convert to twin-engine power required and then to an estimate of fuel efficiency. Furthermore, the few points from this flight can be extrapolated to a wider speed range using the empirical result from Fig. 2-71 that

$$\text{(2.63)}\quad \text{Composite } C_D = 0.07 + 0.06\left(C_L\right)^2 + 0.003\,e^{7.6(C_L - 1.5)}.$$

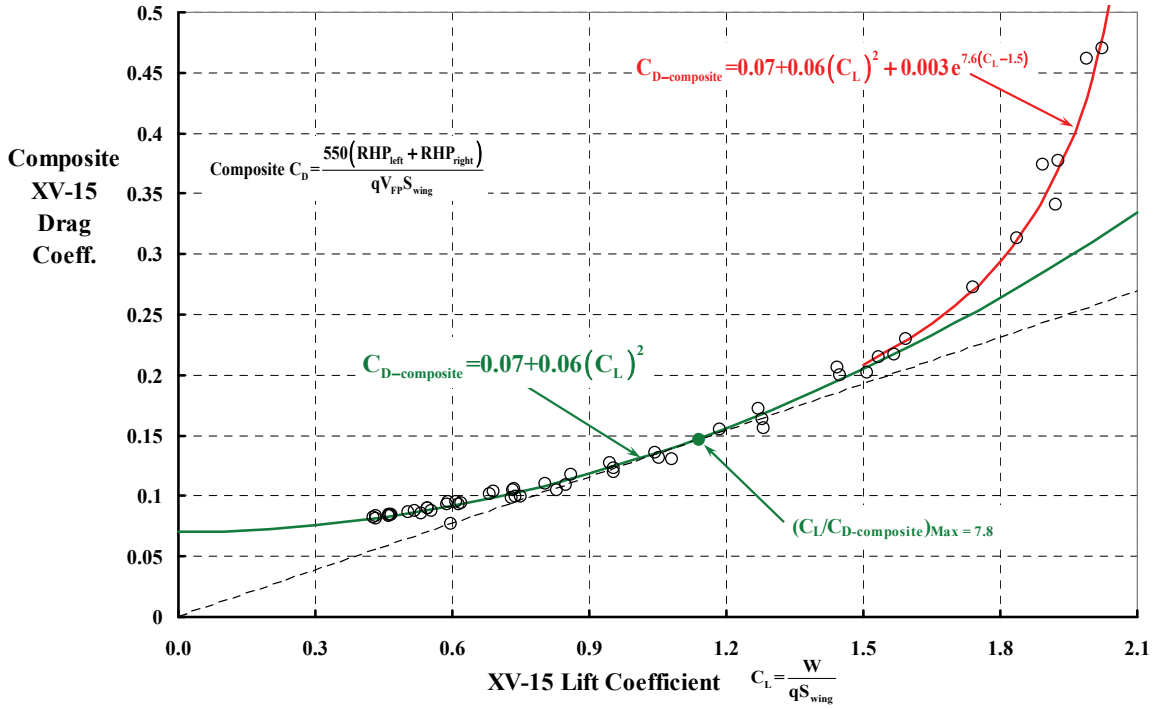

Fig. 2-71. The XV-15 forward-flight-test power required can be collected and describe by a simple curve-fit found empirically.

The propeller shaft horsepower required is converted to engine power required as

$$\text{(2.64)}\quad \text{Twin Engine SHP}_{\text{req'd}} = \frac{\text{Left RHP}_{\text{req'd}} + \text{Right RHP}_{\text{req'd}}}{\eta_{\text{tran}}} + \text{SHP}_{\text{acc}}$$

where, for the XV-15, I have assumed 20 horsepower for accessories and a very low transmission efficiency of 0.91 to estimate the twin-engine power required line shown on Fig. 2-72.[41]

The performance of the XV-15 was primarily limited by rotor shaft torque at 130,000 inch-pounds at density altitudes around 17,000 feet and below. This torque, when the machine is in airplane mode with a rotor speed of 517 revolutions per minute, amounts to 1,067 rotor shaft horsepower. Therefore, the total rotor-shaft power available is 2,134. You can see in Fig. 2-72 that XV-15 operation at a continuous cruise speed of 300 knots (true), even up to a density altitude of 17,400 feet and a gross weight of 13,300 pounds, was within the flight envelope. However, to keep things in perspective, the long-range cruise speed (i.e., the fuel-efficient cruise speed based on specific range) is more like 230 to perhaps 250 knots.

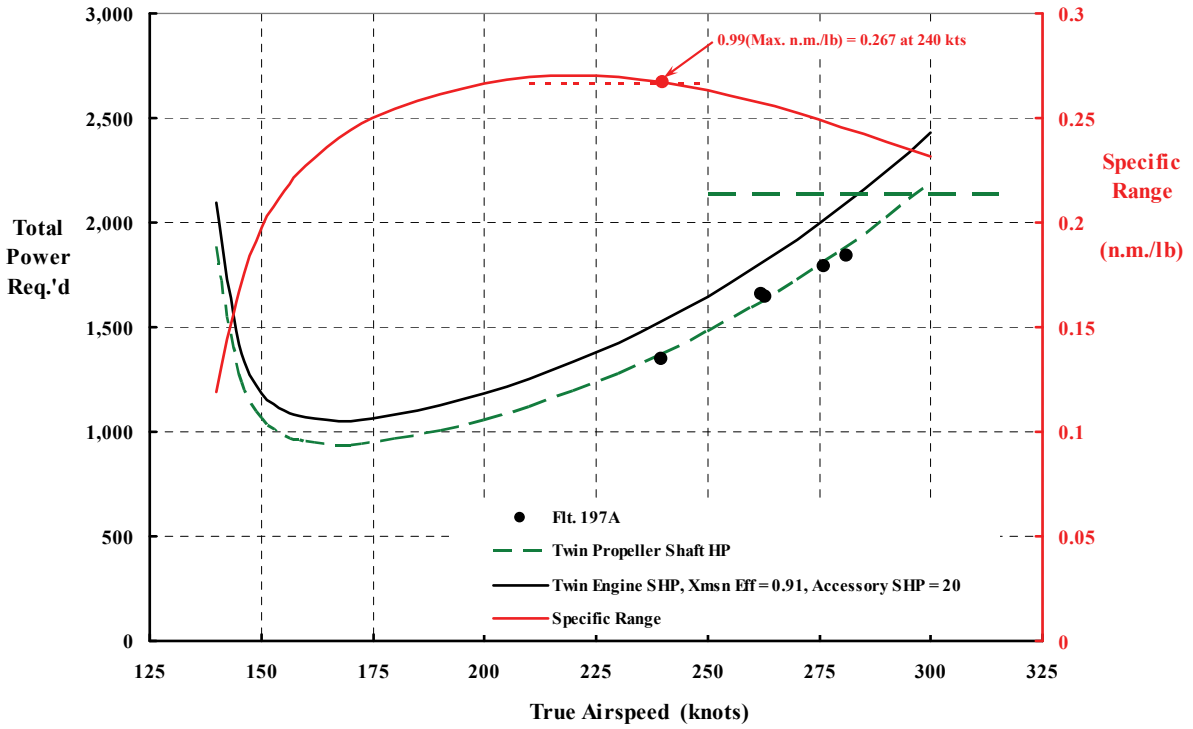

Fig. 2-72. XV-15 performance at a gross weight of 13,300 pounds, density altitude of 17,400 feet, and airplane mode rotor speed of 517 rpm.

[41] Troy Gaffey told me (during a phone conversation in February 2013) that the transmission efficiency was always in doubt. He mentioned that an additional gearbox was required when the decision was made to change from the P&W PT6 to the modified Lycoming T53-L-13B. I estimated the transmission efficiency as 0.91 from the flight test introduction volume [174], figure 1.1-14. Fuel flow data as a function of rotor shaft horsepower contained in reference [174] allowed me to calculate the specific range. You may be able to track down measured fuel flows.

2.10.1 Demonstrator Performance Summary

A summary review of what several companies have accomplished with recent technology demonstrators is provided in Table 2-7. This modern progress, along with compound helicopter research from the 1950s through the 1970s, provides a clear view of the rotorcraft industry's progress to date in combining efficient hovering with airplane-like cruise speeds. My view is shown in Fig. 2-73. There can be no doubt that the industry has made significant progress in reducing installed horsepower per ton of gross weight over the last half century. But from a fixed-wing point of view, rotorcraft advocates still do not have a product that can compete with the propeller-driven airplanes of the 1950s. It is heartwarming to me, however, that there is a growing emphasis on installing enough power for efficient cruise and then seeing what hover performance results. This conceptual design approach is the exact opposite of what we have been doing for decades.

There are a number of points that you might note from Fig. 2-73.[42] The first point is that the performance limit to compounding a helicopter appears approximately set by the Sikorsky X2 TD and the Bell High Performance Helicopter (HPH). Thus, you can imagine a performance band between the conventional helicopter's performance and the upper limit of the compound helicopter. There is a large performance gap between this band and the green line that I have labeled "Boundary of Lowest Performing Airplanes in the 1950s." To get to the right of this imagined band and much closer to the green line, VTOL advocates must reorient the edgewise flying rotor 90 degrees so that the rotor is operating as a propeller. This is the immediate solution to the helicopter's hub drag problem and the rotor limitations of edgewise flying rotors.

The second point deals with the Bell XV-15 tiltrotor data point shown on Fig. 2-73. The Bell XV-15 (Fig. 2-53) has been heralded by many as a major step forward in rotorcraft performance. But I would say that this configuration advancement in rotorcraft technology still falls far short of airplane performance in the 1950s. That is to say, the tiltrotor as now conceived is not good enough. Think about it this way: The Bell XV-15 point says that with a power-loading engine shaft horsepower (ESHP) / (GW/2000) of about 400, this tiltrotor can achieve 300 knots. Modern conventional helicopters—at the same value of power loading—should go 175 knots. So on the positive side, this tiltrotor is an improvement of 125 knots or about 70 percent (i.e., 300/175). On the other side of the coin, 1950's airplanes could achieve 380 knots with a power loading of 400, which is 25 percent (i.e., 380/300) faster than the XV-15. Therefore, there is considerable room for improvement.

Finally, you might argue that these are just technology demonstrators and that performance is not the only requirement. Comparisons including weight empty, payload range, purchase price, operating costs, noise, safety, etc., may ultimately expose the real winner. Being an aerodynamicist at heart, I say, "First things first."

---

[42] You will recognize this coordinate system from the frontispiece in Volume I and from the concluding figure in Volume II on page 702. If an aircraft configuration does not shine on this chart, I am inclined to think negatively. My V/STOL performance goal is, without doubt, von Karman and Gabrielli's limit line [175].

Table 2-7. Five Recent High-Speed Technology Demonstrators

Reference	Perry [143]	Mecklin [144]	Walsh [145]	Harris' Estimate	Maisel [37]
Company	Westland	Boeing	Sikorsky	Eurocopter	Bell
Aircraft	G-Lynx	Model 360	X2 TD	X^3	XV-15
Date	Aug. 11, 1986	Oct. 23, 1989	Sept. 15, 2010	May 12, 2012	June 17, 1980
True airspeed (kts)	216.3	214	250^+	232	301
Advance ratio	0.50	0.517	0.768	0.688	0.752
Mach no. $M_{1,90}$	0.977	0.951	0.883	0.979	na
Mach no. $M_{helical}$	na	na	na	na	0.758
Gross weight (lb)	8,685	30,500	6,000	10,000	13,000
SHP at speed (hp)	2,400	7,000	1,490	3,450	2,500

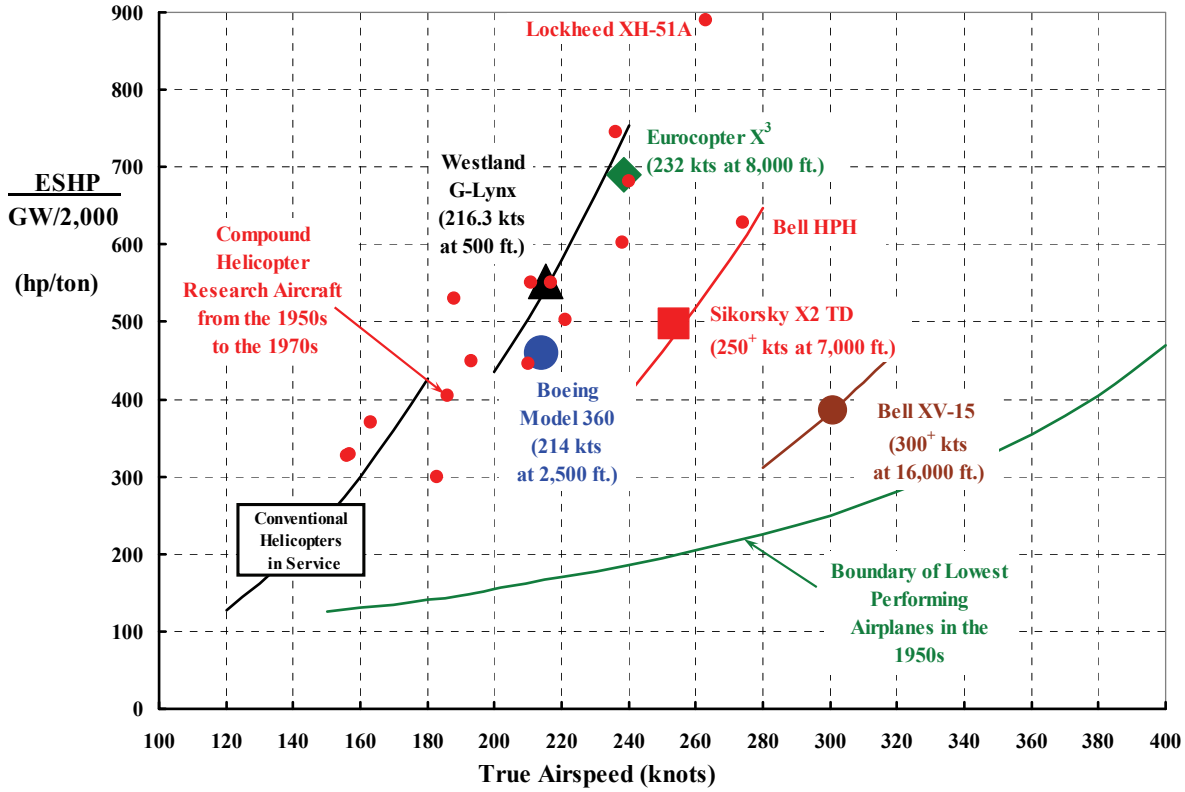

Fig. 2-73. The rotorcraft industry has recently demonstrated several high-speed VTOL concepts. However, achieving this high speed has required installing more power than the industry typically would install when efficient hovering performance is the primary design goal.

2.10.2 Closing Remarks

The theoretical and experimental explorations of rotor propulsion and lifting capability have created some very fundamental implications about the aerodynamic performance of the conventional helicopter. To begin with, a conventional edgewise flying rotor has a very limited propulsive force capability above a forward-speed-to-tip-speed ratio of 0.6. In fact, the edgewise flying rotor cannot propel at all at an advance ratio of 1.0, as simple theoretical considerations such as Eq. (2.7) show. Furthermore, experimental data show that beyond an advance ratio of 0.5 to 0.6 the practical helicopter that we know today ceases to exist because the rotor can hardly overcome its own drag, much less the drag of the rest of the helicopter.[43]

Propulsive force limitations associated with edgewise flying rotors are overcome by adding some form of auxiliary propulsion. However, it is not at all clear that the rotor needs a wing as an auxiliary lifting device—if the rotor can be operated at forward-speed-to-tip-speed ratios of 1.0 or greater. A relatively meager amount of experimental data suggests that a conventional rotor operates like a fixed wing where you can assume that

$$C_L = \frac{L}{\left(\frac{1}{2}\rho V_{FP}^2\right)(bcR)},$$

and maximum lift to drag can be obtained if C_L equals about 0.20.

Let me close this chapter with a short, simple discussion of what it takes to cruise and hover efficiently. Suppose the basic performance equations for the two flight regimes are simply, for a propeller or rotor in hover,

$$\text{(2.65)}\quad \text{Hover } SHP_H = \frac{W}{550(FM)}\sqrt{\frac{W}{2\rho_H A}} \quad \Rightarrow \quad W = \frac{550(FM)SHP_H}{\sqrt{\frac{W}{2\rho_H A}}}$$

and for cruise,

$$\text{(2.66)}\quad \text{Cruise } SHP_{CR} = \frac{W}{550\eta_P (L/D)}V_{CR} \quad \Rightarrow \quad V_{CR} = \frac{550\eta_P (L/D)\, SHP_{CR}}{W}.$$

Now, substitute the expression for weight (W) from the hover equation, Eq. (2.65), into the expression for cruise velocity (V_{CR}), Eq. (2.66), which gives you

$$\text{(2.67)}\quad V_{CR} = 12.61\left(\frac{SHP_{CR}}{SHP_H}\right)\left(\frac{\eta_P}{FM}\right)\left(\frac{L}{D}\right)\sqrt{\frac{W}{(\rho_H/\rho_O)A}} \quad \text{in knots}$$

---

[43] My first paper [176], presented at the American Helicopter Society Annual Forum on May 3, 1961, dealt with this very subject. In that paper, I brashly stated that the conventional rotor "as a helicopter propulsive device, ceases to exist at forward speed between 250 and 260 knots." This statement reached my father and mother through the press while dad was on duty in Formosa (now Taiwan).

where the cruise propulsive efficiency is denoted by (η_P), and a typical value would be at least 0.85 while an ideal value would be 1.0. The hovering Figure of Merit (FM) is about 0.70, up to maybe 0.8, given a breakthrough. The density (ρ_H) depends on a specified hovering ceiling, which could vary from sea level on a standard day (i.e., $\rho_H = \rho_o = 0.002378$ slugs per cubic foot) up to a military hovering ceiling requirement of, say, 6,000 feet (pressure altitude) on a 95 ^oF day where density equals 0.001781 slugs per cubic foot. The weight is lifted in hover by an actuator disc(s) having a total area (A) in square feet. Every configuration I can think of has a lift-to-drag (L/D) ratio in cruise, which I will discuss in more detail shortly.

You can see from Eq. (2.67) that the *ratio* of the cruise power required (SHP_{CR}) to the power required to hover (SHP_H) is a prime variable when discussing VTOL performance. Yes, the choice of an engine is quite key; however, finding a configuration having efficient hover performance matched to efficient cruise performance depends on the ratio (SHP_{CR}/SHP_H), and this is a characteristic of any particular engine. This ratio will vary with the hover and cruise altitudes that are specified, as you can see from Fig. 2-74. Furthermore, the common design practice is to hover at takeoff power and cruise no faster than permitted by the engine's maximum continuous power. This means that the power ratio is less than 1.0, even before considering the altitude specifications.

The lift-to-drag ratio of the VTOL aircraft is also a prime variable in this discussion. Because it appears from Fig. 2-73 that the VTOL aircraft should approximate an airplane in forward flight in order to be competitive, let me assume that any VTOL aircraft has a classical airplane drag polar of the form

$$(2.68)\quad C_D = C_{Do} + \frac{C_L^2}{\pi e AR}\,.$$

Then, from this fundamental, you have the fact that the maximum lift-to-drag ratio will be

$$(2.69)\quad \text{Airplane}\left(\frac{L}{D}\right)_{Max} = \frac{1}{2}\sqrt{\frac{\pi A\,Re}{C_{Do}}}\,,\ \text{which is obtained at } C_L = \sqrt{\pi AR\,e\,C_{Do}}\,.$$

Of course, the actual geometry of any particular VTOL in forward flight will quite likely be more complicated. For instance, a VTOL configuration that uses a rotor to hover (and that rotor only provides lift in forward flight) will need auxiliary propulsion. I have in mind the compound helicopter you saw earlier in Fig. 2-20, which Sikorsky engineers evaluated when they explored the Reverse Velocity Rotor. A configuration of this sort would have a lift-to-drag ratio calculated as

$$(2.70)\quad \frac{L}{D} = \frac{L}{D_E + f_e q_{CR}} = \frac{L/D_E}{1 + \frac{L}{D_E}\left(\frac{f_e}{W}\right) q_{CR}}\,,$$

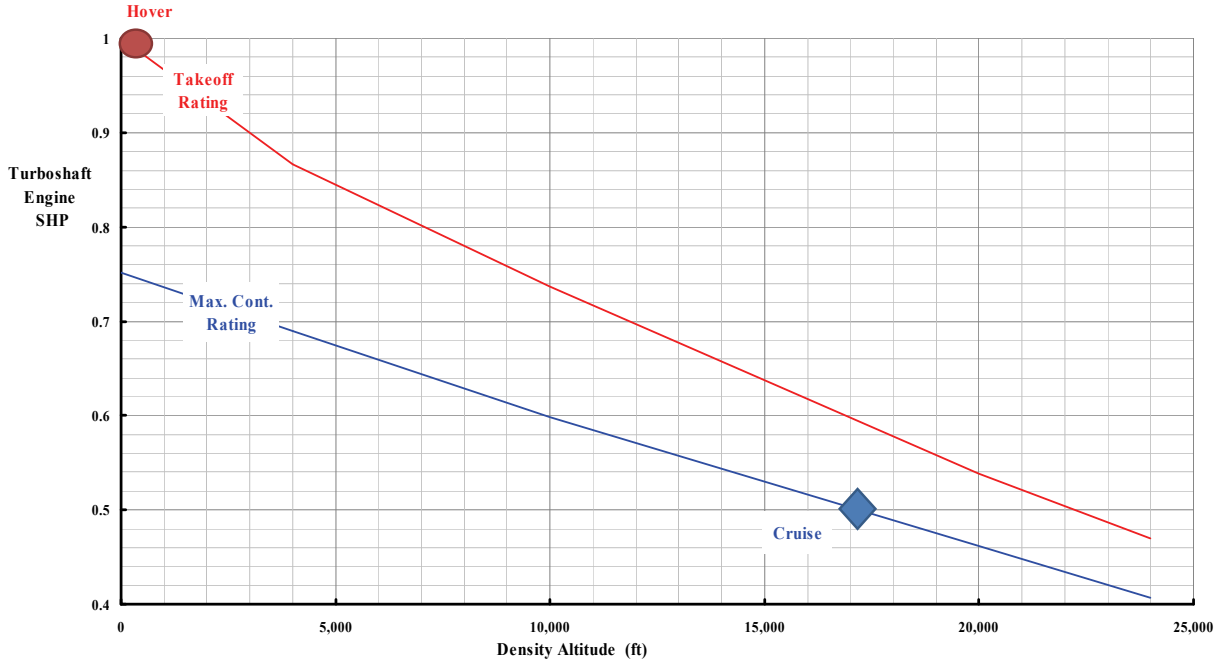

Fig. 2-74. Typical performance of turboshaft engines.[44]

and the maximum lift-to-drag ratio would require a little more study because the parasite drag area (f_e) of the configuration must be established, and the rotor lift to effective drag (L/D_E) must be estimated with reasonable accuracy. Of course, the design cruise speed must be selected before dynamic pressure in cruise $\left(\frac{1}{2}\rho_{CR}V_{CR}^2\right)$ can be calculated.

Lastly, note in Eq. (2.67) that the aircraft disc loading (W/A) and the density ratio ($\sigma = \rho_H/\rho_0$) at the hovering altitude are both important. My nomenclature calls $W/\sigma A$ the density-weighted disc loading in pounds per square foot.

Now let me offer a numerical example so my thoughts are clearly conveyed. Suppose you want to search for a civil transport that might be attractive to, say, Southwest Airlines for a short-haul route structure. Or perhaps the military has a reasonably well defined mission. Maybe the aircraft could have even greater worldwide appeal in countries with less infrastructure than the United States. Suppose marketing department analysis indicates that hovering at 5,000 feet ($\sigma = 0.8616$) and cruising at 23,000 feet would be very attractive to many, many potential buyers. This would mean that the power ratio (SHP_{CR}/SHP_H) would be 0.5 given a trend such as shown in Fig. 2-74. Reasonable engineering experience would suggest that large-diameter rotors down to relatively smaller propellers can be designed that have an FM of, say, 0.75. Just as reasonably, the propulsion device(s)—say, for this example, a set of rotors or even just one propeller—can be provided having an efficiency of 0.85.

[44] Gerardo Nunez, a key member of the Army Concept Development Group at NASA Ames Research Center, was kind enough to prepare this chart for me. I owe him big-time.

This top-level information means that the cruise speed equation, Eq. (2.67), numerically simplifies to

$$(2.71)\quad V_{CR} = 7.146\left(L/D\right)\sqrt{\frac{W}{\sigma A}} \text{ in knots.}$$

Now you can clearly see that cruise speed can be increased by raising the aircraft's lift-to-drag ratio, which is hardly new news. Furthermore, low-density-weighted disc loadings lead to low cruise speeds, which may not be new news. The reason for this latter fact is that low disc loadings mean low installed takeoff power. But low installed takeoff power means lower maximum continuous rated power for cruising as Fig. 2-74 shows.

Equation (2.71), when graphed as you see in Fig. 2-75, offers an interesting perspective of how the key design parameters affect a high-cruise-speed VTOL. Consider the design problem created if the marketing department believes that a maximum continuous cruise speed of 400 knots is absolutely essential to "leap frog" the competition and capture a lion's share of the world market. Four hundred knots can be obtained by a density-weighted disc loading of 30 and a lift-to-drag ratio of 10. That cruise speed can also be obtained with a higher disc loading of about 90 pounds per square foot and an aircraft L/D of 6. Of course, there is a range of choices in between those two points. Naturally, it takes a little more conceptual design work—after gross weight (W) is specified—to define the desired engine takeoff and maximum continuous ratings, then the weight empty and, finally, the selling price.

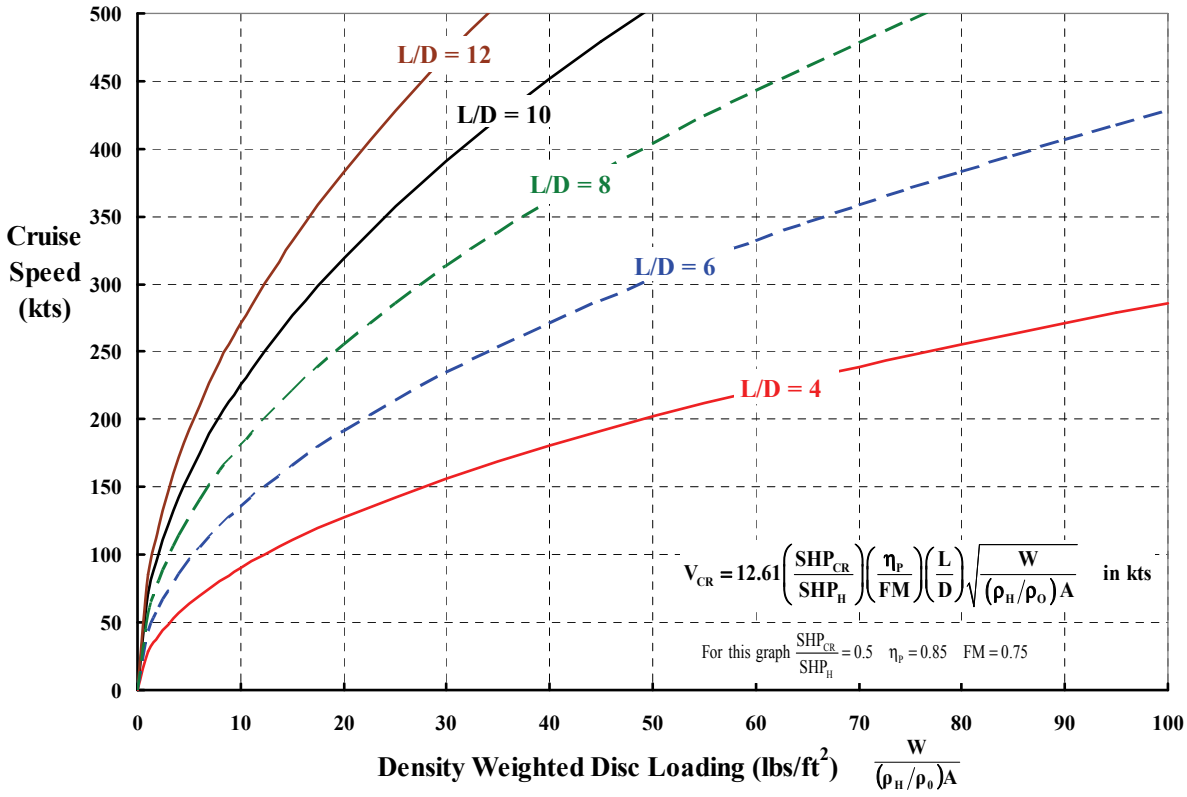

Fig. 2-75. A fundamental top-level-concept design chart.

Fig. 2-75 raises a very important point. Military pilots have experienced considerable trouble with high-disc-loading helicopters (and the U.S. Marines V-22 Osprey, as well) because the downwash velocity in and near hover kicks up a severe dust and debris storm on the generally unprepared landing and takeoff areas that military machines are expected to operate from. These dust storms severely restrict visibility. Therefore, today's military design standard tends to restrict disc loading to approximately 20 pounds per square foot or less. *If* the concept VTOL aircraft can achieve a lift-to-drag ratio of 10, then Fig. 2-75 says that a maximum cruise speed of about 300 knots is all that should be expected. The commercial operator currently does not have such a severe disk loading restriction because most landings and takeoffs are from prepared surfaces. This means that there can be a very big difference between military and commercial VTOL aircraft—a difference so big that a VTOL aircraft developed by and for the military is almost certainly not going to be one that commercial operators might want, given a choice. The commercial operator wants speed and expects to get it with a fuel-efficient aircraft. These are serious considerations that must be kept in mind when there is a perception that a military-developed product can be spun off into a commercial product.

You will notice that the computations leading to Fig. 2-75 were made assuming a propeller efficiency (η_P) of 0.85. Based on Fig. 2-69, you might think that I have been conservative choosing this level of efficiency. However, there are substantial differences in design and performance between heavily loaded propellers such as those used on the Sikorsky X2 and Eurocopter X^3 and lightly loaded proprotors as used on the Bell XV-15. Furthermore, the differences are magnified when compressibility becomes a factor. Historically, propeller diameter has, on more than one occasion, been dictated by tip clearance to the ground despite the fact that the propeller designer would plead for a larger diameter selection. I would suggest that both compound helicopter configurations found this to be the case. With this constraint, the designer is forced to push up propeller tip speed to near, or higher, sonic values and increase solidity by increasing blade chord (and/or number of blades) to absorb the power required to obtain required thrust.

A proprotor as used by the XV-15, in contrast to a propeller, really frees up the designer so that he must only find a configuration that balances hover requirements with forward flight requirements. In my view, this is a much more straightforward design problem. As you learn more about tiltwings and tiltrotors in the following sections, you might keep these last few thoughts in mind.

2.11 THE LTV XC-142 TILTWING AND THE BELL BOEING V-22 TILTROTOR

Finally, after decades of searching, rotorcraft advocates firmly established that configurations using edgewise flying rotors have not given them their "cake and eat it too" solution. In increasing numbers, the community is accepting the fundamental fact that rotors of some diameter must operate and perform like propellers so high-speed cruising comparable to aerodynamically efficient airplanes can be combined with vertical takeoff and landing. In my view, this realization has been slow in coming because there have been far too few helicopter engineers with any fixed-wing background in the design offices. From a technology point of view, helicopter engineers have continually focused on all aspects of rotor systems and the slow-speed helicopter products to which they are attached. But the simple aerodynamic fact is that if you take a typical rotor hub (never mind the blades) and mount it on an efficient airplane (i.e., a maximum lift-to-drag ratio in the range of 12 to 18), you have ruined the airplane's performance. A fixed-wing aerodynamicist will tell you that the *rotor system's hub alone adds drag comparable to unretracted landing gear*. To fixed-wing experts, adding a hub is a big step backwards in airplane design.

The idea that a rotor is wanted for hovering and a propeller is wanted for cruise ultimately boiled down to a tiltwing, Fig. 2-76 [39, 177-179], and a tiltrotor, Fig. 2-77 [34, 180]. The distinction between a rotor and a propeller is more one of size, specifically diameter, rather than function, because both devices can be used to hover an aircraft. A large-diameter propeller is 10 to 20 feet; a large-diameter rotor runs between 40 to 100 feet. The distinction between propeller and rotor became blurred, and this led to the coining of the word "proprotor" by tiltrotor advocates. The examples on the following page should suggest to you that either aircraft can be hovered on heavily loaded propellers or lightly loaded rotors (or anywhere in between for that matter). I use the words *heavy* and *light* but I am really referring to disc loading, which is the ratio of weight to total disc area (W/A_{total}). Let me illustrate the difference using the two examples that follow.

The team of Vought, Hiller, and Ryan (VHR) (Vought later became a division of Ling-Temco-Vought) was the winner of the Tri-Service competition that the Department of Defense ordered the United States Army, Navy, and Air Force to run. This combined effort led to a signed contract with the VHR team for five prototypes on January 5, 1962, and the XC-142 program was off and running. During the development program, the Navy decided against further participation because they felt the downwash from the four propellers would blow people about (and maybe even overboard). The Navy's concern can be quantified this way: The maximum takeoff gross weight of the XC-142 was about 41,500 pounds, and each four-bladed propeller had a diameter of 15.625 feet. Therefore, the total disc area was 4×191.7 or 766.8 square feet, and the disc loading at sea level standard day was 54.1 pounds per square foot. Following simple momentum theory for propellers and rotors, the slipstream velocity hitting a Navy ship deck—or in the Army and Air Force's case, the ground—is calculated as

$$(2.72)\quad V_{downwash} = 2\sqrt{\frac{W}{2\rho A_{total}}} = 2\sqrt{\frac{41{,}500}{2(0.002378)(766.8)}} = 213 \text{ fps} = 145 \text{ mph}.$$

Fig. 2-76. The XC-142 tiltwing was built by Ling-Temco-Vought and Hiller and Ryan after they won the U.S. Air Force Tri-Service competition for an assault transport. The 41,500-pound aircraft, with a weight empty of 24,700 pounds, first flew on September 29, 1964.

Fig. 2-77. The Bell Boeing V-22 tiltrotor is now in service with the U.S. Marines as an assault transport. This 52,600-pound aircraft, with a weight empty of 33,140 pounds, first flew on March 19, 1989.

For the V-22 tiltrotor, two 38-foot-diameter proprotors (2 × 1,134.1 or 2,268.2 square feet) lift a 52,600-pound machine, which gives a disc loading of 23.2 pounds per square foot and a downwash velocity of 95 miles per hour. Because force is proportional to velocity squared, you can say, to the first approximation, that the V-22 is creating about one-fifth of the problem that the Navy was anticipating from the XC-142's downwash. Had the XC-142's proprotor diameter been 23.9 feet, the downwash velocity would have equaled the V-22's.

The other significant difference between the XC-142 tiltwing of the 1960s and the V-22 tiltrotor of the 1980s is the ideal power required to hover. Ideal power required to hover is obtained from

$$\text{(2.73)}\quad \text{Hover } HP_{ideal} = \frac{W}{550}\sqrt{\frac{W}{2\rho A_{total}}}\,.$$

This leads to an ideal power for the XC-142 of 8,049 horsepower versus the installed takeoff power obtained from the four General Electric T64-GE-1 engines (4 × 3,080) of 12,320 shaft horsepower. In contrast, the V-22's ideal power is 6,678 versus its installed 12,300 shaft horsepower from two Rolls-Royce AE-1107C engines. This simple comparison illustrates just how powerful large-diameter proprotors can be in hover performance.

Let me stop right here and say that there is no fundamental reason against putting four larger-diameter proprotors on a tiltwing such as the XC-142. The ideal power of the XC-142 can be made equal to the V-22's 6,678 horsepower simply by increasing the proprotor diameter from 15.625 to 18.68 feet. Nor is there any fundamental reason against decreasing the diameter of the two proprotors on a tiltrotor such as the V-22. The ideal power of the V-22 can be made equal to the XC-142's 8,079 horsepower simply by decreasing the V-22's proprotor diameter from 38 feet to 31.53 feet. This illustrates a fundamental difference between fixed and rotary designers. Fixed-wing advocates have grown up thinking propellers and rotary wing advocates have grown up thinking rotors. To me, it is a rather unfortunate state of affairs, even today, because the XC-142 could have easily accommodated proprotors of a diameter that would have lowered the downwash velocity to values that were acceptable to the Navy. (More design-oriented criteria became available in 1992 [181]). This step might have carried the XC-142 further towards production, and then the aviation world would have had a production VTOL some 20 years before tiltrotors such as the V-22 came along. Of course, this would have required more desire for the tiltwing by the U.S. Army, Air Force, and Navy. In contrast, the U.S. Marines were bound and determined to have a tiltrotor, the V-22, and they got what they wanted from the Bell Boeing team. There are currently some 250 V-22s in service. Now to continue.

Fig. 2-76 and Fig. 2-77 each show aircraft in hover, however the proprotor's horizontal placement has been accomplished in quite different ways. The tiltwing has the engines and propellers hard-mounted to the wing. To reach the airplane state, the wing tilts the whole wing-engine-proprotor assembly forward 90 degrees as a unit. The tiltrotor has the wing hard-mounted to the fuselage, and the wing-tip-mounted engines and proprotors tilt forward 90 degrees to achieve the airplane state. Of course, the details of how the proprotors are varied between 0 and 90 degrees are different, but the primary objective of using the same propulsion package for hover and airplane states is achieved. This is as close to a hummingbird as aeronautics has come after decades of searching.

2.12 THE PATH TO THE EXPERIMENTAL XC-142 TILTWING

The tiltwing configuration began with the Vertol Aircraft Corporation Model 76, (the military designation was VZ-2) shown in Fig. 2-78, which made its first flight in August of 1957. Development of the tiltwing configuration came to an end with the last flight of the XC-142A on May 5, 1970. In between, there was very limited success with the Hiller X-18 and considerable success with the Canadair CL-84, both of which you will read about later. You should know a little bit about each of these VTOLs, so let me start with the Vertol Model 76.

2.12.1 The Vertol Model 76

A very thorough discussion of both the program and the aircraft was published in August of 1963 by the then-Vertol Division of the Boeing Company [182]. This final report was prepared for the U.S. Army under the direction of the Office of Naval Research (ONR). No specific authors are singled out; rather the preface acknowledges the key players in this "Skunk Works" style program. The chronology of the aircraft program, clearly recorded on the insides of the front and back covers of this report, is well worth including here:

Fig. 2-78. The Vertol VZ-2 tiltwing. This 3,500-pound VTOL technology demonstrator, piloted by Leonard Lavassar, made its first hovering flight on August 13, 1957. The first full conversion back and forth from hover was made on July 15, 1958.

"15 APRIL	1956	VERTOL DIVISION AWARDED CONTRACT NOnr 2136(00) TO DESIGN, CONSTRUCT, AND FLIGHT TEST THE U.S. ARMY VZ-2 TILTWING AIRCRAFT
1 APRIL	1957	ROLLOUT OF VZ-2
30 APRIL	1957	FIRST RUN-UP OF VZ-2
25 JULY	1957	COMPLETED 10 HOUR TIEDOWN TEST
13 AUGUST	1957	FIRST HOVER OF VZ-2
7 JANUARY	1958	FIRST AIRPLANE FLIGHT OF VZ-2
28 MARCH	1958	COMPLETED HOVER AND AIRPLANE FLIGHT PROGRAM
10 APRIL	1958	STARTED 50 HOUR TIEDOWN TEST
29 APRIL	1958	COMPLETED 50 HOUR TIEDOWN TEST
16 MAY	1958	STARTED FLIGHT BUILD-UP FOR CONVERSION
15 JULY	1958	FIRST FULL CONVERSION OF VZ-2 FROM HOVER TO FORWARD FLIGHT AND BACK TO HOVER
14 APRIL	1959	COMPLETED FLIGHT PROGRAM
15 APRIL	1959	EJECTION SEAT TESTED AT PHILADELPHIA NAVAL BASE
24 APRIL	1959	ARRIVED AT EDWARDS AIR FORCE BASE FOR ALTITUDE FLIGHT PROGRAM
8 OCTOBER	1959	COMPLETED ALTITUDE FLIGHT PROGRAM AT EDWARDS
20 NOVEMBER	1959	FLIGHT PROGRAM STARTED BY NASA AT LANGLEY FIELD
18 JULY	1960	DROOP SNOOT INSTALLED AND TESTED ON WING AT LANGLEY FIELD
5 JANUARY	1961	COMPLETED FLIGHT PROGRAM AT LANGLEY FIELD
9 FEBRUARY	1961	FULL-SCALE WIND TUNNEL TEST OF VZ-2 BY NASA AT LANGLEY
22 MARCH	1961	VZ-2 RETURNED TO VERTOL DIVISION FOR INSTALLATION OF FULL SPAN FLAP AND AILERONS AND UP-GRADING OF TRANSMISSION
7 NOVEMBER	1961	STARTED 50 HOUR TIEDOWN TEST OF MODIFIED CONFIGURATION
16 NOVEMBER	1961	COMPLETED 50 HOUR TIEDOWN TEST
20 AUGUST	1962	STARTED FLIGHT PROGRAM AT VERTOL DIVISION
7 SEPTEMBER	1962	COMPLETED FLIGHT PROGRAM AT VERTOL DIVISION
18 SEPTEMBER	1962	EXTENDED FLIGHT PROGRAM STARTED BY NASA AT LANGLEY FIELD
17 JANUARY	1963	COMPLETED HOVER FLIGHTS AT LANGLEY FIELD
26 AUGUST	1963	NASA CONTINUING VZ-2 FLIGHT"

Reference [182] points out in the summary:

> "In parallel with the design phase, model force and free flight tests were conducted at NASA, Langley Field, and a dynamically similar model was tested at the Forrestal Research Center of Princeton University. During the earlier phases of development, full-scale propeller tests were performed in the 40 foot by 80 foot wind tunnel at NASA Ames Research Center, Moffett Field, California. Prior to the first hover on 13 August 1957, ground instability tests, preliminary 10 hour tiedown tests, and taxi tests were accomplished. Additional hover and taxi tests indicated various problem areas. However, no modifications were required before airplane flights which were started on 7 January 1958."

I had been at Vertol for just over a year and had the very exciting privilege of witnessing the first try at hovering by Leonard Lavassar on August 13, 1957. I say "try" because after the wheels came off the ground, the aircraft did a few pitch oscillations that Leonard could not damp out. He got back on the ground with perfect timing so that only the tail wheel assembly was damaged. Reference [182] includes a paragraph on this incident, which reads:

> "2. Hover Tests - The initial hover flight attempt showed certain control deficiencies. It was desired to hover a few feet off the ground during the initial flight. However, owing to a

sensitive collective pitch system, the aircraft rose rapidly to an altitude of approximately 10 feet. Difficulty in controlling the aircraft about the pitch axis was encountered. This was due to the low sensitivity of the longitudinal control system near the neutral position. The pilot immediately landed the aircraft.

The collective pitch sensitivity was reduced approximately 40 percent. In addition, the longitudinal control system was modified to provide for a more sensitive stick gradient near neutral and an overall increase in control. The final longitudinal control provided a maximum pitching acceleration of approximately 0.6 radian per second per second in hover. The directional control was also modified in a manner similar to the pitch control."

From then on the program continued without major incidents.

The aircraft was powered by a Lycoming YT53-L-1 engine that was rated at 850 shaft horsepower (SHP), but the maximum useable power was 650 SHP because of limits in the drivetrain, which is shown in Fig. 2-79. The three-blade proprotors had a diameter of 9.67 feet. The blades were of 13-inch constant chord, which makes the solidity (σ) 0.215. The two proprotors operated at 1,416 rpm giving a tip speed of 717 feet per second. With respect to performance, the report [182] shows that in hover at the nominal thrust coefficient (C_T) of 0.0188, the power coefficient (C_P) was 0.0024. This works out to an *aircraft* Figure of Merit of 0.76. In forward flight the aircraft was capable of a maximum speed of 126 knots at a gross weight of 3,500 pounds when flown at the transmission limit of 650 SHP. Thus, the horsepower per ton of gross weight was on the order of 370.

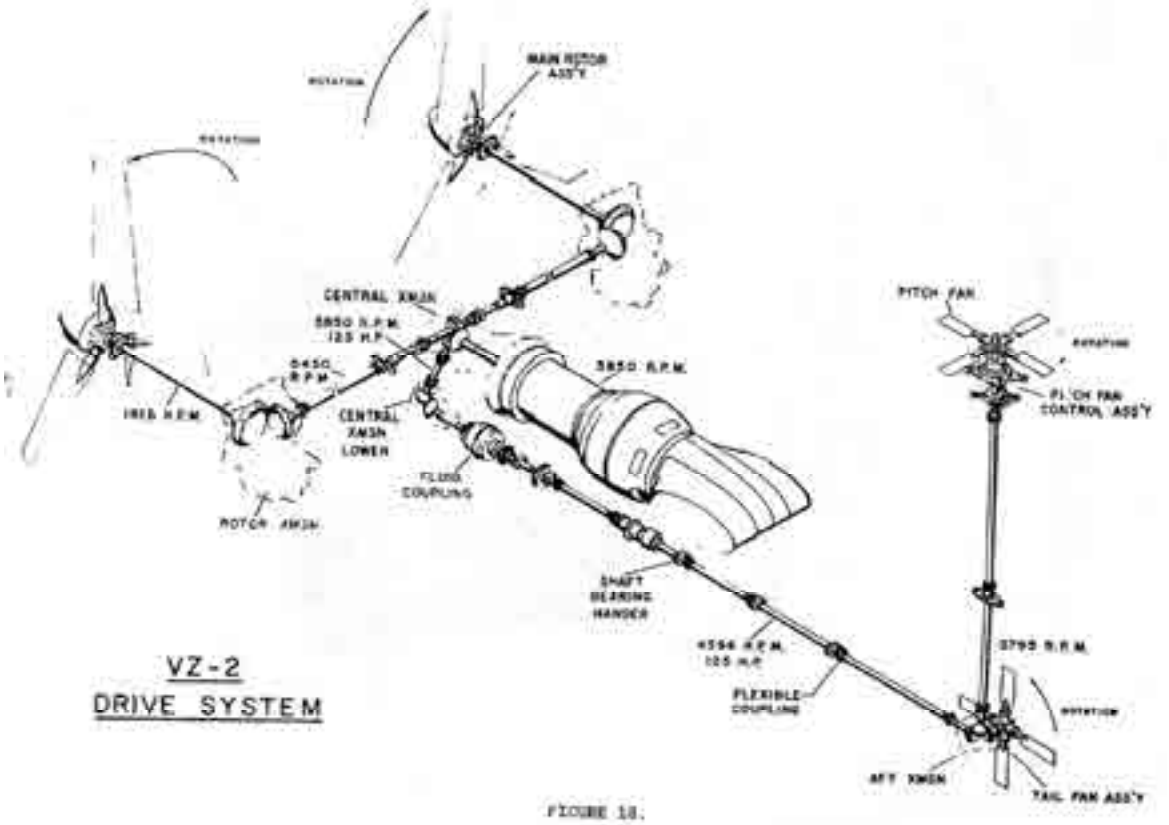

Fig. 2-79. The VZ-2, the first tiltwing, made good use of Piasecki's (then Vertol Aircraft Corporation's and then the Vertol Division of the Boeing Company's) tandem rotor helicopter drivetrain experience.

There is a great deal more technical data and history I might pass on to you just based on the report [182] and its references from the Vertol Division of Boeing, as well as the many NASA reports that were published [183-200]. I will summarized VZ-2 technical data in a table later. However, one technical issue that NASA addressed was the problem of wing stalling during a transition and particularly in descent. After an early flight evaluation, a NASA evaluation was published [183] by Bob Pegg. The conclusions stated:

> "1. Pitch and roll pulse inputs initiated an oscillation which expanded at such a rapid rate as to appear as a divergence on the first swing through the trim position.
>
> 2. The aircraft shows increasing positive speed stability with decreasing airspeed, a condition which can cause large variations in the pitching moment with inadvertent changes in airspeed.
>
> 3. Hovering control power of the aircraft is considered by the pilot to be inadequate in yaw, marginal in pitch, and excessive in roll.
>
> 4. Ground interference causes erratic aircraft motions which, without the use of automatic stabilization, limit operation when the aircraft wheels are within 19 feet of the ground.
>
> 5. Wing stall and separation leading to buffeting, erratic motions, and general difficulty in handling the aircraft result in the desired VTOL velocity-rate-of-climb envelope having regions completely unacceptable for normal flight operations. The addition of a full-span leading-edge droop decreased the regions that were unacceptable for normal flight and thereby permitted an additional 1,100 feet per minute descent capability at airspeed of approximately 60 knots."

The vibration was high and stability and control were poor, all due to the airflow coming off the proprotors and the stalled wing as illustrated in Fig. 2-80. Wing leading-edge slats and trailing-edge flaps were a great help, of course, but the tiltwing's reputation was stained. Today engineers sometimes dismiss out-of-hand this alternate to a tiltrotor based solely on the VZ-2's problems from 50 years ago. Very shortsighted engineers in my opinion!

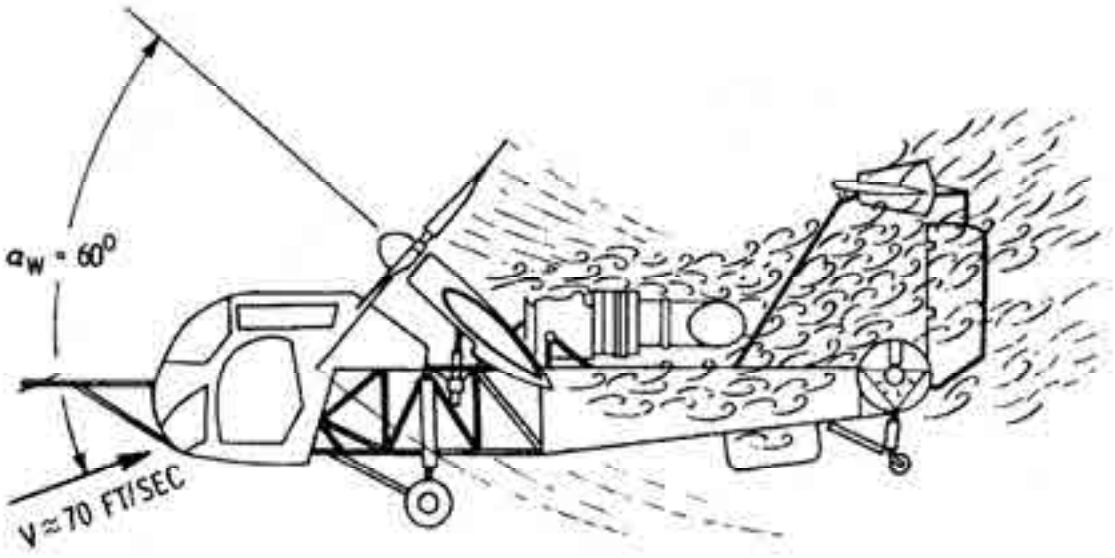

Fig. 2-80. At a rate of descent of 1,500 feet per minute, the vibration level of the VZ-2 was four to five times the level in cruise [193].

The U.S. Navy pilots[45] also took the opportunity to try out the VZ-2 from June 20 to 29, 1960. Their evaluation [201], published October 31, 1960, was based on eight flights for a total of 5.1 hours of testing. Twenty-three partial and complete conversions and reconversions were made. The full report contains 50 paragraphs of findings from which a three-part conclusion is reached. The conclusion by the Navy test pilots is a virtual gold mine of operational shortcomings[46] for this first-generation tiltwing aircraft and deserves inclusion in this volume for historical purposes. They were careful to acknowledge that the VZ-2 was a very simple, proof-of-concept machine, and their conclusions began with paragraph (a), which stated, very encouragingly, that

> "The V-76C tilt wing aircraft can successfully convert and reconvert from hover flight to airplane flight and that the tilt wing design is feasible for many tactical missions (paragraphs 40, 41, 42, 45, 47 and 48)."

Then came the following paragraph (b), so sought by any chief engineer:

> "The following items disclosed during the evaluation of the tilt wing aircraft should be given high priority for study, evaluation, and consideration in future tilt wing and VTOL/STOL aircraft:
>
> (1) Unsatisfactory power-off capability (see paragraphs 40, 41, 42, 45, 47 and 48).
>
> (2) Rotor mass flow, disc loading, recirculation and downwash velocities effects as applied to foreign object damage and over water spray patterns (paragraph 23 and 47).
>
> (3) More durable materials in construction of rotors and engine turbines in regard to foreign object damage (paragraph 23).
>
> (4) Variation of power output with changing mass flow and inflow angles of the rotors during conversion without variation of the pilot power control (paragraph 24).
>
> (5) Multi-engine requirements in future designs and the power load sharing problems inherent in present multi-engine free power turbine installations (paragraphs 28 and 44).
>
> (6) Downwash recirculation effect upon the flying qualities of the aircraft during hover and vertical landings (paragraph 29).
>
> (7) Effect of crosswinds and gusts on the aircraft during ground handling, taxi, take-off, hover and landing with the wing at high incidence angles (paragraphs 19, 22 and 30).
>
> (8) Restrictive rates of descent and glide slope at intermediate and high wing incidence angles (paragraphs 36 and 41).
>
> (9) Reduction of stability and control with reduced power (paragraph 42).
>
> (10) Wing 'DOWN' power-off characteristics (paragraph 43).
>
> (11) Variation of center of gravity (paragraph 46).
>
> (12) Design and aerodynamic problems encountered if wing stores are carried (paragraph 48).
>
> (13) Study of the tilt wing configuration for design with inherent stable static and dynamic stability in all modes of flight (paragraph 34).

[45] You might not know that the U.S. Navy has a Naval Air Test Center in Patuxent River, Maryland. This is home to the headquarters of the Naval Air Systems Command (NAVAIR), which was established on April 1, 1943. In fact, the Naval Test Pilot School is located there, along with some of this country's best test pilots.

[46] Keep in mind that you want test pilots to tell you *everything* that is wrong with your aircraft. This leaves all the reports about the wonderful features of your aircraft to the Marketing Department.

(14) Reliability of any automatic or synthetic stability and control flight systems (paragraph 34).

(15) Improvement of stability and control about all axes at all wing incidence angles (paragraphs 30, 31, 32, 33, 38 and 39).

(16) Effect of increased gross weight and wing loading with respect to the aerodynamic characteristics (paragraph 48).

(17) Marriage into a single instrument of the airspeed, wing angle, sliding maximum-minimum airspeed scale (paragraph 15).

(18) Use of angle-of-attack indicators in operational designs (paragraph 15).

(19) Type of power control to be used in future VTOL/STOL aircraft (paragraph 18).

(20) Complexity of rotor and tail fan drive systems during folding of aircraft for shipboard storage (paragraph 20).

c. The following items, inherent in the test aircraft, should be corrected in future designs:

(1) Restricted field of view (paragraph 13).

(2) Lack of a zero speed ground level ejection seat (paragraphs 16 and 44).

(3) Lack of fire warning indication and in-flight fire extinguishers (paragraph 16).

(4) Awkward arrangement of engine controls (paragraphs 17 and 27).

(5) Lack of cockpit climatic control (paragraph 17).

(6) Inability of ground crew to rotate wing without external power (paragraph 19).

(7) Poor landing gear design (paragraphs 22 and 45).

(8) Power restricted transmission (paragraph 25).

(9) Excessive rotor RPM droop (paragraph 26).

(10) Control force harmony in a hover (paragraphs 32 and 33).

(11) Failure of the stability augmentation system without indication to the ground crew or pilot on pre-flight and in flight (paragraph 34).

RECOMMENDATIONS

52. It is highly recommended that further tilt wing evaluation programs be initiated with application and direction toward an operational requirement and that the programs be directed toward correction of the problems and discrepancies disclosed herein.

53. It is further recommended that in future test programs, procurement not be limited to a single test bed."

From Vertol's point of view [202], the Model 76 showed that "actual experience confirms that small flight research aircraft are a logical means of proving—quickly and at reasonable cost—the basic feasibility of a new concept." And Paul Dancik and Steppy, the authors of reference [202], added:

> "By the end of October, 1958, a total of 17 complete conversions, as well as numerous partial conversions from STOL to hover, or from hover to STOL configurations, were performed. It is believed that, with these conversions, the main goal of the design and construction has been accomplished. But, in addition to fulfilling the main purpose of its existence, the aircraft proved itself a useful research tool. The present paper is written in order to present, without delay, the important topics of our experience, even if some results may still remain of a preliminary or a qualitative nature only."

As I recall, the list that Paul Dancik kept of pilots who flew the VZ-2 numbered over 20, and the NASA research studies just continued to grow. One technology that was tackled immediately was tiltwing aeroelastic behavior. The groundbreaking work was done by Bob Loewy and Bob Yntema who presented a paper at the 25th Annual Meeting of the Institute of Aeronautical Sciences (now the AIAA). This paper was then published in the Journal of the American Helicopter Society [203]. I recommend reading this paper as an example of analytical tools in use during the development of tiltwing aircraft.

2.12.2 The Hiller X-18

Now let me proceed to the second tiltwing. Stanley Hiller's X-18 (Fig. 2-81 and Fig. 2-82) made its first flight on November 24, 1959—some 2 years after the Vertol Model 76 made its marginally successful liftoff. The design takeoff gross weight of the Hiller Aircraft X-18 was 33,000 pounds, and it was virtually 10 times the size of the VZ-2. This first large tiltwing was aimed squarely at a useable military and commercial VTOL transport market. In December 1958, the *American Helicopter Society Newsletter* (now *Vertiflite*) included an article by Percy Dowden titled simply, *Hiller X-18 Research VTOL Aircraft* [13]. Mr. Dowden noted:

> "Overshadowing the increasing speed and comfort of our new commercial air transports is our inability in the future to provide sufficient accessible real estate from which to operate them safely and efficiently. In many of the larger metropolitan areas, the situation is already critical. And with as yet less than 10% of the nations' population ever having set foot in an airplane, airport and airline planners view with concern the maturing of our first true airborne generation. More and more passenger aircraft every year are converging upon a few single spots on the country's topography. The only answer in the future will be to disperse these transportation vortices. VTOL will make this decentralization possible."

This has been an oft repeated refrain by V/STOL advocates over at least the past six decades as I am sure you know.

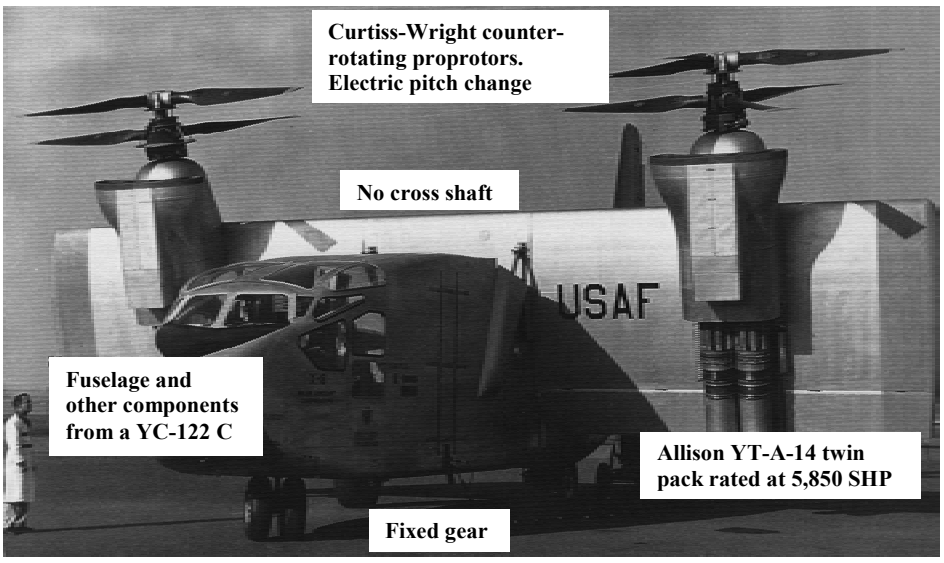

Fig. 2-81. The Hiller X-18 tiltwing 33,000-pound experimental aircraft first flew on November 24, 1959. It had so many proprotor, engine, and other design problems that the U.S. Air Force cancelled the program on January 18, 1964.

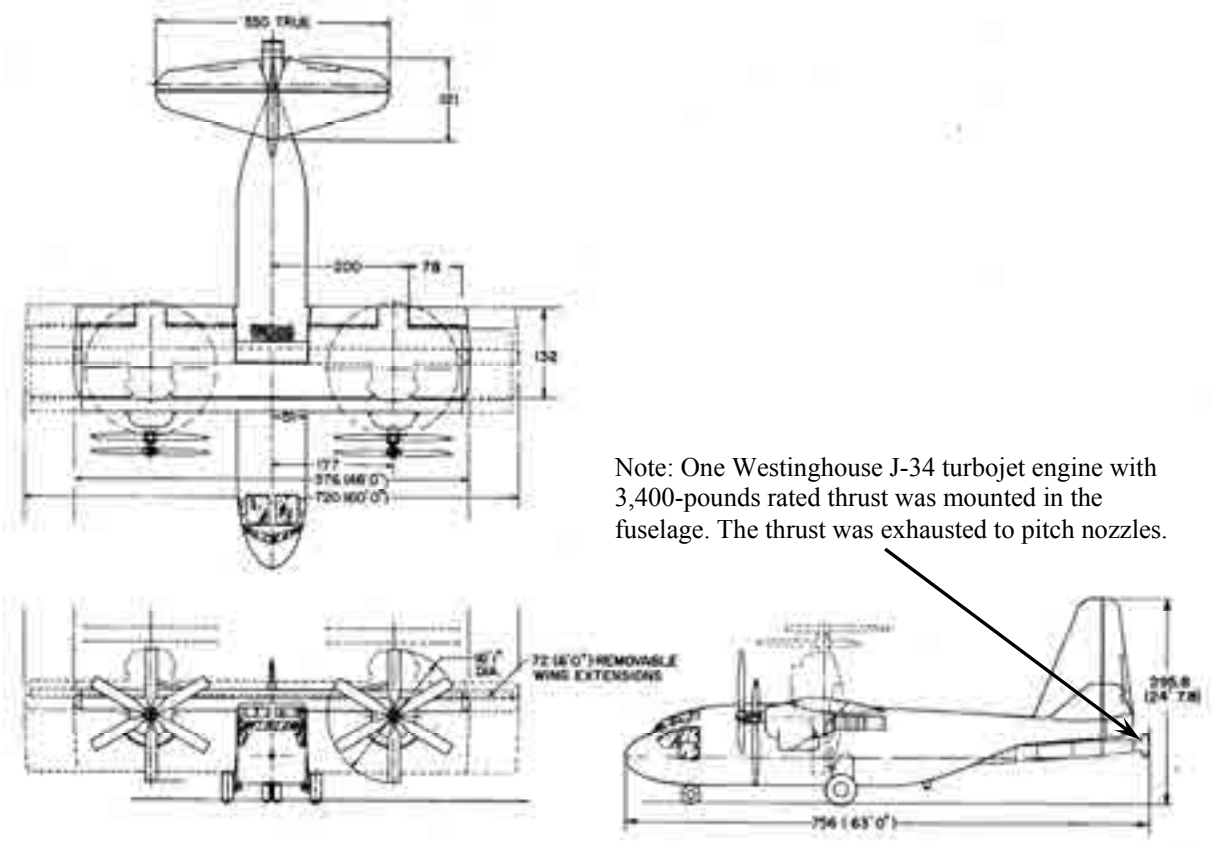

Fig. 2-82. A three-view drawing of the Hiller X-18.

The technical and program data that is available[47] in the open literature is sketchy at best. There are two reasons for this:

1. The program was classified confidential and no effort has been made to request reclassification and,
2. Flight testing was stopped, and the aircraft was grounded after 20 flights because of a nearly catastrophic incident.

In terms of technical data, the best original source I have is the *Vertiflite* article written by Percy Dowden in December 1958, about a year before first flight [13]. You can, of course, find short discussions and data about the X-18 in *Jane's All the World's Aircraft* (starts in 1957 and ends in 1962) and in the popular literature such as references [25, 38, 39]. The Hiller story in toto was superbly written by Jay Spenser [204].

Three subjects that should be of considerable interest to you deal with (a) the shoestring nature of the X-18 program, (b) the design not having an interconnect between the two propulsive units, and (c) the nearly catastrophic incident, which brought the program to its knees. Let me discuss these subjects.

[47] I am sorry not to be able to include in this volume results of a search through Bernie Lindenbaum's files located at Wright State University in Dayton, Ohio. Furthermore, I would have thoroughly enjoyed searching through the Hiller Museum in Palo Alto, California, for the X-18 story.

In 1990, Bernie Lindenbaum convened a meeting about lessons learned from what many describe as the golden age of V/STOL (the decade between 1955 and 1965). The X-18 program was presented by John Nichols [205].[48] John noted:

> "Design and construction of the X-18 took the better part of three years with the largest single task represented by the construction of an entirely new wing with provisions for wing tip extensions and leading edge slats or other devices, engine nacelles and the control integration system. The [YC-122C] fuselage was cut in two and stretched to a length dictated by landing gear and c.g. [center of gravity] requirements. The tail surfaces were recovered with metal since their original fabric was unsuited for use in the vicinity of the pitch control diverter device which ejected the hot exhaust from a J-34 jet engine.
>
> When reviewing the total task in perspective it is questionable as to whether the use of YC-122C components was directly effective in reducing cost since they represented such a small percentage of the total value of the complete machine. If the direct benefits were not very evident, the indirect ones were. The impact of many large size components appearing almost instantaneously in the midst of the project team early in the program provided an impetus and direction to the program at a period when initial fervor would normally be cooling off during the long wait for the arrival of the first pieces and parts as occurs when one is starting off on a brand new hardware project.
>
> In spite of the fact that certain major deviations were allowed in the X-18 with relation to what would be acceptable for a production transport airplane, and in spite of the fact that the engines and propellers came 'free' from the Lockheed [XFV-1] and Convair [XFY-1] pogo stick programs, it was still a remarkable feat to get a 33,000 lb aircraft into the air for less than $4 million. When the project's flights were terminated, somewhat more than $5 million had been spent."

The lack of a cross shaft connecting the port and starboard power and propeller units certainly was an issue. On this point, John wrote:

> "The [U.S. Air Force Flight Dynamics] Laboratories' position with regard to the [Hiller X-18] program was very negative on the basis of the lack of cross-shafting which was considered essential to safety. Upon further questioning as to whether the aircraft would work, the answer was 'probably yes but that without cross shafting it shouldn't be done.' Being informed that if this program was not approved there would be no money for ANY Air Force V/STOL experimental airplane, the Laboratories and ASD [Aeronautical Systems Division] chose to support the program."

The fact that control without cross shafting "could be done" was amply demonstrated by NASA's testing of a powered 1/8-scale model of the X-18 in flight in the Langley Research Center 30- by 60-foot full-scale wind tunnel (Fig. 2-83) in March of 1960 [206]. The same model was pedestal mounted on the full-scale tunnel floor, and force testing was accomplished [207]. Quantitatively and qualitatively, these tests did not uncover any showstoppers to the Hiller design approach of skimping along without a cross shaft. After all, the 1/8-scale model did not have a cross shaft. What was really vital was proprotor blade feathering control—and it was here that the X-18 pilots got shortchanged.

---

[48] Even though John had moved from Hiller to Boeing (Seattle) by the time of this meeting, he was able to draw upon the memories of several key players on the X-18 program. He acknowledged inputs from Percy Dowden, Fred Matteson, Dick Carlson, Joe Stuart III, Ed Bolton, and Stan Hiller. Stan Hiller's company, located on the West Coast, was a terrific center of research as you will conclude after reading Jay Spencer's very well written book [204].

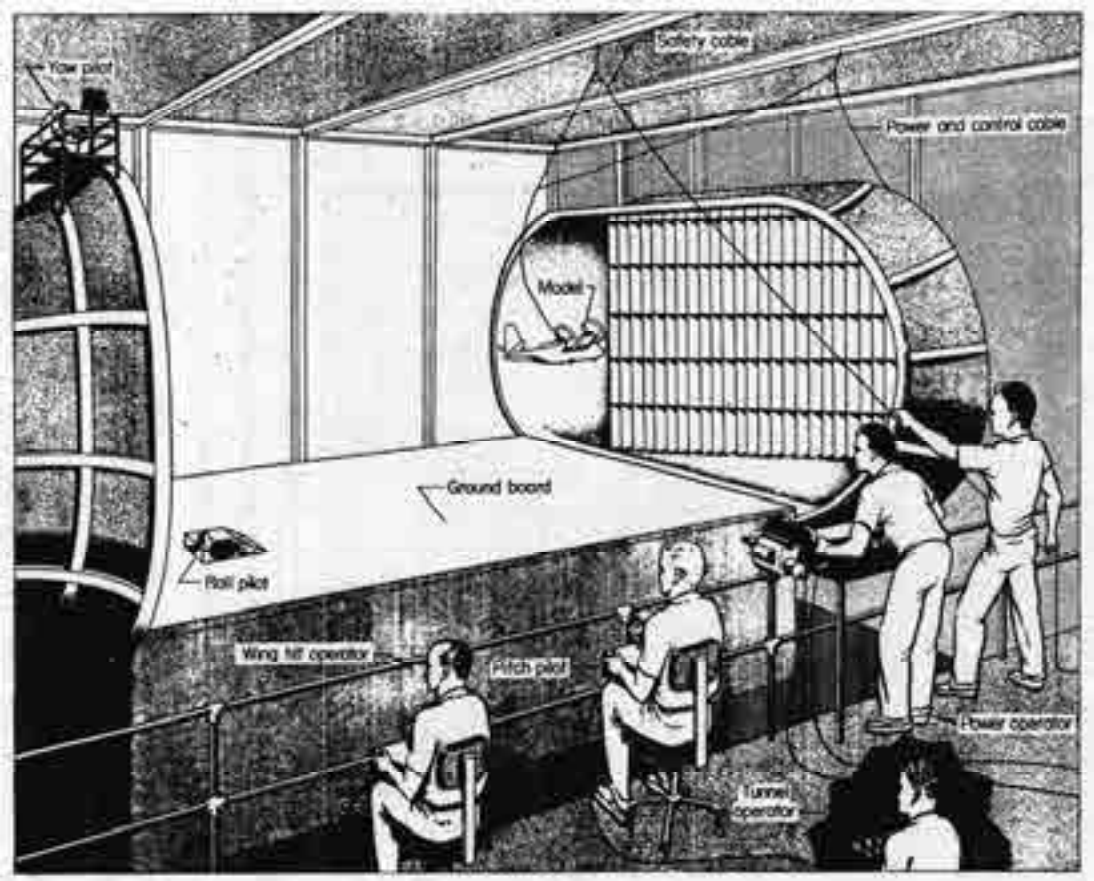

Fig. 2-83. You might not know that this combination of three pilots (pitch, roll, and yaw), a model power operator, and a tunnel operator was used to "fly" many different models in the Langley 30- by 60-foot full-scale wind tunnel. A wing tilt operator was necessary for some V/STOL models.

As to the nearly catastrophic incident, John wrote:

"From the earliest ground runs to the 19th and last flight, the X-18 was plagued by continuous engine and propeller control problems. With one exception, the engines or propellers did not cause flight safety problems, or even fail in flight—they just would not check out satisfactorily in so many pre-flights that adjustment and repair was a continuing problem and employed time and funds which had been planned for flying and collecting data.

That one exception occurred on the ninth flight, on November 4, 1960. While flying at 11,000 ft with a 10 degree wing tilt angle, the X-18 yawed violently to the left, rolled to the right onto its back, and entered an inverted spin. Cool handling of the situation by George Bright, the test pilot, saved the aircraft. Recovery was accomplished at 6,000 ft and, by careful manipulation of the propeller control circuit breakers, propeller control was regained and a safe landing was made. Instrumentation recordings indicated that the propeller blade angle jumped from 20.6 deg. to 34.6 deg. in 0.7 seconds and then back to 8.8 deg. in 1.5 seconds. Upon disassembly of the propeller it was discovered that the reference motor in the governor assembly had stripped all of its gear teeth clean.

> In spite of the calm flight test report submitted by Mr. Bright, 'the X-18 exhibits normal spin recovery characteristics,' the Air Force's confidence in the powerplants and propellers was shaken to the extent that after an engine compressor failure during ground check after the 19th flight, the flight program was terminated. The higher wing angle hovering flights which were scheduled to be done last were eliminated with the intention of attaining hovering static stability derivatives and downwash characteristic data on a ground test stand."

And so ended the Hiller X-18, the first try at an assault transport VTOL. Now let me discuss some performance aspects of the machine.

The total takeoff shaft horsepower amounted to 11,700 horsepower installed in a 33,000-pound machine. Jay Spenser, who wrote the terrific story of Hiller Aircraft—at Stanley Hiller's request, so the story goes—states that the total shaft horsepower available came from two 5,850-horsepower Allison YT40-A-14 engines, but "because each T40 'twin pack' unit incorporated two turboshaft power plants coupled together, the X-18 could also be thought of as a four-engine machine despite its twin-engine appearance." The 11,700 horsepower makes the installed shaft horsepower per ton of gross weight just under 710. The maximum speed was "limited to 220 knots indicated airspeed" because this was the limit imposed on the windshield, which came from a Fairchild C-123 [208]. This limit-indicated airspeed is hardly consistent with such a large amount of installed power, which started me thinking about what the estimated performance envelope (i.e., altitude versus maximum speed) might have been.

My literature search turned up no published data on power required versus airspeed for the X-18. (You may have better luck.) So I turned to the NASA 1/8-scale-model force data published by Lou Tosti [207], which included lift and drag coefficients versus angle-of-attack data with the propellers off. Taking this data (figure 13a) as the cruise configuration even though the Reynolds number based on wing chord was only 770,000, I constructed a lift-drag polar (Fig. 2-84) and concluded that, with propellers off, the X-18 might be approximated by

$$C_D = 0.1346 - 0.07684C_L + 0.16139C_L^2 \tag{2.74}$$

The power-required calculation from this point on is quite straightforward. You only have to pick a gross weight, say the design gross weight of 33,000 pounds, and compute lift coefficient as

$$C_L = \frac{W}{q_{FP}S_W} = \frac{33,000}{q_{FP}(528)} = \frac{33,000}{(\tfrac{1}{2}\rho V_{FP}^2)(528)} \tag{2.75}$$

by picking a flightpath velocity (V_{FP}) range of, say, 100 to 350 knots, and several altitudes such as sea level, 10,000 feet, and 20,000 feet on a standard day where the density of air (ρ) is 0.002378, 0.001756, and 0.001267 slugs per cubic foot, respectively. The dynamic pressure (q_{FP}) is computed using the flightpath velocity in feet per second.

Of course, the aircraft drag coefficient can be found from Eq. (2.74), and the actual drag in pounds is then nothing more than

$$\text{Aircraft Drag} = D_{AC} = q_{FP}S_W C_D \,. \tag{2.76}$$

This drag is equally split between the two propulsive units, which means the thrust of one proprotor (T_p) is $D_{AC}/2$.

Now the power required of one proprotor is calculated according to Eq. (2.57), which, to repeat, is

$$\frac{P_{req'd.}}{q_{FP}V_{FP}D^2} = \frac{1}{2}\left(\frac{T_P}{q_{FP}D^2}\right)\left[\sqrt{1+\frac{4}{\pi}\left(\frac{T_P}{q_{FP}D^2}\right)}-1\right] \leftarrow \text{Induced}$$

$$+\frac{\pi}{16}\left(\sigma C_{d-average}\right)\left\{\frac{1}{\left(V_{FP}/V_t\right)^3}+\frac{3}{\left(V_{FP}/V_t\right)}+\left(\frac{V_{FP}}{V_t}\right)\left[\frac{9}{8}+\frac{3}{2}\ln\left(\frac{2}{V_{FP}/V_t}\right)\right]\right\} \leftarrow \text{Profile} \tag{2.77}$$

$$+\left(\frac{T_P}{q_{FP}D^2}\right) \leftarrow \text{Parasite}$$

The necessary parameters for this computation are the proprotor diameter of 16 feet, 1 inch; the proprotor tip speed, which I guessed was 850 feet per second; the solidity (σ) of 0.347, which I obtained from Fig. 2-82; and the proprotor blade average drag coefficient ($C_{d\text{-average}}$), which I guessed was 0.008. With this input, you have the proprotor power coefficient from Eq. (2.77). Thus, proprotor horsepower (HP_P) for two units amounts to

$$HP_P = 2q_{FP}V_{FP}D^2\left[\frac{P_{req'd.}}{q_{FP}V_{FP}D^2}\right]. \tag{2.78}$$

It only remains to account for the gearbox efficiency and the accessory power to obtain the total shaft horsepower required. Thus,

$$SHP_{AC} = \frac{HP_P}{\eta_{GB}} + SHP_{acc}. \tag{2.79}$$

Lacking any published information, I chose a gearbox efficiency of 0.98 and an accessory power of 150 shaft horsepower. The results of these elementary calculations are shown in Fig. 2-85 along with my rough guess of the shaft horsepower available from two YT40-A-14 turboshaft engines, which decreases with altitude. The dashed line shows the windshield limit true airspeed, which is really a dynamic pressure limit.

It is clear from my rough estimate of the Hiller X-18 performance in forward flight that high speed was not a program objective. You might have guessed this because the landing gear was not retractable, and the wing, having an aspect ratio of 4.3, was very stubby. Wing extensions to increase the wingspan from 48 to 60 feet (an aspect ratio of 5.375) were planned, but the program was cancelled before that experiment could be tried. In closing, I should mention that the X-18 was never flight tested in hover. However, complete faith in the tiltwing concept was not lost, as you will read shortly.

Let me now go on to the Canadian-developed Canadair CL-84.

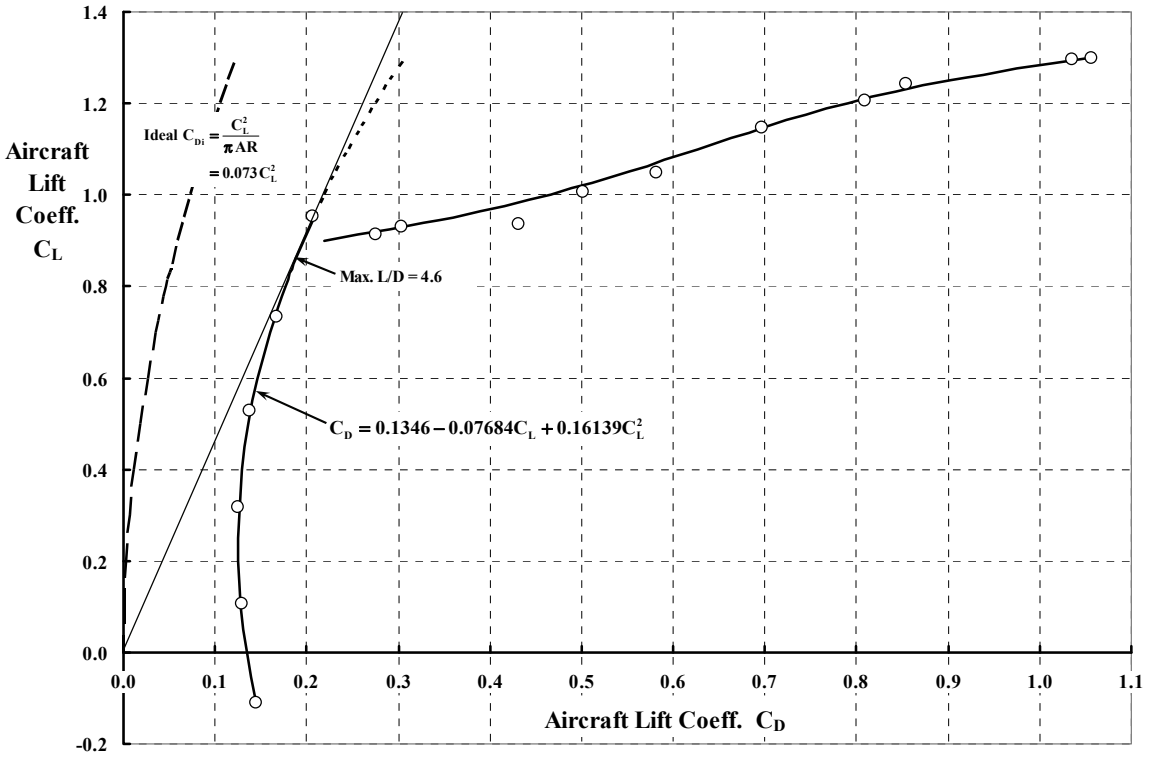

Fig. 2-84. The lift-drag polar of the Hiller X-18.

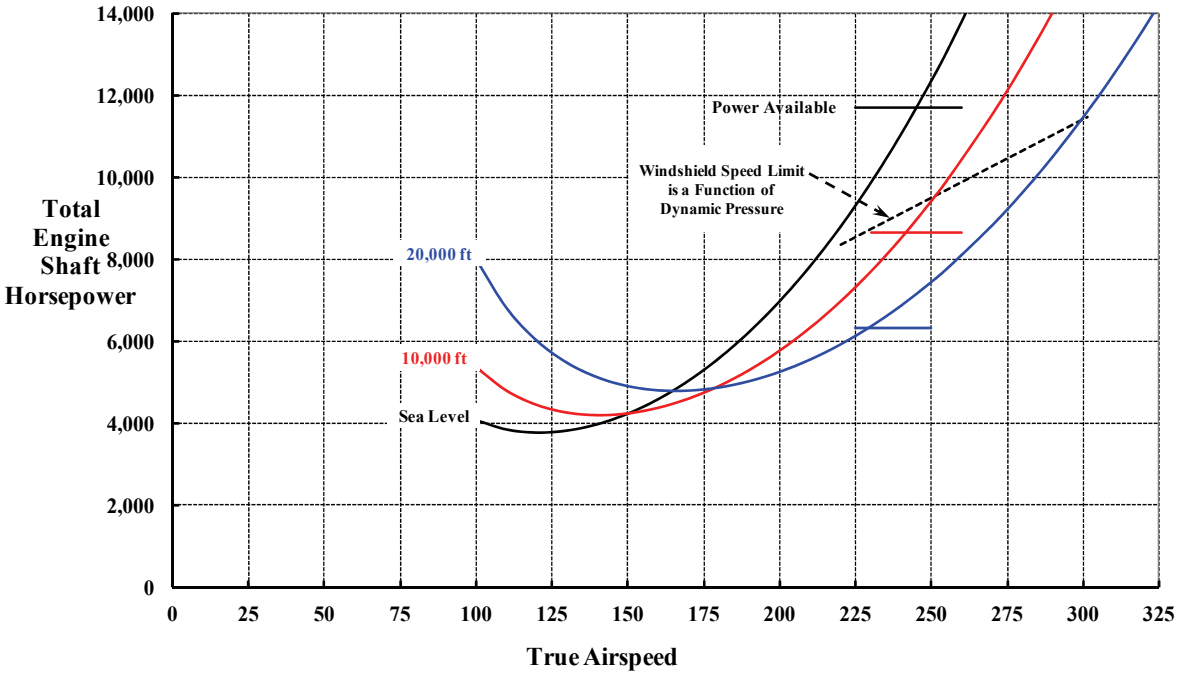

Fig. 2-85. The total engine shaft horsepower required versus speed for the Hiller X-18.

2.12.3 The Canadair CL-84

Canadair Ltd. was created in 1944 by the Canadian Government. It was primarily a fixed-wing manufacturer that much later became the core of Bombardier Inc. and produced regional jet airliners [209]. In the late 1950s, supported in part by Canada's National Research Board and the Defense Research Board, Canadair performed a number of studies suggesting that a tiltwing might be a VTOL product line. In the early 1960s, Canadair obtained a cost-sharing contract with the Canadian Government to design, build, and test a small, twin-engine tiltwing (Fig. 2-86 and Fig. 2-87) that could perform a number of military missions. The U.S. Army had an early interest in what became known as the CL-84 and supplied four prototype engines (Lycoming LTC1K-4A free turbines rated at 1,400 shaft horsepower and similar to the T53-L-13) to the Canadian Government for use in the program.

At that time both the U.S. Navy and Air Force shared the U.S. Army's interest in VTOL because of a requirement for a high-speed search and rescue mission aircraft. The Canadair CL-84 became one of the VTOL aircraft under consideration for this mission. While the Tri-Service[49] deliberations were going on, NASA, with its continuing interest in tiltwing technology based on experience with the Vertol VZ-2, sent two Langley Research Center pilots to Canadair (in Montreal, Quebec) to perform a limited test of the machine in October 1966. The two pilots, Jack Reeder and Bob Champine, both with previous tiltwing experience, along with Hank Kelley as a test engineer, completed their summary of the flight evaluation on August 15, 1969. Their NASA report was formally published in March of 1970 [210]. Shortly after the NASA evaluation, a 20-hour Tri-Service flight evaluation was conducted

Fig. 2-86. The Canadair CL-84. This 10,600-pound VTOL technology demonstrator made its first hovering flight on May 7, 1965. The first full conversion back and forth from hover was made on January 17, 1968. The CL-84's success far exceeded either Vertol's VZ-2 or Hiller's X-18.

[49] This joint interest crystallized into a very serious Tri-Service program, which I will discuss in more detail later.

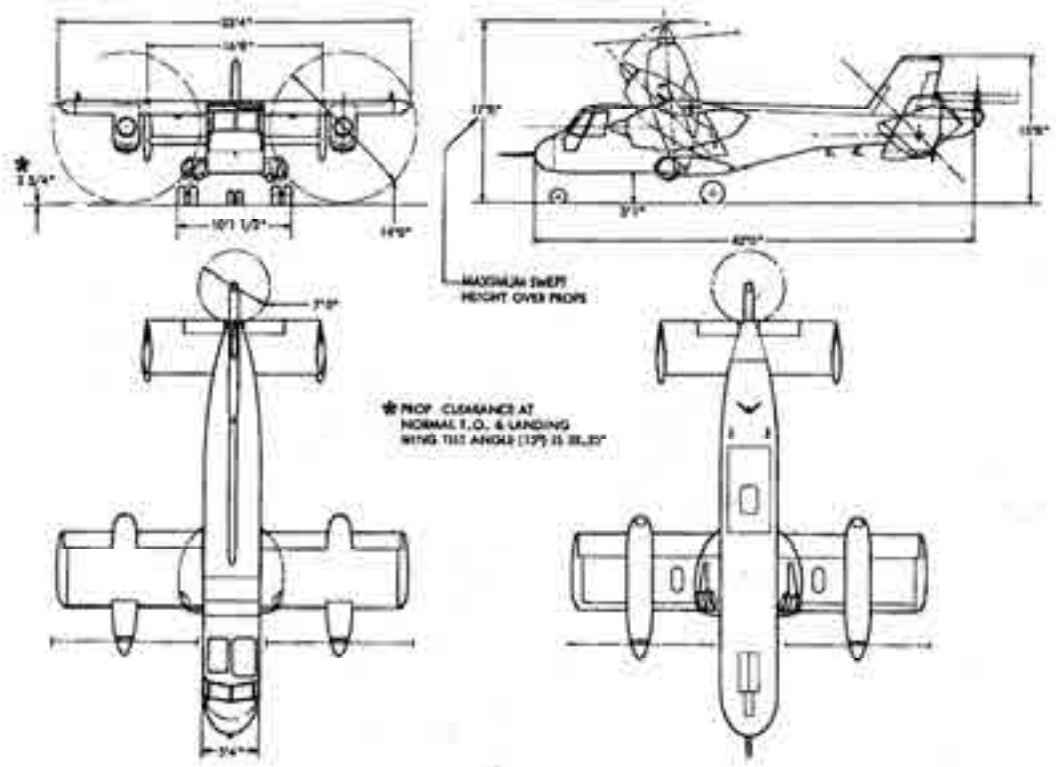

Fig. 2-87. The Canadair CL-84 used a pitch fan for longitudinal attitude control while roll and yaw were controlled by differential proprotor feathering. The gear was retractable. The drivetrain was quite similar to the Vertol VZ-2 [182]. The wing was always set at 15 degrees from horizontal for normal airplane takeoff and landing [211].

(April 28 to August 29, 1967) at the Canadair plant, and a very thorough evaluation report came out in November of 1967 [211]. There was no doubt that this was a Tri-Service evaluation because the six-author team was made up of two Air Force, two Navy, and two Army officers. So that the players all knew their place, the team's report [211] included a paragraph dealing with "responsibilities," and a chain of command chart (Fig. 2-88) was inserted for good measure.

The Canadair CL-84 was considered by many to be a second-generation tiltwing. I think it very much deserved that title when you compare it to the Vertol VZ-2. The NASA authors certainly felt that way because, in their concluding remarks, they wrote:

> "An abbreviated flight-test evaluation of a second-generation tilt-wing V/STOL aircraft, the Canadair CL-84, was conducted to ascertain possible problem areas. In general, based on the limited evaluation possible, most of the flying qualities in the hover, transition, and cruise modes of flight were considered good. However, an indicated rate-of-descent limit of 700 ft/min (3.56 m/sec), defined by loss of control due to stalling, at a typical STOL airspeed of 42 knots, did not appear to provide enough margin for ultimate operational use. Furthermore, low normal-velocity damping was encountered at about 40 knots airspeed at indicated rates of descent desirable for operational use. This characteristic appeared as a

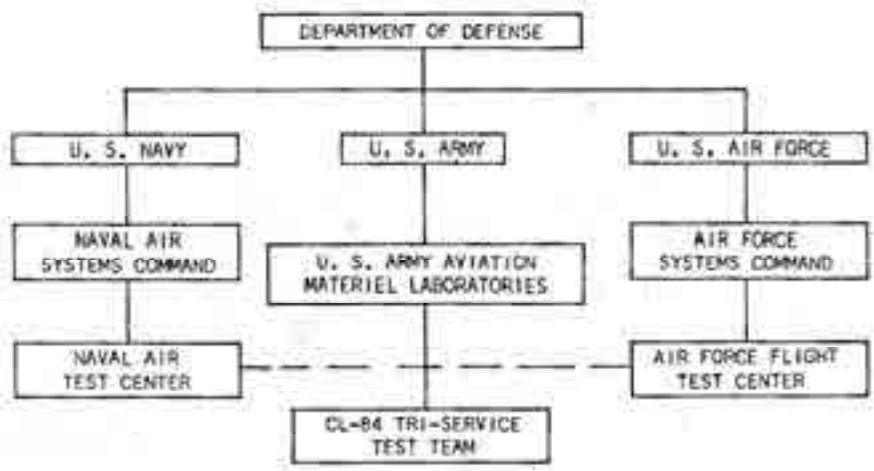

Fig. 2-88. Chain of command for the CL-84 Tri-Service evaluation team [211].

> prolonged increase in rate of descent following a small power reduction, and is thought to be significant for instrument flight. According to pilot observations and the time histories, this characteristic occurred with power settings for initial indicated rates of descent as low as 300 ft/min (1.52 m/sec). Buffeting was not always apparent to the pilot as excessive sink rates developed and, in several descents at altitude, the first indications of approach to limiting stalling were pitch-down and roll-off that occurred at an indicated rate of descent of about 700 ft/min (3.56 m/sec). This behavior may be related to aerodynamic characteristics at angles of attack near maximum lift."

It seems to me that the VZ-2 proved that a tiltwing could—from a performance view point—transition from hover to forward flight and back again with no major problems. The VZ-2's shortcomings in handling qualities were another matter. And the VZ-2 certainly exposed the descent problems in spades, which NASA went right to work on judging from the list of references in its summary report [210]. The Canadair engineers seem to have solved the bulk of the handling quality problems, and this just left the descent problem. It appears (in Fig. 2-89) that the Canadair team installed both slats and flaps to mitigate wing stalling, and yet the Tri-Service test team found that descents approaching 1,000 feet per minute clearly established a limit.

The Tri-Service CL-84 evaluation team's report divided its conclusions into general and specific topics. The general topics' conclusions were quite positive:

> "1. The tilt-wing concept exemplified by the CL-84 aircraft is suitable for search and rescue, surveillance, light-transport, and utility-type missions.
>
> 2. No conceptual features were found which should preclude serious consideration of the concept for STAAS, LIT, SAR, UTTAS, and LTTAS [missions].
>
> 3. The test aircraft is unsuitable for military missions because of many hardware deficiencies resulting from program austerity. However, the CL-84 aircraft has potential for military missions, since the deficiencies are of a nature which can be corrected by hardware design changes currently within the state of the art. Specific discrepancies along with favorable characteristics are outlined below."

Fig. 2-89. Despite slats and flaps for stall mitigation, the Canadair CL-84 still had rates of descent limited to 700 feet per minute, which was well below operational requirements [210].

To me, the list of specific deficiencies, shortcomings, and inadequacies are where flight test evaluations become worth their weight in gold. The evaluation team had a number of specific complaints that, for historical purposes, are quite valuable to future VTOL students and engineers. (What you have next is a long list, I know, but you should be aware that pilots are the end users and you should anticipate their needs.) The evaluators wrote:

"1. The handling qualities of the CL-84 are basically satisfactory but are degraded by control system deficiencies, especially in aerodynamic flight.

a. The following characteristics *enhance* mission suitability:
   (1) Use of a single power lever for height and airspeed control.
   (2) Excellent flying qualities in conversions down to CA 15.
   (3) Excellent agility in formation flying.
   (4) Strong speed stability in powered lift flight.
   (5) Precise control of the aircraft during descent and reconversions, made possible by information provided by the flight path accelerometer.

b. Correction of the following *deficiencies* is *mandatory* for service use:
   (1) Inadequate control force gradients in aerodynamic flight, resulting in over controlling in pitch.
   (2) Inadequate lateral and longitudinal trim rates and trim authority.
   (3) Lack of a satisfactory directional trim system.
   (4) Lack of a proportional wing-tilt rate control.
   (5) Inadequate longitudinal stability in powered lift flight for IFR conditions.
   (6) Inadequate elevator effectiveness for maneuvering in the aerodynamic flight regime.
   (7) Excessive sideslip for tracking tasks in aerodynamic flight.
   (8) Intermittent excessive airframe vibration above 180 KIAS [interesting].
   (9) Lack of adequate stall warning.

c. Correction of the following *deficiencies* is *desirable* for improved service use:
   (1) Excessive control system friction with boost off.
   (2) Weak stick centering.
   (3) Excessive control system hysteresis.
   (4) Insufficient longitudinal stability in powered lift flight for VFR conditions.
   (5) Insufficient height damping in hover for night and IFR operations.
   (6) Insufficient directional control power, sensitivity, and response in hover with SAS on.
   (7) Insufficient static directional stability for small sideslip angles.
   (8) Excessive buffet during landings at CA 50.
   (9) Insufficient buffet warning of impending wing flow separation.
   (10) Loss of height during final stage of level-flight conversions.
   (11) Excessively low tail propeller limit airspeed.
   (12) Restrictions to starting and stopping tail propeller at high main propeller rpm.
   (13) Lack of suitable arrangement of V/STOL-related instruments.
   (14) Moderate longitudinal trim change with power.
   (15) Poor lateral control response, with SAS on in cruise, for stick displacements of one-half and less.
   (l6) Excessive adverse yaw at low airspeeds in aerodynamic flight.
   (17) Low directional force gradients, causing over controlling in aerodynamic flight.
   (18) Excessive gust sensitivity.
   (19) Longitudinal acceleration oscillation during descent.
   (20) Insufficient lateral control response and sensitivity in transitional flight.
   (21) Excessive lateral stick travel for lateral translations in hover.
   (22) Inadequate crosswind capability for taxi.

2. The performance of the CL-84 is inadequate for any mission application, but the aircraft has the potential to meet the performance requirements of most missions.

   a. The following characteristics *enhance* mission suitability:
      (1) Excellent STOL capability, derived from the immersed wing.
      (2) Ability to select optimum wing angle for any given takeoff or landing condition, because of the lack of wing angle restrictions for STOL operations.
      (3) Excellent acceleration and climb capabilities, provided by the high inherent thrust-to-weight ratio.
      (4) Excellent deceleration and descent capabilities, provided by the large propellers.

   b. Correction of the following *deficiencies* is *mandatory* for service use:
      (1) Insufficient installed horsepower for hot-day hover requirements.
      (2) Excessively high drag in aerodynamic flight. Insufficient fuel capacity.

   c. Correction of the following *deficiency* is *desirable* for improved service use:
      (1) Inadequate braking during STOL landings.

3. The CL-84 is *unsuitable* for service use because of numerous hardware deficiencies.

   a. The following characteristics are *desirable*:
      (1) Simplicity and functional operation of the power management system.
      (2) Immediate pressure and temperature indications on the malfunctioning gearbox, provided by an automatic gearbox select feature incorporated with the annunciator panel.
      (3) Mechanical simplicity and ease of maintenance of the CL-84 when compared to other V/STOL aircraft.
      (4) Precise propeller thrust trimming, provided by the yaw.

   b. Correction of the following hardware deficiencies is mandatory for service use:
      (1) Lack of provisions for adequate normal cockpit entry and exit.
      (2) Lack of provisions for adequate emergency exit.

(3) Poor placement of the pilot with respect to the flight controls.
(4) Excessive brake pedal deflection for adequate braking, and lack of a parking brake.
(5) Poor cockpit layout.
(6) Poor power level grip design.
(7) Lack of some warnings and presence of some unnecessary warnings on the annunciator panel.
(8) Use of outmoded instruments and switching functions.
(9) Use of different units of measure for fuel flow and fuel quantity.
(10) Lack of an adequate environmental control system.
(11) Excessive vibration in the nacelle areas. [*Interesting*]
(12) Lack of suitable capability to rig the main propellers statically.
(13) Use of a manual bleed-band lockout feature for low-power operations.
(14) Lack of provisions for emergency propeller rpm control under conditions of dual hydraulic failure or single-order gear-train failure.
(15) Excessive sensitivity of the propeller rpm set switch.
(16) Lack of electro hydraulic interlock feature in the wing control system.
(17) Unsatisfactory design and performance of the fuel system.
(18) Lack of true redundancy in the hydraulic systems.
(19) Unsuitable location of hoist for retrieval of injured personnel.
(20) Lack of adequately designed and qualified ejection seats.
(21) Lack of nose-gear steering.
(22) Lack of adequate over-the-side visibility for confined areas and rescue operations.
(23) Lack of windows/emergency doors in cargo compartment.
(24) Lack of detent on condition levers for ground idle.
(25) Inadequate nose-gear centering capability.
(26) Lack of anti-icing and deicing capabilities.

c. Correction of the following deficiencies is *desirable* for service use:
(1) Lack of single-point refueling.
(2) Lack of gearbox oil level sight gages visible from the ground.
(3) Lack of quick-release latches on engine cowls and on access plates.
(4) Lack of external steps on the fuselage and walkways on top of the aircraft.
(5) Lack of a usable mechanical backup control system.
(6) Lack of a proportional rate controller on the hoist.
(7) Lack of provisions for propeller decoupling and feathering.
(8) Lack of an emergency wing-tilt capability under conditions of dual hydraulic failure.

4. The CL-84 tilt-wing concept is feasible for use in the SAR mission; however, some *deficiencies* limit the capability of the test aircraft in specific phases of the SAR mission.

a. Correction of the following *deficiencies* is *mandatory*:
(1) Inadequate downward field of view to the side of the aircraft.
(2) Lack of windows/escape hatches in the aft compartment.

b. Correction of the following *deficiencies* is *desirable*:
(1) Weak height damping, in hover.
(2) Poor instrument arrangement for night or low-visibility recoveries.

c. The following limitations were determined:
(1) Recovery operations below a 50-foot hover height are not advisable because of high downwash effects.
(2) Certain rescue devices cannot be used in their present configuration."

After the evaluators offered their specific list of items to be corrected before they would accept a CL-84 machine for operational service, they listed their recommendations (with some of my comments in brackets) as follows:

> "1. That the tilt-wing concept exemplified by the CL-84 aircraft be developed to fill search and rescue mission requirements and for use in surveillance, light-transport, and utility type missions.
>
> 2. That if additional testing of this concept is contemplated, sufficient qualification testing of the aircraft, its systems, and its components be accomplished to ensure adequate structural integrity and functional reliability. [This would take the CL-84 class of VTOL from a technology demonstrator to a preproduction classification.]
>
> 3. That all *mandatory* correction items be incorporated into any future version of this aircraft.
>
> 4. That as many of the *desirable* correction items as feasible be incorporated into any future version of this aircraft.
>
> 5. That further analysis of the data included herein be conducted for the purpose of accurately predicting the applicability of the concept to specific missions. [Use their document for code development.]"

The Tri-Service report [211] [50] is a gold mine of technical data and aircraft description information for the Canadair CL-84. As you might have guessed from the list of mandatory and desirable items, flying qualities and human factor data are the most complete. However, noise measurements, for example, are included. Mission potential is discussed, as are cockpit and ground operations evaluations. There is also a very complete data set for the engine. The list of recipients for the report is significant as well. Because the performance data is of particular interest for this introductory volume, let me bring some of this data to your attention.

The CL-84's hover (ceiling performance) out of ground effect (HOGE), shown in Fig. 2-90, was obtained based on (a) the Lycoming LTC1K-4A engine specification, and (b) the nondimensional power required coefficient versus the thrust-coefficient data provide here as Fig. 2-91. In constructing the decision-making format of hover performance (Fig. 2-90), the evaluation team included a decrement in performance that accounted for control. That is, they chose a thrust-to-weight ratio ($2T_P/GW$) of 1.04 when applying Fig. 2-91. You will find that this control margin was as large as 1.15 in other VTOL aircraft. This is in direct opposition to traditional helicopter performance presentations, which very rarely introduce such a margin. Also, you will note that tiltwing and tiltrotor advocates generally account for the gas turbine's residual jet thrust (F_N). Just so there is no misunderstanding, I converted the power and thrust coefficients from reference [211] to rotorcraft form, which is to say that the coordinates of Fig. 2-91 are

$$(2.80)\quad C_W = \frac{(GW - F_N)}{\rho(2A_P)V_t^2} \qquad C_P = \frac{550\,SHP_{Total}}{\rho(2A_P)V_t^3}.$$

You will note on the nondimensional C_P-versus-C_W graph that I have added a curve that you first saw as Eq. 2.41 on page 137 in Volume II. This curve was offered as a mean line of hover performance for some 40 single-rotor helicopters and was derived as

[50] There is no question in my mind that it is in my top five list of flight test reports I have studied.

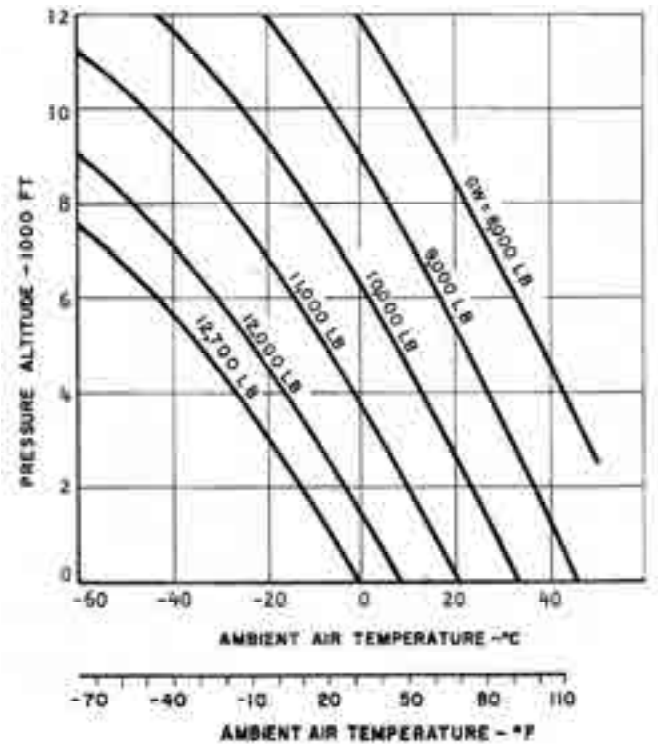

Fig. 2-90. CL-84 hover performance presented in a format useful to a pilot [211].

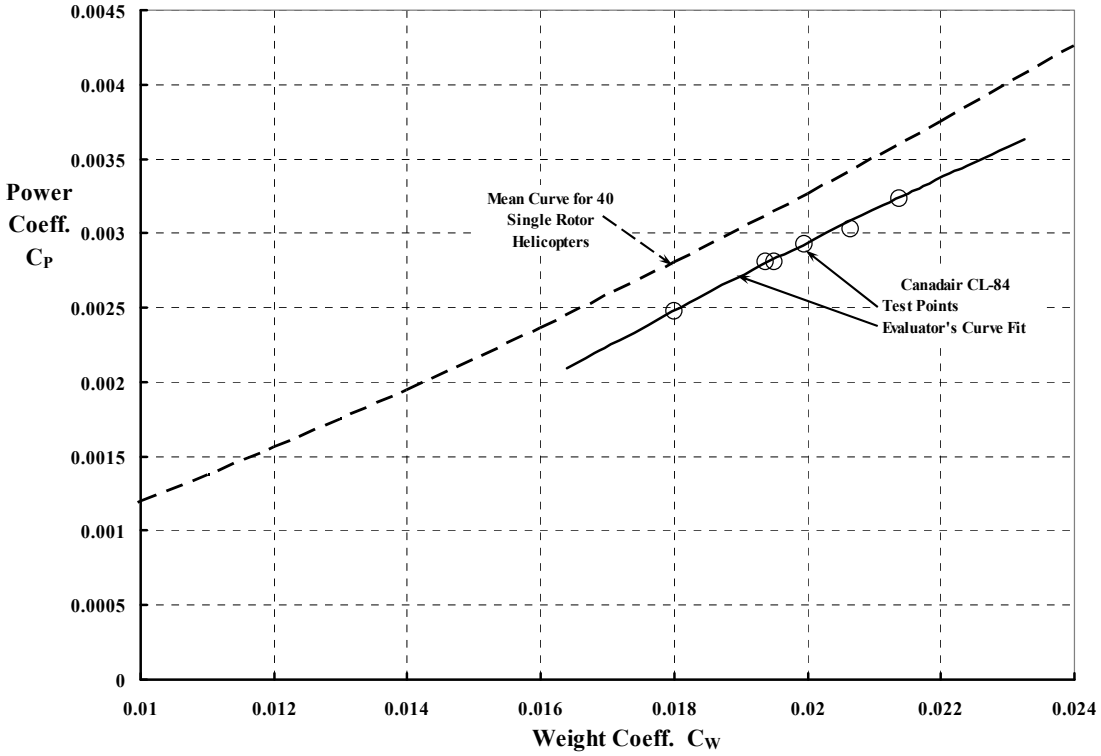

Fig. 2-91. The CL-84's nondimensional hover performance out of ground effect appears to be some 11 percent better than the mean performance for 40 single-rotor helicopters [211].

$$(2.81)\quad C_P = \frac{k_i}{\sqrt{2}} C_T^{3/2} + \frac{\sigma C_{do}}{8} = \frac{k_i}{\sqrt{2}} C_T^{3/2} + \frac{\sigma}{8} \frac{6}{(L/D)_{Airfoil}} \frac{C_T}{\sigma} = \left[\frac{6}{8(L/D)_{Airfoil}} \right] C_T + \frac{k_i}{\sqrt{2}} C_T^{3/2} .$$

An airfoil lift-to-drag ratio of 50 and an induced power constant (k_i) of 1.48 leads to

$$(2.82)\quad C_{P_{Req'd.}} = 0.0157\, C_W + 1.045\, C_W^{3/2} .$$

This result showed that helicopter hover performance was estimated to within a ±12-percent spread. Apparently, the very successful Canadair CL-84 was on the –11-percent side. You should keep in mind that about 4 percent of this comparison will be used up by VTOL advocates asking for a control margin. On the other hand, the VTOL advocates correctly include the turboshaft's residual jet thrust, which for the CL-84 was about 250 pounds from two engines. This positive thrust amounts to about 2.3 percent of the CL-84's 10,600-pound design gross weight. It does seems to me, however, that this one comparison is insufficient to draw a major conclusion about helicopter-versus-tiltwing (or tiltrotor) nondimensional hover performance.

I have included one additional hover performance figure from the CL-84 evaluators' report [211] here as Fig. 2-92. The evaluators apparently felt confident, based on one point, that there was a performance gain to be had by operating the proprotors at a high tip speed. For example, 100 percent "propeller speed" was 1,228 revolutions per minute. This means the design tip speed of the 14-foot-diameter, four-bladed Curtiss-Wright Model 1490A2P3 propeller would be 900 feet per second, which is a tip Mach number slightly over 0.8. Incidentally, the Activity Factor (AF) of this Curtiss-Wright propeller blade is quoted as 90. You will recall that AF is a form of what proprotor advocates call power-weighted solidity. That is,

$$(2.83)\quad AF_{per\ blade} = \frac{100,000}{16} \times \int_{root}^{tip} (r/R)^3 (b/D)\ d(r/R)$$

where propeller advocates use (b) as blade chord. The conversion between the two forms is simply

$$(2.84)\quad \text{Power-Weighted Solidity} = \sigma_P = \frac{128(\text{Blade Number})\, AF_{per\ blade}}{100,000\pi},$$

so that one CL-84 proprotor had a power-weighted solidity of 0.1467. On this basis, the blade loading coefficient (C_T/σ) varied from about 0.145 at 89.5 percent rotor speed down to 0.120 at 100 percent rotor speed. I might add that the "design integrated C_L" of the blade airfoils was 0.498.

Now let me proceed to the power required in forward flight. The Tri-Service test evaluators summarized their view with just one figure, which you see here as Fig. 2-93. The coordinate system is referred power required versus referred speed and is, therefore, useable for all altitude and temperatures where incompressibility flow can be ensured. You encountered this way of presenting airplane performance data in Volume II, pages 213 to 216, and specifically from figures 2-98 and 2-99 on page 215. The high-speed data in referred coordinates was obtained from the rather few dimensional data points that are shown on Fig. 2-94. There are two points of interest on this data that I expect you have noticed.

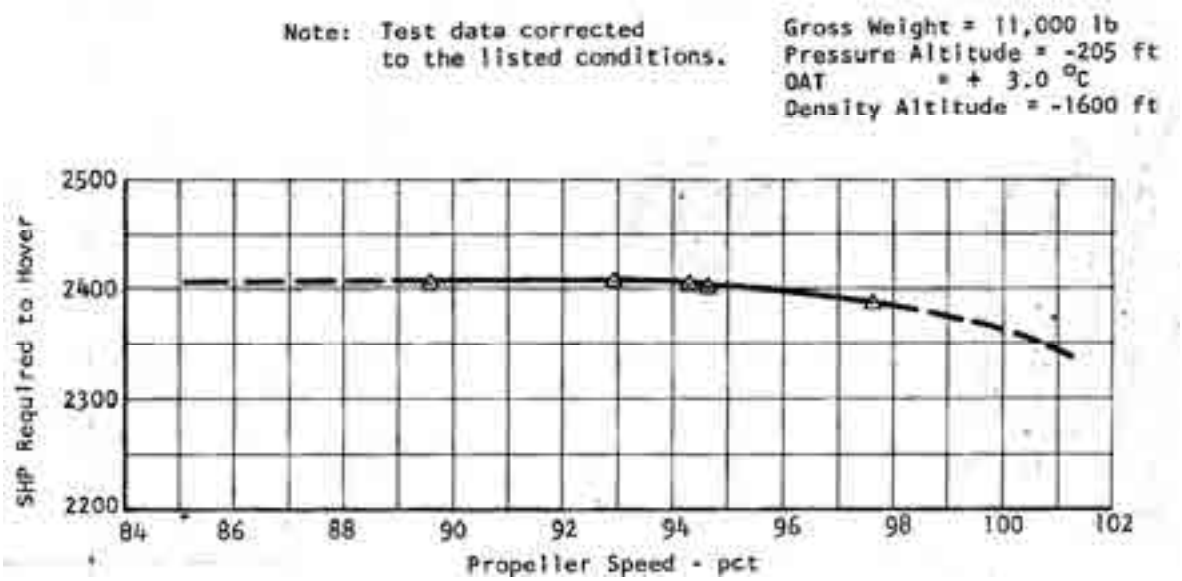

Fig. 2-92. The hover performance of the CL-84 appears to have benefited by operating at 100 percent of the design speed of 1,228 rpm—at least for this altitude and temperature where density (ρ) was 0.002448 slugs per cubic foot [211].

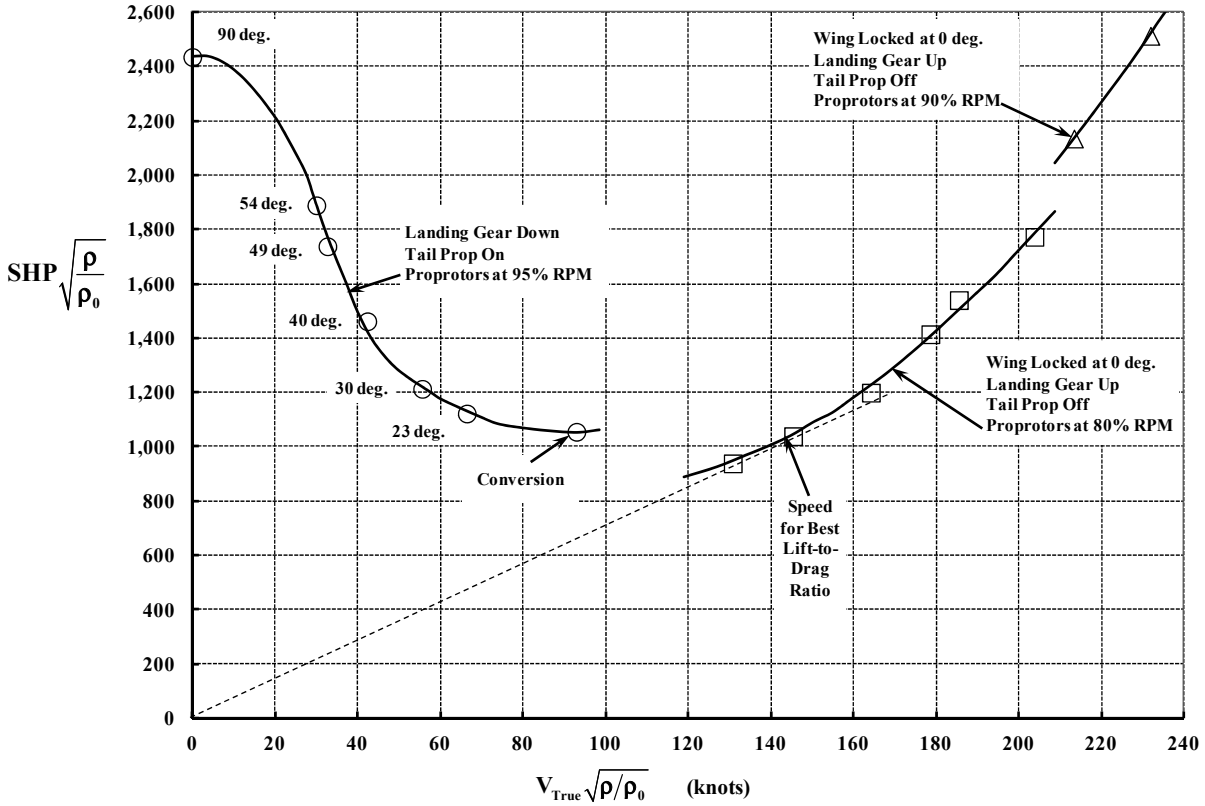

Fig. 2-93. The CL-84's forward-flight power required versus speed performance in referred coordinates (11,000 lb gross weight). (Ref. [211], fig. 62, used density ratio rather than $\sqrt{\rho/\rho_o}$ for high-speed shaft horsepower. I corrected the mistake for this figure. Forward speed was referred correctly.)

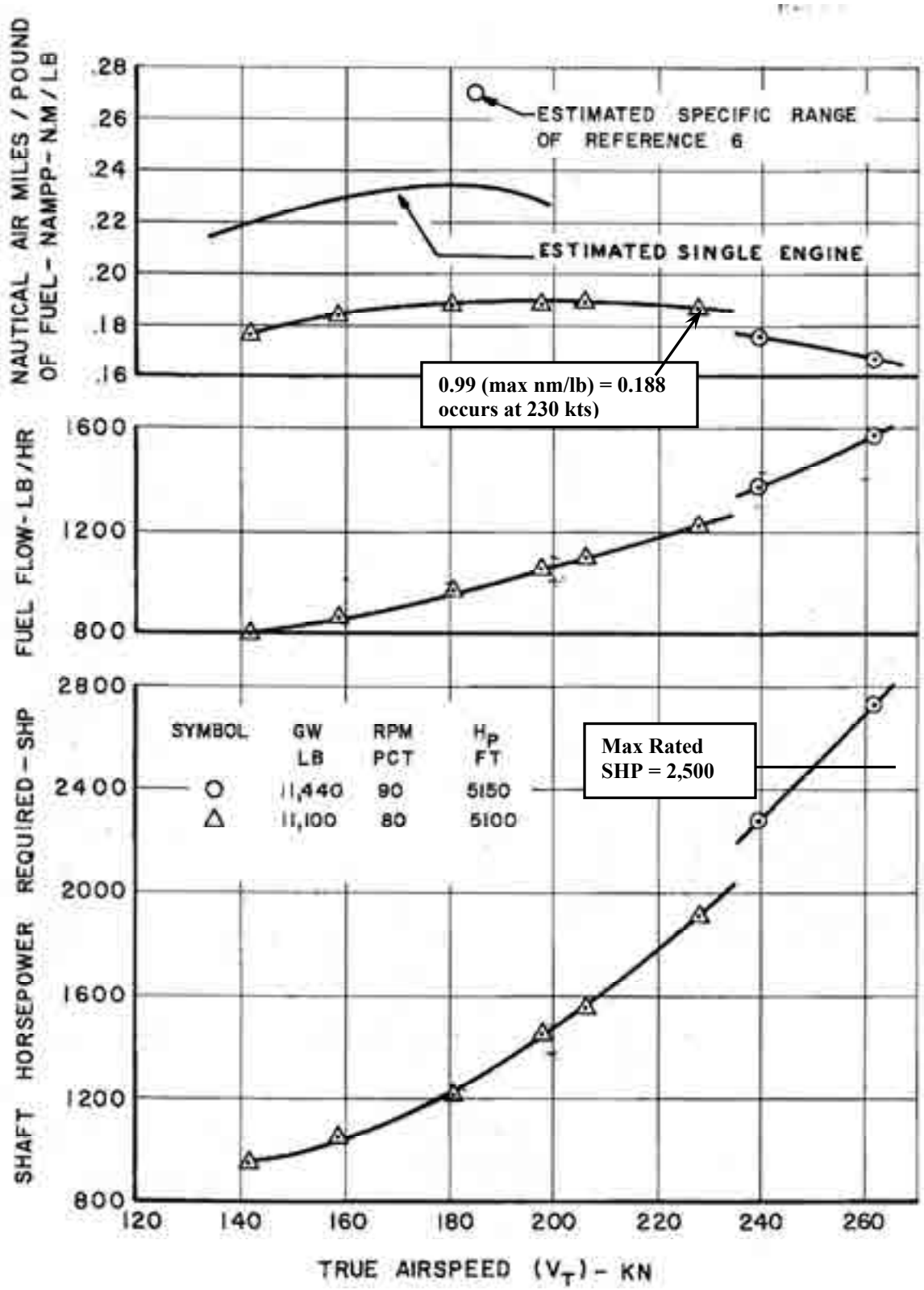

Fig. 2-94. CL-84 performance data [211].

The first point deals with maximum speed. To the power required curve, I have added the takeoff power available at 5,100-foot altitude, which is on the order of 2,500 shaft horsepower. According to the engine specification data in reference [211], the residual turboshaft jet thrust (F_N) is approximately zero at high speed. This means equivalent shaft horsepower (ESHP = SHP + $F_N \times V$) and engine shaft horsepower (SHP) are about the same. Evidently, the Canadair CL-84 had a maximum true airspeed of 250 knots at 5,100 feet. You might note, therefore, that this tiltwing had a horsepower per ton of gross weight of about 440.

Now to the second point. The upper graph on Fig. 2-94 is the specific range (i.e., nautical miles per pound of fuel, or nm/lb for short). Because the speed for best range is associated with 99 percent of maximum nm/lb, you can see that this true airspeed would be about 230 knots. What is also readily apparent from the data is that the actual specific range is about 70 percent of what had been estimated at the start of the design work. This shortfall was mentioned by the Tri-Service evaluation team in their report with the explanation:

> "The maximum range, endurance, and airspeed were less than those estimated in Reference 6 because of the higher-than-predicted drag. To provide an aircraft suitable for military missions, an increase in the fuel capacity and a reduction in drag are mandatory. A considerable number of drag reduction items could be incorporated into the aircraft, with a minimum of modifications. Some of these items were included in the aircraft specification of Reference 6, but they were not installed on the test aircraft during this evaluation. In addition, the removal of externally mounted test and prototype related equipment would improve performance.
>
> The data shown in figure 64 [Fig. 2-94] indicate that propeller rpm had a significant effect on range and endurance. Although this effect was evident, the limited flight time available for this evaluation precluded determination of the exact magnitude of these rpm effects or the establishing of the optimum rpm-to-airspeed relationship for maximum performance."

Let me add one closing paragraph from the evaluators' report dealing with Service Suitability. The evaluators wrote:

> "The test aircraft was unsuitable for use in any mission because of numerous hardware deficiencies and the extreme vulnerability of aircraft systems to enemy fire. However, the concept as exemplified by the CL-84 is considered to be suitable for the types of military missions mentioned above. The high maneuverability at low speed, short takeoff and landing characteristics, high acceleration, and deceleration capabilities peculiar to the concept greatly enhance service suitability. The simplicity of aircraft control, systems, and operating procedures enhances man/machine relationships for improved mission performance."

In my view, the Canadair CL-84's very positive flight evaluation kept the door open for continued tiltwing research and development—and the report [211] made sure the tiltwing would be a configuration included in future studies and requests for proposals. Furthermore, in my opinion, it was a key reason why the U.S. Department of Defense Tri-Service program ultimately selected the larger version—an assault transport proposed by the team of Vought-Hiller-Ryan—for development. The U.S. Tri-Service program was a key step along the path to the Vought-Hiller-Ryan XC-142.

2.12.4 The DoD Tri-Service Program

The Department of Defense saw enough potential in VTOL that it began serious consideration of a program that started in the very early 1960s. Along the way, the Curtiss-Wright X-19 (Fig. 2-95) and the Bell Aerospace X-22A (Fig. 2-96)—as well as the Vought-Hiller-Ryan XC-142 (Fig. 2-76)—all reached flight test with varying degrees of success. The Tri-Service program came to an end in 1970 after flight evaluation of the XC-142 was completed, and the U.S. Air Force changed the emphasis from VTOL to STOL. This change in emphasis ultimately led to the Advanced Medium STOL Transport (AMST) and the YC-14 and YC-15 STOLs, which you will read about later.

There is only one version of the Tri-Service program that tells the story close to what I remember. This version, coauthored by Bernie Lindenbaum[51] and Dan Fraga [212], was published in October 1972. Because I cannot possibly tell the story better than Bernie and Dan did, let me quote their words:

> "Starting in 1961, the United States Department of Defense undertook development of three V/STOL aircraft concepts, as 'Tri-Service' programs. These were the XC-142A, X-19 and X-22A and [they] are examined in this paper. During the same time period there was another tri-service program based on the P-1127. This will not be included, because the nature and objectives of this effort differed substantially from the other three, and also because the P-1127 was basically not a U.S. development.[52] This paper will examine aspects of propeller-based propulsion systems for VTOL aircraft as represented by the three distinctly different design concepts found in the XC-142A, X-19 and X-22A.
>
> While there was no specific overall plan to undertake all of the three tri-service efforts which ultimately developed, the Fall of 1959 can be identified as the starting point for this activity. At that time an Ad Hoc group (called the Perkins' Committee) was convened by Dr. Herbert York, then Director of Defense Research and Engineering (DDR&E), to review military requirements and the state-of-the-art and to make recommendations regarding U.S. national policy on further development of V/STOL aircraft. This resulted in the report 'Evaluation of V/STOL Aircraft' issued on 15 April 1960. The following quoted passage, extracted from the report, set the stage for the program which was to become the XC-142A:
>
> > 'The U.S. VTOL research aircraft program (test beds) demonstrated the technical feasibility that V/STOL aircraft can be built in a number of configurations which contain the vertical take-off and landing capability of rotary wing aircraft, yet do not have the limitations of speed, range and complexity of helicopters; however, the operational suitability of V/STOL to meet military requirements must now be demonstrated. Unless a program for operational suitability is initiated, the uncertainty that exists today will continue.'

---

[51] Bernie was a well-known V/STOL advocate in the more technical side of the U.S. Air Force Flight Dynamics Laboratory in Dayton, Ohio. Between Bernie and Charlie Crawford, who carried the U.S. Army helicopter development efforts on his shoulders for so many years, industry V/STOL champions had two, very technically savvy, very fair, and very influential cohorts. Helicopter and other V/STOL pilots and crew really have them to thank for most of the products that were developed over a nearly four-decade period that began when first-generation machines were converting to gas turbine engines.

[52] The authors might also have mentioned the British program that led to the Short SC.1 [213], which preceded the Hawker P-1127 that ultimately gave us the Harrier. The fighter type SC.1 began conventional airplane flying on April 2, 1957, and tethered hover flying in May of 1957.

One of the actions recommended in the report was the initiation of a program for the development of a tilt-wing assault transport aircraft, designed to satisfy effectively the requirements of the three services.

The VTOL research aircraft program referred to was the series of developments which had taken place during the previous decade wherein numerous configurations were built and flown with varying degrees of success and which proved that there were many promising approaches to VTOL. These efforts covered many concepts from propeller driven tail sitters through tilting rotors, tilting wings, deflected slipstream, lift fans and jet lift types; efforts which represented a substantial monetary investment. It was this proliferation of efforts aimed at finding the 'solution' to VTOL, which led to the formation of the Perkins' Committee. That many of these were based upon propeller propulsion is noteworthy.

In consequence of the Perkins Committee's recommendation, the three services undertook definition of the requirements and the development of a cargo-assault transport type of VTOL airplane. Size and performance were selected to permit establishment of the operational capability and flight characteristics of a reasonably-sized VTOL airplane. It was decided to develop an airplane of approximately 40,000 lb gross weight which would be capable of carrying an 8,000 lb payload one way, outbound, on a 200 NMI radius mission.

The Navy was given the responsibility for managing the ensuing competition, with participation by the other two services. Hence, the requirements which were circulated to industry in January 1961 were put out as a Navy Type Specification (TS-152). Nine companies responded to the request for proposal, and the designs represented an interesting array of concepts. The range covered single tilt wing, tandem tilting wings, tilting ducted propellers, tilting propeller-rotor, direct jet lift and compound helicopter approaches.

Each service made its own evaluation of the proposals and, initially, the services chose different winners. A compromise choice was arrived at, however, in the Vought-Hiller-Ryan design, which was to be later designated as the XC-142A. It was this initial disagreement in concept selection which later led to the other two tri-service programs. In the original evaluation, the Army favored the approach of a single tilt wing with four-propellers because of its superior STOL capability; the Navy preferred the four-ducted propeller tandem wing arrangement because of compactness and inherent safety for shipboard personnel during operations, and the Air Force selected a four-open-propeller tandem tilt wing arrangement because it believed this to be the best configuration for a high speed VTOL machine. It should be noted that the requirements against which the proposals were made, basically were aimed at VTOL operation; STOL was not a requirement.

After the evaluation was completed and a single selection was made, the Air Force assumed management of the program. The contract for the XC-142 was awarded to Chance-Vought (which later became Ling-Temco-Vought) in January 1962 with Hiller and Ryan as major subcontractors. Estimated cost of the program, which was to provide five aircraft, was 76 million dollars; a cost which was to be equally shared by the three services.

Because the original Navy and Air Force preferences differed from the selected concept, the Department of Defense later approved two additional but smaller tri-service programs, the X-19 and X-22A.

The X-19 began as an entirely private development of Curtiss-Wright with the company designation M-200. It was to be a high speed VTOL airplane for the executive transport market. Curtiss-Wright had done considerable development work on the concept, starting with the two-propeller X-100 (Figure 1) and culminating in the M-200. After considerable development effort on this machine, the company decided to seek U.S. Government aid, and the Department of Defense agreed to help fund the completion of the

M-200 (X-19) with the objective of obtaining data for evaluation of this VTOL approach. Since the M-200 configuration was similar to the Air Force's initial concept preference in the XC-142 competition, program management responsibility was assigned to the Air Force XC-142 organization in 1962. Because of the advanced state of the development prior to the contract, the government agreed to exercise only minor control over the design and construction of the machine, the major interest being in the flight test and evaluation of the aircraft. The government funding for the effort was to have been about 8 million dollars and cover both the development and the test phases. Curtiss invested at least as much in the program.

The X-22A program began with the Navy and was based on their need for an aircraft suitable for shipboard operation and one which could be used to explore the area of V/STOL flight control. Since future Navy use of VTOL aircraft would be primarily on ships, the Navy's preference was the shrouded propeller approach. Compared with the open-propeller types, this was considered to be much safer for deck personnel during shipboard operations. A competition was held by the Navy between Bell Aerospace Corp. and Douglas Aircraft Co. Bell won, and in November 1962 was given a 17 million dollar contract to build two vehicles. Bell undertook an extensive development effort and in March 1966 flew an X-22A for the first time. However, it was not until January of 1971 that the Navy accepted the aircraft (one only, the first having been severely damaged in an accident in August 1966). Operation of the X-22A as a flight control research vehicle was contracted to the Cornell Aeronautical Laboratory in January 1971 and that program is still active.

Of the three tri-service programs, only the X-22A is still in use. The XC-142A program was completed and the knowledge gathered was to have provided the basis for the development of a new tilt wing airplane to meet the Air Force's Light Intratheater Transport [LIT] requirement. But change in emphasis from V/STOL to STOL in 1970 caused abandonment of the effort. With regard to the X-19, the contract was terminated shortly after the first aircraft crashed. The second machine was never completed and the progress was abandoned.

While these three concepts differed substantially from each other, all were based on the philosophy that the propeller is a highly effective device for providing both good hover capability and efficient cruise flight."

You read in the second paragraph of Bernie and Dan's story about the Perkins' ad hoc committee in 1959 making "recommendations regarding U.S. national policy on further development of V/STOL aircraft." Twenty years later a similar activity was conducted by the Defense Science Board whose chairman was Eugene Fubini. Fubini turned to Courtland Perkins to marshal a task force to establish the state of the art of V/STOL aircraft in 1979 and recommend a Department of Defense policy for such aircraft. Perkins' task force concluded "that V/STOL aircraft in various subsonic and supersonic configurations are technologically supportable over the next several decades." There was "strong support for V/STOL aircraft in useful military missions. The front-end investment may be high, however, the pay-off is considered to be potentially in excess of that investment." One thing I found quite interesting was that the task force stated that "the Army has little need for V/STOL aircraft beyond the helicopter." Furthermore, the development beyond the Harrier (i.e., the AV-8B) was clearly recommended, and the tiltrotor had been "developed to the point where successful and useful aircraft can be constructed and operated." Much of what the task force recommended was followed as you will find when you read the full report [214].

Fig. 2-95. The Curtiss-Wright X-19. This 10,600-pound VTOL technology demonstrator made its first hovering flight on May 7, 1965. The first full conversion back and forth from hover was made on January 17, 1968.

Fig. 2-96. The Bell Aerospace X-22A. This 15,300-pound VTOL technology demonstrator made its first hovering flight on March 17, 1966. The first full conversion back and forth from hover was made on March 3, 1967.

2.12.5 The Vought-Hiller-Ryan XC-142

The team of Vought-Hiller Aircraft Corporation and Ryan Aeronautical Company won the DoD Tri-Service competition on September 15, 1961, and its tiltwing aircraft was designated as the XC-142A (Fig. 2-97 through Fig. 2-103) by the services. The objective was a cargo/assault transport that could carry 32 troops out 200 nautical miles. Contract go-ahead was given on January 5, 1962, and some 33 months later, the machine made its first flight on September 29, 1964. The first flight was as a conventional airplane. The first hovering flight was made on December 29, 1964, and the first conversion and reconversion was made on January 11, 1965 [215]. The team had sufficient development flying done by early March 1965 to warrant a preliminary Tri-Service V/STOL Test Force evaluation, which was conducted at the Ling-Temco-Vought Corporation in Dallas, Texas. This month-long, Category I evaluation went on from March 17 to April 20 of 1965. The results of this evaluation were reported January 1966 [177].

The Category I evaluation report was not exactly glowing because the opening paragraph of the Conclusions and Recommendations stated:

> "The XC-142A design objective was to provide a full scale tilt-wing V/STOL transport aircraft with which the operational capabilities could be determined for V/STOL aircraft in general and tilt-wing V/STOL aircraft in particular. It was not intended to be a production model. As a concept evaluation vehicle it was satisfactory except for three known safety of flight deficiencies and 22 known deficiencies which would interfere with Category II testing if not corrected. There were 44 additional deficiencies which should be corrected and re-evaluated during Category II tests and 44 more which should be corrected for a production C-142. Most of the known deficiencies were with systems which had not been sufficiently checked out before installation due to the limited funds available. [Talk about penny-wise, pound-short planning!] The novel and critical systems (i.e., flight control system, gearboxes, cross-shafting, wing tilt, etc.) were more completely developed before installation and gave little trouble. The aircraft was safe and simple to fly. Most of the deficiencies were in the aircraft sub-systems. With the correction of 25 items the XC-142A would be ready for Category II tests. The XC-142A was not ready for production.
>
> Each recommendation has the letter A, B, C, or D as a prefix. These letters denote the following:
>
> A—Safety of Flight. Mandatory correction prior to delivery of the first XC-142A for Category II testing.
>
> B—Deficiencies which will interfere with the Category II concept evaluation unless corrected. Mandatory correction prior to delivery of the first XC-142A for Category II testing.
>
> C—Deficiencies which will not interfere with the Category II concept evaluation, but the corrections should be evaluated before the end of Category II. Mandatory correction before the end of Category I testing.
>
> D—Deficiencies which should be corrected for an operational aircraft. Desirable correction before the end of Category I."

The three safety-of-flight deficiencies (the A category) dealt with (a) a poor overhead emergency escape hatch design, (b) no capability for the pilot to monitor the cross shaft bearing temperatures, and (c) overstressing during ground operation of the aileron servo valve.

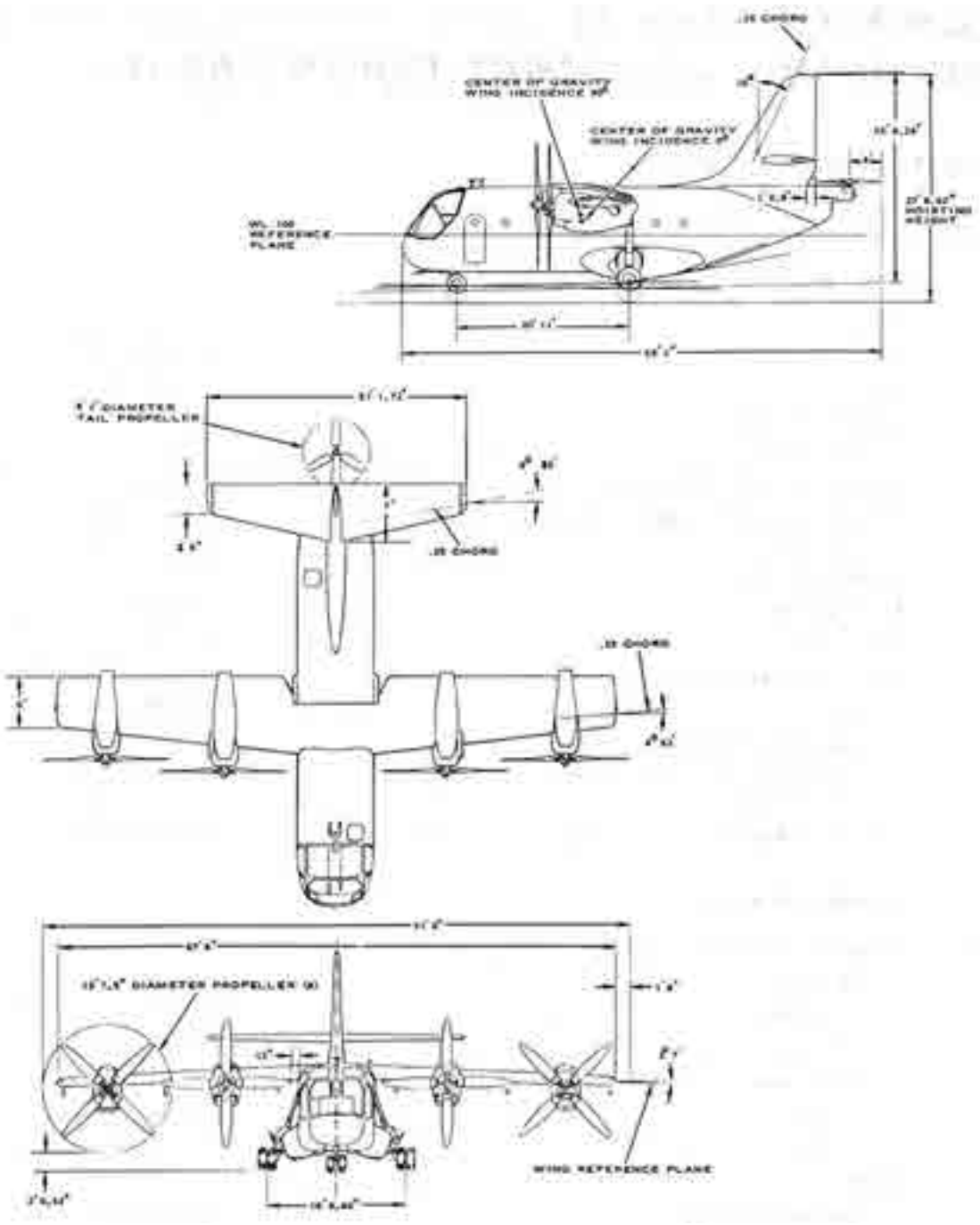

Fig. 2-97. The XC-142A was powered by four T64-GE-1 engines rated at 3,080 shaft horsepower for 10 minutes at sea level standard day. The proprotor was designed for a tip speed of about 1,200 feet per second, but hover testing was conducted at 950 feet per second because of drivetrain limitations. In cruise, proprotor speed was reduced to 750 feet per second [215].

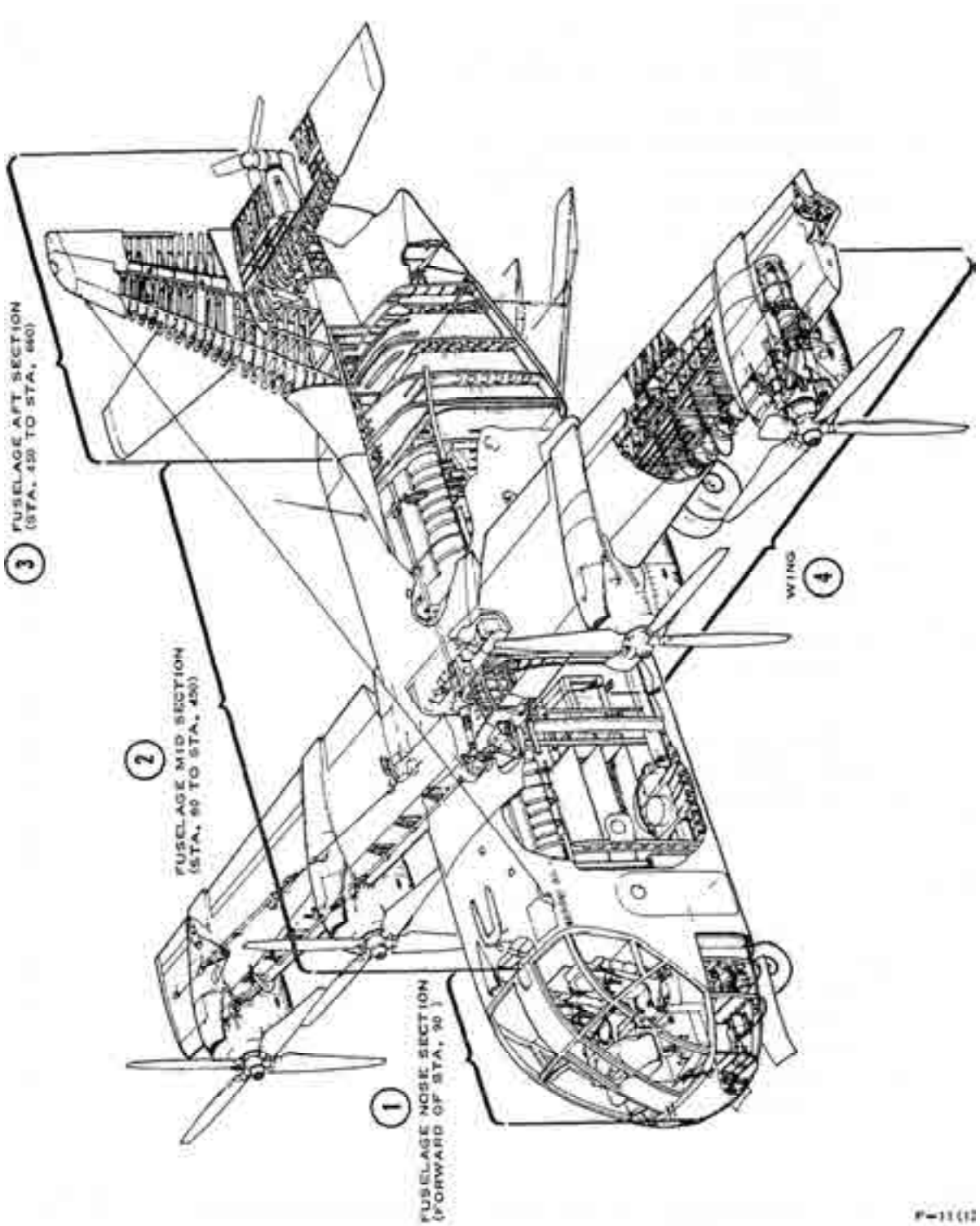

Fig. 2-98. The XC-142A's design weight empty was 23,039 pounds, but when flight testing was stopped, this weight had grown to 25,552 pounds. The design VTOL gross weight was 37,474 pounds, and this was the weight that performance guarantees were based on. Rear ramp loading provisions do not lead to aerodynamically "clean" airplanes [215].

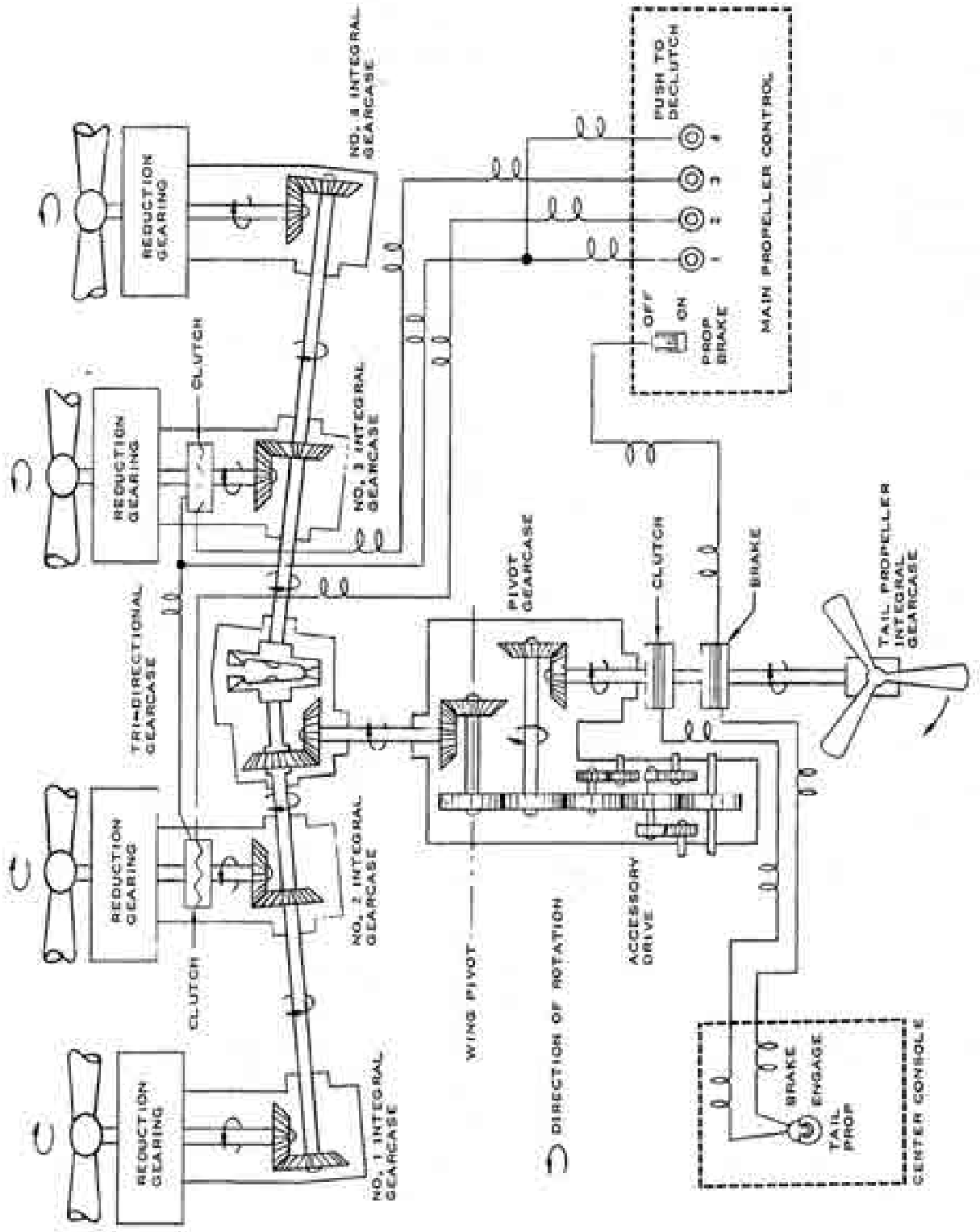

Fig. 2-99. The XC-142A's drivetrain had 26 gears—not counting the two gears in the "tail propeller" gear box [215].

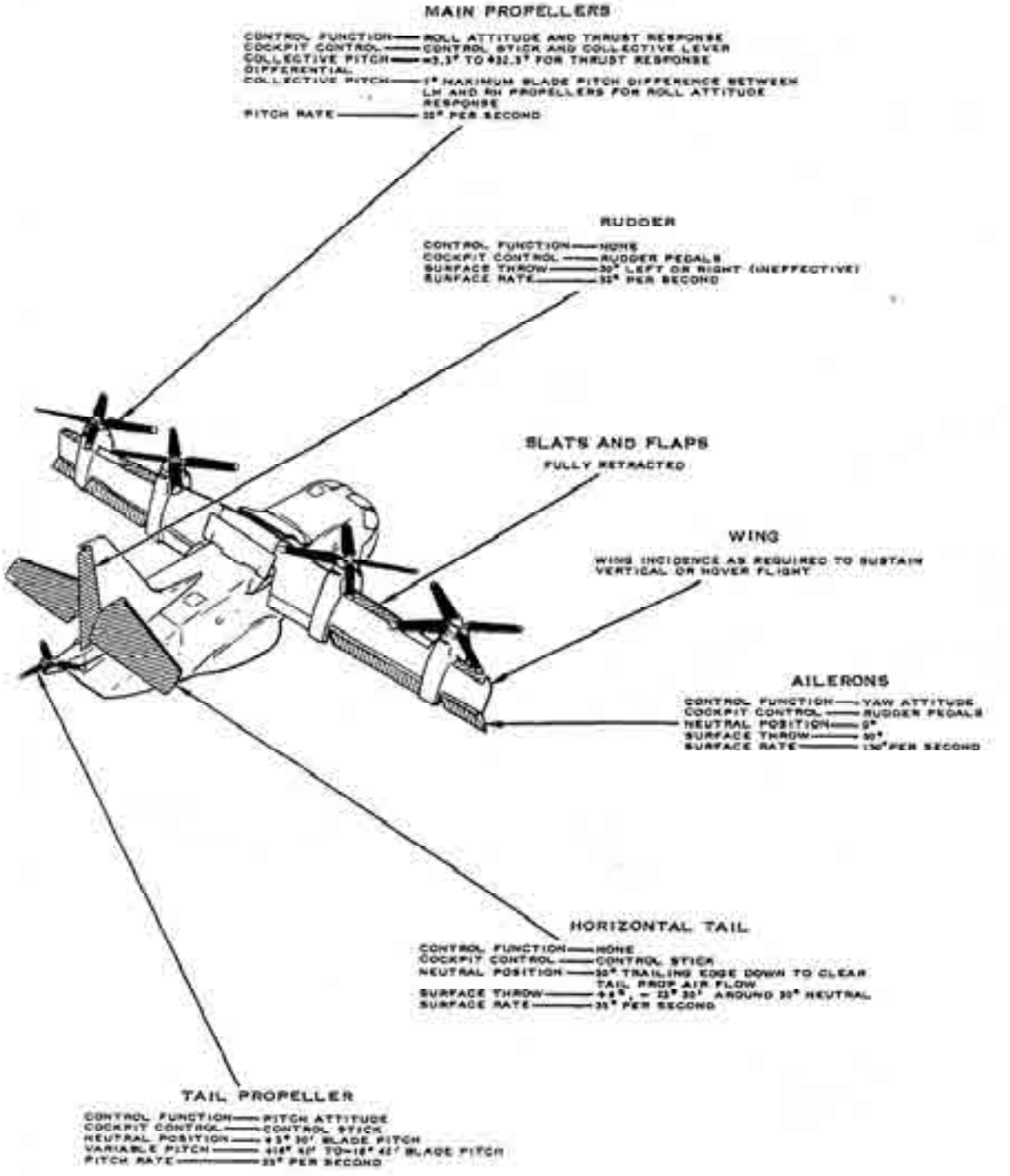

Fig. 2-100. The XC-142A's controls for vertical and hover flight [215].

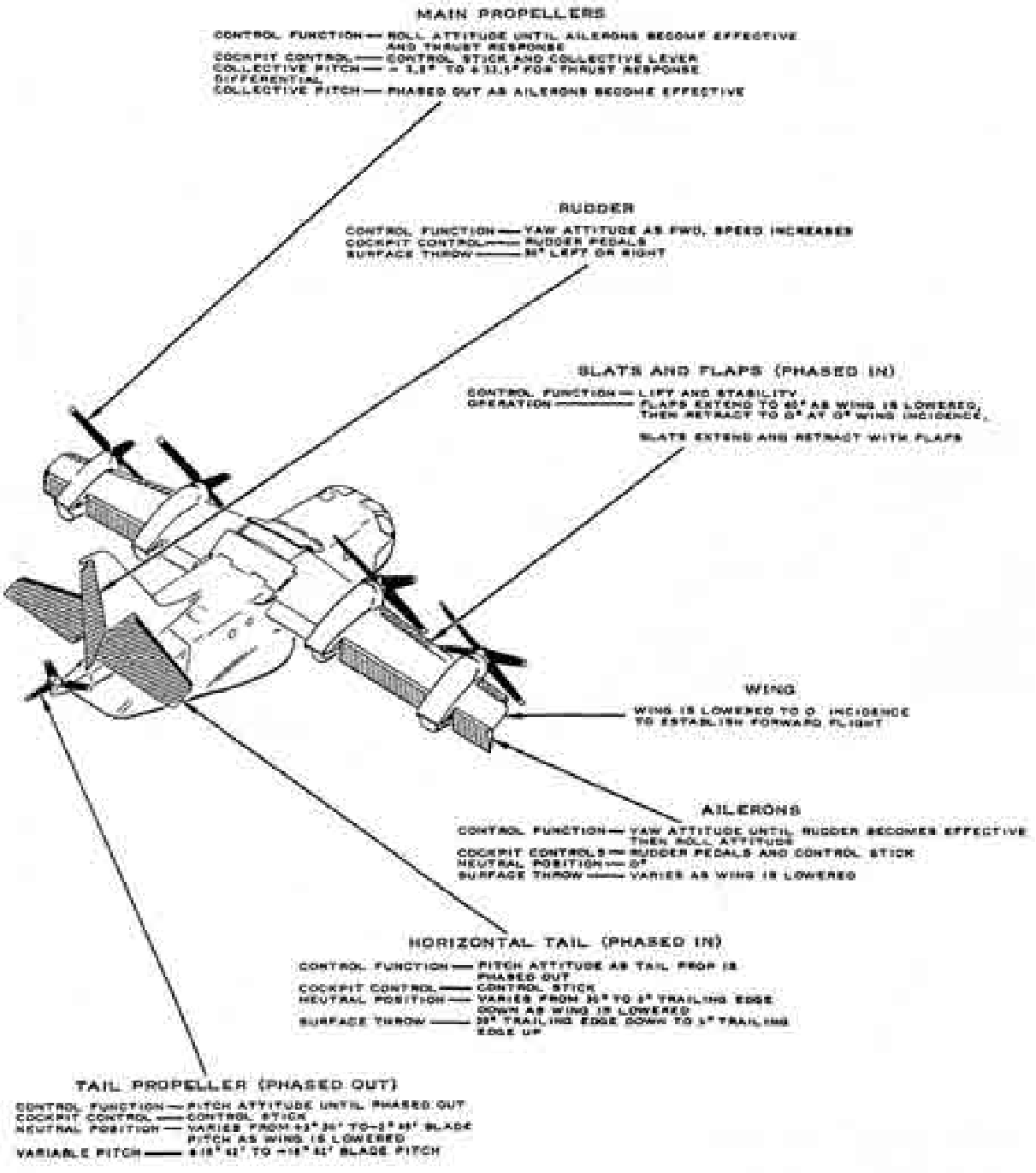

Fig. 2-101. The XC-142A's controls for transition flight [215].

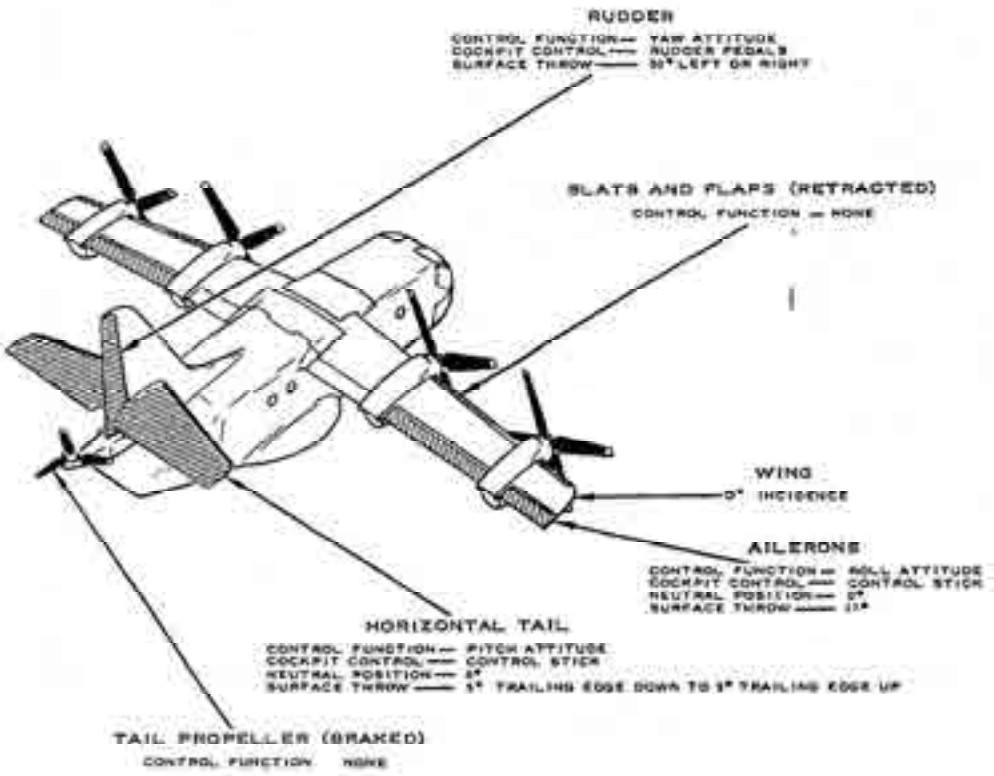

FLIGHT CONTROL RESPONSES

CONTROL FUNCTION	COCKPIT CONTROL	AFFECTED CONTROL SURFACE		
		HOVER	TRANSITION	CRUISE
ROLL	CONTROL STICK	DIFFERENTIAL PROP PITCH	DIFFERENTIAL PROP PITCH AND AILERONS	AILERONS
YAW	RUDDER PEDALS	AILERONS	DIFFERENTIAL PROP PITCH, AILERONS AND RUDDER	RUDDER
PITCH	CONTROL STICK	TAIL PROP	TAIL PROP AND UNIT HORIZONTAL TAIL	UNIT HORIZONTAL TAIL
THRUST	COLLECTIVE LEVER	COLLECTIVE PROP PITCH AND ENGINES	DIFFERENTIAL PROP PITCH AND ENGINES	NO CONTROL
THRUST	THROTTLES	NO CONTROL	NO CONTROL	ENGINES

EFFECTIVE CONTROL SURFACE RESPONSE VARIES WITH WING INCIDENCE AND IS INDEPENDENT OF PILOT INPUTS TO THE FLIGHT CONTROLS. PILOT INPUTS TO THE FLIGHT CONTROLS AFFECT AMOUNT OF SURFACE RESPONSE ONLY.

F-71(3)A

Fig. 2-102. The XC-142A's controls for cruise flight. Note that the tail propeller was declutched and braked in airplane flight [215].

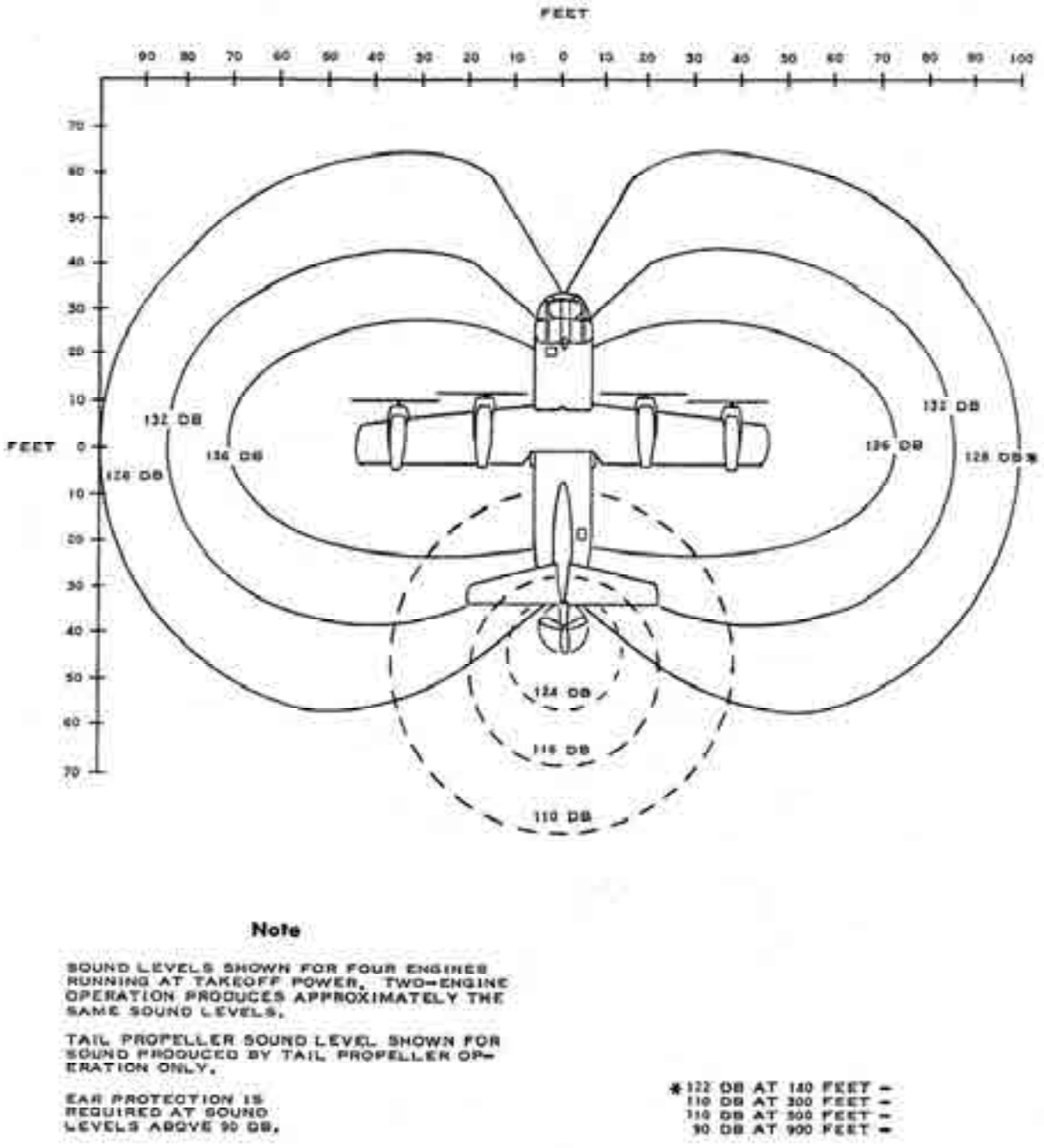

Fig. 2-103. The XC-142A's noise contours clearly made ear protection a requirement even if you were 1,000 feet away from the machine when it was hovering [215].

The test evaluators were dissatisfied with several flight restrictions, but put them all in the C category. However, they wanted several deficiencies fixed before the end of Category I testing. Lastly, the test team felt that a production aircraft—should the aircraft get that far—had a number of shortcomings that needed attention at this stage.

With respect to the aircraft in total, there were a considerable number of deficiencies the evaluating test team sought before Category II testing or production could begin. I have sorted the deficiencies by alphabet in Table 2-8. As you can see, the Vought-Hiller-Ryan team had plenty to do before any XC-142A would be evaluated at the U.S. Air Force Flight Test Center at Edwards Air Force Base in California.

The hover performance was less than predicted by about 12 percent, but a redesigned proprotor was apparently already in the works.[53] The redesign was an increase in Activity Factor per blade from 86 to 105 while retaining the four-blade configuration and diameter at 15.625 feet. In rotorcraft terms, this was a power-weighted solidity increase from 0.148 to 0.171 according to Eq. (2.84). Incidentally, the flight hub moments were much higher than engineering expected, and a hub redesign was required.

Table 2-8. Category I Evaluation of the XC-142A Created 113 Action Items

Item	Total	A	B	C	D	Harris' Comments
Safety	3	3				Poor overhead escape hatch
Flight restrictions	10			9	1	Expand flight envelope to 300 knots
Performance	2			2		Hover performance 12 percent below contract spec
Handling qualities	8		1	6	1	Control forces too high
Airframe	15		3	5	7	Vibration causing windshield distortions
Cockpit	16		3	5	8	Several switches in wrong place; seats not adjustable
Engines	8		3	3	2	Several cracks in airframe/engine interface components
Drivetrain	4		1	1	2	Tri-directional gearbox limited to 10-hour inspections
Propellers	1		1			Strengthen propeller hubs
Fuel system	1		1			Relocate defueling valve
Electrical system	10		2	2	6	High vibration breaking wire bundles
Hydraulic system	8		1	1	6	Power control system 1 and 2 in wrong order
Landing gear	4		1	2	1	Indication system not reliable
Heating system	1				1	System did not function properly
Avionics	6		2	2	2	Numerous noise and interference problems
Auxiliary power unit	2		1		1	APU operation erratic
Flight controls	5		2	3		Pitch trim creep; g loads affect prop pitch; must be able to exceed takeoff power in an OEI emergency
Ice protection	1			1		Not installed; must be installed on aircraft 4 or 5 for Cat. II
Propeller wind blast	1				1	Define hazard areas
Noise	1			1		Levels too high in and about aircraft; P-1 and P-4 helmets inadequate
Crew comfort	3		1		2	Need "cool suits" for Cat. II; cross country is out
Static electricity	1				1	Need permanent static ground wire
Manuals	2			2		Need updating; need cargo loading manual
TOTALS	**113**	**3**	**23**	**45**	**42**	

[53] I know of no new helicopter or V/STOL development program that has met its contractual hover performance specification after early flight test data was acquired. The shortfall seems to be between 5 and 15 percent.

It took the Vought-Hiller-Ryan team a little over 2 years to meet many of the test evaluators' requirements and "fix" its XC-142A so that it was ready for the second go-around at test evaluation. This Category II evaluation by the Tri-Service Test Force was conducted in three segments as the final report for performance[54] dated October 1968 [178] notes in its introduction:

> "The flight testing was accomplished with three aircraft over three separate periods of time. During the first portion of the tests, with aircraft S/N 62-5923, only a pitot-static system calibration was obtained before the airplane crashed during a reconversion. During the second portion of the tests, with aircraft S/N 62-5921, 16 flights were made, totaling approximately 11.5 hours of productive flying time. Tests were limited to those necessary to support the operational suitability test objectives and those tests supporting the assault transport mission evaluation; they consisted mainly of determining the VSTOL capability of the aircraft. The aircraft and instrumentation were maintained by personnel of the Ling-Temco-Vought (LTV) Aerospace Corporation.
>
> The third portion of the Category II tests was conducted with aircraft S/N 62-5922. This aircraft was built by mating the fuselage of the original aircraft of the same serial number, with the wing of aircraft S/N 62-5923. The original aircraft S/N 62-5922 was seriously damaged at the contractor's facility in Dallas, Texas, in October 1965.
>
> During this portion of the tests, 15 flights were made, totaling approximately 15 hours of productive flying time. These tests were made primarily to define the mission capability of the aircraft. The aircraft and instrumentation were maintained by the USAF and the USA with support from the LTV Aerospace Corporation.
>
> During the final phases of the Category II tests the rebuilt aircraft S/N 62-5922, with a contractor crew on board, crashed and was severely damaged on 9 October 1967. This accident terminated the test program prematurely, resulting in incomplete data in some areas.
>
> Persistent subsystem problems contributed to a high percentage of maintenance downtime and a high abort rate throughout the test program. The structural integrity of the aircraft was compromised because of failures of mechanical, hydraulic, and electrical components. These failures were caused by a severe vibration environment, resulting in metal fatigue."

This first major tiltwing aircraft program came to an end in November of 1967, and then a great deal of engineering data was simply put on the shelf. The performance report [178] states that the aircraft met its hover ceiling requirement to hover (out of ground effect) (HOGE) at 6,000 feet on a standard day (density equals 0.001988 slugs per cubic foot). The gross weight was 37,474 pounds, and the four turboshaft engines were at their takeoff rated power of 2,780 SHP per engine at 6,000 feet.

The XC-142A's HOGE performance in engine power (C_P) and weight coefficient (C_W) form is shown in Fig. 2-104. Because of the accident on October 9, 1967, the test evaluators were, in fact, in a data-short position. However, from the hover performance data they did have, they concluded that the XC-142A did meet the contractual requirement. This requirement is shown as the black, solid diamond on Fig. 2-104. One XC-142A propeller was

[54] There is a report on Stability and Control [216] and also one about Operational Suitability [217]. Both of these reports are still restricted, so I can only provide the references.

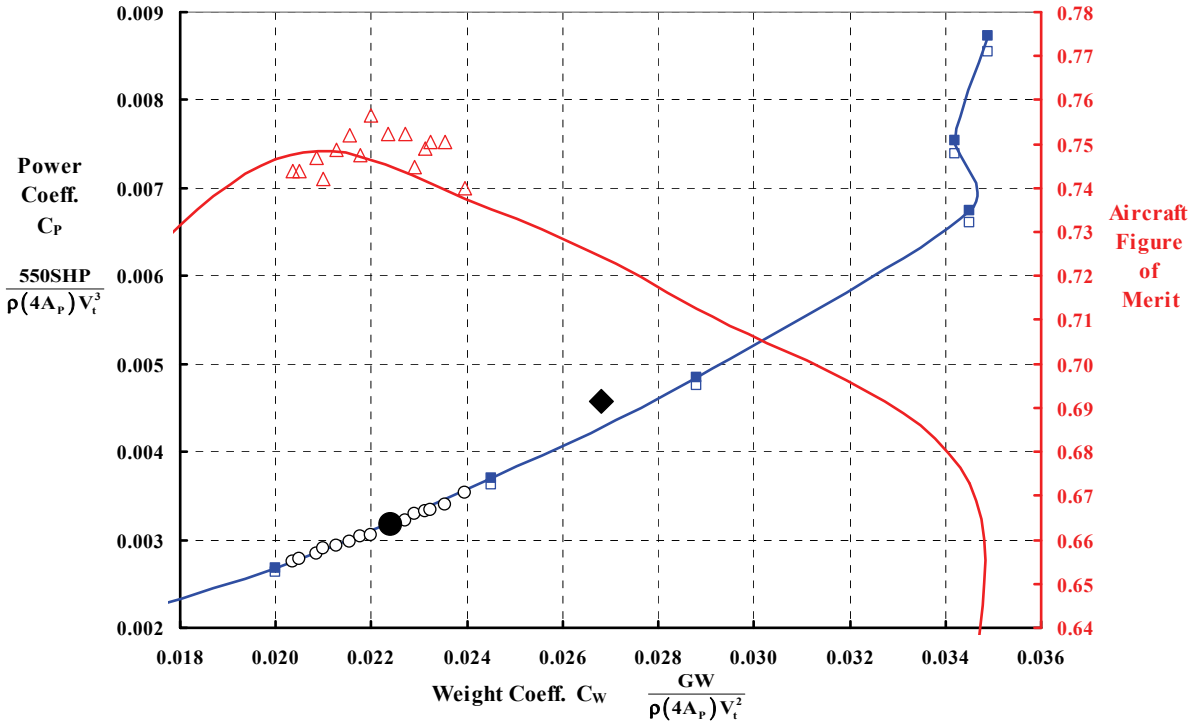

Fig. 2-104. Category II hover performance data out of ground effect was incomplete because of the October 9, 1967 accident and the ending of the XC-142 program in November 1967.

tested on the static propeller test rig at the Air Force Aeronautical Systems Division facility in Ohio. The data was reported in references [218, 219].[55] I have used that isolated propeller data to construct the solid blue line you see on Fig. 2-104. The transmission efficiency was on the order of 0.98, and the accessory power losses were about 44 horsepower. You will note in passing that a tiltwing has virtually no wing download so nearly all the propeller thrust goes to supporting gross weight. This is in direct contrast to a tiltrotor, which gives up anywhere between 10 and 15 percent of its proprotor thrust because the proprotor slipstream impinges on nearly all of the wing area. This impingement creates a wing download, which is negative thrust. You can see the contrasting configurations by comparing Fig. 2-76 to Fig. 2-77.

Fig. 2-104 shows (with the Figure of Merit in red) that the XC-142A was close to its most efficient hovering regime for the 37,474-pound design weight *if* the hovering altitude was sea level on a standard day. Only 9,250 shaft horsepower was required at this condition. This rather minimal power to hover—compared to a military rated power of 3,080 times 4 or

[55] Because of the XC-142A's hover performance shortfall with the low Activity Factor (or solidity, if you prefer) propeller (C-W No. 2FE16A3-4A), the Air Force and the Curtiss-Wright Corporation went right to work to find a better design. The effort involved testing 28 different configurations (plus a calibration baseline). The aerodynamic geometry of the redesigned propeller (C-W No. 2FF16A1-4A) is given in reference [218]. If you ever wanted a gold mine of propeller test results to measure your hover theory against, this reference, and the tabulated data contained in reference [219], will make your task easier. Data up to tip Mach numbers of 1.7 and up to rotorcraft $C_T/\sigma = 0.2$ were obtained.

12,320 total shaft horsepower available—meant that the XC-142A could hover out of ground effect on three engines. Frankly, I found it quite interesting that the test evaluators did not address the XC-142A's ability to hover with one engine inoperative. What was addressed in detail was the nearly unbelievable STOL performance.

The reason I used the word "unbelievable" is because, even at a takeoff weight of 40,000 pounds, test data at sea level showed that the XC-142A pilots could consistently clear a 50-foot obstacle in 410 feet of concrete or carrier deck runway. The pilots only needed 120 feet before they lifted the aircraft off the ground at 41 knots, and they reached 57 knots as they passed over the 50-foot obstacle. In short, a ratio of military rated power to takeoff gross weight of 0.308 horsepower per pound gave the VTOL XC-142A excellent STOL performance off of U.S. Navy ships—without a catapult! The cover of Bill Norton's superb story [39] of the XC-142A, shown in Fig. 2-105, is a great record of the aircraft operating off a carrier deck. Furthermore, the operational suitability test report stated that "the XC-142A's outstanding performance and potential in the STOL mode was a paramount feature." The test evaluators were not so impressed with hover performance on a hot day. In fact, the performance report strongly recommended that the design criteria should be to hover out of ground effect at 6,000 feet with an outside air temperature of 95 ^{o}F. In addition, the thrust-to-weight ratio should be 1.15 to provide a control margin, which really starts to be expensive. Personally, I can only imagine what the aircraft power requirement would cost if pilots wanted to hover with one engine inoperative at 6,000 feet on a hot day.

Fig. 2-105. The XC-142A had installed power for a maximum speed of 355 knots. This excess power equated to exceptional STOL performance. Navy sea trials were quite successful [39] (photo courtesy of Bill Norton).

The test evaluators could make a reasonable case that the XC-142A met the hover requirement. They could not, however, make a similar case for the aircraft meeting forward-flight requirements. The maximum airspeed was to have been 355 knots "at sea level, at military rated shaft power." The combat radius mission was to be 200 nautical miles assuming a mission defined as "on a standard day, at sea level, at a takeoff gross weight of 37,474 pounds, with an outbound/inbound payload weight of 8,000/4,000 pounds, a fuel load of 5,644 pounds, and at a minimum cruise speed of 250 knots."

The evaluators determined from Category II data that the XC-142A only had a maximum speed of 315 knots at the forward center of gravity (c.g.) and only 240 knots at aft c.g. *because of stability and vibration problems*. The combat radius was determined to be 48 nautical miles principally because the evaluators reduced the fuel load to 3,492 pounds to account for the 2,513 pounds lost to weight empty increases of the test aircraft. That is, the design weight empty was 23,039 pounds versus the test aircraft's weight empty of 25,552 pounds. The crew was included at 430 pounds so that the takeoff gross weight was 37,474 pounds. This at least kept the payloads at 8,000/4,000 pounds, which was very important.

The power required data in forward flight that was obtained before the October 9, 1967 accident, was limited. However, the data that was obtained was very thoroughly analyzed and reported in the Category II Performance document [178]. Just for the fun of it and for the historical record, I transferred the tabulated forward-flight data into Microsoft® Excel® and followed the flight test engineering handbook of that time [220] to confirm the test evaluators view of the XC-142A.[56] The results are shown in Fig. 2-106.

The power required and available data shown in Fig. 2-106 suggest that the XC-142A might have demonstrated a maximum speed of 320 to 330 knots—depending on how you extrapolate the available data. Furthermore, the specific range data on Fig. 2-106 gives some indication of the XC-142A's fuel efficiency. The combat radius of 48 nautical miles that the test evaluators arrived at depends on (1) the start-up time, (2) the taxi and/or hover time, (3) the time to climb and the distance traveled, (4) the descent time and distance traveled, (5) the hover time at the combat zone, and (6) the similar return segments. Of course, some fuel must be held in reserve so the crew can get home. Because specifications for these mission segments are not immediately available to me, the one estimate I can make is that 3,492 pounds of fuel, at a specific range of 0.116 nautical miles per pound, equates to a range of 405 nautical miles. On this basis, the radius could hardly exceed 200 nautical miles.

The fuel used in the various mission segments can be roughly estimated using data from the Category II report [178]. The report states that "fuel allowed for engine start, taxi, takeoff and acceleration to climb speed [160 knots] was 500 pounds." The limited data available indicates the machine could climb to 20,000 feet in about 5 minutes after takeoff at a nominal gross weight of 36,000 pounds using military rated power and a propeller RPM of 91 percent. The average fuel burn rate was on the order of 4,300 pounds per hour or about 75 pounds per minute. The average true airspeed was about 210 knots or 3.5 nautical miles per minute. Therefore, in the climb to 20,000 feet, about 375 pounds of fuel was used, and the

[56] My results differed less that 1.5 percent from the data reduction output and graphs in the Category II report.

aircraft covered some 18 nautical miles. Thus, the available 3,492 pounds of fuel was reduced to about 2,617 pounds before the outbound cruise began at 20,000 feet and 250 knots. If you assume the return trip also uses 875 pounds of fuel to reach cruise altitude and speed, then the amount of fuel available for cruise becomes 1,741 pounds. Now, this amount of cruise fuel at a specific range of 0.116 nautical miles per pound means about 200 nautical miles of range, which is 100 nautical miles of combat radius. Add the 18 nautical miles from the climb segment and you might estimate the XC-142A's combat radius at 118 nautical miles versus the test evaluators' 48 nautical miles. *Because I have not included any fuel for reserve*, I would say the test evaluators were generous with their 48 nautical miles versus the specification requirement of 200 nautical miles.

Let me stop for moment and discuss the derivation of the XC-142A's lift-drag polar from the performance data measured during flight testing. This vintage 1960's step-by-step process that arrives at Fig. 2-107 is quite instructive when you see it written out. This process, as you might guess, is the inverse of the process used to predict power required (in advance of flight testing) when given a drag polar—from some source—as the starting point. To begin then, flight test data will give you a torque generally measured from the engine's torque meter, and for modern rotorcraft, a proprotor (propeller if you prefer) shaft torque measured

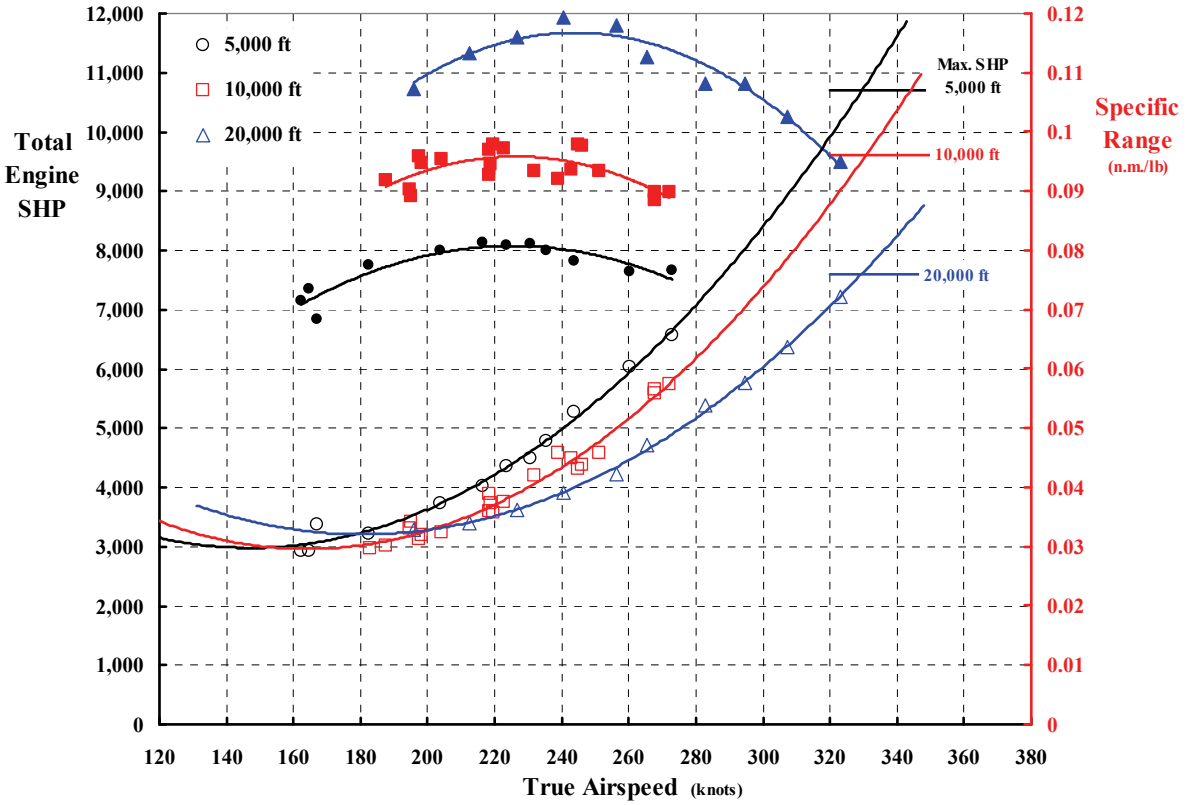

Fig. 2-106. The limited XC-142A power required data that was obtained suggests that the machine would have demonstrated a maximum speed on the order of 320 to 330 knots given the installed power available from four T64-GE-1 turboshaft engines.

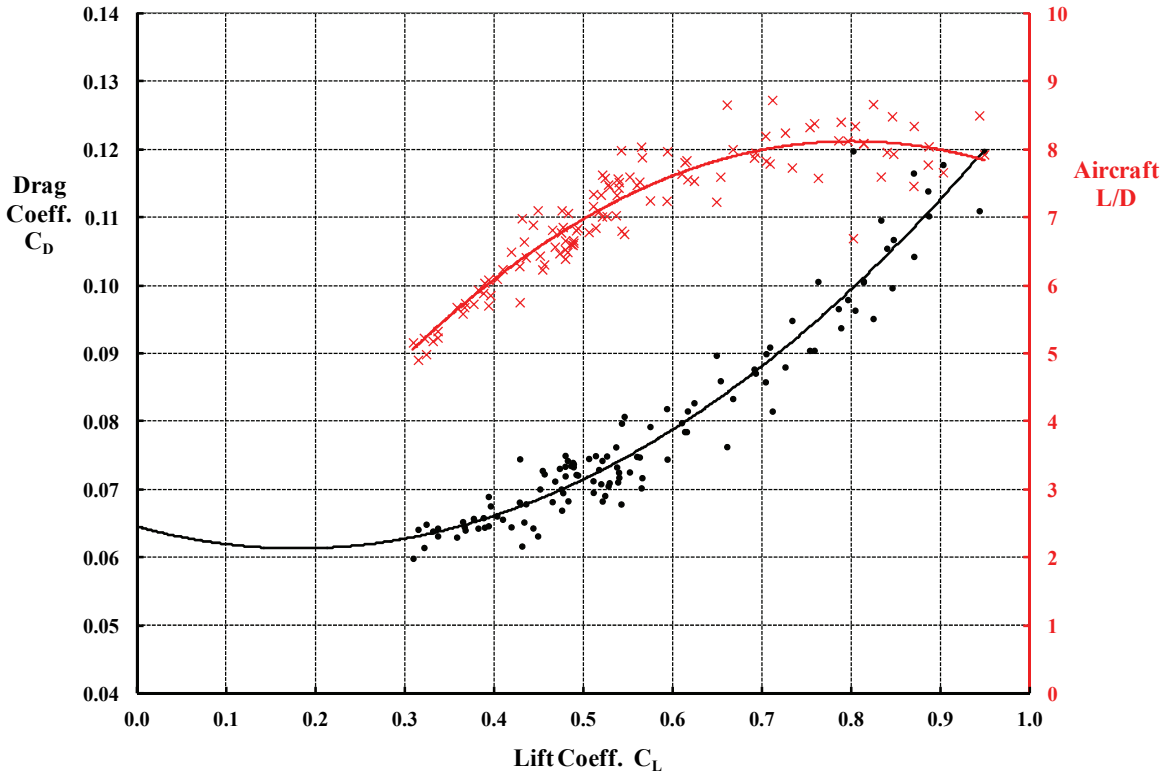

Fig. 2-107. XC-142A drag polar as derived from flight test data.

with a strain gauge. For the XC-142A, only engine torque in percent of the maximum was recorded (but the maximum was set at 1,350 foot pounds). Proprotor speed was also measured and expressed as a percentage of 1,232 rpm. The engine's relatively low torque and relatively high-power turbine speed was transmitted to the proprotor by a gearbox at a ratio of 11.04 to 1. On the XC-142A, the proprotor speed was increased by the gearbox ratio so that the engine shaft horsepower could be computed (and tabulated *and* printed out on paper) using the equation

$$(2.85)\quad SHP_{eng} = \frac{\text{Torque}_{eng}\ (\text{ft}-\text{lbs})\times[\text{Prop Speed (in rad}-\text{sec})]\times\text{Gearbox Ratio}}{550}.$$

The XC-142A's flight test data used an average of the four free-turbine-engine torques and, because of the proprotor interconnect provisions, the average of the four proprotor shaft speeds in Eq. (2.85). My observation was that the engine torques were generally not well matched while the proprotor shaft speeds hardly differed at all. Before this engine horsepower gets to the proprotor, its value is reduced by the transmission efficiency (η_t) and the engine accessory power (SHP_{acc}). That means the proprotor shaft horsepower (PSHP) is calculated as

$$(2.86)\quad PSHP = SHP_{eng}\eta_t - SHP_{acc}.$$

It was interesting to me to see that the propulsion system transmission efficiency of the XC-142 varied with engine shaft horsepower and RPM percentage. In fact, a graph of this dependency was included in the Category II report so I was not required to guess. The transmission efficiency variation was between 0.94 at low power and 100 percent rpm up to

0.985 at a maximum engine shaft horsepower of 3,080 and 60 percent rpm. The accessories were charged with drawing 44 horsepower. I might add that it is quite unusual to have this sort of detail quoted in the data reduction chapter of a flight test report.

Now that you have the horsepower going into the proprotor, the question becomes one of obtaining the proprotor thrust at the operating flight condition. The proprotor shafts of the XC-142A were not instrumented for axial force, which would be called the thrust. As you know, it is rather easy to get close to wing lift from an aircraft's weight, but getting the propulsive force that balances aircraft drag can be quite a challenge. In the case of the XC-142A, the approach was to estimate the thrust horsepower (PTHP) of one proprotor as

$$\text{PTHP} = \text{PSHP} \times \eta_P = \frac{T_P V_{FP}}{550} \quad (2.87)$$

Then the prime contractor—now the Ling-Temco-Vought team—accepted the Curtiss-Wright company's theoretically computed proprotor efficiency (η_P) chart, shown here as Fig. 2-108, as the best data available from which to obtain the thrust of one proprotor

$$T_P = \frac{550 \times \text{PSHP} \times \eta_P}{V_{FP}} \quad (2.88)$$

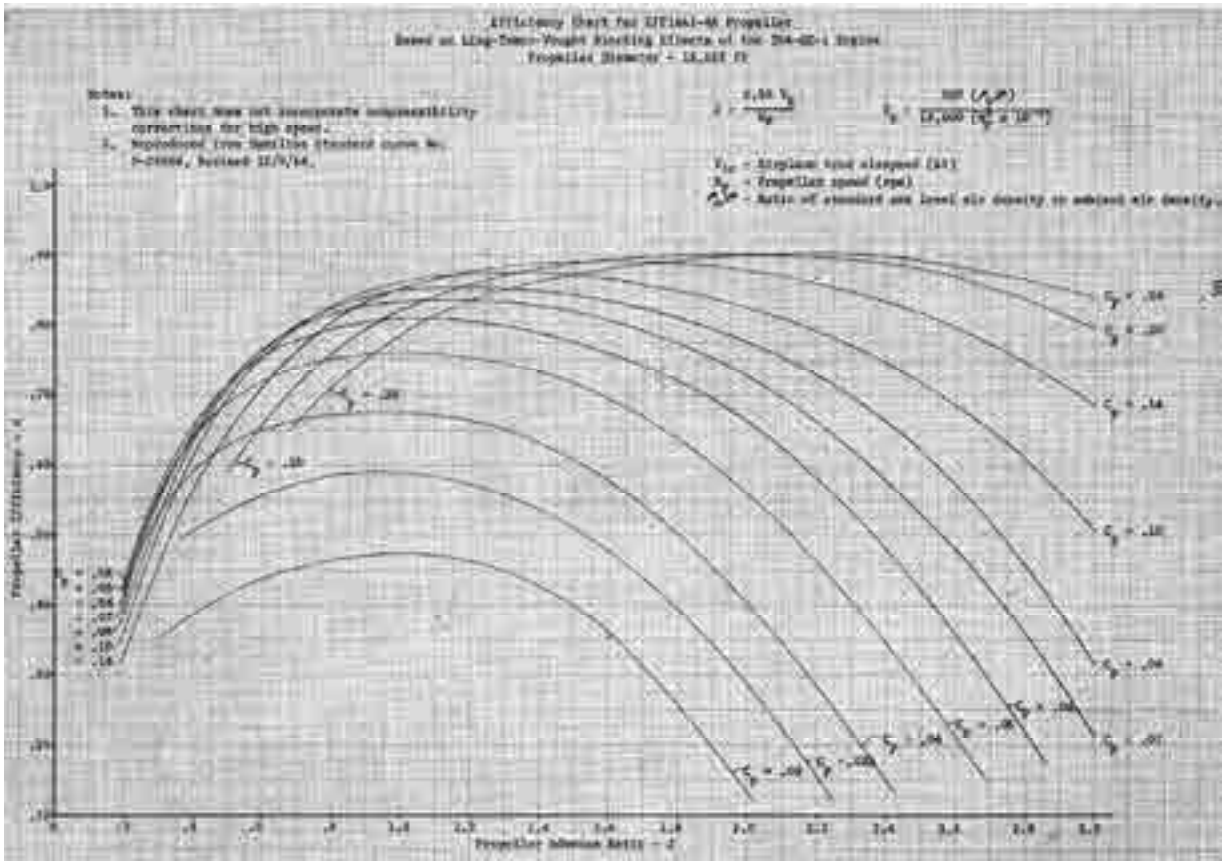

Fig. 2-108. The XC-142A propeller efficiency chart submitted by Curtiss-Wright to Ling-Temco-Vought [178].

The next logical step, because the thrust (T_P) from four proprotors is assumed equal to the aircraft's drag, is to calculate the drag as

(2.89) $D_{A/C} = 4T_P$

and then calculate the conventional drag coefficient as $C_D = D/q_{FP}S_W$.

The propeller efficiency chart, Fig. 2-108, uses the classical coordinate system that I was first exposed to [221] in my freshman year at Rensselaer Polytechnic Institute (RPI) in 1952. The efficiency is defined as the product of advance ratio (J) and thrust coefficient (C_T) divided by power coefficient (C_P). The parameters, in propeller nomenclature, are

$$\text{(2.90)}\quad \eta_P = \frac{J C_T}{C_P} = \frac{\left(\frac{V_{FP}}{nD}\right)\left(\frac{T_P}{\rho n^2 D^4}\right)}{\left(\frac{550\,PSHP}{\rho n^3 D^5}\right)},$$

where the proprotor rotational speed (n) is in radians per second.

In reproducing the test evaluators' performance data in forward flight, I actually took a more direct path that started by creating an equation that fit the curves provided in Fig. 2-108. My experience with efficiency curves such as Fig. 2-108 let me assume that, because C_P equals a function of J and C_T, you can curve-fit propeller efficiency data with

$$\text{(2.91)}\quad \begin{aligned} C_P &= C_{Po} + A_{(J)}C_T + B_{(J)}C_T^2 \\ &= C_{Po} + \left(A_o + A_1 J + A_2 J^2\right)C_T + \left(B_o + B_1 J + B_2 J^2\right)C_T^2 \end{aligned}$$

where $C_T = \eta_P\, C_P/J$ and $C_{Po} = P_o+P_1J+P_2J^2$. Using 160 points from Fig. 2-108, I gave the Microsoft® Excel® regression analysis tool the problem of finding the coefficients and arrived at

$$\text{(2.92)}\quad \begin{aligned} C_P &= 0.015981 + 0.0014024\left(J^2\right) + 0.00036615\left(J^4\right) \\ &+ \left[-0.056282 + 0.877136\left(J\right) - 0.027999\left(J^2\right)\right]C_T \\ &+ \left[1.904649 - 0.733694\left(J\right) + 0.737029\left(J^2\right)\right]C_T^2 \end{aligned}$$

and then I had a curve-fitting of Curtiss-Wright's efficiency data to within 1 percent. Because you know the power coefficient (C_P) and want the thrust (C_T), the quadratic equation, Eq. (2.92), is solved for C_T simply as

$$\text{(2.93)}\quad C_T = \frac{1}{2B}\left[-A + \sqrt{A^2 + 4B\left(C_P - C_{Po}\right)}\right],$$

and it immediately follows that

$$\text{(2.94)}\quad C_D = 4\left[\frac{\rho n^2 D^4}{\left(\frac{1}{2}\rho V_{FP}^2\right)S_W}C_T\right] = \frac{8}{J^2}\left(\frac{D^2}{S_W}\right)C_T.$$

It was a trivial task to mechanize the above steps in an Excel® spreadsheet and reproduce the results shown in Fig. 2-107.

Now let me add some additional thoughts about the Ling-Temco-Vought (LTV) XC-142A before summarizing development progress with tiltwings in toto.

The LTV XC-142A program had a number of technical efforts that contributed to the aircraft's success that you should be aware of. First and foremost are the very interesting NASA reports dealing with trim, performance, descent boundaries created by wing stall, and ground effect (both in hover and low-speed flight). A summary report that Ken Goodson gave at the 1966 NASA Conference on V/STOL and STOL Aircraft [222] contains very helpful information. Ken gathered up NASA test results from three scale models representing the XC-142A, which had a wingspan of 67.55 feet. The model scales and the associated reports were: a 0.11-scale model tested in "free flight" [223] (Fig. 2-109, also see Fig. 2-83); a 0.09-scale powered force model [224]; and a large-scale powered force model [225]. From a trim point of view, Fig. 2-110, the model data and flight test data were in adequate agreement on the wing tilt angle (i_W) required for steady, level flight at all speeds. A key performance chart that Ken presented, reproduced here as Fig. 2-111, illustrates how useful even small-scale models can be in estimating (what amounts to) powered-required-versus-speed data. Note that Ken scaled-up the model data to full scale so that the thrust from four propellers equaled a takeoff gross weight of about 38,000 pounds. The conversion of thrust to proprotor horsepower required is, however, not so easy a task as you now know.

Fig. 2-109. The 0.11-scale model with a wingspan of 7.5 feet was tested in "free flight" in the Langley 30- by 60-foot wind tunnel [223].

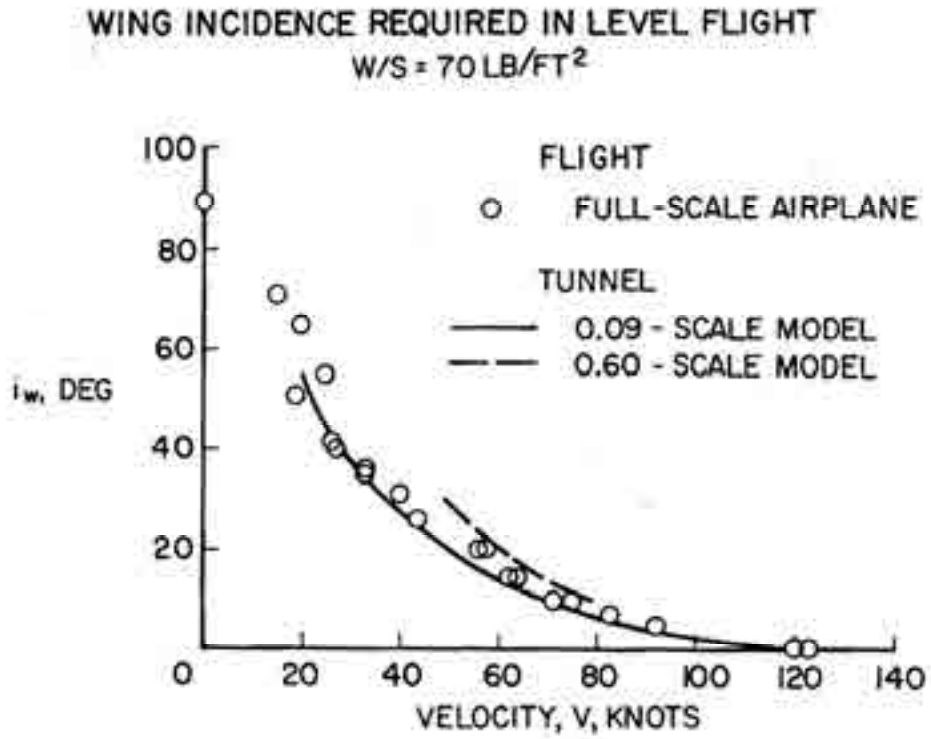

Fig. 2-110. The variation of the wing tilt angle with level flight speed was well established for both the powered force models and the full-scale aircraft [222].

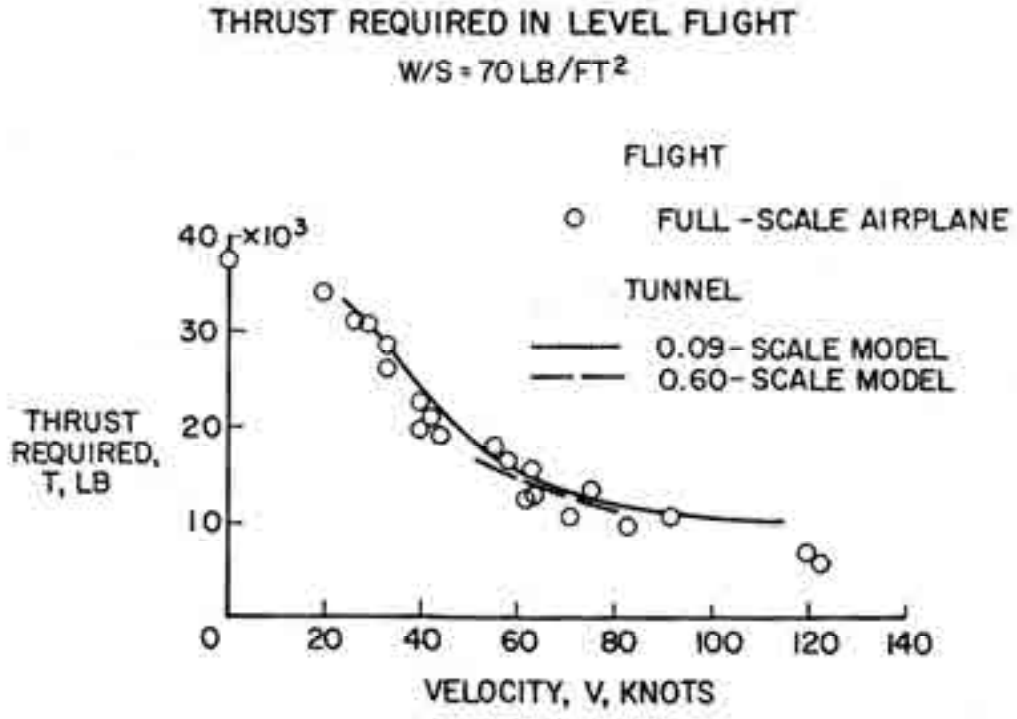

Fig. 2-111. Even small-scale, powered force models are quite valuable when estimating performance as this NASA test data for the XC-142A shows [222].

The descent boundary for the XC-142A (Fig. 2-112) was studied both with the 0.11-scale free-flight model and the 0.09-scale powered-force model using tufts to show separated flow areas on the wing (Fig. 2-113). You will recall that rate of descent (V_Z or R/D) is connected to the flightpath angle (γ) and the forward speed (V_X or V_{FP}) as R/D = V_{FP} sin γ. Therefore, if the XC-142A pilot starts a descent with the wing tilted at, say, 30 degrees corresponding to a speed of 40 knots (from Fig. 2-111), he will experience the onset of wing stall and noticeable aircraft buffeting at a descent angle of about 10 degrees according to Fig. 2-112. This example gives a rate of descent of about 700 feet per minute. From a combat

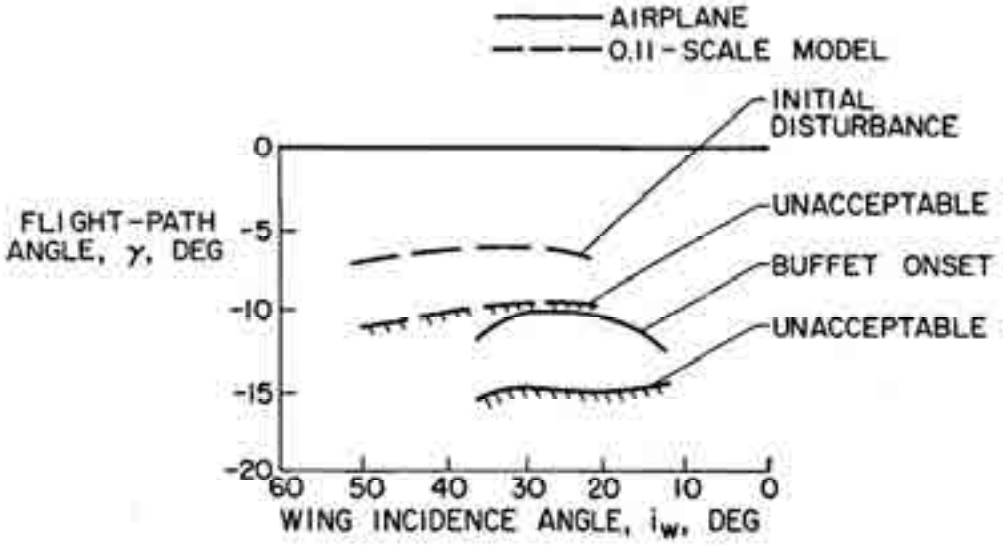

Fig. 2-112. XC-142A descent boundaries from flight test and model scale show the model scale to be quite conservative [222].

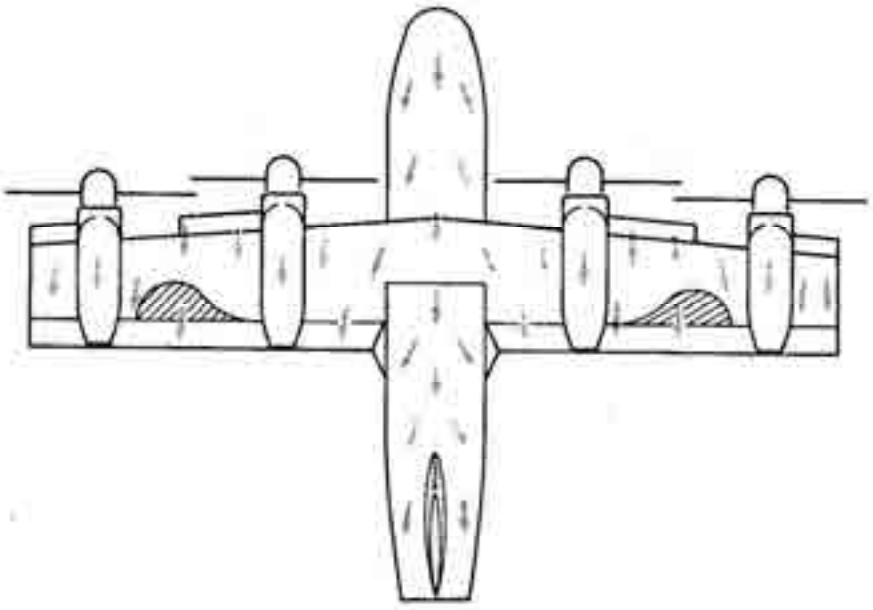

Fig. 2-113. Wing stall between each propeller pair (the shaded areas) defined the buffet onset boundary on the XC-142A [222].

assault mission point of view, a restriction to 700 to 800 feet per minute (7 to 8 knots, or 12 to 13.6 feet per second) in rate of descent is, in my mind, quite unacceptable. Something closer to 1,500 feet per minute with the pilot in absolute control and able to decelerate to a comfortable, controlled landing would be the goal I would shoot for.

You might note from Fig. 2-112 that descents with wing angles between 50 and 90 degrees were not evaluated. As far as I know, this region has never been studied, and yet testing at higher rates of descent at slower forward speeds might disclose that buffeting problems were negligible. Of course, the vortex region might then become a limiting factor.

Ken Goodson's presentation [222] pointed out that hovering and slow-speed flight close to the ground created interesting aircraft behavior. The recirculation of propeller slipstreams, as the sketch in Fig. 2-114 shows, gave the pilots of the XC-142A yaw and roll control problems. Yaw accelerations approaching the control available in hover were measured. Today, you would expect to install a modern autopilot to help the pilot with this kind of distraction. However, the subject of testing models in ground effect received considerable attention in this era as you will appreciate just by reading references [226, 227].

Structural dynamic aspects of the XC-142A received considerable attention at the Chance-Vought Corporation during the design phase. (Many of the internal company reports dealing with all the technology department's efforts are available through the U.S. Air Force Flight Dynamics Laboratory.) The fact that a dynamically similar model was built, tested, and reported on really impressed me then and still does today [228, 229].

During this early VTOL era, the question of handling criteria was still very much under discussion [230-232]. Results from the XC-142A program [233] were of some help, but I think things did not become clearer until high-fidelity simulators came into widespread use. Furthermore, as with the larger helicopters, the first group of VTOLs raised the issue of

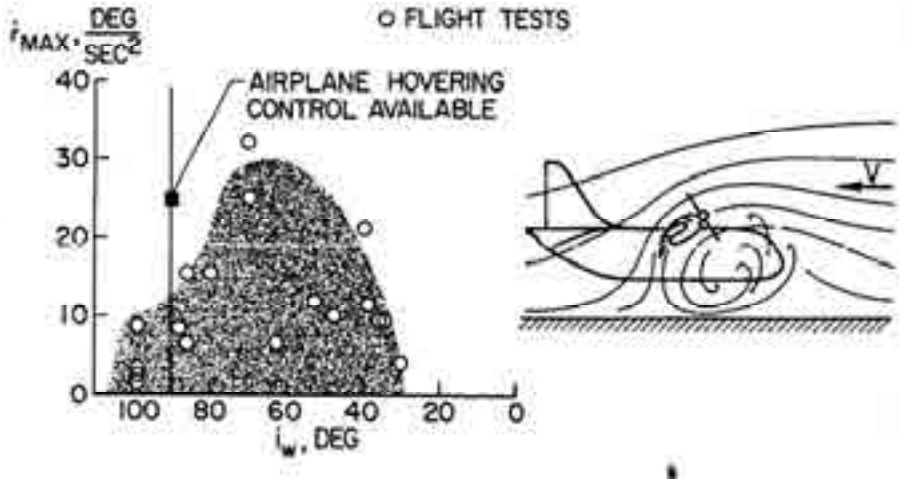

Fig. 2-114. The XC-142A experienced significant yaw accelerations ($\dot{r}$) when the bottom of the fuselage was less than 50 feet above the ground [222].

proprotor slipstreams from hovering aircraft blowing people down. You might find reference [234] of interest. When hovering 75 to 100 feet above the ground, the XC-142A produced ground-level velocities up to 100 knots.

Now for some concluding thoughts about the XC-142A program drawn in part from references [25, 39, 177, 178, 212, 235]. The XC-142A program produced "about" what was sought by the contract (awarded January 1962) between the Tri-Services (the Air Force was in charge) and the Vought-Hiller-Ryan team. What was sought was an experimental VTOL aircraft at a size comparable to the de Havilland/U.S. Army Caribou.[57] For $75.9 million and in 4 years, the LTV team was to produce five machines and one static test article, and get a good, if not glowing, report at the end of Category II evaluation. There may have been some thought that a YC-142A[58] was in the cards because the aircraft was big enough to carry 32 troops in a combat assault mission. The LTV team got the aircraft to first full back and forth conversion on January 11, 1965, which was exactly 3 years after contract award. The program ended up at $135.8 million obligated and spent over 6 years.

There were four very hard landings between the five experimental aircraft and one fatal crash (on May 10, 1967). The final accident on October 9, 1967, brought the program to a halt. This aspect of experimental aircraft—accidents—is one you must always be aware of. Bernie Lindenbaum [212] gave us a detailed summary of XC-142A accidents when he wrote:

> "Aircraft #2—On 19 October 1965, this aircraft experienced a ground loop on landing which caused extensive damage to the wing and propellers. The hydraulic system had a fatigue failure which caused the left outboard propeller actuator to fail during flare-out and landing. This caused an asymmetrical thrust and a ground loop to the left.
>
> Aircraft #3—On 4 January 1966 this aircraft made a hard landing in the vertical mode. The aircraft sustained major damage to the fuselage. The cause of this accident was the pilot's failure to select the proper propeller speed for vertical mode flight. The pilot procedures were revised subsequently to ensure the proper propeller speeds would be selected. The wing of this machine was later mated with the fuselage of the #2 aircraft for further flight testing.
>
> Aircraft #4—On 27 January 1966 there was a turbine failure in the #1 engine caused by the failure of the overriding clutch to engage. This caused extensive damage to the wing, the outboard aileron, the number 2 nacelle, the aft engine shroud and to the fuselage. This aircraft was repaired, used by NASA for flight research, and is now the one which is in the Air Force Museum.
>
> Aircraft #5—On 28 December 1966 this vehicle was taxied into a hangar door causing major damage to the fuselage nose, the wing, the wing hinge and the propellers. This accident was caused by the pilot failing to actuate the hydraulic system; he, therefore, had no brakes or nose wheel steering available.

[57] At a takeoff gross weight of 38,485 pounds, cruise at 250 knots at sea level, have a maximum speed of 380 knots at 20,000 feet, have a combat range of 783 nautical miles and a combat radius of 200 nautical miles, demonstrate a ceiling of 25,000 feet, have a capability to hover out of ground effect at 6,420 feet with a thrust-to-weight (T/W) margin equal to 1.15, and have a STOL capability to take off over a 50-foot obstacle in 288 feet.

[58] To me, a "Y" designation means a preproduction prototype incorporating all the fixes to the XC-142A.

> Aircraft #1—On 10 May 1967 the failure of the spring capsule in the tail rotor pitch control system gave full pitch to the tail rotor, as the aircraft approached the hover configuration. It nosed over at about 200 ft altitude and crashed in an inverted attitude killing the pilots. This is the only accident during the tri-service program that could be directly attributable to the V/STOL configuration.[59]
>
> Aircraft #2—On 9 October 1967 this aircraft experienced a hard landing due to a high sink rate at low forward speed. The pilot reduced power while attempting to go into a hover configuration causing a high rate of descent which could not be stopped prior to ground impact. The hard landing broke the fuselage and the wing, and the aircraft was considered beyond repair."

I would be remiss if I did not say that I think the XC-142A got shortchanged in its development. This tiltwing aircraft was designed to do for the U.S. Army what the tiltrotor—the Bell Boeing V-22—has done for the U.S. Marines. But the experimental XC-142A (comparable to the V-22 in its first phase, the JVX phase) had a raft of reliability and maintenance problems. The aircraft control problems while operating in ground effect were every bit as serious. The shortfall in speed and range performance was also a reason for VTOL critics to want the program cancelled. These technology and engineering shortcomings would have required significant redesign (similar to the FSD V-22 phase) before it could have been cleared even for the Low-Rate Production phase that the V-22 required. And the XC-142A would have required more redesign, as was done on the V-22, before it received go-ahead for full-rate production and widespread use in operation.

The XC-142A and its program never had a champion comparable to the U.S. Marines who wanted the MV-22, a story told by Richard Whittle in his book *The Dream Machine—The Untold Story of the Notorious V-22 Osprey* [34]. You will find Dick's very, very true story absolutely fascinating from start to finish. The XC-142A program, without a glowing Category II flight test report, saw the end of DoD Tri-Service support, and all future tiltwing considerations died. Thoughts turned to the tiltrotor, which I will discuss in a moment, and the U.S. Air Force decided that a STOL assault transport was the way to go. This led to the YC-14 and YC-15 competition that you will read about later.

[59] This accident leads me to mention that while at Boeing Vertol, we began serious work on what we called a monocyclic propeller [236]. The approach was to replace the pitch control fan used on tiltwings such as the VZ-2, CL-84, X-84, and XC-142A with propeller pitching moment. A propeller with cyclic pitch (much like the Sikorsky ABC and X2 TD compound helicopters) would have more than enough longitudinal pitching moment to control the aircraft when operating in ground effect. I was swayed to the idea, in part, because of the VZ-2 flying model tests reported by Lou Tosti at Langley in 1962 [196].

2.12.6 Tiltwings in Summary

Earlier I summarized the feasibility of many rotorcraft demonstrators with one figure, Fig. 2-73. Let me repeat that figure here as Fig. 2-115 so you have a handy reminder. Next I have added the path to the XC-142A to show you where the four tiltwing aircraft (developed between 1955 and 1970) fall. You see this tiltwing progress in Fig. 2-116.

You also have, with Table 2-9,[60] the basic characteristics of the four tiltwing aircraft demonstrated up to the early 1970s. These groundbreaking machines are the VZ-2 developed by the Vertol Aircraft Corporation with support from the U.S. Navy Office of Naval Research (ONR), the CL-84 developed by Canadair with support from the Canadian Government, the X-18 developed by Hiller Aircraft Corporation, and the XC-142 developed initially by the team of Vought-Hiller-Ryan (VHR), later to become the Ling-Temco-Vought (XC-142A). These experimental aircraft (or technology demonstrators, if you prefer) represent six decades of searching by the rotorcraft (and some of the fixed-wing) industry for a product beyond the autogyro and the helicopter.

With respect to Fig. 2-116, you should keep in mind that the Bell XV-15 *tiltrotor* (in gray) was several years away from flying. Therefore, the meaningful comparison is between helicopters and compounds and tiltwings. In this regard I always felt that the XC-142A showed what could be done when you are given a hover requirement of 6,000 feet at 95 ^{o}F. On the other hand, the military assault mission plus U.S. Navy shipboard requirements offer *no* design freedom to create an aerodynamically efficient airplane. This means (to me) that there is very little chance to spin off the military-developed VTOL into an aircraft that the commercial world would buy.

Table 2-9 makes several key points. For example, the ratio of gross weight (GW) to equivalent parasite drag (f_e) is increased over time. Clearly the VZ-2 was only created to demonstrate tiltwing feasibility and basic principles. The CL-84 made a serious effort at high-speed flight because the landing gear was at least partially retractable. However, the installed power would not permit hovering with one engine out, nor was the hover ceiling out of ground effect much above sea level on a standard day with both engines operating. The X-18 was, in my opinion, a very risky adventure because there was no interconnect shafting. Very little was learned from this step and, in fact, the X-18 never even hovered. The XC-142A was the next step toward giving the military a useable VTOL product, but, as I have said, this promising machine did not have the champion needed to look past the aircraft's deficiencies and accidents.

And there you have my summary views about the world of *tiltwings*. Now let me go on to a discussion of *tiltrotors* and how the Bell Boeing MV-22 came about.

---

[60] It would be nice if all the data on this table could be guaranteed. All I can say is that most of the data are at least very representative, and some numbers, obtained from two or three sources, are almost in agreement. In some data cells I put estimate (est.), not applicable (na), and could not find (cnf) in the hope of someone filling in the blanks. Incidentally, I took *Jane's All The World's Aircraft* data with a grain of salt because it comes from manufacturers who tend to be rather optimistic.

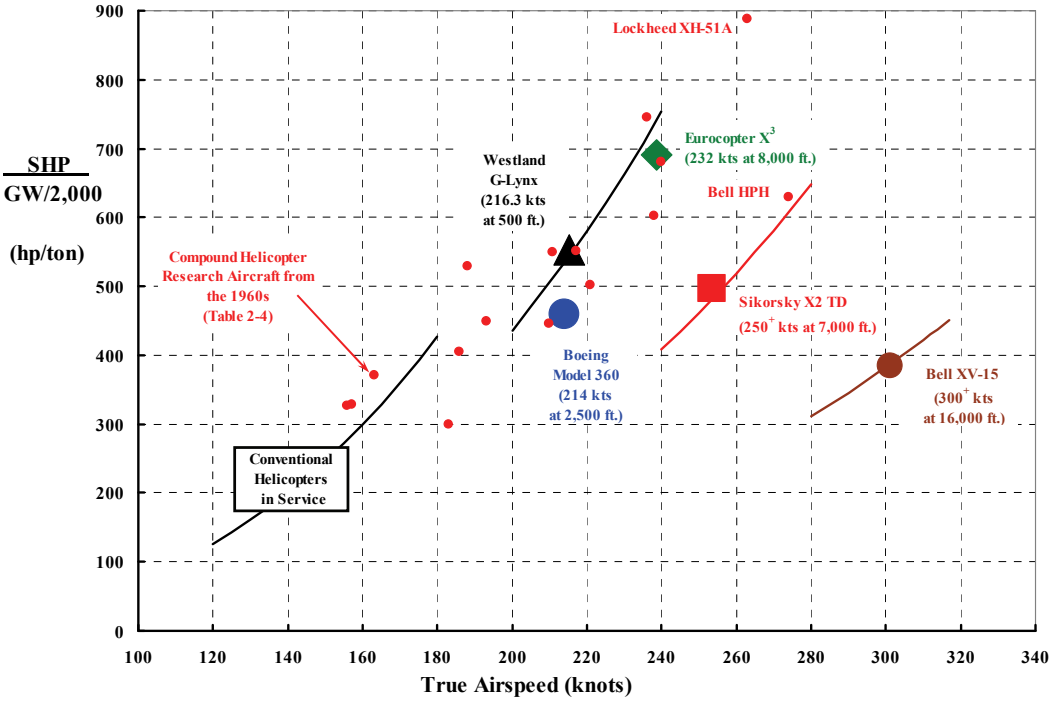

Fig. 2-115. The *rotorcraft* industry has demonstrated many high-speed VTOL concepts.

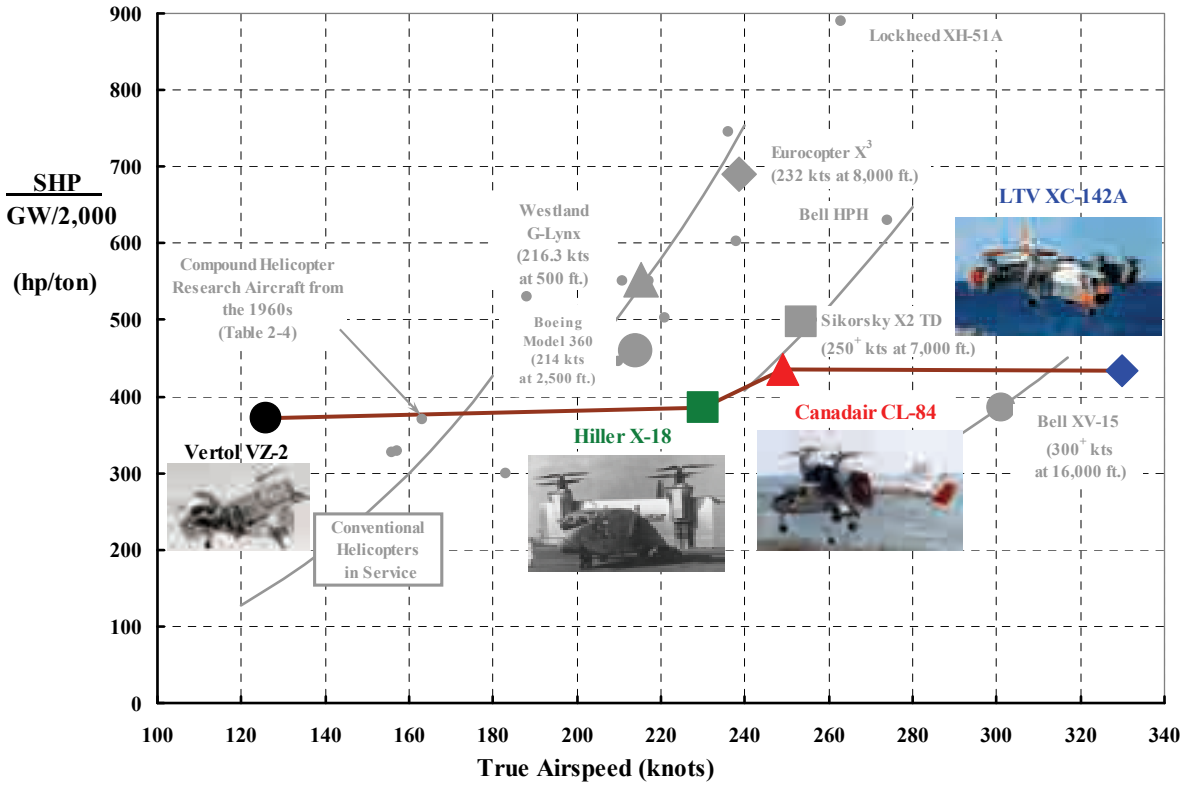

Fig. 2-116. The *aviation* industry demonstrated four tiltwing VTOLs between 1957 and 1970, beginning with the VZ-2 and ending with the XC-142A in October of 1970.

Table 2-9. The Four Tiltwing Demonstrators

Item	Unit	VZ-2	X-18	CL-84	XC-142A
References		[182, 183, 189, 190, 198, 202]	[13, 205-208]	[210, 211]	[28, 39, 177-179, 212]
Manufacturer		Vertol	Hiller	Canadair	Vought-Hiller-Ryan
First flight date		Aug. 13, 1957	Nov. 24, 1959	May 7, 1965	Sept. 29,1964
Crew/passengers		1/0	2/0	2/12	2/32
Type		Research	Research	Prototype	Prototype
Number built		1	1	4	5
Number of accidents		0	1	2	6
Engine (no.)		YT53-L-1 (1)	YT-40-A-14	T53-L-13 (2)	T64-GE-1 (4)
Takeoff rating (SFC)	hp	825 (0.78)	5,850 ()	1,400 (0.58)	3,080 (0.50)
Max continuous rating (SFC)	hp	675 (0.80)	4,954 ()	1,150 (0.613)	2,270 (cnf)
Transmission limit	hp	650	cnf	cnf	11,220
Number of gear boxes		5 (2 for fans)	0	4 (2 for pitch fan)	11 (3 for pitch fan)
Proprotor					
Diameter (blade no.)	ft	9.50 (3)	16.08 (6)	14.0 (4)	15.625 (4)
Activity Factor per blade	na	178	142	90	420
Blade area (total)	ft^2	15.44	70.47	22.63	29.6
Solidity (power weighted)	na	0.2178	0.347	0.147	0.154
Twist	deg	–24	cnf	cnf	cnf
Tip speed hover/cruise	ft/sec	717/717	na	900/900	1010/755
Wingspan	ft	24.875	47.917	34.333	67.55
Wing area (inc. fuselage)	ft^2	118.156	528.0	233.333	534.37
Wing aspect ratio	na	5.24	4.35	5.05	8.53
Horizontal tail area	ft^2	33.00	193	87.5	163.5
Vertical tail area	ft^2	32.00	121	59.1	130.0
Pitch fan					
Diameter (blade no.)		2.0 (4)	J34 turbojet exhaust piped to tail	7.0 (4)	8.17 (3)
Tip speed hover/cruise		613/613		820/stopped	1,005/stopped
Solidity (power weighted)		0.212		0.0664	0.185
Twist	deg	0.0	na	cnf	0.0
Yaw fan		Yes	None	None	None
Diameter (blade no.)		2 (4)	na	na	na
Tip speed hover/cruise		612.6/612.6	na	na	na
Solidity (power weighted)		0.212	na	na	na
Twist	deg	0.0	na	na	na
Flat plate area	ft^2	21.0	63.4	14.4 (est)	32.6
Zero lift drag coefficient	na	0.205	0.135	cnf	0.061
Min drag coefficient at (C_L)		0.135 (0.62)	0.12 (0.30)	0.0616 (0.271)	na
Gross weight/parasite drag area	lb/ft^2	167	520	796	1,208
Normal VTOL takeoff weight	lb	3,500	33,000	11,500	40,149
Maximum takeoff weight	lb	3,500	33,000	14,500	41,500
Max STOL landing weight	lb	3,500	33,000	14,500	37,242
Operational weight empty	lb	3,063	27,272	8,417	25,552
Fuel capacity (U.S. gallons)	gal./lb	cnf	1,000/6,450	247/1,600	1,400/9,000
Maximum (speed/altitude)	kts/ft	126/1,000	235/10,000	249/5,000	330/10,000
Max cruise (speed/altitude)	kts/ft	126/1,000	cnf	230/5,000	251/25,000
Economical (speed/altitude)		100/1,000	cnf	230/5,000	220/20,000
Range	n.m.	130 (est)	cnf	na	3,000
Disc loading	lb/ft^2	24.7	81.2	37.4	51.3
Horsepower per ton of GW	hp/tn	371	709	435	626

2.13 THE PATH TO THE PRODUCTION V-22 TILTROTOR

The first step towards a tiltrotor having fully operational military status was taken when Mario A. Guerrieri and Robert L. Lichten partnered up to start development of what became the Transcendental Model 1-G, which made its first untethered hovering flight on July 6, 1954. Development continued with the Transcendental Model 2, under Bill Cobey as president of Transcendental. At nearly the same time, Bell Helicopter began research and development of the XV-3 with U.S. Army and Air Force sponsorship. When the mechanical instability problems of the XV-3 were solved, Bell won a NASA and U.S. Army competition to design, build, and fly the Bell XV-15. The XV-15 demonstrated that tiltrotor technology was of age and led, finally, to the V-22, which the U.S. Marines first took into combat as the MV-22B on October 4, 2007 [34].

When you add it up, it took 53 years to get from the first experimental tiltrotor to the introduction into combat service of a fully operational, military tiltrotor. This was not exactly an instantaneous birth and application of a new concept. But still, the potential for a commercial VTOL transport that can advance the rotorcraft industry's product line beyond helicopters is now real. A commercial VTOL transport, the Augusta Westland 609, is now in development as I write this in 2013.

This path from the Transcendental Model 1-G to the MV-22B is a story of mixed program and technical issues that easily compares to the tortuous path leading to the first autogyros and early helicopters. It is a relatively easy story to tell in hindsight, but I cannot imagine even drafting a program plan (in advance) that included so many points where the only option appeared to be to simply quit. This is what happened with the XC-142A tiltwing program a decade earlier as you have just read; tiltrotor development fared much better as you are about to learn.

2.13.1 The Transcendental Model 1-G and Model 2

The 1956–1957 issue of *Jane's All the World's Aircraft* has an entry for the groundbreaking Model 1-G that reads, with some italicizing by me, as follows:

"Transcendental Aircraft Corporation

Head Office and Works: Glen Riddle, Pennsylvania[61]
President: William E. Cobey

This small company is engaged in the development of convertiplanes. The original Model 1, which employs two 17-foot rotors which can be swiveled through 84° to provide either lift for vertical flight or thrust for horizontal flight, was designed in 1945 and completed in 1951. Development of the aircraft has progressed through ground tests and modifications to the Model 1-G which, at the time of writing had made successful free vertical flights, the first being achieved on June 15, 1954.

[61] Sue and I had our first house about 2 miles from Glen Riddle. During a Sunday drive in 1960, I noticed the remains of what (I assume now) was a Model 1-G lying by a barn along a back road in Glen Riddle.

Although the development of the Transcendental convertiplane has been mostly privately financed, considerable assistance has been forthcoming through various U.S.A.F. contracts.

In 1952 the company was awarded a contract to investigate the dynamic and structural characteristics of the rotor system. The primary purpose of these tests was to study the action of the rotors during simulated conversion. An additional contract was awarded in 1953 *to investigate mechanical instability problems when tilting the rotors of the convertiplane*. This contract was continued to include limited flight tests.

The Model 1-G, which is illustrated and described hereafter, is strictly a single-seat research aircraft intended to investigate the conversion problems of a convertiplane.

THE TRANSCENDENTAL MODEL 1-G

Type—Single-seat experimental convertiplane.

Rotor System—Two three-blade rotors mounted at tips of fixed wings are arranged to be tilted from horizontal (vertical flight) to point 6° forward of vertical (forward flight) by electric motors. Rotor diameter 17 ft. (5.18 m.). Chord of rotor blades 4 in. (101.6 mm.). Blades have extruded 75 ST aluminum-alloy spar, 24 ST ribs, trailing-edge and skin. Rotors inter-connected to ensure simultaneous tilting. Hubs fully articulated. Controls for collective and cyclic pitch run through wings and over chain and sprocket drive at tips to rotor heads. Rotor transmission from gear box in front of engine, through spanwise shafts to bevel gearing at wing tips to rotor heads. Two-speed gear rotor drive to give required r.p.m. for vertical and forward flight.

Wings—Cantilever monoplane. NACA 23015 wing section. Aspect ratio 7:1. Incidence 4°. Chord 3 ft. (0.915 m.). Aluminum-alloy structure. Ailerons have metal frames and fabric covering. Total aileron area 4 sq. ft. (0.37 m.). Gross wing area 63 sq. ft. (5.85 m.).

Fuselage—Steel tube forward structure. Aluminum-alloy monocoque tail cone.

Tail Unit—Cantilever monoplane type. All-metal structure. Areas: fin 4 sq. ft. (0.37 m^2), rudder 2 sq. ft. (0.186 m^2), tailplane 5 sq. ft. (0.46 m^2), elevators 4 sq. ft. (0.37 m^2). Span of tail 6 ft. 6 in. (1.98 m.).

Landing Gear—Fixed nose-wheel type. Transcendental air-oil shock-absorbers. Wheelbase 6 ft. (1.83 m.). Track 8 ft. (2.44 m.).

Power Plant—One 160 h.p. Lycoming 0-290-A six-cylinder horizontally-opposed air-cooled engine. Fuel capacity 14 U.S. gallons (53 litres).

Accommodations—Pilot's semi-enclosed nacelle forward of wings.

Dimensions.

Wingspan 21 ft. (6.40 m.).
Overall length of fuselage 26 ft. (7.93 m.).
Height 7 ft. (2.13 m.).

Weights and Loadings.

Weight empty 1,450 lb. (658 kg.).
Weight loaded 1,750 lb. (794 kg.).
Disc loading 3.6 lb./sq. ft. (17.54 kg./m^2).
Wing loading 27.7 lb./sq. ft. (135.17 kg./ m^2).
Power loading 10.93 lb./h.p. (4.96 kg./h.p.).

Performance (estimated).

Max. speed as helicopter 120 m.p.h. (192 km.h.).
Max. speed as aeroplane 160 m.p.h. (256 km. h.).
Ceiling as aeroplane 5,000 ft. (1,525 m.).
Endurance 1½ hours."

The tiltrotor that Mario Guerrieri and Bob Lichten envisioned in 1945 was conceived while both were employed at the Kellett Autogyro Company. They left Kellett and started up the Transcendental Aircraft Corporation in October 1946. Bob "established all of the design

criteria and parameters of the aircraft and it was eventually built to these specifications."[62] The partnership lasted until early 1948, but "before detailed design of the aircraft had progressed to any great degree," Bob Lichten[63] left to join the Bell Aircraft Corporation located in Buffalo, New York. A small portion of the Transcendental Brochure [242] states that

> "Mario Guerrieri's first convertiplane was completed in September, 1950. This unique aircraft was basically a fixed wing monoplane with a rotor mounted at each wing tip. The design incorporated a rotor tilting mechanism [Fig. 2-117]. By means of this mechanism, the rotors could be swung from a horizontal hovering plane to a vertical plane once the aircraft had attained sufficient forward speed for the wings to develop enough lift to support the aircraft. With the rotors turning in a vertical plane, they would act like the propellers on a fixed wing airplane, pulling the aircraft forward at speeds far in excess of those possible with a conventional helicopter.
>
> Although Guerrieri's original design was basically sound, he encountered a difficulty which has plagued the designer of virtually every new rotary wing concept. During pre-flight ground testing of his unique configuration [Fig. 2-118], ground resonance was encountered and the aircraft was destroyed in November 1950.
>
> On January 1, 1951, William E. Cobey, an aeronautical engineer with a wealth of practical experience in the design of rotary wing aircraft, joined the organization as Chief Engineer. The experience that Mr. Cobey had gained while employed by Kellett Aircraft Corporation, working on the XR-8, XR-10 and XK-17 helicopters, was invaluable in designing the successor to the Transcendental Model 1, the Model 1-G."

Together, Guerrieri and Cobey carried on until June of 1952 when they entered into a contract with Wright Aeronautical Development Center (WADC) in Dayton, Ohio, to measure blade, rotor shaft, and control stresses. (I would suspect that Transcendental must have been struggling when they got this first of three Air Force contracts). Then in September of 1952, with the company on sounder footing, Mario sold his share of Transcendental to Cobey and left to take a position at Hiller Helicopters in Palo Alto, California.

The story after 1952, when the Model 1 had been rebuilt as the Model 1-G, was written by William Cobey, then Transcendental Aircraft Corporation President, and published

---

[62] Mario Guerrieri sent a letter to *Vertiflite* that was published in the September/October 1988 issue [237]. In November 2013 I decided to see if I could contact him and get some gaps in his story filled in. I was able to track down Mario's son, David, only to find out that his father had died in 2002.

[63] Bob Lichten (born July 3, 1921, in Philadelphia; died September 18, 1971, in a single-car accident near Waco, Texas) graduated from MIT in the class of 1943. He began his career at the Platt-LePage company. He later moved to Kellett as an aerodynamicist [238] and then joined Mario Guerrieri, who also worked at Kellett, and together they formed the Transcendental Aircraft Corporation in October of 1946. Sometime in 1948, Bob moved to Larry Bell's Bell Aircraft Corp. as a project engineer [239]. Bob found a kindred VTOL spirit in Larry Bell, and the two laid the groundwork for the future Bell XV-3. In 1952 Bob moved to what was first known as the Texas Division of Bell Aircraft Corp. Lawrence D. Bell died on October 20, 1956, but by then the nucleus of what was to become Bell Helicopter Textron (in 1960) was thriving, and the XV-3 development was being funded by U.S. Army and Air Force contracts. Bob spearheaded preliminary design and the XV-3 in particular. Robert Lyon Lichten had an amazing career [240]. You will find more about Bob, the XV-3, and many insider antidotes in *the Bell Helicopter Textron Story* [241]. It is well worth your reading time.

in the *American Helicopter Society Newsletter* (later *Vertiflite*) in November 1956 [243]. Cobey noted in his article [with some of my comments in italics] that

> "The Model 1-G Convertiplane [Fig. 2-119] had been designed and built without any financial support from the government. However, as early as March 1951, the United States Air Force [USAF] had shown informal interest in the project. In June, 1952, this interest had developed to the extent that WADC entered into a contract with TRANSCENDENTAL for the purpose of obtaining data on blade, rotor shaft and control stresses, and on blade motions, under various conditions of ground operation. The tests conducted under this contract indicated that the rotor system was structurally sound, that adequate margin of safety would be maintained in flight, *but that mechanical instability would be an important consideration during conversion.*
>
> TRANSCENDENTAL recommended to the USAF that advantage be taken of the fact that the Model 1-G was the most advanced, full-scale convertiplane in existence, and that further development work be pursued on this 'guinea pig' to study mechanical instabilities and to place it in flyable condition. Prior to this time, the Model 1-G had been intended to serve only as a ground research test stand rather than a flight test article.
>
> On June 1, 1953, WADC entered into a second contract with TRANSCENDENTAL 'to establish an experimental and analytical procedure for the elimination of mechanical instabilities in a tilting rotor convertiplane during the design and first article ground test stages of development.' In performing this contract, it was TRANSCENDENTAL's purpose to discover what vibrations are characteristic of tilting rotor convertiplanes and to evaluate the effects of each important mode on the operation of the aircraft.
>
> Tests were conducted on the full-scale convertiplane which was suspended on elastic shock cord, using a mechanical shaker to excite vibration. The amplitude of response vibrations was measured at the rotor hub. Twelve different configurations were tested, varying from each other with respect to rotor shaft length and material (steel and dural), wing struts, tail struts, and/or rotor tilting actuators. Each configuration was tested with the rotor shafts in the vertical, the horizontal, and the intermediate position. Excitation was applied in two planes successively for each rotor shaft position, and excitation frequency was varied over a spectrum of from 200 to 1000 cycles per minute. Test results were expressed in the form of hub response curves. *Based on the results of these tests, a general procedure was developed for the elimination of mechanical instability in tilting rotor convertiplanes. Knowledge gained from these tests was invaluable to advancement of the state of the art, and results were discussed fully by TRANSCENDENTAL engineers with representatives from other manufacturers who were engaged in similar projects* [i.e., Bell with the XV-3].
>
> After the Model 1-G Convertiplane had been modified to place it in flyable condition, TRANSCENDENTAL was awarded a third contract by WADC. Its objective was the determination of forces and moments applied to a convertiplane rotor in flight. As will be noted on the photographs of the Model 1-G accompanying this article, the left rotor of the aircraft was instrumented to record the forces and moments in three mutually perpendicular planes.
>
> During the ensuing six months, conversion flights during which the rotors were tilted forward approximately 70 degrees and back to vertical were performed repeatedly. On July 20, 1955, while in high-speed forward flight with conversion virtually completed, the friction lock on the collective pitch stick slipped, causing the aircraft to enter a steep dive very abruptly. Although the pilot was able to initiate recovery, insufficient altitude was available in which to complete recovery, and the landing gear struck the Delaware River, flipping the aircraft onto its back. At the time of this accident, during which the aircraft suffered major damage, it had accumulated 23 hours of airborne time in over 100 individual flights."

Fig. 2-117. The screw jack conversion actuator assembly of the first tiltrotor, the Transcendental Model 1 (photo courtesy of Howard Levy and Mike Hirschberg).

Fig. 2-118. Mario Guerrieri's Model 1, shown here on its ground test rig, was virtually destroyed in November 1950 because of ground resonance (photo courtesy of Howard Levy and Mike Hirschberg).

Fig. 2-119. The Transcendental Model 1-G. This 1,750-pound VTOL technology demonstrator made its first, untethered, hovering flight on July 6, 1954. The preceding Model 1 was destroyed by ground resonance. This classical, early autogyro and helicopter mechanical instability problem was overcome with the Model 1-G. Only partial conversions from a shaft tilt of 0 degrees (hover) to about 70 degrees forward (airplane) were completed. On July 20, 1955, during a test flight in which the conversion was virtually complete, the aircraft dove, nose first, into the Delaware River (photo courtesy of Howard Levy and Mike Hirschberg).

This first-ever tiltrotor accident did not dissuade the company nor the U.S. Air Force, which gave another contract to Transcendental on March 15, 1956. Initial design efforts to pursue a warmed-over Model 1-G were not encouraging, so Transcendental decided on a completely new, larger machine, the Model 2, shown in Fig. 2-120 and Fig. 2-121. As to the Model 2, Cobey went on in his article [243] to describe the aircraft saying:

> "The Model 2 is the same basic configuration as its predecessor, the Model 1-G, but it is structurally much stronger, it is aerodynamically much cleaner, and it has 50% more power. Design parameters are maintained as close as possible to the Model 1-G to minimize the effect of modifying the power plant. It has been designed with growth potential from its present estimated gross weight of 2249 lbs. to a gross weight of 4000 lbs. The Model 2 has a useful load more than double that of the Model 1-G, while the increase in weight empty (attributable to the increased power) is less than 9%.
>
> The increase in power from 160 to 250 hp necessitated a new center transmission. In order to provide for growth potential and future installation of a much higher powered shaft turbine, the new center transmission is designed to absorb up to 1,000 hp. This redesign has been accomplished with a weight increase of only 40 lbs. over the previous 160 hp transmission.
>
> The gear ratio of the new center transmission has been changed so that the tip speed of the 18-foot-diameter rotors of the Model 2 is the same as that of the 17-foot-diameter rotors of the Model 1-G. The rotor blades of the Model 2 are of greater length and chord than those of the Model 1-G in order to accommodate the increased gross weight. Wing area of the Model 2 has been increased over that of the Model 1-G by 40% with no increase in wing

weight. The increased wing area results from the greater span (increased about one foot to provide clearance for the larger rotors) and from sweeping back the trailing edge.

Construction of the Model 2 is complete, and ground tests are in an advanced stage. With the exception of gears and Government Furnished Equipment [G.F.E.] consisting of engine, instruments, wheels, and tires, the entire aircraft was fabricated within TRANSCENDENTAL's own shop, by the organization's own personnel, using company owned tooling. The aircraft is scheduled to make its first flight by the end of 1956—approximately nine months from the start of manufacture. This significant achievement is considered to be eloquent testimony to the effectiveness of TRANSCENDENTAL's competent administrative and engineering staff and to the versatility of its shop team."

That the Model 2 was at least lifted to a hover seems to be indisputable. However, it appears that the exact date of when the aircraft first hovered is, at present, not known. At any rate, the 1957–1958 issue of *Jane's All the World's Aircraft* reported in part:

"In March 1956 Transcendental was awarded a further contract to continue development of the convertiplane. The new Model 2, while having the same basic configuration as its predecessor, is structurally stronger, aerodynamically much cleaner, and has 50 percent more power. The Model 2 was completed only seven months after U.S.A.F. contract for its construction was placed.

Type—Two seat. Experimental Convertiplane.

Rotor System—Two three-blade rotors mounted at tips of fixed wings are arranged to be tilted from horizontal (vertical flight) to point 6° forward of vertical (forward flight) by electric motors. Rotor diameter 18 ft. (5.49 m.). Chord of rotor blades 0.356 ft. (108 mm.). Blades have extruded 75 ST aluminum-alloy spar, 24 ST ribs, trailing-edge and skin. Rotors inter-connected to ensure simultaneous tilting. Hubs fully articulated.

Fig. 2-120. According to Bill Norton [244], this photo is the only known proof that the Model 2 actually flew. The best guess is that the first flight was in very late 1956 or early 1957 (photo courtesy of Howard Levy and Mike Hirschberg).

Controls—Collective and cyclic pitch run through wings and over chain and sprocket drive at tips to rotor heads. Rotor transmission from gear box in front of engine, through spanwise shafts to bevel gearing at wing tips to rotor heads. Two-speed gear in rotor drive to give required r.p.m. for vertical and forward flight.

Wings—Cantilever monoplane. NACA 23015 wing section. Aluminum-alloy structure. Ailerons have metal frames and fabric covering. Gross wing area 100 sq. ft. (9.29 m^2).

Fuselage—All-metal structure.

Tail Unit—Cantilever monoplane type. All-metal structure. Span of tail 6 ft. 4 in. (1.92 m.).

Landing Gear—Fixed nose-wheel type. Transcendental air-oil shock-absorbers.

Power Plant—One 250 h.p. Lycoming 0-435-23 six-cylinder horizontally-opposed air-cooled engine. Fuel capacity 14 U.S. gallons (53 litres).

Accommodations—Enclosed cockpit seating two side-by-side in nose of fuselage.

Dimensions.

Wingspan 22 ft. 9 in. (6.93 m.).

Overall length of fuselage 22 ft. 1 in. (6.74 m.).

Height 9 ft. 5 in. (2.86 m.).

Weights.

Weight empty 1,579 lb. (717 kg.).

Weight loaded 2,249 lb. (1,021 kg.).”

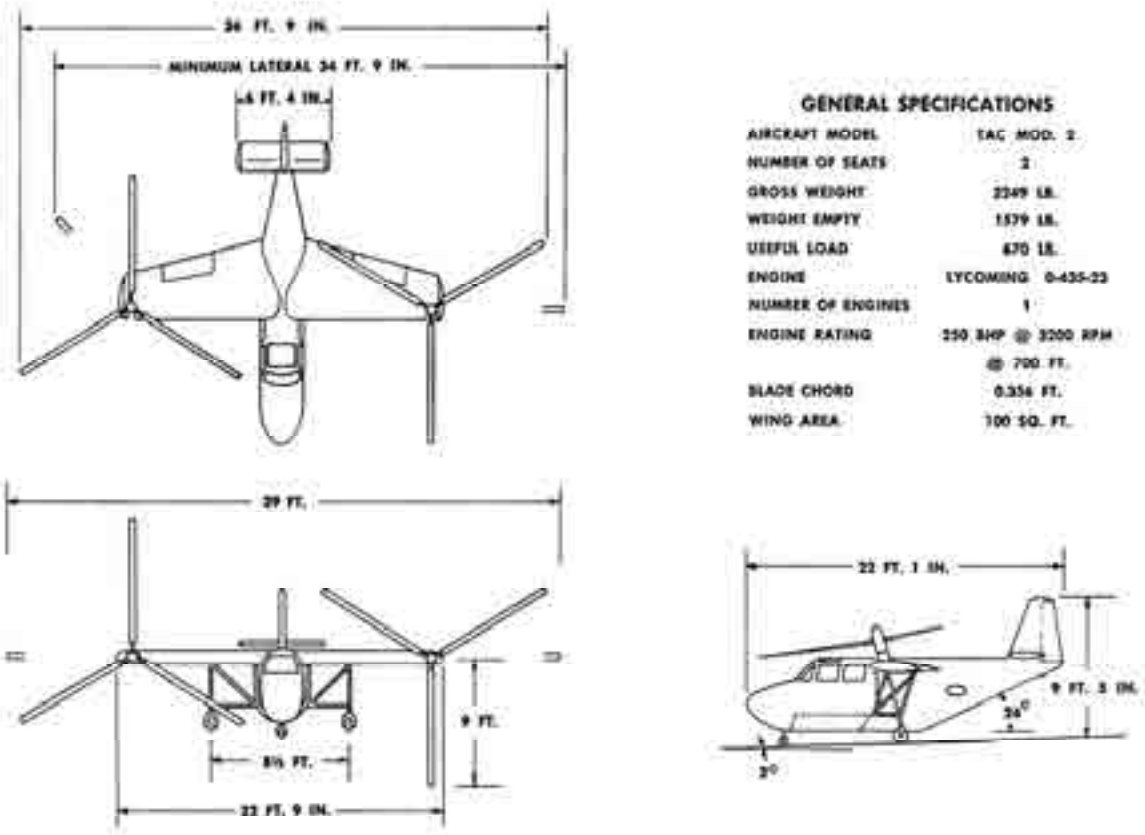

Fig. 2-121. The Transcendental Model 2. This 2,249-pound tiltrotor was designed with growth potential to 4,000 pounds at a future date when a turboshaft engine was to be installed.

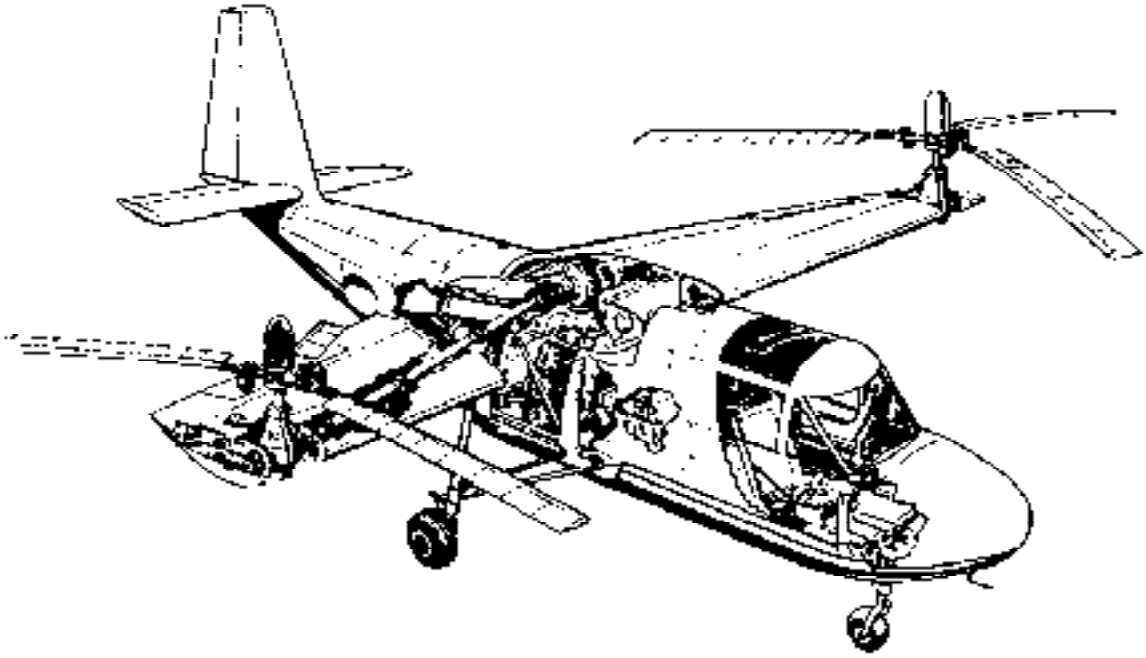

Fig. 2-122. The Model 2 showed some attention to airplane aerodynamics although retractable landing gear was not a feature. Bill Norton states [244] that the Air Force was surprised by the Model 2's development and that they cancelled the March 15, 1956 contract (aimed at further Model 1-G data gathering) in February of 1957.

Even as the Model 2 was being developed, Transcendental, under Cobey's leadership, was looking forward to the Model 3, Fig. 2-123. But without U.S. military financial support, the company was doomed. In December of 1957, Republic Aviation, located in Long Island, New York, established a Helicopter Division. It appears that Cobey sold Transcendental to Republic Aviation in early 1958; all the talent went on to other adventures and Transcendental's story ended.

I would be quite remiss if I did not remind you that the origins of tiltrotors can easily be traced back to Britain and Germany before World War II as Bob Lynn (retired Senior Vice President of Research and Engineering for Bell Helicopter) reported in his 1992 AHS Nikolsky Lecture [245]. One very interesting additional fact came to light in October of 2013. At the 75th Celebration of the 1938 Rotating Wing Aircraft Meeting [246], which was held at the Franklin Institute in Philadelphia, Pennsylvania, Fred Piasecki, Frank Piasecki's son, gave a presentation with wonderful pictures of many pioneers. Mike Hirschberg, the Director of the AHS, sent me a copy of the presentation with a note that slide 6 would be of real interest. The artwork that Fred sent me, included here as Fig. 2-124, had the caption:

> "The lower artwork was done by F.N. Piasecki while employed at Platt-LePage Aircraft as a draftsman with Allen Price and Elliot Deland. The story is: the artist made a fine sketch of the tilt rotor yet never finished on time for the next morning Washington visit planned by Platt. FNP completed the art showing the rotors in their hover mode."

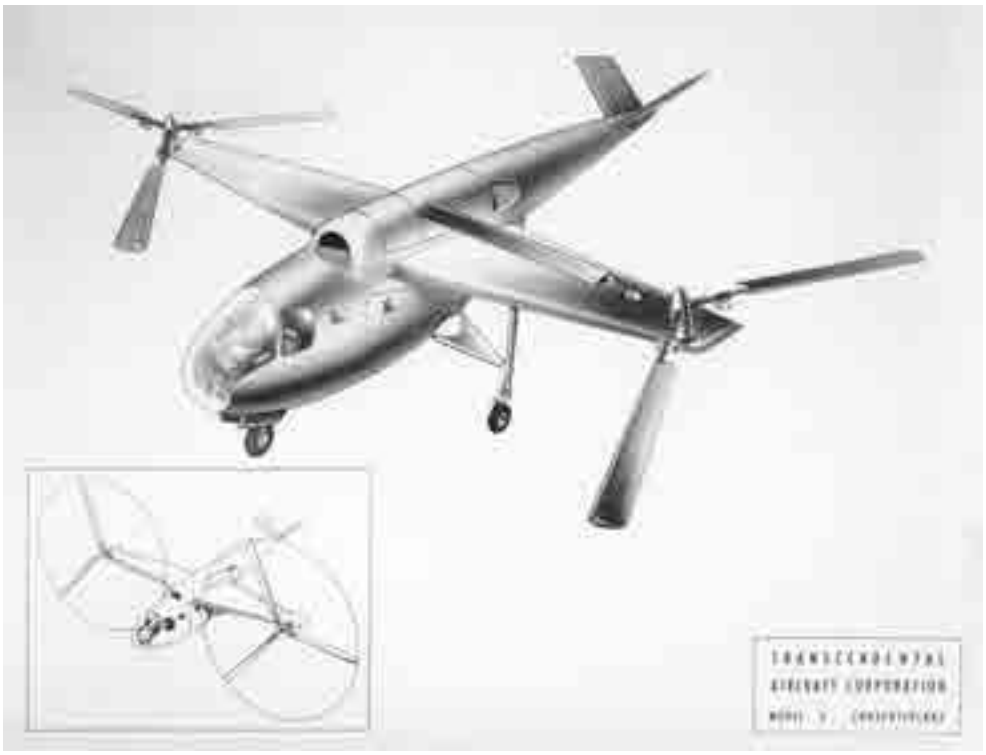

Fig. 2-123. The Transcendental Model 3 never got beyond the drawing board stage.

Fig. 2-124. It is easy to see this 1945 concept as a growth of the Platt-LePage XR-1, which was itself a scaled version of Focke's F.61 shown on the cover of Volume II (photo courtesy of Fred Piasecki).

2.13.2 The Bell XV-3

When Bob Lichten arrived at Bell Aircraft Corporation in Buffalo, New York, sometime in 1948 (with his 5 years of experience from employment at Kellett and Transcendental), you can well imagine that he was able to absorb much of Larry Bell's engineering VTOL studies conducted up to that time. As luck would have it, both the U.S. Army and the U.S. Air Force were warming to the idea of VTOL aircraft. The management aspect was that the Air Force would act as the contractual agency for the Army. This joint military thinking began to crystallize by August of 1950, and in May of 1951 they issued a Request for Proposal (RFP) for convertible aircraft. Larry Bell and Bob Lichten's response was the Bell Model 200, and Bob became the project engineer.

In October of 1951, the two services agreed on three winners:

1. The McDonnell Aircraft XV-1, a compound helicopter that you saw earlier in Fig. 2-6 on page 49.
2. The Sikorsky XV-2, a stopped rotor compound that only reached preliminary design.
3. The Bell Aircraft Corporation and then Bell Helicopter Textron XV-3 (Fig. 2-125 and Fig. 2-126), a tiltrotor—the world's second when you include Transcendental's efforts.

Let me stop right here to point out that the *XV series* went up to XV-15, at which point I stopped searching beyond Mike Rogers' terrific book, *VTOL Military Research Aircraft* [25]. You should be aware, however, that the U.S. Army Transportation Research and Engineering Command (TRECOM), the U.S. Air Force Wright Aeronautical Development Center (WADC), and the U.S. Navy Office of Naval Research (ONR) supported VTOL aircraft development of the *VZ series*, which Rogers also discusses. The VZ series went from the VZ-1 up to the VZ-12. The Doak VZ-4[64] that you see in Fig. 2-127 and Fig. 2-128 was, in my opinion, one of the most successful of the VZ series and was a VTOL aircraft having technology quite comparable to the Vertol VZ-2 tiltwing (Fig. 2-78, page 138), the Bell Aerospace X-14[65] shown in Fig. 2-129, and the Bell Helicopter XV-3, which you will learn more about shortly.

---

[64] You will find NASA Langley testing of the Doak VZ-4 reported in references [247-249]. Separate test reports of the 4-foot-diameter ducted fan, including a detailed configuration description, is provided in references [250-255]. The VZ-4 was evaluated by the Air Force, and results were reported in reference [249].

[65] Jay Miller made a very, very thorough study in *The X-Planes* [38] and he covers the X-14 and its predecessor, the Bell ATV, in great detail starting on page 107. Miller notes that the X-14 made its first "complete VTOL cycle on May 24, 1958." Following Bell's testing, the U.S. Air Force took delivery and immediately turned the only X-14 over to NASA Ames Research Center during October of 1959. NASA operated the aircraft primarily as a variable stability machine nearly continuously for the next 22 years. Miller states that "few accidents and no major injuries marred its distinguished career."

Fig. 2-125. The Bell XV-3 (s/n 54-4147) started out with three-bladed, articulated hinged proprotors. A dynamic instability referred to as rotor-pylon instability, and later as whirl flutter, finally caused a catastrophic crash on October 25, 1956 (photo courtesy of Tommy Thomason).

Fig. 2-126. The XV-3 (s/n 54-4148), the second aircraft, used Bell's "standard" two-bladed, teetering proprotor, which, along with several other fixes, suppressed whirl flutter enough that military flight test evaluation could be completed [256].

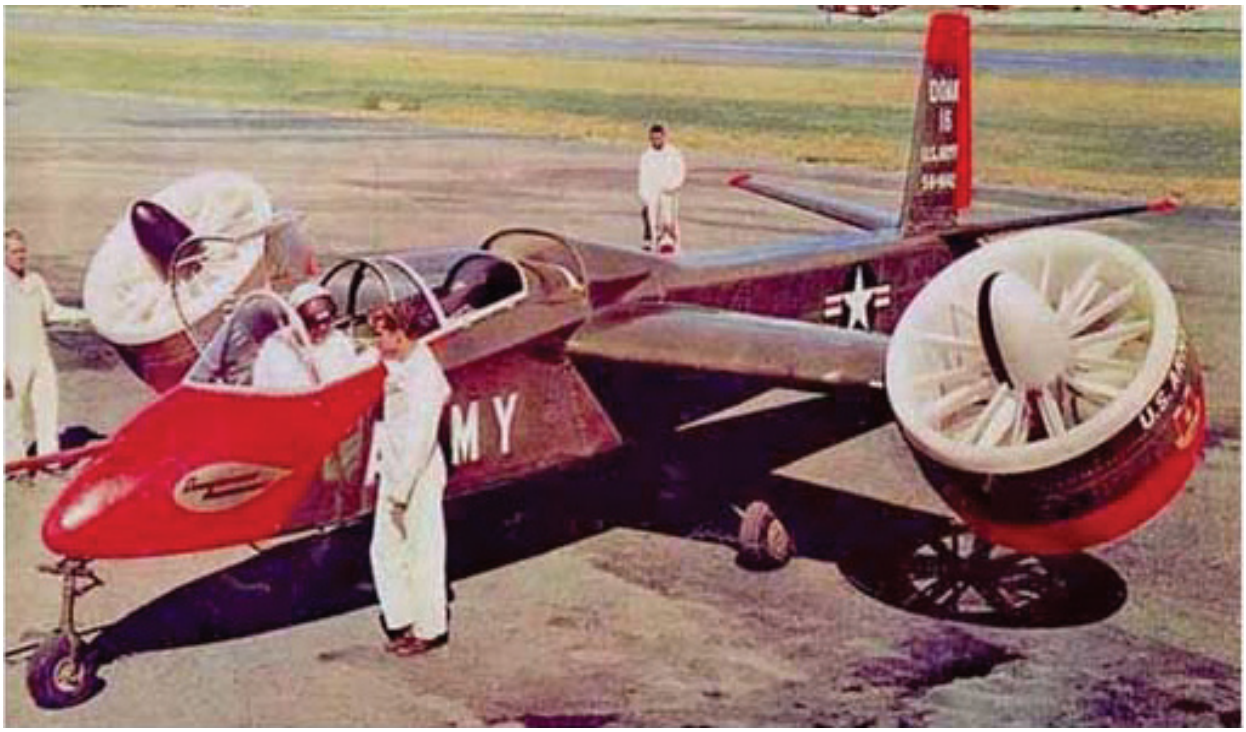

Fig. 2-127. Only one Doak VZ-4A was built.

Fig. 2-128. The Doak VZ-4A made its first flight on February 25, 1958. This 3,200-pound aircraft was initially powered with an 840-horsepower Lycoming YT-53 turboshaft engine, which was later upgraded to a 1,000-horsepower YT-53A.

Fig. 2-129. Larry Bell's Bell Aircraft Corporation became Bell Aerospace in 1965. The company obtained a contract for the X-14 in July of 1955. This 4,270-pound aircraft was initially powered by two Armstrong Siddeley ASV8 Viper turbojet engines slung under the nose and exhausting through vane cascades beneath mid-fuselage. Each Viper was rated at 1,750 pounds thrust. It first hovered on February 17, 1957.

The Bell XV-3 program extended from October of 1951 to November of 1968—say 17 years. Two machines were built. The aircraft began with two, three-bladed proprotors and, after a first hovering flight on August 11, 1955, the first aircraft (s/n 54-4147) flew on and off with an inherent proprotor dynamic instability until October 25, 1956. That day saw the end of the three-bladed version and most of the rest of the aircraft.

Robert (Bob) L. Lynn had the honor of giving the 1992 Nikolsky Lecture [245]. He chose to speak on *The Rebirth of the Tiltrotor*. In his lecture, he recounted the early evidence of the dynamic instability problem and the events on that heartbreaking day in October of 1956 with these words (plus my additions in brackets):

> "At Bell [Aircraft Corporation] in 1951, Bob [Lichten] was successful in selling a tiltrotor as part of the U.S. Army and Air Force Convertiplane Program that was to provide demonstrations of different approaches to convertiplane requirements. The aircraft in that program, the McDonnell XV-1, the Sikorsky XV-2, and Bob Lichten's XV-3, are shown in figure 5.
>
> Aided by many good people, Bob also was successful in overcoming normal development difficulties and in keeping the program sold during its design, manufacture, and early wind tunnel test phases. Figure 6 shows the as-designed, [three-bladed] articulated rotor version of the XV-3 just before its first ground test [on June 23, 1955]. Aircraft always look best before their test programs, with all their fairings on and before they 'grow' feathers (vortex generators), tufts, and dents.

> As is usually the case, things became more difficult as the aircraft entered into ground and flight tests. Intermittently throughout the next several years, its flight development was delayed due to recurring dynamics problems, referred to as 'rotor-pylon instability.' Although the dynamicists of the day and their contemporary analyses provided much needed guidance, they couldn't handle these very difficult problems adequately, and solutions were left to trial and error.
>
> The first occurrence of a dynamics problem was during the initial hover flight [on August 11, 1955] when the pilot, Floyd Carlson, suddenly encountered a very high vertical cockpit vibration. He recovered by setting the aircraft down hard. Figure 7 shows a photograph of that flight. Floyd had encountered a form of mechanical instability while airborne. No one was hurt and the damage to the aircraft was minimal, but nearly a full year was spent on tie-down seeking fixes.
>
> Dick Stansbury, the project pilot and my good friend, recently told me that during these ground tests (fig. 8) the instability was encountered often. The pilot was protected with a one-half-inch armor-plate 'house' that moved back to allow entry into the cockpit, and rotor 'snubbers' were provided to recover from the instability when the normal recovery technique of lowering the collective failed to arrest it. An increased mast length, increased controls stiffness, and additional pylon damping and stiffness allowed flight to resume [on March 24, 1956].
>
> In flight, 'nibbles' of the problem were again encountered, and this led to the addition of struts to stiffen the wing (fig. 10). At first the struts appeared to fix the problem, but at about 70 knots at zero pylon angle (vertical), a mild instability occurred (ref. 7). The problem seemed benign and controllable, so Dick backed off speed a little to evaluate the effect of pylon angle. As he lowered the pylon toward 15 deg from the vertical, it struck again. This time the consequences were catastrophic. Violent vertical cockpit vibration caused Dick to black out—and the aircraft crashed. At the beginning of the episode, Dick somehow had enough presence of mind to turn on the instrumentation. Later study of the records confirmed airborne mechanical instability. As a result of this accident Dick Stansbury was crippled for life. He contributed much to the program, just as he did to the development of Bell's helicopters, both before and after the accident. As one of a crowd, I acknowledge my admiration for Dick Stansbury for his courage and spirit, as well as his accomplishments."[66]

Whirl flutter as it came to be called, became, as you might guess, a research topic of intense interest for tiltrotor advocates until well after the XV-15 had demonstrated a performance-limited flight envelope free of this dynamic instability. (You might not know that Lockheed's Electra, a four-turboprop airliner, suffered the same plight, and three aircraft disintegrated in flight between February 1959 and March 1960. The FAA put a speed limit on that airplane after the third accident. I will discuss whirl flutter shortly.)

---

[66] Bob Lynn was one of my mentors. While he was on a visit to Boeing Vertol, I was asked to give him a tour of the Boeing V/STOL wind tunnel. That meeting led to me moving to Bell in July of 1977. I went from Director of Research to Chief of Aero. Fortunately, I have always been big on the work and unimpressed by titles and offices. I just wanted a change from a military customer to the world of commercial helicopters. At that time the Bell family include more than a few (some would say) matured and maturing mavericks. This group was quietly guided and encouraged by real leaders. As Bell's chief engineer after Bart Kelley, Bob made sure I became an apprentice maverick. I was hardly aware of it at the time and certainly returned little appreciation. Bob steered me toward very useful tasks and quietly swept up my debris as I thrived and grew. Now that is a mentor.

Bell offered me a perfect blend of Skunk Works with enormous production and product support capability. They could make one or two prototypes or a couple of thousand machines with equal dexterity.

After the XV-3's October 25, 1956 setback, Bell engineers immediately replaced the three-bladed articulated design with a two-bladed semirigid rotor. The rotor configuration changes were more than just a change from three to two blades. These details, and some chronology of the XV-3 program, are provided in Table 2-10 and Table 2-11.

You might note on Table 2-10 that I use reference [257] most in following the chronology of the XV-3 program. This reference is an article in *Aerophile*, Volume 2, Number 1, dated June 1979, and I believe this is the most complete and authoritative story you can read on the subject. Jay Miller was both the editor and publisher of this magazine for the several years that it existed. Jay's lead-in to the very detailed article titled *Bell's XV-3* shows just how much work went into providing considerable depth about the program. He wrote:

> "A number of folks get a note of credit for assisting AEROPHILE in the gathering of information and data for the completion of this in-depth XV-3 story. Special thanks go to Tommy Thomason, present-day director of Tilt Rotor Programs for Bell Helicopter Textron, who busted his butt getting us literally every available reference item needed in order to do this unique aircraft historical justice. Thanks is also due to Bell Helicopter Textron's Martin Reisch who made sure that all available p.r. releases were in our hands for reference; Ted Carrigan who came through with color transparencies for our cover; NASA's Stanley Miller; [Bell] test pilot Dick Stansbury; [Bell] test pilot Bill Quinlan; [Bell] project engineer Bob Mertens; and [Bell] flight test engineer Claude Leibensberger."[67]

It is interesting to me to see so many similarities between the XV-3 and Transcendental's Model 1-G. In particular, the fuselage shapes clearly show Bob Lichten's influence, which is not too surprising considering the fact that Mario Guerrieri mentions that Bob did the preliminary design on the Model 1-G before leaving Transcendental. And then at Bell (starting in 1948) Bob began as the project engineer and later became head of the Advance Design Group soon after Bell Helicopter moved to Hurst, Texas. The choice of three blades and an articulated hub for the XV-3 clearly duplicates the Model 1-G.

What the XV-3 development team lacked was a firm foundation in whirl flutter dynamics. Furthermore, the machine was very overweight or, as others have said, the machine was grossly underpowered, and I might add under-rotored with the smaller diameter. The aircraft, as evaluated at the U.S. Air Force Flight Test Center at Edwards Air Force Base in California, had a nominal takeoff gross weight of 4,890 pounds. The weight empty of the two-bladed version was 4,205 pounds, and the equipped pilot weighed 245 pounds. Instrumentation added another 160 pounds, and that left only 280 pounds for fuel. The takeoff rating of the Pratt & Whitney R-985-AN-1 supercharged piston engine was 450 horsepower at 2,300 revolutions per minute, however only about 400 horsepower reached the two proprotors [256, 260]. The aircraft could barely hover out of ground effect (HOGE) at Bell in Texas and could not hover HOGE at Edwards Air Force Base in California. I imagine that this must have been disappointing to Bob Lichten because his primary skill was aerodynamics—I have been told—and he was widely acknowledged as a leader and the driving force behind the XV-3.

---

[67] Claude Leibensberger led a team of Bell retirees who restored the one remaining XV-3 (s/n 54-4148) [258, 259].

Table 2-10. The Bell XV-3 Program

Item	Three Bladed	Two Bladed	Remarks
Configuration Data	Articulated with flap and lag hinges	Teetering with stiff inplane blades	
Diameter (ft)	25.0	23.0	
Chord (in.)	6.28	11.0	
Solidity (nd)	0.04	0.046	
Airfoil	NACA 23015	NACA 0015	
Chronology	**Date/[Ref]**		
Contract award	October 1951 [257]		One of 3 winners
Rollout of s/n 54-4147	Feb. 10, 1955 [257, 260-262]		Fig. 2-125
Rollout of s/n 54-4148	April 1955 [257]		
First hover s/n 54-4147	Aug. 11, 1955 [257, 260-262]		Pilot: Floyd Carlson
Envelope expansion began	June 1956 [257]		Limited progress
Hard landing	Aug. 18, 1956 [257]		Dynamic instability
200-hr tie-down test completed	Early March 1956 [257]		Many “fixes”
Restart s/n 54-4147 hovering	March 24, 1956 [257]		
First in-flight pylon tilt	July 11, 1956 [257]		Pylon tilt to 5 deg
Severe damage incident	July 25, 1956 [257]		Instability; back to tie-down
Returned to flight status	Sept. 26, 1956 [257]		After many more “fixes”
Partial conversions	Early Oct. 1956 [257]		Got to 80 knots
Crash of s/n 54-4147	Oct. 25, 1956 [257, 261]		Pilot: Dick Stansbury
Decision to use s/n 54-4148 as two-blade test vehicle	Nov. 1956 (best guess)	**Date/[Ref]**	Standard Bell Helicopter design
Initial whirl testing began		April 22, 1957	Okay in ground tie-down
Wind tunnel testing first		August 4, 1957	Shipped to NASA Ames
First 40 x 80 test (no. 114)		Sept.–Oct. 1957 [263]	Exposed instability
First hover s/n 54-4148		Jan. 21, 1958 [257]	Encouraging
Partial conversion (to 30 deg)		April 1, 1958 [257]	Weaving
Second 40 x 80 test (no. 125)		Oct. 1958	Aircraft intact
Returned to flight status		Dec. 11, 1958 [257]	At Bell
First full conversion		Dec. 18, 1958 [257]	Pilot: Bill Quinlan
First gear shift		March 13/14, 1959 [257]	Looses altitude
Bell flight testing concluded		April 24, 1959 [257]	No show stoppers
S/N 54-4148 shipped to Air Force Flight Test Ctr (AFFTC)		April 30, 1959 [257]	By Lockheed C-130
AFFTC limited flight evaluation conducted		May 21–July 3, 1959 [256, 264, 265]	Evaluation generally positive; underpowered and overweight
Preliminary Report		July 22, 1959 [264]	Shows some promise
Final AFFTC Report		May 1960 [256]	Publically available
Third 40 x 80 test (no. 172)		June/July 1962 [266]	Sustained rotor/pylon oscillations encountered
Fourth 40 x 80 test (no. 267)		May 1966 [267]	Fatigue failure at 8:00 p.m. PDT on May 20th

Table 2-11. The Bell XV-3 Configuration Properties [264]

Airplane:
- Length ..... 30.3 ft
- Ground to top of vertical stabilizer ..... 13.6 ft
- Proprotor span (distance between outboard edges of disks) ..... 52.5 ft
- Distance from wing MAC quarter chord to horizontal tail MAC quarter chord ..... 164.5 in.

Wing Group:

Wing
- Area (total) ..... 116.0 sq ft
- Span ..... 31.2 ft
- Root chord ..... 45.0 in.
- Elevator movement ..... 20 deg above, 15 deg below
- Tip chord ..... 45.0 in.
- Mean aerodynamic chord ..... 45.0 in.
- Airfoil section ..... NACA 23021
- Thickness ..... 21 %
- Incidence ..... +5.0 deg
- Sweepback and dihedral ..... 0 deg
- Aspect ratio 8.4

Aileron
- Sweep of leading edge ..... 20 deg
- Area (aft of hinge line) ..... 9.4 sq ft
- Span ..... 66.6 in.
- Chord (average percent wing chord excluding overhang balance) ..... 22.5 %
- Movement ..... 20 deg above, 20 deg below

Flaps
- Single slotted, 0.20 wing chord
- Half-span flaps are incorporated

Horizontal tail
- Area (total) ..... 32.6 sq ft
- Stabilizer area (to elevator hinge) ..... 18.7 sq ft
- Span ..... 133.1 in.
- Root chord ..... 46.4 in.
- Airfoil section, root ..... NACA 0015
- tip ..... NACA 0012
- Incidence, normal 0 deg
- Sweep of leading edge ..... 9.5 deg
- Dihedral ..... 0 deg
- Aspect ratio 3.8

Vertical tail
- Area (total) ..... 32.8 sq ft
- Fin area (to rudder hinge) ..... 27.3 sq ft
- Rudder area (aft of hinge) ..... 5.5 sq ft
- Airfoil section ..... NACA 0012
- Aspect ratio 1.33
- Rudder movement ..... 20 deg right, 20 deg left

Proprotor:
- Type ..... Semi-rigid UFA
- Number of blades 2
- Delta-3 ..... –20 deg
- Diameter ..... 23 ft
- Chord, constant ..... 11.0 in.
- Solidity 0.51
- Disc loading (based on 4,700 lb gross weight) ..... 5.66 lb/sq ft

2.13.2.1 Performance

That the XV-3, with two-bladed hubs and 23-foot-diameter proprotors, appeared woefully underpowered (and overweight) became immediately clear when hover testing began at Edwards. Two other points were also clear. The change from an articulated hub with three blades to a stiff inplane teetering hub (Fig. 2-130) was made with a reduction of 2 feet in rotor diameter! The change was made expeditiously, of course, to remove ground resonance as a factor in the aircraft's dynamic instability problems. The other key point was that it appeared that 60 horsepower from the engine was lost before it ever got to the proprotor hubs. This last point is made abundantly clear in Fig. 2-131. Because the test gross weight was nominally 4,700 to 4,800 pounds and the brake horsepower of the Pratt & Whitney R-985-AN-1 engine was about 450, you have, roughly speaking, a power loading of 10 pounds per horsepower. Therefore, the 60 lost horsepower meant something like 600 pounds of lost gross weight. This seems to me to be high by a factor of two. A drivetrain efficiency more on the order of 3 to 5 percent and 5 to 10 horsepower for accessories would be reasonable. This would amount to 30 horsepower and some 300 pounds of lost gross weight.

This situation received minor consideration as the flight evaluation report [256] notes in its power determination paragraph. The report, by Wally Deckert and Bob Ferry, states (with some editing by me):

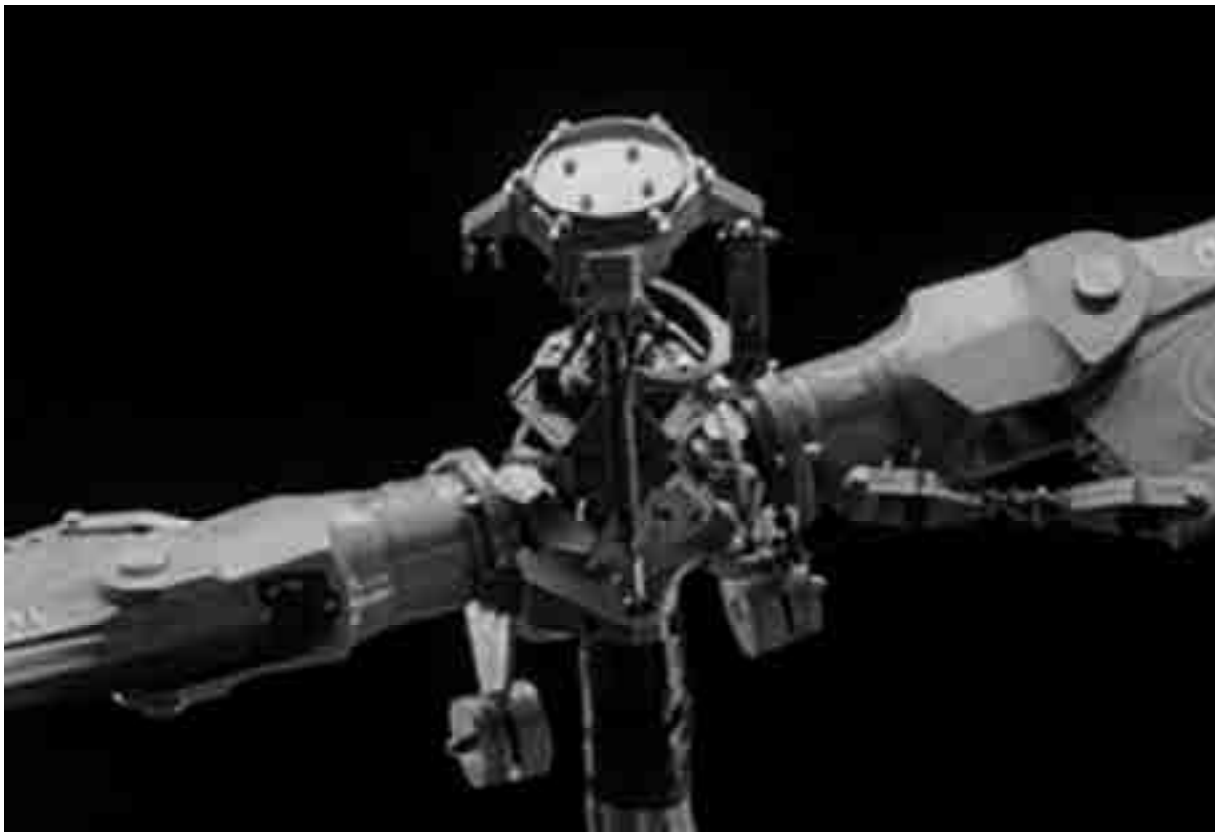

Fig. 2-130. The two-bladed, semirigid rotor configuration used on the XV-3 (photo courtesy of Bill Warmbrodt).

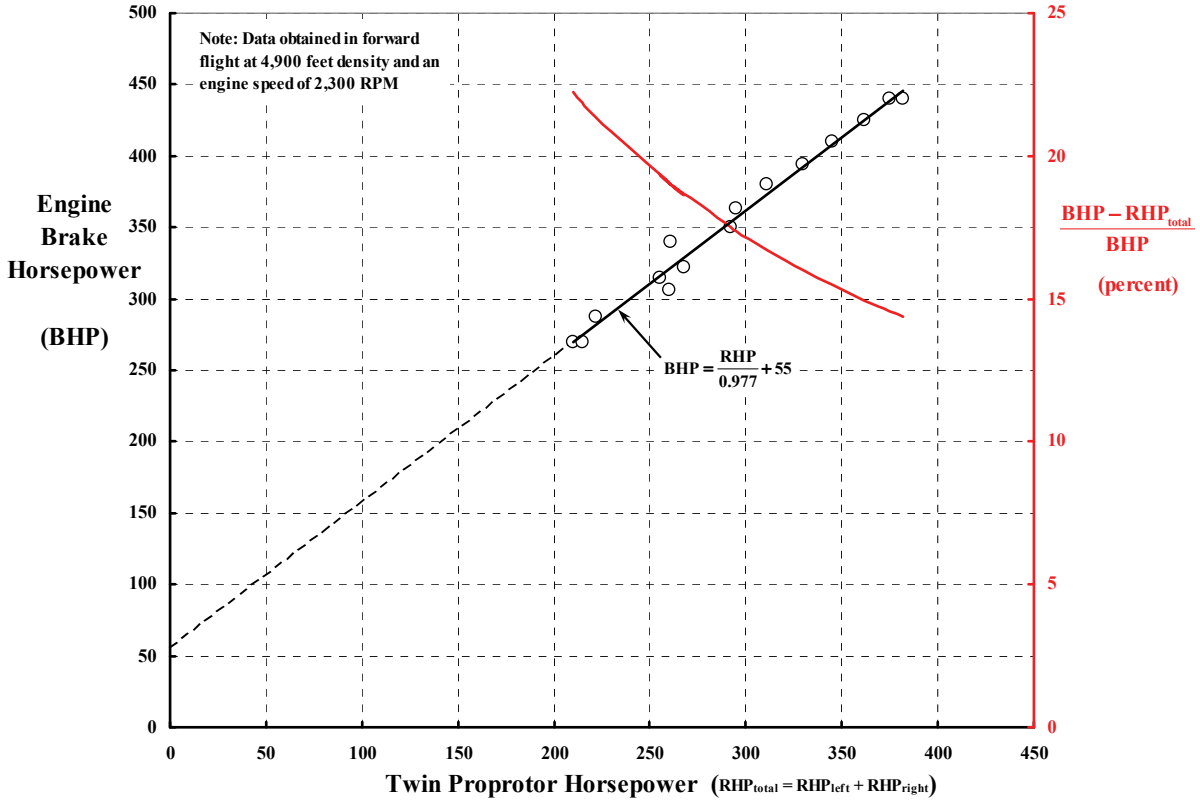

Fig. 2-131. The difference between proprotor power required and engine power required measured during the XV-3's limited flight evaluation appears excessive (to me). However, little attention was paid to this performance aspect because of other more important considerations such as dynamic instabilities and flying qualities.

"*A calibrated engine was not available for the test program.* Due to the nature of the test program and test vehicle, little effort was expended in rigidly determining the power characteristics of the R-985 engine. Test brake horsepower was determined by recording the manifold absolute pressure, engine rpm, carburetor air temperature, and atmospheric condition. These conditions were used to enter the Pratt and Whitney power chart (fig. 23) to obtain BHP_e. This was corrected to BHP_t by the following relationship. There was essentially no carburetor air temperature rise noted during the evaluation. No corrections were made for humidity since the relative humidity was always less than 20 percent and corrections were negligible. A full rich mixture was used during all the quantitative test work. The full throttle lines on the Pratt and Whitney power chart may be used with essentially no error by entering the chart at a given engine rpm and altitude. That is, full throttle manifold pressure versus altitude occurred essentially as shown on the power chart.

Proprotor torque was measured by a strain gage installation on the proprotor masts [shafts]. The performance in this report, however, is based on brake horsepower for consistency. *Proprotor torque was not obtained during the STOL evaluation and the* [free in-flight] *hovering tests because gross weight considerations necessitated the removal of all oscillograph-recorded parameters.* However, to show the power relationship (fig. 22) [Fig. 2-131] presents BHP versus RHP at one density altitude. [I imagine one result is not a universal result for all altitudes and, in particular, all engine and rotor speeds.]

> The high test gross weights and density altitudes prohibited a free-flight, quantitative definition of hovering performance. To obtain hovering performance a special hovering rig was designed and fabricated to accommodate the XV-3. As shown in the accompanying photograph, the XV-3 was mounted on a loading platform. This loading platform could be raised from ground level to desired heights to a maximum of 13 feet. The skids of the XV-3 were rigidly attached to a piece of boiler plate. Four load cells were inserted between the boiler plate and the loading platform. Load cell readout was by oscillograph. Several hundred pounds of weight placed on the boiler plate provided aircraft stability at high power settings and more accurate load cell readings. It is believed that downwash effects on the boiler plate were negligible due to its small size and location (see photograph). Using 2400 engine rpm [a proprotor speed of 555 rpm] a manifold sweep was then conducted at 0, 5, 10 and 13 foot skid heights. [The distance from bottom of the skids to the proprotor planes was 8.8 feet.] The load cells thus recorded the thrust of the proprotors minus the download on the wings, which gave a simulated hovering gross weight of the aircraft.
>
> In the absence of compressibility effects, dimensional analysis of the major parameters affecting hovering performance will yield two dimensionless parameters, namely C_P and C_W.
>
> $$C_P = \frac{550 \times BHP}{\rho A (\Omega R)^3} \qquad C_W = \frac{W}{\rho A (\Omega R)^2}$$
>
> These parameters were used to present non-dimensional hovering performance (fig. 1) [Fig. 2-132]. The validity of this simulated hovering performance was substantiated by qualitative observations during the test program *although it should be noted that the tests were conducted in a 4-knot crosswind*. In some respects this tethered technique is more desirable than free-flight hover. For example, power and aircraft stabilization can be obtained readily and reliably. However, the technique does require previous free-flight determination of the hovering cyclic stick positions or tests at several cyclic stick positions."

I became intrigued with this drivetrain and hover data and, just for the fun of it, I decided to reverse analyze both the in and nearly out of ground effect (IGE and OGE) hover data to estimate the aircraft's proprotor C_P versus C_W using the relationship that

$$(2.95) \quad RHP_{total} = 0.977(BHP) - 55.$$

The results I obtained are shown in Fig. 2-132. There are relatively few points to quantify the XV-3's hover performance from the flight evaluation [256]. However, the aircraft was tested in the NASA full-scale 40- by 80-foot wind tunnel (Fig. 2-133) and Dave Koenig, Dick Greif, and Mark Kelly authored a NASA Technical Note [263] on the investigation. They provided five more HOGE points with direct measurement of mast torque. The five points were obtained with the wind tunnel roof removed and the proprotor shafts inclined forward by 5 degrees—the thought being that recirculation of tunnel air would be, at least, minimized. These points, also included on Fig. 2-132, help establish just what the XV-3's hover performance was when expressed as a classical proprotor C_P-versus-C_W curve. However, flight testing continued on to obtain transition and forward-flight performance using the Pratt & Whitney engine specification chart as the "correct" basis for power.[68] Of course, as an aerodynamicist at heart, I was disappointed that more accurate quantitative flight test data were not obtained for the Bell XV-3. My view is that engine power and proprotor torque should also (and always) be measured at near zero thrust. Nor was I satisfied with the test being conducted without a calibrated engine and the fact that the aircraft weight empty had

[68] See figure 23, page 74 of reference [256].

grown substantially by the time the aircraft was shipped to Edwards. But, if you keep in mind the trials and tribulations that were overcome, you must appreciate that hover performance was really a very minor point in the development of the first tiltrotor to complete transition from hover to forward flight and back again.

As you might imagine from Fig. 2-125, Fig. 2-126, and Fig. 2-133, the forward-flight performance confirmed the high drag and poor maximum lift-to-drag ratio of the XV-3. The situation became very clear during testing of the machine in NASA's 40- by 80-foot wind tunnel. *This was the first wind tunnel test of a full-scale tiltrotor*. The measured aerodynamic characteristics (i.e., lift coefficient, C_L, and drag coefficient, C_D, versus fuselage angle of attack, α_f) with the *proprotor blades off* is shown in Fig. 2-134. Because the two teetering hubs were not removed, the aircraft's minimum drag coefficient (C_{Dmin}) equal to 0.1126 left something to be desired in terms of aerodynamic efficiency. This minimum drag corresponds to an equivalent parasite drag area (f_e) of about 13 square feet and, at a gross weight (GW) of 4,800 pounds, you have GW/f_e equal to 367 pounds per square foot. A quick look back to Volume II, page 292, figure 2-146, will show you that the XV-3 had only slighter lower drag for its gross weight than the first-generation helicopters. In the region below stall, say below a lift coefficient of 1.1, data on Fig. 2-134 can be approximated by the following equation:

$$C_L = 0.08281\left(\alpha_f + 4.3495\right) \quad \text{with angle of attack } (\alpha_f) \text{ in degrees}$$

(2.96)

$$C_D = 0.1152 - 0.02816C_L + \left(0.03926 + \frac{1}{\pi AR}\right)C_L^2 \quad \text{with an aspect ratio (AR) of 8.6.}$$

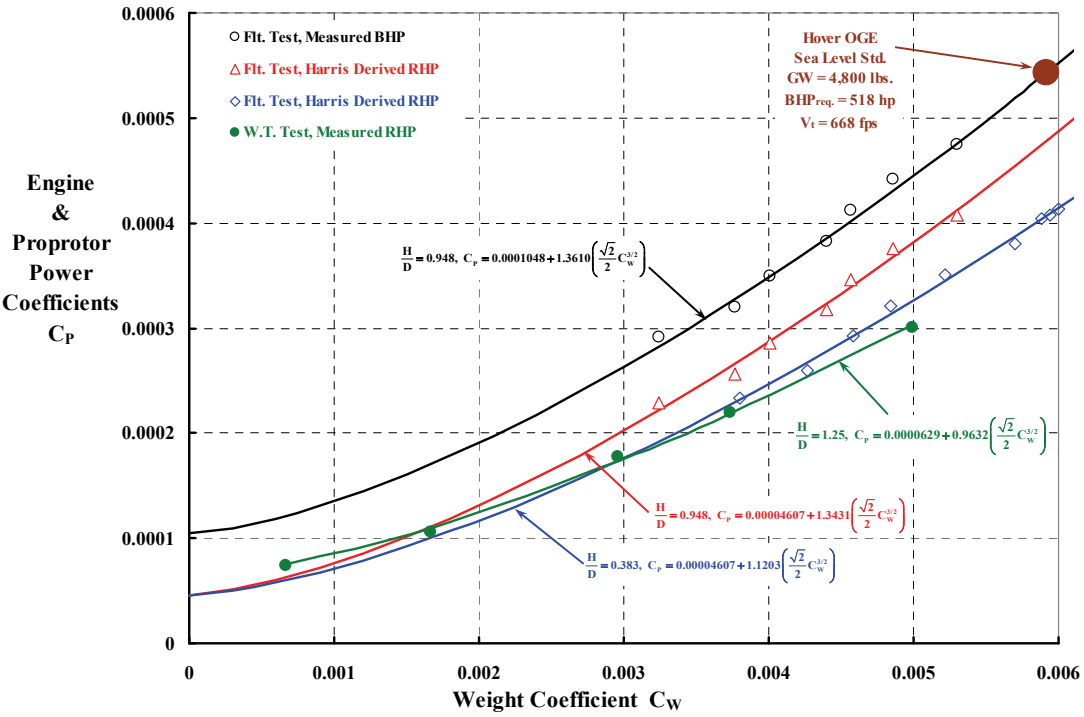

Fig. 2-132. According to the limited flight evaluation [256], the Bell XV-3 needed 518 horsepower out of the P&W 985 engine just to hover OGE on a standard day at sea level.

Therefore, the XV-3—with proprotor blades off but hubs on—had a maximum lift-to-drag ratio of 6.2 at a lift coefficient of 1.1, which is just before stall. Data with the proprotor shafts in the hover position simply increased the zero lift drag coefficient from 0.1152 to 0.1536.

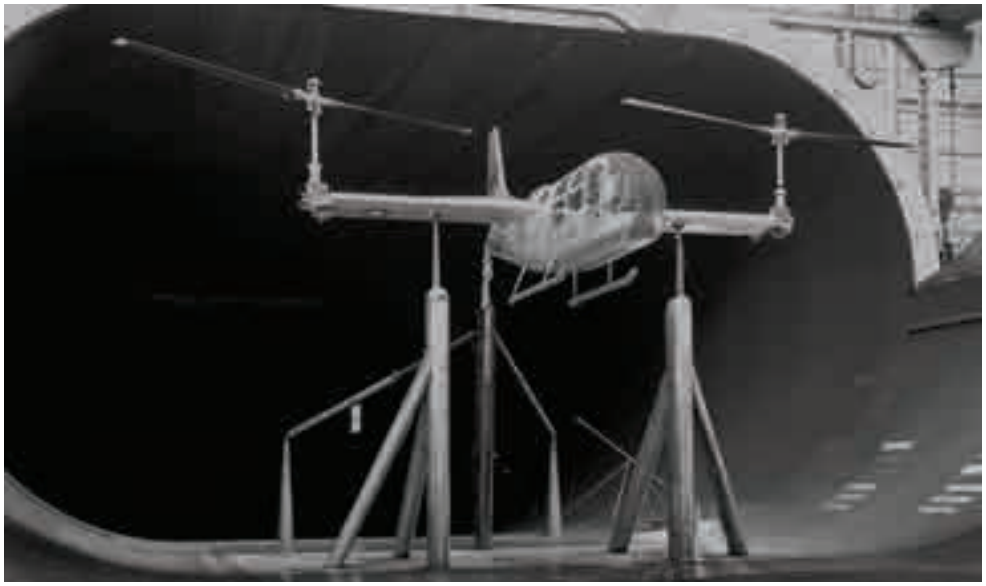

Fig. 2-133. Before flight testing at Edwards Air Force Base, the XV-3 was tested in NASA's large-scale wind tunnel (photo courtesy of Bill Warmbrodt).

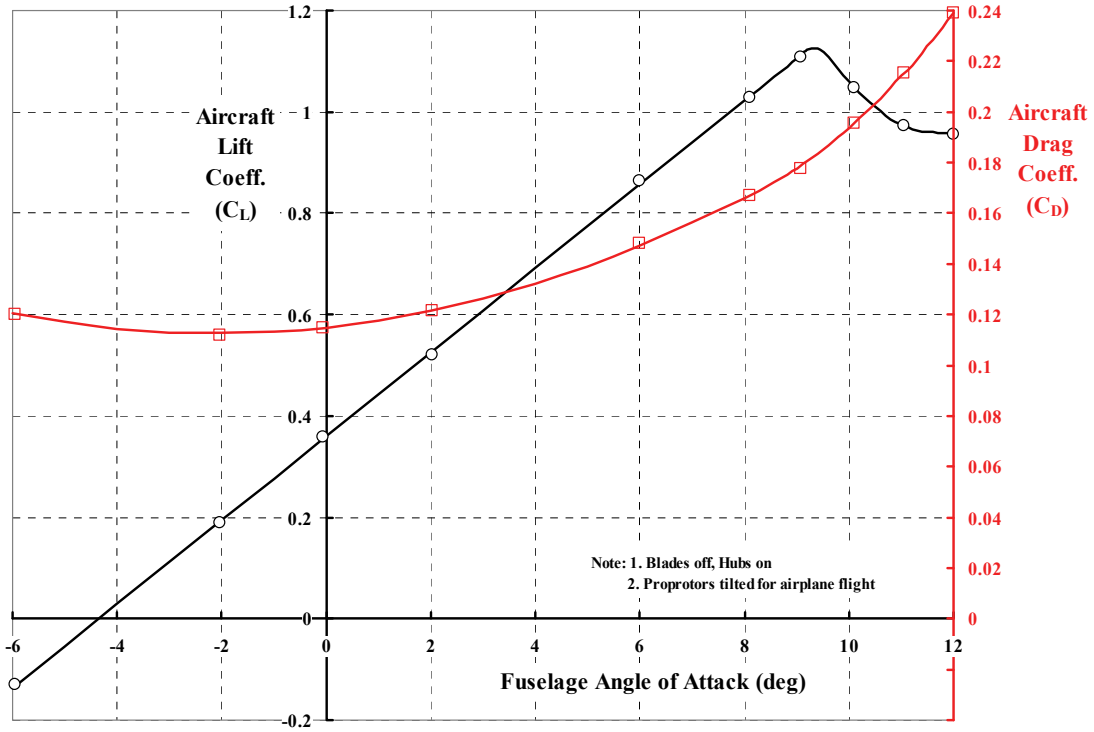

Fig. 2-134. The Bell XV-3 was not aerodynamically "clean." The L/D_{max} was only 6.2 occurring at a C_L of 1.1. Retractable skids would have helped reduce drag, of course.

Dave Koenig, Dick Greif, and Mark Kelly also conducted power-on testing of the XV-3 when it was in the 40- by 80-foot wind tunnel at NASA Ames. All controls were operated remotely from the control room [263]. The testing procedure was quite unique. They chose four pylon tilt angles of 10 (near hover position of 0 degrees), 30, 60, and 90 (airplane mode) degrees. At each pylon (or shaft tilt, if you prefer) angle, they fixed the proprotor power and varied the fuselage angle of attack while holding the tunnel speed constant. During a fuselage angle-of-attack sweep, they recorded primary forces and moments, as well as the usual rotor flapping and blade feathering parameters. I have included two examples of their performance data, Fig. 2-135 and Fig. 2-136, which are for pylon tilt angles of 10 and 30 degrees measured forward from the angle (0 degrees) used for hovering. You might note that the authors presented their data (figure 8, page 30 of reference [263]) in coefficient form, but I have found the dimensional form much easier to grasp for this introduction because it is closer to the dimensional flight test data you will see shortly.

From Fig. 2-135 you can see that the dimensional presentation form allows a simple interpolation for the speed (at total proprotor power of 242 horsepower and a gross weight of 4,700 pounds). Thus, based on wind tunnel data, the XV-3 should reach steady, level flight at 76 knots with the proprotor shafts tilted forward to 10 degrees. The situation at a 30-degree shaft tilt (see Fig. 2-136) begins to show the XV-3's performance limitations that were later confirmed in flight test.

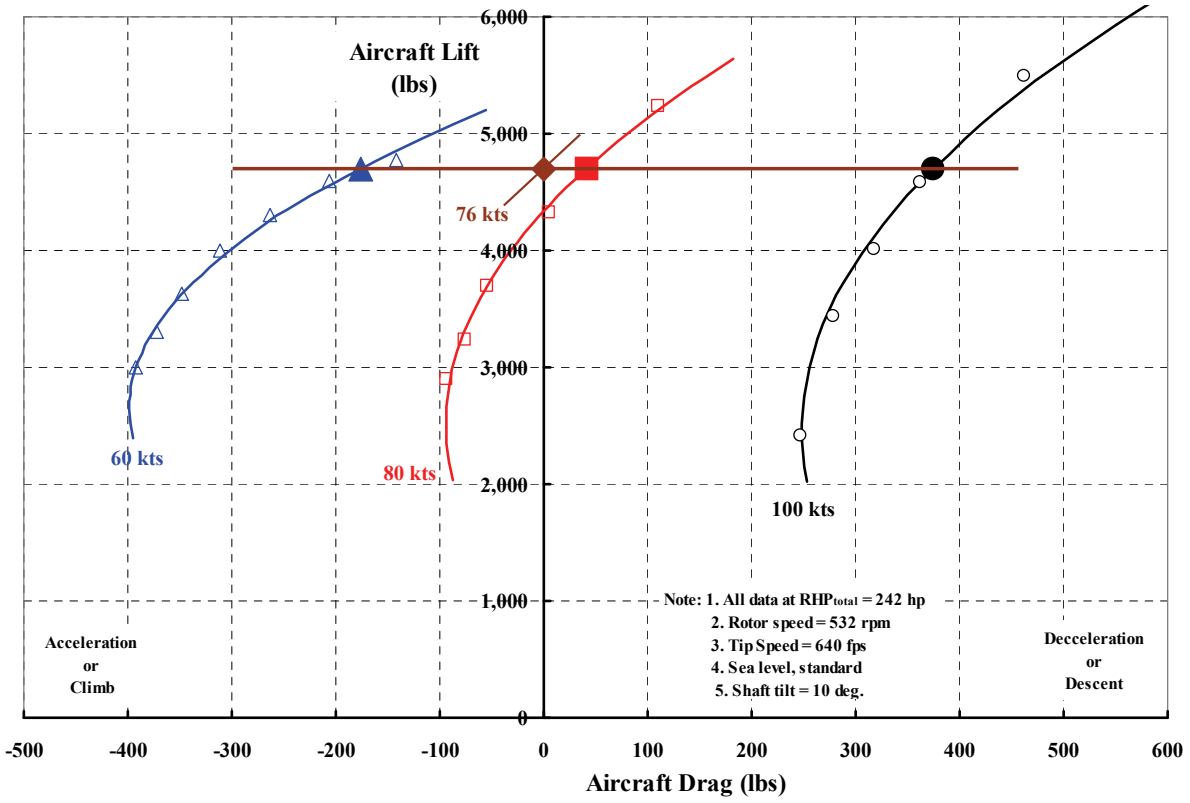

Fig. 2-135. Wind tunnel lift-drag measurements at a shaft tilt of 10 degrees forward from the hover angle showed the XV-3 had quite adequate performance capability.

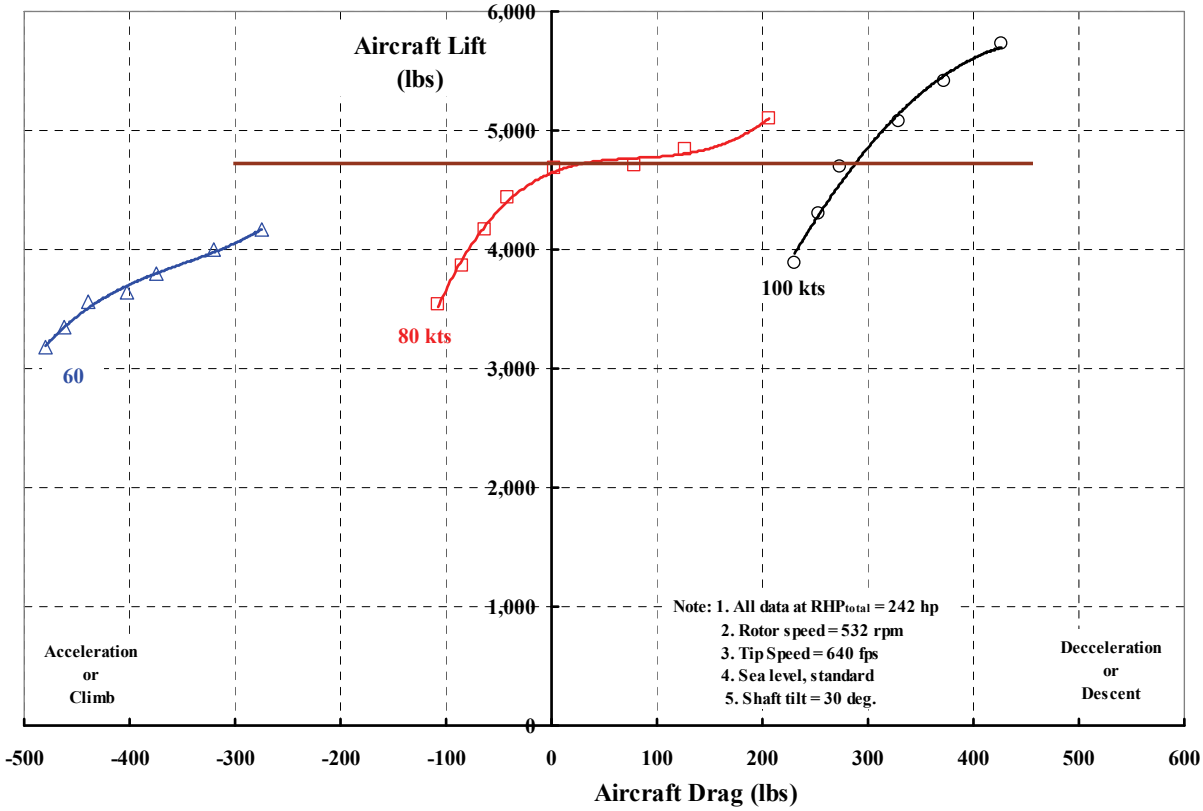

Fig. 2-136. Wind tunnel lift-drag measurements at a shaft tilt of 30 degrees showed the XV-3 had insufficient wing area (S_W = 116 sq ft).

After NASA Ames completed XV-3 wind tunnel testing in late October of 1958, the aircraft was shipped by a Lockheed C-130 transport airplane back to Bell where contractor testing was finished. On April 30, 1959, Bell then shipped its one flyable XV-3 (s/n 54-4148) to the U.S. Air Force Flight Test Center (AFFTC) at Edwards Air Force Base again by C-130 transport airplane and, finally, a limited flight evaluation was conducted from May 21 to July 3, 1959. While a preliminary flight evaluation report was available in late July of 1959 [264], the final limited evaluation report did not become publically available until May of 1960 [256].

The final evaluation report was deemed "limited" because the XV-3—as tested—was over design gross weight, and performance data acquired at about a 5,000-foot altitude showed a usable speed range of only 15 to 110 knots because the maximum power of the Pratt & Whitney reciprocating engine was about 420 horsepower. In fact, a large number of flights required the flaps down at 20 degrees, and *this included all 45 data points obtained in steady, level flight*. As Fig. 2-137 shows, the flight envelope was severely restricted in its "high-speed" capability because of insufficient engine power available. Just as bad a situation was created by the insufficient wing area (S_W of 116 square feet) that, even with flaps down at 20 degrees, led to a stalling speed of 100 knots. On the bright side, no aeromechanical instabilities raised their head, and conversions from hover to airplane flight and back again could be accomplished on a regular basis.

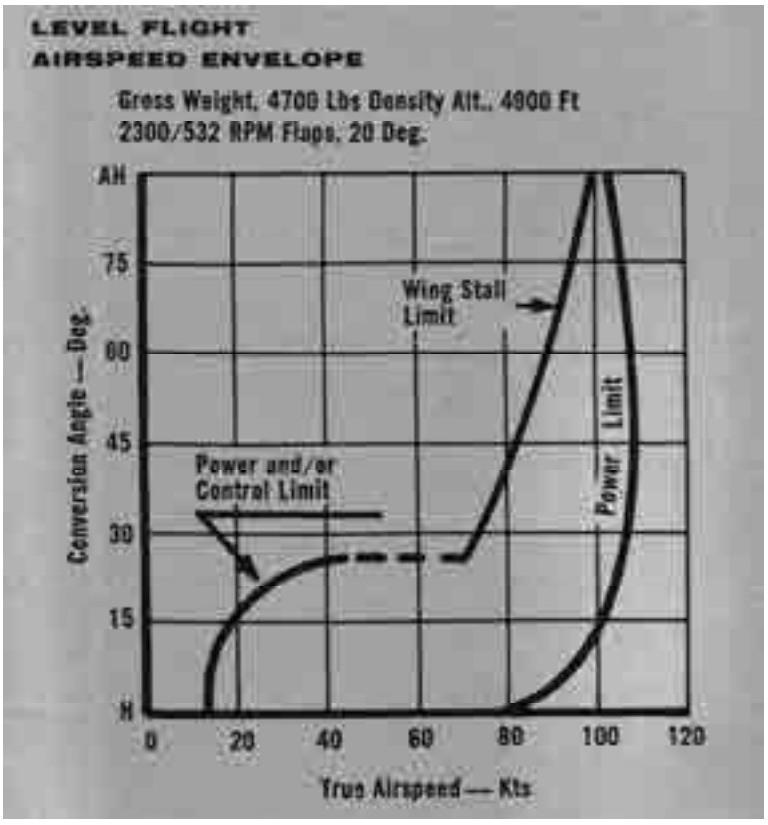

Fig. 2-137. Even though the Bell XV-3 was an overweight, underpowered, experimental machine, it proved that the tiltrotor concept was quite feasible [256].

The flight envelope you see in Fig. 2-137 was based on 45 data points that provided the power-required-versus-speed curves shown in Fig. 2-138. This data peaked my curiosity as to what engine power available would have been needed in airplane mode so that true high speed (well in excess of the 100 knots achieved by current in-service helicopters) might have been demonstrated. To make this airplane mode estimate, I used Eq. (2.96) for the XV-3's drag level and Eq. (2.55), repeated here for convenience,

$$
\begin{aligned}
P_{req'd.} &= P_{induced} + P_{profile} + P_{propulsion} \\
&= T_P\left(\frac{T_P}{2\rho\pi R^2 V_{FP}}\right) \\
&+\rho\left(\pi R^2\right)V_t^3\left(\frac{\sigma C_{d-average}}{8}\right)\left\{1+3\left(\frac{V_{FP}}{V_t}\right)^2+\left[\frac{9}{8}+\frac{3}{2}\ln\left(\frac{2}{V_{FP}/V_t}\right)\right]\left(\frac{V_{FP}}{V_t}\right)^4\right\} \\
&+T_P V_{FP}
\end{aligned}
\tag{2.97}
$$

for the power required by one of the two proprotors. The total engine brake horsepower required was then obtained from Eq. (2.95) after doubling the results from Eq. (2.97). The estimate from this simple calculation is shown with the heavy lines I have added to Fig. 2-138.

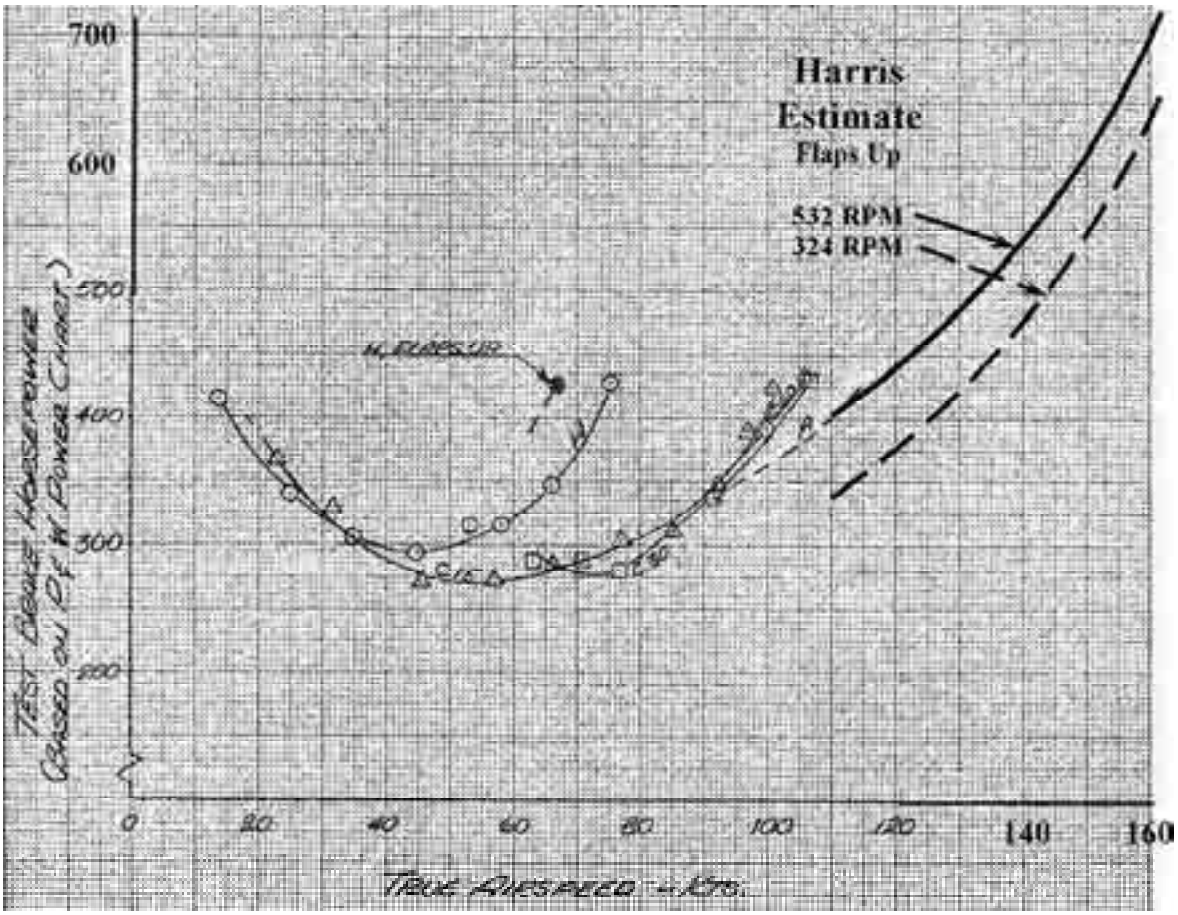

Fig. 2-138. XV-3 engine brake horsepower required versus speed at several shaft tilt angles (i.e., conversion angles labeled by C or H for hover position) [256].

What the XV-3 needed, of course, was a turboshaft engine rated at about 800 horsepower to offset the aircraft's very high parasite drag. The wing area of 116 square feet was marginally sufficient for altitudes up to, say, 10,000 feet, given more power. However, all conversions and reconversions clearly benefitted by putting the flaps down.

The general opinion of the pilots was that the XV-3 had insufficient thrust margin in hover and that the aircraft was "squirrely" in ground effect. In forward flight, the aircraft's performance, stability, and control in level flight and maneuvers was compromised because of the teetering proprotors flapping. This latter point led to the XV-3 being sent to NASA Ames for a dynamic stability flight study. The very valuable results of this follow-on flight testing were reported in reference [268]. Hervey Quigley and Dave Koenig's introduction is a very good summary of the XV-3. They wrote, with some additions by me, that

> "The Bell XV-3 convertiplane has been extensively tested over the past several years. An investigation was conducted in the Ames 40- by 80-foot tunnel to study the effectiveness of a number of modifications to correct the wing-pylon oscillation which was evident on the initial flights of the airplane. This investigation, reported in reference 1 [263], showed that the airplane could be flown through transition and gear-shifted to low prop-rotor rotational speed in airplane flight without serious airplane or rotor stability problems. A limited flight evaluation was performed by the Air Force Flight Test Center and is reported in

reference 2 [256]. The flight evaluation explored the flight characteristics of the airplane from near hover to about 155 knots. Since the completion [July 3, 1959] of the Air Force tests, the airplane has been flight-tested by the National Aeronautics and Space Administration at the Ames Research Center to explore further some of the problem areas noted in previous tests and to study general handling-qualities requirements for V/STOL aircraft. *Much of the recent flight testing of the XV-3 has centered around the cruise configuration of the airplane in order to study the effect of the large flapping rotors on the handling qualities at cruising speed and above.* This paper will deal with what is considered to be *one of the basic problems of the tilt-rotor concept in cruise* when flapping prop-rotors are used for propellers. This problem can be divided into four separate but related problem areas:

(1) The high blade-flapping amplitude with steady-state angles of attack and sideslip

(2) The increase in flapping due to maneuvering

(3) The prop-rotor normal force associated with pitching and yawing angular velocities of the airplane

(4) The airframe vibration which accompanies airplane angular velocities."

In this very short (10-page, 7-figure) report, the authors got right to the point. They wrote in the discussion that

"As airspeed is increased, the steady-state flapping decreases for both prop-rotor rotational speeds [532 and 362 rpm]. Thus, it would appear that flapping should become less of a problem as speed is increased; however, any type of maneuver will introduce additional flapping. The flapping due to maneuvering in pitch at 130 knots air-speed is presented in figures 3 and 4 [Fig. 2-139] where the change in blade flapping due to angle of attack and due to pitch angular velocity are presented. The change in blade flapping angle due to angle of attack alone (fig. 3) is relatively small, but the blade flapping due to pitch angular velocity (fig. 4) can be quite large. A pitch angular velocity of only – 0.2 radian per second results in a change in blade flapping angle of over 4°. In dynamic maneuvers, the change in blade flapping angle due to angle of attack and pitch angular velocity can add to give even higher blade flapping angles. The XV-3 is provided with a maximum available blade flapping angle of 11.2° which should prove adequate for any normal maneuver. It can be seen in figure 4 that the change in blade flapping angles is positive when the pitching angular velocity is negative; because of inertial effects, the prop-rotor disk is lagging the angular motion.

In evaluation flights of the airplane at high airspeeds, pilots have reported a condition in which the airplane oscillated about all axes simultaneously. An analysis of the time histories taken during this maneuver has shown that it consisted of longitudinal and lateral-directional oscillations that were very lightly damped. The damping ratio and period for the two oscillations over the speed range that could be covered with this airplane are presented in figure 5. These data are for the low prop-rotor rotational speed. The longitudinal and lateral-directional oscillations are not directly coupled. They are at different frequencies and oscillations can be performed in either mode without exciting the other, but with such low damping it is easy to excite both modes at the same time. These damping ratios are much lower than are considered acceptable by any of the criteria for airplanes in cruise. Damping ratios of 0.34 for the longitudinal mode and 0.18 for the lateral-directional mode have been specified as the minimum allowable by military handling qualities specifications.

The damping ratios are not only low but also change appreciably over this relatively small airspeed range, approaching zero at the higher speeds [Fig. 2-140]... . Due to the low tail volume of the XV-3, the force on the prop-rotor hub had a large effect on the dynamic stability of the airplane."

With this first-ever measured data [256, 263, 268], tiltrotor advocates got a quick reminder about airplane stability and control. Just imagine if the XV-3 had been powered with an 800-horsepower turboshaft engine. Then level flight forward speeds on the order of 160 would have been possible. This would have forced the pilots to quickly learn how to fly an unstable airplane—just the situation the Wright Brothers faced at Kitty Hawk on Dec. 17, 1903. Most certainly, the vertical and horizontal tail surfaces would have been resized before envelope expansion could have continued but with potential whirl flutter problems.

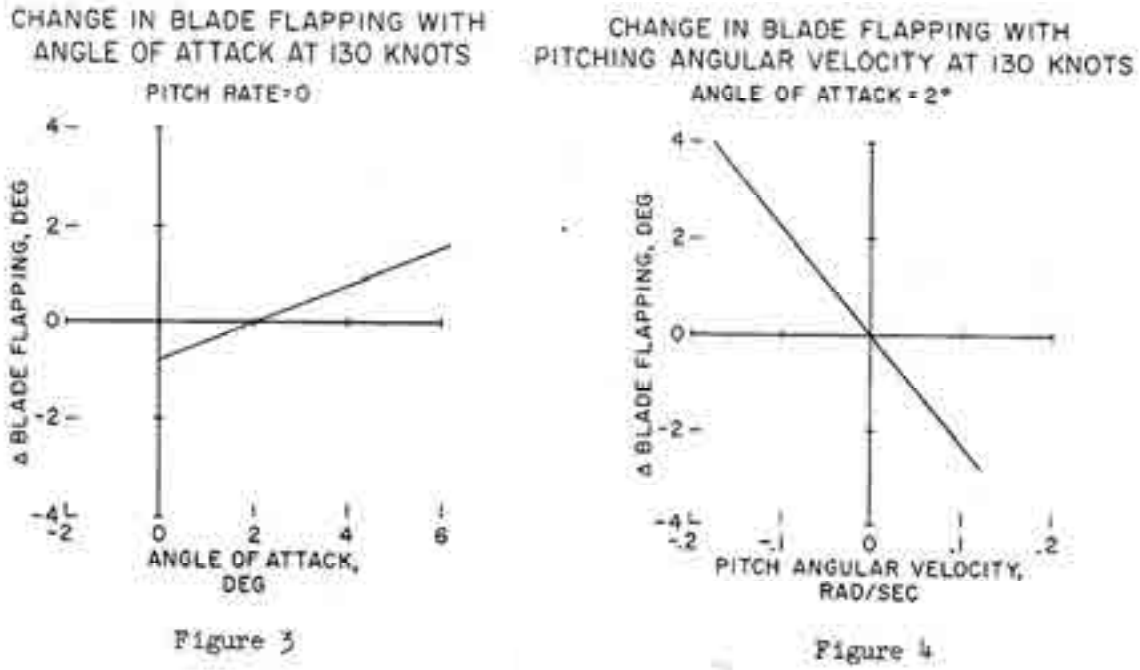

Fig. 2-139. The teetering proprotor flapping contributed negative damping to the longitudinal stability of the Bell XV-3 tiltrotor [268].

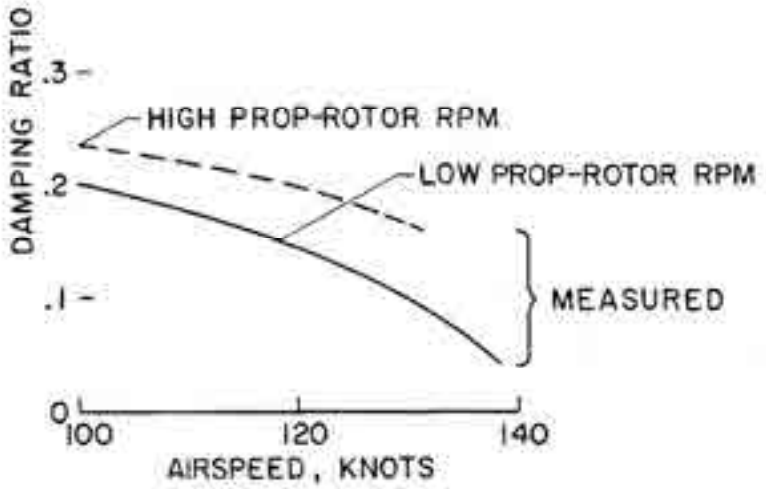

Fig. 2-140. The Bell XV-3 would have had negative damping in longitudinal dynamic stability (of the short-period mode with 2-second period) beyond 160 knots. Lowering the proprotor speed to achieve greater propulsive efficiency would have created a serious quality-of-flight problem [268].

The stability behavior of the XV-3 that was being commented about so negatively was captured on an oscillograph strip chart[69] and reported in the flight evaluations conducted at Edwards Air Force Base and NASA Ames [256, 264, 268]. I have reproduced one example for you to see here as Fig. 2-141 [256]. In this example, sensors recorded what the pilot did with the longitudinal stick (the top curve on the figure) and what the XV-3 did in response. Five channels of data were recorded: pitch acceleration, normal acceleration, pitch rate, angle of attack, and blade flap angle. In this particular flight, the pilot agreed to put in an aft pulse, which is commonly defined as "deflect stick 1 inch from the trim position, hold aft stick for 1 second, and then return stick to the trim position." In essence, his task was to create a square wave. While you might think he did a poor job, I will tell you that his "pulsing" of the stick was actually quite good. The issue is more of an academic one because dynamists of all stripes can mathematically create a square wave and are quite dissatisfied with anything less than perfection. This example was aimed at obtaining *stick-fixed* behavior after the aircraft was disturbed from trim, level flight at 94 knots.

As ragged as you might think the pilot's disturbing stick motion was (in comparison to a square wave), the XV-3 clearly returned to a trimmed condition in about 5 to 6 seconds. The time that it took for the aircraft to return to trimmed, level flight was considered by all the pilots to be quite long. Furthermore, the time to regain trim increased as the procedure was repeated at successively higher speeds. I imagine the test crew, based on a rough curve of time to regain trim versus speed, projected that the XV-3 would not ever return to trim at, oh say, 140 to 150 knots. This is a characteristic of an unsatisfactory airplane, and the flight reports said so in no uncertain terms. In fact, if you take a moment to reread the requirements for an airplane to win the Daniel Guggenheim Safe Aircraft Competition (page 3 of this Volume) you will see that requirement 6 stated that the airplane should "remain in stable flight for at least 5 minutes with hands (and feet) off all controls for any airspeed between 45 mph and 100 mph, even in gusty air." There is absolutely no evidence that the Bell XV-3 could meet *this* 1930's requirement.

2.13.2.2 Longitudinal Stability

The subject of longitudinal stability when the pilot holds the controls fixed in the trim position and then the aircraft is hit by a gust—or some other disturbance occurs—is quite interesting. You could say it is more than interesting because it plays a very, very important part in configuring any aircraft, even at the beginning of conceptual design. To see what aircraft design parameters are involved, you need at least an introductory knowledge of the theory behind this subject.

So let me start with an examination of Fig. 2-141 in a little more detail. I have chosen the oscillograph trace for rate of pitch from this figure to begin the study. To help, I converted this waveform from its original analog tracing to a digital graph so the small vertical scale is enlarged. This graph is shown in Fig. 2-142. The first thing to notice from this waveform

[69] These are the kind of charts I grew up with. I learned how to interpret the data at nearly a glance as did most of my peers.

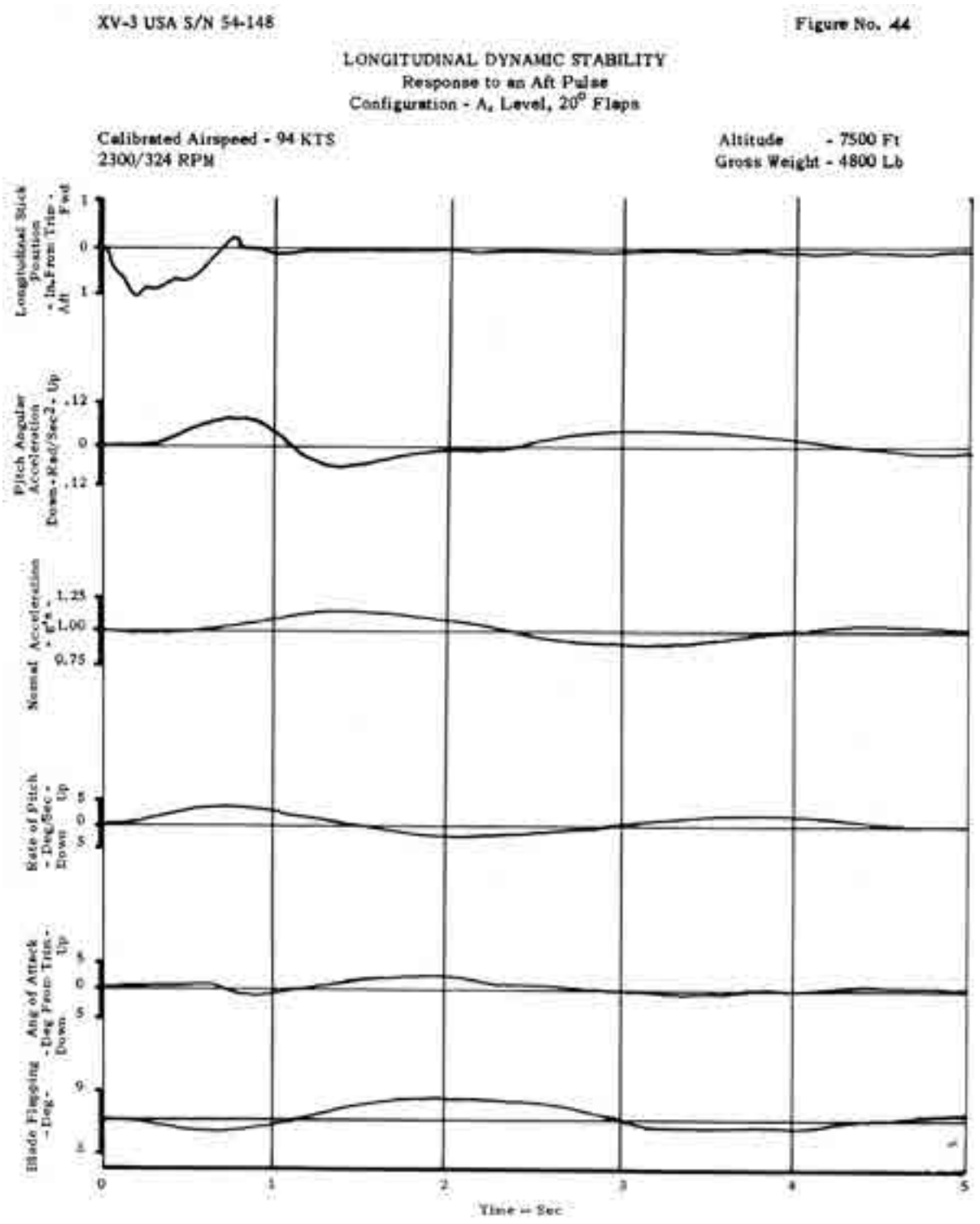

Fig. 2-141. Oscillograph strip chart showing the stability behavior of the XV-3 from flight evaluations conducted at Edwards Air Force Base and NASA Ames [256].

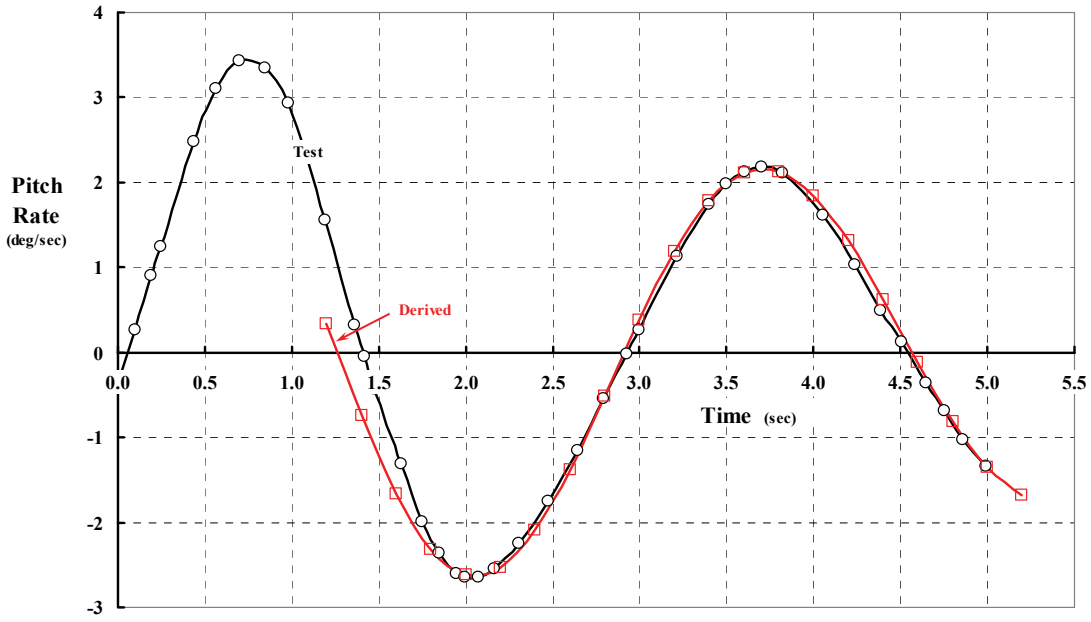

Fig. 2-142. The XV-3's short-period longitudinal stability appeared lightly damped.

is that after the pilot completed his "square wave disturbance" at time equal to about 0.75 seconds, the XV-3 reached a maximum pitch rate of about 3.5 degrees per second in the nose-up direction. Pitch *angle* is generally denoted by the symbol (θ) and, because pitch *rate* is a change (Δ) in pitch angle with time (t), you would write in mathematical terms

$$\frac{\Delta\theta}{\Delta t} = 3.5 \text{ degrees per second.}$$

When the change is virtually infinitesimal, then a dynamist will change the symbol from Δ to a "d" and write

$$\frac{\Delta\theta}{\Delta t} \rightarrow \frac{d\theta}{dt} = 3.5 \text{ deg/sec as } \Delta \text{ approaches zero.}$$

When the mathematics consume too much pencil lead and paper, you will see shorthand brought into equations so that $d\theta/dt \equiv \dot{\theta}$. Personally, I have often found that the dot above the Greek symbol frequently disappears by the second reproduction of a technical work. Therefore, I will stick to the Δθ/Δt notation as much as possible.

The second thing to notice about the pitch rate waveform in Fig. 2-142 is that the curve looks like a trigonometric sine or cosine function where, after each repetition, the maximum (and minimum) pitch rate is getting smaller. In fact, dynamists have found that acceptable airplanes have a pitch angle that behaves—mathematically—in accordance with

$$\theta = e^{Ct}\left[A\sin(\text{freq})t + B\cos(\text{freq})t\right] \quad (2.98)$$

where (C) is a constant (with units of 1/second) that accounts for the damping that makes the oscillation die out (one hopes). The oscillating frequency (freq) is in radians per second. The constants (A and B) determine the amplitude of the oscillation.

It is a relatively simple matter to take the derivative of Eq. (2.98) and arrive at a pitch rate equation, which appears as

$$(2.99)\quad \frac{d\theta}{dt} = e^{Ct}\left[(B\times freq - AC)\sin(freq)t - (BC + A\times freq)\cos(freq)t\right].$$

My approximation of Eq. (2.99) to the flight test results is shown in Fig. 2-142. The constants that I believe best apply to the XV-3 are:

Oscillating frequency (freq)	1.9 radians per second
Damping constant (C)	-0.12
Coefficient (A)	$+0.0195$
Coefficient (B)	-0.0240
Sin amplitude (Bω – AC)	-0.04322 radians per seconds
Cos amplitude (BC + Aω)	-0.03993 radians per second

On this basis, you can fit the XV-3 flight test measured waveform with

$$(2.100)\quad \frac{d\theta}{dt} = -e^{-0.12t}\left[(0.04322)\sin 1.9t - (0.03993)\cos 1.9t\right].$$

Keep in mind that the effect of the pilot's stick input causes what dynamists call a transient input. In this example, this whole transient period occupies about the first 2 seconds of the experiment. Therefore, my approximation equation, Eq. (2.100), only applies after the transient input is completed. That is why my result only applies to the XV-3's response after 2 seconds and why my curve starts at time equal to 2 seconds. Using advanced dynamic stability theory, you can predict the aircraft's behavior during the transient period, but that is a discussion beyond my intentions for this introductory volume.

Dynamists use a few other terms that you should know about. For instance, they will interchange oscillating frequency in radians per second and period (T_{Period}) in seconds. A period is the time it takes for the waveform to complete one cycle. Because a cycle is one revolution or 2π radians, you have

$$(2.101)\quad T_{Period} = \frac{2\pi}{freq},$$

so when you have a waveform, you can "eyeball" the time to complete a cycle and, in your head, calculate the frequency as freq = $2\pi/T_{Period}$, which has the units of radians per second.

Another term dynamists and flying qualities specifications use is damping ratio, which relies on a denominator in the ratio called critical damping. You encountered this damping ratio term as the label on the vertical axis in Fig. 2-140. Furthermore, reference [268] noted that "Damping ratios of 0.34 for the longitudinal mode and 0.18 for the lateral-directional mode have been specified as the minimum allowable by military handling qualities specifications." For Bell's XV-3 it appears that

$$(2.102)\quad \text{Critical Damping Ratio (CDR)} = \frac{-C}{2(freq)} \approx 0.032.$$

This result differs markedly from the data in Fig. 2-140 and certainly shows that the XV-3 fell far short of the minimum of 0.34 specified by the military (in the 1960s).

There are, in fact, just two key numbers from the preceding discussion that a competent stability and control engineer needs in order to make a preliminary judgment about the longitudinal stability of a conceptual design. These two numbers are the damping constant (C) and the natural frequency. Engineers "know" from experience that the acceptable aircraft will oscillate, after experiencing a disturbance, according to the displacement equation

(2.103) $\text{Displacement} = e^{Ct}\left[A\sin(\text{freq})t + B\cos(\text{freq})t\right]$.

They want to see the damping constant (C) come out negative, which means that any disturbance to the aircraft will die away quickly, and the aircraft will return to its trim state. They initially ignore the amplitudes (i.e., A and B) of the oscillation (or waveform, if you prefer). Furthermore, they have a mathematical approach that solves for the damping constant and frequency in a most direct manner—given some detail about the machine. This mathematical approach contracts Eq. (2.103) to its complex number form, which is written as

(2.104) $\text{Displacement} = \bar{A}e^{St}$

where S is a complex number defined as Real + Imaginary $\times \sqrt{-1}$. Because $i = \sqrt{-1}$, I like to write that S = Re + Im i.[70] Do not forget that (Im) is really a real number.

Let me stop right here for a moment to discuss the fundamentals of how dynamists use applied mathematics and complex numbers to solve many F = ma equations. As an example, think about the mass (m) – damper (c) – spring (k) problem stated as

(a) $$m\frac{d^2x}{dt^2} + c\frac{dx}{dt} + kx = 0$$

or, more in line with the way dynamists think,

(b) $$\frac{d^2x}{dt^2} + \left(C = \frac{c}{m}\right)\frac{dx}{dt} + \left(\omega^2 = \frac{k}{m}\right)x = 0.$$

The solution giving the displacement (x) is "simply"

(c) $$\begin{aligned} x &= e^{(Re)t}\left\{K_1\left[\cos(Im)t + i\sin(Im)t\right] + K_2\left[\cos(Im)t - i\sin(Im)t\right]\right\} \\ &= e^{(Re)t}\left\{(K_1 + K_2)\cos(Im)t + (iK_1 - iK_2)\sin(Im)t\right\} \end{aligned}.$$

[70] I wish that the theory of complex numbers was just called advanced trigonometry. Furthermore, I wish there had been a slide rule for adding, subtracting, multiplying, and dividing complex numbers when I was in college. Frankly, I have never been comfortable with the concept that $i = \sqrt{-1}$, but what else could you call it?

Because K_1 and K_2 are just arbitrary constants, then $(K_1 + K_2)$ and $(iK_1 - iK_2)$ are also just arbitrary constants that you might as well label as A and B. Therefore the solution to Eq. (b) is more simply written as

(d) $$x = e^{(Re)t}\left[A\sin(Im)t + B\cos(Im)t\right].$$

To the practicing engineer, Eq. (d) is quite incomplete because the real numbers (i.e., Re and Im) are not related back to the original problem given by Eq. (a). You must be reminded that

$$Re = -\frac{1}{m}\left(\frac{c}{2}\right)$$

(e) and that

$$Im = \sqrt{\omega^2 - (Re)^2} = \sqrt{\left(\frac{k}{m}\right)^2 - \left(-\frac{c}{2m}\right)^2} = \frac{1}{m}\sqrt{k^2 - c^2}.$$

Let me add that when a curve fit is made to an experimental waveform, it is quite handy to know that

$$c = (-2m)Re$$

(f) and that

$$\omega^2 = Re^2 + Im^2 \text{ or, better yet, that } k = m\sqrt{Re^2 + Im^2}.$$

Given that relatively short interruption, you can immediately see that my curve fit of the XV-3's short-period response to the pilot's stick input by

(2.100) $$\frac{d\theta}{dt} = -e^{-0.12t}\left[(0.04322)\sin 1.9t - (0.03993)\cos 1.9t\right]$$

is the solution of the F = ma problem stated as

(2.105) (a) $$\frac{d^2\theta}{dt^2} + (0.24)\frac{d\theta}{dt} + (1.9^2)\theta = 0.$$

You should know that when aircraft behavior such as that shown in Fig. 2-141 is in hand, the techniques of solving backwards for key flying qualities and flight control details have been advanced to a very high-level state by Mark B. Tischler,[71] a U.S. Army Senior Technologist at the Aeroflightdynamics Directorate at NASA Ames Research Center. Mark led the development of two very successful and widely used software tools (CIFER® and CONDUIT®) that can identify an aircraft's stability and control details. Knowing these details has contributed handsomely to the development of unmanned aircraft and significantly improved the handling qualities of manned aircraft.

[71] Mark's father is equally famous because he invented the pacemaker. Many of us, myself included, are quite happy knowing the high-tech modern version is quietly working away in its pocket just under the skin.

Now that you have the necessary mathematics, let me return to the subject.

Longitudinal stability analyses (and performance analyses, for that matter) start by first finding the aircraft's trim condition in curvilinear flight prior to any disturbance. To do this, you would normally create a side view of the aircraft showing the forces and moments acting on the machine. You see such a drawing for the XV-3 here in Fig. 2-143. I have positioned the aircraft as if it were pulling up to start a loop. This view allows you to establish two force equations and one moment equation using the wind axis (wa) shown on the figure with green vectors as the $X_{wa} - Z_{wa}$ system.

$$F_Z = ma_Z = \left(2T\alpha_{trim} + 2H\right) + L_{BSW} + L_T - W$$

$$F_X = m\,a_Z = \left(2T - 2H\alpha_{trim}\right) - D_{BSW} - W\theta \tag{2.106}$$

$$M_{cg} = I_y\ddot{\theta} = 2M_{hub} + 2Hx_{pr} + M_{BSW} - x_{ac}L_{BSW} - x_t L_T$$

You will immediately notice that I have included the aerodynamic forces plus the aircraft's weight contribution in these equations with a number of assumptions, such as: (a) angles are small so the sine of an angle is the angle and the cosine of an angle is 1.0, and (b) major forces pass through or close to the aircraft's center of gravity (cg), etc. Furthermore, the pitch angle (θ), as I am using it, is measured between the horizon and the wind axis—*not* between the horizon and the fuselage reference line. This is a subtle point of stability analyses not well pointed out in many textbooks. The interpretation is that the aircraft can pitch up and down (±θ) while both the trim airspeed and trim angle of attack remain unchanged. In other words, the angle of attack and the pitch angle are not necessarily equal.

With respect to the inertia forces, a little more care is needed. You see here that by choosing the wind axis system, the accelerations[72] are calculated as

$$a_Z = \frac{d^2Z_{wa}}{dt^2} = V\left[\frac{d\theta}{dt} - \frac{d\alpha}{dt}\right] \quad \text{and} \quad a_X = \frac{d^2X_{wa}}{dt^2} = \frac{dV}{dt} \quad \text{and} \quad \ddot{\theta} = \frac{d^2\theta}{dt^2}. \tag{2.107}$$

Of course today you have digital computers available, and the equations of motion can be written with any degree of complexity you desire and in any axis most convenient. In the era up to the invention of the digital computer, however, we were limited to paper, pencil, and a slide rule, plus the analog computer. Frequently two of us would work together so each calculation was checked. Still, mistakes crept in, and we had to triple check our work to find the error.

Fortunately, enough information from the XV-3 program is available to compute the trim associated with the flight-measured-stability example you have in Fig. 2-141. I have included this necessary data in Appendix E. You also have the calculations for the trim at a calibrated airspeed of 94 knots (true airspeed of 105 knots or 177 feet per second), an altitude of 7,500 feet (density of 0.001889 slugs per cubic foot), a rotor speed of 342 revolutions per

[72] Valuable textbooks about airplane dynamics and aeroelasticity [269-271] and corresponding ones for helicopters [103, 272] go to great lengths to derive inertia terms in each of the several axis systems available. Personally, I favor the wind axis system.

minute (tip speed of 390 feet per second), a gross weight of 4,800 pounds, and the aircraft's flaps deflected 20 degrees trailing edge down.

Solution of the trim equations is, generally, a solution of nonlinear equations, if for no other reason than that the airframe drag contains a parabolic drag term. In the XV-3 and similar proprotor-driven airplanes, the calculation of proprotor forces requires the usual detailed algebra (and some calculus). Appendix E shows you my method for calculating both the proprotor thrust (T), the H-force, and for good measure, the blade motions of longitudinal and lateral flapping and the blade control angles. These control angles first determine the blade motions of longitudinal and lateral flapping. These blade motion angles are very important when you are looking for possible blade-to-airframe clearances. My trim results are shown in Table 2-12.

Table 2-12. The Bell XV-3 Trim Solution at 105 Knots

Fuselage angle of attack (α_{trim})	2.7 degrees (nose up)
Elevator angle (δev)	– 3.53 degrees (tail-end up)
Thrust of one proprotor (T)	287.0 pounds
H-force of one proprotor (H)	approximately 0 pounds
Hub moment of one proprotor (M_{Hub})	0 foot pounds (teetering rotor)
Airframe lift (L)	3,247 pounds
Airframe drag (D)	574 pounds
Airframe moment (M)	0 foot pounds (nose up)
Proprotor blade angles	Appendix E

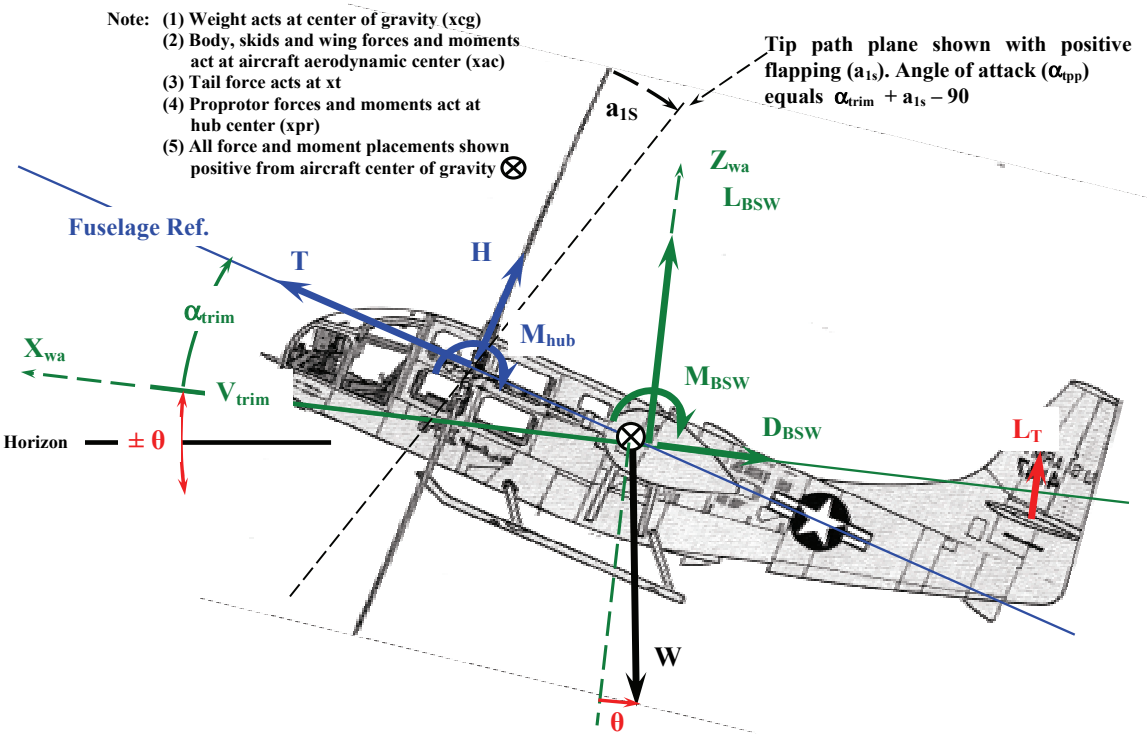

Fig. 2-143. A longitudinal stability analysis in curvilinear flight starts with establishing the aircraft's position in space. The subscript (BSW) indicates the total force due to just body + skids + wing + hubs forces. This baseline, blades-off configuration was tested at full scale and reported in reference [263].

Now, a longitudinal stability analysis at the early design stage only searches for the aircraft's behavior as a small perturbation (i.e., a $\pm\Delta$) away from trim. Decades of experience with satisfactory airplanes have shown that any small disturbance will set the aircraft oscillating about the trim point, but inherent stability will cause (i.e., damp) the oscillation to die out, and the aircraft will return to its original trim condition. But remember, the aircraft will not deviate from trim without an unbalance in forces and/or moments to begin with.[73] You see this occurrence in Fig. 2-141 when the pilot deliberately pulled aft on the longitudinal stick. This action caused the elevator's trailing edge to go up, and this added a downward increment in the stabilizer lift. The result was that the aircraft pitched (θ) nose up, which, incidentally, is taken as the positive direction in flying qualities analyses.

Longitudinal stability analysis has its basis in rather easy to understand concepts. First of all, everything that happens is caused by the forces and moments changing with time. If, for example, there is a change from trim in the vertical force (i.e., a ΔF_Z), then the aircraft will react with a change in vertical acceleration (Δa_Z). This thinking is expressed mathematically as

$$(2.108)\quad F_{Z-trim} + \Delta F_Z = m\,a_{Z-trim} + mV\left[\frac{\Delta\theta}{\Delta t} - \frac{\Delta\alpha}{\Delta t}\right].$$

Of course, because $F_{Z\text{-}trim} = ma_{Z\text{-}trim}$, these terms disappear from the discussion and, therefore, the analysis applies around any selected trim point. Furthermore, all the changes are infinitesimal, so $\Delta\theta/\Delta t \rightarrow d\theta/dt$ as Δ approaches 0 can be used anytime you want to change symbology as you will see in Appendix E. I will not change symbology for this discussion, therefore the ΔF_Z is calculated from

$$(2.109)\quad \Delta F_Z = mV\left[\frac{d\theta}{dt} - \frac{d\alpha}{dt}\right].$$

Following similar logic, you have

$$(2.110)\quad \Delta F_X = m\frac{dV}{dt} \qquad \text{and} \qquad \Delta M = I_Y\frac{d^2\theta}{dt^2}\ .$$

It does, of course, take a considerable effort to include theoretical estimates for how all the forces and moments change with all the variables. You will find my theoretical estimates in Appendix E should you want to pursue the problem in more detail.

Now that you have some flying qualities theory and some details provided by Appendix E, let me discuss some historical and technical details of the XV-3 development.

Wally Deckert and Bob Ferry reported [256, 264] that the XV-3 tiltrotor had quite unsatisfactory longitudinal stability when the aircraft was flown with the pilot's controls held fixed. At this time the XV-3, with two-bladed proprotors, had finished testing at Bell and had been shipped to the Air Force at Edwards. The limited flight test program conducted from

[73] There are many examples where a vibration (which is, after all, what airplane stability is) is virtually self excited. Wing flutter and proprotor whirl flutter are two of concern for all airplanes as you will learn shortly.

May 21 to July 3 of 1959 was immediately followed by a "quick look report" dated July 22, 1959. In this preliminary report [264] by Wally and Bob, they wrote that

> "The high speed regime was incrementally extended from 110 knots TAS [true airspeed] in level flight to 155 knots in a dive using the low rotor rpm gear ratio. The test work terminated at 155 knots because all the available collective pitch was utilized. Faster speeds could only be obtained by over speeding the rpm (or modifying the collective system to increase available pitch).
>
> In the 120 to 140 knot TAS regime the pilot of the chase ship reported that the horizontal stabilizer and elevator were buffeting although the XV 3 pilot could not detect this tail buffet. Accelerometers were installed in the tips of the horizontal tail to define this phenomenon.[74] Results showed that in AH mode [airplane mode with 20-degrees-down flaps and a hover rpm of 525] a 4/rev (34 cps) frequency predominated with some 2/rev (17 cps) evident and in the A mode [flaps up and rotor slowed to 324 rpm] the 2/rev (11 cps) predominated with some 4/rev evident. Double amplitudes were a maximum of about l/2 inch. The mode of the horizontal tail was the asymmetric see-saw type. The amplitudes increased only slightly with airspeed. Because tail flutter was not evident and airspeed not an important factor, the high-speed investigation was continued. The pilot was still unable to detect any tail buffet at the maximum 155 knot TAS dive point.
>
> A stability and controllability investigation was conducted in incremental steps up to and including 150 knots TAS. The stability and controllability characteristics deteriorated in this high-speed region. The dynamic characteristics were excellent at 105 knots. Above 123 knots TAS, a weakly damped pitching oscillation (the short-period mode) begins to appear.
>
> One possible reason for the weakness of the short-period longitudinal dynamic stability is the short distance between the horizontal tail and wing. Another is the destabilizing effect of the relatively large propeller blade area. At the time of this writing [July 22, 1959] insufficient data has been reduced and analyzed to positively define this phenomenon."

What had become immediately apparent (it seems to me) was that the XV-3's tail configuration and short tail moment arm had been sized without adequately considering the impact of a large diameter, slowly turning rotor versus a small diameter, high-tip-speed propeller.[75] (Today you would probably dismiss the problem and tell the pilots and upper management that a larger tail will fix the problem and, don't worry, one is in the works.) But you have to keep in mind that in that era, say 1945 to 1960, only (a) textbooks such as Perkins and Hage [269] were in use; (b) experimental results from propeller-driven aircraft designed many years earlier were widely available; and (c) the aviation industry, after World War II, was done developing the propeller and was concentrating on jet-engine-powered machines.

---

[74] I was taught by Teddy Hoffman during the OH-58D program that "smart" engineers never used the word phenomenon because it means cost overrun and schedule delay to upper management.

[75] Both Jack Vaughen [273] and Ken Wernicke confirmed this situation. Jack worked at Bell for 4 years after graduating from MIT. He was the test engineer for the XV-3 1/4-scale-model test conducted at Wright Field's 20-foot-diameter wind tunnel. He wrote the test report and the accompanying analysis report. Deliveries of the two contractually required documents were up against a delivery date. At Bob Lichten's direction, the analysis report was completed on time but without including proprotor influences. After test pilot criticism, Lichten had Ken, who had recently graduated from the University of Kansas, do a review of the stability analysis report. He found the analysis satisfactory but also noted the lack of proprotor influence. This influence could have been included based on Ken Amer's theory [274]. (Many an aircraft development program has been stymied when engineers assume some parameter is small with no justification other than a time crunch, opinion, or betting on the come.)

In fact my study of the XV-3's longitudinal stick-fixed stability, and both its long-period and short-period modes, suggests that, *with blades off*, the XV-3 was a marginally adequately designed *experimental* airplane using standards of the day. What had not been included during the analysis efforts was the substantial influence of the two proprotors. You can get a sense of the situation simply by dividing the aerodynamic forces and moments into airplane components that do not rotate (i.e., what I will call the airframe) and proprotor components that do. Then you would write

$$\begin{aligned} \Delta F_{Z-\text{proprotor}} + \Delta F_{Z-\text{airframe}} &= mV\left[\frac{d\theta}{dt} - \frac{d\alpha}{dt}\right] \\ \Delta F_{X-\text{proprotor}} + \Delta F_{X-\text{airframe}} &= m\frac{dV}{dt} \\ \Delta M_{\text{proprotor}} + \Delta M_{\text{airframe}} &= I_Y \frac{d^2\theta}{dt^2} \end{aligned} \qquad (2.111)$$

Obviously, if you neglect the proprotor influence—for whatever reason—you will get one solution for these three equations of motion. And just as obviously, inclusion of the proprotor will likely alter your outlook on the stability of the aircraft and cause some redesigning.

The fact that the XV-3 had—by my calculations—adequate stick-fixed longitudinal stability may have been comforting as the aircraft design progressed (when you assume no large effects from either of the two proprotors). After all, the configuration really did not depart far from the vintage 1941 Bell Aircraft P-39 that you see in the exploded view below. This fighter airplane had a takeoff gross weight of about 7,400 pounds, a wingspan of 34 feet, and a propeller diameter of 12 feet. One unique feature of this fighter was that the engine was *behind* the pilot just like the Transcendental Model 1-G. The propeller was driven by a long shaft. Now, in your mind, replace the single propeller with two 23-foot-diameter proprotors. Mount one at each wingtip to give clearance between the blade tips and the fuselage and the wing. Then move the pilot to the nose for better visibility and to make space for the engine gearbox and drivetrain to the two proprotors. Move the wing up to a shoulder position just like the Transcendental machine. Then you submit a proposal, you win a contract, and you proceed with preliminary and detail design. Of course, the conceptual design thinking may not have flowed *quite* like my guess, but if the early pictures such as Fig. 2-114 through Fig. 2-124 are any indication, Bob Lichten and Larry Bell were, I venture to say, satisfied with the 3-view drawings of the Bell Aircraft Model 200, which became the Bell Helicopter XV-3.

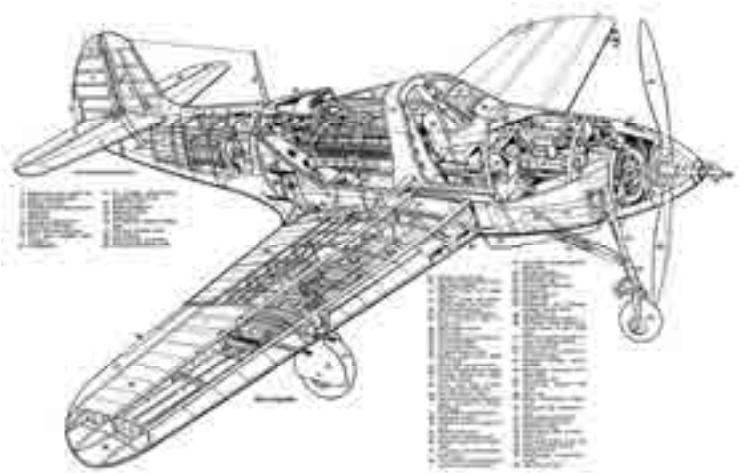

In following the story of the XV-3, a nagging thought grew in my mind as I reread Wally Deckert and Bob Ferry's statement that "One possible reason for the *weakness* of the short-period longitudinal dynamic stability is the short distance between the horizontal tail and wing. Another is the destabilizing effect of the relatively *large propeller blade area*."

The speculation at the time was that the proprotors' H-forces (Eq. 2.106) and, to a lesser extent, their thrusts (2T) were a much larger destabilizing force than had been thought. The opinion appears to have been that the total change in either (or both) of the forces could be the source of the "weakness" in the short-period mode. The fact that there might be a hub moment involved could be discounted because both the three-bladed and two-bladed proprotor configurations could not introduce a significant hub moment. After all, the XV-3's original three-bladed design had nearly zero flapping hinge offset, and changing to the two-bladed teetering rotor hub virtually removed hub moment as a player.

You can begin to appreciate the influence of the large diameter proprotors by expanding the proprotors' forces and moments contribution to Eq. (2.111). Concentrating on just the H-force, you have

$$\Delta F_{Z-\text{proprotor H}} = \Delta H = \frac{\Delta H}{\Delta V}\Delta V + \frac{\Delta H}{\Delta \alpha}\Delta \alpha + \frac{\Delta H}{\Delta \theta}\Delta \theta + \frac{\Delta H}{\Delta (d\theta/dt)}\Delta (d\theta/dt) + \frac{\Delta H}{\Delta (d\alpha/dt)}\Delta (d\alpha/dt) \quad (2.112)$$

$$\Delta M_{\text{proprotor H}} = \Delta H (\text{distance hub in front of center of gravity})$$

Here, I have introduced what flying quality engineers call a stability derivative or, in their shorthand notation, the terms $\Delta H/\Delta V$, $\Delta H/\Delta \alpha$, $\Delta H/\Delta \theta$, etc. You are quite likely to see these derivatives written as dH/dV, $dH/d\alpha$, $dH/d\theta$, or $\partial H/\partial V$, $\partial H/\partial \alpha$, $\partial H/\partial \theta$, etc. in textbooks, reports, and papers. But notation preciseness is of little concern for this discussion. Because the contribution of H-force to drag along the wind axis is known (today) to be small, I have dropped discussion of this contribution to the longitudinal stability to keep things simple. Furthermore, in a more detailed analysis suited to a computer, there can be many more independent variables than just V, α, θ, etc., but the question remains as to which of these stability derivatives lies at the heart of the XV-3's "*weakness*." And then, how do you fix it? One thing is clear, Bell engineers and other tiltrotor advocates mounted major test and theory efforts to find the culprits and implement more than a few fixes [37, 275]. Troy Gaffey, Jing Yen, and Ray Kvaternik provided a particularly good overview in a paper they presented in September of 1969 [276]. This paper is well worth your reading time.

Just for the fun of it, I decided to put myself back in time and imagine some quantitative data that could shed light on the shortfall in the XV-3's longitudinal stability.

Given that the best bet was that $\Delta H/\Delta \alpha$ and $\Delta H/\Delta (d\theta/dt)$ were the real culprits, I used a longitudinal stability analysis to determine the influence of *just* these two stability derivatives. In essence, I wanted to see pitch rate ($d\theta/dt$) waveforms with proprotors on and with proprotors off. My results, shown in Fig. 2-144, were quite interesting, because I found that the damping was dictated primarily by $\Delta H/\Delta (d\theta/dt)$ and the oscillating frequency was controlled by $\Delta H/\Delta \alpha$. This, in itself, makes sense because any derivative associated with a

rate of change with respect to time acts like a damper—if it has a negative value. But, in the case of the XV-3, the proprotor contribution has a positive sign. That is, if the aircraft is in trim with some H-force and the aircraft begins to pitch nose-up at some rate, say +0.1 radian (about 5.7 degrees) in 1 second, the H-force will change from the trim H-force by an additional ΔH of about 250 pounds (i.e., 2,550 × 0.1).

This is not all of the XV-3's proprotor contribution. My calculations show that the proprotors acted like a negative spring because $\Delta H/\Delta\alpha$ appears to be on the order of +490 pounds per radian. Therefore a change of +0.1 radian will add an additional 49 pounds for a potential total of, say, 300 pounds, should the angle of attack and pitch rate motions coalesce at a particular time in the oscillation.

In July of 1959, Wally Deckert and Bob Ferry [264] stated that

> "One possible reason for the weakness of the short-period longitudinal dynamic stability is the short distance between the horizontal tail and wing. Another is the destabilizing effect of the relatively large propeller blade area. At the time of this writing [July 22, 1959] insufficient data has been reduced and analyzed to positively define this phenomenon."

As it turned out, that was really just one-third of the aircraft's problem. In late March of 2014, I had several lengthy conversations with Troy Gaffey[76] and Ken Wernicke.[77] Both of these engineers were quite involved in learning from the XV-3 program and were determined not to repeat the experience with the XV-15 and MV-22 designs. Their view, as Troy explained it, was that the cause of the pilot's complaints about the XV-3 *was not* the inherent aircraft stability—even including proprotor classical aerodynamic influences and the tail design. The problem was, in fact, three-fold because

(1) the proprotor mountings to each wingtip were not even close to rigid mountings,

(2) the wing's torsional stiffness was compromised because the wing's major spar, thought to be a closed-wall box section, was in fact more like a C-section in structural stiffness, and

(3) the teetering rotor had pitch-flap coupling (i.e., delta-3 of – 20 degrees) that caused coupling with blade inplane bending at a coupled frequency above once per revolution.

The combined aeroelastic properties of these three design variables led to low-frequency aircraft oscillation. Troy made the specific point that when the XV-3 was hard-mounted in the NASA Ames large-scale wind tunnel, Bill Quinlan (who was in the cockpit and "flying" the aircraft during the 1962 test) clearly experienced proprotor hub and wing torsion deflections at low frequency on the order of 0.2 per rev (about 1 to 2 cycles per second). Troy's view was that the XV-3 was lucky to be underpowered because at speeds much beyond 130 knots it would have encountered whirl flutter and, I would add, might well have been destroyed in flight.

---

[76] Troy became Bell's Vice President of Engineering when Bob Lynn retired. He befriended me when I went to Bell, and I quickly learned that he was a giant in the field of aeromechanics. He remains today a close friend and has provide you many, many thoughts in this three-volume book.

[77] Ken was the chief of the XV-15 program and Bell, the rotorcraft industry, and you and I owe him a world of thanks. Read his thoughts about the XV-3 in Appendix F.

Now let me close this discussion about longitudinal stability by adding a waveform that meets the then-current military minimum specification of a critical damping ratio of 0.34. You see this result as the green line on Fig. 2-144. My general impression is that a lot more than a simple "quick and dirty" change to the XV-3's airframe was needed. And this meant considerably more engineering homework was needed before another step could be taken along the path to the Marine's MV-22B. The homework took about 5 years of jam-packed efforts, which included:

a. analyses,
b. science experiments,
c. model tests,
d. full-scale component testing,
e. an intermediate preliminary design competition, and
f. a competition for a new experimental tiltrotor

before the combined talents of Bell, NASA, and the U.S. Army could proudly point to the XV-15 tiltrotor. During this 5-year period, the team encountered a show-stopping aeroelastic instability that became known as proprotor whirl flutter *after* it was fully understood. And then Bell engineers had enough confidence to begin detailed design.

Aircraft trim, longitudinal stability, and whirl flutter subjects all require a better understanding of proprotor forces, particularly when the shaft has some motion. This is the next subject to be discussed.

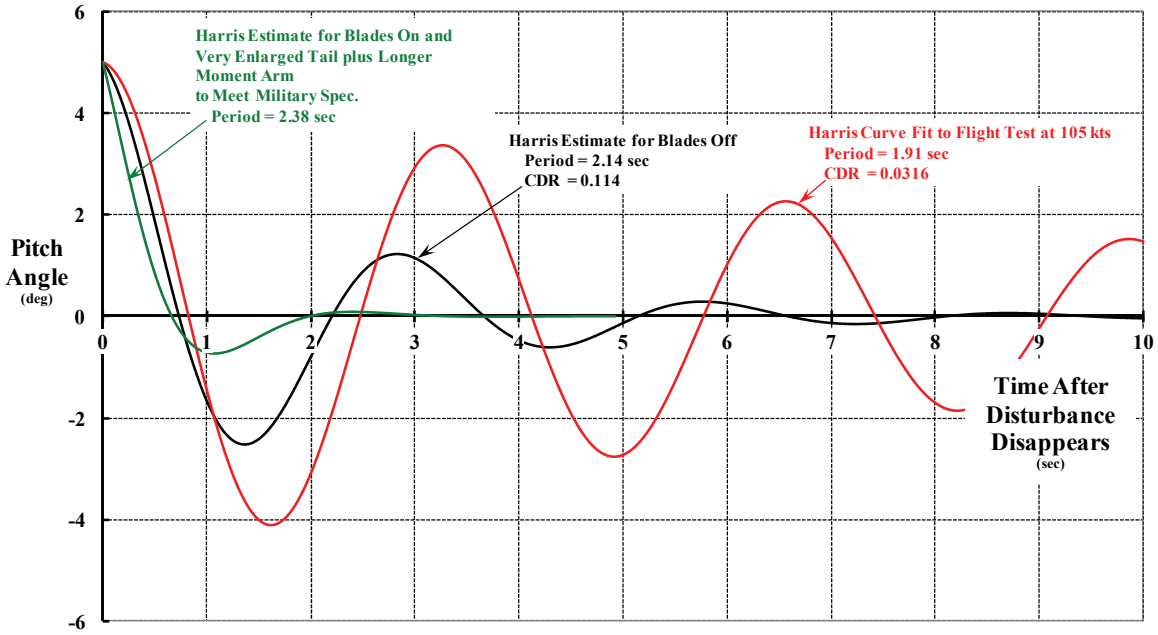

Fig. 2-144. The XV-3 appears to have been a marginally well designed experimental airplane for that era—*if you do not include the contribution of the two proprotors*. The XV-3's short-period stability was very, very dependent on the values of the proprotor stability derivatives $\partial H/\partial \alpha$ and $\partial H/\partial \dot{\theta}$. The $\partial H/\partial \alpha$ acts like a negative spring and the $\partial H/\partial \dot{\theta}$ decreases the aircraft's overall pitch damping.

2.13.2.3 Proprotor Thrust and H-Force, Including Shaft Motion

As test data from the XV-3 was acquired, it became clearer to the researchers that proprotors acting as propellers were a quite different problem than rotors acting as a helicopter's lifting and propulsive system. The full-scale wind tunnel testing conducted in 1959 [263], and then the flight test data available by mid-1961 [256, 268], all pointed to marginal longitudinal stability in the short-period mode as you have just read.

The importance of shaft motion first became clear in relation to the XV-3's longitudinal stability. In this case, the shaft motion is created by aircraft motion, and the aircraft motion goes on at quite low frequencies compared to the proprotor's rotational speed. A ratio of the two frequencies of less than 0.1 would be representative. But then, more data analysis questions begin to be asked about shaft motion created by wing structural dynamics, even when the aircraft is flying in straight and level flight. In this second case, the frequency of the shaft motion increased considerably, to the point where coupled bending and torsion of the wing could couple with blade motion and cause whirl flutter.

I found Hervey Quigley and Dave Koenig's April 1961 discussion [268] of the shaft motion and associated rotor forces especially interesting. They wrote, in discussing Fig. 2-145, that

> "It was predicted in reference 3 [Ken Amer's NACA TN 2136 dated October 1950] that convertiplanes which use flapping prop-rotors would have this problem [i.e., proprotors may contribute negative damping to aircraft stability]. Being consistent with helicopter theory, a flapping rotor is essentially a gyroscope and requires a couple across the rotor disk 90 degrees out of phase with the angular motion of the airplane to make it precess and follow its shaft. (See ref. 3.) When airplane pitching motion is introduced, the prop-rotor disk lags the airplane angular motion until sufficient flapping is present to produce the necessary couple aerodynamically by increasing lift on one side of the disk and decreasing lift on the opposite side; thus, the increase in flapping due to airplane angular velocity. The change in aerodynamic force on a blade due to flapping can be resolved into two forces, one perpendicular and one parallel to the prop-rotor disk. These forces are shown schematically in figure 7 [see Fig. 2-145]. This sketch indicates that when the airplane is pitching down the components of the forces due to flapping are forward and down on the inboard side, and rearward and down on the outboard side of the prop-rotor disk. For a constant prop-rotor rotational speed, Ω, the magnitude of the precessing force changes little with airplane flight conditions, but the in-plane force depends on blade angle. It can be seen in figure 7 that the in-plane force is in the direction of the angular motion of the airplane and tends to produce a negative damping moment about the airplane's center of gravity. Also, because of the flapping, the tip path plane and, therefore, the thrust vector is tilted and an additional force is produced on the prop rotor hub which is proportional to the prop-rotor thrust and in a direction to give a positive damping moment. At low advance ratios, such as in helicopter mode at low speed, the in-plane force due to blade flapping is small, and the prop-rotor contributes positive damping. However, at high advance ratios, when the blade angles are large, the in-plane forces due to flapping become sufficiently large to offset the force produced by the tilt of the thrust vector and the resultant force is in a direction to give a negative damping moment. *The method in reference 3 of calculating these forces and moments was developed for helicopters in hover and low-speed flight and will require expansion to analyze damping moments due to flapping prop-rotors at high advance ratios [in axial flight].*"

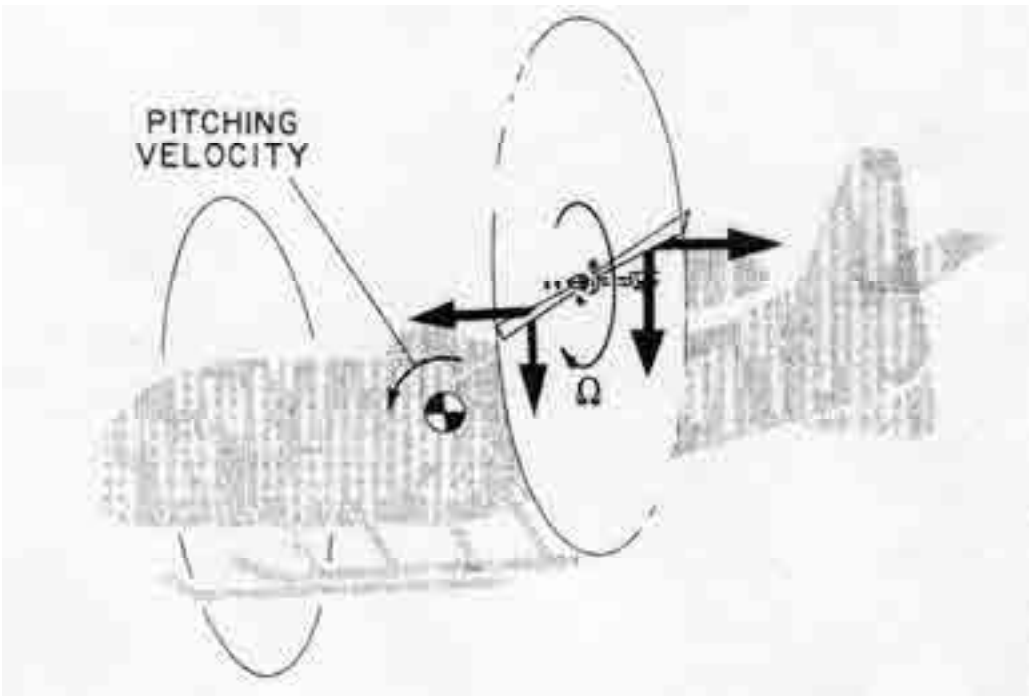

Fig. 2-145. Proprotor vertical forces can be very large.

You may be rather surprised to know that by the end of 1952 (a decade earlier than Hervey and Dave's closing words), helicopter engineers had all the analytical tools needed to calculate proprotor thrust and the aerodynamic component of H-force[78] in considerable detail—including the situation where there was shaft motion. However, the technology was not very well known and only a very, very few even bothered with it because helicopter development was the driving interest. The technology, while not assembled into the comprehensive analyses that we have today, was available in six technical reports. Historically, I would point to:

a. Zbrozek's study of the oscillating shaft problem reported in April 1949 [277],

b. Britland and Fail's experiments in Britain in May 1950 [278],

c. Ken Amer's well referenced paper published as NACA TN 2136 in October 1950,

d. Sissingh's two reports analyzing the British 1950 experimental data, which became available in August 1951 [279] and November 1951 [280],

e. And my hands-down favorite, Walter Castles and Noah New's jewel published as NACA TN 2656 that came out in July of 1952 [281].

From just these few reports, you can make a very reasonable estimate of the XV-3's proprotor force and moment characteristics, and the stability derivatives required by Eq. (2.112). The key methodology lies within Castle and New's report [281], *A Blade-Element Analysis for Lifting Rotors That is Applicable for Large Inflow and Blade Angles and Any Reasonable Blade Geometry.*

[78] In all of my discussions of H-force, I have ignored the inertia component. See Appendix E.

2.13.2.3.1 Problem Formulation

Castle and New's words about the reason for their work make for fascinating reading. For example, in the first paragraph of their introduction they wrote:

> "This project, which was conducted at the Georgia Institute of Technology Engineering Experiment Station under the sponsorship and with the financial assistance of the National Advisory Committee for Aeronautics, was undertaken in order to develop a blade-element analysis for lifting rotors that would be *useful for convertiplane calculation*s [my italics]. This necessitated the elimination of the usual approximations that the blade-element inflow angle φ and the blade angle θ are small angles and required a reasonably exact treatment of the blade geometry."

They offered (in my opinion) a neat way around the then-current helicopter starting point, which was that blade element lift would be calculated based on the assumption that any airfoil along a proprotor blade span would produce lift following classical aerodynamic behavior. This fundamental was that $C_\ell = a\alpha$, and many small angle assumptions were made to develop a rotor aerodynamic analysis. This is where John Wheatley began with his famous study of autogyro rotor aerodynamic forces and moment theory [282] that you read about in Volume I. (You might recall that Appendix E of Volume I also has all the equations you need to make excruciatingly detailed calculations of helicopter rotor forces and moments.)

In contrast, Castle and New stated that

> "Two-dimensional thin-airfoil theory demonstrates that
>
> $$C_\ell = a \sin\alpha \tag{33}$$
>
> For two-dimensional airfoils, equation (33) is modified by a multiplying function of the solidity, chord spacing, and blade angles that is very nearly unity for average lifting-rotor configurations as shown in reference 4. Thus, within the approximation that the radial components of flow may be neglected, equation (33) should be applicable for blade-element rotor theory over the unstalled range of blade-element angles of attack. Beyond the stall, equation (33) is somewhat less in error than the usual relation $C_\ell = a\alpha$ as can be seen from figure 3, which is a plot of the above expressions and the experimental values of C_ℓ against α for an NACA 0015 airfoil. The use of equation (33), rather than the usual approximation that $C_\ell = a\alpha$, allows the thrust and tangential components of lift on a blade element to be exactly expressed, within the approximations involved in neglecting radial components of the flow, in terms of the easily integrated in-plane and normal components of the velocity at the blade element U cos φ and U sin φ. Thus the usual approximation that the inflow angle φ is a small angle may be eliminated. This may be demonstrated as follows:"

I based my analysis of proprotor behavior in axial flight on Castle and New's suggestions. The details are shown in Appendix E.

Now let me turn to what I believe is the heart of the shaft motion problem. As I see it, the discussion centers around the classical rotorcraft differential equation, which, when solved, determines a blade's flapping motion (β). The subsequent calculation for forces and moments is rather straightforward. To review then, Cierva [283, 284] began with the now familiar differential equation from which *rigid blade* flapping is found by solving

$$\frac{d^2\beta}{d\psi^2} + \varpi^2\beta = \frac{1}{I_{flap}\Omega^2}\left(M_{aero}\right)_\psi + \frac{1}{I_{flap}\Omega^2}\left(M_{gyro}\right)_\psi \tag{2.113}$$

where the system's natural frequency (ω), when divided by rotor speed (Ω), is denoted by (ϖ). The aerodynamic moment about a flapping hinge is found, in the very simplest of cases as discussed in both Volume I and Volume II, from

$$(2.114) \quad \left(M_{aero}\right)_{\psi} = \int_0^R r\, dT_{r,\psi} \ .$$

Shaft motion adds a gyroscopic moment about the flapping hinge in the amount of

$$(2.115) \quad \left(M_{gyro}\right)_{\psi} = \left(-2I_{flap}\Omega \frac{d\theta_{shaft}}{dt}\sin\psi + I_{flap}\frac{d^2\theta_{shaft}}{dt^2}\cos\psi \right) .$$

Of course, answers to even simple questions are hidden when the problem is stated at such a summary level as I have with Eqs. (2.113), (2.114), and (2.115). For example, if the pilot moves the stick, how does the rotor respond? Or, when shaft motion is caused by aircraft pitching rate ($d\theta_{shaft}/dt$) as Fig. 2-145 illustrates, how does a blade's flapping motion respond?

The answer to these and many other questions falls rather naturally into three basic rotorcraft technologies. I think of the three technologies as follows:

1. Aerodynamic trim calculations where little concern for aircraft motion is required. The direct application for this group is the follow-on estimates of aircraft performance. To rotorcraft engineers making these trim calculations on an everyday basis, the differential equation is reduced to

$$(2.116) \quad \frac{d^2\beta}{d\psi^2} + \varpi^2\beta = \frac{1}{I_{flap}\Omega^2}\left(M_{aero}\right)_{\psi} ,$$

and there is little need to include the gyroscopic moments.

2. Flying quality calculations are frequently made knowing that aircraft motion (and thus the shaft motion if the aircraft is structurally rigid) is quite slow relative to rotor rotational speed (Ω). These rotorcraft engineers generally accept a small error by setting shaft acceleration ($d^2\theta_{shaft}/dt^2$) to zero and letting ($d\theta_{shaft}/dt$) equal a constant, say $\dot{\theta}_{shaft}$. This lets them deal with a differential equation in the form

$$(2.117) \quad \begin{aligned} \frac{d^2\beta}{d\psi^2} + \varpi^2\beta &= \frac{1}{I_{flap}\Omega^2}\left(M_{aero}\right)_{\psi} - \frac{1}{I_{flap}\Omega^2}\left[2I_{flap}\Omega\left(\frac{d\theta_{shaft}}{dt} = \text{constant} \right)\sin\psi \right] . \\ &= \frac{1}{I_{flap}\Omega^2}\left(M_{aero}\right)_{\psi} - 2\left(\frac{\dot{\theta}_{shaft}}{\Omega} \right)\sin\psi \end{aligned}$$

Because the pitch rate $d\theta_{shaft}/dt$ in radians per second is assumed constant, and given that the rotor speed (Ω in radians per second) is also assumed constant, it follows that the gyroscopic moment in this flying qualities calculation is simply

$$(2.118) \quad \text{Flying Qualities } \left(M_{gyro}\right)_{\psi} = -2\left(\frac{\dot{\theta}_{shaft}}{\Omega} \right)\sin\psi = -2\left(\nu_{FQ}\right)\sin\psi \ .$$

This puts all of the flying quality differential equation in terms of blade azimuth. The presumption here is that dynamic motion can be analyzed as a "quasi-steady" motion. The result of this approach is that a steady shaft-pitch-rate ratio (ν_{FQ}) is nothing more than a form of cyclic pitch that a pilot might reproduce with a longitudinal cyclic movement. Said another way, a pilot's fore and aft stick input produces a ($B_{1C}\sin\psi$) term to blade feathering, which is known to produce longitudinal flapping. A steady pitch rate produces a [(ν_{FQ}) $\sin\psi$] term, which, therefore, also produces longitudinal flapping. Thinking about shaft motion this way means that decades of autogyro and helicopter knowledge and experience is immediately applicable.

3. Aeromechanic (or dynamic or aeroelastic or structural dynamic, if you prefer) calculations require the inclusion of both the pitching rate and acceleration terms, resulting in the complete differential equation in the expanded form of

$$\frac{d^2\beta}{d\psi^2}+\varpi^2\beta=\frac{1}{I_{flap}\Omega^2}\left(M_{aero}\right)_\psi-\frac{2}{\Omega}\frac{d\theta_{shaft}}{dt}\sin\psi+\frac{1}{\Omega^2}\frac{d^2\theta_{shaft}}{dt^2}\cos\psi\,. \tag{2.119}$$

Here the assumption has generally been made that the shaft motion may depend more on the structural dynamics of the aircraft wing than on the aircraft motion. In this case, the shaft motion may well be at an oscillating frequency (ω_{shaft} in radians per second) much closer to the proprotor rotational speed (Ω). Therefore, a more general assumption is frequently made, which is that the shaft motion is an oscillation described as

$$\theta_{shaft}=A\sin\left(\omega_{shaft}t\right), \tag{2.120}$$

where the coefficient (A) is an amplitude in radians. On this basis, the derivatives for shaft pitch rate and pitch acceleration become

$$\frac{d\theta_{shaft}}{dt}=A\left(\omega_{shaft}\right)\cos\left(\omega_{shaft}t\right)\quad\text{and}\quad\frac{d^2\theta_{shaft}}{dt^2}=-A\left(\omega_{shaft}^2\right)\sin\left(\omega_{shaft}t\right). \tag{2.121}$$

These derivatives can be substituted into Eq. (2.119) so that the differential equation becomes

$$\begin{aligned}\frac{d^2\beta}{d\psi^2}+\varpi^2\beta=\frac{1}{I_{flap}\Omega^2}\left(M_{aero}\right)_\psi&-\frac{2}{\Omega}\left[A\left(\omega_{shaft}\right)\cos\left(\omega_{shaft}t\right)\right]\sin\psi\\&-\frac{1}{\Omega^2}\left[A\left(\omega_{shaft}^2\right)\sin\left(\omega_{shaft}t\right)\right]\cos\psi\end{aligned}\,. \tag{2.122}$$

You will immediately note that the gyroscopic terms are a mix of time (t) and blade azimuth (ψ). Many researchers prefer to introduce the ratio (ν) of shaft oscillation frequency to proprotor speed, which puts everything in the blade azimuth world. That is, they state

$$\nu=\frac{\omega_{shaft}}{\Omega},$$

and this shorthand contracts the differential equation to

$$\frac{d^2\beta}{d\psi^2}+\varpi^2\beta=\frac{1}{I_{flap}\Omega^2}\left(M_{aero}\right)_\psi-2\left[A\left(\nu\right)\cos\left(\nu\psi\right)\right]\sin\psi-\left[A\left(\nu^2\right)\sin\left(\nu\psi\right)\right]\cos\psi\,. \tag{2.123}$$

A most interesting additional step is to use trigonometry to expand the products of [cos(νψ)sinψ] and [sin(νψ)cosψ] so the differential equation to be solved in the aeromechanics world appears, after some simplification, as

$$\frac{d^2\beta}{d\psi^2}+\varpi^2\beta=\frac{1}{I_{flap}\Omega^2}\left(M_{aero}\right)_\psi-\frac{1}{2}A(\nu)\left\{(2-\nu)\sin\left[(1-\nu)\psi\right]+(2+\nu)\sin\left[(1+\nu)\psi\right]\right\}. \tag{2.124}$$

Aeromechanics researchers in the later portion of the XV-3's development became increasingly worried that the aircraft had some form of aeroelastic instability lurking in it. As they dug deeper, they began to see a possibility of a rotor-pylon-wing coupling that might cause a severe vibration—a vibration so severe that the rotor assembly might be torn from the wingtip. This possibility was confirmed by Earl Hall [285] when he presented his landmark paper in April of 1966.

With the preceding introductory background in hand, let me discuss thrust and the aerodynamic component of H-force for each of the three technology groups I have outlined. You will find, I hope, that Appendix E provides adequate details[79] as to how I arrived at the results that follow. In the following discussion you will see numerical examples for the XV-3. The calculations have been made assuming the XV-3 properties listed in Table 2-13. *Additionally, all of my calculations have been made assuming the induced velocity at a blade element is zero.*

Finally, remember that this discussion is cast as if we were back in the 1950s and 1960s—well before the full breadth of proprotor aeromechanics requirements had been realized. And well before the full needs of proprotor technology had been stated, which was not completed until Wayne Johnson at NASA Ames published reference [286] in July of 1975.

Now let me begin with the subject of proprotor thrust and H-force required by aerodynamic trim calculations.

Table 2-13. Bell XV-3 Teetering Rotor Properties Used for Shaft Motion Calculations

Item	Symbol	Units	Values	Notes
Diameter	D	ft	23	
Chord	c	ft	0.9167	11/12
Blade twist	θ_t	deg	– 40	washout
Tip speed	V_t	ft/sec	390	RPM = 324, Ω = 33.9292 rad/sec
Airfoil lift curve slope	a	per radian	5.73	
Delta-3	δ_3	deg	– 20	$\Delta\theta/\Delta\beta$ = – 0.36397
Density altitude	h_D	ft	7,500	ρ = 0.001898 slug/ft^3
Flap inertia	I_F	slug-ft^2	82.7	per blade
Lock number	γ	nd	2.1084	$\gamma = \rho acR^4/I_F$
Hub-to-tilt-axis distance	Xpr	ft	3.76	

[79] To me, solving the flap motion differential equation at any of the three levels categorized just gets you the blade motion. This is, of course, a necessary step in calculating proprotor forces, which are of primary interest. For the sake of completeness, Appendix E does include my approach to solving the differential equation, but the objective is to calculate thrust, H-force, and Y-force after finding solutions for the blade flapping motion. Keep in mind that I have used a rigid blade to outline the details, and remember that the complete aeromechanics solution is a subject for experts having a combination of aeroelasticity, structural dynamics, and aerodynamics skills, and, I might add, a strong foundation in applied mathematics.

2.13.2.3.2 Aerodynamic Trim Results

Consider first the fact that the thrust and H-force of *just one XV-3 blade* creates hub forces that vary as a blade goes around (i.e., completes a revolution of 360 degrees in azimuth angle, ψ). Suppose, for example, the aircraft is flying in trim at 105 knots according to my calculation for the XV-3 in Table 2-12. Following the analysis presented in Appendix E, the thrust and H-force of one blade will vary with blade azimuth as you see in Fig. 2-146. This is the type of waveform you would get from an oscillograph much as you saw earlier in Fig. 2-141. Here I have shown the repetitive nature of the thrust and H-force waveforms with just two revolutions of blade azimuth travel.

Rotorcraft engineers have found that much of their analyses and experimental data result in waveforms that behave as a Fourier series. This is the case presented in Fig. 2-146, and I have included the Fourier series for both thrust and H-force for one blade as you can see.

It is only the steady forces or zero harmonic (i.e., $T_0 = 143.2$ and $H_0 = 12.53$) that are important to calculating the trim of the aircraft. Everything else is a vibration and/or structural load (to be studied by other rotorcraft researchers). The question you might now ask is, given that the waveforms shown in Fig. 2-146 are for one blade in the XV-3's two-bladed proprotor, what do the waveforms look like for the pair of blades arranged as one teetering proprotor in near axial flight? The answer is provided in Fig. 2-147 where you can see that the H-force for two blades has become dominated by a two-per-rev harmonic. It is here that Fourier series and some knowledge of trigonometry have great value. Let me stop for a moment and elaborate.

A Fourier series—say, for example, the H-force provided in Fig. 2-146—is written mathematically in shorthand as

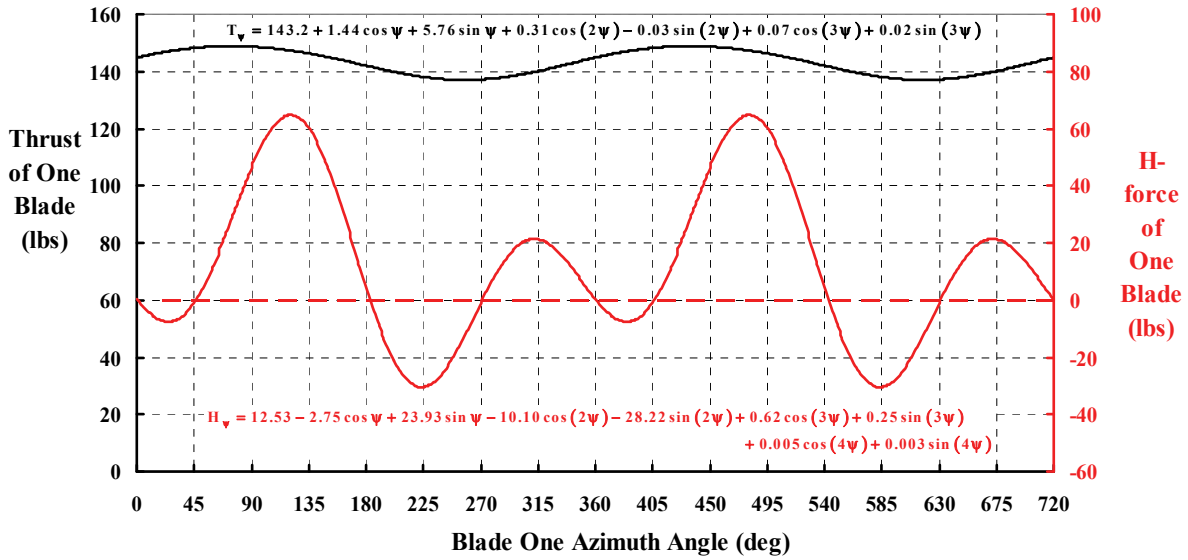

Fig. 2-146. A single, rigid flapping blade creates vibratory hub loads. However, only the steady (i.e., zero harmonic) load is required for trim calculations.

$$H_\psi = H_0 + \sum_{n=1}^{\infty} H_{nc}\cos(n\psi) + \sum_{n=1}^{\infty} H_{ns}\sin(n\psi). \tag{2.125}$$

Fourier series express summation with the Greek letter (Σ). The harmonic coefficients are identified by (H_{nc} and H_{ns}). Then the sum is obtained from the first term (n = 1) up to (n = ∞). For a single blade, the series converges rather quickly. That is to say, you need not have the sum of an infinite number of terms (i.e., n = ∞) to have very useful results.

Fourier series come in very handy when you want to add a waveform from a second flapping blade to the results for one flapping blade to obtain the H-force of a two-bladed rotor. The process is to define a master blade and call it blade 1, and denote its azimuth angle by (ψ_1). Then blade 2 is positioned as trailing blade 1 by 180 degrees. Thus, $\psi_2 = \psi_1 - \pi$ with all angles in radians. You then add the Fourier series for each blade as follows

$$\begin{aligned}\text{Two bladed rotor } H_\psi = &\left\{H_0 + \sum_{n=1}^{\infty} H_{nc}\cos(n\psi_1) + \sum_{n=1}^{\infty} H_{ns}\sin(n\psi_1)\right\} \\ &+\left\{H_0 + \sum_{n=1}^{\infty} H_{nc}\cos(n(\psi_1-\pi)) + \sum_{n=1}^{\infty} H_{ns}\sin(n(\psi_1-\pi))\right\}\end{aligned} \tag{2.126}$$

where the harmonic coefficients are always for blade 1 *assuming the two blades are absolutely identical*. I might note in passing that the situation of having two identical blades on one rotorcraft has never happened in the history of the industry. An expansion of Eq. (2.126) using trigonometry leads immediately to

$$\begin{aligned}\text{Two bladed rotor } H_\psi = &\,2H_0 + 2H_{2c}\cos(2\psi_1) + 2H_{2s}\sin(2\psi_1) \\ &+2H_{4c}\cos(4\psi_1) + 2H_{4s}\sin(4\psi_1)\end{aligned}. \tag{2.127}$$

A comparison of the H-force for both one- and two-blade rotors is shown in Fig. 2-147.

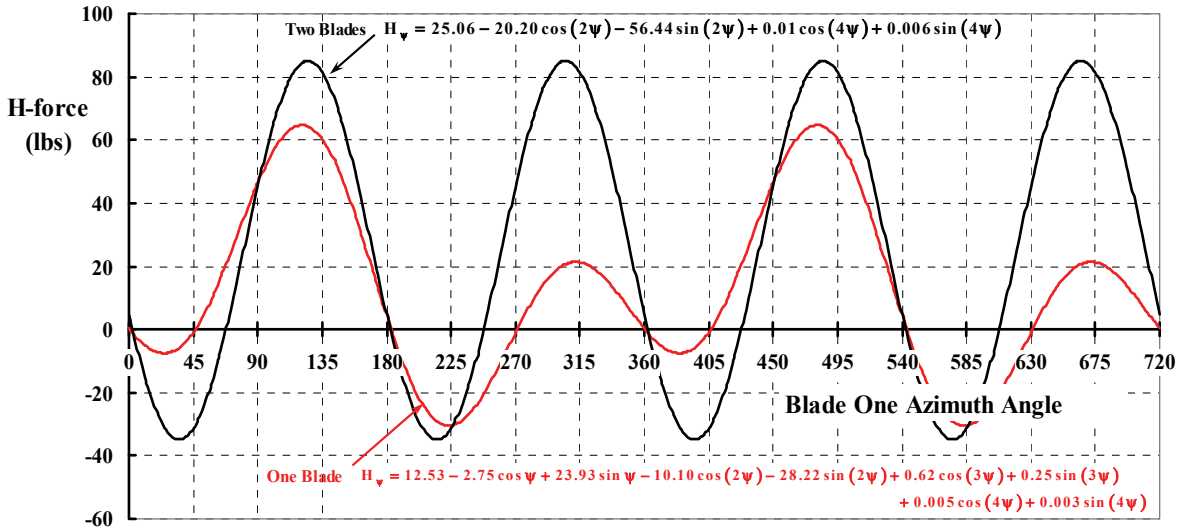

Fig. 2-147. The teetering rotor with rigid blades creates a steady load and vibratory hub loads only at two, four, etc. per revolution. Harmonics above two per rev are quite small for proprotors in axial flight with longitudinal and lateral cyclic set at zero.

I have taken a liberty in the preceding example of trim forces by saying that a two-blade teetering rotor system can be approximated as two blades, each having its own flapping hinge. In fact, with the teetering two-bladed rotor system, each blade produces a moment at the teetering hinge, and it is the difference of the two moments that creates teetering motion. The resultant "flapping" angle really should be called the teetering angle, but you will rarely hear it called that. This is a quite accurate liberty particularly with a proprotor in near axial flight and when the waveforms can be described by a simple Fourier series having integer harmonics (i.e., 1ψ, 2ψ, 3ψ, etc.). However, the two-bladed teetering rotor must be treated more carefully when nonharmonic motion is a factor.

Appendix E shows that the algebra is rather complex before you arrive at simple expressions for thrust and H-force well suited to calculating aerodynamic trim, but the results are very simple for the proprotor in nearly axial flight and with zero cyclic. For the XV-3, I found that the forces for *one proprotor* can be calculated from

$$\text{(2.128)}\qquad \begin{aligned} T &= T_0 + T_1\theta_0 + T_2\alpha_f^2 \qquad \text{so } \theta_0 = \frac{T - T_0 - T_2\alpha_f^2}{T_1} \qquad \text{Note: All angles in radians} \\ H &= \left(H_0 + H_1\theta_0 + H_2\theta_0^2\right)\alpha_f \end{aligned}$$

where all angles are in radians and the forces are in units of pounds. The coefficients (i.e., T_0 through H_2) have the units of pounds and vary with the trim speed (V_{FP}). Values for the XV-3 are given in Table 2-14. This handy result is directly applicable to the trim discussion that you read in section 2.13.2.2 starting on page 222. You will recall from Table 2-12 on page 229 that at 105 knots and an altitude of 7,500 feet, the aircraft was estimated to trim with the fuselage angle of attack (α_f) 2.7 degrees nose-up. Just the thrust of *one* proprotor amounted to 287 pounds.

The first step in using Eq. (2.128) is to find the collective pitch that produces a thrust of 287 pounds. Using Eq. (2.128) and values of the coefficients from Table 2-14 you find that

$$\text{(2.129)}\qquad \theta_0 = \frac{T_{trim} - T_0 - T_2\alpha_f^2}{T_1} = \frac{287 - (-7,061) - (2,321)(2.7/57.3)^2}{6,404} = 1.14756 \text{ rad.} = 65.75 \text{ deg.}$$

Then the H-force is calculated as

$$\text{(2.130)}\qquad \begin{aligned} H &= \left(H_0 + H_1\theta_0 + H_2\theta_0^2\right)\alpha_f \\ &= \left[9,327 + (-16,895)\theta_0 + 8,037\theta_0^2\right]\frac{2.7}{57.3} = 24.7 \text{ pounds.} \end{aligned}$$

2.13.2.3.3 Flying Quality Results

The flying quality calculations, when a quasi-steady motion assumption is made, simply add a steady pitch rate term to the trim solution given with Eq. (2.128). Following Appendix E, you have the quite useful result that

$$T = T_0 + T_1\theta_0 + T_2\alpha_f^2 \quad \text{so} \quad \theta_0 = \frac{T - T_0 - T_2\alpha_f^2}{T_1} \qquad \text{Note: All angles in radians.}$$

$$H = \left(H_0 + H_1\theta_0 + H_2\theta_0^2\right)\alpha_f + \left(H_3 + H_4\theta_0\right)\frac{d\theta_{shaft}}{dt} \tag{2.131}$$

The question uppermost in my mind was how the XV-3's proprotor thrust derivatives and, in particular, the H-force derivatives, vary with speed. As you can see from Eq. (2.131), these derivatives are quite dependent on the trim at each speed under study because thrust changes with speed to ensure trim. And if trim thrust changes, so does the collective pitch to produce that trim thrust. Then the H-force, being dependent on trim collective pitch, is immediately affected. The coefficients (i.e., T_0 through H_4) are listed on Table 2-14. Given the trim point and Eq. (2.131), the stability derivatives become:

$$\frac{\Delta T}{\Delta\alpha_f} = 2T_2\left(\alpha_f\right)_{trim} \quad \text{and} \quad \frac{\Delta T}{\Delta\left(d\theta_{shaft}/dt\right)} = 0$$

$$\frac{\Delta H}{\Delta\alpha_f} = \left(H_0 + H_1\theta_0 + H_2\theta_0^2\right) \quad \text{and} \quad \frac{\Delta H}{\Delta\left(d\theta_{shaft}/dt\right)} = \left(H_3 + H_4\theta_0\right). \tag{2.132}$$

Table 2-14. XV-3 Proprotor Stability Derivatives for the XV-3 (density altitude 7,500 feet, geometry per Table 2-13)

Item	Symbol	Unit	Value			
Flight speed	V_{FP}	knot	105	120	140	160
Thrust	T	lb	287	375	510	666
H-force	H	lb	24.7	36.5	58.3	88.9
Angle of attack	α_f	deg	2.70	2.36	2.03	1.77
Collective	θ_0	deg	65.75	69.09	73.05	76.52
Thrust constants	T_0	lb	–7,061.4	–7,776.7	–8,735.7	–9,714.0
	T_1	lb	6,403.6	6,687.3	7,076.5	7,488.8
	T_2	lb	2,320.7	2,740.1	3,439.1	3,986.6
H-force constants	H_0	lb	9,327.4	13,625.4	18,486.1	28,571.6
	H_1	lb	–16,894.8	–23,573.7	–30,899.1	-45,671.0
	H_2	lb	8,036.7	10,712.2	13,624.4	19,236.3
	H_3	lb	2,264.8	2,638.3	96.5	115.5
	H_4	lb	–1,547.8	–1,757.5	–63.3	–74.7
Flying qualities derivatives	$\Delta T/\Delta\alpha_f$	lb/rad	218.7	226.0	243.1	246.6
	$\Delta H/\Delta\alpha_f$	lb/rad	523.1	775.4	1238.0	1886.8
	$\Delta T/\Delta(d\theta_{shaft}/dt)$	lb/rad per sec	0.0	0.0	0.0	0.0
	$\Delta H/\Delta(d\theta_{shaft}/dt)$	lb/rad per sec	488.6	519.1	15.9	15.8
	$\Delta M_{cg}/\Delta\alpha_f$	ft-lb/rad	1966.9	2915.5	4654.7	7094.4
	$\Delta M_{cg}/\Delta(d\theta_{shaft}/dt)$	ft-lb/rad per	1837.0	1951.8	59.7	59.3

2.13.2.3.4 Aeromechanics Results

Researchers who deal with this more complicated dynamics problem can no longer assume that shaft motion is a constant pitch rate. Nor can they assume that rigid blade motion is simple harmonic motion. In this case, the calculations are very dependent on the hub geometry and the shaft oscillation frequency (ω_{shaft}), which is in radians per second. That is, two blades each attached to the hub with flapping hinges are not the same as two blades attached to a teetering hub of the XV-3 type. Furthermore, the three blades attached to a universal joint hub require that each configuration must be modeled carefully. The XV-15 uses a hook joint, which introduces an inplane two-per-rev harmonic. The MV-22 uses a constant velocity joint, which does not introduce a two-per-rev harmonic.

For my purposes here, let me first deal with just the XV-3's teetering hub configuration using Eq. (2.119) as the starting point. Six things happen with this configuration. First, the flapping moment of inertia of a single blade must be increased by a factor of two so that both blades are accounted for. Second, the aerodynamic moment that causes the teetering is the difference between the flapping moment of each blade. Third, the flapping angle becomes the teetering angle (β_T). Fourth, each blade must derive its flap angle from the teetering angle. To accomplish this fourth step, I have assigned one blade to be a master blade (call it blade 1) and the blade associated with the teetering angle. Then it follows that blade 2, which trails blade 1 by 180 degrees, is at the negative flapping angle of blade 1. Stated mathematically, you would write

$$\beta_{Blade1} = \beta_T \quad \text{and} \quad \beta_{Blade2} = -\beta_T . \tag{2.133}$$

Just think of a playground seesaw (or teeter-totter, if you prefer). When one person on the seesaw goes up (plus) the other person goes down (minus). Fifth, the azimuth angle (ψ_1) of blade 1 becomes the reference azimuth angle (ψ). Sixth, blade 2 trails blade 1 by 180 degrees so the azimuth angle of blade 2 is ($\psi_2 = \psi - \pi$).

Given the above six points, for the XV-3 configuration you have

$$\begin{aligned}\frac{d^2\beta_T}{d\psi^2} + \varpi^2\beta_T = {} & \frac{1}{2I_{flap}\Omega^2}\left[\left(\text{Blade 1 } M_{aero}\right)_\psi - \left(\text{Blade 2 } M_{aero}\right)_{\psi-\pi}\right] \\ & + \frac{1}{2I_{flap}\Omega^2}\left[\left(\text{Blade 1}M_{gyro}\right)_\psi - \left(\text{Blade 2}M_{gyro}\right)_{\psi-\pi}\right].\end{aligned} \tag{2.134}$$

Now, the aerodynamic moment for blade 1 is summarized in Appendix E and, when applied to blade 1 with reference to the teetering angle, you have

$$\text{Blade1}\left(M_{aero}\right)_\psi = \left(\tfrac{1}{2}\rho V_t^2 acR^2\right)\left[K0_\psi + K1_\psi\frac{d\beta_T}{d\psi} + K2_\psi\beta_T\right]. \tag{2.135}$$

Then it follows from Eq. (2.133) that the flapping moment of blade 2 must be

$$\text{Blade2}\left(M_{aero}\right)_\psi = \left(\tfrac{1}{2}\rho V_t^2 acR^2\right)\left[K0_{\psi-\pi} - K1_{\psi-\pi}\frac{d\beta_T}{d\psi} - K2_{\psi-\pi}\beta_T\right]. \tag{2.136}$$

With this understanding, the aerodynamic moment about the teetering hinge becomes

$$(2.137)\qquad \left(M_{aero}\right)_{\psi}-\left(M_{aero}\right)_{\psi-\pi}=\left(\tfrac{1}{2}\rho V_t^2 acR^2\right)\left\{\left[K0_{\psi}+K1_{\psi}\frac{d\beta_T}{d\psi}+K2_{\psi}\beta_T\right]-\left[K0_{\psi-\pi}-K1_{\psi-\pi}\frac{d\beta_T}{d\psi}-K2_{\psi-\pi}\beta_T\right]\right\},$$

and when you gather the terms up you have

$$(2.138)\qquad \left(M_{aero}\right)_{\psi}-\left(M_{aero}\right)_{\psi-\pi}=\left(\tfrac{1}{2}\rho V_t^2 acR^2\right)\left[\left(K0_{\psi}-K0_{\psi-\pi}\right)+\left(K1_{\psi}+K1_{\psi-\pi}\right)\frac{d\beta_T}{d\psi}+\left(K2_{\psi}+K2_{\psi-\pi}\right)\beta_T\right].$$

The gyroscopic moment for the two-bladed teetering rotor is constructed in a similar manner so that the differential equation expands to

$$\begin{aligned}(2.139)\qquad \frac{d^2\beta_T}{d\psi^2}+\varpi^2\beta_T=&\frac{1}{2I_{flap}\Omega^2}\left(\tfrac{1}{2}\rho V_t^2 acR^2\right)\left[\left(K0_{\psi}-K0_{\psi-\pi}\right)+\left(K1_{\psi}+K1_{\psi-\pi}\right)\frac{d\beta_T}{d\psi}+\left(K2_{\psi}+K2_{\psi-\pi}\right)\beta_T\right]\\&+\frac{1}{2I_{flap}\Omega^2}\left\{-\frac{2}{\Omega}\frac{d\theta_{shaft}}{dt}\sin\psi+\frac{1}{\Omega^2}\frac{d^2\theta_{shaft}}{dt^2}\cos\psi\right\}\\&-\frac{1}{2I_{flap}\Omega^2}\left\{-\frac{2}{\Omega}\frac{d\theta_{shaft}}{dt}\sin(\psi-\pi)+\frac{1}{\Omega^2}\frac{d^2\theta_{shaft}}{dt^2}\cos(\psi-\pi)\right\}.\end{aligned}$$

Some simplification to Eq. (2.139) can be obtained by using a Lock number for a single blade, in which case

$$\frac{1}{2I_{flap}\Omega^2}\left(\tfrac{1}{2}\rho V_t^2 acR^2\right)=\frac{\gamma}{4},$$

and when you remember that $\sin(\psi-\pi)=-\sin\psi$ and $\cos(\psi-\pi)=-\cos\psi$, the gyroscopic terms are easily collected. Therefore, the final form of the two-bladed rotor teetering equation is

$$\begin{aligned}(2.140)\qquad \frac{d^2\beta_T}{d\psi^2}+\varpi^2\beta_T=&\frac{\gamma}{4}\left[\left(K0_{\psi}-K0_{\psi-\pi}\right)+\left(K1_{\psi}+K1_{\psi-\pi}\right)\frac{d\beta_T}{d\psi}+\left(K2_{\psi}+K2_{\psi-\pi}\right)\beta_T\right]\\&+\left\{-\frac{2}{\Omega}\frac{d\theta_{shaft}}{dt}\sin\psi+\frac{1}{\Omega^2}\frac{d^2\theta_{shaft}}{dt^2}\cos\psi\right\}.\end{aligned}$$

Admittedly, when written out completely as you might have seen in the 1950s, Eq. (2.139) appears rather complex. But skillful aeromechanic engineers (even back then) used advanced mathematics to derive their theories and make computations. Much of this work is conveyed to others in—what amounts to—mathematical shorthand. Earl Hall's paper [285] is a very good example.

Now let me show you some results that follow from solving Eq. (2.140) using the XV-3 geometry as configured in Table 2-13. Suppose the shaft is oscillating in a sinusoidal pitching motion according to $\theta_{shaft}=A\sin(\omega_{shaft}t)$, and the question is, what do the blade flapping motion, thrust, H-force, and Y-force waveforms look like for, say, a shaft motion frequency (ω_{shaft}) to rotor speed (Ω) ratio (ν) of 0.25? Place this configuration in steady, level

flight (a) at 105 knots, (b) with a fuselage angle of attack of 0 degrees, (c) with zero cyclic, and (d) producing the 287 pounds thrust required for trim. Keep in mind that while the fuselage angle of attack is not varying, the rotor shaft at the wingtip is changing the angle of attack according to Asin (ω_{shaft} t). This input data gives the textbook results for a two-bladed, teetering rotor system that you see in Fig. 2-148 through Fig. 2-151.

The first thing to notice in these results is that the proprotor's teetering motion does not follow the shaft motion as you can plainly see from Fig. 2-148. Keep in mind that if the teetering angle was zero at all times, the proprotor's tip path plane would be perpendicular to the shaft. For this XV-3 case, the misalignment, at times on the order of 6 degrees, is substantial based on helicopter experience. Furthermore, the XV-3 had a delta-3 of –20 degrees (i.e., $\Delta\theta/\Delta\beta_T = -0.364$), which is intended to reduce teetering motion.

The second thing to notice is the magnitude of the inplane forces (i.e., H- and Y-forces) shown in Fig. 2-150 and Fig. 2-151, respectively. These hub forces act perpendicular to the shaft and have a moment arm of 3.76 feet. Thus, the vibratory moment created by the H-force is ±350 pounds times 3.76 feet, or roughly ±1,300 foot-pounds. This moment is twisting the wing and should be considered a very serious fatigue load. The Y-force is applying a moment at the wingtip, tending to bend the wing in the chordwise sense. From Fig. 2-149 you can see that the vibratory thrust is only about ±40 pounds. However this force acts at a moment arm of half the wingspan (15.6 feet), which adds another ±625 foot-pound fatigue load.

In short, proprotors as used on the XV-3 were capable of introducing substantial loads. These loads affected the aircraft's flying qualities and added fatigue loads to the structure.

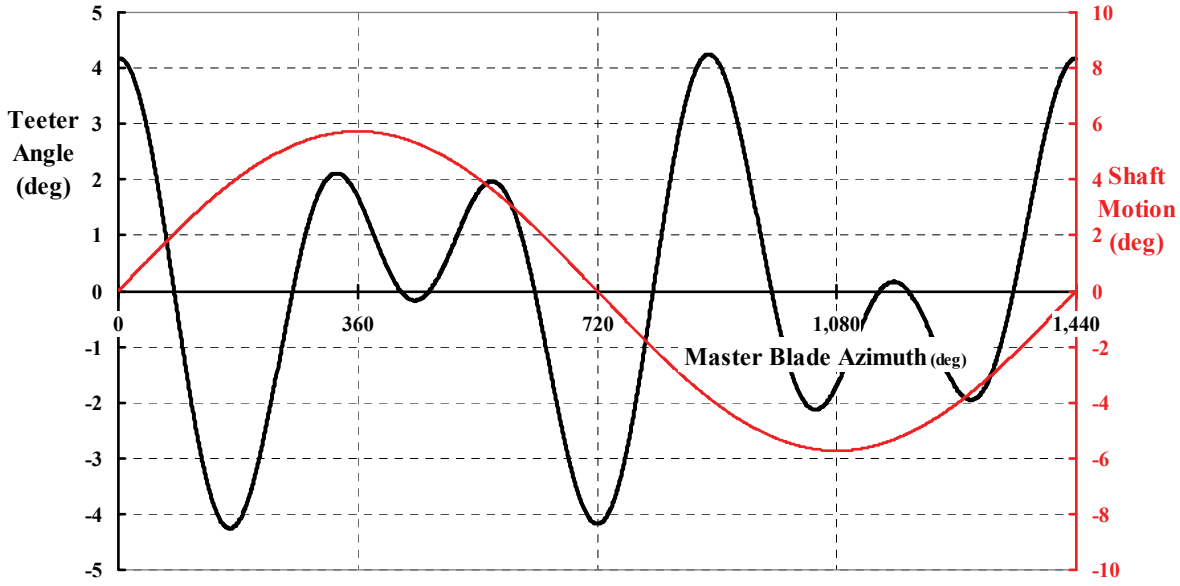

Fig. 2-148. The teetering angle is measured relative to the shaft. Zero teetering angle means that the tip path plane is perpendicular to the shaft.

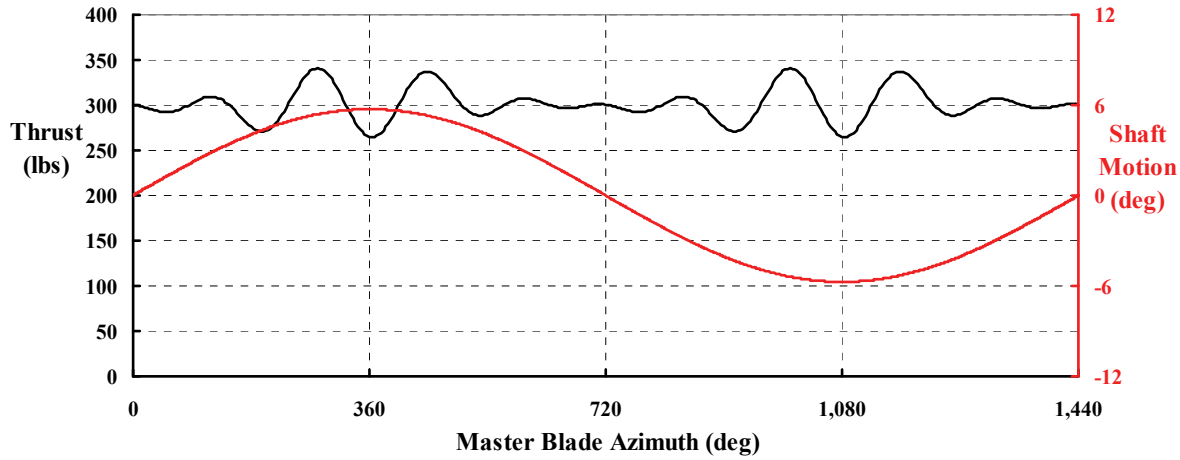

Fig. 2-149. The teetering proprotor thrust has a minor vibratory component, however this can add significant yawing moments to the aircraft.

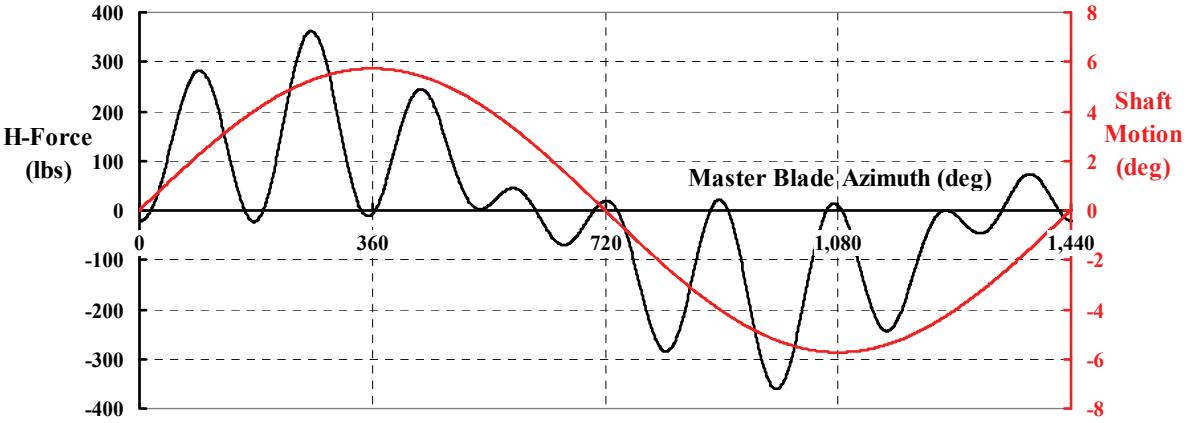

Fig. 2-150. H-force tends to be in phase with shaft motion, which is negative damping.

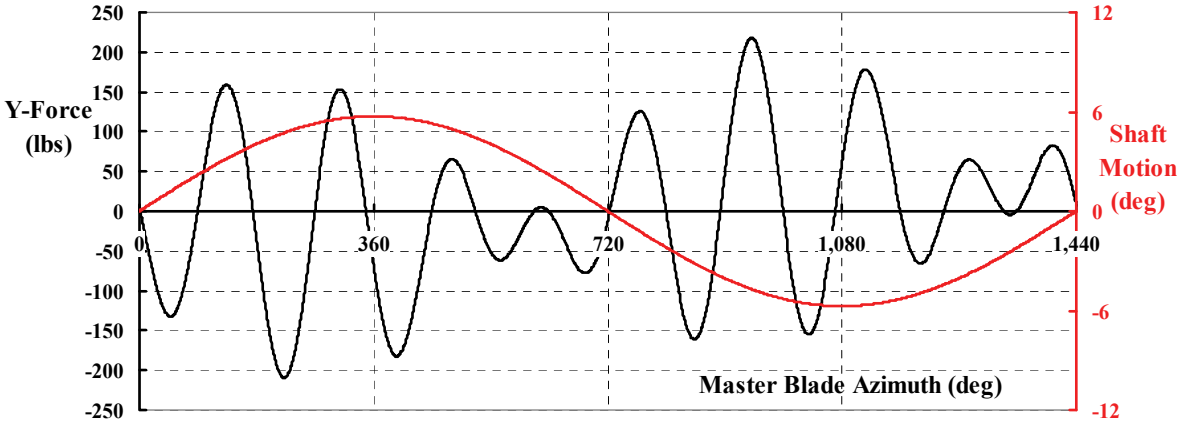

Fig. 2-151. Y-force with shaft pitching motion is significant.

To provide an example of the three-bladed flapping hub configuration, let me just add a blade to the XV-3. After all, the three-bladed rotor system was what the XV-3 started out with (Fig. 2-125, page 204). I will assume this third blade is identical to those on the teetering system as described in Table 2-13. Again, place this three-bladed configuration in steady, level flight (a) at 105 knots, (b) with a fuselage angle of attack of 0 degrees, (c) with zero cyclic, and (d) producing the 287 pounds of thrust required for trim.

As to the equations for flapping and proprotor forces, the approach is quite different than those developed for the two-blade teetering proprotor system as you can see from Appendix E. So let me just convey flapping, thrust, H-force, and Y-force results. Again, I will assume that only the shaft is oscillating in a sinusoidal pitching motion according to $\theta_{shaft} = A \sin(\omega_{shaft} t)$ with a shaft motion frequency (ω_{shaft}) to rotor speed (Ω) ratio (ν) of 0.25. The amplitude (A) is 0.10 radians.

The flapping, thrust, and H- and Y-forces for the three-bladed, flapping proprotor systems (Fig. 2-152 through Fig. 2-155) are considerably different than those you saw for the two-bladed, teetering proprotor system. With three blades attached to a flapping hinge hub, the higher frequency response to shaft motion virtually disappears and, in fact, what little waviness you do see is an artifact of the numerical integration I used.

Consider first the flapping motion as conveyed in Fig. 2-152. The flapping hinge hub with three rigid blades attached to it is just like a three-arm seesaw mounted at the hub's centerline. This configuration has a plane that can tilt in any direction. Said another way, the tips of the three blades form a plane. You might also think of it as a three-legged stool where the stool's seat is the tip path plane. The plane can tilt in any one of the 360 degrees of the compass depending on the length of each leg of the stool. This plane is called the tip path plane.

Fig. 2-152 shows that as the shaft moves up, the tip path plane lags behind, which you can see from the small sketch included on the figure. Later in the shaft's sinusoidal motion the situation reverses. The tip path plane also tilts right to left (or left to right, depending on the proprotor rotation) when you are looking down on the setup. Note that the tip path plane's motion is not exactly synchronized to the shaft's motion, which is to say that there is a phase shift. This phase shift is caused by the mutual interdependence of the gyroscopic and aerodynamic moments. The tip path plane appears to be wobbling relative to the shaft.

The three forces shown in Fig. 2-153 through Fig. 2-155 are now seen to be very smooth waveforms when compared to the two-bladed, teetering configuration. This means the higher harmonic vibratory loads at two per rev, four per rev, etc., are virtually removed, which is a substantial benefit for the three-bladed system. However, the H-force is now clearly a negative damping contributor and deserves more detailed discussion. You can see from the H-force graph in Fig. 2-154 that the force is out of phase with the shaft motion. In fact, the H-force is not exactly in phase with the shaft pitch rate ($d\theta_{shaft}/dt$) either. Rather the H-force behaves in accordance with

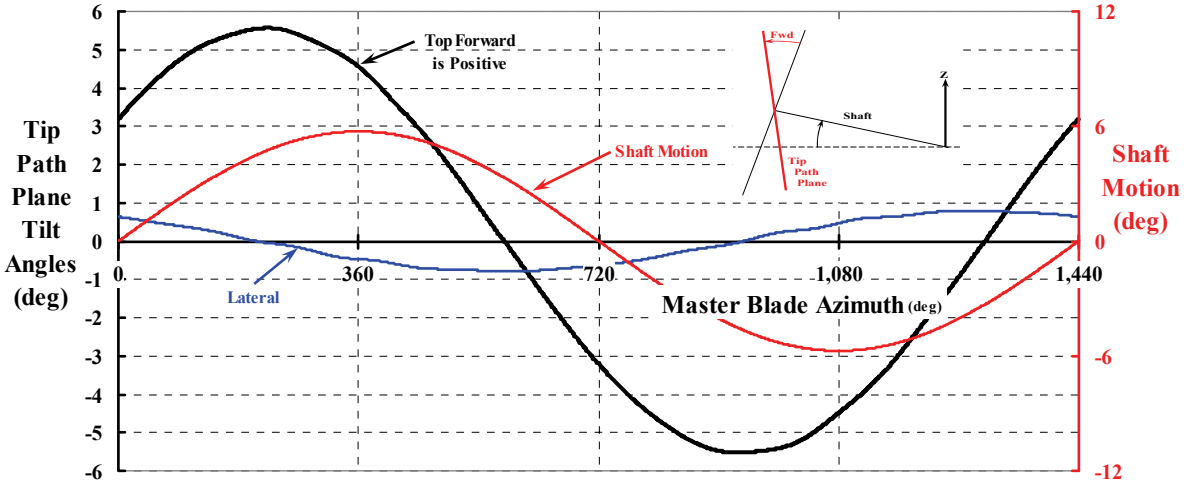

Fig. 2-152. The tip path plane angle can be referenced to the aircraft's axis system.

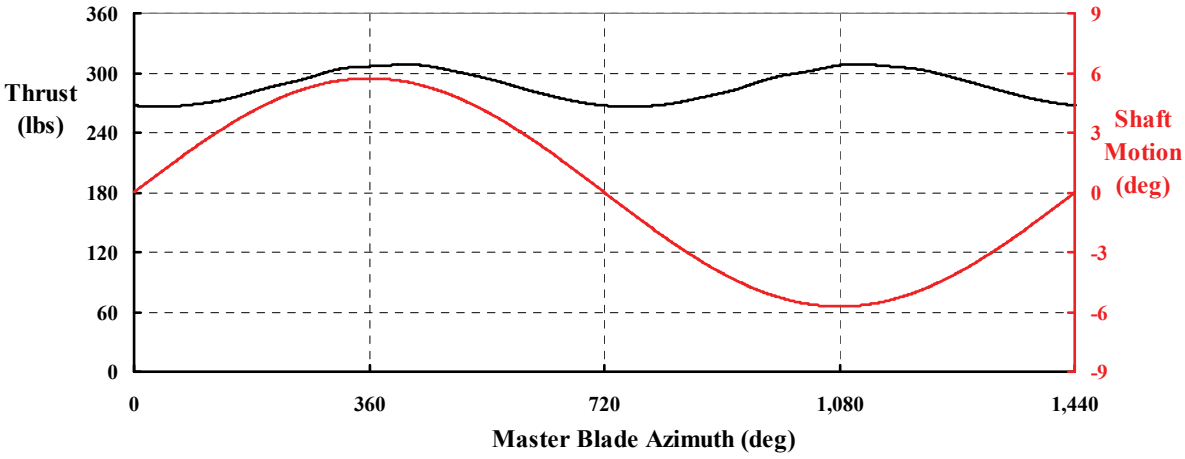

Fig. 2-153. The gimbaled, three-bladed proprotor's thrust is virtually independent of shaft motion.

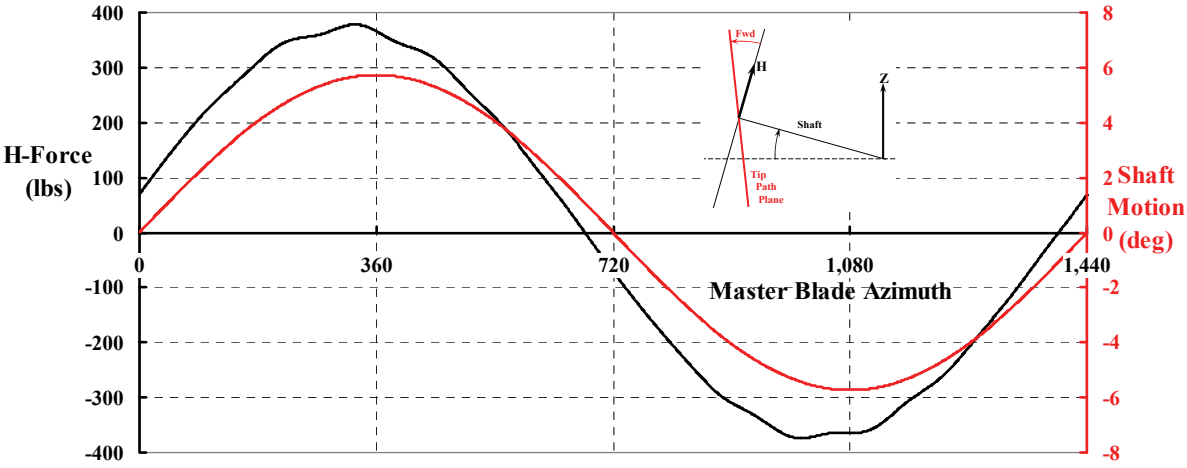

Fig. 2-154. H-force is nearly in phase with shaft motion, which is negative damping.

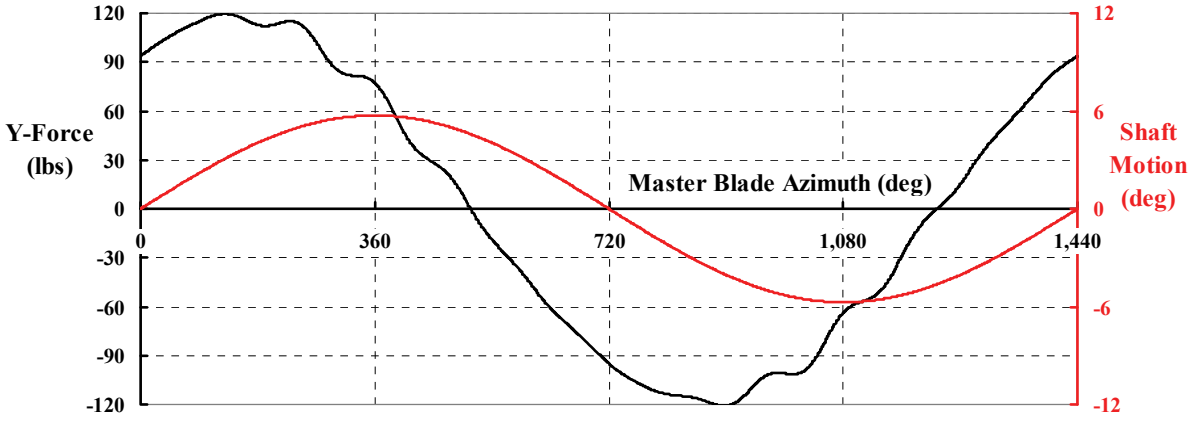

Fig. 2-155. Y-force due to shaft pitching motion is significant.

$$H = S_1 \sin(\nu\psi_M) + C_1 \cos(\nu\psi_M)$$
$$= K_0 A \sin(\nu\psi_M) + K_1 A\Omega\nu \cos(\nu\psi_M) = H_0\theta_{shaft} + H_1 \frac{d\theta_{shaft}}{dt}. \quad (2.141)$$

Because the shaft motion is sinusoidal (Fig. 2-156), it is quite reasonable to represent the H-force in terms of the H_0 and H_1 coefficients. The constants (S_1 and C_1, or K_0 and K_1, or H_0 and H_1) themselves depend on the shaft motion frequency (ω_{shaft}), the flight condition, and the rotor geometry. Keep in mind that each set of coefficients you might choose includes the aerodynamic force parameter of $\left(\frac{1}{2}\rho V_t^2\right)(b\,c\,R)$, which has the units of pounds. Note that H_0 and H_1 are simply derivatives. That is

$$H_0 = \frac{\Delta H}{\Delta\theta_{shaft}} = H_\theta \quad \text{and} \quad H_1 = \frac{\Delta H}{\Delta\theta_{shaft}/dt} = H_{\dot\theta}. \quad (2.142)$$

There is a tendency to think of H-force as a function of shaft pitch rate and, therefore, an indication of damping. But a simple plot of H-force versus the shaft pitch rate shows an elliptical pattern as you can see in Fig. 2-157. *Clearly, displacement* (θ_{shaft}) *is as important as shaft pitch rate* ($d\theta_{shaft}/dt$) *in determining the magnitude of H-force.*

Additional insight is provided by noting that when the shaft motion is $\theta_{shaft} = A\sin(\omega_{shaft}t)$—as I have used for this discussion—then the pitch rate is

$$\frac{d\theta_{shaft}}{dt} = A(\omega_{shaft})\cos(\omega_{shaft}t) = A\Omega\left(\frac{\omega_{shaft}}{\Omega}\right)\cos\left(\frac{\omega_{shaft}}{\Omega}\psi_M\right) = A\Omega(\nu)\cos(\nu\psi_M). \quad (2.143)$$

Therefore, pitch rate can be factored out of Eq. (2.141), which gives you

$$H = H_0 \frac{d\theta_{shaft}}{dt}\left[1 + \frac{(H_1 A\Omega^2\nu^2)\sin(\nu\psi_M)}{(H_0 A\Omega\nu)\cos(\nu\psi_M)}\right] = H_0 \frac{d\theta_{shaft}}{dt}\left[1 + (H_2 A\Omega\nu)\tan(\nu\psi_M)\right]. \quad (2.144)$$

This is a very important result because as the pitch frequency ratio (ν) becomes very small at a given rotor speed (Ω), $\cos(\nu\psi_M)$ approaches 1.0 and $\tan(\nu\psi_M)$ approaches $(\nu\psi_M)$, so H-force can be approximated by

$$(2.145) \quad H \approx H_0 \frac{d\theta_{shaft}}{dt}\left[1+\left(H_2 A\Omega\nu^2\psi_M\right)\right] \approx H_0 \frac{d\theta_{shaft}}{dt} = H_0\dot{\theta}_{shaft}\,.$$

This is some justification for the 1950's approximation used in early flying qualities work—specifically for Eq. (2.131). In effect, a series of very short azimuth steps ($\Delta\psi_M$) are used.

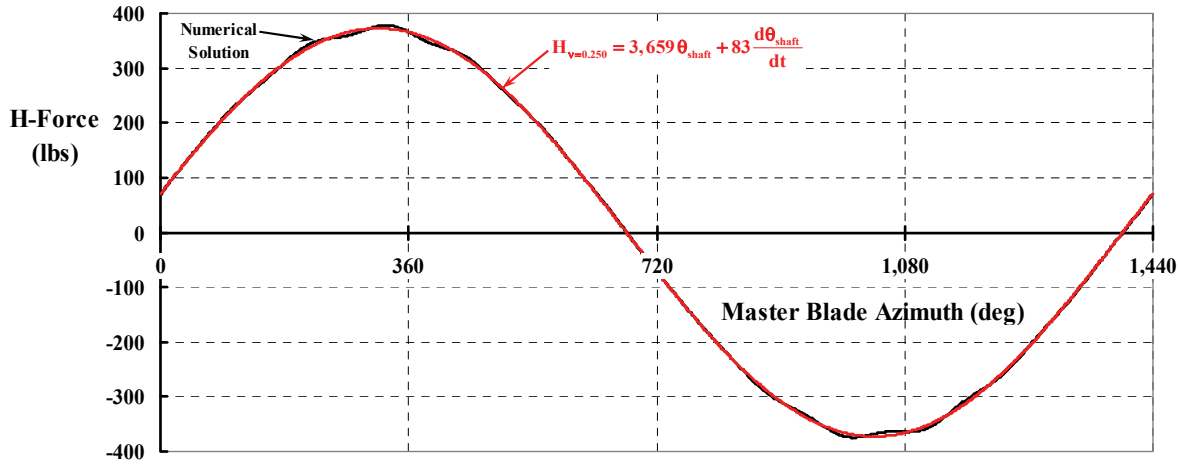

Fig. 2-156. H-force is dependent on both shaft pitch angle and pitch rate (for XV-3 with a three-bladed, flapping rotor, and A = 0.10, ν = 0.250).

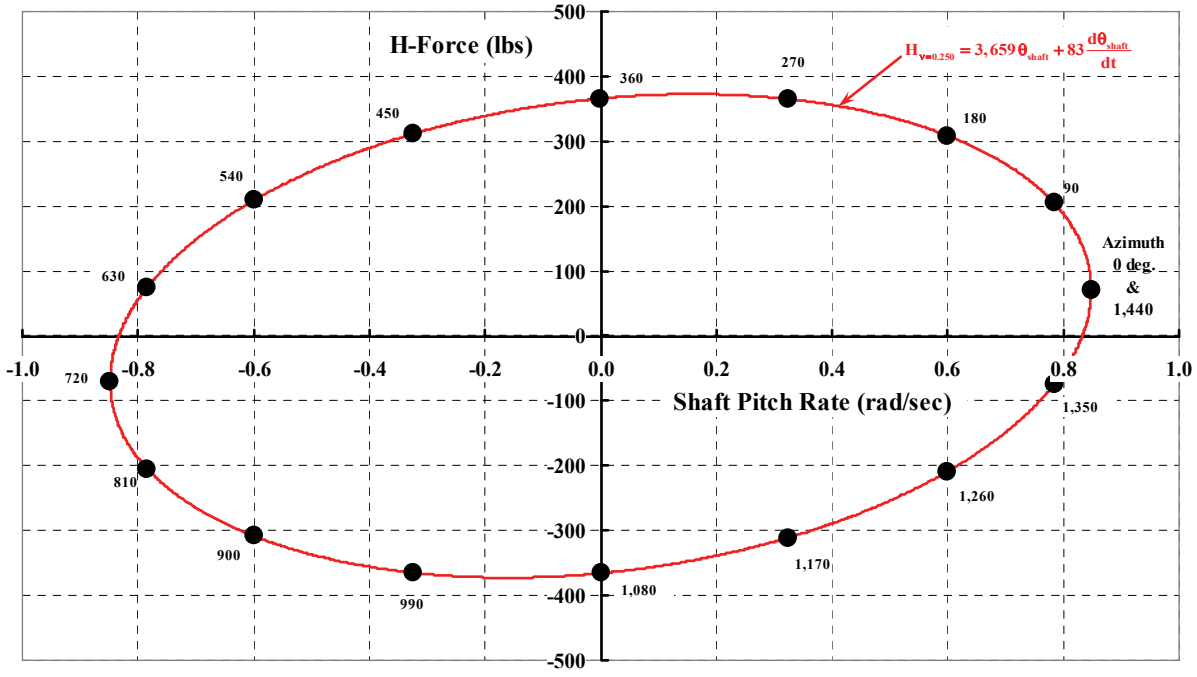

Fig. 2-157. Because H-force is not in phase with shaft pitch rate, you have an elliptical pattern (for XV-3 with a three-bladed, flapping rotor, and A = 0.10, ν = 0.250).

Now let me use methodology from Appendix E to answer two reasonable questions[80] about the preceding results. The questions are:

1. How does H-force behave with increasing shaft frequencies at constant amplitude (A) and at the same flight condition?
2. How does H-force behave over a speed range at constant amplitude and constant shaft frequency?

You have my answer to the first question with Fig. 2-158 and Fig. 2-159. Here I have just sequenced the pitch frequency ratio (ν) from 0.05 to 1.25. The more complete trends of the derivatives H_0, H_1, Y_0, and Y_1 (to be discussed shortly) are tabulated in Table 2-15. The computations have been made with a collective pitch of 64.78 degrees. This ensured that the trim thrust of 287 pounds at a flight velocity of 105 knots was obtained at each pitch frequency ratio (because thrust is unaffected by pitch frequency or pitch amplitude). The rotor speed (Ω) was held constant at 33.93 radians per second for these computations.

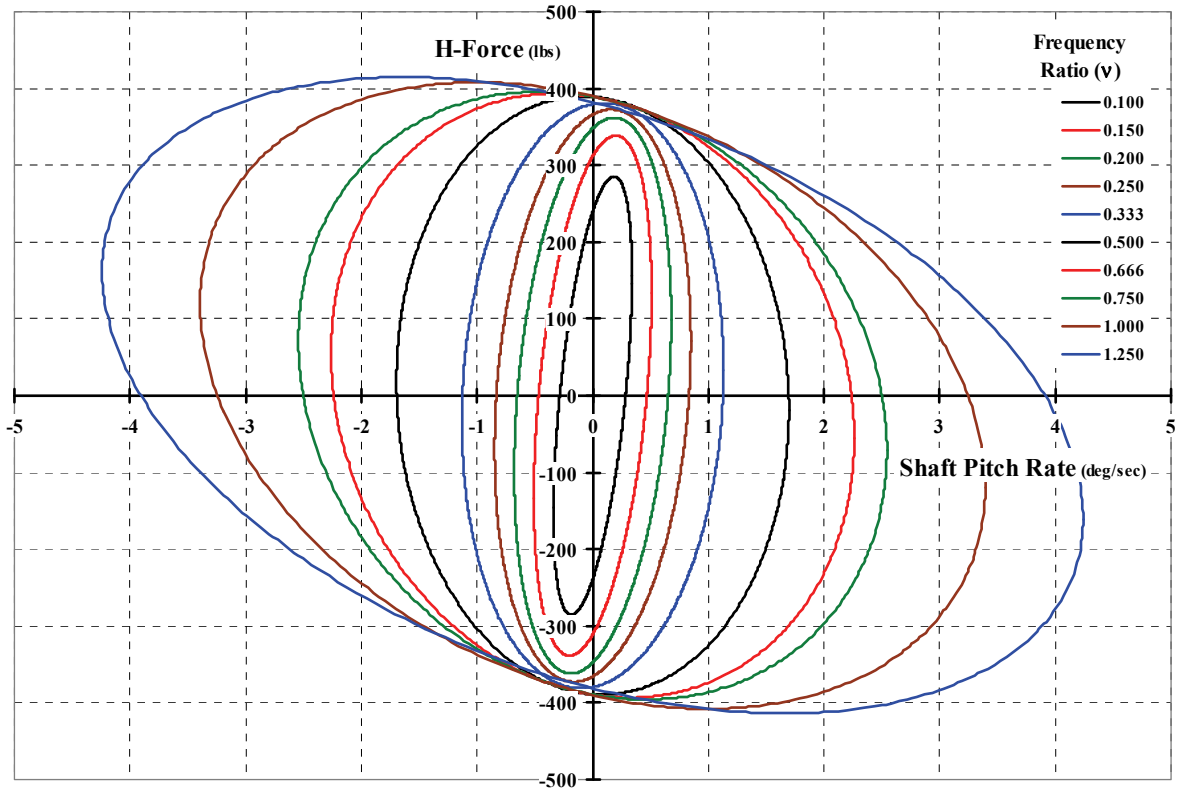

Fig. 2-158. H-force depends on both shaft pitch angle and shaft pitch rate.

[80] Troy Gaffey studied these two questions in a paper he presented in November of 1969. At that time, Troy was Group Engineer of VTOL Dynamics. He was, in my mind, later Chief Engineer of the MV-22 program. In February 1991, Troy became Vice President of Bell Engineering and Research when Bob Lynn retired. Troy successfully piloted Bell Engineering through a very rough 10-year patch as Textron repeatedly tried to find a president that could bring out the best in their Helicopter Division. Troy retired in June of 2002 and is now President of AVX Aircraft. In my view, he has excellent management skills. I count him as one of my longtime best friends—and one of the top five dynamists in the rotorcraft industry.

Table 2-15. XV-3 Proprotor (V = 105 knots, Ω = 33.929 rad/sec)

$\nu = \omega_{shaft}/\Omega$ (nd)	$H_0 = \frac{\Delta H}{\Delta\theta_{shaft}}$	$H_1 = \frac{\Delta H}{\Delta\, d\theta_{shaft}/dt}$	$Y_0 = \frac{\Delta Y}{\Delta\theta_{shaft}}$	$Y_1 = \frac{\Delta Y}{\Delta\left(d\theta_{shaft}/dt\right)}$
0.050	1,396.0	686.3	–294.6	108.1
0.075	1,896.5	577.9	–317.8	163.4
0.100	2,393.3	458.0	–229.4	194.0
0.150	3,112.9	262.3	129.4	186.0
0.200	3,478.8	147.0	458.7	146.7
0.250	3,659.4	83.1	706.6	111.4
0.333	3,795.3	29.5	940.3	72.4
0.500	3,889.4	–10.9	1,132.7	36.6
0.667	3,893.3	–24.5	1,215.5	22.1
0.750	3,892.9	–28.1	1,215.5	18.5
1.000	3,900.3	–35.3	1,199.6	11.5
1.250	3,812.8	–38.0	1,195.9	0.0

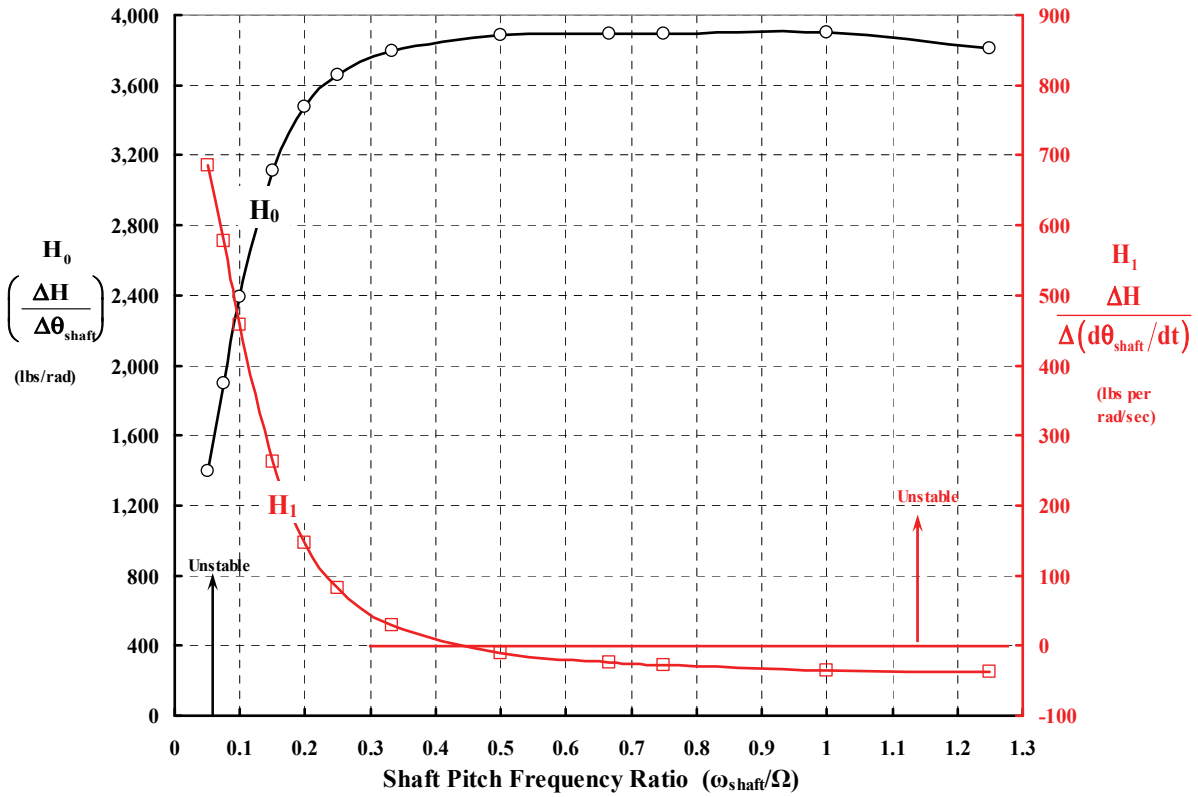

Fig. 2-159. A positive H_0 means a negative spring. A positive H_1 indicates negative damping. Thus, the rotor is a very destabilizing force contributor.

The second question deals with how the four derivatives (H_0 thru Y_1) vary with speed. The answer to this question requires a little more information about the flight condition chosen at each speed. I assumed that as the speed increased from 105 knots, the thrust required for trim (and therefore collective pitch) increased in accordance with Table 2-14. For this calculation, I set the shaft amplitude (A) at 0.1 and the shaft pitch rate ratio (ν) constant at 0.500. You see the results of this computation in Table 2-16 and Fig. 2-160. Notice that I made no computations below 40 knots. This is because my calculations do not include the induced velocity at each blade element, which is, as you know, an important factor at low speed.

You will find a very fundamental case in Appendix E. In this case, I assumed the velocity was zero, the blades had no twist, the collective pitch was zero (i.e., zero thrust), there was no cyclic, and there was no delta-3. This case simulates a very, very simple experiment. Of course, the rotor tip path plane lags the shaft pitching motion. However, the H-force due to aerodynamics is virtually zero because thrust is near zero throughout the cyclic. But keep in mind that a wind tunnel balance would measure inertia forces.

Table 2-16. XV-3 Proprotor ($\nu = \omega_{shaft}/\Omega = 0.5$)

V (kts)	Root Collective (deg)	Thrust (lb)	$H_0 = \frac{\Delta H}{\Delta\theta_{shaft}}$	$H_1 = \frac{\Delta H}{\Delta\, d\theta_{shaft}/dt}$	$Y_0 = \frac{\Delta Y}{\Delta\theta_{shaft}}$	$Y_1 = \frac{\Delta Y}{\Delta\left(d\theta_{shaft}/dt\right)}$
40	37.39	44.49	41	1151.70	4.15	313.49
80	51.34	57.65	167	2672.42	–2.14	746.41
80	57.61	64.78	287	3889.40	–10.86	1132.71
105	64.60	68.65	376	4729.59	–17.73	1411.94
160	68.49	77.54	667	7406.90	–41.71	2335.19
190	73.11	83.04	929	9844.10	–65.39	3196.01

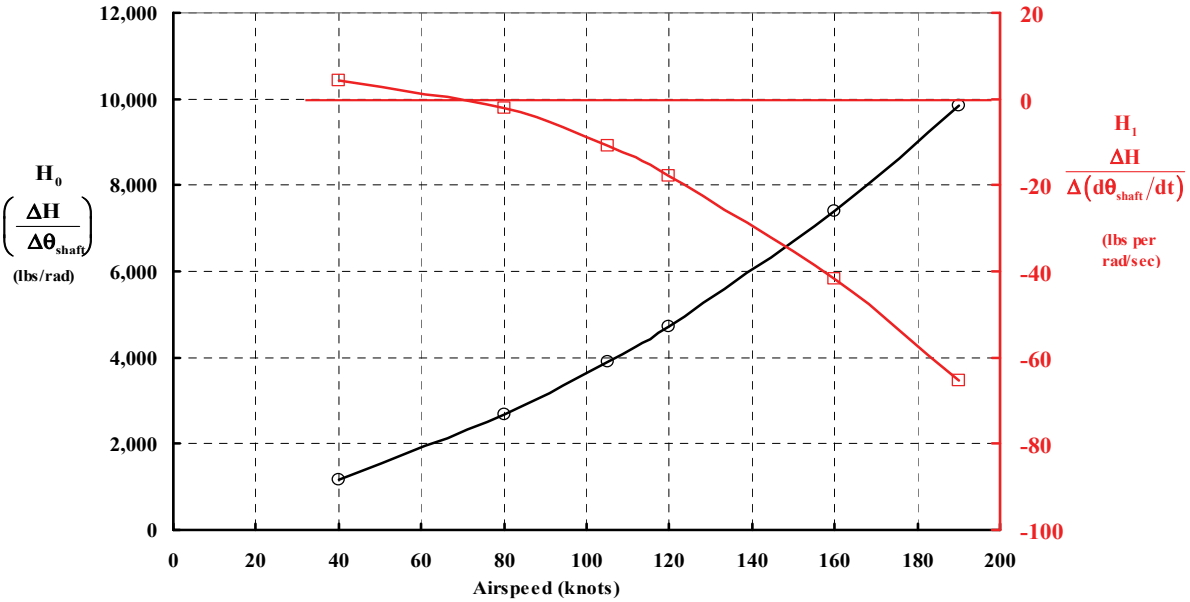

Fig. 2-160. H-force derivatives as a function of airspeed for $\omega_{shaft}/\Omega = 0.5$.

Now consider the inclusion of Y-force in the discussion. You see from Table 2-15 and Table 2-16 that shaft pitching motion (θ_{shaft}) has a by-product, which is a Y-force. That is, the two forces behave as

(2.146) $$H_{\text{due to pitch}} = \frac{\Delta H}{\Delta \theta_s}\theta_{shaft} + \frac{\Delta H}{\Delta \dot{\theta}_s}\frac{d\theta_{shaft}}{dt} \quad \text{and} \quad Y_{\text{due to pitch}} = \frac{\Delta Y}{\Delta \theta_s}\theta_{shaft} + \frac{\Delta Y}{\Delta \dot{\theta}_s}\frac{d\theta_{shaft}}{dt}.$$

Note that I have used the derivatives in their long form and used a symbol with a dot above it to indicate a rate. This makes things a lot clearer to me. Now, it is just as easy to imagine, as Fig. 2-161 suggests, that the shaft is oscillating in yaw (ϕ_{shaft}). For this shaft motion, Y-force is the prime force and H-force becomes the by-product. That is,

(2.147) $$Y_{\text{due to yaw}} = \frac{\Delta Y}{\Delta \phi_s}\phi_{shaft} + \frac{\Delta Y}{\Delta \dot{\phi}_s}\frac{d\phi_{shaft}}{dt} \quad \text{and} \quad H_{\text{due to yaw}} = \frac{\Delta H}{\Delta \phi_s}\phi_{shaft} + \frac{\Delta H}{\Delta \dot{\phi}_s}\frac{d\phi_{shaft}}{dt}.$$

You can immediately see that the total H- and Y-forces must include terms accounting for both pitch and yaw shaft motion. That is,

(2.148) $$H = H_{\text{due to pitch}} + H_{\text{due to yaw}} \quad \text{and} \quad Y = Y_{\text{due to yaw}} + Y_{\text{due to pitch}},$$

which is illustrated in Fig. 2-162. Just as importantly, you can immediately see that Y-force is just H-force rotated 90 degrees. This means that everything you have learned about H-force can be applied to Y-force just by changing H to Y and changing θ_{shaft} to ϕ_{shaft}. Therefore, the trends shown in Fig. 2-159 and Fig. 2-160 are applicable to Y-force. Of course, there is no reason that the shaft motion in yaw is the same as the pitch motion. To make this clear, let me reinforce this point by stating that

(2.149) $$\text{in pitch } \theta_{shaft} = A_\theta \sin(\omega_\theta t) \quad \text{and in yaw } \phi_{shaft} = A_\phi \sin(\omega_\phi t)$$

being careful to pay attention to the subscripts for each symbol.

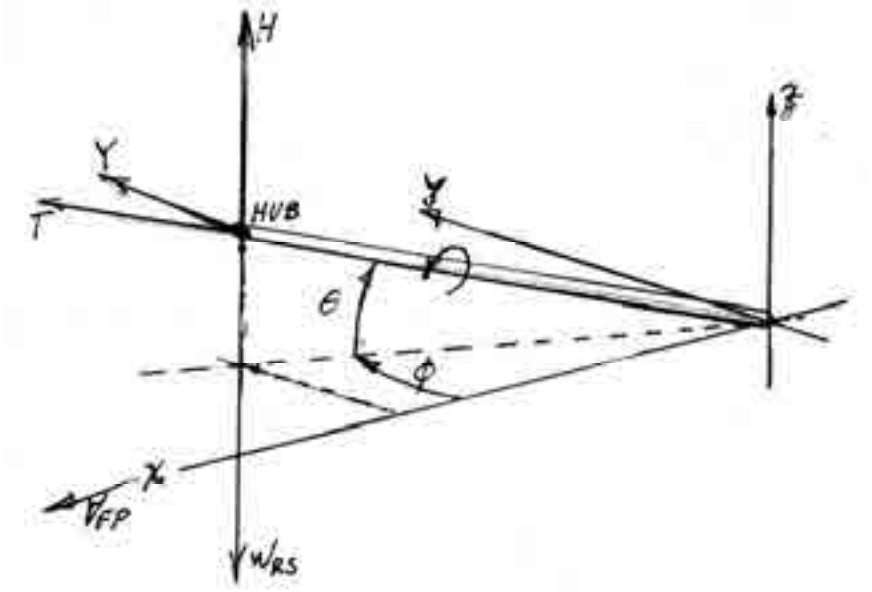

Fig. 2-161. The H- and Y-forces depend on both shaft motions.

The question now arises as to how the shaft motion might come about. In a simple experiment, the shaft could be driven by an actuator, and the two forces could be measured with a balance. This is the experiment that was conducted in May of 1950 by Britland and Fail [278]. The computations you have just reviewed are nothing more than an analytical experiment that parallels their experiment.

The shaft motion can also come about by some disturbance to the aircraft or, in the extreme, a self-excited vibration. To examine the self-excited situation, suppose the hub is initially deflected in both the pitch and yaw directions with restoring moments being created by the springs shown in Fig. 2-162. Let the springs have constants of ($K_{\theta shaft}$) and ($K_{\phi shaft}$), both being in units of foot-pounds per radian. Imagine now that the deflected hub is released and the question becomes, Will the hub return to its equilibrium position, or will it simply increase the amplitude of vibration until destruction occurs?

The vibration is resisted by the inertia moment due to the rotor weight (W_{RS}) acting at the moment arm (X_{PR}). The vibratory motion after the hub is released is governed by two second-order differential equations, which are

$$\left(\frac{W_{RS}}{32.17}X_{PR}^2\right)\frac{d^2\theta_{shaft}}{dt^2}+K_{\theta_s}\theta_s = X_{PR}H = X_{PR}\left[\frac{\Delta H}{\Delta\theta_s}\theta_{shaft}+\frac{\Delta H}{\Delta\dot{\theta}_s}\frac{d\theta_{shaft}}{dt}+\frac{\Delta H}{\Delta\phi_s}\phi_{shaft}+\frac{\Delta H}{\Delta\dot{\phi}_s}\frac{d\phi_{shaft}}{dt}\right]$$
$$\left(\frac{W_{RS}}{32.17}X_{PR}^2\right)\frac{d^2\phi_{shaft}}{dt^2}+K_{\phi_s}\phi_s = X_{PR}Y = X_{PR}\left[\frac{\Delta Y}{\Delta\phi_s}\phi_{shaft}+\frac{\Delta Y}{\Delta\dot{\phi}_s}\frac{d\phi_{shaft}}{dt}+\frac{\Delta Y}{\Delta\theta_s}\theta_{shaft}+\frac{\Delta Y}{\Delta\dot{\theta}_s}\frac{d\theta_{shaft}}{dt}\right]. \quad (2.150)$$

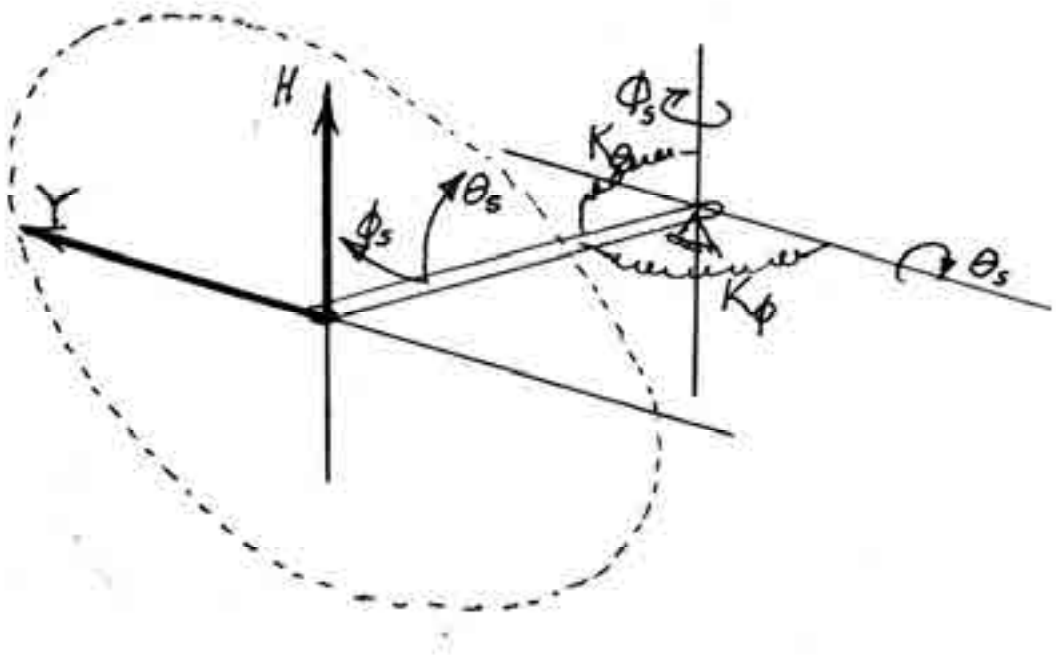

Fig. 2-162. In many aeromechanic problems you must allow for a shaft yawing motion in combination with a shaft pitching motion. Early whirl flutter analyses were based on this simple representation.

These two equations are coupled, which is to say that motion in pitch affects yaw motion and vice versa. Aeromechanics engineers generally condense these two equations with shorthand before solving them. Therefore, you may see Eq. (2.150) written as

$$\begin{aligned}\frac{d^2\theta}{dt^2}+\omega_\theta^2\theta &= \frac{X_{PR}}{I_\theta}\left[H_\theta\theta+H_{\dot\theta}\dot\theta+H_\phi\phi+H_{\dot\phi}\dot\phi\right]\\ \frac{d^2\phi}{dt^2}+\omega_\phi^2\phi &= \frac{X_{PR}}{I_\theta}\left[Y_\phi\phi+Y_{\dot\phi}\dot\phi+Y_\theta\theta+Y_{\dot\theta}\dot\theta\right]\end{aligned} \tag{2.151}$$

where the moments of inertia (I_θ and I_ϕ) replace ($W_{RS}X_{PR}^2/g$), the natural frequencies of the configuration (ω_θ^2 and ω_ϕ^2) equal (K_θ/I_θ and K_ϕ/I_ϕ) respectively, and all eight of the force derivatives (i.e., H_θ to $Y_{\dot\theta}$) are denoted by a subscript rather than the cumbersome ($\Delta H/\Delta\theta$ to $\Delta Y/\Delta\dot\theta$). Keep in mind that the derivatives vary with frequency, aircraft flight condition, and proprotor physical properties—not to mention the structural design of the whole aircraft.

The solution of Eq. (2.151) was hardly straightforward in the era of propeller and proprotor development when researchers faced initially unexplained oscillations that threatened to (and did) destroy an aircraft. But as the equations of motion became more complex, computer evolution came to the rescue. Earl Hall made the statement is his 1966 paper discussing the XV-3's whirl flutter problem that

> "The first step in these investigations was a detailed analysis of the XV-3 data from the tunnel tests. Effort was then turned to the formulation of a simple closed form solution to explain the recorded pylon prop-rotor system behavior. However, it was soon realized that the problem involved the specification of more variables than could then tractably be related. Therefore, an open digital analysis (appendix B) and a test program of models dynamically scaled from the XV-3 (appendix C) were developed. The analysis and the model tests represented a two-pronged attack on the problem, with each method relying heavily on the other. In addition to the techniques described herein, analytical work has been completed on a simplified linear analysis of the system described in appendix B. *This analysis has been programmed for the analog computer* [my italics].[81] The linear analysis has also been used to generate closed form stability criteria for pylon stability. These criteria have provided guidance to the model and open form analytical studies."

From this introductory discussion of how shaft motion affects proprotor forces, you can appreciate the complexity of rotorcraft technology. Even the preliminary design process involves no less than 12 variables as Eq. (2.151) shows for this one technology example. I have illustrated the example at the simplest level I could construct as Appendix E shows. However, there are additional details dealing with the hub geometry that you must consider. These details are illustrated by the XV-15 and V-22 hubs.

[81] During the early 1960s while at Vertol I was assigned to work for Maury Young as sort of a technical aid. One subject Maury took up was solution of whirl flutter equations. Maury had me go up to Electronic Associates Inc. in New Jersey, program the equations on their analog computer, and run a bunch of cases. It was a fun job, and I learned a great deal. I remember the EA Inc. staff as a terrific group.

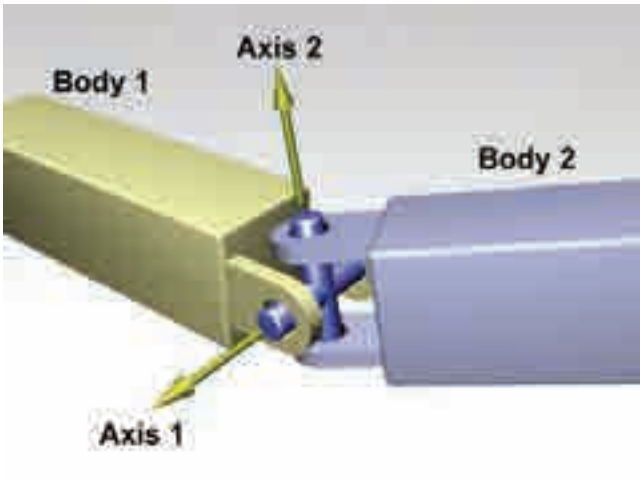

Consider the three-bladed rotor systems flown on the Bell XV-15 (Fig. 2-53, page 104) and the U.S. Marines MV-22 (Fig. 2-77, page 136). The three-bladed hub used on the XV-15 and the MV-22 is generally called a gimbaled hub. That is, the blades are attached rigidly to the hub as with the XV-3 (Fig. 2-130), and the hub is attached to the shaft with a joint that can transmit torque and thrust while allowing hub tilting. The two configurations, shown in Fig. 2-163 and Fig. 2-164, while functionally similar, are, in fact, quite different. The XV-15's hub-to-shaft joint is commonly called a universal joint. This type of joint, as shown in the picture above, allows misalignment in two axes just like the joint used in rear-drive power trains for automobiles and trucks. The misalignment between the two shafts is general designed to be rather small because the universal joint introduces a twice-per-revolution torsional vibration.

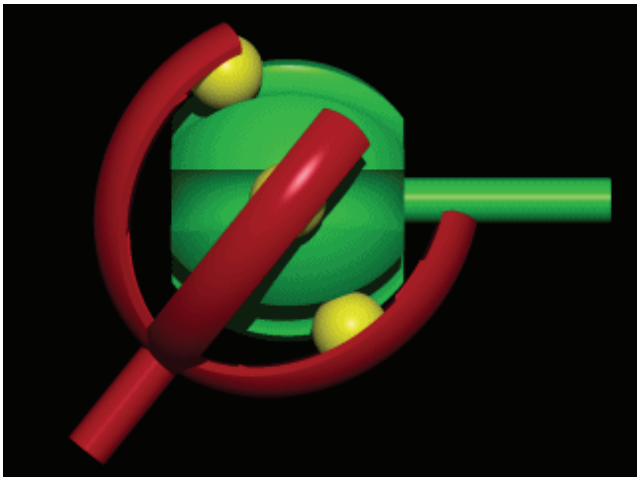

The MV-22 hub is attached to the shaft with a constant velocity joint. You are probably more familiar with this class of coupling because it is used on front-wheel-drive cars, and auto mechanics refer to it as a CV joint. A simple example is shown in this picture on the right. Here you get a sense that the misalignment between the two shafts can be quite large and yet both the input and output shafts remain at equal rotational speeds. There is virtually no twice-per-revolution torsional vibration with the constant velocity coupling, which reduces inplane vibration. The constant velocity joint used on the MV-22 is an elastomeric assembly as I have pointed out on Fig. 2-164.

You will note that there is also a significant difference between the two designs in how the blade is retained against centrifugal force while accommodating blade feathering. The XV-15 design uses a strap that twists during a pitch change while the MV-22 reacts to centrifugal force with an elastomeric bearing that can accommodate blade feathering. Pitch link loads and all control system loads are significantly affected by such hub and blade retention design details as Fig. 2-163 and Fig. 2-164 illustrate.

With the preceding thoughts in mind, let me go on to the subject of proprotor whirl flutter.

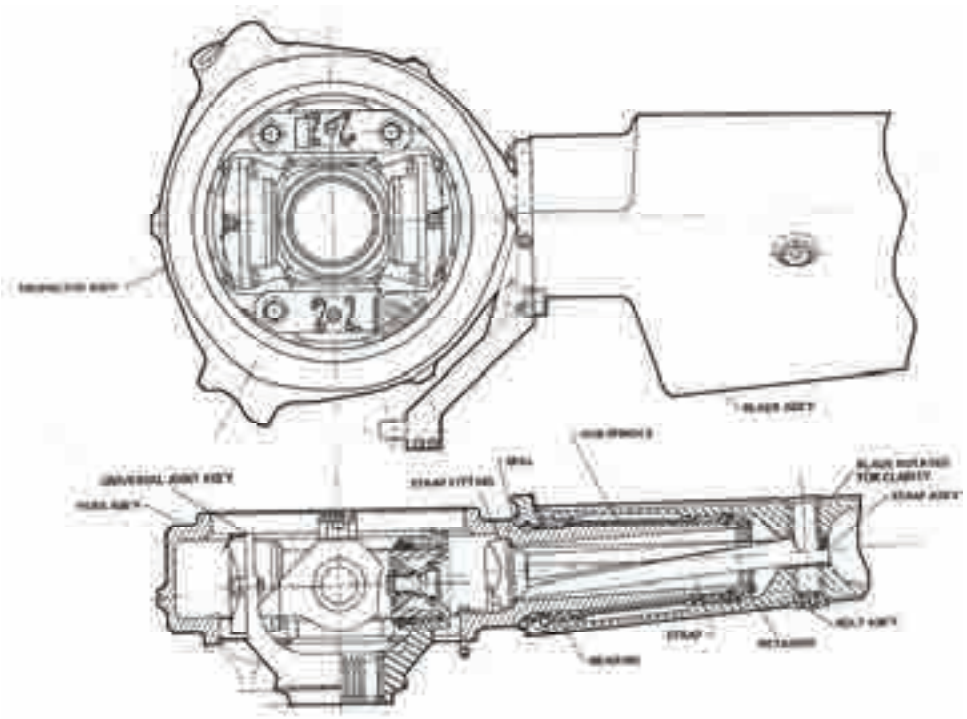

Fig. 2-163. The XV-15 hub had a universal joint attached to the proprotor shaft (courtesy of Ken Wernicke).

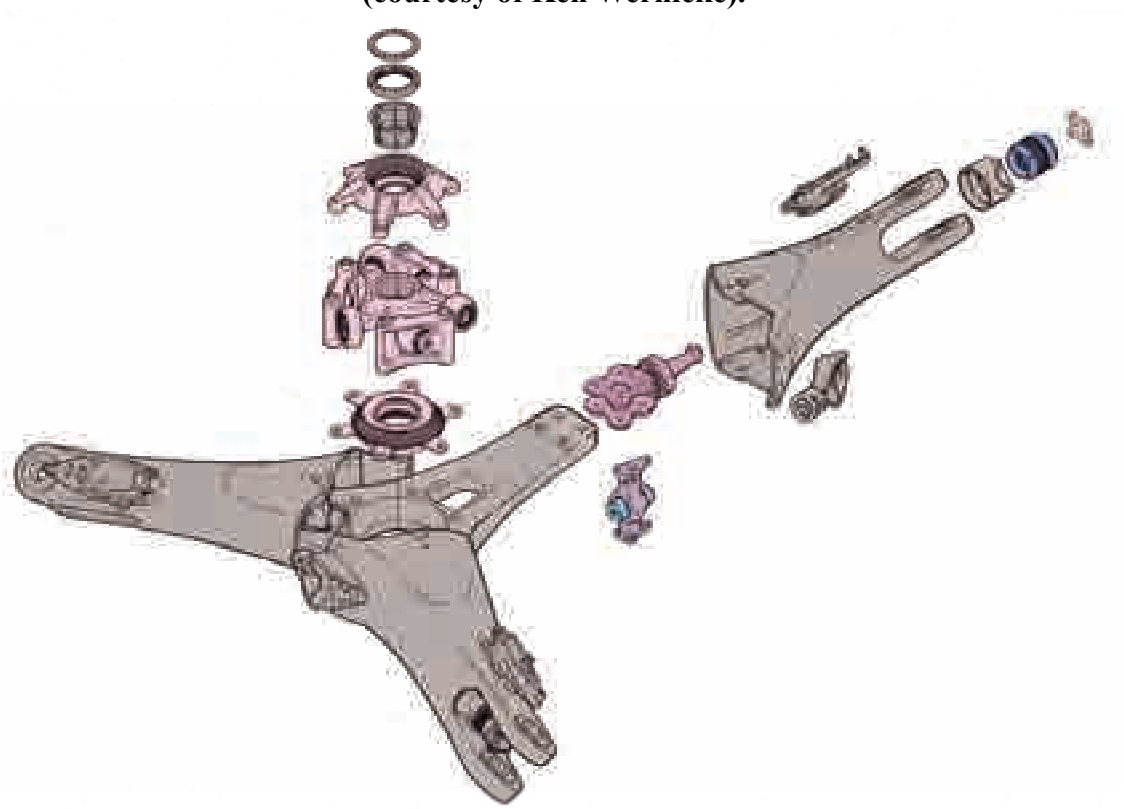

Fig. 2-164. The MV-22 hub has a constant velocity joint attached to the proprotor shaft (courtesy of Meridith Segall, Ames Research Center).

2.13.2.4 Proprotor Whirl Flutter

Proprotor whirl flutter is just one problem falling within the broader category of flutter. For over a century, flutter has been the most serious aircraft-destroying aeroelastic phenomenon the aviation industry has dealt with. There are, however, also a number of everyday sights where flutter is at play. For example, there are (a) flags fluttering in the breeze, (b) stop signs on their poles twisting back and forth in the wind, (c) stop lights—suspended across the intersection on a wire—swinging every which way from Sunday in a strong breeze, and (d) venetian blinds in an open window creating a racket when the wind blows. One very well known incident of the destructive power of this aeroelastic instability was the Tacoma Narrows Bridge rising, falling, and twisting in a 40-mile-per-hour wind. The bridge completely collapsed on the morning of November 7, 1940. You might note in passing that when wind speed increases, so does the chance that flutter will occur. Odds are that at some speed the dynamic system will become unstable, and then you have a full-blown case of flutter.

That aeroelasticity and flutter were reasonably well researched subjects is hard to deny. You need only read Professor A. R. Collar's two historical reviews [287, 288] and Isaac Garrick and Wilmer Reed's history of aircraft flutter [289]. Even closer to home, you have Taylor and Browne's 1938 paper [290]. Bob Loewy [291] gave us an excellent review of rotorcraft dynamic and aeroelastic problems in 1969. Finally, you can read a review of U.S. Army/NASA rotorcraft aeroelastic research written by Bob Ormiston, Bill Warmbrodt, Dewey Hodges, and Dave Peters, and published in October of 1988. Their report [292] contains 311 references.

Aviation was particularly hard hit by flutter when several four-propeller-driven Lockheed L-188 Electras disintegrated in flight during 1959 and 1960. The accident investigations pointed toward some aspect of whirl fluttering of the propeller and turboshaft engine assembly. Researchers began to suspect that the engine was less than rigidly mounted to the wing. In fact, Taylor and Browne's 1938 paper [290] (page 48) raised the point that the structural components that mount the propeller/engine assembly to the airframe could—if not properly chosen—lead to instabilities. A part of the Electra accident investigation was supported by NASA Langley Research Center and put the talents of John Houbolt, Wilmer Reed, and several staff members to work. You will find their respective reports [293-297] of great interest. The overview Wilmer provided [296] in July of 1967 is particularly worthwhile.

And then in 1962, Bell's XV-3, with its two-bladed proprotor, became infected.

Bell's XV-3 (s/n 54-4147) made its first hovering flight on August 11, 1955, with three-bladed, 25-foot-diameter proprotors. It experienced a number of aeromechanical stability problems that ended with a crash of the aircraft on October 25, 1956. This crash caused the development team to change to the two-bladed, 23-foot-diameter teetering hub configuration, and flight and wind tunnel testing proceeded—at least with the threat of ground resonance removed because Bell's teetering hub used stiff inplane blades. It was during the full-scale testing in the NASA Ames large-scale tunnel in 1962 that, as Bob Lynn [245] wrote, "Many had nagging questions about the pylon oscillations." These nagging questions

led to a thorough research effort to uncover what was going on. The effort began to bear fruit. Bob went on to say that "Jan Drees[82] was the first to connect an existing explanation [Ken Amer's NACA TN 2136 dated October 1950] of the negative damping with the XV-3's problem." This hint culminated when Earl Hall presented a paper at the American Helicopter Society Southwest Regional meeting in December of 1965. His presentation turned into a paper [285] published in the AHS Journal in April of 1966. The paper's title was simple: *Prop-Rotor Stability at High Advance Ratio*. The number of reports and papers that followed was clear evidence that the subject deserved some attention as you will note from several references [266, 276, 285, 286, 298-309].

Earl Hall's paper provided a clear picture of the XV-3's proprotor whirl flutter with his figure 5, which I have included here as Fig. 2-165. His theoretical work was supported with model testing. The first test in a series was performed by Bell Helicopter's Mike Paine with the "birdcage" model shown in Fig. 2-166. The theoretical and experimental work showed that there was a rather sharply defined flight speed where the wing-pylon-proprotor dynamic system would definitely become unstable. To me, Earl Hall's figure 5, accompanied by the rest of his April 1966 paper, summed up the essence of proprotor whirl flutter. You should know, however, that Wilmer Reed's paper in June of 1963 [297] and other studies [295] certainly gave many V/STOL advocates—and tiltrotor members of the development effort, in particular—cause for concern.

You are now probably asking, just what does whirl flutter look like anyway? There are, of course, a number of high-speed moving pictures now converted to digital videos that you can look at.[83] My favorite came in 1998 when Rick Peyran, then a member of the Army Mobility Research and Development Laboratory (AMRDL) located at NASA Ames, performed a science experiment with a desktop model (Fig. 2-167) as part of a research study to find ways to improve stability margins and achieve higher speeds with new tiltrotor aircraft. This experiment was referred to in a paper [304] prepared by Rick, Wally Acree, and Wayne Johnson. Their comment about the model was that "The research began with a very simple, unpowered table-top model of a wing and rotor, built of balsa wood and driven by an ordinary window box fan. The model was built by Rick and operated as a windmill. The wing was a ladder-frame structure with no aerodynamic shell, and the rotor was a two-bladed teetering [17-inch-diameter] design." Their view was that "This was the simplest design possible for testing whirl flutter."[84] When I saw this model demonstrate proprotor whirl flutter, I was absolutely delighted. Fig. 2-168 is a series of time-lapse frames of whirl flutter collected from Rick's model, which you can study at your leisure. A video of the experiment that the time-lapse frames were taken from can been seen at http://rotorcraft.arc.nasa.gov.

---

[82] Bob said that "Jan was the most creative engineer that I have ever known." I completely agree. When I moved to Bell in July of 1977, I reported to Jan who was Directory of Technology. Jan had the most amazing gift of being able to present his thoughts with such conciseness and clarity that even the youngest engineer could immediately grasp the idea.

[83] I was quite fortunate to receive a CD with his collection, courtesy of Wayne Johnson (February 15, 2014). When you have watched the videos several times, you will see why flutter is so dangerous.

[84] One could, of course, power the rotor with rubber bands—an unnecessary addition since the flutter can easily be demonstrated with the rotor in a windmill state.

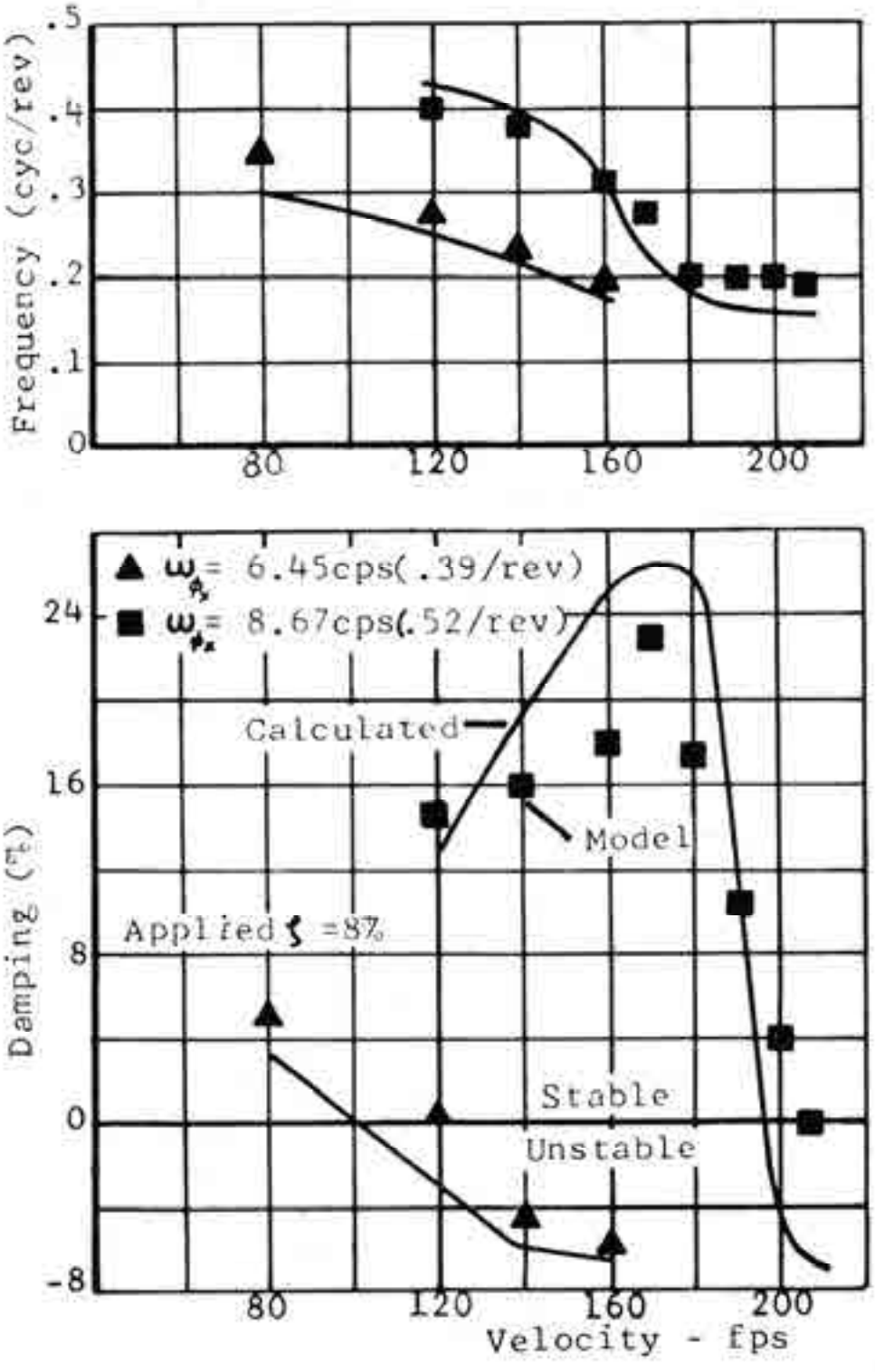

Fig. 2-165. The XV-3's proprotor whirl flutter was predictable [285].

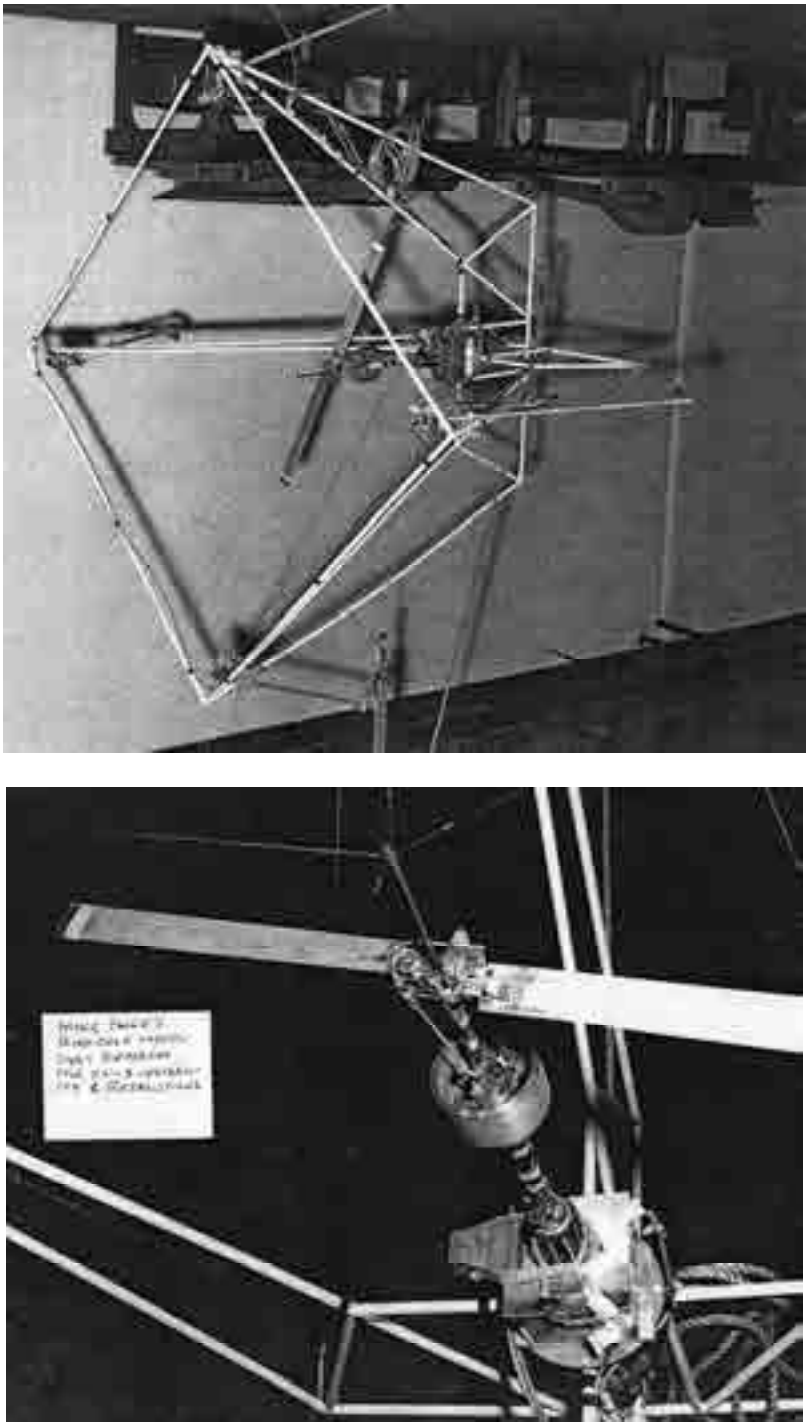

Fig. 2-166. The first proprotor whirl flutter experiment was performed by Bell Helicopter's Mike Paine. Forward flight was simulated by a large fan providing a wind-tunnel-like airstream. The model, which was called the "birdcage," was unpowered and operated like a windmill. The configuration simulated an XV-3 proprotor's potential for a very serious instability (photo courtesy of Ken Wernicke).

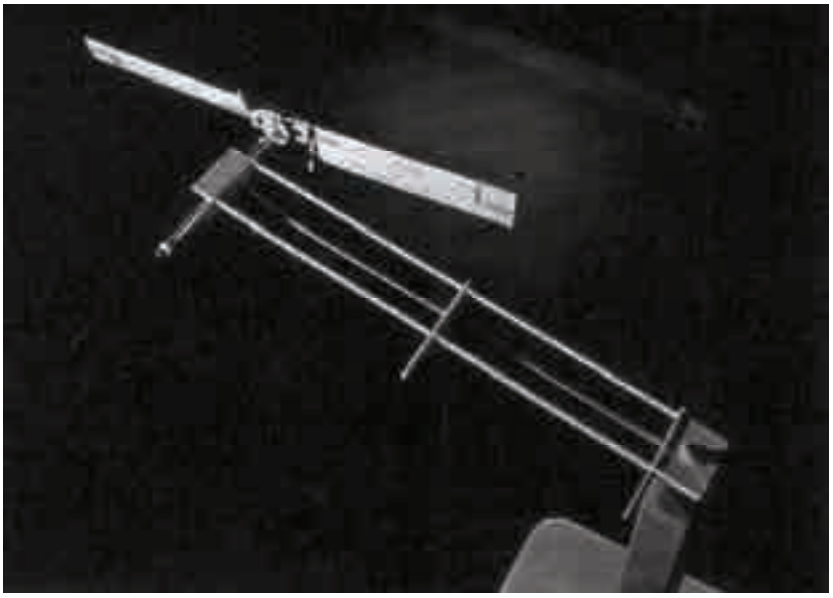

Fig. 2-167. In 1998 Rick Peyran of the AMRDL at NASA Ames built and experimented with this desktop model. He found several configurations that demonstrated whirl flutter in 1998. The 17-inch-diameter model operated as a windmill when the window fan was turned on (photo courtesy of Rick Peyran and Paul Langston).

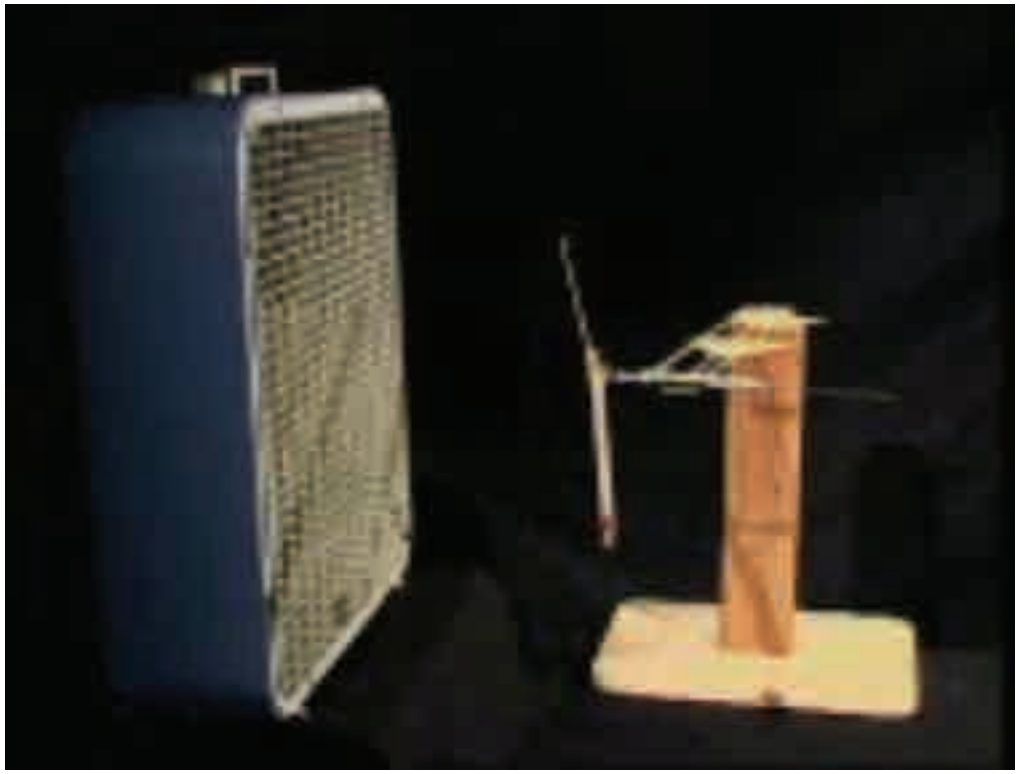

Frame 296. Wind off, model static

Fig. 2-168. An example of whirl flutter.

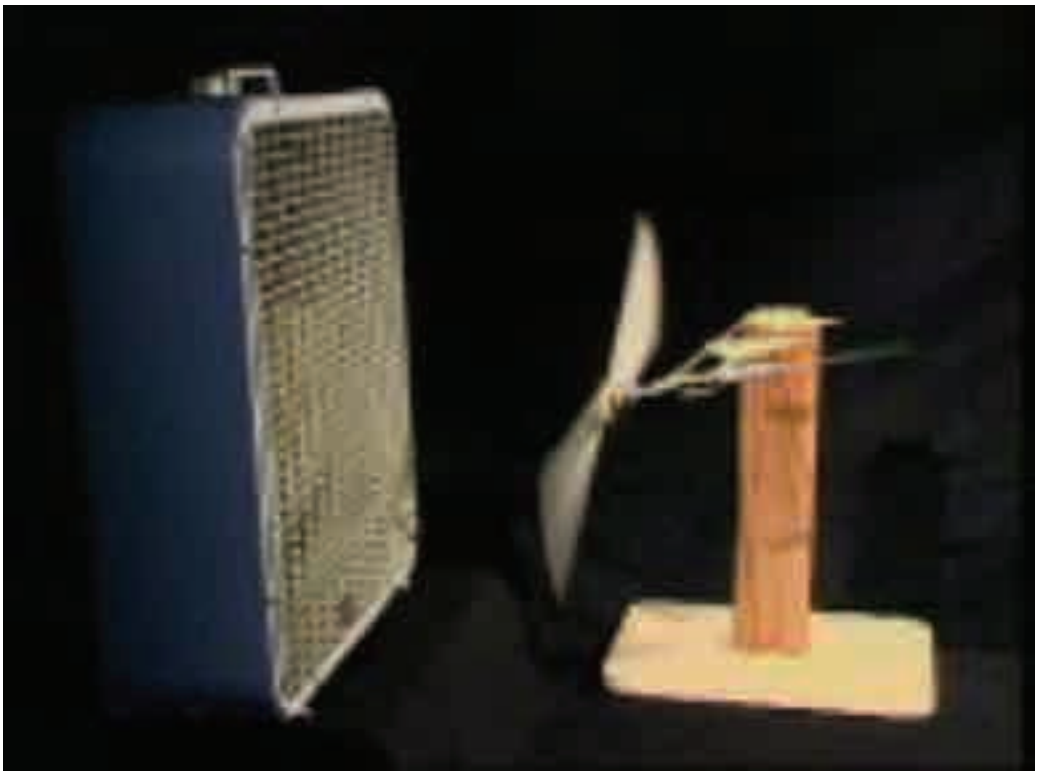

Frame 1645. Most negative twisting (i.e., pitched down) in cycle.

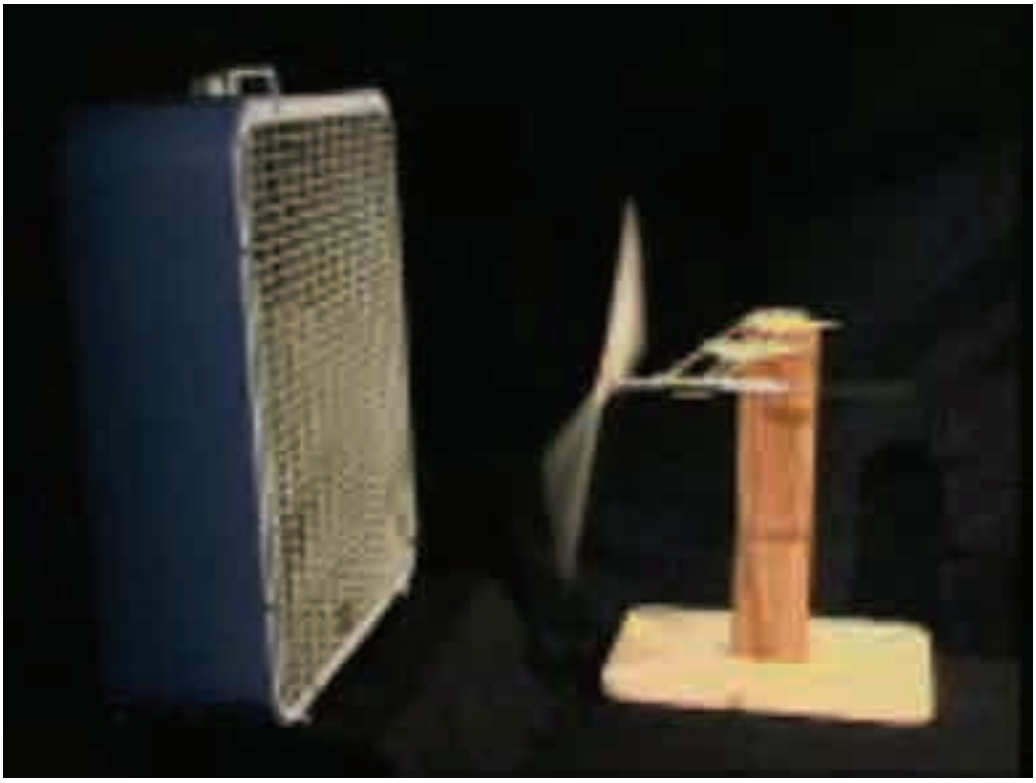

Frame 1646. Pitching up.

Figure 2-168. Continued.

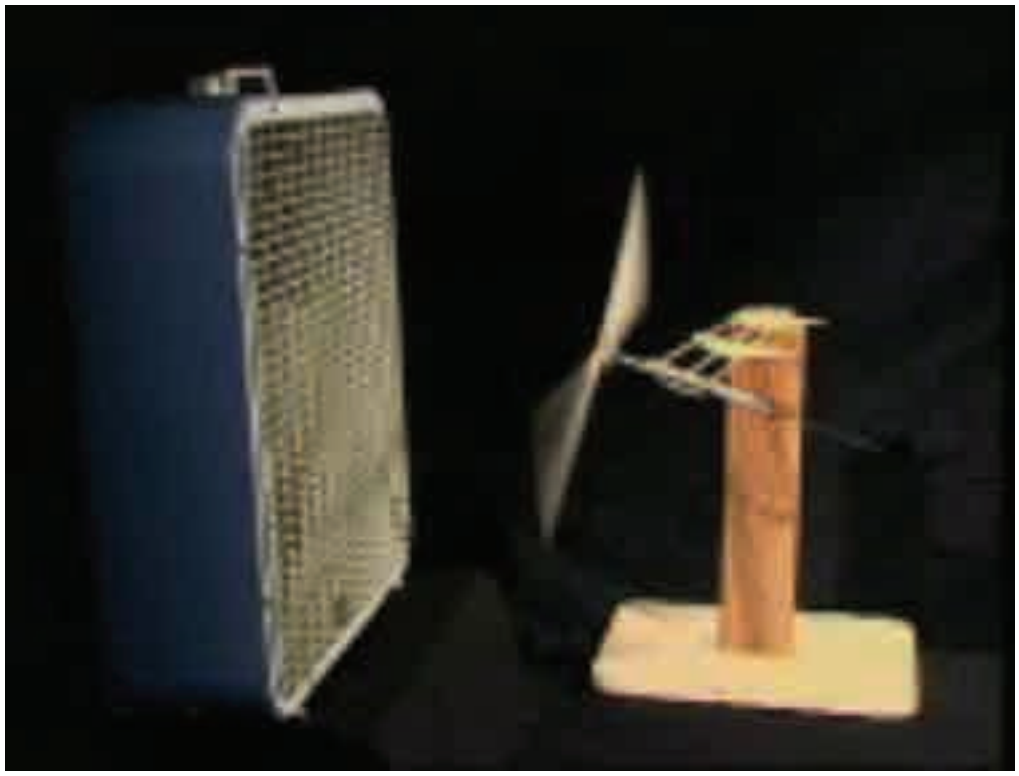

Frame 1647. Maximum pitch up in cycle.

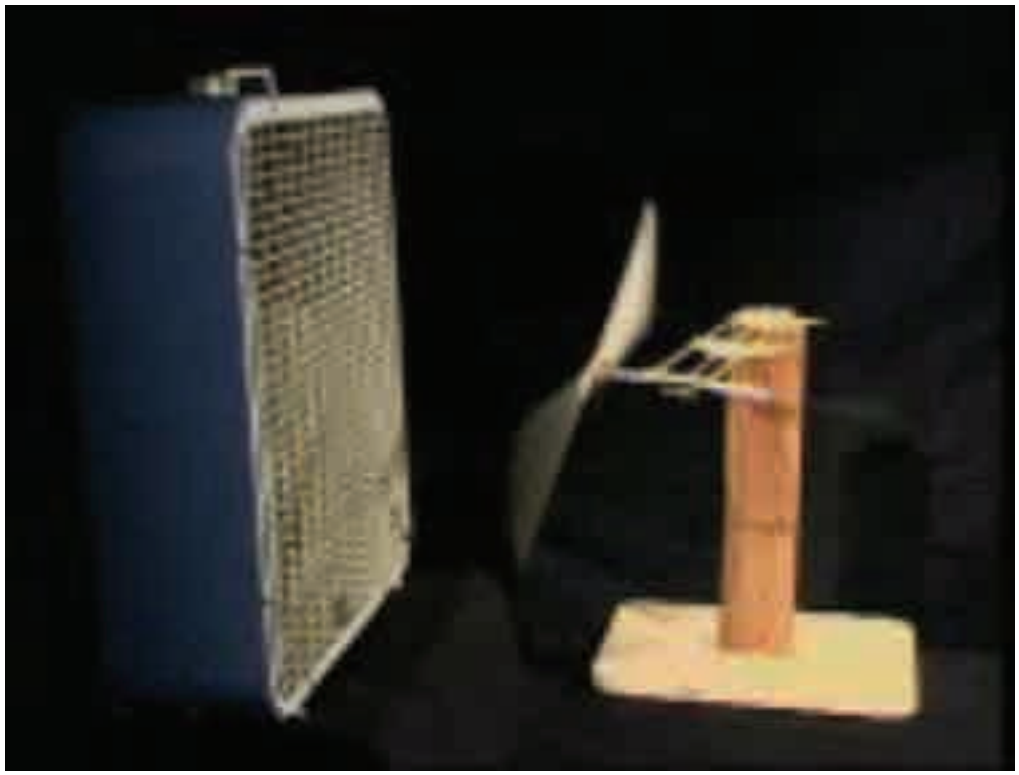

Frame 1648. Pitching down.

Fig. 2-168. Continued.

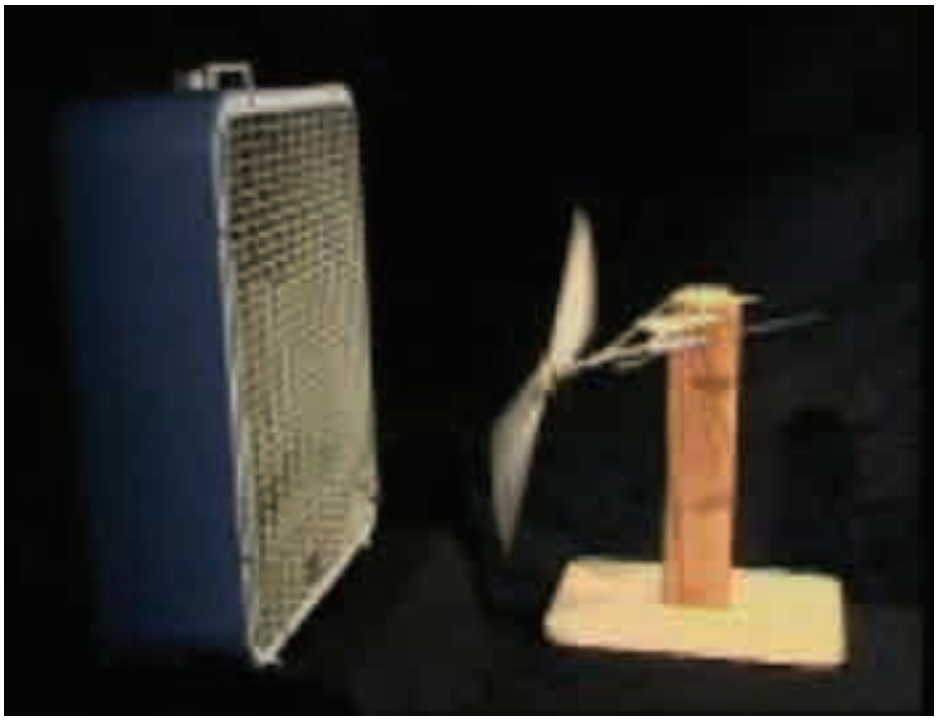

Frame 1649. Back to most negative twist in cycle (Rick Peyran grabbed the model a split second after frame 1649 to stop the twisting motion).

Fig. 2-168. Concluded.

After demonstrating how violent whirl flutter could be, Rick continued the experiment by adjusting the proprotor blades' chordwise center of gravity well forward of the quarter chord with tip weights. This simple design change completely stabilized the proprotor-wing system as you will see from the video at http://rotorcraft.arc.nasa.gov. With this insight, Acree, Peyran, and Johnson published a very significant paper (in my mind) [304] showing how the airspeed at which whirl flutter occurs might be raised—*even with thin wings better suited to high-speed performance*.

Based on the stop-action photos alone shown above, you should have no doubt about how violent proprotor whirl flutter can be. The model proprotor's plane of rotation is clearly not perpendicular to the shaft, and the "wing" is being twisted to an extreme. Watching such a vibration event from the cockpit or as a passenger on a Lockheed Electra would be scary, even if you did not know that in a few more seconds the proprotor, and perhaps the whole wing, were coming off—and you were sure to die.

I would be remiss if I did not provide a bare-bones analysis of whirl flutter in this volume. Let me start with Fig. 2-169, drawn from any frame of the preceding stop-action photos you like. You can immediately see that I have replaced the rotor with one vibratory force, which is the proprotor's H-force. You were first introduced to this force during the discussion about longitudinal stability. To keep things as simple as possible, the thrust (T) and Y-force are dismissed. *This would be quite unacceptable in any modern, computer-based analysis.* As to the wing, it has been replaced with an elastic axis (ea) of length (L) equal to

one-half of the wingspan. This elastic axis has a constant bending stiffness (EI) and constant torsional stiffness (GJ). These stiffness parameters have the units of pound-foot squared. The root end of the wing is hard-mounted to a wall, and this cross section cannot twist or warp. At the free end of the wing (i.e., the tip) I have attached a beam placing the proprotor hub a distance (X_{pr}) ahead of the wing's elastic axis. This beam, representing the proprotor shaft, is absolutely rigid in bending and torsion, and is attached to the elastic axis with a rigid joint. At the free end of the beam, I have replaced the rotor with just one force—the H-force, which varies with time (i.e., $H_{(t)}$) in some manner not immediately known. Note that I have assumed that the center of gravity of this analysis model lies somewhat ahead (X_{cg}) of the wing's elastic axis but behind the proprotor hub.

I have shown the dynamic system at rest with Fig. 2-169 because it fits what I saw before the Peyran, Acree, and Johnson science experiment began. Because the dead weight of the model acts at the model's center of gravity, I placed this force ahead of the elastic axis. And I saw the deflection of the hub (Z_{pr}) and the center of gravity (Z_{cg}) as downward. The deflections depend on both elastic bending *and* torsional deflection. These static deflections are easily determined simply by inspection as

$$(2.152) \quad Z_{pr} = \delta_{ea} + \theta X_{pr} \quad \text{and} \quad Z_{cg} = \delta_{ea} + \theta X_{cg} .$$

Roark, in his standard handbook of beam formulas [310], gives the deflection due to bending as

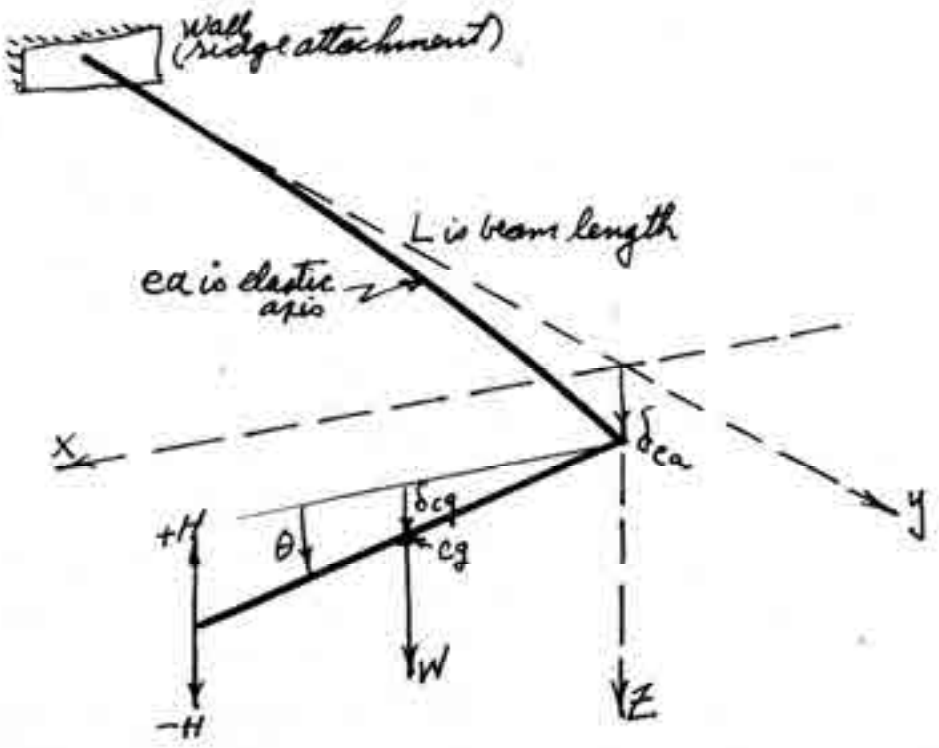

Fig. 2-169. Wing bending and twisting couples with proprotor hub motions and can lead to whirl flutter.

$$(2.153) \quad \delta_{ea} = \left(\frac{L^3}{3EI} \right) \left(W - H_{(t)} \right)$$

and deflection due to twisting of the elastic axis as

$$(2.154) \quad \theta = \left(K_{root} \frac{L}{GJ} \right) \left(W X_{cg} - H_{(t)} X_{pr} \right),$$

where the constant (K_{root}) can vary from one-third (i.e., stiff) up to unity (i.e., soft) and is very dependent on how rigidly the wing is attached to the wall (i.e., the fuselage). You should stay alert about this fact of life when dealing with real hardware. Generally, a beam is calibrated by applying load and measuring the deflection. But in dynamic analyses, the reverse is used because deflections are calculated, and you want the resulting loads to determine if the material is going to break. Thinking of the problem this way gives you spring constants as

$$(2.155) \quad \left(W - H_{(t)} \right) = \left(\frac{3EI}{L^3} \right) \delta_{ea} = K_\delta \delta,$$

and moment due to twisting of the elastic axis is calculated from

$$(2.156) \quad \left(W X_{cg} - H_{(t)} X_{pr} \right) = \left(\frac{GJ}{K_{root} L} \right) \theta = K_\theta \theta.$$

I followed Bisplinghoff, Ashley, and Halfman [271] in deriving the two deflection equations of motion. Skipping the derivation details, let me state directly that

$$(2.157) \quad \begin{aligned} &\frac{W}{g} \frac{d^2\delta}{dt^2} + \frac{W}{g} X_{cg} \frac{d^2\theta}{dt^2} + K_\delta \delta = H_{(t)} && \text{Bending where } K_\delta = \left(\frac{3EI}{L^3} \right) \\ &\frac{W}{g} X_{cg}^2 \frac{d^2\theta}{dt^2} + \frac{W}{g} X_{cg} \frac{d^2\delta}{dt^2} + + K_\theta \theta = X_{pr} H_{(t)} && \text{Torsion where } K_\theta = \left(\frac{3GJ}{L} \right). \end{aligned}$$

With Eq. (2.157) you have a two-degrees-of-freedom (i.e., δ and θ) problem where there is coupling. You see that the two equations of motion are coupled together because a bending deflection term is embedded in the torsion equation, and a torsion deflection term exists in the bending equation. Most unsettling is that both F = ma equations are very dependent on how H-force behaves with time (t).

It is precisely at this point that a useful solution to these differential equations becomes very iffy. Without any better thinking, H-force will be dependent on both deflections involved in the two-degrees-of-freedom equations. Putting myself back in the 1950s, I would be inclined to assume that

$$(2.158) \quad H_{(t)} = \frac{dH}{d\theta} \theta + \frac{dH}{d\dot{\theta}} \dot{\theta} + \frac{dH}{d\ddot{\theta}} \ddot{\theta} + \frac{dH}{d\delta} \delta + \frac{dH}{d\dot{\delta}} \dot{\delta} + \frac{dH}{d\ddot{\delta}} \ddot{\delta}.$$

However this assumption immediately raises the question of how to calculate these six stability derivatives. Fortunately, Earl Hall at Bell developed a more comprehensive solution approach that you can see in his paper [285].

From this brief discussion, I hope you can appreciate why Bob Lynn wrote "that many had *nagging questions* about the pylon oscillations."

Stop for a moment and think about some of the questions that were probably on many tiltrotor advocates' minds just by looking at Eqs. (2.157) and (2.158). Just think about what was left out of the simplest equations of motion that I have constructed, and then begin to worry. For example,

a. Just how complicated is this dynamics problem anyway?

b. What about proprotor thrust and side force? After all, the subject is whirl flutter and these simple equations only permit the hub to rise and fall, not whirl.

c. Where are the standard wing lift, drag, and moment terms?

d. I don't see any terms accounting for the whole aircraft's elastic deflections! What about them?

e. The XV-3's proprotors are going to flap and the blades are flying wings. How are we going to include this third degree of motion with blade elastic deflections?

f. Suppose there is a hub moment due to teetering. What then?

g What happens if we change to a bearingless hub or want to try the Messerschmitt-Bölkow-Blohm (MBB) hingeless blade retention system?

h. Is whirl flutter a showstopper to building large tiltrotors suited to commercial airline operations?

I am sure you get my drift from this starting list of "nagging questions" and, of course, you could add many more. Furthermore, the list of questions is, even today, being added to [306] as experimentation continues [307].

Now let me proceed to what the pilots thought about the XV-3.

2.13.2.5 Pilot Evaluation

A preliminary evaluation of the XV-3 as a VTOL was published on July 22, 1959 [264]. This evaluation for acceptance for more formal military testing was made after military pilots flew the machine at Bell's facility. Then the aircraft was shipped to Edwards Air Force flight test center. The XV-3 was overweight and underpowered, which allowed the Air Force only a very limited amount of flight testing. Still, a report [256] was published in May of 1960 that was favorable for the tiltrotor's future. The conclusions of the report authored by First Lieutenant Wally Deckert, the Project Engineer, and Major Bob Ferry, the Project Pilot, stated (with some of my additions and emphasis) first that

> "Within the scope of the flight test evaluation, it appears that the fixed-wing prop-rotor principle is feasible and should he given serious consideration in future V/STOL design competition. The XV-3 demonstrated that the fixed-wing prop-rotor concept is operationally practical with safety and complexity comparable to helicopters.

> The XV-3 exhibited several features that are considered highly desirable for any V/STOL aircraft. Conversions and reconversions can be easily conducted without scheduling variables such as airspeed, conversion angle, and fuselage attitude. The autorotational and *power-off reconversion capability*, and the prop-rotor damping and inertia provide safety. The XV-3 is operationally practical because of the low downwash velocity and temperature, low vibration levels, reasonable noise levels, and excellent reliability and availability (based upon limited usage). The XV-3 also exhibited good aircraft and prop-rotor control and behavior during wing stall, good rolling take-off performance, and basic controllability *without electronic or mechanical* [stability] *augmentation*."

I recall that even V/STOL advocates who favored high-disc-loading tiltwing machines such as the Vertol VZ-2 (Fig. 2-78, page 138) and the Canadian CL-84 (Fig. 2-86, page 151) were very impressed with the XV-3 and very happy for Bell. Today, I think that this was the beginning of the low-disc-loading versus high-disc-loading choice that V/STOL advocates would offer to the aviation world right down to the present day.

As you know, I believe that the deficiencies pilots find with an aircraft and pass on to a chief engineer are much more valuable than the accolades. After all, a new design is suppose to have great features of considerable value. On the other hand, the new design is suppose to be free of unsatisfactory characteristics, and the XV-3 certainly was no different than the other several hundred aircraft that obtained a thorough military pilot evaluation. For example, Wally and Bob, in their report, stated in the conclusions that

> "The unacceptable deficiencies of the XV-3 that may or may not be inherent were: the erratic lateral darting tendencies and the persistent roll oscillation during hovering flight in ground effect; the sudden requirement for a large increase in power as hovering flight is approached; weak longitudinal and directional controllability coupled with weak lateral-directional stability throughout the low speed, small conversion angle regime; excessive transient prop-rotor blade flapping during longitudinal and directional maneuvering in airplane flight; weak longitudinal dynamic stability in airplane flight at dive speeds; and the high parasite drag in all configurations at high speeds.
>
> Several additional unacceptable deficiencies of the XV-3 were noted during the test program. However, the solutions to these additional deficiencies are of the hardware type and are not inherent in the principle. In this category the unacceptable deficiencies are: the excessive pilot effort required due to the multitude of cockpit controls required for some normal flight maneuvers; the ejection system because it is downward and powered by bungee cords; the skid-type landing gear; and the poor hovering performance and modest performance in airplane flight."

You will find the expanded discussion of these deficiencies in Wally and Bob's report to be of considerable interest.

There was one subject addressed in the evaluation of the XV-3 that tiltrotor advocates forgot to remember, and it became a factor when Bell Boeing and the U.S. Marines were learning how to use the MV-22. You will read about this later. The subject was the behavior of the XV-3 in descent; Wally and Bob stated (with some emphasis by me) that

> "Partial power and power-off descents were conducted in configurations C15, C30, C45, C60 and C75.[85] With partial power, the flying qualities were satisfactory. With power-

[85] The C stands for conversion angle. The numbers that follow state the tilt angle measured from proprotors set for hovering (i.e., C0) down to airplane flight (i.e., C90).

off severe buffet due to wing stall was the primary limiting factor. Some low speed steep power-off descents at C30 to C75 were aborted due to severe buffet, although the prop-rotor rpm could be maintained. *In an emergency this buffet would be a good warning to change the configurations, as necessarily required*. If the airspeed was maintained at 90 knots CAS or greater, the stall buffet was absent or minimized. *In configuration C15 or less, a mild buffet was encountered in a high power descent at low airspeeds. This buffet was characteristic of the buffet commonly experienced in helicopters operating in their own rotor wash.*

During high rates of descent at mid conversion angles with the wing stalled, lateral stability and control was reduced. As previously mentioned, at C15 and low speeds, longitudinal and directional control were inadequate, preventing a precision low speed approach. Interference from wing stall (buffeting) was not encountered during a partial power approach in configuration C15 or less.

Steady state and transient blade flapping were as high in partial power descents as in any other regime (9- to 10-degree peaks were recorded; stops were at 11.5 degrees). These characteristics are acceptable. This is because partial power characteristics were satisfactory, and there was no flight requirement for low speed steady state, power-off descents from configuration C15 to C75. *In the event of a power failure while operating at C15 or more, a continuous reconversion into autorotation could be safely conducted*."

2.13.2.6 Closing Remarks

On the surface, the XV-3 program was a superb achievement given the technology available in the 1950s. V/STOL advocates in the rotorcraft camp were very enthusiastic because their decades-long search culminated in the XV-3. If you think back for a moment, you will recall that Gene Liberatore (Fig. 1-16), Bernie Lindenbaum (Fig. 1-19), and Hal Andrews (Fig. 1-21) sketched out a wide waterfront of configurations that might do what the XV-3 did. However, just below the surface lay the proprotor-pylon-wing dynamic instabilities, which were not well understood at all.

To me, discovering the source of what was first thought to be a flying qualities problem with the XV-3 was the breakthrough that the tiltrotor configuration needed before it could advance one step further. Perhaps it was fate that Ken Amer published his NACA TN 2136 in October of 1950. Ken's report explained a helicopter flying qualities parameter that nobody had thought about before. Perhaps it was also fate that Jan Drees, Bell's chief of technology, and a young Ken Wernicke (see Appendix F) connected and used Ken Amer's finding to start a search for a solution to the whirl flutter phenomena that—without a doubt—blocked any further tiltrotor development. Or perhaps it was just darn good engineers staying abreast of every bit of helicopter technology progress being discovered and then letting their minds wander over all the possible applications. At any rate, to the relief of many, the tiltrotor again became a viable VTOL configuration.

In the meantime, by the mid-1960s the aviation industry had a very good sense of what the tiltwing design offered because the Ling-Temco-Vought (LTV) XC-142A (Fig. 2-76) had been evaluated [177-179]. What had not been settled was whether a stopped and stowed rotor configuration—also offered by a segment of the rotorcraft industry—was to be weeded out. I think this question got settled with the Composite Research Aircraft (CRA) program.

2.13.3 The Composite Research Aircraft Program

There was a preliminary design program sandwiched in between the XV-3 and XV-15 tiltrotor developments. The program began in mid-1967 by the U.S. Army Aviation Material Laboratories (AVLABS) branch located at Fort Eustis, Virginia. The program was formally known as the Army VTOL Rotary Wing Composite Research Aircraft (CRA) program, but was generally referred to as the CRA preliminary design study, or just the CRA for short. The general objective of the CRA was to combine the efficient hovering characteristics of a helicopter and the high-speed-cruise characteristics of a fixed-wing aircraft into one research aircraft. Today you might wonder about the use of the word composite because we are now inclined to think of composite as a material; but in the 1960s, what was sought was a composite of two aircraft. Nevertheless, the objective has been periodically examined for decades, and the CRA was one of many searches made. In fact, there appears to be no end to the search for such a "composite" aircraft—tiltrotors and tiltwings not withstanding.

AVLABS established eight key aircraft requirements, and three aviation manufacturing companies completed preliminary designs to meet the requirements. The CRA requirements were:

1. Payload—3, 000 pounds,
2. Fuel—3, 000 pounds,
3. Vertical takeoff and landing,
4. Hover (OGE) at 95°F and 6,000-foot pressure altitude (density ratio of 0.74936),
5. Disc loading—10 pounds per square foot or less,
6. Speed—300 knots required (400 knots desired),
7. Lift-to-drag ratio—at least 10, and
8. Cargo compartment size—5.5 feet wide by 6 feet high by 14.5 feet long.

Two companies, Bell Helicopter Textron and Lockheed California, were paid $1.9 million each to complete their efforts [311]. A third company, Hughes Tool Company, Aircraft Division, also received a contract, but I have not been able to determine how much money it was paid for its effort. The contractual start date was March 24, 1967, and by January 1969, AVLABS had a sizable summary volume from each company. The Army's view was that if development of the Bell, Lockheed, and Hughes "convertible" aircraft was "as successful as anticipated, engineers foresee a VTOL/STOL advance that could be adjudged a major aeronautical achievement of this decade."

As you will read in the following pages, Lockheed designed a stopped and stowed rotor compound, Hughes designed a tip-driven hot cycle rotor for hover that also was stopped and became the wing for airplane flight, and Bell designed a tiltrotor. Let me discuss each composite aircraft configuration in turn, and then provide a table and a few summary remarks comparing the three designs.

2.13.3.1 The Lockheed Stopped-Stowed Rotor (AVLABS TR 68-40)

Lockheed's 406-page report [312] introduces their design with two major points. First they point out that the U.S. Air Force program from the 1950s that led to flight test evaluation of the McDonnell XV-1 compound and the Bell XV-3 tiltrotor left the Sikorsky stopped and stowed XV-2 behind. The report states that "the stopped-rotor concept, however, was not carried through a flight test program and therefore has not had the opportunity of a demonstrated acceptance." Then the report proceeds to its second introductory point, stating that

> "Recent development of the rigid-rotor [called bearingless rotor today] system, which eliminates the need for conventional flapping and lead-lag hinges, offers an opportunity for developing a successful stopped-and-stowed-rotor concept. Such programs as the XH-51A helicopter and the testing on a modified compound XH-51A, which led to the award of the Advanced Aerial Fire Support System (AAFSS), form the basis for the design, as presented in this report of a stopped-rotor system.
>
> Recently, technical feasibility of the stopped-rotor concept was positively confirmed with the successful completion of a wind tunnel test program using a full-scale 33-foot-diameter rotor in the NASA Ames 40- x 80-foot wind tunnel, reference BuWeps Contract, NOw 66-0246-f [313]. Rotor start and stop testing, with blade folding and extending, was performed in the tunnel tests. Start/stop tests were made at wind tunnel speeds and rotor angles of attack of 80 knots from 0 to 12 degrees, 100 knots from 0 to 6 degrees, 120 knots from 0 to 2 degrees, and 140 knots at 0 degrees. A total of 55 start/stops were successfully completed. In conjunction with the start/stop tests, blade folding and extending tests were conducted at speeds up to 140 knots. Results of these tests can be used to substantiate the analysis and design of the stowed-rotor concept. This wind tunnel test vehicle was designed to transition at a forward speed of 120 knots with a margin over transition to 140 knots.
>
> The preliminary design of the Composite Research Aircraft (CRA) incorporates design features of this test rotor. Control actuators are close coupled with the swashplate. A simple fold mechanism developed on the test rotor has also been employed. These tested mechanical design features, coupled with the successful completion of the wind tunnel tests, provide a high degree of confidence that the stowed-rotor concept will be successfully developed."

Thus, Lockheed established both the need for, and the technical confidence in, their design and hopefully a follow-on program of flight research. You can find several additional papers of interest in references [314-318].

Lockheed's stopped and stowed rotor composite aircraft (Fig. 2-170) met AVLABS' objectives with a design gross weight of 24,500 pounds (Table 2-17) using a 60-foot-diameter, three-bladed rotor. The disc loading at sea level was 8.66 pounds per square foot, which increased to 10 pounds per square foot for the hot and high design condition. Each T64-GE-16 could deliver a maximum of 3,435 horsepower at zero speed and at sea level on a standard day. Performance calculations indicated that the machine was capable of hovering at 6,800-foot pressure altitude on a 95 ^{o}F day, thus exceeding the requirement by 800 feet.

As to meeting the forward-flight requirements, the aircraft's wingspan was 50 feet and the area was 279 square feet, which gives an aspect ratio of just under 10. The four-bladed propellers had a diameter of 10 feet, and the blade activity factor was 120. The clearance between the propeller's blade tips and the fuselage was 7 inches. Based on the estimated

power required of 1,270 horsepower at 175 knots and 24,500 pounds design weight, Lockheed achieved a lift-to-drag ratio of 10.4 when calculated by $\frac{L}{D}=\frac{W(1.69V_{knots})}{550SHP}$. The minimum equivalent parasite drag area was estimated at 11.21 square feet. Calculations showed the configuration would achieve about 350 knots at sea level on a standard day with both engines at military rated power and producing 7,600 horsepower.

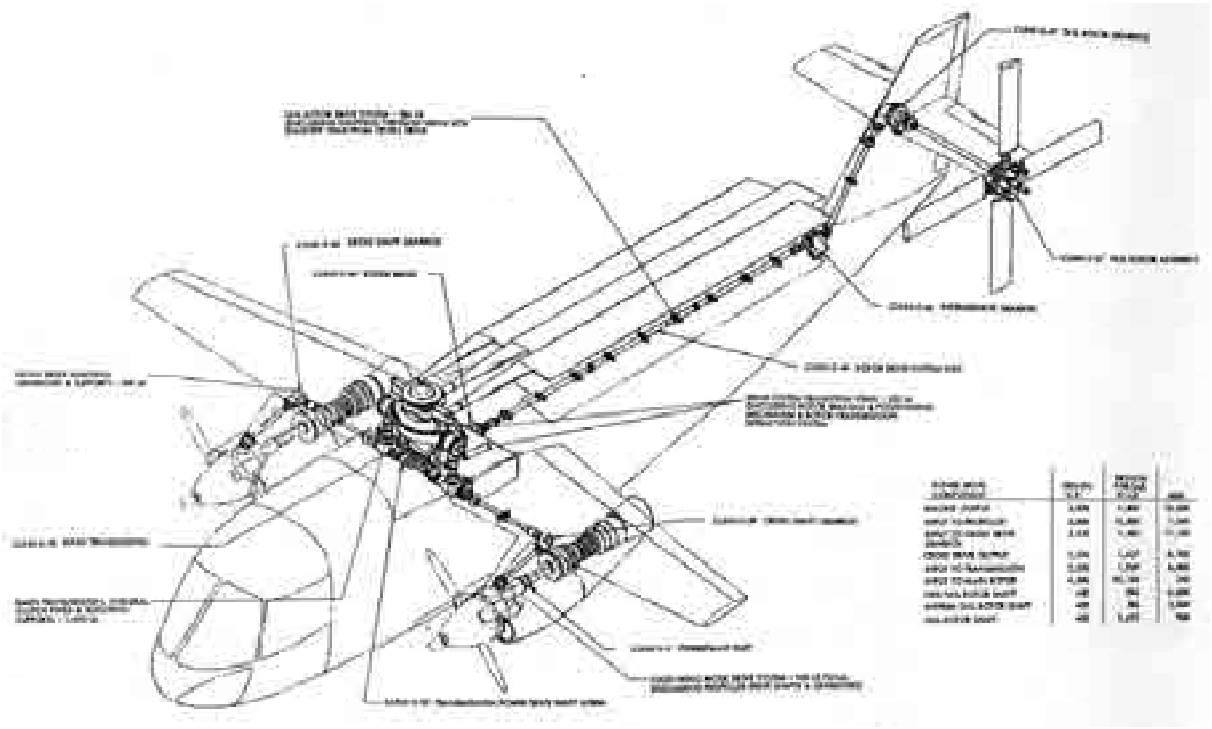

Fig. 2-170. The rotor blades were only partially enclosed for forward flight with Lockheed's stopped and stowed composite research aircraft [312].

Table 2-17. Summary Weight Statement for the Lockheed CRA

Item	Weight (lb)
Weight empty	17,961
Pilot	200
Copilot	200
Oil (including unusable)	119
Unusable fuel	20
Payload	3,000
Fuel	3,000
Design gross weight	24,500
Overload gross weight	28,800
Ferry takeoff weight	31,200
Hover OGE 6,000 feet, 95 ^{o}F	24,900

2.13.3.2 The Hughes Hot Cycle Rotor/Wing (AVLABS TR 68-31)

Hughes' 307-page report [319] presents a VTOL having a maximum speed of nearly 500 knots. The tip-driven rotor was based on the Hughes hot cycle XV-9A research helicopter [320] developed during the early 1960s. The report's introduction states that

> "The Hot, Cycle Rotor/Wing combines, for the first time, the helicopter and the jet airplane in the form of the Hot Cycle Rotor/Wing lifting system. This is a tip-jet powered helicopter rotor with a very large hub. The Rotor/Wing can be stopped in flight to become a fixed wing (figure 2), and the aircraft flies as a jet airplane.
>
> The Hot Cycle Rotor/Wing CRA provides the advantages of hovering efficiency, low downwash velocity, and helicopter-like flying qualities for vertical and low-speed flight, in addition to the high-speed capability and cruise efficiency of the jet airplane. Its simplicity and light weight is made possible through the combined use of the all-pneumatic Hot Cycle drive system and the dual-purpose Rotor/Wing lift system. This eliminates the need for heavy and complex mechanical drive components and antitorque tail rotor; it permits flight as a helicopter and as an airplane without recourse to duplicate lifting systems or to folding, tilting, or retracting of lift systems to effect conversion.
>
> With excellent hover and payload capabilities, a maximum speed of 490 knots, and maximum lift-to-drag ratio of 12, the Hot Cycle Rotor/Wing will exceed all CRA performance requirements and will make possible a major advance in vertical-lift aircraft technology.
>
> Substantiation of all basic technical aspects of the CRA design is available from the results of the USAAVLABS XV-9A Hot Cycle Research Aircraft program and from extensive Hughes- and Government-sponsored analysis, whirl testing, and wind tunnel testing that have defined basic aerodynamic characteristics of the Rotor/Wing in all modes of flight. The Composite Research Aircraft based on the Rotor/Wing will further substantiate and refine the concept."

The Hughes hot cycle composite aircraft (Fig. 2-171) met AVLABS' objectives with a design gross weight of 19,635 pounds (Table 2-18) using a 50-foot-diameter, three-bladed rotor with a very large hub (Fig. 2-172) and relatively short blades (Fig. 2-173). The disc loading at sea level was 10 pounds per square foot, which increased to 11.5 pounds per square foot for the hot and high design condition. The single Pratt & Whitney J52-P-8A could deliver a maximum static thrust of 9,300 pounds at sea level on a standard day with a fuel flow of 8,000 pounds per hour. Performance calculations indicated that the machine would be capable of hovering out of ground effect at 13,100-foot pressure altitude on a 95 ^{o}F day. At 6,000 feet on a 95 ^{o}F day, the aircraft was calculated to hover at a gross weight of 26,000 pounds, which meant a payload of 9,365 pounds versus the 3,000-pound requirement. The hover C_T versus C_Q (Fig. 2-174) was based on corrected whirl tower test data.

As to meeting the forward-flight requirements, the aircraft's wing area was 526 square feet assuming just two swept blades giving a wingspan of 44.8 feet. This was an aspect ratio of 3.81. The maximum speed of 490 knots was to be obtained at 13,000 feet on a standard day. Hughes calculated a maximum lift-to-drag ratio of 12.0 at a lift coefficient of about 0.3. The minimum equivalent parasite drag area in airplane mode was estimated at 8.8 square feet, and the Oswald span efficiency factor used in the performance calculations was 0.895.

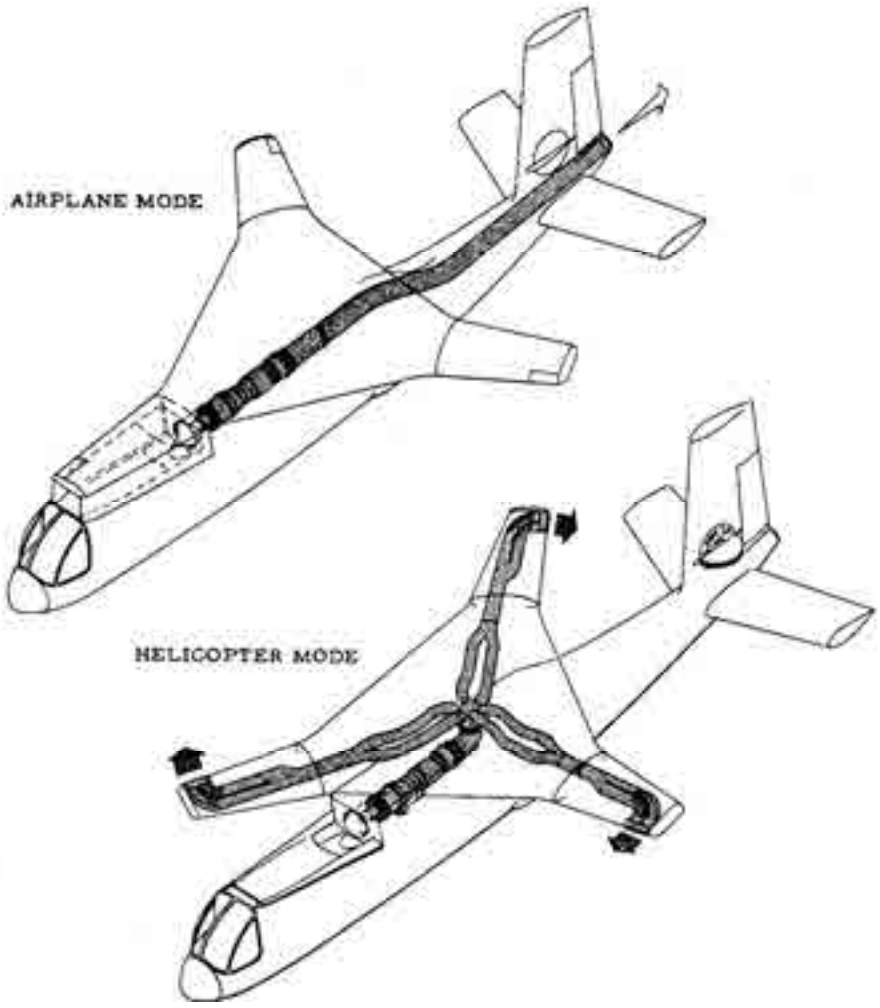

Fig. 2-171. The Hughes composite aircraft with its tip-driven rotor required a 4.7-foot shaft-driven tail rotor for yaw control [319].

Table 2-18. Summary Weight Statement for the Hughes CRA

Item	Weight (lb)
Weight empty	13,169
Pilot	200
Copilot	200
Oil (including unusable)	36
Unusable fuel	30
Payload	3,000
Fuel	3,000
Design gross weight	19,635
Overload gross weight	30,000
Ferry takeoff weight	30,000
Hover OGE 6,000 feet, 95 ^{o}F	26,000

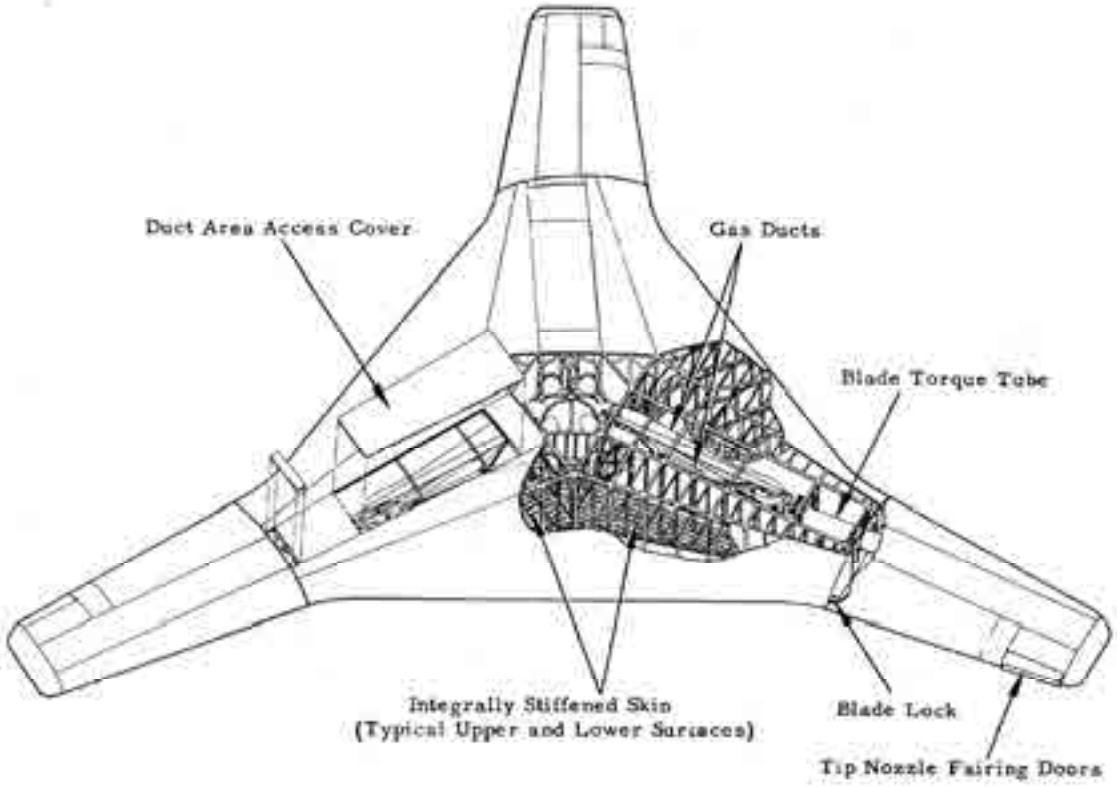

Fig. 2-172. The Hughes CRA hub was an integral part of the "wing" [319].

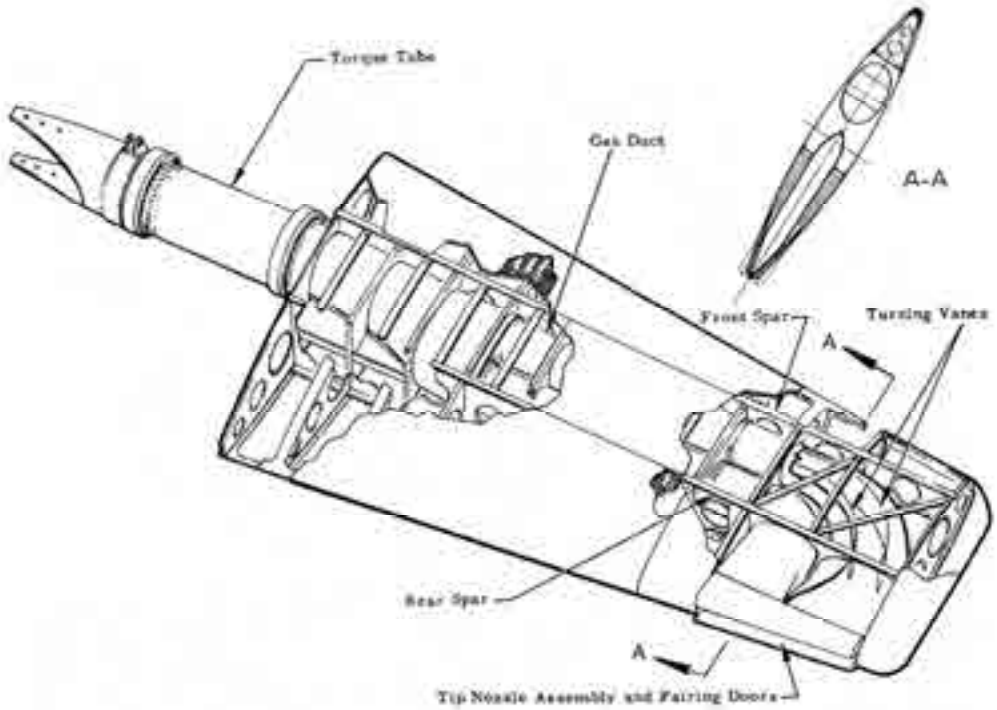

Fig. 2-173. The "rotor blades" were very short compared to those of a conventional helicopter [319].

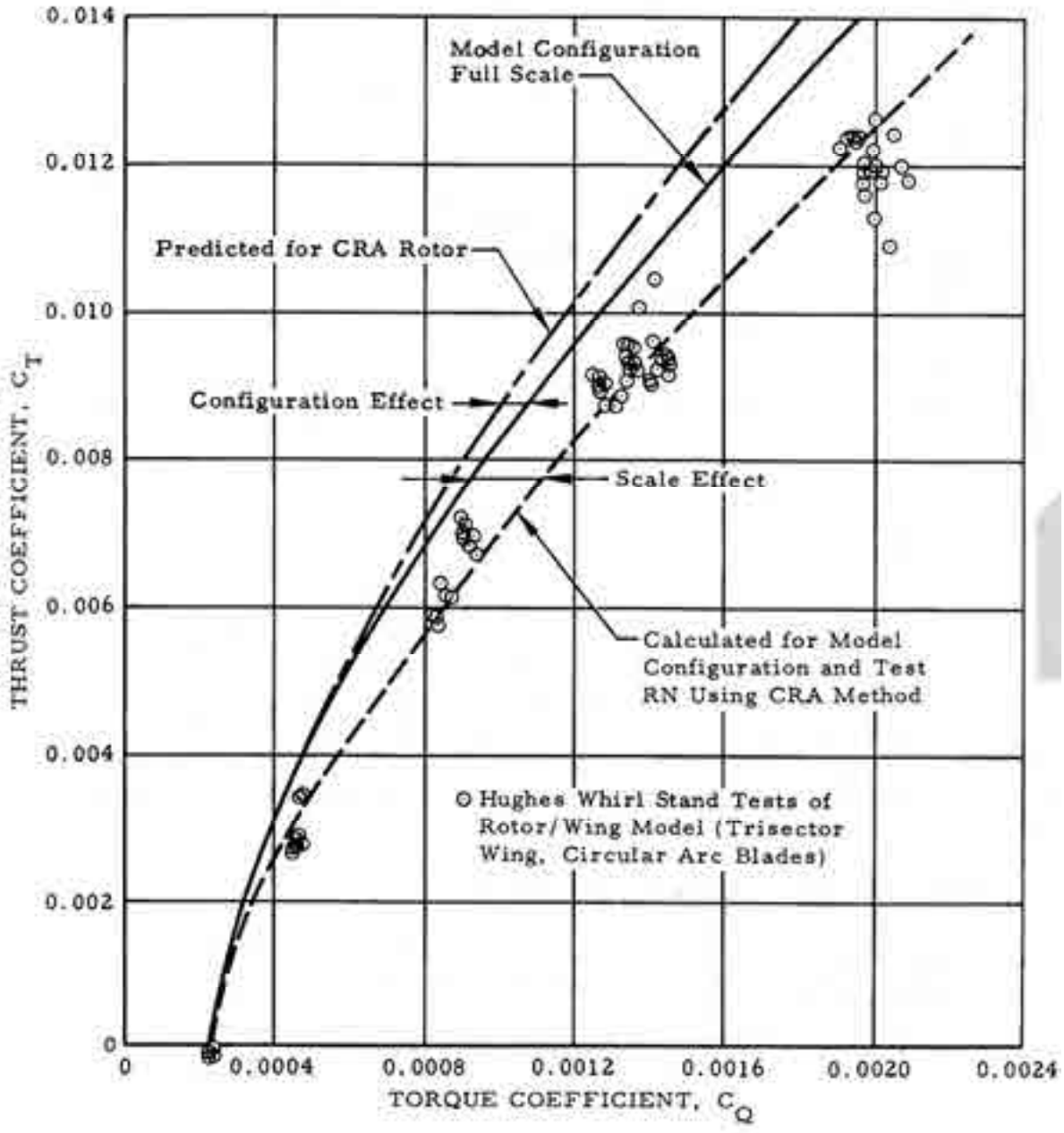

Fig. 2-174. Hughes based the estimate of hover performance on model tests. The three-bladed model had a diameter of 80 inches and a nominal solidity of 0.159 [319].

2.13.3.3 The Bell Tilt Proprotor (AVLABS TR 68-32)

In its introduction, Bell's 447-page report [321] authored by Ken Wernicke advocates the tiltrotor configuration by stating that

> "The basic objective of the Bell D266 Composite Aircraft design is to achieve efficient vertical flight and efficient fixed-wing cruise flight with the simplest possible mechanical systems and pilot-control procedures. The tilt-rotor configuration makes it possible to avoid duplicating systems—such as dual powerplants, one kind for lift and another for cruise; or dual propulsion elements, such as rotors for low speed and propellers, shrouded fans, or jets for fixed-wing flight, each with its associated drive gearing and clutching or diverter-valve arrangements. This approach is a factor in designing an aircraft with a low empty weight and therefore a high useful-load-to-gross-weight ratio—a key factor that determines the effectiveness of any aircraft."

Bell pointed to its experience with the XV-3 as substantiation for its Model 266 composite research aircraft design. The report notes that

> "Following its initial development and flight testing by Bell, the XV-3 was put through an extensive series of flight tests by U.S. Air Force, NASA, and U.S. Army test groups. The total test program has included over 500 hours of flight, wind-tunnel, and ground-run time, including over 250 test flights in 125 hours of flight time. The test aircraft was flown by ten Government test pilots as well as two Bell pilots, who made over 110 full conversions to fixed-wing configuration and over 30 gear shifts to low-rpm cruise operation. *Five of the Government test pilots made power-off reconversions from cruise flight to helicopter autorotation* [my italics].
>
> In addition to the basic XV-3 program, several related Government-sponsored R&D programs have been conducted. These include a preliminary design study of an 80,000-pound gross weight machine for the USAF, two series of wind-tunnel tests of powered quarter-scale tilt-rotor models, and extensive computer studies of the aerodynamics of rotors in axial flight operation. Since 1961, work has been intensified to expand the tilt-rotor design base established by the XV-3 program. This work has included several detailed design studies of tilt-rotor aircraft for a variety of military and civil applications. A specific example is Bell's D252 Tri-Service Transport Aircraft, designed for a 4-ton payload.
>
> Extensive dynamic model testing and analytical work have been conducted to explore characteristics of rotor-pylon systems operating at speeds up to 500 knots. As a result of the model and analytical programs, design tools are now available which should lead to development of tilt-rotor aircraft more nearly free of dynamic problems. All of this work, especially the XV-3 program, where full-scale problems have been encountered and solved, is directly applicable to the composite research aircraft."

Bell's technical substantiation data and experience with models (specifically with whirl flutter) are documented in reference [322].

Bell's tiltrotor (Fig. 2-175 through Fig. 2-178) met AVLABS' objectives with a design gross weight of 23,000 pounds (Table 2-19) using two 38.5-foot-diameter, three-bladed rotors. The disc loading at sea level was 9.88 pounds per square foot, which increased to 11.4 pounds per square foot for the hot and high design condition. Each T64-GE-12 engine could deliver a maximum of 3,435 horsepower at zero speed and at sea level on a standard day. The proprotor speed in hover was 372 rpm. Performance calculations indicated that the machine would be capable of hovering out of ground effect (HOGE) at 11,050-foot pressure altitude on a 95 ^{o}F day at the design gross weight. At 6,000 feet, the aircraft was calculated to hover

HOGE at a gross weight of 28,000 pounds. The report indicates that the machine could hover OGE on one engine at sea level on a 95 ^{o}F day and at 6,000 feet on a standard day. Bell's cargo compartment size was extended beyond the requirement by 6 feet, 9 inches, thus providing space for 24 troops. The drivetrain schematic is shown in Fig. 2-179, and the proprotor hub assembly is shown in Fig. 2-180.

As to meeting the forward-flight requirements, the aircraft's wing area was 330.5 square feet and the span was 46.8 feet, which is an aspect ratio of 7.44. The maximum speed was estimated to be 385 knots at 12,000 feet on a standard day. In airplane mode, proprotor speed could vary between 198 and 297 rpm as determined by drivetrain torque limits. Bell calculated its aircraft would have a maximum lift-to-drag ratio of 10.0. The minimum equivalent parasite drag area in airplane mode was estimated at 9.51 square feet.

Fig. 2-175. Bell pointed to several model tests as substantiation for its Model 266 design [321].

Table 2-19. Summary Weight Statement for the Bell CRA

Item	Weight (lb)
Weight empty	15,994
Pilot	200
Copilot	200
Oil (including unusable)	55
Unusable fuel	20
Payload	3,000
Fuel	3,000
Growth potential	440
Design gross weight	23,000
Overload gross weight	30,800
Ferry takeoff weight	41,500
Hover OGE 6,000 feet, 95 ^{o}F	28,000

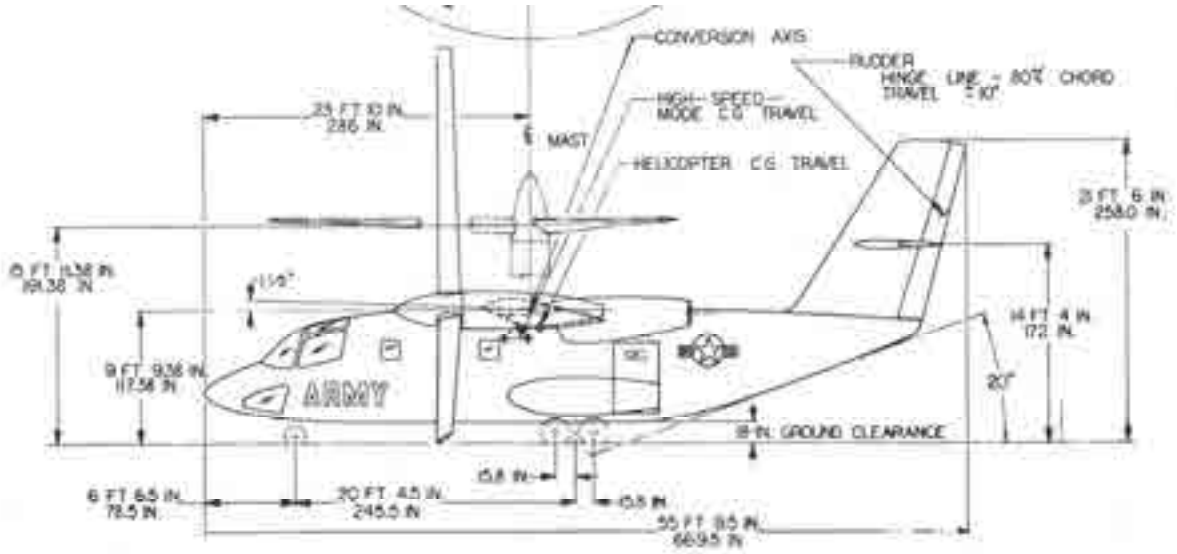

Fig. 2-176. The Bell CRA was rather short coupled, but it still had a cargo compartment sized for 24 troops [321].

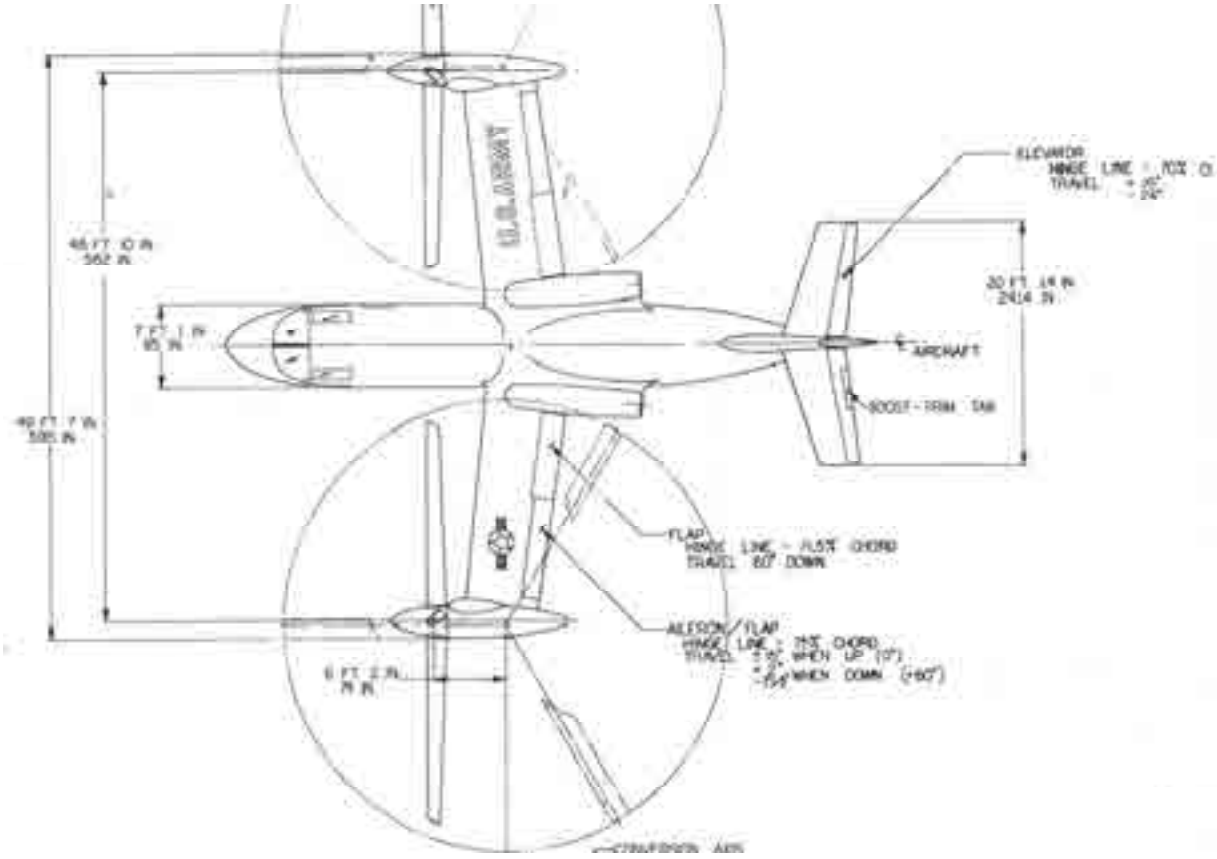

Fig. 2-177. The engines were mounted close to the fuselage, and they did not tilt as the rotors tilted [321].

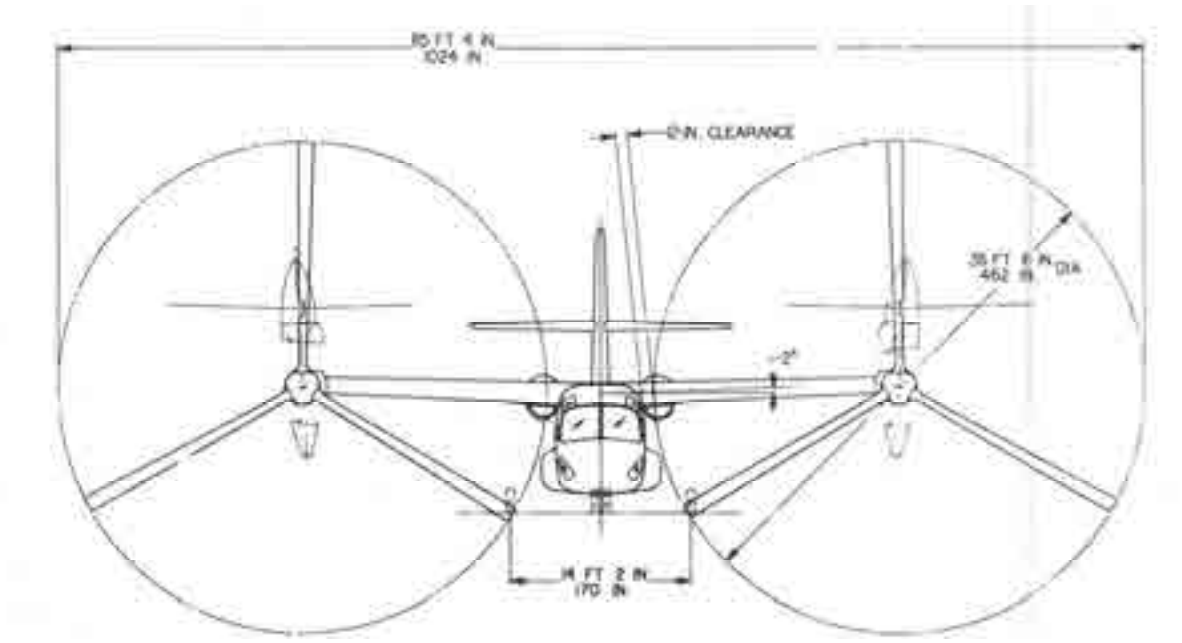

Fig. 2-178. This view shows that a power-off landing *might* be made with the rotors still in airplane mode [321].

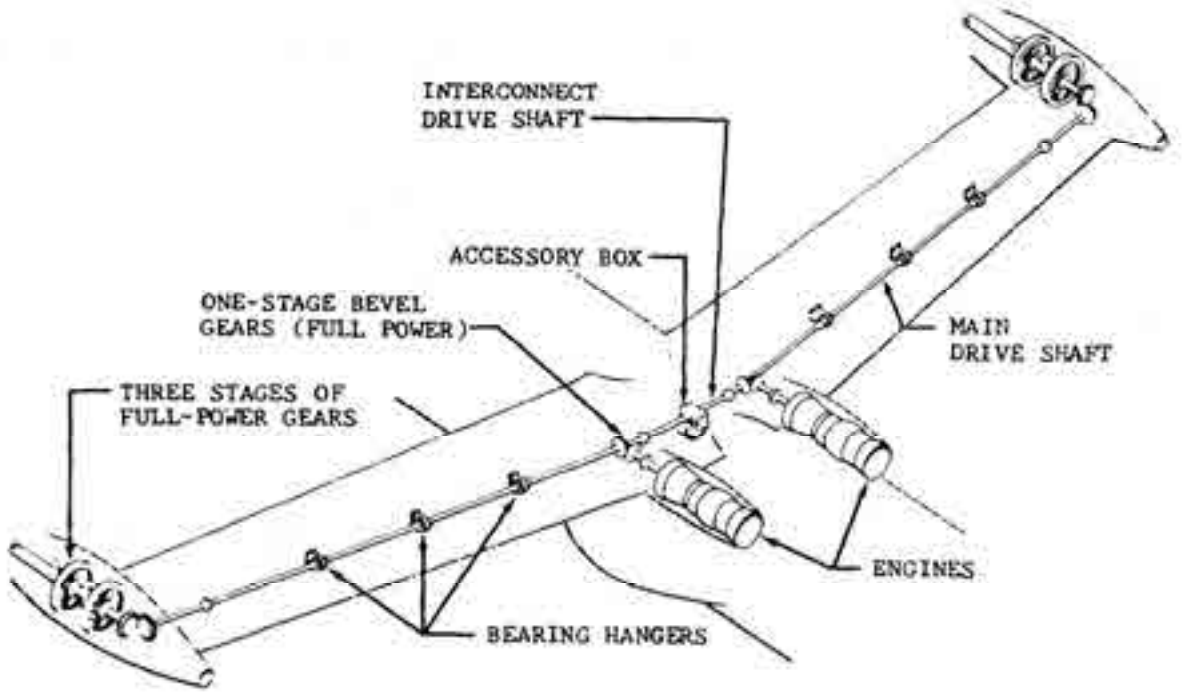

Fig. 2-179. The interconnecting shafts must carry full engine power with this drivetrain arrangement [321].

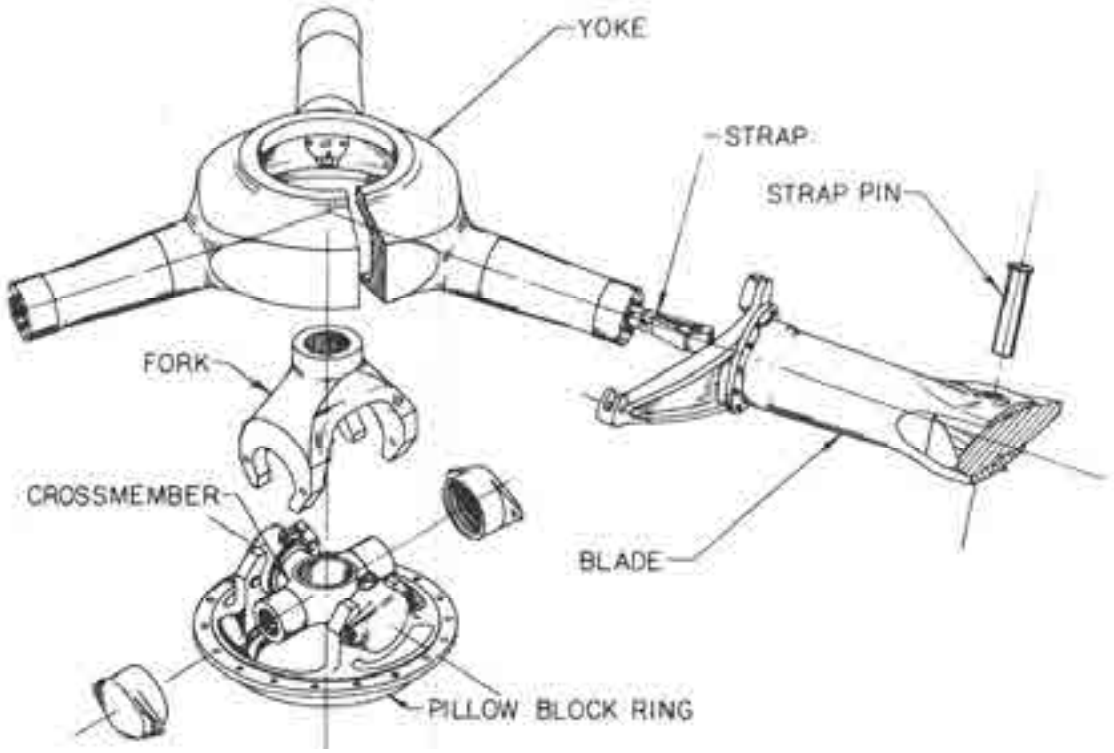

Fig. 2-180. The Bell CRA proprotor hubs had a universal joint to provide a gimbal degree of freedom. This was a simple variation of Bell's two-bladed seesaw rotor hub design [321].

2.13.3.4 Composite Research Aircraft Comparisons

Each of the CRA design reports provides a wealth of information. In my mind, the advocates reported more thorough preliminary design results than you are likely to find in many later studies the industry has made. The data from this 1960's effort leads to several comparisons that you may find quite interesting. To begin with, all three designs met or exceeded the eight key requirements. The design gross weight was to include a useful load of 6,000 pounds distributed equally between fuel and payload. Enough power was to be installed so that hovering out of ground effect at 6,000-foot pressure altitude with an outside air temperature of 95 ^{o}F was ensured. Table 2-20 shows the weight and uninstalled engine power required to satisfy these requirements. The rotor diameter necessary to meet the low-disc-loading requirement led to large rotor diameters typical of helicopters. The three designs met the 300-knot speed requirement and, in fact, did much better as Table 2-20 shows.

The CRA contracts required tabulation of each aircraft's weight empty in MIL-STD-451, Part 1 format. In my experience, component weights at this level of detail are not always published unless a contractual requirement is included. In this instance, Table 2-21 shows that some very creative design thinking was employed by the three contractors. On the other hand, no contingency weight was included, which makes the total weight empty calculations quite optimistic considering the aviation industry's poor track record in meeting any weight empty objective.

Table 2-20. All CRA Designs Met or Exceeded AVLABS' Requirements

Objective	Lockheed Stopped-Stowed	Hughes Hot Cycle	Bell Tiltrotor
Design gross weight and hover OGE ceiling on a 95 °F day with 6,000 lb useful load	24,500 lb 6,800 ft	19,635 lb 13,100 ft	23,000 lb 11,050 ft
Weight empty	17,961 lb	13,169 lb	15,994 lb
Engine (number)	T64-GE 14 (2)	J52-P-8A (1)	T64-GE 12 (2)
Uninstalled military rated power (SL, std)	3,435 hp	9,300 lb	3,435 hp
Fuel flow (all engines, MRP at SL, std)	1,650 lb/hr	8,000 lb/hr	1,650 lb/hr
Number of rotors	One	One	Two
Rotor diameter (disc loading at SL, std)	60 ft (10)	50 ft (10)	38.5 ft (9.88)
Wing area	279.0 sq ft	526.0 sq ft	330.5 sq ft
Wingspan	50 ft	44.8 ft	46.8 ft
Speed Altitude Uninstalled engine horsepower at altitude	378 kts 10,000 ft 5,400 hp	490 kts 13,000 ft 9,000 hp (est)	385 kts 12,000 ft 4,300 hp
Lift-to-drag ratio (10 or better)	10.4	12.0	10.0
Minimum parasite drag area (f_e)	11.21 sq ft	8.80 sq ft	9.51 sq ft
Cargo compartment size—5.5 feet wide by 6 feet high by 14.5 feet long	14.5 feet long	14.5 feet long	21.4 feet long

Table 2-21. The CRA Design Reports Provided Weight Empty Data in MIL-STD-541, Part 1 Format

Item	Lockheed Stopped-Stowed	Hughes Hot Cycle	Bell Tiltrotor
Rotor group	2,150	700	2,439
Wing group	1,540	2,053	1,886
Tail group	611	704	444
Body group	3,046	2,098	2,048
Alighting gear group	889	600	776
Flight controls group	1,010	729	865
Nacelle group	804	240	353
Propulsion group	5,361	3,545	4,633
Auxiliary power plant	150	150	150
Instruments group	178	120	116
Hydraulics group	181	205	144
Electrical group	524	300	307
Electronics group	900	900	900
Armament group	300	250	300
Furnishings and equipment group	262	527	533
Air conditioning group	55	40	100
Other	0	8	0
Weight empty	17,961	13,169	15,994

2.13.3.5 Closing Remarks

There are several observations about the aircraft designs that industry provided to AVLABS that I found quite interesting. For instance, each company calculated a payload-versus-range graph although no formal requirement was stated. I assume AVLABS did not have a mission requirement because it was research aircraft (a technology demonstrator, if you prefer) that they wanted. Therefore, the fuel requirement was just to have 3,000 pounds of fuel available for flight testing. Nevertheless, the payload–range comparison between the three VTOLs shown here in Fig. 2-181 is quite informative. Of course, making the comparison at 10,000 feet on a standard day shows the Hughes hot cycle design in a poor light. The Hughes design was more like a jet fighter than a propeller or proprotor-driven troop transport design as envisioned by Lockheed and Bell.

The three reports made estimates of ferry range, which is also of interest. Table 2-22 shows that designs from both Lockheed and Hughes could make the passage from the West Coast to Hawaii. Bell selected a more ambitious objective of "unescorted flight capability across the Atlantic and Pacific Oceans." However, a rolling takeoff was required in Bell's CRA.

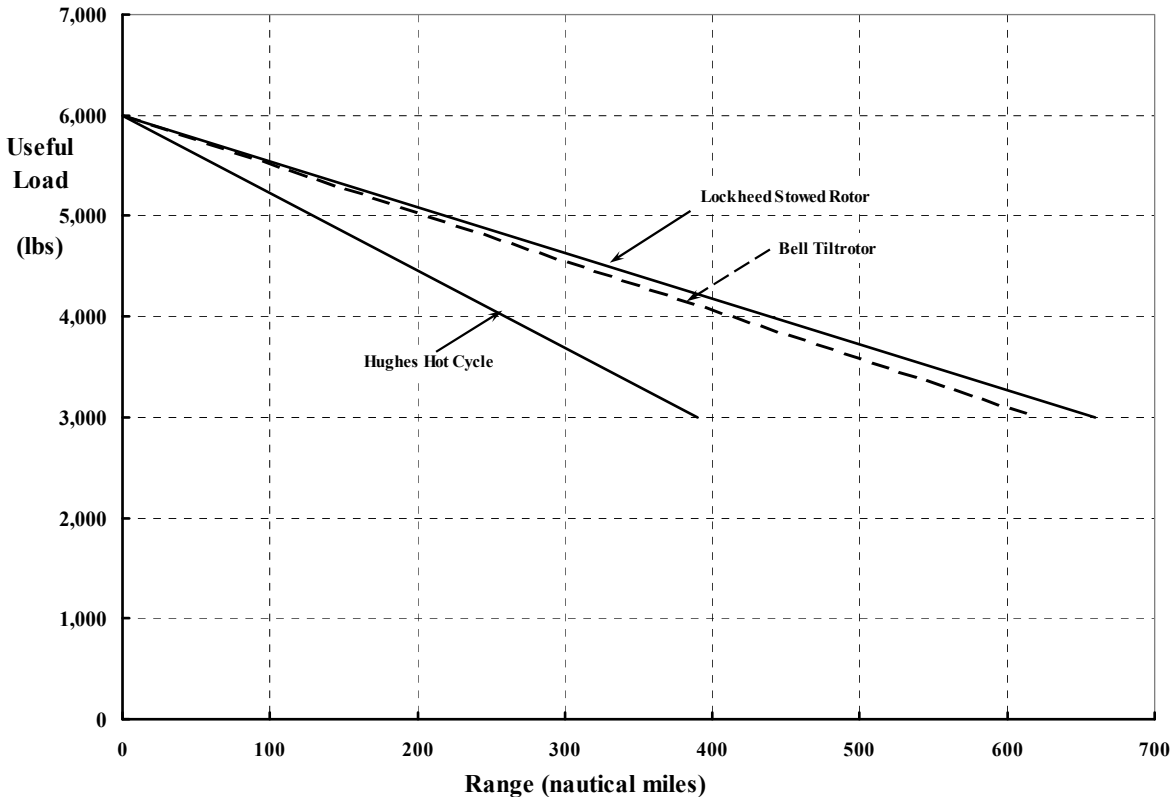

Fig. 2-181. Payload–range comparison for cruising at 10,000 feet on a standard day after taking off at the design gross weight. Delivery of no less than 3,000 pounds of cargo was the basis for this comparison.

Table 2-22. All CRA Designs Were Capable of Long Ferry Ranges

Designer	Configuration	TOGW (lb)	Fuel Burned (lb)	Range (nm)	Cruise Altitude (ft)	Average Nautical Miles per Pound
Lockheed	Stowed rotor	30,000	9,819	2,600	25,000	0.265
Hughes	Hot cycle	30,000	14,042	2,575	35,000	0.183
Bell	Tiltrotor	41,500	22,965	4,275	25,000	0.207

Another example that you may find interesting in the three reports was minimum drag coefficient level and the attention to substantiating this very important coefficient. The Lockheed designers, having a long history of airplane design (but considerably less rotary wing background), included a very comprehensive set of airplane drag coefficient data shown here in Fig. 2-182. Lockheed's report [312] emphasized the drag estimating approach where the minimum drag of the ideal airplane is found when all components (i.e., wings, fuselage, tail, etc.) only have skin friction drag, and no component has separated flow, which causes pressure drag. Early airplanes of the World War I era had excessive pressure drag that gave very high values of the aerodynamic cleanness coefficient (CD_f). Lockheed's design had a minimum equivalent parasite drag area (f_e) of 11.81 square feet, of which 9.01 square feet was due to skin friction drag and the rest was attributed to pressure drag.

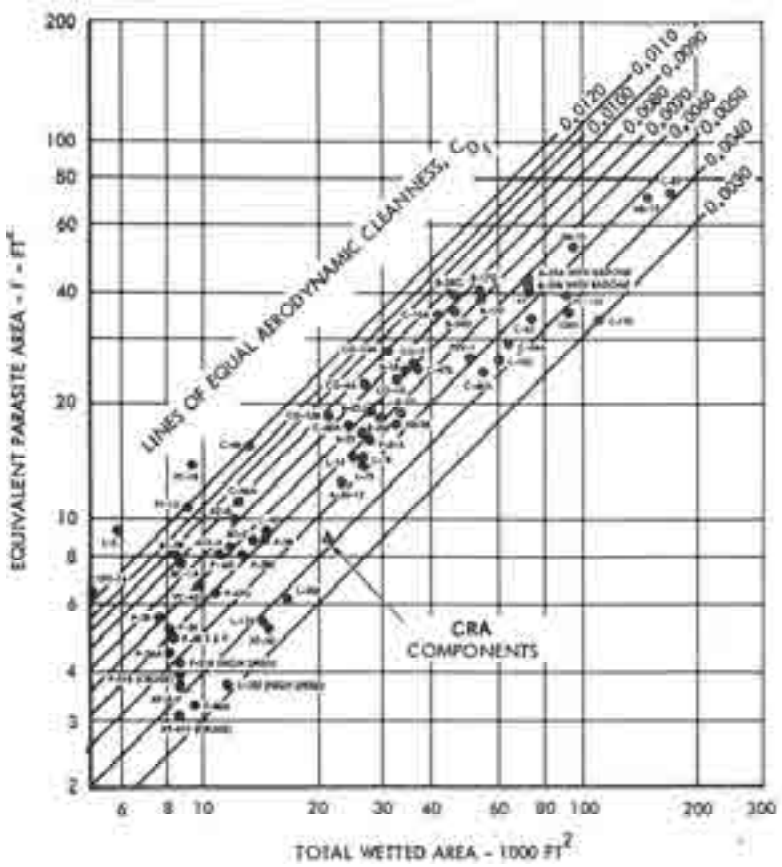

Fig. 2-182. Aircraft drag contains both skin friction and pressure elements. The ideal airplane has only skin friction drag; then minimizing wetted area will get you a very low equivalent parasite drag area (f_e) [312].

A last example of interest to me was a comparison of the three configurations on what I refer to as the von Karman chart. Therefore, I added the results of the three CRA designs to Fig. 2-116 on page 191. This comparison is shown in Fig. 2-183. I found it quite interesting that AVLABS specified that each configuration must have a lift-to-drag ratio of 10 or greater when calculated by $\frac{L}{D}=\frac{W\left(1.69V_{knots}\right)}{550HP}=10$. This requirement translates to the ideal line I have added on Fig. 2-183, which assumes that the L/D of 10 (as measured by the best power-off-glide slope) is achieved at all flightpath velocities along the line. However, the horsepower is ideal power when, in fact, each configuration has very real losses such as propeller efficiency, transmission efficiency, and accessory power. Frankly, I prefer to use the engine shaft horsepower in the denominator and then rename the L/D as an equivalent lift-to-drag ratio, in which case you have $\left(\frac{L}{D}\right)_E=\frac{W\left(1.69V_{knots}\right)}{550\ SHP}$.

And last but not least, AVLABS did not require that the lift-to-drag ratio of 10 be at the highest speed of 300 knots (or greater). To illustrate this point, Bell's tiltrotor achieved a maximum lift-to-drag ratio of 11.1 at a speed of 240 knots at 25,000 feet. Thus, the AVLABS lift-to-drag-ratio requirement was one way of establishing fuel-efficient cruise. The high-speed requirement of 300 knots was one way of establishing a dash speed.

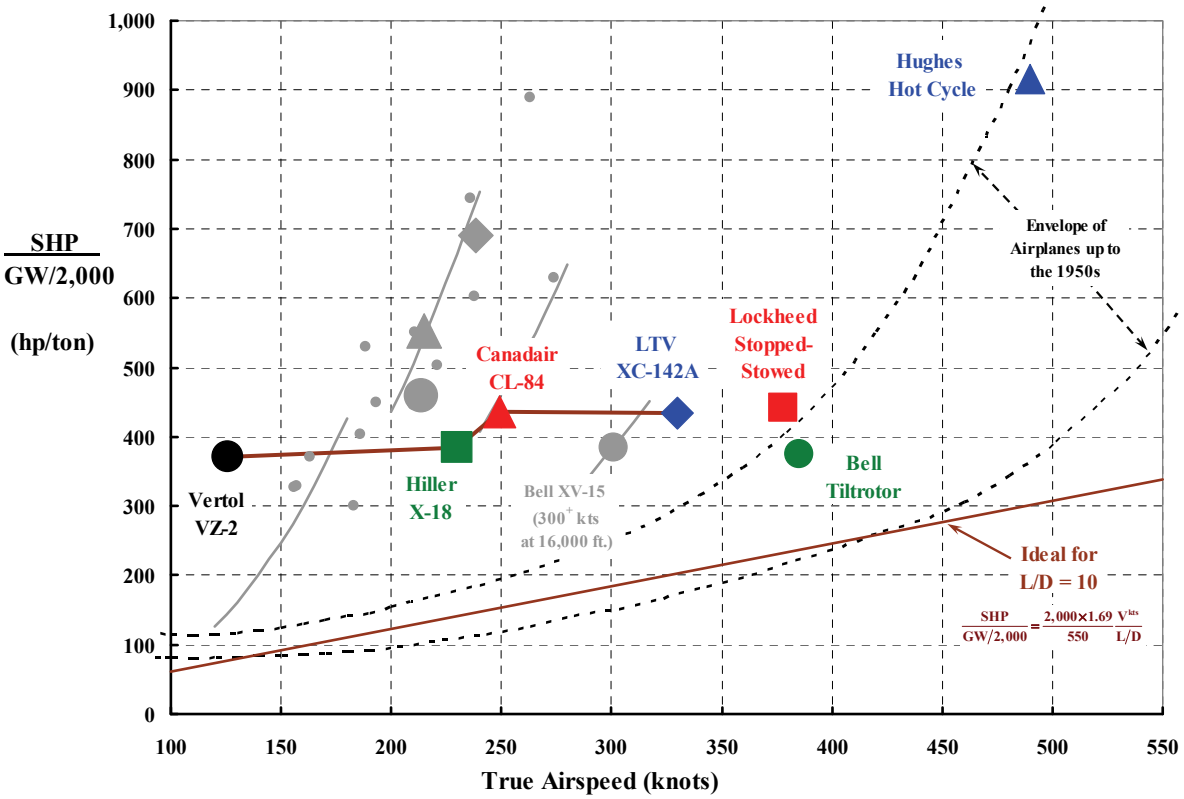

Fig. 2-183. Von Karman and Gabrielli's chart from their paper *What Price Speed* [175] is a favorite of mine. Clearly, the AVLABS study yielded three VTOL configurations with maximum speed capability in the class of some 1950's era airplanes.

2.13.4 The Bell XV-15

The AVLABS Composite Research Aircraft program came to an end with the submittal of the Lockheed, Hughes, and Bell reports. The hoped for follow-on did not happen, and government support and funding dried up in December 1967. Once again rotorcraft VTOL advocates saw their hopes dashed. But 10 years later—on May 3, 1977, to be specific—the first hover and low-speed flight was made with the Bell / NASA / U.S. Army XV-15 experimental aircraft. Bell's Ken Wernicke was the chief engineer and guiding architect, and Ron Erhart and Dorman Cannon were the pilots. It was the XV-15 that finally demonstrated that a practical combination of desirable helicopter features and desirable airplane features could, in fact, be incorporated in one machine.

There is one, and only one, book [37] that tells you the story of the XV-15. It was written by Marty Maisel, Demo Giulianetti, and Dan Dugan. They titled the book *The History of the XV-15 Tilt Rotor Research Aircraft: From Concept to Flight*. It was published as a Monograph in Aerospace History (#17) by the National Aeronautics and Space Administration in 2000. You can find it online today just by typing NASA SP-2000-4517 into your search engine. Marty, Demo, and Dan's book is only 222 pages long, yet every key bit of the XV-15's evolution is extraordinarily well documented. For example, if you want to know who all the key players were in the development of the XV-15, you need only read appendix B. And for a very complete chronology, just turn to appendix C.

The XV-15 came about primarily because of a competition between Boeing Vertol and Bell Helicopter that started out in the early 1970s. The competition was created when tiltrotor advocates at the highest level in NASA and the U.S. Army were convinced of the machine's value to the aeronautical world. It seems to me that by January 1971 the tiltrotor was—after decades of searching—the rotorcraft industry's low-disc-loading VTOL of choice.

Initial efforts by the two companies were simply for (a) configuration experiments, (b) preliminary aircraft design studies, and then (c) development of a program for a minimum-size tiltrotor research aircraft that could meet proof-of-concept objectives. A step along the way was a V/STOL Tilt Rotor Aircraft Study funded by NASA that produced several well-focused reports [323-327] in March of 1972. The reports—in the Task I volumes—designed a range of aircraft that would be quite satisfactory for both civil and military applications. Having established ultimate end-use products, the two competitors conveyed—in the Task II volumes—design aspects of a relatively small research aircraft that needed to be built and tested. This was considered a major step that would provide a successful technology demonstrator that advocates could show to the world. These competing proof-of-concept research aircraft were quite similar as you can see from Fig. 2-184 and Fig. 2-185. What jumps out at you first in this comparison is that in Boeing Vertol's design, the engines did not tilt as the rotors tilt. Secondly, the vertical stabilizers are quite different. Beyond that I only see two light turboprop airplanes, which, of course, is quite a broad simplification.

In March of 1972 NASA and the U.S. Army were able to compare Bell's Model 300 to Boeing Vertol's Model 222 in a number of areas. From references [323-330], I have constructed the typical configuration and program overview shown in Table 2-23. Perhaps

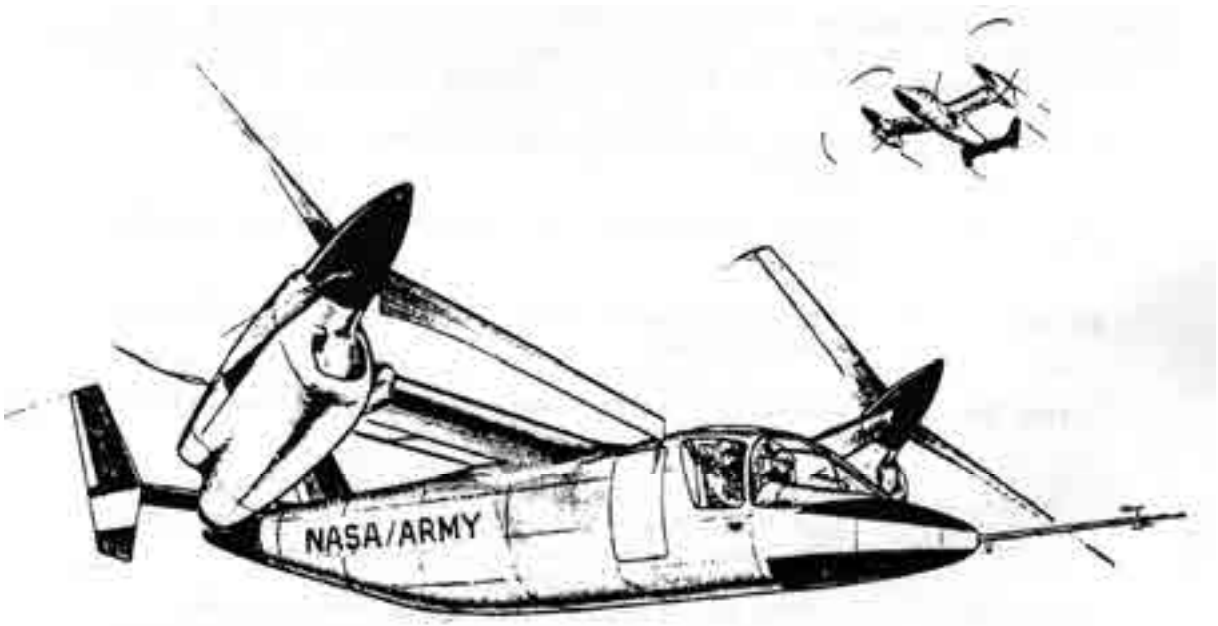

Fig. 2-184. Bell's vision of a tiltrotor research aircraft began as the Model 300.

Fig. 2-185. Boeing Vertol's vision of a tiltrotor research aircraft began as the Model 222.

you have already noticed from this table that the Bell Model 300 engine (i.e., the Pratt & Whitney PT6C-40 VX) had a maximum rated power about 350 horsepower less than Boeing Vertol's choice, the Lycoming T53-L-13B. That is a difference of 700 horsepower on a 12,000-pound machine! NASA preferred the Lycoming LTC1K-41K rated at 1,550 horsepower. Bell made the change with a redesigned engine nacelle and the addition of an "engine-coupling gearbox" as discussed in reference [37]. Thus, the Bell 301 was born.

Table 2-23. Tiltrotor Research Aircraft Envisioned in March of 1972

Item	Unit	Boeing Vertol Model 222	Bell Helicopter Model 300
References		[324-327]	[323, 328-330]
Crew		2	2
Engine (number)		Lyc. T53-L-13B (2)	P&W PT6C-40 (VX)
Maximum horsepower SL, standard day, V = 0	hp	1,500	1,150
Normal rated horsepower SL, standard day, V = 0	hp	675	995
Transmission limit	hp	2,300	2,140
Number of gear boxes		5	3
Dimensions			
Wingspan	ft	33.25	34.6
Wing area (including fuselage)	ft^2	200.0	181.0
Wing aspect ratio	na	5.61	6.6
Horizontal tail area	ft^2	56.3	50.2
Vertical tail area	ft^2	43.3	50.2
Proprotor			
Hub type		Hingeless/ soft inplane	Gimbaled/ stiff inplane
Diameter (blade number)	ft	26.0 (3)	25.0 (3)
Solidity	na	0.115	0.089
Twist	deg	–40	–45
Tip speed hover/cruise	ft/sec	750/525	740/600
Aerodynamics			
Minimum drag coefficient, proprotors off	na	0.0314	0.0360
Equivalent flat plate area, proprotors off	ft^2	6.28	6.52
Gross weight/parasite drag area (GW/f_e)	lb/ft^2	1910	1,900
Weights			
Weight empty	lb	9,230	7,390
Crew	lb	360	400
Fuel (includes trapped fuel) and tank capacity	lb/gal.	2,000/308	1,614/248
Oil (includes engine, xmsn, gearboxes, trapped)	lb	40	105
Payload	lb	370	2,891
Design gross weight	lb	12,000	12,400
Maximum STOL takeoff weight	lb	14,400	15,000
Performance			
Hover ceiling OGE standard day at DGW	ft	12,000	4,600
Maximum speed at 30 min HP (speed/altitude)	kts/ft	310/16,000	312/8,000
Economical cruise (speed/altitude)	kts/ft	230/10,000	242/20,000
Range (distance/altitude)	nm/ft	na/na	567/20,000
Disc Loading (sea level, standard day)	lb/ft^2	11.3	12.6
Uninstalled horsepower per ton of gross weight	hp/ton	500	371
Planning-Type Cost Estimate			
Total cost		$29,197,382	$31,361,000
Total price		$31,241,198	$33,556,000 (est)

Planning-type cost estimates are provided in Table 2-23 in the next to the last row. The comparison shows that the cost to design and build two research aircraft, plus spares, plus ground and flight testing, plus delivering the machines to NASA, plus conducting a full-scale test in the NASA 40- by 80-foot wind tunnel with one of the aircraft was, in my opinion, simply a wash. I believe that cost estimating is one of the most inexact efforts in the world. So if you imagine the estimates are most likely off (i.e., will be low 80 percent of the time) by a factor of two (which is my general rule of thumb), then estimated cost is hardly a deciding factor in choosing between Boeing Vertol and Bell in this example.

In late October of 1972, Boeing Vertol and Bell were placed under contract to deliver what were, in essence, proposals for the small research aircraft they had been championing. Each company received $500,000 for its effort, and a deadline of January 22, 1973, was set. Tommy Thomason reported in *Aerophile Magazine* [331] that Bell's proposal "weighed no less than 774 pounds of paper in the form of twenty five [copies] of 12 volumes." Then, on April 13, 1973, Bell was selected for *negotiations* leading to a contract for the design, fabrication, and testing of two machines.

The negotiations stretched out as Marty and his coauthors describe [37]. They wrote that

> "These negotiations, initiated in late April 1973, engaged the Government and Bell in debates over a series of difficult issues for three months. One of the most contentious areas was the Government's requirement for either a cost ceiling or a negative fee approach to motivate the contractor to control costs. After a meeting between Bell President James F. Atkins and Ames Director Dr. Hans Mark in June, the possible use of company funds to share the cost of an overrun was accepted by Bell. With that important decision made, other issues such as cost reduction items were soon resolved and a contract for the Phase II-A effort was awarded on July 31, 1973. This was to be a 60-day planning level of effort (not to exceed $0.2M). Following a Government assessment of the plans presented at the end of that period, a 'go-ahead' for the Phase II-B for the design, fabrication, and test of two V/STOL tilt rotor research aircraft was given on September 30, 1973.
>
> Phase II[B] - Program Formulation
>
> The work was to be performed under cost-plus-incentive-fee (CPIF) contract. The incentive fee was based on the ability to meet the target cost of $26.415M. If the contract was completed at the target cost, the contractor would earn a 6-percent fee. The fee would be increased to 12 percent if the final cost fell to $23.2M, and would be decreased to a negative fee of about –5.6 percent if the cost grew to $32.4M. This arrangement resulted in the contractor and the Government sharing equally in any overrun or underrun from the target cost."

On this basis you would have to say that the Bell 301 (soon to be designated the XV-15) had a start date of September 30, 1973. On May 3, 1977, the first aircraft (N702NA) was hovered and then taken into low-speed flight by Bell pilots Ron Erhart and Dorman Cannon. Just for the record, the Bell XV-3 made its first flight on August 11, 1955. The Transcendental Model 1-G made its first flight on June 15, 1954. Clearly, a very successful tiltrotor did not just appear overnight.

One very interesting difference between the Bell XV-3 and the XV-15 is shown by the top view drawings overlaid—*at equal scale*—in Fig. 2-186. Here you can immediately appreciate the payoff for a 22-year investment in technology. Just stop and think of the differences for a moment. At equal proprotor diameters, the total uninstalled engine shaft horsepower was increased by a factor of nearly seven. That is, the XV-3 had one piston engine manufactured by Pratt & Whitney (the R985-AN-1 rated at 450 horsepower and weighing about 800 pounds) while the Bell Model 301, or the XV-15 if you prefer, had two Lycoming LTC1K-41K turboshaft engines rated at 1,550 horsepower each for a total installed weight of about a 1,150 pounds. The design gross weight went from 4,700 pounds to 13,000 pounds while the actual weight empties went from 4,205 to 10,083 pounds. The XV-3 could barely hover out of ground effect at sea level on a standard day, but the XV-15 could hover at 7,000 feet on a standard day. The XV-15 was free of flying quality and dynamic instabilities, while the XV-3 was plagued by both instabilities. The XV-3 barely achieved 130 knots, but the XV-15 demonstrated a maximum speed of 300-plus knots at slightly over 20,000 feet.

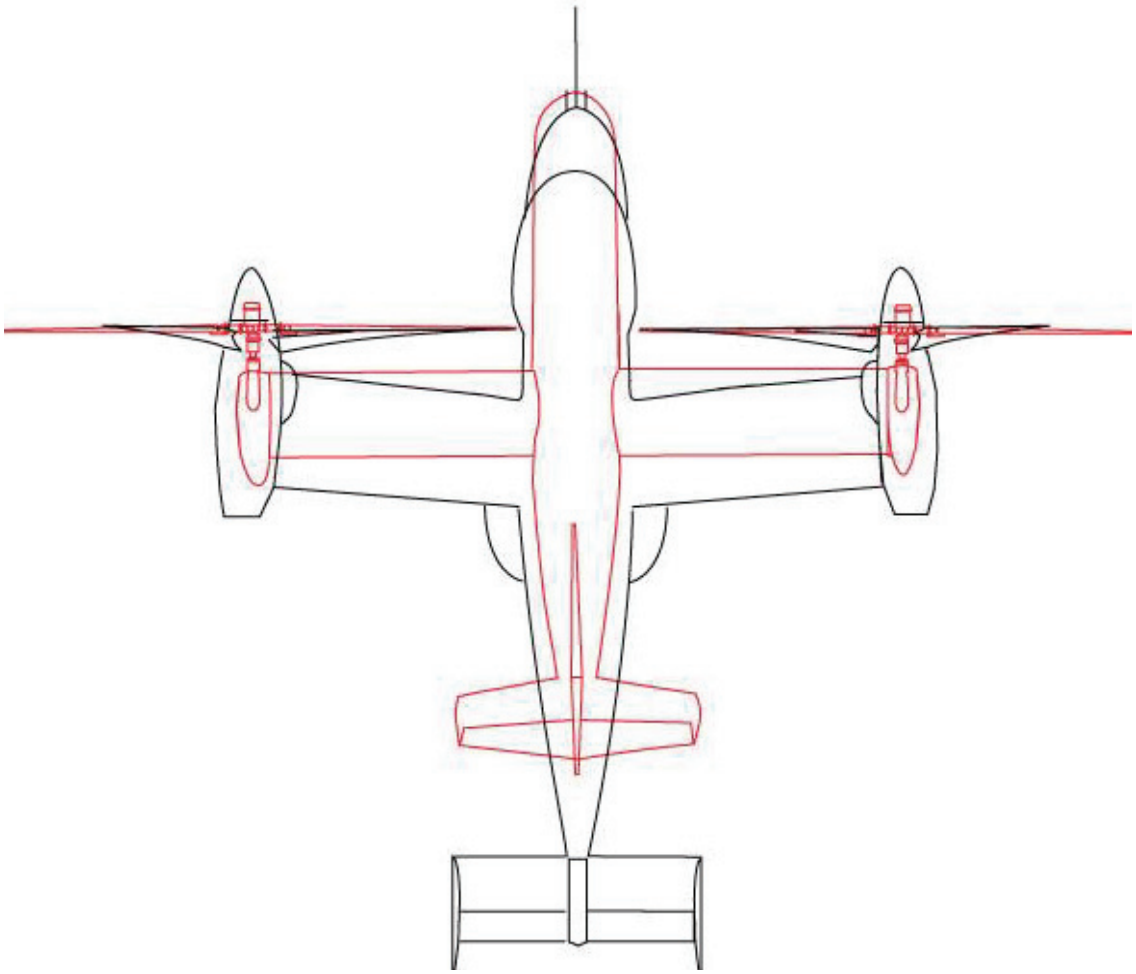

Fig. 2-186. The contrast between the XV-3 and the XV-15 shows the payoff for 22 years of Research and Development money. The red outline is the XV-3; the black is the XV-15 (illustration courtesy of Meridith Segall, Ames Research Center).

Out of curiosity, I began to wonder roughly just how much money did NASA and the three services invest to bring this first truly successful tiltrotor into being. From old notes [332] that John Zuk, NASA's primary advocate of V/STOL, prepared in 1982, you have the following table (then-year dollars in millions).

Government	1974	1975	1976	1976T	1977	1978	1979	1980	1981	1982	Total
NASA	7.0	11.3	1.9	0.3	0.8	3.35	0.3	3.1	0.4	2.6	31.05
Army	10.2	3.0	3.3	0.9	2.6	2.30	0.3	1.6	0.8	0.1	25.10
Navy							1.8	2.4			4.20
Air Force								0.1			0.10
Total	17.2	14.3	5.2	1.2	3.4	5.65	2.4	7.2	1.2	2.7	60.45

As I have mentioned, Marty Maisel, Demo Giulianetti, and Dan Dugan's book, *The History of the XV-15 Tilt Rotor Research Aircraft: From Concept to Flight* [37], provides a very thorough story of the evolution of the XV-15. However, should you want even more technical information, I suggest you start with Marty Maisel's XV-15 familiarization document [169]. Beyond that you can turn to the Bell contractor reports [172-174, 333, 334], which document a great deal of the flight test data and experience gathered up to 1983. In short, the XV-15 tiltrotor technology was not, and will not be, lost.

In my opinion, the XV-15 (Fig. 2-187) opened the door to a third product line for the rotorcraft industry. As it turned out, the first production tiltrotor through the door was the MV-22, built for the U.S. Marines. This MV-22 is a medium high speed rotorcraft that can hover efficiently and is, I believe, a true V/STOL transport.

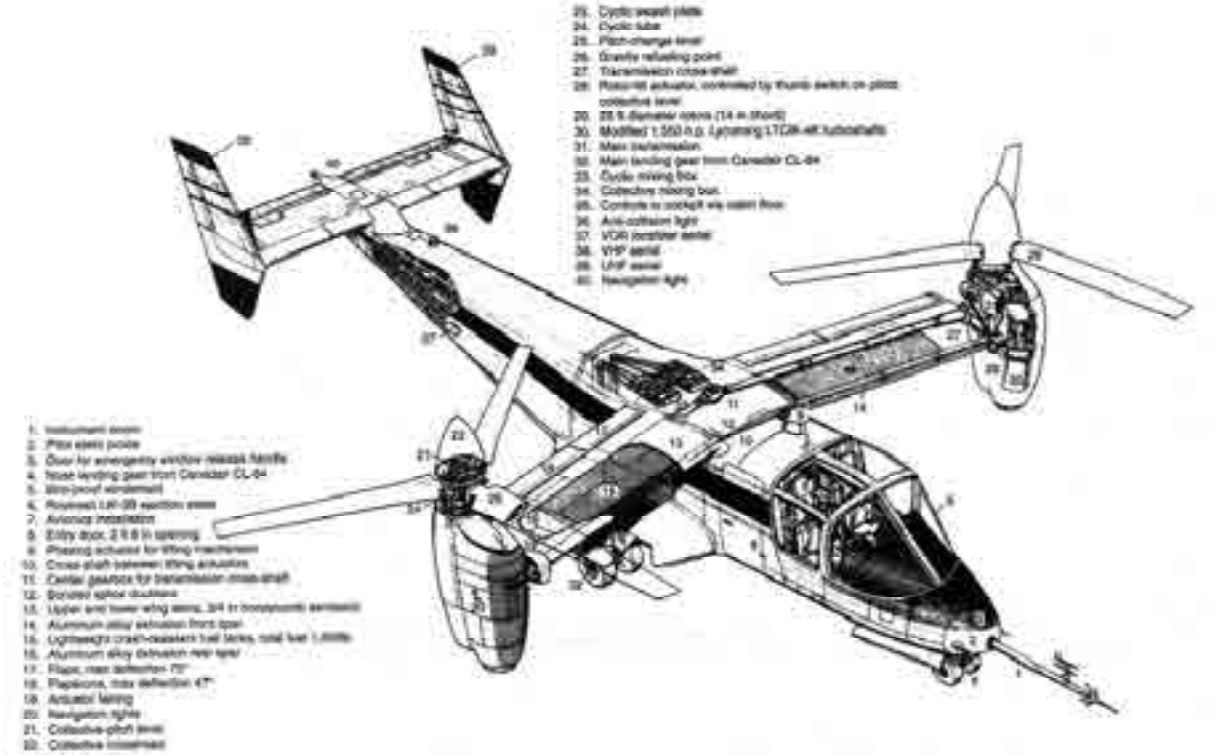

Fig. 2-187. The Bell/NASA/Army XV-15 laid a firm foundation for a production tiltrotor [37]. The first production tiltrotor was the Bell Boeing MV-22.

2.13.5 The Bell Boeing MV-22

All the debates about how to apply the tiltrotor technology summarized with the XV-15 came to an end on April 25, 1983. On that day the partnership of Bell and Boeing Vertol was awarded a contract for $68.7 million for preliminary design of the JVX. The letters JVX stood for Joint Services, Advanced Vertical Lift, and Experimental. It was not until January 1985 that the aircraft officially became the V-22. The Secretary of the U.S. Navy, John Lehman, a strong tiltrotor advocate, came up with the addition that the V-22 would be called the Osprey [34].[86]

The final step towards the U.S. Marines MV-22 Osprey began when the U.S. Department of Defense (DoD) established its JVX program on December 30, 1981.[87] At the direction of Deputy Defense Secretary Frank Carlucci, the three services put up $1.5 million each to fund a program office. A memorandum of understanding, dated June 4, 1982, established that development costs of the JVX would be split three ways. The U.S. Army would ante up 34 percent, the U.S. Navy would ante up 50 percent, and the U.S. Air Force 16 percent. Initially, the Army took the lead task to create the System Specification, which was to be attached to a Request for Proposal (RFP) for preliminary design of the JVX. On May 3, 1982, the JVX program office invited representatives of 25 companies to a briefing where program officials told them that the tiltrotor was the favored configuration. This opinion was based quite heavily on an internal technology assessment of aircraft that could meet the evolving system specification. This document [336] was released in May of 1983, and its preparation was guided by Charlie Crawford (then the U.S. Army's chief engineer for the Aviation Research and Development Command (AVRADCOM)). Charlie drew from a wide pool of engineering talent to produce this technology assessment document. The conclusions and recommendations reached in the 191-page assessment document are as follows:

> **"11. CONCLUSIONS AND RECOMMENDATIONS**
>
> **11.1 Conclusions.**
>
> **11.1.1 Technical Feasibility of a Common Design**. The JVX JSOR missions can be accomplished by a multiservice VTOL aircraft with a high degree of inter-service commonality. The key requirements drivers are: shipboard (LHA) compatibility, seating for 24 troops plus two gunners, long range (world-wide) self-deployment and long range special

[86] There are only two books that capture the V-22's history. The first was written by Bill Norton and was published in January of 2004 [40]. Bill's book is a superb documentation of many of the technical and manufacturing details of the V-22 before it reached full-rate production and deployment. The facts and figures Bill compiled are an absolutely invaluable source to study when you want an authoritative account of the tiltrotor's development.

The second book was written by Richard Whittle and was published in April of 2010 [34] when the, by then, MV-22B had been deployed to the Middle East. The story he put into words reads like a novel. Every twist and turn, every up and down, every successful step forward, and every setback in the program are recounted in—sometimes painfully—great detail. Dick's interviews with nearly every member of the cast of players simply adds to the accurate retelling of the story. Nobody I've talked too about Dick's story disputes his history even though it is difficult to read about the several mistakes that were made in development and fielding the V-22.

[87] The most "official" recounting of the V-22 up to July 1986 is contained in a general accounting office (GAO) report [335].

operations, and high altitude (SEMA). The key technology helpers are: advanced composite materials, fly-by-wire flight controls, emphasis on aerodynamic efficiency, advanced drive system technology, advanced high-speed VTOL configurations, and modern fuel efficient engines.

11.1.2 Lift/Cruise Fan Configuration. The LCF configuration needs higher speed (450 kt) missions, with more time at high altitude, to be efficient. The higher fuel consumption than helicopter or tilt rotor leads to higher mission gross weights for all JVX missions. The very high disc loading produces an adverse downwash environment for rough field or external load operations. Engineering development of a new configuration, such as this, is high risk without a flight demonstration program.

11.1.3 Aux Propulsion Compound Helicopter and ABC Configurations. These configurations are heavier, require larger engines, and consume more fuel than either the helicopter or the tilt rotor for all JVX missions. They are not suitable for the high altitude (25,000 to 30,000 ft) SEMA mission. They cannot perform the JVX world-wide self-deployment mission. They are faster than the helicopter, but still do not satisfy all of the JVX mission requirements. The aerodynamics of the ABC configuration at high speed (when the rotor is slowed down) are high risk without successful flight demonstration.

11.1.4 Helicopter. The helicopter cannot perform the Air Force Long Range Special Operations or the World-wide Self-deployment missions. The helicopter is not suitable for the high altitude (25,000 to 30,000 ft) SEMA mission. The helicopter cannot satisfy the overall 250 to 300 kt JVX speed requirement or the specific speed requirements in the Army high altitude SEMA mission, the Navy CSAR mission, and the two Marine Amphibious Assault missions. If these limitations are acceptable, then the helicopter is the lightest solution for the Marine missions and for the Army low altitude SEMA mission.

11.1.5 Tilt Rotor. A multi-service VTOL aircraft of the tilt rotor configuration can perform all of the JVX missions with a high degree of inter-service commonality. The tilt rotor can perform all of the Navy and Marine missions, including worldwide self-deployment, using the T64-GE-418 engine, however it cannot perform the more demanding Army and Air Force missions. The tilt rotor can perform all of the JVX missions using the Modern Technology Engine (MTE).

11.2 Recommendations.

Based on analysis conducted herein, the Joint Technology Team makes the following recommendations:

a. The Joint Services requirements document should be finalized with full consideration given to the mission tradeoffs contained in this report. Such mission tradeoffs make a common design for all services feasible. Consideration should be given to additional multi-service missions such as: Navy CV-ASW (SH-3H), VOD (CH-53), AEW (E-2), ASW (S-2), and Utility (UH-46); US Air Force FAC X (OV-10); and Medical Evacuation, Special Forces, and Medium Lift missions for the US Army.

b. Establish joint services team to define joint MTE program (JVX/E-2/P-3/CH-47C/C-130 application).

c. Enhance the probability of competition by funding Preliminary Design efforts preceding Full Scale Development proposals.

d. Prior to finalizing the budget, have an independent cost analysis performance by OSD CAIG or other independent out-of-house consulting agency."

What the exact effect was on the 25 companies that attended the JVX program office bidders' conference on May 3, 1982, is not too hard to guess. I imagine most executives walking out of the meeting and conceding the $2 billion to $40 billion program to the Bell Helicopter Company. It was at about this time that Bell teamed with Boeing on a 50-50 basis (in June of 1982), and James Ambrose, Under Secretary of the Army for Research and Development, turned over management of JVX to the Navy.

The Joint Services Operational Requirement [337] and the JVX System Specification [338] were both well in hand when the RFP went on the street (January 17, 1983). When the dust settled, the Bell Boeing team was the only bidder. The team submitted its proposal February 22, 1983, and on April 25, 1983, it was rewarded with a contract for $68.7 million for preliminary design of the JVX as a tiltrotor. Then, on May 13, 1983, Secretary Ambrose reneged on the U.S. Army's commitment to the JVX program, choosing instead to start the Light Helicopter Experimental (LHX, later to become the Sikorsky RH–66 Comanche) program. Fortunately, follow-on discussions between Army Secretary John March, and Secretary of the Navy, John Lehman, established an Army agreement to buy 231 of the 913 total planned production procurement. At the end of this interruption by the Army, the U.S. Marine Corps was in charge of the JVX's future.

The Bell Boeing team's preliminary design passed Critical Design Review (CDR) in December of 1986. Anticipating passing the CDR successfully, the Marines had requested a quote in May of 1985 for the V-22 Full-Scale Development (FSD) program to build and test the machine. Bell's and Boeing's upper management negotiated with Naval Air Systems Command (NAVAIR) for several months and then briefly with Secretary Lehman, who demanded a fixed-price contractual arrangement for FSD or there would be no deal. Finally, on March 19, 1986, a contract was signed that set a target price of $1.714 billion and a ceiling price of $1.810 billion over 7 years. The contract called for five prototypes and one ground test article plus all the testing. If FSD cost more than the target price, the government would pay 60 percent of the overrun up to the ceiling price. Secretary Lehman was very firm in negotiations. His position was summed up by an article in *Defense Week* [339] stating that "Lehman says any contractor who suffers cost overruns on firm fixed-price contracts will have to live with the deal or go bankrupt." In essence, the Bell Boeing team had a fixed-price contract for $1.810 billion and 7 years to complete the work statement. Take it or leave it. As you must know, Bell (with its parent Textron's agreement) and the Boeing Company took the deal. Then on May 1, 1986, Under Secretary of the Navy William Taft IV sent a memo (for the Secretary of the Navy) to the V-22 Program Office [340] that read:

> "Subject to the conditions outlined below, the Navy is authorized to enter into Full Scale Development of the V-22 Osprey Program.
>
> Because of the significant cost of the V-22 Program, the question of its affordability still presents substantial concern. The Full Scale Development contract must allow program cancellation with minimum penalty to the Government if it is determined, as discussed below, that it would be desirable for the Government to do so.
>
> You have advised us that the Critical Design Review for the V-22 will take place in September 1986. We also understand that both Bell and Boeing Vertol will provide not to exceed prices for the next three lots of aircraft production (450 aircraft) by 30 November 1986. This data will be reviewed with the DSARC principals no later than 15 December 1986.

> The CAIG, in conjunction with the Navy and based in part on these bids, will reassess the total V-22 program costs to determine affordability.
>
> Additionally, you have begun a study to determine the potential of the V-22 in anti-submarine warfare as a replacement for the S-3 aircraft. The results of this study will also be of great importance in determining the future of the V-22. During the first quarter of FY 1987, all of this information will be used by the DSARC in consultation with this office to determine whether to continue Full Scale Development of the V-22."

From then on, cost at every level became a crucial factor in keeping the V-22 program alive.

On May 23, 1988, just 2 years after Secretary Taft sent his memo, the first of six prototypes was rolled out in what was described in the *Bell Helicopter News* [341] as a colorful and dramatic ceremony. Dick Tipton's article went on to say:

> "When the curtain rose and the lights went up to reveal the V-22 in the hangar at the flight Research Center, it was as if everyone present was mesmerized. The stillness was uncanny. Several Bell and Boeing employees admitted they had to hold back tears after witnessing the unveiling of the aircraft. It was an emotional experience to see the Osprey when the curtains, which had hidden the V-22 throughout the ceremony, finally parted. Dramatic music and special lighting effects sent more chills down the spine. And as if to salute the crowd, the aircraft then tilted its rotors vertically.
>
> With the 4th Marine Aircraft Wing Band leading the way, the camouflaged aircraft was rolled out of the hangar onto the flight line so visitors could inspect the latest in American aerospace technology. 'It's the biggest and most impressive rollout I've ever seen in my 40 year career of reporting,' said freelancer Pete Bulban, who retired five years ago as senior editor of Aviation Week's Dallas Bureau. Marine Corps pilots and enlisted men—some of whom will eventually be assigned to Osprey units—were also complimentary of the rollout and the V-22 as a technical masterpiece.
>
> 'It's a terrific machine,' one pilot commented after inspecting the cockpit. 'I can hardly wait to fly it.' 'This rollout is special, because I think the V-22 represents a level of advancements in aviation technology we've not seen in a long time,' said Frank Shrontz, Boeing Company's chairman and chief executive officer.
>
> Nearly 2,000 people attended the May 23 event, including local, state and national politicians, military officers, suppliers and subcontractor representatives, aviation leaders, and members of the press. Employees from all facilities and all shifts also were invited to see the V-22 during the afternoon. 'You don't get an opportunity except maybe once in a lifetime to be involved in something as new and as different as the Osprey,' said Bell President Jack Homer. 'Seeing this rollout is the culmination of a dream.'"

Twelve months after the rollout ceremony—on March 19, 1989, to be precise—the first prototype (S/N 16391) completed its first hovering and slow-speed flight. The test pilots for the flight were Dorman Cannon of Bell and Dick Balzer of Boeing. *Helicopter News* reported in its March 31, 1989, flyer [342] that the "V-22 first flight met all NAVAIR requirements." The article also pointed out that the first flight had, 4 years earlier, been scheduled for August of 1988. Clearly V-22 development was already behind schedule due primarily (in my opinion) to time spent on upper management's contractual discussions. I should add that I have never seen a program plan that included time for upper management to do their job—or the impact on cost and schedule when they are too slow.

On September 14, 1989, the Osprey completed its first full in-flight conversion [343], and the flight envelope was quickly expanded up to 8,300 feet and 280 knots in the next several months. Despite this clear demonstration of FSD progress with the prototypes, the follow-on production program took a hit when Secretary of Defense Richard Cheney chose to cancel all V-22 advance production contracts. The Navy got the official word by memorandum from Deputy Defense Secretary Donald Atwood on December 1, 1989. The memo [344] read as follows:

> "SUBJECT: Protection of the Public Fiscal Interest in Termination of V-22 Osprey Aircraft Procurement
>
> In the submission of the FY 1990 budget the Administration reached a firm decision not to procure the V-22 Osprey aircraft, in light of national security priorities and constraints on defense resources.
>
> The Department of Defense Appropriations Act, 1989, appropriated 3334 million in the Aircraft Procurement, Navy (AP, N) account for advance procurement of V-22-related items. That entire amount was obligated, but much of it remains unexpended. In light of the decision not to procure the V-22, it is incumbent upon the Department of Defense to protect the public fiscal interest by ending expenditure of taxpayers' resources on advance procurement for the V-22 aircraft that the Department of Defense will not be procuring.
>
> I direct you to terminate forthwith all contracts relating to the V-22 aircraft that are funded by the FY89 AP, NV-22 advance procurement funds. Report to the Comptroller of the Department of Defense the amount of FY89 AP, N funds deobligated as a result of this termination."

Aviation Week & Space Technology noted in its December 11, 1989, issue [345] that "Atwood's order affected only the $334 million in advance procurement funds that were appropriated for Fiscal 1989, which ended Sept. 30, 1989. The money was to prepare for production of the first 12 V-22s under an option in the Bell Boeing development contract. The development program, funded over Cheney's objections at $255 million for Fiscal 1990, will continue as planned."

The $1.810 billion—give or take $100 million—for full-scale development covering a 7-year period from, say, March 19, 1986, to March 19, 1993, was still in place. By June of 1991, four more prototypes were flying. The sixth aircraft did not fly and became a source of spares. But on June 11, 1991, the V-22 FSD program suffered its first aircraft accident. On that date ship number 5 rolled completely upside down during its first takeoff to a hover [346]. Fortunately the two pilots escaped with only minor injuries. The accident investigation concluded that lateral control (a fly-by-wire system) had been miswired. Then on July 21, 1992, ship number 4 crashed after an engine fire erupted in the port nacelle.

Heartbreakingly, this second accident took the lives of seven aircrew and test team members.

The loss of seven humans and the destruction of ships 4 and 5 brought the Full-Scale Development program to a halt. The three intact V-22s were grounded, and then a protracted period was spent by all concerned trying to decide what to do next. Unlike many other very advanced technology aircraft development programs, the influential advocates in Congress

and at the Department of Defense decided to give the U.S. Marines, the Naval Air System Command, and the Bell Boeing team another chance.

This second chance was called the EMD phase. The letters EMD stood for engineering and manufacturing development. This phase was far from a clean-sheet-of-paper redo. The first five V-22 prototypes had shown that the design was not ready for a simple conversion to a production configuration, which would have been designated as the MV-22A (the "M" standing for Marines). The FSD design was overweight and fell short in meeting the system specification in more ways than I can list in this introduction you are reading. Most importantly, the production price for whatever number that might be ordered could not be firmly established by either the government or the Bell Boeing cost estimators. What was clear was that the tiltrotor concept was not fundamentally flawed.

The bridge from FSD to production was crossed when, in June 1996, Bell and Boeing were given a contract to build five more V-22s. The DoD, perhaps to convey faith in the Marines' desire to have a fleet of V-22s, defined this group of five redesigned machines as Lot 1 of a phase called low-rate initial production (which was shortened to LRIP). Everything that had been learned about this first all-composite aircraft, with many leading-edge technologies in several areas of the machine, was available to Bell Boeing and NAVAIR engineers, and this staff put their knowledge to good use as the EMD unfolded.

The EMD Ospreys were designated as the B model, and the V-22 became known as the MV-22B (Fig. 2-188). The first flight of an MV-22B was made on April 30, 1999. This aircraft was accepted by the Marines in May of 1999, and they took the aircraft to the Navy flight test facility located at Patuxent River, Maryland, where the government's developmental test flying began in earnest. As the following MV-22Bs came online, the government took delivery, and the Marines began operational evaluation of the aircraft. You can read about the many facets of operational testing just by scanning through Bill Norton's book [40].

Then, on April 8, 2000, another, even more heartbreaking, accident occurred while a small formation of MV-22Bs was trying a simulated tactical mission. All 19 Marines on board died. This accident occurred during a low-forward-speed, high-rate-of-descent condition which led into the vortex ring state, a well-known flight regime that helicopter pilots avoid. Unfortunately, the MV-22B's vortex ring state boundary was not well mapped out at the time the operational evaluation was attempted in April 2000. All V-22s were grounded, and the Secretary of Defense established an independent panel to review the program. The Panel, chaired by John R. Dailey, submitted a 200-page report [347] on April 30, 2001. It offered 70 recommendations developed from a quite detailed analysis of 23 different areas. Several other reviews were conducted in support of Dailey's "Blue Ribbon Panel." For example, the U.S. Navy requested that NASA perform an independent assessment of tiltrotor aeromechanics phenomena that might adversely impact the safety or performance of the V-22. The panel Henry McDonald convened was directed to focus on the vortex ring state and autorotation. This panel's work [348] was finally published on August 17, 2001. Another example was a General Accounting Office (GAO) report [349] that went to the Secretary of Defense, Donald Rumsfeld, on February 20, 2001.

The consensus—after everybody did their homework and reported in—was that only low-rate initial production (LRIP) of the MV-22B should be considered at that time. The NAVAIR-Bell Boeing team was to go back and fill in all the end runs and shortcuts they had taken to meet schedule. Establishing a very accurate picture of the boundary of the vortex ring state that the pilots could refer to in their flight manuals was just one of the 70 recommendations that Dailey made.

Despite many naysayers, the V-22 was given a third chance, and another CDR was successfully passed in December 1994. Then LRIP began in June of 1996 and manufacturing the first of five Lot 1 aircraft began on May 7, 1997. This aircraft hovered for the first time on April 30, 1999. It took another several years of flying and fixing before full-rate production was authorized in September 2005.

The original program premise was that the "Joint Services" would buy their share of aircraft. The Marines would buy 552, the Navy 50, the Air Force 50, and the Army 231. The latest actuals [350] show that as of fiscal year 2014, the Marines have bought and taken delivery of 213, the Navy has apparently opted out, the Air Force now has 44, and the Army has decide to not buy any. NAVAIR quotes the latest flyaway unit cost in July of 2010 as $64 million for the MV-22B and $76 million for the Air Force CV-22B [350].

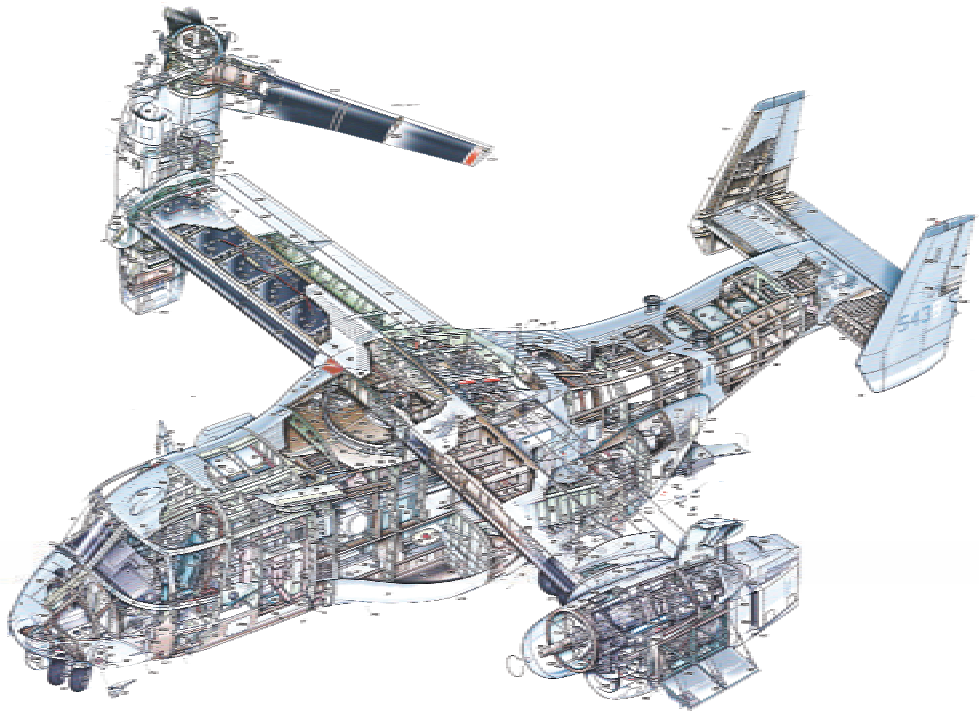

Fig. 2-188. The U.S. Marines 24-troop-carrying MV-22B designed and built by the Bell Boeing team is the first rotorcraft to *operationally* demonstrate helicopter-like hovering efficiency with turboprop airplane-like performance (*Flight International*).

2.13.6 Tiltrotors in Summary

There is no doubt that the path to the first operationally successful tiltrotor was a long one. The tiltrotor began, in my view, with the Transcendental Company in the early 1950s. Despite their early successes, the company did not have the money or manufacturing capability to follow through. However, their efforts brought the tiltrotor to the attention of all three military branches in the United States. A small band of tiltwing advocates passed their enthusiasm from generation to generation until—some six decades later—the U.S. Marines deployed the MV-22B to the Middle East. A simple comparison might be made that the Wright Brothers offered the U.S. Army their Wright Flyer in December 1903. Within three decades, we had the very advanced Douglas DC-1, then -2, and then -3, which was the first airplane that the commercial airlines could make a profit with without government subsidies.

The six-decade path was so long for several reasons. First and foremost, it was difficult to find a ground swell of demand for the machine. It took the U.S. Marine's requirements and tenacity over the long haul to give birth to the MV-22B tiltrotor. As a reminder, the LTV XC-142A *tiltwing* program never made it beyond development flight testing. It also had a major crash, which killed two pilots and brought the program to a halt on October 9, 1967. No group of influential advocates came forward to give the tiltwing a second chance. This has left the MV-22B as the only successful rotorcraft to operationally demonstrate helicopter-like hovering efficiency with turboprop airplane-like performance.

When you look at Table 2-24 you can get a sense of several other reasons for the six-decades-long path. First of all, tiltrotor development could not proceed very far without adopting gas turbine engines. Of course, this statement can be applied to the aviation industry in general, but I think it is especially true in the development of V/STOL aircraft. Secondly, adopting composite materials improved structural design options, and this meant more useful load for a given design gross weight. Finally, while the table might not show it, it took considerable research (including access to a digital computer) to get to the bottom of proprotor whirl flutter. One message that you might take away is that a small research aircraft (i.e., the Model 1-G or the XV-3) can demonstrate a concept, but it often takes major evolution, and even breakthroughs in other fields, to get a useful product. Thus, a very good idea can hibernate until just the right time to wake up and be noticed.

Now let me offer a concluding thought or two. The MV-22B is not an optimum tiltrotor—far from it (Fig. 2-189). In fact, I would go on to say that the only driving specification [338] for the 24-troop-carrying machine was that it must go down an existing elevator on some existing U.S. Navy ship or forget it. It is quite reasonable for the Navy to say that it will not change its elevators for any old VTOL that comes along. Nor will it build a few ships just to act as a fleet of floating VTOL ports. There does not seem to be a compromise other than for the VTOL to fold itself up while on the ship deck. That was the design limitation for the V-22, and it met the requirement as Fig. 2-189 shows—but at an extreme price in dollars, installed engine power, and weight empty. Lastly let me say that when you embark on a development effort using a Joint Program approach so that enough Department of Defense money is extracted from all three services, you create too many sullen

generals and admirals. I might add as a personal opinion (and from a working engineer's point of view) that in the time it takes upper management to do their job, it is quite likely that *any* new aircraft—V/STOLs included—can be designed, built, and tested. However, I must admit that the V-22 development story you have just read might be an exception to my statement.

Table 2-24. The Four Tiltrotors Developed So Far

Item	Unit	Model 1-G	XV-3 (note 1)	XV-15	MV-22B (note 2)
References (also various *Jane's All The World's Aircraft*)			[256, 257, 261, 263]	[169, 172-174, 256, 257, 263, 333, 334]	[40]
Manufacturer		Transcendental	Bell	Bell	Bell & Boeing
First flight date		June 15,1954	January 21, 1958	May 3, 1977	April 30, 1999
Crew/passengers		1/0	1/4	2/6	3/24
Number built		1	2	2	125 as of FY08
Accidents during development		1	2	0	5
Engine (number)		Lyc O-290-A (1)	P&W R 985 (1)	LTC1K-41K (2)	RR AE-1107C (2)
Takeoff rating	hp	160	450	1,550	6,150
Maximum continuous rating	hp	na	400	1,250	5,256
Drivetrain limit	hp	na	na	2,920	11,248
Number of gear boxes		3	3	5	5
Dimensions					
Wingspan (between rotor centers)	ft	21.0	31.17	32.17	46.83
Wing area (including fuselage)	ft^2	63.0	116.0	169.0	382.0
Wing aspect ratio	na	7.1	8.4	6.12	5.74
Horizontal tail area	ft^2	9.0	32.6	50.25	88.5
Vertical tail area	ft^2	6.0	32.8	50.5	35.2
Proprotor					
Diameter (blades)	ft	17 (3)	23.0 (2)	25.0 (3)	38.0 (3)
Blade chord	in.	4.0	11.0	14.0	27.6 (mean)
Solidity	na	0.025	0.0507	0.089	0.116
Twist (note 3)	deg	0	– 1.6	– 36	–47.5
Tip speed hover/cruise	ft/sec	na/na	640/390	771/676	821/664
Aerodynamics					
Reference drag area, f_e (note 4)	ft^2	na/na	13.0	9.24	34.6
Minimum drag coefficient at (C_L)		na (na)	0.1126 (0.2)	0.0547	na
GW/f_e	lb/ft^2	na	369	1,406	1,520
Weights					
Design VTOL takeoff weight	lb	1,750	4,800	13,000	52,600
Maximum takeoff weight	lb	1,750	5,000	15,000	60,500
Basic weight empty (note 5)	lb	1,450	4,205	10,083	33,459
Fuel capacity (U.S. gallons)	lb/gal.	95 (14)	600 (90)	1,436 (220)	9,400 (1,448)
Performance					
Hover ceiling (note 6)	ft	na	0	4,500	1,000
Maximum (speed/altitude)	kts/ft	139 (0)	130 (4,900)	301 (26,000)	291 (15,000)
Economical (speed/altitude)	kts/ft	na	85 (4,900)	242 (20,000)	269 (20,000)
Economical specific range	nm/lb	na	0.50	0.28	0.090
Disc loading (note 7)	lb/ft^2	3.85	5.78	13.24	23.19
SHP per ton of design GW (note 8)	hp/ton	182	187	477	468

Notes:
1. With two blades. First flight with three-bladed version was August 11, 1955. 2. EMD version. First flight of V-22 FSD version (s/n 16391) March 19, 1989. 3. Washout is negative. 4. Blades off, hub on. 5. No crew, trapped fluids only, no payload. 6. Design weight, standard day. 7. Sea level, standard day. 8. SHP based on total engine(s) uninstalled takeoff rating.

Fig. 2-189. Military specifications such as the Navy's requirement for shipboard compatibility for the MV-22B severely compromise any commercial spin-off.

Fig. 2-190. Bell's D326 is a tiltrotor design that can compete with turboprop airplanes.

2.14 FINAL THOUGHTS ABOUT ROTORCRAFT

The rotorcraft industry has finally established two V/STOL aircraft that can be added to its autogyro and helicopter product lines. These two aircraft, shown in useful military configurations on page 136, are the XC-142A tiltwing (Fig. 2-76) and the MV-22B tiltrotor (Fig. 2-77). Arriving at these two VTOLs has taken decades of research and development. The primary discriminator between these two types of VTOL aircraft is the ratio of gross weight to total proprotor disc area for a given design objective. For example, the XC-142A tiltwing's disc loading is 52 pounds per square foot while the MV-22B's disc loading is 21 pounds per square foot. When comparisons are made between the tiltwing and the tiltrotor, many studies have shown that the high-disc-loading tiltwing requires more uninstalled horsepower than the tiltrotor—*at equal takeoff gross weight and density altitude*—so that the power loading (i.e., the ratio of power to weight) is greater with a tiltwing than a tiltrotor. The difference in disc loadings, say between the XC-142A and the MV-22B, translates immediately into a substantial difference in power loading. To be more specific, the XC-142A uses four T64-GE-1 engines providing a total uninstalled takeoff power of 12,320 horsepower, which gives a power loading (at its 40,141-pound vertical takeoff weight) of about 614 horsepower per ton of gross weight. In contrast, the MV-22B uses two AE-1107C engines providing 12,300 total uninstalled horsepower, which gives a power loading (at its 52,600-pound vertical takeoff weight) of about 468 horsepower per ton of gross weight. There are, of course, many other considerations that affect this simple comparison. One very important consideration is the XC-142A's military requirement to hover at 6,000 feet on a 95 ^{o}F day with 24 troops on board, and to move the troops 300 or 400 or 500 nautical miles comfortably enough so that they arrive ready to fight. On the other hand, the original V-22 design altitudes were sea level on a 103 °F day for ship-based operations and 3,000 feet, 91°F for land operations.

There is a second, nearly as important discriminator that has emerged during the more recent decades. This discriminator is the design objective for speed. The exact design speed requirement has been found to separate edgewise flying rotor VTOL configurations from tiltwing and tiltrotor configurations such as Bell's Model D326 shown in Fig. 2-190. If you take a moment and refer back to Fig. 2-73 on page 129, you will be reminded of several edgewise flying rotor VTOL machines. None of these edgewise flying rotor designs have shown fuel efficient, airplane-like high speeds. In fact, the edgewise flying rotor configurations have, so far, obtained high speed by brute force. That is to say, an inordinate amount of power is installed per ton of takeoff gross weight. If I were asked what I thought the practical upper limit speed for edgewise flying rotor configurations is, I would refer to Fig. 2-73 and pick 250 knots for a dash speed and 175 knots for fuel-efficient cruising.

Finally, there is a third discriminator of great importance to high-speed rotorcraft and airplane designers alike. This discriminator is the classical lift-to-drag ratio (L/D). Any aircraft has a power-off glide ratio (i.e., the longest distance traveled for the least loss in altitude when power is turned off) from which you can establish its L/D. Alternately, a simple wind tunnel test can provide a graph of lift versus drag from which the maximum L/D can be obtained. In this regard, airplane designers have perfected the art of getting the least drag for a

given amount of lift. Conversely, rotorcraft designers, with only a few exceptions, have perfected the art of getting the most lift in hover for the least amount of installed power and to heck (there is no other printable word for it) with an aerodynamically low-drag machine. But the design of V/STOL aircraft by rotorcraft engineers requires skills this group does not apply, or does not have, based on the products they have fielded.

To bring the preceding three points into focus, let me remind you of the discussion in paragraph 2.10.2 by repeating a conceptual design graph for V/STOL aircraft; Fig. 2-75 from page 133 is repeated here as Fig. 2-191. I believe that enough of the key parameters needed to create a rotorcraft V/STOL concept are captured by this one graph and the simple equation shown on the graph. Very little discussion is required about this very fundamental graph, however Fig. 2-191 immediately makes it quite clear that military V/STOL requirements for low disc loading and high speed are extremely challenging. For example, the U.S. Army currently desires low disc loadings, say, below 20 pounds per square foot on a high, hot day to minimize the cloud of dust and debris that gets stirred up during landings. When a low-disc-loading requirement is coupled with a high-cruise-speed requirement, then a design team is faced with finding a way to maximize the machine's L/D. This becomes especially challenging if the requirement is for a troop transport, and very difficult when a rear ramp configuration is demanded and a nose ramp configuration is deemed impracticable. It becomes completely impractical when a large machine is designed for ship duty.

I need add very little to Fig. 2-189 about other U.S. Navy requirements. One clear thing, at least to me, is that Navy requirements are rather incompatible with U.S. Army and Air Force requirements. This makes the concept of a joint program producing a satisfactory

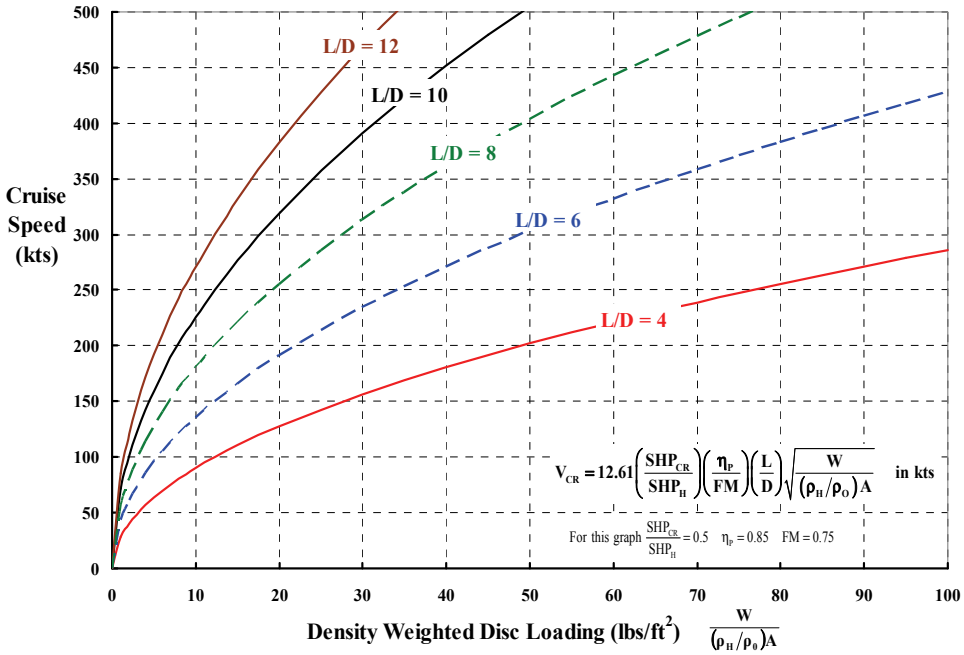

Fig. 2-191. A fundamental top-level-concept design chart. Military helicopters have achieved L/Ds of 4; tiltrotors and tiltwings have achieved L/Ds of 6 to 8.

VTOL very difficult. With respect to the U.S. Air Force, you would think their requirements might be the most in line with what a rotorcraft V/STOL has to offer. After all, this military branch favors efficient cruise at high speed *and* high altitude. But my experience has repeatedly shown that the Air Force acquired a disdain for propellers—in any form—nearly on the day practical turbojet engines arrived on the scene. The U.S. Army does not share this view, and so a joint Army and Air Force V/STOL program, say, to replace the Air Force C-130 with a V/STOL, seems rather unlikely. I need not add that interservice rivalries have continually stretched out decision making points in new aircraft schedules.

As you have surmised, von Karman and Gabrielli's chart from their paper [175] *What Price Speed* is a favorite of mine even though it can be difficult at times to precisely establish power, gross weight, and speed data for any given aircraft. Nevertheless, you have, in Fig. 2-192, my summary view of several rotorcraft under discussion in this introduction. What jumps out at me is that no rotorcraft tested so far compares very well to airplanes in operation up to the 1950s.[88] To emphasize this point, I have added to the figure two airplanes (Lockheed Electra and Saab 2000) that commercial airlines bought. As you can see, even a tiltrotor as represented by the MV-22B fails to be competitive with what airlines might be attracted to.

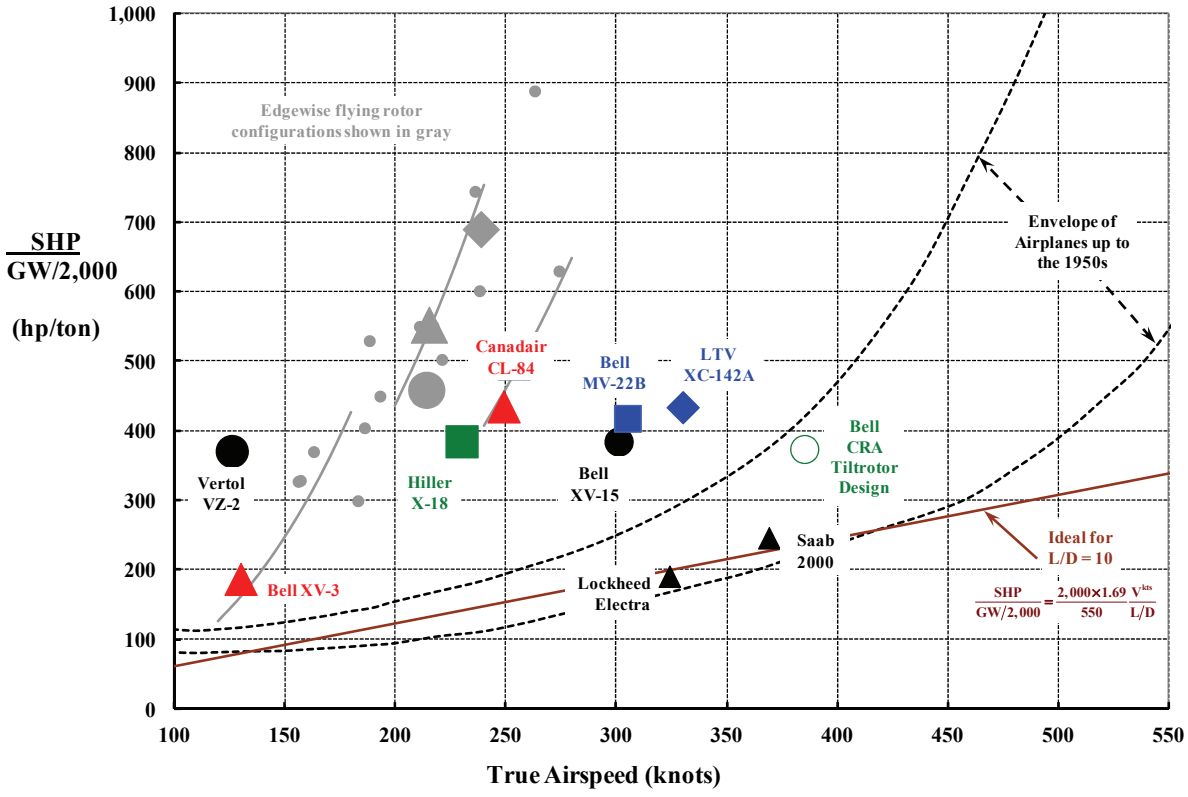

Fig. 2-192. It appears that the rotorcraft side of the industry can produce VTOLs capable of 300 to 375 knots at 20,000-foot altitude without giving up hovering efficiency.

[88] While I see the Hughes Hot Cycle configuration as having merit, its low fuel efficiency (see Fig. 2-181) makes it a no contender in my mind. The Lockheed Stopped-Stowed has too many gearboxes (see Fig. 2-170).

This makes the point that those high-speed VTOLs that have been explored for the military are not, so far, well suited to direct conversion into a commercial product.

Of course, it is possible that any given VTOL product can appear quite competitive when placed on a summary performance graph such as Fig. 2-192. However, maximum speed in itself is not the only performance characteristic that makes an aircraft desirable. Using fuel efficiently is equally important to both the military and commercial customer. You will recall that the Middle East initiated an oil embargo in 1973. The effects of fuel shortages, high prices, and dependence on foreign oil supplies significantly affected the U.S. economy and continue to today.[89] The issue of fuel efficiency became a national priority, and in 1975 the U.S. Senate directed NASA to look at every fuel-saving concept aviation technology had to offer. In the foreword to reference [33] you will read that

> "Although several concepts were identified and pursued, the advanced turboprop promised the highest potential fuel savings for high-speed subsonic aircraft. It was, however, the most challenging concept technically and was initially resisted almost entirely by U.S. engine and airframe manufacturers, the airlines, and the military.
>
> In spite of the challenges, NASA decided to pursue the program because the potential payoff was too large to ignore. The Advanced Turboprop Project Office was formed at the NASA Lewis Research Center in Cleveland, Ohio, to manage and integrate the program. A systems approach was followed that looked at the entire aircraft in designing the propulsion system. This included elements such as the propeller and the nacelle, the drive system, installation aerodynamics, and the aircraft interior and community environments and the effect of these elements on meeting the goals of reduced fuel consumption, low operating costs, and passenger acceptance.
>
> In 1987 the advanced turboprop propulsion concept was proven by three flight programs using large-scale hardware. The NASA-General Electric-Boeing flight test and the General Electric-McDonnell Douglas flight test used the Unducted Fan as a proof-of-concept demonstrator for the gearless counterrotating concept. The NASA-Lockheed-Georgia Propfan Test Assessment test used the single-rotating, large-scale advanced turboprop to record verification data for propfan design codes. On the basis of the success of these tests and previous scale-model work, Pratt & Whitney-Allison built a geared counterrotating propulsion system that they plan to fly on the MD-80 in early 1988.
>
> These tests have demonstrated that the advanced turboprop uses 25 to 30 percent less fuel than equivalent technology turbofan engines. The subsequent reduction in aircraft direct operating costs is 7 to 15 percent depending on fuel prices. The advanced turboprop has the required structural integrity and safety, aircraft interior environment, and community and enroute noise levels to be competitive with turbofan engines in commercial service. U.S. aircraft manufacturers plan to introduce new, highly efficient propfan-powered aircraft with vastly improved performance into the commercial fleet in the early 1990s."

The idea was to replace commercial turbofan aircraft with somewhat slower, but more fuel efficient, turboprop-driven airplanes. However, the embargo was declared over by the Organization of Petroleum Exporting Countries (OPEC) in March of 1974 and, because the traveling public had become extremely satisfied with airplanes that did not have propellers, all

[89] Many of us can remember very long lines at gas stations just to get a few gallons for our cars. The days of just "filling her up" had come to—what turned out to be—a relatively short interruption. Incidentally, fuel-efficient Japanese cars were then in very short supply.

the NASA research fell on deaf ears. No advanced turboprop airplanes entered the world of commercial airlines.

One outcome of the oil embargo was that V/STOL advocates increased their marketing with the theme that V/STOLs should complement (or even replace) helicopters because V/STOLs were more fuel efficient and could go faster. On engineering grounds, this is a valid claim for speed as you can see from Fig. 2-192. The fuel efficiency claim is equally true as you can see from Fig. 2-193. You will recall that in Volume II, on pages 271 to 277, I discussed fuel efficiency in some depth and offered a rather simple equation to calculate specific range (SR) in nautical miles per pound of fuel burned. I repeat this equation here as

$$(2.159)\quad SR = 350\left[\frac{(L/D)_{a/c}}{SFC}\right]_{avg.}\frac{1}{W_{initial}} \quad \text{in nautical miles per pound.}$$

The simple message quantified by Eq. (2.159) is that, for a given aircraft size ($W_{initial}$), engine manufacturers must minimize the fuel required to produce a given power required (SFC), and airframe manufacturers must minimize aircraft drag (D) for a given amount of lift (L). The aviation industry has been well aware of these two requirements for over a century, thus research and development have always been ongoing.

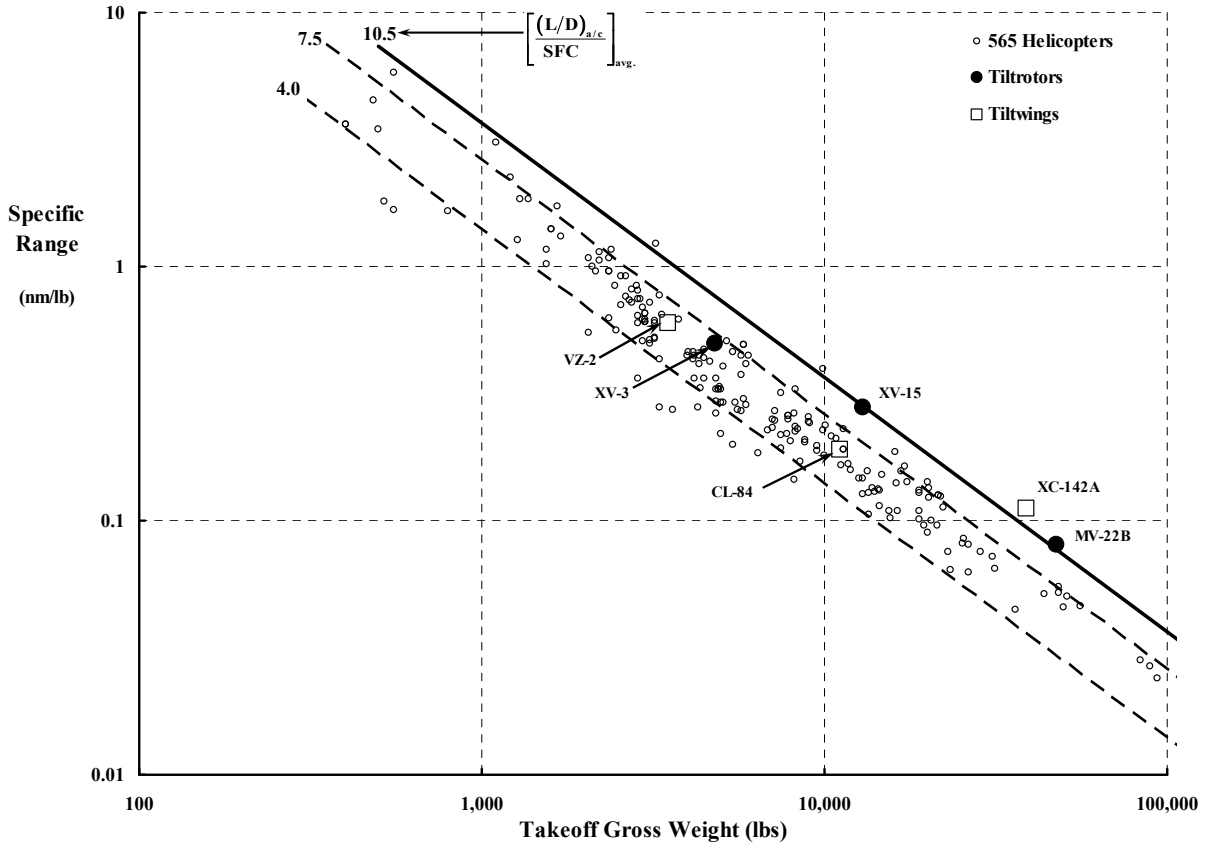

Fig. 2-193. Tiltrotor and tiltwing V/STOLs offer improved fuel efficiency compared to helicopters.

It is possible, of course, that any given VTOL product can appear quite competitive when placed on summary performance graphs such as Fig. 2-192 and Fig. 2-193. However, the issue of how much of the designed gross weight is available for useful load is not addressed. You will recall from Volume II that design gross weight is split between useful load (i.e., fuel, passengers, cargo, etc.) and weight empty (i.e., structure, engines, furnishings, etc.). Therefore, a display of this split is as important as the performance at design gross weight. In Fig. 2-194 you see weight empty graphed versus design VTOL takeoff gross weight. The relative positions of the four tiltwings and four tiltrotors that have been designed, built, and flight tested are compared to 615 helicopters. The comparison is quite interesting. You should expect that experimental machines hardly ever appear favorable in such a comparison because concept evaluation is the only goal. You see that fairly clearly in Fig. 2-194. Concept evaluation by the XV- and VZ-series aircraft appear to have a ratio of weight empty to design VTOL gross weight on the order of 0.85. But then, when a concept proves worth pursuing and engineers pay aggressive attention to detailed design, the weight empty fraction improves to something in the range of 0.65 (the preproduction XC-142A) to 0.73 (the CL-84).

Sometimes a data collection such as Fig. 2-194 can be rather misleading, however. For example, when you examine the XV-15's weight statement [174] you quickly see that this experimental VTOL had ejection seats that weighed a total of 230 pounds. This weight is equivalent to a passenger and would become useful load in a commercial machine. Furthermore, ejection seats distort the relative merits of the CL-84 and the XV-15 to make the point clearer. Another example is apparent when discussing the relative weights of the MV-22B and the XC-142A. The MV-22B started out as the FSD V-22, which should have been designated as the XV-22 in my opinion. The FSD V-22 had a design gross weight of 47,500 pounds and a weight empty of 32,340 pounds, which, I might add, included all the weight devoted to folding the aircraft to go down a ship's elevator. Thus the FSD V-22's weight empty fraction is 0.681, which is more comparable to the XC-142A's 0.650.

I should add the reminder from my experience that paper studies—such as that conducted during the AVLABS Composite Research Aircraft program—often offer considerable departures from past trends, from reality, and occasionally even from the laws of physics. The CRA study concluded that the weight empty fraction for each of the three designs was:

Configuration	Design Gross Weight (lb)	Weight Empty (lb)	Weight Fraction
Lockheed Stowed Rotor	24,500	17,961	0.733
Hughes Hot Cycle	19,635	13,169	0.671
Bell Tiltrotor	23,000	15,994	0.695

One can only wonder what the production aircraft weight fractions would have been if the CRA program had continued to its logical end. There is little evidence that weight empty fractions go down as an aircraft goes from conceptual design and paper study to operational use. The most successful way to reduce the weight empty fraction is to increase the denominator (i.e., the gross weight) as successive versions of the aircraft with uprated engines go into production.

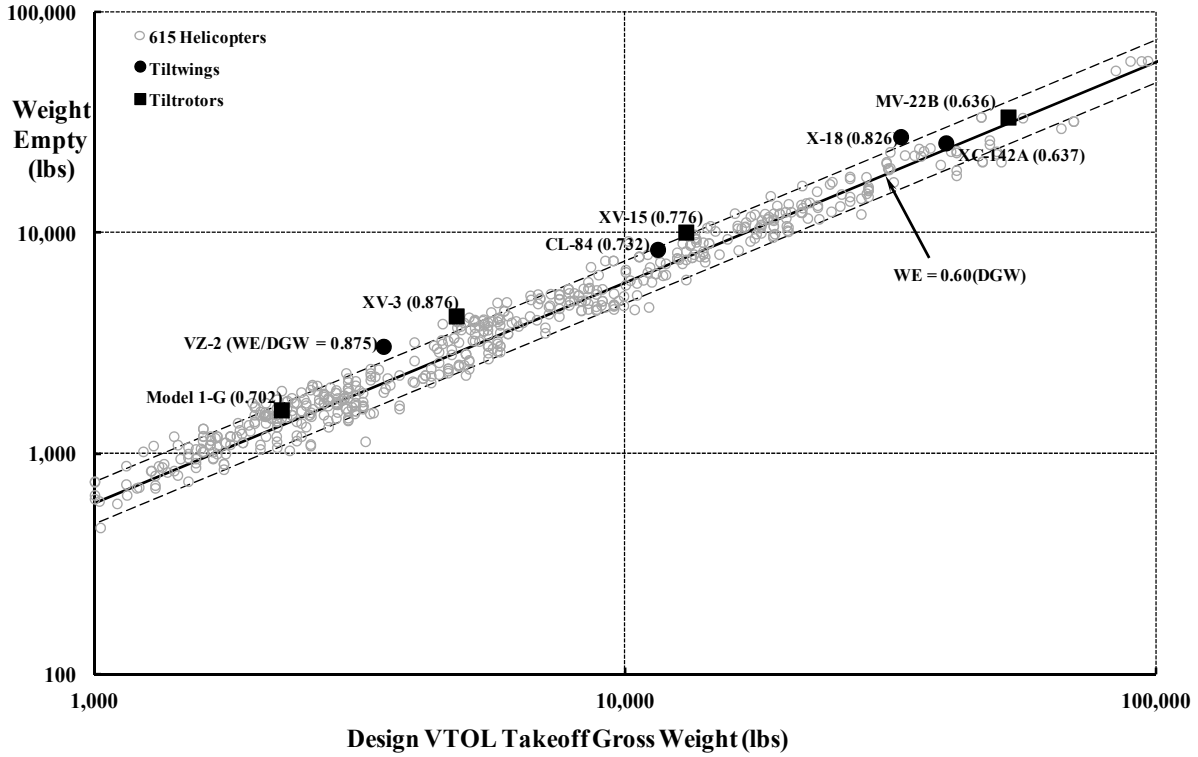

Fig. 2-194. There are not enough VTOL data points to draw a conclusion about the average weight empty fractions of this aircraft class.

Consider the subject of cost next. Here let me turn to Norm Augustine's classic book of laws [351][90] and specifically his chapter titled *The High Cost of Buying*. Norm makes the point that

> "It can be shown that the unit cost of military equipment, as is the case with much other high-technology hardware, is increasing at an exponential rate with time. Figure 9 shows, for example, the historical trend of rising unit cost in the case of tactical aircraft. From the days of the Wright Brothers' airplane to the era of modern high-performance fighter aircraft, the cost of an individual aircraft has unwaveringly grown by six db per decade . . . a factor of four every ten years. *This rate of growth seems to be an inherent characteristic of such systems, with the unit cost being most closely correlated with the passage of time rather than with changes in maneuverability, speed, weight, or other technical parameters* [my italics]. The same inexorable trend is shown in figures 10 through 13 to apply to commercial aircraft, helicopters, and even ships and tanks, although in the last two somewhat less technologically sophisticated instances, the rate of growth is a factor of two every ten years."

After this introduction and the data provided, Norm goes on to state one of his most famous laws:

> **"In the year 2054, the entire defense budget will purchase just one tactical aircraft. This aircraft will have to be shared by the Air Force and Navy 3 1/2 days each per week except for leap year, when it will be made available to the Marines for the extra day."**
>
> **(LAW NUMBER IX)**

[90] The Second Edition; first printing dated 1983 is my favorite version.

I have selected his chart for helicopters (his figure 11), and I have added a point for the Bell Boeing MV-22B tiltrotor. The results are shown here in Fig. 2-195. The data point is plotted at the Year of Initial Operational Capability of 2007 and a unit cost of $84 million based on my reading of the Selected Acquisition Report dated December 31, 2012 [352]. Because of the many trials and tribulations of the V-22 program that you read about earlier, you might see things a little differently. I like to think that the rotorcraft industry, with help from the fixed-wing manufacturers, can, in the future, design, build, and deliver tiltrotor and tiltwing aircraft that are priced well below Norm's trend line and my extrapolation, which is shown in red.

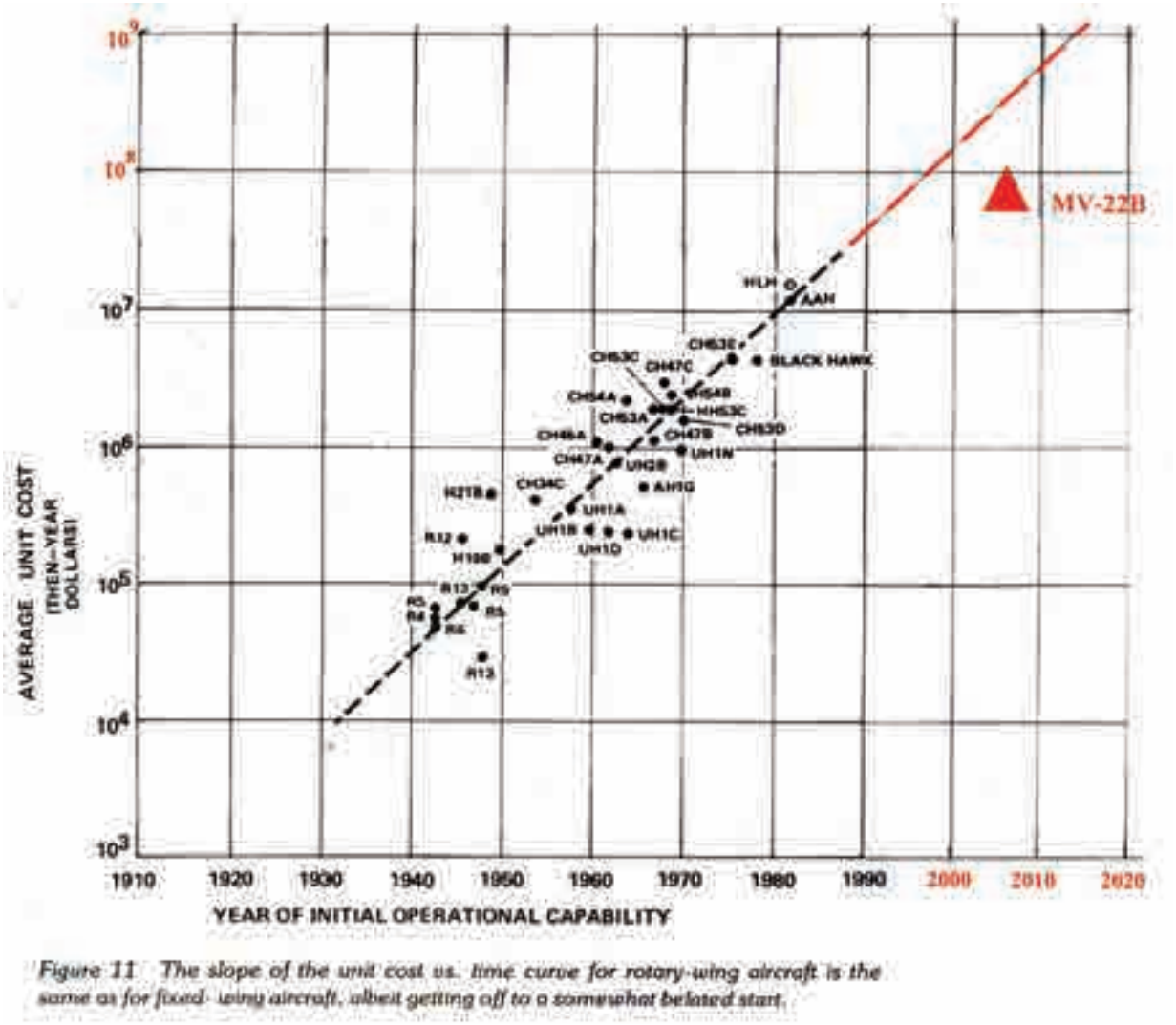

Figure 11 The slope of the unit cost vs. time curve for rotary-wing aircraft is the same as for fixed-wing aircraft, albeit getting off to a somewhat belated start.

Fig. 2-195. Based on Norm Augustine's statistical trend for helicopters, it appears that the Bell Boeing MV-22B tiltrotor is not as expensive as one might think. Had the program gone smoothly, its initial operational capability (IOC) would have been a decade earlier and, I suspect, its unit cost to the Marines would have been less.

Now let me go on to discuss the prospects for commercial (or if you prefer, civil) VTOLs. There is only one near-term commercial VTOL being prepared for the market that you should be aware of. It is the AW609 tiltrotor. This two-crew, nine-passenger VTOL shown in Fig. 2-196 was to be developed and marketed by Bell (51 percent share) and Boeing (49 percent share) as the Bell Boeing Model 609. Boeing declined to participate in March of 1998, so Bell teamed with Agusta, an Italian firm, in September of 2009. Later, Bell's interests in the 609 were completely acquired by Agusta. Then Agusta teamed with Westland, a British company, and by November of 2011 the Bell 609, and then the Bell Agusta 609, had finally become the AgustaWestland 609.

The AgustaWestland partnership announced at the February 25, 2014, Helicopter Association International annual trade show (HAI Heli-Expo) that certification to FAA standards had progressed enough for the aircraft to be used for demonstrations at the show. *Aviation Week* reported [353] that

> "The first [AW609] prototype, AC1, which is based in Arlington, Texas, with the AgustaWestland Tiltrotor Company (AWTC), is being used for the demo flights. It was flown from Texas [to Long Beach, California for the HAI show] in 6 hr.; officials are particularly pleased with the final leg of the journey, which saw the AW609 fly between Mesa, Ariz., and Long Beach nonstop with a 20-kt. headwind in 1 hr., 35 min. at 20,000 ft., burning 1,000 lb. of fuel per hour. The straight-line distance between the two [cities] is around 365 mi."

Fig. 2-196. The AW609 has a 16,800-pound VTOL design weight and a weight empty of 11,300 pounds. It is powered by two P&W PT6C-67A turboprop engines, each rated at 1,940 horsepower for takeoff at sea level standard day. It has demonstrated 333-knots maximum speed, and 275-knots maximum cruise speed. Note that the frontal area of the proprotor spinners and the nacelles behind appear nearly as large as the fuselage frontal area (photo courtesy of AgustaWestland).

This *Aviation Week* information is quite interesting because it can be translated into some basic performance data. *Assuming* that the quoted straight-line distance was in statute miles, you have a distance of roughly 320 nautical miles. A 20-knot headwind means that the equivalent still air distance was more like 350 nautical miles. Therefore, the flight time suggests that the *average* trip speed was about 220 knots. Additionally, the fuel burn for the flight time amounts to 1,500 pounds for the 350-nautical-mile flight, and this gives an *average* specific range of 0.233 nautical miles per pound of fuel. You might be interested to know that U.S. Airways—with its 79-passenger Bombardier CRJ900 that cruises at near Mach 0.8 (about 460 knots at 35,000 feet)—quotes the gate-to-gate travel time for virtually the same route as 1 hour and 15 minutes. The one-way ticket price when I called on November 26, 2014, was $184.00. Incidentally, a key airline economic parameter is cents per passenger seat mile. For this U.S. Airways' example, the parameter is calculated as one seat times 184 dollars divided by 365 statute miles, which comes out to about 50 cents per seat mile. Because I based the calculation on price not cost, 50 cents per seat mile is probably a little high in terms of cost, but airlines are not known as an industry with very high (if any at all) profit.

From this simple illustration, you can see that the AW609 and, I suspect, many other VTOLs, can compete on gate-to-gate travel time with a regional jet, at least up to a range of 400 nautical miles. To offer any airline a way to make a profit with a ticket price of $184.00 when operating a VTOL over, say, the Phoenix to Long Beach route is another matter entirely. Of course, you might argue that a passenger may not have to arrive an hour and a half before boarding time if he or she is flying on a VTOL-equipped airline. So far, that is a wishful consideration and not even close to a demonstrated fact.

The introduction of VTOL aircraft into the United States airspace is not as easy a matter as you might think given today's regulatory world. While the engineering world began to read more details about the FSD V-22 and MV-22B,[91] the FAA, NASA, and the DoD commissioned a joint civil tiltrotor study about how to capitalize on development of the military tiltrotor and document the potential of the commercial tiltrotor transport market. John Zuk at NASA Ames Research Center became the Study Director, Cliff McKeithan, the Study Manager, and Tom Galloway, the Technical Monitor. A contract (NAS2-12393) was given to the Boeing Commercial Airplane Company that, in turn, enlisted the aid of Bell Helicopter Textron and the Vertol Division of Boeing to fulfill the objectives of the study. A Summary Final Report [378] was published in July of 1987, and a Phase II effort was reported [379] in January of 1991. As you might expect, Boeing's Summary Report was comprehensive, authoritative, and very encouraging. The summary highlighted:

"National Issues

V-22 technology addresses several national issues.
- U.S. prominence in aviation
- Airport congestion relief
- Technical and industrial competitiveness
- Balance of trade

[91] You will find a representative sample of technical papers and reports in references [354-377]. The subject of the vortex ring state (which caused one MV-22B accident) is examined in several of these references.

Market Summary

Civil tiltrotor is a unique vehicle with a large market potential, particularly in high-density market. Pressurized versions show especially high potential.
Tiltrotor is superior to multi-engine helicopters under most conditions.
- Twice the speed and longer range
- Lower operating costs
- Better community acceptance
- Better passenger comfort

Tiltrotor is competitive with fixed-wing aircraft under certain conditions.
- VTOL capability and time savings are key to success
- Greater convenience could result in capture up to 2/3 of high-density markets

Market penetration depends on configuration, economics, and size.
- Assessment is difficult because of new transportation system
- All new design: 300–1400 units
- V-22 derivatives: 50–700 units
- Primary market is in North America (65%–75%)

Technical Summary

Six configurations analyzed (8–75 passenger).
- Includes V-22 derivatives and new designs
- All designs based on V-22 technology

V-22 derivatives with pressurized fuselages can accommodate 50 passengers and meet design range objective (600 nmi).
Passenger and community acceptance is anticipated (low noise, vibration and emissions).
Tiltrotors can operate in current airspace; however, improvements are needed to exploit tiltrotor capabilities for competitive service.
Early development of certification criteria is a high priority.

Potential Risk Areas Identified

Technical validation.
- Pressurized composite fuselage
- Competitive cost designs
- Aerodynamic improvement
- High performance configurations

Certification validation.
- Engine out criteria
- Failure mode criteria
- Flight deck operations
- All weather operation

Infrastructure.
- Vertiport design, location, availability
- Adaption into National Airspace System

Operational characteristics.
- Route proving
- Terminal access

Marketing.
- Public perception and acceptance (safety, noise, ride comfort)
- Economic competitiveness
- Development of supporting infrastructure
- Business payoff 10 years plus”

The Summary Report included quite definitive recommendations:

"**Recommendations:** Develop a National Plan for a tiltrotor transportation system, including:

Civil Tiltrotor Technology Development

Reduce risks and costs through design concepts, materials, and production methods.
Optimize aerodynamics and configurations.
Validate key technologies.
Canard configuration
Pressurized composite fuselage
Rotor/wing interaction

Infrastructure Planning and Development

Vertiports conveniently located in metropolitan areas.
New terminal instrument procedures to take advantage of precision navigation equipment.
Integration into the National Aerospace System.
Certification criteria for powered lift.
Continued development of airworthiness criteria.

Flight Technology Demonstration Plan

Identify key technologies.
Identify vehicle candidates.
Support certification criteria.
Define relationship to infrastructure needs.
Develop financial options and schedule.

Near-term Actions

Continue FAA/NASA/DOD/Industry cooperation for civil tiltrotor development.
Follow-on work on civil tiltrotor technology development.
Work on infrastructure and flight demonstration development plans.
Key civil tiltrotor development to V-22 program."

This vintage 1987 Boeing Commercial Airplane Company report increased momentum of the commercial tiltrotor like no report before or since. The tiltrotor was continually portrayed as a "National" resource and needed national economic development. The report stated:

> "Manufacture of the CTR [Commercial Tiltrotor] aircraft and development of supporting vertiports has a positive effect on national employment. Besides the direct CTR and vertiport development jobs, employment diversification results as manufacturing and service industries develop around the new hubs of transportation (vertiports). Quantifying national economic development was not the principal focus of this study, but it can be noted that industry would have to invest at least $2 billion more to produce the United States' first commercial tiltrotors. Additionally, an initial network of 25 vertiports would require private or local investment of $1 billion to $2 billion. Relatively speaking, vertiports are economical to build and conserving of land—as little as $40 million and 5 acres. A system of vertiports would serve to distribute the demonstrated favorable economic impact of urban airports throughout the community. Considering multiplier effects, a study done for the Department of Commerce concluded the increased national economic activity would be approximately $80 billion for every 1,000 commercial tiltrotors produced."

And then the Phase II report was published, which stated, based on the market survey, that the market "demand was more than 2,600 tiltrotors (passenger service only)." The survey concluded that the demand would come as geographically shown in Fig. 2-197.

It was a pretty exciting period as I recall it. *The* commercial VTOL had been found, both the Bell XV-15 and the FSD V-22 showed performance well in excess of what helicopters could do or ever promise, and the military had their machine. Even "Big Boeing"

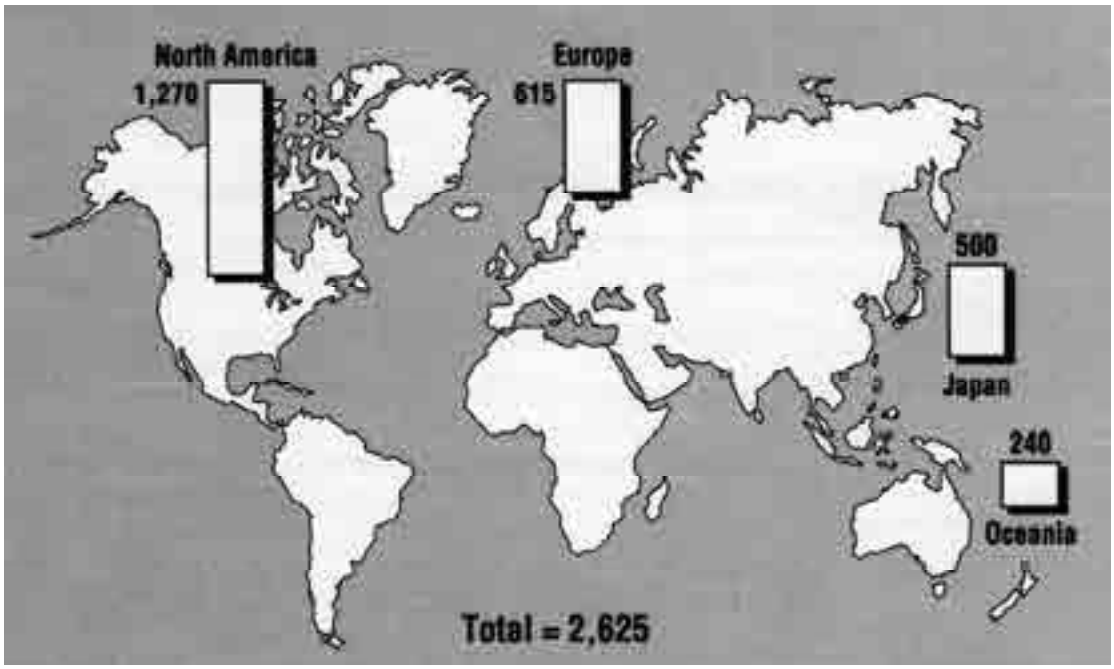

Fig. 2-197. Boeing's 1987 marketing survey predicted a bright sales future for the civil tiltrotor [379].

was behind it, and the U.S. economy was bright enough. The potential use of tiltrotors in the Canadian transportation system was even studied in some detail [380].

And then hopes for a commercial tiltrotor began to fade. The V-22 program began to have problems, and Secretary of Defense Cheney started a campaign to cancel MV-22B production [381]. Then Boeing backed out in bringing the Bell Boeing 609 to market. Nevertheless, The U.S. Department of Transportation went forward, at the 1992 direction of the U.S. House of Representatives (H.R. 6168) [382], with its plans to form a Civil Tiltrotor Development Advisory Committee. The committee was chaired by Frank Kruesi, Assistant Secretary for Transportation Policy, and he gathered 31 members, all top-level people in the world of aviation, banking, operations, law, economics, etc. The final report, dated December 29, 1995, was sent, along with a cover letter, to Albert Gore, President of the Senate, and to Newt Gingrich, Speaker of the House of Representatives. This was in accordance with Public Law 102-581, which required a report to Congress. The final report was also widely distributed, as you might guess. The cover letter included these paragraphs to which I have added some emphasis with italics:

> "The Committee has evaluated the technical feasibility and economic viability of developing civil tiltrotor (CTR) aircraft and a national system of infrastructure to support incorporation of tiltrotor technology into the national transportation system. *It found that the CTR is technically feasible and under certain circumstances could be economically viable and operate profitably without government subsidies.* Introduction of CTR for scheduled transportation service would depend upon overcoming a number of significant uncertainties and risks. One of the most important of these is the ability to locate vertiports at central city locations in large metropolitan areas, as well as suburban points close to major employment and economic centers. The successful completion of additional vehicle and infrastructure research would be required along with many interdependent decisions involving

> manufacturers, operators and various levels of government. In the Committee's view, the potential benefits, primarily delay reduction at congested airports and improved service to travelers, could be significant.
>
> The report recommends expanding the existing CTR research program and the creation of a public/private partnership to address these institutional, infrastructure, and coordination issues. *The report recommends that research costs be shared by industry and government while aircraft development costs be the responsibility of industry. Infrastructure costs would be borne by system users and aircraft operators with local government airport financing practices.* Clearly, *obtaining the significant Federal funding* envisioned for the cooperative research, test, and demonstration effort *will be difficult in this time of budget stringency.* Similarly, local funding for vertiport development is likely to be limited.
>
> *The report also recognizes that there may be other competing technologies for highly traveled transportation corridors* and recommends that DOT initiate a multimodal study of options, including CTR, for increasing intercity transportation capacity.
>
> As Chairman I can personally attest to the excellent qualifications and experience represented on the Committee and the dedication and commitment the members demonstrated over the course of the Committee's work. The report represents a general consensus of the CTRDAC membership, although individual Committee members had concerns with specific findings and recommendations. Although several members of the Committee are executives within the Administration, the report should not be interpreted as representing Administration policy. Copies of the report will be furnished to the Secretary of Transportation, Secretary of Defense, and the Administrator of NASA for consideration."

One member of the committee, Dr. Janet Welsh Brown (a Senior Fellow at the World Resources Institute) was unable to sign on to the final committee report because she believed "that continuing Federal support of the 40-passenger civil tiltrotor is not in the public interest at this time." In fact, for any number of reasons, this was the position that ultimately prevailed right up to the time this Volume III was published. And so the introduction of any commercial VTOL other than the AW 309 lies in hibernation.

The recommendation of the committee to "expand the existing CTR research program" was heeded from 1993–2001 by a NASA-sponsored program aimed at a Short Haul Civil Tiltrotor. After that period, NASA significantly reduced its investment in aeronautics in general, and rotorcraft in particular, until 2006. Since 2006, aeronautics investment at NASA has been approximately 3 percent of the NASA budget, and the investment in VTOL has been a miniscule part of the budget [383-385]. Fortunately, the U.S. Army maintained a foundation in rotorcraft research, primarily because helicopters and a VTOL follow-on are such vital machines for its missions. Most recently, the Army embarked on a new rotorcraft program called the Joint MultiRole Rotorcraft Technology Demonstrator (JMR-TD) aimed at first replacing its UH-60s, the 11 troop-carrying Black Hawks [386, 387]. Any hopes of a strong U.S. Government push for a commercial V/STOL appear dashed. In short, that 1991 view that the United States had a "National" resource in tiltrotor aircraft and technology was killed in virtually 15 years. In contrast to U.S. efforts, AgustaWestland, with its acquisition of Bell's 609 and with considerable support from the European Union, is moving ahead with research very applicable to commercial tiltrotors of any size through the Enhanced Rotorcraft Innovative Concept Achievement (ERICA) and CleanSky programs, Fig. 2-198 [388, 389].

Fig. 2-198. The European Union is investing in AgustaWestland's ERICA and CleanSky programs [388].

Now before proceeding to the fixed-wing world, let me add a note about two V/STOL configurations that I believe have received virtually no attention when future civil or military V/STOL transport configurations have been discussed. The first configuration, Fig. 2-199, is a compound helicopter suited to speeds from 200 to 250 knots and ranges perhaps up to 400 nautical miles. It was the Sikorsky work done in regard to the Reverse Velocity Rotor [79] and discussed earlier that set me to thinking. My curiosity was more along the lines of what can be done if you accept, say, eight blades, run the rotor at an advance ratio (V_{FP}/Vt) of 1.5 or even higher, and cruise at an altitude of 10,000 to 20,000 feet. Fig. 2-41 on page 91 and Eq. (2.44) suggest that a rotor can produce sufficient lift without a wing. Fig. 2-40 on page 90 suggests that the rotor blades alone may offer quite useable lift-to-effective-drag values.

The second configuration is a low-disc-loading tiltwing that came to me by a letter in 1991 from George Schairer, then retired Vice President of Research and Development at the Boeing Company. Mr. Schairer said, "Take a good look at tiltwings with rotors instead of propellers. They may be much simpler." He retired from Boeing in 1978 and died in late October 2004. Then in 2008, Tommy Thomason invited me to sit on a special panel he was putting together for the 46th Annual Forum of the American Helicopter Society to be held in Montreal, Canada. The panel's discussion centered on the Joint Heavy Lift program that the U.S. Army was embarking on in support of the Future Combat Systems program. At that time, the Army was seriously exploring a vehicle weighing from 20 to 36 tons. They wanted a V/STOL that could pick up this vehicle and move it a considerable distance. The VTOL designs under consideration at the time did not include a *low-disc-loading* tiltwing. Therefore,

Fig. 2-199. Suppose you accept, say, eight blades attached to a hingeless hub, forget the wing, and operate the rotor at high speed at an advance ratio of 1.5 or higher. A Sikorsky paper [79] got me thinking.

A JHL Tiltwing For Any Global Mission.

We Should Be Considering This Aircraft.

Art work courtesy of Gerardo Nunez

Tactical Engagements	Strategic Deployment
VTOL at 4,000 ft. on a 95°F day	VTOL at 4,000 ft. on a 95°F day
Margin for 1 engine out HOGE	4 Engs. at 11,000 SHP (10 min rating)
Design TOGW = 176,000 lbs	Overload TOGW = 206,000 lbs
WE = 94,000 lbs	WE = 94,000 lbs
Payload = 56,000 lbs	Payload = 56,000 lbs
Fuel = 26,000 lbs	Fuel = 56,000 lbs
Hover tip speed of 730 fps	Cruise tip speed of 350 fps
V_{max} of 350^{+} kts at V_{Tip} = 350 fps	Cruise at 250^{+} kts at 30,000 ft. Std.
Conversion Complete by 160 kts	Range 2,500 n.m., 20 kts headwind
Terrain Adapting Landing Gear	Reserve Range 500 n.m.
	Cruise L/D $[W*V/(550*SHP)]$ = 14

Fig. 2-200. A low-disc-loading tiltwing is one viable alternative to a tiltrotor [390].

I used my presentation time to make a sales pitch for a tiltwing that should be included in the selection process—but was not. The low-disc-loading tiltwing approach that Mr. Schairer suggested led to the configuration you see in Fig. 2-200. Of course, this conceptual design needs some careful preliminary design. Should you be interested in the complete presentation, it is available in reference [390].

2.14.1 Thoughts About the Future

It seems to me that the rotorcraft industry is not getting enough performance and productivity per "buck" for the power it installs in any given VTOL concept it has come up with so far. However, I do believe that the industry can design machines that have quite respectable weight empty to design gross weight fractions. Furthermore, I believe the technology tools are becoming adequate so that structural and aeromechanic problems that arise can be solved quickly and most likely even in advance of final drawing releases.

It bothers me that commercial airlines appear to now be assuming that there is no place for VTOL in the world's transportation system. Based on what they have seen so far, their presumption may be well founded as pointed out by the comparison of the AW609 to the Bombardier CRJ900 that U.S. Airways operates. In 1998 Mike Scully and I published a paper titled *Rotorcraft Cost Too Much* [391] that included a summary chart I have reproduced here as Fig. 2-201.[92] We have now progressed some 16 years to the AW609, which is shown on Fig. 2-201 as the D-609 point right above the MV-22 point. Let me draw your attention to two other commercial airplane data points on this figure. The airplanes are the 1960's era Lockheed Electra and the 1990's era Saab 2000. Both of these fixed-wing, passenger carrying aircraft fall close to the dashed line of constant productivity per "buck" equal to 300 ton-knots per $1 million. In contrast, the two tiltrotor aircraft appear to fall on an extension of the helicopter trend, which is along the dashed line labeled 100 ton-knots per $1 million. This is a substantial problem for the rotorcraft industry when selling their VTOL products. It continually relegates VTOL to niche markets.

Let me suggest that, from an engineering point of view, the rotorcraft industry *can* produce a commercial passenger carrying tiltrotor or tiltwing that could equal the performance of, say, the Saab 2000 data point shown in Fig. 2-201 [392]. To acquaint you with this nearly successful turboprop airliner,[93] it was a 50-passenger-seat airplane (Fig. 2-202) that could take off over a 50-foot obstacle in Denver, Colorado, in just over 5,500 feet of runway at its maximum takeoff gross weight of 50,265 pounds. Its landing distance was about 1,000 feet shorter. The aircraft was powered by two Allison AE 2100A turboprop

[92] Mike and I included this figure at the suggestion of Evan Fradenburgh, an engineer who we, along with the rest of the rotorcraft industry, really respected. At that time, Evan had recently retired from Sikorsky. Evan's suggested chart was probably the best piece of trend data in our paper.

[93] The airlines turned to regional jets when they became available in part because of public preference for the jet ride quality first experienced with the Boeing 707. Turboprop-driven aircraft just had too big an uphill battle for widespread acceptance.

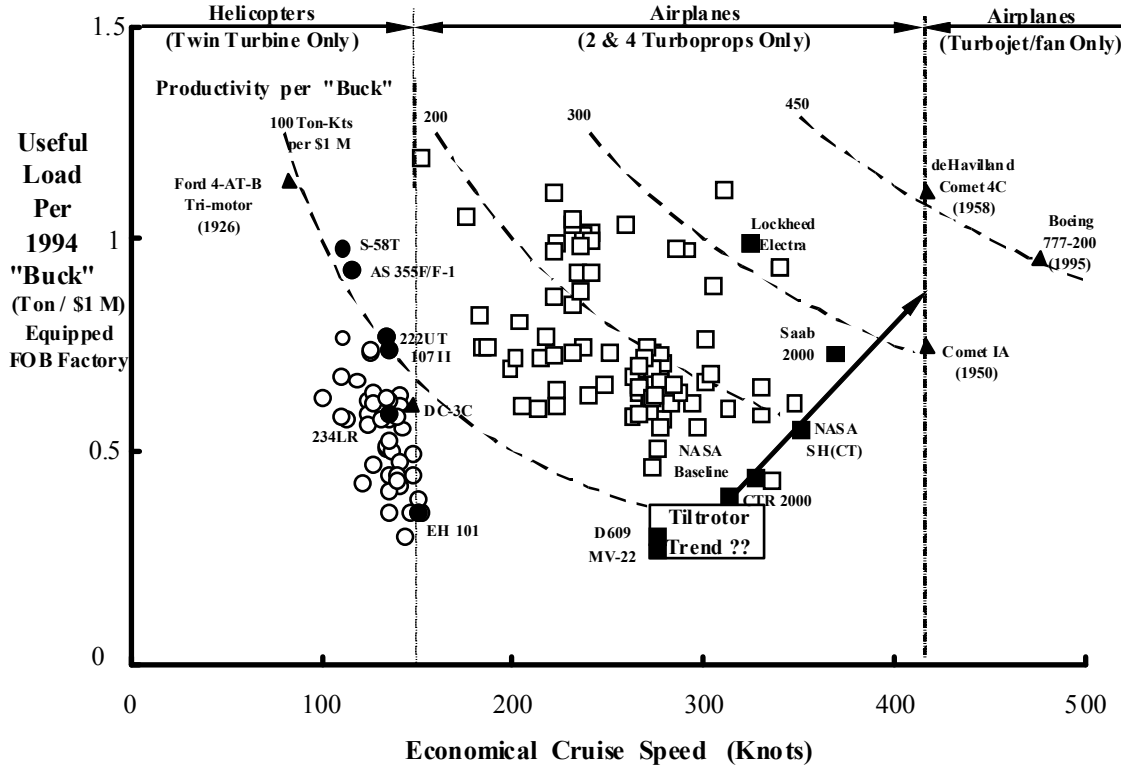

Fig. 2-201. The rotorcraft industry does not appear to be making any progress in raising its products' productivity per "buck" [391].

engines, each having a takeoff rating of 6,000 shaft horsepower. Saab derated the engines to 4,125 as a takeoff rating, which certainly would have ensured the 30,000-hour life that Allison quoted. For the Saab 2000 data point on Fig. 2-201, Mike and I credited it with a selling price of $14 million in 1994 ($22.5 million in 2014, according to the U.S. Bureau of Labor Statistics), a weight empty of 29,770 pounds, a useful load of 20,495 pounds, and a maximum cruise speed of 369 knots at 25,000 feet. This information leads to a useful load per 1994 "buck" of 0.732. Additionally, we estimated the fuel burn rate at 2,170 pounds per hour, which gives a specific range of 0.17. The long-range cruising speed was more like 300 knots at 31,000 feet.

Now consider these three points:

1. Based on the Harris and Scully aircraft price estimating trends [391], the rotorcraft industry *cannot now* produce a Saab 2000 VTOL derivative for $22.5 million, which is what a Saab 2000 would probably sell for in 2014 dollars.
2. NASA, for example, perceives the introduction of the civil tiltrotor into U.S. airspace as using a portion of current airports. Tiltrotor operations would be done with vertical takeoff and landings [393, 394].
3. The National Intelligence Council, for example, projects that from now to 2030, "most countries will be increasingly urban" [395].

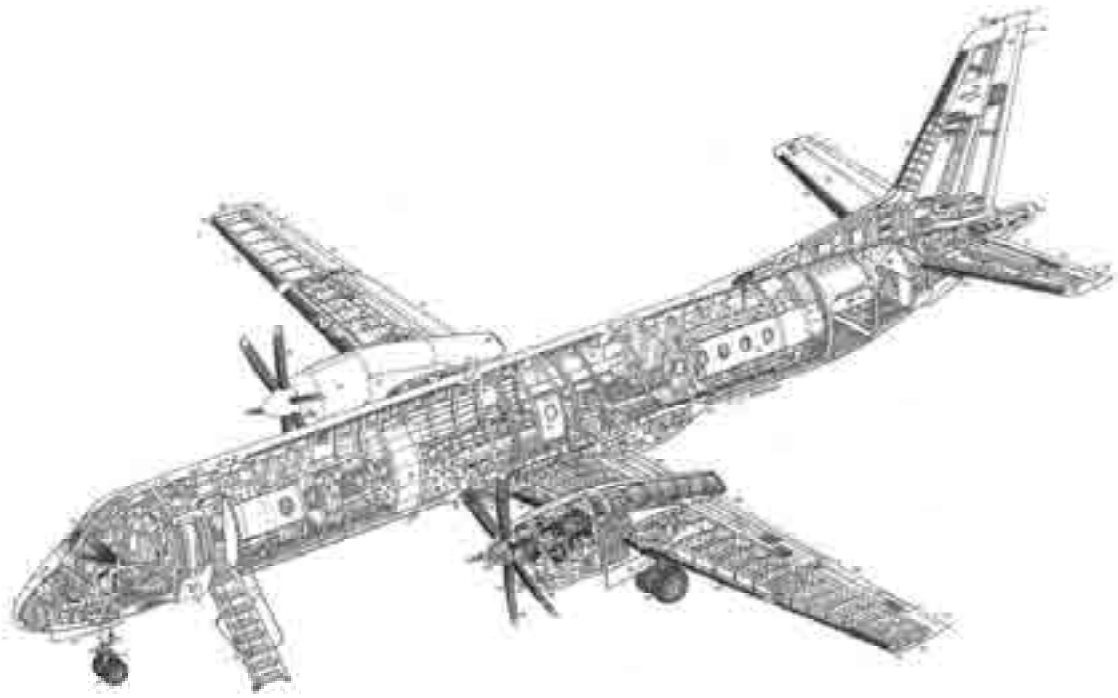

Fig. 2-202. The Saab 2000 [396] operated as a 50-passenger CTOL at a design gross weight of 50,265 pounds using two Allison AE 2100A turboprop engines derated to a total of 8,250 shaft horsepower at takeoff. It required a 4,000-foot runway at sea level [392] (*Flight International*).

Let me discuss these three points in order. To start with, Harris and Scully's price estimating equation is of the form

$$\text{(2.160)} \quad \text{Selling Price} = \left[\text{K} \left(\text{Weight Empty} \right)^{0.4854} \left(\text{Engines Rated SHP} \right)^{0.5843} \right] (\text{Inflation}),$$

and the equation is equally applicable to helicopters, tiltrotors, general aviation airplanes, and airliners. That is to say, Harris and Scully could not find a statistical difference in the exponents of weight empty and horsepower because of aircraft type. What they did find, however, was that the constant (K) depends on a number of configuration variables. For example, gas-turbine-engine-powered aircraft were considerably more expensive than piston-engine-powered aircraft by a factor of 1.779. And pressurized aircraft were more expensive than unpressurized aircraft by a factor of 1.135. Any inflation was based on prices indexed to 1.0 in 1994. According to the U.S. Bureau of Labor Statistics, inflation has increased prices by a factor of 1.6 as of 2014. Following Harris and Scully, the Saab 2000, if manufactured and sold in the United States in 2014, would carry a selling price of

$$\text{(2.161)} \quad \text{Saab 2000} = \left[\$593 \times (29,770)^{0.4854} \left(2 \times 4,125 \right)^{0.5843} \right] 1.6 = \left[\$17.1 \text{ m} \right] 1.6 = \$27.5 \text{ million}.$$

In contrast, a civil tiltrotor (CTR) at equal weight empty and installed power—produced by the U.S. rotorcraft industry—would have a price tag of

$$(2.162)\quad \text{Saab 2000 CTR} = \left[\$934\times(29{,}770)^{0.4854}\,(2\times 4{,}125)^{0.5843}\right]1.6 = [\$26.9\,\text{m}]1.6 = \$43.3\,\text{million}.$$

This comparison immediately raises the question of whether the U.S. rotorcraft industry could manufacture and sell a Saab 2000 today for $27.5 million. My guess would be no, because their manufacturing cost history has perpetuated a high-price V/STOL product.

But suppose the rotorcraft industry was just converting a Saab 2000 into a tiltrotor or a tiltwing rather than starting from a clean sheet of paper. The challenge to the industry would then be to redesign *just* the wing, wing-fuselage interface, and propulsion subassembly for V/STOL with two Rolls-Royce AE 2100A turboshaft engines, each flat-rated at 4,125 shaft horsepower for takeoff. The pressurized fuselage with its commercial interior would be retained along with as many Saab 2000 subassemblies as possible. The objective would be a V/STOL aircraft with a weight empty on the order of 30,000 pounds. The selling price objective would be to minimize the increase of the constant (K) from $593 which, I suggest, might be easier if just the wing and proprotor were at issue. Keep in mind that each of the Saab 2000's Dowdy Aerospace Propellers (Model (c) R381/6-123-F/5) weighing 500 pounds [397] would be removed, and the AE 2100A turboshaft engines [398] might have to be modified to operate vertically.

Now I suggest that this V/STOL aircraft would have superb STOL performance (forget its VTOL performance for the moment) that would let the useful load be much greater than a Saab 2000's 20,495 pounds. This would mean that the Saab's design gross weight of 50,265 pounds would be increased, which would, of course, increase the weight empty somewhat. However, the designers would be selectively strengthening key areas based on a known design—not starting from scratch. Most importantly, the V/STOL I have suggested would take off in much less distance than the Saab's 5,500-foot runway—probably more on the order of 550 feet.

Imagine now that this V/STOL derivative of a Saab 2000 has a useful load increase of, say, 10,000 pounds, and operating as a STOL it can take off and land on 550 feet of concrete. The design gross weight would be about 60,000 pounds, and the weight empty would still be close to 30,000 pounds. Then the useful load would be about 30,000 pounds, verses the Saab 2000's 20,495 pounds. You might note that the MV-22B has a weight empty of about 33,500 pounds, and its normal vertical takeoff weight is about 52,600 pounds. More importantly, its maximum takeoff weight for self ferrying is 60,500 pounds. Of course, there is no reason to shoot for anything less than a maximum cruise speed of 369 knots. This leaves the selling price as the only remaining significant issue. Suppose a member of the rotorcraft industry teamed with Sweden's Saab company so that together they had an average 1994 constant (K) of $763. On this basis, you would have productivity per 1994 buck of

$$(2.163)\quad \frac{\text{Productivity}}{1994\ \$\text{million}} = \frac{\text{Useful Load}\times\text{Max. Cruise Speed}}{1994\ \$\text{million}} = \frac{15\,\text{tons}\times 369\,\text{knots}}{\$22\ \text{million}} = 251.$$

The marketing theme would be that the rotorcraft industry has a superb STOL that can perform VTOL at reduced useful load. The production Saab 2000 CTR might be stretched to accommodate, say, 70 passengers, and the full rated power of 6,000 horsepower from the Rolls-Royce AE2100A engine would be used based on the technology demonstrator development. At any rate, I hope you get my line of thinking because I believe this is a path to a commercial V/STOL that would be worth peddling to the airlines.

The second point deals with how VTOL aircraft can fit into existing airspace. References [393, 394] illustrate a number of patterns a VTOL aircraft could take during takeoff and landing without interrupting normal flight operations of fixed-wing airliners. My review of these references suggests that VTOL was hardly essential to meet FAA criteria as studied by William Chung, et al. Both the XV-142A and the V-22 demonstrated that there is very little difference between a vertical takeoff and a STOL takeoff in terms of real estate required. So I ask the question, Why bother installing the power for VTOL when perhaps half as much installed power would do for STOL? Of course, the drawback here is that with less installed power, the machine may not cruise as fast as a Saab 2000. Therefore, drag reduction would be a significant part of any program. This design direction would lower the CTR's selling price, and this one step might attract some in the airline business to convince the FAA to initiate at least an experiment of CTRs operating in commercial transportation airspace. Just imagine an experiment with 5 to 10 technology demonstrators showing what V/STOL can really do. The whole program could be funded by NASA, the Department of Transportation, and several airlines.

The last point I will comment on deals with where people will congregate over the next 15 to 20 years and what this means to the future of commercial V/STOL aircraft. Reference [395] suggests that urban sprawl will simply continue. An excellent, concise discussion of congregation was provided by R.E.G. Davies in a paper [399] adapted from his Wings Club 37th "Sight" Lecture delivered in New York on May 17, 2000. In my opinion, Davies wrote the book on commercial aviation [2]. In his 2000 lecture, he gives a very clear picture of urban sprawl around the world in the future. Despite his long career of advocating the value of airplanes, Davies' lecture includes a strong suggestion that the United States should invest heavily in high-speed rail. These sort of projections have been repeated over and over again for decades. It seems to me that these projections can now be taken as a fact of life and hardly need re-quantification until, oh say, 2050. By then I can imagine, for example, that Phoenix, Arizona, and Los Angeles, California, will have sprawled together to make another "corridor."

These projections suggest two things to me. First, V/STOL advocates have repeatedly shown (analytically) that their aircraft can increase throughput of urban air transportation centers without adding new runways. This is a good point because airport authorities continually tell us that it is virtually impossible to get new runways added at existing airports. And getting another 10,000-foot airport like the one recently constructed in Denver, Colorado, does not appear on the horizon (i.e., the next 20 to 50 years). More importantly, using VTOL aircraft or STOL aircraft to increase the throughput appears to be splitting hairs because both aircraft types can be accommodated by current traffic patterns around 10,000-foot runways.

The real problem is offering airlines an aircraft they can buy and operate at a profit. I suggest that designing tiltrotor and tiltwing aircraft with only enough installed power for STOL is a big step toward attracting airlines.

Secondly, I see urban sprawl as simply surrounding regional airports, which are now in rural areas. A good example from the past is the way Palo Alto's 2,500-foot, asphalt-paved airport now exists between San Jose's and San Francisco's International Airports in California. Closer to my home in Piedmont, Oklahoma (now a rural farmland area) are two examples of the future. Suburbs of Oklahoma City are engulfing both Wiley Post Airport and Sundance Airpark quite quickly. These two regional airports are about 15 miles west of Oklahoma City. At issue, of course, is just what aircraft gross weights can be accommodated without breaking asphalt and concrete or rutting ground. It seems to me that regional airports act like train stations of the past in that every town wanted one so that it would grow. Based on these examples, I would say that vertical takeoff and landing aircraft are not required. What is required are inexpensive STOL aircraft, and the rotorcraft industry has just the product for the airlines—if it stops installing power for VTOL and begins installing just the power needed for STOL.

To summarize then, the rotorcraft industry has tried unsuccessfully to sell commercial VTOLs for decades in a market that is dominated by fixed-wing, turbojet and turbofan aircraft using 5,000- to 10,000-foot runways. Secondly, the fixed-wing side of the industry seems to continually shy away from providing service to the several thousand regional airports that exist in the United States. Imagine now that the world's population grows to the point where airlines *want* to provide service to connecting pairs of regional airports with runways 2,000 feet long or less. In the next chapter, you will read that designing fixed-wing commercial airliners for operation out of airports with such short runways requires quite a different engineering and marketing expertise than what the fixed-wing industry has been using for decades. Here the rotorcraft industry has a clear advantage because it has already demonstrated technology to design and manufacture VTOLs that have outstanding STOL performance. Both the LTV XC-142A [178] and the V-22 Osprey [392] can easily operate from 500- (i.e., Ultra STOL) to 1,000-foot runways at overload gross weight. *Therefore, I suggest that the rotorcraft industry stop selling VTOLs and start designing and marketing STOL aircraft:*

(a) that can operate safely from any of the current 5,000- to 10,000-foot runways and, more importantly, from virtually all regional airports;

(b) that, at reduced weight, can do vertical takeoff and landings whenever a profitable route appears; and

(c) that have realistic selling prices and operating costs that attract airlines.

Now let me change the subject from rotorcraft at high speed to the other side of the coin—fixed-wing aircraft at low speed.

3 FIXED-WING PERFORMANCE AT LOW SPEED

Ever since the convincing demonstration of the airplane, the autogyro, and the helicopter,[94] the aviation industry has continually focused on two fundamental objectives. These two objectives have been to:

1. Offer fixed-wing machines that carry more, go faster, fly higher, and yet still take off and land within rationally sized airports. This aviation branch has pursued its objective with metal monoplanes, retractable landing gear, variable-pitch propellers, swept wings, gas turbine engines, and of course, high-wing-lift devices such as the Fowler flap.
2. Offer rotary wing machines that carry more, go faster, fly higher, and yet still take off and land vertically (VTOL). This side of the aviation industry has pursued its objective by making successive improvements to the helicopter (including use of the gas turbine engine) and with a decades-long search for airplane-like speeds. Today, the tiltrotor configuration has emerged as the first positive rotorcraft step to a VTOL machine that flies at significantly higher speeds than a helicopter.

In the fixed-wing world, requirements for short takeoff and landing (STOL) have come almost entirely from the military. Over the years, the United States Army has frequently asked the United States Air Force (USAF) for logistical support much closer to the battle area. In my opinion, the USAF has given relatively little weight to the Army's need in this regard. Over the years, this situation has prompted the Army to develop helicopters with increasing lift capacity. The vast majority of studies and programs that yield USAF logistical support airplanes having STOL capability show that combining STOL with other USAF missions has led to an unacceptably compromised airplane. Perhaps the best example of this is the USAF experiment with the Advanced Medium STOL Transport program, which officially started with an Air Force Request for Proposal on January 20, 1972, and officially ended in February 1978. In this program, the Air Force selected two contractors (McDonnell Douglas with its YC-15 and Boeing with its YC-14) to demonstrate prototypes of a STOL transport that could complement the Lockheed C-130. Despite quite reasonable success, neither aircraft was placed in production, and the Air Force decided instead to embark on a strategic heavy-lift aircraft that became the C-17. A comprehensive discussion of many STOL aircraft is offered by Bill Norton in his AIAA Case Study, *STOL Progenitors: The Technology Path to a Large STOL Aircraft and the C-17A* [26]. The story of Boeing's YC-14 program is told by Jack Wimpress in his AIAA Case Study, *The YC-14 STOL Prototype: Its Design, Development, and Flight* [400]. I have read few in-depth stories about prototype development that can hold a candle to Jack Wimpress' book.

[94] I suggest that Wilber and Orville Wright accomplished this in 1908. After rather secretive development from 1903 to 1907, Wilber gave widely attended demonstrations in Europe, and Orville fulfilled their U.S. Army contract at Ft. Myer, Virginia. In 1924, Juan de la Cierva demonstrated his C-4 Autogyro to the Royal Aeronautical Society in England. And then Henrich Focke's helicopter was flown before thousands inside the Deutschland Halle sports stadium in Berlin in 1936.

In the commercial fixed-wing world, the early rule of thumb was that the ratio of maximum speed to landing speed was about 3. This situation continued until landing speeds began to approach pilots' tolerance. Landing speeds beyond 50 to 75 miles per hour were reason enough for pilots to complain, particularly because runways at the vast majority of airports were (and still are) well under 5,000 feet. With the advent of the jet transport, landing speeds approached 125 to 150 miles per hour. As a result, successful, modern day, public air transportation depends on runways being 10,000 feet or longer.

Designing an airplane that can land on a short runway (2,000 feet or less appears to qualify an airplane for the STOL designation) *seems*, on the surface, not particularly challenging. You only need to lay aside such issues as pilot workload, control at low speed, performance should one engine fail, and of course, cost. To illustrate this point, consider Fig. 3-1. Imagine the aircraft is on a glide slope of between 2 and 15 degrees as it passes over a 50-foot obstacle. The immediate question is: What horizontal distance will the aircraft travel before it strikes the ground? Given a glide slope and glide speed, this is a simple geometry problem. There are, however, some less than subtle factors raised by Fig. 3-1. First, think about a naval aircraft landing on a carrier deck. In this extreme, a fighter aircraft approaches the carrier at somewhere between 100 and 125 knots, aiming for the intended deck spot. And then, for all intents and purposes, the pilot simply slams the aircraft down on the deck with approximately 600- to 800-feet-per-minute vertical velocity. Thanks to the aircraft's landing gear and tail hook, and the cables stretched across the deck, the aircraft is arrested within 1 second after traveling some 300 feet. Coming to a stop from 125 knots in 300 feet, leads to an average deceleration of 75 feet per second squared or 2.3 g's.

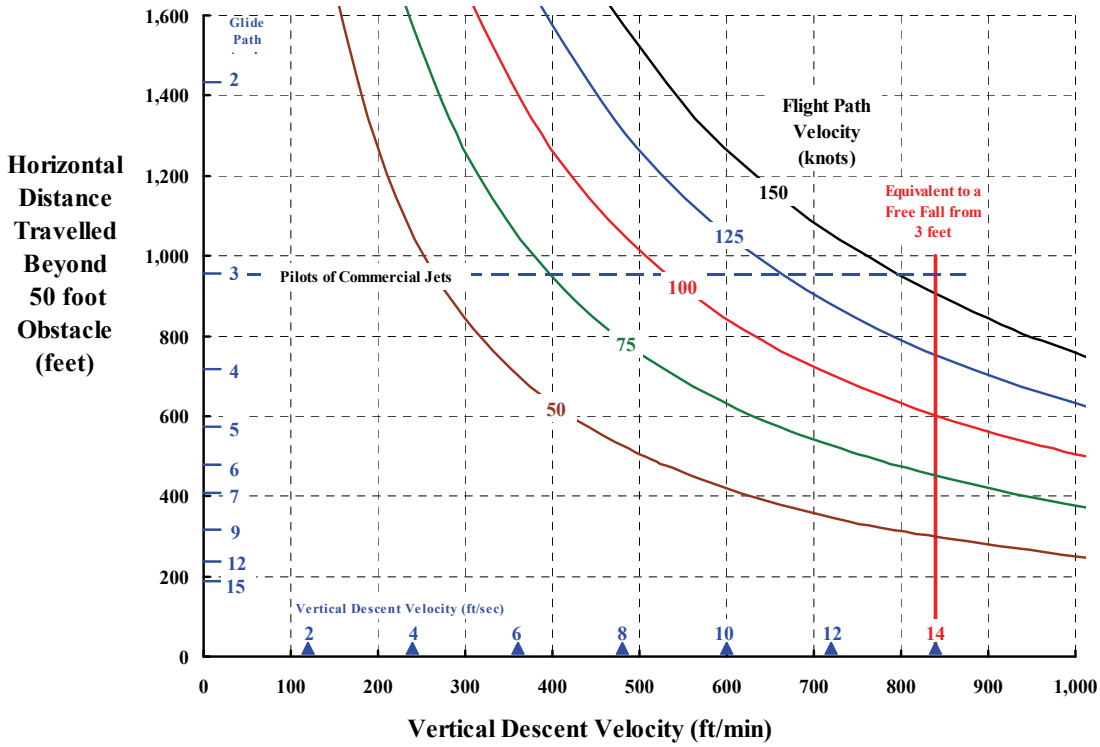

Fig. 3-1. The geometry and constraints surrounding landing.

Laying aside the naval-carrier-assisted STOL as one end of the spectrum, the situation faced in the commercial world presents the more pleasant extreme. The fundamental problem faced by the commercial pilot is how to arrest the rate of descent and touch down at well under 200-feet-per-minute descent velocity. Of course, passengers are always complimentary when they hardly know the wheels have touched the runway. To accomplish this landing the pilot must flare the aircraft. A fixed-wing aircraft's flare reduces the glide slope from about 3 degrees to virtually zero, or at most 1/2 degree, given a 125-knot landing speed. This is the major difference between STOL and VTOL. A fixed-wing airplane—even with an approach speed as low as 75 knots—has very little capability to decelerate along the final glide path. Reducing the glide slope is the only realistic option, and this maneuver extends the landing distance. On the other hand, the pilot of a VTOL aircraft can decelerate his aircraft, even to a hover, anywhere along the final glide path. It takes very little imagination to extend the curves in Fig. 3-1 to zero speed and then appreciate the operational flexibility that VTOL provides.

3.1 LIMITATIONS OF CIRCULATION LIFT

Shortly after I graduated from Rensselaer Polytechnic Institute (RPI) and joined Vertol (June 1956), an article appeared in the Readers' Forum of the March 1957 issue of the *Journal of the Aeronautical Sciences*. The two-page article was written by Heinrich Helmbold [401], and he reasoned that a wing could not achieve a maximum lift coefficient greater than 1.9 times the wing aspect ratio ($AR = b^2/S$). This was an absolutely fascinating thought to me, and one that no professor imparted to me during my 4 years at RPI.

Helmbold included just one figure in his article, and you see it here as Fig. 3-2. His theory accounted for a distorted wake that, unlike classical Prandtl-Glauert wing theory, does not remain in the plane of the wing.[95] My aerodynamics class was first taught using Paul

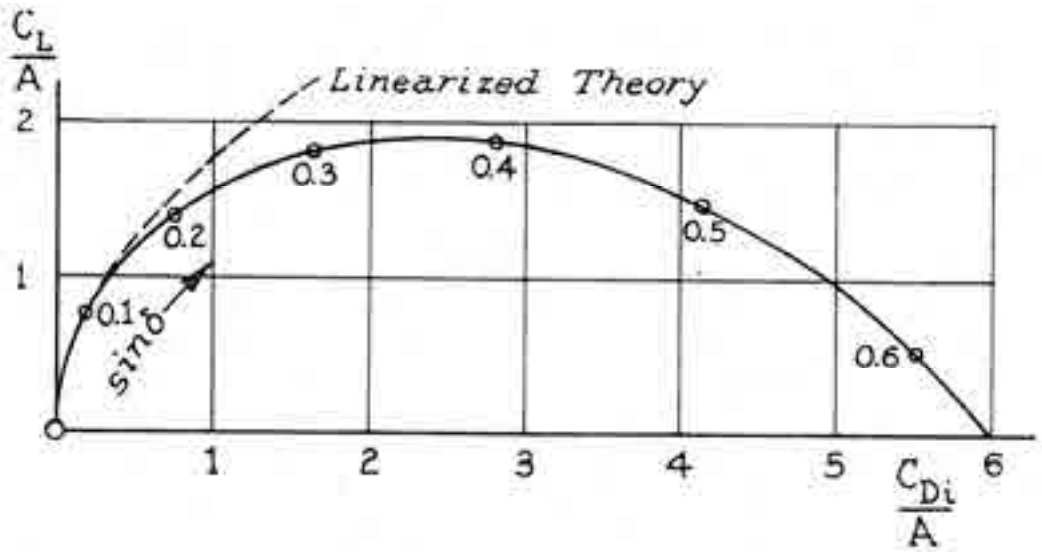

Fig. 3-2. Heinrich Helmbold's nonlinear wing theory [401].

[95] A similar investigation was published by Clarence Cone in April 1961 [402].

Hemke's *Elementary Applied Aerodynamics* [221]. Later, Alan Pope's book, *Basic Wing and Airfoil Theory* [403], along with Perkins and Hage's *Airplane Performance, Stability and Control* [269], became our primary textbooks. This undergraduate study always used the sketch—from which wing lift and drag equations were created—illustrated here in Fig. 3-3.

We learned that the actual wing could be replaced with a lifting line and that the ideal circulation (Γ) varies elliptically along the lifting line from wingtip to wingtip as

$$\Gamma = \Gamma_0 \sqrt{1 - \left(\frac{2y}{b}\right)^2} \quad . \tag{3.1}$$

This fundamental wing theory says that wing-induced drag (D_i) in pounds is calculated quite simply as

$$D_i = \frac{L^2}{(\rho/2)V^2 \pi b_w^2} \quad , \tag{3.2}$$

where the primary variables are the wing lift (L) in pounds, the air density (ρ) in slugs per cubic foot, the flightpath velocity (V) in feet per second, and the wingspan (b) in feet. I was taught that the nondimensional form of induced drag was

$$\frac{D_i}{q b_w^2} = \frac{1}{\pi}\left(\frac{L}{q b_w^2}\right)^2 \quad \text{or, occasionally,} \quad \frac{C_{Di}}{AR} = \frac{1}{\pi}\left(\frac{C_L}{AR}\right)^2 \quad . \tag{3.3}$$

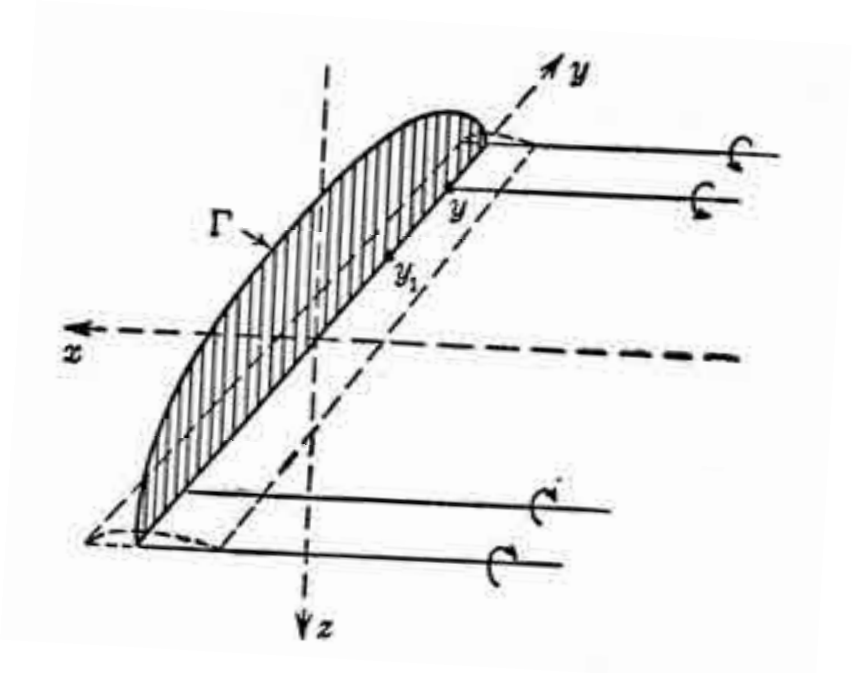

Fig. 3-3. The classical Prandtl-Glauert wing theory assumes that the wake is flat and it lies in the plane of the wing.

Heinrich Helmbold made it quite clear, however, that the flat wake approximation left something to be desired and that the wake actually forms behind the wing at an angle (δ) as I have sketched here. When the wake deformation is included, Helmbold found that

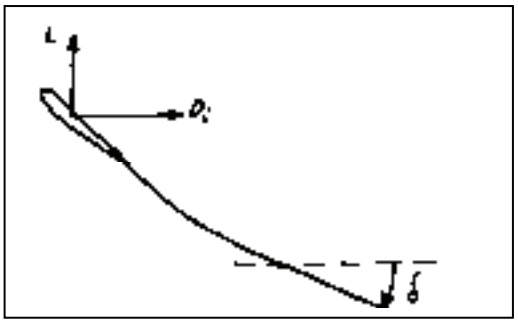

$$(3.4)\qquad \frac{D_i}{qb_w^2}=\frac{1}{\pi}\left(\frac{L}{qb_w^2}\right)^2\left\{\frac{\sqrt{1-\sin^2\delta}}{\left(1-\frac{\pi^2}{4}\sin^2\delta\right)^2}\right\}=\frac{C_{Di}}{AR},$$

and that wing lift was also dependent on the wake angle (δ) as

$$(3.5)\qquad \frac{L}{qb_w^2}=\frac{\pi^3}{4}\sin\delta\left(1-\frac{\pi^2}{4}\sin^2\delta\right)=\frac{C_L}{AR}.$$

It is worth noting that the lift and drag coefficients have the alternate forms C_L/AR and C_{Di}/AR. Furthermore, Eq. (3.5) is a cubic equation, which has the solution

$$(3.6)\qquad \sin\delta=\frac{4\sqrt{3}}{3\pi}\cos\left[\frac{5\pi}{3}-\frac{1}{3}\arccos\left(\frac{3\sqrt{3}}{\pi^2}\frac{C_L}{AR}\right)\right]\quad \text{for } 0\le\frac{C_L}{AR}\le\frac{\pi^2\sqrt{3}}{9}.$$

To graph lift versus induced drag, you need only pick a few wake angles and compute lift from Eq. (3.5) and induced drag from Eq. (3.4). You see the results here in Fig. 3-4.

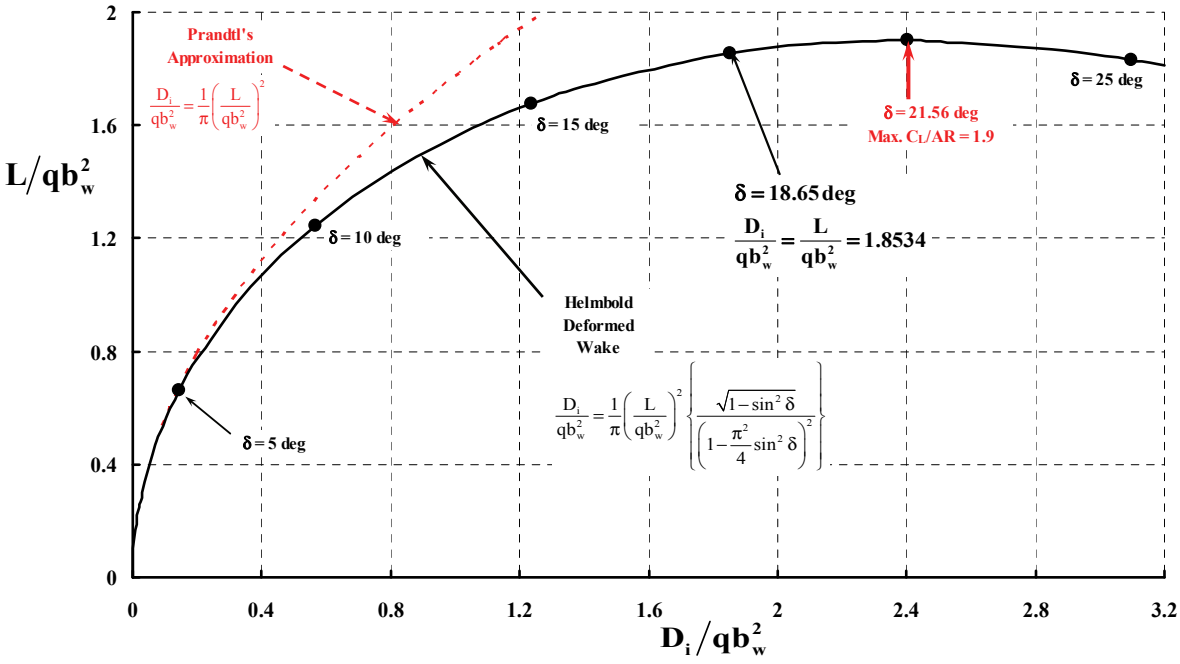

Fig. 3-4. The wake behind the lifting wing is not flat, and this leads to induced drag being greater than what you would calculate with the Prandtl-Glauert theory.

What made such an impression on me was that the ideal fixed wing could never have a lift coefficient greater than

$$(3.7) \quad \text{Wing Max. } C_L = \frac{\pi^2\sqrt{3}}{9}\,AR \approx 1.9\,AR,$$

and this result says that the slowest a fixed wing can fly would be determined by

$$(3.8) \quad \text{Minimum Airspeed } V_{min} \approx \sqrt{\frac{L}{0.95\rho b_w^2}} \text{ in ft/sec} \approx 12.45\sqrt{\frac{L}{\sigma b_w^2}} \text{ in knots},$$

where the density ratio is ($\sigma = \rho/\rho_o$), the wingspan is (b_w) in feet, and the wing lift (L) is aircraft gross weight in pounds.

The second major point that Helmbold's analysis offers is that induced drag (D_i) equals lift (L) when L/qb^2 (or, if you prefer, C_L/AR) equals 1.8534, which occurs when the wake angle is 18.65 degrees as you can see from Fig. 3-4. Take a minute to absorb this second point. The fixed-wing aircraft's induced drag will equal its weight at an airspeed slightly above its minimum flight speed. *If the propulsion unit force (say from a propeller) must balance the wing-induced drag, and this drag equals the aircraft's weight, why not just direct the force vertically and hover?*[96]

The confusing thing to me about Helmbold's theory was that in order to obtain maximum wing lift coefficients on the order of $C_L = 1.9\,AR$, the wing airfoils would have to be extraordinarily high. After all, if the wing aspect ratio (AR) was, say, 10, the airfoil would be operating at a two-dimensional airfoil lift coefficient (C_ℓ) of 19, and this flew in the face of what I had learned about two-dimensional airfoils. Thin airfoil theory for uncambered mean lines, as I learned it, says the two-dimensional lift coefficient behaves as

$$(3.9) \quad C_\ell = \frac{dL}{q(c\,dy)} = 2\pi\sin\alpha.$$

When the Joukowski transformation is extended to cambered mean lines, the reference chord (c) shrinks to the point where the airfoil appears as a circle, the circulation becomes so strong that the two stagnation points coincide, and the reference chord becomes the cylinder's diameter. At this limiting case you often see the maximum lift coefficient quoted as 4π.[97] (To me, this progression from 2π to 4π is more a change in the magnitude of the reference chord.) The way I like to think about the limiting case of circulation lift is illustrated in Fig. 3-5. The thing to keep in mind is that when the angle of attack is 90 degrees, the sharp "nose" of the flat plate is providing all of the lift. The velocity around the nose is infinite. The lower and upper surface stagnation points coincide with the trailing edge. This is the type of solution one gets with circulation around a circular cylinder in a free stream.

---

[96] John Nichols pointed this out to the rotorcraft industry in May of 1957 [404].

[97] Mr. Apollo M. O. Smith (1911–1997) was honored to give the 37th Wright Brothers' Lecture in August 1974. In the published paper [405], he provides the clearest explanation of how camber alters Eq. (3.9).

In August of 1970, Mr. Frank (Al) Cleveland (1923–1983) presented the 33rd Wright Brothers' Lecture. In his published paper [406], he gave a snapshot of the trend in "nonaugmented maximum lift coefficients" that you see here as Fig. 3-6. Clearly, all the arrangements of mechanical flaps, slots, etc. were only capable of yielding a maximum lift coefficient on the order of $C_{Lmax} = \pi$.

Fig. 3-5. The uncambered airfoil has a theoretical maximum lift coefficient of 2π.

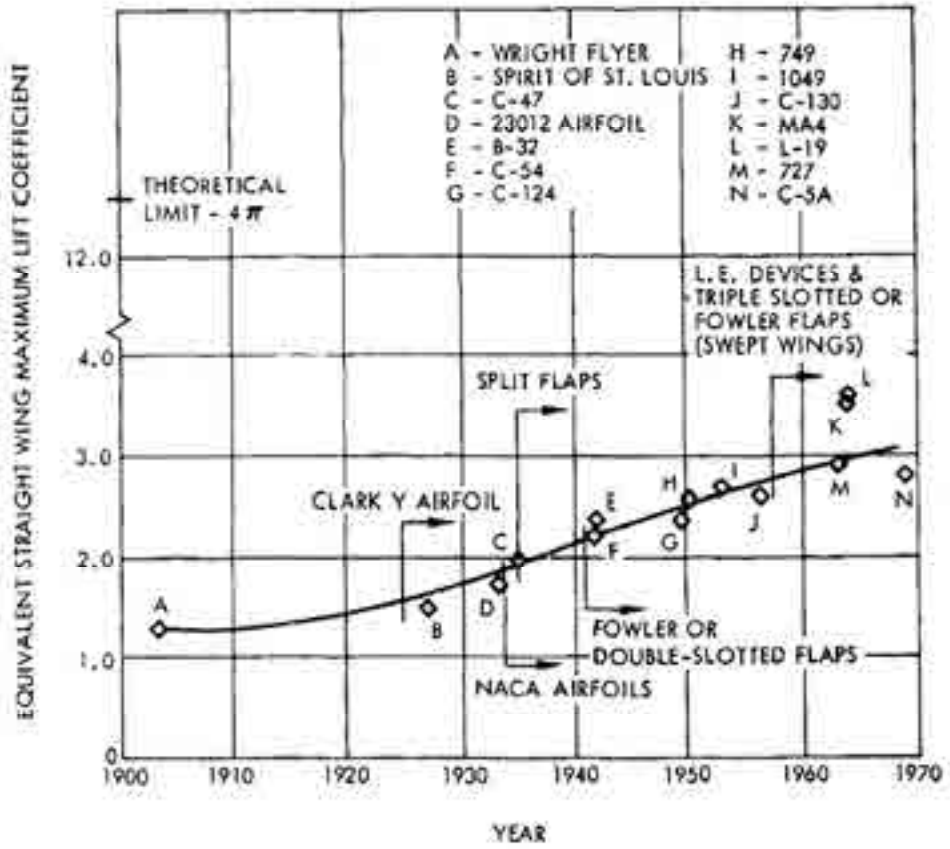

Fig. 3-6. Wing "nonaugmented" maximum lift coefficients of about $C_{Lmax} = \pi$ can be obtained. Higher values require some form of powered lift [406].

The ability to increase wing maximum lift was given a significant boost in November 1931. In that year, Harlan D. Fowler [407] published a technical note in *Western Flying* magazine. His article is, in my view, of such historical importance that I have included it as Appendix G in this volume. The NACA Langley Memorial Aeronautical Laboratory was particularly enthusiastic about Fowler's invention, which led to an experiment that Fred Weick and Bob Platt reported in May of 1932 [408]. They wrote in the introduction:

> "The Fowler wing, developed by Harlan D. Fowler, is the result of an attempt to combine three different methods of increasing the maximum lift.
>
> 1. Increasing the area by means of an extension surface.
> 2. Increasing the effective camber by means of a flap.
> 3. Providing a slot to help maintain unburbled flow at high angles of attack.
>
> The combining of these methods is accomplished by means of an extension surface, which is a sort of flap having an airfoil section. The extension airfoil is retracted into the lower rear portion of the wing when not in use but is extended to the rear and downward when high lift is desired. (Fig. 1.) The gap that is left between the main wing and the extension airfoil forms a slot to maintain unburbled air flow over the rear airfoil at the high angles of attack.
>
> Previous wind-tunnel tests on models of 3-inch chord at both Massachusetts Institute of Technology and New York University, and full-scale flight tests have all shown exceptionally high lift coefficients with the Fowler wing arrangement. (Reference l.) The present tests were made as part of a series on high-lift devices in the 7- by 10-foot wind tunnel of the National Advisory Committee for Aeronautics. The Clark Y airfoil section was used for both the basic wing and the extension airfoil, and the tests were made to cover a range of slots and angular deflections of the extension airfoil.

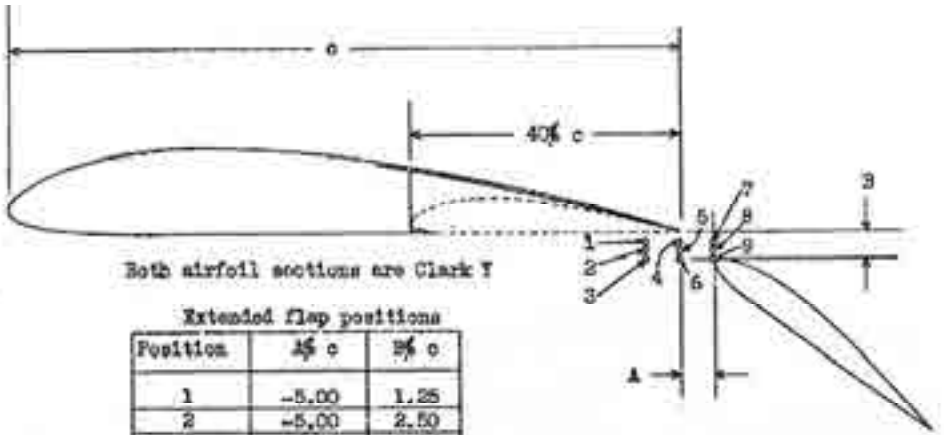

Extended flap positions

Position	A% c	B% c
1	-5.00	1.25
2	-5.00	2.50
3	-5.00	3.75
4	0.00	1.25
5	0.00	2.50
6	0.00	3.75
7	5.00	1.25
8	5.00	2.50
9	5.00	3.75

Fig. 1 Section of Fowler wing."

The wing was rectangular and had a reference chord of 10 inches; the span was 60 inches. The test was conducted at 80 miles per hour giving a Reynolds Number of 609,000. Weick and Platt noted that "The highest value of C_{Lmax}, 3.17, was obtained with the nose of the extension airfoil in position 5 (see fig. 1). This is the location suggested by Mr. Fowler. It is believed that the lift coefficient of 3.17 is the highest that has been obtained to date from a device readily applicable to normal airplane construction." The flap deflection was 40 degrees.

The concept of a variable-area wing created a situation that has received relatively little notice, at least as far as I know. So let me bring the situation to your attention with this simple question: Given that "the highest value of C_{Lmax}" was 3.17, what do you suppose is the reference area? Weick and Pratt felt compelled to write that "curves of C_{Lmax} (based on the area of the basic wing)…" and I think their 11 words answered the question for all time. The basic wing with the flap retracted experimentally achieved a maximum lift coefficient of 1.28 in Weick and Pratt's test, which means that a 250-percent increase in maximum lift had been obtained. In his article [407], Harlan Fowler stated that the increase was obtained approximately distributed as "variable camber, 43 percent, variable area, 28 percent, recessed camber, 7 percent, and slots, 22 percent."

The lift and drag data from both Fowler's and Weick and Pratt's experiments are shown in Fig. 3-7. It is important to note that Fowler's basic wing had a span of 21 inches and

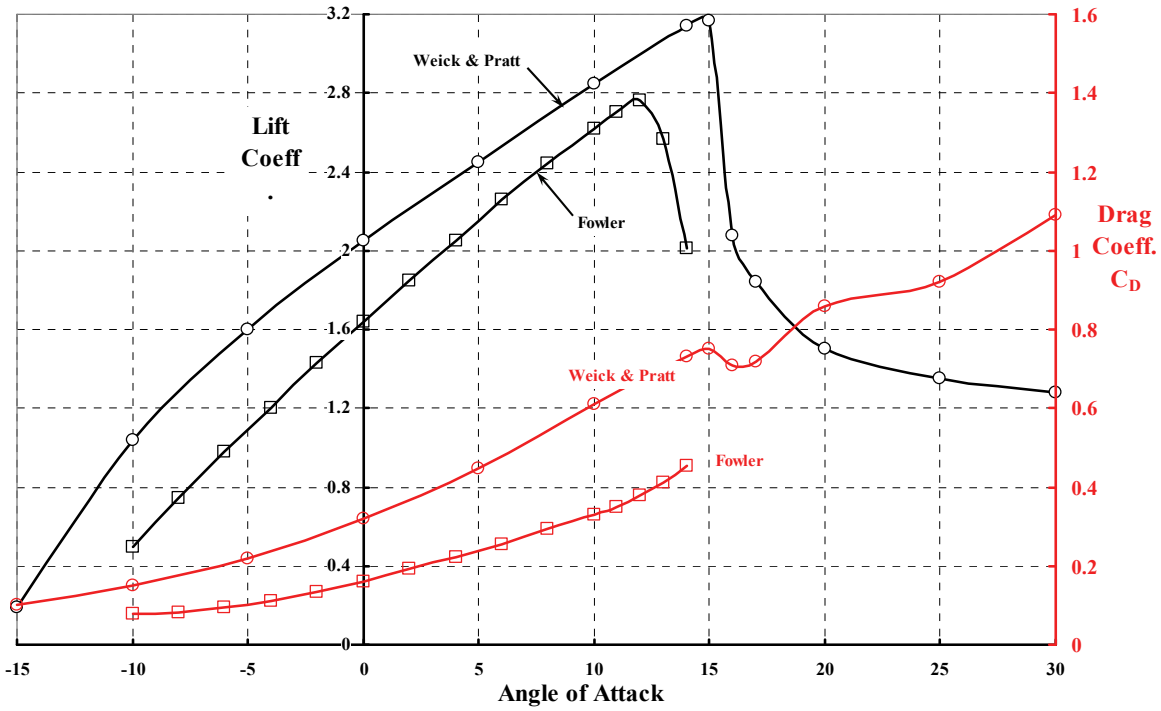

Fig. 3-7. The earliest lift and drag data for the Fowler flap showed that maximum lift coefficients (based on the retracted flap wing area) on the order of $C_{Lmax} = \pi$ could be obtained "from a device readily applicable to normal airplane construction."

a chord of 3 inches. The flap itself had a span of 18 inches and a chord of 1.25 inches. The Weick and Platt model had a span of 60 inches, and the basic wing chord was 10 inches. The flap had a span of 60 inches and a chord of 4 inches. The flap deflection was 40 degrees in both experiments.

Now let me gather up the wing lift and drag data I have selected for your review. You have seen Prandtl's test results for wings of several aspect ratios (Fig. 1-3), and you have seen the improvement in maximum lift coefficient offered by Harlan Fowler's flap (Fig. 3-7). The comparison I want to emphasize is how the practical lift-drag data looks relative to ideal. You see this comparison in Fig. 3-8, which shows what I would call unaugmented wing performance. To me, the term "unaugmented" means that powered lift technology associated with propeller slipstream, boundary layer control (BLC), jet flap, etc., is yet to be included in the effort to improve STOL performance. It should be clear from Fig. 3-8 that without wing stalling, wing lift-versus-drag polars behave very much as predicted by ideal theory. This fact will be used later to establish absolute ideal STOL performance using a C-130 as the example.

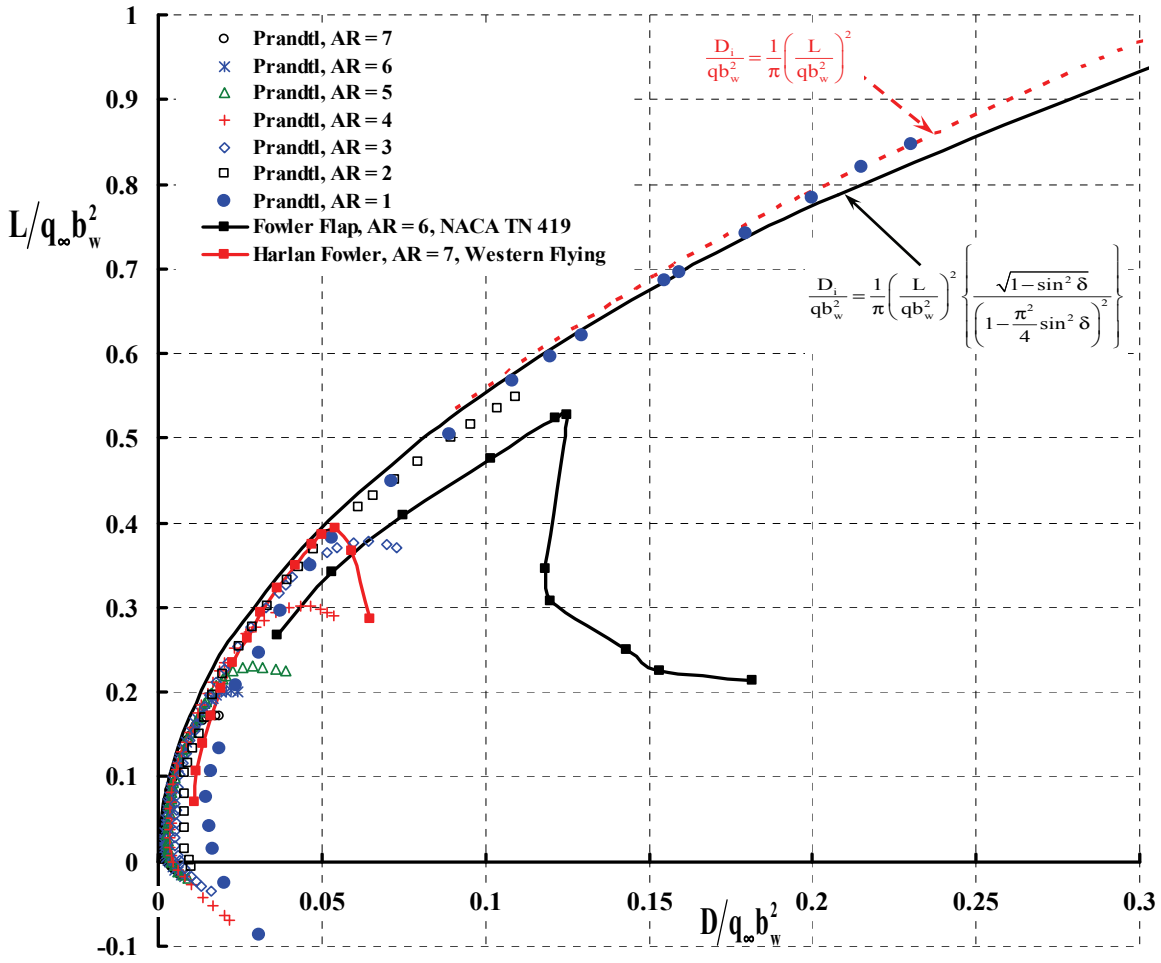

Fig. 3-8. Without wing stalling, wing lift-versus-drag polars behave very much as predicted by ideal theory.

3.2 SOME KEY STEPS

At the start of the 1950s, fixed-wing engineers had a very good idea of what high-lift performance they might obtain with mechanical arrangements of flaps, slats, and slots.[98] Much of this technology was ready for application to the jet transports that were already on the horizon. And so aerodynamic research turned to what further gains could be made by (1) redirecting propeller slipstreams downward with the flaps; (2) adding BLC to delay the onset of separated flows; and (3) the direct, downward ejection of air from the wing trailing edge in what was called a jet flap. A great deal of this research was conducted at the N.A.C.A. Langley and Ames Research Centers, and it continued when the N.A.C.A. was revamped into today's NASA. You will find literally hundreds of N.A.C.A./NASA reports providing experimental data for all manner of propeller/flap/slot combinations. Furthermore, many of these combinations were evaluated with and without some form of BLC. As research began to show what was possible with two-dimensional airfoil configurations, the more promising combinations were evaluated with finite wings, and the best of these combinations were experimentally studied as representative airplanes at full scale, or nearly so, in the NASA Ames 40- by 80-foot wind tunnel. From this wealth of research, I have selected only a few examples to show you the foundation that was laid for STOL airplane technology. You will see that the examples are aligned with (1) the Fairchild C-123, which was then in production; (2) what Lockheed later demonstrated by adding BLC to the flaps of its propeller-driven C-130; and (3) what McDonnell Douglas (YC-15) and Boeing (YC-14) accomplished by directing exhaust from their aircraft turbofans over flaps. I might just as easily have selected examples of lowering fighter airplane landing and takeoff speeds, but keep in mind that my emphasis in this volume about other V/STOL aircraft is on what civil aviation transports might need.

3.3 WINGS, FLAPS, PROPELLERS, AND JET FLAPS

During the mid-1950s the U.S. Air Force and U.S. Army were having a roles-and-mission debate about who should provide tactical transport aircraft. The Army wanted a medium-size logistical support aircraft capable of landing as close to the battlefront as humanly possible. Their view was that the logistical support airplane should land on unpaved, hastily prepared landing strips, and they saw the de Havilland Canada C-8 Buffalo as just the aircraft for them. The Air Force saw the C-8 as being too slow, too small, and quite short on range to be of use in other missions beyond what the Army wanted the aircraft for. The Air Force decided that the Fairchild C-123 (Fig. 3-9) was more aircraft for the money, and proceeded to fund Fairchild in developing and producing several hundred C-123s. This production was pursued in parallel with the larger Lockheed C-130 tactical transport (shown later), which the Air Force saw as an ideal, all-around transport. The Fairchild C-123 airplane did yeoman service during the Vietnam War, and NASA saw the machine as a very good baseline aircraft to conduct fundamental STOL research on.

[98] The well-known British engineer, A. D. Young, published a very thorough survey of flap aerodynamics in February of 1947 [409].

Fig. 3-9. The Fairchild C-123 logistical transport was modeled at 0.4 scale by the N.A.C.A. as the baseline for STOL research.

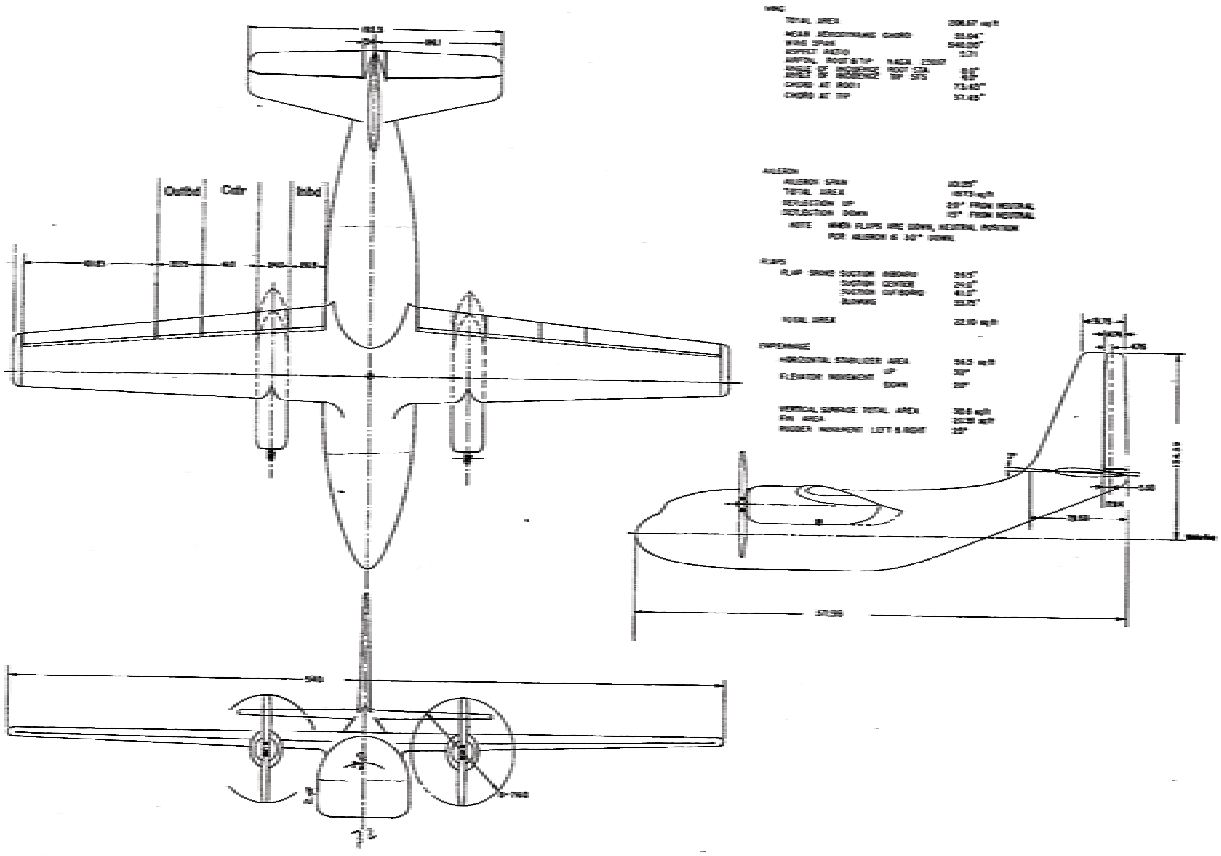

Fig. 3-10. The N.A.C.A. 45-foot-wingspan model of the Fairchild C-123 [410].

The N.A.C.A. built a 0.4-scale model of the C-123 (Fig. 3-10) that was first tested in the Langley Research Center 30- by 60-foot large-scale wind tunnel [410]. After initial testing at Langley, the 45-foot-wingspan "model" was transferred to Ames Research Center specifically for additional testing in their 40- by 80-foot wind tunnel (Fig. 3-11). Data from three test entries were reported in the 1958–1959 period [411-413].

The initial testing of this model was with suction as the means of BLC [411], followed immediately with results obtained by blowing [412]. It appears that suction BLC, particularly as it was applied for obtaining laminar flow control over the aircraft surfaces, was a relatively impractical approach to improving lift and reducing drag because of system clogging, among other reasons [414]. Therefore, let me describe some results with blowing BLC.

The NACA 23017 airfoil was the model's basic airfoil for the complete wing from tip to tip. The slotted-flap arrangement shown in Fig. 3-12 was used for both the flap-span and aileron-span portions of the wing. Both the flaps and the ailerons were equipped with thin

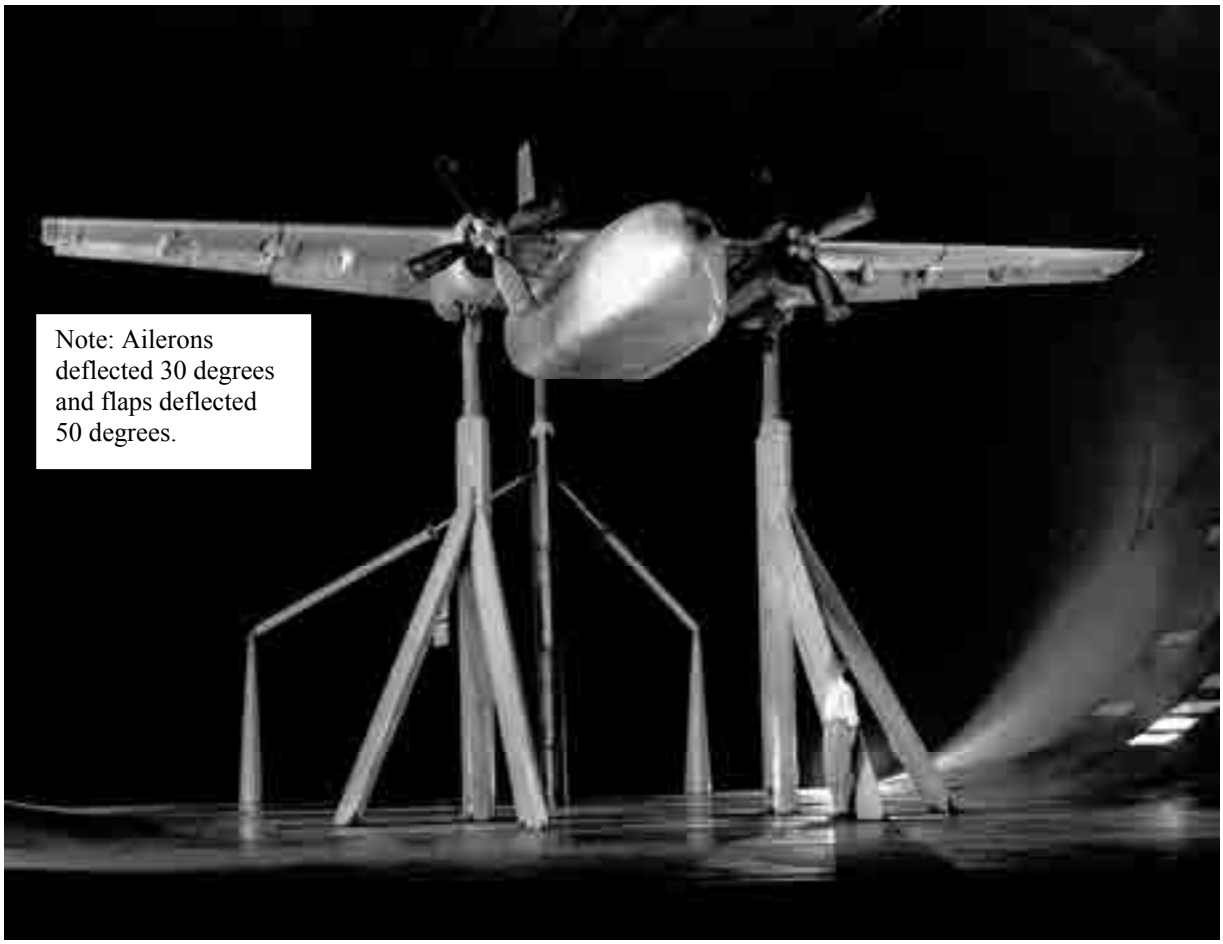

Fig. 3-11. The 0.4-scale model of the Fairchild C-123 (a tactical transport airplane) installed in the NASA Ames 40- by 80-foot wind tunnel. The model's wingspan was 45 feet.

Fig. 3-12. The NACA/Handley Page slotted-flap airfoil used in both the flap-span and the aileron-span portions of the wing of the 0.4-scale-model Fairchild C-123. The basic airfoil was the NACA 23017. The flap chord was 0.26 of the chord when the flap was undeflected.

slots providing energized air for BLC. The details of the blowing system had been worked out in earlier experiments with a full-scale F-86 fighter [415].

To understand the lift and drag data for the C-123 that you will see shortly, you need a little information about flaps and propellers, including their slipstreams. Let me start with flaps.

3.3.1 Airfoil Behavior With Deflected Flaps

It is worth a minute to see how flap deflection affects two-dimensional airfoil lift and drag coefficients. Experimental data obtained by the N.A.C.A. for their 23012 airfoil [416] is the closest data source (that I could find) for a configuration comparable to that shown in Fig. 3-12. You see typical airfoil section lift coefficient versus angle of attack and drag coefficient versus lift coefficient data on the facing page. This data is reproduced from figure 15 on page 425 of reference [416]. From Fig. 3-13 you can see that up to a flap deflection of about 40 degrees, airfoil lift curves appear to extend nearly linearly with flap deflection. That is, the angle of attack for zero lift becomes progressively more negative, which is a characteristic of cambering an airfoil, and that is approximately what flap deflection does. Furthermore, the maximum lift coefficient increases in a nearly linear fashion with increasing flap deflection. Beyond a flap deflection of 30 degrees, the lift curves display evidence of airfoil stalling.

From Fig. 3-14, you see that flap deflection significantly increases the airfoil drag at zero lift. Perhaps the more informative trend is illustrated by the brown dashed line on Fig. 3-14, which shows airfoil lift and drag increasing with flap deflection when the airfoil angle of attack is zero. I have illustrated this basic data of lift and drag coefficients as a function of flap deflection with the airfoil at zero angle of attack in Fig. 3-15.

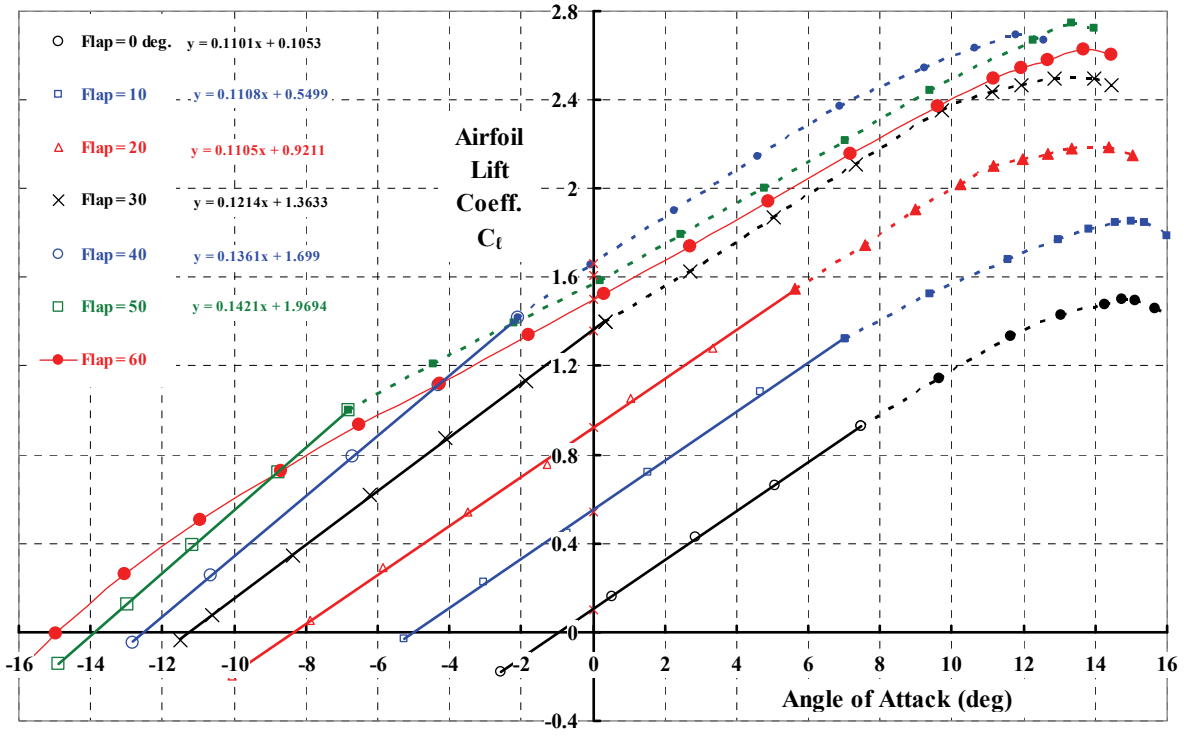

Fig. 3-13. Airfoil lift coefficient data for the NACA 23012 with a 0.26-chord flap deflected at several angles [416].

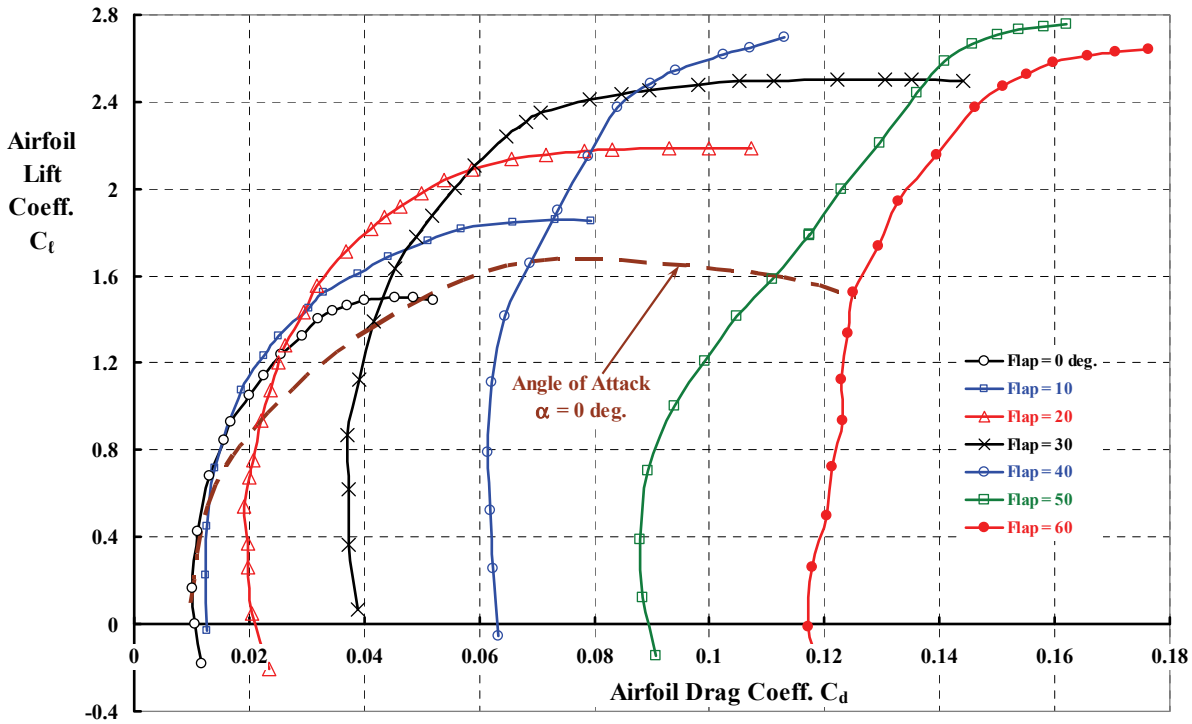

Fig. 3-14. Airfoil drag coefficient data for the NACA 23012 with a 0.26-chord flap deflected at several angles [416].

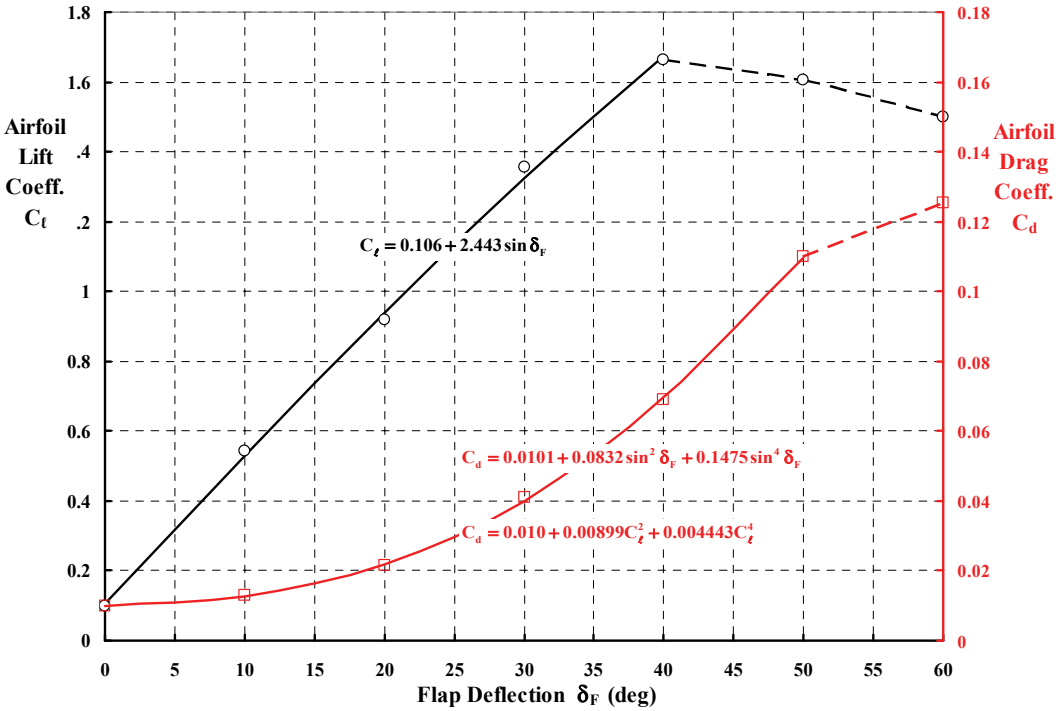

Fig. 3-15. Airfoil lift and drag coefficient data for the NACA 23012 at zero angle of attack with a 0.26-chord flap deflected at several angles [416].

The above figure shows that two-dimensional airfoil data is quite well behaved up to flap deflections of about 40 degrees. Airfoil stalling with associated separated flow becomes a factor beyond the stalling angle as the dashed lines suggest. Note that up to stall, the airfoil lift coefficient follows a linear equation while the drag coefficient is more parabolic in character. Keep in mind that all kinds of mechanical flaps have been developed as A. D. Young informs you [409], and remember that the theory of high-lift devices is rather empirical in nature. The 0.4-scale model of the Fairchild C-123 with its 0.26-chord slotted flap is just one example. Now let me proceed to propellers and their slipstreams.[99]

3.3.2 Propeller Slipstreams

The study of how wings were affected by propeller slipstreams began to receive serious attention in the mid-1920s. Then, in February of 1937, one of the most referenced reports about how wing lift increases due to propeller slipstream, and how that lift increase might be estimated, was published. The report, R&M No. 1788 [417], was written by R. Smelt and H. Davies, two British engineers who worked at the Royal Aircraft Establishment. Their first-order estimate was simply based on momentum theory for propellers, and they were careful to account for how the diameter of the slipstream contracts

[99] A draft created by a ceiling fan in your sitting room is a low-velocity slipstream in propeller terms.

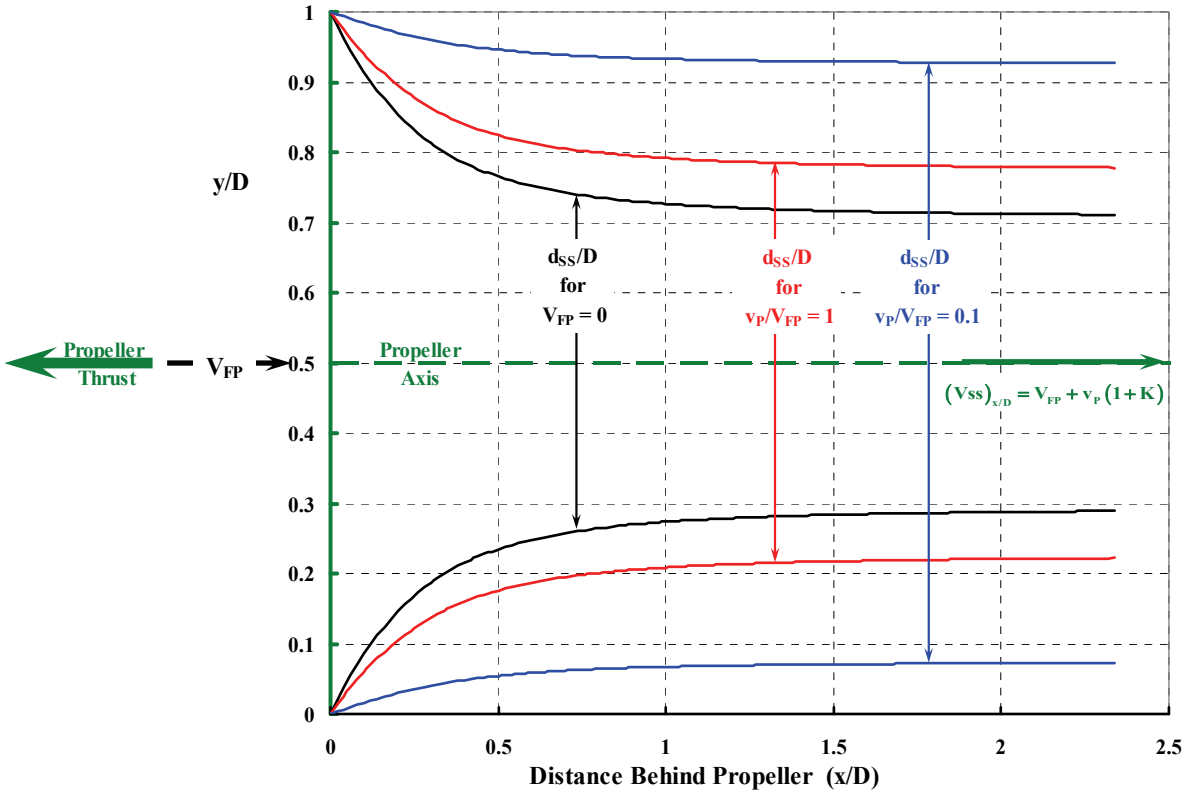

Fig. 3-16. A thrusting propeller creates a slipstream (i.e., a column of moving air), and the diameter of this column of air contracts behind the propeller. The propeller plane is shown as the heavy green line acting as the ordinate. Aerodynamic physics make the slipstream act just like a nozzle but with a phantom shape.

behind the propeller. This contraction behavior for several ratios of x/D is illustrated in Fig. 3-16. The velocity and diameter of the slipstream are determined by the conditions right at the propeller plane, which I have placed at station zero along the propeller axis in Fig. 3-16. The thrusting propeller itself adds an increment in velocity (v_P) to the flightpath velocity (V_{FP}). This incremental velocity (i.e., named induced velocity) is calculated using momentum theory by

$$(3.10)\quad v_P = \sqrt{\left(\frac{V_{FP}}{2}\right)^2 + \frac{T_P}{2\rho A_P}} - \frac{V_{FP}}{2},$$

and this means that the total velocity *immediately* behind the propeller (i.e., $V_{slipstream}$ or V_{SS} for short) is

$$(3.11)\quad (Vss)_{x/D=0} = V_{FP} + v_P = V_{FP} + \sqrt{\left(\frac{V_{FP}}{2}\right)^2 + \frac{T_P}{2\rho A_P}} - \frac{V_{FP}}{2} = \frac{V_{FP}}{2} + \sqrt{\left(\frac{V_{FP}}{2}\right)^2 + \frac{T_P}{2\rho A_P}}$$

where the velocities are in feet per second, the propeller thrust (T_P) is in pounds, the air density (ρ) is in slugs per cubic foot, and the propeller area ($A_P = \pi D^2/4$) is in square feet.

Smelt and Davies found that this slipstream velocity (V_{SS}) increased the further behind the propeller you go. They also found that the slipstream velocity increase depended on the ratio of the distance (x) divided by propeller diameter (D) and expressed this velocity as a function of (x/D) as

(3.12) $$(Vss)_{x/D} = V_{FP} + v_P(1+K) \quad \text{where} \quad K = \frac{x/D}{\sqrt{\frac{1}{4}+\left(\frac{x}{D}\right)^2}}.$$

You might note in passing that infinitely far behind the propeller plane (that is, where $x/D = \infty$) K equals 1.0, and the slipstream velocity equals $V_{FP} + 2v_P$, which is the highest possible slipstream velocity—according to momentum theory.

The corollary to the increasing slipstream velocity behavior given by Eq. (3.12) is that the diameter of the slipstream (d_{SS}) contracts. Smelt and Davies were satisfied with momentum theory, which yields

(3.13) $$\text{At } x/D, \quad \frac{d_{SS}}{D} = \sqrt{\frac{V_{FP}+2v_P}{V_{FP}+2v_P(1+K)}} = \sqrt{\frac{1+2v_P/V_{FP}}{1+\frac{2v_P}{V_{FP}}(1+K)}}.$$

You can now see that slipstream contraction depends on the ratio of the increment in velocity that the propeller produces (v_P) to the flightpath velocity (V_{FP}) and also on the nondimensional distance behind the propeller plane (x/D). This shows you that Fig. 3-16 is a generalized picture of the propeller slipstream geometry.

When the propeller is producing thrust in a static condition (i.e., $V_{FP} = 0$), the momentum theory calculates the slipstream velocity as

(3.14) $$(Vss)_{x/D} = v_P(1+K) = \sqrt{\frac{T_P}{2\rho A_P}}\ (1+K) \text{ where } K = \frac{x/D}{\sqrt{\frac{1}{4}+\left(\frac{x}{D}\right)^2}},$$

and the contraction rate is the greatest because

(3.15) $$\text{At } x/D, \quad \frac{d_{SS}}{D} = \sqrt{\frac{1}{(1+K)}}.$$

The other extreme is when you are very far behind the propeller plane and well behind the airplane itself. At that point the slipstream velocity is

(3.16) $$(Vss)_{x/D=\infty} = V_{FP} + 2v_P,$$

and the slipstream is fully contracted because

(3.17) $$\text{At } x/D = \infty, \quad \frac{d_{SS}}{D} = \sqrt{\frac{1}{2}}$$

regardless of the value of the flightpath velocity.

The slipstream geometry and velocity are, of course, very key parameters in estimating how much lift will be produced by the portion of the wing that is immersed in the slipstream. You get that sense from Fig. 3-17. This figure represents the slipstream as a column of air. This figure also suggests that the deflected flap will redirect the propeller's column of air downward.

The aerodynamic complexity of the problem presented by Fig. 3-17 cannot be taken lightly. Before tackling the problem, Barney McCormick, in his excellent textbook *Aerodynamics of V/STOL Flight* published in 1967 [27], states on page 220 that "Several approaches to the problem of a wing in a propeller slipstream can be found in the literature. None of these is quite satisfactory. Either the physical model is too simplified and restricted in its range of application or more exact solutions are too complicated for practical application." Personally, I think Barney's thoughts are an understatement, even today. I would say that computational fluid dynamics (CFD) is the only reasonable solution approach in today's world.

Just think about some of the problem's variables for a minute. To begin with, most STOL wings are not covered by a large group of slipstreams. Next, the slipstream velocity depends on propeller thrust, which is a major variable. Taken together, the spanwise distribution of lift and drag is far from ideal. Experiments have shown that slipstreams do not follow the flap deflection angle exactly, and furthermore, the actual deflection of the "column of air" is very influenced by the size of the flap. These are just my tip-of-the-iceberg thoughts when I look at Fig. 3-17, and that is why pre-computer theory is of questionable use today—even for conceptual design, in my opinion. This makes early model experiments in a wind tunnel of immense value to any new STOL aircraft development. You can appreciate the value of wind tunnels just by considering what NASA learned from the 0.4-scale-model tests of the Fairchild C-123 (Fig. 3-11).

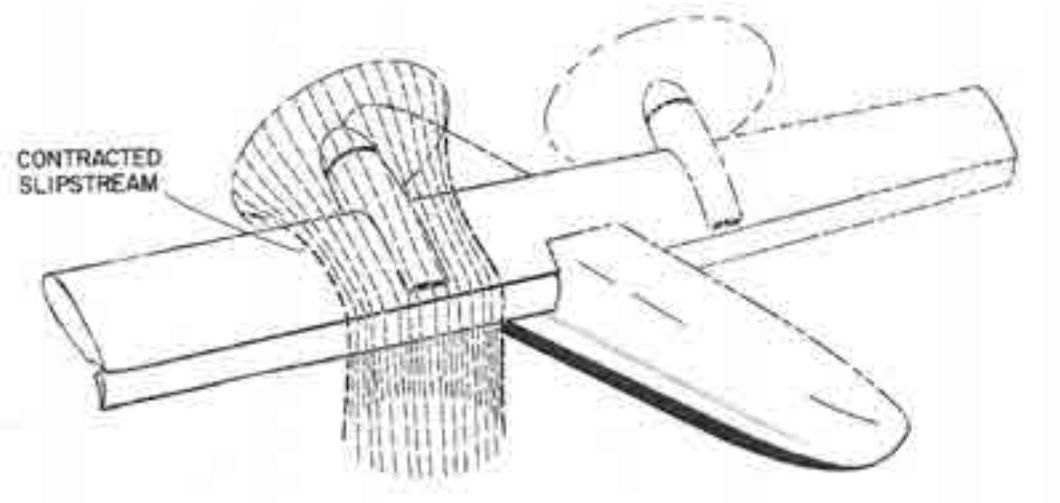

Fig. 3-17. Propeller, wing, and flap aerodynamics have been studied primarily with momentum theory for the propeller in conjunction with classical wing and flap theory—along with considerable empiricism based on wind tunnel data [417, 418] (figure courtesy of Gerardo Nunez).

3.3.3 Propellers at Angle of Attack

You see from Fig. 3-17 that a propeller can be at a considerable angle of attack even with conventional takeoff and landing (CTOL) aircraft, to say nothing about STOLs or VTOLs such as a tiltwing or tiltrotor. This angle can range well beyond the axial flight condition most fixed-wing engineers assume. Furthermore, this is a range that rotorcraft engineers have little experience with. I say this because, in their sign convention, Rotorcraft engineers would say this propeller angle-of-attack range is -90 to -15 degrees. Regardless of the sign convention, when the propeller is at such large angles of attack, the propeller slipstream is not the simple picture shown in Fig. 3-16. More importantly, the slipstream is no longer a column of air that you can assume is perpendicular to the propeller's face. The situation becomes clear when you study Fig. 3-18, which is the classical sketch used by many authors to apply Glauert's momentum theory to the inclined propeller. Because there are very little, if any, CFD calculations for this problem in the literature I perused, I will follow classical teachings.

Glauert's assumption about using momentum theory to calculate the propeller-induced velocity (v_P) right behind the propeller plane is quite straightforward. He was the first to propose that

$$(3.18)\quad v_P = \frac{T}{2\rho A V'} = \left(\frac{T}{2\rho A}\right)\frac{1}{\left[\left(V_{local}\cos\alpha_P + v_P\right)^2 + \left(V_{local}\sin\alpha_P\right)^2\right]^{1/2}},$$

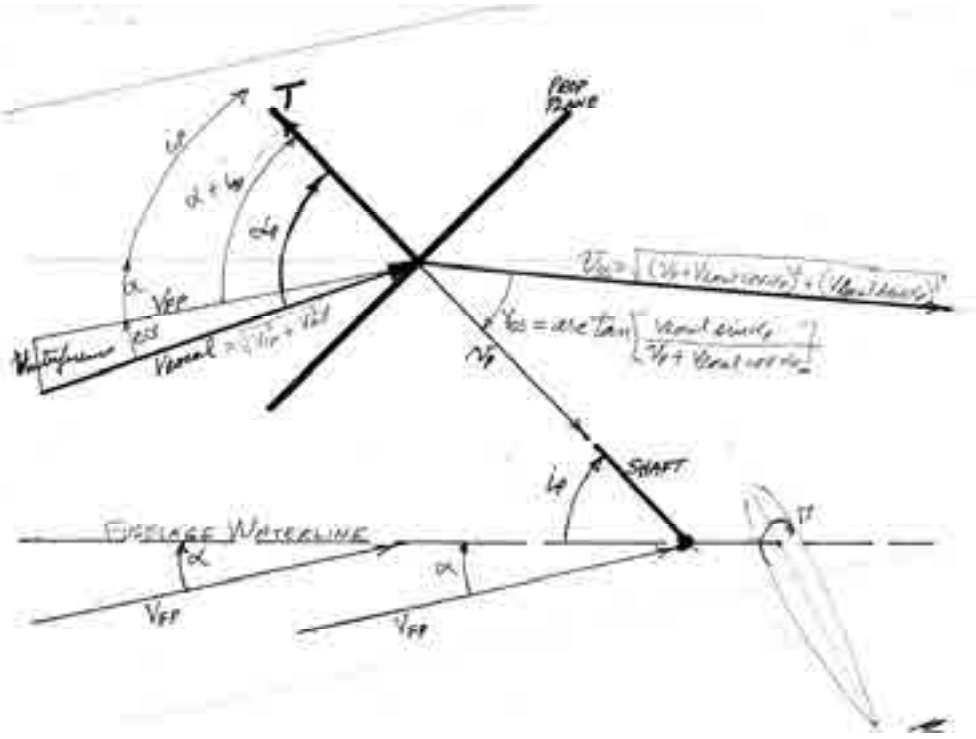

Fig. 3-18. Even a simple analysis of a propeller at angle of attack requires careful attention to many angles and velocities.

and this immediately creates a quartic equation in propeller-induced velocity of the form

$$(3.19)\quad v_P^4 + \left(2V_{local}\cos\alpha_P\right)v_P^3 + V_{local}^2 v_P^2 - \left(\frac{T}{2\rho A}\right)^2 = 0\,.$$

Classically, Eq. (3.19) is put in a velocity ratio form by defining the propeller-induced velocity, when the local velocity (V_{local}) is zero, as

$$(3.20)\quad v_{P-static} = \sqrt{\frac{T}{2\rho A}} \quad \text{or} \quad v_{P-static}^4 = \left(\frac{T}{2\rho A}\right)^2$$

so the quartic is transformed into the ratio $\bar{v} = v_P / v_{P-static}$ being a function of $\bar{V} = v_{local} / v_{P-static}$, and the quartic to solve looks like

$$(3.21)\quad \bar{v}^4 + \left(2\bar{V}\cos\alpha_P\right)\bar{v}^3 + \left(\bar{V}^2\right)\bar{v}^2 - 1 = 0\,.$$

You no doubt know that a quartic equation has four roots. Furthermore, this quartic can be solved with a variety of numerical schemes. I prefer the direct method that follows.

The root you want from Eq. (3.21) is given by

$$(3.22)\quad \bar{v} = D - \frac{\bar{V}}{2}\cos\alpha_P + \left[\frac{\pi/2 - \alpha_P}{\sqrt{\left(\pi/2 - \alpha_P\right)^2}}\right]\sqrt{(A+B) - C}$$

where the propeller-shaft angle of attack (α_P) is used in radians. The alphabet parameters (i.e., A, B, C, D) depend on a primary function, G, and whether G is positive or negative. The primary function, G, is calculated from

$$(3.23)\quad G = \bar{V}^8\sin^2\alpha_P + \bar{V}^4\left(27\sin^4\alpha_P - 18\sin^2\alpha_P - 1\right) + 16\,.$$

To save paper, you then calculate

$$(3.24)\quad \begin{aligned} F &= \frac{\bar{V}^2}{1,728}\left(\bar{V}^4 - 18 + 54\sin^2\alpha_P\right) \qquad H = \frac{\sqrt{3}}{288}\sqrt[4]{G^2} \\ A &= \sqrt[3]{F+H} \qquad B = \sqrt[3]{F-H} \qquad C = \frac{\bar{V}^2}{12}\left(3\sin^2\alpha_P - 1\right) \end{aligned}\,.$$

Now, the sum of A and B depends on the sign of G. This means an "IF–THEN" logic statement is required that goes like this

$$(3.25)\quad \begin{aligned} &\text{IF } G > 0 \quad \text{THEN} \quad A + B = \sqrt[3]{F+H} + \sqrt[3]{F-H} \\ &\text{IF } G < 0 \quad \text{THEN} \quad A + B = 2\left[\sqrt[6]{F^2+H^2}\right]\left\{\cos\left[\frac{1}{3}\arccos\left(\frac{F}{\sqrt{F^2+H^2}}\right)\right]\right\}. \end{aligned}$$

This step lets you calculate D as

$$(3.26)\quad D=\left[2\sqrt{(A+B)^2+C(A+B)-3(AB)}-(A+B+2C)\right]^{1/2},$$

and then you have all the alphabet parameters to calculate $\bar{v}=v_P/v_{P-static}$ using Eq. (3.22). The only restriction to this method is that propeller-shaft angles of attack beyond $\alpha_P = 160$ are not covered. In fact, decades of autogyro and helicopter development have confirmed that the Glauert assumption is in serious error for angles of attack much beyond +110 degrees.

The obligatory graph that shows the curves created by the preceding method is provided in Fig. 3-19. One key point worth noting immediately is that if the propeller-shaft angle of attack is in the range of $-30 < \alpha_P < +30$ degrees, the propeller-induced velocity is quite adequately estimated by

$$(3.27)\quad \bar{v}=\sqrt{\left(\frac{\bar{V}}{2}\right)^2+1}\ -\frac{\bar{V}}{2}\qquad \text{for}\quad -30^o<\alpha_P<30^o,$$

which is just the induced velocity you calculate when the propeller-shaft angle of attack is zero.

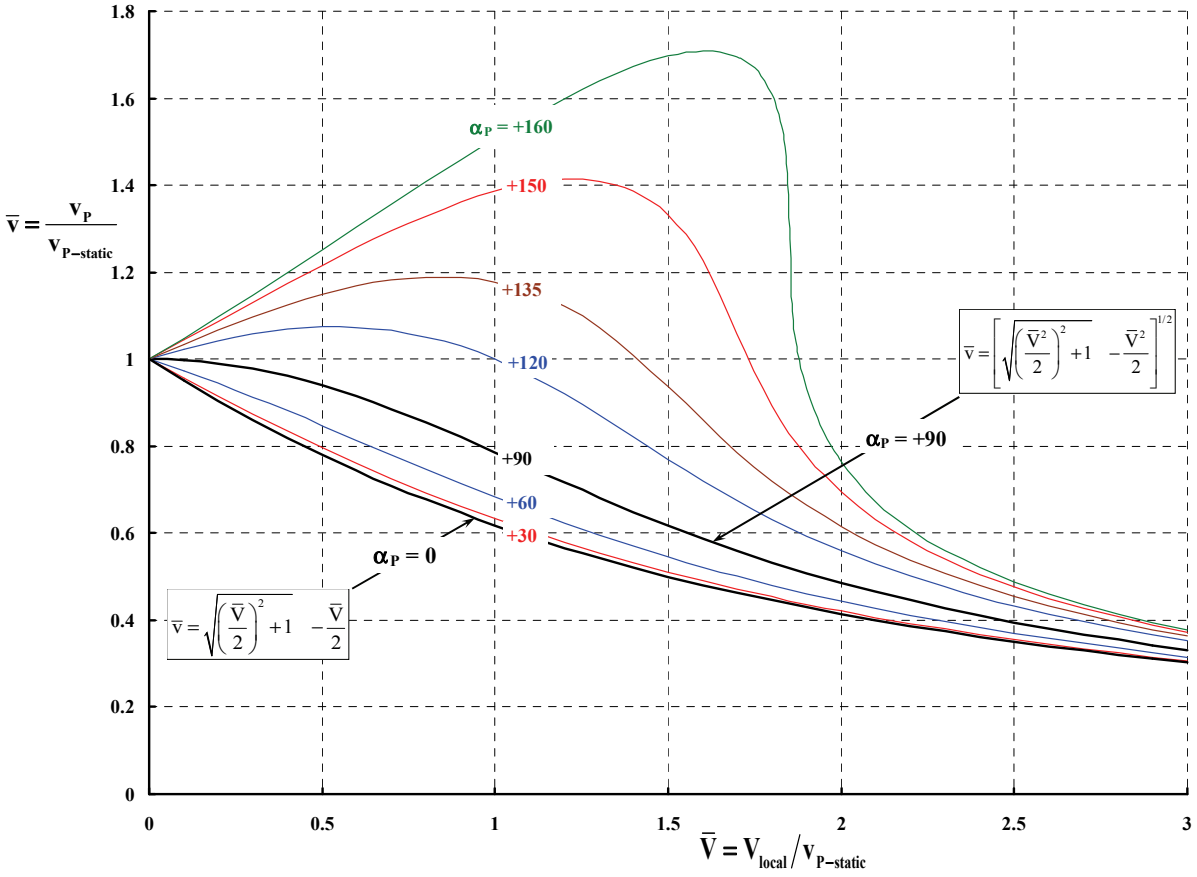

Fig. 3-19. Glauert's assumption of Eq. (3.21) in graphical form.

Now turn your attention back to Fig. 3-18, and note that the column of air leaving the propeller can be represented by the slipstream velocity (V_{ss}). The magnitude of this slipstream velocity is, of course, important and can be calculated by

$$(3.28)\quad V_{SS} = \sqrt{V_{local}^2 + v_P^2 + 2V_{local}v_P \cos\alpha_P}$$

but, more importantly, the slipstream velocity is not perpendicular to the propeller plane, and this has an effect on the wing angle of attack—at least that portion of the wingspan immersed in the propeller slipstream. This slipstream velocity is inclined to the propeller shaft by the slipstream angle (γ_{SS}), which you calculate as

$$(3.29)\quad \gamma_{SS} = \arctan\left(\frac{V_{local}\sin\alpha_P}{v_P + V_{local}\cos\alpha_P}\right).$$

Next, consider the propeller slipstream influence on the distribution of lift along the span of the wing from the left wingtip to right wingtip.

3.3.4 Propeller Slipstream Effect on Wings

Of the relatively few reports quantifying how the spanwise distribution of lift is distorted by a slipstream, I would suggest starting with J. Stüper's April 1938 report. This German work was quickly translated by the N.A.C.A. [419]. It is well worth your reading time because, as Stüper reported:

> "The results of wind-tunnel tests for the determination of the effect of a jet on the lift and downwash of a wing are presented in this report. In the first part, a jet without rotation [i.e., propeller swirl velocity is zero] and with constant velocity distribution is considered—the jet being produced by a specially designed fan. Three-component, pressure distribution, and downwash measurements were made and the results compared with existing theory. The effect of a propeller slipstream was investigated in the second part. In the two cases the jet axis coincided with the undisturbed wind direction. In the third part the effect of the inclination of the propeller axis to the wing chord was considered, the results being obtained for a model wing with running propeller."

More powerful theoretical and experimental methods to address the slipstream/wing aerodynamics came with the development of computational fluid dynamics and the use of particle image velocimetry [420-424].

Let me give you a little more insight about this propeller-wing interaction problem. You might prefer to not call this a problem, but rather call it powered lift aerodynamics. I will draw my example from data Weiberg and Page reported [413] for the four-propeller configuration of the Fairchild C-123. They included one example of airfoil normal force coefficient (C_n) varying spanwise "on the left wing panel." This "wing panel" had sufficient chordwise pressure taps at nine spanwise stations to obtain the airfoil normal force loading (dN/dy) at each span station (y). They integrated the chordwise pressure times local area (cdy) from the leading edge to the trailing edge and then calculated a normal force coefficient as

$$(3.30)\quad C_n = \frac{dN/dy}{q_{FP}c} \approx \frac{dL/dy}{q_{FP}c}.$$

You might think that the local velocity at each spanwise station should be used to calculate dynamic pressure ($q = \frac{1}{2}\rho V^2$), but that is not general practice in experimental work. That is why you see the dynamic pressure (q_{FP}) based on flightpath velocity (V_{FP}) used in Eq. (3.30). When the airfoil angle of attack is less than 10 to 15 degrees, the normal force coefficient is a sufficiently accurate approximation for airfoil lift coefficient (C_ℓ) in a surprising number of analyses.

The spanwise distribution of normal force coefficient that Weiberg and Page provided is reproduced here as Fig. 3-20. My curve fairing, the red line passing through their nine data points, was guided by some experience [419] and *smoothed out with imagination* based on propeller, flap, and aileron locations. When viewed from the front as in Fig. 3-20, both propellers on the port-side wing panel (shown in blue) rotated counterclockwise. This is the rotation for the propellers on the starboard wing panel also.

The insight I want to offer using Weiberg and Page's data is best done with quantitative values. To begin with, the data in Fig. 3-20 was obtained with the test configuration tabulated in Table 3-1. The normal force coefficient (C_n) is based on the wind

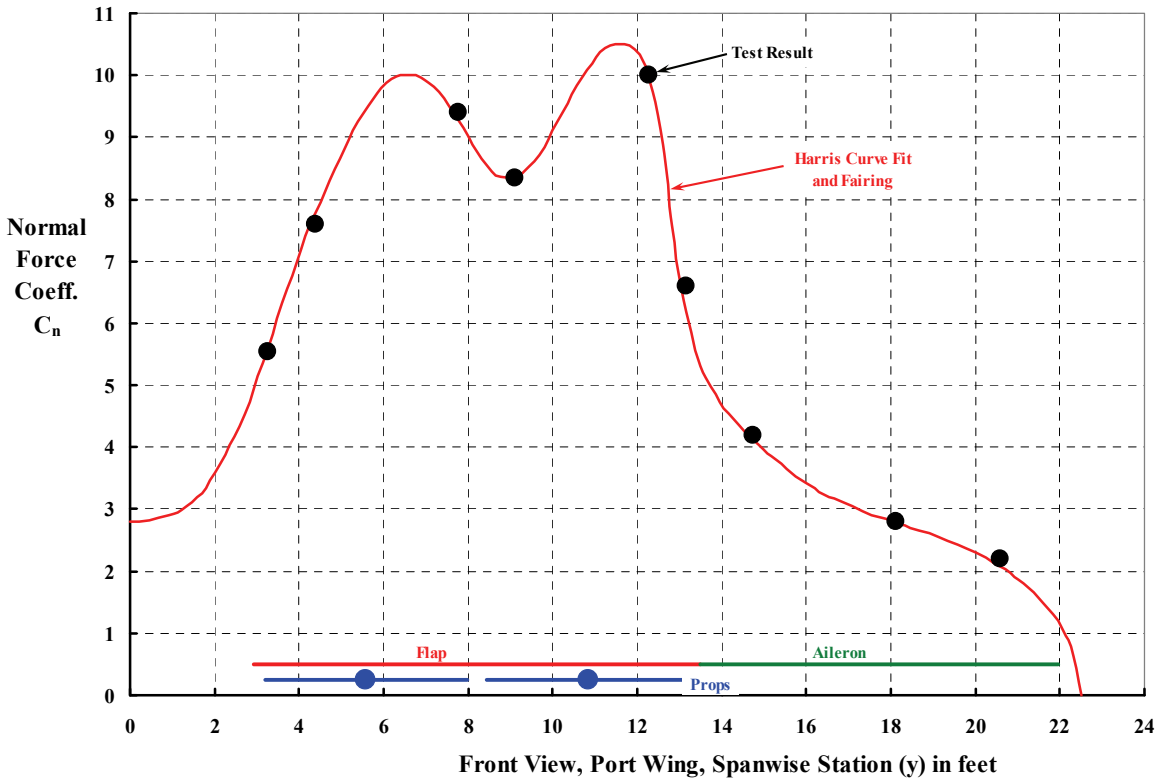

Fig. 3-20. Normal force coefficient loading over the port wing panel was published for one test condition [413]. The tunnel speed was 71 feet per second.

Table 3-1. Test Configuration for Normal Force Coefficient Data Provided in Fig. 3-20 (the wing aspect ratio was 9.86, the span was 45 feet, and the area was 205 square feet; the propeller thrust axis incidence to the fuselage water line is unknown)

Item	Symbol	Units	Value
Fuselage angle of attack	α	deg	1
Wing root incidence	i_w	deg	8.3
Flap deflection	δ_F	deg	60
Aileron deflection	δ_A	deg	30
Flap BLC coefficient	$C_{\mu f}$	na	0.029
Aileron BLC coefficient	$C_{\mu a}$	na	0.006
Propeller thrust coefficient	T_C	na	2.15/4
Vertical force coefficient	$C_{Z\text{-}wa}$	na	5.0
Horizontal force coefficient	$C_{X\text{-}wa}$	na	1.55
Vertical force	F_Z	lb	6,165
Horizontal force	F_X	lb	615.5
Wind tunnel dynamic pressure	q_{FP}	psf	6.0
Wing geometry			
Area	S_W	ft^2	205.4
Root chord	c_R	ft	6.30
Tip chord	c_T	ft	3.15
Root incidence	i_R	deg	8.3
Tip incidence	i_T	deg	3.5
Propeller geometry			
Diameter	D	ft	4.770
Area	A_P	ft^2	17.870
Static induced velocity	$v_{p\text{-}static}$	fps	10.847
Lift coefficient	C_L	na	5.781
Lift	L	lb	7125

tunnel free-stream velocity, which makes it rather easy to calculate the dimensional spanwise loading (dL/dy). Fig. 3-21 shows the calculation result for the full wingspan, which starts at the starboard wingtip (y = –22.5 feet) and ends at the port wingtip where y = +22.5 feet.

Two lines are shown on Fig. 3-21. My fairing of the experimental data is shown with the dashed line. The additional line shown in green illustrates how the loading should be distributed to obtain minimum induced drag. You will recall from classical wing theory [221, 403] that the loading must have an elliptical shape. That is, when the ideal elemental loading (dL/dy) is found from the bound circulation (Γ_y) as classically defined according to

$$\frac{dL}{dy} = \rho V_y \Gamma_y , \tag{3.31}$$

then the total wing lift follows by integration from wingtip to wingtip. In this conventional lifting wing problem (say for a glider), the velocity (V_y) is taken as a constant equal to flightpath velocity (V_{FP}) in feet per second. The air density (ρ) has the units of slugs per cubic

foot. The wing is assumed to be a lifting line along which the bound circulation,[100] in square feet per second, is distributed elliptically according to

$$(3.32)\quad \Gamma_y = \frac{\Gamma_o}{b/2}\sqrt{(b/2)^2 - y^2}$$

where the wingspan is denoted by (b), and the maximum circulation (Γ_o) becomes a variable that is ultimately chosen to set the magnitude of wing lift.

The integration to obtain wing lift is carried out rather simply:

$$(3.33)\quad L = \int_{-b/2}^{+b/2} \rho V_y \Gamma_y dy = \int_{-b/2}^{+b/2} \left(\rho V_{FP} \frac{\Gamma_o}{b/2}\sqrt{(b/2)^2 - y^2} \right) dy = \frac{\pi}{4}\rho V_{FP} b \Gamma_o .$$

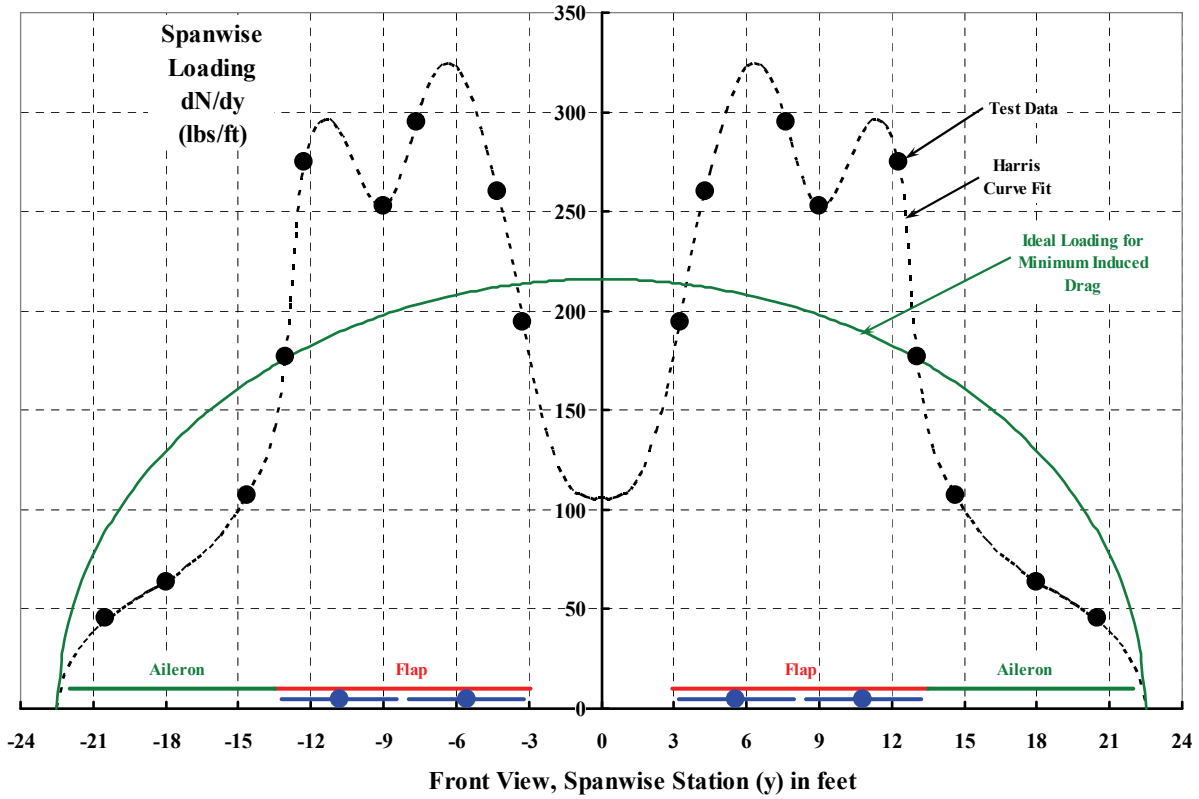

Fig. 3-21. Powered lift systems can produce span loadings significantly different from the classical ideal. The integrated lift is 7,600 pounds for both examples shown here.

[100] I like to think of the wing being replaced by a lifting line and that the lifting line is the centerline of a horizontal tornado, which is easy for me to picture because I live in Oklahoma. The strength of the tornado is Γ, which weather people classify as EF1 to EF5. An EF5 classification means maximum swirl velocities of over 200 mph (293 fps) if the tornado is right on top of you. If you are some distance (d) away from the center of the tornado, the velocity is considerably less with a variation approximated as 293/d.

The corollary to the lift equation is that the wing trails a wake back to infinity. This wake induces a velocity (w_y) along the lifting line. This velocity does not vary from the starboard wingtip to the port wingtip for a wing that is ideally loaded. This induced velocity for the ideal wing-loading case has the magnitude

$$w_y = -\frac{\Gamma_o}{2b} = -\frac{2L}{\pi\rho V_{FP} b^2} . \tag{3.34}$$

The induced velocity tilts the lift vector aft by the induced angle (α_i) equal to an assumed small angle, w_y/V_{FP}, and this gives rise to induced drag, which you calculate with

$$D_i = \alpha_i L = \left(\frac{w_i}{V_{FP}}\right) L = \frac{1}{V_{FP}}\left(\frac{2L}{\pi\rho V_{FP} b^2}\right) L = \frac{1}{\pi}\left(\frac{L^2}{qb^2}\right) \quad \text{or} \quad C_{Di} = \frac{C_L^2}{\pi AR} . \tag{3.35}$$

I suspect you quickly observed from Fig. 3-21 just how non-elliptical the loading becomes when the flaps are deflected 60 degrees and ailerons are deflected 30 degrees. Of course, propeller slipstreams add analytical complications because the velocity (V_y) cannot be assumed constant from tip to tip. Perhaps when you study Fig. 3-21 you have the same sense I did. It appears to me that a better first approximation of the loading would be two ellipses, one for the port wingspan and a mirror image for the starboard wingspan. That would mean that half of the lift would be carried on the port side by one-half of the span and one-half of the wing area. From Eq. (3.34), the induced velocity over the port wing panel (and the starboard wing panel) would therefore be substantially higher than for the ideal loading. Numerically, you have

$$\begin{aligned} w_y &= -\frac{2L}{\pi\rho V_{FP} b^2} = -\frac{2(7,600)}{\pi(0.002378)(71)(45)^2} = -14.15 \text{ fps for ideal wing} \\ w_y &= -\frac{2L}{\pi\rho V_{FP} b^2} = -\frac{2(7,600/2)}{\pi(0.002378)(71)(45/2)^2} = -2\times 14.15 = 28.3 \text{ fps for port wing panel} \end{aligned} \tag{3.36}$$

This, of course, increases the total induced drag substantially because, from Eq. (3.35),

$$\begin{aligned} D_i &= \left(\frac{w_y}{V_{FP}}\right) L = \left(\frac{14.15}{71}\right)(7,600) = 1,514 \text{ lb for ideal wing} \\ D_i &= \left(\frac{w_y}{V_{FP}}\right) L = \left(\frac{28.3}{71}\right)\left(\frac{7,600}{2}\right) = 1,514 \text{ lb for port wing panel} \end{aligned} \tag{3.37}$$

so the total induced drag of the two-ellipse loading approximation for the wing panels is 3,028 pounds.

This simple illustration leads to wing-induced drag coefficients of

$$\begin{aligned} C_{Di} &= \frac{D_i}{q_{FP} S_W} = \frac{1,514}{(6)(204)} = 1.24 \text{ for ideal wing} \\ C_{Di} &= \frac{2(\text{port } D_i)}{q_{FP} S_W} = \frac{3,028}{(6)(204)} = 2.48 \end{aligned} \tag{3.38}$$

while the lift coefficient, $C_L = 7{,}600/(6)(204) = 6.2$, remains the same because one-half of the lift is carried on one-half of the wing area.

You could have arrived at the same conclusion quite quickly from Eq. (3.35) with the induced drag coefficient in the form of $C_{Di} = C_L^2 / \pi AR$. The two-ellipse loading approximation means that the same lift coefficient (i.e., $C_L = 6.2$) is carried by a wing panel of one-half of the aspect ratio (i.e., 9.86/2), and this immediately doubles the induced drag coefficient.

Perhaps you noticed from Fig. 3-21 that the integration of span loading yielded a lift of 7,600 pounds while the wind tunnel balance recorded only 7,125 pounds as shown in Table 3-1. The difference comes primarily from negative lift created by the horizontal stabilizer. This is a fundamental characteristic of statically stable airplanes. The requirement for negative stabilizer lift can be significantly increased when powered lift is accompanied by a large, nose-down aircraft pitching moment. This is particularly true when extra wing lift is obtained with flaps and further aggravated when propeller slipstreams increase flap lift.

Now let me take the discussion one further step. You see from Eq. (3.31) that the elemental lift ($dL/dy \approx dN/dy$) variation along the span depends on how the product of velocity (V_y) and bound circulation (Γ_y) varies along the span. Unfortunately, Weiberg and Page offer no test data for either variable in their report [413]. That leads me to some speculating to continue the discussion. Therefore, consider the results of my speculation with Fig. 3-22, and then let me use classical wing theory [403] to obtain the result you see. Keep in mind that the fairing between the test points is my best guess.

You immediately see from Fig. 3-22 that the span loading is significantly increased in the span region where the propellers are located. The propeller slipstream offers a large increase in dynamic pressure over what the flightpath velocity provides, and this augments the lift provided by the 60-degree flap deflection. It is very interesting to see how nonuniform the slipstream velocity is in contrast to what you might expect based on momentum theory. This classical theory, which you encountered in the discussion surrounding Fig. 3-16 on page 345, stated that propeller-induced velocity right at the propeller plane (v_P) could be estimated by Eq. (3.10), repeated here for convenience, as

$$(3.39) \quad v_P = \sqrt{\left(\frac{V_{FP}}{2}\right)^2 + \frac{T_P}{2\rho A_P}} - \frac{V_{FP}}{2}.$$

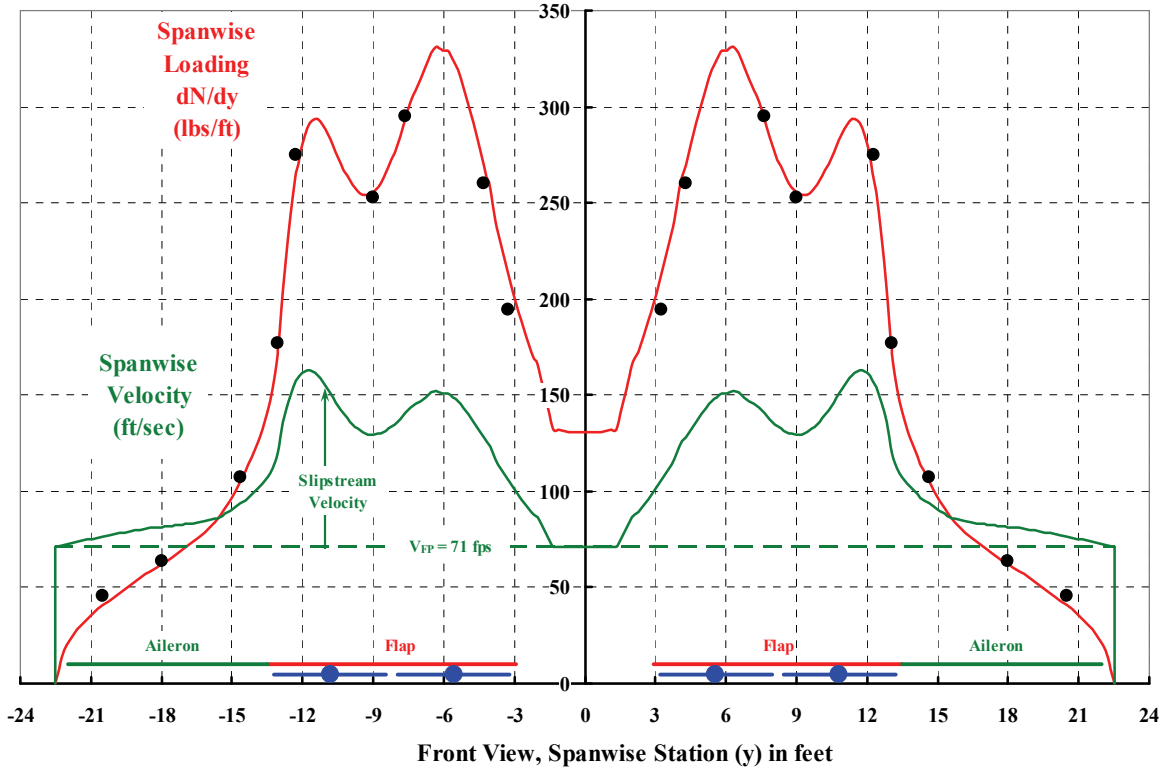

Fig. 3-22. For this data, the flaps were deflected 60 degrees and the ailerons were deflected 30 degrees. The flightpath velocity was 71 feet per second, and each 4.77-foot-diameter propeller was producing 662 pounds of thrust. Wing lift was integrated to 7,790 pounds.

The operating conditions corresponding to the example under discussion yield

$$(3.40)\quad v_P = \sqrt{\left(\frac{71}{2}\right)^2 + \frac{662}{2(0.002378)(17.87)}} - \frac{71}{2} = 59.6 \text{ ft/sec}.$$

The total velocity (V_{SS}) in the slipstream right at the propeller plane is the sum of the flightpath velocity (V_{FP}) and the propeller-induced velocity, or 120.6 feet per second. However, the propeller planes are approximately one diameter ahead of the wing quarter-chord line (i.e., the lifting line, and therefore x/D = 0.89), so the propeller-induced velocity will increase according to Eq. (3.12) as

$$(3.41)\quad (Vss)_{x/D} = V_{FP} + v_P(1+K) \quad \text{where } K = \frac{x/D}{\sqrt{\frac{1}{4} + \left(\frac{x}{D}\right)^2}},$$

and then V_{SS} equals 184 feet per second. You also learned that the propeller slipstream diameter will contract according to Eq. (3-13), repeated here for convenience, as

(3.42) At x/D, $\frac{d_{SS}}{D} = \sqrt{\frac{V_{FP} + 2v_P}{V_{FP} + 2v_P(1+K)}} = \sqrt{\frac{1 + 2v_P/V_{FP}}{1 + \frac{2v_P}{V_{FP}}(1+K)}}$,

and therefore the wing is seeing a 4.77-foot-diameter column of air shrunk to about 0.8 of 4.77 feet, or to 3.82 feet at the wing quarter chord.

These propeller slipstream calculations using momentum theory must only be thought of as a first approximation. In my opinion, Fig. 3-22 strongly suggests the approximation is not good enough even for conceptual design.

Let me go on and describe how the results shown in Fig. 3-22 were obtained. The objective was to solve for a spanwise velocity and bound circulation (Γ_y) that reproduced my curve fitting of the experimental loading (dL/dy). Taking it step by step, you

1. Divide the wing lifting line into many station points (I used 200).
2. Define the airfoil lift coefficient versus local angle of attack for each station. I used Fig. 3-13 as my source and let the airfoils in the flap-span region follow $C_\ell = 0.1481\alpha + 2.2215$. The aileron-span airfoils followed $C_\ell = 0.1214\alpha + 1.363$ and, after mulling it over, I decided to use the flap equation for the wingspan region over the fuselage. A computational fluid dynamics approach with the aircraft modeled in some detail should clarify how wing lift carries over the fuselage from the left wing panel to the right wing panel. I assumed that the boundary layer flow coefficients ensure that no airfoil stall would occur.
3. Note the wing geometry provided in Table 3.1, which gives you the geometric angle of attack to which an induced angle of attack must be added. That is, the angle of attack to be used in the airfoil lift-curve equations is $\alpha = \alpha_{fuselage} + i_{airfoil} + \alpha_i$.

Now you are in a position to start the calculation. You first:

4. Guess a spanwise velocity distribution $[(V_{SS})_y]$ to start with. I chose to let this velocity distribution be the flightpath velocity of 71 feet per second all along the wingspan, with a constant 59 feet per second added for the span regions behind the propellers.
5. And then you calculate the first and subsequent bound circulations from classical theory, $\Gamma_y = \frac{(dN/dy)_y}{\rho(V_{SS})_y}$. You have the nine experimental loading (dL/dy) values (plus my guess to fill in between test points) from Fig. 3-22. And you have a spanwise velocity from step 4, so this step is quite straightforward.

6. Now you must calculate the induced velocity (w_y) at the lifting line due to the complete trailing-wake structure. This wake structure is classically referred to as a multitude of horseshoe vortices. The representation is by a series of nearly straight lines trailing from the wing lifting line. The lines braid themselves together the farther behind the wing you look. I am sure you have seen contrails behind high-flying jet transport airplanes. Frequently you can see these contrails in pairs. One trails the airplane's port wingtip and the second trails the starboard wingtip. Each contrail contains the braided-up vortices from the left or right side of the airplane's plane of symmetry, as the sketch shows. The calculation is made from the equation $w_{yo} = \frac{1}{4\pi}\int_{-b/2}^{+b/2} \frac{d\Gamma_y/dy}{y_o - y} dy$ where the span station at which you want the induced velocity is denoted by (y_o). This equation says that each trailed vortex will contribute to the induced velocity at the span station you are interested in—hence the integration. Because I took so many span stations, the formal integration can be replaced as a sum of small increments. That is how I calculated the induced velocity by

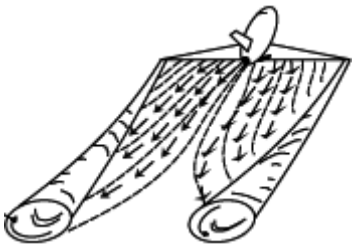

$$w_{yo} = \frac{1}{4\pi}\sum_{-b/2}^{+b/2} \frac{\Delta\Gamma_y}{y_o - y}.$$

There are any number of ways to tackle this induced velocity calculation. I did it with a Microsoft® Excel® spreadsheet. The pictorial view of the calculations looks like this:

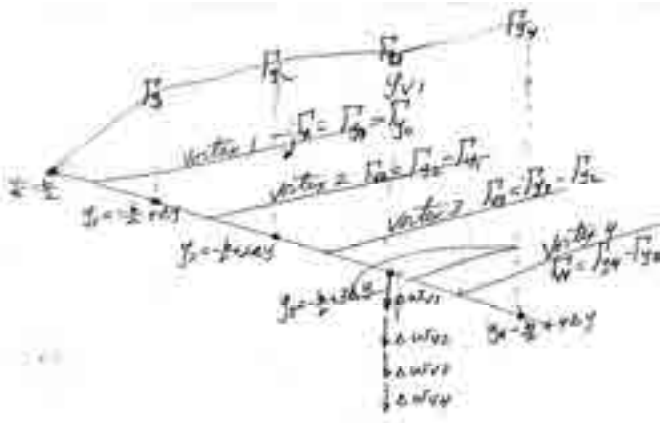

(I am indebted to Wayne Johnson for his suggestions on the best way to make this calculation for induced velocity along the lifting line.)

With the induced velocity (w) in hand, you can calculate the spanwise loading from the airfoil lift-curve representation. You proceed by:

7. Calculating the induced angle of attack as $\alpha_i = w_y/V_{SS}$, and then the local angle of attack (α) along the wingspan is obtained from

$$\alpha = \alpha_{fuselage} + i_{airfoil} + \frac{w_y}{V_{SS}}.$$

8. And from the airfoil angle of attack you have the lift coefficient (C_ℓ) of each airfoil from wingtip to wingtip.
9. Then with the lift coefficient and the first guess at the velocity along the span in hand, you obtain a loading (dL/dy) that can be compared to the loading you started with at step 4.

At this point you will find that the loading (dL/dy) at step 9 does not agree with the loading (dL/dy) at step 4. This means that iteration must be performed until the initial loading and final loading agree. Following another of Wayne Johnson's suggestions, a relaxation technique, to ensure reasonably fast convergence you:

10. Create a new step 4 loading equal to

0.01[previous (dL/dy) step 4] + 0.99[(dL/dy) step 9]

and start the whole calculation over again. After several copy/paste keystrokes you will find that the beginning loading and final loading agree, so you are done. Be aware that convergence and speed are rather sensitive to the 0.01 and 0.99 coefficients. I started with 0.05 and 0.95 and got nowhere, so a more gentle relaxation was necessary.

The preceding process constitutes an explanation of classical lifting-line wing theory as developed by Prandtl, Betz, and Munk [425]. You will find this lifting-line problem solved with more advanced mathematics in reference [421].

My first results with the initial velocity distribution at step 4 provided a converged outcome where step 4 loading equaled step 9 loading. However, the spanwise loading did not pass through the nine experimental points nor did it reproduce my curve fit to the experimental data. To arrive at the results shown in Fig. 3-22, I kept changing the velocity distribution along the span until the classical wing theory was satisfied *and* reasonable agreement with experimental data (plus my curve fit) was achieved.

It is very clear that propellers and other powered lift systems that depend on a high-exhaust velocity (e.g., a jet engine) can substantially increase lift. What might be considered a downside, however, is the amount of drag that is produced. In fact high drag is a benefit in short field landings as Bill Norton recounts in his excellent book [26] about STOL aircraft. Therefore, this discussion would be incomplete without a calculation of drag for the example under discussion. In the first place, the wing drag, as you most likely know, is the sum of induced drag and profile drag. The common equation you are likely to see that calculates total wing drag [269] for a well-designed airplane *in cruise flight* is

$$\text{Wing total } C_D = C_{Do} + \frac{C_L^2}{\pi AR}(1+\delta). \tag{3.43}$$

In this oft-used approximation, the profile drag and the lift coefficients are based on forces divided by flightpath dynamic pressure and wing area. The factor (δ) increases the induced drag when the span loading is not ideal.

The total wing drag for my example of a wing with flaps down and propellers thrusting needs a more thorough calculation than Eq. (3.43) suggests. Because detailed spanwise data is available from the calculation of the span loading (dL/dy), I used a spanwise integral. That is,

$$(3.44)\quad \text{Wing Drag} = D_w = \int_{-b/2}^{b/2} \left[q_y c_y C_{do} + \alpha_i \frac{dL}{dy} \right] dy \,.$$

The profile drag coefficient (C_{do}) equations for the airfoils with flap and aileron deflection are derived from Fig. 3-14 and assume that the boundary control blowing coefficient (C_μ) obviates separated flow. The airfoil properties I used were

$$(3.45)\quad \begin{aligned} C_d &= 0.0366 + 0.000768\, C_\ell + 0.000973\, C_\ell^2 \qquad \text{for } \delta_{aileron} = 30 \text{ deg} \\ C_d &= 0.1191 + 0.00160\, C_\ell + 0.000599\, C_\ell^2 \qquad \text{for } \delta_{flap} = 60 \text{ deg} \end{aligned} \,,$$

and the distribution of induced drag (D_i) and profile drag (D_o) for the NASA four-propeller version of the Fairchild C-123 is shown in Fig. 3-23.

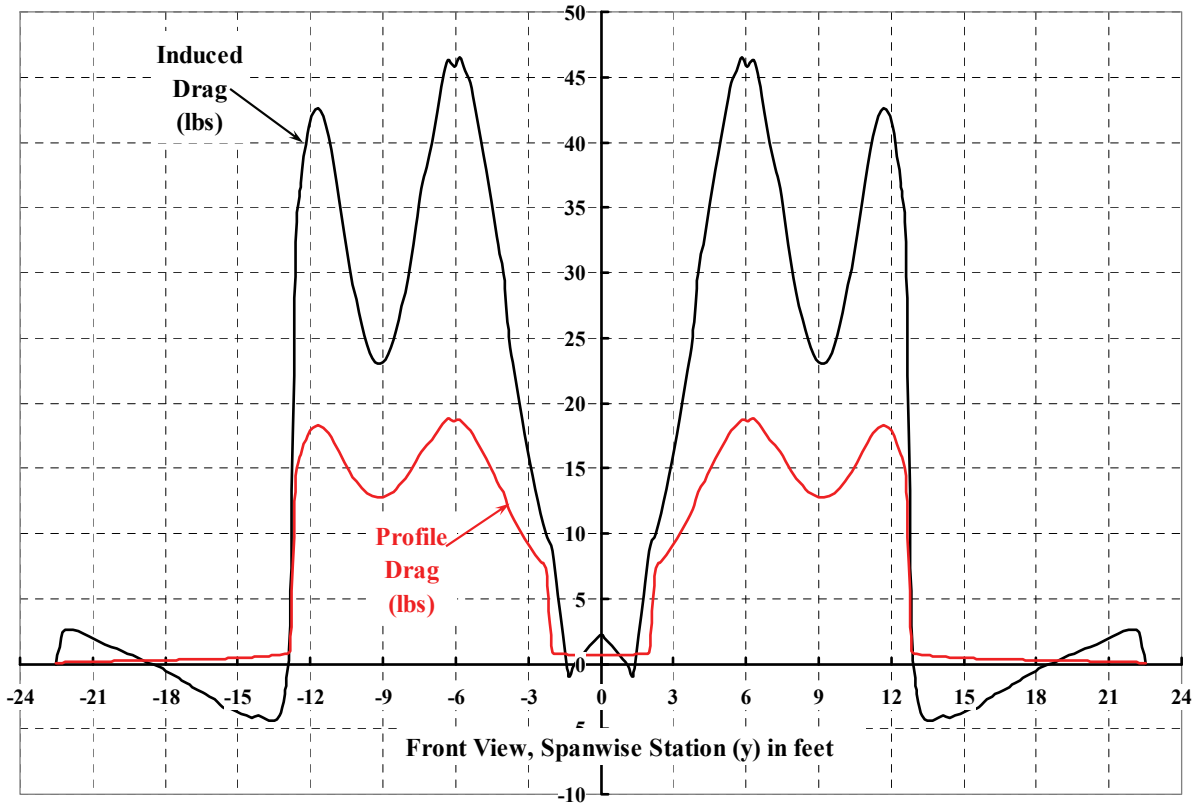

Fig. 3-23. The induced drag and profile drag distributions sum up to a D_i of 674 pounds and a D_o of 321 pounds in this example. The lift distribution integrates to 7,790 pounds.

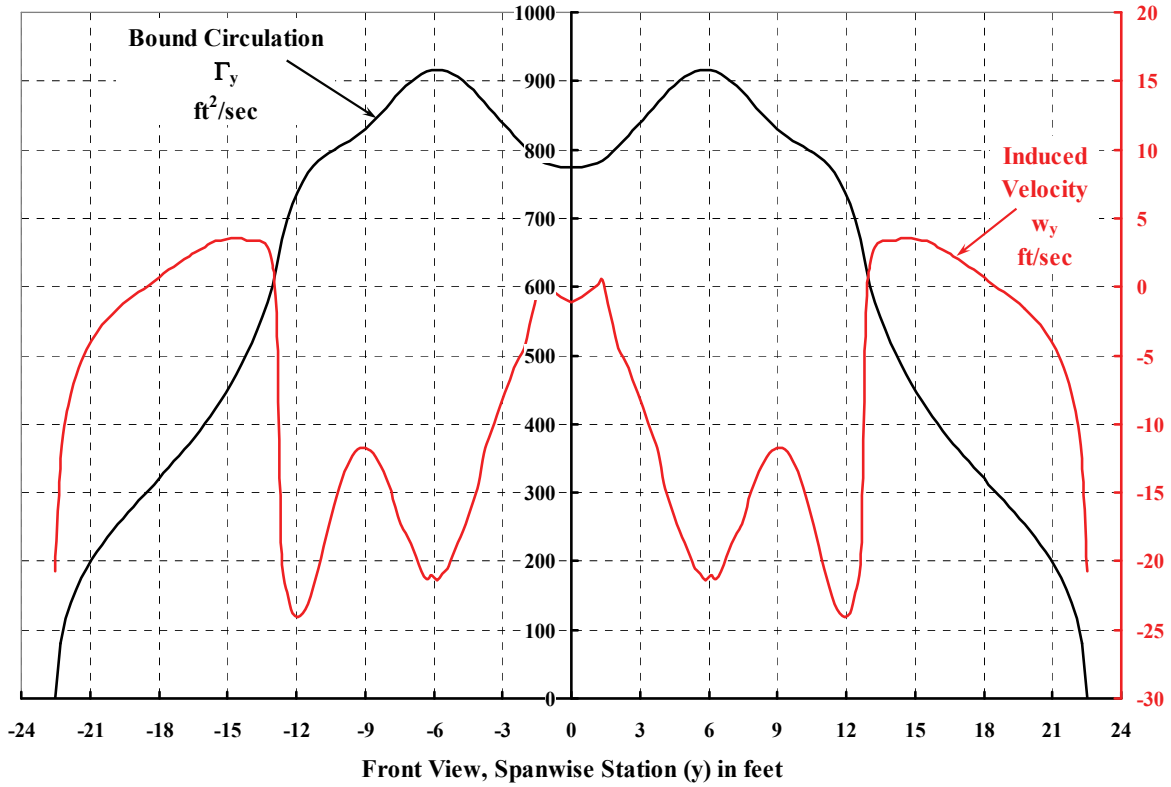

Fig. 3-24. Simple theoretical calculations of spanwise distribution of bound circulation and induced velocity along the wing lifting line for the example problem.

It is worth noting that this landing configuration gives a wing lift-to-drag ratio of 7,790/995 or 7.8, which corresponds to an approach angle of slightly over 7 degrees, even before the rest of the airframe drag is included.

3.3.5 Wing Lift Effect on Propeller

The preceding illustrations, Fig. 3-23 and Fig. 3-24, introduce you to the large effect the propeller has on the wing. Of course, the reverse is true—the lifting wing considerably alters the air flow coming into the propeller. The wing adds an upwash velocity and/or downwash velocity to the flightpath velocity, and this changes the angle of attack and velocity that should be used as inflow to the propeller. Let me give you a rough approximation of the propeller inflow conditions using results from the example just discussed in section 3.3.4.

Consider the case of a wing lifting line that is loaded as shown in Fig. 3-22 and Fig. 3-24. The bound circulation (Γ_y) *does not* vary elliptically from wingtip to wingtip as you see in Fig. 3-24. Nevertheless, each small length of the lifting line contributes a small increment of induced velocity at, say, the propeller hubs. The problem is how to calculate the induced velocity—not along the lifting line, but at the propeller hubs. This requires application of the Biot-Savart law and starts with calculating the flow around a vortex. Glauert [426] used this simple sketch to visualize the lifting line (A to B) as the center of the elemental vortex; the induced velocity (w) then depends on the distance (h) from the vortex centerline. The fundamental equation that will calculate this induced velocity for you is

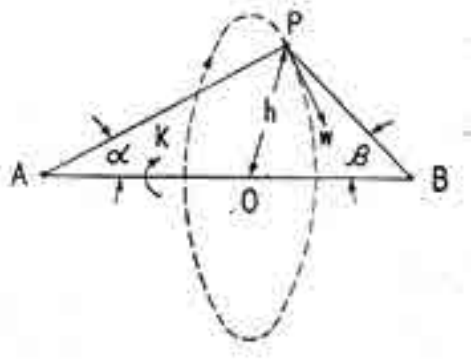

$$(3.46)\quad w = \frac{\Gamma}{4\pi h}\left(\cos\alpha + \cos\beta\right).$$

In the above sketch, the elemental vortex extends from point A to point B. The vortex has a bound circulation strength of Γ (labeled K in the sketch), which is constant all along the vortex. The point where you want to find the induced velocity is labeled P. The location of this point is determined by simple geometry. I think of the A-to-B vortex as a mini tornado creating a swirl velocity (w). Looking down the vortex centerline at A towards B, the swirl is clockwise if the bound circulation is positive. You can create all kinds of wakes behind a lifting line by stringing together a number of very short A–B vortices, including curved wakes behind helicopter rotor blades and propeller blades. The bookkeeping can mount up as the number of A–B vortex segments grows, but today's computer power more than accommodates the artistic imagination of most engineers.

For my purposes here, I will only be using a relatively few vortex segments as you can see from Fig. 3-25. Again, the wing itself is replaced by a lifting line along which the bound circulation varies as shown in Fig. 3-24. I have chosen the y-axis to coincide with the lifting line. And, as you can see from Fig. 3-25, the x-axis is forward so the propeller planes are located at x equals 4.77 feet ahead of the lifting line, which corresponds to (h) on the sketch. The inboard propeller hub is located at y equals 5.58 feet; the outboard hub is located at y equals 10.83 feet. This is the configuration of the NASA four-propeller version of the Fairchild C-123 as reported by Weiberg and Page [413].

Now concentrate on the short vortex segment that spans the distance y_n to y_{n-1}. This geometry corresponds to the sketch because A is y_n and B is y_{n-1}. There are two other vortex segments included in Fig. 3-25. The first vortex trails aft to infinity from span station y_n (i.e., point A on the sketch), and the second vortex, in a similar manner, trails aft to infinity at station y_{n-1} (i.e., point B). This vortex geometry is sort of shaped like a $\cap$ and is referred to as a horseshoe vortex in the classical literature. The bound circulation is assumed constant from y_n to y_{n-1} and has a value Γ equal to the average of Γ_n and Γ_{n-1}.

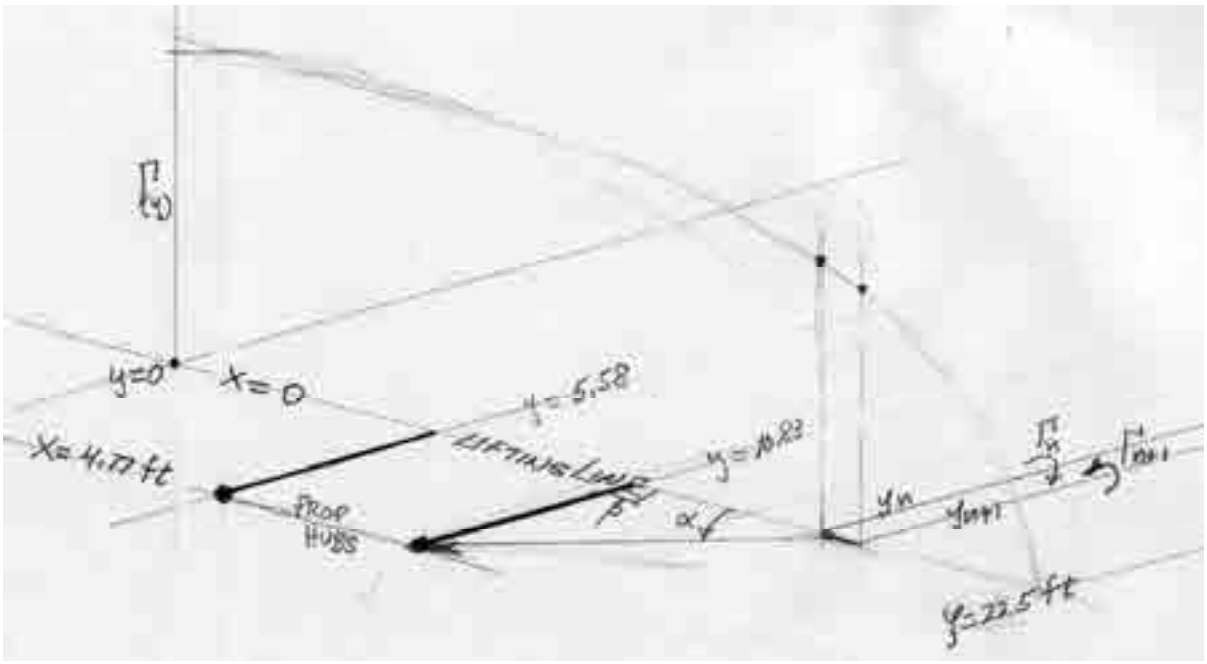

Fig. 3-25. The wing can be represented by straight-line vortex segments.

With this understanding of the problem's geometry, you can immediately calculate the contribution of the short vortex segment along the lifting line to the induced velocity at, say, the outboard hub. The contribution is, following the sketch, simply

$$(3.47)\quad \text{Outboard Hub } \Delta w = \frac{(\Gamma_n + \Gamma_{n-1})/2}{4\pi(4.77)}\left(\cos\alpha_n - \cos\alpha_{n-1}\right).$$

Note that the β angle is 90 degrees, which leads to the zero in Eq. (3.47). As to the cosine of the other angles (α_n and α_{n-1},), you have

$$(3.48)\quad \left(\cos\alpha_n - \cos\alpha_{n-1}\right) = \frac{\left(y_n - y_{\text{outboard hub}}\right)}{\sqrt{h^2 + \left(y_n - y_{\text{outboard hub}}\right)^2}} - \frac{\left(y_{n-1} - 10.88\right)}{\sqrt{(4.77)^2 + \left(y_{n-1} - 10.88\right)^2}}.$$

Now, recall that I divided the wing lifting line up into 200 stations for analysis purposes in the earlier discussion. In essence, there will be 200 short vortex segments of length A to B or, preferably, y_n to y_{n-1}, each contributing its own Δw at the propeller hub. The sum of all the incremental, induced velocity contributions is written in mathematical shorthand as

$$(3.49)\quad \text{Outboard Hub Upwash } w = \frac{1}{4\pi(4.77)}\sum_{-b/2}^{+b/2}\left(\frac{\Gamma_n + \Gamma_{n+1}}{2}\right)\left(\cos\alpha_n - \cos\alpha_{n-1}\right).$$

I obtained this sum quite easily using an Excel® spreadsheet. The result was an upwash velocity of 22.6 feet per second at the outboard hub and about 18 percent higher (26.6 feet per second) at the inboard hub. For the sake of completeness, you have the distribution of contributions to the upwash at both hubs shown in Fig. 3-26. It is the area under the curves that gives the two values of upwash I have just quoted.

The vortices trailing back from the lifting line contribute a downwash at the propeller hubs, which somewhat offsets the upwash just calculated. A first-order approximation for this downwash at the hubs can be made given the induced velocity along the lifting line found earlier (Fig. 3-24). That is,

(3.50) Outboard Hub Downwash $w = w_{\text{lifting line}} \left(1 - \frac{x}{\sqrt{(b/2)^2 + x^2}} \right)$.

In this example, the upwash, Eq. (3.49), and downwash, Eq. (3.50), are added together to give interference velocities of

(3.51) $$\begin{aligned} w_{\text{at outboard hub}} &= 22.6 + (-15.0) = +7.6 \text{ ft/sec} \\ w_{\text{at inboard hub}} &= 26.6 + (-17.0) = +9.6 \text{ ft/sec} \end{aligned}$$.

Because the aircraft has symmetry, the story is the same for the propellers on the starboard side.

Recall now that the flightpath velocity for this example was 71 feet per second. This means that the angle of attack at the propeller hubs has been increased by a wing-induced interference angle of about 6 degrees (i.e., 7.6/71 times 57.3) for the outboard hub and about

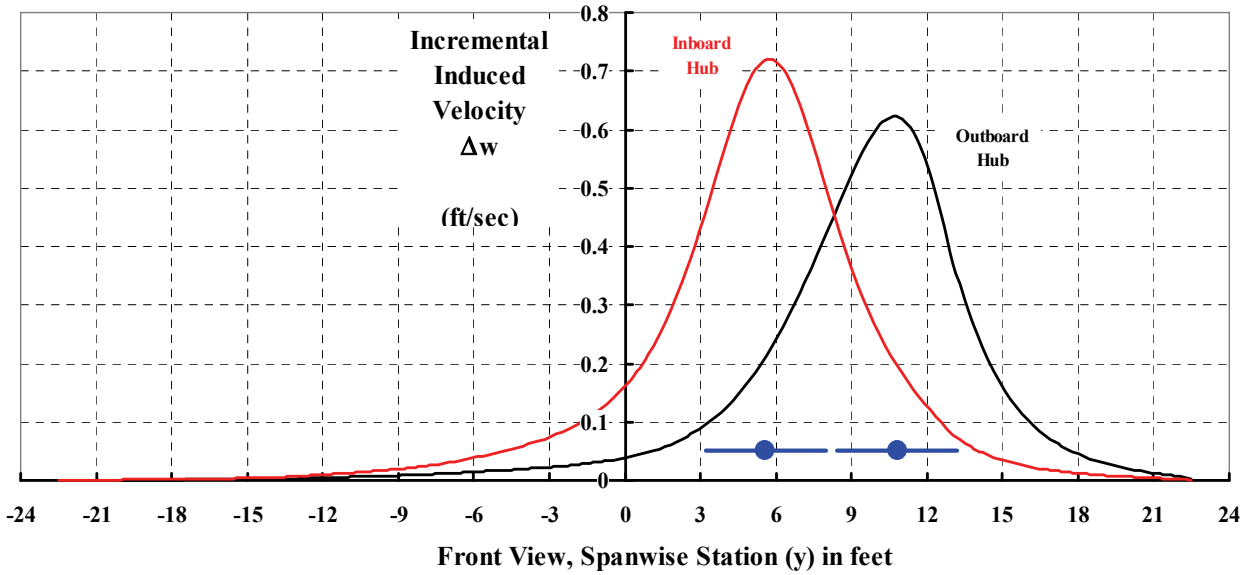

Fig. 3-26. The increments in induced velocity at a propeller hub contributed by 200 vortex segments spanning y_{n-1} to y_n.

2 degrees more for the inboard hub. In and of themselves, these interference angles are not very large, but the interference velocity can vary across the diameter of the propeller. In fact the wing will create a very nonuniform interference velocity over the whole face of the propeller, and this can lead to substantial vibratory stress on the propeller blades. Also keep in mind that propellers are mounted at the end of nacelles, which in themselves alter the inflow to the propeller. Once the blades of the propeller have vibratory loads, you can bet that those loads are transmitted to the wing and then throughout the airframe. Once in the airframe, those vibratory loads immediately find *every* passenger's seat (not to mention the pilot's and copilot's seats). And then you have a problem.

The preceding introductory discussion is just that, an introduction, because the propeller-wing interference problem requires a much more in-depth analysis than I have offered. Should you care to study the problem further, I suggest you start with the thorough set of experimental data in reference [427]. After that you should find references [428] and [429] interesting. Finally, you only need to read Gennaretti and his coauthors' paper [422] to appreciate what analysis level is required to begin dealing with propeller-wing interference.

The research during nearly all of the 20th century certainly concentrated on understanding and improving propeller-wing-flap landing and takeoff performance. However, augmentation of wing lift with flaps and propellers was not the only avenue researchers pursued to improve an airplane's low-speed performance. There was an interlude when the high-lift potential of a jet flap was given very serious consideration.

3.3.6 Wing With Jet Flaps

In January 1933, Mr. G. B. Schubauer completed a test dealing with jet propulsion and thrust augmentors while working at the Bureau of Standards. The work was paid for by the recently formed National Advisory Committee for Aeronautics. Schubauer's experiment was reported in NACA TN 442 [430]. The tail end of this report contains experimental data for a wing with a jet flap. You have to fast-forward to the 1950s before you again find reports [431-438]—many of them from British researchers—dealing with the jet flap concept because so much effort was devoted to boundary layer control, flaps, and propellers.

One paper written by Lowry, Riebe, and Campbell [438] is particularly enjoyable because of its historical tracings, clarity, and simplicity. For example, the authors began their paper with a simple figure, reproduced here as Fig. 3-27, and wrote:

> "Just what is this device known as a jet flap or jet-augmented flap? In simple terms it is the simulation of a flap by a jet sheet which augments the lift by inducing circulation around the wing (fig. l). The sketch shows the lift forces acting on the airfoil. The reaction lift is the component of the jet reaction in the lift direction, jet reaction times sin δ, where δ is the deflection of the jet stream from the wing-chord plane in degrees. The total lift includes both the circulation or pressure lift and the reaction lift. Thus, there is lift augmentation when the total lift is greater than the reaction lift. It can be seen that the ratio of total lift/reaction lift is always greater than one. This ratio does decrease as the jet reaction is increased at a constant forward velocity but always shows some augmentation even at the high-thrust conditions."

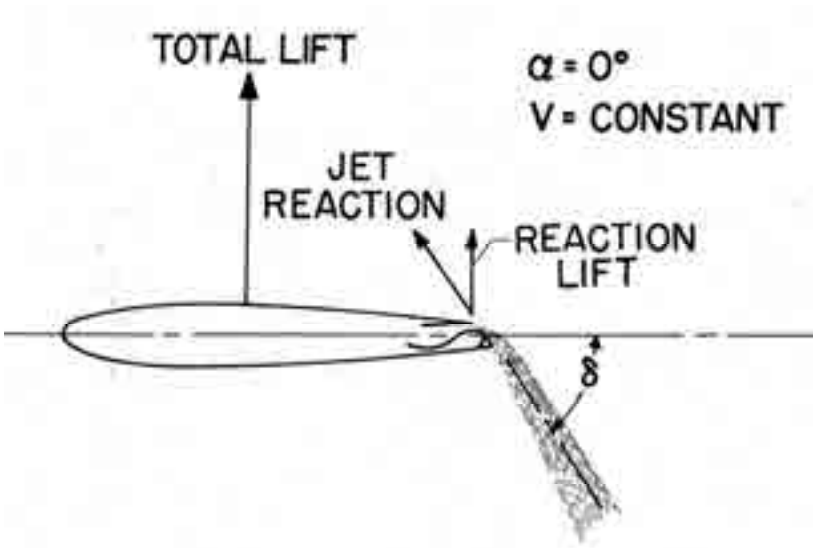

Fig. 3-27. The original jet flap concept was called a jet-augmented flap or a blown flap. The ultimate application was with jet engine exhaust being blown over the upper surface of a wing and deflected flap. This application was used on the Boeing YC-14, for example, and became known as upper surface blowing (USB) [438].

The authors go on to give credit to Schubauer's work by noting:

> "The principle of the jet flap was proposed, probably for the first time, by Schubauer in 1932, reference 2 [430]. In his work in thrust augmentation *he proposed integrating the wing and engine* [my italics] since he reasoned he could get lift augmentation by deflecting the jet sheet at the wing trailing edge and hoped to get thrust augmentation [i.e., propulsive force] by tilting the wing forward in the same manner as the helicopter gets its thrust. In discussing the principle, he wrote, 'The jet as it impinges upon the air gives rise to a superposed external flow of the spreading type. In short, when we consider this flow, the jet is producing the same type of motion in the surrounding air as an airfoil would produce if, from its shape or angle of attack, it were deriving a lift. The jet should then, aside from its reaction, give rise to a lift upon the airfoil.' His experimental results are reproduced in figure 2 since they are probably the first results of an airfoil equipped with a jet flap. These results, incidentally, agree very well with recently obtained data. It can be seen that considerable lift in excess of the reaction lift, V = 0, was induced on the airfoil. Unfortunately there were no practical jet engines at that time, and since the device did not augment the thrust in the longitudinal direction (thought to be a requirement for successful application of jet propulsion to aircraft) the idea was filed away for some 10 years. In 1942 it was proposed, upon re-analysis of these data, that jets may, if integrated into the wing, be effectively utilized for both the propulsion and sustentation of aircraft. This proposal came at an inopportune time and was not pursued further until some few years ago when the idea was studied both here and abroad, references 3 to 5. The idea of *integrating the wing and engine was again proposed by Rogallo* [my italics] in a paper presented at the IAS Annual Meeting in 1946 (ref. 6) as a means of increasing the propulsive efficiency of a jet airplane. So even though we may give it a new name, the integration of the wing and engine is not really a new idea. It is realized that this is a very brief and incomplete resume of the history of jet-lift augmentation and that many contributions have not been recognized. References 7 to 14 are included to give some of the early studies on blowing as a boundary-layer control and as a substitute for a physical flap or control."

3.3.6.1 Schubauer's 1932 Jet Flap Experiment

The configuration Schubauer tested in 1932 and reported in 1933 [430] is shown in Fig. 3-28. The 14-inch-long wing was supported about in the middle of the 3-foot (I will guess square) test section of the Bureau of Standards wind tunnel and on the end of a 1-inch-diameter, 9-inch-long brass tube. This brass-tube wing support connected to the tunnel balance and was not faired, so drag measurements include a large tare drag. The brass tube served as a pressurized air path into the wing, which became a plenum for the nozzle. Schubauer quotes the nozzle as having a jet flap angle of 70 degrees. For analysis purposes, the nozzle exit area is 0.00583 square feet, the wing area is 0.3281 square feet, and the rectangular wing aspect ratio is 4.148. In addition, in my study of Schubauer's report, I assumed the test was conducted at sea level on a standard day.

Schubauer presented all of his test results in figure 36 of NACA TN 442. From his figure, I reconstructed tabulated data only for the zero wing angle of attack, and included this data here as Table 3-2. (I seriously doubt that the original tabulated data had as many digits as Table 3-2 provides.) Of course this exploratory test provided very interesting results and, just as certainly, any number of new questions were raised as so frequently happens with experiments.

Table 3-2. Jet Flap Test Data From 1933
(NACA TN 442, fig. 36 data, wing angle of attack equals 0 degrees)

Tunnel Speed (fps)	Differential Pressure (cm of Hg)	Pressure Ratio (PR)	System Lift (lb)	System Drag (lb)	Measured Jet Thrust (lb)	Apparent Jet Angle (deg)	Theory Jet Thrust (lb)	Theory Ideal Compressor (HP)
0	0.00	1.0000	0.0000	0.0000	0.0000	58.0	0.000	0.0000
0	1.22	1.0160	0.1351	–0.0844	0.1593	58.0271	0.393	0.0602
0	3.00	1.0395	0.3695	–0.2384	0.4398	57.1691	0.686	0.1386
0	4.54	1.0598	0.5578	–0.3379	0.6522	58.7951	1.445	0.4240
0	6.13	1.0806	0.7693	–0.4643	0.8986	58.8863	1.936	0.6573
0	7.92	1.1042	0.9922	–0.5767	1.1476	59.8307	2.483	0.9548

Tunnel Speed (fps)	Differential Pressure (cm of Hg)	Pressure Ratio (PR)	System Lift (lb)	System Drag (lb)	Apparent Wing Lift (lb)	Apparent Wing + Brass Tube Drag (lb)	System C_D/AR_W	System C_L/AR_w	C_{ll}/AR_w
94	0.00	1.0000	0.0000	0.540	0.0000	0.54	0.0378	0.0000	0.0000
94	1.22	1.0160	1.7486	0.5070	1.6134	0.5914	0.0355	0.1223	0.0111
94	3.00	1.0280	2.7601	0.4590	2.3906	0.6974	0.0321	0.1930	0.0308
94	4.52	1.0598	3.4022	0.4230	2.8444	0.7609	0.0296	0.2379	0.0456
94	6.12	1.0806	4.0349	0.3800	3.2656	0.8443	0.0266	0.2822	0.0628
94	7.93	1.1042	4.6876	0.3350	3.6955	0.9119	0.0234	0.3278	0.0803

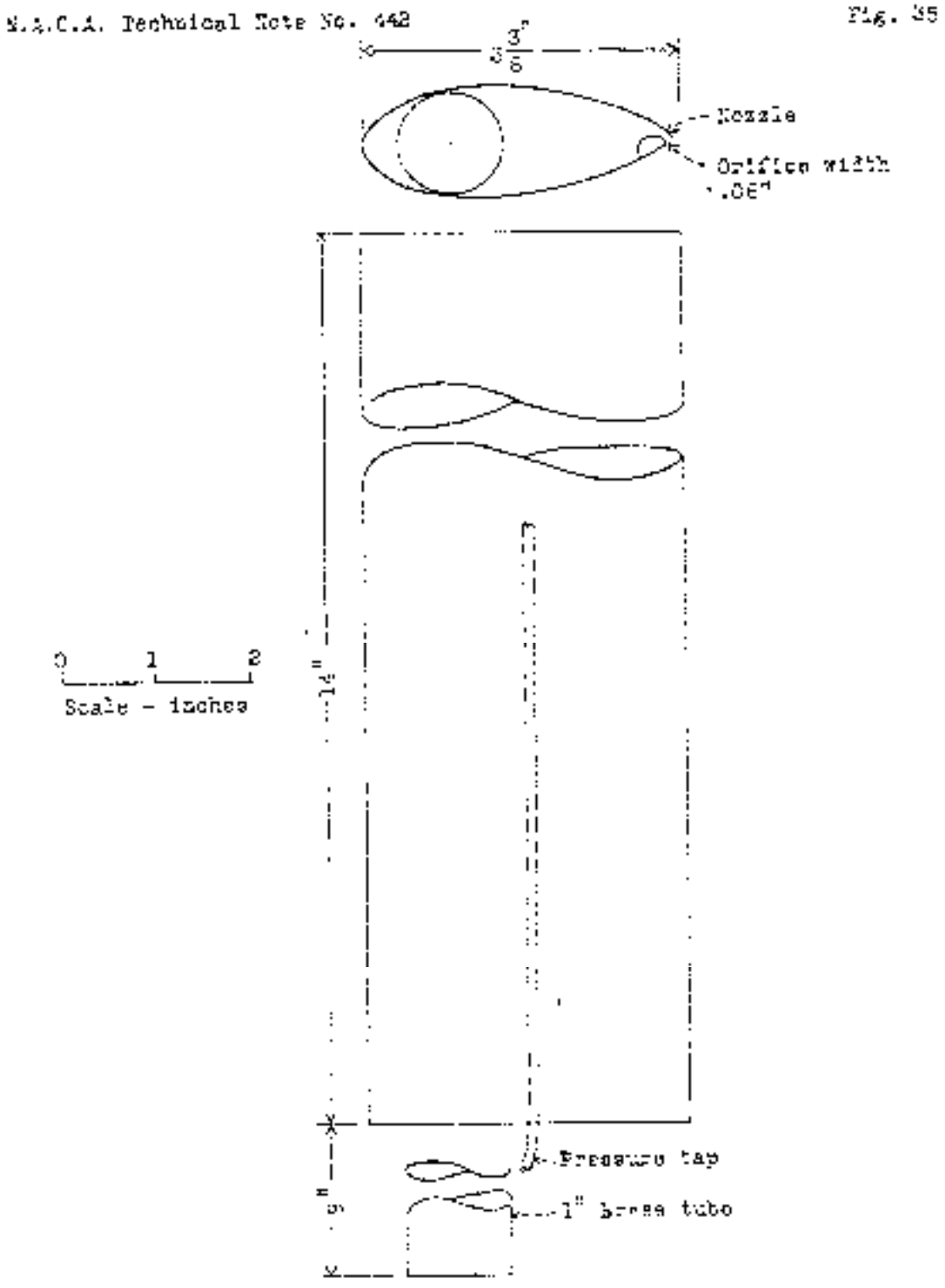

Fig. 3-28. Schubauer's experimental jet flap model was quite small. The nozzle area was 0.00583 square feet.

Consider first the wind-off data in Table 3-2, which calibrated the nozzle's jet thrust. The increasing differential pressure between the wing plenum and the atmosphere was measured in centimeters of mercury. (This gauge pressure translates into relatively low pressure ratios.) The balance lift and drag forces lead to a resultant force equal to jet thrust. Contrary to Schubauer's statement that the nozzle angle was "70 degrees," the lift-to-drag ratio suggests that the nozzle thrust acted at a jet deflection angle (δ_{jet}) slightly less than 60 degrees.

From a theoretical point of view, the measured pressure ratios lead to calculated jet thrusts more than double what the static calibration showed. That is, when the convergent nozzle is not choked and the fluid is air, the jet thrust is theoretically given by

$$(3.52)\quad \text{Thrust}_{jet} = 7 A_{exit} P_{atm} \sqrt{1 + PR^{4/7} - 2\,PR^{2/7}} \quad \text{for } 1 \le PR \le 1.893 .$$

The nozzle exit area was 0.00583 square feet, and I will assume the test was conducted on a standard day so the atmospheric pressure (P_{atm}) was 2,116.23 pounds per square foot. From Table 3-2, the highest pressure ratio tested was 1.1042, so the ideal nozzle theory says the jet thrust should have been 2.483 pounds. This is considerably more than the jet thrust of 1.1476 pounds that Schubauer measured. No doubt Schubauer's nozzle was very inefficient compared to technology today, but even modern nozzles fall 10 to 20 percent below ideal.

From ideal nozzle theory when the pressure ratio is equal to or less than 1.893, the compressor horsepower required to produce that ideal jet thrust from Eq.(3.52) is given by

$$(3.53)\quad HP_{compressor} = \frac{0.6973}{\eta_c}\left[A_{exit} P_{atm} \sqrt{T_{atm}}\, PR^{6/7} \left(PR^{2/7} - 1 \right) \sqrt{\left[\left(\frac{1}{PR} \right)^{\frac{10}{7}} - \left(\frac{1}{PR} \right)^{\frac{12}{7}} \right]} \right]$$

where the compressor efficiency (η_c) could be on the order of 0.9. You will calculate that an *ideal* compressor horsepower ($HP_{compressor}$) of about 1 horsepower is required to produce 2.483 pounds of ideal jet thrust.

Frequently you may want to know what the jet velocity is. Ideal convergent nozzle theory offers this equation

$$(3.54)\quad V_{jet} = 109.6172 \sqrt{\left(T_{atm} \right)\left(PR^{2/7} - 1 \right)} \quad \text{for } 1 \le PR \le 1.893 ,$$

and for Schubauer's test at the highest pressure ratio and again, assuming sea level standard day where the atmospheric temperature (T_{atm}) is 518.4 degrees Rankine (i.e., 459.4 ^{o}F + 59 ^{o}F), you will calculate about 423 feet per second. Occasionally, you may want to know the mass flow (in slugs per second). You can turn to ideal theory, which says

$$(3.55)\quad \frac{d\,m_{jet}}{d\,t} = 0.063859 \frac{A_{exit} P_{atm}}{\sqrt{T_{atm}}} PR^{\frac{6}{7}} \sqrt{\left[\left(\frac{1}{PR} \right)^{\frac{1}{7}} - \left(\frac{1}{PR} \right)^{\frac{12}{7}} \right]} \quad \text{for } 1 \le PR \le 1.893 .$$

Now consider the wind-on portion of Table 3-2. The wind tunnel speed of 94 feet per second gives a flightpath dynamic pressure (q_{FP}) of 10.51 pounds per square foot at sea level on a standard day. Even though the wing was at zero angle of attack, the system lift approached nearly 4.7 pounds, but from the static calibration, only 1 pound of vertical force is provided by the jet thrust at the differential pressure of 7.92 centimeters of mercury. The conclusion is that the apparent wing lift is on the order of 3.7 pounds. This amount of apparent wing lift corresponds to a wing lift coefficient of 1.07. This would mean that the wing thinks it is at about 10 degrees angle of attack. It would seem that the jet thrust forced the wing's lower surface stagnation point well aft of the airfoil leading edge, along the bottom surface.

The wind-on drag data is also of interest. Note that Table 3-2 shows that with the jet velocity off (i.e., differential pressure equals zero) and the wind tunnel at 94 feet per second, the drag is 0.54 pounds. About 0.4 pounds of this drag is due to the unshielded brass tube, assuming a drag coefficient of 0.6 and the tunnel speed of 94 feet per second. That makes the wing drag about 0.14 pounds or a zero lift-drag coefficient of 0.04, which is not too unreasonable for a symmetrical airfoil having a thickness-to-chord ratio of 0.34 and a cutoff trailing edge—particularly when you consider that the Reynolds number was about 174,000.

You will frequently see a graphical presentation of the data from Table 3-2 as shown in Fig. 3-29. Here the two components of the system lift coefficient are plotted versus the jet

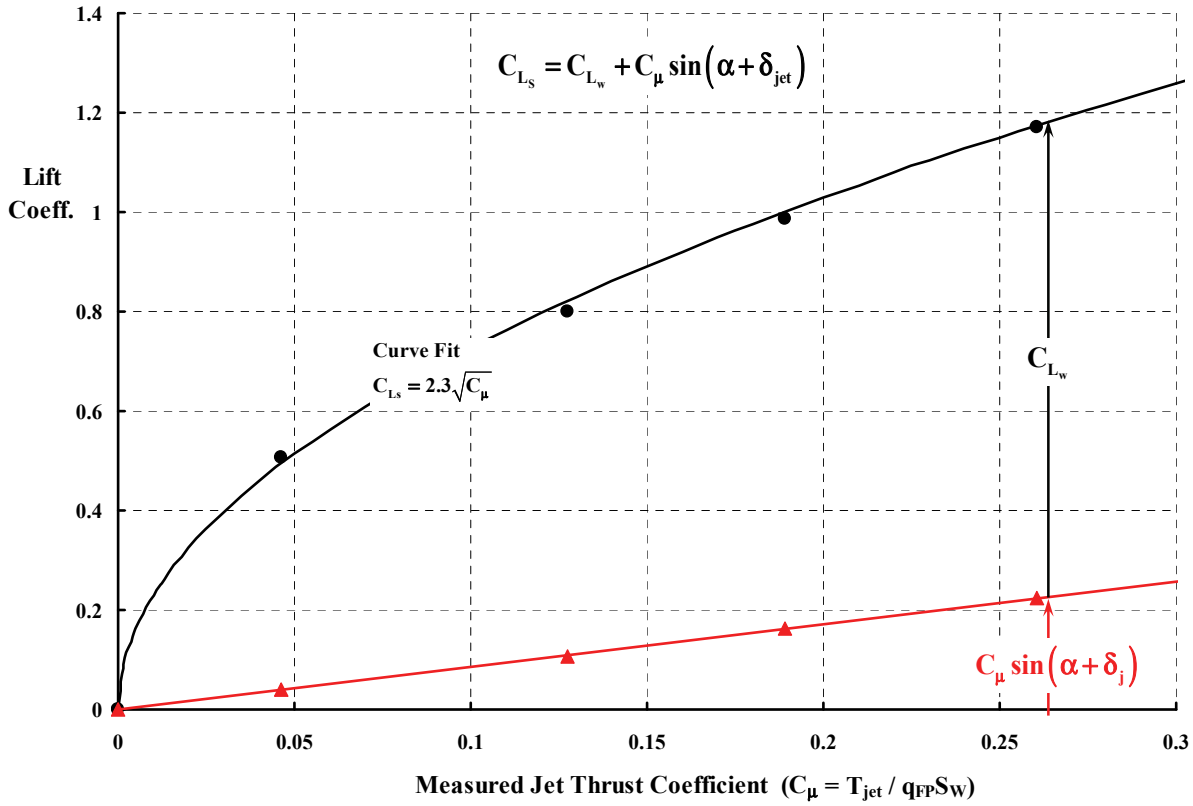

Fig. 3-29. Schubauer's test results at 94 feet per second from Table 3-2. The wing angle of attack was zero, and the jet flap deflection was approximately 58 degrees.

thrust coefficient based on the measured jet thrust. Notice how quickly wing lift builds up with relatively little jet thrust. This data suggests that there is, however, a limit to just how much incremental wing lift coefficient can be created with more jet thrust. When the system lift coefficient has a slope that parallels the jet thrust component, the wing lift component appears to be nearly a constant. The theory that calculates the wing lift due to the jet thrust was presented by two British engineers, Spence [431, 439] and Maskell [437] in the mid-1950s. You will find that Barney McCormick [27] provided a thorough review of the semiempirical theory. Because even the theoretical results are algebraically complicated, I have not included the results in this volume.

The basic force diagram for the jet flap configuration is shown in Fig. 3-30. Here the jet flap is added at the trailing edge of a wing, and the jet thrust force appears as sketched. Clearly the jet thrust adds lift to the system and, just as clearly, the jet thrust offsets the wing drag. While of concern, the jet thrust also has the potential to create a very large nose-down pitching moment that must ultimately be dealt with by the horizontal stabilizer. Keep in mind that achieving pitching moment equilibrium requires a stabilizer download (i.e., negative lift) that will detract from 5 to 30 percent of the wing's lift. But from a force point of view, the system behaves as if

$$\begin{aligned} L_S &= L_w + T_j \sin\left(\alpha + \delta_j\right) \\ D_S &= D_i - T_j \cos\left(\alpha + \delta_j\right) \end{aligned} \quad . \tag{3.56}$$

Notice that I have chosen the drag direction as positive and preordained that the jet thrust component in the drag axis is in the positive propulsive force direction, which is the negative-drag direction. Now consider the nondimensionalizing of the system forces using the flightpath velocity (V_{FP}) as the velocity to calculate dynamic pressure (q_{FP}), and base the system lift and drag coefficients on the wing area (S_W). Then

$$\begin{aligned} C_{Ls} &= C_{Lw} + \frac{T_j}{q_{FP} S_W} \sin\left(\alpha + \delta_j\right) = C_{Lw} + C_\mu \sin\left(\alpha + \delta_j\right) \\ C_{Ds} &= C_{Dw} - \frac{T_j}{q_{FP} S_W} \cos\left(\alpha + \delta_j\right) = C_{Dw} - C_\mu \cos\left(\alpha + \delta_j\right) \end{aligned} \quad . \tag{3.57}$$

The Helmbold theory gives values for wing lift and induced drag as discussed above. Furthermore, the most common coefficient used to deal with jet thrust divided by (q_{FP}) and (S_W) is written as C_μ. Therefore, in the bulk of literature dealing with boundary layer control (BLC), including the jet flap under discussion here, the force equations are as shown in Eq. (3.57). Generally, the system coefficients are written without the subscript, s. Finally, division by the wing aspect ratio (AR_w) gives the Helmbold form of

$$\begin{aligned} \frac{L_{system}}{q\, b^2} &= \frac{C_{Ls}}{AR_w} = \frac{C_{Lw}}{AR_w} + \frac{C_\mu}{AR_w} \sin\left(\alpha + \delta_j\right) \\ \frac{D_{system}}{q\, b^2} &= \frac{C_{D_S}}{AR_w} = \frac{C_{Dw}}{AR_w} - \frac{C_\mu}{AR_w} \cos\left(\alpha + \delta_j\right) \end{aligned} \quad . \tag{3.58}$$

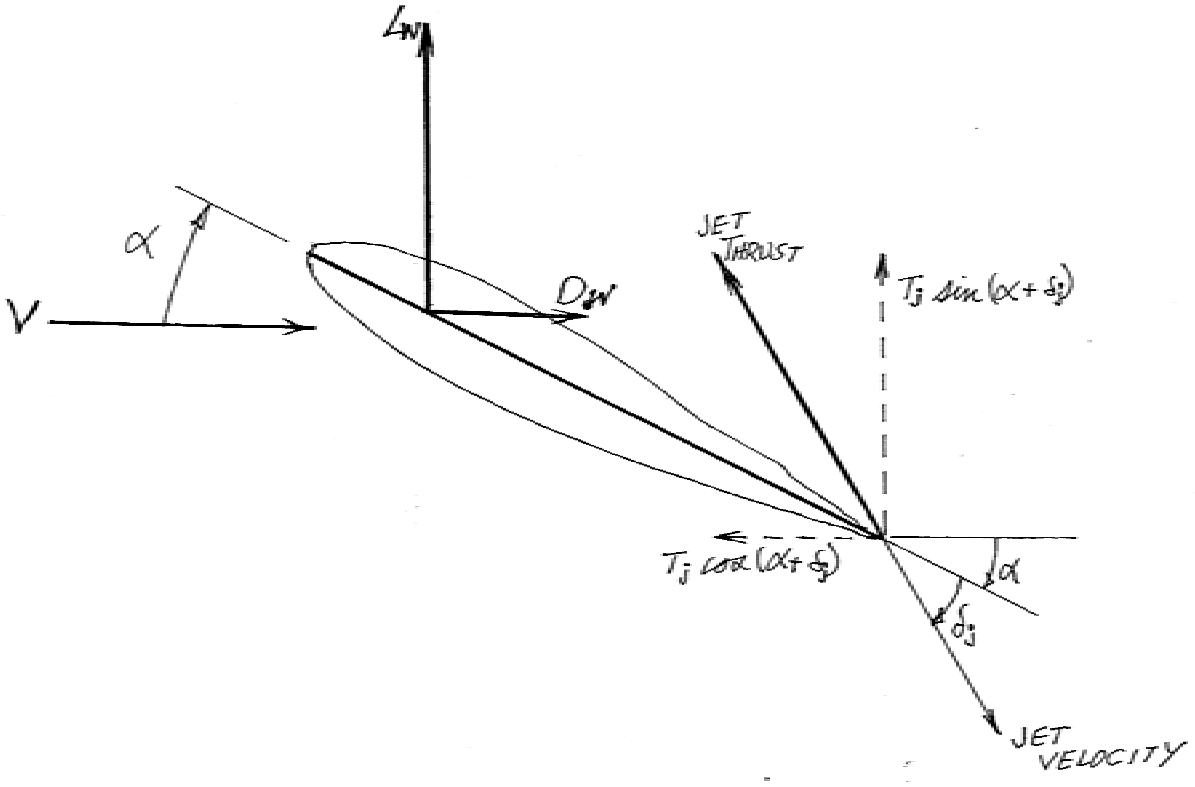

Fig. 3-30. Jet flap force diagram.

Note that if the jet thrust coefficient (C_μ) is large, the wing-induced drag *and* profile drag will be overcome and you obtain a negative wing drag, which is just another way of labeling a propulsive force. In fact, with a very large jet thrust, all of an aircraft's drag can be overcome and equilibrium flight is achieved. I believe this is what Schubauer envisioned.

The question now arises as to how close is Schubauer's experimental system lift and drag to a simple theory. Let me relate the theory first and then make a theory test comparison. Recall that the drag polar of a practical wing *without a jet flap* is reasonable well predicted by

$$(3.59)\quad C_{Dw} = \left(C_{Do} + KC_{Lw}^2\right) + \frac{C_{Lw}^2}{\pi AR_w}(1+\varepsilon)$$

according to Perkins and Hage's [269] *Airplane Peformance, Stability and Control*, page 95. The profile drag is accounted for by the drag at zero lift (C_{Do}) plus the increase in profile drag due to wing lift $\left(KC_{Lw}^2\right)$. The ideal induced drag, the third term in Eq. (3.59), is increased by the factor (1+ε) to account for a non-elliptical wing loading.

A simple theory for the wing *with a jet flap* is obtained by modifying the induced drag term. There have been a number of approximations to calculating the drag polar of a practical

wing with a jet flap.[101] One helpful approximation for the system induced drag—when the wake is assumed to be flat as in Prandtl-Glauert theory—is that[102]

$$\text{(3.60)}\quad \text{System Induced Drag } C_{Di} = \frac{C_{Ls}^2}{2C_\mu + \pi AR_w}(1+\varepsilon) \text{ for flat wake.}$$

Note that the wing lift coefficient (C_{Lw}) has now become the system lift coefficient (C_{Ls}). It is a simple additional step to replace the wing lift coefficient with the system lift coefficient in the profile drag due to lift term (which I have done without theoretical justification), and then you have another semiempirical view that the system drag polar for a wing-jet flap system is given by

$$\text{(3.61)}\quad C_{Ds} = \left(C_{Do} + KC_{Ls}^2\right) + \frac{C_{Ls}^2}{2C_\mu + \pi AR_w}(1+\varepsilon) - C_\mu \cos\left(\alpha + \delta_{jet}\right) \quad \text{for a flat wake.}$$

Now let me take the final step of offering my semiempirical theory in Helmbold's format. That is,

$$\text{(3.62)}\quad \begin{aligned} \frac{L_{system}}{q\,b^2} &= \frac{C_{Ls}}{AR_w} = \frac{C_{Lw}}{AR_w} + \frac{C_\mu}{AR_w}\sin\left(\alpha + \delta_{jet}\right) \\ \frac{D_{system}}{q\,b^2} &= \frac{C_{D_S}}{AR_w} = \frac{C_{Do}}{AR_w} + K\left(AR_w\right)\left(\frac{C_{Ls}}{AR_w}\right)^2 + \frac{(1+\varepsilon)}{\left(2C_\mu/AR_w + \pi\right)}\left(\frac{C_{Ls}}{AR_w}\right)^2 - \frac{C_\mu}{AR_w}\cos\left(\alpha + \delta_{jet}\right). \end{aligned}$$

Equation (3.62) offers you a way of judging how close to ideal performance Schubauer got with his small model. Let me first get you oriented. As you study Fig. 3-31, you see a lift-drag polar coordinate system. The heavy, solid black curve is the base of the discussion. This is Helmbold's lift-drag polar for the ideal wing, which was discussed at the beginning of this chapter. Next you see Schubauer's test data from Table 3-2 in Helmbold's coefficient form shown as the red triangles. His test data rise upwards from zero lift and toward a condition of negative drag as the jet thrust coefficient (C_μ) increases. Now notice the black circles. Here I have applied Eq. (3.62) by simply subtracting lift and drag jet-thrust components from the system lift and drag coefficients as the figure shows. Finally, as a reference to ideal, I have added the light, dashed black line, which is Helmbold's theory, zero shifted along the abscissa. Fig. 3-31 shows that within Schubauer's experimental accuracy, and within the limits of simple jet flap theory, the system does behave as Eq. (3.62) predicts.

It does not take very much studying of Fig. 3-31 to imagine that if the jet thrust coefficient were larger by 5 to 10 percent because of experimental error, the black circles would string out to the other side of Helmbold's zero-shifted ideal.

[101] For instance, see references [433] and [440].

[102] Barney McCormick [27] included the clearest derivation I have seen.

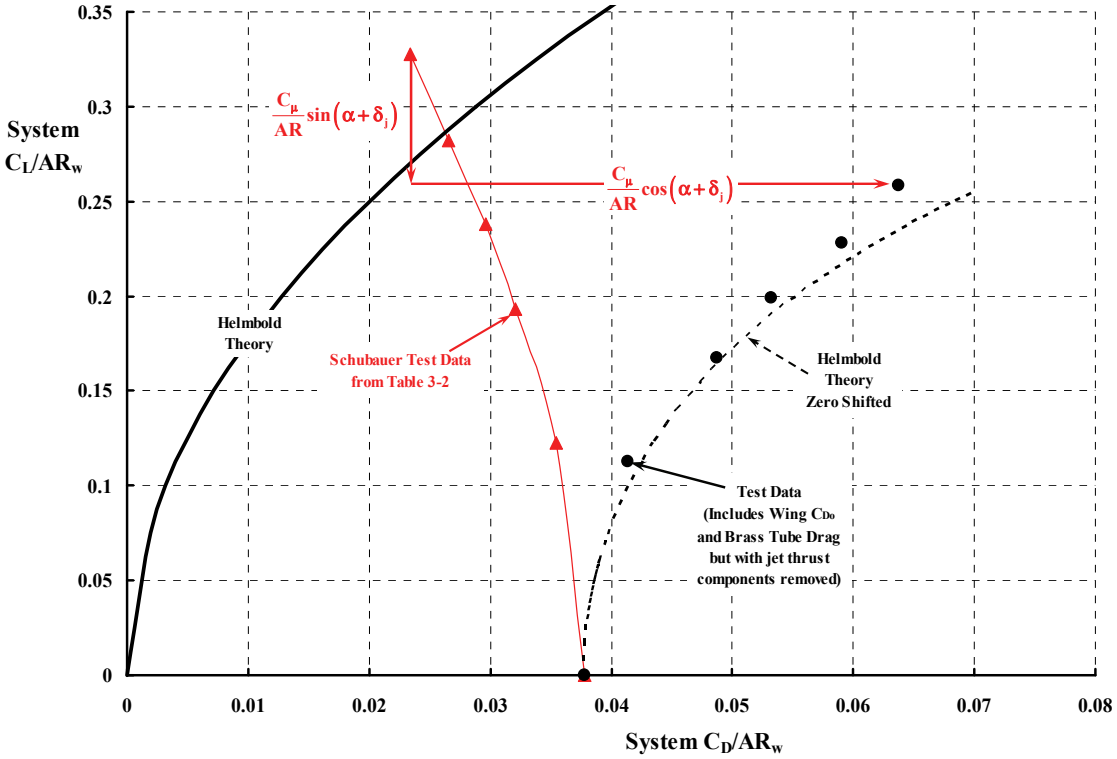

Fig. 3-31. Schubauer's data demonstrated that high lift and propulsion could be obtained.

Let me suggest another way of comparing test data to ideal using Schubauer's data from 1932. To do this I must create a different form of what a system ideal lift-drag polar looks like. Only one point from Schubauer's data on Fig. 3-31 is actually required to convey my new ideal, so I will use the highest red triangle on Fig. 3-31 for the example. From Table 3-2 this point corresponds to a jet thrust of 1.1476 pounds, which is a jet thrust coefficient divided by a wing aspect ratio of 0.0803. Suppose now that you accept, for the moment, an ideal defined as Helmbold's theory plus the jet thrust component assuming, from Eq. (3.61), that $(\alpha + \delta_{jet})$ is a small angle so that $\cos(\alpha + \delta_{jet})$ is 1.0. Then you have an approximation for the ideal system drag coefficient divide by wing aspect ratio that appears as

$$(3.63)\quad \frac{D_{system}}{q\,b^2} = \frac{C_{D_S}}{AR_w} = \frac{1}{\left(2C_\mu/AR_w + \pi\right)}\left(\frac{C_{Ls}}{AR_w}\right)^2 - \frac{C_\mu}{AR_w}.$$

Note that I have assumed that the lift distribution from wingtip to wingtip is elliptical (i.e., $\varepsilon = 0$), which is the minimum-induced-drag span loading. Furthermore, at zero system lift coefficient, the ideal system drag coefficient is simply

$$(3.64)\quad \frac{D_{system}}{q\,b^2} = \frac{C_{D_S}}{AR_w} = -\frac{C_\mu}{AR_w}.$$

Now turn your attention to Fig. 3-32 where I have shown Schubauer's test results in comparison to Eq. (3.63) with C_μ/AR_w equal to 0.0803.

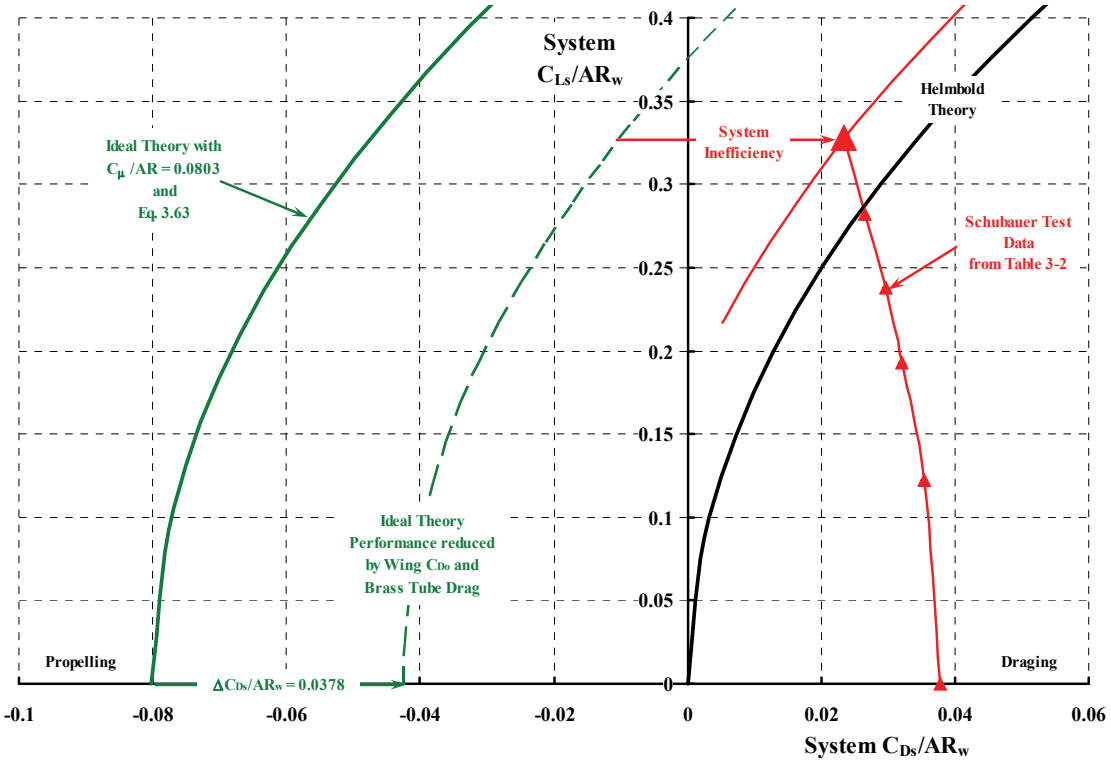

Fig. 3-32. Schubauer's model was not very efficient when compared to ideal theory.

The results of using Eq. (3.63) with C_μ/AR_w equal to 0.0803 are shown with the heavy green line on Fig. 3-32, but you can see that the highest lift point Schubauer measured (i.e., the large red triangle) is not in the propelling quadrant at all. It would be quite something if the large red triangle fell on the heavy green line and would, of course, delight jet flap advocates. In fact, Schubauer's model had considerable drag at zero lift, so it is unreasonable to expect such an ideal. To be more realistic, on Fig. 3-32 I have shown the ideal theory shifted toward the drag quadrant by the drag at zero lift (i.e., C_{Do}/AR_w equal to 0.0378) and identified this performance level with the dashed green line. It does not seem so unreasonable to expect Schubauer's highest point to fall on this line because it reflects induced drag and ideal jet thrust components. But, as you can see, this expectation is not met by a considerable margin, which is a real measure of system inefficiency in my mind.

You should keep in mind that the preceding analysis would apply to any experimental data point Schubauer obtained and only depend on what jet-thrust-coefficient level the point had. Therefore, your imagination should see a red curved line paralleling the ideal theory, passing through each red triangle and labeled with its own jet thrust coefficient.

The impression that the system drag polar Schubauer obtained was hardly close to what the ideal theory might predict was a small point to many researchers. The fact that very large lift coefficients might be obtained with jet thrust coefficients much larger than what researchers were thinking about for BLC was a new research avenue. Schubauer thus opened the door to powered lift for STOL.

3.3.6.2 Modern Jet Flap Results—NACA TN 3865

There was a gap of two decades after Schubauer's report was published (in 1933) before the aviation industry came back to his ideas. The industry's motivation was the success that the gas turbine engine demonstrated in practical use on both military and commercial aircraft. Researchers in all the major countries made significant contributions, but I would say that the British took the early lead. Of the hundreds of reports and papers on the subject of jet flaps, I have selected one experimental contribution by NACA Langley Aeronautical Laboratory because of its introductory nature *and because it appears to confirm Helmbold's theory* [401], which shows the limit to wing lift you read about in paragraph 3.1. The experimental results were published in NACA TN 3865. This experiment almost became a bible of test data—judging by the number of times it is referenced in other boundary layer control and jet flap reports and books. This December 1956 report [433] by Lockwood, Turner, and Riebe is titled *Wind-Tunnel Investigation of Jet-Augmented Flaps on a Rectangular Wing to High Momentum Coefficients*. Their test configuration, shown here as Fig. 3-33, was quite similar to Schubauer's, but it involved pressure ratios up to nearly 6 and the jet thrust coefficient (C_μ) reached 57! With a rectangular wing aspect ratio of 8.4, the maximum tested C_μ/AR was 6.78, which was over 20 times the value that Schubauer reported with his 4.14-aspect-ratio rectangular wing in NACA TN 442 [430].

The authors of NACA TN 3865 began their discussion of their experimental results by addressing the jet thrust coefficient, which is commonly called the momentum coefficient by many authors. What they wrote is terribly important because comparisons between test and theory depend heavily on the values of C_μ used. With some additions of mine in brackets, they wrote:

> "A brief discussion of the momentum coefficient is necessary because the data presented are dependent upon the basis used for calculating this coefficient. *The momentum coefficient used herein is based upon the product of the [measured] mass of air discharged through the slot and the theoretical velocity obtained by assuming isentropic expansion to free-stream static pressure* [my italics]. In a converging nozzle, efficiencies of nearly 100 percent are obtained up to choking velocity [the speed of sound], above which a slight loss occurs as the pressure ratio is increased. The nozzle used in the present investigation is shown in figures 1 [Fig. 3-33] and 2 and the calibration of the 57° and 86° jet nozzles is shown in figure 4 [Fig. 3-34]. (Several values of the ratio of plenum-chamber pressure to free-stream static pressure that existed for the calibration are indicated in the figure.) These data indicate that the measured reaction [i.e., thrust] is approximately 75 percent of the calculated value for either jet angle. *It should be emphasized that the theoretical momentum coefficient has been used* [my italics] because it is believed that the momentum of the jet at the nozzle exit is largely responsible for the change in circulation around the wing, and because the losses in the jet due to over expanding, turning, and base pressure could not be individually evaluated from the results of these data."

Lockwood and his coauthors chose to use the calculated thrust to compute the jet thrust coefficient ($C_\mu = T_j/q_{FP}S_w$), which is a very key point. Frankly, I would have debated that choice because the measured static thrust was 0.75 times the calculated thrust as Fig. 3-34 shows. On the other hand, the authors included no test-versus-theory material, and that left the problem squarely on the shoulders of other researchers to deal with. Whether the measured thrust with zero tunnel velocity applies when the wind is on is a very serious question that has never been addressed. This is the first of three issues that bother me.

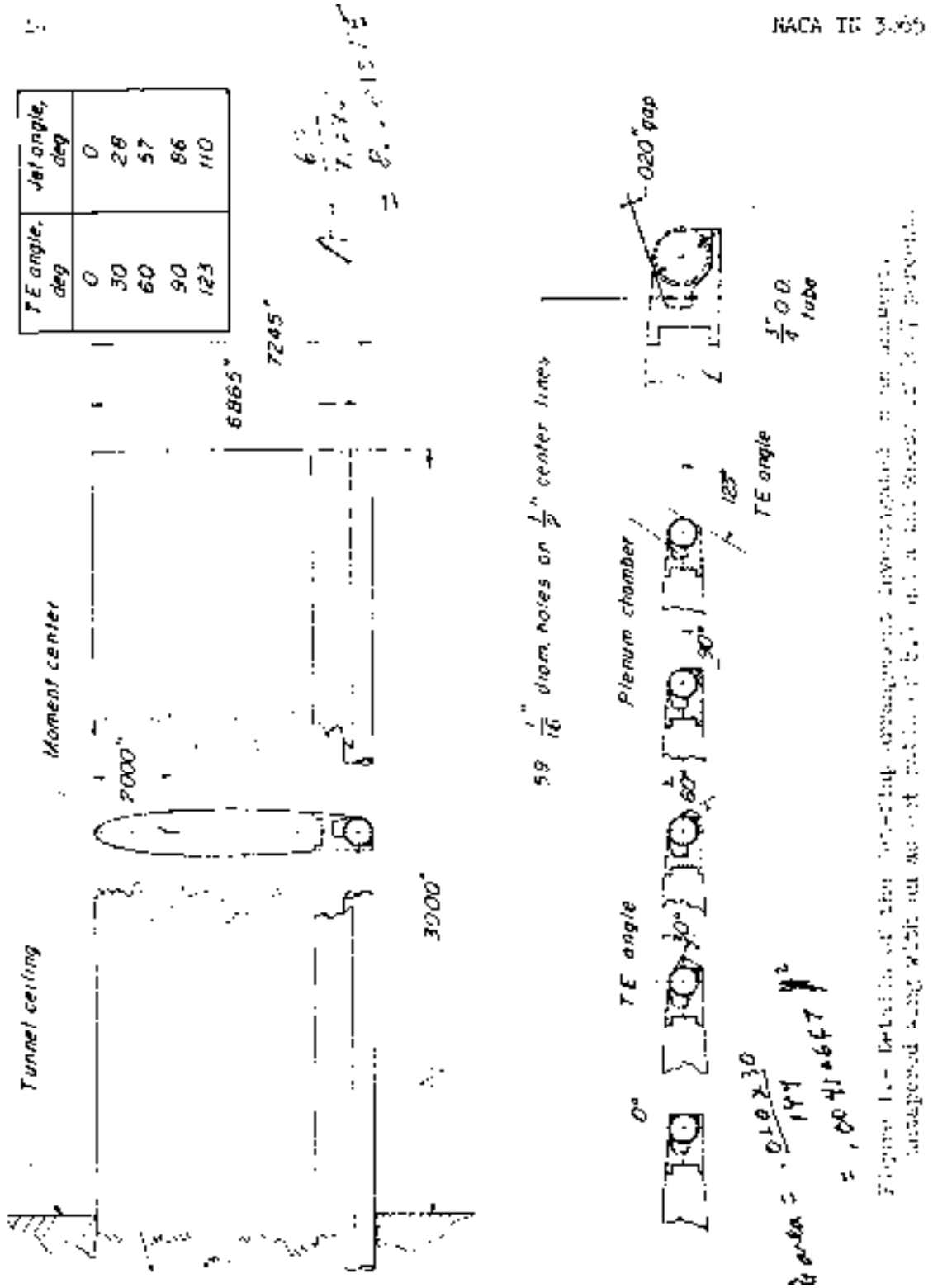

Fig. 3-33. The test configuration from NACA TN 3865 (pressure ratios up to nearly 6 were involved, and the jet thrust coefficient (C_μ) reached 57)!

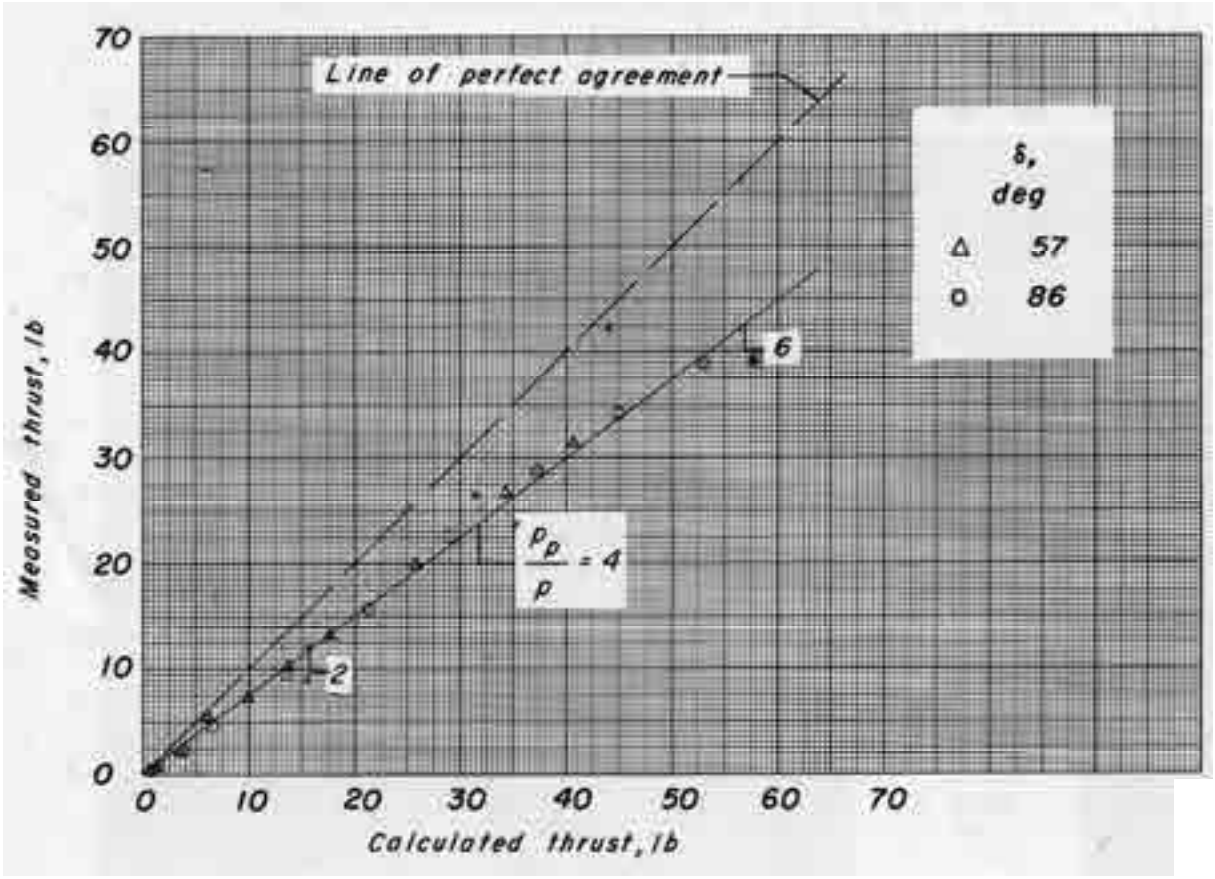

Fig. 3-34. Calculated thrust was used to compute the jet thrust coefficient (from NACA TN 3865).

The *calculation* of the nozzle thrust and other parameters is rather interesting. The nozzle thrust is fundamentally defined as $T_{jet} = \frac{dm_{jet}}{dt} V_{jet}$. The researchers stated in their report:

> "The weight rate of flow of air [i.e., mass flow] was determined by means of a calibrated sharp-edge orifice in the pipe line before the air came onto the balance frame, and the pressures and temperatures for determining the jet-exit velocities were measured in the plenum chamber in the wing."

Based on these statements, you can see that the mass flow $\left(\frac{dm_{jet}}{dt} = \frac{dW_{jet}}{g\,dt} \right)$ was obtained from a "calibrated sharp-edge orifice" and the jet velocity (V_{jet}) was obtained from ideal nozzle theory, which states that for a *choked nozzle*

$$(3.65)\quad V_{jet} = \sqrt{\frac{2\gamma}{\gamma-1} RTg \left[1 - \left(\frac{p}{P_p} \right)^{\frac{\gamma-1}{\gamma}} \right]} = 44.751 \sqrt{T_{atm} PR^{2/7}} \quad \text{for } PR \geq 1.893.$$

The researchers noted that the "pressures and temperatures for determining the jet-exit velocities were measured in the plenum chamber in the wing." You might not know that when a convergent nozzle is choked (i.e., at the flow exit point to the atmosphere from the plenum chamber), it means that the nozzle velocity (V_{jet}) cannot exceed a Mach number of 1.0. If the mass flow had not been measured, you would calculate thrust based totally on ideal choked nozzle theory, in which case the mass flow in slugs per second would be calculated from

$$(3.66)\quad \frac{d\,m_{jet}}{d\,t} = 0.016527\,\frac{A_{exit}P_{atm}}{\sqrt{T_{atm}}}PR^{6/7} \quad \text{for} \quad PR \geq 1.893,$$

and the jet velocity, in feet per second, would be calculated from Eq. (3.65). In a direct form, the jet thrust can be found from

$$(3.67)\quad Thrust_{jet} = A_{exit}P_{atm}\left(1.267881\,PR - 1\right) \quad \text{for} \quad PR \geq 1.893.$$

You should keep in mind that a STOL with jet flaps must carry within itself the power to create the jet thrust. This becomes an additional power required for the configuration. The ideal compressor horsepower required to produce the jet thrust found with Eq. (3.67) is simply

$$(3.68)\quad HP_{compressor} = \frac{0.18047}{\eta_c}\left[A_{exit}P_{atm}\sqrt{T_{atm}}PR^{6/7}\left(PR^{2/7} - 1\right)\right] \quad \text{for} \quad PR \geq 1.893.$$

There is a second interesting ideal-versus-actual deficiency that Lockwood, Turner, and Riebe reported [433]. It has to do with the shortfall in the actual direction of the nozzle flow and the actual jet-thrust-vector orientation versus the geometric angle. Note the table on Fig. 3-33 that shows the trailing-edge angle and the jet thrust angle (δ_{jet}). For instance, the highest trailing-edge angle of 123 degrees was found to only provide a measured jet thrust angle of 110 degrees. This followed Schubauer's experience where the geometric 70-degree flap angle actually achieved slightly less than 60 degrees when tested. The researchers noted that "all data in NACA TN 3865 is referenced to the measured jet thrust angles" of 0, 28, 57, 86, or 110 degrees. The researchers did not comment on the difference or how they obtained the jet thrust angle, but with balance readings of lift and drag, and at zero tunnel velocity, the angle may well have been found by

$$(3.69)\quad \delta_{jet} = \text{arc tangent}\left(\frac{D}{L}\right).$$

Now let me go on to discuss the experimental results documented in NACA TN 3865.

I have taken the test condition section of NACA TN 3865 nearly verbatim and added the last column: "The tests were made in the Langley 300 MPH 7- by 10-foot tunnel at conditions tabulated below. The angle-of-attack range for the investigation extended from –12 to about +20 degrees. All five jet thrust angles were tested at the primary, *theoretical* jet thrust coefficients (C_μ) of 56.75, 28.5, 14.37, 7.1, 1.96, and 0. The 86-degree jet thrust angle was tested more thoroughly at every jet thrust coefficient."

Test Conditions From NACA TN 3865

Dynamic Pressure q, lb/sq ft	Velocity V, ft/sec	Reynolds Number	Mach Number	Theory Jet Thrust Momentum Coefficient, C_μ	Measured Jet Thrust Momentum Coefficient, C_μ
0.56	21.8	84,000	0.02	56.75	42.56
1.13	30.8	119,000	0.03	28.50	21.38
2.26	43.7	168,000	0.04	14.37	10.78
4.5	61.7	238,000	0.06	7.10	5.33
8.5	84.7	326,000	0.08	0, 1.96, 0.15 to 4.5	0, 1.47, 0.11 to 3.375
16.9	119.7	460,000	0.11	0.96	0.72
110.6	340	1,230,000	0.30	0 and 0.079	0 and 0.059
164.2	373	1,300,000	0.33	0.008 to 0.058	0.006 to 0.0435

To give you a sample of the lift and drag data for this wing and jet flap model, I have reproduced one set of data where wing angle of attack is varied from –8 to +20 degrees, and the jet thrust angle is constant at 0 degrees. The secondary variable is the jet thrust coefficient, which varies from 0 to 55.60. *Do not forget that the researchers felt that the actual value of the coefficient was nominally 0.75 times the values tabulated on the figures.* The system lift coefficient as it varies with wing angle of attack is shown in Fig. 3-35, and the accompanying system drag polar is provided in Fig. 3-36.

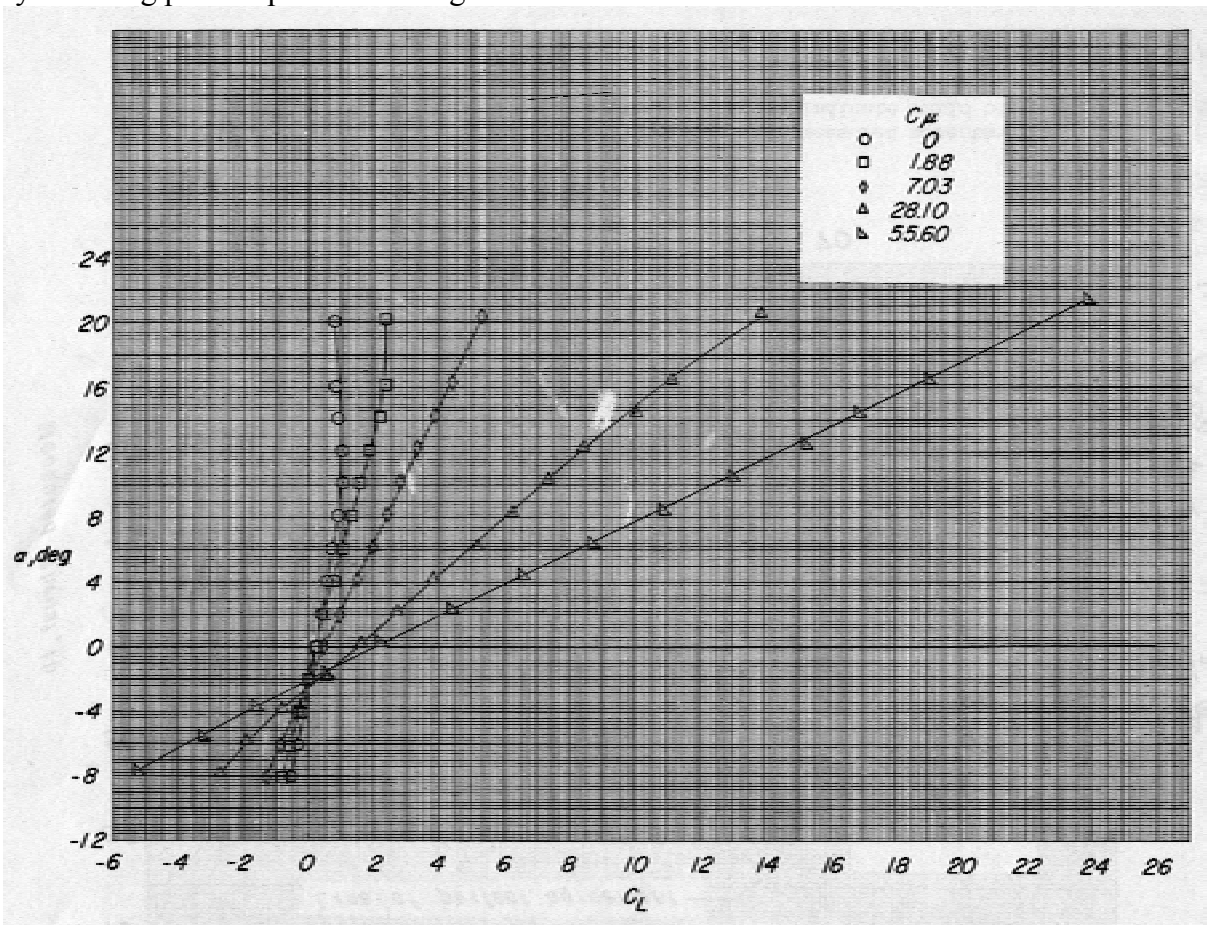

Fig. 3-35. Wing angle of attack versus system lift coefficient as affected by jet thrust coefficient. Jet thrust angle is 0 degrees.

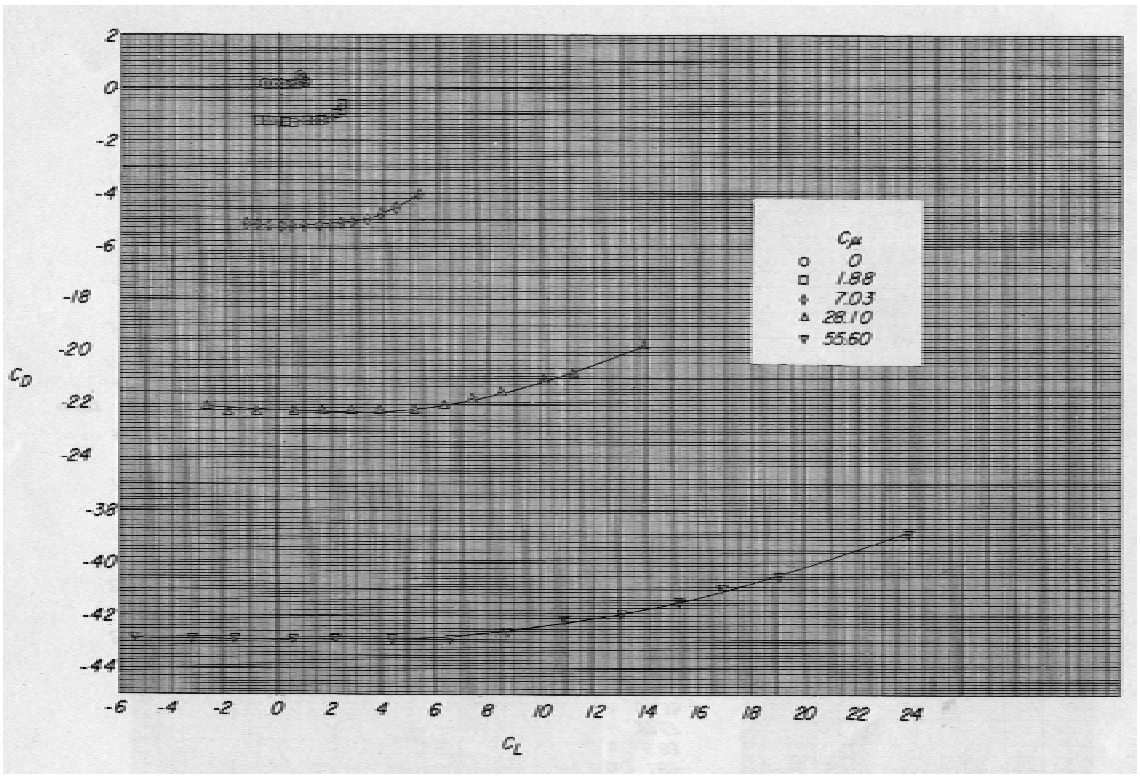

Fig. 3-36. System drag polar as affected by jet thrust coefficient (jet thrust angle is 0 degrees).

In discussing the aerodynamic data provided by NACA TN 3865, you will see that the jet thrust becomes a dominate force as the jet thrust coefficient is increased. This is the core meaning of the words "powered lift" that many STOL advocates use. To illustrate this fact, I begin by extracting the wing lift and drag from the test data. That is, from Eq. (3.57) you have

$$\begin{aligned} C_{Lw} &= C_{Ls} - C_\mu \sin\left(\alpha + \delta_{jet}\right) \\ C_{Dw} &= C_{Ds} + C_\mu \cos\left(\alpha + \delta_{jet}\right) \end{aligned}, \tag{3.70}$$

and remember that $C_\mu\cos(\alpha+\delta_{jet})$ is a positive number, but it acts in a negative drag direction.

Now that Fig. 3-35 and Fig. 3-36 lay the cornerstone, let me discuss the lift coefficient versus wing angle of attack first. You see from the lift versus angle-of-attack data in Fig. 3-35 that the lift-curve slope ($dC_{Ls}/d\alpha$) increases dramatically as the jet thrust coefficient increases. In contrast, the data indicate that the angle of attack for zero system lift appears virtually independent of the jet thrust coefficient, staying at about –2.3 degrees. There is evidence of the system stalling at low-jet-thrust coefficient. However, that evidence disappears at higher values of C_μ, starting at 7 and continuing on up to 55. A simple regression analysis shows that the system lift coefficient (C_{Ls}) behaves as

$$C_{Ls} = \left(0.083 + 0.02407\sqrt{C_\mu} + 0.018423C_\mu\right)\left(\alpha + 2.307\right) \tag{3.71}$$
$$\text{Note}: \alpha \text{ in degrees and } \delta_{jet} = 0 \text{ degrees.}$$

In Eq. (3.71), the jet thrust coefficient is not as tabulated on Fig. 3-35 but is rather the measured values, which is to say, the researchers' calculated values times 0.75. This is a quagmire in which the researchers placed the readers of their report and users of their data.

Finally, there is a third important issue that I would raise about the experimental data. It is not at all clear why the angle of attack for zero lift is on the order of –2.3 degrees, as you see from Fig. 3-35.[103] The authors of NACA TN 3865 stated:

> "The jet-flap wing was constructed by removing the rear 30 percent of a 10-inch-chord wing that had NACA 0012 airfoil sections and installing a 0.750-inch-diameter tube and a plenum chamber, as shown in figure 1 [Fig. 3-33]. High-pressure air was brought in through the tube and ejected into the wing plenum chamber through 59 holes of 1/16-inch diameter located in the tube at spanwise intervals of one-half inch. For the jet-flap configurations, wedges were attached to the trailing edge of the wing to fix the angle δ that the resulting jet made with the wing chord line. The slight increase of wing area resulting from addition of the wedges was not considered a part of the basic wing area."

You would expect that a symmetrical airfoil such as the NACA 0012 would have a zero angle of attack for zero lift, not the –2.3 degrees shown in Fig. 3-35. Because the data for all geometric jet flap angles and zero jet thrust coefficient showed this surprising "zero shift" in the angle of attack for zero lift, I suspect a flow angularity in the wind tunnel of about –2.3 degrees. Whether this angle is constant is open to question.

Because of the three issues that bother me, I have chosen to convey the researchers' data assuming that:

a. the measured jet thrust coefficient rather than the calculated value is the one to use,
b. the jet thrust angle rather than the geometric angle is the one to use, and
c. the tabulated angle of attack must have 2.3 degrees added so that zero lift occurs at near zero angle of attack.

With these "corrections," I believe you will have a much better grasp of jet-flap-system aerodynamics when the "calculated" jet thrust coefficient (C_μ) varies from 0 to 57, and the jet thrust angle varies from 0 to 110 degrees.

Now let me extract the wing lift (C_{Lw}) from the system lift (C_{Ls}) using Eq. (3.70) and the redigitized data I obtained from Fig. 3-35. The objective is to see how the wing lift coefficient varies with angle of attack and the several jet thrust coefficients tested. The results of the extraction are shown in Fig. 3-37. A simple regression analysis of this data shows that the wing lift coefficient contribution to the system lift coefficient behaves as

$$C_{Lw} = \left(0.083 + 0.024365\sqrt{C_\mu} + 0.0012867 C_\mu\right)(\alpha + 2.307) \quad (3.72)$$

$$\text{Note: } \alpha \text{ in degrees and } \delta_{jet} = 0 \text{ degrees}$$

and therefore the system lift coefficient with $\delta_{jet} = 0$ degrees is adequately described by

$$C_{Ls} = \left(0.083 + 0.024365\sqrt{C_\mu} + 0.0012867 C_\mu\right)\alpha + C_\mu \sin\left(\alpha + \delta_{jet}\right). \quad (3.73)$$

[103] I have often wondered why it always seems that finding and setting a zero reference point in an experiment is so time consuming. Frequently, I have just given up and resorted to "deltas." However, if the absolute is suspect, how can you depend on the deltas?

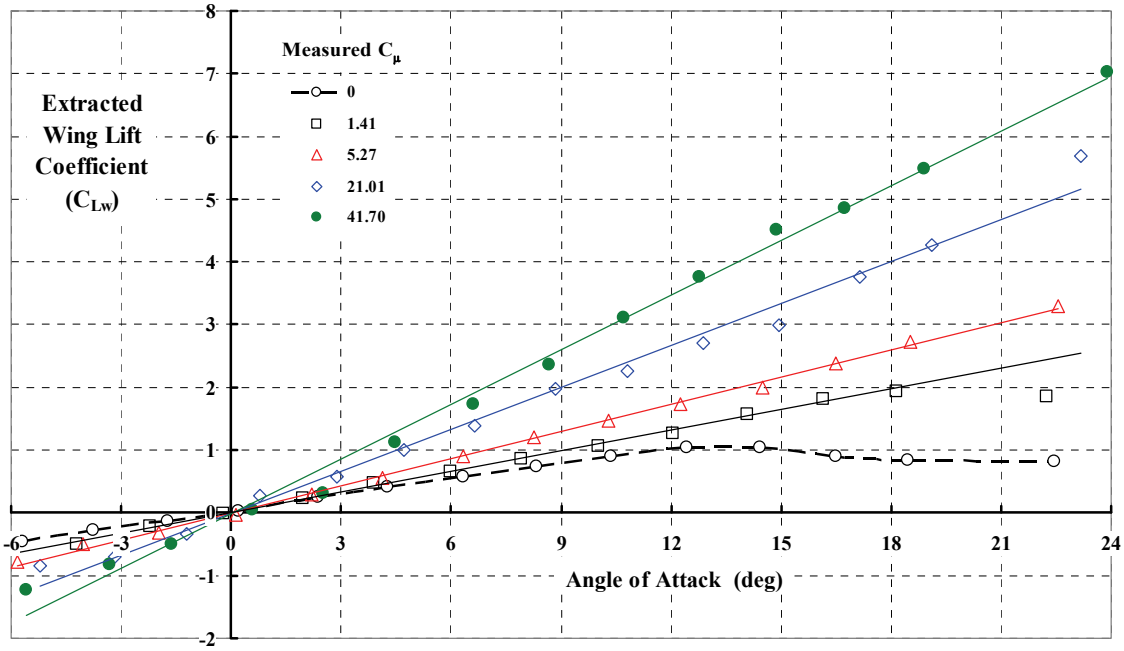

Fig. 3-37. Wing contribution to the jet flap system. Jet thrust vectored at 0 degrees relative to the cutoff NACA 0012 airfoil chord line. Note that the data has been corrected for an unexplained angle of zero lift of –2.3 degrees and that the measured jet thrust coefficient has been used.

It is worth a minute to see how the system lift and extracted wing lift behave as the jet thrust angle (δ_{jet}) varies while the measured jet thrust coefficient (C_μ) remains nearly constant. You see the behavior at a nominal jet thrust coefficient value of 21 in Fig. 3-38 and Fig. 3-39.

The system lift coefficient (Fig. 3-38) shows immediately that the jet flap system has a maximum lift coefficient on the order of 42. This maximum is reached, with a C_μ of 21, when the jet flap angle is near 90 degrees. This maximum is predictable using Helmbold's theory by redefining the wing aspect ratio (AR_w) to account for jet thrust. On page 206 of Barney McCormick's book [27] you will find that the *system* aspect ratio (AR_s) must be defined as

$$(3.74)\quad AR_s = AR_w + \frac{2C_\mu}{\pi}.$$

For the NACA TN 3865 model, the wing aspect ratio of 8.28 is increased to 21.64. Now Helmbold's theory says that the maximum ratio of system lift coefficient (C_{Ls}) to system aspect ratio is 1.9, based on Fig. 3-4. Therefore, you have

$$(3.75)\quad \text{Maximum } C_{Ls} = 1.9\left(AR_w + \frac{2C_\mu}{\pi}\right) = 41.1.$$

This result provides some experimental evidence that Helmbold's theory is correct.

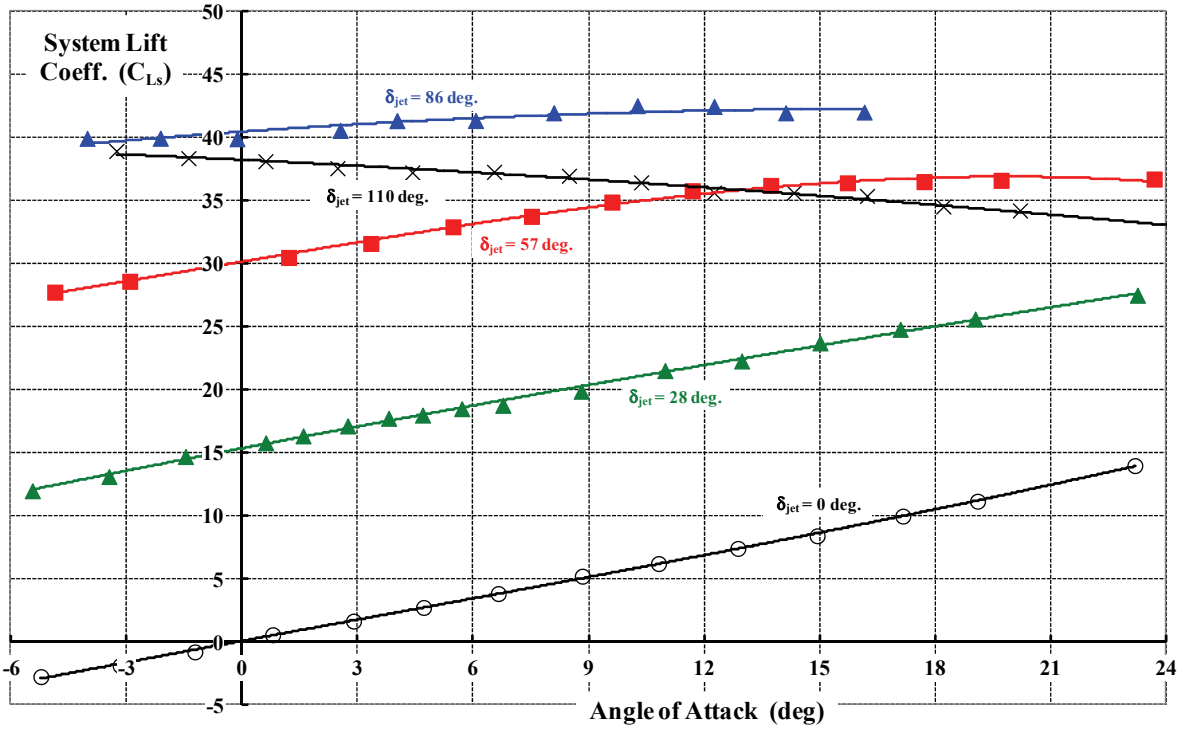

Fig. 3-38. *System lift* coefficient as affected by jet thrust angle. Nominal jet thrust coefficient is 21 (C_μ), which is the measured coefficient.

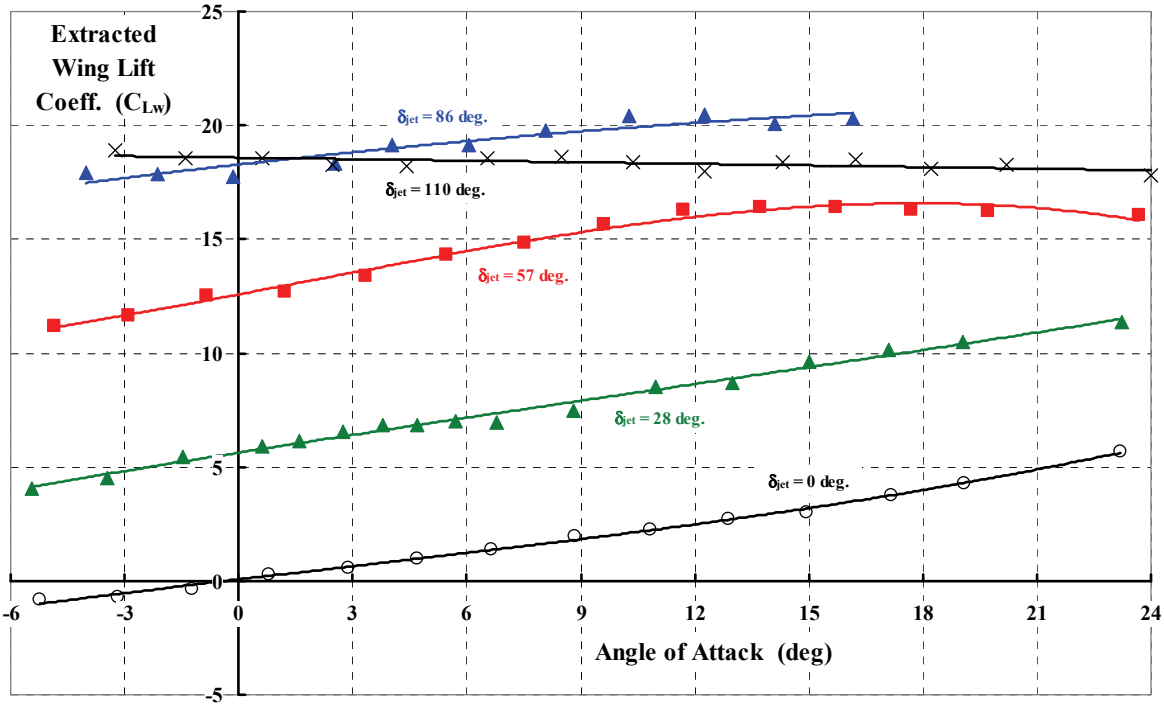

Fig. 3-39. *Wing lift* contribution to system lift as affected by jet thrust angle. Nominal jet thrust coefficient is 21 (C_μ), which is the measured coefficient.

You might note from Fig. 3-38 and Fig. 3-39 that the lift-curve slopes for both the system and the wing are relatively independent of jet thrust angles up to at least 57 degrees where some evidence of system maximum lift is seen.

Now consider the system drag polar data that you saw in Fig. 3-36. You see the wing's contribution to the system drag polar here in Fig. 3-40. Two points of interest are apparent from this figure. The first is how little jet thrust is required to unstall the wing. That is, the characteristic drag polar of a normal wing that you see with the jet thrust coefficients of 0 and 1.41 is hardly evident with a C_μ of 5.27 and greater. Second, in order to clearly see the wing drag polar, I have had to increase the ordinate by a factor of 30 relative to Fig. 3-36. You can see what I suspect is a zero drift in the drag at zero lift. You would expect the wing drag polar to always be positive as the data at 0 and 1.41 C_μ exhibits. In this introductory discussion, I will ignore what amounts to a zero shift of about 3 percent caused, I imagine, by the very small drag levels (in pounds) being measured when the jet thrust *coefficient* is large.

The more interesting data set is seen when the jet thrust angle (δ_{jet}) varies while the measured jet thrust coefficient (C_μ) remains nearly constant. You see this behavior at a nominal jet thrust coefficient of 21 in Fig. 3-41 and Fig. 3-42.

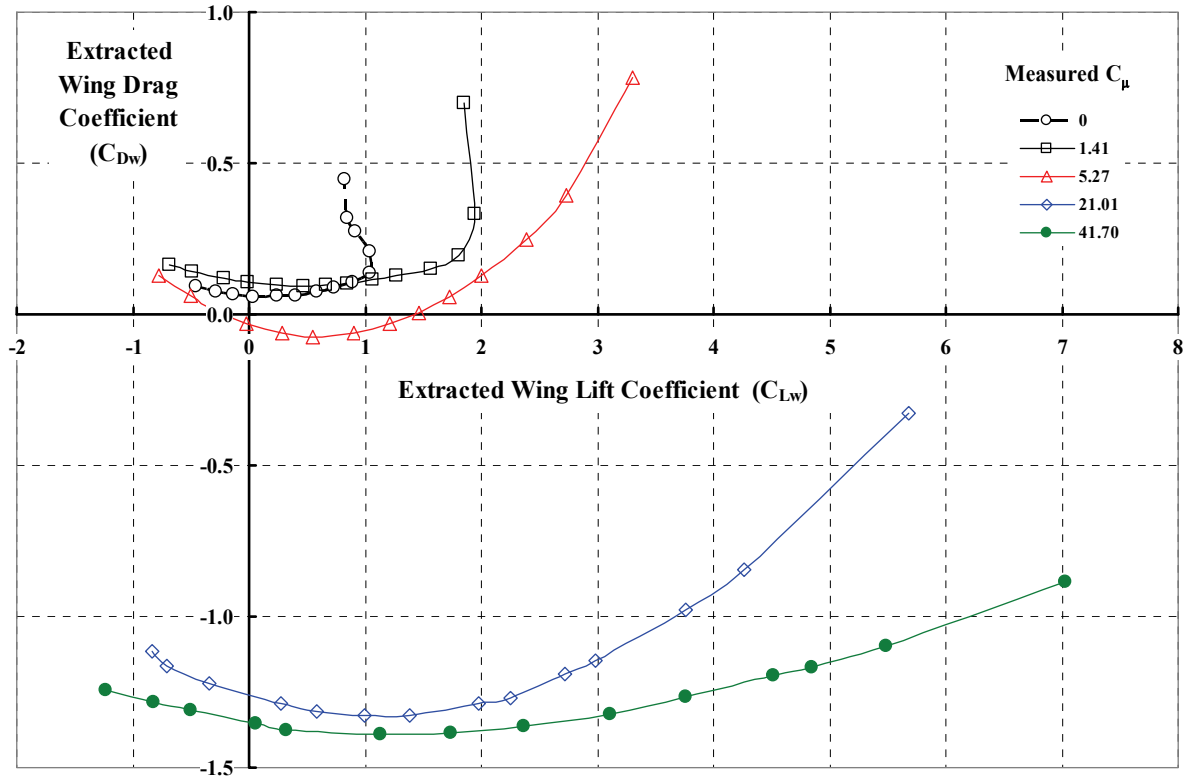

Fig. 3-40. Wing contribution to the jet-flap-system drag polar. Jet thrust vectored at 0 degrees relative to the cutoff NACA 0012 airfoil chord line. Note that the measured jet thrust coefficient has been used.

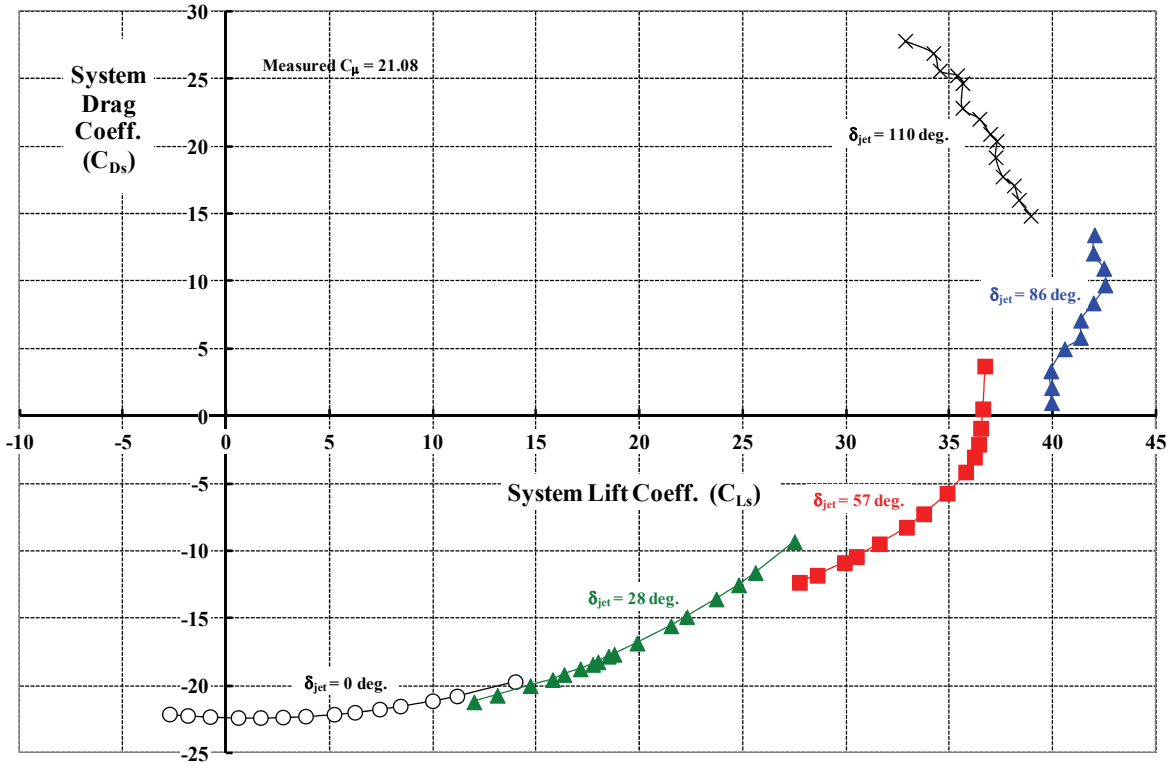

Fig. 3-41. System drag polar as affected by jet thrust angle. Jet thrust coefficient is nominally 21, which is the measured coefficient.

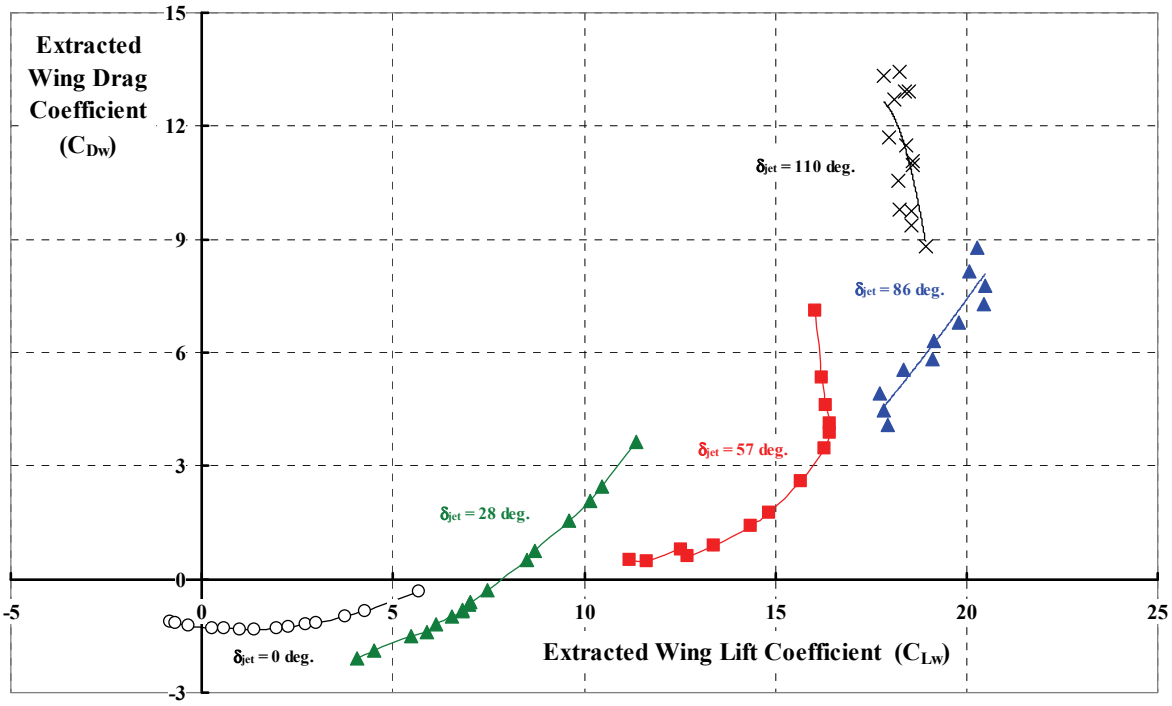

Fig. 3-42. Wing drag polar as affected by jet thrust angle. Jet thrust coefficient is nominally 21, which is the measured coefficient.

A theory to estimate the drag polar for a wing combined with a jet flap is available [27, 434, 440]. For this introductory conversation, you will find that Barney McCormick's discussion [27] is more than adequate. Barney (as well as several other researchers in that era) offers equation 7-31 on page 206 of *Aerodynamics of V/STOL Flight*, which, in my notation, becomes

$$(3.76)\quad \frac{\text{System Induced Drag}}{q_{FP}S_w} = C_{Di} = \frac{1}{\pi}\frac{C_{Ls}^2}{\left(AR_w + 2C_\mu/\pi\right)}.$$

This simple relation does not account for the trailed, flat wake rolling up.

Because the test data provided by Lockwood, Turner, and Riebe in NACA TN 3865 extends well beyond the region where a flat wake assumption is valid, I have approached the calculation with Helmbold's deformed wake theory. This means that the parameters of interest must be recast using a system aspect ratio defined as $AR_s = AR_w + 2C_\mu/\pi$. Then the system induced drag divided by system aspect ratio becomes a function of the system lift coefficient divided by system aspect ratio. That is

$$(3.77)\quad \frac{C_{Di}}{AR_w + 2C_\mu/\pi} = f\left(\frac{C_{Ls}}{AR_w + 2C_\mu/\pi}\right).$$

It is a simple process to use Helmbold's equations [i.e., Eq. (3.4) through Eq. (3.6)] that you encountered earlier. The calculations become

$$(3.78)\quad \frac{C_{Di}}{AR_w + 2C_\mu/\pi} = \frac{1}{\pi}\left(\frac{C_{Ls}}{AR_w + 2C_\mu/\pi}\right)^2 \left\{\frac{\sqrt{1-\sin^2\delta_{jet}}}{\left(1-\frac{\pi^2}{4}\sin^2\delta_{jet}\right)^2}\right\},$$

$$(3.79)\quad \frac{C_{Ls}}{AR_w + 2C_\mu/\pi} = \frac{\pi^3}{4}\sin\delta_{jet}\left(1-\frac{\pi^2}{4}\sin^2\delta_{jet}\right), \text{ and}$$

$$(3.80)\quad \sin\delta_{jet} = \frac{4\sqrt{3}}{3\pi}\cos\left[\frac{5\pi}{3} - \frac{1}{3}\arccos\left(\frac{3\sqrt{3}}{\pi^2}\frac{C_{Ls}}{AR_w + 2C_\mu/\pi}\right)\right].$$

$$\text{for } 0 \le \frac{C_L}{AR_w + 2C_\mu/\pi} \le \frac{\pi^2\sqrt{3}}{9} \text{ and } \delta_{jet} \le 25.1 \text{ deg}.$$

Keep in mind that the system induced drag is, in fact, an ideal drag. Furthermore, to obtain the total system drag, the component of jet thrust in the drag direction must be included. Thus,

$$(3.81)\quad \text{Ideal } C_{Ds} = C_{Di} - C_\mu\cos\left(\alpha + \delta_{jet}\right).$$

No profile drag has been included and, therefore, I believe Eq. (3.81) represents the ideal drag polar for a wing with a jet flap, and experimental data, if reasonably accurate, should not be better than the preceding theory offers. Of course, the roll-up of the trailing vortex wake is not included, which means a computational fluid dynamic (CFD) calculation needs to be

made. I am not aware of any calculations along the CFD line having been made or published. However, a more extensive literature search will quite likely find papers of interest.

Using this vintage 1950's technology, you obtain the comparison provided in Fig. 3-43. This result uses the measured system lift coefficient (C_{Ls}), wing angle of attack (α), and jet thrust angle (δ_{jet}). The abscissa is the measured system lift coefficient. This technology does capture the data trend of NACA TN 3865 as you can see with the comparisons in Fig. 3-43. That is to say, the drag polars have the characteristic parabola shape, but I would say that this technology is not good enough even for conceptual design today. The experimental data appears to exceed ideal, and the disparity becomes more evident as the jet thrust angle and coefficient increase. For example, even at zero system lift and zero jet-thrust angle, the measured system drag (shown with open symbols) is always more negative than the ideal theory (the red lines). Remember that negative drag is a positive propulsive force, so this experimental data says that an airplane equipped with this NACA type of jet flap could appear particularly attractive from an aerodynamic point of view.[104]

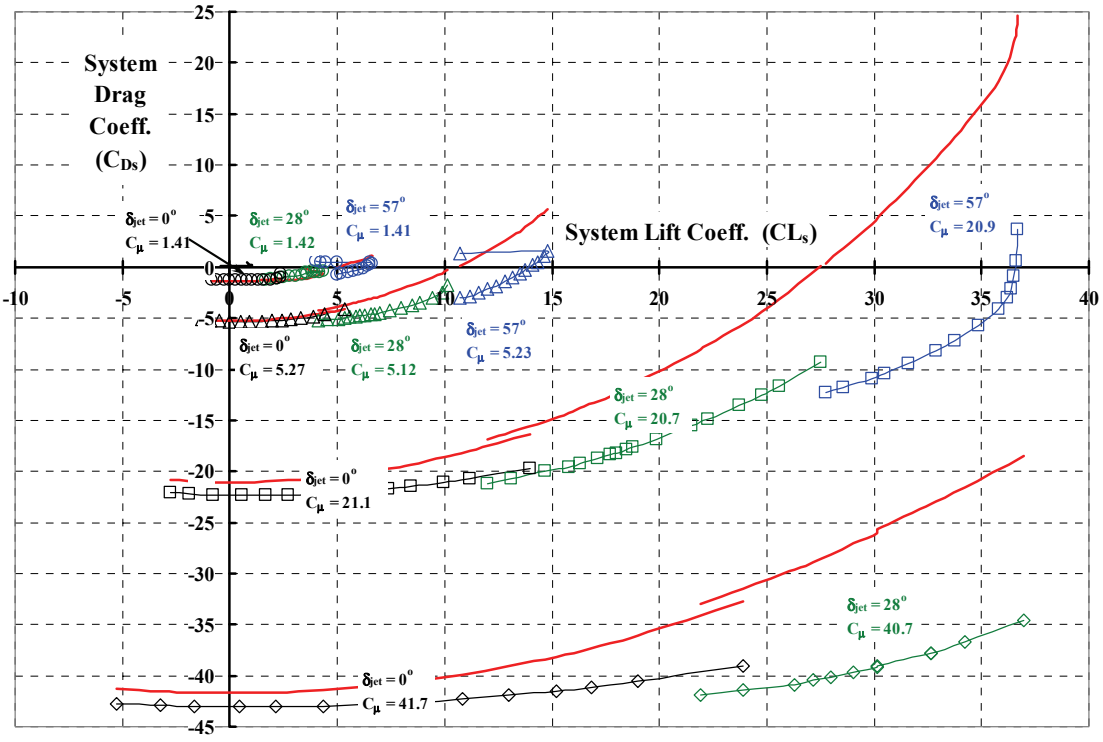

Fig. 3-43. Comparison of vintage 1956 jet-flap drag polar theory to experimental data. The theory and experimental data appear to become more at odds with each other as the jet thrust angle and coefficient increase.

[104] There was a follow-on test to the test reported in NACA TN 3865 that may interest you [432]. The model had its span reduced from 30 inches to 20 inches and then to 10 inches. This varied the aspect ratio from 8.4 to 5.6 to 2.8. The jet thrust angle was set at 85 degrees. The objective of this follow-on test was to establish the effect of aspect ratio combined with jet thrust on maximum system lift. As usual, the experiment just opened the door to many new questions. One thing was clear—calculated jet thrust was only a crutch.

3.3.7 George Schairer's 1961 Powered Lift Theory

The availability of experimental data gives me an opportunity to show you another way to compare powered lift aircraft lift-drag polar data to theory.[105] For lack of a better name, I will call the theory the Schairer powered lift theory. George Schairer's theory in graphical form is simplicity at its best, and the philosophy behind the graph is even more fundamental.

The fundamental is this: you can add any kind of powered lift thrusting device to a wing. However, the wing itself cannot have a better lift-drag polar than that ideal obtained by Helmbold's theory, which I showed you in Fig. 3-2. The thrusting device (say propellers operating at a given thrust coefficient, C_T or T_C, or as with jet flaps and BLC, nozzle thrust coefficient, C_J or C_μ, etc.) moves you from the drag quadrant of the lift-drag polar to the propulsion quadrant, as you saw in Fig. 3-32, Fig. 3-36, and Fig. 3-41. However, the *maximum* movement from the ideal Helmbold-induced-drag side to the propulsion quadrant cannot be more than the sum of thrusting force and the induced drag. The summation is done by adding a thrust vector to the Helmbold lift-drag polar to produce a new system lift coefficient (C_{Ls}) versus system propulsive force coefficient (C_{Xs}) curve that lies in the propulsion quadrant. This new curve is the limit of lift-propulsive-force performance for that particular powered lift configuration.

Let me show you an example of how to apply Mr. Schairer's theory in graphical form. Then I will point out how quickly you can get an opinion about lift-drag performance—for any powered lift V/STOL configuration—that experimental data or conceptual analysis is showing you.

The constructed Schairer graph is shown in Fig. 3-44. The coordinate system reflects the wing aspect ratio because

$$(3.82)\quad \frac{C_{Ls}}{AR} = \frac{L_S}{q_{FP} b_W^2} \quad \text{and} \quad \frac{C_{Xs}}{AR} = \frac{X_S}{q_{FP} b_W^2} = -\frac{D_S}{q_{FP} b_W^2}.$$

Now suppose you have experimental force data for the thrust coefficient of $T_C = T/q_{FP}S_W = 24$. Suppose the wing aspect ratio (AR) is 5.54. Therefore the thrust vector has a magnitude of $T_C/AR = 24/5.54 = 4.33$. The base for the Schairer graph is Helmbold's wing theory. The equations you use to calculate Helmbold's curved line are Eqs. (3.4), (3.5), and (3.6), which you will find on page 333. The blue circle point that you see on Helmbold's wing theory line on Fig. 3-44 was calculated with a wing wake angle (δ) of 13.18 degrees, which returned a C_{Xs} of 0.968 at a C_{Ls} of 1.54. Next you create a line that is tangent to Helmbold's theory line. This tangent line is shown as a red line on the figure and makes an angle (β) with the C_{Xs}/AR axis. This angle is calculated with

[105] The approach was shown to me by George Schairer when he was preparing his 1961 paper, *Looking Ahead in V/STOL* [16]. I was, at best, a junior engineer at that time. See footnote 10 on page 21.

$$(3.83)\quad \beta = \text{arc tangent}\left[\frac{1}{\pi^2}\left(\frac{\cos\delta}{\sin\delta}\right)\left(\frac{4-3\pi^2+3\pi^2\cos^2\delta}{3\cos^2\delta-1}\right)\right].$$

The thrust vector of magnitude, $T_C/AR = 4.33$, is perpendicular to the tangent line, and this defines the ideal maximum value of C_{Ls}/AR and C_{Xs}/AR. Thus, the tail of the thrust vector is anchored to a C_{Xs} of 0.968 at a C_{Ls} of 1.54, the lower blue circle point. Now, to anchor the arrowhead point (the upper blue circle), you note that the thrust vector makes the same angle (β) to the C_{Ls}/AR axis. The coordinates of the thrust vector arrowhead are, therefore, at

$$(3.84)\quad \begin{aligned}\frac{C_{Ls}}{AR} &= \frac{T_C}{AR}\sin\beta + \left(\frac{L_S}{q_{FP}b_W^2}\right)_{\text{Helmbold}}\\ \frac{C_{Xs}}{AR} &= \frac{T_C}{AR}\cos\beta - \left(\frac{D_S}{q_{FP}b_W^2}\right)_{\text{Helmbold}}\end{aligned}.$$

Do not forget that Helmbold's lift and drag polar equations on page 333 give you positive values, but Mr. Schairer's graph treats drag as being a negative contribution to C_{Xs}.

It is nearly a trivial matter to "program" a spreadsheet in Microsoft® Excel® to create Mr. Schairer's graph by just picking several wake angles (δ). In 1961, we did it with a compass and a piece of graph paper as Mr. Schairer shows in his paper [16].

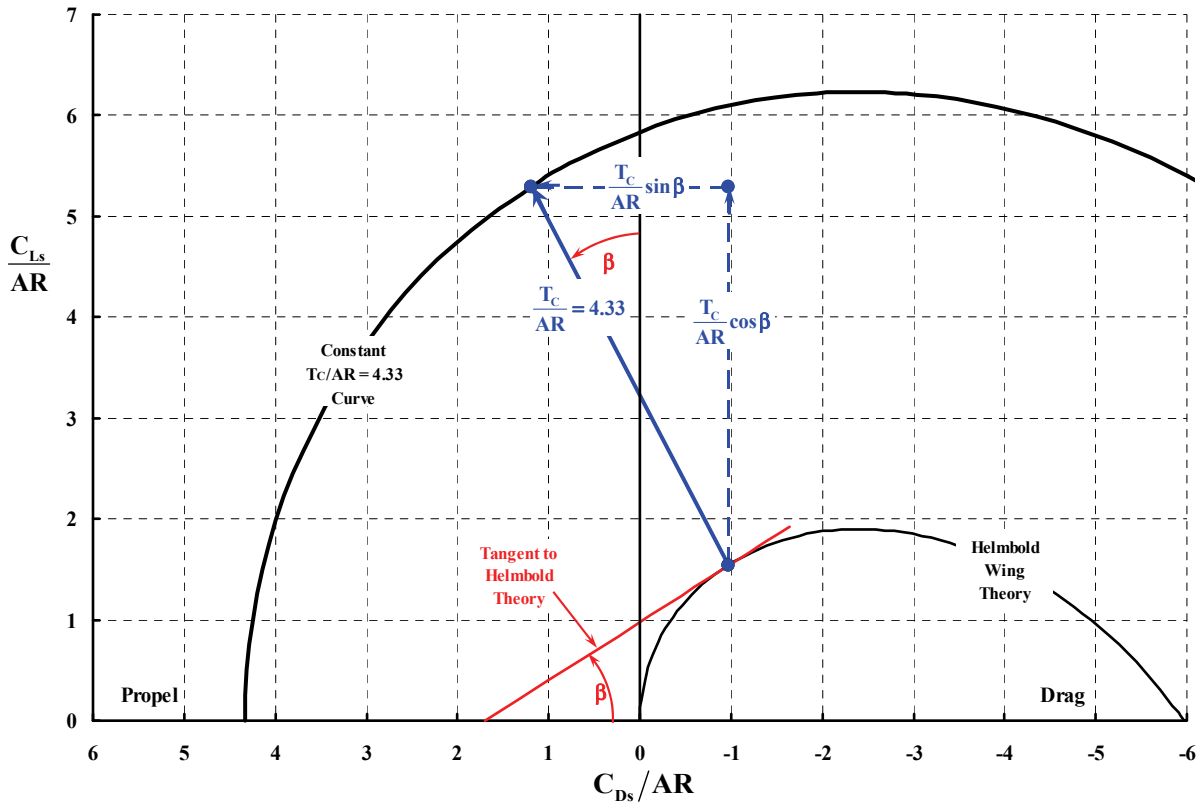

Fig. 3-44. Schairer's graph for powered lift aircraft and systems.

The preceding jet flap experimental data from Schubauer [430] and Lockwood, Turner, and Riebe's data [433] can be compared to the Schairer theory, which will let you appreciate, as I do, the contribution this man made to V/STOL aircraft development. In fact, you might not realize it, but Fig. 3-32 was an introductory comparison. Therefore, let me concentrate on Lockwood's data as reported in NACA TN 3865, which you examined with one popular theory on Fig. 3-43.

You see the comparison of data from NACA TN 3865 reformatted from Fig. 3-43 to Schairer's graph in Fig. 3-45. I have shown Schairer's theory at two values of the jet thrust coefficient (C_μ) because the authors of NACA TN 3865 chose to use calculated values of the jet thrust coefficient. I believe the measured value (i.e., 0.75 times the calculated value) cannot be ignored in any theory-versus-test comparison.

Because a comparison at just one jet thrust coefficient as shown in Fig. 3-45 can only be treated as encouraging, I have included an additional example from Lockwood's NACA TN at a lower C_μ on Fig. 3-46.

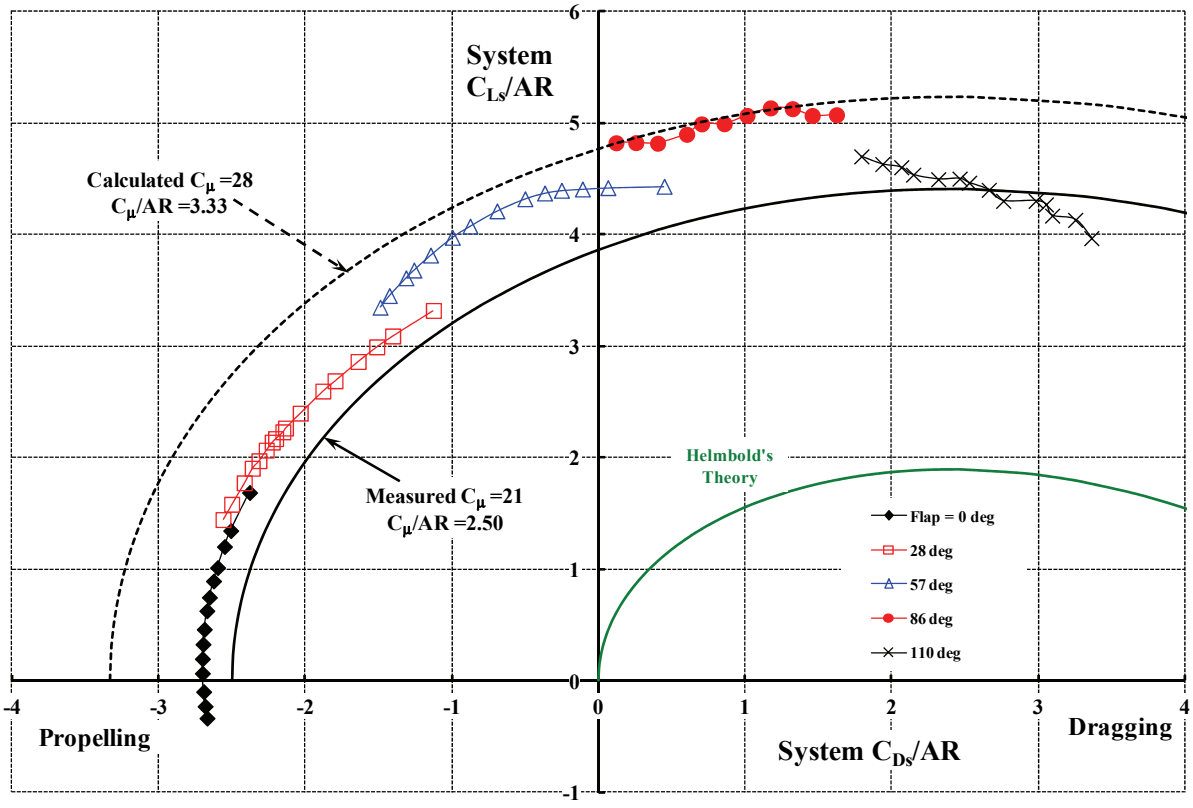

Fig. 3-45. NACA TN 3865 data compared to George Schairer's theory at measured and calculated jet thrust coefficient bracketing values. The wing aspect ratio is nominally 8.40.

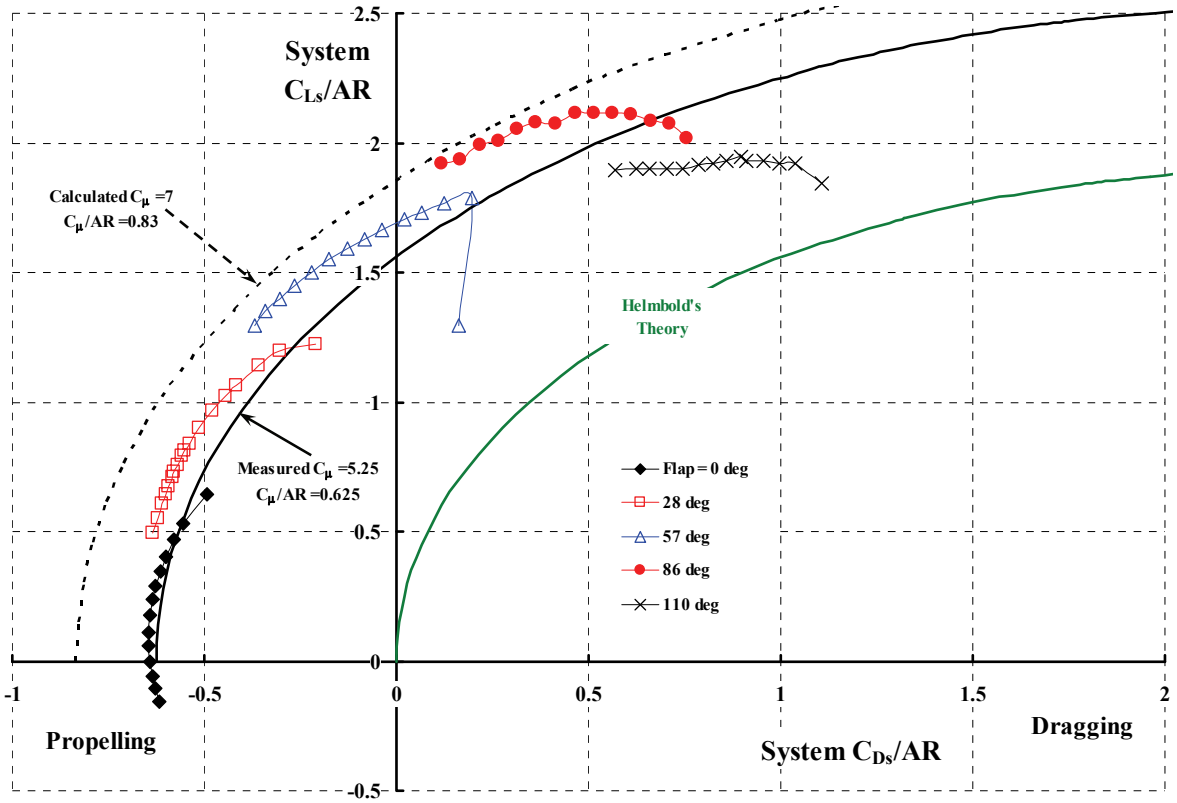

Fig. 3-46. NACA TN 3865 data compared to George Schairer's theory at lower measured and calculated jet thrust coefficients. The wing aspect ratio is nominally 8.40.

You will find many more examples of experimental data compared to Mr. Schairer's theory in his September 1961 paper, *Looking Ahead in V/STOL* [16]. In the 1961 study, Mr. Schairer forecast the future of each major class of aircraft. With respect to STOL, he had this to say:

> "In the area of short takeoff and landing, it is evident that much attention will be given to vectoring the lifting thrust in the directions which will give shortest possible takeoff and landings. It is probable that most current arrangements are inadequate in this matter, but it is likely that the deficiencies can be readily corrected.
>
> Of special interest in the short takeoff and landing discussion is the question of blown flaps. It is entirely possible that flaps with extensive blowing will be very attractive for the STOL mode of operation. Further testing of blown flap arrangements is urgently needed to clarify their characteristics.
>
> When aircraft with a vertical landing capability are to be flown long ranges, such as across oceans, it is difficult to understand why the takeoff should not be made in the short takeoff mode. It would appear that much attention should be given to aircraft in which short takeoffs are used for flight ranges beyond about 1000 miles but which provide for vertical takeoff with full payload and vertical landing with full payload for short range operation. The compromises possible in such aircraft are likely to result in the maximum utility for many types of missions."

Mr. Schairer had some other considerations that he included in his paper. He wrote:

> "The development of wind tunnel testing procedures for V/STOL aircraft is in its infancy. Much attention to such techniques is urgently needed. V/STOL configurations have not been adequately tested in wind tunnels and much basic test data on various fundamental configurations is urgently needed in order to sort out those arrangements which are likely to work from those with low chance of success. Such cut and try work can probably be done very well in a wind tunnel rather than in more expensive flight testing.
>
> Stalling is a major consideration in the design of V/STOL aircraft and is likely to be the central theme of the aerodynamic design. Ground effects and their influence on stalling are likely to be exceedingly important."

Mr. Schairer's summary was quite succinct:

> "In final summary, the author finds that the technology of vertical lift aircraft is reasonably well developed in the case of the helicopter but hardly explored for other arrangements. Much progress is possible in the helicopter and very great improvements can be expected in other vertical takeoff schemes. The application of the design methods used for large fixed wing aircraft are likely to result in a marked rate of improvement in V/STOL aircraft."

As it turned out, Mr. Schairer's prognosis was quite correct. By the end of the decade, the research on V/STOL had, in fact, settled on extracting performance from blown flap concepts. In the United States, industry plus NASA and the U.S. military had reduced the whole V/STOL waterfront to the four configurations you see in Fig. 3-47. The weeding-out process *did* involve substantial wind tunnel testing as Mr. Schairer recommended and just a small sample of the literature will tell you. By the early 1970s, the four promising configurations shown in Fig. 3-47 had been reduced to just three: (1) trailing-edge flap blowing, (2) external nozzle under wing, and (3) external nozzle above wing. Propeller-driven configurations were no longer even included in the discussion. It was simply a case of wanting our cake (i.e., jet transport cruise performance) and eating it too (i.e., STOL performance).

Powered lift theory was carried as far as researchers of that era could go, and considerable empirical constants were derived from experimental data both in wind tunnels and with small research aircraft. One thing that has really interested me is that Helmbold's theory (which Mr. Schairer and others used as a jumping-off point) was never adequately proven—at least by my standards. This is an ideal problem for CFD experts to tackle.

Nevertheless, variations on the jet flap concept began to emerge as the most promising path to STOL aircraft powered with gas turbine engines. In 1961, Williams, Butler, and Wood, three British researchers, had their paper published [440]. They wrote in their introduction:

> "From one aspect, the Jet flap scheme is a natural extension of slot blowing over trailing-edge flaps for B.L.C., using much higher quantities with a view to increasing the effective chord of the flap to produce so-called 'super-circulation' about the wing. Examples of this were available more than 20 years ago, from the experiments of Lyon in Britain, Bamber in the U.S.A., Hagedorn in Germany, and Valensi in France. However, the concept

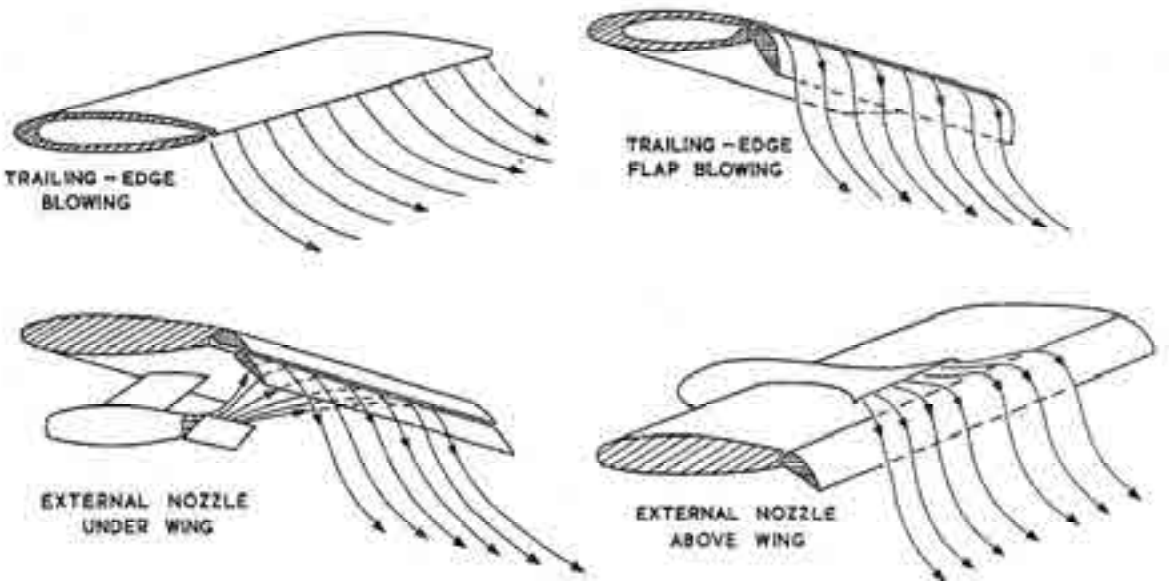

Fig. 3-47. In the early 1960s, STOL advocates had a reasonable appreciation of jet thrust, and they began to see how jet engine exhaust could, more practically, be used to provide high lift at low speed—without giving up efficient high-cruise speed. This was the vision that Schubauer had in 1932 [430].

> proper originated much more recently, from a search for methods of using the efflux of turbo-jet engines not merely to provide propulsion and direct jet lift by tilting, but also to generate significant favourable lift on the wing with the minimum reduction of propulsive thrust. *Ideally, the lifting and propulsive systems of turbo-jet aircraft might then be completely integrated with advantage (Fig. 1)* [my italics and see Fig. 3-47]."

3.3.7.1 The Working Engineer's View

Now let me jump ahead a decade or so to 1974 and a paper published by Ya-Tung Chin, Tom Aiken, and Garland Oates [441], which gives an excellent picture of the practical side of powered lift experimental data. The introduction of their paper summed up the early 1970's situation rather well I think. They wrote:

> "A new generation of subsonic turbofan transport aircraft with takeoff and landing field lengths from 1500–2000 ft may eventually be required by the military and by the commercial airlines. For aircraft to attain such basic short takeoff and landing (STOL) performance, they must operate at takeoff and landing speeds substantially slower than those of today's jet transports. To reduce takeoff and landing speeds, the most effective method is to increase the maximum lift coefficient of the wing. The widely accepted approach is to *integrate the propulsion and the high-lift systems* [my italics] so that propulsive thrust is used to augment aerodynamic lift during low-speed operation."

The authors go on to provide a careful discussion of the Lockheed-Georgia idea for an improved version of the trailing-edge flap blowing approach, which was called an AIBF (Advanced Internal Blown Flap). More details of the Lockheed configuration are shown in Fig. 3-48. The need for large-scale model testing was apparent to Lockheed, the U.S. Air

Force, and NASA Ames Research Center. And so, in a joint program, a model was built (Fig. 3-49) and tested [442]. The test results, put in a form quite useful to the practicing aeronautical engineer, were include in Chin, Aiken, and Oates' paper [441]. These test results, reproduced here as Fig. 3-50, show that aerodynamic data must establish performance in both takeoff and landing configurations. There is, of course, a major difference as to where on the general lift-drag graph (or lift-propulsive-force graph, if you prefer) the two operational flight regimes fall. It would, however, take a book to tell you how to translate the wind tunnel data into an aircraft with both optimized takeoff *and* landing performance. Being more of a rotorcraft advocate, I am hardly qualified to write such a design manual. However, the key principle appears to be twofold. First, you want the *best* ratio of powered lift to propulsive force for takeoff (i.e., a very high propulsive-thrust-to-weight ratio) and second, you want the *worst* ratio of powered lift to system drag (i.e., low L/D but high L and lots of drag) for landing.

Chin, Aiken, and Oates describe the performance of an AIBF-STOL design having a wingspan of 123.5 feet, a wing area of 2,180 square feet, a payload of 28,000 pounds, and fuel for a 500-nautical-mile-radius mission. This design was to take off and land (over a 50-foot obstacle) at 160,000 pounds from a 1,900-foot field.

It is of particular interest for this introductory discussion to see how the aerodynamic data from Fig. 3-50 compares to George Schairer's ideal performance theory. You see the results of my analysis in Fig. 3-51. Here I have indicated that the data is for the complete aircraft with the jet flap operating by a lift coefficient (C_{Ls}/AR) and a drag coefficient (C_{Ds}/AR). Furthermore, notice that I have retained the sign convention that drag is positive. On this figure I have first separated the comparison into landing data identified by the circle symbol. This landing data has a flap deflection angle (δ_F) of 60 degrees. The takeoff data is denoted by a square symbol, and the flap deflection angle is 30 degrees. To avoid a cluttered graph, the comparison is made at only three jet thrust coefficient (C_J) values of 0.0, 0.52, and 1.59.

Lockheed-Georgia aerodynamic engineers recommended a flap deflection angle of 60 degrees for landing, and this configuration had relatively high drag as the circle symbols show. This permitted quite steep descent angles as you can see on both Fig. 3-50 and Fig. 3-51. For takeoff, the Lockheed aerodynamic engineers recommended a flap deflection angle of only 30 degrees. You should note from Fig. 3-51 that the takeoff curves at all three jet thrust values are closer to Schairer's ideal than the landing curves. Both sets of curves reflect the drag at zero lift.

One additional comparison that may interest you is provided in Fig. 3-52. Here I have shown the performance of the components (wing, fuselage, etc.) as a wing lift coefficient (C_{Lw}/AR) versus a drag coefficient (C_{Dw}/AR). This data was obtained following Eq. (3.70), which means that

$$(3.85)\quad \frac{C_{Lw}}{AR} = \frac{C_{Ls}}{AR} - \frac{C_J}{AR}\sin\left(\alpha + \delta_F\right) \qquad \frac{C_{Dw}}{AR} = \frac{C_{Ds}}{AR} + \frac{C_J}{AR}\cos\left(\alpha + \delta_F\right).$$

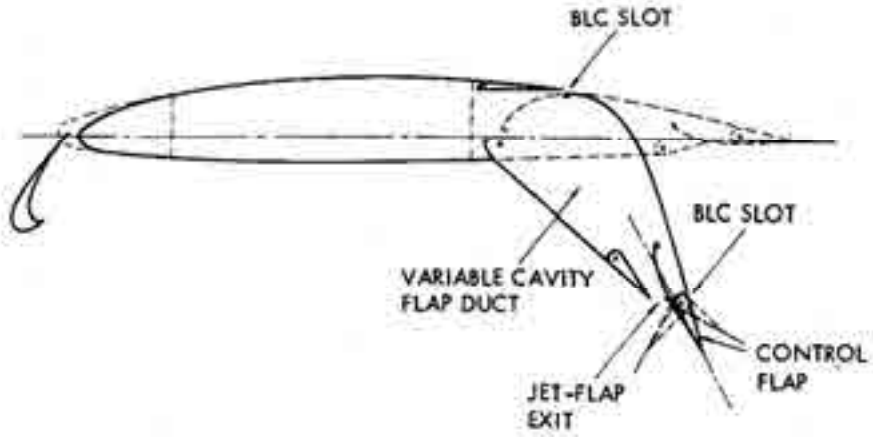

Fig. 3-48. The Lockheed-Georgia AIBF circa 1973 [441].

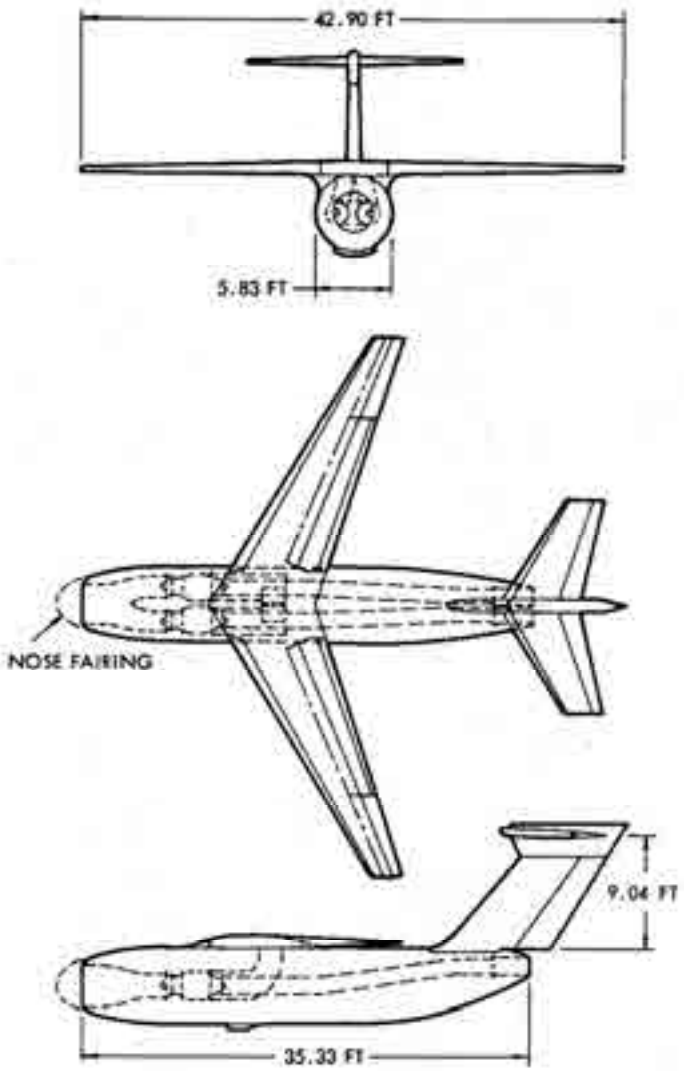

Fig. 3-49. NASA Ames built a large-scale powered lift model for testing in their 40- by 80-foot wind tunnel [442].

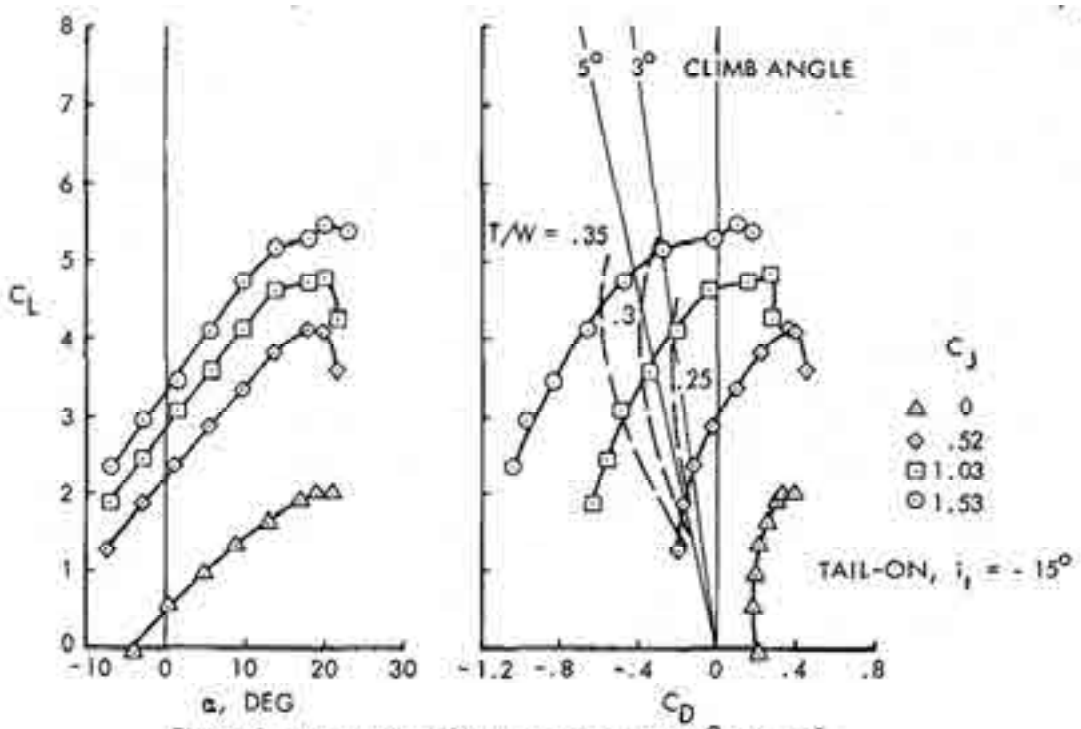

Figure 5. Longitudinal Characteristics, $\delta_f = 30°$, $\delta_c = 0°$

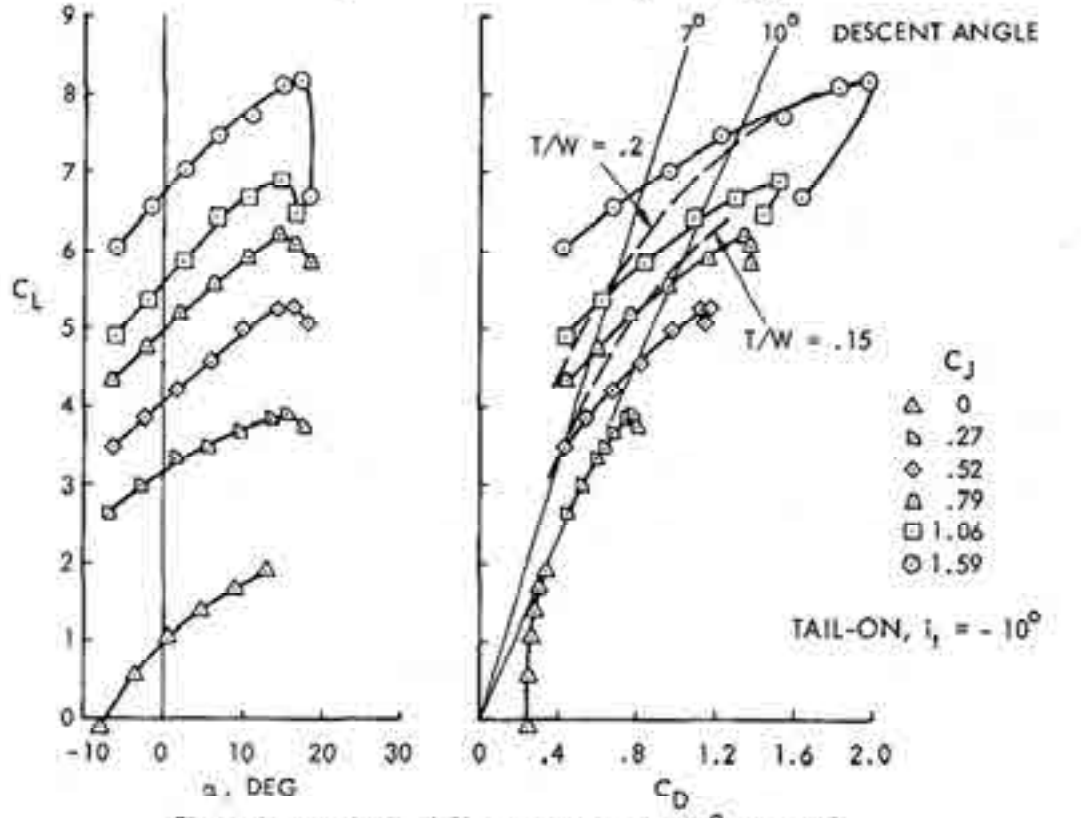

Figure 6. Longitudinal Characteristics, $\delta_f = 60°$, $\delta_c = 20°$

Fig. 3-50. Aerodynamic data required for STOL performance analysis.

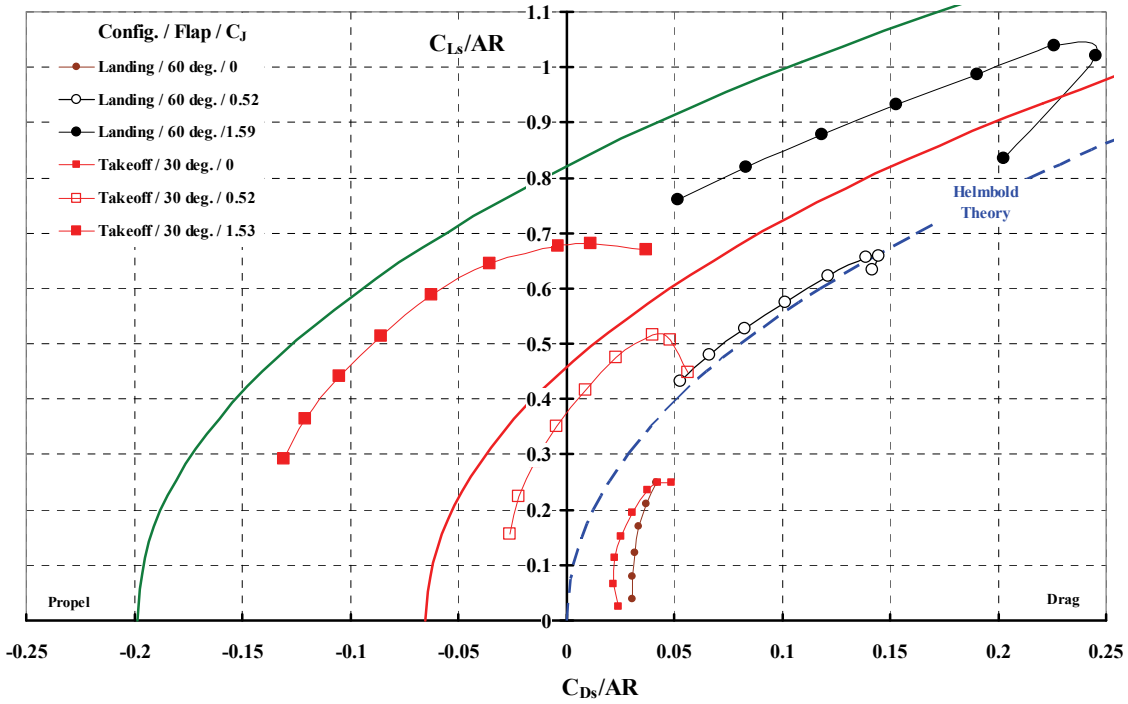

Fig. 3-51. Schairer's ideal theory versus Lockheed-Georgia performance data obtained from a NASA Ames powered lift model.

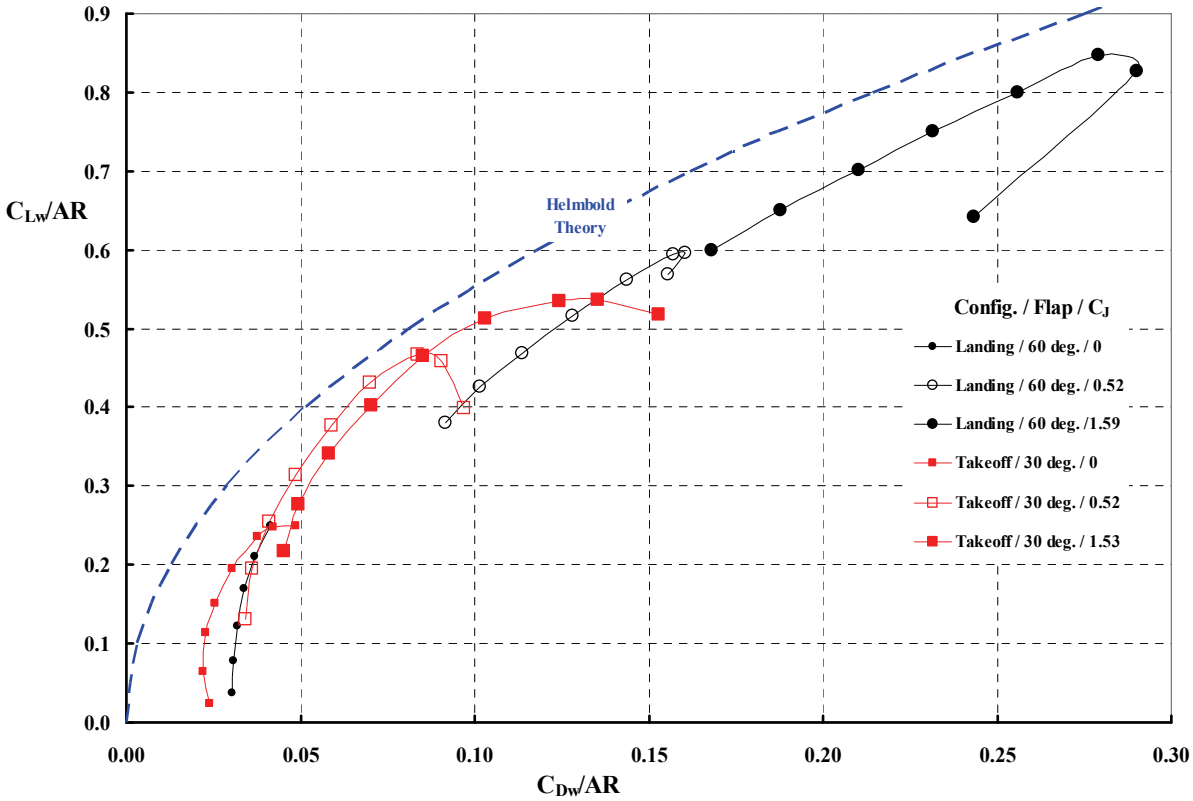

Fig. 3-52. Derived wing performance versus Helmbold's theory.

As I come to a close discussing how a working engineer came to see STOL performance data, I would be quite remiss if I did not point out the nearly overwhelming number of reports that came out of the N.A.C.A. and NASA from the early 1950s, 1960s, and throughout most of the 1970s. It was very little trouble[106] to compile a short reference list [432, 433, 442-459] of some 20 reports that could be of immense value to you. The experimental results from these documents will, just by their titles, convince you that the start-up work by the British in the 1950s was continued in the United States at a feverish pace for the next 25 years. Experimentation began in small scale at the Langley Research Center, and then, as jet flap performance in all its many forms became clear, large-scale tests in the Ames Research Center 40- by 80-foot wind tunnel became increasingly numerous. I find it very interesting that many people point to the N.A.C.A. work on airfoils and engine cowls as a major contribution (which it was), but I also think the N.A.C.A and NASA work on STOL aircraft development and, in particular, the test results provided by NASA Ames Research Center with its large-scale wind tunnel, also deserve recognition as major contributions. This was a major research effort that many men contributed to over a 25-year period. The path led to today's McDonnell Douglas (now Boeing) C-17, which made its first flight on September 15, 1991, that I will discuss later.

As the 1970s began, all the wind tunnel testing let the fixed-wing STOL proponents focus on fewer and fewer variations of the jet flap concept. Lockheed-Georgia, Boeing, McDonnell Douglas, de Havilland Canada, the United States Air Force, NASA, and companies in France and Russia—in short, a wide-ranging group—were all taking a hard look at external nozzles (i.e., jet engine exhaust) blowing very hot air *over* the wing and *under* the wing, configurations you see in Fig. 3-47. The STOL waterfront was indeed narrowing.

You might be interested in three technology demonstrators developed between the early 1960s and the early 1970s. The first was the Hunting H.126 developed in Britain, which first flew in March of 1963. The second was developed in the United States in 1973 by the Ball-Bartoe Aircraft Corporation, located in Boulder, Colorado, which was formed to specifically build the Jetwing. The Jetwing's first flight was on July 11, 1977, but you should know that Bartoe, the designer of the Jetwing, tested his aircraft in the NASA Ames Research Center large wind tunnel in December 1976. The third was explored by de Havilland Canada with NASA Ames support, and it had its first flight on May 1, 1972. The next several pages discuss these three aircraft that demonstrated "external nozzle above wing" technology. You might recall that these early efforts were followed in the 1970s by the U.S. Air Force competition for an Advanced Medium STOL Transport (AMST). And you might recognize that (1) the external nozzle *under* wing was the configuration McDonnell chose for its YC-15 STOL in the competition (the YC-15 first flew on August 26, 1975), and (2) the external nozzle *above* wing was the configuration Boeing selected for its YC-14 STOL entry, which first flew on August 9, 1976.

---

[106] Actually, all I did was send a list of the reports that I thought you would need to Bill Warmbrodt, Wayne Johnson, and Kathy Ponce at NASA Ames and, in a blink of an eye, I had PDF documents. Access to most of these N.A.C.A./NASA documents required some level of official need because they are—if you can believe it after 60 years—somewhat restricted. Furthermore, the original data was published unrestricted!

3.3.7.2 The Hunting H.126

Schubauer's idea became very attractive when the gas turbine engine reached the commercial market place. As the idea presented in Fig. 3-27 and the words "*integrating of the wing and engine"* were sinking in, designers began to think about using the exhaust from the jet engine (i.e., the jet engine's thrust) in a way that increased lift at low speed. Just stop and think about this design challenge for a moment. The turbojet engine has two places where you can get high-pressure air to blow over a deflected flap. In Volume II (pages 63 to 67, specifically) you learned a great deal about gas turbine engines and their compressor stage. Therefore, the first place to look for some compressed air is just after the air leaves the compressor. This was the place that aerodynamicists said was ideal because then they could have a *small amount of relatively cool air* for boundary layer control (BLC) and thus get more lift from flaps. I am afraid that many of these aerodynamicists did not think much about the reduction in overall gas turbine engine performance when you bleed off (i.e., steal) some air after the compressor stage and before it goes on to the power stages of the engine. Their emphasis was getting BLC flow coefficients (C_μ) on the order of 0.1 or less, so bigger flaps could be deflected to larger angles without separated flow.

The second source of air from a turbojet engine is the engine's exhaust, which is where the thousands of pounds of thrust come from. Now you are talking about jet thrust flow coefficients (C_μ or C_J, if you prefer) of 1 to 100 because

$$C_\mu = \frac{\text{Jet engine thrust in pounds}}{q_{FP} S_W} . \tag{3.86}$$

To illustrate, suppose the takeoff jet thrust from all engines is about one-half of the takeoff weight of the STOL aircraft. Because jet transports are designed for high-speed cruise at high altitudes [460, 461], imagine that the ratio of design weight to wing area (W/S_W) is 75 pounds per square foot. Then you can calculate that the jet thrust flow coefficient at takeoff would be $C_\mu = 38/q_{FP}$. Now set the requirement that fully controlled level flight shall be maintained at, say, 54.3 knots at sea level on a standard day (density equals 0.002378 slugs per cubic foot). Then dynamic pressure (q_{FP}) at this flightpath velocity would be $54.3^2/295$ or 10 pounds per square foot. On this basis, the jet thrust coefficient would be a C_μ of about 3.8. Now, if the jet engine thrust could be deflected downward by 90 degrees, you could say the aircraft lift coefficient (C_L) equals, at a minimum, the flow coefficient and, therefore, C_L equals 3.8. Of course, if the installed jet engine thrust of all engines equaled the takeoff gross weight of the STOL aircraft, you would have an aircraft operating at a lift coefficient of 7.6 at 54.3 knots.

Looking back on history, I would say there was some considerable poetic license taken with the words "jet flap." From my knowledge, the only aircraft that was built somewhat along the lines of Fig. 3-27 was the Hunting H.126, which you see here as Fig. 3-53. This British STOL research demonstrator first flew in March of 1963, and after nearly 150 hours of test flying, the aircraft was loaned to NASA Ames Research Center for testing in their 40- by 80-foot wind tunnel, Fig. 3-54. This testing was done during June and July of 1969, and test results are documented in reference [462]. Subsequently, a 1/7-scale powered force model was tested in the NASA/Army 7- by 10-foot wind tunnel, and those results were also published [463].

Fig. 3-53. The Hunting H.126 was a small, one-man British research demonstrator.

Fig. 3-54. The Hunting H.126 was tested in the NASA Ames 40- by 80-foot wind tunnel during June and July of 1969. The H.126 had a wingspan of 45.33 feet, a wing area of 221 square feet, and a wing aspect ratio of 9.3 (photo courtesy of Bill Warmbrodt, Ames Research Center).

According to the Aircraft Specification ER. 189D [464], the Hunting H.126 was powered with one Bristol Siddeley Orpheus BOr.3 Mk.805 turbojet that had a takeoff rating of 4,000 pounds. The specification's Amendment List 22, dated September 1964, states the basic weight empty as 8,077.8 pounds. With a pilot (180 lb), full fuel (2,324.8 lb), test equipment (302.0 lb), and miscellaneous items (51.7 lb), the takeoff gross weight was 10,640 pounds. Thus, the thrust-to-weight ratio was about 0.4. By the way, the landing gear did not retract because it was only the low-speed region that was under investigation.

The British Hunting H.126 is particularly noteworthy in my mind because it was the first aircraft to demonstrate a step toward Schubauer's "*integration of the wing and engine.*" The story of this aircraft is wonderfully summed up by Mr. K. D. Harris (no relation) who wrote [465] in his opening paragraphs:

> "The jet-flap principle, and the possibilities of applying this principle to a jet-propelled aeroplane, were first conceived at the National Gas Turbine Establishment, UK, in 1952. The concept was made public in 1955 in a lecture to the Royal Aeronautical Society by I. M. Davidson, the leading protagonist of the scheme. The pioneer investigations at NGTE and NPL during this early period were followed over the next decade by extensive experimental and theoretical studies, in Britain particularly at the RAE and Huntings.

The exceptionally high lift-coefficients that the jet-flap offered, together with the remarkable promise of substantial thrust recovery, led to the early decision in 1956 by the British Ministry of Aviation to order a piloted research aircraft. The H.126 jet-flap research aircraft was then designed and built by Huntings (Luton, UK) under contract for a flight research programme at the Royal Aircraft Establishment. This work was intended not only to ensure essential flight research to complement wind-tunnel and theoretical studies, but also to provide flight-handling experience of value more generally for STOL aircraft with high-lift wings.

The desirability of a piloted vehicle was obvious, if only because of the very large C_L range that would be made possible. However, it was also envisaged that novel means of aircraft control entailing deflection of the jet-flap and variation of the jet-flap thrust might be investigated, and these considerations made a piloted vehicle essential.

In the 1950s by-pass engines had not been developed, and it was quickly realized that a major problem would be met in ducting the very hot and relatively low-pressure gas from the engine(s) to the trailing-edge of the wing.

In view of the extreme cost of developing a new type of engine, it was decided that the research aircraft would have to be powered by an existing unit of proven reliability. This meant that the aircraft would inevitably have a very poor overall performance when judged against contemporary aircraft. This fact must always be kept in mind, and no deductions regarding the potential performance of the jet-flap should be drawn from the H.126 without making full allowance for this very severe handicap imposed on the research aircraft."

K. D. Harris' paper includes considerable detail, and even more configuration specifics are contained in Tom Aiken and Tony Cook's report of NASA testing at full scale [462]. As you can see from Fig. 3-55, the Orpheus gas turbine exhaust was ducted not only to the 18 wing

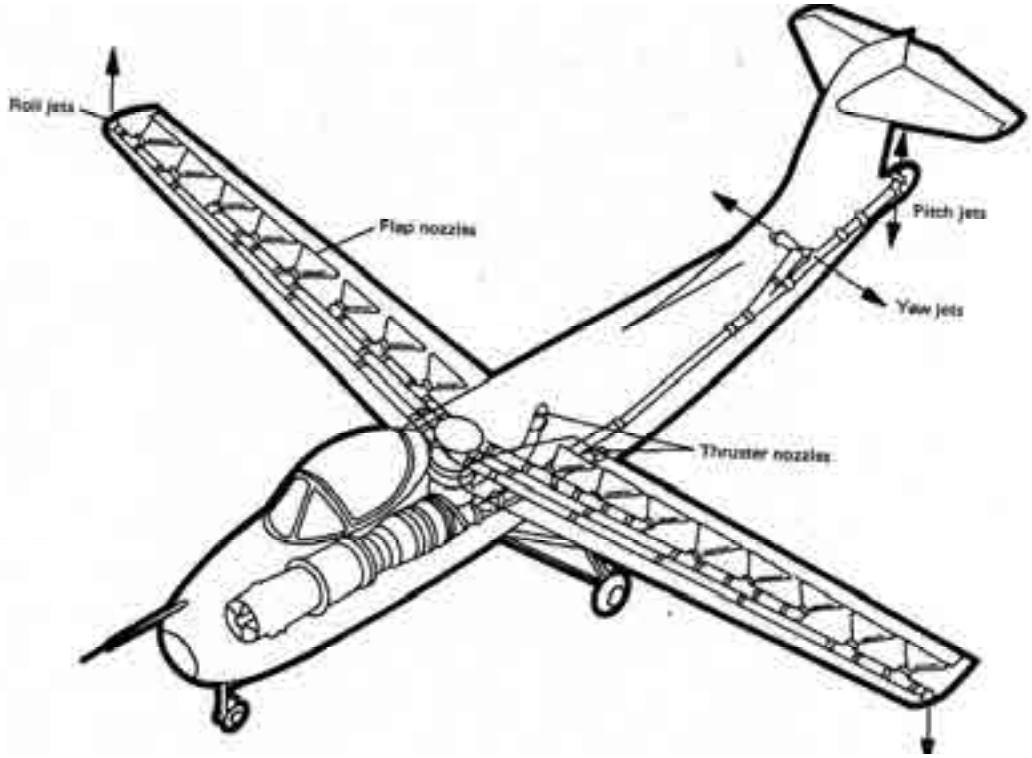

Fig. 3-55. The Hunting H.126 general arrangement drawing as tested in the NASA Ames 40- by 80-foot wind tunnel [462].

nozzles, but also to the aircraft's tail to provide pitch and yaw control at very low speeds where the normal aircraft control surfaces were woefully undersized. K. D. Harris [465] made a particularly important point during his discussion of the general arrangement (Fig. 3-55), the NACA 4424 airfoil (Fig. 3-56), and the three-view drawing (Fig. 3-57) when he noted:

> "A general arrangement drawing of the aircraft is shown in Figure 1 [Fig. 3-55]. The main features are the fairly large aspect-ratio, shoulder-high wing; the large fin and high-set tailplane and the rather deep fuselage housing an Orpheus turbo-jet engine under the single seat cockpit. The tricycle undercarriage was not made retractable because interest was mainly in low-speed flight.
>
> With a maximum all-up weight of about 10,700 lb (47,600 newtons) and a wing area of 217 ft^2 (20.1 m^2), the wing loading is about 50 lb/ft^2 (2,370 N/m^2). To keep the engine jet temperature to not more than 620°C, the basic Orpheus engine had to be derated from a test-bed thrust of about 5,000 lb (22,200 N) to about 4,300 lb (19,100 N). However, since 15% of the engine efflux is continuously used for control and autostabilization purposes, and because of the large thrust losses incurred in ducting the efflux through the fuselage and wings, the effective propulsive thrust from the nozzles is slightly less than 3,000 lb (13,300 N). The ducting system is illustrated in Figure 1. Division of the engine efflux is as follows:
>
> | | | |
> |---|---|---|
> | Jet-flap | 55% | |
> | Direct thrust nozzles | 30% | i.e. 85% for propulsion |
> | Pitch control jets | 5% | used for control purposes |
> | Yaw control jets | 5% | used for control purposes |
> | Roll control jets | 5% | used for auto-stabilization |
>
> In the early project schemes, all the propulsion was to have been supplied in the form of a jet-flap, as in the original NGTE concept. However, it was found that the overall propulsive efficiency could be much improved by restricting the jet-flap to a strength just sufficient to generate the specified lift-coefficient [C_{Ls} of 6]. The jet flow released by this was ducted to direct thrust nozzles positioned at such a distance below the centre of gravity that a nose-up pitching moment was produced approximately cancelling out the nose-down moment of the jet flap."

The cross-sectional view through the flap or aileron shown in Fig. 3-56 indicates the basic airfoil was a NACA 4424, which gave the room needed for ducting.

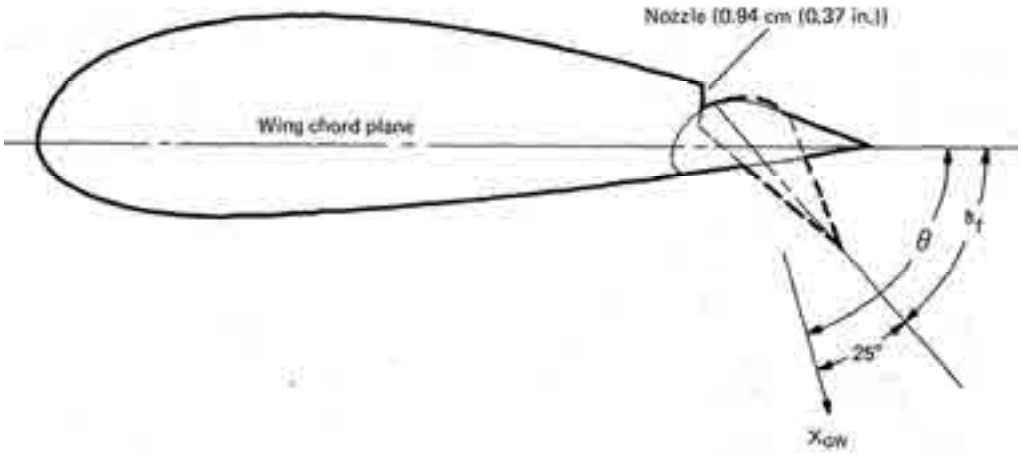

Fig. 3-56. The Hunting H.126 basic wing airfoil was a NACA 4424. The flap chord was nominally 12 percent of the wing chord [462].

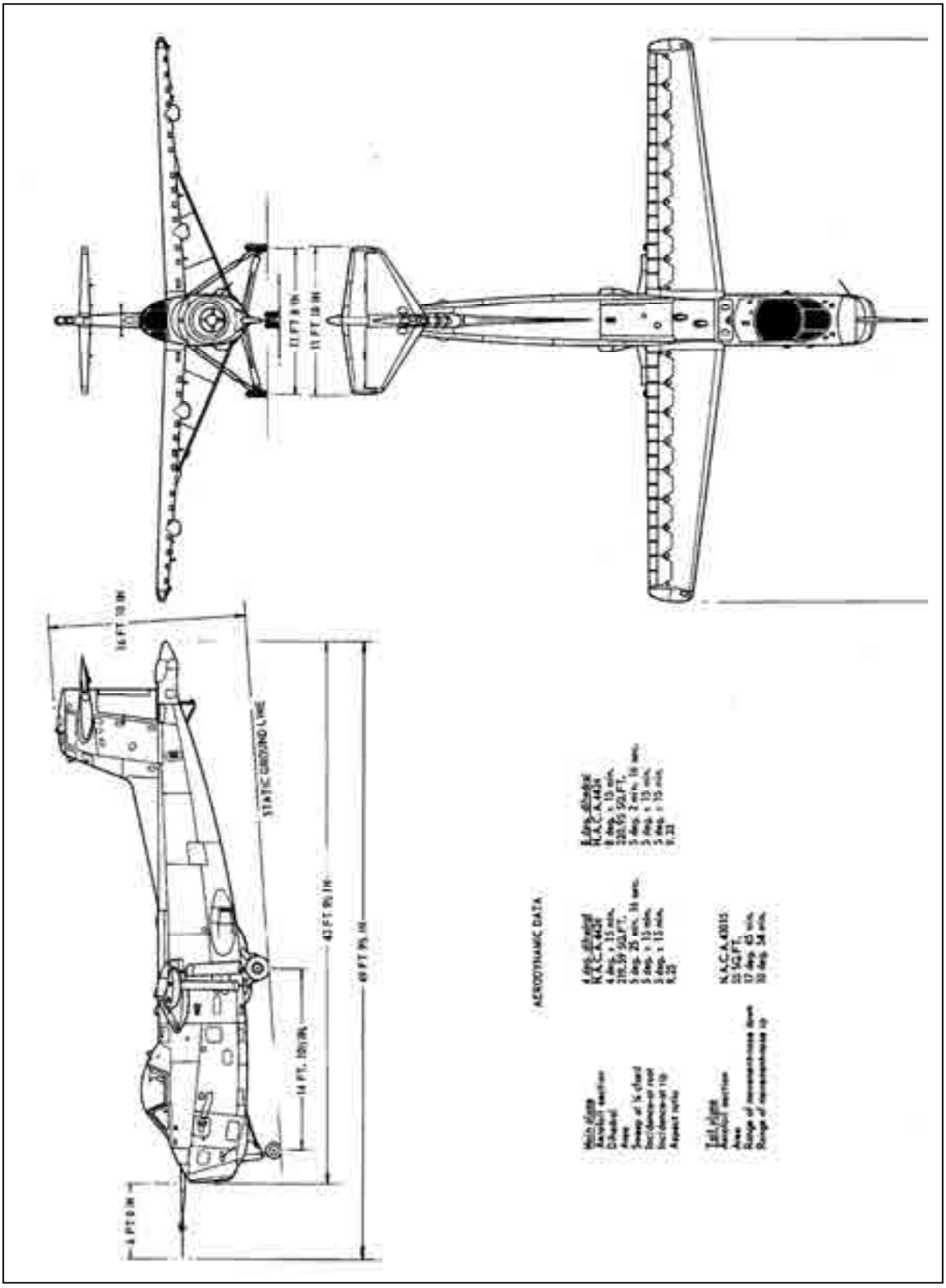

Fig. 3-57. The Hunting H.126 three-view drawing [464].

For slow-speed flight, about one-half of the turbojet's 4,000-pound thrust was diverted through ducting until finally a thin sheet of air[107] was blown over the top surface of very short chord flaps. This sheet of air followed the contour and deflection angle of a flap. Additional ducting provided air to wingtip nozzles, and this augmented roll control provided by the ailerons. Air delivered to nozzles in the tail area gave pitch and yaw control. The other half of the engine thrust output provided thrust to overcome drag through two exhaust pipes on either side of the fuselage. Guest pilots were told not to fly slower than 35 miles per hour (30 knots). At a gross weight of 10,740 pounds, flight at 30 knots, and at sea level on a standard day (q_{FP} = 3), the lift coefficient was about 16! Clearly, a great deal of the lifting was thought to come from the wing having "super circulation."

After completing its flight test and demonstration program, the Hunting H.126 was shipped to NASA Ames Research Center for testing in their large-scale wind tunnel. This testing was done in June and July of 1969, but a test report [462] by Tom Aiken and Tony Cook was not published until April of 1973. I found figure 7(b) of Tom and Tony's report very interesting because, as far as I know, it was the first test where the aerodynamic properties of a landmark jet flap aircraft (the first flight was in 1961) were obtained under very controlled conditions. You see the fundamental lift versus angle of attack and lift versus drag polar of this jet flap demonstrator in Fig. 3-58 and Fig. 3-59, respectively.

The first thing I took notice of in the lift versus angle-of-attack data (Fig. 3-58) was that the maximum lift measured was a powered-on lift coefficient (C_{Ls}) of 6.9 obtained with a jet thrust coefficient (C_J) of 0.87. According to Tom and Tony's report, this point was obtained with the jet engine operating at 97 percent of design engine speed and at a wind tunnel dynamic pressure (q_{FP}) of 7.3 pounds per square foot. At sea level on a standard day, this dynamic pressure corresponds to a flightpath velocity (V_{FP}) of 43 knots. The H.126 had a wing area of 221 square feet, which means the aircraft lift was on the order of 11,130 pounds. How the H.126 could maintain level flight at 30 knots (35 miles per hour) is not at all clear to me, given the NASA Ames wind tunnel data. In my opinion, this is nothing less than an example of marketing overstating engineering facts, or the aircraft was descending.

The first thing I took notice of from the drag polar shown in Fig. 3-59 was that the maximum tested condition of C_J equal to 0.87 and C_{Ls} equal to 6.9 corresponds to a descent angle of over 7 degrees. Keep in mind that *equilibrium level flight* is obtained when drag is zero, which is to say $\Sigma F_X = 0$ and $\Sigma F_Z = \text{Weight}$. The second point I want to bring to your attention deals with George Schairer's theory. Fig. 3-59 shows Mr. Schairer's theory compared to H.126 wind tunnel test data at the lowest and highest jet thrust coefficient values. At both jet thrust coefficient values (and at the intermediate values as well) it is apparent that the configuration falls short of ideal performance by a significant amount. Still in all, the British Hunting H.126 gave jet flap advocates a starting point configuration and enthusiasm to continue their search for significant improvements in jet flap aircraft STOL performance.

[107] I have referred to the turbojet exhaust simply as air but, as I am sure you know after reading the discussion of engines in Volume II, the temperature of this air was on the order of 1,000 ^{o}F. This meant that insulated heat shielding had to be used around the ducts and as coverings for the wing and flaps.

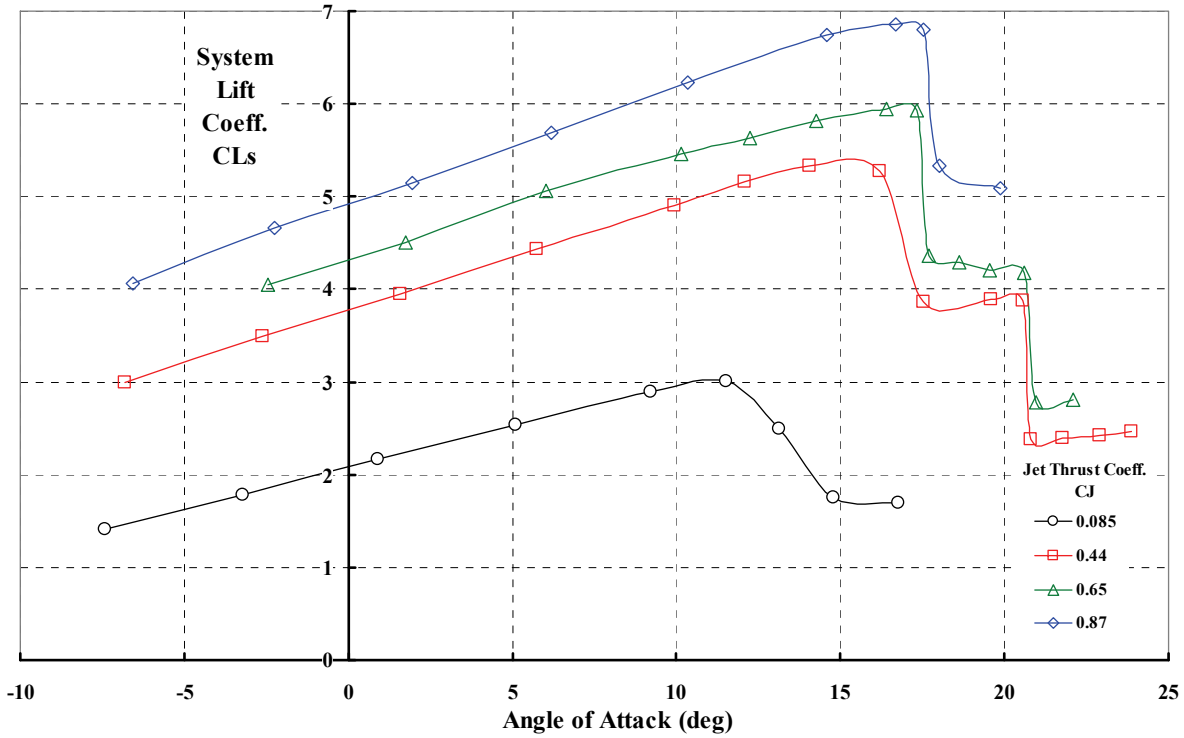

Fig. 3-58. Lift versus angle-of-attack characteristics of the British Hunting H.126.

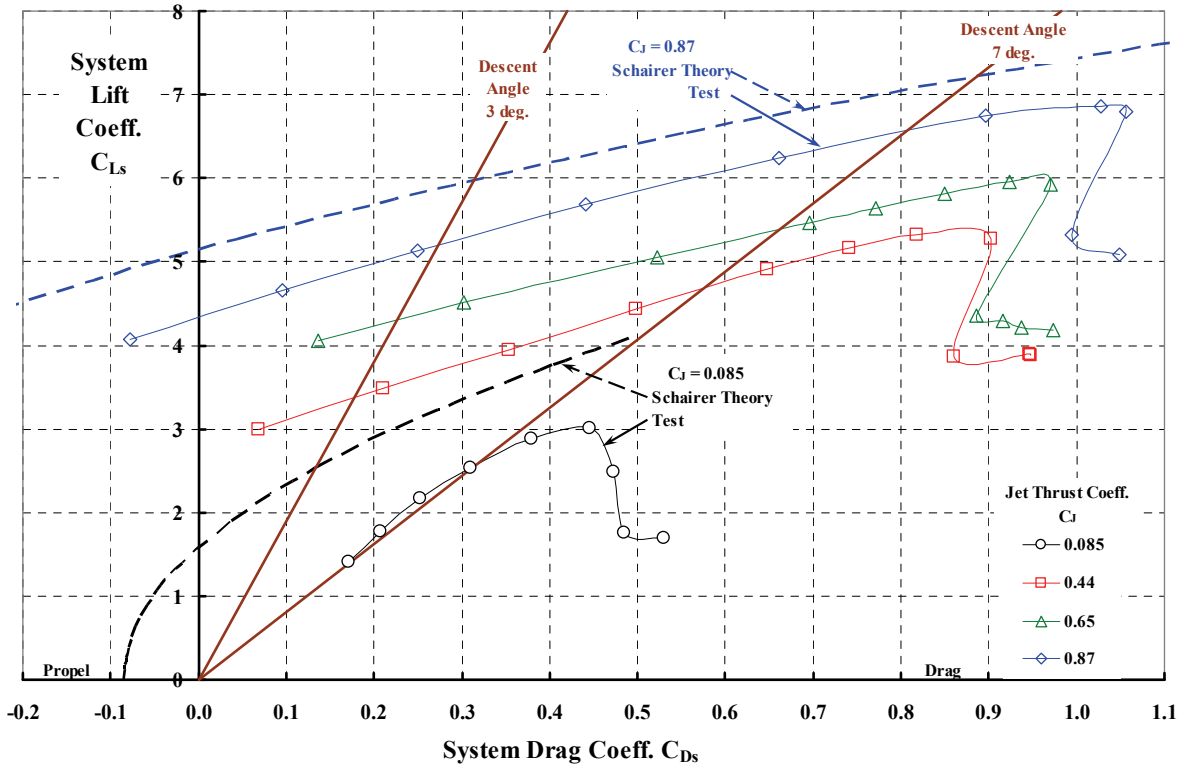

Fig. 3-59. The lift-versus-drag performance of the H.126 was less than George Schairer's ideal, but this first-of-its-kind aircraft spurred jet flap research.

3.3.7.3 The Ball-Bartoe Jetwing

In 1973 the Ball-Bartoe Aircraft Corporation, located in Boulder, Colorado, was formed specifically to build the Jetwing (Fig. 3-60), which Otto Bartoe (he went by Pete) had conceived and designed.[108] The first flight of this STOL aircraft was on July 11, 1977, and *Air International* [466] reported a great deal of information in February 1978. Following about 70 hours of test flying, the Ball-Bartoe company denoted the aircraft and conceptual patents to the University of Tennessee in December 1978 [467]. The university received a contract (N00019-80-C-0126) from the Naval Air System Command on February 19, 1980, which funded 60 hours of flying time and 108 hours of ground test time. The results of this program were reported by Associate Professor Ralph Kimberlin [468] on July 1, 1981. A follow-on contract (N00019-81-C-0506) was awarded on September 30, 1981, to evaluate the Jetwing with the ejector wing removed. Professor Kimberlin was the author of the final report [469] for this second phase. Between these two University of Tennessee reports you have an extremely thorough description of the Jetwing and a clear picture of its performance. For example, Professor Kimberlin included some background [468] that reads [with some editing on my part] as follows:

Fig. 3-60. The Ball-Bartoe Jetwing was another small, one-man research demonstrator. It made its first flight on July 11, 1977 [466].

[108] Pete Bartoe, born in 1927, was one of a handful of people who started the Ball Brothers Research Corporation as a division of the Ball Corporation in 1956. He was their first engineer, later became president, and in 1973 became the chief operating officer of the division. Apparently he was an engineer with a real passion for inventions. He was honored by the Colorado Aviation Historical Society in 2004, and the article about him is quite interesting. He died in 2010.

> "Development started on the Jetwing research airplane in 1973. The airplane was completed and ready for testing by December of 1976. Full scale testing started [and was completed] in December of 1976 in the NASA Ames Research Center 40' x 80' wind tunnel [test number 498]. An evaluation of the wind tunnel data revealed that the aircraft was neutrally stable to unstable longitudinally at the centers of gravity where it was likely to be flown. As a result about 300 pounds of lead ballast was added to the nose of the aircraft prior to the start of flight testing.
>
> The first flight was conducted at Mojave, California on July 11, 1977, by Mr. H. R. Salmon [pilot]. This flight confirmed the instability, and as a result an additional 100 pounds of lead ballast was added. Forty-seven flights were flown at Mojave for a total of 34 hours. During this testing it was discovered that the horizontal tail would stall whenever the flaps were lowered to angles in excess of 40° in combination with flight speeds of about 50 knots indicated airspeed. As a result a safe flap deflection of 35° was established. A certain amount of quantitative performance data were gathered during the Mojave testing, but its usefulness is limited due to the lack of calibrations on instruments and airspeed system. Upon completion of testing at Mojave, the aircraft was ferried to the Ball-Bartoe Aircraft Company facility at Boulder, Colorado, where some testing and demonstration flying continued. An additional 44 flights and 32 flight hours were accumulated upon the aircraft during the ferry trip and test flying at Boulder."

Let me stop for a moment to point out that the Hunting H.126 and the Jetwing really did not have an engine wing interface as Schubauer conceptualized and tested, and as I have illustrated in Fig. 3-27. The historical evolution from 1933 to the late 1960s led to what was called an upper-surface blown flap. The evolution was completed with the Boeing YC-14, which I will discuss in more detail shortly. Schubauer's sheet of high-velocity air was squirted in the desired direction mechanically. The two aircraft under discussion squirted a sheet of high-velocity air nearly tangent to the wing's upper surface as you see with the Ball-Bartoe Jetwing in Fig. 3-61. Then a mechanically deflected flap bent the sheet of air in the desired direction. This is an application of the Coandă effect, which says that a stream of air wants to follow any nearby surface even if the surface is curved. *Thus, a turbo jet engine's thrust can be deflected down for low-speed flight* ***and still provide a forward-force component*** *so level flight can be maintained. Alternately, the mechanical flap can be retracted, and the full jet thrust can propel the aircraft as in the conventional jet transport we see flying today.* Now let me continue.

The Ball-Bartoe Jetwing (JW-1) was a small aircraft powered by one Pratt & Whitney JT15B-1 turbofan engine rated at 2,200 pounds static thrust. The engine was rated at 1,750-pounds maximum continuous static thrust when installed in the Jetwing. Its maximum takeoff gross weight was 3,750 pounds, but the normal takeoff weight (from the weight statement that Professor Kimberlin included in reference [468]) was 3,600 pounds:

Fuselage	1,083	
Engine	633	
Pilot and equipment	200	
Fuel	672	(106-gallon capacity)
Ballast	412	(the aircraft was tail heavy)
Wings	600	
	3,600	

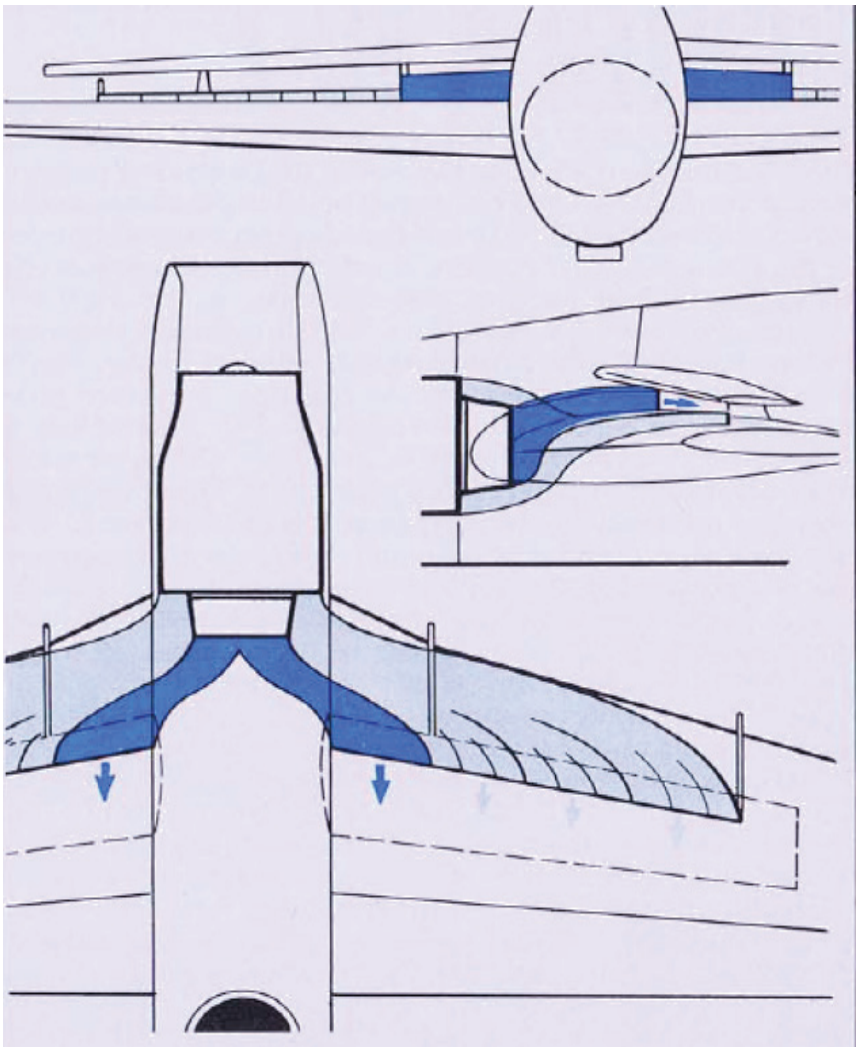

Fig. 3-61. The turbofan's hot gas shown in dark blue was ducted to the inboard span of the wing. The cooler air from the bypass part of the engine was ducted to the outer part of the wing [468].

Now let me describe the Jetwing in further detail based Kimberlin's reports [468, 469] and with the three-view from Fig. 3-62 in hand. The untwisted wingspan was 21.75 feet, and its aspect ratio was 4.48. The wing area was 105.6 square feet, and the ratio of tip chord to root chord (i.e., the taper ratio) was 0.46. The engine inlet area was about 126 square inches, and the hot gas exhaust nozzle area was 156.2 square inches; the bypass air from the gas generator exited through a 96.3-square-inch nozzle. The aircraft was constructed primarily of aluminum with some titanium used in critical areas. The fuselage, for example, was constructed of welded steel-tube frames covered with titanium and aluminum sheet stock.

As you can see, the pilot's cockpit was situated well aft, and this gave him, as you might have already guessed, very poor visibility when the aircraft was at high angles of attack.

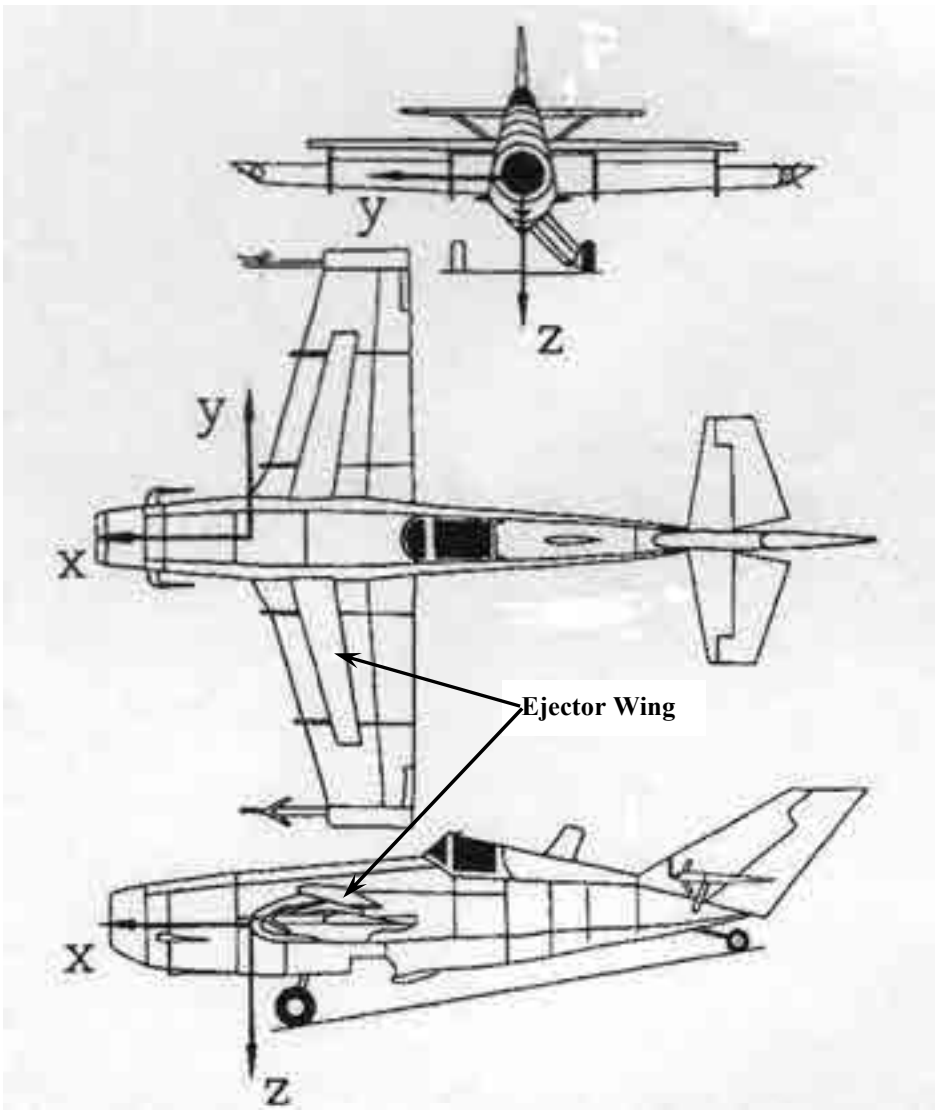

Fig. 3-62. The Ball-Bartoe Jetwing general arrangement drawing [468].

I would be remiss if I did not point out the small "ejector wing" with my callout on Fig. 3-62. Professor Kimberlin notes that in both flight and wind tunnel testing, with and without this little wing, none of the researchers—or, more importantly, the pilots—could see any value to this "device." Therefore, I will only draw your attention to ejector-wing-*off* data.

Before the Jetwing was ever flown it was tested in the NASA Ames large-scale wind tunnel (Fig. 3-63).[109] The performance data indicated the aircraft had potential, but the center

[109] This wind tunnel is officially known as the NFAC (National Full-Scale Aerodynamic Complex). In May 2003, after an accounting ploy called full-cost accounting, NASA Headquarters no longer thought the tunnel was worth its keep and they mothballed the complex. Fortunately, people with a less myopic view showed Congress, the Department of Defense, and the U.S. Air Force the value of the NFAC, and the Air Force took operational control in September of 2005. Restoration was completed in the fall of 2009, and the 40- by 80-foot and its 80- by 120-foot companion are now so busy that people are standing in line to get wind tunnel time [470].

(a)

(b)

(c)

Fig. 3-63. The Jetwing was tested in the NFAC (December 1976) before its first flight in January 1977 (photo courtesy of Bill Warmbrodt, Ames Research Center).

of gravity was too far aft and the aircraft was statically unstable about the longitudinal axis. The immediate and simple fix was to added 300 pounds of ballast in the nose. After first flight, the nose ballast was increased to 412 pounds. I believe this is just one simple example of "test before you fly." No doubt a smaller scale, powered force model would have found the same static stability problem, but that little model would have been very expensive relative to the overall program costs, which were minimal given the "Skunk Works" approach that Pete Bartoe took.

Now let me show you some low-speed flight performance data [469] that was obtained at the University of Tennessee Space Institute under Professor Kimberlin's leadership. In the Professor's words:

> "This report [469] covers the flight test program of the Jetwing research airplane which was conducted for Naval Air Systems Command. The purpose of the flight test program was to validate NASA Ames Research Center 40 x 80 foot wind tunnel data on the aircraft by flight test, and to obtain performance, stability, and control data sufficient to evaluate the Jetwing concept for future application to other flight vehicles."

NASA Ames appears to have had little trouble in testing Pete Bartoe's aircraft in just one month (December of 1976).[110] A key graph from the NASA data found its way into the Professor's report, and I have reproduced it here as Fig. 3-64. As a first step in the discussion,

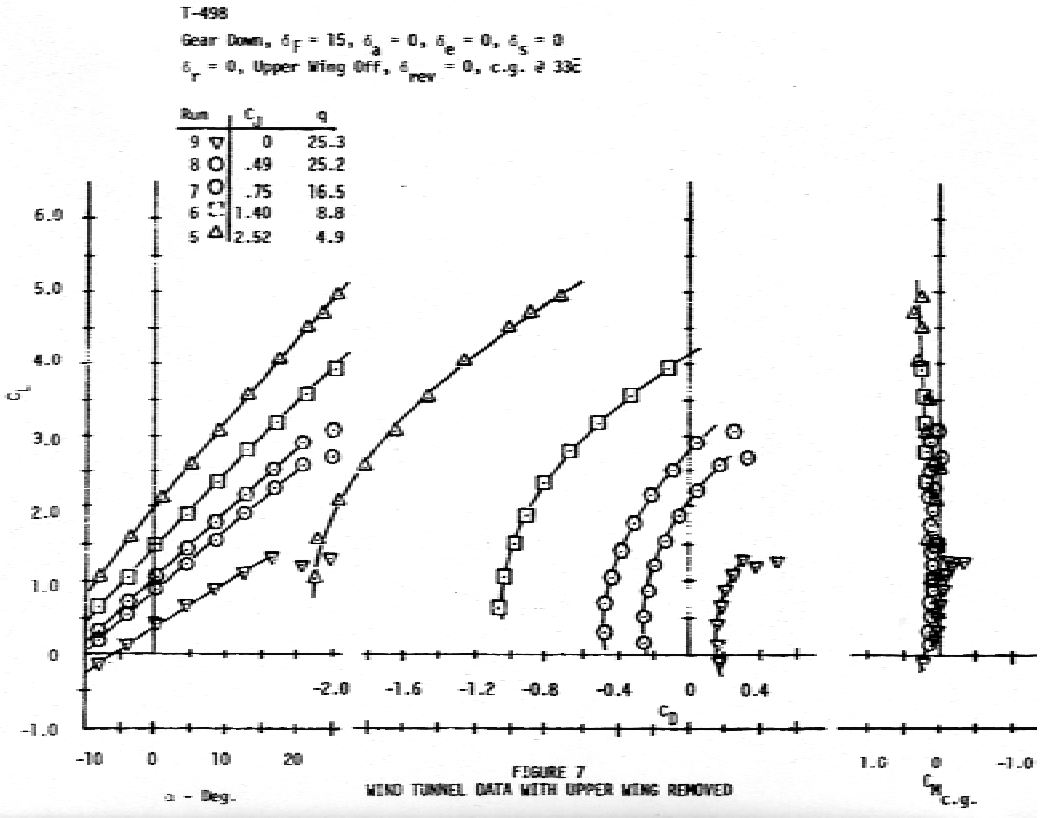

Fig. 3-64. NASA Ames provided 40- by 80-foot wind tunnel data in support of the Jetwing program. This data was available *before* first flight [469].

[110] Try as I might, I have been unable to find a NASA report with data from this test.

I have compared Kimberlin's flight test data for the Jetwing to the NASA Ames wind tunnel test data and shown the results in Fig. 3-65. For good measure, I have also included George Schairer's ideal performance theory as dashed lines on the figure. The stated objective of the professor's program was flight (solid data symbols) versus wind tunnel data (open data symbols), and you can see from Fig. 3-65 that the agreement is quite remarkable. As to ideal theory versus test, you can see that the gap between theory and test widens as the jet thrust coefficient (C_J) increases. Of course, you would expect a disagreement with C_J equal to zero, because the ideal drag polar has no drag (C_{Ds}) at zero system lift (C_{Ls}). But note that at a C_J of 2.52 (the brown dashed line), adding an increment of drag equal to, say, about +0.2 will not close the gap between theory and test. It takes another + 0.2 to bring theory and test into agreement. The implication is that the jet flap is not 100 percent efficient, and this inefficiency appears to be a percentage of the reference jet thrust coefficient. My crude examination came to the conclusion that if you multiply the reference C_J by about 0.9, and add a drag at zero lift of + 0.2 to the ideal theory, every dashed theory line will closely approximate the test data, at least up to the onset of wing stall.

Another point of interest is just how little jet thrust is required to unstall the wing. You see this by the departure of the test data from a parabolic shape at high system lift coefficients. There is no evidence of stall at jet thrust coefficients of 1.4 and 2.52, up to angles of attack of 22 degrees, which is well beyond what a paying customer would tolerate. And as a final point, I have shown rate-of-climb lines on Fig. 3-65 to give you some appreciation of the takeoff capability of the Jetwing. The flap angle is only 15 degrees for this data, which would be satisfactory for takeoff. Landings would require at least 30 degrees and probably all of the 52 degrees of flap angle available.

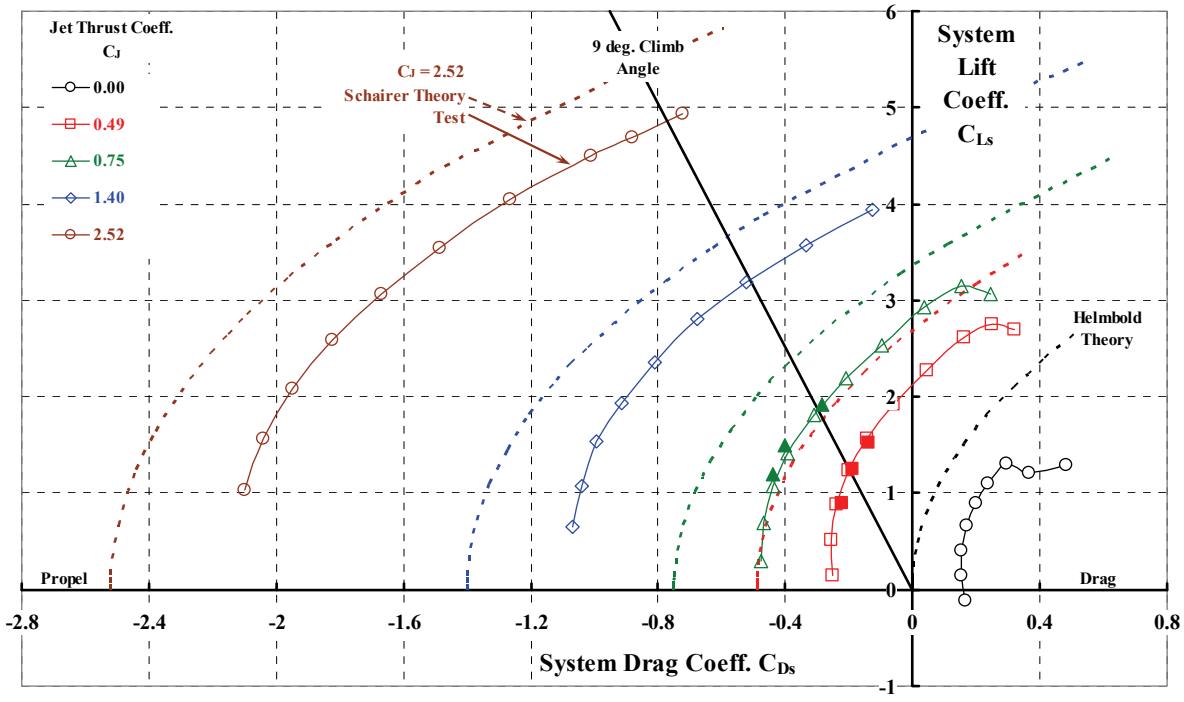

Fig. 3-65. Flight test data (solid symbols) and ideal theory (dashed lines) compared to NASA Ames wind tunnel test data (open symbols) for the Jetwing.

The second objective of the Jetwing flight test program was flight evaluation. The STOL capability was clearly number one in the program, and Professor Kimberlin wrote [468] that the aircraft configurations, speeds, and power settings used for the tests were as follows:

"TAKEOFF

1. Gear Down, Flaps 15 degrees
2. Power Setting—95% N1
3. Liftoff Speed—60 to 65 KIAS
4. Climb Speed—70 KIAS (target)

LANDING

1. Gear Down, Flaps 30 degrees
2. Power Setting—74% N1
3. Approach Speed—70 KIAS (target)
4. Touchdown Speed—65 to 55 KIAS
5. Thrust Reverser—Deployed after touchdown
6. Braking—Maximum after touchdown

The takeoff weight and center of gravity for these tests was 3608 lb at 35.51 M.A.C. [mean aerodynamic chord]. The aircraft was refueled after a maximum of three test runs in order to keep weight and center of gravity excursions small. Since takeoff and landing tests are prone to have large data scatter due to pilot technique, sufficient number of runs were made in order to have a reasonable statistical sample. Thrust reversing was used on each run since the thrust reverser is an integral part of the Jetwing concept."

From this test procedure, the professor concluded [468] that the Jetwing, at 3,600-pounds flight weight on a standard day with no wind, had the following STOL performance:

Item	Ground Roll	Air Distance Over 50 Feet	Total Distance Over 50 Feet
Takeoff	954 ft	308 ft	1,262 ft
Landing	842 ft	719 ft	1,561 ft

It is interesting to note from this table that on takeoff the air distance, over a 50-foot obstacle of 308 feet, works out to about a 9-degree average climb angle. In contrast, the landing air distance of 719 feet gives an average final approach angle of 4 degrees, less than half of the climb angle. It is also interesting to note that at the 70-knot approach, and at the climb speed of 70 knots, the aircraft was operating in equilibrium flight at a system lift coefficient of

$$(3.87)\quad C_{Ls} = \frac{W}{q_{FP} S_W} = \frac{3,600}{\left(70^2 / 295\right) 105.6} = 2.05\,,$$

which is really quite conservative (in my mind) considering the data on Fig. 3-65. Clearly the Jetwing could be flown very easily at a system lift coefficient of 4, and at a jet thrust coefficient of 1.8 on takeoff or 1.4 on the landing approach. This would mean that the approach and climb speed could easily have been 50 knots. One test pilot, "Fish" Salmon, was quoted in *Air International* [466] as saying:

"...that the Ball-Bartoe Jetwing has positive handling characteristics down to speeds of 45 kts (83 km/h) and has experienced no control difficulties, although he would like the centre of gravity to be shifted forward a little. The entire tailplane can be varied in incidence for trimming and the elevator also incorporates trim tabs which were originally connected with a stability augmentation system but have since been locked in place, since stability was found to be satisfactory. The Jetwing has negative stability in some flight modes but remains controllable."

The Ball-Bartoe Jetwing was considered to be a relatively quiet jet-engine-powered aircraft. Professor Kimberlin included several examples of fly-by noise in sound pressure levels (dB). A page from his report [468] is reproduced here as Fig. 3-66 because noise on takeoff was the loudest he reported.

Finally, the professor thoroughly recounted the handling qualities in both of his reports, but I will leave that for your reading (it is well worth your time). His final recommendation dealt with the need for measurement and analysis of downwash, particularly at the tail. A Mr. U. P. Solies at the University of Tennessee took on that task [467].

Now let me discuss the work that de Havilland Canada and NASA Ames Research Center did to develop a refined trailing-edge jet flap configuration, one of the four basic configurations you see in Fig. 3-47. De Havilland called this refinement an "augmented jet flap."

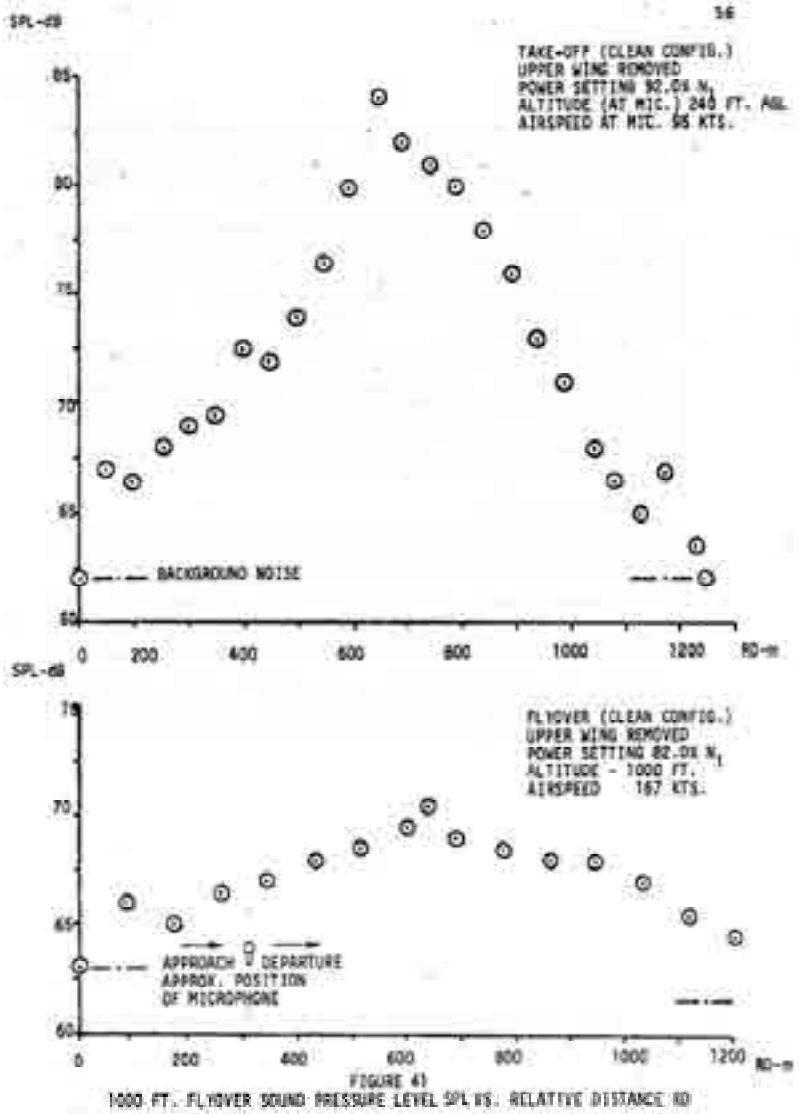

Fig. 3-66. Jetwing noise levels during takeoff (upper figure) and during a flyover (lower figure) were considered quite low [469].

3.3.7.4 The de Havilland/NASA Ames/Boeing C-8A Augmentor Wing Research Aircraft (AWRA)

De Havilland Canada came into being in 1928 as a subsidiary of the famous British de Havilland Aircraft Company founded by Geoffrey de Havilland on September 25, 1920 [471]. The Canadian company started making the Tiger Moth (a two-place trainer) and then saw the need for STOL aircraft all over Canada and Alaska, and then in many countries around the world. Later you will learn how they filled that need. In the early 1960s they saw the need for larger utility transport STOLs, and they had the expertise to start a research program on what they called an "Augmentor Wing," the details of which you will read shortly. Don Whittley, Chief Research Engineer for the subsidiary, first divulged the concept and its development in 1961 at a 1964 AIAA meeting [472]. He followed up 3 years later with more information [473]. In his first paper, Don offered a very interesting graph, which I have reproduced here as Fig. 3-67. He was illustrating a boundary between STOL and VTOL that I had never seen before. In discussing his view, Don wrote, with some of my thoughts interjected, that

> "The main objective of STOL technology from an aerodynamic standpoint is to develop wing lift to a maximum while keeping installed power to a minimum in order to satisfy an overall aircraft requirement which includes a specified short field length. The subject under consideration here concerns the ultimate in STOL technology. This is not to suggest that the augmentor-wing concept is necessarily the ultimate solution to STOL aircraft design, but rather that there is a limit to the development of such aircraft beyond which the law of diminishing returns sets in. This is illustrated in Fig. 1 [Fig. 3-67]. The diagram shows clearly that, at a given value of thrust/weight ratio (T/W), the take-off distance can be reduced by increasing the value of C_{Lmax},[111] but that at values of C_{Lmax} = 6 or more the gain in terms of take-off distance diminishes rapidly. In the particular case under consideration (wing loading, W/S = 50), this corresponds to a take-off distance to the 50 ft. obstacle in the region of 750 ft. provided that we restrict ourselves to *reasonable values of installed thrust/weight ratio, say not in excess of 0.6* [my italics]."

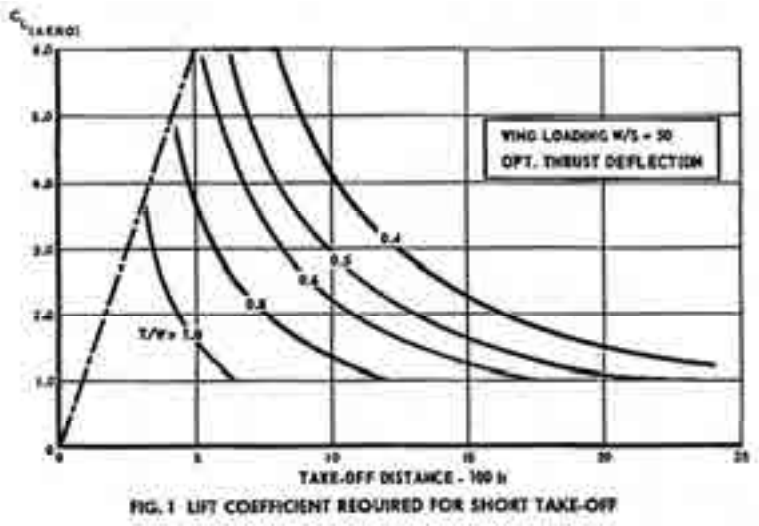

Fig. 3-67. Don Whittley's line between VTOL and STOL [472].

[111] Whittley referred to this C_{Lmax} saying that the parameter "does not include the lift component of the deflected jet." Since Helmbold's theory says that C_{Lmax}/AR cannot exceed 1.9, Whittley's requirement means that the wing aspect ratio (AR) must be greater than about 3, and this practical wing must not exhibit any stalling.

> "When the installed thrust to weight ratio exceeds 0.80 approximately, then it is necessary to re-examine the whole question and decide whether it might not pay to go all the way and provide a VTOL capability with STOL performance at maximum or overload weights. In order to illustrate this possibility an arbitrary cut-off at $C_{Lmax} = 6.0$ is shown on Fig. 1 and a second line is drawn through the axis (the VTOL point) to define approximate boundaries for V/STOL operation. *Note that, using the safety rules of Ref. 1* [474]*, a thrust/weight ratio greater than one is required for VTOL* [my italics]. The economy and flexibility of a VTOL design can be improved considerably by taking advantage of the STOL mode and so this realm of operation assumes considerable importance. *When thrust/weight ratio is close to unity, as in the VTOL design, then there is no longer any requirement for very high lift coefficients, and the opportunity to exchange the complication and weight of a high lift STOL wing for a corresponding VTOL penalty due to greater installed power becomes a most interesting possibility* [my italics]. So there would appear to be two quite distinct ways of achieving 'ultra-short' take-off and landing; one by overloading a VTOL design and the other by development of the STOL aircraft to the ultimate practical limit. (The word ultra-short is used here to indicate distance to the 50 ft. obstacle of 750 ft. or less, the corresponding ground roll being 300 ft. or less, approximately.) The relative merits of these two approaches will become evident only after some years of operational experience and it may be found that the two concepts are complementary rather than competitive to the extent of exclusion of one or the other, but it would appear that STOL aircraft must be developed toward ultra-short field lengths if they are to retain a place in the future, in view of increasing competition from V/STOL."

With this statement I think Whittley set the goal for STOL performance. He obviously thought that the augmentor wing concept could lead to an "ultra" STOL aircraft capable of getting on and off a runway that was only 750 feet long. I might add, however, that STOL advocates (including Don) rarely raise the question of how much surrounding airport land and airspace are required to permit operation from a 750-foot-long piece of farmland or concrete. Of course, my opinion applies to VTOL advocates as well.

The augmentor wing concept shown in Fig. 3-68 was perfected for flight testing with a succession of two-dimensional tests and a few large-scale tests in NASA's NFAC. By the early 1970s, it was being called a wing with an "augmented jet flap." What is shown as a trailing-edge blown flap in Fig. 3-47 was "augmented" by the addition of a second, short chord flap mounted in the fashion of a biplane. You might argue that the additional components and the duct-within-a-duct arrangement just added more complexity to the wing, and I suppose you would be right, but Whittley and others had already conceded that STOL came with a penalty, just not as great a penalty as VTOL. The design task was simply to get the most lift and the shortest runway with the least cost and complexity, and without giving up high-speed cruise performance.

In April of 1973, Don reported again on the progress of his program [475].[112] His paper includes a great deal of history that I think is quite valuable. He wrote:

> "The collaboration between de Havilland (Canada) and NASA (Ames) in STOL dates back to early 1964, at which time, generally, there was much preoccupation with VTOL but very little real interest in STOL. However, in that period, de Havilland, Canada, designed and built a large 42 foot span model (Fig. 2) [Fig. 3-69] of a transport based on the

[112] By then he was deputy director for research and clearly championing the augmentor wing concept.

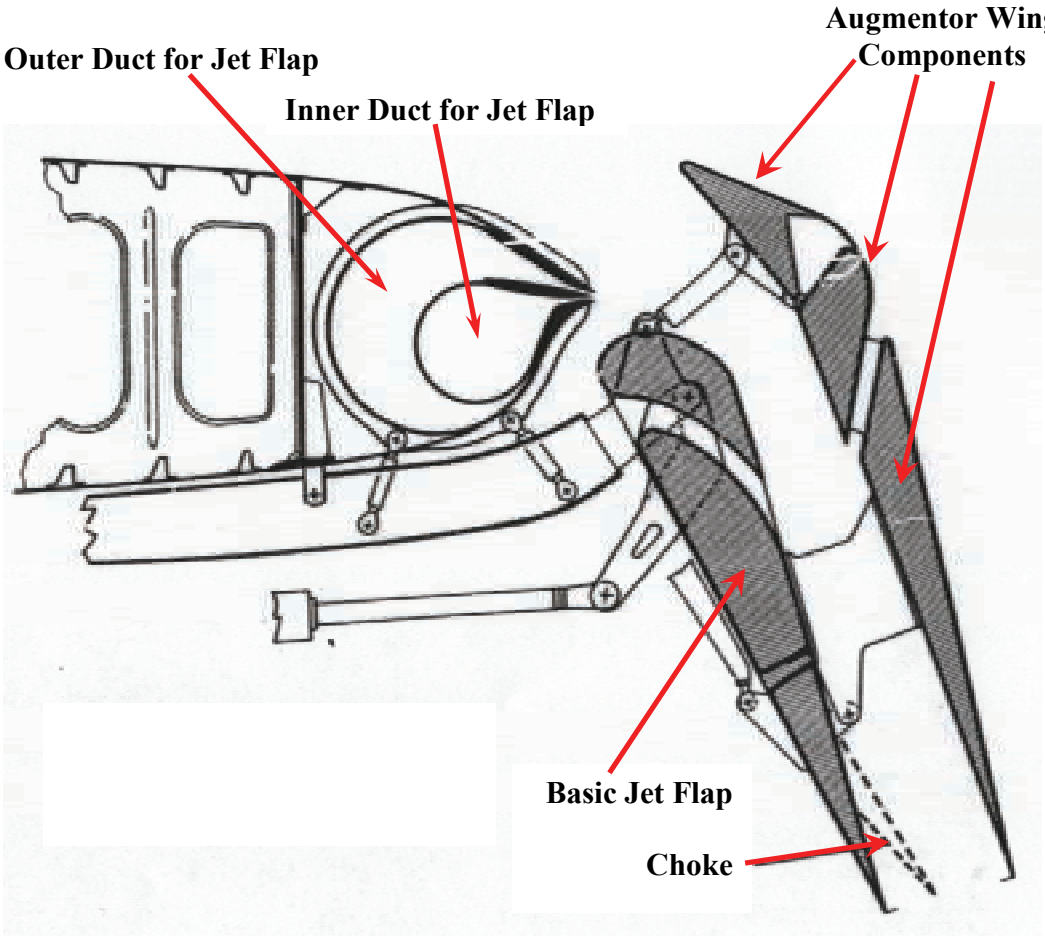

Fig. 3-68. The de Havilland augmented jet flap was created by adding a biplane "wing" above the basic trailing-edge jet flap.

Augmentor Wing concept for tests [Fig. 3-70] in the Ames 40' x 80' tunnel with funding from the Canadian Defense Research Board. The first two series of tests in the NASA 40' x 80' tunnel took place in November 1965 [Test No. 248] and March 1966 [Test No. 260]. It was the immediate success of these tunnel tests which prompted NASA to approach the Canadian Defense Department with a view to establishing a joint program to design and build a 'proof of concept' aircraft based on the de Havilland Buffalo airframe incorporating the augmentor flap principle.

The original design study for such an aircraft was carried out by de Havilland during the first six months of 1967. The Rolls-Royce Spey was identified as being the most suitable engine available for the conversion. De Havilland proposed a 'split-flow' version of the engine separating the two jet streams so that all the by-pass flow could be ducted to the wing for flap blowing. The engine would be fitted with a thrust reverser which could be modulated in flight to give partial reverse and thereby achieve control of flightpath angle during approach to land. The design incorporated a completely new wing and required relocation of the landing gear from the nacelles to the fuselage—otherwise the fuselage and empennage remained essentially unchanged. (Fig. 3.) Upon review, the program was found to be too costly and therefore it was temporarily abandoned.

> The program was re-started in 1968 when NASA led a study contract to North American Rockwell to investigate a minimum cost, one aircraft program which retained the Buffalo [DHC C8] wing box and landing gear. De Havilland assisted NAR in a consultant capacity for that study. Consideration was given to the use of separate engines for propulsion and blowing as well as to various types of 'split-flow' engines. In the former case, using readily available hardware, the design solutions showed a requirement for four turbo-compressor units plus two propulsion engines. This resulted in a rather cumbersome arrangement. In the latter case, the Rolls-Royce Spey was identified again as the most suitable engine but the layout required an off-set relative to the existing landing gear to avoid conflict with the jet. Once again, the resulting configuration was not particularly attractive. (Fig. 4.)
>
> A compromise solution was suggested by the author early in 1969 which formed the basis of the final configuration, that was, to fit existing Pegasus type vectoring nozzles to the Spey engine and leave the landing gear locked down at all times. The bifurcated jet pipe arrangement would permit the engine to remain in line with the landing gear while deflection and vectoring of the jet would be used for descent and flightpath control. With this solution, the vectored hot thrust would introduce a roll imbalance if an engine failed during approach to land but this could be off-set by the large roll control power available due to blowing the wing, and, in particular, by augmentor choke control. A general arrangement of the final configuration as developed by de Havilland and the Boeing Company is shown in Fig. 5. The research aircraft is a joint Canada/USA project which is funded by The Canadian Department of Industry, Trade, and Commerce and by the Ames Research Center of NASA.
>
> Some of the engineering design aspects of the Buffalo/Spey aircraft are now reviewed with specific reference to the integration of airframe and engine."

The two Ames Research Center tests that Don spoke of as being of "immediate success" were test numbers 248 and 260,[113] and results were published as NASA TN D-4610 [447] by Dave Koeing, Vic Corsiglia, and Joseph Morelli, and NASA TM X-62017 [448] by Tony Cook and Tom Aiken.[114] The "model" of a transport STOL with augmentor wing, Fig. 3-69 and Fig. 3-70, had a span of 42 feet, as you can see from the three-view drawing. The blowing for the first-ever test of the augmentor wing was provide by a J-85 gas turbine engine and two Viper 8 load compressors (Fig. 3-71 and Fig. 3-72). During this first test, maximum system lift coefficients (C_{Ls}) between 5 and a little over 7 were measured, depending on the blowing configuration.

This first test was so encouraging with respect to high maximum lift coefficients that a second test was conducted in March of 1966. For this entry, two J-85 jet engines for cruise were underslung from the wing (Fig. 3-73 and Fig. 3-74). The report written by Tony Cook and Tom Aiken [448] noted:

---

[113] The first test in the N.A.C.A. 40- by 80-foot wind tunnel at Ames Research Center was in August of 1944. When NASA Headquarters decided to shut the NFAC down in 1987 (even though it was going strong), 568 tests had been performed in the facility! This works out, on the average, to 13 tests per year. The United States of America (and the aerospace industry) was certainly getting its overhead money's worth out of this national facility—in my opinion.

[114] Woody Cook, Dave Koeing, and Tom Aiken played major roles as leaders of the NASA Ames V/STOL program in this era.

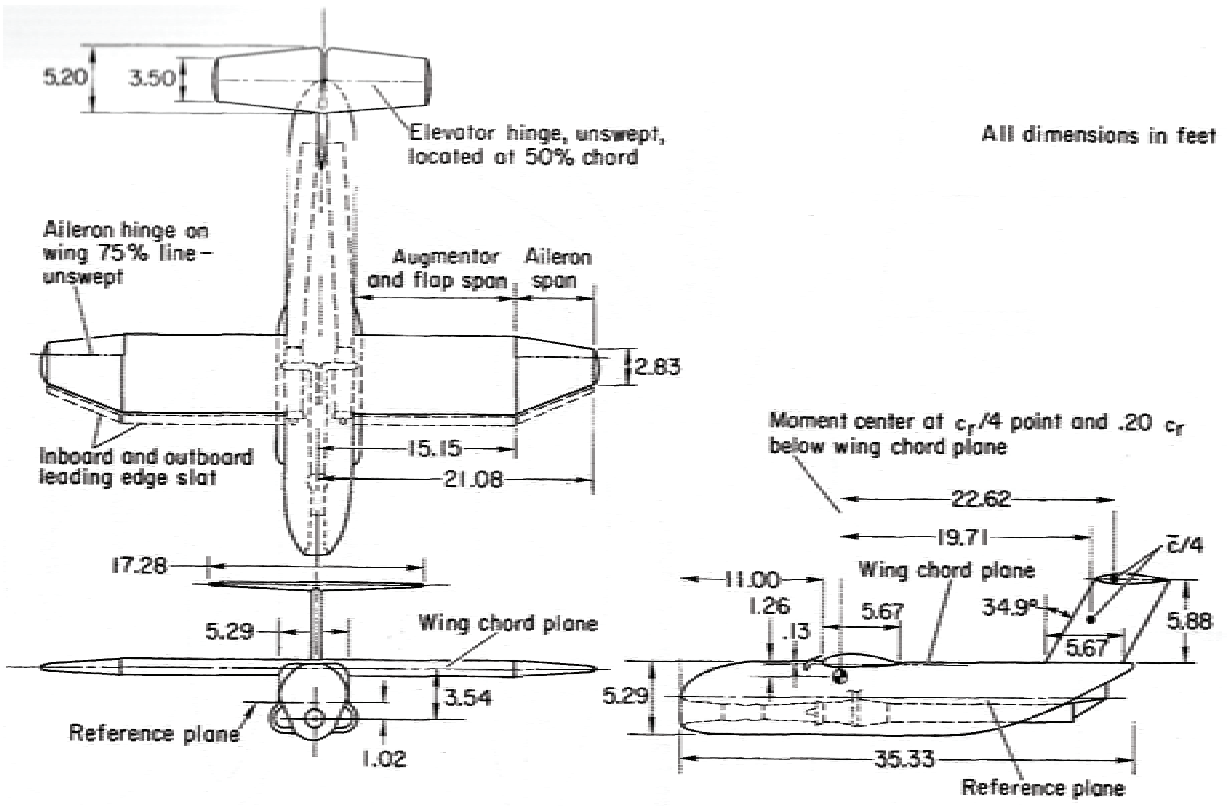

Fig. 3-69. The de Havilland Canada 42-foot-wingspan model was tested in November of 1965 [447].

Fig. 3-70. The first-ever, large-scale augmentor wing test was made with only the compressors that provided BLC and jet flap blowing [447] (photo courtesy of Bill Warmbrodt, Ames Research Center).

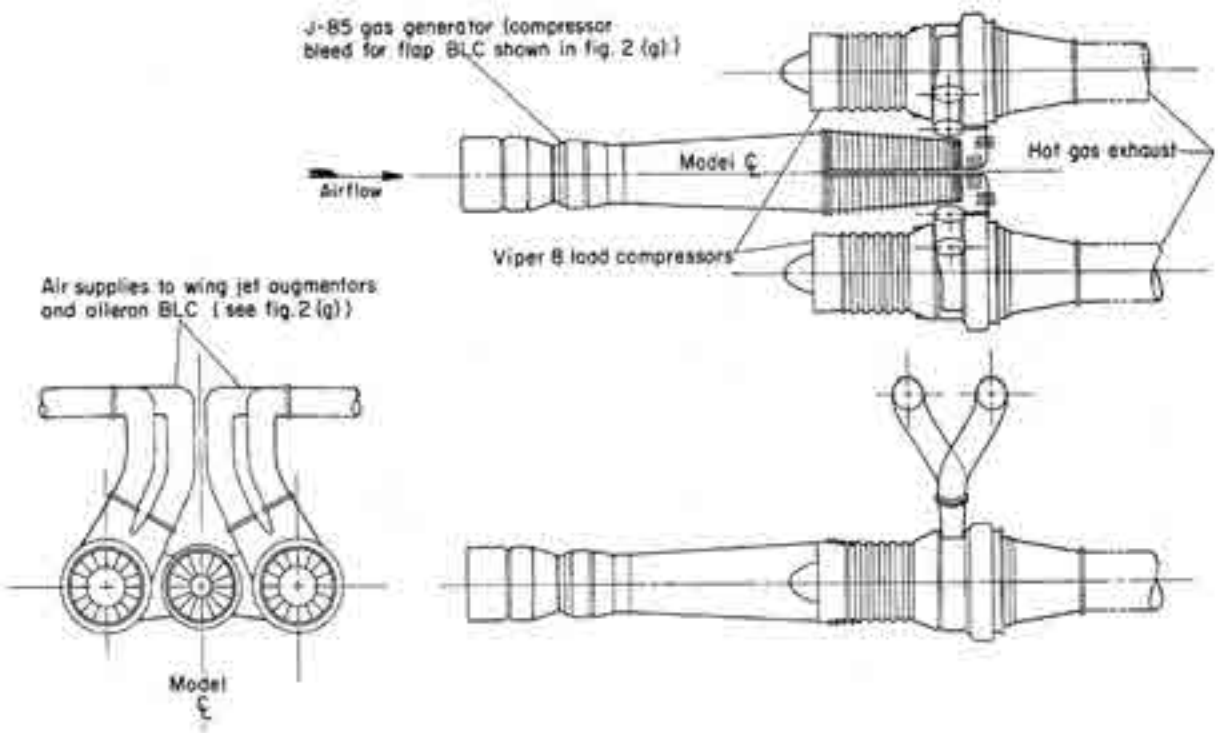

Fig. 3-71. Air from the J-85 jet engine drove the two Viper 8 compressors [447].

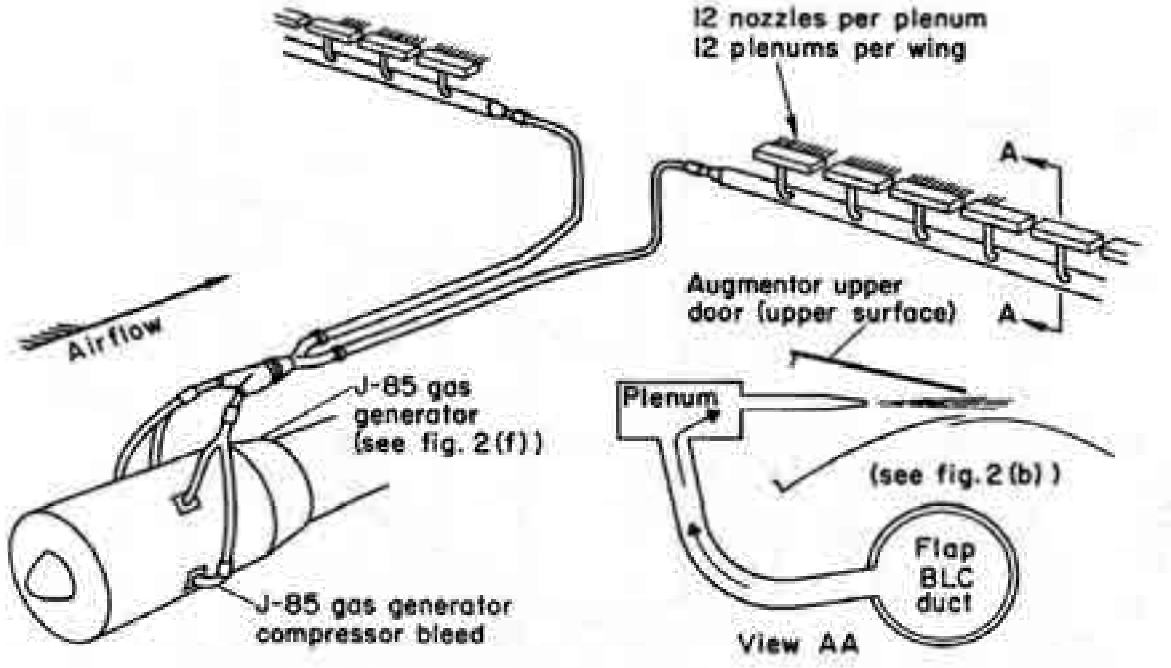

Fig. 3-72. There is no question that the first-ever augmentor wing needed an extensive piping system [447]. This was true for all the internally blown (i.e., duct works within the wing) jet flap concepts.

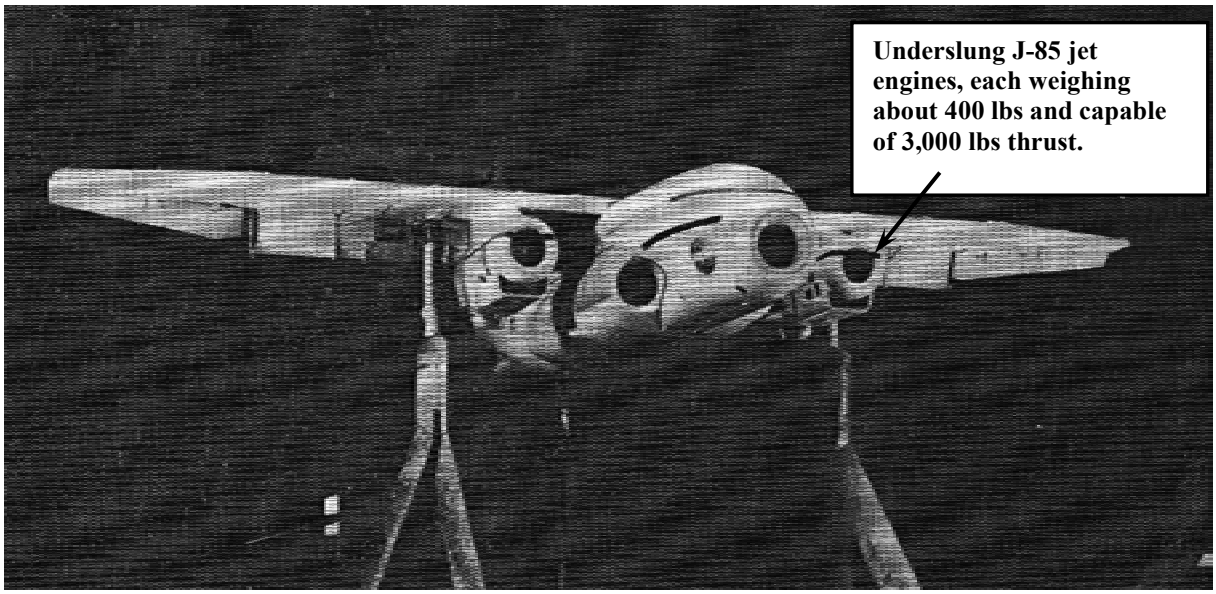

Fig. 3-73. The de Havilland augmentor wing added two J-85 cruise engines underslung from the wing for its second entry into NASA's 40- by 80-foot wind tunnel. The wing area was 222 square feet, and the aspect ratio was 8.0 [448].

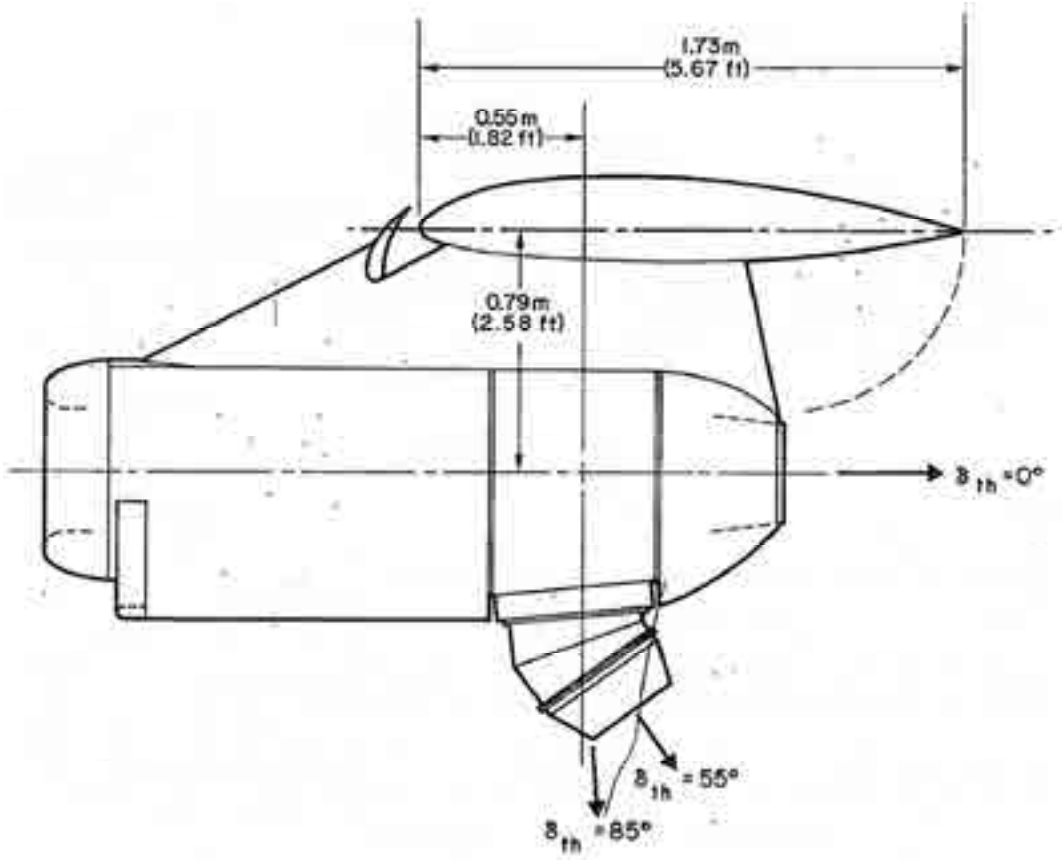

Fig. 3-74. The underwing J-85 jet engines had thrust diverter nozzles ground adjustable to three angles [448].

> "The tests reported herein are the most recent large scale tests in a continuing effort to simplify the augmentor flap geometry for consideration of application to a proposed research aircraft (CV-7A 'Buffalo' aircraft). The augmentor flap design was simplified from the design of the flaps tested in reference 1 [447] by removing the blowing BLC nozzle on the trailing edge flaps, removing the flap secondary air inlet, and in general reducing the complexity of mechanism of the various portions of the flap and their relative motions to each other. The model geometrically simulated a CV-7A aircraft with an augmented jet flap extending over 55 percent of the wingspan. In addition, underwing cruise engines were mounted on the model. These were provided with deflectable thrust capability for simulation of landing conditions."

The second test of de Havilland's concept was quite comprehensive because some very early groundwork was being laid for an "Augmentor Wing Research Aircraft." Not only were longitudinal characteristics measured, but lateral (directional, control power, and engine-out) characteristics were measured as well. The stability and control were found to be satisfactory and behavior following engine failure at low speed appeared to be rather benign, as you can see from data that Tony Cook and Tom Aiken [448] provided. I can only imagine that the de Havilland team, and Don Whittley in particular, must have been quite pleased.

The performance of the twin J-85 cruise engine configuration is rather interesting to share with you because of the many powered lift components that could both lift and propel the aircraft. Just think about this for a moment. There were, of course, (1) the jet flap components with their jet thrust coefficient (C_J) and angles (δ_{flap}), (2) the ailerons with their BLC blowing coefficients (C_μ) and angles ($\delta_{aileron}$), and (3) the cruise engines with their thrust coefficients (C_T) and angles (δ_{thrust}). These components each contributed to the system lift coefficient (C_{Ls}) and system drag coefficient (C_{Ds}). Just writing the equations for lift and drag requires keeping track of both port and starboard components. For the sake of simplicity in this introductory volume, I have studied the augmentor wing performance at the system level assuming that port and starboard components are equal. Still in all, the lift and drag equations are lengthy because you have

$$C_{Ls} = C_{L-airframe} + C_J \sin\left(\alpha + \delta_{flap}\right) + C_\mu \sin\left(\alpha + \delta_{aileron}\right) + C_{T-J85} \sin\left(\alpha + \delta_{thrust}\right) \tag{3.88}$$

and

$$C_{Ds} = C_{D-airframe} - C_J \cos\left(\alpha + \delta_{flap}\right) - C_\mu \cos\left(\alpha + \delta_{aileron}\right) - C_{T-J85} \cos\left(\alpha + \delta_{thrust}\right) \tag{3.89}$$

where the angle of attack (α) is referenced to the fuselage waterline. Do not forget that all the coefficients are based on flightpath velocity (V_{FP})—so dynamic pressure is (q_{FP})—and wing area (S_w). You might also keep in mind that the takeoff and landing configurations are definitely different, so the influence of no less than six parameters must be examined in a very thorough experiment—the objective being to optimize the aircraft's STOL performance with all engines operating and with one engine inoperative (OEI). The NASA and de Havilland team really just got to the tip of the iceberg with two entries in NASA's NFAC facility.

Let me start with one example of the landing configuration first, which is the experimental data including a comparison with Schairer's theory shown in Fig. 3-75. Then I will proceed to one example of performance for a takeoff configuration as shown in Fig. 3-76.

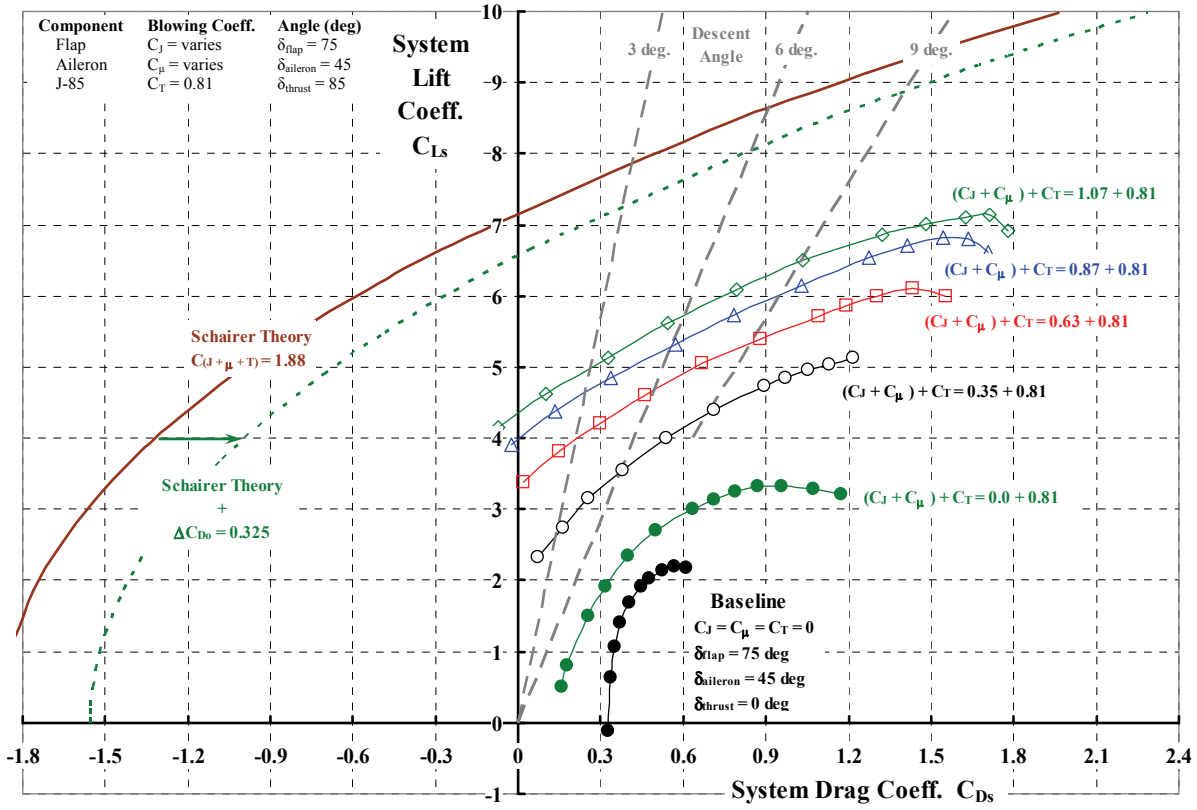

Fig. 3-75. Landing performance of the de Havilland augmentor wing model. Flap deflection is 75 degrees; J-85 thrust coefficient is 0.81.

Performance data for de Havilland's augmentor wing aircraft in the landing configuration is shown in Fig. 3-75. This graph conveys several important points. The most important point is the influence of blowing air over the complete wingspan (i.e., $C_J + C_\mu$ increases in magnitude), and holding the cruise engine thrust (C_T) constant at 0.81 illustrates the aerodynamic feasibility of the concept. While Don Whittley had suggested that wing lift coefficients in the presence of blowing air needed to be about 6 for the "ultra" STOL, the augmentor wing concept offered system lift coefficients (C_{Ls}) of at least 6 to 7 at very steep descent angles. This 42.16-foot-wingspan model was considered to be a 0.53-scale model of the full-size C-8 Buffalo research aircraft, which had a span of 78.75 feet and a wing area of 865 square feet. The C-8 Augmentor Wing Research Aircraft (AWRA) was expected to land at a flightpath velocity of 50 to 65 knots at a gross weight of 43,000 pounds. When you think about it, 50 knots resolved into X and Y velocities at a descent angle of 9 degrees means a descent velocity of 7.82 knots or 13.2 feet per minute or, more importantly, 790 feet per second. If you refer back to Fig. 3-1 on page 330, you will see that 50 knots at 760 feet per second is right at the limits of the design envelope. Certainly this qualifies the adjective in "ultra" STOL. At 50 knots on a standard day, you have a flightpath dynamic pressure (q_{FP}) of 8.47 pounds per square foot, which results in a system lift coefficient of 5.86. To me, this says the de Havilland augmentor wing concept had been proven by wind tunnel testing to be worth pursuing with a flight research aircraft, and that is exactly what happened as you will read shortly.

You might note on Fig. 3-75 that the model of the augmentor wing concept fell far short of what George Schairer's theory said was ideal performance.

Now let me discuss the takeoff performance chart shown in Fig. 3-76. For takeoff the flaps were set at 50 degrees, and the J-85 cruise engines exhausted straight aft at a thrust coefficient of 1.46. This configuration moved the performance into the negative drag quadrant of the longitudinal performance chart. Furthermore, the augmentor wing appears to have exceptional capability to climb at a very steep angle following liftoff. Suppose, for example, that the liftoff speed of the contemplated research aircraft was 50 knots, and the takeoff gross weight was 45,000 pounds. At sea level, standard day conditions, the system lift coefficient would be 6.13 and, from Fig. 3-76, the climb angle would be about 6 degrees, assuming the full system thrust coefficient of $C_{J+\mu+T} = 2.47$ (i.e., the green line with diamond symbols). To clear a 50-foot obstacle at the 6-degree climb angle would require about 475 feet, and this would take about 5.6 seconds at 50 knots. Now suppose that Schairer's ideal performance was reached by some magic of "advanced technology." This would allow a climb angle of about 11 degrees, which means the ground distance would be reduced to 257 feet.

From this example, you can see that liftoff speed and climb angle are major variables when it comes to talking about a STOL takeoff. An "ultra" STOL needs a large ratio of thrust (i.e., power) to weight to accelerate to a liftoff speed in a short ground run. Then it needs a high-liftoff system lift coefficient so that the liftoff speed is low. And then a very large negative system drag coefficient (i.e., positive propulsive force coefficient and power) is needed to get to a steep climb angle to clear the 50-foot obstacle.

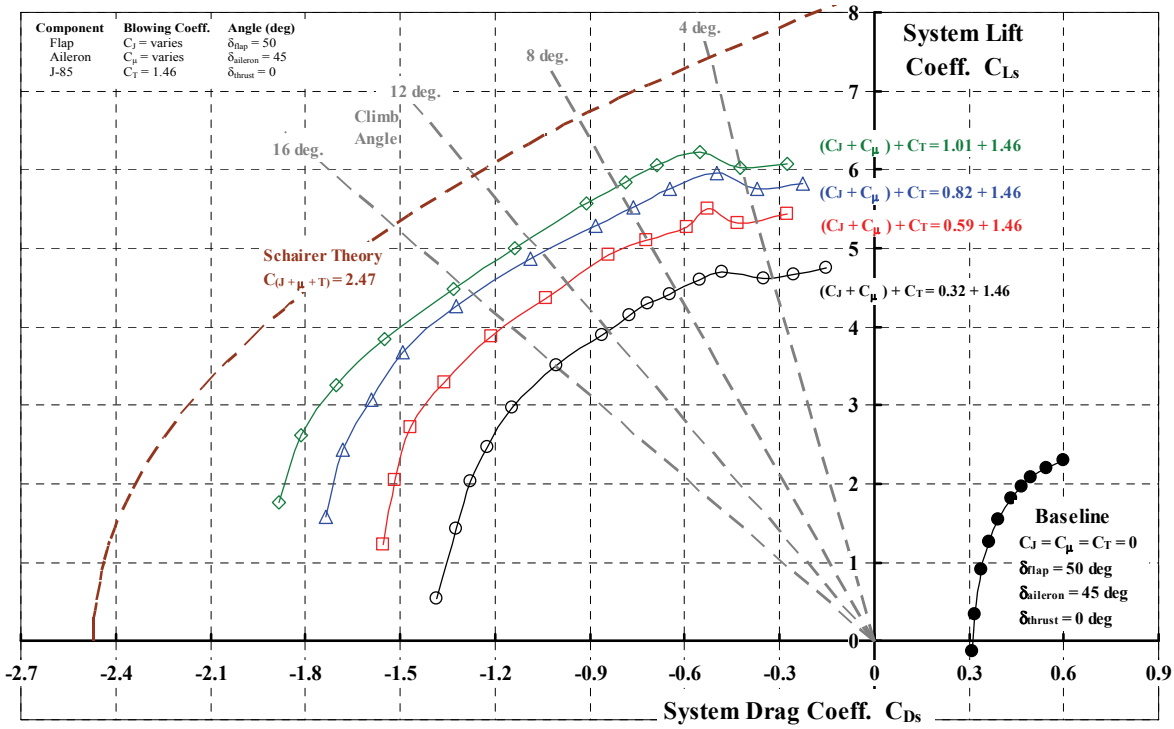

Fig. 3-76. Takeoff performance of the de Havilland augmentor wing model. Flap deflection is 50 degrees; J-85 thrust coefficient is 1.46.

The next step in the augmentor wing aircraft proof-of-concept program was to build a research aircraft—a technology demonstrator, if you prefer. This aircraft, shown in Fig. 3-77 and Fig. 3-78, was first known as the Buffalo/Spey research aircraft and was later called the C-8A AWRA. The de Havilland C-8A AWRA was created from a C-8A Buffalo. In their flight test report [476] covering "the first 8 months of proof-of-concept testing of the aircraft in STOL configuration," Hervey Quigley, Bob Innis, and Seth Grossmith wrote in the introduction:

> "A cooperative NASA/Canadian Government research program on the augmented jet flap concept began in 1965. The program included analysis and small-scale static and wind-tunnel tests (ref. 5); large-scale tests in the Ames 40- by 80-Ft Wind Tunnel (refs. 6-8) conducted by NASA in cooperation with the Canadian Defense Research Board using a de Havilland built model; and NASA design feasibility and simulator studies. Research progress by early 1970 warranted development of a proof-of-concept aircraft to test the jet STOL principle in flight. The U.S. and Canadian Governments entered into an international agreement whereby the NASA and the Canadian Department of Industry Trade and Commerce (DITC) would modify a de Havilland C-8A Buffalo to an augmented jet flap STOL research aircraft. The DITC contracted with the de Havilland Aircraft of Canada, Ltd., and their subcontractor, Rolls-Royce of Canada, Ltd., to provide and modify the jet engines and modify the nacelles. The NASA contracted with The Boeing Company to modify the aircraft, provide the augmented jet flap system, install the propulsion system, and perform the initial flight tests. Reference 9 [477, 478] summarizes the contractor development program and describes the augmented jet flap STOL research aircraft.
>
> The C-8A Buffalo aircraft was chosen on the basis of a design feasibility study, which showed that with required aircraft modifications, the primary research objective could be achieved at a reasonable cost and within an acceptable time span. In addition, considerable design data were available from extensive testing in the Ames 40- by 80-Ft Wind Tunnel of a large-scale model having a wing planform similar to the C-8A (refs. 6-8) [447-449]. (Simulation inputs to the development of the aircraft are discussed in refs. 10-12.)
>
> The first flight of the aircraft was made on May 1, 1972, at Seattle, Washington. The initial airworthiness flight test program was conducted by The Boeing Company (ref. 13) [478]. During these tests the aircraft was flown within a flight envelope of from 50 to 180 knots and at load factors sufficient to demonstrate that the aircraft flight loads were within design and the airplane flutter free. The aircraft was delivered to NASA on July 31, 1972."

Fig. 3-77. The C-8A AWRA made its first flight on May 1, 1972.

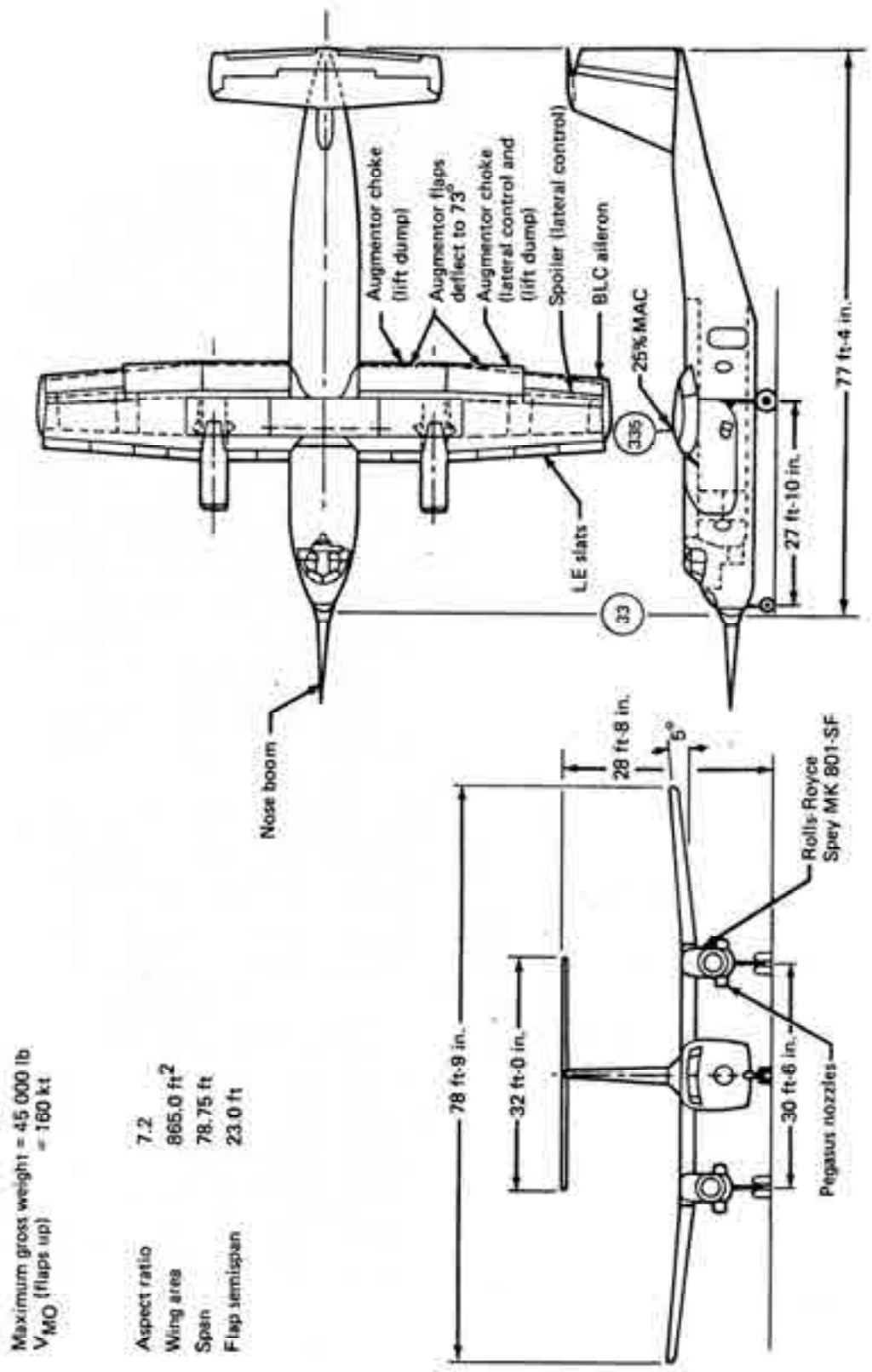

Fig. 3-78. The maximum takeoff gross weight of the C-8A AWRA was 45,000 pounds [477].

The C-8A AWRA was created from a standard de Havilland C-8A Buffalo (initially in service as the U.S. Army CV-7A, de Havilland DHC-5, or U.S. Air Force C-8A), which was delivered to Boeing for modification weighing 25,255 pounds, empty. Boeing's summary report [477] states that 11,138 pounds were removed to give a "stripped" configuration as the starting point. From this stripped configuration, you have the weight statement shown in Table 3-3. The items added back into the stripped aircraft are listed in Table 3-4. You might note that de Havilland, which was responsible for the propulsion system, installed the modified Rolls-Royce (of Canada) Spey engines with Pegasus nozzles for slightly over 7,000 pounds. Boeing (Seattle), which was responsible for the wing, spent 1,800 pounds just for the augmentor duct system and another 1,600 pounds for the flaps.

Table 3-3. The C-8A AWRA Weight Statement [477]

Item	Weight (lb)
"Stripped" configuration	14,117
DHC additions	9,357
Boeing additions	7,233
Trapped fuel	110
Engine oil	28
Weight empty	**30,845**
Pilot and copilot	400
Operating weight empty	**31,245**
Flight test equipment	1,320
Fuel	12,435
Design takeoff gross weight	**45,000**

Table 3-4. Items Added Back Into the "Stripped" C-8A AWRA [477]

DHC Additions	Weight (lb)		Boeing Additions	Weight (lb)
Inlet	132		Flaps	1,604
Upper cowl	193		Ailerons	262
Lower cowl	486		Spoilers	63
Aft fairing	38		Leading edge	800
Fixed structure	570		Trailing-edge shroud	169
Engine mount	274		Flap supports	500
Firewall	45		Aileron supports	50
Systems	412		Wingtips	15
Nozzle actuation	163		Hydraulics	825
Spey with Pegasus nozzles	7,044		Electrical and electronics	250
Total DHC additions	**9,357**		Instruments and flight deck	75
			Flight controls	400
			ECS	30
			Fuel system	–175
			Augmentor duct system	1,800
			Nose boom	115
			Main gear modifications	250
			Fuselage modifications	50
			Paint	150
			Total Boeing additions	**7,233**

Based on these weight statements, you would have to say that the increment in weight empty for STOL performance (expected to be considerably better than a standard C-8A) was about 6,000 pounds (i.e., 25,255 growing to 30,845) out of a design weight of 45,000 pounds. This is a 23-percent increase in weight empty.

The change in the propulsion system was significant. A standard propeller-driven C-8A in its mid-1960s-era configuration was powered by two General Electric T64-GE-10 turboprop engines, each having a takeoff rating of 2,850 horsepower and weighing about 1,200 pounds. The propellers were three-bladed, 14.5-foot-diameter, Hamilton Standard 63E60-11's, each weighing about 1,000 pounds. The modification replaced the GE engines with Rolls-Royce Spey Mk 801-SF engines and Pegasus MK 5 nozzles. Each engine could produce about 6,100 pounds thrust from the core and 3,450 pounds thrust at takeoff at sea level on a standard day.

This information about engine powers and thrust led me to wonder about VTOL performance versus STOL performance. The takeoff thrust of two propellers on a standard C-8A must be on the order of 20,740 pounds based on simple Figure of Merit theory as follows:

$$(3.90)\quad \mathrm{HP}_{\mathrm{available}} = 0.95\left(2{,}850_{\mathrm{T64}}\right) = \frac{1}{\mathrm{FM}=0.8}\,\frac{\mathrm{T}=10{,}370}{550}\sqrt{\frac{10{,}370}{2\left(\rho=0.002378\right)\left(\mathrm{A}=165\right)}}\,.$$

It would seem then that one Rolls-Royce Spey engine had a takeoff thrust about on a par with one G.E. T64 engine plus one Hamilton Standard propeller. Having satisfied myself on this point, I wondered what size propeller would allow VTOL at 45,000-pound takeoff gross weight with two engines, each rated at 2,850 horsepower. The answer, using Eq. (3.90), is two 46.4-foot-diameter proprotors. These two proprotors would, of course, have to be spaced along a wing having a span of 78 feet, 9 inches, in such a manner as to leave space for a fuselage. Of course, you might imagine a four-proprotor configuration, in which case the diameter of each proprotor would be 32.8 feet, and the proprotors would have to be tiltable in some manner to avoid the blade tips striking the ground during VTOL operations.

The joint program that de Havilland, NASA Ames, and Boeing put together might easily be a model for any technology demonstrator effort. The Boeing summary report [477] states that a contract was awarded to Boeing on July 1, 1970, and the aircraft was delivered to NASA Ames on July 31, 1972. *Flight International* reported [479, 480] that of the $9 million spent on the effort, $4.5 went to Boeing to make the augmentor wing and aircraft conversion, and $3 million was paid to de Havilland and Rolls-Royce for the power plant and its modifications. Presumably, NASA received the remaining $1.5 million from the Canadian Department of Industry, Trade, and Commerce. You might now ask, Just what STOL performance did this augmentor wing research aircraft demonstrate for $9 million? The results of the 1-month Boeing flight qualification effort were reported by Skavdahl and Patterson [478], and the 8 months of flight testing by NASA were reported by Hervey Quigley, Bob Innis, and Seth Grossmith in reference [476]. From these two reports, you have a very comprehensive picture of the aircraft's performance and handling qualities with both engines operating and, much more importantly, the aircraft's behavior with one engine inoperative.

Table 3-5. STOL Takeoff and Landing Performance [476]

Takeoff Parameters	Values		Landing Parameters	Values
Gross weight (max), lb	45,000		Gross weight (max), lb	43,000
Engine thrust, percent	99		Engine thrust, percent	93
Flap deflection, deg	30		Flap deflection, deg	65
Aileron droop, deg	17		Aileron droop, deg	30
Nozzle position, deg	6		Nozzle position, deg	80
Rotation speed, kts	65		Approach speed, kts	65
Liftoff speed, kts	75		Touchdown speed, kts	60
Climb speed, kts	86		Ground roll distance, ft	840
Climb angle, deg	16		Total distance over a 35-ft obstacle, ft	1,200
Ground roll distance, ft	700			
Total distance over a 35-ft obstacle, ft	1,100			

The performance data is of most interest in this introductory volume because the aircraft was quite safe to fly as you will see by reading both reports at your leisure. The NASA authors included a summary of the aircraft's STOL performance in table 10 of their report, which I have reproduced here as Table 3-5.

The NASA authors provided the total distance over a 35-foot obstacle for 23 takeoffs in their figure 77. I have reproduce their data here, in a slightly different form, as Fig. 3-79 and added my theory, which will be discussed shortly. Note that the ground roll distance at a takeoff gross weight of 45,000 pounds from Table 3-5 is also shown. In discussing this data, the NASA authors wrote:

> "A compilation of several takeoffs in figure 77 shows the effect of takeoff weight on the distance required to clear 35 ft (10 m). These data were corrected for wind conditions but not temperature. Large variations in performance are present, as expected, but a lower boundary is fairly well defined. The data show that the performance is about as predicted (ref. 10) [481].

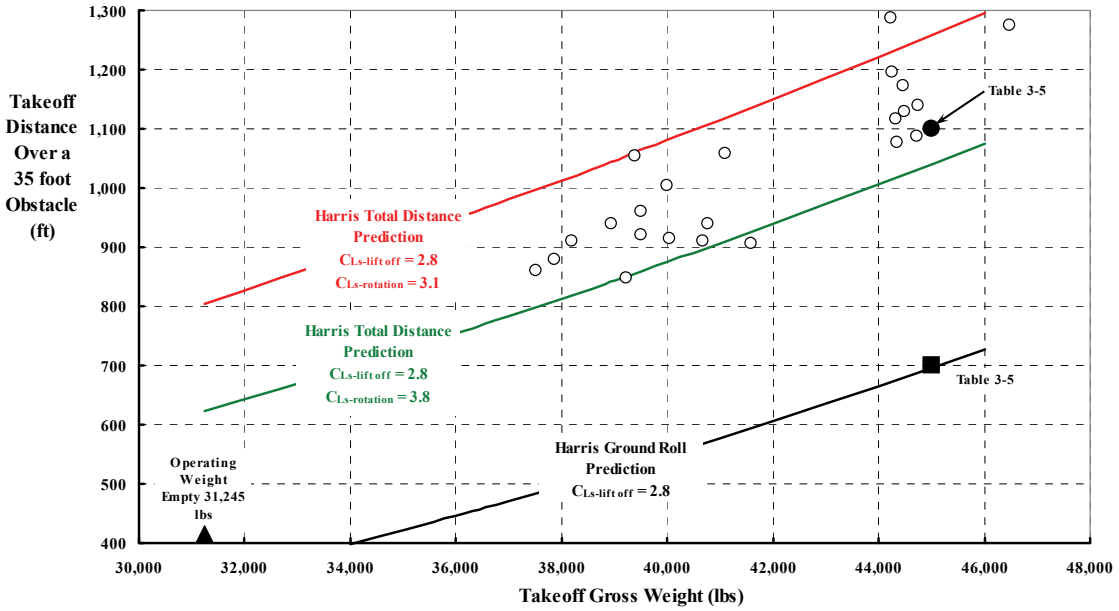

Fig. 3-79. Takeoff performance is always accompanied by data scatter.

> During these tests no attempt was made to determine the optimum flap deflection for minimum takeoff performance; 30° flap deflection was chosen as the nominal takeoff flap deflection for engine considerations.
>
> Except for the rapid rotation necessary for these takeoffs and the poor visibility over the nose of the aircraft during the initial climb, the pilots considered the takeoffs comfortable, with little change in control techniques required for STOL operation."

In Fig. 3-79 you see my predictions of the C-8A AWRA flight test data obtained by NASA Ames [476]. Let me discuss these results. There were, in fact, 23 carefully documented STOL takeoff data points obtained with the Fairchild camera records. From time-lapse photographs (like Fig. 3-80 below) combined with aircraft instrumentation, technicians were able to produce time histories of a takeoff such as the one you see in Fig. 3-81 and Fig. 3-82. I reproduced these two figures from figure 75 of reference [476].

There is a great deal to be learned from this time history data that you have before you. To begin with, you can see from Fig. 3-81 that I have estimated the velocity between 0 and 115 feet per second (68 knots) with a simple linear extrapolation from the recorded data. In addition, I have estimated the aircraft acceleration by curve fitting the velocity and then taking the derivative of the velocity curve fit equation with respect to time (i.e., dV/dt). These estimates mean that the ground roll distance can be calculated assuming a constant acceleration and using the classical equation $F = ma = (W/g)a$.

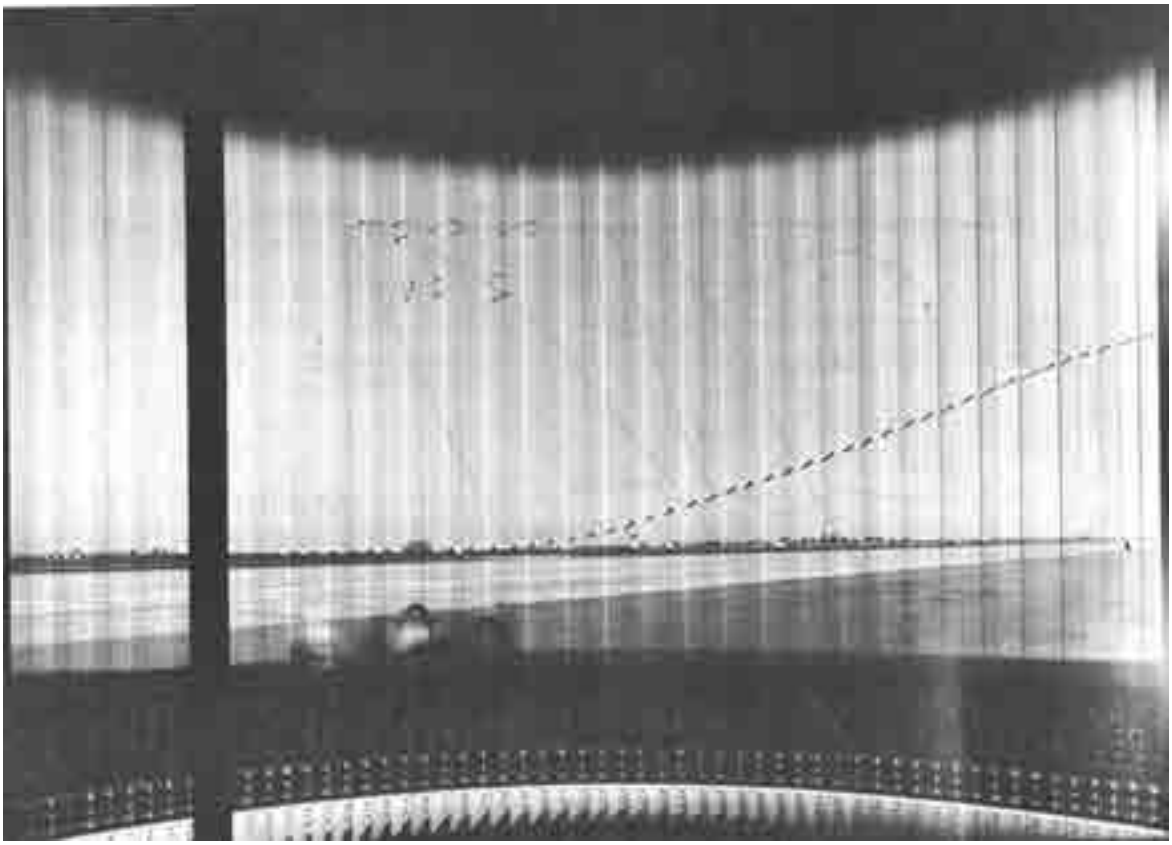

Fig. 3-80. One example of the Fairchild camera time-lapse photography of a takeoff.

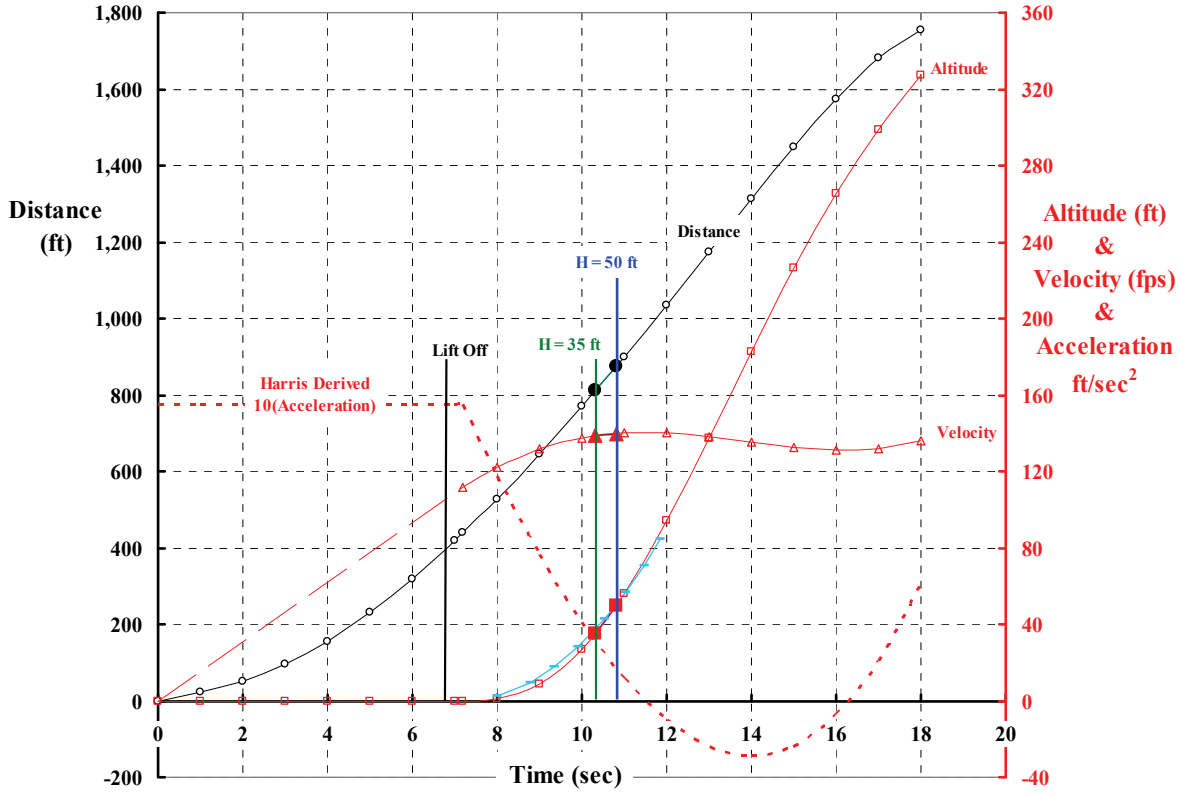

Fig. 3-81. Typical takeoff time history data. Takeoff gross weight (TOGW) of 39,220 pounds, flaps deflected to 30 degrees, engine speed at 99 percent (thrust about 9,550 pounds from each engine).

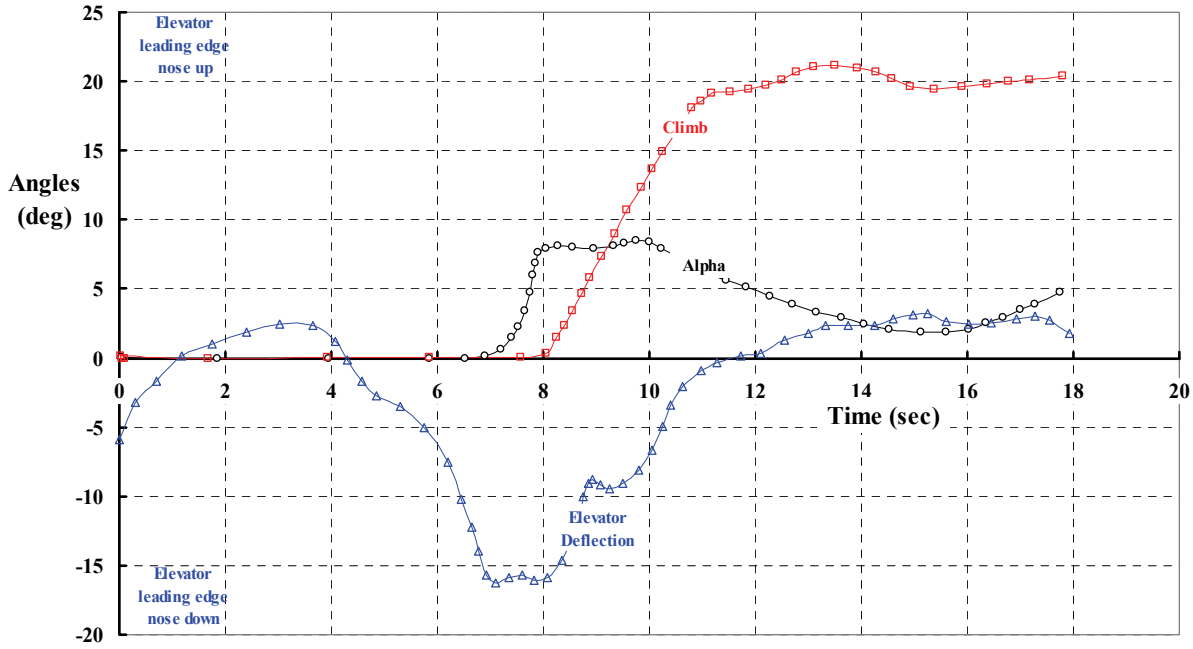

Fig. 3-82. Additional typical takeoff time history data.

If you assume the ground run is performed at a constant acceleration as suggested by the distance-versus-time line on Fig. 3-81, simple physics says that

$$(3.91)\quad D_{grd.roll} = \frac{1}{2} a_{ave} t^2 = \frac{1}{2} \frac{V_{liftoff}^2}{a_{ave}} \quad \text{and} \quad F_{net} = \frac{TOGW}{g} a_{ave} .$$

Now Table 3-5 quotes the liftoff velocity as 75 knots (126 feet per second) and the ground roll distance as 700 feet. This translates to an average horizontal acceleration of 11.34 feet per second squared using Eq. (3.91). The implication is that average propulsive force during the ground roll is about 15,700 pounds. The no-wind liftoff speed of 75 knots suggests the system lift coefficient is on the order of

$$(3.92)\quad C_{Ls-liftoff} = \frac{TOGW}{q_{liftoff} S_w} = \frac{45{,}000}{\left(75^2/295\right)865} = 2.78 .$$

Suppose now that the system lift coefficient is the design constant for all takeoff gross weights, and suppose the propulsive force available is at a maximum and is constant at that maximum regardless of gross weight and speed; then it follows that

$$(3.93)\quad \begin{aligned} D_{grd.\,roll} &= \frac{1}{2} \frac{\rho V_{liftoff}^2}{\rho a_{ave}} = \frac{q_{liftoff}}{\rho} \frac{TOGW}{g F_{net-available}} \\ &= \frac{1}{\rho} \left(\frac{TOGW}{S_w C_{Ls-liftoff}} \right) \frac{TOGW}{g F_{net-available}} = \frac{TOGW^2}{\rho g S_w C_{Ls-liftoff} F_{net-available}} \end{aligned} .$$

Now consider the horizontal distance traveled after liftoff and climbing to clear an obstacle. This horizontal distance traveled depends primarily on the time, after liftoff, that it takes to clear the obstacle, which I will name (T_{obs}). This maneuver is a transient one that is very dependent on pilot technique, which is the primary reason for the data scatter in Fig. 3-79. You see in Fig. 3-82 that the C-8A AWRA maneuver begins with the pilot pulling aft on the longitudinal control to drop the elevator's leading edge and create an elevator negative lift. This negative lift times a moment arm creates an aircraft nose-up pitching moment. The C-8A AWRA, having a tricycle landing gear, rotates about the main landing gear wheels as the nose wheel leaves the ground.[115] As a result of pilot input, the aircraft angle of attack is substantially increased (perhaps to a recommended angle), the aircraft lift is increased beyond that required for just supporting the takeoff gross weight, and a vertical acceleration is obtained. And so the aircraft lifts off and transitions to a climb angle that increases with time in a nearly linear manner. This transient maneuver is not very repeatable when controlled by a human.

From Fig. 3-81 you see that the altitude above ground increases in a parabolic manner, which suggests that the vertical acceleration (a_Z) is a constant and that altitude (H_t) therefore increases as

[115] This maneuver raises many questions about the control power to create the rotation and the aircraft's geometry providing clearance before the rear of the aircraft strikes the ground. These are major design issues.

(3.94) $H_t = \frac{1}{2} a_Z \left(t - t_{\text{liftoff}} \right)^2$.

The vertical acceleration for the C-8A AWRA, at a takeoff gross weight of 39,220 pounds during this maneuver, can be calculated. Think about it this way. During the time frame between about 7.2 seconds when liftoff occurs (i.e., t_{liftoff} = 7.2 seconds) and 10.2 seconds—a time span of 3 seconds—the aircraft gains 35 feet in height above the ground. During this time period, the aircraft lift must be greater than the takeoff gross weight by some average lift increment (ΔL_{ave}). Thus, the vertical acceleration must be on the order of

(3.95) $a_Z = \frac{2H_t}{\left(t - t_{\text{liftoff}} \right)^2} = \frac{2(35)}{3^2} = 7.8 \text{ ft/sec}^2$.

Turning again to F = ma, the additional lift force over and above the takeoff gross weight must therefore be

(3.96) $F_Z = \Delta L_{ave} = \left(\frac{TOGW}{g} \right) a_Z = \left(\frac{39,220}{g} \right) 7.8 = 9,500 \text{ pounds}$.

This result says that after rotation to about an 8-degree angle of attack, the C-8A AWRA was operating at a system lift coefficient of

(3.97) $C_{Ls-rotation} = \frac{TOGW + \Delta L_{ave}}{\left(\frac{1}{2} \rho V_{\text{liftoff}}^2 \right) S_w} = \frac{39,220 + 9,500}{\left[\frac{1}{2} (0.002378)(111)^2 \right] (865)} = 3.84$.

Note that at 39,220 pounds and at 65 knots, the system lift coefficient is 2.88. However, the real capability of the C-8A AWRA depends on a system lift coefficient being slightly over 3.8. While this might not be close to the aircraft's maximum system lift coefficient of about 6, it represents a prudent margin for gusts, engine failure, etc.

Suppose the aircraft's takeoff design criteria is based on the system lift coefficient after rotation ($C_{Ls\text{-}rotation}$). Then the average incremental lift (ΔL_{ave}) will depend on the difference between this available lift and the takeoff gross weight. That is,

(3.98) $\Delta L_{ave} = C_{Ls-rotation} \left(\frac{1}{2} \rho V_{\text{liftoff}}^2 \right) S_w - TOGW$,

and the vertical acceleration can be established as

(3.99) $a_Z = \frac{g}{TOGW} \Delta L_{ave} = \frac{g}{TOGW} \left[C_{Ls-rotation} \left(\frac{1}{2} \rho V_{\text{liftoff}}^2 \right) S_w - TOGW \right] = g \left[\frac{C_{Ls-rotation}}{C_{Ls-liftoff}} - 1 \right]$,

which makes the vertical acceleration totally dependent on the selected values of the liftoff system lift coefficient and the rotation system lift coefficient. These values might be thought of as design goals, and later they would find their way, probably as a chart, into the Flight Manual.

The objective of the preceding discussion and associated equations has been to obtain an estimate for the time (T_{obs}) at which the obstacle is cleared. That time depends on the height of the obstacle and the vertical acceleration obtained from Eq. (3.99). Thus, Eq. (3.95) becomes

$$(3.100)\ T_{obs} - t_{liftoff} = \sqrt{\frac{2H_{obs}}{a_Z}} = \sqrt{\frac{2H_{obs}}{g\left[\frac{C_{Ls-rotation}}{C_{Ls-liftoff}} - 1\right]}}.$$

You should now be suspecting my next simplifying approximation. To keep things easy, I will assume that the aircraft continues after liftoff at a ground speed equal to the velocity at liftoff. Then the total distance to clear the obstacle will be

$$(3.101)\ D_{Total} = D_{grd.roll} + V_{liftoff}\left(T_{obs} - t_{liftoff}\right) = D_{liftoff} + V_{liftoff}\sqrt{\frac{2H_{obs}}{g\left[\frac{C_{Ls-rotation}}{C_{Ls-liftoff}} - 1\right]}}.$$

It is, of course, a nonconservative assumption that the speed after liftoff remains constant at $V_{lift\ off}$ because Fig. 3-81 shows that by the time the 35-foot obstacle is cleared, the speed has increased from 111 feet per second at liftoff up to about 130 feet per second.

The final takeoff distance (D_{Total}) can now be written because you know the liftoff velocity is calculated based on $C_{Ls\text{-}lift\ off}$, and you know the ground run distance to liftoff from Eq. (3.93). Therefore,

$$(3.102)\ D_{Total} = \frac{g}{\rho}\frac{TOGW^2}{\left(S_w C_{L-liftoff} F_{net}\right)} + \sqrt{\frac{2}{\rho}\left(\frac{TOGW}{S_w C_{L-liftoff}}\right)}\sqrt{\frac{2H_{obs}}{g\left(\frac{C_{Ls-rotation}}{C_{L-liftoff}} - 1\right)}},$$

and there you have my approximation for calculating takeoff distance over an obstacle of any height (H_{obs}). There are, of course, many, many other approaches and approximations to the STOL takeoff problem that you might want to consider.

Let me add a note about the propulsive force (F_{net}). I solved for this force based on the data in Table 3-5 and using Eq. (3.91). At 45,000 pounds takeoff gross weight, the average acceleration came out at 11.65 feet per second squared. Therefore the force, following $F_X = ma_X$, comes out at 15,720 pounds, which you might recall is about 70 percent of the 22,800 pounds thrust that a pair of Rolls-Royce Spey engines gave in the test cell. The thing to keep in mind is that some of the engine thrust is given up to provide boundary layer control to the flaps and ailerons as this simple sketch suggests (Fig. 3-83). Furthermore, as soon as the aircraft begins its ground roll, aircraft drag in the form of rolling friction detracts from the engine thrust. Then, aircraft aerodynamic drag and engine ram drag (see footnote next page) build up with velocity. In short, it appears that using 100 percent of the jet engine manufacturer's quoted static takeoff thrust for the takeoff calculation of powered lift STOL

configurations would be widely optimistic when determining ground roll distance during the conceptual design phase.[116]

Naturally you want some confidence in my simplistic result. Fig. 3-79 showed that the scatter can be bracketed solely on the basis of two system lift coefficients. In my experience, pilots will control the aircraft during the ground roll in a very repeatable manner up until the liftoff speed is reached. But then the rotation to an aircraft angle of attack for climb is probably done in a very unrepeatable manner. The variations in flight control motions between pilots, and even for an individual pilot on any given day, can hardly be expected to be repeatable. Such is the life when analyzing experimental data that contains a transient.

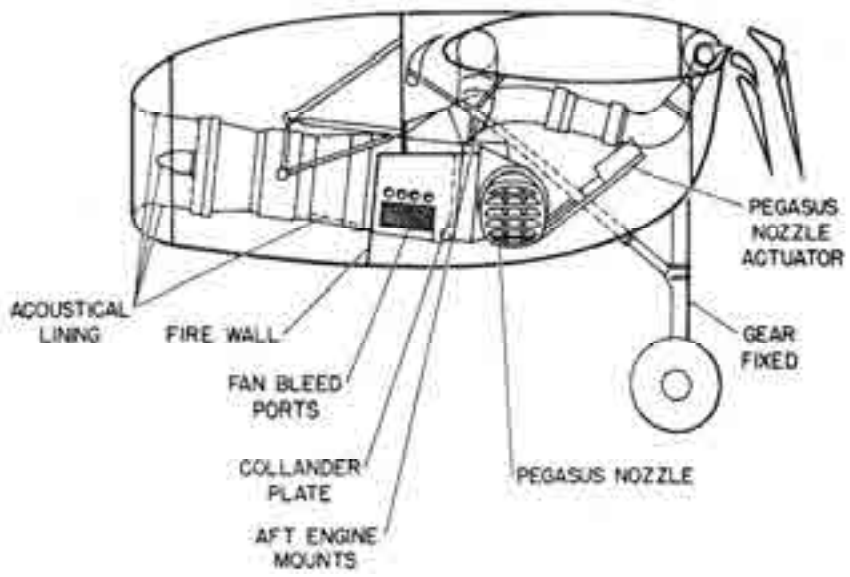

Fig. 3-83. Installation of the Rolls-Royce Spey MK 801 Split Flow engine with the vectorable nozzle from a Pegasus engine [481].

[116] Jet engine experts consider engine net thrust defined by $F_{net} = (\dot{m}_{air} + \dot{m}_{fuel}) V_{jet} - \dot{m}_{air} V_{FP}$. Ram drag is the $\dot{m}_{air} V_{FP}$ term and is sometimes called the inlet momentum drag. I learned this (again) after bothering Mike Scully with a thermodynamics question. Though he kindly did not express (out loud) his frustration with me, he told me to buy the book [482] by Nicholas Cumpsty (a British professor at the University of Cambridge) titled *Jet Propulsion: A Simple Guide to the Aerodynamic and Thermodynamic Design and Performance of Jet Engines* and read it. You will find Professor Cumpsty's discussion of ram drag on pages 26 and 83.

The Boeing reports [477, 478] provide a wealth of engineering data and led Boeing to the conclusion that the C-8A AWRA was "demonstrated to be airworthy." There is one key graph from these reports that you should see before I close this discussion. The forward-flight performance of the aircraft in its cruise configuration—but with landing gear not retracted—is shown in Fig. 3-84.

Now let me go back to the era when the baseline aircraft was propeller driven and STOL performance was the objective.

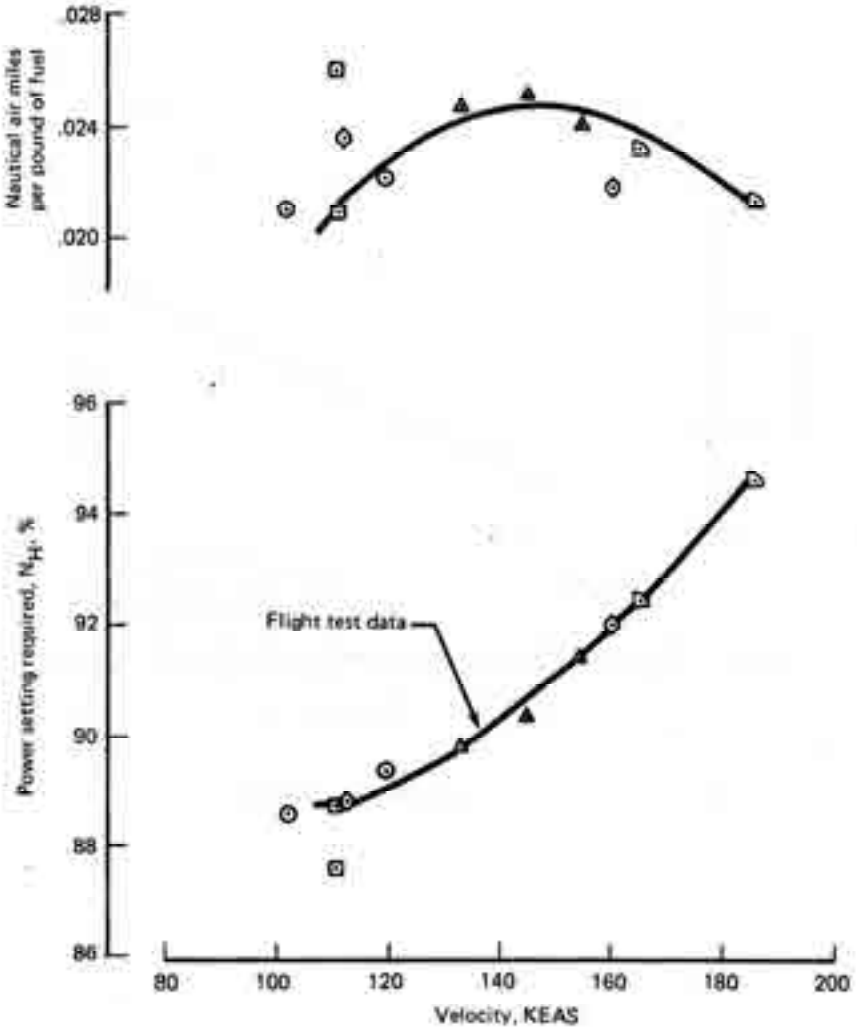

Fig. 3-84. The C-8A AWRA demonstrated that key principles of powered lift and cruise performance were not severely compromised [478]. Data was for a gross weight of 40,000 pounds. Note that the landing gear could not be retracted.

3.4 MODEL TEST OF THE FAIRCHILD C-123—2 PROPS

An examination of the lift and drag aerodynamic characteristics of the 0.4-scale-model C-123 (Fig. 3-9) must begin with a very fundamental baseline. For this discussion, I have chosen one baseline configuration from the initial model testing conducted at Langley Research Center [410]. This starting point had the *two nacelles on* but with the propellers off and with the horizontal stabilizer (i.e., the tail) incidence set at –3 degrees. The flaps and ailerons were set to zero deflection. For the second baseline, I selected the configuration closest to what Ames Research Center started with after they received the model from Langley [411]. The Ames testing began with the *two nacelles off*, the propellers off, a tail incidence of –3 degrees, and the flaps and ailerons set to zero deflection. This, unfortunately, complicates the comparison of baselines and makes it difficult to ever make an exact comparison between model and full scale, but that was not the researchers' objective. I only made these baseline comparisons as something that might be of interest to you. For the discussion here, it is the test results from Ames Research Center [411-413] that are of primary importance. (However, you should know that the Langley report [410] has a number of very interesting data in it such as the spanwise distribution of normal force coefficient. The Ames report [411] adds chordwise pressure distribution data at several spanwise stations.)

Lift and drag coefficient baseline data for the 0.4-scale-model Fairchild C-123 is shown in Fig. 3-85 and Fig. 3-86. Notice that I have also included the Ames data when the

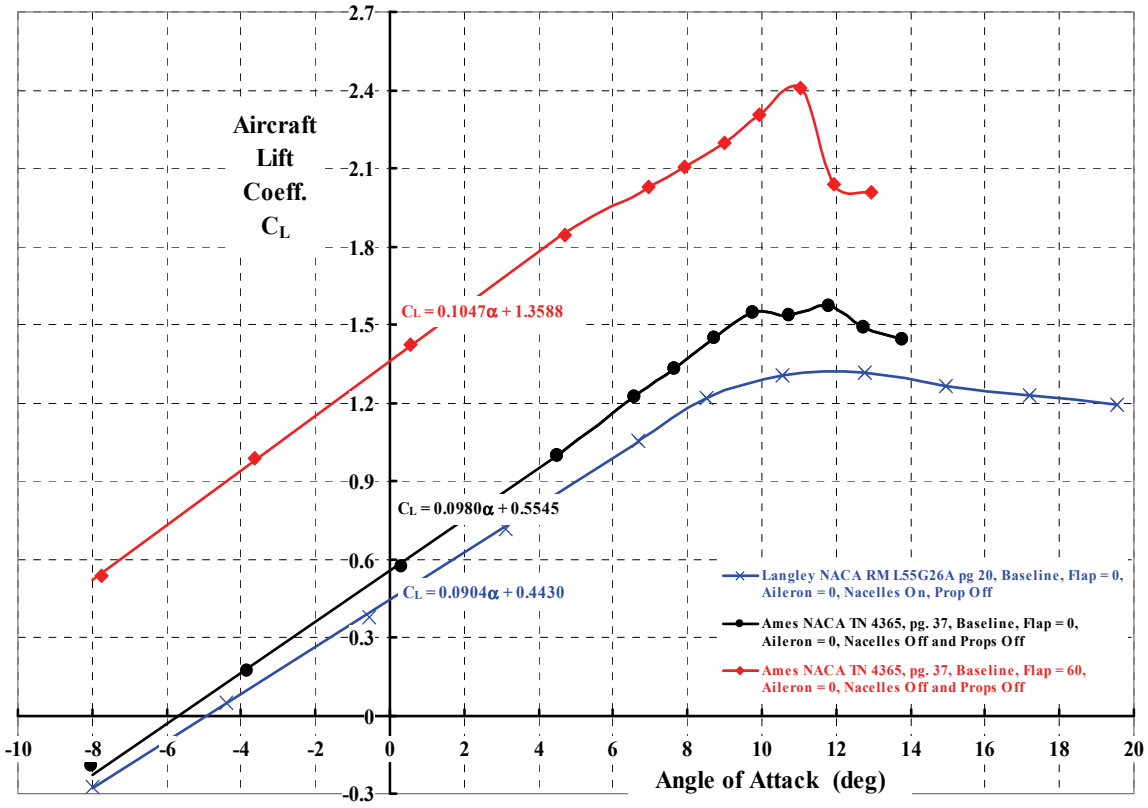

Fig. 3-85. Model C-123 lift coefficient versus angle of attack with propellers removed.

flap deflection was 60 degrees. For convenience, I have also added regression analysis results in equation form. Notice on the Ames data in Fig. 3-85 that when the flap is deflected from 0 to 60 degrees, the lift-curve slope ($dC_L/d\alpha$ per degree) increases slightly from 0.098 to 0.1047. This is in line with the linear theory that says that lift from angle of attack (α) and from flap deflection (δ_F) can be added. That is,

$$(3.103)\ C_L = \frac{dC_L}{d\alpha}\left(\alpha + \alpha_{L0} + k\delta_F\right),$$

which, quoting from reference [221], says "that the slope of the lift curve is not significantly altered when the flap is deflected. Rather the C_L versus α is shifted upward when the flap is deflected and remains parallel to the original C_L-versus-α curve of the wing [at least to the first approximation]." That is certainly the behavior of the flapped *airfoil* as you learned from Fig. 3-13 and Fig. 3-15. Of course, the difficult task is to calculate, or at least estimate, the constant (k) in Eq. (3.103) before preliminary design begins.

The *wing* drag polars shown in Fig. 3-86 that accompany the lift behavior shown in Fig. 3-85 are particularly interesting in my mind because they so closely follow the trend of *airfoil* data you saw earlier. You might consider that a rather trivial statement, but remember that most airplanes do not have flapped airfoils all along the trailing edge. In the case of the model C-123, the flap span is less than one-half of the wingspan. In fact, the total flap area is

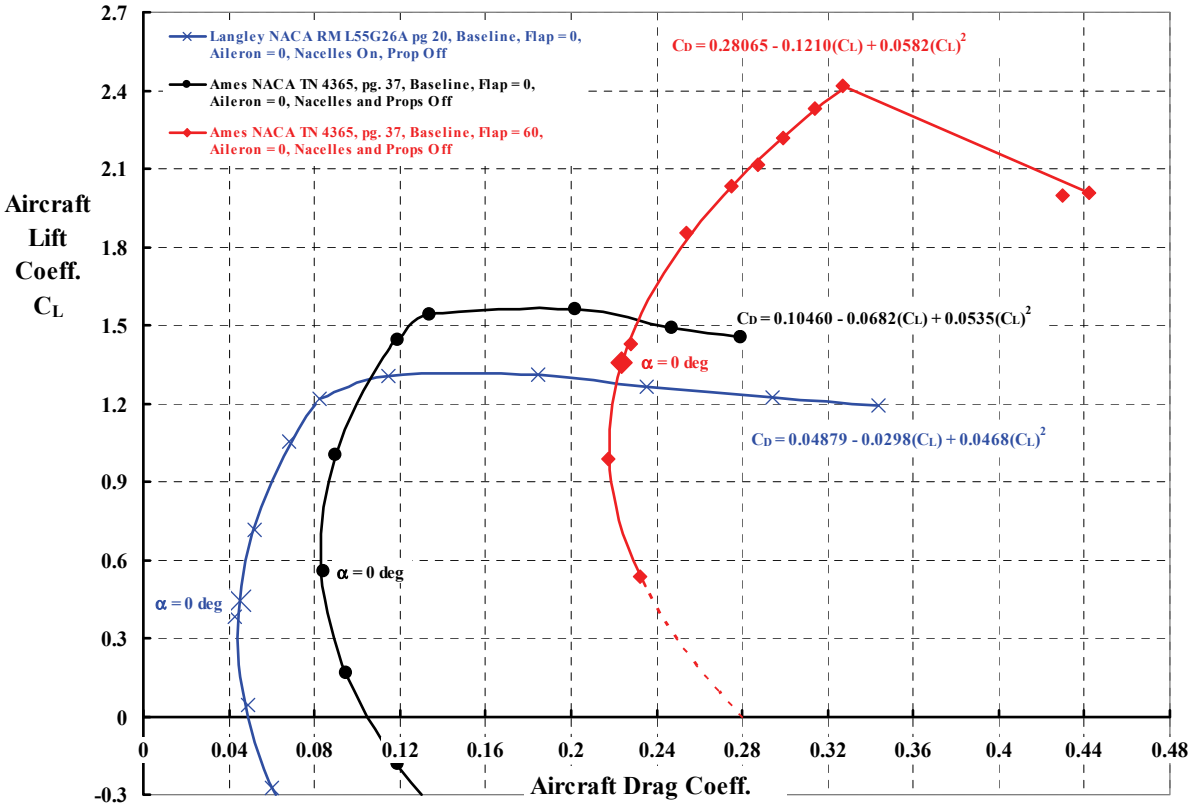

Fig. 3-86. Model C-123 lift-drag polar with propellers removed.

only slightly greater than one-tenth of the total wing area, which you will note from Fig. 3-10. This illustrates that maximum lift capability can be significantly raised without unreasonable modifications to a wing designed for maximum efficiency in cruise flight.

Prior to the onset of wing stall, the three aircraft drag polars shown in Fig. 3-86 follow the classical parabolic behavior. Should it be of value in the future, the regression analysis "curve fits" up to stall onset are as follows:

$$C_D = 0.0488 - .0298\,C_L + 0.04681\,C_L^2 \Rightarrow \text{Langley } \delta_F = 0\,\text{deg}.$$
$$C_D = 0.1046 - .0682\,C_L + 0.05345\,C_L^2 \Rightarrow \text{Ames } \delta_F = 0\,\text{deg}.$$
$$C_D = 0.2806 - .1210\,C_L + 0.05818\,C_L^2 \Rightarrow \text{Ames } \delta_F = 60\,\text{deg}.$$

Remember that drag coefficient is calculated as $C_D = D/q_{FP}S_W$ where the dynamic pressure (q_{FP}) is based on the flightpath velocity (V_{FP}), and the wing area (S_W) for the model C-123 is 206.6 square feet.

The ideal-induced-drag portion of the aircraft drag coefficient is dependent on the lift-coefficient squared and the wing aspect ratio (AR), so you have

$$(3.104)\quad C_{Di} = \frac{C_L^2}{\pi AR}$$

and, because the model C-123 aspect ratio is 9.71 according to Fig. 3-10, you have an ideal-induced-drag coefficient of $C_{Di} = 0.03278\,(C_L)^2$.

The initial testing of the 0.4-scale model of the Fairchild C-123 was reported by Ames Research Center in early July [411]. It appears that this initial exploration, which examined boundary layer control (BLC) with suction, convinced the researchers that BLC by blowing showed more promise, so a second test entry was undertaken. This testing [412] concentrated first on the influence of propeller thrust on the model's lift, drag, and pitching moment coefficient. The sum of thrust from the two propellers was designated simply as (T), and this thrust sum—*when nondimensionalized by the wind tunnel dynamic pressure (q_{FP}) and the model's wing area*—was designated by T_C'. In the discussions that follow, I think it is clear enough after dropping the prime to say that

$$(3.105)\quad T_C = \frac{\text{Left } T_P + \text{Right } T_P}{\left(\frac{1}{2}\rho V_{FP}^2\right)S_W}.$$

It is worth a moment to discuss the propellers and the measurement of T_C. The propeller geometry was discussed by Weiberg and his coauthors [411] who wrote:

> "The propellers were made from four-bladed Aeroproducts propellers (hub designation A-542-B1, blade designation H20-156-23M5) modified by cutting off the tips (no tip planform rounding) to give a propeller diameter of 6.75 feet. The geometric blade characteristics of the modified propellers are shown in figure 5 [Fig. 3-87]. The blade angle at 0.75 blade radius was set at 29.5°. This blade angle was chosen to allow the propellers to absorb the maximum power output of the drive motors at the maximum propeller rotational speed determined from considerations of propeller strength. Both propellers were rotated in a

clockwise direction (viewed from the rear). Each propeller was driven through a gearbox by a variable-speed electric motor. The gearbox and motor were housed in the engine nacelles shown in figure 1(a) [Fig. 3-11].

A calibration was made to determine the propeller thrust for a given condition of tunnel free-stream velocity and propeller rotational speed. The calibration was made with the model with flaps and ailerons undeflected and with the model at the angle of attack for zero lift. Measurements were made of the drag force for various values of propeller rotational speed and tunnel dynamic pressure. The gross propeller thrust (with slip-stream effect neglected) was assumed to be the difference between the measured drag force with propeller operating and with propeller removed. The propeller thrust thus determined was converted to a dimensionless coefficient by means of the relationship T_C' = thrust/$q_\infty S$. The propeller rotational speed was converted to the usual dimensionless form of propeller advance ratio, $J = V_\infty nD$. The variation of T_C' with J is shown in figure 6 [Fig. 3-88] (for the 29.5 blade used in the tests) and for the purposes of this report was assumed to be independent of the angle of flow into the propeller as affected by angle of attack, wing lift, and flap deflection. In the tests, propeller rotational speed and tunnel dynamic pressure were set to give the value of J required (fig. 6) [Fig. 3-88] to obtain the desired thrust coefficient T_C'."

Now for some test results showing how propeller thrust affects aircraft lift and drag.

During this part of the second test at Ames Research Center [412], BLC was turned off, and the lift and drag coefficient results for several propeller thrust levels (T_C) were obtained. Consider first the lift-curve data reproduced here in Fig. 3-89. You can immediately see that the lowest thrust coefficient (i.e., $T_C = 0.15$) has a lift curve that is virtually equivalent to the propellers-off Ames baseline shown as the red diamond data points on Fig. 3-85. Next, notice that the lift curves remain linear up to the onset of stall. From the equations (found by linear regression analysis) listed in the legend, the lift-curve slope ($dC_L/d\alpha$ per degree) increases nearly linearly with propeller thrust. Furthermore, the lift at zero angle of attack (C_L at $\alpha = 0$ degrees) does, in fact, vary linearly with propeller thrust. A little more analysis shows

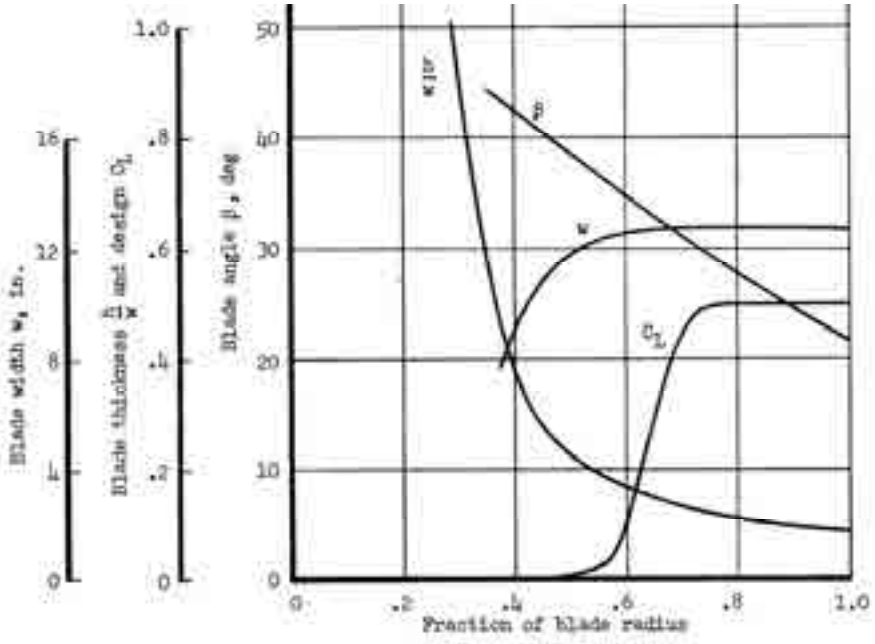

Fig. 3-87. Propeller geometry of the 0.4-scale model of the Fairchild C-123 [411].

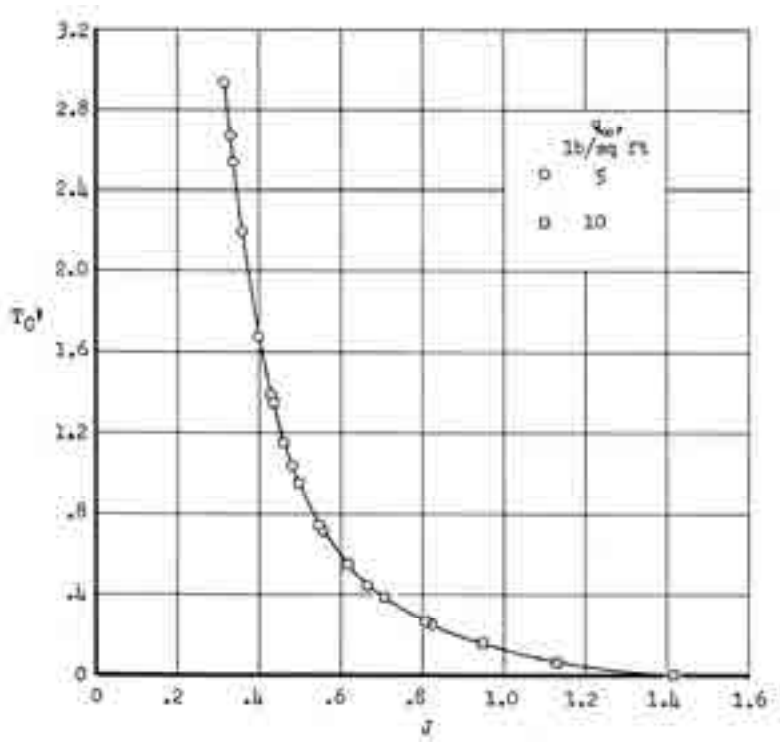

Fig. 3-88. Calibration of model propeller thrust coefficient [411].

that the complete data set shown in Fig. 3-89 can be represented by one semiempirical equation. That is, given that

$$(3.106)\quad C_L = f(\alpha, \delta_F, T_C),$$

you have, for the results shown in Fig. 3-89 with a 60-degree flap deflection angle,

$$(3.107)\quad \frac{dC_L}{d\alpha} = 0.1094 + 0.02159\,T_C$$
$$C_{L,\alpha=0} = 1.2179 + 0.7535\,T_C$$

or, if you prefer,

$$(3.108)\quad C_L = (1.2179 + 0.7535\,T_C) + (0.1094 + 0.02159\,T_C)\,\alpha \quad \text{for } \delta_F = 60 \text{ deg}.$$

I must remind you that finding the several constants in Eq. (3.108) with the technology available during the 1950s was a daunting and speculative task. However, with computational fluid dynamics, I like to think that it could be successfully done today—but I do not have any references to offer in support of this belief.

Now let me discuss the aircraft lift-drag aerodynamics with propellers on and thrusting. This portion of the discussion is helped by first studying the aircraft trim equations using Fig. 3-90 as a guide. To apply wind tunnel data, the flightpath becomes the axis system, and you must keep in mind that the angle of attack (α) is the sum of a descent angle (γ) and the angle (θ), which is the angle that the aircraft's waterline reference makes with the horizon. Now the forces acting parallel to the flightpath velocity sum as

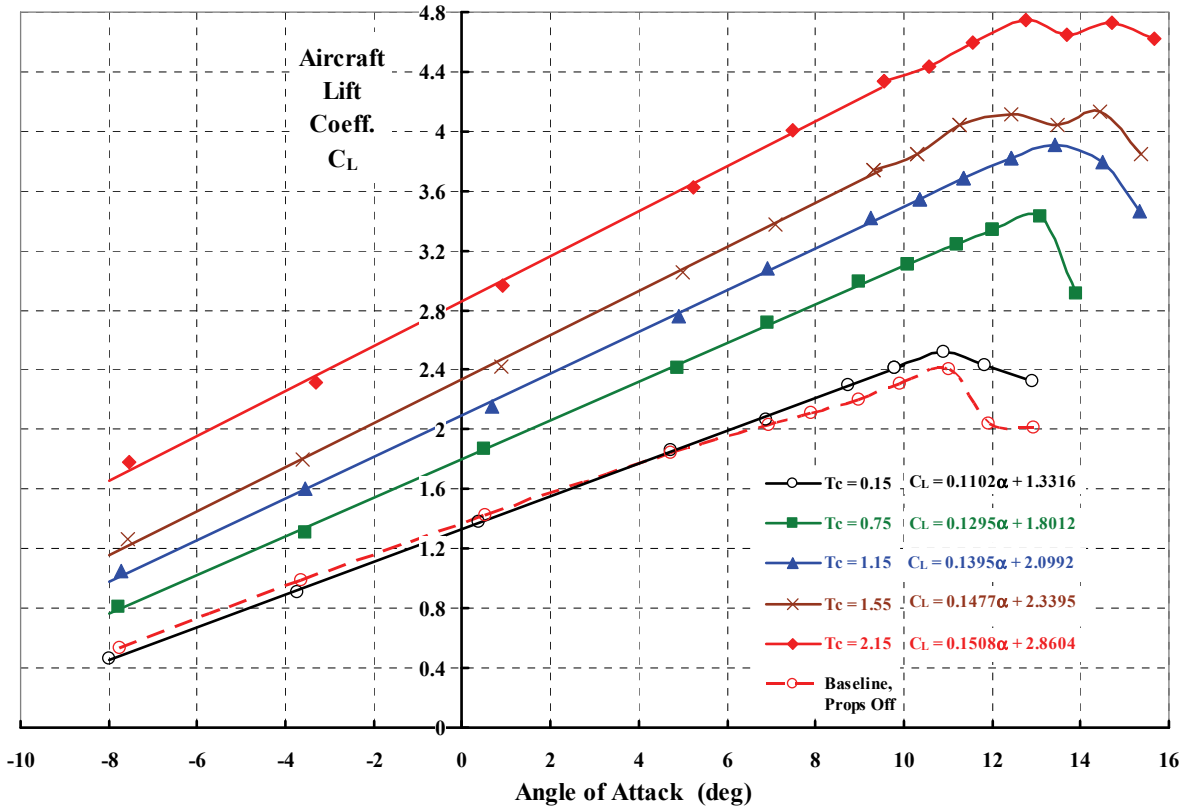

Fig. 3-89. The effect of propeller thrust on aircraft lift with a flap deflection (δ_F) of 60 degrees [412].

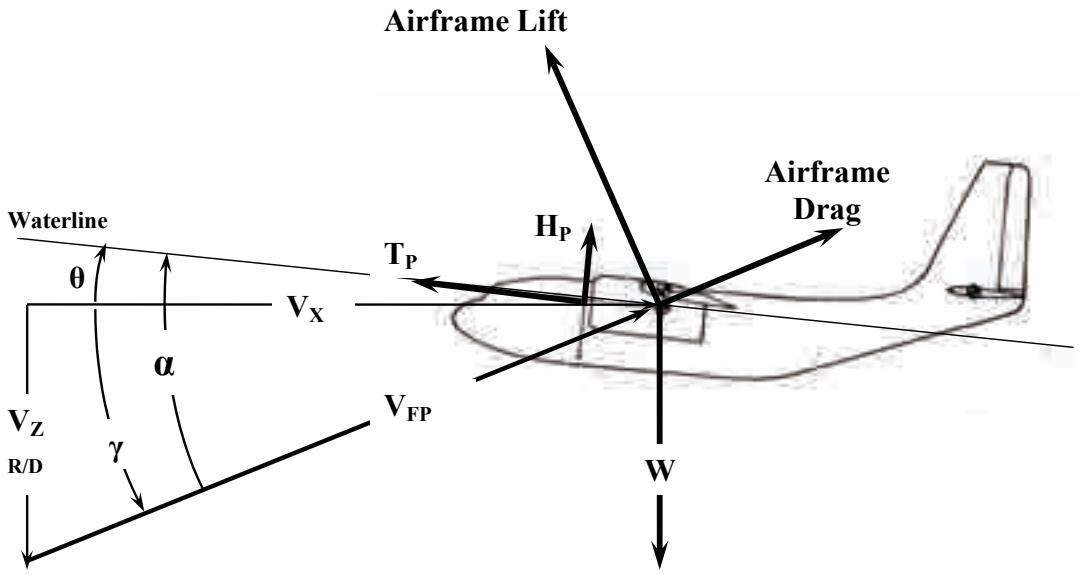

Fig. 3-90. Primary forces involved in a simple longitudinal trim analysis. For clarity, no horizontal or vertical stabilizer forces, or pitching moments, are shown.

(3.109) $C_{Ls} = \sum F_{\perp FP} = (\text{Net } T_X)\cos(\theta+\gamma) - H_P \sin(\theta+\gamma) - D_{af} + W\sin\gamma$,

and the forces acting perpendicular to the flightpath velocity sum as

(3.110) $C_{Ds} = \sum F_{\parallel FP} = (\text{Net } T_Z)\sin(\theta+\gamma) + H_P \cos(\theta+\gamma) + L_{af} - W\cos\gamma$.

Of course, for trimmed flight, both $\sum F_{\parallel FP}$ and $\sum F_{\perp FP}$ must be zero. Aerodynamic engineers refer to this axis system as the wind axis system.

The designation of the propeller thrust contribution to the two trim equations (Net T_X and Net T_Z) requires additional insight, which I will provide shortly.

I have introduced you to these trim equations because they highlight a symbology issue that can lead to rather "sloppy" notations. You see on Fig. 3-89 that lift is denoted as Aircraft Lift Coefficient (C_L). You have every right to ask me if this lift coefficient includes the propeller thrust component ($T_P \sin\alpha$) from Eq. (3.109). The answer is yes, and that is what I meant by the preface *aircraft*, which is really an insufficient adjective. Furthermore, the wind tunnel data includes a propeller force normal to the thrust axis that acts at the propeller hub and is called the H-force by rotorcraft engineers. In fact, in a more complete set of longitudinal trim equations, there is a summation of pitching moments that would include all propeller moments. And to top it off, the horizontal and vertical stabilizers are in place, and the horizontal stabilizer is set at an incidence angle of –3 degrees, therefore it contributes to the measured "aircraft" lift and drag shown in Fig. 3-89 and Fig. 3-91. I have lumped all the airframe surfaces as L_{af} and D_{af} in the simple trim equations. With these thoughts in mind, in the following discussion about the aircraft's "drag" polar, I will use the coefficient notation that

(3.111) $$C_{Z-wa} = \frac{\sum F_{\perp FP}}{q_{FP} S_W} \quad \text{and} \quad C_{X-wa} = \frac{\sum F_{\parallel FP}}{q_{FP} S_W}$$

where Z-wa is positive upwards and X-wa is positive forward, which may be called negative drag if you like. Note that I have tacked on a "-wa" so you will know I mean wind axis. In a wind tunnel, it follows that the rate-of-descent velocity (V_z = R/D) is zero. Therefore, the descent angle (γ) is zero, and the pitch attitude (θ) is the angle of attack (α).

Now take a look at the "drag" polar data that accompanies the "lift" data (Fig. 3-89), which you see here as Fig. 3-91. I consider this a force polar because the propeller thrust is a major variable. Notice that I have added several curved lines representing my curve fitting to the experimental data, which are shown with symbols. My curve fitting was done with a regression analysis of all the data points below stall onset on Fig. 3-91, and I found that

(3.112) $C_{X-wa} = 0.8019 T_C - \left[0.2152 - 0.01408 C_{Z-wa} + 0.04381 C_{Z-wa}^2\right]$.

This semiempirical equation had an error factor (R^2) of 0.9971. The arched lines on Fig. 3-91 were graphed in accordance with Eq. (3.112). If data only between a zero angle of attack and α = +10 degrees is analyzed, you have reasonable curve fitting with

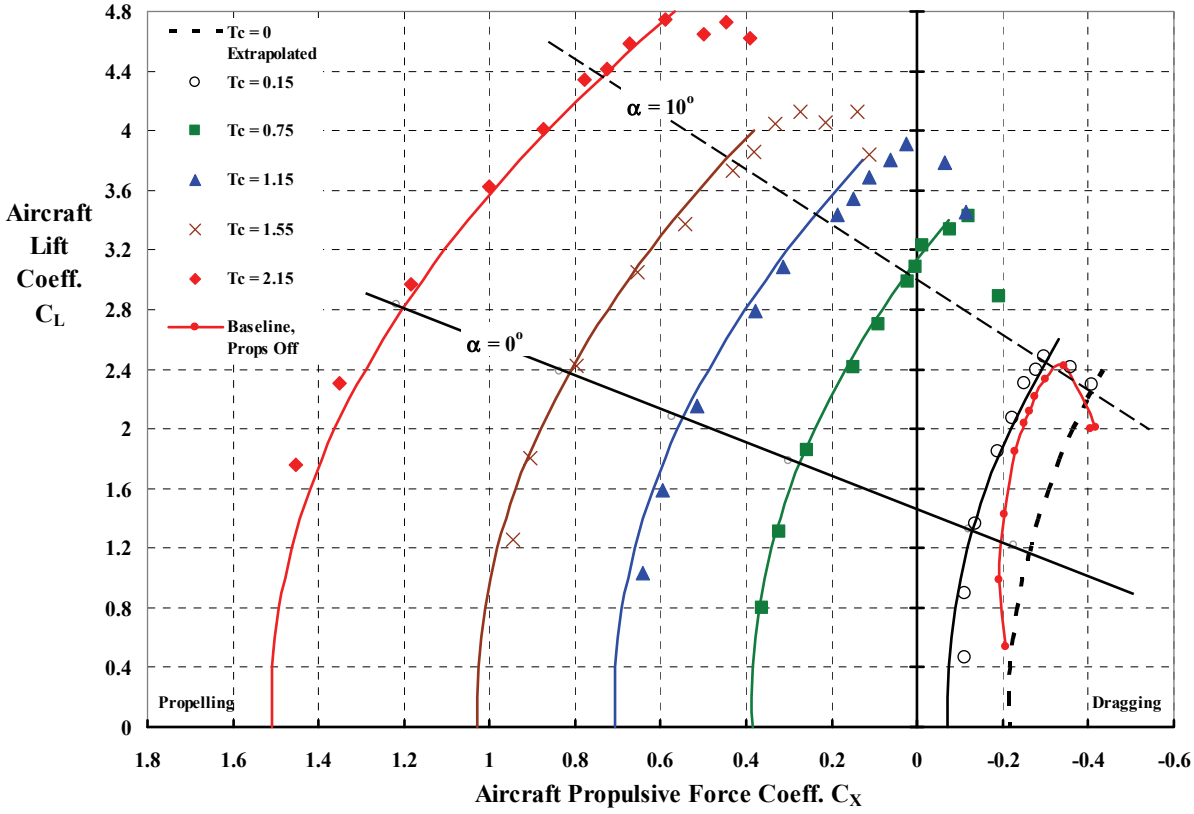

Fig. 3-91. The 0.4-scale model of Fairchild C-123 illustrates a typical powered force graph for a STOL aircraft. Note that $\gamma = 0$, and therefore $\theta = \alpha$.

$$(3.113)\ C_{X-wa} = 0.8139T_C - \left[0.206 + 0.04103C_{Z-wa}^2\right].$$

This result suggests that the Oswald efficiency factor (e) is 0.807 as determined by

$$0.04103C_{Z-wa}^2 = \frac{C_{Z-wa}^2}{\pi AR\, e} = \frac{C_{Z-wa}^2}{\pi(9.61)(0.807)}.$$

Next, note that I have extrapolated the family of curves down to $T_C = 0$ using Eq. (3.112) and have shown this result in Fig. 3-91 as the dashed black line in the drag quadrant. You might observe in passing that the force curve at the lowest measured propeller force coefficient ($T_C = 0.15$) is in the drag quadrant but definitely displaced from the propellers-off baseline data shown with the red circle symbols and line. Also notice that the zero-propeller-thrust (the black dashed line) and baseline data are not in agreement, and this suggests a considerable amount of mutual interference between propellers and wing, even if the propellers are at zero thrust. But beyond that, there is an orderly progression further into the positive $C_{X\text{-}wa}$ quadrant as propeller thrust is applied. Now look at the diagonal line that is labeled $\alpha = 0$. Following this diagonal line shows you that increasing propeller thrust (and H-force, too) adds a considerable amount of lift as well as propulsive force. For example, increasing T_C from 0 to 2.15 increases the $C_{Z\text{-}wa}$ (i.e., the "lift coefficient" if you prefer) from 1.17 to 2.81, an increment of 1.64—or more than a doubling of the propeller thrust equal to

zero, $C_{Z\text{-}wa}$ value. The increase of T_C from 0 to 2.15 moves you to the propulsion quadrant of the force graph. The propulsion increment at a constant $C_{Z\text{-}wa}$ of 1.17 moves you from $C_{X\text{-}wa}$ equal to -0.26 to $+1.2$, an increment of +1.46, which is slightly *less* than the incremental "lift" of 1.64.

This brings me to the calculation of net thrust (Net T_P). Perhaps the most important information to catch your eye is that the arched lines on Fig. 3-91, given by Eq. (3.112), begin at zero $C_{Z\text{-}wa}$ with $C_{X\text{-}wa}$ values significantly less than the propeller force coefficient (T_C) values. Let me state this point as a question: How come, for example, a T_C of 2.15 does not produce a $C_{X\text{-}wa}$ of 2.15 less some drag of, say, -0.2? Both T_C and $C_{X\text{-}wa}$ (and $C_{Z\text{-}wa}$ for that matter) are nondimensionalized by dynamic pressure based on flightpath velocity (V_{FP}) and wing area (S_W), so this is not a definition issue. Fig. 3-91 says there is a significant loss in thrust, roughly (2.15 –1.45)/2.15, or about one-third of the T_C is gone. The question is: Where did it go?

The answer to this question requires a glance at Fig. 3-92 plus a little explanation and, of course, a few equations. Think of the propeller slipstream as a contracting column of air. This contracting air column leaves the propeller plane and travels nearly straight back. Then the air column impinges on the deflected flap. The deflected flap forces the air column to change direction by the flap deflected angle (δ_F). Turning the air column downward requires forces on the wing component of the airframe. I have labeled these forces R_Z and R_X. Simplistically, I have aligned the axis system parallel to, and perpendicular to, the flightpath velocity. (A simple illustration of fluid mechanics at work is when you watch two or three firemen controlling the water direction from their hose. They can only relax if the hose is straight. Any other squirting direction requires them to bend the hose, and that takes strength.)

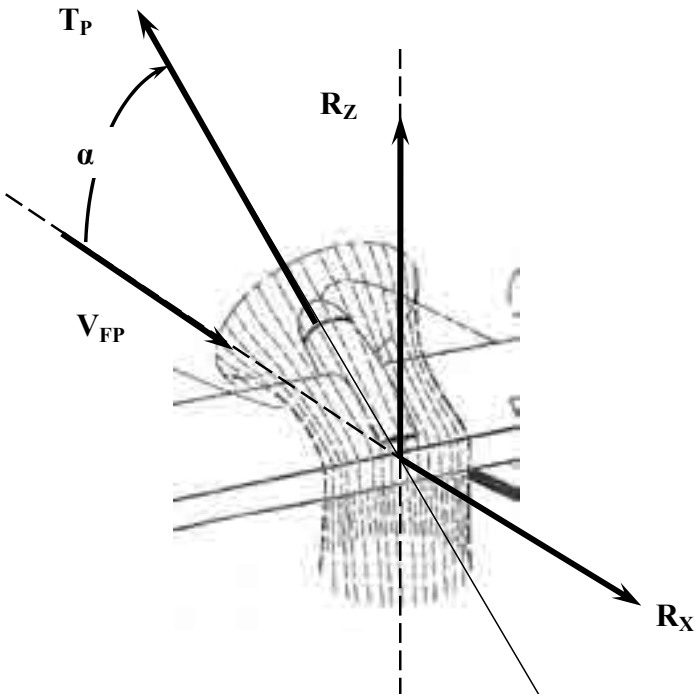

Fig. 3-92. Turning a column of air takes forces.

In the practical case, the air column is actually split into two pieces by the wing and the flap. Experimental data has shown that when the two pieces regroup behind the flapped wing, the "effective" air-column turning angle ($K_e\delta_F$) is quite a bit less than the physical flap deflection angle (δ_F). This experience is applied by the constant (K_e), which lies between zero and unity, and is primarily dependent on the ratio of flap chord to propeller diameter. Thus, with Fig. 3-92 in mind, for one propeller having a thrust (T_P), you have

$$\begin{matrix} \text{Net } T_Z = T_P \sin\alpha + R_Z \\ \text{Net } T_X = T_P \cos\alpha - R_X \end{matrix} . \tag{3.114}$$

Barney McCormick [27] stated in his V/STOL book that "Several approaches to the problem of a wing in a propeller slipstream can be found in the literature. None of these is quite satisfactory."

With Barney's quote in mind, here is an introductory approach that answers the question I posed earlier. The forces R_Z and R_X can be estimated by elementary fluid mechanics.[117] The basic principle is that force equals mass flow times a change in fluid velocity. Applying this principle to the problem at hand means that

$$\begin{matrix} R_Z = \text{Mass Flow}\left[V_{SS} \sin\left(K_Z\delta_F + \alpha \right) \right] \\ R_X = \text{Mass Flow}\left[V_{SS} - V_{SS} \cos\left(K_X\delta_F + \alpha \right) \right] \end{matrix} . \tag{3.115}$$

Let me use these two equations with several simplifying assumptions. First of all, assume that the mass flow is the quantity immediately behind the propeller. From what you learned earlier about propellers and their slipstreams, this means

$$\text{Mass Flow} = \rho A_P \left(V_{FP} + v_p \right), \tag{3.116}$$

where (ρ) is the density of air in slugs per cubic foot, (A_P) is the propeller disc area in square feet, and the slipstream velocity (V_{SS}) immediately behind the propeller ($V_{FP}+v_P$) is in feet per second. Thus, the units of mass flow are slugs per second.[118] I will assume the mass flow is constant from behind the propeller to well behind the airplane.

Second, I have assumed in Eq. (3.115) that the slipstream velocity lies along the flightpath velocity axis. One hopes that this is not too serious an assumption, but the actual direction is influenced by the propeller being at an angle of attack. Furthermore, a tractor propeller is in front of the wing and, therefore, will be influenced by the wing's upwash.

Third, let me include the constant (K_e) that interjects some empiricism into the theory because the column of air is not turned completely to the mechanical flap deflection angle (δ_F). More precisely, I need some constant (K_e) to make the theoretical answer come out

[117] *Fluid Mechanics* by Streeter [483] was my textbook; it was copyrighted in 1951. Beginning at chapter IV, pages 95 and 96, Mr. Streeter teaches about the forces on an elbow pipe through which a fluid flows.

[118] Multiplying mass flow in slugs per second by velocity in feet per second gives you slug-ft/sec^2, which you know is a pound of force (i.e., F = ma, so m = F/a).

"right." Finally, I will assume the slipstream is fully contracted in the distance between the propeller plane and the leading edge of the flap. This defines the slipstream velocity (V_{SS}) as

$$(3.117)\quad V_{SS} = V_{FP} + 2v_p = V_{FP}\left(1 + \frac{2v_P}{V_{FP}}\right).$$

Applying these four assumptions (plus many more hidden behind the scene), the forces added to the wing to turn the propeller slipstream can now be written as

$$(3.118)\quad \begin{aligned} R_Z &= \rho A_P V_{FP}^2 \left(1 + \frac{v_p}{V_{FP}}\right)\left(1 + \frac{2v_p}{V_{FP}}\right)\left[\sin\left(K_e\delta_F + \alpha\right)\right] \\ R_X &= \rho A_P V_{FP}^2 \left(1 + \frac{v_p}{V_{FP}}\right)\left(1 + \frac{2v_p}{V_{FP}}\right)\left[1 - \cos\left(K_e\delta_F + \alpha\right)\right] \end{aligned}.$$

Now, for the ratio of propeller-induced velocity (v_P) to flightpath velocity (V_{FP}), you need only recall Eq. (3.10), repeated here for convenience, as

$$(3.119)\quad v_P = \sqrt{\left(\frac{V_{FP}}{2}\right)^2 + \frac{T_P}{2\rho A_P}} - \frac{V_{FP}}{2} \quad \text{or} \quad \frac{v_P}{V_{FP}} = \frac{1}{2}\left[\sqrt{1 + \frac{2T_P}{\rho A_P V_{FP}^2}} - 1\right].$$

To connect with many test reports that define T_C as $NT_P/q_{FP}S_W$ where (N) is the number of propellers and, to repeat, dynamic pressure is $q_{FP} = \frac{1}{2}\rho V_{FP}^2$, make the substitution of $T_P = q_{FP}S_W T_C/N$ into Eq. (3.119), and then you have

$$(3.120)\quad \frac{v_P}{V_{FP}} = \frac{1}{2}\left[\sqrt{1 + \left(\frac{S_W}{N A_P}\right)T_C} - 1\right].$$

The next to the last step is to nondimensionalize the forces by $q_{FP}S_W$, which gives you the net thrust in coefficient form for any number (N) of propellers. Thus, in summary

$$(3.121)\quad \begin{aligned} \text{Net } CT_Z &= T_C \sin\alpha + \left(2\frac{NA_P}{S_W}\right)\left(1 + \frac{v_p}{V_{FP}}\right)\left(1 + \frac{2v_p}{V_{FP}}\right)\left[\sin\left(K_e\delta_F + \alpha\right)\right] \\ \text{Net } CT_X &= T_C \cos\alpha - \left(2\frac{NA_P}{S_W}\right)\left(1 + \frac{v_p}{V_{FP}}\right)\left(1 + \frac{2v_p}{V_{FP}}\right)\left[1 - \cos\left(K_e\delta_F + \alpha\right)\right] \end{aligned}.$$

The preceding theory development is a variation of what you will find in Barney McCormick's book [27] and in Dick Kuhn's very well known semiempirical theory [418]. In fact, I have left you with the same problem Dick found. The problem is this: when the thrust is zero, which is to say the induced velocity (v_P) is zero, Eq. (3.121) *is not zero*. The common assumption is that the net thrust component should be zero if thrust is zero. The expedient solution is to "correct" Eq. (3.121) by adding in the residual at zero thrust so that the final result, with a little arithmetic, becomes

$$\text{Net } CT_Z = T_C \sin\alpha + \left(2\frac{NA_P}{S_W}\right)\left[3\frac{v_p}{V_{FP}} + 2\left(\frac{v_p}{V_{FP}}\right)^2\right]\left[\sin\left(K_e\delta_F + \alpha\right)\right]$$

(3.122)

$$\text{Net } CT_X = T_C \cos\alpha - \left(2\frac{NA_P}{S_W}\right)\left[3\frac{v_p}{V_{FP}} + 2\left(\frac{v_p}{V_{FP}}\right)^2\right]\left[1 - \cos\left(K_e\delta_F + \alpha\right)\right]$$

All that remains to complete a theory to calculate $C_{Z\text{-}wa}$ and $C_{X\text{-}wa}$ is to add in the airframe forces at zero thrust. The complete result for the $C_{Z\text{-}wa}$ coefficient is

$$(3.123)\quad C_{Z-wa} = T_C \sin\alpha + \left(2\frac{NA_P}{S_W}\right)\left[3\frac{v_p}{V_{FP}} + 2\left(\frac{v_p}{V_{FP}}\right)^2\right]\left[\sin\left(K_e\delta_F + \alpha\right)\right] + C_{L\text{ at }Tc=0}.$$

To use this result you must have the lift curve of the aircraft at zero thrust and for the selected flap configuration and flap deflection. For the 0.4-scale model of the Fairchild C-123, you have test data to use as given by Eq. (3.108), repeated here as

$$(3.124)\quad C_L = \left(1.2179 + 0.7535\,T_C\right) + \left(0.1094 + 0.02159\,T_C\right)\alpha \quad \text{for } \delta_F = 60 \text{ deg}.$$

This result suggests that $C_{L\text{ at }Tc\,=\,0}$ equals $1.2179+0.1094\alpha$ and it can be used in Eq. (3.123).

To calculate $C_{X\text{-}wa}$ you have

$$(3.125)\quad C_{X-wa} = T_C \cos\alpha - \left(2\frac{NA_P}{S_W}\right)\left[3\frac{v_p}{V_{FP}} + 2\left(\frac{v_p}{V_{FP}}\right)^2\right]\left[1 - \cos\left(K_e\delta_F + \alpha\right)\right] - C_{D\text{ at }Tc=0},$$

and you need the aircraft zero drag coefficient ($C_{D\text{ at }Tc\,=\,0}$) as a function of angle of attack. Here you can turn to Eq. (3.112) and, because at zero thrust $C_{Z\text{-}wa}$ equals $C_{L\text{ at }Tc\,=\,0}$, you have

$$(3.126)\quad C_{D\text{ at }Tc=0} = 0.2152 - 0.01408\left(C_{L\text{ at }Tc=0}\right) + 0.04381\left(C_{L\text{ at }Tc=0}\right)^2.$$

If you make computations with Eqs. (3.123) through (3.126), keep in mind that I have used the angles in degrees, and remember that this discussion centers on a flap deflection angle of 60 degrees. Furthermore, the flap configuration is as shown in Fig. 3-12, so this is just one very specific example.

I would be quite remiss if I closed this discussion without *some* evidence that the preceding theoretical discussion and resulting equations are "in the ballpark"—at least for this one example. The correlation of this semiempirical theory for $C_{Z\text{-}wa}$ and $C_{X\text{-}wa}$ is shown in Fig. 3-93 and Fig. 3-94. The constant came out $K_e = 0.68$ based on several trial comparisons and my judgment.

What you have just read is how we did it with a slide rule "way back then." We thought we were doing pretty good.

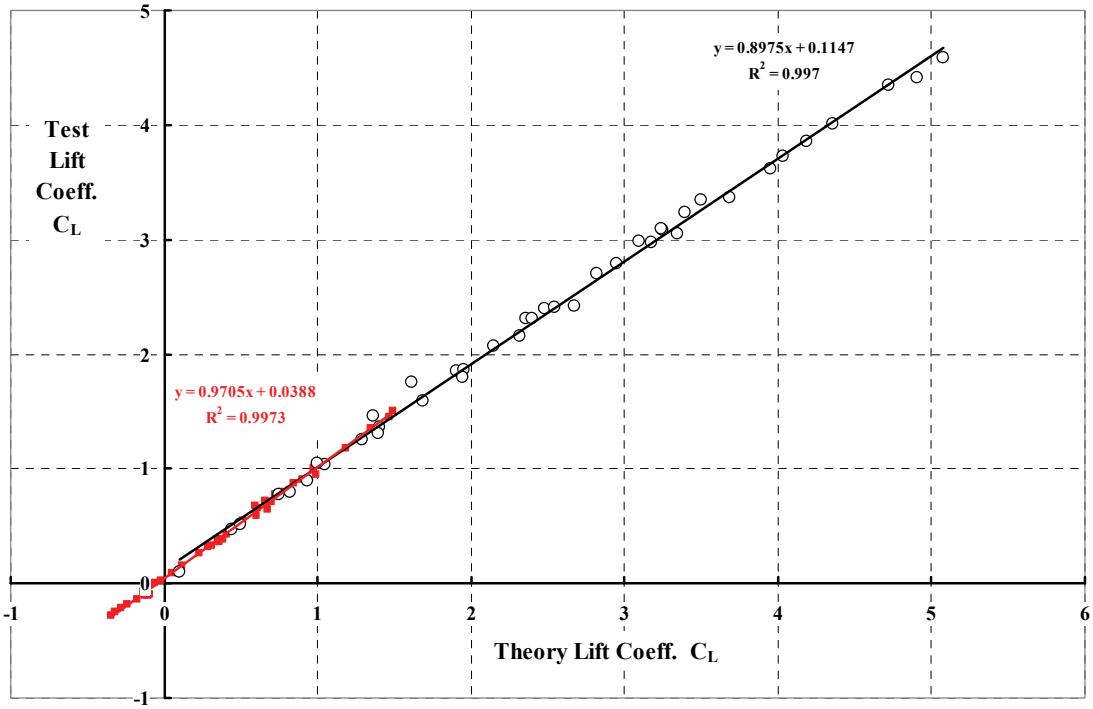

Fig. 3-93. Lift correlation: test versus theory following Eq. (3.123).

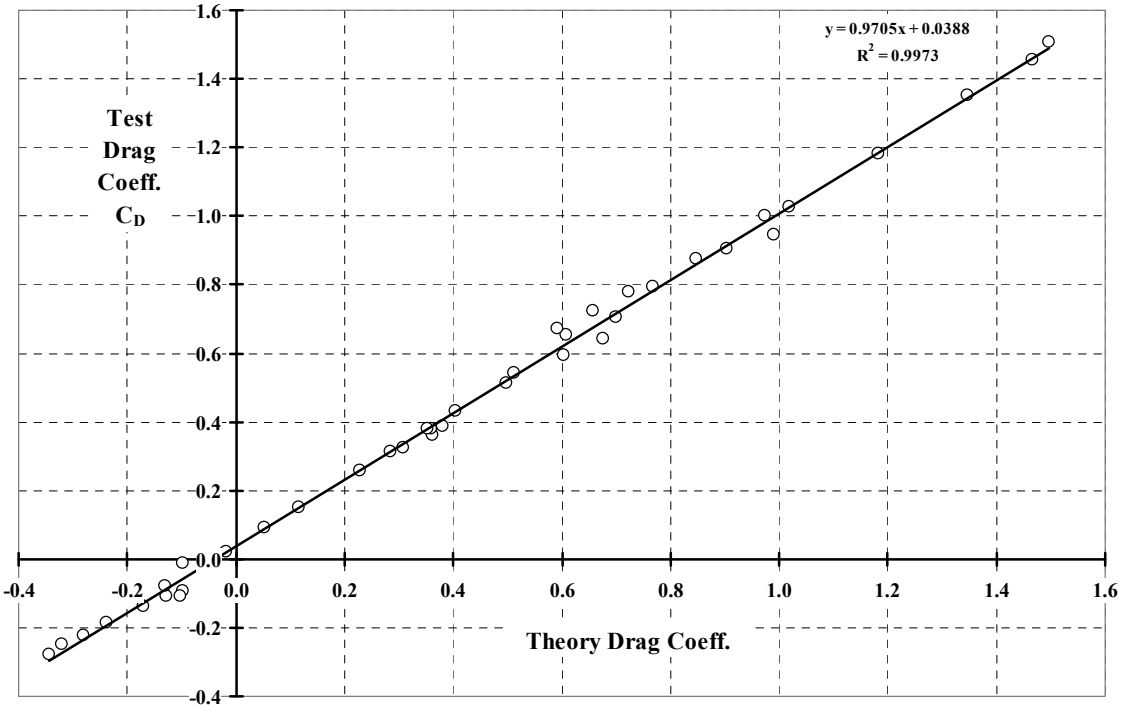

Fig. 3-94. Drag correlation: test versus theory following Eq. (3.126).

I must interrupt this STOL discussion for a brief moment to tell you about a rather thorough theoretical and experimental VTOL effort that the N.A.C.A./NASA mounted in the mid-1950s. The sole objective of this effort was to find a configuration where hovering flight could be obtained just by redirecting all propeller slipstreams completely through 90 degrees and, in fact, beyond to about 110 degrees. The N.A.C.A. Langley Research Center took the lead in this vigorous attack, and Dick Kuhn, Ken Spreemann, and John Draper were the champions as I recall. The effort began somewhat before the Ryan Aeronautical Company developed the VZ-3, which is shown in Fig. 3-95. This aircraft came into being because of money provided by the Office of Naval Research (ONR) and the Army Transportation Research and Engineering Command (TRECOM). The aircraft's first flight was on December 29, 1958. The multielement flap system deflected the thrust from two, 9.167-foot, three-bladed propellers that were powered with a single Lycoming T-53 engine producing 825 horsepower. As you can see from Fig. 3-95 and by reading one NASA report [484], the aircraft used leading-edge slats, and about two-thirds of the wing chord was devoted to two slotted-flap segments. I do not think I have ever seen a more cambered airfoil. Limited success with the VZ-3 led to a larger version, the 4,000-pound VZ-5, which had four propellers powered by a General Electric YT58-GE-2 engine providing about 1,000 horsepower [485-487]. An even larger version (in model scale) with six propellers was

Fig. 3-95. The Ryan VZ-3, along with several NASA wind tunnel experiments, established what potential the deflected slipstream concept had for VTOL. The wingspan was 23 feet and the gross weight was about 2,600 pounds. The general conclusion was that the approach was not too promising, and now the aircraft is on display at the U.S. Army Aviation Museum in Ft. Rucker, Alabama.

Fig. 3-96. The Vertol VZ-2 tiltwing proved more promising than the Ryan VZ-3. The first hovering flight of this 3,500-pound VTOL was on August 13, 1957, and the first full conversion back and forth from hover was made on July 15, 1958.

wind tunnel tested [488]. As it turned out, the VZ-2 tiltwing approach shown in Fig. 3-96 showed much greater promise [182, 183] than the Ryan VZ-3, and deflected slipstream approaches to vertical takeoff and landing were slowly discontinued.

On a personal note, it was a great thrill for me at age 23 to witness the first hover, and first complete back and forth transition of the VZ-2 because I had done a longitudinal stability and control analysis of that tiltwing under Phil Sheridan's guidance. With help from the analog computer guys, I "programmed" a wiring board to solve the trim equations and had an 8-inch CRT scope showing pitch attitude and airspeed. Leonard LaVassar, our chief pilot who did almost all the early flight testing, sat in a wooden chair with a makeshift joystick watching the scope and "flew" the contraption through transition. By the time the wing tilt was 45 degrees, the "flight simulator" flew like an airplane, which was the general consensus from flight testing. (Nobody paid much attention to those theoretical and flight simulator efforts, but I was happy.)

Now to continue. The theoretical and experimental study of propeller-wing-flap aerodynamics did not, of course, stop just because hovering configurations (e.g., the Ryan VZ-3) were proving to have many shortcomings. In February of 1959, Dick Kuhn [418] at NASA Langley updated earlier work [417] by Smelt and Davies, which gave propeller-wing-flap aerodynamics at least a firmer foundation for V/STOL aircraft development. And the researchers at NASA Ames saw what propeller slipstreams plus flaps could do to increase the maximum lift capability of the basic C-123 model. You saw an example of their experimental work in Fig. 3-91. They found that practical aspects of airfoil stall kept the wing-flap-propeller combination from achieving *very high* values of the total aircraft lift coefficient as

used by Heinrich Helmbold (i.e., $L/q_{FP}b_w^2$), which you first encountered in Fig. 3-4. To make this important point quite clear, let me add the Ames researchers' model C-123 data from Fig. 3-91 to Helmbold's theoretical graph (Fig. 3-4). Referring to Fig. 3-91, I simply subtracted the value of $C_{X\text{-}wa}$ at zero $C_{Z\text{-}wa}$ from the experimental data for each constant propeller thrust curve and called it aircraft drag due to lift (i.e., $D/q_{FP}b_w^2$). You see the results in Fig. 3-97. Simply stated, propeller-wing-flap aerodynamics was still quite susceptible to basic airfoil and flap stalling.

This fact has driven the fixed-wing side of the industry to find an additional stream of air (somewhere on the airplane) to add to the normal air (created by the flightpath velocity) flowing about a wing. A simple example of this approach is to add more slipstreams by adding more propellers and raising the total thrust. Another example is releasing compressed air obtained, say, from the compressor stage of a turboshaft, turbofan, or turbojet engine and directing the air through pipes to strategic portions of the wing. This approach falls into the category of BLC. A third approach is to nozzle compressed air as a sheet from the trailing edge of a wing, which makes the wing think it has a jet flap. Each of these approaches gives the wingspan, or a portion of the wingspan, a dynamic pressure higher than that created by the flightpath velocity. However, no matter how the lift is distributed along the wingspan, and no matter how much additional velocity and dynamic pressure are added, the ideal induced drag is still the lowest induced drag you can have. This is the message you are beginning to see with the fundamental chart shown in Fig. 3-97.

I would be remiss if I did not remind you of the enormous contribution the NACA research center at Langley [24, 489], and later the NACA/NASA research center at Ames [47, 490], made towards giving fixed-wing aircraft some hope of STOL performance. The scope of experimentation, coupled with theoretical development, accomplished at these two research facilities is simply mind-boggling to me. Reports just seem to pour out from the relatively few, but very creative, engineers. With very little trouble, you can obtain a file of over 5,000 NACA, and then NASA, reports dealing with V/STOL alone, never mind the early autogyro and helicopter reports.[119] What became invaluable in my mind was the testing accomplished in the NASA Ames 40- by 80-foot, and the later 80- by 120-foot, full-scale wind tunnels. And then when the wind tunnel experiments revealed a promising feature, flight research became the icing on the cake. The performance and flying qualities research, particularly with aircraft configurations ideally suited to answer key questions, gave the aviation industry enormous guidance in development of practical STOL machines. The 1960s and 1970s were two decades of really exciting discoveries in the world of V/STOLs and I, for one, just reveled in the progress.

[119] My literature folder has a subfolder containing 6,480 NACA/NASA reports in PDF form. They all relate aeronautically to V/STOL in some way.

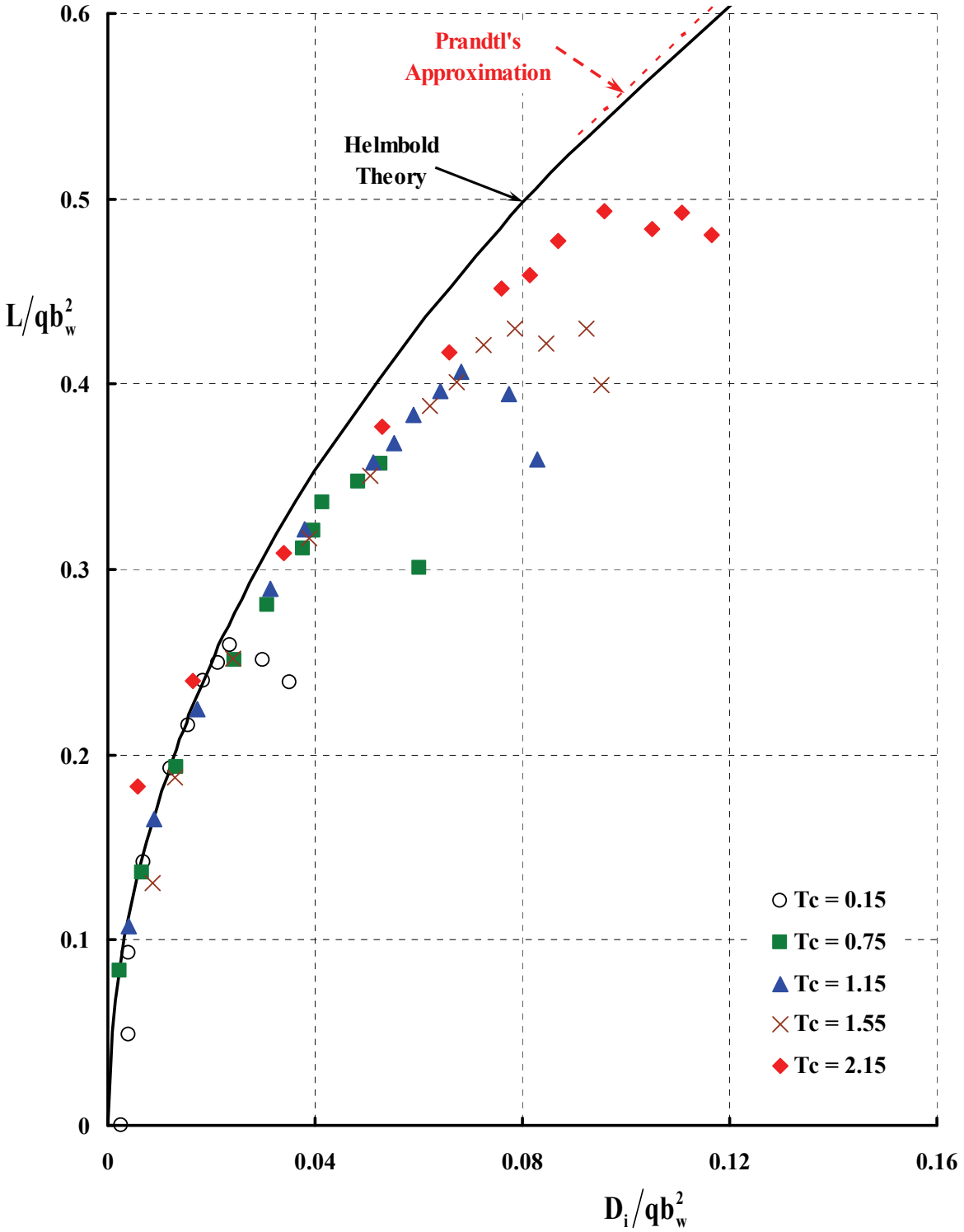

Fig. 3-97. Lift-versus-drag behavior of the Fairchild C-123 at model scale. Note: minimum profile drag removed.

3.5 MODEL TEST OF THE FAIRCHILD C-123—4 PROPS

At test completion of the 0.4-scale Fairchild C-123, NASA Ames researchers had in their hands an excellent "model" to use to further investigate V/STOL configurations. Next, they decided to modify the model by adding two more propellers (Fig. 3-98) and repeat the test program they had done with the twin-propeller model. The researchers also expanded the study of boundary layer control (BLC) from the preceding test. As I see it today, they were intent on getting much higher values of lift (i.e., $L/q_{FP}b_w^2$) by wringing everything they could out of at least one wing-flap-propeller plus-BLC configuration. This objective certainly fit the needs continually expressed by the fixed-wing side of the industry, even today.

You see results for the configuration that produced the highest force coefficient perpendicular to the flightpath (i.e., the wind axis, $C_{Z\text{-}wa}$) in Fig. 3-99 and Fig. 3-100. The thrust coefficient of the four propellers reached a maximum T_C equal to 4.10. The flap deflection angle (δ_F) was increased from 60 degrees in the two-propeller test to 80 degrees for the four-propeller test. The ailerons, which were undeflected in the first test, were deflected (δ_A) at 30 degrees in the follow-on test. Finally, BLC was activated for both the flaps and the ailerons. The two figures on the facing page show you that, compared to the two-propeller test, maximum vertical force was virtually doubled. The force polar data is adequately approximated by

$$(3.127)\ C_{X-wa} = 0.8139T_C - \left[0.300 + 0.04103C_{Z-wa}^2\right],$$

which differs from the two-propeller data, Eq. (3.113), only in additional parasite drag due to the two additional nacelles (i.e., 0.300 versus 0.206). A very key point is made by the force polar in Fig. 3-100. You will recall from Fig. 3-90 that equilibrium flight requires the force parallel to the flightpath velocity ($C_{X\text{-}wa}$) to be zero. This condition of $C_{X\text{-}wa}$ equals zero was achieved with a propeller thrust coefficient of T_C = 4.1, which produced a "lift" coefficient of 8.5.

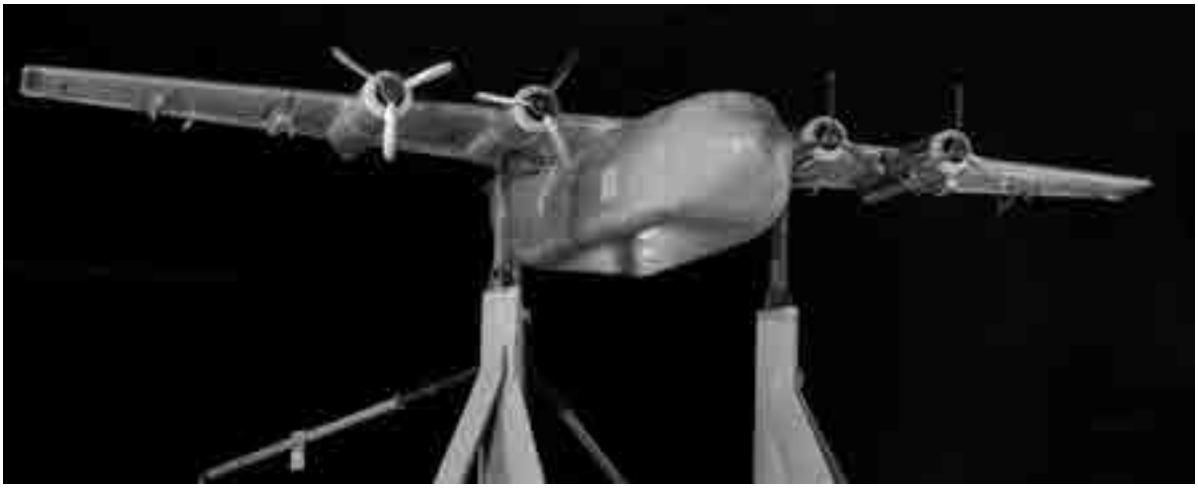

Fig. 3-98. Tested in the NASA Ames 40- by 80-foot wind tunnel, the Fairchild C-123, at 0.4 scale with four propellers, bore a striking similarity to the Lockheed C-130 (photo courtesy of Bill Warmbrodt, Ames Research Center).

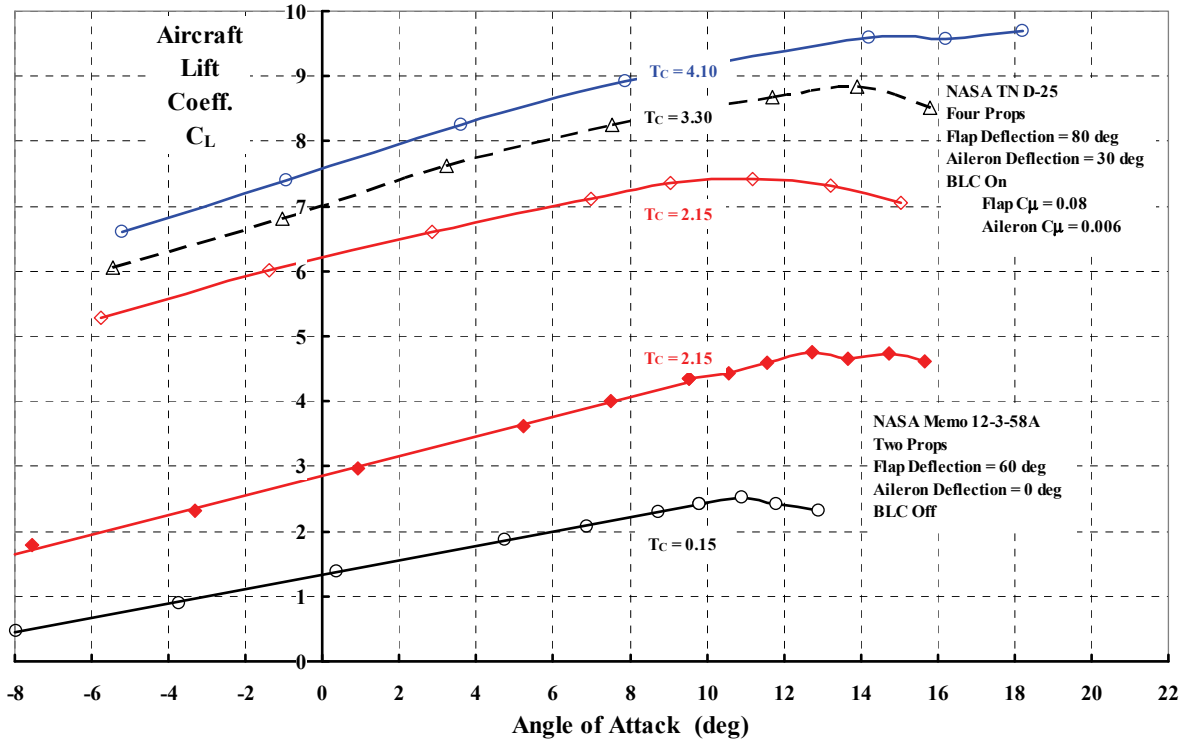

Fig. 3-99. Powered "lift" coefficients far in excess of typical wing-alone values can be obtained by adding flaps, propellers, and BLC.

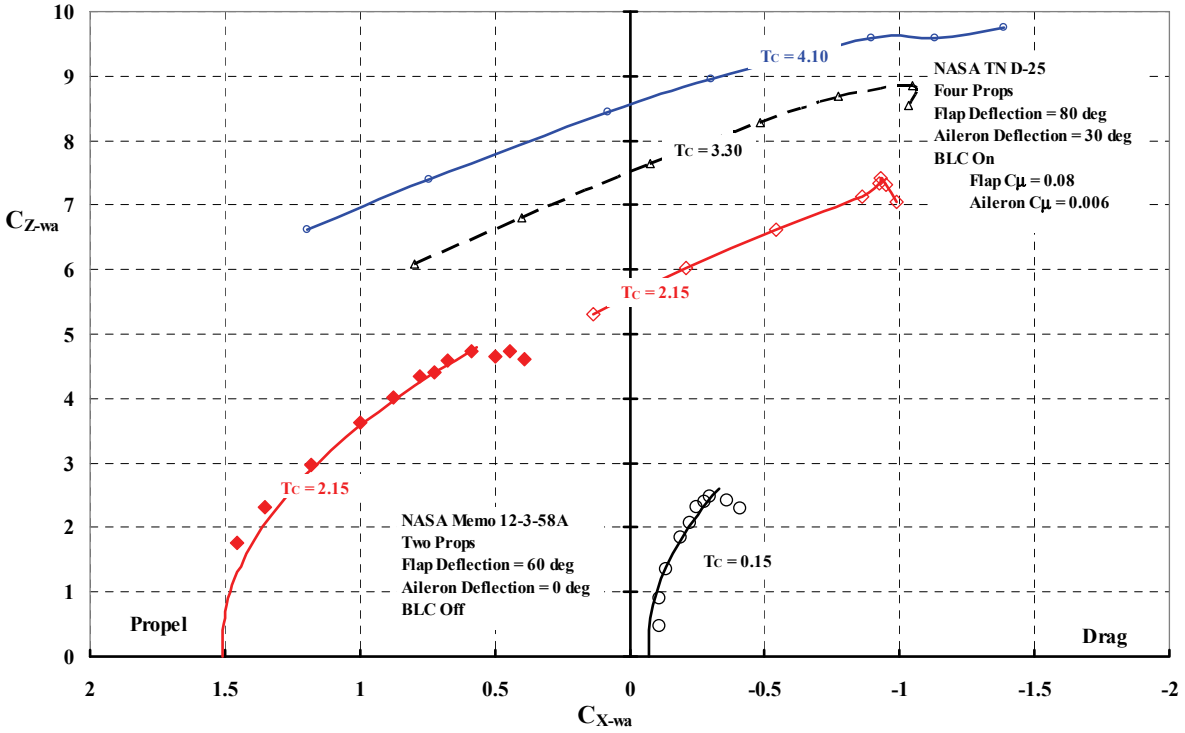

Fig. 3-100. BLC keeps the flaps and ailerons from stalling. The resulting force polar shows that trim, level flight (i.e., $C_{X\text{-}wa} = 0$) can be maintained at a $C_{Z\text{-}wa}$ of 8.5.

Of course, the immediate practical question is this: If the $C_{Z\text{-}wa}$ coefficient is 8.5, how slow could a four-engine C-123 fly in steady, level flight, say at sea level on a standard day? The maximum takeoff weight of the Fairchild C-123 was about 60,000 pounds, and the aircraft had a wing area of 1,223 square feet. The aircraft was powered with two Pratt & Whitney R-2800-99W piston engines, each having a takeoff rating of 2,500 horsepower. The C-123 stall speed is generally quoted as 83 knots.[120] However, with a "lift" coefficient of 8.5 and landing at sea level on a standard day where the air density is 0.002378 slugs per cubic foot, you can calculate from

$$(3.128)\ C_{Z-wa} = \frac{W}{q_{FP} S_W} = 8.5 = \frac{295}{V_{kts}^2}\left(\frac{60,000}{1,223}\right) \text{ at S.L. Std.}$$

that the flight speed (V_{FP}) is 41 knots given a high-powered lift coefficient of 8.5. This is an impressive improvement in low-speed performance.

There is a follow-up question dealing with the glide slope for landing. Fig. 3-100 shows that at a T_C of about 3.30, the C-123 could operate at a $C_{Z\text{-}wa}$ of 8.5 and a negative propulsive force (i.e., a drag) coefficient ($C_{X\text{-}wa}$) of -0.9. This negative propulsive force is available for descent to balance the term W sin γ in Eq. (3.109). Roughly speaking then, at 41 knots (q_{FP} of 5.7) and 60,000 pounds on a standard day, you have

$$(3.129)\ C_{X-wa} = -0.9 = \frac{W}{q_{FP} S_W}\sin\gamma = \frac{60,000}{(5.7)(1,223)}\sin\gamma,$$

which yields a glide slope (γ) of about 6 degrees. Many engineers use the simpler statement that glide slope (γ) in degrees equals $C_{X\text{-}wa}/C_{Z\text{-}wa}$ times 57.3 degrees per radian. If you look again at Fig. 3-100, you can see that the highest $C_{Z\text{-}wa}$ data point for a thrust coefficient of 4.1 has the ratio $C_{X\text{-}wa}/C_{Z\text{-}wa}$ of –1.38/9.75, which gives a glide slope of 8 degrees. In short, such slow approach speeds and considerably steeper than airliner approach angles (see Fig. 3-1) mean a four-engine C-123 with BLC could reasonably land within a 1,000-foot field following George Schairer's criteria, which you learned about from Fig. 1-15 (on page 21). Clearly, obtaining the capability to land and take off in a short field is hardly insurmountable. That just leaves stability and control as a major technical issue [184], and of course, engines, cost, and weight (not necessarily in that order) are always of paramount concern.

It is worth a moment to make a rough calculation of the power required for a four-engine/propeller, conceptual version of the full-scale C-123 at the 41-knot level flight speed. The total thrust of the four propellers at the thrust coefficient of $T_C = 4.1$ amounts to

$$(3.130)\ \text{Total thrust, 4 props} = q_{FP} S_W T_C = (5.7)(1,223)(4.1) = 28,580 \text{ pounds},$$

which, you might notice immediately, is about one-half of the 60,000-pound flight weight. On this basis, the thrust of one propeller (T_P) is 7,150 pounds. The power required by one propeller to produce its portion of the total thrust is made up of induced power, propulsive power, and profile power. Let me assume that this four-propeller version of the C-123 would

[120] See, for instance, *Jane's All the World's Aircraft* for 1969–1970, pages 323 to 324.

use 13-foot-diameter propellers, which give a disc area (A_P) of 133 square feet. Then the induced power (i.e., $K_i \times v_P \times T_P$), using Eq. (3.119) to first calculate the induced velocity (v_P), follows as

$$(3.131)\ v_P = \sqrt{\left(\frac{1.15\times 41}{2}\right)^2 + \frac{7{,}150}{2(0.002378)(133)}} - \frac{1.15\times 41}{2} = 108.9 - 23.6 = 85.4 \text{ ft/sec.}$$

Next, induced power, with a correction factor (K_i = 1.15) that accounts for nonuniform induced velocity, blade tip, and root losses and swirl, becomes

$$(3.132)\ HP_{induced} = (1.15)\frac{(7{,}150)(85.3)}{550} = 1{,}277 \text{ hp}.$$

The propulsive power (i.e., $T_P \times V_{FP}$) is simply

$$(3.133)\ HP_{propulsion} = \frac{(7{,}150)(1.69\times 41)}{550} = 900 \text{ hp}.$$

The calculation of profile power, following Eq. (2.57), would require more detailed propeller design work, so to expedite the discussion, let me make an educated guess using simple rotor theory. That is, I will assume the propeller is designed for optimum static thrust performance with the design blade-loading coefficient (in rotorcraft nomenclature) of C_T/σ equal to 0.15. Because I have assumed four, 13-foot-diameter propellers, the disc loading (T_P/A_P) is on the order of 53 pounds per square foot, which is very high as any rotorcraft engineer will tell you. Propeller designers would suggest a tip speed (V_t) of 850 feet per second. Now, simple rotor theory gives you the starting point that

$$(3.134)\ HP_{profile} = \frac{\rho A_P V_t^3}{550}\left(C_{Po} = \frac{\sigma C_{do}}{8}\right).$$

However, because you can obtain solidity (σ) from the design blade-loading coefficient as

$$(3.135)\ \sigma = \frac{T_P}{\rho A_P V_t^2 (C_T/\sigma)_{design}} = \frac{7{,}150}{(.002378)(133)(850^2)(0.15)} = 0.21,$$

and because you can assume the propeller airfoils have an average drag coefficient (C_{do}) of 0.025 at the design airfoil lift coefficient, with some compressibility effects you now have a more informative way to calculate profile power as

$$(3.136)\ HP_{profile} = \frac{C_{do} V_t}{4{,}400 (C_T/\sigma)_{design}} T_P = \frac{(0.025)(850)}{4{,}400(0.15)}(7{,}150) = 230 \text{ hp}.$$

Summing up these three power elements gives you the power required from one engine of 2,407 horsepower and, therefore, a total power of roughly 9,630 horsepower.

This leads me to the subject of how much power is required by the BLC system. Reference [412] states:

> "The air for boundary-layer control was supplied by a centrifugal compressor driven by a variable-speed electric motor. The maximum compressor pressure ratio used during the test was 1.65. The compressed air flowed from the compressor to a plenum chamber. Separate ducts were used to transmit the compressed air from the plenum chamber into each of the flaps and ailerons. Each of these ducts contained a thin-plate orifice meter with pressure orifices and a thermocouple for measuring the pressures and temperature required for determining the boundary-layer-control flow and jet momentum coefficients. The air flow to each of the flaps and ailerons was controlled by electrically actuated butterfly valves located within the ducts."

I have used an enlargement of a previous drawing (Fig. 3-12) to give you more details about the BLC system, which you see in Fig. 3-101. We are not told from the reference just where the compressor and plenum chamber were physically located, but I can imagine they were in the 45-foot-wingspan model itself. At any rate, separate ducts guided the compressed air into each flap and aileron. I suggest by Fig. 3-101 that the spar of the flap (and aileron) acted as the final compressed air chamber before the compressed air escaped, at high velocity, out through a slot that was 0.04 inches high.

An estimate of the horsepower required for the 0.4-scale-model BLC system—without getting into a thermodynamic approach that is provided by Mark Kelly and Bill Tolhurst [415]—is that

$$(3.137)\quad HP_{BLC} = \frac{T_{Jet} V_{Jet}}{550}.$$

The thrust is stated in nondimensional form with a jet thrust coefficient denoted almost universally by the symbol (C_μ), which is nothing more than $T_{Jet}/q_{FP}S_w$. For the four-prop testing, the NASA Ames researchers set the flap BLC flow to produce a jet thrust coefficient of 0.08; for the ailerons, C_μ was set to 0.006. Therefore, for my conceptual design study where the aircraft is flying at 41 knots in steady, level flight, the jet thrust from the flaps and ailerons amounts to

$$(3.138)\quad \begin{matrix} \text{Flap } T_{Jet} = q_{FP}S_W C_\mu = (5.7)(1,223)(0.08) = 558 \text{ pounds} \\ \text{Aileron } T_{Jet} = q_{FP}S_W C_\mu = (5.7)(1,223)(0.006) = 42 \text{ pounds} \end{matrix},$$

or a total of 600 pounds. This is clearly not a significant contributor to lifting the 60,000-pound aircraft under discussion. Now think about the slot area at the 0.4-scale model that these jet thrusts are associated with. The slot height for the 0.4-scale model was only 0.04 inches and, from Fig. 3-10, the total flap span (port and starboard) was about 21 feet and the total aileron span was about 17 feet. This gives a BLC flap slot area, scaled up to the 60,000-pound concept size, of 0.175 square feet. Similarly, the BLC aileron slot area, scaled up, equals 0.142 square feet. If you think in terms of a "disc loading," then the flaps are operating at about 3,200 pounds per square foot! The ailerons are loaded more modestly at about 295 pounds per square foot.

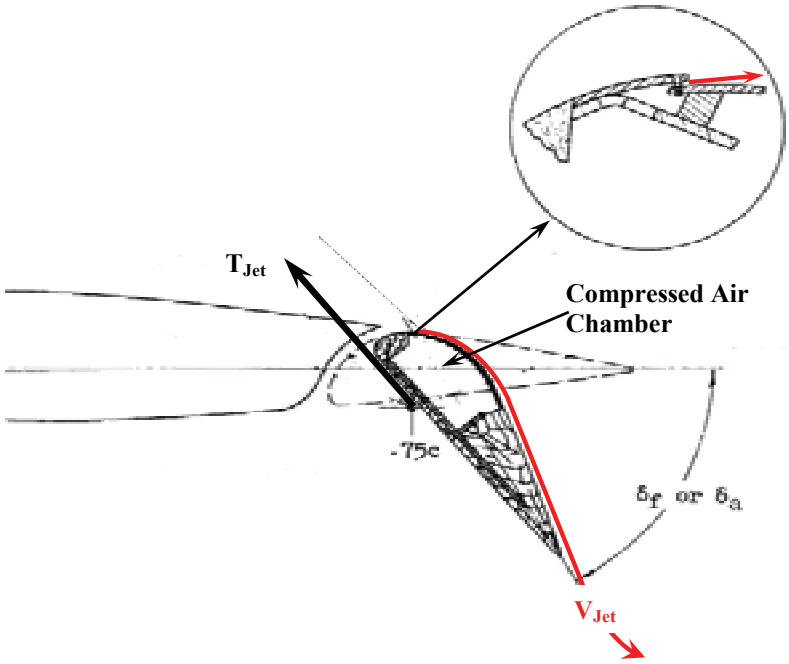

Fig. 3-101. The hollow spars of the flap and the aileron were the final chamber for compressed air. The air escaped at high velocity to the atmosphere through a 0.04-inch-high slot.

To complete the estimate, I will assume that the compressor can provide sufficient air quantity and mass flow at a reasonable pressure ratio so that the jet velocity (V_{Jet}) is at the speed of sound, say 1,116 feet per second. This assumption is known—by more knowledgeable engineers than me—as the velocity that chokes the nozzle. You can immediately see that the BLC system *could* require a great deal of power because

$$(3.139)\quad HP_{BLC} = \frac{(T_{Jet}V_{Jet})_{Flaps} + (T_{Jet}V_{Jet})_{Ailerons}}{550} = \frac{(558+42)(1{,}116)}{550} = 1{,}220 \text{ hp}.$$

This result of 1,220 horsepower assumes, of course, an ideal compressor driven by an ideal engine (or motor) and that there are no losses in piping the compressed air to the flap and aileron slots, or, if you prefer, nozzles. (Recall that an equation to calculate ideal compressor power was given earlier on page 370.)

The rough power-required estimates I have made can be summed up for the complete, four-engine aircraft as follows:

Induced	5,108
Propulsion	3,602
Profile	920
BLC	1,220 (ideal)
Total	10,850

and you now see that decreasing the approach speed from 83 knots to 41 knots requires virtually doubling the power available. As an aside, it might interest you to know that if the diameter of each of the four propellers was increased from 13 to 33.6 feet, 10,850 horsepower would lift the 60,000-pound weight vertically at sea level on a standard day (assuming an aircraft Figure of Merit of 0.6). Of course, positioning four 38-foot-diameter props along a 110-foot wingspan would require considerable overlapping and, of course, wing redesigning.

The drag-due-to-lift data from this four-propeller test can be added to the Helmbold graph that you see evolving. The results are shown in Fig. 3-102.

With the completion of testing with the NASA four-propeller version of the Fairchild C-123, the NASA Ames researchers reported an application of their test results in NASA TN D-1032 [491]. The authors of this report, James Weiberg and Curt Holzhauser, wrote:

> "Interest in obtaining short take-off and landing (STOL) performance led to the wind-tunnel tests of a large-scale propeller-driven transport-type model reported in references 1 to 4 [410-413]. Boundary-layer control (BLC) applied to trailing-edge flaps and ailerons provided large increases in lift because of the increased effectiveness of the flap in the propeller slipstream. However, the data [410-413] were not presented in terms of STOL performance improvements possible, nor were the limitations pointed out. Subsequent to the wind-tunnel tests, flight experience was obtained with an airplane similar to the model of reference 2 [411]. Some of the problems that resulted when STOL-type approaches and landings were made are reported in reference 5 [492].
>
> A study is presented of the improvements in take-off and landing distances possible with a conventional propeller-driven transport-type airplane when the available lift is increased by propeller slipstream effects and by very effective trailing-edge flaps and ailerons. This study is based on wind-tunnel tests of a 45-foot-span, powered model, with BLC on the trailing-edge flaps and controls. The data were applied to an assumed airplane with four propellers and a wing loading of 50 pounds per square foot. Also included is an examination of the stability and control problems that may result in the landing and take-off speed range of such a vehicle.
>
> The results indicated that the landing and take-off distances could be more than halved by the use of highly effective flaps in combination with large amounts of engine power to augment lift (STOL). At the lowest speeds considered (about 50 knots), adequate longitudinal stability was obtained but the lateral and directional stability were unsatisfactory. At these low speeds, the conventional aerodynamic control surfaces may not be able to cope with the forces and moments produced by symmetric, as well as asymmetric, engine operation. This problem was alleviated by BLC applied to the control surfaces."

The last sentence of their conclusion reads:

> "Further reductions in the landing and take-off speeds to obtain shorter distances probably will result in the need to supplement the aerodynamic controls, the need for counterrotating propellers, and possibly the need for interconnected shafting on the propellers."

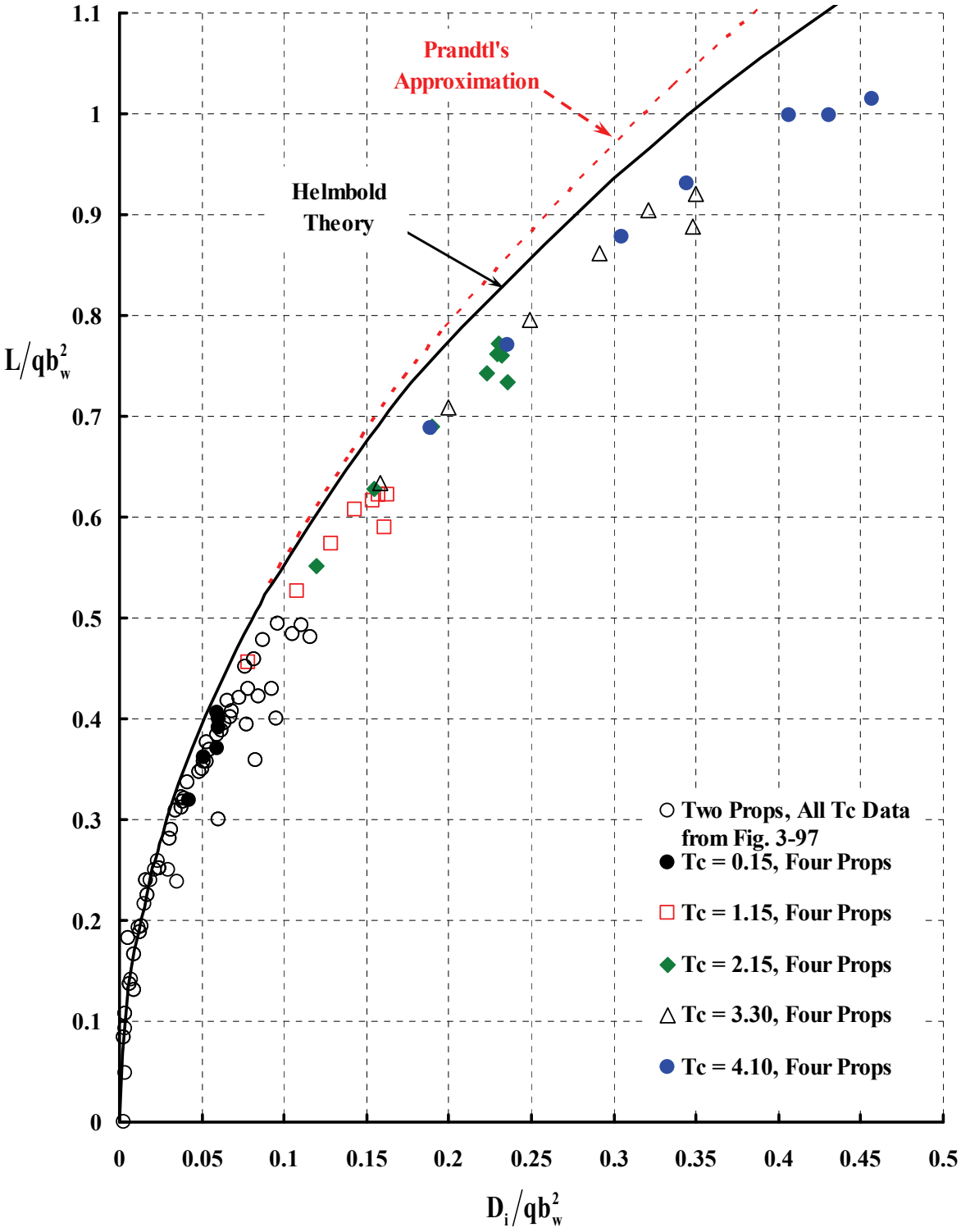

Fig. 3-102. Lift-versus-drag behavior of the four-propeller Fairchild C-123 at model scale. Note: Minimum profile drag removed.

3.6 TILTING WING, FOUR PROPELLERS, FLAPS, AND BLC

In 1960, the researchers at NASA Ames decided to take their 0.4-scale model of the Fairchild C-123 one step further—a step that went well beyond the conventional STOL of that day and age. They modified the model into a tiltwing while retaining the four propellers, the flaps, and for good measure, BLC. In their test report [493] they wrote:

> "The model shown in figure 1 [shown here as Fig. 3-103] was used for the tests reported in reference 1 [four-prop test just discussed] but for the present tests was modified to incorporate wing tilt. The wing could be tilted 30° and 50° from a wing-down position at which incidence of the root-chord was 8.3° with respect to the fuselage reference line. The wingspan was shortened by removing the outboard 40 percent of the wingspan. The geometry of the model tested is shown in figure 2(a) [see Fig. 3-104] and pertinent dimensions are given in table I.
>
> The blowing boundary-layer control system on the flaps is described in reference 2 [the two-prop test]. Details of the jet nozzle are shown in figure 2(b) [see Fig. 3-101]. The height of the jet nozzle was 0.060 inch.
>
> The model was equipped with 4 three-bladed propellers. The geometric characteristics of these propellers are given in reference 1. The blade angle at 0.75 blade radius was 21.5°. The propellers were rotated in a clockwise direction, viewed from the rear."

From a fixed-wing aerodynamicist's point of view, this step—to make a tiltwing aircraft—converted a very well designed airplane with an aspect ratio 9.61 wing into a stubby, awkward looking, not-worth-trying machine with an aspect ratio 5.54 wing. The researchers had turned a silk purse into a sow's ear—as the saying goes. Frankly, after studying Fig. 3-103 and Fig. 3-104, I would have to agree with that view. Of course, testing went on.

Fig. 3-103. The 0.4-scale model of the Fairchild C-123 after conversion to a severely cropped tiltwing (photo courtesy of Bill Warmbrodt, Ames Research Center).

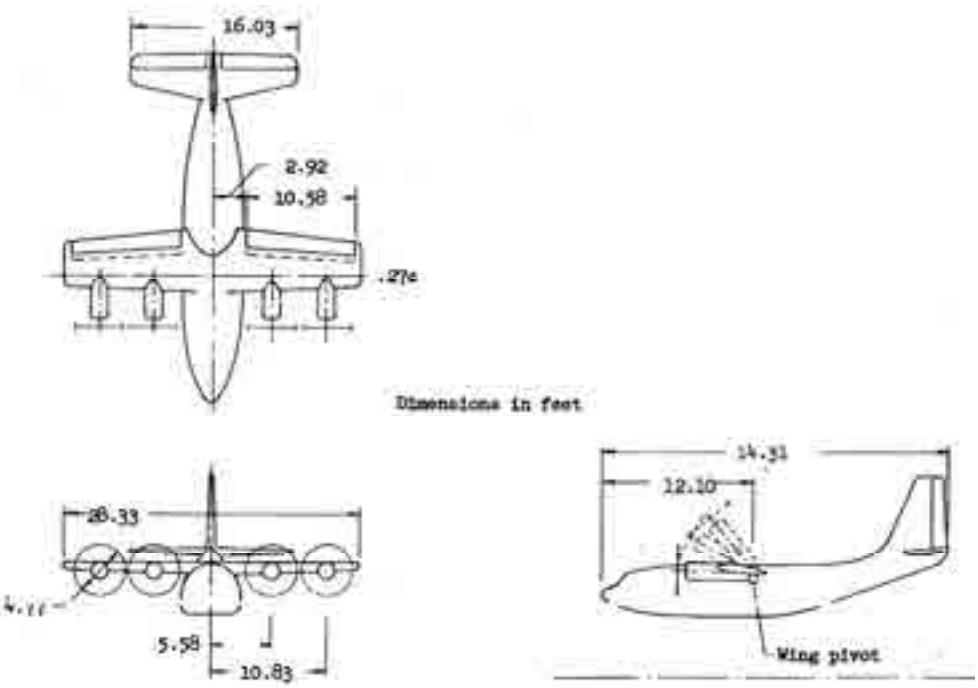

Fig. 3-104. The geometry of the 0.4-scale model of the Fairchild C-123 after conversion to a severely cropped tiltwing. The wing had an aspect ratio of 5.54 and an area of 145 square feet. The mean aerodynamic chord was 5.18 feet [493].

In the introduction to their report [493], the researchers stated that "the data are presented without analysis." More importantly, they stated in a footnote that "because of the difficulty in maintaining constant thrust coefficient [T_C] at values of 9 and above [they reached a T_C of 24], the data obtained were cross-plotted against thrust coefficient to obtain the curves shown in figures 4 to 6 for constant thrust coefficient [9, 15, and 24 T_C] and hence are presented without data points." I first chose the data at a T_C of 24 with a flap deflection (δ_F) of 80 degrees and a blowing BLC coefficient (C_μ) of 0.092 to study in depth for the following discussion. The primary variable is reduced to wing-tilt-incidence angles (i_W) of 0, 30, and 50 degrees to which 8.3 degrees must be added because the "incidence of the root-chord was 8.3 degrees with respect to the fuselage reference line." The angle of attack was measured between the wind tunnel airstream and a fuselage water line.

Study the comparison shown in Fig. 3-105 at a propeller thrust coefficient of $T_C = 3.9$ for the tilting wing versus $T_C = 4.1$ for the non-tilting wing (both at the same incidence angle of $i_w = 0$). Both have BLC on, and the flaps are deflected to 80 degrees. At first glance, you might say the two configurations have nearly equal force polars, give or take some differences in stalling effects, therefore either configuration is worth pursuing. But that would be misleading because the forces are nondimensionalized by different wing areas, and the aspect ratios are quite different, which the tabulated data on the figure make very clear. It is this type of potential incorrect conclusion from data presented in coefficient form that has trapped many an engineer and can lead to incorrect business decisions by upper management.

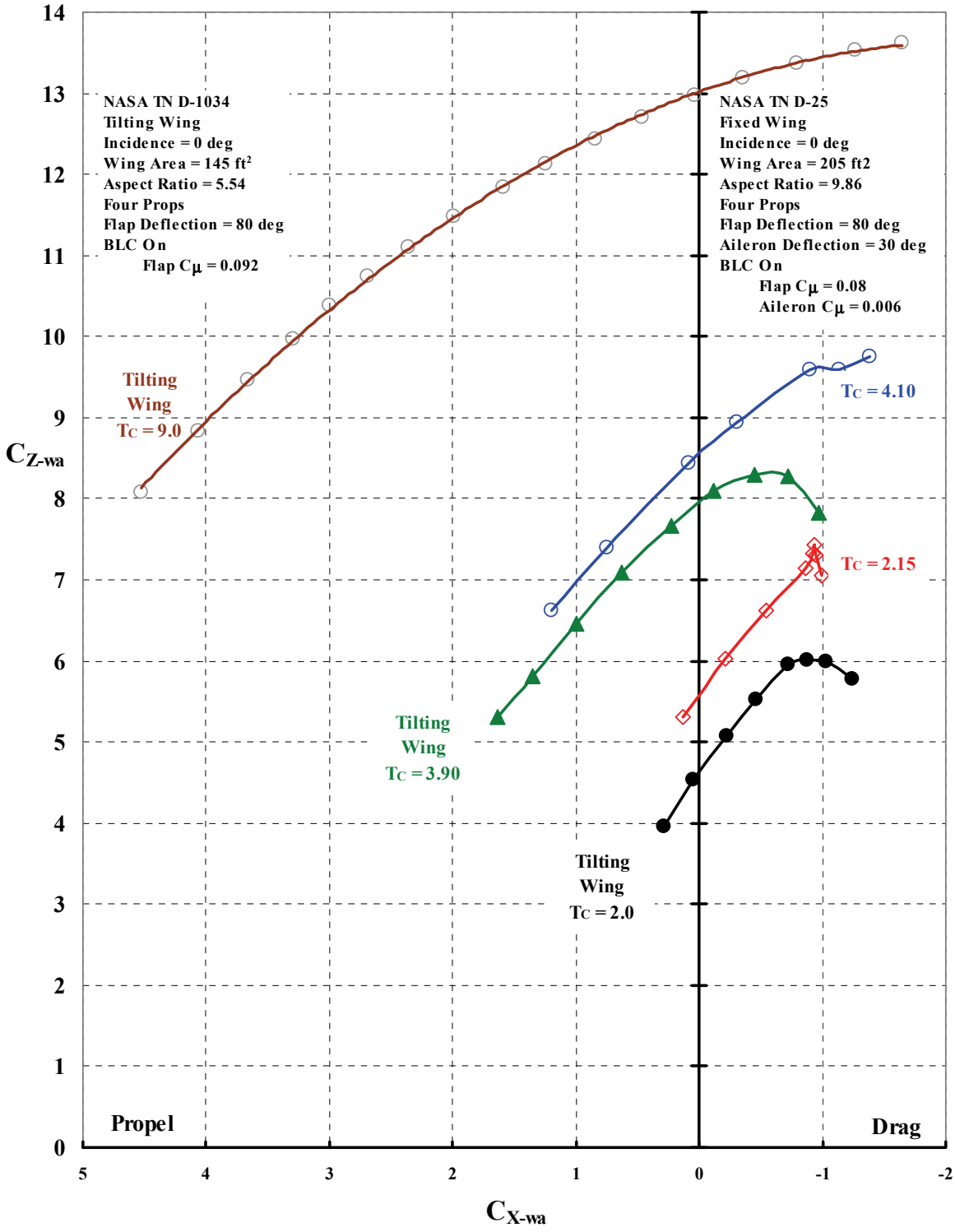

Fig. 3-105. Force polars comparing a tilting wing at an aspect ratio of 5.54 to a fixed-wing at an aspect ratio of 9.86, both at the same incidence angle (i_w = 0 degrees). Note the difference in wing area information that is included for both configurations.

It is, of course, relatively easy to transform the comparison in Fig. 3-105 into the coordinates of

$$\frac{C_{Z-wa}}{AR} = \frac{L}{q_{FP} b_W^2} \quad \text{versus} \quad \frac{C_{x-wa}}{AR} = \frac{X}{q_{FP} b_W^2}$$

and have a quite different comparison, which you see in Fig. 3-106.

The Schairer theory and graph offer one way to compare experimental data to an ideal. The ideal is based on simple physics and, as you can tell, I am a strong believer in its use.

The researchers at NASA Ames investigated the tilting wing force polars at wing incidences of 0, 30, and 50 degrees. For analysis purposes, you must add in the 8.3 degrees of wing root incidence relative to the fuselage waterline, which was the reference line for angle of attack. The baseline configuration was zero flap deflection (δ_F = 0 degrees), with BLC off (i.e., C_μ = 0). At that time, many tiltwing advocates thought the use of flaps and BLC by fixed-wing advocates was a poor choice if *real* STOL performance was the objective. They argued (a) that a tiltwing would always have a VTOL capability at some takeoff weight with the wing at 90-degree incidence and (b) that the VTOL takeoff weight could be substantially increased with partial wing tilting if a STOL requirement was in the cards. The argument deserved to be studied experimentally, and the NASA researchers had just the right model and test procedures to put data on the table.

In Fig. 3-107 and Fig. 3-108 you see the influence of wing incidence (i_w) at several ratios of propeller thrust coefficient (T_C) to aspect ratio (AR). Consider Fig. 3-107 first. All points shown are with zero flap deflection (δ_F = 0 degrees) and with BLC off (i.e., C_μ = 0). This data does not immediately make a case for the VTOL advocates because neither a 38- nor 58-degree incidence shows a force polar comparable to the baseline 8.3-degree built-in incidence. You might note in passing that there is evidence that propeller thrust is slightly improving the 58-degree-incidence configurations relative to the 38-degree incidence.

The more important consideration for VTOL and STOL advocates is fuselage attitude during takeoff and landing. To identify this factor, I have used solid symbols to show you where zero angle of attack is along each force polar in Fig. 3-107. This would correspond to zero pitch attitude, which would be a pleasant benefit to passengers on a civil transport.[121] Now think of the zero-pitch-attitude points in relation to takeoff. The three baseline points, the solid black circles, illustrate the conventional takeoff and landing (CTOL) airplane because the propeller thrust is used primarily to accelerate the aircraft with a maximum $C_{X\text{-}wa}$ and little lift. The three red solid triangles can be thought of as the thrust vectored for STOL. The three blue solid diamonds begin to approximate a near-VTOL condition. You can appreciate from Fig. 3-107 that arriving at an optimum STOL for the shortest field length required can be a rather interesting engineering problem. Now take a look at Fig. 3-108.

[121] Please keep in mind that my emphasis in this volume is heavily slanted toward V/STOL use in commercial transportation.

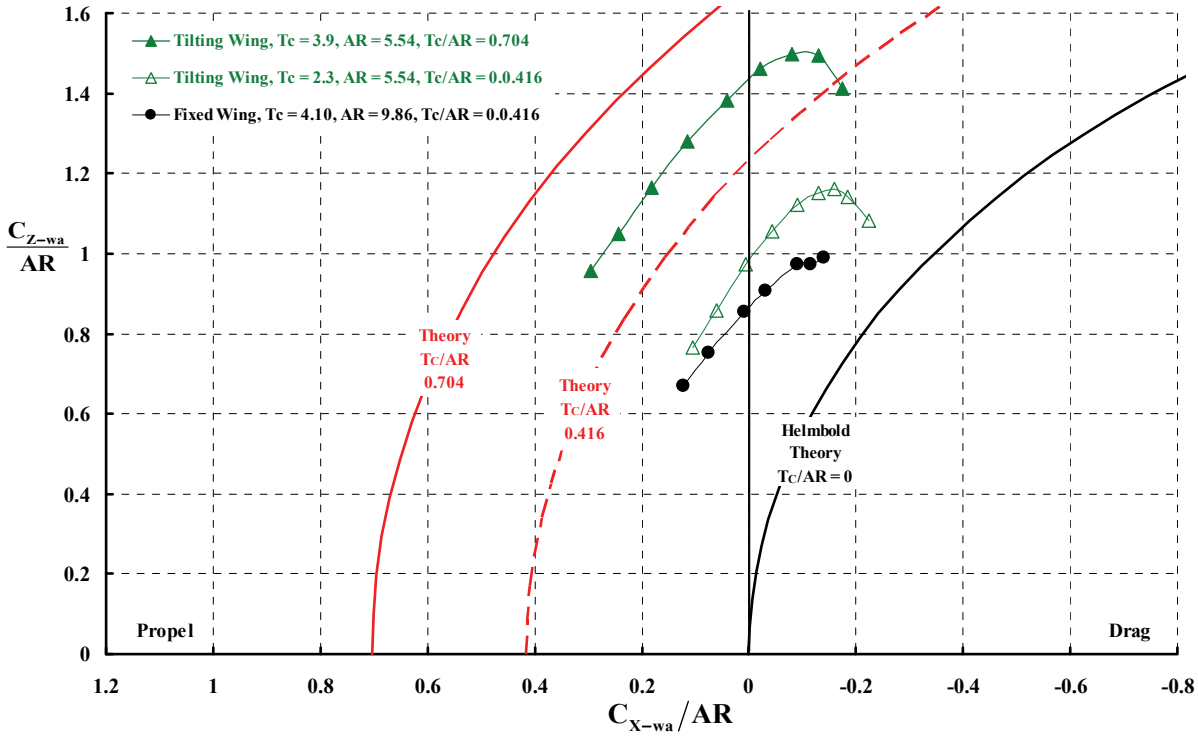

Fig. 3-106. Force polars comparing tilting wing versus fixed wing at the same incidence angle (i_w = 0 degrees). The configurations are shown in Fig. 3-105.

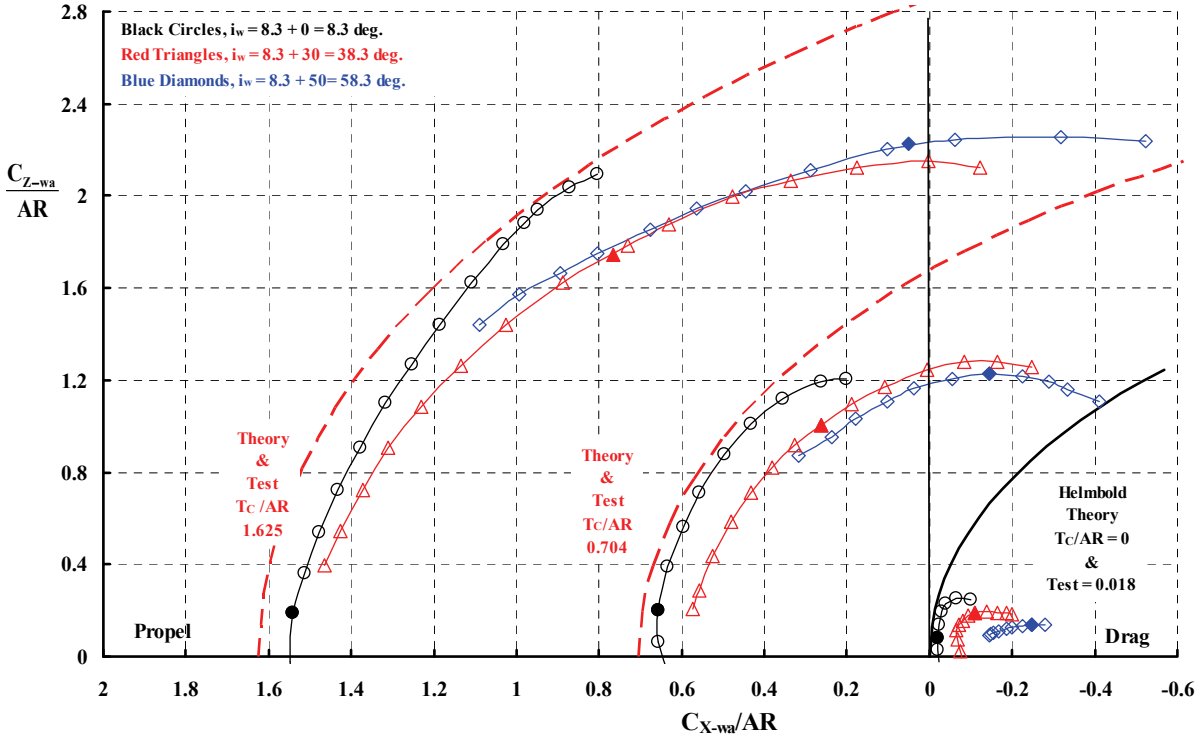

Fig. 3-107. Effect of wing incidence and thrust coefficient on low-speed performance. Flap deflection is zero, and BLC is off for all data points.

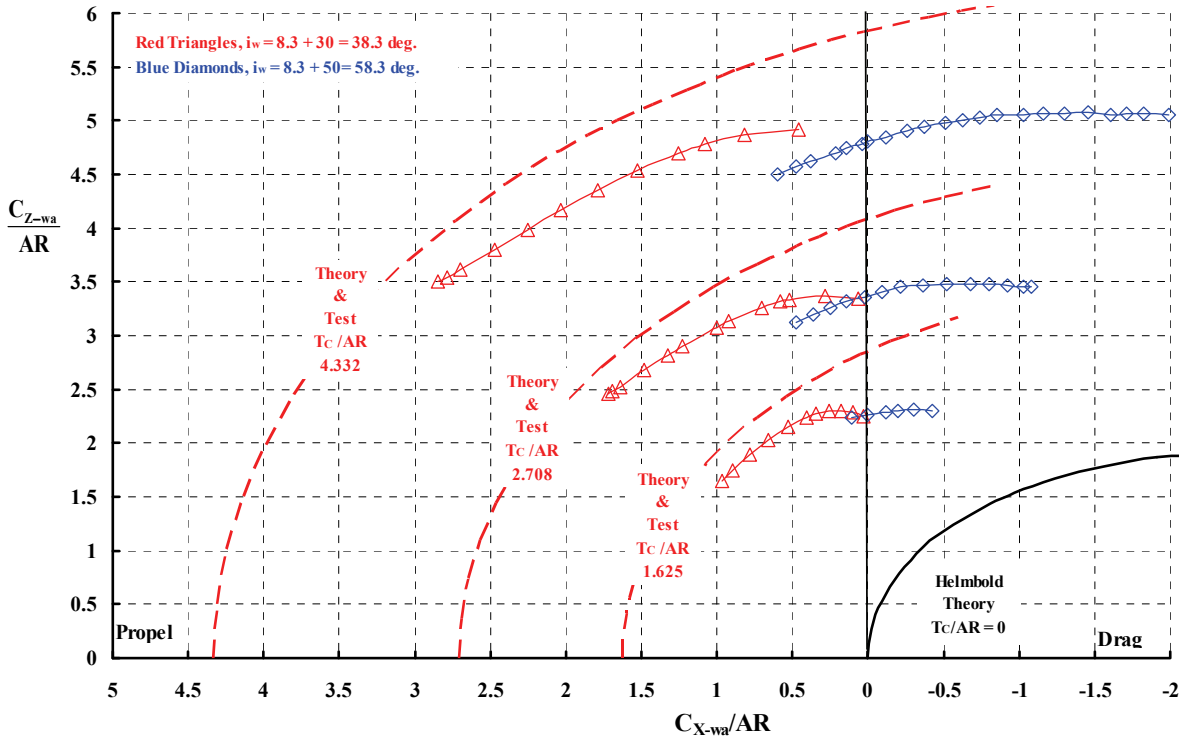

Fig. 3-108. Effect of wing incidence and thrust coefficient on low-speed performance. Flap deflection is 50 degrees, and BLC is on for all data points.

The NASA researchers concluded their experiment with the stubby tilting wing STOL by obtaining data with flap deflection and enough BLC to delay wing stalling. During this last portion of the testing they increased thrust coefficient from 9, which you saw as the maximum on Fig. 3-107, to 14 and 24 T_C for both wing incidences (i_w) of 38.3 and 58.3 degrees as you see on Fig. 3-108. I chose the results for a flap deflection (δ_F) of 50 degrees and a BLC blowing coefficient (C_μ) of 0.065 to give you a feeling for the scope of this NASA Ames research.

Let me conclude on a personal note. In January of 1957, about 6 months after starting my career at Vertol, I was sent up to New York City for the day to the 25th Annual Meeting of the Institute of the Aeronautical Sciences. Why I was given this privilege is still beyond me, although it might have been because "they" had me working on the Model 76 around that time. Nevertheless, I listened to Dick Kuhn (up from the Langley Research Center) present a terrific paper [494] about the propeller-driven STOL research the N.A.C.A. was doing. He contrasted the performance of "tiltingwing types (Fig. 3-96) with deflected-slipstream types (Fig. 3-95)." Dick's paper, which I bought with my own money, has an appendix giving the neatest and simplest summary of takeoff and landing theory I have ever seen.

3.7 FOUR PROPELLER-DRIVEN STOLS

There are literally hundreds of thousands of airplanes that can be labeled as STOLs if you use a small runway as the criteria. You need only scan all of the *Jane's All the World's Aircraft* books published since 1910 to see pages and pages of light, one-, two-, three-, or four-seaters that did, and can, operate quite comfortably from any 1,500- to 2,500-foot-long strip of semi-prepared ground. Alternately, you can re-examine Fig. 1-2. No special features for STOL operation drove these designs. By their very nature—low installed power and relatively high drag—they do not cruise much above 150 knots and have approach speeds of 50 knots or less without flaps or boundary layer control, or any other powered lift devices. Just think about the fabulously popular Piper J-3 Cub of the pre-World War II era as one example. Not one of these light machines is on my list of STOL aircraft that you saw early in Fig. 1-22 on page 30. My selection from the hundreds of thousands of machines amounts to the 36 STOL transports powered by piston and gas turbine engines. Within this narrowed-down group, most are propeller driven, and it is from this even narrower group that I want to give you more detailed background.

The last hundred pages or so you read dealt primarily with aerodynamics and with performance in particular. That is a traditional way of beginning a discussion about STOLs, but it is the operational characteristics that really matter. Therefore, the aircraft I have selected to discuss in more depth have each contributed a long list of characteristics, operational data, and lessons learned that, you will see, make or break a successful STOL. I will begin with the production success de Havilland Canada had with STOL airplanes and then follow up with two STOL demonstrator programs that should have turned into production programs but did not. Later, in Chapter 4, I want to discuss some general trends that may be of use should an airplane with real STOL performance be required in the future.

3.7.1 De Havilland Canada (DHC) Production STOLs

Geoffrey de Havilland opened the de Havilland Aircraft Co. Ltd. in England on September 25, 1920. He and his company quickly became world famous with his D.H. 60 Moth, a two-seater training airplane. The history of the company is well discussed in A. J. Jackson's book [471]. Perhaps you will recall that the first commercial jet was the de Havilland Comet, which British Overseas Airways Corporation started using to carry fare-paying passengers on May 2, 1952.

The Canadian arm of the company (DHC) was established in 1928. In 1993, the then-retired Vice President of Engineering, Richard D. Hiscocks, wrote *A Case Study of the de Havilland Family of STOL Commuter Aircraft* [495]. The general information and the detailed data about the STOL aircraft that the company produced is absolutely fascinating, and I would say you should not start any STOL discussion until you have read this engineer's writings.

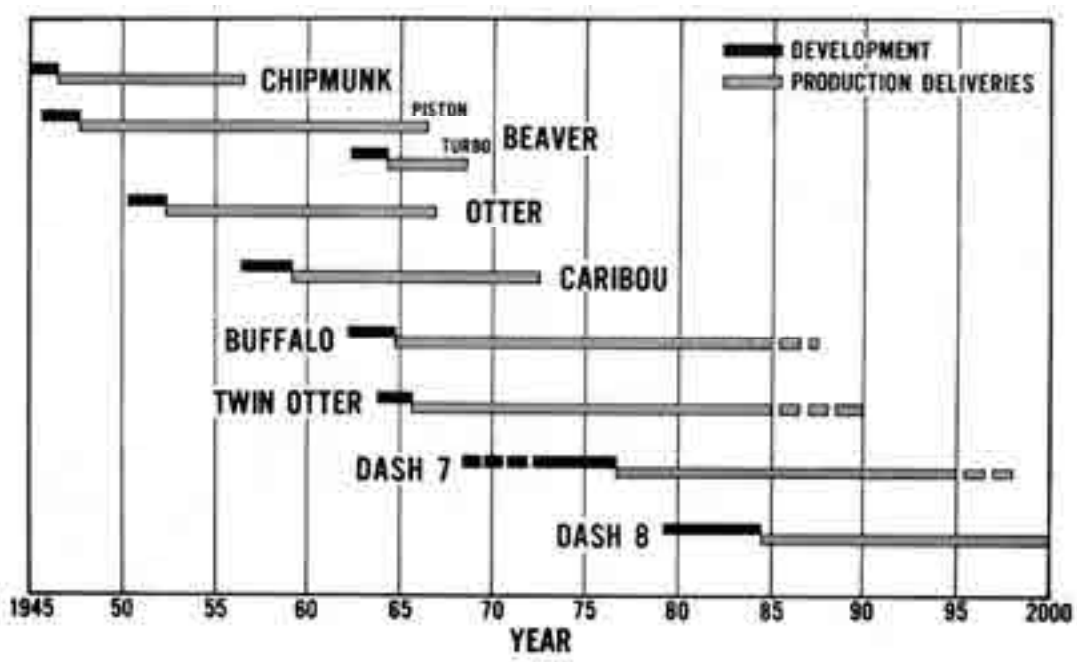

Fig. 3-109. De Havilland Aircraft of Canada Ltd. produced many aircraft before it was sold to the Boeing Company in early December of 1985 [495].

The family of aircraft Mr. Hiscocks discusses in his figure 2 is shown here as Fig. 3-109, and he notes that between 1945 and through 1981, his company produced just under 5,000 machines. He conveys the design philosophy for these aircraft as follows:

> "All of the members of this family of aircraft are designed to clear a 50 foot obstacle in approximately 1,000 feet under takeoff power, to descend on a 7½ degree glide path and land over a 50 foot obstacle in a total distance of 1,000 feet using maximum performance techniques."

He then goes on to write:

> "With the safety standards required in civil transport operations this distance is increased. For example, in multi-engined aircraft, the ability is required to fail an engine at any point in the takeoff and perform an accelerated stop or to continue the takeoff on the surviving engines and clear an obstacle. Under these conditions, the field length requirements of the DHC aircraft are approximately doubled on a standard day at sea level.
>
> This performance will permit the use of 'stub' runways on a 'non-interference with existing traffic' basis at crowded airports and, for small communities, the cost of runways is reasonable.
>
> To design for runways shorter than these, in the company experience, implies a high cost and excessive complexity of systems."

To me, these approaches lie at the heart of the STOL design philosophy. Maximum performance can only be used if all engines are operating, but the true design criterion is STOL with an engine inoperative and with considerable control margins. This is exactly the modern design criteria for multiengine helicopters designed to FAA Category A requirements, which you learned about in Volume II.

When you read Mr. Hiscocks' case study you will come across his figure 26, reproduced here as Fig. 3-110. Now you can see that the de Havilland design approach is squarely aimed at offering aircraft that can operate in and out of at least 75 percent of the 10,692 runways (in 1971) that the FAA keeps track of. If an aircraft has STOL performance equal to a 1,500-foot runway, then the 75 percent increases to about 93 percent of all runways in the United States (and islands). Mr. Hiscocks[122] is an engineer after my own heart because his intent seems to me to be to simply capture the STOL market in toto.

Before discussing several key features that a designer must incorporate to create a better-than-satisfactory STOL aircraft, let me summarize some configuration and performance data for each aircraft the case study examines. I can do this rather easily because Mr. Hiscocks included a great deal of descriptive material in his appendices. Only a few holes needed to be filled in from other sources, such as references [496-499] and *Jane's All the World's Aircraft*, to produce Table 3-6.

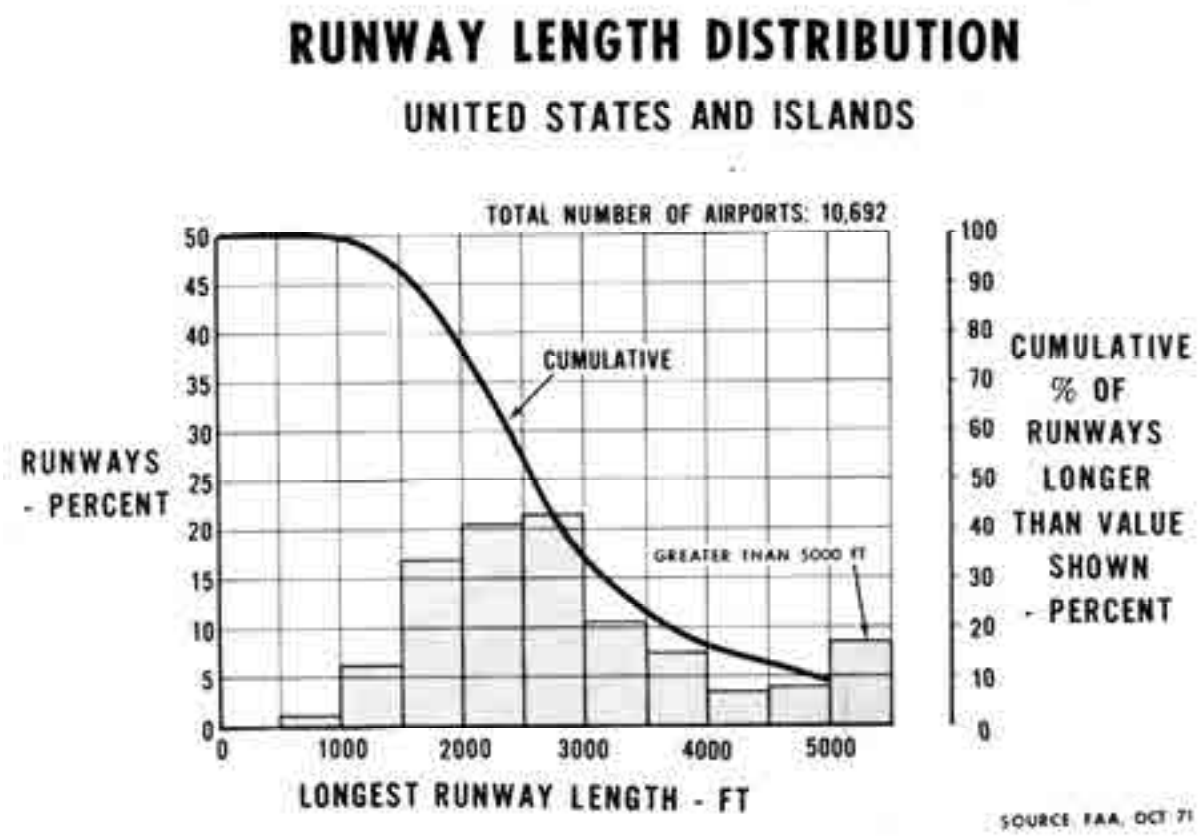

Fig. 3-110. The vast majority of runways are under 3,000 feet in length [495].

[122] I seem to naturally add "Mr." when a gentleman's piece of work just seems downright outstanding—and doubly so for this chief engineer. Mr. Hiscocks died in early December of 1996. I would have liked to work for him.

Table 3-6. De Havilland Production STOLs

Item	Unit	DHC-1	DHC-2	DHC-3	DHC-4	DHC-5D	DHC-6-300	DHC-7
Common name		Chipmunk	Beaver	Otter	Caribou	Buffalo	Twin Otter	Dash 7
Military designation		Landplane	Army L-20	Army U-1A	Army CV-2B	Army CV-7A	Army UV-18A	Army EO-5C
First flight date		May 22, 1946	Aug. 16, 1947	Dec. 12, 1951	July 30, 1958	Sept. 22, 1961	May 20, 1965	Mar. 27, 1975
References (plus FAA type certificate data sheets)		[495, 500-502]	[495, 502, 503]	[495, 502, 504]	[495-498, 502, 505]	[495, 499, 502, 506]	[495, 502, 507]	[495] TCDS A20EA
Crew/passengers		1/1	1/7	1/10	2/30	3/41	2/20	2/50
Type		Two-seat trainer	STOL utility transport	STOL utility transport	STOL utility transport	STOL tactical transport	STOL utility transport	Quiet STOL airliner
Engine and (no.)		DH Gipsey Major 10 (1)	P&W R. 985 Wasp Jr. (1)	P&W R-1340-S1H2-G (1)	P&W R2000-7M2 (2)	GE CT64-820-4 (2)	P&W PT6A-27 (2)	P&W PT6A-50 (4)
Takeoff rating (SFC)	hp	142 (0.57)	450 (0.70)	600 (0.68)	1,450 (0.65)	3,133 (0.49)	620 (0.612)	1,120 (0.587)
Max continuous rating (SFC)	hp	138 (0.56)	400/0.50	400 (0.48)	725 (0.46)	2,745 (0.51)	620 (0.612)	973 (0.607)
Propeller (diameter/blade no.)	ft	6.75/2	8.50/2	11.0/3	13.083/3	14.50/3	8.5/3	11.25/4
Propeller speed (TO/Cruise)	rpm	2,400/2,100	2,300/2,200	2,250/2,000	2,700/2,550	1,160/1,015	2,100/2,100	1,210/1,210
Wingspan	ft	34.33	48	58	95.625	96	65	93
Wing area	ft^2	172.5	250	375	912	945	420	860
Wing aspect ratio	na	6.83	9.22	8.97	10.02	9.75	10.06	10.00
Horizontal tail area	ft^2	na	48.4	85.0	230.0	233.0	100.0	217
Vertical tail area	ft^2	na	25.4	69.0	211.0	152.0	82.0	170
Maximum gross weight	lb	1,930	5,100	8,000	31,300	49,200	12,500	44,000
Normal STOL takeoff weight	lb	1,900	5,100	8,000	28,500	41,000	12,500	44,000
Maximum landing weight	lb	1,900	5,100	8,000	28,500	39,100	12,300	42,000
Basic weight empty	lb	1,277	2,827	4,100	17,800	22,337	5,850	27,030
Operational weight empty*	lb	1,695	3,294	4,431	18,260	23,197	7,415	27,680
Fuel capacity (U.S. gal.)	gal./lb	32.4/194	96/576	216/1,295	807/4,842	2,107/13,695	378/2,459	1,480/10,060
Maximum (speed/altitude)	kts/ft	122/SL	142/5,000	139/5,000	188/6,500	250/10,000	200/10,000	231/8,000
Max cruise (speed/altitude)	kts/ft	na/SL	124/5,000	120/5,000	158/7,500	227/10,000	235/10,000	244/15,000
Economical (speed/altitude)	kts/ft	98/SL	113/5,000	105/SL	137/7,500	181/10,000	181/10,000	227/15,000
Range	nm	385	395	820	1,307	1,887	775	690
Takeoff (grd run/over 50 ft)	ft	775/1,165	560/1,015	630/1,155	670/1,235	1,040/1,540	700/1,200	1,100/2,260**
Landing (grd run/over 50 ft)	ft	465	500/1,000	440/880	725/1,185	610/1,120	515/1,050	900/1,950**
Horsepower/ton of GW		147	200	150	204	306	198	203

* Basic weight + crew and equipment + trapped liquids. ** FAR 25 sea level, zero wind, dry, hard, level surface.

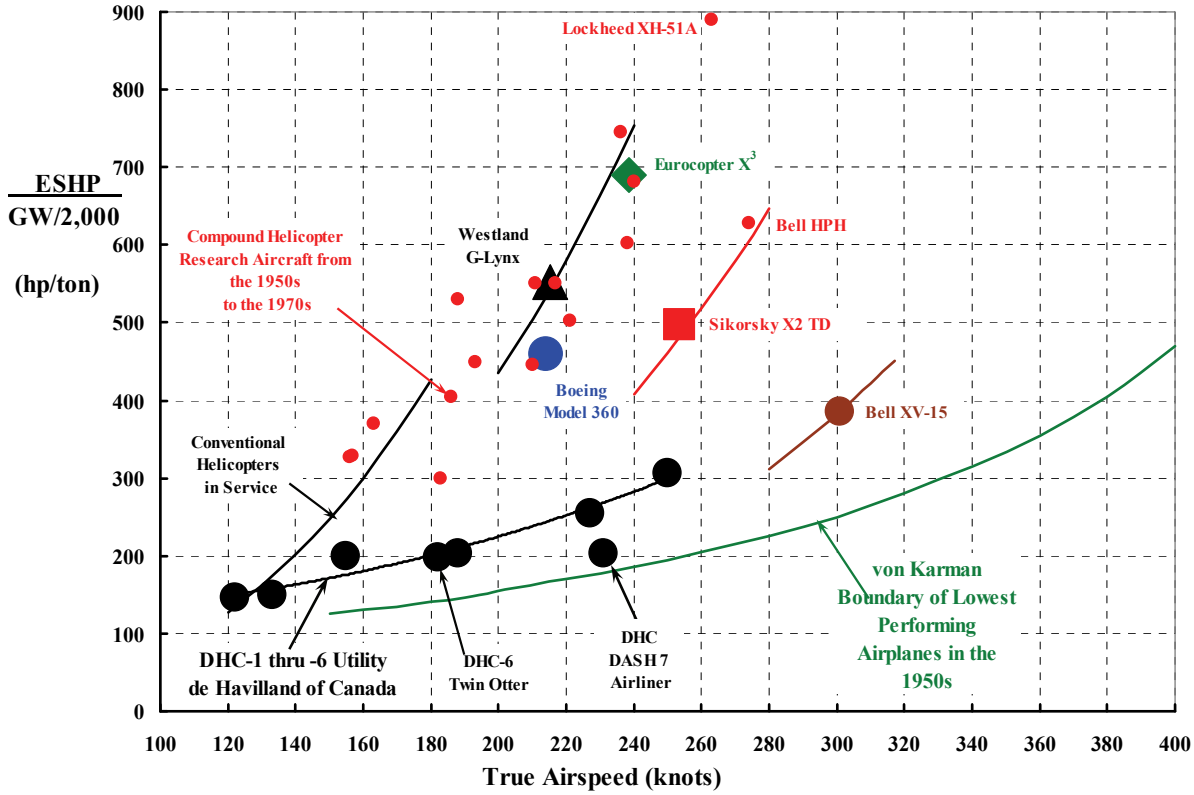

Fig. 3-111. There appears to be a penalty for incorporating STOL capability—at least based on de Havilland's product line trends.

The key trend data of installed horsepower per ton of gross weight versus maximum true airspeed for de Havilland products is illustrated in Fig. 3-111. Here I have shown the de Havilland STOL data compared to several high-speed rotorcraft you saw earlier. This comparison says to me that there is a penalty for incorporating STOL capability into a conventional airplane just as there is for incorporating VTOL capability. I am using von Karman's boundary for lowest performing airplanes in the 1950s as a reference and assuming more installed power than what the green line suggests is a measure of the penalty.

You will note on Fig. 3-111 that the de Havilland Twin Otter (the DHC-6) is singled out with a label. The reason for this is because the Twin Otter and the Bell XV-15 are twin-engine aircraft with approximately the same normal gross weight. That is, the Twin Otter (Table 3-6) has a normal gross weight of 12,500 pounds, and the Bell XV-15 tiltrotor (Table 2-7 on page 129) has a normal gross weight of 13,000 pounds. The aircraft are quite different in terms of installed horsepower. The Twin Otter has two 620-horsepower Pratt & Whitney turboprop engines while the Bell XV-15 uses two Lycoming LTC1K-4K turboshaft engines, each having a takeoff rating of 1,550 horsepower. In short, the VTOL aircraft has 2.5 times the installed power of a similarly sized STOL. This, of course, is an apples-to-oranges comparison in many respects. For example, increasing the installed power of the Twin Otter by a factor of 2.5 would certainly increase its true airspeed to something on the order of 250 knots and much more if the Twin Otter's fixed gear was retractable as it is on the XV-15.

3.7.2 The Bréguet 941 Demonstrator

The Bréguet 941 (Fig. 3-112, Fig. 3-113, and Fig. 3-114) brought the *propeller-driven* STOL, capable of takeoff and landing from a 1,000-foot runway, to the most advanced state the industry was going to see. This 1960's aircraft saw the end of an era because the addition of a bypass fan to a turboshaft engine (i.e., a turboshaft engine driving a ducted fan) provided a large column of relatively cool air that could be directed over deflected flaps. Thus, turbojet aircraft cruise speeds with shorter takeoff and landing speeds were no longer a dream to the fixed-wing community as you will read in more detail later.

The history of how the Bréguet 941 series came into being is quite interesting. During the early 1960s, the United States Army and the North Atlantic Treaty Organization (N.A.T.O.) in Europe saw a need for a light tactical transport. By light, these armed services meant somewhere around 45,000 pounds takeoff gross weight. The French company, Bréguet Aviation,[123] anticipated the need and began development of a proof-of-concept machine called

Fig. 3-112. The four propellers were interconnected on the Bréguet 941 because of success demonstrated by the smaller Bréguet 940 (photo courtesy of Bill Warmbrodt, Ames Research Center).

[123] Bréguet Aviation was short for Société des Ateliers d'Aviation Louis Bréguet. You might recall from Volume II that Louis Bréguet developed a successful coaxial helicopter with help from Richet. After seeing the German Henrich Focke's side-by-side machine, Bréguet ceased further helicopter interest and turned to developing and producing fixed-wing aircraft. His company was very successful, and in 1971 he merged with Marcel Dassault to form the Avions Marcel Dassault-Bréguet Aviation.

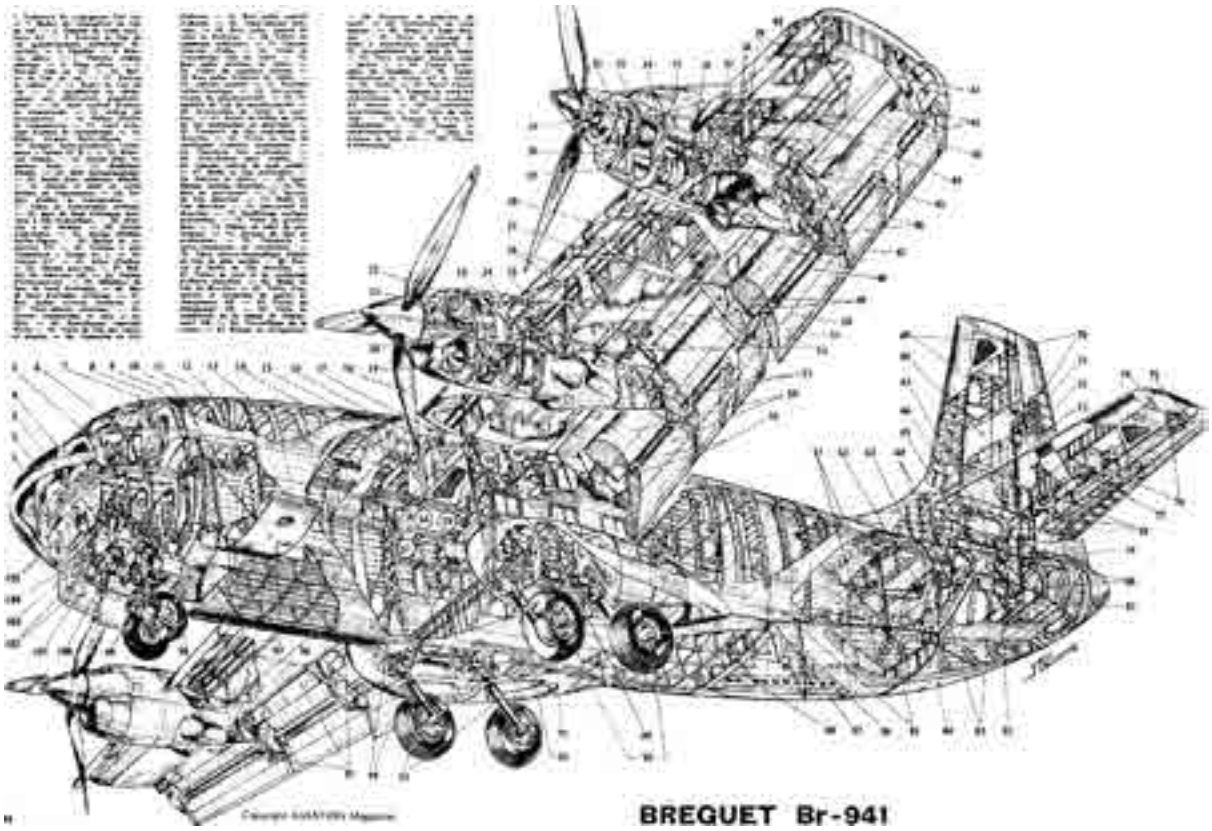

Fig. 3-113. In front view, the outboard port and inboard starboard propellers turned clockwise; the inboard port and outboard starboard propellers turned counter-clockwise. This minimized antitorque creating a rolling moment.

the Bréguet 940, which first flew on May 21, 1958. This technology demonstrator aircraft had a wingspan of 57 feet, 5 inches, and was powered by four 400-shaft-horsepower Turbomeca Turmo II free-turbine engines. The propellers were three-bladed with a diameter of 13 feet, 1 inch, and they were manufactured by Ratier-Figeac.[124] The maximum takeoff gross weight of the Bréguet 940 was 16,180 pounds.

The key feature of the Bréguet 940, and then the 941, was—in my opinion—that the four propellers were interconnected through each engine's gearbox with a transverse shaft (Fig. 3-115). With this one design decision, the whole issue of a single engine failure on takeoff or landing was relegated to a manageable reduction in power. The whole question of handling qualities during this emergency was simply taken off the table, and all the associated aircraft compromises normally worried about became of minimum concern. A corollary to the interconnect decision was that the two propellers on the starboard side were counterrotating as were the two on the port side, which, because of equal propeller RPM, removed the majority of any rolling moment caused by propeller torques being unequal. Another beauty of this design decision was that, on landing, two propellers could be propelling and the other two could be "dragging" because of the variable pitch capability. This design decision helped the

[124] Paulin Ratier started the company in 1904 and specialized in wooden propellers. Figeac is a town in France.

pilot hold the descent angle nearly constant while providing nearly instantaneous positive thrust for an emergency go-around. I can only imagine the trade studies and discussions that went on at the Bréguet Company prior to the final decision being made on this key feature.

The thought process behind these design decisions was explained by General Henri Ziegler, General Manager of the Bréguet Aviation Company, when he gave the 14th Louis Bleriot Lecture before the Royal Aeronautical Society [175]. In discussing the approach, General Ziegler stated:

"Actually, most of the difficulties [of STOL] are encountered, not during takeoff which is an accelerated transient configuration, but in landing. The idea is to utilize power in approach. But, if the aircraft is to remain at a reasonable attitude, the thrust of the propellers is to be compensated for by drag; otherwise, although the deflected slipstream aircraft can fly at low minimum speed, in that configuration it has a very low angle of descent, or even, with more power, climbs.

The Aerodynamics Department of Bréguet was then in the paradoxical position of having to build up more drag—drag which is usually the aerodynamicist's personal enemy!

Here is their approach to the problem:

As is probably known, for safety reasons on which I will comment later, the four engines and the four propellers are interconnected by a shaft. The idea has been to create induced drag or achieve an artificial reduction of the aspect ratio. In order to do this, the two external propellers are set at zero equivalent pitch, while all the available power of the four engines is transferred on to the two central propellers, thus largely increasing the blowing effect on the central part of the wing.

This configuration, that we call *transparency*, permits a stabilized descent with over 60 percent of the maximum power on the four engines, under steep slopes up to 20 percent and at low speed less than 45 kts (52 m.p.h.).

Just after touchdown, the aircraft must brake efficiently and any second spent in doing so means a big loss on the landing run, since the speed is still appreciable. In order to achieve efficient braking in a split second, the four propellers are reversed, which has the effect of aerodynamically braking the aircraft and also, instantly, destroying the lift, thus allowing good braking effect on the wheels. There again, the interconnecting shaft is of assistance since, at the moment of touch-down, the pitches of the outboard propellers are already zero, they go immediately into reverse pitch while the positive pitches of the inboard propellers are progressively reduced, then grow negative. At no time are the pitches of all the propellers zero, so that there is no tendency to over-speed [the engines] and the engines do not have to be throttled back."

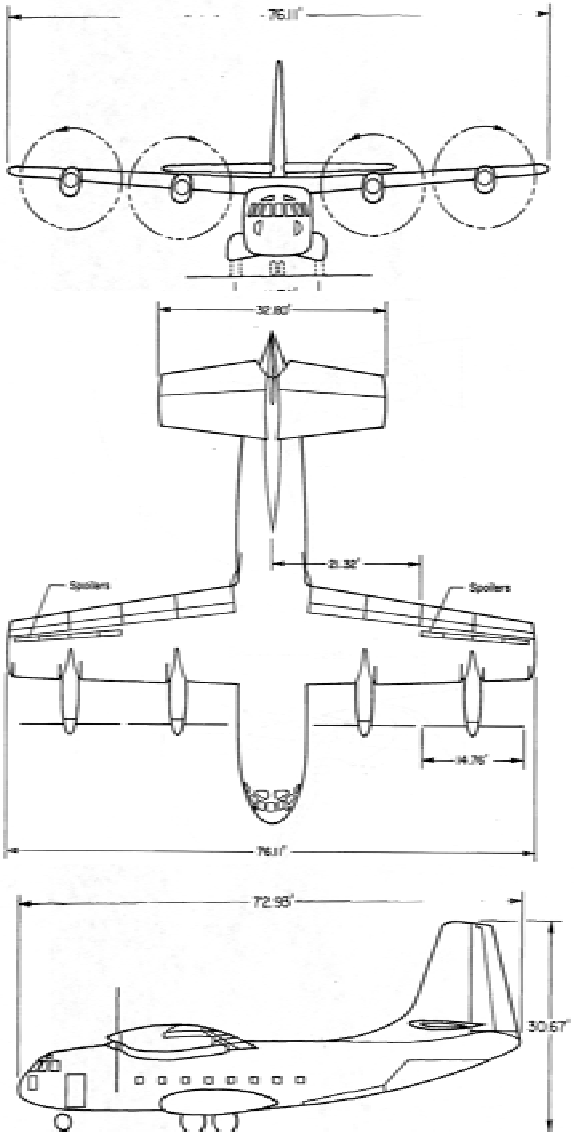

Fig. 3-114. Bréguet 941 three-view drawing [508].

The success of using interconnected propellers was noted worldwide. Furthermore, the demonstrated use of propeller thrust to augment aircraft lift (while still providing propulsion) with the slipstream from four propellers acting on the inboard triple-slotted flaps and the outboard double-slotted flaps was impressive. And then, in the 1961 to 1962 period, N.A.T.O. put out a Basic Military Requirement (NBMR number 4) that called for a larger aircraft than the Bréguet 940. Manufacturers from several countries responded to the request for proposal including de Havilland of Canada with its DHC-4 (the Caribou) and, of course, Bréguet with a larger version of the 940, the Bréguet Type 941.

The Bréguet 941 was a preproduction prototype ordered by the French Air Ministry on February 22, 1960. This aircraft was a 33-percent scaled-up version of the 940 with improvements that corrected most of the shortcomings of the technology demonstrator machine. The aircraft first flew on June 1, 1961. The wingspan was 76.1 feet, the wing area was 886 square feet (versus the 940's 512 square feet) and the maximum takeoff gross weight was 44,000 pounds when powered by four 1,250-shaft-horsepower Turbomeca Turmo III engines. This aircraft was demonstrated both in Europe and in the United States. In fact, NASA and U.S. Air Force pilots had the opportunity to fly the machine in France at the Bréguet factory. The NASA study led to two reports [508, 509] that provided considerable technological data about the Bréguet 941, which I will discuss shortly.

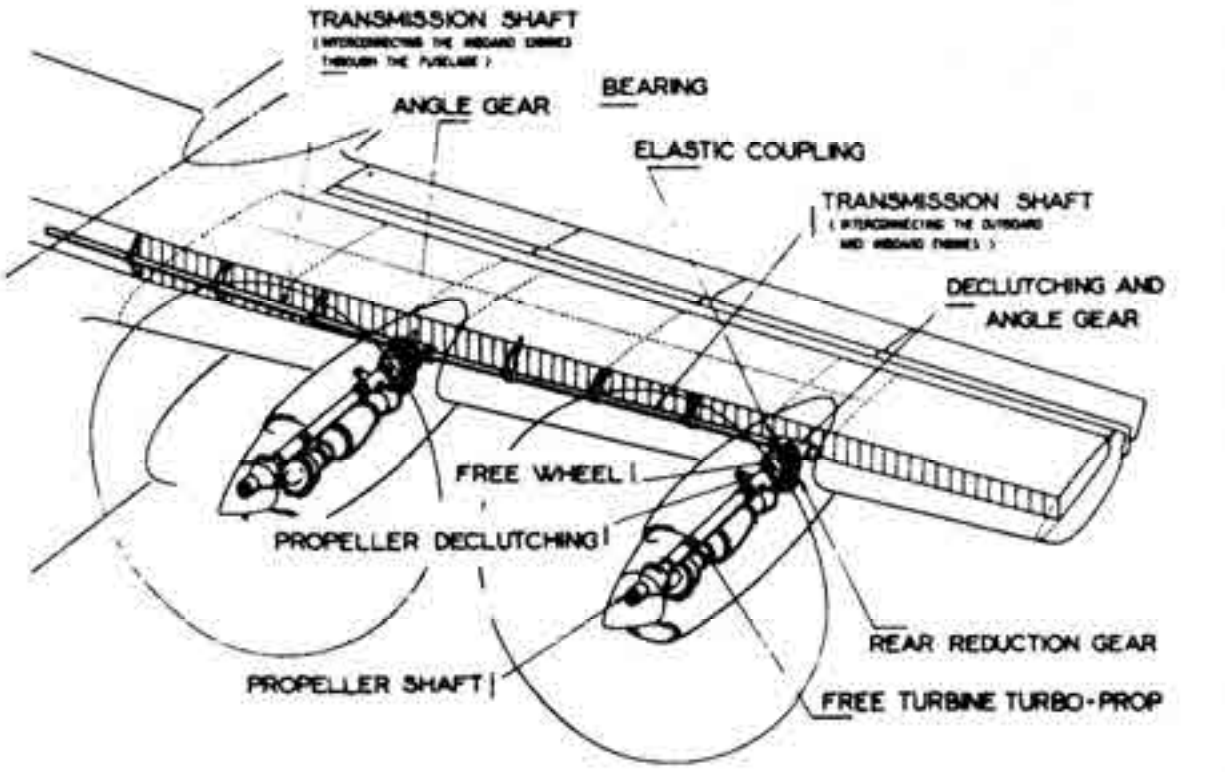

Fig. 3-115. Bréguet 940 and 941 propellers were interconnected just like the typical tandem rotor helicopter [510]. It is probable that fixed-wing STOL advocates strongly resisted the mechanical complexity.

It appears that the N.A.T.O. countries could not agree on the selection of one aircraft to meet their NBMR-4 requirements, and the expected STOL program was dropped. However, the French Air Force knew what they wanted and so funding for four production aircraft was ordered on November 29, 1965. This aircraft was designated the Bréguet 941S. The first aircraft off the production assembly line first flew April 19, 1967. By the Spring of 1968, all four Bréguet 941S aircraft were flying. The slight enlargement in the cargo compartment was considered adequate for 93 percent of the vehicles used by a U.S. airborne division (in the 1960s).

The Bréguet 941S was the top-of-the-line "ultra" STOL configuration that emerged after two decades of research and development by industry and other organizations (e.g., NASA). The only real competitor was the de Havilland DHC-5 Buffalo, which was of serious interest to the Canadian Ministry of Defense and the U.S. Army. The maximum takeoff gross weight of the 941S for the STOL assault mission was 48,500 pounds, but for the long-range mission, the aircraft could be loaded to 58,420 pounds and then the pilots did a conventional takeoff. A comparison of the de Havilland DHC-5D Buffalo to the three versions of the Bréguet 940 series is provided in Table 3-7.

In the late 1960s, McDonnell Douglas became interested in the Bréguet 941S, and a series of demonstrations were carried out in the United States. Aircraft were repainted in American Airlines' and Eastern Airlines' colors and designated the McDonnell 188. The goal was to show the commercial airline world, including the FAA, just what STOL aircraft could do for the transportation system in the United States. The campaign went on for 2 years but ended with no takers. I suppose there were many reasons for this outcome. It might have been that the Bréguet 941S was too expensive to operate on short-haul routes or that the FAA was reluctant to disrupt the then-current air traffic control system. But I am inclined to think that the economical benefits of STOL, and even VTOL, were (and still are) just not there. To me, even buses and trains (with government subsidies) cannot compete with the automobile in the United States—at least until congestion becomes overwhelming. After 14 years of demonstrations, STOL advocates gave up selling a commercial STOL in 1974. However, the U.S. Air Force still was interested in a medium-size STOL, and they initiated a competition that led to the Boeing YC-14 and McDonnell Douglas YC-15, which you will read about a little later on.

The technology demonstrated by the Bréguet 941, powered with four Turbomeca Turmo II engines rated at 1,165 shaft horsepower, was reported by NASA in references [508, 509]. The concluding remarks in Quigley, Innis, and Holzhauser's report [508] is quite interesting. They wrote that

> "A flight investigation of a typical STOL transport aircraft was undertaken, utilizing the Bréguet 94l airplane. The study has shown that the airplane has acceptable performance, handling qualities, and operational characteristics for the STOL mission. The evaluating pilot found the airplane comfortable to fly at the low airspeeds required for STOL operation. Many of the satisfactory characteristics can be attributed either directly or indirectly to the cross shafting of the propellers. The safety aspect of interconnecting the propellers is obvious in case of engine failure and adds much to the pilot's sense of well being when flying at low airspeeds and high power. Lateral control power and adverse yaw characteristics are improved

> to a satisfactory level by the use of differential propeller pitch. Finally, opposite rotating propellers gave aerodynamic symmetry and no lateral or directional moment changes with changes in airspeed or engine power.
>
> The pilot considered both longitudinal and lateral-directional stability too low for a completely satisfactory rating. Low stability, particularly inherent in an airplane with high moments of inertia operating at low airspeeds, results in low restoring moments and long periods which complicate the pilot's control task. More research is required to determine ways to cope with the problem and to adequately define stability and control requirements of STOL airplanes."

There is no question in my mind that with today's fly-by-wire (or light) and computer assistance technology, the Bréguet 941's flight control system, Fig. 3-116 and Fig. 3-117, could be modified to reduce the pilot's workload to virtually zero. As it was, the machine's

Table 3-7. The de Havilland DHC-5D Was the Only Real Competitor to the Bréguet 941S as the 1960s Drew to a Close

Item	Unit	DHC-5D	Bréguet 940	Bréguet 941	Bréguet 941S
Common name		Buffalo	Tech demo	Prototype	Production
Reference		[495, 499, 502, 506]	[511]	[508, 510, 512]	Jane's 1971-72
First flight date		Sept. 22, 1961	May 21, 1958	June 1,1961	April 19, 1967
Crew/passengers		3/41	2/0	2/48	2/56
Pressurized		No	No	No	Maybe
Cabin length	ft	31.4	na	35.0	36.6
Engine and (number)		GE CT64-820-4 (2)	Turbomeca Turmo II (2)	Turbomeca Turmo IIID (4)	Turbomeca Turmo $IIID_3$ (4)
Takeoff rating	hp	3,133	400	1,250	1,500
Propeller diameter and (blade no.)	ft	14.50 (3)	12.47 (3)	14.76 (3)	14.76 (3)
Propeller RPM	rpm	1,160	1,027	1,200	1,200
Wingspan	ft	96.00	58.50	76.08	76.71
Wing area	ft^2	945	512	889	902
Wing aspect ratio	na	9.75	6.66	6.52	6.52
Horizontal tail area	ft^2	233	na	320	320
Vertical tail area	ft^2	152	na	219	219
Maximum takeoff weight	lb	49,200	16,182	45,000	58,420
Operational weight empty	lb	23,197	na	26,950	29,674
Fuel capacity (U.S. gal.)	gal./lb	2,107/13,695	na	1,720/11,150	2,640/17,160
Maximum (speed/altitude)	kts/ft	250/10,000	na	248/SL	243/SL
Maximum cruise (speed/altitude)	kts/ft	227/10,000	na	225/10,000	235/10,000
Economical (speed/altitude)	kts/ft	181/10,000	na	205/10,000	215/15,000
Range	nm	1,887	na	1,375	1,650
Stall (speed/GW)	kts/lb	65/39,000	40/15,400	48/44,100	46/44,100
STOL performance at sea level					
Takeoff weight	lb	41,000	15,400	45,000	48,500
Ground run distance	ft	1,040	280	700	655
Distance over 50 feet	ft	1,540	620	1,150	1,050
Landing weight	lb	39,100	15,400	41,000	44,100
Ground run distance	ft	610	200	400	345
Distance over 50 feet	ft	1,120	520	780	820

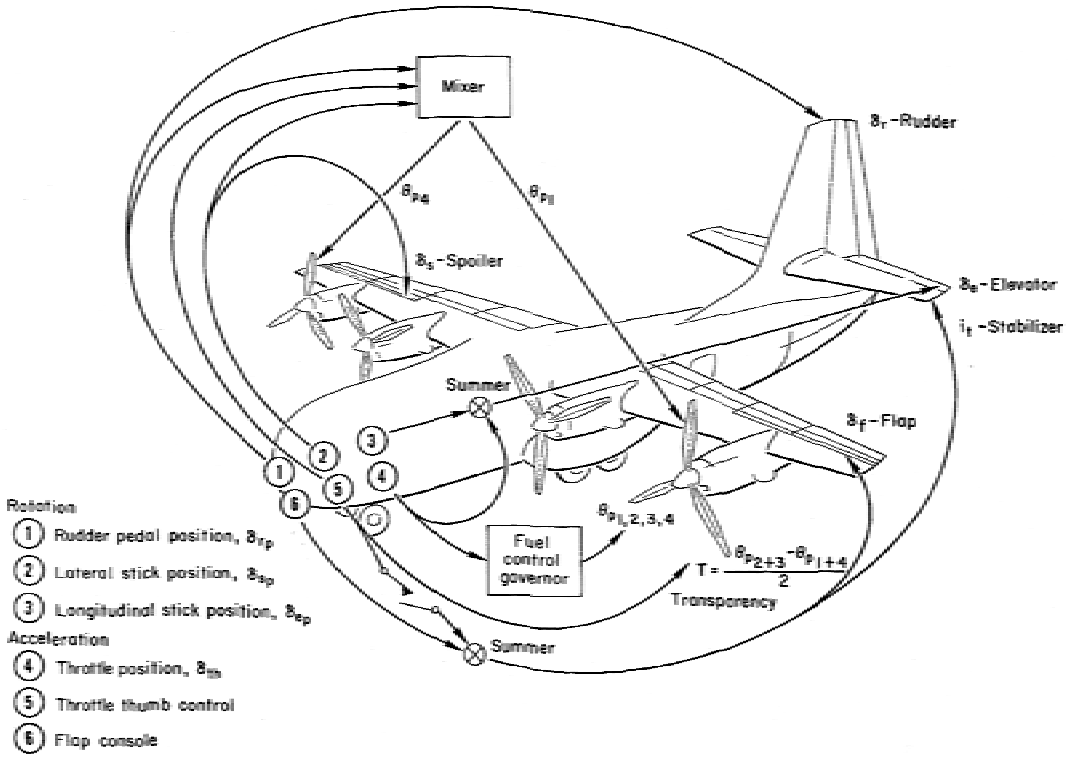

Fig. 3-116. This flight control system was accomplished without a computer [509].

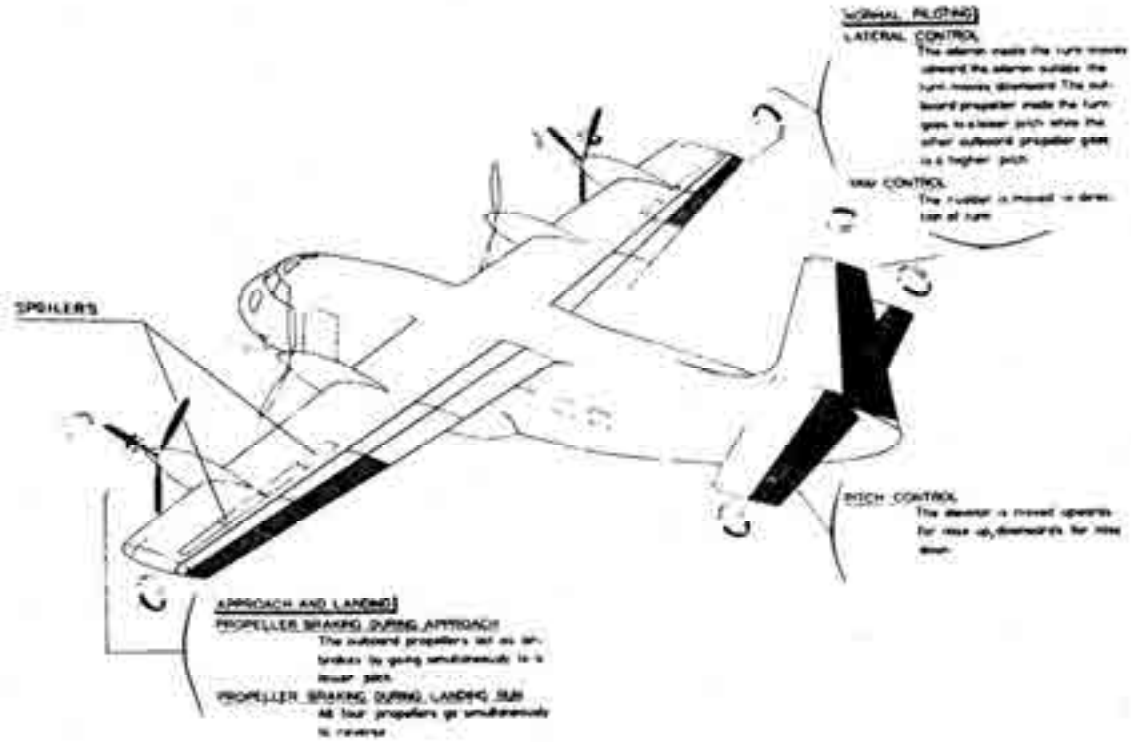

Fig. 3-117. Low-speed STOL operation relied on both the propeller and the flap control system [510].

flight control system was a setup for today's advanced fly-by-wire or light systems. Certainly the control power could be increased somewhat so that the demonstrated "slow speed of less than 60 knots and glide slope of about 8 degrees" would define what STOL means. Therefore, let me go on to the performance aspects of the machine.

The performance data that was reported by Quigley and his coauthors included both takeoff and landings by Bréguet and NASA pilots. These operations were conducted from a concrete runway and from a grass strip with the results shown with Fig. 3-118. It appears to me from this figure that the NASA fairings of the data with lines does not fully point out the scatter. This scatter amounts to at least ±100 feet at low weight, and more like ±200 feet at the heaviest takeoff gross weights. It is clear that a takeoff from a grass strip can easily add 250 feet to the distance required to clear a 35-foot obstacle. The authors' description of the "operational techniques" used to obtain the data shown on Fig. 3-118 is quite informative. They wrote:

> "The takeoff technique was quite easy and straightforward in that no requirement for minimum control speed had to be considered. A time history of a typical take-off is shown in figure 8. The engines can be advanced to full power and checked before the brakes are released. Nose-wheel steering which was provided by a separate control was adequate during take-off, but rudder pedal steering would have been preferable to allow the pilot to keep his left hand on the throttle. Lateral control was adequate for maintaining a wings-level attitude during the take-off roll under all crosswind conditions tested. Up elevator can be applied early in the takeoff roll to obtain nose-wheel liftoff as soon as possible without an apparent drag increase. With this technique, rotation and takeoff occur almost simultaneously at about 55 knots at a gross weight of 38,500 pounds. The recommended procedure is to rotate to an angle of attack between 7° and 10° and maintain this angle until the resultant climb angle has been established. Although this was considered a safe procedure, it does not produce maximum performance. In addition, angle of attack tends to overshoot initially and it is difficult to stabilize at the desired value since pitch attitude, airspeed, and angle of attack are continually changing during the rotation and liftoff. In order to obtain more consistent take-off performance a better guide is needed during rotation and liftoff. An instrument combining longitudinal acceleration with angle of attack would allow the pilot to rotate to a higher angle initially while still maintaining a safe margin from the stall.
>
> Airspeed and angle of attack can be stabilized rapidly in the climb (65 knots and 7° angle of attack at the gross weight tested) and the airplane is easily maneuvered in this configuration. Satisfactory turn entries can be made using only lateral control, and steep turns close to the ground with bank angles up to 45° are relatively comfortable. A slight amount of bottom rudder is required to maintain steady-state turns; however, this was not particularly objectionable to the pilot. The effect of engine failure during take-off was of relatively little concern because of the interconnected propellers; engine failure results only in a reduced rate of climb."

You have, of course, taken note of the U.S. Army's official view [512][125] of the takeoff capability of the prototype Bréguet 941. Their opinion of the aircraft was published in January 1964 after Army representatives participated in a joint U.S. Air Force/French Air Force

[125] This view included charts and tables that the French Air Force prepared, presumably based on their flight test experience and their expectation of what the 941S was expected to achieve with the Turbomeca Turmo IIID rated for takeoff at 1,500 shaft horsepower.

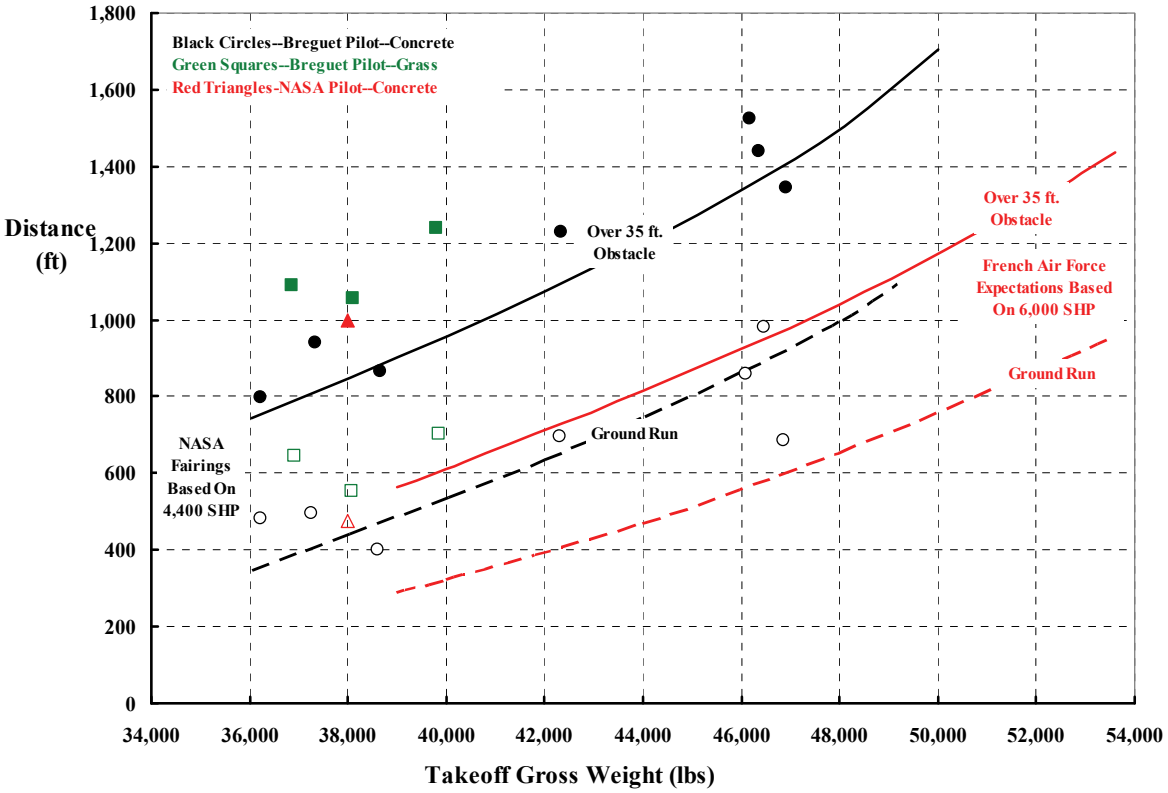

Fig. 3-118. The takeoff performance of the Bréguet 941 was achieved with 1,100 shaft horsepower from each of four engines. The total 18,480 pounds of static thrust from the four propellers was "derived from tests of a 0.55-scale propeller, which gave 4.2 pounds of thrust per shaft horsepower (Figure of Merit equal to 0.57)." French Air Force performance expectations were based (I think) on 1,500 shaft horsepower per engine for the production 941S [508, 512].

evaluation conducted during November 1963. At that time the 941 prototype was the only version flying and was powered by four Turbomeca Turmo IIID engines, each with a takeoff rating of 1,200 shaft horsepower. The most comparative STOL aircraft in U.S. Army service at that time was the de Havilland Caribou II, the CV-7A or the C-8A as designated by the U.S. Air Force after the roles and mission debate with the Army was settled. Incidentally, in response to a question about cost by the Army representative, the statement was made that "the French project pilots estimated the cost of the production version [the 941S] at between 2.0 and 2.5 million dollars per airplane. Bréguet personnel quoted a price of 1.5 million dollars per airplane in a lot of 100 minus radio equipment." This was, I suppose, in 1963 dollars.

While some landing performance data is contained in reference [508], the much more interesting report, by Innis, Holzhauser, and Gallant [509], deals with tests under Instrument Flying Rules (IFR). The major variable they flight tested and reported deals with the approach angle or the descent angle, or glide slope if you prefer. Data is presented for a standard

2.5-degree approach and a 7.5-degree approach. As to the reason for the testing, the authors wrote in their introduction that

> "STOL aircraft can be flown slowly and steeply and therefore can be operated into small airfields and restricted spaces. This capability has aroused interest [in the early 1960s] by airlines and governmental agencies for their use in commercial air travel (refs. 1 to 6). In addition to providing added convenience to the air traveler, landing and taking off slowly and steeply also offers potential for improved all-weather reliability, reduced nonproductive time, and increased safety (ref. 7).[126] Several STOL aircraft have shown the desired low-speed performance in visual flight conditions (refs. 8 and 9), and some helicopter work has been done at STOL speeds on instruments (refs. 10 and 11). However, practically no flight work has been done with STOL aircraft operating in the terminal area under Instrument Flight Rules (IFR) to ascertain their potential as well as limitations and to examine the effect this environment has on the required performance, handling qualities, and operational characteristics.
>
> Tests were conducted with the Bréguet 941, an STOL propeller driven transport, because previous tests by NASA (ref. 9) [508] showed it to have good STOL performance with satisfactory to acceptable handling qualities under Visual Flight Rules (VFR). The airplane was comfortable to fly at low speeds and was capable of descending or climbing at angles greater than 10° at 60 knots. Landing and takeoff distances of 1000 feet over an obstacle were safely attained because the propellers were interconnected and good control was provided about each axis.
>
> The tests were made on a standard 2-1/2° Instrument Landing System (ILS) and on its 7-1/2° secondary lobe to determine the difficulty in tracking an ILS at low speeds to low altitudes. It was anticipated that this task would expose any handling qualities problems. The tests included transitions to the ILS at various altitudes to find acceptable intercept altitudes and operational procedures. Some maneuvering flight work at low altitudes was done to ascertain the capabilities of STOL aircraft operating in restricted airspaces. These results were then used to look at nonproductive time of STOL aircraft when operated in the terminal area.
>
> The tests were conducted by NASA and USAARL in cooperation with Société Anonyme des Ateliers D'Aviation, Louis Bréguet, and the French Air Force. The chief pilot of New York Airways also participated in a portion of the tests."

The profile of the 7.5-degree final approach and landing is illustrated in Fig. 3-119. One of the first questions answered by testing was, What was the minimum altitude at which the pilot felt comfortable when intercepting the ILS signal? When flying at 4,500 feet, the intercept was made over 5.46 nautical miles from touchdown, which was considered rather time-consuming. By working the intercept problem down in altitude, the pilots felt that at an intercept altitude of 1,500 feet above ground level (AGL) they would have about 90 seconds on the glide slope before the 200-foot altitude was reached, and a decision to land or to go around needed to be made.

A key point about the flight along the glide slope that you need to keep in mind is that the aircraft must not be flown right at stall. A speed margin of at least 10 knots must be

[126] This reason—or something similar—for V/STOL has been advanced so many times over the last 60 years that I have lost count. Frankly, I wonder if a better reason for V/STOL might simply be that all the airlines could pick up gates at every terminal they wanted to expand their route structure to. Just imagine if the number of gates at Ronald Reagan Washington National Airport was suddenly expanded by a factor of two nearly overnight.

maintained to allow for correction to any deviation from the glide slope. (In fact, I have heard pilots say they add 10 knots for every child they have.) Data presented in reference [508] show that stalling of the Bréguet 941 was quite benign because:

> "The airplane had no definitive stall in the usual sense. The stall or minimum airspeed was that airspeed at which further increases in angle of attack did not appreciably change airspeed. The lift curve is quite flat at CLmax as shown in the discussion of the aerodynamic characteristics in the appendix. Therefore, it was difficult to determine exact angle of attack for minimum airspeed.
>
> Figure 25 [Fig. 3-120] presents the stall-speed variation with engine power for take-off, landing, and wave-off configurations. At high engine power in the landing configuration, stall speeds of less than 45 knots are possible.
>
> The only stall warning noted was some light buffeting in both landing and take-off configuration when stalls were performed at low engine power. At the higher engine power there was no natural stall warning. A stick shaker, which was actuated by angle of attack, was provided for stall warning. Although the pilot would desire natural stall warning, the stick shaker was considered satisfactory.
>
> The handling qualities of the airplane near minimum airspeed were considered to be acceptable by the pilot. There was no tendency to roll-off or to pitch up or down near the stall if the sideslip angle was kept low. However, there was a tendency for the airplane to pitch up with an increase in sideslip angle at the very high angles of attack (above the angles of attack used in normal take-off rotations or landing flares). The directional stability was almost neutral near minimum airspeed, but the rudder control was adequate to control sideslip. The lateral control was also adequate near the stall, and there was sufficient longitudinal control for a rapid decrease in angle of attack for recovery."

The time history of the Bréguet 941 landing is very interesting. Longitudinal parameters during a landing were reported in reference [509]. The authors noted that this was just "1 of the 25 landings." I have reproduced their figure here as Fig. 3-121. Notice immediately that the whole landing after the ILS intercept only took about 125 seconds. This is unmatchable by today's commercial jet transports, as I am sure you appreciate.

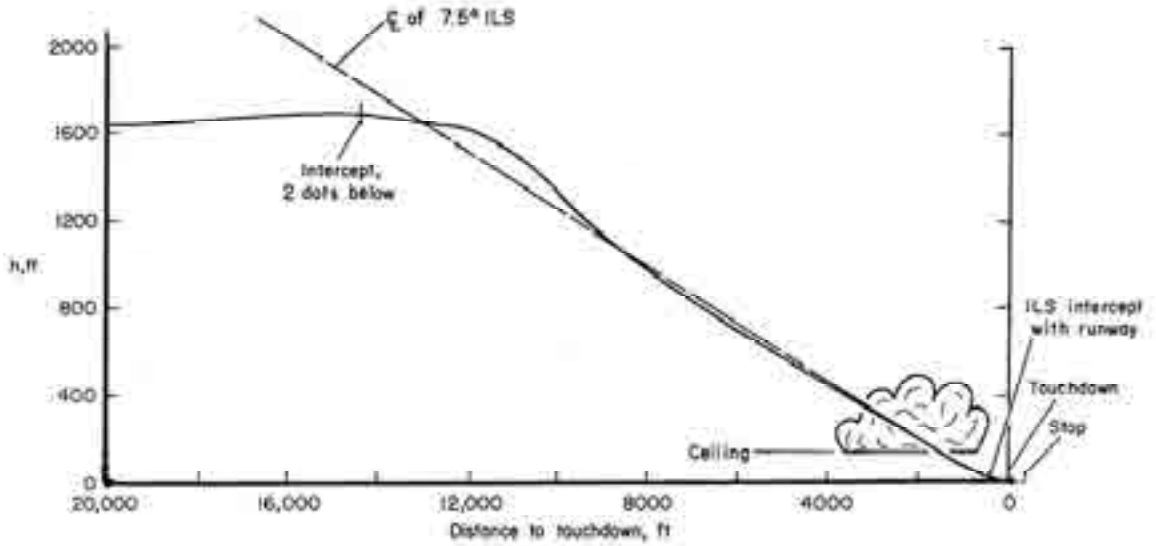

Fig. 3-119. The final approach and landing profile with a 7.5-degree descent angle [509].

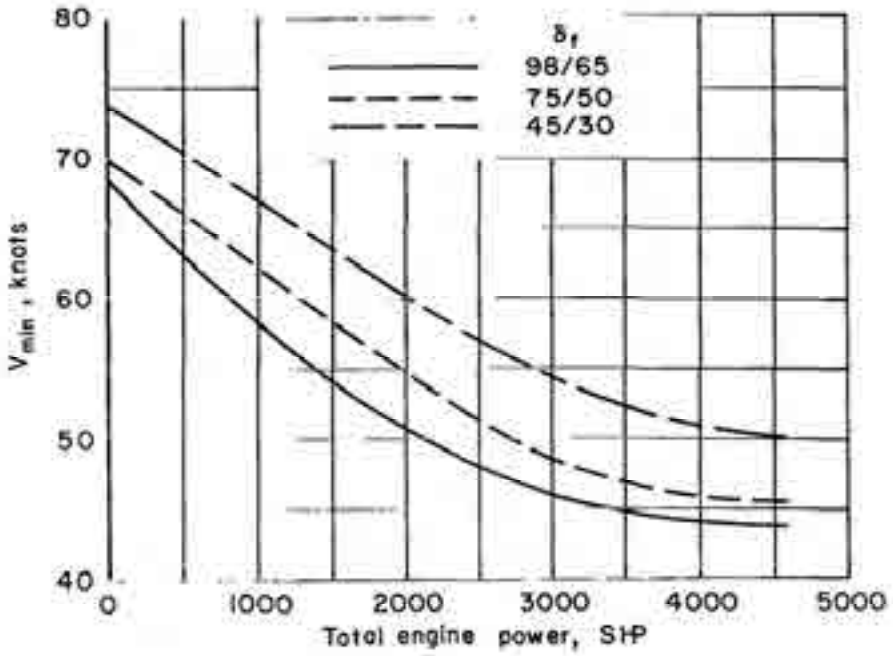

Fig. 3-120. The Bréguet 941 was quite capable of controlled flight at 45 knots [508].

The intercept of the ILS signal was accompanied by a rather large overshoot as you can see by following the Height Above Ground graph, which is the top graph on Fig. 3-121. However, the pilot was able to correct the error rather quickly as shown by the time history of this error on the second graph down from the top. Once stabilized on the glide slope, the pilot was able to use the differential propeller thrust setting and power changes to stay on the ILS signal to within ±0.25 degrees.

The true airspeed graph shows that the pilot reduced speed rather slowly from 75 to 65 knots as he brought the aircraft along the ILS signal. It is interesting that during this deceleration, the aircraft's pitch attitude (θ) was nose down about – 8 degrees. You get a sense of this nose-down attitude from Fig. 3-112, but as a spectator the approach was rather disconcerting. Once the pilot began his flare—at about 145 seconds—he brought the nose up in preparation for touchdown. Henri Ziegler made the point that quick reversal of propeller pitch (β in degrees) is very important if the ground run is to be minimized. Just think about this very important point for a second. A touchdown speed of 65 knots is about 110 feet per second, which is a great deal of runway used up in 1 or probably more like 2 seconds, particularly if the objective is landing within 1,000 feet. After all, the distance traveled after passing over a 50-foot obstacle on a 7.5-degree slope is slightly over 380 feet of runway. Thus, nearly one-half of the 1,000 feet is used up if the pilot takes 2 seconds to reverse propeller pitch and put the brakes on. And this does not even count the distance used up in the flare or braking to a stop.

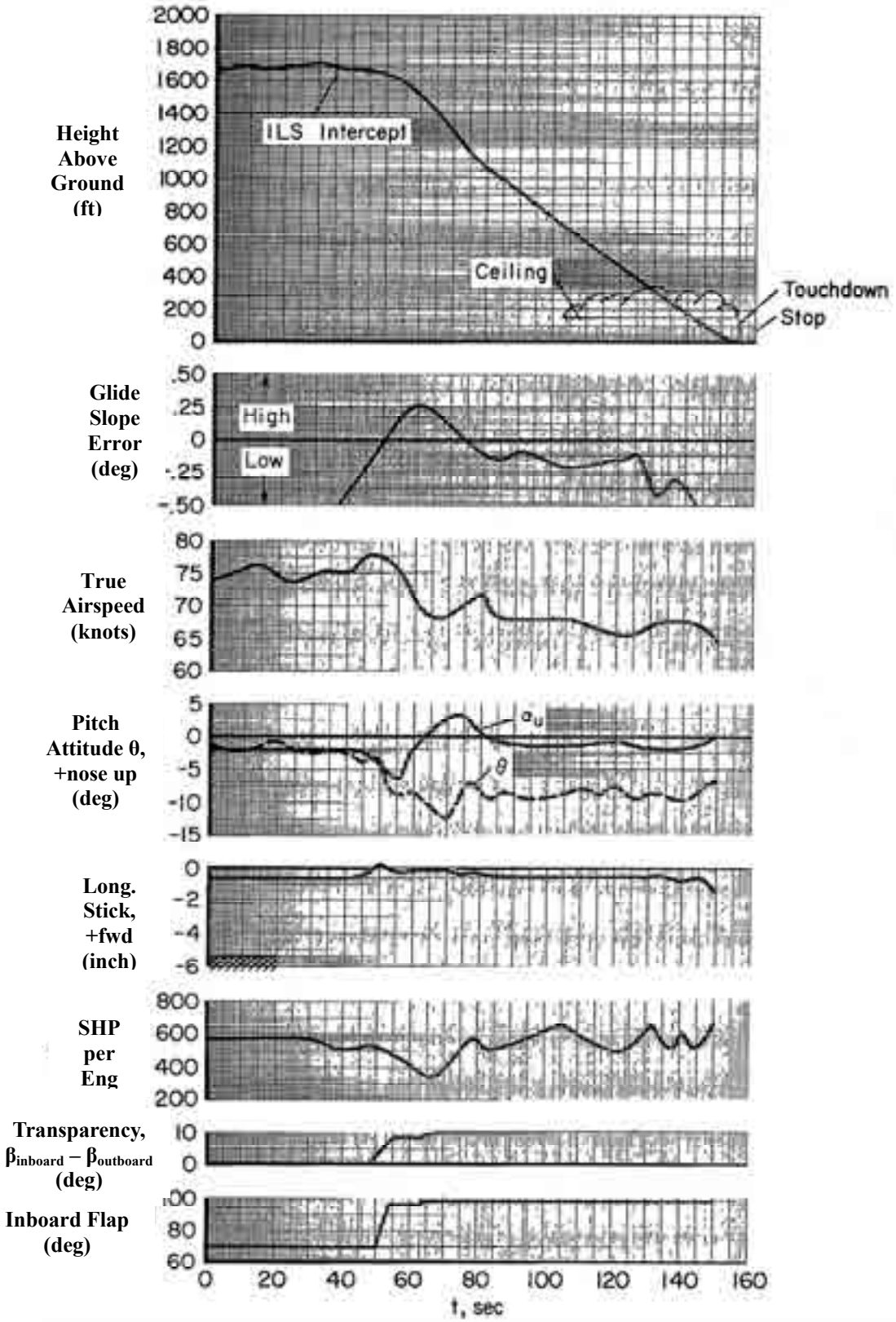

Fig. 3-121. The time history of the Bréguet 941 during an ILS landing [509].

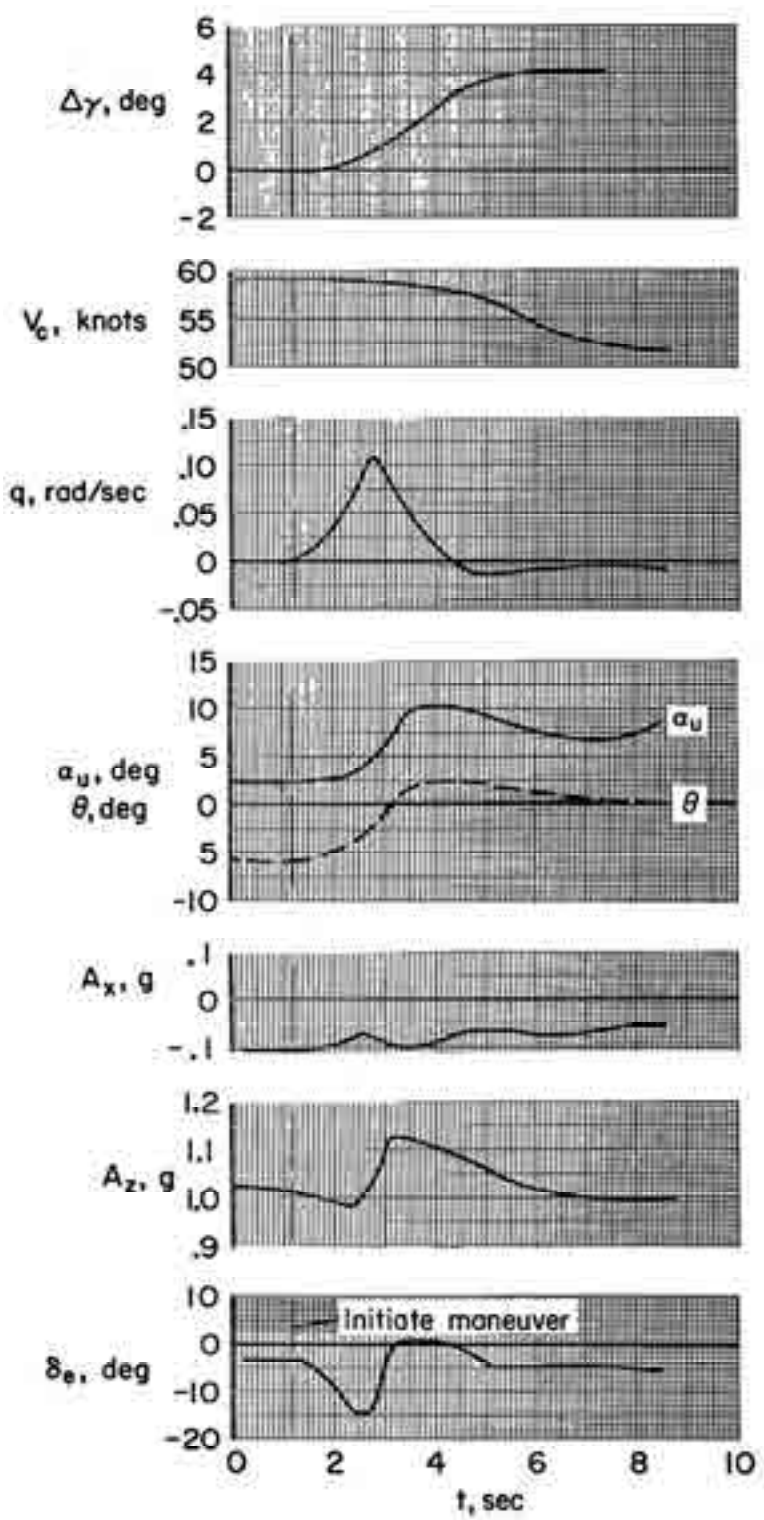

Fig. 3-122. The "half flare" maneuver with a medium-hard landing (300 feet per minute vertical velocity at touchdown) allowed pilots to increase precision in touchdown. This provided the maximum amount of concrete for braking [509].

The flare is used to transition from a 7.5-degree glide slope to a 0-degree glide slope (i.e., parallel to the ground). It is the flare, and when to start the flare, that—in my opinion—exposes differences in piloting. Incidentally, this same when and how to flare issue also exists for helicopter pilots doing a power-off full-autorotation landing. Innis, Holzhauser, and Gallant made a point of discussing this flare technique in their report. They wrote, with a few notes I have added, that

> "The normal landing procedure is to initiate a flare about 20 feet above the ground. The aircraft is rotated to at least a level attitude, and the increase in angle of attack produces sufficient vertical acceleration to reduce the descent velocity from about 800 to about 300 ft/min at touchdown. This "half flare" takes about 4 seconds. [That is 440 feet of runway used at 65 knots.] It was made at altitude for better documentation. The results, fig. 17 [Fig. 3-122], show that 0.1 g vertical acceleration is developed within 2 seconds, the glide angle is reduced 4 degrees, and the airspeed is reduced 5 knots. The maximum vertical acceleration measured for an abrupt attitude change at altitude was 0.25 g; when power was applied in addition to elevator, 0.4 g was obtained. It was found that the maximum acceleration used during any approach or landing was 0.1 g. The pilots felt that sufficient vertical acceleration was available for STOL type approaches and landings.
>
> The half flare landing increases precision in touchdown because the contact point is closer to a straight line extension of the approach flightpath, and hence, eases the judgment problem. Further, the large dispersions associated with floating down the runway when a fully flared landing is performed are eliminated. The pilots also reported greater consistency in landing performance with transparency than without transparency. While this was not documented, it seems reasonable to expect that the aircraft would be less disturbed near the ground with transparency since the span loading is distorted to simulate a lower aspect-ratio wing.
>
> Landing gear design is important in making these half flare landings; not only do the higher touchdown velocities necessitate a higher design sink speed, but more important, the energy absorption characteristics must avoid rebound and impart low acceleration to the passengers. The 'soft' gear of the Bréguet satisfied these requirements, and the peak vertical acceleration at the c.g. was 0.5 g at 300 ft/min touchdown velocity."

Perhaps the most interesting paper to come out of the Bréguet 940/941/941S program was written in 1963 by a Mr. P. E. Lecomte who was a "Service Technique Aeronautique" at Bréguet Aviation [510]. In discussing the operational aspects, he wrote:

> "OPERATIONAL ASPECTS - At the present time, operational aspects are the least known because experience has been insufficient. However, two aspects to which attention has already been drawn to a certain extent are the variability of take-off and landing lengths and the design of the undercarriage in connection with the use of unimproved fields.
>
> Take-off and Landing Length Variability - Experience has shown that with the technique used, take-off lengths are perfectly constant with a VTOL. This is less evident in the case of landing. As a matter of fact, although approach is possible along a glide path with slope of 8 deg, a certain dispersion of touchdown points is noted. This is not crucial because the landing lengths are (on purpose) shorter than the take-off lengths. Nevertheless a visual device has been tried at landing. For the first experiment, a deck landing mirror, set in such a way as to give an approach along a slope of about 8 deg, has been used. The first results were encouraging and showed that more than 92 percent of landings took place within a distance of 165 ft. Assuming a Gaussian distribution, a root mean square deviation of 44 ft has been found, which means one chance in a hundred of exceeding a deviation of 137 ft (and even in that case it would be possible to reopen the throttle; see Fig. 17).

Use of Unimproved Fields - The "Jockey" landing gear has been specially designed to accommodate unimproved fields. The operation of this landing gear, equipped with low pressure tires, is shown in figure 18 [Fig. 3-123] and has given satisfactory results for various types of landing conditions. It should be pointed out that the landing gear design data (vertical speed of –13 fps) are compatible with landing at a steep path.

Finally, the landing gear permits the attitude of the aircraft to be changed on the ground, in order to facilitate loading and unloading."

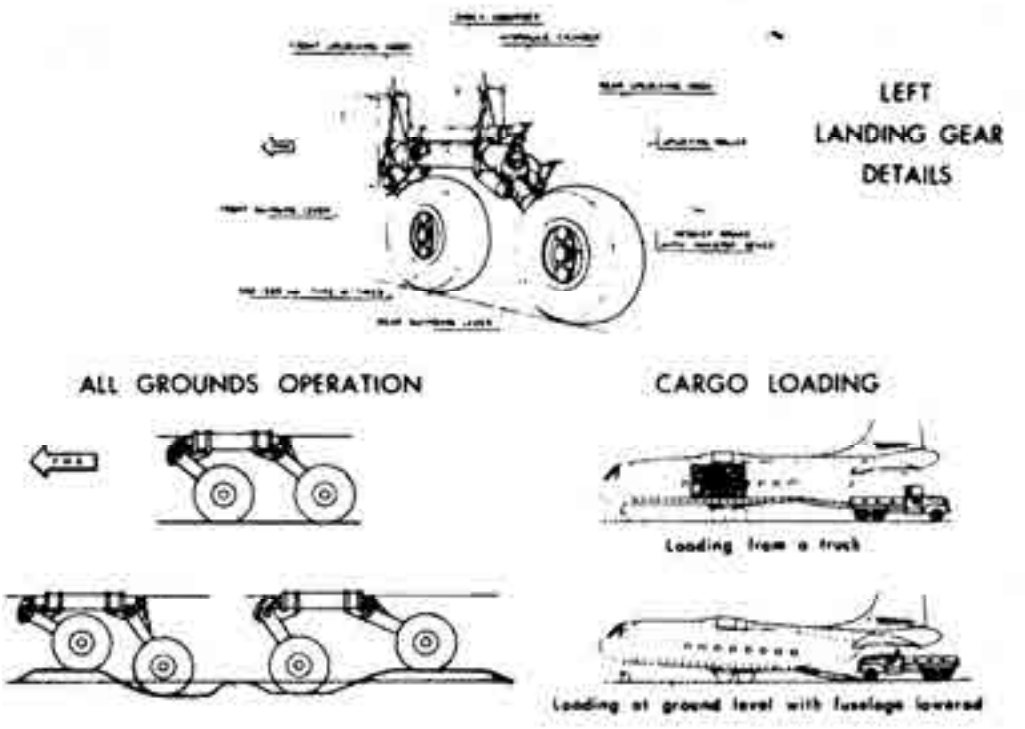

Fig. 3-123. Bréguet Aviation designed the Bréguet 941 landing gear for a 13-feet-per-second descent speed at touchdown [510].

In closing this discussion, I would say that the Bréguet 941 must be considered a very successful demonstrator by any standard. Its handling qualities, even without today's advanced technology, should have satisfied NASA Langley's most experienced test pilot, Jack Reeder [184, 513]. The aircraft thrust horsepower-required data (i.e., includes propeller efficiency, η_p) shown on Fig. 3-124 suggests the Bréguet 941 could have cruised comfortably above 200 knots. Given more powerful engines as were later demonstrated with the Bréguet 941S, you would think that a cruise speed of 230 knots would have been common place in service. The lift-drag polar, Fig. 3-125, showed that the configuration had a maximum C_L/C_D of 12.3, which seems quite reasonable after combining STOL with cruise efficiency. The follow-on, the Bréguet 941S, required very few changes beyond the usual installation of more powerful engines. Thus, by 1970 we had a candidate for both military STOL and commercial short-haul needs. However, the potential customers did not materialize, and in 1974 the French effort came to an end. One reason I have most often heard during Monday morning quarterbacking is simply that the aircraft was propeller driven.

Airline passengers really favored the jet-engine-powered aircraft over an old fashion, propeller-driven airplane. Certainly, the U.S. Air Force was not (and is still not) really interested—in my opinion—in having any "propeller-driven aircraft in their fleet." And the airlines appeared not to be able to make a profit from short-haul routes back then. I suppose that congestion in the future will dictate a solution.

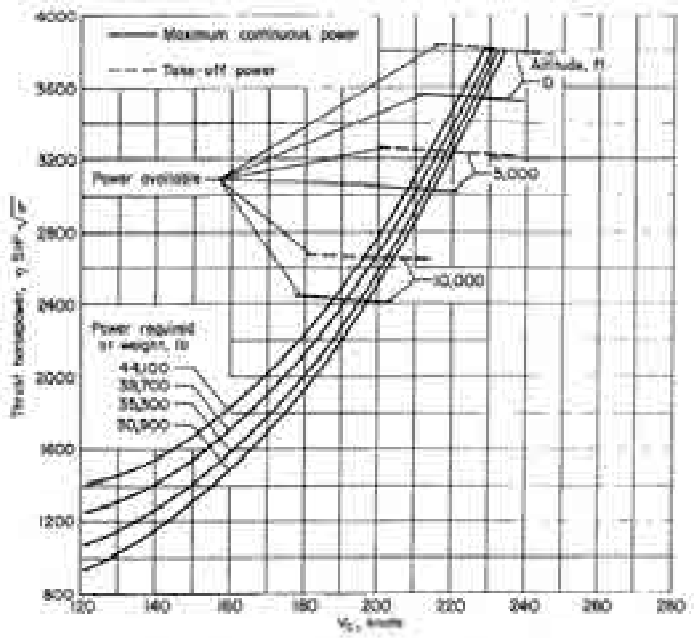

Fig. 3-124. Power-required curves for the Bréguet 941 suggest that high-speed cruise at over 220 knots was in the cards—given more power and a higher cruise altitude [508].

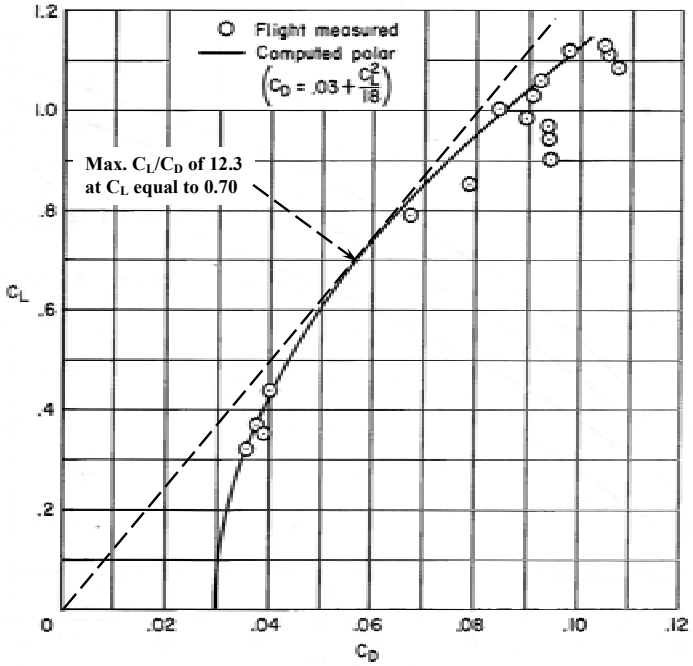

Fig. 3-125. The Bréguet 941 had a maximum lift-to-drag ratio of 12.3 at a lift coefficient of 0.70 [508]. This was certainly on a par with a Douglas DC-3 and well above what rotorcraft advocates had to offer.

3.7.3 The Lockheed C-130 (With BLC) Demonstrator

The Lockheed Georgia[127] C-130 tactical transport must be the most successful propeller-driven airplane the U.S. Air Force has ever seen in service [515]. When you follow the history of this aircraft—designated the Hercules—in *Jane's All the World's Aircraft*, you will read that:

1. The C-130 was designed to a specification from the U.S.A.F. Tactical Air Command in 1951. Lockheed was awarded a production contract in September 1952.
2. The first of two YC-130s flew on August 23, 1954.
3. The C-130A [516] was the initial production version. It was powered with 3,750 shaft horsepower Allison T56-A-1A or -9 turboprops driving Aeroproducts three-blade, constant speed, reversible pitch airscrews. The propeller diameter was 15 feet. Fuel capacity, originally 5,250 U.S. gallons, was later supplemented with two, 450 U.S. gallon underwing pylon tanks. The equipped weight empty was 63,000 pounds, and the normal gross weight was 124,200 pounds. Maximum cruise speed was 315 knots. The A model first flew on April 7, 1955; deliveries to the U.S.A.F. began in December 1956, and 231 were built before production ended in February 1959.
4. The C-130B [517] first flew on November 20, 1958; this improved version entered service on June 12, 1959, and about 100 were delivered by March 1961. It had an additional 1,710 U.S. gallons of fuel in the wings inboard of the inner engine nacelles. Landing gear was strengthened and installed power increased to four 4,050 hp Allison T56-A-7A turboprops driving four-bladed, Hamilton Standard airscrews.
5. Product improvement programs kept production going with C, D, E, and H models.
6. The 2,000th Hercules was delivered on May 14, 1992. More than half have gone to the U.S.A.F. The final C-130H was delivered in January 1998. An H model is shown in Fig. 3-126 with details of the turboprop engine provided in Fig. 3-127.
7. Lockheed began privately funded development of the J model (Fig. 3-128) in 1991, including FAA certification of the aircraft as the L-100J. In late August 1998, the aircraft began acceptance testing by the British. The C-130J is still in production, and as of 2008, the U.S.A.F. has bought well over 100. The C-130J is powered with four Rolls-Royce AE 2100D3 turboprop engines, each flat rated to 4,591 shaft horsepower. The propellers are Dowty Aerospace R391s with six composite blades. The aircraft's maximum cruise speed is 356 knots at 25,000 feet, and the economical cruise speed is 339 knots at 28,000 feet. The operating weight empty is 75,562 pounds, and the normal gross weight is 155,000 pounds.

[127] The Georgia Division of Lockheed grew out of U.S.A.F. Plant No. 6, which opened in March 1943 with 500 employees. The Georgia Division opened in Plant No. 6 in 1951 and was busy refurbishing 120 Boeing B-29s flown from Pytoe, Texas, to Marietta, Georgia. On February 2, 1951, the Air Force issued RFPs to Lockheed, Boeing, Douglas, and Fairchild for a medium-weight transport. Lockheed was awarded a contract for two YC-130 prototypes on July 2, 1951. These prototypes were developed and built at the Lockheed Aircraft Corporation in Burbank, California. On March 10, 1955, the first production model of the C-130 rolled out of the Georgia Division [514].

Fig. 3-126. The Lockheed C-130H is a real workhorse for the U.S. Air Force.

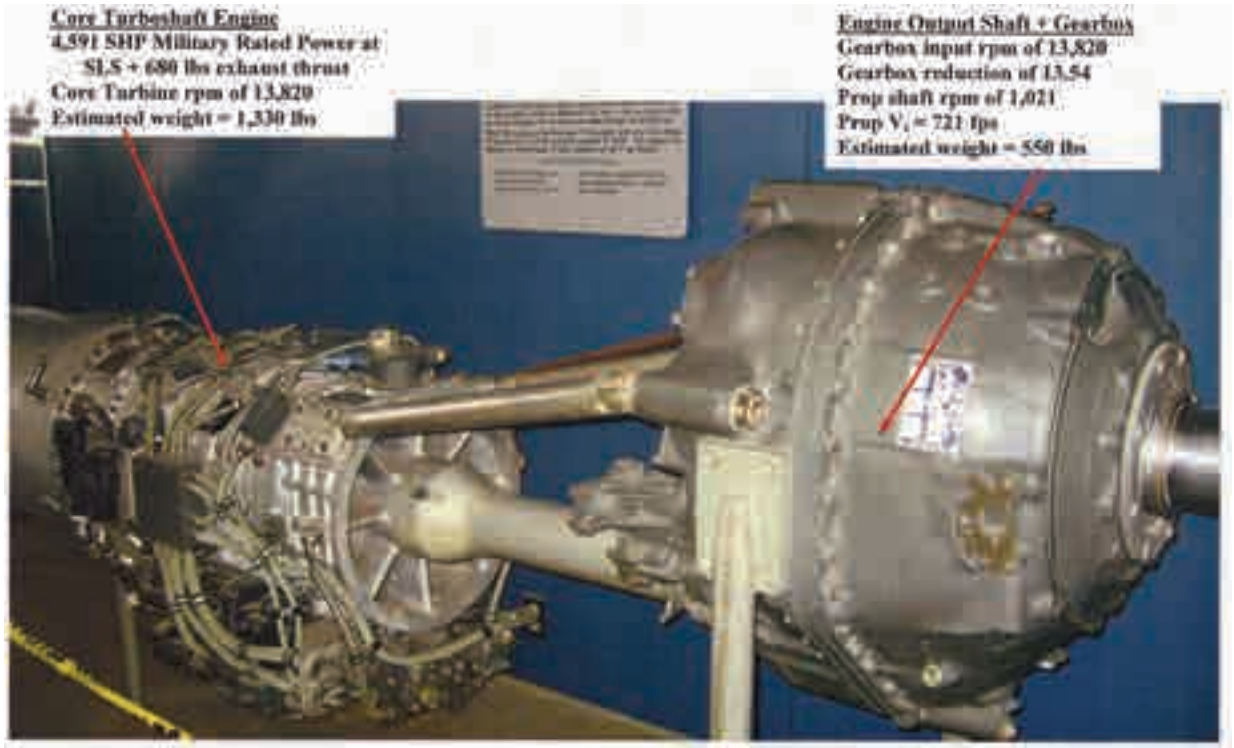

Fig. 3-127. The Lockheed C-130H uses four Allison T56 turboshaft engines.

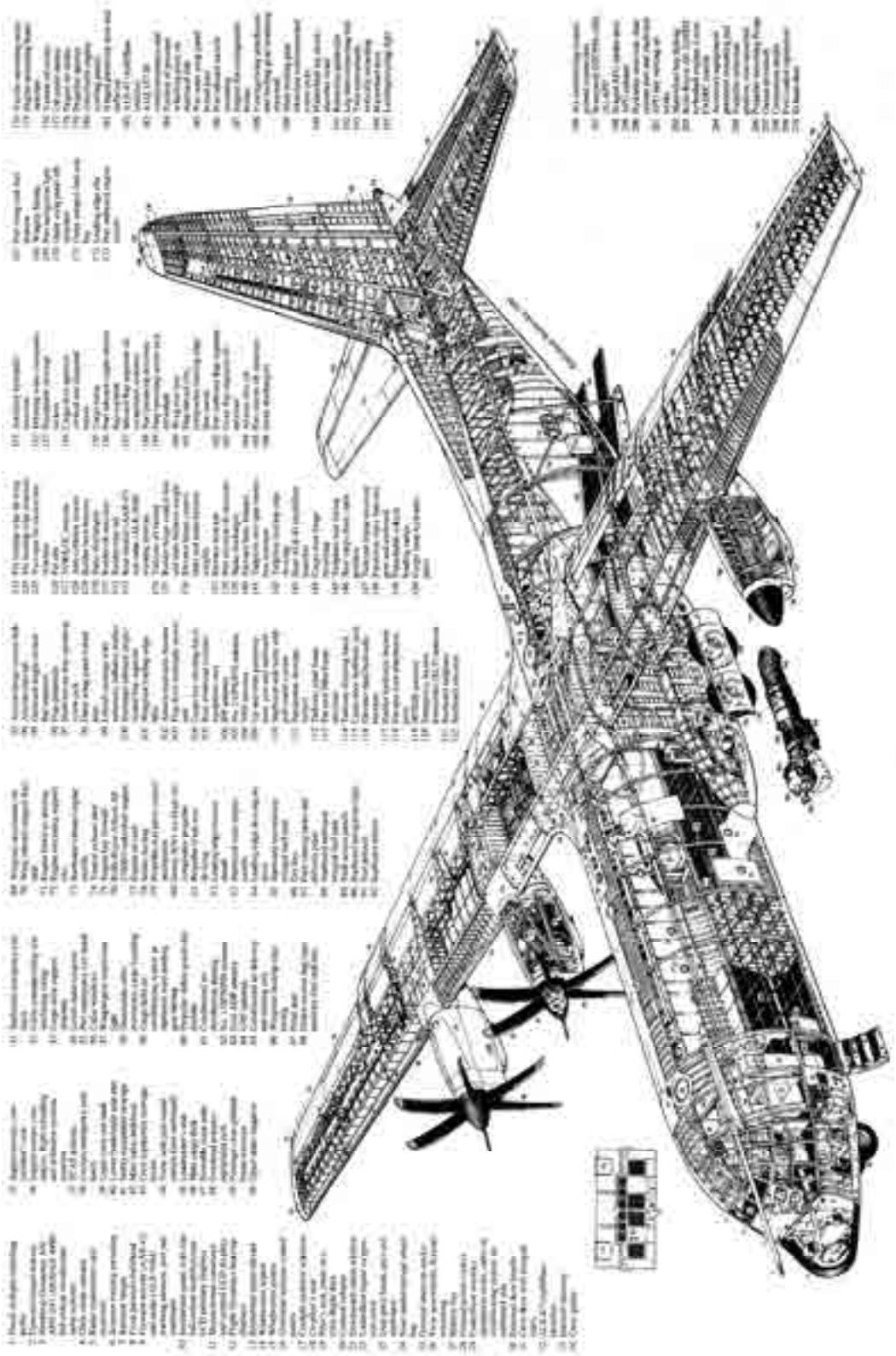

Fig. 3-128. Cutaway of the Lockheed C-130J as shown in *Jane's All the World's Aircraft, 2004/2005*.

A key reference point in the series of Lockheed C-130 aircraft was the E model. This model added range-extension fuel tanks to the C-130B model. The maximum takeoff gross weight was increased from 130,000 pounds for the B model to 155,000 pounds for the E model. The C-130E was very, very thoroughly tested by the U.S. Air Force, and the performance data was reported in references [518-520]. The C-130E, like the B model, is powered by four Allison T56-A-7 turboprop engines rated at 4,050 equivalent shaft horsepower at military rated power and standard day, sea level conditions. Each engine drives a Hamilton Standard four-blade, reversible, full-feathering 541160-91 propeller. An external, non-droppable pylon-mounted fuel tank has been attached to the lower side of each wing midway between the inboard and outboard engines. Each 1,400-gallon pylon tank has a usable fuel quantity of 1,360 gallons or 8,840 pounds of JP-4 at 6.5 pounds per gallon. This increases the total usable fuel from 6,960 gallons (C-130B) to 9,680 gallons.

It is worth a moment to stop and look at some of the performance data for the C-130E because it can be used as a basis for what might be achieved with a V/STOL replacement having both long-range logistical and shorter range assault transport capability. In fact, I would suggest that the C-130E's performance can be used as a goal for any commercial V/STOL airliner as well. To begin with, the E model significantly improved the payload-range envelope for this class of aircraft as Fig. 3-129 shows. I might add that in my view, the Lockheed C-130 started out with the A model as an assault transport with near-STOL performance *at light weight*. And then over time the aircraft became a long-range logistical support aircraft with no real claim to STOL performance.

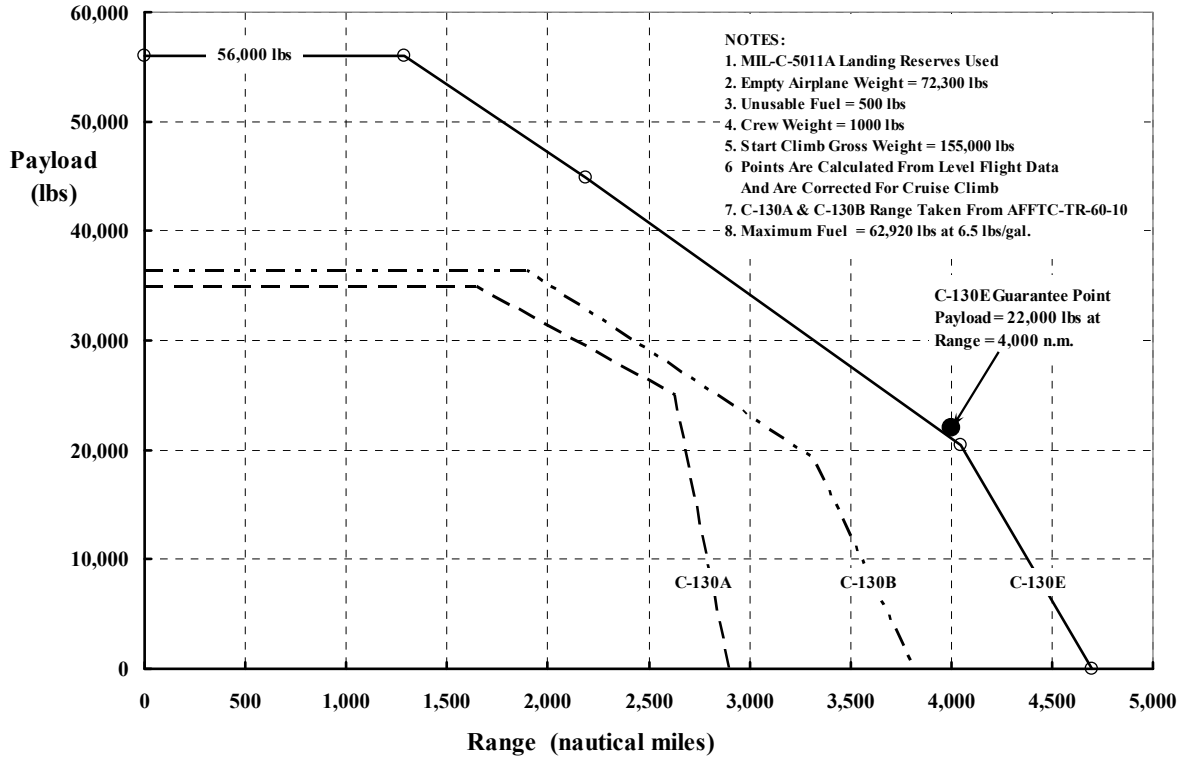

Fig. 3-129. The Lockheed C-130E significantly expanded the payload-range envelope of this logistical support aircraft series.

The classical forward flight performance curves of the Lockheed C-130E are shown in Fig. 3-130 and Fig. 3-131. From the engine power required and available data given in Fig. 3-130, you can see that the aircraft can cruise most efficiently at 300 knots true airspeed at 25,000 feet on a standard day and at 130,000 pounds gross weight. This places each engine at normal rated power, which is just over 2,000 horsepower. This means the total engine power is about 8,000 horsepower, and therefore the horsepower per ton of gross weight is on the order of 123. You might look at it another way and say that because each engine's military rated power at standard day, sea level conditions is 4,050, then the horsepower per ton of gross weight is about 250.

Note the light gray line on Fig. 3-130. This power required data corresponds to performance with the external fuel tanks and pylon attachments to wing assemblies removed. The data suggest that these range extension devices increase power required by about 100 horsepower per engine or nearly 400 horsepower total. These assemblies also decrease optimum cruise speed by about 7 knots.

The specific range (SR) performance measured by nautical air miles per pound of fuel burned is provided in Fig. 3-131. This data illustrates the basic trend that if an aircraft weighs more it will burn more fuel, a fact I am sure you are well aware of. You will recall that in Volume II, on pages 271 to 277, I discussed fuel efficiency in some depth and offered a rather simple equation to calculate specific range in nautical miles per pound of fuel burned. I repeat that equation here as

$$(3.140)\quad SR = 350\left[\frac{(L/D)_{a/c}}{SFC}\right]_{avg.}\frac{1}{W_{initial}} \quad \text{in nautical miles per pound.}$$

The simple message quantified by Eq. (3.140) is that, for a given aircraft weight ($W_{initial}$), engine manufacturers must minimize the fuel required to produce a given power (SFC), and airframe manufacturers must minimize aircraft drag (D) for a given amount of lift (L).

Let me illustrate the use Eq. (3.140) in finding the bracketed term based on C-130E information. Reference [518] states that with a maximum fuel load of 62,920 pounds (i.e., 9,680 U.S. gallons at 6.5 pounds per gallon), the E model can take off at 155,000 pounds and fly 4,700 nautical miles. This gives a specific range of 0.0747 (4,700/62,920). On this basis, you have

$$(3.141)\quad \left[\frac{(L/D)_{a/c}}{SFC}\right]_{avg.} = \frac{SR \times W_{initial}}{350} = \frac{(0.0747)(155,000)}{350} = 33.1.$$

Now the nominal specific fuel consumption (SFC) of the Allison T56-A-7 turboprop engine is on the order of 0.55 pounds per hour per horsepower for one engine or 2.22 for the four engines. It therefore follows that the average aircraft lift-to-drag ratio $(L/D)_{a/c}$ is on the order of 15.

This brings me to a discussion of the C-130E lift-coefficient versus drag-coefficient curve (more commonly referred to as a lift-drag polar) for the aircraft.

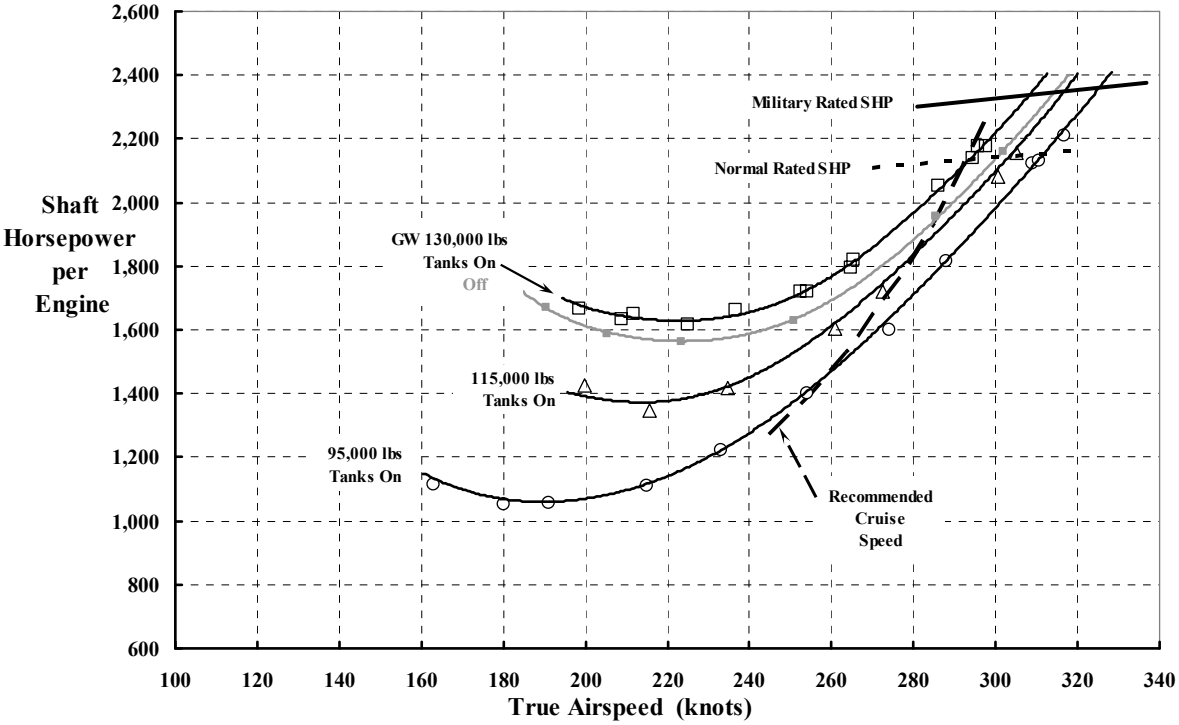

Fig. 3-130. The Lockheed C-130E can cruise continuously at around 300 knots true airspeed at 25,000 feet.

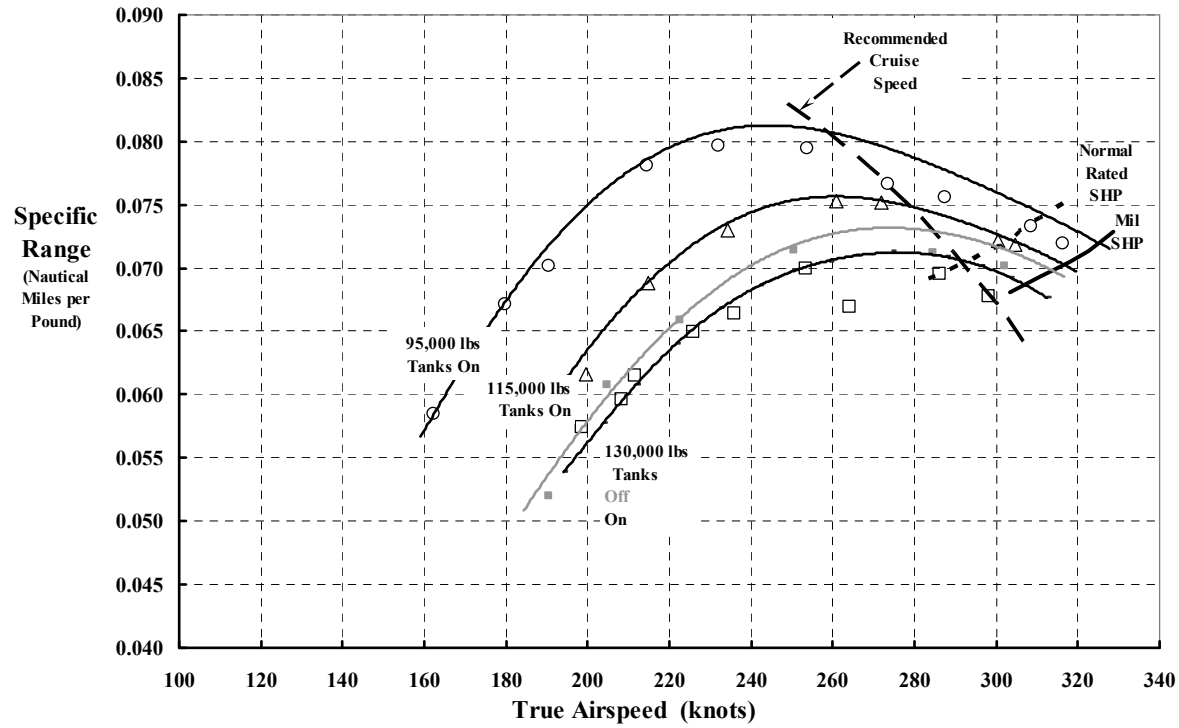

Fig. 3-131. The C-130E is very efficient in cruise compared to helicopters and even tiltrotor aircraft (see Fig. 2-193 on page 311).

The authors of reference [518] used the measured engine shaft horsepower required to "back out" the C-130E's lift-drag polar. The results of their calculation are shown in Fig. 3-132. This data was obtained by first deducting engine gearbox and accessory power (ΔSHP_{GBL}) from engine shaft horsepower to give the propeller shaft horsepower. This power loss per engine was established as

(3.142) $\Delta SHP_{GBL} = 51 + 0.005(SHP)$.

The propeller shaft horsepower was then multiplied by the propeller efficiency (furnished by Hamilton Standard) to give the thrust horsepower, which in turn was converted to airplane drag for each true airspeed tested. This drag, and the corresponding test weight, yields the lift and drag coefficients you see on Fig. 3-132. These coefficients were based on a wing area of 1745.5 square feet, which, incidentally, includes 226 square feet of fuselage.

Considerable attention to the stall boundary at idle, normal, and military rated powers was given in reference [518]. The data was summarized on pages 155 to 157 of this report and indicated that in the cruise configuration at flight idle, the maximum safe operating lift coefficient was about 1.88. Testing the cruise configuration at normal rated power yielded a practical lift coefficient of 2.48, which illustrates the beneficial effect of the propeller slipstreams. In the takeoff configuration at military power, the deflected flaps (18 degrees) raised the lift coefficient to 3.88. Finally, the landing configuration test results indicated that at military power, the C-130E could be operated safely at a lift coefficient of 4.20. However, with engines at flight idle, the safe operating lift coefficient was reduced to about 3.0 because of the lost propeller slipstreams.

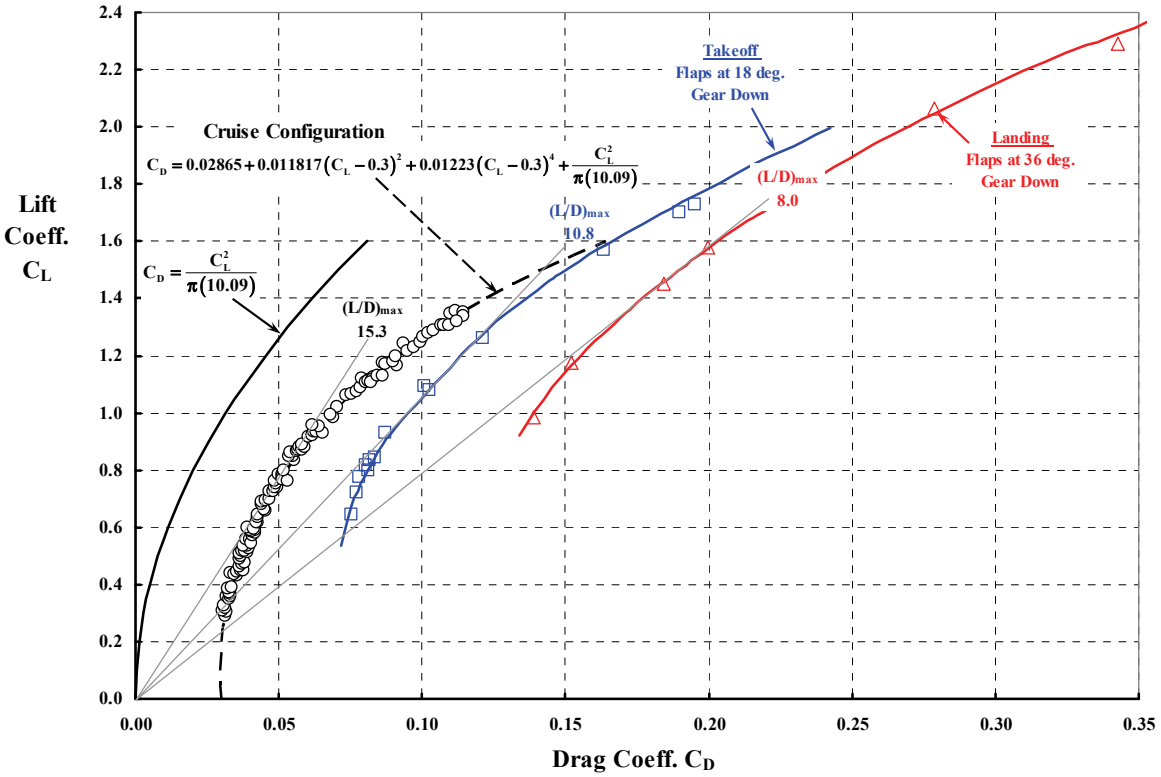

Fig. 3-132. C-130E lift-drag polars (assumes propeller blades off).

Now consider first, takeoff distances, and then second, landing distances, for the Lockheed C-130E. These were key aspects of testing because the data found a prominent place in the pilots' Flight Manual [521] for the aircraft. For my purposes here, I have collected the raw data before it was corrected for headwind, altitude, temperature, reference gross weight, etc. These corrections are necessary for an accurate Flight Manual, but are not necessary to see the first-order effects, which are pilot technique and takeoff gross weight.

The recorded data for many takeoffs is tabulated in references [518] and [520]. A sample graph of this time history is illustrated in Fig. 3-133. Here you see the time histories for takeoffs at a low gross weight of 99,000 pounds and the highest gross weight of 155,900 pounds. In both extremes, each of the four engines was operating at a military power of 3,755 shaft horsepower with an exhaust jet thrust of 740 pounds when the brakes were released.[128] These examples represent takeoff from a solid concrete runway at approximately 1,000 feet altitude on a standard, calm day.

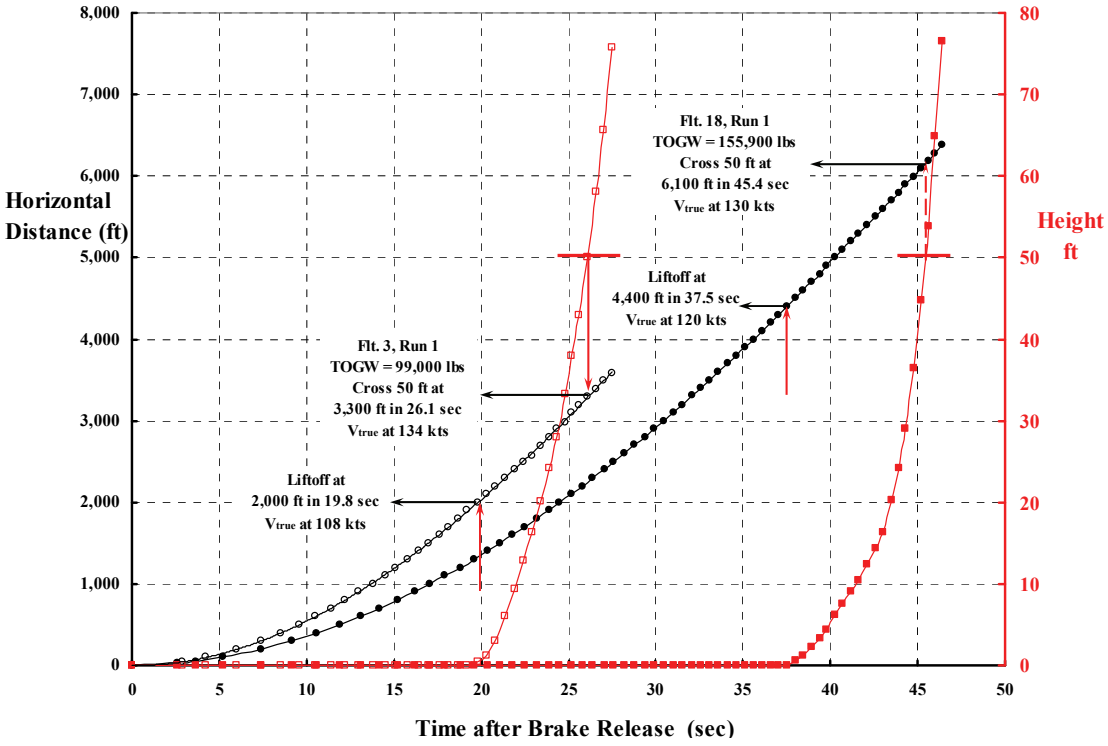

Fig. 3-133. C-130E takeoffs with each of the four engines producing a military rated power of 3,755 horsepower and exhaust jet thrust of 740 pounds. Power at the propeller was 3,685 horsepower based on Eq. (3.142). The flaps were set 18 degrees down.

[128] You may not know that manufacturers of turboshaft engines generally have a rating that includes the jet thrust. For the Allison (now Rolls-Royce) T56-A-7, the military takeoff rating is 4,050 horsepower, which is really an equivalent horsepower (ESHP). Allison engineers computed this equivalent power approximately as ESHP = SHP + T_{jet}/2.5. Of course, the introduction of the constant 2.5 is rather arbitrary because no universally accepted way has been set for how much power jet thrust represents at zero speed. In the case of the T56 engine, 3,755 horsepower, less gearbox and accessory losses, goes directly to the propeller. The 740 pounds of jet thrust acts as an accelerating force on the aircraft.

The basis of takeoff is, of course, to gain enough ground speed so the aircraft can lift off and then climb over a "spec" 50-foot-high obstacle.[129] This liftoff speed and the associated distance, as well as the distance at the 50-foot obstacle, were key pieces of data reported in references [518, 520]. In Fig. 3-134 you have my summary of the tabulated takeoff data obtained during a portion of the 121 hours of flying conducted at Edwards Air Force Base from March 21 to June 8, 1962. I have also included data from reference [520] because it gave C-130E takeoff performance simulating an "Emergency-Wartime-Use-Only" condition, which extended the takeoff gross weight from 155,000 pounds to 175,000 pounds.

This figure represents the capability of the Lockheed C-130E during takeoff with all four engines operating at military rated power. You might think that the data offered in Fig. 3-134 has considerable "scatter" in the points for any one takeoff gross weight, say for example around 155,000 pounds. But that is not what is happening. The spread in the points is, in fact, created mostly because of pilot technique at any given gross weight and power setting.

As you might well expect, C-130E takeoffs during which an engine failed were simulated, and time history data recorded and then published. Engine failure is a major safety issue with airplanes in both takeoff and landing, although an engine failure during takeoff is

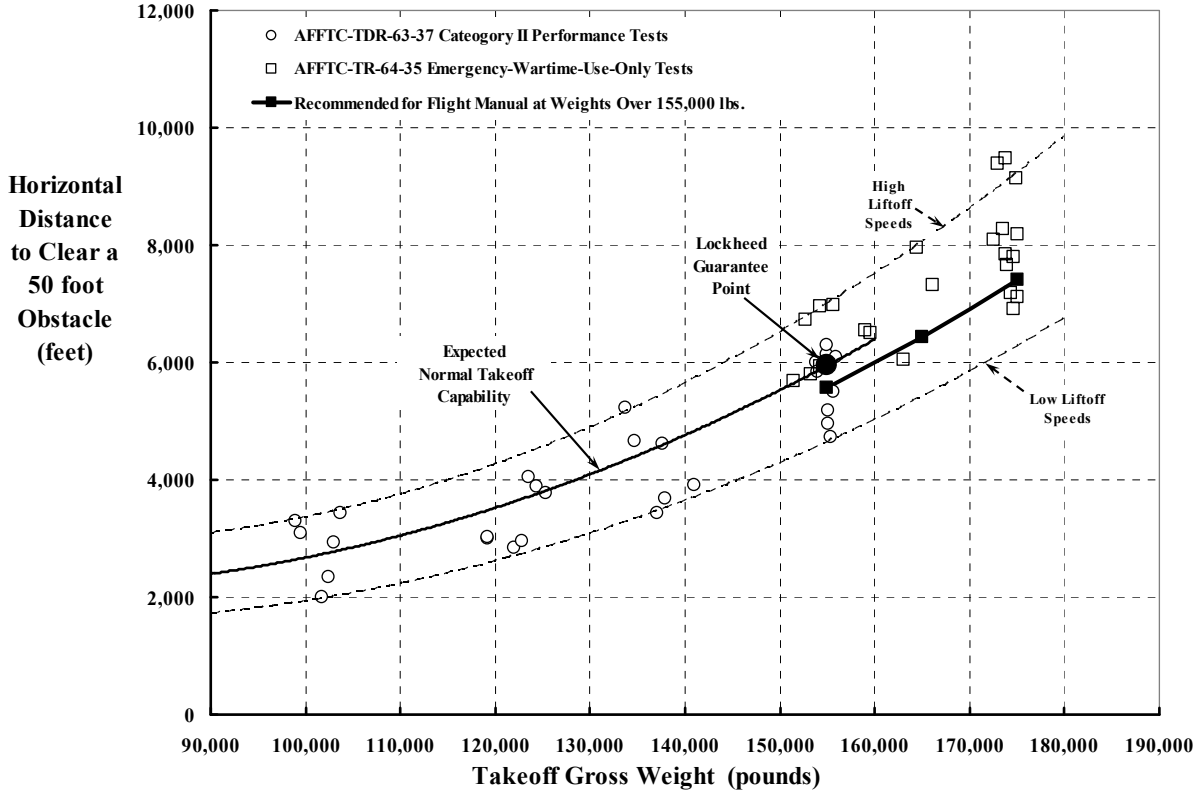

Fig. 3-134. Quoting takeoff distances based on flight test data is not easy—frequently it is simply a judgment call. Nominal altitude is 1,000 feet, standard day.

[129] One hopes that a considerably higher obstacle is not looming just ahead.

frequently the more critical situation. Just imagine the pilot's situation in having to decide whether to abort the takeoff and brake to a stop or continue the takeoff with one engine (of four or, even worst, of two) having failed. And suppose the engine failure occurs right near a ground speed where the Flight Manual says flight is possible. Because this situation is addressed in flight evaluation, the adequate Flight Manual does offer decision point advice. But other factors are, of course, at play. For example, in the case of the C-130E, brakes overheating were a significant factor during an aborted takeoff. This is just one issue that you can read about by studying references [518-520] in detail.

Now let me briefly examine the Lockheed C-130E's landing performance. You see in Fig. 3-135 that at a light weight (92,300 pounds) the aircraft passes over the 50-foot obstacle nearly in a steady descent at a glide path angle of about 4 degrees and an airspeed of about 105 knots. The pilot begins a flare (i.e., increases angle of attack to arrest rate of descent) at about 15 to 20 feet above the ground. This flare maneuver to reduce rate of descent adds about 750 feet to the landing distance, but may not require any use of runway concrete (in this example) if the touchdown is precise. Another way of thinking about this is to imagine that the 50-foot obstacle is located 1,500 feet from the beginning of the concrete runway. After touchdown, the pilot "quickly" reverses propeller thrust and applies brakes to bring the aircraft to a full stop in about 1,000 feet. In essence, the landing field proper must be considerably larger than just a 1,000-foot strip of concrete. I would suggest that for this light gross weight, the landing field must be a clearing of about 2,600 feet.

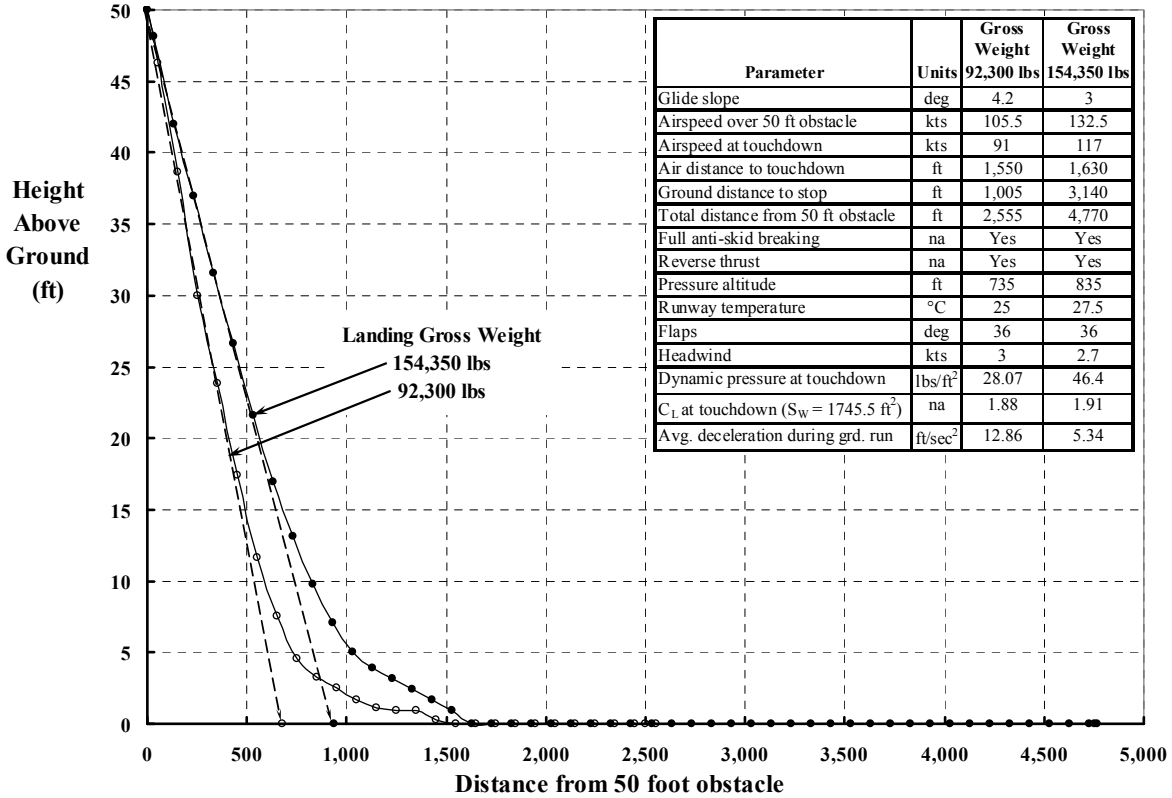

Parameter	Units	Gross Weight 92,300 lbs	Gross Weight 154,350 lbs
Glide slope	deg	4.2	3
Airspeed over 50 ft obstacle	kts	105.5	132.5
Airspeed at touchdown	kts	91	117
Air distance to touchdown	ft	1,550	1,630
Ground distance to stop	ft	1,005	3,140
Total distance from 50 ft obstacle	ft	2,555	4,770
Full anti-skid breaking	na	Yes	Yes
Reverse thrust	na	Yes	Yes
Pressure altitude	ft	735	835
Runway temperature	°C	25	27.5
Flaps	deg	36	36
Headwind	kts	3	2.7
Dynamic pressure at touchdown	lbs/ft^2	28.07	46.4
C_L at touchdown (S_W = 1745.5 ft^2)	na	1.88	1.91
Avg. deceleration during grd. run	ft/sec^2	12.86	5.34

Fig. 3-135. C-130E landings were accomplished with full flaps down (36 degrees) and at very low power. Nominal altitude is 1,000 feet, standard day.

Landing data provided in reference [518] yielded a sufficient number of points to see how the total landing distance and the air distance to touchdown varied with gross weight. You see this data in Fig. 3-136. Keep in mind that the air distance to touchdown includes the flare maneuver that pilots use to reduce rate of descent to an acceptable level. In these examples the glide slope ranged between 3 and 4 degrees, so the flare to touchdown added about 800 to 1,000 feet to the total landing distance. The alternative would be a carrier-type touchdown, which I would call just slamming down, and the landing gear collapses. After touchdown, C-130E pilots apply reverse thrust and brakes to slow the machine to a stop. This phase of the landing gives nearly a constant decelerating force, and therefore the greater the gross weight, the more runway required. Simple physics shows that ground run is approximated by

$$(3.143)\quad D_{\text{Grd. Run}} = \frac{W_{\text{at Touchdown}}\left(V_{\text{at Touchdown}}\right)^2}{2(32.17)F_{\text{Decel}}}.$$

My analysis suggested that the decelerating force (F_{Decel}) was about 31,000 pounds due to reverse thrust, anti-skid braking, and ground friction drag.

The C-130E Category II Performance Tests concluded with a statement by the authors that the "aircraft performance guarantees are essentially met or exceeded in all areas." To support this conclusion, a table was included, which I have reproduced here (with some of my additions) as Table 3-8. You might note, in passing, the third note below the table.

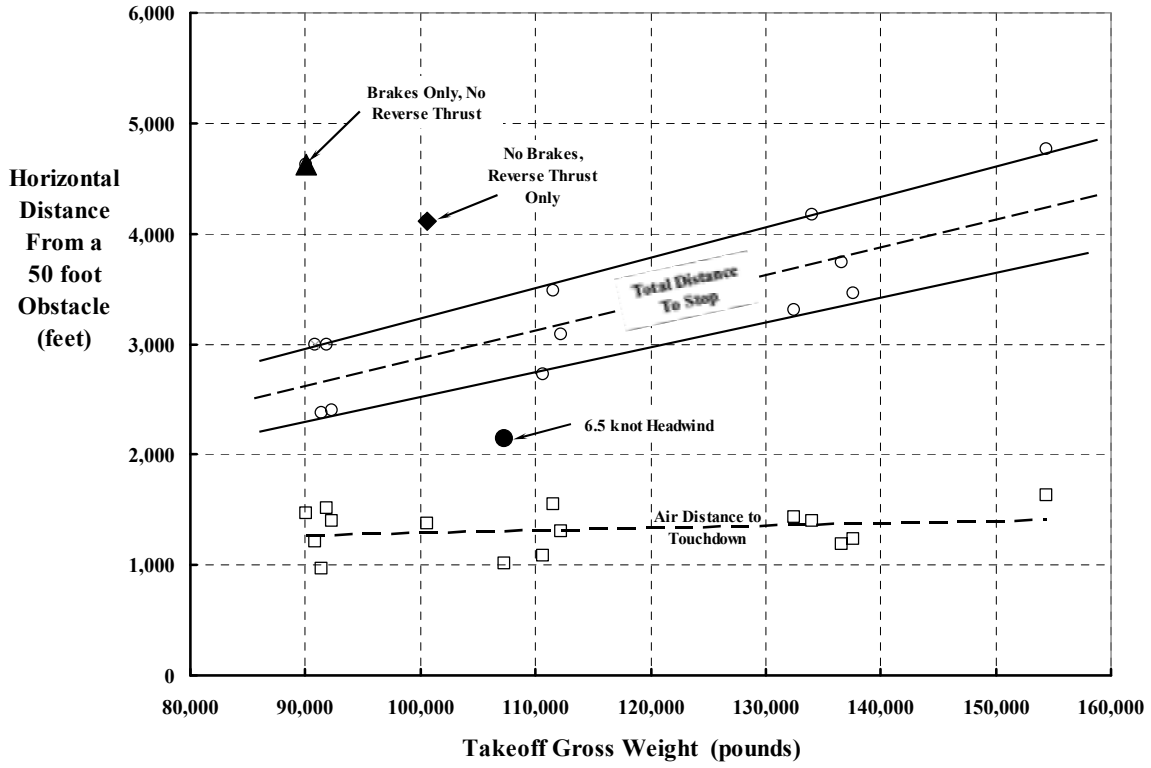

Fig. 3-136. Quoting landing distances based on flight test data is not easy—frequently it is simply a judgment call. Nominal altitude is 1,000 feet, standard day.

Table 3-8. Lockheed's Performance Guarantees Versus Air Force Test Results [518]

Performance	Guarantees[1]	Flight Test
Takeoff over a 50-foot obstacle, sea level[2]	5,950 ft	5,925 ft
Takeoff ground roll, sea level[2]	4,250 ft	4,250 ft
Landing over a 50-foot obstacle at 130,000 pounds landing weight, sea level	3,175 ft	3,225 ft[3]
Landing ground roll at 130,000 pounds landing weight, sea level	2,300 ft	2,400 ft[3]
Rate of climb at sea level with normal rated power (4 engines)	1,450 ft/min	1,530 ft/min
Service ceiling, normal rated power (4 engines)	22,000 ft	24,100 ft
Rate of climb at sea level with one engine inoperative, normal rated power	750 ft/min	760 ft/min
Service ceiling with one engine inoperative, normal rated power	13,500 ft	15,500 ft
Power-off stalling speed at 130,000 pounds weight in the landing configuration	96 KEAS	94 KEAS
Cruising speed at 151,500 pounds, 20,000 feet, and normal rated power	290 KTAS	298 KTAS
Range—22,000 pounds of cargo at long-range cruising speed and altitudes with MIL-C-5011A landing fuel reserves	4,000 nmi	3,925 nmi

Notes: 1. Lockheed Georgia Company Report ER 5200M, revised 15 November 1960.
2. Fifty percent flaps [18 degrees] and Military Rated Power [3,755 hp + 740 lb thrust].
3. The 130,000-pound landing distance of 3,175 feet over a 50-foot obstacle can be met by skilled pilots utilizing 1.28 V_{SL} at 50 feet and 1.2 V_{SL} at touchdown [V_{SL} means stall speed], no reverse thrust, maximum anti-skid braking, and 100 percent flaps. *It is doubtful that the average service pilot could achieve these distances without considerable practice*. As a consequence, the Flight Manual should not be based on guaranteed landing distances.

It may be hard to imagine, but the C-130 that first flew as the A model in April of 1955 is still in production some 60 years later as the J model. Deliveries of the C-130J to the U.S.A.F. are anticipated through 2020 [522]. Despite 60 years of evolution, the wingspan (132.6 feet) and area (1,745.5 square feet) are still the same!

A valuable benchmark for V/STOL advocates is the cost (really purchase price) to the U.S.A.F. for the C-130J. This data, from the Selected Acquisition Report (SAR) dated May 21, 2013 [522], is provided in Fig. 3-137. This data raises two questions: Could the aviation community provide commercial airlines with a 75- to 100-passenger, vertical or ultra-short STOL (say from a 1,000-foot field with 500 feet of concrete), with high-speed performance like the C-130J, for a selling price of $100 million in 2020? And secondly: Would any airline operating in the world's air transportation system buy one?

It might interest you to know that Lockheed Martin got a signed letter of intent from the ASL Aviation Group ordering "up to 10 LM-100J commercial freighters" at the July 2014 Farnborough air show [523]. Lockheed is now in the process of getting its LM-100J (Model L-382J) type certificated with the FAA [524, 525].

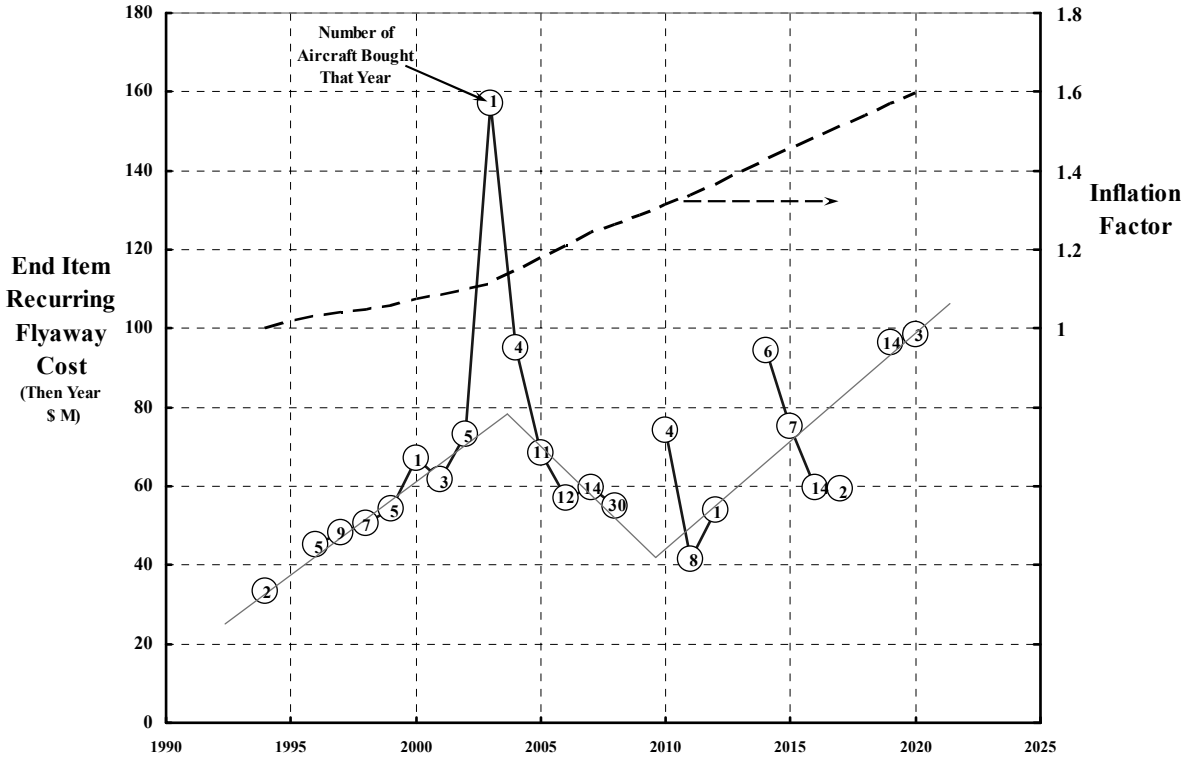

Fig. 3-137. U.S. Air Force procurement of Lockheed C-130Js is planned through 2020.

Now let me address Lockheed's effort to operationally apply boundary layer control (BLC) to a C-130. For this discussion I will rely heavily on a paper presented by the then assistant chief engineer at Lockheed Georgia, Mr. F. N. Dickerman, and Mr. C. F. Branson, on November 1, 1960 [526]. Key phrases and words from the paper are in quotes.

The United States Army and Air Force finally "crystallized" their thinking for an "assault transport" with better short-field performance than the A and B models of the C-130 in February 1958. Their need was documented by an Air Force General Operations Requirement (GOR) for a Troop Carrier Assault Aircraft (Fixed Wing) Support System (Revised).[130] The GOR was number 130 and specified an aircraft able "to carry 20,000 pounds of cargo on a radius mission of 1,000 nautical miles to a midpoint unprepared field with only 500 feet for ground roll available." I interpret this statement as: fly out 500 nautical miles, off-load 20,000 pounds very near the battlefront, and return. What exactly was meant by "unprepared" was not clarified until completion of Project Rough Road, a project that you will read about later.

Lockheed was convinced, based on a series of internal studies, that a C-130 with some form of BLC could satisfy the GOR. Lockheed's generic identification of the aircraft was the GL-128—should the BLC aircraft go into production. What was needed first was a flight

[130] The first draft of the GOR 130 came out in late 1955.

research aircraft—a demonstrator or a test bed if you prefer—"to demonstrate the capability of the complete boundary layer control concept in providing the performance, stability, and control required for assault transport operation." The proposal for this test bed was favorably received by the Air Force, and they awarded a contract to Lockheed in October 1958. The test-bed configuration, shown in Fig. 3-138, was a "one of a kind" research aircraft, and when rolled out was given the tail number 58-0712. The aircraft was more generally referred to as the NC-130B. As you read Dickerman's paper you will quickly see that *without stability and control at very low speeds, full STOL performance cannot be obtained*.

As it turned out, "before the initial flight of the test-bed airplane was made, budgetary considerations in the Air Force necessitated the cancellation of the contract. The Lockheed Aircraft Corp. realized the potential of the BLC concept and provided funds for a minimum feasibility flight test program." Dickerman included a table of dates and accomplishments that you may find interesting. He recorded:

First flight occurred on February 8, 1960
First BLC-on flight performed on March 31, 1960
Total test time of 23 hours as of June 22, 1960
Total BLC test time of 19 hours as of June 22, 1960
Stalls performed, 155
BLC takeoffs accomplished, 13
BLC landings accomplished, 15.

He concludes that "this [23 hours in 4-1/2 months] flight test program has now been successfully completed and showed the BLC Hercules to be a practical STOL Cargo Transport."

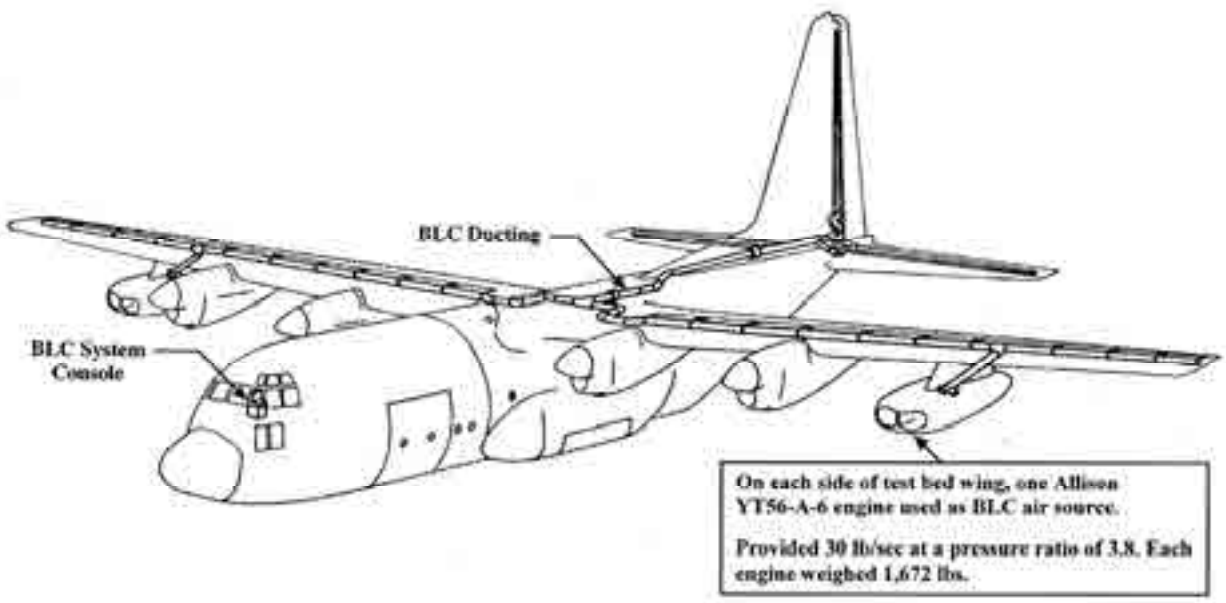

Fig. 3-138. The Lockheed NC-130B was a "one of a kind" BLC-equipped C-130B [526, 527].

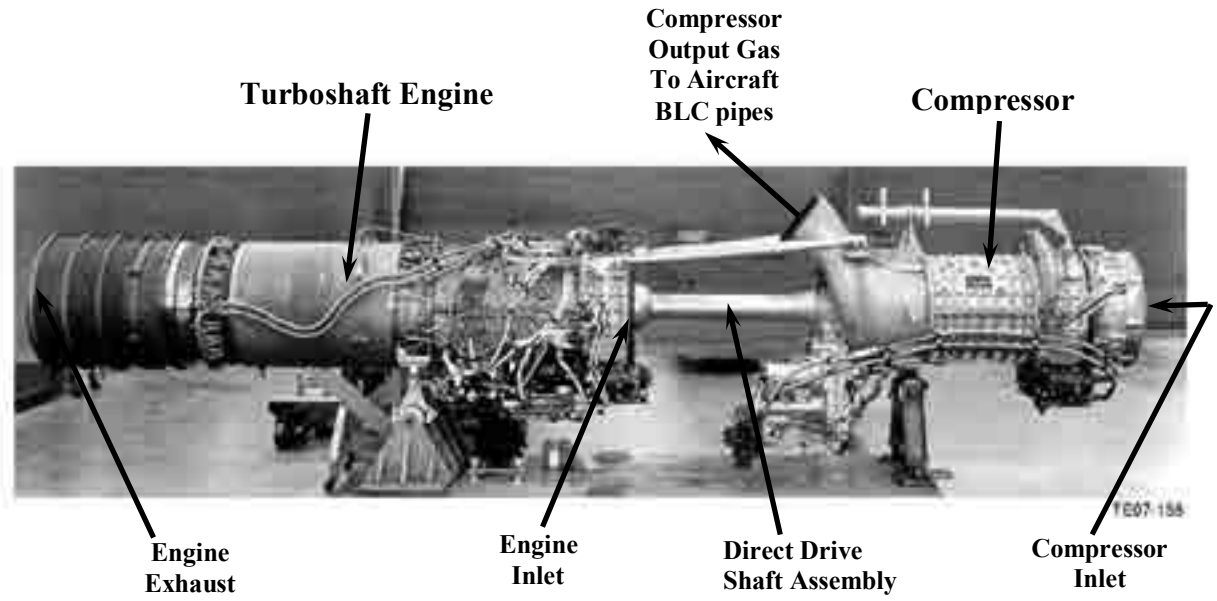

Fig. 3-139. Contrast this YT56-A-6 engine and compressor assembly with the standard T56 shown in Fig. 3-127 [528] (photo courtesy of Rolls-Royce Heritage Trust, Allison Branch, Inc., Indianapolis, IN).

The artist's rendition of the NC-130B shown in Fig. 3-138 immediately draws your eye to the two additional under-wing pods, one on the port side and one on the starboard. You can contrast the BLC test bed to the standard C-130 shown in Fig. 3-126. You might assume that there were two turbojet engines in a pod because of the two inlets on the nose of the pod, but you would be wrong. In the 1960s, a number of turboprop engines had their gearbox and propeller removed so the engine's output shaft could direct drive a compressor that provided air for BLC designs. For Lockheed, Allison (now Rolls-Royce) did this with a couple of their T56 turboshaft engines, and the converted assembly was designated as a YT56-A-6, which you see here in Fig. 3-139.

The characteristics of the YT56-A-6 shown in Table 3-9 were somewhat of a surprise to me when I first saw them.131 The reason I was surprised was that it took two 3,860-shaft-horsepower engines to deliver all the BLC air for the flaps and control surfaces of the NC-130B. Just think about this for a moment. This large assault transport STOL test bed required four turboshaft engines rated at 4,050 equivalent shaft horsepower plus two BLC engines rated at 3,860 equivalent shaft horsepower—a total of 23,920 shaft horsepower—to achieve the performance required by the U.S. Air Force COR 130. This means that the ratio of test bed gross weight (100,000 pounds) to installed power was on the order of 4.2 pounds per horsepower. My immediate thought was that any rotorcraft worth its salt could do a vertical

131 At Mike Scully's suggestion, I contacted David Newill, President of the Allison Branch of Rolls-Royce Heritage Trust. This is a historical repository for virtually everything about Allison and Rolls-Royce, and is located in Indianapolis, Indiana. As we talked he reached for his Allison engine bible compiled by John Leonard [528], and he quickly sent me an email with the photo and table you now have. It was an absolute delight to spend the time with David.

Table 3-9. The YT56-A-6 Gas Turbine Engine/Compressor Package Delivered 30 Pounds Per Second of BLC Air at a Pressure Ratio of 3.80 When Operating at 3,860 hp [528]

Characteristics	
Engine	Engine length: 90.9 in.
Engine type: Turboshaft driving an air compressor	Compressor rotor diameter: 14.7 in.
Compressor type: Axial	Turbine rotor diameter: 18.0 in.
Combustor type: Cannular	Total weight: 1,635 lb
No. of spools: 1	Maximum shaft horsepower: 3,860 hp
No. of compressor stages: 14	Jet thrust: 580 lb
No. of fuel nozzles: 6	Direction of rotation: CCW
No. of turbine stages: 4	
Turbine inlet temperature: 1,780 °F	**Air Compressor**
Engine speed: 13,820 rpm	No. of compressor stages: 8
Overall length: 165.3 in.	Compressor rotor diameter: 14.7 in.

takeoff at this power loading. For example, assuming an aircraft Figure of Merit of 0.7 (see Fig. 2-104), a tiltwing with four 28-foot-diameter proprotors distributed along a 132.6-foot wing (see Fig. 2-105) would work quite well. Or, if you are a tiltrotor advocate, two 40-foot-diameter proprotors would do just fine. Of course, if the design altitude is higher, the diameters would grow.

Dickerman noted that several aerodynamic considerations were important. He said,

"To meet the requirements of a 500-ft airport established by GOR 130, it was necessary to achieve much higher maximum lift coefficients on the C-130 airplane. It was estimated the required lift could be achieved by a combination of blowing boundary layer control and propeller slipstream deflection. *The maximum lift coefficient required for take-off is approximately 7.0 at a speed of 50 knots* [my italics]. Fig. 2 shows the variation of propeller thrust coefficient at take-off power setting with airspeed for the BLC Hercules. Propeller thrust coefficient is defined by:

$$T_C = \frac{\text{propeller thrust of one engine}}{2 \times \text{dynamic pressure} \times \text{propeller diameter}^2} = \frac{T}{2qD^2}$$

At a speed of 50 knots, the thrust coefficient is 3.0.

The blowing coefficient varies with airspeed as shown in Fig. 3. The blowing coefficients shown here are for the production airplane and are slightly higher than those available for the test-bed airplane. The blowing flow coefficient is defined by:

$$C_\mu = \frac{\text{blowing air mass flow} \times \text{blowing airjet velocity}}{\text{dynamic pressure} \times \text{area affected}} = \frac{m_j V_j}{qS_j}$$

On the basis of references 2 and 3, the variations of maximum lift with blowing and thrust coefficients were derived for the BLC Hercules. Fig. 4 shows the power of maximum lift for 60 and 90 deg of flap and 30 deg of aileron droop versus blowing coefficient. For the 60-deg flap deflection and a C_μ of 0.20, the maximum lift is 3.40. Fig. 5 shows the additional maximum lift due to propeller slipstream. For a thrust coefficient of 3.0, corresponding to take-off power at a speed of 50 knots, the increment in maximum lift is 3.80. The total maximum lift [coefficient] at 50 knots is 7.20, slightly greater than that required to provide the desired take-off performance. [Harris' note: It took *both* propeller slipstream and BLC to achieve the maximum lift coefficient of 7.2.]

With the drag due to the much larger flap deflections possible with boundary layer control and the propeller slipstream deflection, the power settings during the landing maneuver are much greater than those normally experienced. For example, the BLC Hercules requires approximately 75% power for level flight with 90 deg of flap. From Fig. 5 it is seen the propeller slipstream makes a substantial contribution to the landing maximum lift, also. The performance of the BLC Hercules is achieved, then, by the use of power-on stall speeds.

It was recognized early in the design of the BLC Hercules that the large thrust coefficients experienced would create stability and control difficulties. Experience on the C-130 had shown that, as power effect is increased to the maximum, stability in all three directions decreases to minimum levels; yet, the maximum thrust coefficients on the BLC airplane are four times those for the C-130. The concept derived to provide satisfactory flying qualities despite low stability levels is the use of complete boundary layer control. Not only is BLC applied to the flaps, but also to ailerons, rudder, and elevator. On the rudder and elevator, it is applied to both sides. In addition to the use of boundary layer control, all surfaces have deflections approximately double those of the standard C-130. With the highly effective controls the following are possible as shown in Table 2.

1. Reduced minimum control speeds, with either a main propulsion engine or BLC engine inoperative, which are below the reduced liftoff and touchdown speeds.
2. Reduced nose wheel liftoff speeds below the takeoff speed.
3. Reduced minimum flare speed below the landing touchdown speed.
4. Stabilized low-speed flight using the control surfaces.

Highly effective controls are necessary for stabilized flight with neutral or negative stability whether an autopilot is used or, as on the BLC Hercules, the pilot flies the airplane. With reduced stability and airspeed, the response of the BLC airplane is slow compared to the human pilot reaction time. It was conceived that the pilot could conveniently fly the airplane in the same manner as a helicopter is flown or a car is driven.

Continuous small deflections would be required to provide the necessary stability. This becomes a practical consideration for the relatively short periods of operation in the BLC regime if, in addition, small control forces are used."

The second major change to the C-130B was to increase the rudder area from 75.0 to 98.6 square feet by increasing the rudder chord. Beyond that, all deflecting surfaces had much greater travel than a standard C-130, which Dickerman reported as follows:

Surface Deflections—C-130 and BLC Hercules [526]

		BLC Hercules (deg)	C-130 (deg)
Flaps:	Take Off	40	18
	Landing	60	36
Ailerons:	Droop	30	None
	Up	BLC 30 Normal 30	25
	Down	BLC 60 Normal 18	15
Elevator:	Up	50	40
	Down	39	15
Rudder:	Right	60	35
	Left	60	35

Dickerman's report about the flight test program is so fascinating that I have included it nearly verbatim:

"The Lockheed funded flight-test program consisted of these two basic parts:

1. Slow-speed flight with BLC and power, including stalls to determine handling characteristics.
2. Take-off and landing performance.

The first part included handling characteristics with an outboard main propulsion engine or a BLC engine inoperative. Since the purpose of the program was to demonstrate performance, the weight and center of gravity were limited to median values of approximately 100,000 lb and 25%, respectively.

The initial phase of the program was concerned with evaluation of the new full power control system and the artificial feel forces. The rudder rotary actuator was sluggish around neutral and required increased flow. The increased flow created an unstable system requiring dampers on the valve, which increased the rudder breakout force to a value which is acceptable for the test bed airplane, but not for operational aircraft. The aileron wheel forces were reduced to a maximum of 20 lb before they were considered acceptable. The elevator feel was produced originally by a q-bellows in series with the wheel. The response of this arrangement proved unsatisfactory, and a simple spring was substituted for the test bed. Since the test bed was structurally limited in speed [to 200 knots], the stick force per g could be made acceptable.

All operation up to this point was without BLC. After considerable ground running to check the system, the first BLC on flight was made on March 31, 1960. Very rapidly, the tests progressed to the point where full take off power stalls were being made. The stalls on the BLC airplane with power are characterized by wingtip stall outboard of the propeller. Due to the propeller slipstream, no significant stalling occurs over the flap. With the tip stall, a corresponding decrease in aileron effectiveness occurs. *This decrease in aileron effectiveness limits the minimum speed available*. The pilot feels this decrease in the response of the airplane to aileron control input and breaks off the approach to the stall. During the approach to the stall, there is a slight tendency for the nose to rise and, at the stall, the left wing tends to drop, due to the relatively large effects of engine torque. The wind-tunnel tests [with a one-tenth-scale powered force model with BLC] had predicted these stall characteristics, and the estimated stall speeds reflected them. Fig. 12 shows a comparison of the estimated stall speeds with those attained with the test bed airplane. These speeds do not include the airspeed position error correction, which would reduce them several knots, since the airspeed calibration tests were conducted down only to 60 knots. The extrapolation was considered to be too far.

The problem of horizontal tail stall failed to develop during the flight-test program. As a precautionary measure, the uptilted leading edge was installed to see what effect it could have on the airplane. However, it stalled on the upper surface with the low flap deflections used during the initial part of the program and it could not be reattached. It was then discarded in favor of the leading edge blowing slot. Thus far in the program, which has not attained the lowest speeds nor explored the forward center of gravity, the tail has not stalled and the leading edge blowing has not been required. There is a hand-operated valve in the airplane to turn the blowing on, and its affect has been checked several times with no noticeable change in the airplane.

The effect of the failure of a main outboard engine was considered at length in the design. The wind tunnel tests showed initially, and the flight test substantiated, that roll control would be critical, since the minimum control speed becomes a three-engine stall speed. The loss in lift behind the dead engine creates an asymmetric lift that cannot be

controlled by the ailerons. This speed is approximately 10% above the all engine stall speed. Assuming the three engine stall speed varies with altitude similar to the *all engine stall speed, the minimum control speed at sea level is 55 knots*.

The effect of a BLC engine failure was demonstrated to be very small. The BLC engine was cut at 70 knots and the speed reduced to 62 knots before the airplane stalled. Again applying an altitude correction would reduce this speed to 57 knots. Small trim changes were required when the engine was cut and adequate control was available down to the stall.

At flight speeds from 70 knots and above, control and stability are more than adequate. Low altitude flights with the ramp doors open simulating aerial drop capability have been made at 70 knots with a flap deflection of 40 deg. Below this speed, there is a gradual deterioration of stability until the airplane stalls. In this region, the pilot flies the BLC airplane with continuous small control movements in a manner similar to flying a helicopter. The low control forces were necessary in this region to reduce fatigue. As determined on the simulator, the pilot demonstrated with the airplane that he would control the flightpath very well. *The speed stability, that is, the ability to maintain airspeed, seemed much better on the airplane than on the simulator.* The most important criticisms of the control system were the lack of centering and the loss in aileron effectiveness at the stall. Again, the similarity to helicopter experience is apparent. The acceptable values of control breakout force are influenced by the control force level and the stability of the aircraft. These criticisms were not serious, however, and the flight test program had demonstrated that adequate flying qualities existed for flight at the low speeds required for short-field take-offs and landings.

The first step in making the short-field takeoff was to determine the acceleration characteristics during taxi runs. Immediately, difficulty was experienced in keeping the airplane on the ground beyond 60 knots with 60-deg flap. The main gear lifted off and the pilot forced the nose wheel back on the ground. The airplane flew down the runway, wheelbarrow fashion. Reducing the flap deflection to 40 deg increased the acceleration and reduced the attitude problem. Normal short-field procedures were used, except that the airplane accelerated during the climb out. The results of the takeoff tests are shown in Fig. 13, compared to the estimated data based on the wind-tunnel tests. Despite the higher lift off speeds experienced in the flight testing, the data show reasonable agreement. *For a gross weight of 100,000 lb, the BLC airplane can get off the ground in 750 ft, and over the 50-ft height in 1,390 ft.*

The landing distance tests were set up to obtain the minimum ground roll distance. Standard short-field procedures were used, except that the approaches were flat to utilize higher power settings and slower touchdown speeds. Fig. 14 shows the test results compared to the estimated distances. *The ground distance is 690 ft for a gross weight of 100,000 lb. The touchdown speed is 70 knots compared to an estimate of 65 knots.* The pilot was able to obtain full braking and reverse thrust sooner than was estimated. These landings are made with 60 deg of flap. The use of 90 degree will require more power, and can either reduce the air distances or decrease the touchdown speed and ground-roll distance.

The BLC equipment worked exceptionally well during the flight test program. We experienced no difficulties with the main BLC ducts. The nozzles were adjusted once, to even out the flow near the tips. Except for the q-bellows, the feel and control systems worked satisfactorily. The production airplane will require very little in the way of detail system design change from the test bed, except for the BLC engines."

As to the paper's conclusions, Dickerman ended on a very positive note saying,

"Further flight-testing of the BLC Hercules will develop the following:

1. Increased aileron effectiveness at the stall.

2. *More accurate low-speed airspeed system* [my italics].
3. Decreased breakout forces and improved control centering.
4. Elevator control forces within specification requirements throughout the speed range.
5. Landing procedures for minimum over-the-obstacle performance.

The test-bed flight-test program has demonstrated that the BLC Hercules is a practical STOL airplane. With the use of Continental engines for boundary layer control air on the production airplane, the flow is increased and the takeoff and landing distances are decreased to approximately 500 ft on an unprepared field, as required by GOR 130. The complete boundary layer control system provides the stability and control required for assault transport operation."

It seems to me that the test bed served its purpose rather well as most test beds do. It did provide confidence that landing and taking off from a 500-foot unprepared field should be possible with a production airplane at a gross weight of 100,000 pounds. *The primary task was clearly to get very satisfactory stability and control characteristics so the BLC and propeller thrust could be used to their fullest.*

Following Lockheed's 23-hour test program, during the early summer of 1961 the test bed was flown on a demonstration tour in England, West Germany, Italy, and France [527]. The aircraft then participated in Project Rough Road, as you will read later. Then the issue of stability and control at very low speeds was taken up by NASA Ames shortly after the NC-130B's Rough Road evaluation was completed. Lockheed flew its test bed to Ames where primarily flying qualities testing was conducted from June 30, 1961, to December 20, 1961 [490]. Findings were report in NASA TN D-1647 [529] by Hervey Quigley and Bob Innis, who summarized the collective opinion as follows:

"A flight investigation was conducted to evaluate the operational problems and handling qualities of a large transport airplane that had been equipped with blowing boundary-layer control on highly deflected flaps, drooped ailerons, and control surfaces to give it STOL capabilities. The airplane was capable of landing and taking off over a 50-foot obstacle at distances of less than 1,500 feet and at airspeeds of less than 65 knots. The results of the study have indicated that some standard operational techniques and procedures will have to be revised before full advantage can be taken of the STOL vehicle. The pilot's major control problem at low airspeeds was the large sideslip excursion caused by the unsatisfactory lateral-directional handling qualities. The longitudinal handling qualities were considered satisfactory."

Given these flight test results, Ames launched a flight simulator study of the NC-130B. The emphasis was primarily on the lateral-directional handling qualities as reported in reference [530]. This study showed that the handling qualities of the NC-130B would be satisfactory *if* the directional stability and sideslip rate damping were increased. In essence, the pilots needed some stability augmentation to help fly the aircraft at very low speeds. Furthermore, additional flight testing with a stability augmented aircraft was clearly required. The NC-130B was sent back to Lockheed Georgia where an augmentation system was incorporated to drive the rudder in response to several inputs with variable gains. By early 1963, the aircraft was back at Ames for a follow-on flight test program from February 27, 1963, to May 23, 1963 [490]. The report [531], published in May of 1967, summarized the results saying:

> "This flight and simulator study investigated techniques for augmenting the lateral-directional characteristics of a large STOL transport airplane to improve handling qualities in the landing approach.
>
> For the airplane tested, augmentation was required to help the pilot control sideslip when maneuvering in the approach or when making approaches in gusty weather. With augmentation to improve the turn coordination and directional damping, the sideslip excursions could be reduced satisfactorily.
>
> Turn coordination was augmented with a system that drove the rudder in proportion to roll rate and aileron deflection. For satisfactory turn coordination the system did not eliminate all sideslip, but the peak sideslip to peak bank angle ratio was reduced to less than 0.3 in a rudder-pedal-fixed turn entry.
>
> Directional damping was augmented with a system that drove the rudder in proportion to the rate change of sideslip relative to the airplane flightpath. This damper system derived its inputs from internally mounted instruments (roll attitude, yaw rate, and lateral acceleration) and, therefore, excluded the random inputs due to sharp edged gusts. The gain of the side-slip rate damper was adjusted to give a damping ratio of between 0.4 and 0.5.
>
> The rudder authority for augmentation depends on the maneuvering required of the airplane in the landing approach. For the NC-130B airplane of this investigation, 25-percent rudder authority (15 degrees) enabled the airplane to be maneuvered to a bank angle of about 15 degrees at the 70-knot landing approach speed. Higher maneuvering capability and, therefore, higher rudder authority, will be demanded for most STOL missions."

The report included a table giving the pilots' opinions using what became known as the Cooper-Harper rating system. That table is included here as Table 3-10 and shows that the level of stability and control was definitely improved to a satisfactory level under normal operation with the NC-130B. What was not accomplished was enough stability and control should an emergency occur. Even more significant was the pilots' opinion that, should the stability augmentation system fail with the aircraft in very slow speed flight, it was doubtful that the average pilot could even land the aircraft on a very short field.

Throughout this time of NC-130B design, development, and evaluation, Lockheed was continuing their study of what they generically called the GL-128, which was to be the production STOL. This production STOL was frequently compared to a standard C-130E that Lockheed saw as the next model in the series of C-130s. Of course, improvements to the test bed to offer a production model was always kept in mind. This BLC-130 was designated as the GL 128-17; the -17 gives you a sense of the wide scope of Lockheed's studies. A hint of what Lockheed saw as a production C-130 with boundary layer control was presented in a paper by T. Dansby and his coauthors [527] at the AIAA General Aviation Aircraft Design and Operations Meeting held in Wichita, Kansas, on May 25–27, 1963.

Dansby stated that there would be four compressors in a production design and showed a figure detailing the arrangement, which you see here as Fig. 3-140. For the production C-130 with BLC, Allison offered its commercial version of the T56 designated as the 501-M5. This turboprop engine was to drive Hamilton Standard's four-bladed, 15-foot-diameter propeller. In addition, the 501-M5 gearbox had a rearward drive shaft to the compressor as I have noted on Fig. 3-140. As to the maximum power available and its distribution, Dansby stated that

"At maximum power at sea level the 501-M5 engine develops 6,500 shp, of which 2,000 hp is absorbed by the BLC compressor when the clutch is engaged; the remaining 4,500 shp drives the propeller. When the clutch is disengaged, and the BLC system is not in use, all of the power of the engine drives the propeller with a limitation of 5,000 shp, which is imposed by the gear box capacity. This reduces the size and weight of the gear box, and the power limitation does not restrict the altitude cruise performance. …Each compressor delivers 20 pounds per second at a pressure ratio of 3.80, or 41 psig [pounds per square foot gauge]."

STOL performance from a soft, dry field at sea level on a standard day and over a 50-foot obstacle was projected to be about 1,000 feet at a gross weight of 110,000 pounds.

Table 3-10. Lockheed and NASA Improved the NC-130B's Flying Qualities Up to the Satisfactory Level, but the Pilots Thought the STOL Was Unsatisfactory Should an Emergency Occur at Very Low Speeds [531]

	Adjective Rating	Numerical Rating	Description	Primary Mission Accomplished	Can Be Landed
Normal operation	Satisfactory	1	Excellent, includes optimum	Yes	Yes
		2	Good, pleasant to fly	Yes	Yes
		3	Satisfactory, but with some mildly unpleasant characteristics	Yes	Yes
Emergency operation	Unsatisfactory	4	Acceptable, but with unpleasant characteristics	Yes	Yes
		5	Unacceptable for normal operation	Doubtful	Yes
		6	Acceptable for emergency condition only*	Doubtful	Yes
No operation	Unacceptable	7	Unacceptable even for emergency condition*	No	Doubtful
		8	Unacceptable—dangerous	No	No
		9	Unacceptable—dangerous	No	No

* Failure of a stability augmentor.

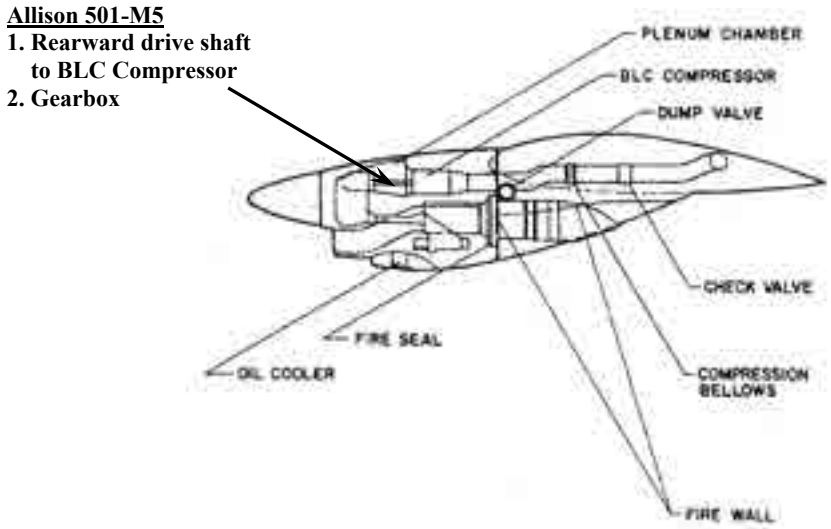

Fig. 3-140. A design of a production C-130 with BLC was designated as the GL-128-17 and was to use four Allison 501-M5 turboprop engines rated at 6,500 horsepower. The 501-M5 turboshaft engine is described by John Leonard [528], page 74.

In the early 1960s, when demonstrations of practical aircraft using BLC were being given considerable attention, there were any number of papers and reports available [412, 432, 532-552] dealing with getting very high maximum wing lift coefficients, say, on the order of 6 to 8. And, of course, there were any number of reports and papers dealing with takeoff and landing calculation methods, as well as aircraft design [553-563]. What struck me from my limited collection was that only one report [544] gave the method to calculate the ideal power to produce the amount of blowing air required to achieve maximum lift coefficients. You will recall an even simpler equation on page 66 of Volume II, which I repeat here as

$$(3.144)\quad \frac{\text{HP}_{\text{compressor}}}{\text{Airflow lbs/sec}} \approx \frac{0.33949}{\eta_C}\left(459.67 + \text{T}_{\text{T2}} \text{ in } ^\circ\text{F}\right)\left(\text{PR}^{0.2857} - 1\right).$$

The compressor for the GL-128-17 was designed to a pressure ratio (PR) of 3.8. The air at the compressor inlet (T_{T2}) at sea level standard day is 59 ^{o}F, and *if* the compressor is 100 percent efficient (i.e., $\eta_C = 1$) then the compressor power required is about 1,600 horsepower for an airflow of 20 pounds per second. Dansby stated that he expected that 2,000 horsepower of the 501-M5 was allocated to the BLC compressor. That would imply that the effective efficiency was on the order of 0.8, which seems reasonable to me.

Clearly, significant power is required for boundary layer control in large transport aircraft such as the Lockheed C-130. In my experience, BLC advocates rarely mention this power required fact—or its cost—when they present their designs.

Dansby addressed the cost of three approaches to V/STOL in his paper. Cost data is—in my experience—quite unusual to find in technical papers. The flyaway (i.e., unit) costs dealt with a minimal STOL 130, a BLC STOL 130, and a VTOL C-130. The cost numbers were based on production of 100 aircraft. I have included both tabulated data (Table 3-11) and a very, very interesting summary figure (Fig. 3-141) showing cost data referenced to a standard production C-130 designed for assault transport missions.

Table 3-11. Lockheed's Cost Estimate for Three Levels of V/STOL Aircraft Performance [527] (Costs Normalized to a 1960's Production C-130); Production Materials Appear to be a Major Cost Driver

Performance	STOL C-130	BLC-130	VTOL C-130
Development			
Design	2.63	10.62	14.35
Static and flight test	1.71	2.77	6.16
Production (additional to standard C-130E)			
Tooling	3.48	5.49	9.55
Material	2.71	24.57	123.05
Labor, overhead, and misc	6.65	11.89	15.52
Standard C-130E	100.00	100.00	100.00
Unit cost, 100 aircraft*	117.23	155.34	268.63

* Unit (flyaway) cost includes the airframe, engines, propellers, and equipment.

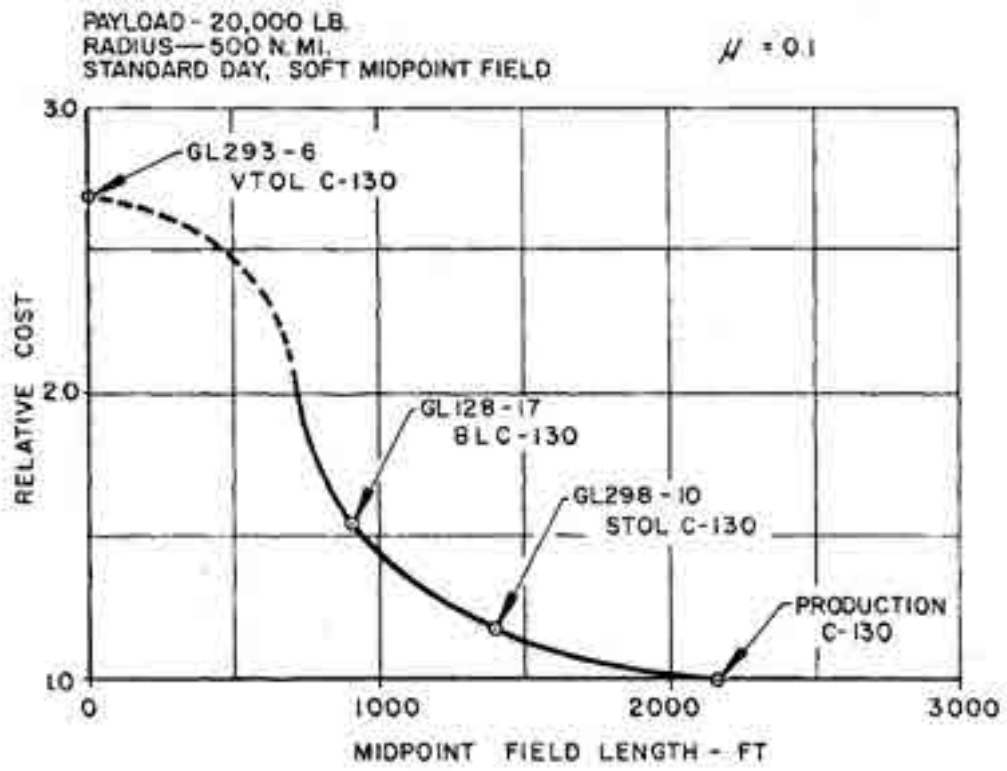

Fig. 3-141. Lockheed's estimate of aircraft cost increases depending on the field length available at the midpoint of a 1,000-nautical-mile assault transport mission. In my opinion, this is a very pessimistic trend given the technology available today such as tiltrotor, tiltwing, and other powered lift aircraft [527].

The VTOL C-130 that Dansby offered, the GL293-6 on Fig. 3-141, was a direct lift with a number of turbojets stored in pods as you see in this sketch below. The two "lift pods" were to be identical and interchangeable, and each pod was to contain 11 Allison 610-D1 10,000-pound-thrust turbofan lift engines, together with the systems and instrumentation necessary for their operation. The lift pods were to be located beneath the wing, midway between the T56 engines, and be attached to the wing by two struts and to the rear fuselage by two additional struts, forming an A-frame. Dansby emphasized that the pods were designed to be removable from the airplane and to be readily stowed within the airplane cargo compartment for deployment. By my count that amounts to 26 engines in this VTOL design! No wonder Dansby placed the VTOL C-130 at a "relative cost" of 2.7 on Fig. 3-141.

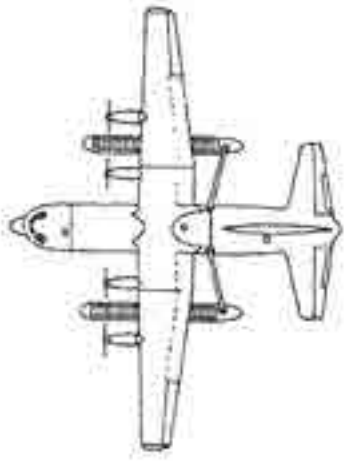

Now let me discuss what I believe was one of the U.S. military's most important experiments—Project Rough Road.

3.8 PROJECT ROUGH ROAD

By the 1960s the United States had, primarily, three operational airplanes representative of what many would call assault transports. That some thought of them as STOLs is rather a mute point because no universally accepted definition of STOL existed at that time. Nevertheless, the three aircraft were:

1. The Lockheed C-130 Hercules (Fig. 3-126) with a maximum takeoff gross weight of 155,000 pounds.
2. The Fairchild C-123 Provider (Fig. 3-142) with a maximum takeoff gross weight of 60,000 pounds.
3. The de Havilland of Canada CV-2B Caribou (Fig. 3-143) with a maximum takeoff gross weight of 28,500 pounds.

This range in gross weight capability meant that between these three airplanes the U.S. Air Force with its C-130s and C-123s and—to a lesser extent the Army with its Caribou—could transport jeeps or tanks or anything in between (even helicopters) when acting as logistics support aircraft. And of course, with seats, large numbers of troops could be moved about.

You will immediately notice from the three photographs of these assault transports just how similar they are. To me, it is as if they are just scaled versions of one another. But the one defining characteristic of the assault transport is the rear ramp loading and unloading feature. You get a sense of this feature with the upswept tail end of the fuselage on all three airplanes.[132] It appears, in my view, that nearly half the fuselage is missing!

Then, between mid-June of 1962 and the end of July in 1963, the Air Force and the Army faced the issue of what the words "unprepared landing field" might mean to both operational pilots and aircraft designers. It seems to me that with their operational experience, pilots could qualitatively describe what unprepared meant, but takeoff and landing performance is hardly defined in a qualitative sense. Manufacturers were prone to quote takeoff and landing distances over a 50-foot obstacle most favorably without stating that the field was paved with concrete. And so, the question of performance when the field was made of clay—or even just a stretch of sand—needed to be answered. The experiment that provided considerable quantitative insight about "unprepared" was named Project Rough Road.

Project Rough Road was conducted by the Air Force Flight Test Center (AFFTC) and directed by the Air Force Aeronautical Systems Division (ASD). There were three elements supporting the project: the three airplanes mentioned above plus two derivatives, the pilots and their airplanes plus all the support staff, and a small group of soil analysis engineers. This team (Fig. 3-144) established takeoff and landing distances as a function of gross weight for, primarily, three landing areas—paved, clay, and sand. When you think about it, this is quite a test matrix: two flight maneuvers on three soils with five airplanes tested at two to three

[132] This rear ramp design requirement is also seen on such military helicopters as the Boeing CH-46 and CH-47, as well as the Bell Boeing V22 and LTV XC-142A.

Fig. 3-142. The Fairchild C-123B Provider had a maximum takeoff gross weight of 60,000 pounds [564-569].

Fig. 3-143. The de Havilland of Canada CV-2B Caribou had a maximum takeoff gross weight of 28,500 pounds [495-498, 502, 505, 570].

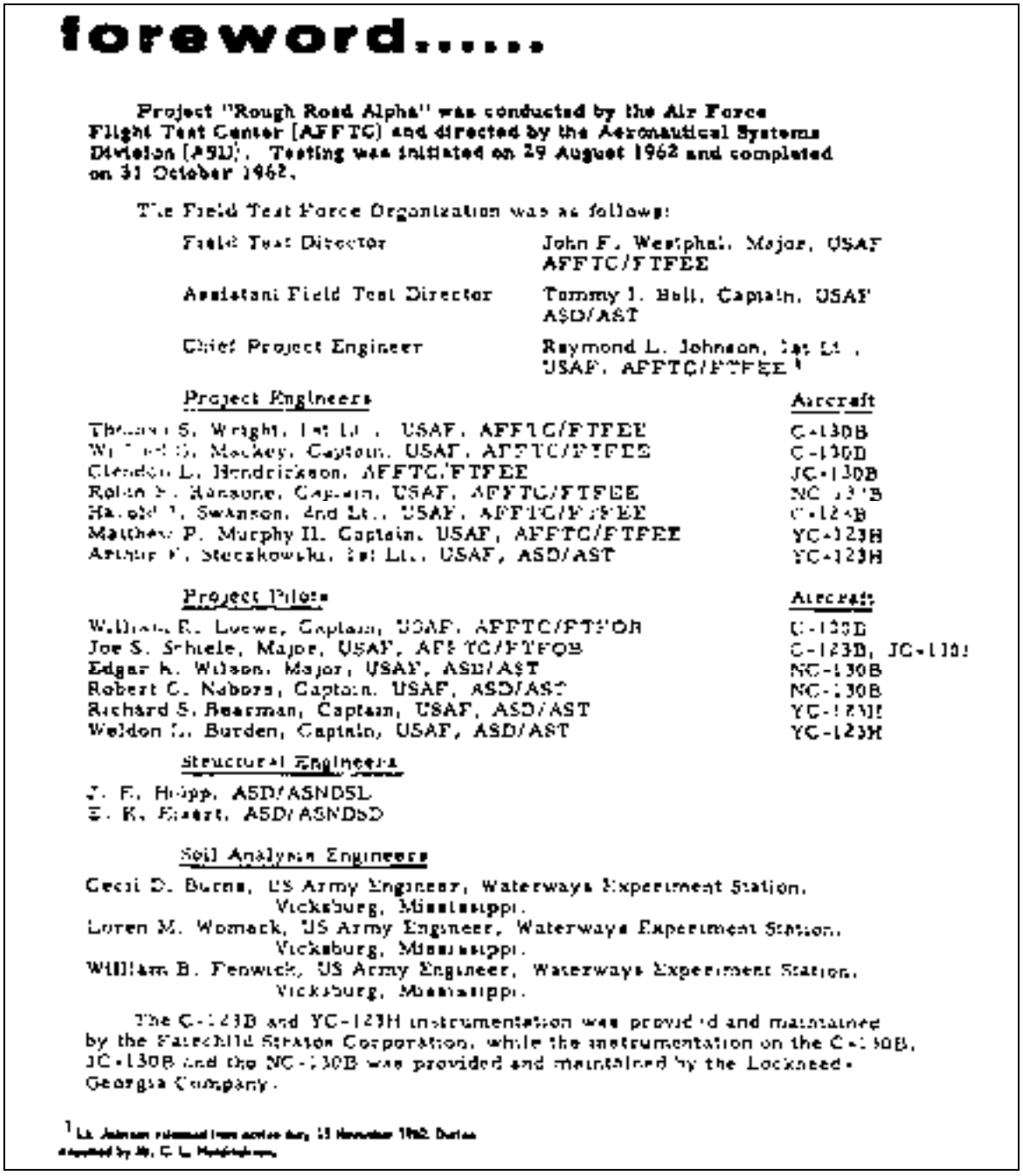

foreword.....

Project "Rough Road Alpha" was conducted by the Air Force Flight Test Center [AFFTC] and directed by the Aeronautical Systems Division [ASD]. Testing was initiated on 29 August 1962 and completed on 31 October 1962.

The Field Test Force Organization was as follows:

Field Test Director	John F. Westphal, Major, USAF AFFTC/FTFEE
Assistant Field Test Director	Tommy J. Bell, Captain, USAF ASD/AST
Chief Project Engineer	Raymond L. Johnson, 1st Lt., USAF, AFFTC/FTFEE [1]

Project Engineers	Aircraft
Thomas S. Wright, 1st Lt., USAF, AFFTC/FTFEE	C-130B
William G. Mackey, Captain, USAF, AFFTC/FTFEE	C-130B
Clendon L. Hendrickson, AFFTC/FTFEE	JC-130B
Robert F. Ransone, Captain, USAF, AFFTC/FTFEE	NC-130B
Harold T. Swanson, 2nd Lt., USAF, AFFTC/FTFEE	C-123B
Matthew P. Murphy II, Captain, USAF, AFFTC/FTFEE	YC-123H
Arthur F. Steczkowski, 1st Lt., USAF, ASD/AST	YC-123H

Project Pilots	Aircraft
William R. Lowe, Captain, USAF, AFFTC/FTFOB	C-130B
Joe S. Schiele, Major, USAF, AFFTC/FTFOB	C-123B, JC-130B
Edgar H. Wilson, Major, USAF, ASD/AST	NC-130B
Robert C. Nabors, Captain, USAF, ASD/AST	NC-130B
Richard S. Bearman, Captain, USAF, ASD/AST	YC-123H
Weldon L. Burden, Captain, USAF, ASD/AST	YC-123H

Structural Engineers

J. F. Hopp, ASD/ASNDSL
E. K. Ehert, ASD/ASNDbD

Soil Analysis Engineers

Cecil D. Burns, US Army Engineer, Waterways Experiment Station, Vicksburg, Mississippi.
Loren M. Womack, US Army Engineer, Waterways Experiment Station, Vicksburg, Mississippi.
William B. Fenwick, US Army Engineer, Waterways Experiment Station, Vicksburg, Mississippi.

The C-123B and YC-123H instrumentation was provided and maintained by the Fairchild Stratos Corporation, while the instrumentation on the C-130B, JC-130B and the NC-130B was provided and maintained by the Lockheed-Georgia Company.

[1] Lt. Johnson [illegible] active duty, 15 November 1962. Duties [illegible] by Mr. C. L. Hendrickson.

Fig. 3-144. It is quite unusual for the forward of a technical report [564] to provide the names of all the key players who contributed to the effort. The fact that six pilots were a part of this experiment is noteworthy.

gross weights, and all to be done for takeoff and then again for landing. The actual experimental data was acquired over about 2-1/2 months from June 13, 1962, to August 1, 1963. Several very key reports [564, 571-573] became available by September 1963.

The Air Force concentrated their first efforts on testing Lockheed's B model of the C-130 series during June and July of 1962. Two reports about these efforts were published as Phase I [571] and Phase II [572] of Project Rough Road. You will find that Phase I contains data for a standard C-130B while Phase II provides data for a somewhat modified C-130B.

In the introduction of the Phase I report, the authors state that the objective was to establish the "short field" capabilities of the production C-130B. At that time it appears to me that "STOL" capabilities were measured against what the C-130 A and B models had. The test gross weight was 101,000 pounds, which "simulates [landing and takeoff at the end of] the outboard portion of a 500-nautical-mile-range support radius mission with a 20,000-pound payload." The Air Force had several test sites where takeoff and landings were performed. The engineers used the paved runway at Elgin Air Force Base (AFB) in Florida to establish the baseline capabilities of the production C-130B. After that they used the following off-site locations, which had different soil types:

Wright-Patterson AFB, Ohio	Hard clay
Eglin AFB, Florida	Firm sand
Eglin Auxiliary Field No. 2	Soft sand
Barksdale AFB, Louisiana	Soft clay

The Naval Air Station in New Orleans, Louisiana, was also initially considered because it had a runway with soft clay but this site was "rejected when it was found that the area would not support the aircraft." The soil engineers established the California Bearing Ratio (CBR) for each site, and the Phase I and II reports discuss several other characteristics of the unprepared runways in considerable detail.[133]

From the 11 figures of detailed test results, the Phase I report provided a simple table of takeoff and landing distances over a 50-foot obstacle, which you have here as Table 3-12.

Table 3-12. Air Force Established "STOL" Performance of Its Production C-130B [571]

	MAXIMUM PERFORMANCE Gross Weight 101,000 lb Standard Sea Level, No Wind Conditions	
Surface	**Total Takeoff Distance/ft Flaps 50 Percent (18°)**	**Total Landing Distance/ft Flaps 100 Percent (36°)**
Paved	1,550	1,870
Hard clay	1,600	2,000
Firm sand	1,820	1,700
Soft sand	2,150	1,780
Soft clay	1,950	1,710

[133] The subject of how soil is classified for supporting vehicles is quite interesting, but it is beyond the scope of this discussion.

From this data you can see that soft soil, in which the aircraft can leave ruts, significantly increases takeoff distances but hardly affects landing distances. It is immediately obvious that a clearing of no less than 2,200 feet, with a runway probably on the order of 1,000 feet, was what the C-130B needed at any place in the world to have operational flexibility. You might also note the words "MAXIMUM PERFORMANCE" on the table. Earlier you read the words "Emergency-Wartime-Use-Only." These words mean that the pilot is not required to follow the Flight Manual. This permission allowed pilots to be as aggressive in flying the aircraft as they felt during takeoff and landing maneuvers. In short, the pilots were to extract every ounce of performance from the aircraft that they could. It is quite significant that in the hands of a well-practiced pilot, the C-130B could take off and land from a paved runway some 1,000 feet shorter than if flown "by the book" (see Fig. 3-134 and Fig. 3-136).

While Phase I was in progress, the Air Force loaned a C-130B test bed (S/N 57-0525) back to Lockheed for modifications intended to improve the short field performance of the production model. The modifications included (a) changing the propeller gear boxes to increase propeller RPM, (b) allowing more negative propeller pitch to increase reverse thrust, (c) increasing maximum flap deflection from 36 to 50 degrees, and (d) altering the nose gear strut to reduce transient loads. Tire pressure was maintained at 60 pounds per square inch. This modified C-130B was designated as the JC-130B and used in the Phase II test program.

The Phase II program went on from July 14 through July 17 of 1962 with testing on the same soft sand used during Phase I. The primary test gross weight was 101,000 pounds. As the Phase II reports [572], "compared to the production C-130B, the 'short field' takeoff performance of the modified aircraft is not significantly improved." The tabulated results for takeoff are provided here in Table 3-13.

On the positive side, the landing performance was substantially improved on both paved and soft sand surfaces as the tabulated data in Table 3-14 shows. The authors of the Phase II report concluded that "landing speeds are generally 10 knots lower than those used for maximum performance landings with the production C-130B." The primary concern in landings was nose gear loads, particularly in the landings on soft sand. On three of the five landings, the nose gear loads "were 14 percent over the design limit strength."

Table 3-13. The Modified C-130B, the JC-130B, Offered No Takeoff Performance Improvement Over the Production C-130B [572]

	COMPARISON OF SHORT FIELD TAKEOFF DISTANCES PRODUCTION C-130B VS. MODIFIED C-130B Gross Weight - 101,000 lb Takeoff Rated Power Standard Sea Level, No Wind Conditions Flaps - Production Aircraft 18°, Modified Aircraft 20°			
	Ground Roll - ft		**Total Distance - ft**	
Surface	**Production C-130B**	**Modified C-130B**	**Production C-130B**	**Modified C-130B**
Paved	1,050	1,050	1,550	1,550
Soft sand	1,650	1,600	2,150	2,100

Table 3-14. The JC-130B Offered Significant Landing Performance Improvement Over the Production C-130B [518, 572]

COMPARISON OF "SHORT FIELD" LANDING PERFORMANCE PRODUCTION C-130B VS. MODIFIED C-130B Gross Weight - 101,000 lb Standard Sea Level, No Wind Conditions Modified Flap 50°, Production Flap 36°						
	Ground Distance (ft)		Total Distance (ft) Method A		Total Distance (ft) Method B	
Surface	Production	Modified	Production	Modified	Production	Modified
Paved	1,270	880	1,870	1,620	2,260	2,020
Soft sand	1,180	860	1,780	1,600	2,170	2,000

	LANDING SPEEDS			
	Indicated Airspeed - Kts		True Airspeed - Kts	
	Touchdown	50 ft	Touchdown	50 ft
Production	87	95	91.0	97.5
Modified	77	85	86.5	87.5

The recommendations published in the Phase II report stated:

"Should the modifications tested during Phase II be incorporated on the production aircraft, it is recommended that:

1. Further testing be conducted to evaluate the changes in the specific range of the aircraft due to the increased propeller speed (page 1).
2. Additional tests be conducted to define, and if possible to improve the stability and control characteristics of the aircraft in the landing configuration at the low speeds required for "short field" landings (page 2). [I would add that this is a recurring recommendation for short field landings with fixed-wing aircraft.]
3. The nose landing gear and the main landing gear along with the associated back-up structures be structurally investigated and modified as necessary to provide adequate static and fatigue strengths for off-runway operations (page 9)."

At the completion of Phase II, it surely must have become clear to all concerned that any further improvements in landing performance would require significant improvements to both stability and control at much lower speeds than 80 to 90 knots. Apparently, takeoff performance could be improved with increased thrust, which *just* meant more powerful engines, different propellers, and selective increases in airframe strength.

The final phase of Project Rough Road was conducted from August 29 to October 31 of 1962. This phase added the word "Alpha" after Road in the report title [564]. The abstract of the report states:

> "Project Rough Road Alpha was conducted to determine the limits of off-runway capability of five aircraft, the C-130B (Production), JC-130B (Modified), NC-130B (Boundary Layer Control), YC-123H Modified, and C-123B (Production). Areas used for the test were representative of the minimum soil strength conditions feasible for assault operations. Relatively smooth unprepared surfaces were selected: soft sand at Yuma, Arizona, and soft clay at Harper Lake, California. The main runway at Edwards AFB, California, was

> utilized for base line data. The requirements for operations under conditions such as soft sand are not wide spread and would be accomplished only in emergency situations.
>
> It was concluded that all the test aircraft can maneuver on any sand area (except quick sands), regardless of bearing strength, where the terrain (roughness, obstructions, etc.) is suitable. Soft clay similar to that at Harper Lake with a California Bearing Ratio (CBR) of 3 or more will support both the C-123 and C-130 aircraft at the gross weights tested."

Let me stop right here before discussing the results of Project Rough Road Alpha. The Rough Road project report that was published by the U.S. Air Force in April 1963 dealt with the C-130 and C-123 assault transports. However, the report was missing data for the U.S. Army's CV-2B, the Caribou built by de Havilland of Canada. To rectify this oversight, the U.S. Army Aviation Test Activity (also located at Edwards Air Force Base in California) conducted its own tests of the Caribou following Air Force procedures and test sites. The Army's report [497] was published in September of 1963. Let me add that the Army's report had the parenthetical subtitle "(Similar to Air Force Project Rough Road Alpha)."[134] The Army's report included Caribou results added to the Air Force's table of data for the C-130 and C-123.

The two tables—for takeoff and landing—from the Rough Road experiment are of such value that I have reproduced them here as Fig. 3-145 and Fig. 3-146. I found two interesting aspects from the project in toto. The first was how much a sand surface affected takeoff and landing distances in comparison to a paved surface. This interesting result is shown in Fig. 3-147. It appears that an "unprepared" sand runway increases takeoff distance over a 50-foot obstacle by about 25 percent. The sand's retarding influence appears to reduce landing distance over a 50-foot obstacle by about 10 percent. I might also note in passing that the C-130 with boundary layer control, the NC-130B, did not produce a significant improvement over the production C-130B in this experiment. This disappointing result was quite likely because stability and control at low speed was insufficient to allow use of the high lift performance available. On the other side of the coin, the addition of two CJ-610-1 turbojet engines slung under the wing of the C-123B to create a YC-123H significantly shortened the takeoff distance. Of course, the turbojet engines were of no significant use in landing.

The second interesting aspect was the aircraft lift coefficients at liftoff and touchdown. Fortunately, the tables in the Army report (Fig. 3-145 and Fig. 3-146) provided sufficient data to calculate lift coefficients based on nominal test gross weight and true airspeeds for these key phases of the maneuver, plus the note that the data was for standard day at sea level. Using this information, I found that a nominal lift coefficient at liftoff and touchdown speeds was in the range of 2.3 to 2.5 for the standard aircraft and considerably higher for the NC-130B, which had boundary layer control. My results are shown in Fig. 3-148.

---

[134] You might not remember the raging interservice roles and mission debate between the Air Force and the Army that was going on in the 1960s. The Army's CV-2B Caribou was swept up in the debate. As Dr. Ian Horwood wrote [574], "the Army's position was that if an aircraft [fixed wing, rotary wing, or V/STOL] flew in support of ground operations, that aircraft belonged to the Army. The use of the CV-2B in Vietnam by the Army was to prove particularly galling for Air Force officers, many of whom believed that all fixed-wing aircraft should be operated by the Air Force." Horwood noted that "the dispute over the CV-2B was to result in a 1966 decision by which the Army renounced its CV-2s to the Air Force (where they were re-designated C-7s) in return for the Army's retention of the armed helicopter [Bell's AH-1G Cobra attack helicopter]."

TABLE III
TAKEOFF PERFORMANCE SUMMARY***
Standard Sea Level - No Wind Conditions

Takeoff Distances - Feet **Recommended Airspeed - Knots**

Aircraft	Gross Weight (lb)	Ground Roll Surface			Total Distance to Clear 50 Feet Surface			Recommended Flaps % (°)	$V_{Lift-off}$		$V_{50\ Feet}$		Basic Weight	Test Weight Design $GW^{\times 100}$
		Paved	Sand	Clay	Paved	Sand	Clay		KIAS	KTAS	KIAS	KTAS		
CV-2B	28,500	550	875	655	920	1195	1025	25	--	57.0	--	58.0	19,777	100%
C-130B	85,000	700	980	890	1100	1380	1290	50 (18)	70.0	77.5	83.5	82.5	70,570	63%
	101,000	1060	1480	--	1560	1980	--	50 (18)	75.5	84.5	88.5	88.0	70,750	75%
	125,000	1690	2390	2110 (2260)*	2390	3090	2810 (2960)*	50 (18)	83.0	94.0	97.5	97.0	70,570	93%
JC-130B	85,000	670	950	--	1070	1350	--	40 (20)	70.0	77.5	82.0	82.5	79,017	63%
	101,000	1000	1440	--	1500	1940	--	40 (20)	79.0	84.5	88.5	88.0	79,017	75%
	125,000	1640	2290	--	2340	2990	--	40 (20)	90.5	94.0	97.0	97.0	79,017	93%
NC-130B	101,000	820	1010	860	1400	1590	1440	33 (30)	--	71.0	--	80.0	81,439	63%
	115,000	1220**	1420	--	1840**	2040	--	33 (30)	--	78.0	--	85.0	81,439	75%
	125,000	1510	--	1570	2160	--	2220	33 (30)	--	83.0	--	90.0	81,439	93%
C-123B	47,000	900	1670	1180	1300	2070	1580	33 (20)	73.0	75.0	74.0	78.0	34,407	87%
	54,000	1230	2280	1660	1850	2900	2280	33 (20)	79.0	80.0	81.0	83.0	34,407	100%
YC-123H	47,000	590	690	670	960	1060	1040	50 (30)	--	68.0	--	72.0	40,086	76%
	54,000	790	920	890	1260	1390	1360	50 (30)	--	73.0	--	77.0	40,086	87%
	62,000	1020	1230	1170	1610	1820	1760	50 (30)	--	78.0	--	83.0	40,086	100%

* Soft clay with wet surface.
** Estimated.
*** This table is a reproduction of the table presented in FTC-TDR-63-8, page 17, (Project Rough Road Alpha), with the CV-2B test data added.

Fig. 3-145. Takeoff Performance Summary.

TABLE IV
LANDING PERFORMANCE SUMMARY**
Standard Sea Level - No Wind Conditions

Landing Distances - Feet **Recommended Airspeed - Knots**

Aircraft	Gross Weight (lb)	To Clear 50 Feet Surface			Ground Roll Surface			Recommended Flaps % (°)	$V_{50\ Feet}$		$V_{Touchdown}$		Basic Weight	Test Weight Design $GW^{\times 100}$
		Paved	Sand	Clay	Paved	Sand	Clay		KIAS	KTAS	KIAS	KTAS		
CV-2B[1]	28,500	925	850	925	500	450	485	100 (40)	--	65.0	--	62.0	19,777	100%
CV-2B[2]	28,500	1250	1050	1194	825	650	755	100 (40)	--	65.0	--	62.0	19,777	100%
C-130B	85,000	1500	1400	1380	800	700	680	100 (36)	85.5	85.5	77.5	80.0	70,570	63%
	101,000	1870	1720	--	1080	930	--	100 (36)	92.0	93.0	84.0	87.0	70,750	75%
	125,000	2720	2510	2100 (2850)*	1620	1410	1000 (1750)*	100 (36)	101.5	103.5	93.0	97.0	70,570	93%
JC-130B	85,000	1400	--	--	750	--	--	100 (50)	80.5	80.5	71.0	77.0	79,017	63%
	101,000	1630	--	--	910	--	--	100 (50)	88.0	87.0	77.0	83.5	79,017	75%
	125,000	2400	--	--	1400	--	--	100 (50)	98.0	97.0	87.0	93.0	79,017	93%
NC-130B	101,000	1650	1650	1650	650	650	650	78 (70)	--	72.0	--	71.0	81,439	63%
	115,000	--	1980	--	--	980	--	78 (70)	--	75.0	--	74.0	81,439	75%
	125,000	1900	--	1900	900	--	900	78 (70)	--	78.0	--	77.0	81,439	93%
C-123B	47,000	1500	1270	1355	760	530	615	100 (60)	81.0	83.0	74.0	76.0	34,407	87%
	54,000	1730	--	1410	970	--	650	100 (60)	87.0	90.0	79.0	81.0	34,407	100%
YC-123H	47,000	1250	1170	1120	700	620	570	100 (60)	79.0	76.0	--	75.5	40,086	76%
	54,000	1370	1270	1190	820	720	640	100 (60)	85.0	78.0	--	78.0	40,086	87%
	62,000	1550	1400	1310	1000	850	760	100 (60)	90.0	82.0	--	82.0	40,086	100%

* Soft clay with wet surface.
** This table is a reproduction of the table presented in FTC-TDR-63-8, page 18, (Project Rough Road Alpha), with the CV-2B test data added.
1 Reversing propellers and braking action.
2 Braking action only.

Fig. 3-146. Landing Performance Summary.

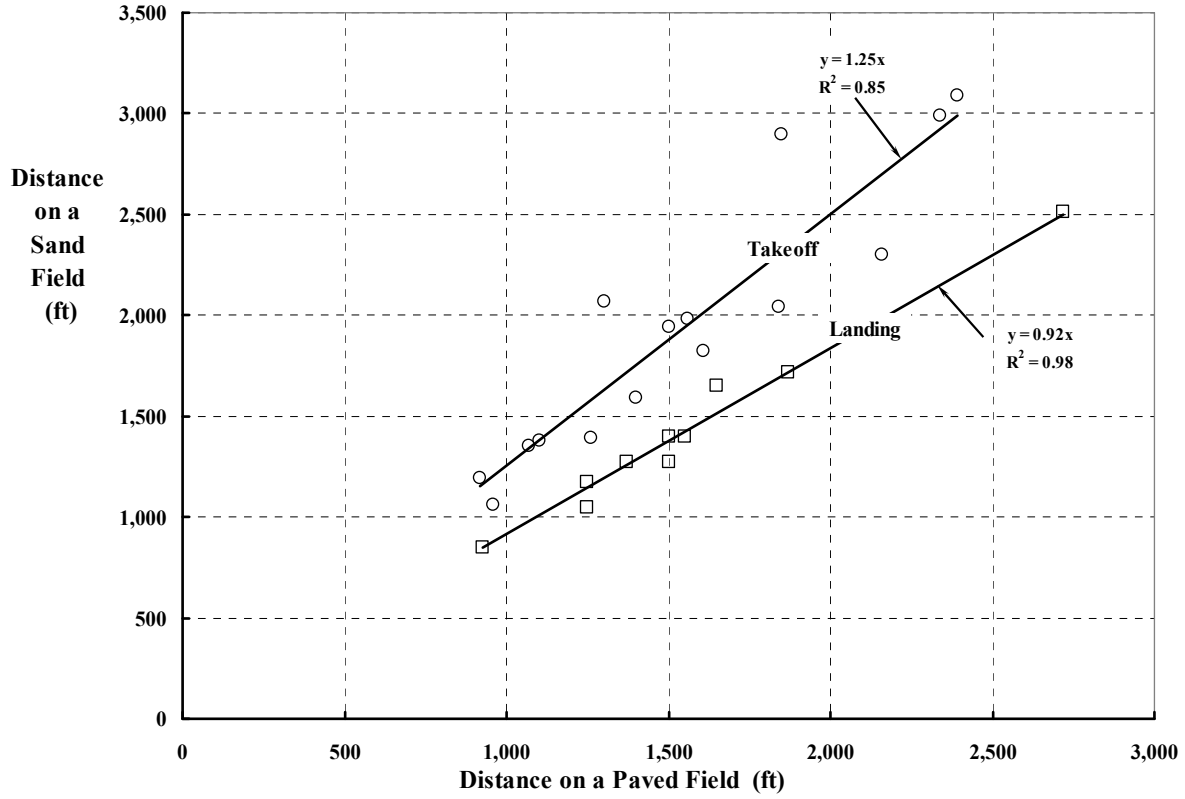

Fig. 3-147. When clearing a 50-foot obstacle, the performance difference between paved and sand "unprepared" runways is substantial.

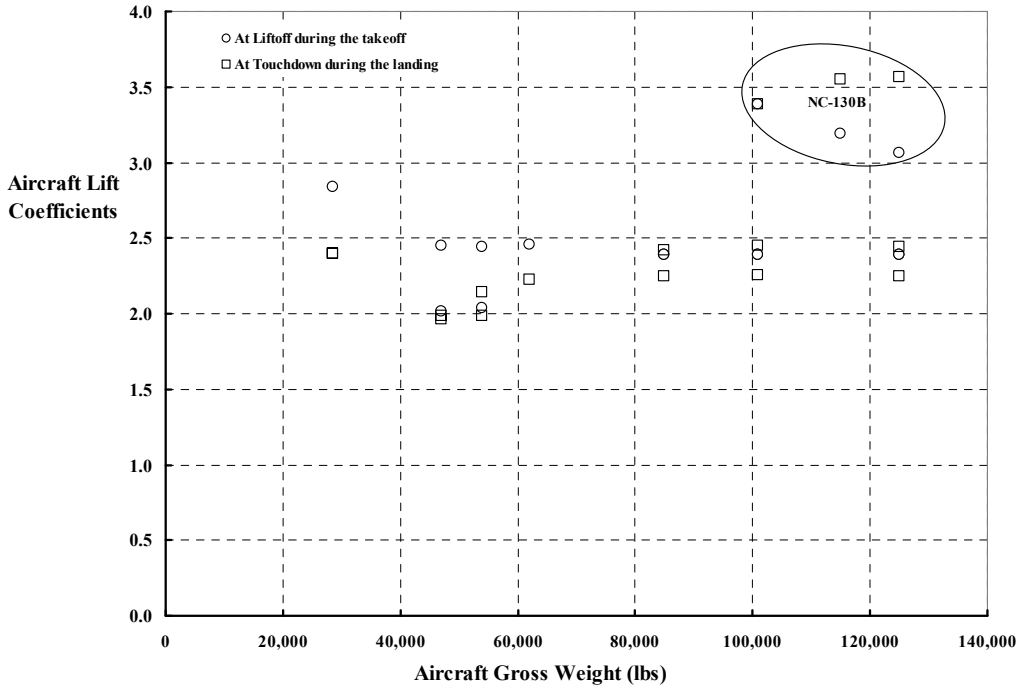

Fig. 3-148. Lockheed's NC-130B demonstrated practical BLC.

The results from Project Rough Road provide sufficient information to examine the takeoff results and the landing results with several different aircraft in some detail using a rudimentary—but still adequate—manner for this Volume III. Consider the takeoff problem first.

3.8.1 Takeoff Results

Let me approximate the takeoff maneuver with just the two phases that you see with the simple sketch below. Rather than using a much more thorough analysis, I have replaced the phase after liftoff, the transition to climb, and the climb to 50 feet with just a horizontal distance, which I have labeled air distance. Because the air distance after liftoff and the 50-foot-high obstacle form a right triangle, Project Rough Road's data establishes an effective climb angle, which is a small angle. The assumption here is that the Rough Road data were obtained by relatively skilled pilots. I recognize that this is taking considerable poetic license with the actual transition and climb-out maneuver because every pilot is different.

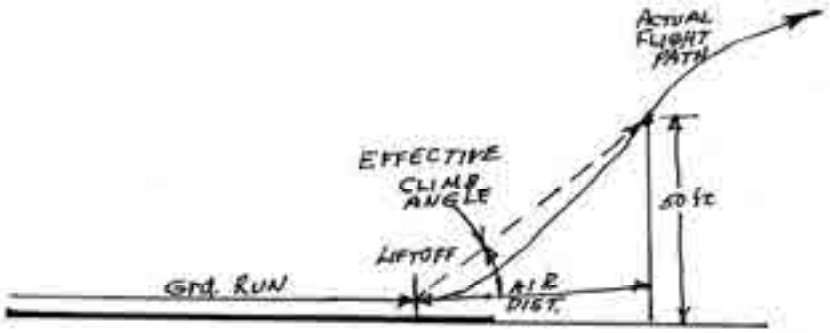

Now first consider the ground run distance (D_{gr}) that several Rough Road aircraft pilots demonstrated from a *paved* runway. The immediate objective is to get an order-of-magnitude feeling for what the average acceleration (a_{avg}) is so that the measured ground run distances and associated liftoff airspeeds are achieved. Simple physics says that the ground run distance is calculated as

$$D_{gr} = \frac{V_{liftoff}^2}{2a_{avg}} \tag{3.145}$$

where the airspeed at liftoff ($V_{liftoff}$) is in feet per second, and the average acceleration (a_{avg}) is in feet per second squared.

The behavior of ground run distance with liftoff airspeed that I found is illustrated in Fig. 3-149. Clearly nothing beats accelerating fast to a low liftoff airspeed if the requirement is to take off from, say, a 500-foot-long runway. And the fundamental is to have a large accelerating force acting on a lightweight machine. This is a basic fact of physics for all drag racing, as I am sure you are aware. These statements and Fig. 3-149 raise the immediate question as to just what was the range in accelerating force for the aircraft in the Road Rough experiment. My answer to this question, using simple F = ma, is shown in Fig. 3-150. Keep

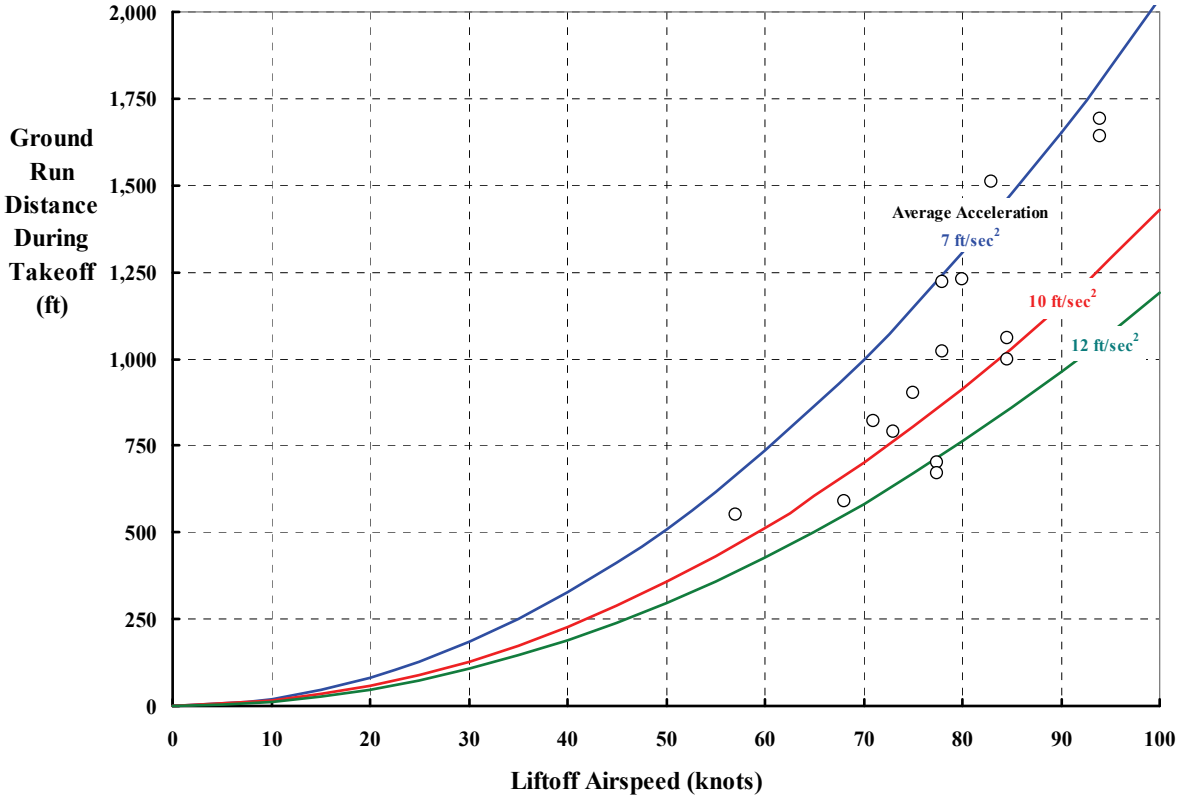

Fig. 3-149. Liftoff airspeed is the most important parameter in the problem.

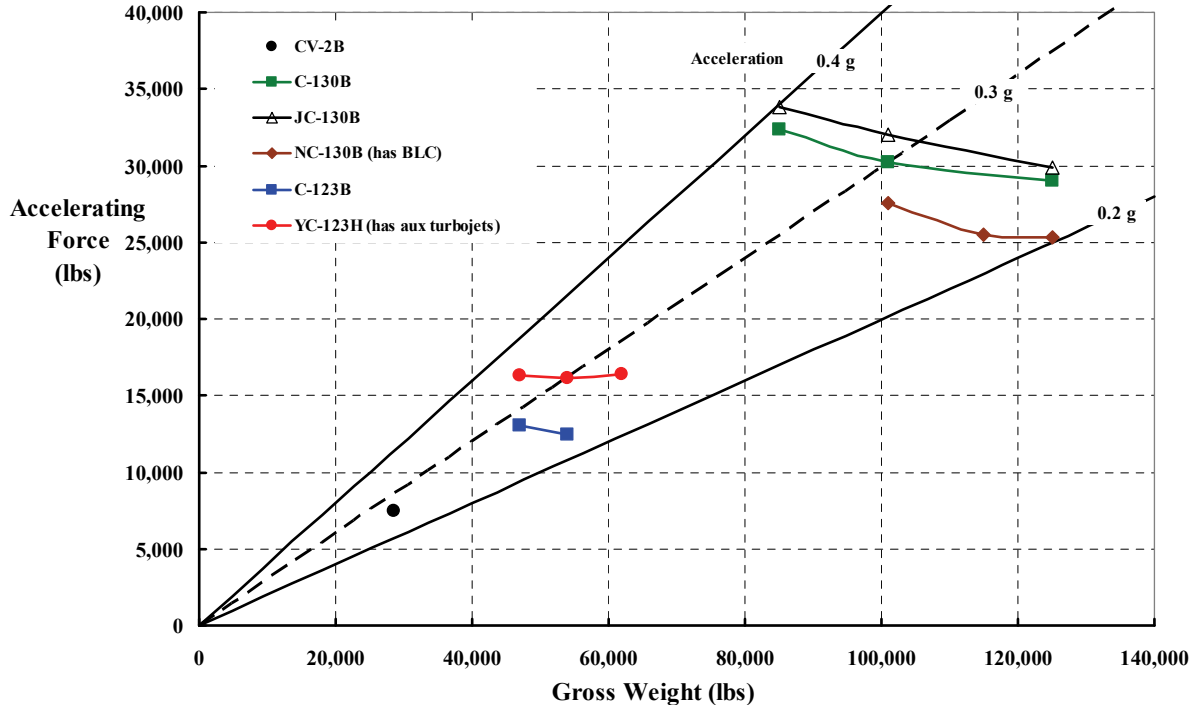

Fig. 3-150. Accelerating force *cannot* be assumed constant in the ground run calculation.

in mind that the accelerating force is the net sum of all forces acting nearly parallel with the runway. This means the propeller thrusts, the engine residual jet thrust, the rolling friction, and the aircraft's drag all must be considered for an airplane in ground effect before the net accelerating force can be accurately calculated.

An interesting facet of the ground run portion of the takeoff is how propeller thrust varies with increasing ground speed when the engine is operating at constant power. Let me use the C-130B for the example, and let me use simple, ideal momentum theory to establish the trend. As you will recall from momentum theory, propeller horsepower required ($PHP_{req'd}$) to produce a given thrust (T) in pounds at a given flightpath velocity (V_{FP}) in feet per second is simply

$$(3.146)\quad PHP_{req'd.} = \frac{T\left(V_{FP} + v_i\right)}{550},$$

where the induced velocity (v_i) is calculated from

$$(3.147)\quad v_i = \sqrt{\left(\frac{V_{FP}}{2}\right)^2 + \frac{T}{2\rho A_P}} - \frac{V_{FP}}{2} \qquad \text{(see paragraph 3.3.2, page 344)}.$$

Suppose you assume that the available power (SHP_{avail}) to one C-130B, 15-foot-diameter propeller from its T56 turboshaft engine is 3,755 horsepower. Assume that this power available is constant throughout the takeoff. Now, to solve the problem, you are looking for the thrust that makes propeller power required equal engine power available at each velocity under study.[135] My solution shows that thrust will decrease as the ground speed increases, which you can see from Fig. 3-151.

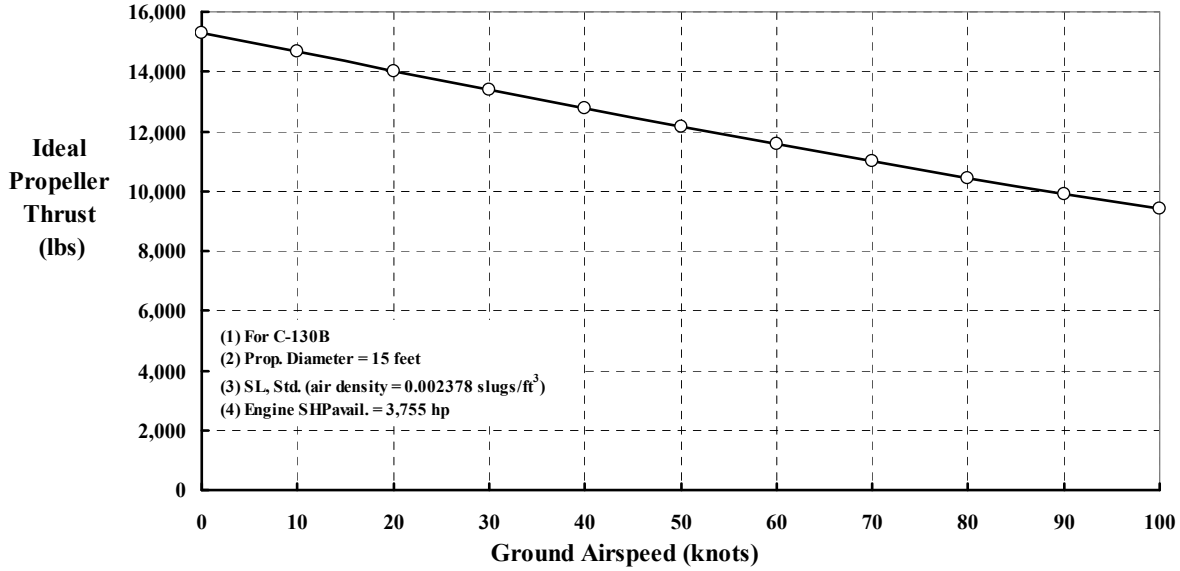

Fig. 3-151. Propeller thrust decreases with ground speed and is a significant factor in takeoff distance calculations.

[135] I set the problem up in Microsoft® Excel® and then used the Goal Seek tool to find the thrust that matched power required with power available.

Roughly speaking, the average thrust from four C-130B propellers during the ground run would be 48,000 pounds. But Fig. 3-150 shows that the net accelerating force is about 33,000 pounds, which means that 15,000 (i.e., 48,000 minus 33,000) pounds of accelerating force is lost due to the rolling friction and the aircraft's drag plus several other items I have neglected. Being a rotorcraft advocate, I would say that this is an enormous loss in available thrust just to get off the ground. In fact, I can easily imagine increasing each of the four propellers' diameters to 32 feet and redesigning the wing to tilt. Then this modified C-130B could land *and* take off vertically after traveling outbound 500 nautical miles and arriving at a gross weight of 101,000 pounds where 20,000 pounds of cargo would be off-loaded. At the very least, one could think of somewhat smaller diameter propellers mounted on a wing that partially tilts. This would at least vector some of the thrust in the lift direction and would ensure that a modified C-130B could operate off a 500-foot runway.

Now let me discuss the air distance that the Rough Road aircraft traveled before clearing a 50-foot obstacle. In order for the aircraft to climb after liftoff, additional lift beyond gross weight must be obtained. To get this additional lift the pilot raises the aircraft's nose, which increases the aircraft's angle of attack. This action occurs in the transition phase of the takeoff. The additional lift over and above weight gives the aircraft a vertical acceleration (a_{vert}), which, by following F = ma, amounts to

$$(3.148)\quad a_{vert} = \frac{\text{Lift} - W}{W} 32.17 .$$

This vertical acceleration occurs during the time the aircraft is traveling forward. The 50-foot obstacle will be crossed in an amount of air time (t_{air}) equal to

$$(3.149)\quad t_{air} = \sqrt{\frac{2(50\,\text{ft})}{a_{vert}}} .$$

But, to a first approximation, the horizontal distance traveled will be the liftoff velocity times the air time, which, from Eqs. (3.149) and (3.148), says that

$$(3.150)\quad D_{air} = V_{liftoff} t_{air} = V_{liftoff} \sqrt{\frac{2(50\,\text{ft})}{a_{vert}}} = V_{liftoff} \sqrt{\frac{2(50)W}{(\text{Lift} - W)(32.17)}} = 1.763 \frac{V_{liftoff}}{\sqrt{L/W - 1}} .$$

Using the definition of lift coefficient (i.e., $C_L = L/qS$), I am inclined to write

$$(3.151)\quad D_{air} = 1.763 \frac{V_{liftoff}}{\sqrt{\text{Climb}\, C_L / \text{Liftoff}\, C_L - 1}} .$$

Given these simple concepts, you can see just how the pilots of the Rough Road aircraft varied the air distance portion of the takeoff. My view, shown in Fig. 3-152, is that the pilots were careful in asking the aircraft for more lift in order to clear the 50-foot obstacle so that a large margin remained before the onset of stall. Recall that the maximum safe operating lift coefficient during takeoff was established as 3.2. Looking back at Fig. 3-148, you will see that lift coefficients at liftoff were on the order of 2.5. A 10-percent increase in lift coefficient would mean a coefficient of 2.75, which, I would say, was still well away from the onset of stall. Of course, the whole experiment was conducted virtually at sea level.

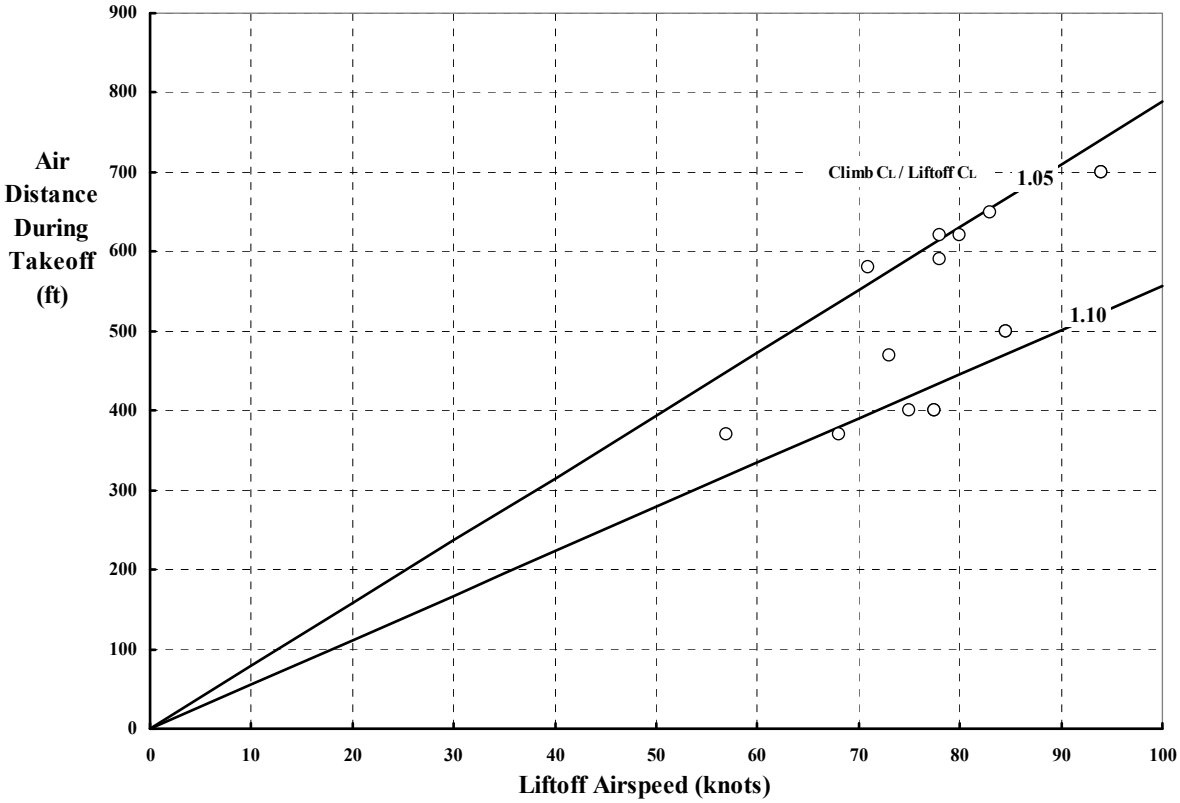

Fig. 3-152. Even a relatively small increase in aircraft lift coefficient at liftoff will reduce the air distance needed to clear a 50-foot obstacle.

3.8.2 The Landing Problem

Now consider the landing problem. This subject was addressed by Hermann Glauert [575] in 1920. Glauert was one of aviation's most famous aerodynamicists as you will recall from Volume I. Jumping ahead nearly 100 years, you have an artist's illustration of a landing, Fig. 3-153, taken from the Flight Manual for the Army's L-19 Bird Dog [576]. Here you see the several phases of the landing maneuver. Let me start by examining the last part of the air distance portion of landing, which is the distance traveled from, say, a 50-foot obstacle until touchdown. In Fig. 3-154 you see the demonstrated capability of several aircraft participating in Project Rough Road. The air distance from the 50-foot obstacle to touchdown is determined by the airspeed of the aircraft at the 50-foot obstacle times the time spent in descending 50 feet. Assuming an average rate of descent (R/D_{avg}), the descent air time will be

$$t_{air} = \frac{50\,\text{ft}}{R/D_{avg.}}. \tag{3.152}$$

And, therefore, the air distance will be

$$D_{air} = V_{50\,\text{ft}}\, t_{air} = V_{50\,\text{ft}} \frac{50\,\text{ft}}{R/D_{avg.}}. \tag{3.153}$$

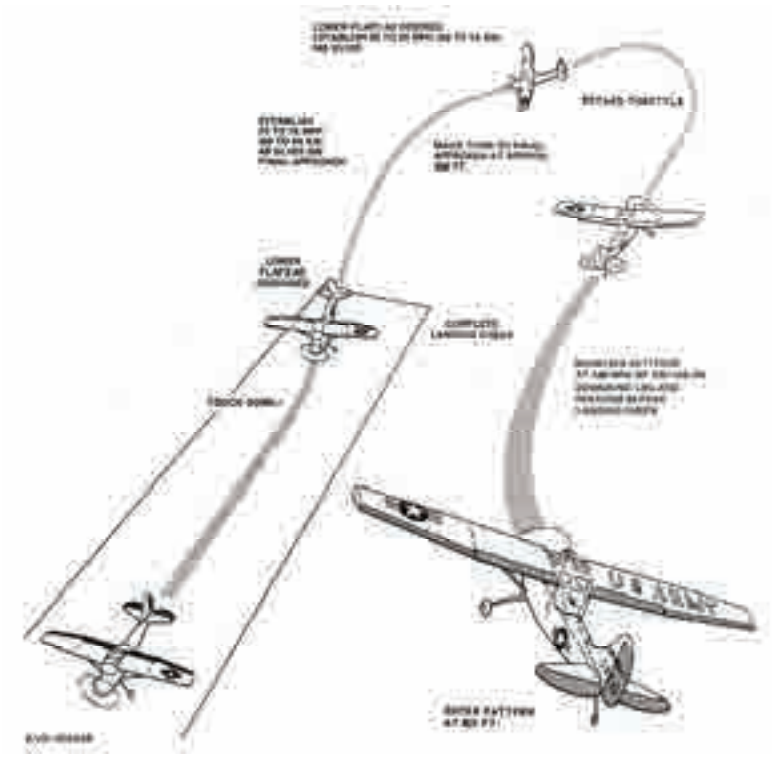

Fig. 3-153. Artist's illustration of a landing taken from the Flight Manual for the Army's L-19 Bird Dog [576].

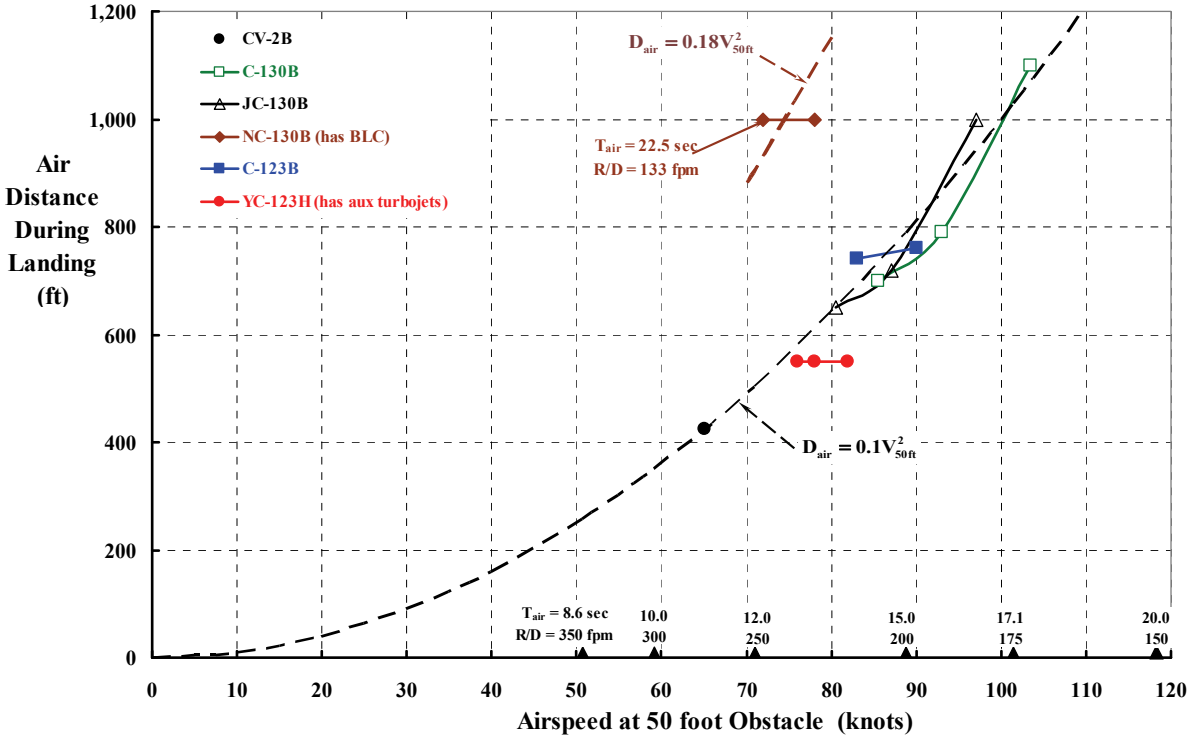

Fig. 3-154. Demonstrated capabilities of the Project Rough Road aircraft.

Because both air distance from the 50-foot obstacle and airspeed at the obstacle are known from the test data, it follows that the average rate of descent can be approximated as

$$(3.154)\quad R/D_{avg.} = V_{50\,ft}\frac{50\,ft}{D_{air}}.$$

You will note on Fig. 3-154 that the BLC test bed of the C-130B, the NC-130B, shows no evidence that the pilots were taking advantage of the aircraft's capability. While the aircraft certainly could approach slower and descend faster, the pilots flew the aircraft very conservatively, in my view.

Now consider the ground run portion of the landing. As previously stated, the ground run distance is calculated from basic physics as

$$(3.155)\quad D_{Ground\ Run} = \frac{W_{at\ Touchdown}\left(V_{at\ Touchdown}\right)^2}{2(32.17)F_{Decel}}.$$

The capabilities of the aircraft tested are summarized in Fig. 3-155. I found these results quite interesting. First of all, the ability to reverse propeller thrust is clearly a mandatory requirement for an aircraft with "short field" capability. The CV-2B Caribou data makes this point very clear. Secondly, the C-130B data establishes just how much more decelerating force the aircraft would need to have if the touchdown speed was not reduced by some means. The Joint Air Force and Army requirement (COR 130) you read about earlier specified a 500-foot runway. The other mission requirement (20,000 pounds delivered 500 nautical miles) appears to lead to a C-130B landing at the battlefront at a gross weight of 101,000 pounds. On this basis, the decelerating force would need to be at least doubled to bring such a large aircraft to a stop in 500 feet. To mitigate this design problem, Lockheed turned to boundary layer control and its NC-130B test bed. At a gross weight of 101,000 pounds, the NC-130B needed only to demonstrate a touchdown speed of about 60 knots—about the touchdown speed of the CV-2B Caribou—so that the "standard" C-130B reverse thrust and braking capability would be retained. Unfortunately, the pilots did not know enough about the stability and control of the NC-130B at very low speeds to even attempt such a slow touchdown. And this, I think, gave boundary layer control a very bad reputation, which killed upper management's enthusiasm.

When you look at the two CV-2B Caribou data points on Fig. 3-155, I expect you are as impressed as I am to see how valuable thrust reversal has been in obtaining short field landing capability. The Caribou, with only ground rolling friction and brakes plus some (or perhaps no) assistance from the propellers, had a ground run distance of 825 feet on a paved surface. With a touchdown speed of 62 knots, this equates to a ratio of average decelerating force (F_{decel}) to landing weight (W) of 0.075. As a rotorcraft advocate dealing mostly with zero ground run distance aircraft, I began to think more about the details of the ground run distance calculation that fixed-wing advocates must deal with.

On the surface, the calculation of ground run distance does not seem to be very difficult. After all, F = ma can be applied by stating in the X direction (i.e., horizontal) that

$$(3.156)\quad \sum F_X = ma = \frac{W}{g}a = \frac{W}{g}\frac{dV}{dt} = \frac{W}{g}\frac{dV}{dD}\frac{dD}{dt} = \frac{W}{g}V\frac{dV}{dD}.$$

It follows then that the ground run distance ($D_{Grd\ Run}$) *only* requires solving an integral of the form

$$(3.157)\quad D_{Grd\,Run} = \frac{W}{g}\int_{V_{Touchdown}}^{0}\frac{V}{\sum F_x}dV.$$

You can find the components making up the horizontal force summation (ΣF_x) in any number of textbooks and reports. For me, the U.S. Air Force textbook [577] studied by students at the Test Pilot School at Edwards Air Force Base in California is a very good introductory source. This textbook offers the summation of horizontal forces as

$$(3.158)\quad \sum F_X = F_P - D - \mu_{roll}(W - L) = F_P - \mu_{roll}W - (qS_W)(C_D - \mu_{roll}C_L)$$

where the thrust of one propeller (T_P) in pounds is multiplied by the number of propellers (N) so that F_P equals N times T_P. Keep in mind that the thrust is generally negative for the ground run calculation. The aircraft's drag (D), lift (L), and weight (W) are in pounds. The aircraft's conventional lift and drag forces can be expressed in coefficient form, and this illuminates the dependence of the force summation on dynamic pressure ($q = \frac{1}{2}\rho V^2$). The coefficient of rolling friction (μ_{roll}) on paved surfaces with brakes off is nominally 0.03.

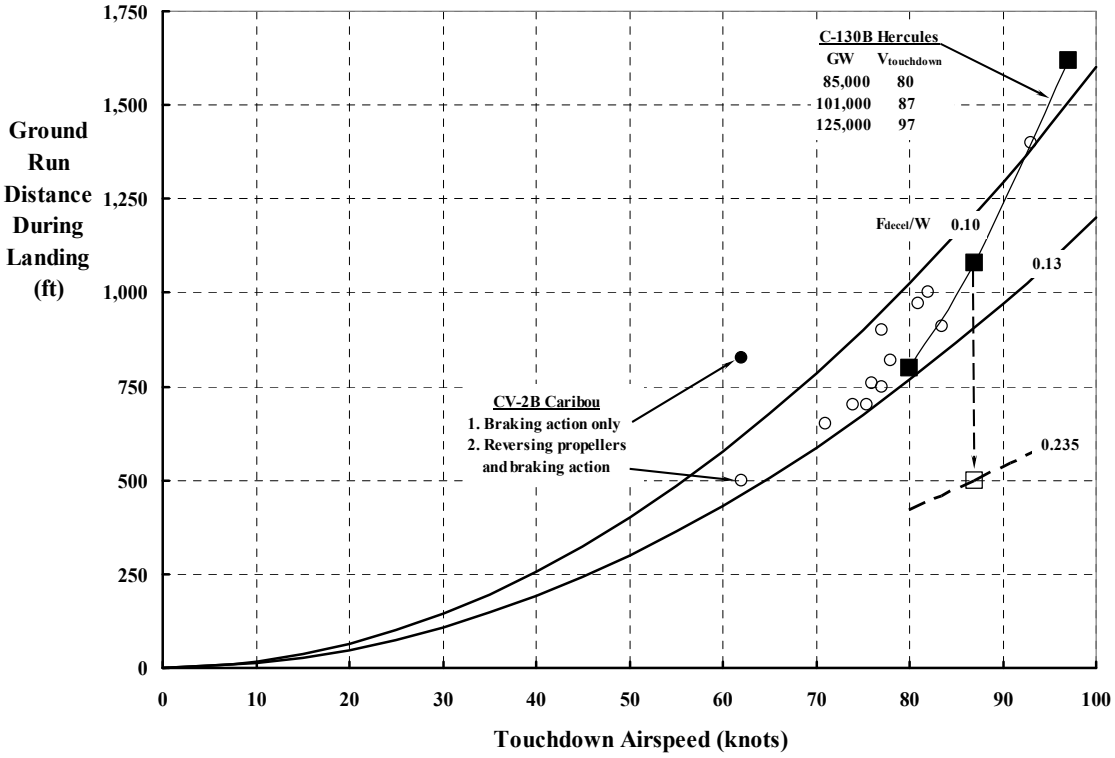

Fig. 3-155. Nominal ratios of deceleration force to landing weight.

When brakes are applied, an additional braking force (F_{Brake}) must be included in Eq. (3.158). This force deserves some discussion. You will see in the literature that it is quite common to simply increase the rolling friction constant a significant amount. You might see the "friction" coefficient raised by a factor of 10 [578]. Personally, I find this approach a little too crude because the "equivalent" rolling friction coefficient is really a constant force divided by a weight. That is, aircraft brakes are frequently designed to provide a 10-foot-per-second squared deceleration (a_{dec}) at the design landing weight to meet Federal Aviation Agency requirements [579]. This guideline translates to a braking force of

$$(3.159)\quad F_{Brake} = \frac{\text{Design W}}{g}\left(\text{design deceleration constant}\right) = \frac{W_{Des}}{g} a_{dec} = \text{constant}.$$

Finally, from an aircraft design point of view, turboshaft engines have a residual jet thrust that comes with the direct shaft horsepower provided to the propeller. Recalling footnote 128 on page 499, the Allison T56-A-7 had a jet thrust of about 740 pounds while sending 3,755 horsepower to the propeller. This jet thrust (T_{jet}) acts to accelerate the aircraft during the landing ground run, which is not helpful—to say the least.

Taken altogether, I suggest that a more complete summation of horizontal forces would be

$$(3.160)\quad \sum F_X = F_P - D - \mu_{roll}\left(W - L\right) - F_{Brake} + T_{jet} = \left(F_P - \mu_{roll} W - F_{Brake} + T_{jet}\right) - \left(qS_W\right)\left(C_D - \mu_{roll} C_L\right).$$

Of course, the ground run distance calculation would be incomplete without some consideration of the time it takes for the pilot to reconfigure the machine and the aircraft to transition from flying to beginning the landing. It takes a finite time to apply brakes even in a dead stick landing, and it takes even more time to obtain full reverse thrust. Therefore, I suggest that every ground run distance ever quoted or measured includes a distance of

$$(3.161)\quad D_{Pilot} = V_{touchdown} t_{Pilot}.$$

Based on Eqs. (3.160) and (3.161), you can now see that the total ground run distance calculation takes the form

$$(3.162)\quad \begin{aligned} \text{Total } D_{Ground\,Run} &= V_{touchdown} t_{Pilot} \\ &+ \frac{W}{g}\int_{V_{Touchdown}}^{0} \frac{V}{\left(NF_P - \mu_{roll} W - F_{Brake} + NT_{jet}\right) - \left[\left(\tfrac{1}{2}\rho S_W\right)\left(C_D - \mu_{roll} C_L\right)\right] V^2} dV, \end{aligned}$$

which results—*when the propeller force (NF_P) and jet thrust (NT_{jet}) are assumed to be zero*—in the solution

$$(3.163)\quad D_{Ground\,Run} = V_{touchdown} t_{Pilot} + \frac{W}{g}\left[\frac{1}{2\left(\tfrac{1}{2}\rho S_W\right)\left(C_D - \mu_{roll} C_L\right)}\right] \ln\left[1 - \frac{\left(\tfrac{1}{2}\rho S_W\right)\left(C_D - \mu_{roll} C_L\right)}{0 - \mu_{roll} W - F_{Brake}}\right].$$

Now suppose, using the Caribou with its 912-square-foot wing area as an example, you first consider a case where the pilot touches the aircraft down at 62 knots on a long, flat, paved runway located at sea level (density of 0.002378 slugs per cubic foot). Assume he or she leaves the flaps down so that the lift coefficient (C_L) equals 2.4, and the aircraft drag

coefficient (C_D) is, say, 0.15. Assume that both engines are off (i.e., F_P and T_{jet} equal zero) throughout the ground run. This leaves the pilot with little reconfiguring to do, so assume pilot time is zero. With a rolling coefficient of 0.03, and the pilot not using brakes and following Eq. (3.163), you will calculate that the aircraft rolls slowly to a stop in just under 3,900 feet.

But now assume that the Caribou's pilot applies brakes designed to a deceleration constant of 10 feet per second squared at a design gross weight of 28,500 pounds. You can immediately calculate a braking force of 3,540 pounds following Eq. (3.159). Then the aircraft comes to a stop in about 1,000 feet. The pilot actually demonstrated a slightly lower ground run distance of 825 feet as Fig. 3-155 shows. This suggests that the Caribou's designers provided a deceleration constant more on the order of 13 feet per second squared. Naturally, pilots are very careful using brakes because tires can heat up and blow out, brakes can fade or fail, the whole landing gear assembly can collapse, or—pick several other reasons. On smaller tail-wheel type aircraft, pilots use brakes very cautiously because the aircraft can tip nose over if the main wheels stop turning (i.e., lock up) or—perhaps more embarrassingly—cause a ground loop. On tricycle landing gear aircraft, severe braking puts a large drag load on the nose gear assembly, which can fail. Finally, it would seem to me that anti-lock brakes should be a requirement for STOL aircraft.

The question now arises as to what reverse thrust can do to further reduce the ground run distance. First of all, you have a typical example of experimental data for a *propeller* thrust coefficient variation with *propeller* advance ratio (J) shown in Fig. 3-156. This data

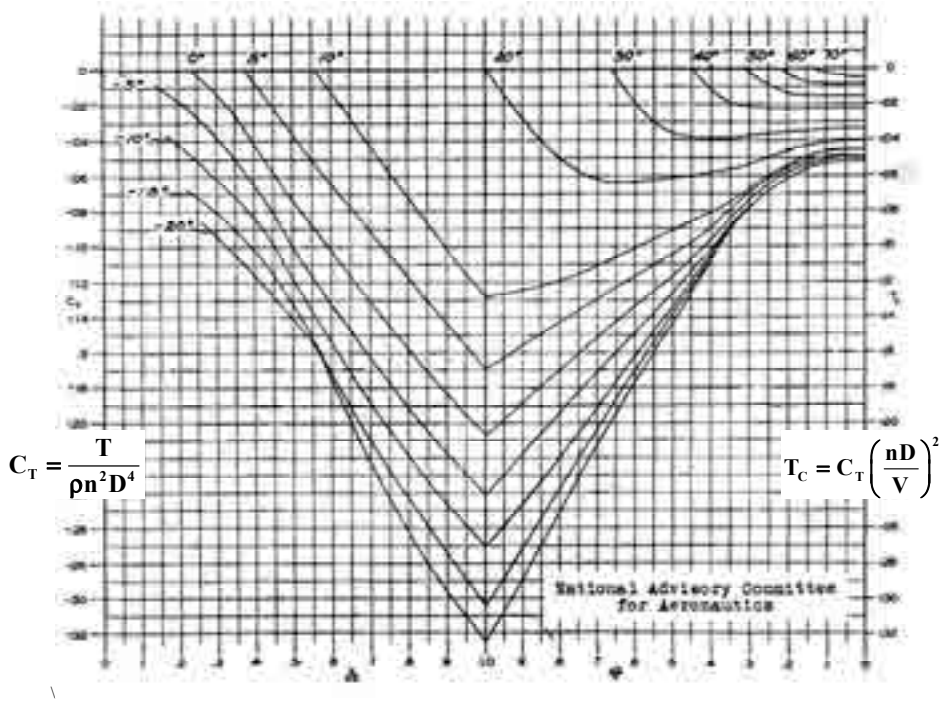

Fig. 3-156. Typical trend of propeller negative thrust coefficient with propeller advance ratio (J = V/nD) for a four-bladed configuration in 1944 [580].

was taken from reference [580], which is a very interesting experiment conducted during the period when variable pitch propellers were being widely used, particularly on dive-bombers during World War II. From Fig. 3-156 you can see that the braking force of this propeller varies with the pitch angle at the three-quarter radius station ($\beta_{0.75}$). This experimental data suggests that reverse propeller thrust (F_P) behaves approximately as

$$(3.164)\quad F_P = -\left(\rho A_P V_t^2\right)\left(\frac{\sigma_P a_{airfoil}}{2}\right)\left[C_0 + C_1\frac{V_{GR}}{V_t} + C_2\left(\frac{V_{GR}^2}{V_t}\right) + \text{etc} + C_3\beta_{0.75R} + \text{etc}\right]$$

for this introductory discussion. Furthermore, it is clear that the coefficients (i.e., C_0, C_1, etc.) may depend on the blade pitch angle at the three-quarter radius ($\beta_{0.75R}$). Note that the propeller braking force depends on the propeller disc area (A_P) in square feet and the propeller solidity (σ_P). The blade airfoil section has the lift curve slope ($a_{airfoil}$) of 5.73 per radian. The propeller tip speed (V_t) in feet per second is calculated from the propeller shaft speed (RPM) and radius (R) as $V_t = (\pi R)RPM/30$. The ground run velocity (V_{GR}) is in feet per second. The difficult task is to obtain values of the constants. These constants are best obtained from test data. Appendix H discusses some theoretical aspects involved in calculating the constants, including complications that may arise because of blade element stall and the vortex ring state.

For rotorcraft advocates who might not be familiar with propeller coefficients (or propeller experts unfamiliar with rotor notation), the relationships are

$$(3.165)\quad \text{Advance Ratio}\qquad \frac{V}{V_t} = \frac{1}{\pi}J = \frac{1}{\pi}\left(\frac{V}{nD}\right)$$

$$\text{Thrust Coefficient}\qquad \text{Rotor}\,C_T = \frac{T}{\rho A V_t^2} = \frac{4}{\pi^3}\left(\text{Propeller}\,C_T\right) = \frac{4}{\pi^3}\left(\frac{T}{\rho n^2 D^4}\right)$$

where propeller shaft rotational speed (n) is in revolutions per second and propeller diameter (D) is in feet. Also, propeller experts use blade Activity Factor (AF) *per blade* as their measure of what rotorcraft engineers call power-weighted solidity. The conversion is

$$(3.166)\quad \text{Rotor power-weighted solidity}\ \sigma_P = \left(\frac{128}{100{,}000\pi}\right)(bAF)$$

where, again, the number of blades is denoted by (b) in the rotorcraft world. A blade in the four-bladed set used to obtain the data shown in Fig. 3-156 had an Activity Factor per blade of about 160, which becomes a power-weighted solidity of 0.263.

I might add that the example data provided in Fig. 3-156 behaves approximately as

$$(3.167)\quad T_P = \left(\rho A_P V_t^2\right)\left(\frac{\sigma_p a_{airfoil}}{2}\right)\left(-0.0321\frac{V}{V_t} - 0.0734\left(\frac{V}{V_t}\right)^2 + 1.3062\left(\frac{V}{V_t}\right)^3 + 0.05658\left(\beta_{0.75R}\right)\right)$$

after I made several rather arbitrary changes to the nominal, test recorded blade angle as discussed more fully in Appendix H. I am quite certain that this *is not* a universal equation for all propellers; it only serves as an illustration of the requirement to establish *how propeller negative thrust behaves as a function of ground speed*.

As you might now be suspecting, the variation of propeller braking force with ground speed is rather ill defined. In fact, Hank Borst[136] in his 1973 review of propellers [581] summarized the situation by dismissing theory and showed ways to extrapolate available test data to make performance estimates.

If you want to examine more experimental results from reverse thrust testing, I suggest starting with references [582-590]. From a theory point of view, I suggest references [581, 591-598]. You will find the clearest explanation of a proprotor's flow states (and the vortex ring region, in particular) in Chapter 4 of Wayne Johnson's book, *Rotorcraft Aeromechanics* [598], and his excellent summary report of available data [599]. You will gain even more insight about the complexity of the vortex ring state from references [600, 601].

Appendix H presents my effort at developing a landing ground run distance theory, which I then used for a theory-versus-test study that you will read about next. You will also see that I made good use of a NACA report [580] published in August of 1944.

Now consider the results of ground run distance calculations, using the theory developed in Appendix H, for 12 aircraft of interest. (Details about each aircraft are provided in Table 3-15.) You have already studied the Fairchild C-123 (Fig. 3-142 and references [564-567]) and the C-130 (Fig. 3-126 and references [516-520, 571, 572]) and its BLC version, the NC-130B (Fig. 3-138). The other aircraft I have selected, along with a photo and a few interesting facts about each machine, are shown in Fig. 3-157 through Fig. 3-165.

Fig. 3-157. The Glenn Curtiss Tanager was the outright winner of the Guggenheim Safe Aircraft Competition. It featured manually controlled flaps, floating ailerons, long-stroke rugged landing gear, and independently operated brakes. The propeller was fixed pitch [602, 603].

[136] Hank was a key player in developing the Curtiss X-19. I came to know him for a short period when he left Curtiss and worked at Boeing Vertol. He was a real propeller expert. Furthermore, after Dr. Horner, author of *Fluid Dynamic Drag*, died, Hank completed the volume titled *Fluid-Dynamic Lift*. These two books are worth their weight in gold in my opinion.

Fig. 3-158. The de Havilland DHC-1 Chipmunk was a small trainer that put the company back in the commercial business at the close of World War II. It was a monoplane rebirth of England's D.H. 82 Tiger Moth biplane. The brakes were hydraulic and the flaps were fabric-covered metal structures. Full-down flap setting was 30 degrees. De Havilland manufactured the wooden 78.8-inch-diameter propeller, which had an 18-degree pitch at the three-quarter radius [495, 500, 501, 604].

Fig. 3-159. The Cessna 305, the U.S. military L-19 (Bird Dog), replaced the Piper Cub L-4. With DOD Directive 4505 dated July 6, 1962, aircraft designations were changed, and the L-19 became the O-1 ("O" for observation). The brakes were mechanical. Full-down flap setting was 60 degrees. The McCauley 1A200/FM 9047, 7.5-foot-diameter propeller was fixed pitch. The blade angle at the 30-inch radius (r/R = 2/3) was 14 degrees. Minimum ground run distance was obtained with power-off landing. At a gross weight of 2,200 pounds and touchdown airspeed of 43 knots, distance was about 320 feet [576, 605-607].

Fig. 3-160. The de Havilland DHC-2 Beaver established itself as a very rugged STOL for the backwoods. The aircraft was all metal. At its typical gross weight of 5,100 pounds, it could operate in and out of a 1,000-foot field surrounded by 50-foot obstacles. It was powered by a P&W 450 bhp R985 Wasp Jr. engine, and its first flight was August 16, 1947 [495, 503, 604].

Fig. 3-161. The de Havilland DHC-2 Mk III Turbo Beaver was powered by a P&W PT6A-20, a turboprop engine rated at 550 ESHP. The takeoff gross weight was 5,370 pounds and the STOL performance was on par with the piston-engine-powered Beaver, while providing about a 200 pound increase in useful load. The aircraft could be flown with floats and skis as well as in land plane configuration [495, 604].

Fig. 3-162. The de Havilland DHC-3 Otter was bought by all the U.S. services. This 8,000-pound aircraft was powered by a 600 bph P&W piston R-1340-S1H2-G engine. It could cruise economically at 120 knots at 5,000 feet. It's first flight was on December 12, 1951, and the aircraft continued de Havilland of Canada's reputation for rugged STOL performance [495, 504, 604].

Fig. 3-163. The de Havilland DHC-6 Twin Otter first flew on May 20, 1965. This all-metal, 12,500-pound-gross-weight aircraft was powered by two P&W PT6A-27 turboprops, each having a 620 ESHP rating for takeoff. The Twin Otter continued de Havilland's design philosophy of 1,000-foot STOL performance. The rights to build the aircraft are now in the hands of Viking Air of Victoria, British Columbia [495, 507, 604].

Fig. 3-164. The de Havilland DHC-4 Caribou made its first flight on July 30, 1958. This STOL aircraft became a favorite of the U.S. Army. However, in the mid 1960s, the U.S. Air Force took control of nearly all of the Army's fixed-wing machines. At a gross weight of 31,300 pounds and powered by P&W R2000 piston engines (1,450 bhp each), the Caribou could still operate out of 1,300-foot unprepared fields [495-498, 505, 604].

Fig. 3-165. The de Havilland of Canada CC-115 or the U.S. Army CV-7A Buffalo [477, 478, 495, 499, 506, 604]. The maximum STOL takeoff gross weight was 49,200 pounds, which put it in competition with the Air Force Fairchild C-123B. The Buffalo was powered by two turboshaft CT64-820-4 General Electric engines, each with a takeoff rating of 3,133 ESHP. The three-bladed, 14.5-foot-diameter propellers were Hamilton Standard (model 63E60-13) and normally operated at 1,160 rpm. Of course, the U.S. Army Buffalo became U.S. Air Force property in the roles and mission settlements and was redesignated as the C-8.

Table 3-15. Aircraft Input Data for Ground Run Distance Calculation[1,2,3]

Item	Symbol	Unit	Tanager	Chipmunk	Cessna L-19	Beaver	Turbo Beaver	Otter
Normal weight	GW	lb	2,840	1,860	2,400	4,500	5,100	8,000
Engine manufacturer			Curtiss	de Havilland	Continental	P&W	P&W	P&W
Engine model			Challenger	Major 1C	0-470-11-C1	R985 Wasp	PT6A-20	R1340
Takeoff power	ESHP	hp	170	140	213	450	550	600
Wing area	S_W	ft^2	333.0	172.5	174.0	250	250	375
Number of propellers	N	na	1	1	1	1	1	1
Propeller pitch type			Fixed	Fixed	Fixed	Variable	Variable	Variable
Propeller diameter	D	ft	8.35	6.567	7.5	8.5	8.5	10.833
Prop. Activity Factor	AF	na	60	100	120	120	100	93
At touchdown								
Weight	W_{TD}	lb	2,840	1,860	2,200	4,500	5,100	8,000
Propeller reverse thrust	T_{TD}	lb	0	0	0	– 525	–1,090	–890
RPM	RPM_{TD}	rpm	0	0	0	2,000	2,000	1,800
Velocity	V_{TD}	kts	26.6	50	43	52	52	50
Drag coefficient	C_D	na	0.25	0.15	0.35	0.315	0.315	0.315
Lift coefficient	C_L	na	3.57	1.30	2.0	1.96	2.22	2.48
Blade pitch [4]	$\beta_{0.75}$	deg	15	13	12.4	–10	–10	–5
Rolling friction coeff	μ	na	0.03	0.05	0.03	0.03	0.03	0.03
Braking force	F_{Brake}	lb	880	0/290	340	1,400	1,580	2,490
Pilot time [5]	T_{pilot}	sec	0	0	0	2	2	2
Ground roll distance [6]	D_{GR}	ft		[7]				
Test or manual			90	1,398/465	320	500	360	440
Prediction			165	1,388/459	373	425	393	410

Table 3-15. Concluded[1,2,3]

Parameter	Symbol	Unit	Twin Otter	Caribou	Buffalo	C-123B	C-130B	NC-130B
Normal weight	GW	lb	12,500	28,500	49,200	47,000	125,000	125,000
Engine manufacturer			P&W	P&W	GE	P&W	Allison	Allison
Engine model			PT6A-27	R2000-7M3	CT64-820-4	R2800-99W	T56-A-7	T56-A-7
Takeoff power	ESHP	hp	1,240	2,900	6,266	5,000	16,200	16,200
Wing area	S_W	ft^2	420	912	945	1223.2	1745.5	1745.5
Number of propellers	N	na	2	2	2	2	4	4
Propeller pitch type			Variable	Variable	Variable	Variable	Variable	Variable
Propeller diameter	D	ft	8.5	13.083	14.5	15.5	15.0	15.0
Propeller Activity Factor	AF	na	90	99	120	112	177	177
At touchdown								
Weight	W_{TD}	lb	12,500	28,500	49,200	47,000	101,000	101,000
Propeller reverse thrust	T_{TD}	lb	– 1,245	– 15,750	– 9,740	– 5,905	– 18,690	– 14,980
RPM	RPM_{TD}	rpm	1,800	2,500	1,160	1,000	1,022	1,022
Velocity	V_{TD}	kts	74	62	105	76	87	71
Drag coefficient	C_D	na	0.2	0.2	0.3	0.315	0.315	0.40
Lift coefficient	C_L	na	1.47	1.69	1.4	1.96	2.25	3.12
Blade pitch [4]	$\beta_{0.75}$	deg	– 5	– 15	– 15	– 10	– 6	– 6
Rolling friction coeff	μ	na	0.03	0.03	0.03	0.03	0.03	0.03
Braking force	F_{Brake}	lb	3,886	7,973	22,941	14,610	31,085	31,085
Pilot time [5]	T_{pilot}	sec	2	3	2	2	3	3
Ground roll distance [6]	D_{GR}	ft						
Test or manual			950	500	850	760	1080	650
Prediction			806	515	1,040	781	1,149	741

Notes: (1) Airfoil lift curve slope is 5.73 per radian. (2) Air density is 0.002378 slugs per cubic foot. (3) Propeller thrust per Eq. 3-167. (4) Blade pitch at 3/4 radius during ground run. (5) Pilot time used to apply brakes and reverse pitch. (6) See Appendix H. (7) Chipmunk test data for brakes off and on.

You will note on Table 3-15 that the smaller machines used fixed-pitch wooden or metal propellers. It was interesting to me that T.P. Wright wrote in his paper about the Curtiss Tanager [602] that

> "Considerations of economy of weight and increased climbing efficiency, combined with the absence of need for higher speed, prompted the selection of a wooden propeller. Had the contest occurred three or four months later, without question a metal controllable-pitch propeller would have been used, as subsequent flight-tests have shown that substantial improvement in certain performance characteristics, notably climb and take-off, are obtainable by this means."

As to landing, Mr. Wright stated that "to land the Tanager, it is necessary merely to hold the stick all the way back and wait for the earth to come up, which it will appear to do rapidly but with no more shock on landing than with a conventional airplane." You might recall from Volume I that autogyro pilots made similar observations about their rotary wing machines.

You will also note from Table 3-15 that power-off landings were quite normal for the small machines if the runways were very short. For example, the L-19A's flight test report [605] states:

> "[Power off] landing tests were conducted at altitudes of 4000 and 7000 feet. The technique used was to approach with 60 degree flaps while carrying partial power (2,000 rpm) at an airspeed (44 knots IAS) just above stall buffet. Roundout was accomplished by the combined use of longitudinal control and engine power. Touchdown was made in a three-point attitude or tail wheel first. Touchdown was complicated by the spring landing gear that tends to produce a bounce during even a gentle approach. *Both brakes were applied as hard as possible without skidding the tires as soon as the airplane touched down* [my italics]. Directional control was accomplished by both differential braking and by rudder-tail wheel steering.
>
> The test results are presented in figs. 26 and 27, appendix I. These results show that the distance required for landing over a 50-foot obstacle is longer than shown in the Flight Handbook."

A later model of the L-19, the TL-19D—redesignated as the O-1D [606]—used McCauley's[137] 2A36CI-U/90-0 constant speed propeller. This was an early type of variable pitch propeller produced by several manufacturers, including Hamilton Standard, the industry leader.[138] The constant speed propeller was a very big step up from fixed-pitch propellers [608-610]. As a rotorcraft engineer, I would point to pilot-controlled blade angle as the key feature. In Fig. 3-166 it is quite easy to see the similarity of the constant speed propeller and a helicopter rotor because both devices allow the pilot to change collective pitch. Beyond that, the constant speed propeller, unlike the rotor, does not have any cyclic pitch capability. The feature of constant speed is that when the pilot makes a collective change—say an increase in pitch by 5 degrees—the increased demand for thrust is an increased load on the engine, which would normally drag engine speed down. The propeller engineers added a hydraulic coupling to the engine throttle so a small addition of power was automatically made. I liken the constant speed feature to a car's automatic cruise control. When the car encounters a hill, the

[137] McCauley is now a member of Textron, as is Bell Helicopter.

[138] Hamilton Standard is now called United Technology Aerospace, a member of United Technology Inc.

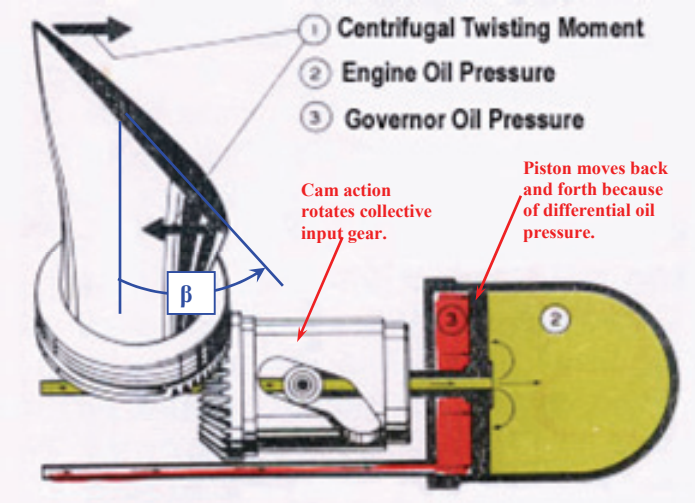

Fig. 3-166. Propeller blades get their pitch control with a right-angle gear set. The blade pitch angle ($\beta_{0.75R}$) range is from about a +100 degrees, so full feathering is available should the engine quit. For a braking force on landing, the blade pitch angle can be set to as much as a –20 degrees.

accelerator pedal is stepped on by some unseen foot, and the car stays at 65 miles per hour both on the flat road and over the hills and valleys. The major benefit of the constant pitch propeller is that the pilot can have an optimum pitch for takeoff and can change thrust by adjusting engine RPM. Then in cruise, the pilot can change the blade pitch to an optimum angle, which makes the propeller the equivalent of a fixed-pitch thrusting device. Then he or she can adjust the engine speed for maximum nautical miles per pound of fuel burned.

You should keep in mind that a helicopter's rotor control includes both collective and cyclic inputs, which have been mechanically perfected with a swashplate and pitch links. Because propellers used on conventional airplanes only need collective pitch, a much simpler mechanical design can be used as you see from Fig. 3-166.

Now on to the results of my Appendix H calculations[139] of ground run distance—they are shown in Fig. 3-167.

There is no question that a detailed calculation of ground run distance—even during conceptual and preliminary design phases—requires a great deal of information. It also requires intimate knowledge of what the certificating agency demands as you will see from reading through reference [579] for example. However, I was rather pleased to see from my Appendix H calculations that the distance was dominated by three key aircraft design parameters. Furthermore, I am satisfied that the fourth parameter, the pilot's reaction time,

[139] In carrying out the calculations, I needed the Activity Factor for several Hamilton Standard propellers. After a thorough search I came up empty-handed. My contacts, like George Rosen [611], at Hamilton Standard have passed away, so I called Alan Egolf at Sikorsky for some help. Alan and Mike Torak referred me to Henry Healy at what is now United Technology Aerospace. And now I owe Alan and Mike thanks; and I owe Henry, along with Ira Keiter, big-time for the data they dug up and sent me.

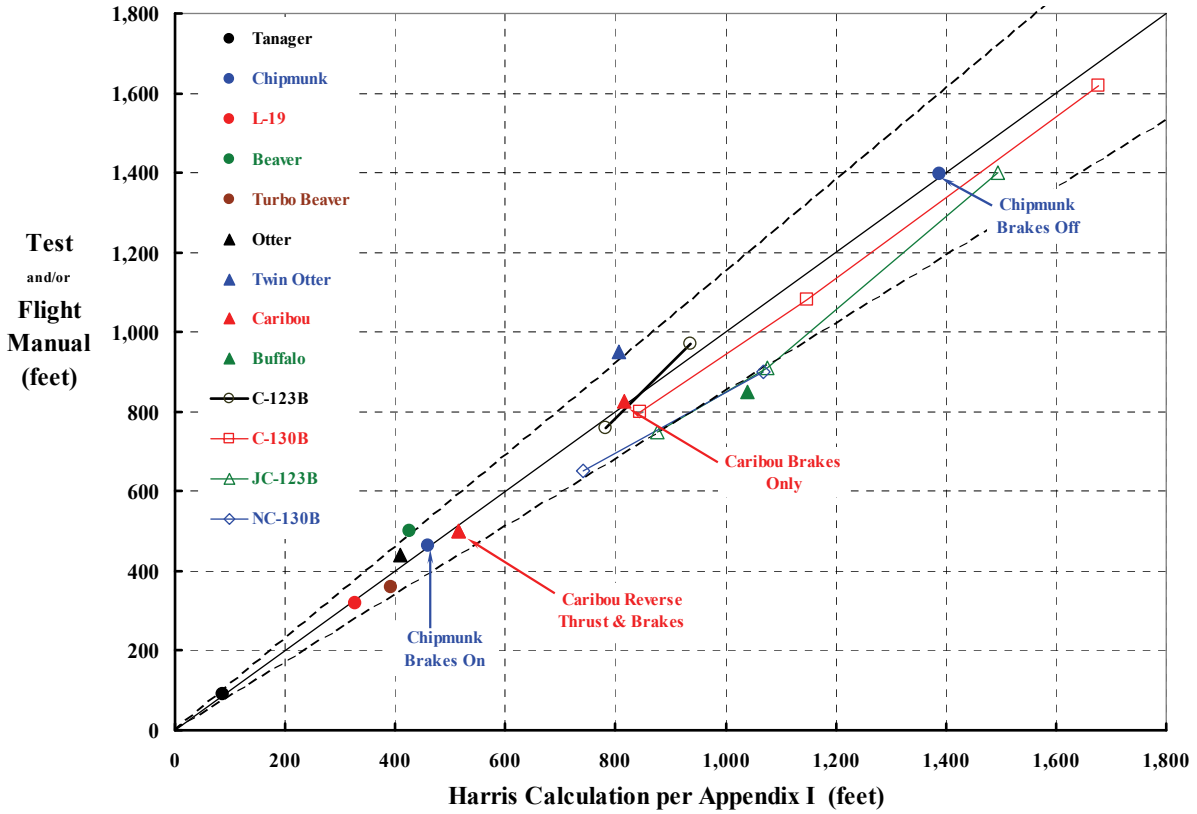

Fig. 3-167. An airplane's ground run distance can be estimated to within ±15% with a *relatively simple* theory and a few key pieces of information such as (1) propeller negative thrust variation with ground speed, (2) design landing gear brake force, and of course (3) touchdown speed and (4) pilot/aircraft reaction time.

accounts for the bulk of the scatter in test results. For example the C-130B, at a landing weight of 125,000 pounds, has a nominal touchdown speed of about 160 feet per second. If the requirement is to land on a 500-foot-long piece of runway, then more than one-half of the ground is used up in 2 seconds as the pilots reconfigure their machine. In comparison, having an eight-propeller C-130 versus the current four only reduces ground run distance by 210 feet. Or suppose the design braking capability is doubled from 10 to 20 feet per second squared; I found that distance was only reduced by 150 feet. Or suppose the touchdown speed is reduced by half, then the distance is reduced by about 300 feet, not counting the pilot's reaction time. I am sure that you can now see just how difficult a problem fixed-wing designers face when "short field" performance is a firm requirement.

To close this discussion, it may come in handy for you to see how recommended landing performance is provided to C-130 pilots via the aircraft Flight Manual [521], which incidentally, is a little over 600 pages long and has many valuable illustrations. You see the two key charts as Fig. 3-168 for landing speeds and Fig. 3-169 for landing distance. Keep in mind that up to the age of computers, engineering equations and calculations had no place in a Flight Manual. Thus, it was up to the pilot and copilot to thumb through a manual and find aircraft operating features, answers to mission-related questions, and of course, actions to be taken in an emergency.

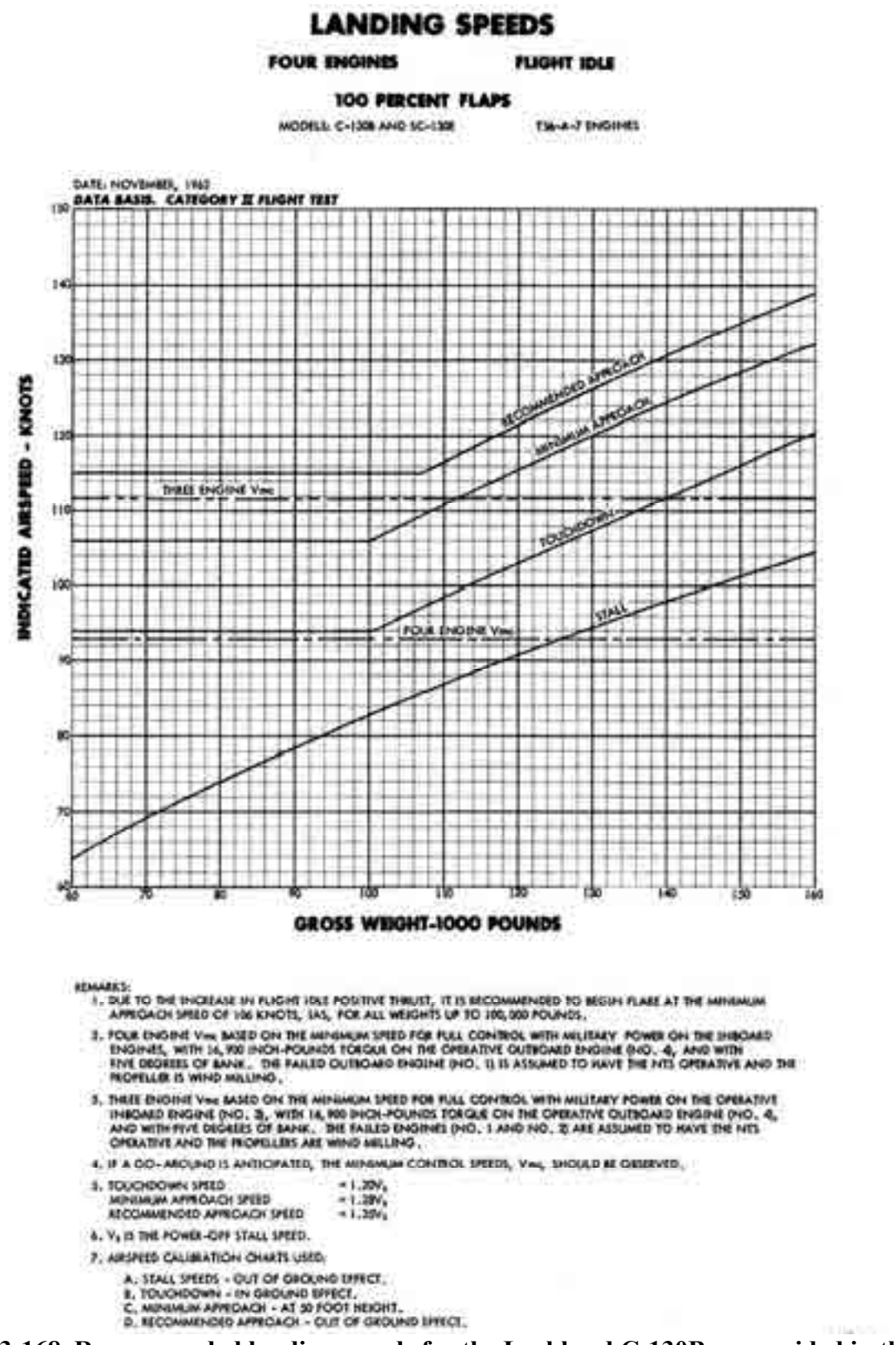

Fig. 3-168. Recommended landing speeds for the Lockheed C-130B as provided in the Flight Manual [521].

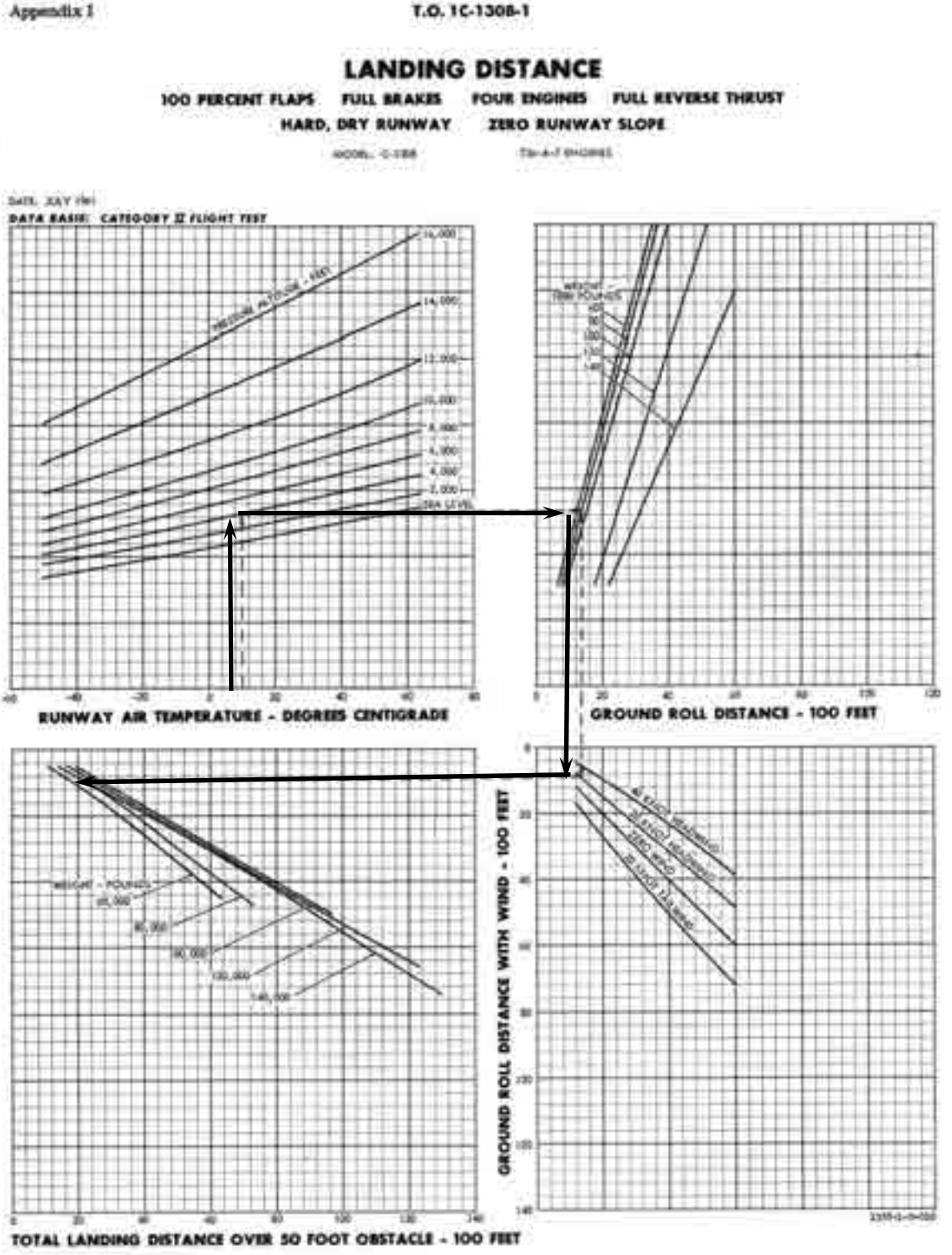

Fig. 3-169. Expected landing distances for the Lockheed C-130B as provided in the Flight Manual [521].

3.9 THE "SHORT FIELD" AIRCRAFT STATUS AS OF 1970

In January and February of 1920,[140] Hermann Glauert [613], Britain's leading aerodynamicist, published a two-part paper titled *The Landing of Aeroplanes* [575]. Then, in January 1926, Glauert's report about the necessary size of "aerodromes" was published [614]. This later report contained a very interesting figure that you see here as Fig. 3-170.

Then it seems to me that the interest—and then the military need—for fixed-wing aircraft operations from a "short field" did not change much from the late 1920s up to when Project Rough Road came to an end and the results were fully absorbed in the mid-1970s. You will recall that the Daniel Guggenheim Fund sponsored a Safe Aircraft Competition in 1927. The objective "of this competition was to achieve a real advance in the safety of flying through improvement in the aerodynamic characteristics of heavier-than-air [machines], without sacrificing the good, practical qualities of the present day aircraft." Back then, aviators were talking about obstacles 35 feet high, and they became 50 feet high by 1970. Back then, the objective was to take off over the obstacle in 500 feet after a ground run of 300 feet. Back then, the objective was to "glide over a 35-foot-high obstruction and, after touchdown, come to a rest within a distance of 300 feet from the base of the obstruction."

By 1960 the U.S. Army and Air Force were agreeing on the need for future assault transports that could land and take off from 500-foot-long "unprepared" runways. The aircraft then in the U.S. military fleet had shown, I think, that only de Havilland of Canada was capable of producing a family of true "short field" fixed-wing airplanes. It struck me that the Army even tried to get this point across to upper management with their report [497] in which they had added CV-2B Caribou data to the Air Force Rough Road report [564]. The Army author's first two conclusions were:

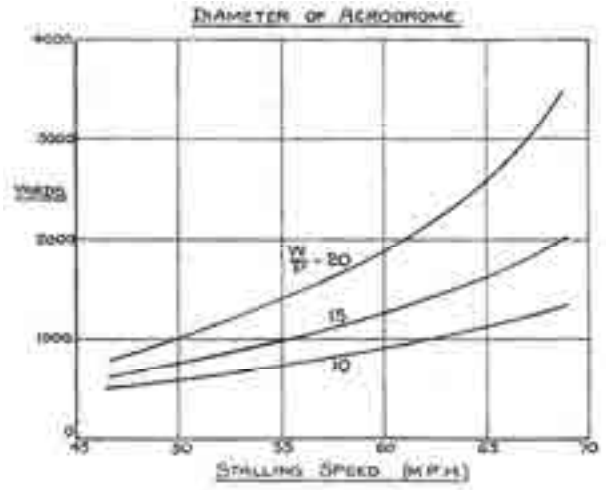

Fig. 3-170. H. Glauert's view in 1926 about the *Necessary Size of Aerodromes in Order That a Landing May be Made if the Engine Fails When Getting Off* [614].

[140] By 1910, the question of whether the dirigible or the airplane was superior was settled [612]. World War I came to an end when the Armistice was signed on November 11, 1919. And the dawn of civil aviation was marked by the Premier Congrés International de la Navigation Aérienne held in November 1921 in Paris.

> "1. The takeoff and landing performance of the CV-2B airplane operating at maximum gross weight exceeds that of the C-130B, JC-130B, NC-130B, and the C-123B.
>
> 2. The takeoff and landing performance of the CV-2B operations at maximum gross weight exceeds that of the YC-123H at all gross weights and conditions tested except for takeoff in soft sand at a gross weight of 47,000 pounds. At this gross weight, the YC-123H could carry little, if any, payload on a normal combat mission."

In short, there was nothing in the current U.S. Air Force transport fleet that could meet what the Army felt were the takeoff and landing requirements—requirements that gave the Army both troops and supplies wherever they could clear an area (i.e., an aerodrome) and "prepare" a 500-foot runway.

Then, to top it off, the Army fielded another fixed-wing aircraft to its fleet as the Rough Road results were being absorbed. This aircraft, designated as the CV-7A [499] by the U.S. Army and the CC-115 in Canada (Fig. 3-165), was a larger version of the Caribou and manufactured (you might have guessed) by de Havilland of Canada. The CV-7A was given the name Buffalo. When the Air Force/Army roles and mission debate was settled, the Buffalo became Air Force property and was redesignated as the C-8 in 1962.

Given this insight, it appears to me that the status of "short field" aircraft in the late 1960s was well defined by seven fixed-wing airplanes described in Table 3-16. Just for the fun of it, I have added the rotorcraft industry's MV-22B tiltrotor, vintage 1990s, for comparison even though it came three decades after demonstrated fixed-wing progress.

Table 3-16. Typical Aircraft "Short Field" Capability as of 1970[1,2]

Item	DHC 5D C-8	Fairchild C-123B	Bréguet 941	Bréguet 941S	Lockheed NC-130B	Lockheed GL-128-17	Lockheed C-130B	Marine MV-22B
Status	Fielded	Fielded	Demo	Proto	Demo	Design	Fielded	Fielded
Reference	[495, 499, 502, 506]	[564-569]	[508-510, 512, 513, 615]	Jane's 1971-72	[526, 527]	[527]	[516, 517, 521, 564, 571, 572]	See Table 2-24
Max TOGW	49,200	54,000	46,000	58,420	135,000	155,000	135,000	60,500
Max land GW	39,100	47,000	40,000	44,100	125,000	130,000	125,000	52,600
Takeoff ESHP	6,266	5,000	5,000	6,000	23,920	26,000	16,200	12,300
Weight empty	23,197	30,900	27,000	32,400	73,260	83,000	73,260	33,459
TOGW/ESHP	7.85	9.4	11.68	9.73	5.64	5.96	8.33	4.92
No. of troops	41	60	56	40	92	92	92	24
Takeoff distance at gross weight	41,000	47,000	40,000	48,500	125,000	110,000	125,000	52,600
Ground run	949	1,180	610	655	1,570	na	2,110	0
Over 50 feet	1,250	1,580	860	1,020	2,220	1,000	2,810	0
Landing distance at gross weight	39,100	47,000	40,000	44,100	101,000	110,000	101,000	52,600
Landing speed	67	76	48	50	71	55–60	87	0
Ground run	552	615	250	345	650	600	930	0
Over 50 feet	1,136	1,355	650	820	1650	900	1,720	0

Notes: (1) Weight is in pounds, speed is in knots at sea level on a standard day, and distance is in feet. (2) Power is equivalent horsepower at sea level on a standard day. (3) STOL assault mission from "unprepared" (clay or sand, whichever is shorter) airfield.

The very abbreviated summary table you have just reviewed is, of course, simply a selected overview of a few STOL aircraft that existed worldwide. To grasp the breadth of all of the examples, I suggest you read Bill Norton's superb book, *STOL Progenitors: The Technology Path to a Large STOL Aircraft and the C-17A* [26].

Over five decades, the fixed-wing industry had, by 1970, honed technologies such as (1) high-lift devices, (2) propellers, and (3) takeoff and landing theory and practice. Airplane engineers had established that STOL demanded, first and foremost, low-speed control and stability. Without those capabilities, no pilot could take full advantage of the performance that aerodynamicists were quite able to incorporate in any fixed-wing airplane. In my view, the Bréguet 941, with its cross shafting to interconnect propellers, was the only demonstrated way to achieve real STOL performance with stability and control. And I would add, achieving very "short field" performance with boundary layer control required additional power on the order of what VTOL requires.

Such was the propeller-driven STOL situation when the U.S. Air Force began efforts to obtain a much needed replacement for the Lockheed C-130. Air Force thinking was also heavily influenced by their aircraft experiences during war. On this subject, you will find a summary prepared by the Historical Office of the Air Force Flight Test Center [616] quite interesting. This report is titled *USAF Aircraft in Southeast Asia Tested by the Air Force Flight Test Center*. Finally, Jack Wimpress [400] expressed his view about future plans for Air Force STOL transports and included a statement by General William (Spike) Momyer that I found most interesting. Jack wrote:

> "The Vietnam conflict highlighted the fact that the Air Force had an airlift dilemma. The C-141 and C-5A had good payloads, range, and speeds but required elaborate and complex air bases to operate effectively. At the other extreme, helicopters were independent of air bases but were slow, vulnerable, and could move heavy cargo only short distances. Between these two extremes were several fixed-wing airplanes, including the C-7, C-123, and C-130. These aircraft were less dependent on paved runways when carrying light loads, but were limited in speed, range, and payload weight and volume. There was no aircraft that could interface effectively with the heavy logistics transports and carry the men and materiel (including large vehicles) to a point where they could be used directly by the operational troops or picked up and delivered efficiently by helicopters. During the 1960s, the Air Force spent considerable effort developing the Light Intratheater Transport (LIT) to meet this need. This airplane was to have vertical takeoff and landing (VTOL) capability and was meant to replace the old C-7 and the C-123. However, Gen. Spike Momyer had been made Commanding Officer of the Tactical Air Command (TAC) just after being in charge of air operations in Vietnam, and he was convinced a larger airplane was needed—a true C-130 replacement. In a memo written in December 1969, he gave the following guidance to TAC to prepare a new airlift modernization requirements document:
>
> 1) VTOL is too expensive—2000 ft field length is about right.
> 2) C-130 cargo box is too small. It must carry pallets and troops at the same time; 12 ft by 12 ft by 45 ft is OK.
> 3) No turboprops should be used."

In my view, this spelled the end of propeller-driven, large-size STOL aircraft development. Furthermore, General Momyer's position about VTOL seems to still stand, even today.

3.10 YC-14 AND YC-15

Bill Norton begins his 220-page book [26] about STOLs with 62 pages that give you a very clear picture of events leading up to what became known as the Advanced Medium STOL Transport (AMST) program. The plan was to select two companies to build STOL technology demonstrator/prototypes. This program was expected to yield a production STOL transport meeting U.S. Air Force requirements as guided by General Momyer's December 1969 memo. The requirements were spelled out in Required Operational Capability number 52-69 issued May 6, 1970. The ensuing competition between five companies ended on November 10, 1972, when McDonnell Douglas was selected to develop the YC-15 aircraft (Fig. 3-171, Fig. 3-173, and reference [617]), and Boeing was selected to develop the YC-14 (Fig. 3-172, Fig. 3-173, Fig. 3-174, and references [618, 619]). Both companies were given identical objectives:

> "• Design, fabricate, and evaluate [two] prototype aircraft which will demonstrate in hardware, new technology, which after additional engineering development, will provide a medium size (C-130 class) jet STOL transport.
>
> • Provide a low cost development option for modernization of the tactical airlift force.
>
> • Obtain visibility on costs associated with short field performance.
>
> • Define STOL operational rules, safety rules, and related design criteria."

Now let me first show you a timeline of the AMST program using, in part, key dates that Bill Norton provides in his book.

1. U.S. Air Force Requirement 52-69 issued May 6, 1970.
2. Program launched in December 1971 under Secretary of Defense Melvin Laird's direction with $6 million provided by Congress.
3. Request for Proposal on the street January 24, 1972.[141]
4. On March 31, 1972, six proposals were received by the Prototype Program Office at Aeronautical Systems Division (ASD) located at Wright-Patterson Air Force Base, Dayton, Ohio.
5. ASD evaluation completed on July 7, 1972.
6. Boeing and McDonnell Douglas announced as winners on November 10, 1972.
7. Phase I contracts let on December 10, 1972, lead to both contractors unit cost estimates in excess of goal. Air Force reduced design requirements.
8. Phase II contracts authorized on January 9, 1973.
9. On May 2, 1973, Air Force designates the two competing aircraft as YC-14 and YC-15, which indicated a preproduction status as opposed to an experimental designation of XC-. This added requirements to make demonstration of cargo handling systems a part of the ultimate down-select. Original program concept of technology demonstrator with an empty shell had been brushed aside.

[141] Nine firms were given the Request for Proposal (RFP); four firms and one team responded—Bell, Boeing, Fairchild, McDonnell Douglas, and a joint proposal from Lockheed/North American Rockwell.

10. New contracts negotiated in April 1974 to reflect increased requirements, less Congressional funding and changes in first flight dates.
11. First flight of McDonnell Douglas YC-15 on August 26, 1975.
12. First flight of Boeing YC-14 on August 9, 1976.
13. USAF completed flight evaluation of the McDonnell Douglas YC-15 on August 18, 1976, after two prototypes had completed 473 flight hours.
14. USAF completed flight evaluation of the Boeing YC-14 on August 5, 1977, after two prototypes had completed 603 flight hours.
15. RFP for full-scale development of production aircraft issued September 16, 1977.
16. Technical proposals received on November 15, 1977; cost and risk proposals submitted on November 22, 1977.
17. Source selection anticipated in April 1978 was placed on hold January 5, 1978.
18. Source selection officially terminated by Secretary of Defense Harold Brown in February 1978.
19. On October 31, 1979, Secretary of Defense Harold Brown cancelled the AMST program, and the aircraft ended up in the Military Aircraft Storage and Disposition Center at Davis-Monthan Air Force Base in Tucson, Arizona.

You might note in passing that release of the Air Force AMST requirement was in May of 1970, and a down-select to one contractor for production was anticipated in April of 1978. This amounts to 8 years, or more precisely, two presidential terms. In that time-lapse, (a) Congressional funding slowly dried up, (b) Air Force and Army support dwindled, and (c) the requirement began to shift from a short-range tactical assault aircraft to replace the Lockheed C-130 over to a long-range strategic airlifter that could deliver tons of payload anywhere in the world. And so began a new program that started in 1978 and ended when the McDonnell Douglas C-17 Globemaster III [620-622] went into service in January of 1995.

To work around reduced Congressional support, the Air Force delayed the first flight of Boeing's YC-14 by 1 year. This staggering gave Boeing extra time to refine their design, albeit mostly with their own money. A key design aspect was that both companies had to make do with available engines. Norton writes about McDonnell Douglas that

> "Douglas had initially proposed using the Pratt & Whitney (P&W) TF33 turbofan engine to power their prototype. This was to have featured a nozzle with greater diameter than the nacelle to direct surrounding airflow into the exhaust to aid in cooling. However, by early 1973 they had instead chosen to use four 16,000-lbf (71-kN, uninstalled and sea level) thrust low-bypass ratio (1:1) Pratt & Whitney JT8D-17 turbofans for their candidate prototype. The company was familiar with the JT8D power plant as they were employed on all models of their DC-9, from which the YC-15s nacelles were adopted. This was an old and comparatively inefficient engine nearing the end of its growth cycle and would likely not be in production for much longer. However, it was the only suitable power plant readily available at the time and, being well matured, it was expected to offer few problems. The choice was easy in the respect that the engine was familiar and P&W leased the units to DAC at practically no cost. However, it was clear that the aircraft really required turbofan engines

> in the 20,000–25,000-lbf (89–111-kN) thrust class, but none were then available 'off the shelf.' Because there were a number of new engines in the class that were expected to be available soon, and with the likelihood of improved performance, the engine installation was designed such that three alternative power plants could be fitted for tests at a later date. Those developmental engines that held promise were the P&W JT8D-209 and JT10D and General Electric/Snecma CFM56L, all in the 18,000–22,000-lbf (80–98-kN) thrust class.
>
> The 121,000-lb (54,885-kg) gross weight DC-9-50 used just two JT8D-17s, so the YC-15 had considerable thrust by comparison for STOL operations. At its maximum takeoff weight, the YC-15's excess thrust yielded a thrust-to-weight ratio (T/W) of 0.30. Wing loading (weight divided by wing area, or W/S) was 87 psi (864 bar). Low wing loading and high T/W is the desired combination for high maneuverability. This would have a tactical advantage and was of interest to the military developers. Roll rate, for example, was vital in evading threats and yet the C-141 had failed to meet specifications in this regard. The YC-15's characteristics compared favorably with the C-130's W/S of 88 psf (874 bar) and T/W of 0.25."

Boeing also changed their initial engine selection as Norton[142] writes:

> "By early 1973 Boeing had decided against their initial selection of the Pratt & Whitney JT9D engine to power their aircraft. They chose instead two enormous and powerful 51,000-lbf (227-kN) thrust (48,680 lbf installed at sea level standard day conditions) General Electric F103-GE-100 turbofans (also designated YF-103-F2). More commonly known as the CF6-50D, this was the new commercial "fanjet" with a 4.2:1 bypass ratio. This was then the largest high-bypass turbofan engine in the world, and just one of these power plants had more thrust than all three engines on a Boeing 727. For the YC-14, the large fan section helped in cooling the core exhaust flow and ameliorating somewhat the design challenge of hot efflux onto the top of the wing and flaps.
>
> The GE engine had been recently used on the McDonnell Douglas DC-10-30, the Airbus A-300, and the Boeing E-4 (747 airframe) then in design and had accumulated more than a million flight hours. But, the power plant was still fairly new with only about 3000 h on any one unit in service. They would prove quite reliable, however, with few problems and no engine change except as a demonstration. The engines yielded a thrust-to-weight ratio of 0.43 compared with the YC-15's T/W of 0.30. This revealed another advantage of the twin-engine design. The high level of available engine power to operate safely in the event of a single-engine failure meant that T/W with both engines running would be suitably high for STOL and tactical operations. So, with half the number of engines, the YC-14 possessed more overall thrust in seeking the same performance as the YC-15. Most pilots would comment on the considerable excess thrust available compared with most other transports. The JT9D and the Rolls-Royce RB.211 engines were considered potential alternative engines for future commercial customers of the aircraft."

This engine selection aspect opened up a real difference between the machines, and the flight test evaluations reflected the difference. The burden then fell on the Aeronautical Systems Division to establish a more apples-to-apples comparison between each competitor's very advanced STOL aircraft. As it turned out, the Source Selection Board never had to make a decision.

In retrospect, the whole YC-14, YC-15, and then C-17 story fits quite nicely into Norm Augustine's book of program laws [351].

---

[142] The amount of aircraft and systems detail you will find in Bill Norton's book is quite extraordinary. I bought two extra copies because I found I was underlining and highlighting darn near every other sentence.

Fig. 3-171. The McDonnell Douglas YC-15 first flew on August 26, 1975. The go-ahead contract was signed on January 9, 1973 [617, 623, 624].

Fig. 3-172. Boeing's contract was also signed on January 9, 1973. However, the first flight of the YC-14 was delayed until August 9, 1976, due to Air Force funding being pared down by the U.S. Congress [400, 618, 619, 625].

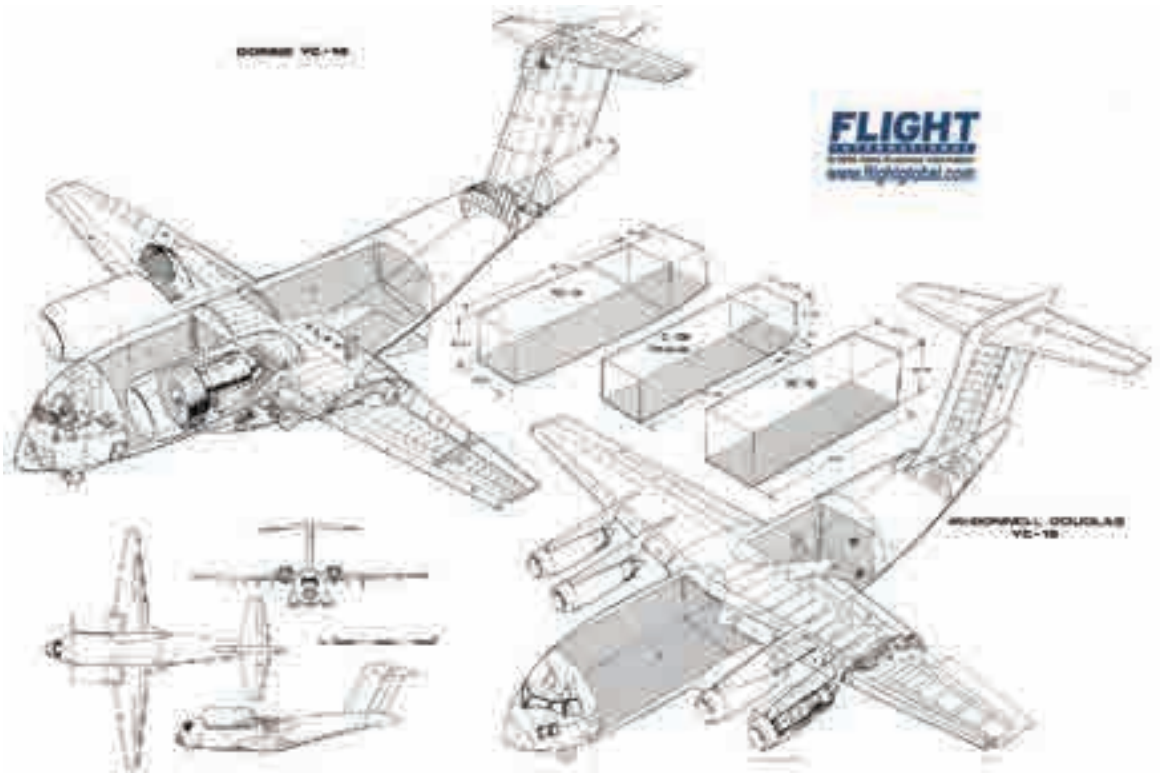

Fig. 3-173. McDonnell Douglas and Boeing designed their aircraft around a 47-foot-long, nearly 12- by 12-foot box requirement with rear ramp loading.

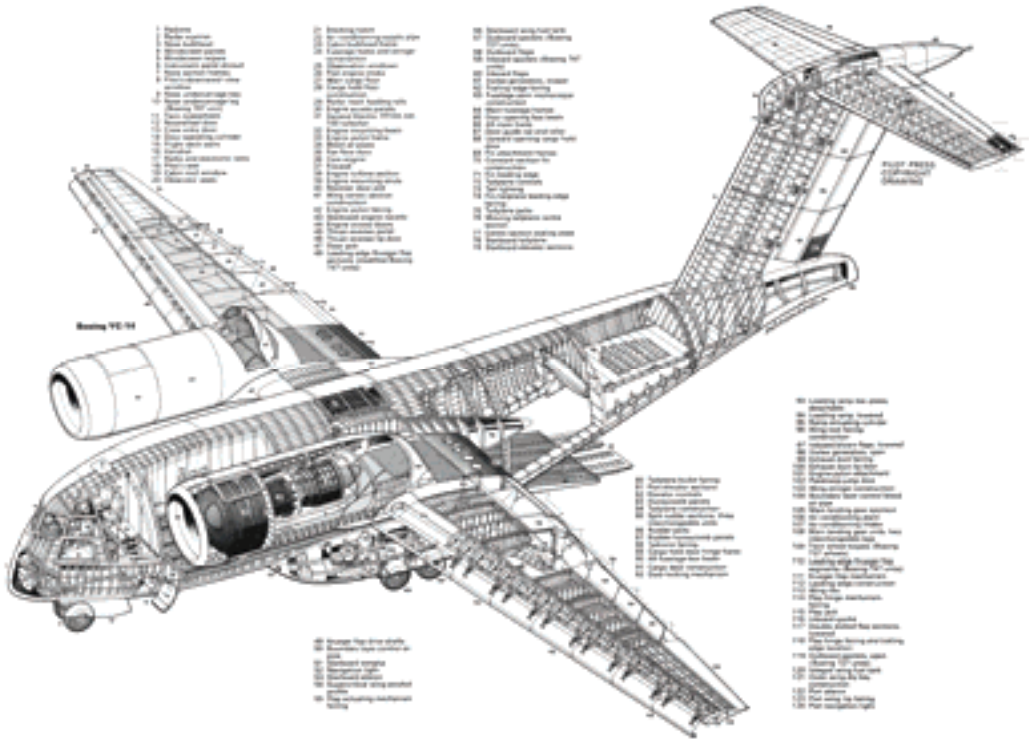

Fig. 3-174. Of the two AMST aircraft, Boeing's YC-14 was the more advanced STOL.

3.10.1 Design Requirements

The U.S. Air Force request for AMST proposals was quite short and, as Bill Norton notes, industry proposals were limited to no more than 50 pages. The requirements themselves were a minimum, and goals were the byword. In my mind, this is the most desirable form of an RFP. Procurement philosophy was being guided by the catchy phrase "Fly before you buy." In fact, I would describe the January 1972 RFP as a modern day update of the Wright Brothers' 1907 contract with the U.S. Army,[143] which was only one page long. The key AMST requirements were simply:

> "1. Cargo cabin shall be 55 feet long and 12 by 12 feet in width and height. [This was ultimately reduced to 47 feet long (including the ramp) and 11.7 feet wide by 11.3 feet high, because of affordability].
>
> 2. Routinely operate out of a 2,000 foot long landing zone with a 30,000 pound payload at the midpoint of a 500 nautical mile mission [radius] (with at least half of the internal fuel remaining). This was to be done at sea level on a 103°F day. [This requirement was ultimately reduced to 27,000 lb and a mission radius of 400 nm, again because of affordability].
>
> 3. A zero payload, 2,600 nautical miles, self deployment ferry mission without refueling with fuel contained only in the wings [this requirement remained unchanged]."

The two aircraft that evolved based on these requirements are summarized in Table 3-17. I have added comparable physical and performance characteristic for the Lockheed C-130H/E to emphasize the STOL advancement being achieved in the 1970s using turbofan thrust (instead of propellers) for powered lift.

With this short introduction, let me examine the two key performance requirements in some detail based primarily on the flight test reports [617, 618]. You can read about all the other characteristics of the two aircraft, as well as the program's ebb and flow, in Bill Norton's book [26].

3.10.2 STOL Mission

Both the YC-14 [618] and YC-15 [617] flight evaluation reports provide a wealth of STOL technology gleaned from the AMST program. First of all, the performance testing yielded quite accurate data about the fuel consumption as a function of speed, altitude, and weight. From this data, performance engineers accurately established aircraft weight at the midpoint of the 800-nautical-mile mission. An interesting point about the mission was the assumption that the aircraft would fly out with 27,000 pounds of payload, drop this load off, and pick up 27,000 pounds of cargo to return. This meant that the midpoint mission weight was about the same for both the landing and the subsequent takeoff. The key weights established from experimental data were as follows:

Key STOL Mission	Boeing YC-14 (lb)	McDonnell Douglas YC-15 (lb)
Start engine weight	174,804	166,000
Midpoint weight	160,920	149,300

[143] The U.S. Army Signal Corps Specification No. 486, *Advertisement and Specification for a Heavier-Than-Air Flying Machine,* was dated December 23, 1907. You might be interested in other thoughts I have on this matter, which I expressed with five slides while part of a panel at the AHS 64th Annual Forum in April 2008 [626].

Table 3-17. The YC-14 and YC-15 Offered Improvements When Compared to the Lockheed C-130H/E

Item	Unit	Lockheed C-130H/E	Boeing YC-14 (1)	McDonnell YC-15 (1)
Fuselage diameter	ft	15.1	17.90	18.00
Fuselage length	ft	97.74	131.67	109.83
Cargo floor width	ft	10.00	11.70	11.70
Cargo compartment height/length	ft	9.12/41	11.20/47.30	11.33/45.33
Cargo compartment length with ramp	ft	66.70	61.50	57.20
Wingspan	ft	132.6	129.00	110.36 (2)
Wing area	sq ft	1745.5	1,762.4	1,740.0 (2)
Wing aspect ratio	na	10	9.44	7.00
Wing taper ratio	na	0.52	0.35	0.30
Horizontal tail span	ft	52.7	54.90	56.70
Horizontal tail area	sq ft	545	603.00	643.00
Vertical tail area	sq ft	300	518.00	462.22
Fuel capacity in wing	lb	44,330	62,736	51,961 (2)
Auxiliary fuel in cabin tanks	lb	0.00	0.00	11,691
Empty weight + 27,000-lb payload	lb	101,000	145,143	129,921
Maximum ramp gross weight	lb	175,000	230,000	220,000
Maximum takeoff weight	lb	175,000	225,000	216,680
Maximum landing weight (unpaved)	lb	155,000	175,000	na
Number of engines		4	2	4
Engine type	na	Allison T56-A-15	GE CF6-50D	P&W JT8D-17
Takeoff thrust per engine, SL, std day	lb	9,600	49,327	16,000 (3)
STOL midpoint weight	lb	112,500	160,920	149,300
Takeoff thrust/STOL midpoint weight	na	0.34	0.613	0.4287
STOL performance, sea level, 103 °F day at midpoint weight				
Landing flap setting	deg	36	60	45
Landing ground run distance	ft	1,300–1,650	1,152	1,325
Landing distance over 50 feet	ft	2,300–3,100	1,713	1,945
Takeoff flap setting	deg	18	30	14
Takeoff ground run distance	ft	1,000–1,600	1,469	1,950
Takeoff distance over 50 feet	ft	1,500–2,400	2,090	2,600
Cruise Mach number	na	0.494	0.64	0.65
Cruise airspeed/altitude	kts	300/23,000	362/35,000	368/35,000
Maximum range (basic wing)	nm	3,700	2,363	1,760 (4)
Maximum range (basic wing + cabin aux)	nm	na	na	2,590

Notes: 1. Both AMST aircraft met the requirement to have a crew of two pilots and only one loadmaster. The C-130 has a crew of three plus the loadmaster.
2. Production configuration to have a larger wing with span of 132.58 feet, area of 2,107 square feet, aspect ratio of 8.4, and able to carry 72,900 pounds of fuel internally.
3. Expected to increase to 22,000 pounds with the GE/Snecma CFM56 engine so that thrust-to-weight ratio would be more on the order of 0.4.
4. Expected to be about 2,425 nautical miles with larger wing.

The STOL mission, you will recall, was to arrive at a sea level landing site on a day when the temperature was 103 ^{o}F. The site was to be "semi-prepared" and only 2,000 feet long with 50-foot obstacles at either end. Presumably this would be something like a dirt or grass strip only a couple of hundred feet wide. After landing, dropping off the cargo, and reloading in a rapid turnaround, the aircraft was to be off again. Table 3-17 shows that each design approach (i.e., upper surface blowing (USB) and external blown flap (EBF)) needed some improvements before the Y-designation could be removed and the aircraft could go into production. In my mind, both design approaches demonstrated the ability to ultimately meet the U.S. Air Force requirements. However, the reports taken together listed over 40 specific items addressing both mandatory and desired fixes that should be addressed in a production aircraft. My view is that (a) both of these very advanced STOLs were really experimental aircraft, (b) five or six additional aircraft from one or the other company needed to be built as true preproduction machines, and (c) the parallel to the MV-22B tiltrotor program you read about earlier is uncanny.

Now let me discuss some technical points about takeoff and then go on to landing. Keep in mind that both aircraft were the most advanced examples of STOL performance with turbofan engines that the fixed-wing industry had ever put on the table. The amount of STOL technology provided in the two flight test reports at the end of the AMST program truly represents a major step forward in the evolution of STOL aircraft. The number of landings and takeoffs that each aircraft made, the pile of time histories digitally recorded, and the depth of analysis of raw data simply boggles my mind. I will point out, however, that the report evaluating the Boeing YC-14 is the more informative report, presumably because it came a year after the McDonnell Douglas YC-15 test and analysis program was completed, and everyone involved had more experience dealing with this new type of transport machine.

3.10.2.1 Takeoff

You have, with Fig. 3-175 and Fig. 3-176, the raw data of takeoff results for both STOL aircraft. I have made little distinction in the data shown on Fig. 3-175 beyond the two symbols because the major difference between the two design approaches is the ratio of engine takeoff thrust to mid-mission gross weight. This raw data includes takeoffs made (a) from concrete, asphalt, and "semi-prepared" runways, (b) from a variety of pressure altitudes and outside temperatures, and (c) with all engines operating at takeoff thrust. Consider first, Fig. 3-175. No doubt your impression of "scatter" in the data is perplexing. However, the scatter is primarily due to (1) the lift coefficient at liftoff, and (2) the thrust available at takeoff, which depends, in turn, on pressure altitude and outside temperature. You see this explanation of the scatter from the small graph in the top left corner of Fig. 3-175.

VTOL advocates will note that the Boeing YC-14 could make vertical takeoffs at a gross weight of about 80,000 pounds. That is to say, if the aircraft was reconfigured with two additional General Electric F103-GE-100 turbofans it could perform a vertical takeoff at about 160,000 pound gross weight. The extra installed takeoff thrust would most certainly add to higher cruise speeds at higher altitudes. Of course, the weight empty would increase with additional engines. Let me add that the McDonnell Douglas design used four P&W JT8D-17

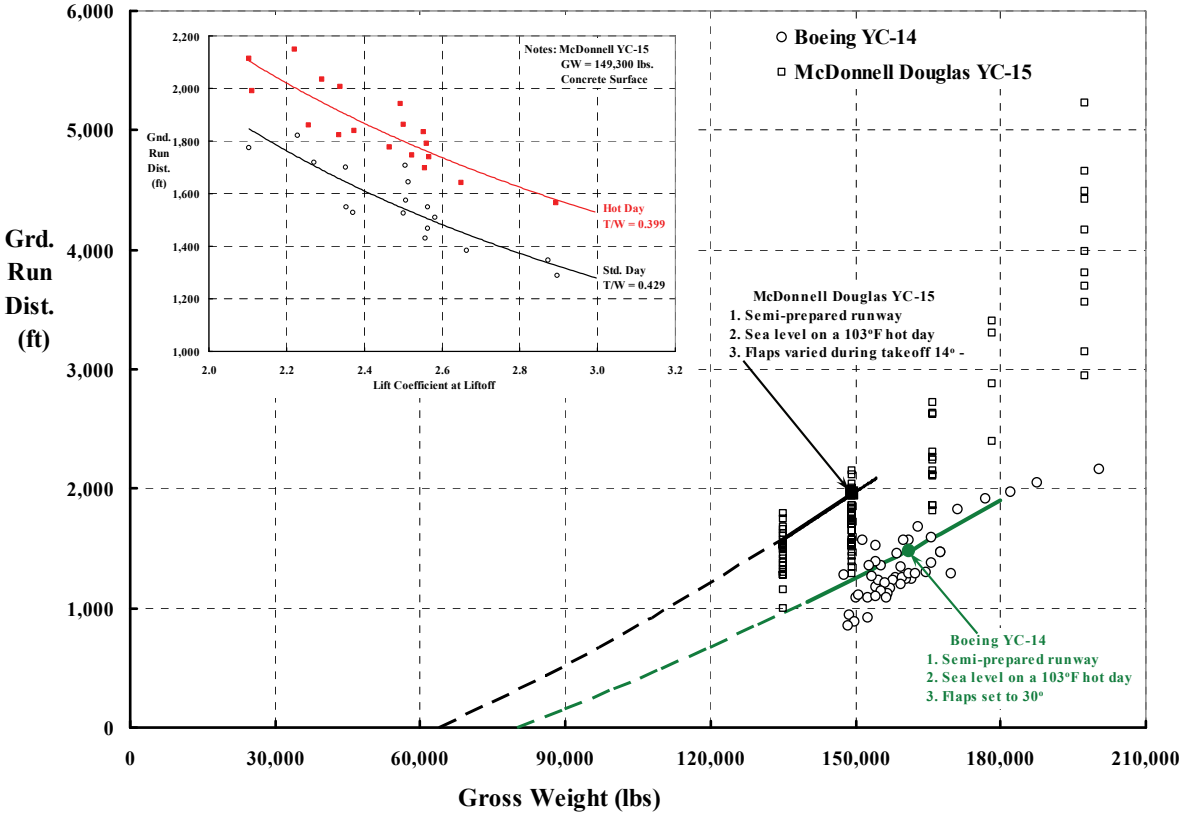

Fig. 3-175. The primary difference between the takeoff performances of these two STOL aircraft is the ratio of installed thrust per pound of weight.

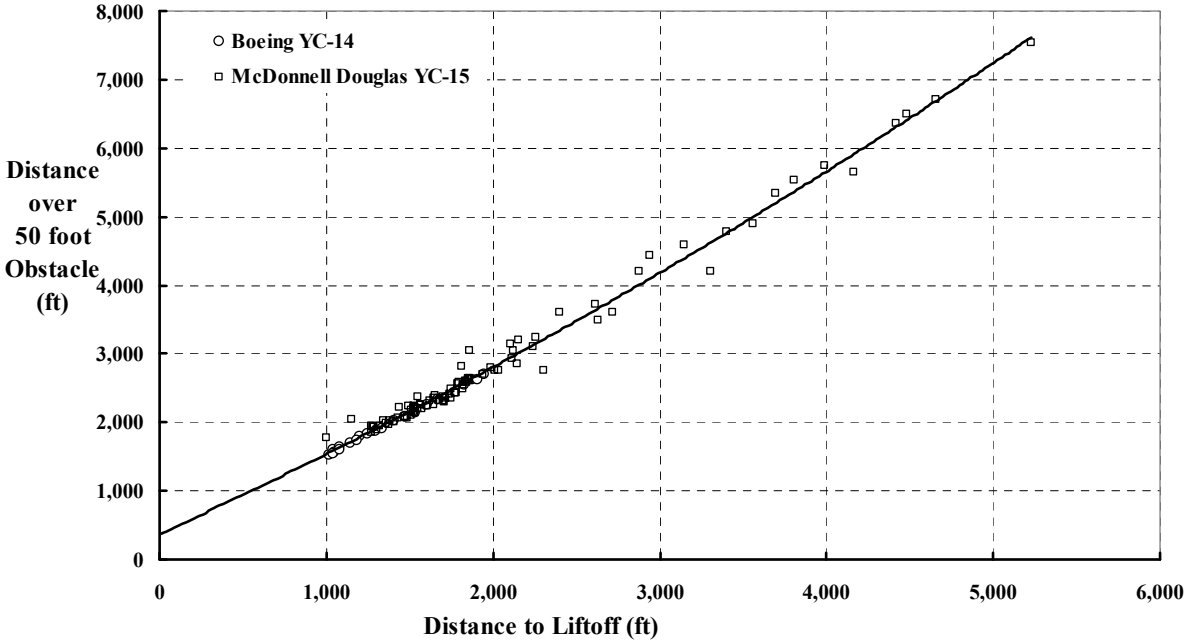

Fig. 3-176. It appears that both aircraft types followed the relationship that $D_{50ft} = 373 + 1.112 D_{Liftoff} + 0.0000523 \left(D_{Liftoff} \right)^2$.

turbofan engines. This engine produces 16,000 pounds of static thrust at sea level on a standard day with an air flow of 327 pounds per second, which is a mass flow ($dm/dt = \dot{m}$) of 10.16 slugs per second. Simple theory ($hp = T^2/1100\dot{m}$) shows that this amount of thrust carried on such a small nozzle disc area equals about 22,900 horsepower. This suggests that the STOL mission could easily be met with a proprotor configuration. It is not so clear, however, that the requirement for high-speed cruise would be met. Debates of this sort between STOL and VTOL advocates have been going on for decades.

Now consider Fig. 3-176. Here you see that the total distance traveled from brake release to where the aircraft passes over the 50-foot obstacle is—to a first approximation—just dependent on the ground run distance. What I found interesting was that both aircraft appear to have this same relationship. That is,

(3.168) $D_{50\text{ft}} = 373 + 1.112 D_{\text{Liftoff}} + 0.0000523 \left(D_{\text{Liftoff}}\right)^2$,

and this suggests that F is approximately equal to ma, give or take the 373 feet.

Let me now go on to a more detailed discussion of takeoff.

While both test reports provide appendices outlining the takeoff data reduction and analysis, Boeing's YC-14 report [618] is clearly the more informative. I found it quite interesting that the three primary authors of the report each carried the title, YC-14 Performance Engineer. They wrote in appendix A (Data Analysis Methods) that "Conventional jet aircraft exhibit predictable performance characteristics and the data reduction task is simplified." You will find that the McDonnell Douglas YC-15 report [617] assumes the reader is quite knowledgeable about "conventional jet aircraft" and that this report is rather lacking in details. It seems to me that the YC-15 with its EBF was just another example of turbofan engines substituted for propellers, which was, of course, a major step forward in its own right. The YC-14 was the final, practical demonstration of decades of research on USB flap performance characteristics. As such it deserved the efforts of three performance engineers (Lee Trlica, Robert Kennington, and Robert Springer) who, in my opinion, did a superb job of providing a very practical summary of the USB configuration.

That said, let me give you a brief overview of the methodology developed by Trlica, Kennington, and Springer[144] to interpolate takeoff performance between the many circle points you see on Fig. 3-175. By demonstrating a semiempirical approach to calculating the test data, these performance engineers could establish performance at the Air Force requirement points and thus determine whether the aircraft "met spec." Consider first the calculation of the ground run portion of the takeoff.

The determination of not only takeoff performance, but landing performance as well, depends first and foremost on several key speeds defining the maneuver. The authors referred to the several speeds as an airspeed schedule and stated:

[144] There is no question in my mind that all that Boeing performance engineers had learned about upper surface blowing (USB) technology was transferred to these three Air Force Performance Engineers.

> "Ground rules for the determination of the takeoff airspeed schedule were contained in the YC-14 Estimated Performance document (reference 3).[145] This document specified that (1) rotation speed (V_g) be greater than or equal to the minimum control airspeed on the ground without nose-wheel steering (V_{mcg}), (2) liftoff airspeed (V_{lo}) be greater than or equal to 1.08 times the minimum liftoff airspeed (V_{mu}), (3) climb out airspeed (V_{CO}) be greater than or equal to 1.20 times the power-on minimum airspeed with the critical engine inoperative (V_{min}), and (4) refusal speed (V_1) must be equal to or greater than minimum control speed on the ground with nose wheel steering (V_{mcg}).
>
> Minimum liftoff speed determination tests were conducted on the main base runway. The objective was to determine the lift coefficient of the aircraft at the minimum airspeed at which the airplane becomes airborne.
>
> Minimum liftoff airspeed, commonly referred to as minimum unstick airspeed (V_{mu}), was considered by The Boeing Company to be one of the more important parameters that determines runway length requirements. It was defined as the minimum airspeed at which the aircraft would lift off the ground during the takeoff roll. Minimum liftoff air speed could be limited by angle of attack, aircraft geometry, or air minimum control speed. In the case of the YC-14, the minimum liftoff airspeed was limited by geometry. This meant that the liftoff angle of attack was limited to that pitch attitude at which the tail of the aircraft would be in contact with the runway surface. The minimum liftoff airspeed was determined by the lift coefficient that existed when the aircraft lifted off the ground with the tail in contact with the runway surface.
>
> Original predictions made by The Boeing Company indicated that it was unlikely that a tail strike could be achieved during rotation of the YC-14 with both engines operating at takeoff rated thrust at sea level on a hot day. These predictions indicated that the aircraft would lift off when sufficient forward airspeed was attained to rotate the aircraft. For this reason, all engines operating (AEO) minimum liftoff airspeed tests were not planned during this evaluation. Subsequent operations showed that adequate clearance between the tail cone and the runway surface did exist on all but one AEO takeoff. On this takeoff minor damage to the fiberglass tail cone occurred because the pilot used a very high rotation rate. This rotation rate, approximately 16 degrees per second, was considered too high when compared with the normal rotation rate of approximately 6 degrees per second. Tail strike with all engines operating at takeoff rated thrust was not considered probable at normal rotation rates."

Given this starting point, both the airspeed (do not forget about head winds) at rotation (V_g) and at liftoff (V_{lo}) were quite accurately established and agreed upon.

The calculation of the ground run distance during takeoff was therefore divided into two parts. The first part was the calculation from brake release up to the airspeed where the aircraft was rotated from all wheels on the ground to only main wheels on the ground. The second part added the distance traveled up to liftoff. That is,

$$(3.169)\quad D_{Grd.Run} = \frac{W}{g}\int_0^{V_g} \frac{V}{\sum F_x} dV + \frac{W}{g}\int_{V_g}^{V_{lo}} \frac{V}{\sum F_x} dV .$$

The summation of forces is expanded to

$$(3.170)\quad \sum F_X = F_g - F_e - D - \mu_{roll}(W - L) - \phi W = F_g - F_e - (D - \mu_{roll} L) - \mu_{roll} W - \phi W$$

[145] Rengstorff, A. E., et al., YC-14 Estimated Performance. D748-10101-1, Rev. A, The Boeing Company, Seattle, Washington, June 1976.

by following the simple sketch the performance engineers provided below. *Keep in mind that Eq. (3.169) expects all forces that contribute to ΣF_X to be a function of speed.* The regrouping of the terms in Eq. (3.170) exposes the parameter ($D - \mu_{roll}L$), which was uniquely (perhaps fortuitously would be a better word) related to the turbofan thrust (F_g). The engine ram drag (F_e) is a normal penalty associated with gas turbine engines. The data reduction methodology found a simple equation for each of the terms in Eq. (3.170). This, to me, summarizes all of the key USB technology obtained from decades of powered lift research [60-63].[146]

Now as to the individual modeling of each term in Eq. (3.170), first you have the following for the gas turbine engine thrust (F_g):

$$F_g = N\left(A_0 + A_1 M + A_2 M^2\right) \qquad M \equiv \text{Mach Number} = \frac{V_{fps}}{a_s} = \frac{V_{fps}}{1116.74\sqrt{\theta}}$$

(3.171)

$$F_g = N\left[A_0 + A_1\left(\frac{V_{fps}}{a_s}\right) + A_2\left(\frac{V_{fps}}{a_s}\right)^2\right]$$

where the number of engines is denoted by (N). The engine manufacturer can easily provide tables and graphs of how the engine thrust varies with speed for any atmospheric condition. The performance engineers simply curve fit this sort of data, and this produces the three constants A_1, A_2, and A_3. Recall that (θ) is the ratio of outside temperature for the flight condition to the standard temperature at sea level. The airspeed (V_{fps}) is in feet per second.

The methodology makes considerable use of the nondimensional form of the engine's jet thrust using the coefficient (C_J), which is defined as $C_J = F_g / qS_W$ where the dynamic pressure is, as you know, ($q = {}^1/_2\rho V^2$). I have chosen to avoid this generally accepted nondimensional form (C_J) in favor of hard numbers. For example, the ram drag (F_e) is characterized by the performance engineers as $CF_e = \dfrac{F_e}{qS_W} = A_3\left(\sqrt{C_{J-one}} + \sqrt{C_{J-two}}\right)$.

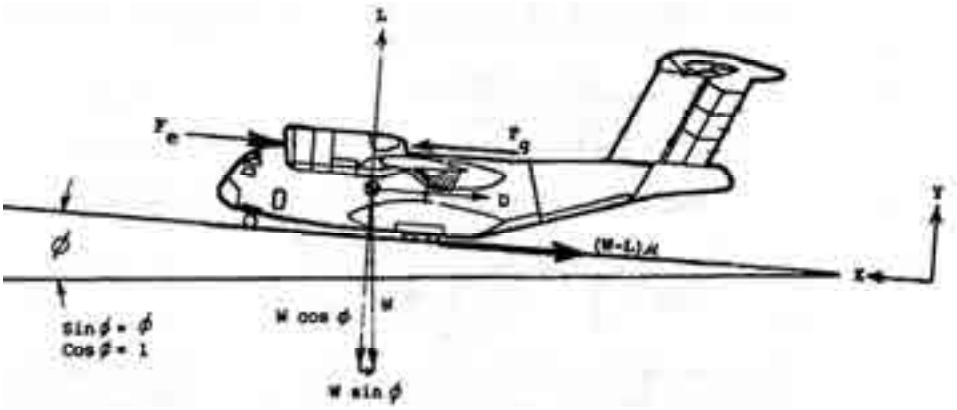

Fig. 3-177. Forces to be accounted for in the ground run calculation.

[146] Can you imagine calculating the time history of a YC-14's takeoff and landing using computational fluid dynamics now available in 2015?

Thus, ram drag in a dimensional form becomes

$$(3.172)\quad F_e = A_3\sqrt{2\rho S_W V\left(\frac{F_g}{N}\right)}.$$

This brings me to the most interesting term in Eq. (3.170), which is $(D-\mu_{roll}L)$, or in its nondimensional form $(C_D-\mu_{roll}C_L)$. I was absolutely fascinated by figure B13 on page 180 of the YC-14 report. You see it here as Fig. 3-178 where time histories of many takeoffs at varying conditions with all engines operating (AEO) lead to such a simple graph of

$$\frac{(C_D-\mu_{roll}C_L)}{C_J} \quad \text{versus} \quad \frac{1}{C_J}.$$

Virtually all of the aerodynamics embodied in the USB approach are reduced to two straight lines. The first straight line models the aircraft during its ground run up to the rotation speed (V_g). These lines are simply

$$(3.173)\quad \frac{(C_D-\mu_{roll}C_L)}{C_J} = A_4 + A_5\left(\frac{1}{C_J}\right) \quad \text{for} \quad 0 \le V \le V_g \quad \text{and}$$

$$(3.174)\quad \frac{(C_D-\mu_{roll}C_L)}{C_J} = A_6 + A_7\left(\frac{1}{C_J}\right) \quad \text{for} \quad V_g \le V \le V_{lo}.$$

When dimensionalized, these key aerodynamic decelerating forces are seen as

$$(3.175)\quad \begin{aligned} (D-\mu_{roll}L) &= A_4F_g + A_5\left(\tfrac{1}{2}\rho V^2 S_W\right) \quad \text{for} \quad 0 \le V \le V_g \\ (D-\mu_{roll}L) &= A_6F_g + A_7\left(\tfrac{1}{2}\rho V^2 S_W\right) \quad \text{for} \quad V_g \le V \le V_{lo} \end{aligned}.$$

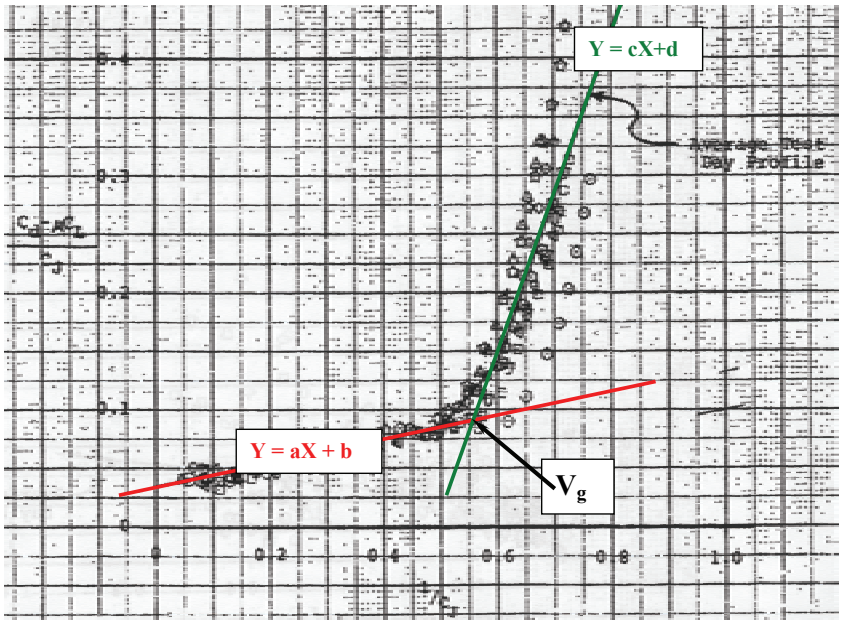

Fig. 3-178. The aerodynamic drag of the YC-14 changes substantially as the aircraft rotates from all wheels on the ground to just main wheels on the ground.

These aerodynamic decelerating forces are the only forces that change in the ground run calculation. The two-part representation reflects the change from the aircraft angle of attack with all wheels on the ground to the angle of attack used to initiate the climb over the 50-foot obstacle.

I would be remiss if I did not mention that the performance engineers devised a few simple test runs that established the ground rolling friction coefficient (μ_{roll}) as 0.037 for operations from a concrete runway and 0.055 from the semi-prepared runway. Testing with the McDonnell Douglas YC-15 arrived at about the same order of magnitude for this coefficient.

The last two terms in Eq. (3.170), $\mu_{roll}W$ and ϕW, are self explanatory.

You now have all the components of ΣF_X (it is only required to perform the integration with velocity called for by Eq. (3.169)). Of course, given the use of the digital computer, the YC-14 Performance Engineers had no trouble programming the complete ground run model. I certainly found it quite easy to reproduce their results using PTC Mathcad software. And, in fact, I found a quite accurate closed-form solution that was very illuminating. After reconstructing the solution in Mathcad as the performance engineers described, I found ΣF_X could be expressed as a polynomial in airspeed using a series expansion. The polynomial was of the form

$$\sum F_X \approx B_0 + B_1 V + B_2 V^2$$

where the coefficients B_0, B_1, and B_2 were simply

(3.176)
$$B_0 = A_1 N\left(1 - A_5\right) - \mu_{roll} W - \phi W$$

$$B_1 = A_1 N \frac{A_2}{a_S}\left(1 - A_5\right) - A_4\sqrt{2\rho S_W A_1}$$

$$B_2 = A_1 N \frac{A_2}{a_S^2}\left(1 - A_5\right) - \frac{1}{2a_S} A_2 A_4 \sqrt{\frac{2\rho S_W}{A_1}} - \frac{1}{2} A_6 \rho S_W .$$

Of course, the value of the straight line coefficients model the aerodynamic drag force change with the speed range as Fig. 3-178 suggests and Eq. (3.175) represents. Therefore, to complete the calculation you need

(3.177)
$$C_0 = A_1 N\left(1 - A_7\right) - \mu_{roll} W - \phi W$$

$$C_1 = A_1 N \frac{A_2}{a_S}\left(1 - A_7\right) - A_4\sqrt{2\rho S_W A_1}$$

$$C_2 = A_1 N \frac{A_2}{a_S^2}\left(1 - A_7\right) - \frac{1}{2a_S} A_2 A_4 \sqrt{\frac{2\rho S_W}{A_1}} - \frac{1}{2} A_8 \rho S_W .$$

What this regrouping approach gives you is a closed-form solution for the integration over speed. This closed-form solution was, I found, also expandable in a series. Thus, the two parts of the total ground run distance can be estimated for the distance traveled with all wheels on the ground from Eq. (3.178) and then the additional distance with just the main wheels on the ground from Eq. (3.179).

$$\text{(3.178)}\quad \text{Part 1 } D_{\text{Grd.Run}} = \frac{W}{2gB_1} V_g^2 \left[\begin{array}{l} 1 - \frac{2}{3}\left(\frac{B_2}{B_1}\right) V_g - \frac{1}{2B_1^2}\left(B_1 B_3 - B_2^2\right) V_g^2 \\ + \frac{2B_2}{5B_1^3}\left(2B_1 B_3 - B_2^2\right) V_g^3 \end{array} \right] \quad \text{for} \quad 0 \le V \le V_g \,.$$

$$\text{(3.179)}\quad \text{Part 2 } D_{\text{Grd.Run}} = \frac{W}{2gC_0 C_2} V_g^2 \left[\begin{array}{l} C_0 \ln\left(\frac{C_0 + C_1 V_{lo} + C_2 V_{lo}^2}{C_0 + C_1 V_g + C_2 V_g^2} \right) \\ - C_1 \left(V_{lo} - V_g \right) \end{array} \right] \quad \text{for} \quad V_g \le V \le V_{lo} \,.$$

One of the more interesting graphs that the above results give you is how much runway is used up as the aircraft gathers enough speed to lift off. Fig. 3-179 offers one example that I obtained by "programming" Eqs. (3.178) and (3.179) using Microsoft® Excel® software.

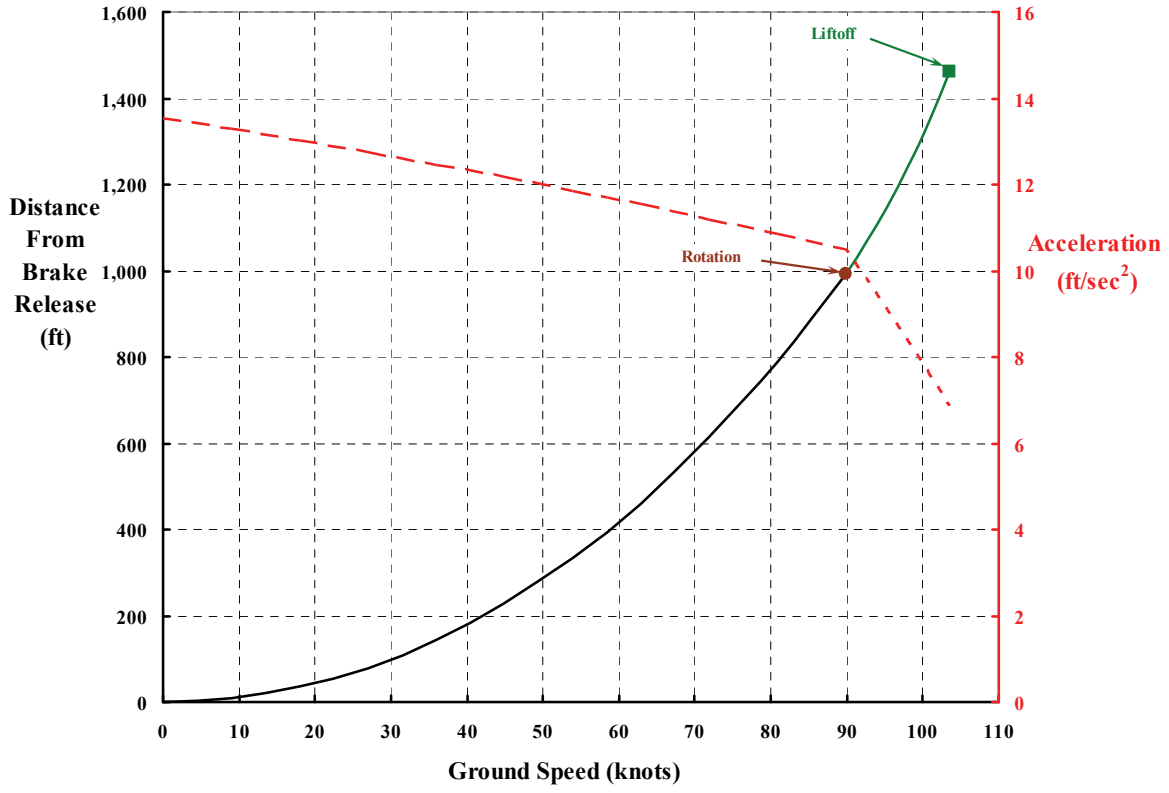

Fig. 3-179. Typical ground run distance calculation. While rotation increases drag and decreases acceleration, ground speed still builds up very rapidly.

Now consider the horizontal distance traveled after liftoff as the aircraft climbs and passes over the 50-foot obstacle. You saw from Fig. 3-176 that, for some reason, this horizontal distance adds to the ground run distance making the total distance to clear a 50-foot obstacle immediately known by Eq. (3.168). While this is an interesting observation for a very "quick and dirty" guess, it is hardly a methodology for conceptual or preliminary design in this day and age. To add to this, I found that both the YC-14 and -15 test reports were rather unsatisfactory in their analysis of this last segment of the takeoff. This dissatisfaction prompted me to propose a more careful calculation, which follows.

Let me use the Boeing YC-14 as the example. Roughly speaking, the whole takeoff maneuver takes about 19 seconds as the aircraft travels the 2,090 feet from brake release. (You might note that this distance is 90 feet longer than the requirement for takeoff from a semi-prepared field located at sea level on a 103 ^{o}F day.[147]) With such a high inertia machine, it seems to me that changing its velocity more than a few knots in 3 or 4 seconds is not a reasonable assumption. Of course, failure of an engine during takeoff or landing is quite another matter. However, aircraft performance after engine failure is a very important subject that is beyond the scope of this Volume. Therefore I suggest that after liftoff—with all engines operating—the aircraft continues to gain airspeed in the nearly linear manner shown on Fig. 3-179, which means that airspeed and horizontal distance traveled after liftoff are simply calculated as if the aircraft did not lift off. To be more precise, Eqs. (3.169) through (3.179) are used until the aircraft has passed the 50-foot obstacle. When you follow this set of equations, you have engine thrust (F_g), horizontal distance (D), horizontal velocity (V_X), and stopwatch time (T) during the complete takeoff.

The calculation of height above ground level (H) is better approached as an F = ma problem. I suggest that creating a time history of the maneuver is the approach to use, and this means

$$(3.180)\quad V_Z = \int_0^T a_Z \, dt \,,$$

and then integrating vertical velocity (V_Z) again so that

$$(3.181)\quad H = \int_0^T V_Z \, dt \,.$$

Following this approach only requires three things.

First, the vertical acceleration must be calculated. This is rather simple, because the increasing angle of attack of the aircraft, from the brake release to the rotation point through liftoff to over the 50-foot obstacle, produces lift (L_t) that varies with time. Therefore, you have

$$(3.182)\quad \sum F_Z = L_t - W = \frac{W}{g} a_Z \,.$$

[147] Missing a key performance requirement by 4.5 percent when your competitor meets, or even beats, spec could well mean you will lose the contract.

Of course, obtaining some estimate of this time-varying lift requires the very basic curve(s) of the aircraft's lift coefficient versus angle of attack. With turbofan-powered-lift aircraft such as the YC-14 and YC-15, the lift coefficient depends not only on angle of attack, but on the turbofan thrust. The three performance engineers who wrote the YC-14 report [618] provided a representative example for the YC-14 in its takeoff configuration, which you see here as Fig. 3-180. I found it convenient to use this family of curves in my calculations with an equation of the form

$$C_L = L_0 + L_1(\alpha) + L_2(C_J) + L_3(C_J\alpha) + L_4(\alpha^2) + L_5(C_J^2) \tag{3.183}$$

rather than some table look-up scheme. You may find references [627, 628] useful in developing curves such as Fig. 3-180 from theory. I would remind you, however, that curves of lift coefficient versus angle of attack for several jet thrust coefficients are very configuration specific.[148]

Second, some representation of the aircraft's pitch attitude during the maneuver must be made. In this regard, I found a time history of a takeoff in the YC-14 Flying Qualities Evaluation report [619]. This data confirmed my experience that pilots tend to control the aircraft such that pitch attitude (θ_t) changes linearly with time. You might think of this as equivalent to the pilot establishing a pitch rate ($d\theta_t/dt$) and holding that pitch rate until the aircraft's nose-up attitude becomes uncomfortable (or even dangerously near stall) until he clears the obstacle. However, that is a very simplistic view. Nevertheless, I suggest that the pitch attitude at the beginning of rotation is zero, and after that time you have

$$\theta_t = R(t - t_{rot}). \tag{3.184}$$

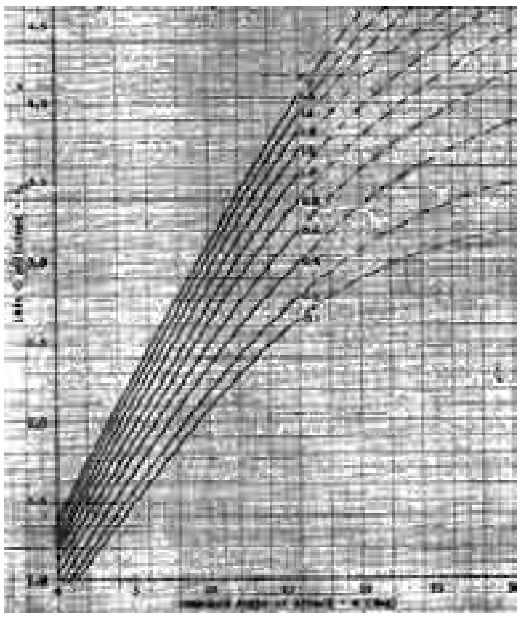

Fig. 3-180. Typical lift coefficient behavior of a powered lift STOL aircraft.

[148] During the last year I managed Boeing's V/STOL wind tunnel (located at the Vertol division near Philadelphia), the Boeing Seattle airplane guys came in with their YC-14 powered force model. The tunnel's annual report for the year [629] shows that of the 3,900 hours of productive testing time, 1,900 hours were devoted to 11 tests of the YC-14. I spent many free hours analyzing the performance data we recorded from this model just to understand its powered lift aerodynamics both in and out of ground effect. At that time we were also up to our eyeballs in testing that supported Boeing Vertol's UTTAS program. I remember it as a fun time even though we had a three-shift operation going on. My wife, Sue, remembers it as a series of 50- to 70-hour work weeks when she had to call and say, "Get home for dinner at 6:00 p.m. sharp!" But she never said, "or else."

This second assumption requires further discussion. First of all, the horizontal elevator on both the YC-14 and YC-15 was very powerful in the sense that it could produce a large amount of negative lift. This negative lift times the moment arm was easily able to raise the nose very quickly should the pilot, for some reason, need to do so. The pilot's ability to drag the underside of the fuselage in the tail cone area was a concern, as you might guess from Fig. 3-177. The report [617] discussing the McDonnell Douglas YC-15 states that "Upon reaching rotation speed, the aircraft was rotated at the aim rotation rate of approximately 3 to 4 degrees per second toward a target initial climb out attitude (θ) of 15 degrees." The Boeing YC-14 report [618] is more informative because the writers state (with some condensing and editing by me) that

> "Original predictions made by The Boeing Company indicated that it was unlikely that a tail strike could be achieved during rotation of the YC-14, *with both engines operating at takeoff rated thrust at sea level on a hot day*. Subsequent operations showed that adequate clearance between the tail cone and the runway surface did exist on all but one AEO takeoff. On this takeoff minor damage to the fiberglass tail cone occurred because the pilot used a very high rotation rate. This rotation rate, approximately 16 degrees per second, was considered too high when compared with the normal rotation rate of approximately 6 degrees per second. Tail strike with all engines operating at takeoff rated thrust was not considered probable at normal rotation rates. This did not preclude damage to the fiberglass tail cone. *With the main landing gear struts fully extended, the tail cone would contact the runway surface at approximately 15.6 degrees pitch attitude*. Structural damage to the metal airframe would not occur until a pitch attitude of approximately 17 degrees was attained. The Boeing Company defined the geometry limited pitch attitude for minimum liftoff airspeed to be 17 degrees. *Damage to the tail cone would be unacceptable for the C-14 aircraft."*

The report goes on to say that

> "Numerous buildup tests were conducted to familiarize the pilots with the single-engine takeoff characteristics by conducting takeoffs with one engine at idle and the other engine set at the aim thrust-to-weight (T/W) ratio. Then, actual single-engine takeoffs were accomplished with one engine shutdown. Thrust was advanced on the operating engine at a rate where the pilot could maintain directional control with rudder pedal steering only. Rotation to the desired pitch attitude usually began between 55 and 60 KIAS while the desired thrust was being established. Target T/W ratio was usually established by approximately 80 KIAS with liftoff occurring at approximately 85 KIAS. Full rudder pedal deflection was usually required to maintain directional control at liftoff. The aircraft was allowed to climb to approximately 30 feet above ground level and to accelerate to approximately 100 KIAS. Then, for reasons of safety, the takeoff test was terminated and a landing made on the runway remaining. This was easily accomplished, and the pilot experienced no difficulty in lining up the aircraft with the runway centerline.
>
> The test conditions flown are tabulated in table 2. The lift coefficient at main landing gear liftoff was calculated from the airspeed and gross weight that existed when the angle of the main landing gear lever beam indicated that the struts were fully extended. Flightpath normal acceleration was assumed to be equal to one g [I think this was not a good assumption because of scatter in the data]. These results were plotted as a function of pitch attitude at liftoff (assumed equal to angle of attack) and are shown in figure B1 along with the predicted values. *The test results indicated that higher minimum liftoff airspeed lift coefficient values were achieved than were predicted by the contractor.* Extrapolating the test results to the limiting angle of attack of 17 degrees proposed by The Boeing Company yielded a lift coefficient value of 3.78. This lift coefficient value was used to compute minimum liftoff airspeed as a function of gross weight as shown in figure B2."

The primary point I wish to make here is that takeoff and landing analyses based on assuming the aircraft is a point mass[149] are really not good enough today—even for conceptual design. Such issues as ground–airframe clearance are just one example. Tradeoff studies between cost, performance, *aircraft geometry,* and weight quickly show what is practical and what is quite unrealistic.

Now, to calculate the height gained after liftoff as more runway is used up, consider this step-by-step method programmed into Microsoft® Excel®, which I have summarized as follows:

1. Because the distance up to rotation is available from Eq. (3.178), only the equations leading up to Eq. (3.177) and (3.179) need be considered.
2. Establish (or pick, or guess) the ground speed at which rotation should begin considering the aircraft's configuration, and the altitude and temperature on the runway. Beyond the rotation speed, select additional speeds that extend the speed 5 or 10 knots beyond what you might expect the liftoff speed to be.
3. Complete all the calculations required by Eq. (3.177) and (3.179). This gives you inputs for engine thrust (F_g), horizontal distance (D), horizontal velocity (V_X), and horizontal acceleration (a_X). Stopwatch time (t) to use for this time history calculation is easily calculated by the integral
$$t = \int_{V_g}^{V} \frac{1}{a_X} dV_X,$$
which can be performed numerically to any level of accuracy.
4. Now define a piloted-input aircraft pitch attitude (θ_t). For the two cases that you will see shortly, I selected the YC-14 taking off at sea level on the spec hot day and at the mid-mission gross weight of 160,920 pounds as the example. The two cases are:

   Case 1. Pilot uses excessive aft stick so that the aircraft's tail cone is scraped on the ground when the wheels come off the ground. This pitch rate (R) of 6 degrees per second with Eq. (3.184) lets the aircraft's center of gravity rise up from ground level by about 3 feet at which point the pitch attitude is 16 degrees as measured by a line joining the wheels of the extended landing gear and the tail cone.

   Case 2. Pitch rate varied until the test results of 2,090 feet total takeoff distance at the 50-foot obstacle are obtained by my methodology (i.e., *find the pitch attitude rate that makes the answer come out right*).

Given information from steps 1, 2, 3, and 4, it is rather straightforward to proceed with:

[149] During my literature search for this volume, I came across a Master's Thesis dated December of 1978. The thesis was written by a 35-year-old engineer by the name of David Powell LeMaster. He was then graduating from the Air Force Institute of Technology at Wright Patterson Air Force Base in Ohio. You should read his work [630] because he tackles the takeoff and landing performance methodology for both the YC-14 and YC-15 STOLs right in the middle of the competition. It is a very nice piece of work.

5. Calculate:
   a. The dynamic pressure as $q = 1/2\rho V^2$.
   b. The jet thrust coefficient from $C_J = F_g/qS_W$.
   c. The aircraft lift coefficient (C_L) from Eq. (3.183) assuming angle of attack equals pitch attitude.[150] I used the following for the YC-14:

$$C_L = 0.657825 + 0.1533315(\alpha) + 0.7607435(C_J) - 0.002321244(\alpha^2)$$
$$+ 0.03098411(C_J\alpha) - 0.2350437(C_J^2) \quad \text{Note: } \alpha \text{ in degrees}$$

   d. Aircraft lift as $L = qS_W$.
   e. Vertical acceleration from Eq. (3.182) so that $a_Z = \frac{g}{W}(L_t - W)$.
   f. Vertical velocity (V_Z) given vertical acceleration and time.
   g. Height above ground level (H) of the bottom of the wheels.

The results for my two cases are shown in Fig. 3-181. You can see from these results that if the pilot chooses a more aggressive takeoff maneuver that would be permitted under emergency conditions (such as in wartime), the aircraft is quite capable of clearing the 50-foot obstacle in some 1,840 feet. While this might cause some damage to the tail cone, the takeoff distance is considerably shorter than the 2,090 feet that the YC-14 was credited with in the flight evaluation report.

Let me hasten to point out that rate of climb, with its associated climb angle (γ), reduces angle of attack to less than the pitch attitude with high performance STOL aircraft as you can surmise from Fig. 3-181. For the Case 1 example, as the YC-14 passes over the 50-foot obstacle, the pitch attitude (θ) is 23 degrees nose up. The climb angle is 14.7 degrees. Therefore, the better angle to use in calculating lift coefficient is $\alpha = \theta - \gamma$ or 9.3 degrees. When you add this connection between climb angle and angle of attack you immediately interject an iteration in the calculation, which I chose not to do for this introductory examination of YC-14 takeoff performance. My main points are that (a) climb after the wheels lift off is a calculation that should be made following F = ma, and (b) aircraft geometry cannot be excluded from the methodology.

Finally, let me remind you again that curves of lift coefficient versus angle of attack for several jet thrust coefficients are very configuration specific. I believe that wind tunnel testing of even the smallest, simplest powered force models is a mandatory step in estimating takeoff performance, even in the conceptual design phase.

Now let me proceed to a relatively brief discussion of the STOL landing performance demonstrated by the two AMST aircraft.

---

[150] This is not a very good assumption for accurate calculations.

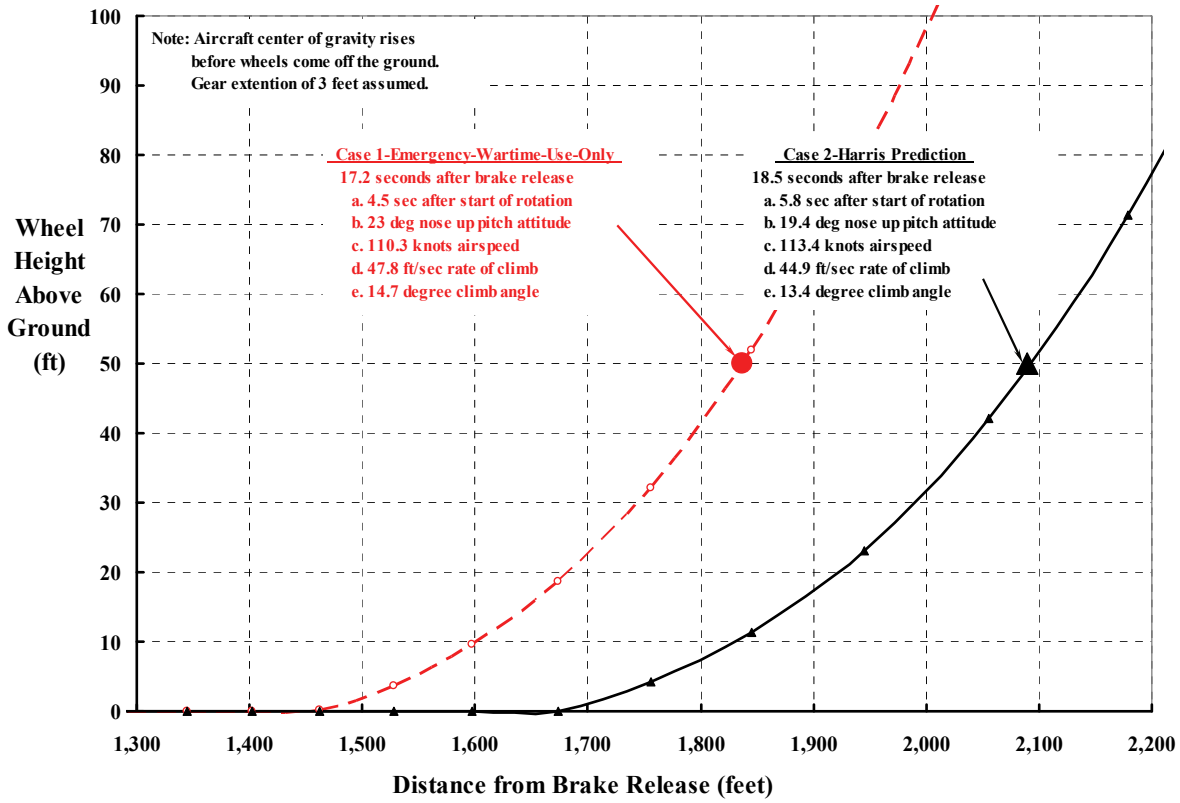

Fig. 3-181. Under "Emergency-Wartime-Use-Only" conditions, YC-14 pilots could expect to clear a 50-foot obstacle in about 1,840 feet from brake release by just *slightly* scraping the tail cone on the runway at liftoff.

3.10.2.2 Landing

Both the YC-14 and YC-15 were credited with meeting the landing specification as you can read from the flight evaluation reports. I have recorded this accomplishment on Table 3-17. Because both aircraft met the landing requirement, you will find considerably fewer report pages devoted to landing performance than to takeoff performance. However, there was considerable attention paid in the reports as to how the pilots felt about controlling the aircraft during approach. Therefore, let me start this discussion of landing with the approach and touchdown phase of the maneuver.

A key requirement was to pass over the 50-foot obstacle on a 6-degree glide slope. Stop and think about this requirement for a moment. A 6-degree glide slope means that a direct line from a height of 50 feet to *touchdown of the wheels* equates to a horizontal distance, while in the air, of 475 feet. Now these two very large, very advanced STOL aircraft had comparable wingspans of, say, 125 feet, and overall lengths of about 110 feet (see Table 3-17). The pilot's eyes were approximately 15 feet above the ground when the aircraft was at rest. In the air, the main wheels were uncompressed and dangling (I could not think of a better word) down another 3 feet. All in all, I would say that given that the objective was to hit a spot 475 feet from the 50-foot obstacle with an object weighing on the order of 150,000

pounds, it sounds rather difficult to me. An even greater restraint was that the landing gear for both aircraft was designed for only a vertical descent speed of about 13 feet per second. This meant that some flaring by the pilot must be made or he (or she) would have a landing much like Navy fighters make onto a carrier deck. In fact, the pilots of these large machines began the flare between 30 and 50 feet above the ground, which meant their eyes had virtually landed. The McDonnell Douglas YC-15 report [617] describes the whole landing problem in engineering terms shown here as Fig. 3-182. While necessary for accurate engineering calculations, Fig. 3-182 hardly conveys the practical view you see with Fig. 3-183. Here I have overlaid the scaled YC-15 profile on the 50-foot-high, 475-foot-long triangle under discussion. The pilot, while travelling at about 150 miles per hour, is looking at a horizontal distance about four times the length of the aircraft. I might mention in passing that a pilot of a 22-foot-long Piper Cub would view the triangular space as generous—particularly because his (or her) aircraft is only landing at about 35 miles per hour.

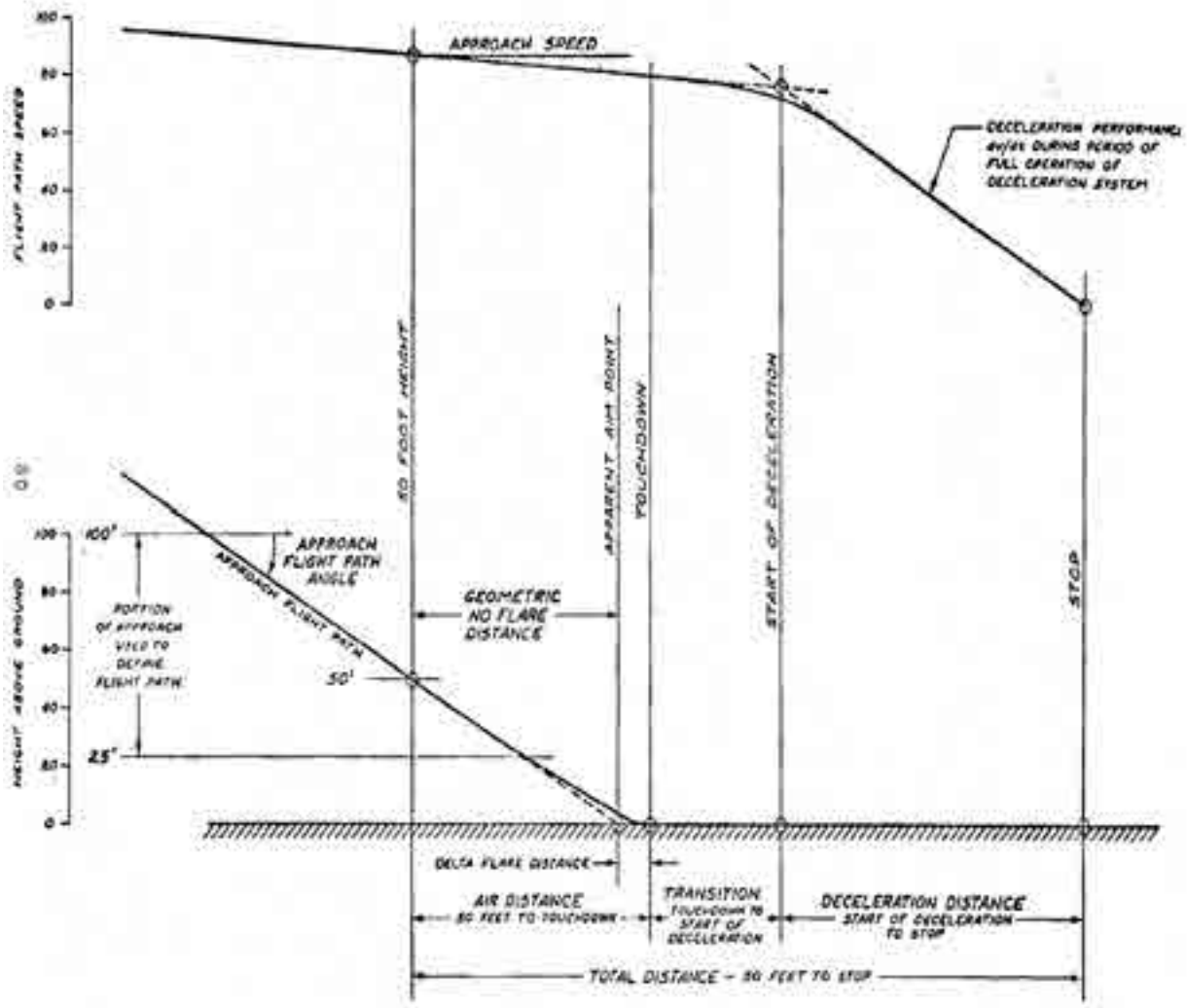

Fig. 3-182. Typical engineering geometry and definitions for a landing performance calculation [617].

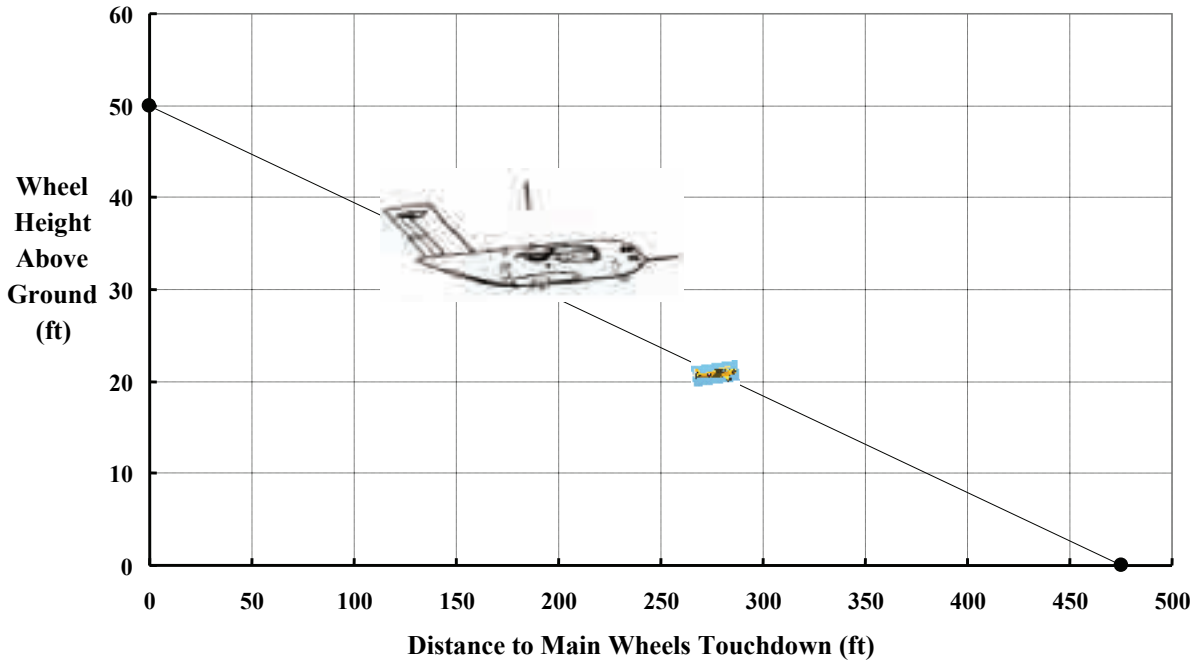

Fig. 3-183. Landing distances such as 50 feet and 475 feet, or glide angles like 6 degrees, must seem very small to pilots of large, turbofan-powered STOL aircraft. You will recall from Fig. 3-1 that commercial jets follow a 3-degree approach angle.

This size factor was quite significant because the ratio of wing height above the ground to wingspan was about 0.2 and made ground effect important. I found it quite interesting that pilots of the Boeing YC-14 said that ground effect influenced their flying during approach. The authors of the YC-14 report stated (with some italics by me) that

> "The STOL mode approaches were initiated from conventional traffic patterns and altitudes. After configuring the aircraft in Flap Detent 60 [degrees], the approach was initiated upon capturing a six-degree glidepath angle to the touchdown aim point. Various visual aids were used by the pilot to capture and maintain a six-degree approach angle. These aids are described in the Touchdown Dispersion section of this report.
>
> Analysis of the approaches conducted during the STOL mode landing performance tests indicated that the average approach angle at a height of 50 feet above the runway was 4.7 degrees. This decrease of the approach angle from the *specified six-degree approach* yielded longer air distances and, therefore, adversely affected the total landing distance. The fact that the average glidepath angle at 50 feet was significantly less than six degrees was attributed to a combination of factors. The pilots indicated some reluctance in holding the six-degree approach through a height of 50 feet because of the concern for exceeding the landing gear touchdown sink rate limits. Additionally, the aircraft exhibited positive ground effect, requiring the pilot to apply forward pressure on the control wheel as the aircraft neared the ground in order to maintain the approach angle. *Pushing on the control wheel as the aircraft neared the ground was initially uncomfortable, and hence for most of the landings the pilot allowed the approach angle to shallow as the aircraft approached the runway.* Twenty-one approaches were flown after the landing tests were performed to determine if the six-degree approach could indeed be held through a height of 50 feet above the runway without exceeding landing gear touchdown sink rate limits and to evaluate the ground effect characteristics. The average approach angle at a height of 50 feet above the runway for these

approaches was 5.6 degrees with an average touchdown rate of sink of -10.3 feet per second. (The minimum sink rate was -7.5 feet per second and the maximum was -12.7 feet per second.) The landing gear touchdown rate of sink limit for the STOL midmission gross weight was -13.5 feet per second (based on 80 percent of design limit). These tests demonstrated that the six-degree approach glidepath was difficult to obtain. *In order to present performance figures consistent with demonstrated approach angles, the landing performance in this report is based on a 5.6-degree approach angle.*

The average height above the runway at which flare commenced was 34 feet. For this report, flare *height is defined as the wheel height* at which the flightpath diverged from the tangent to the glidepath which existed at 50 feet above the runway. Thus, flare heights of only 50 feet and below were averaged. In order to minimize the air distance from a height of 50 feet to touchdown, the pilots attempted to minimize the manual flare. All STOL mode landings exhibited some degree of flare, however. *Even when the pilot made no flare inputs at all, the aircraft exhibited a flare due to ground effect.* In the majority of approaches conducted the flare observed was due to a combination of pilot inputs and ground effect."

The relationship of flightpath angle (γ_{50}) at 50 feet to the "air distance" (i.e., horizontal distance) traveled to touchdown (D_{Air}) is illustrated in Fig. 3-184. The basic geometry of what I would call the approach triangle is that

(3.185) $D_{Air} = K/\gamma_{50}$ where K is in feet and γ is in degrees.

Data obtained with the McDonnell Douglas YC-15 shows that flaring significantly increases air distance above what a straight line, slam into the ground, distance would be. Furthermore,

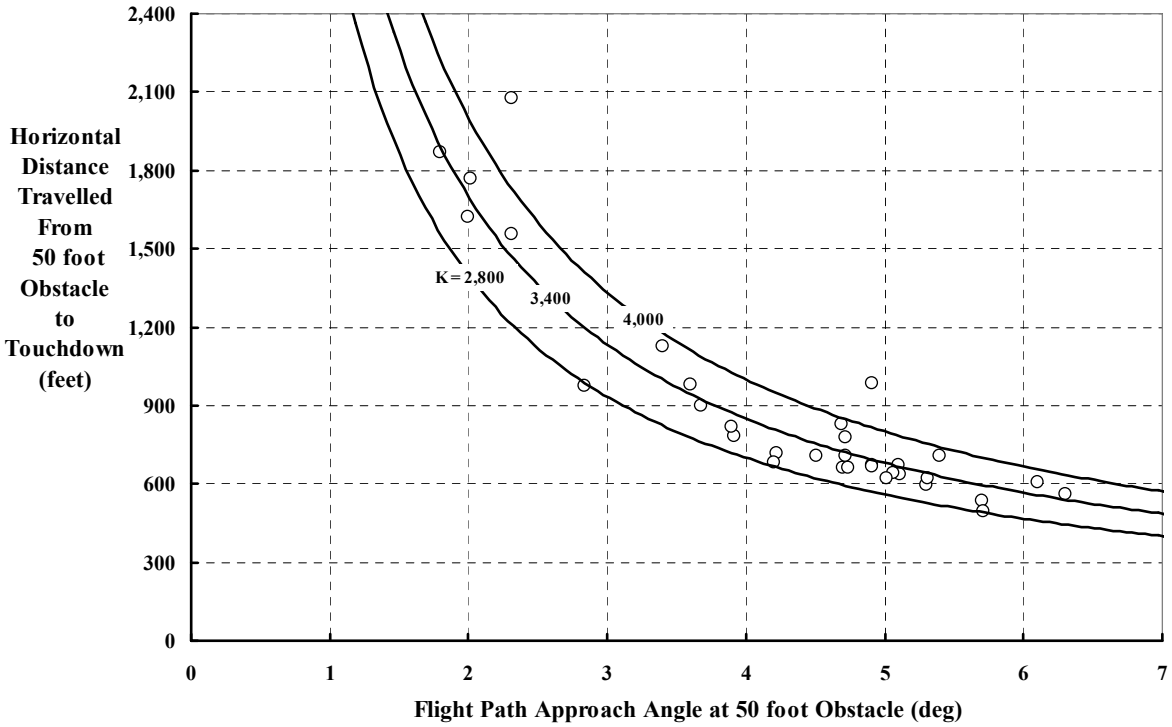

Fig. 3-184. Consistent landing distances to touchdown from the 50-foot obstacle require a very high level of pilot skill—at least with the two AMST STOL aircraft.

flaring was not consistent, and this led both STOL aircraft reports to discuss what was referred to as "touchdown dispersion." I have reduced the two touchdown dispersion discussions to the three curves you see on Fig. 3-184. The slam-into-the-ground approach behaves as if K equals 2,800 feet. The statistic mean of the YC-15 data is approximated with a K of 3,400 feet. The upper bound to the data is represented with K equal 4,000. In short, the touchdown aim point from the 50-foot obstacle can be missed—in my opinion—by as much as ±300 feet. In engineering terms, I suggest that the air distance is estimated by

(3.186) $D_{Air} = 3,400 \pm 600/\gamma_{50}$ where γ_{50} is in degrees.

The corollary to air distance is the rate of sink at touchdown. You will recall from the discussion surrounding Fig. 3-1 (which began this chapter 3) that the rate of sink (V_Z) is estimated from the flightpath velocity at touchdown (V_{TD}) much as air distance is. That is, if the flightpath angle at touchdown (γ_{TD}) is known, then the sink rate (assuming γ_{TD} is a small angle) will be

(3.187) $V_Z = (1.687 V_{FP})(\gamma_{TD} / 57.3) \approx 0.03 (V_{FP})(\gamma_{TD})$

where (V_Z) is in feet per second with (V_{FP}) in knots and (γ_{TD}) in degrees when the conversion constants are applied. Equation (3.187), when graphed as shown in Fig. 3-185, gives you a good sense of the rather small box the pilot must maneuver in so that the aircraft is not damaged at touchdown.

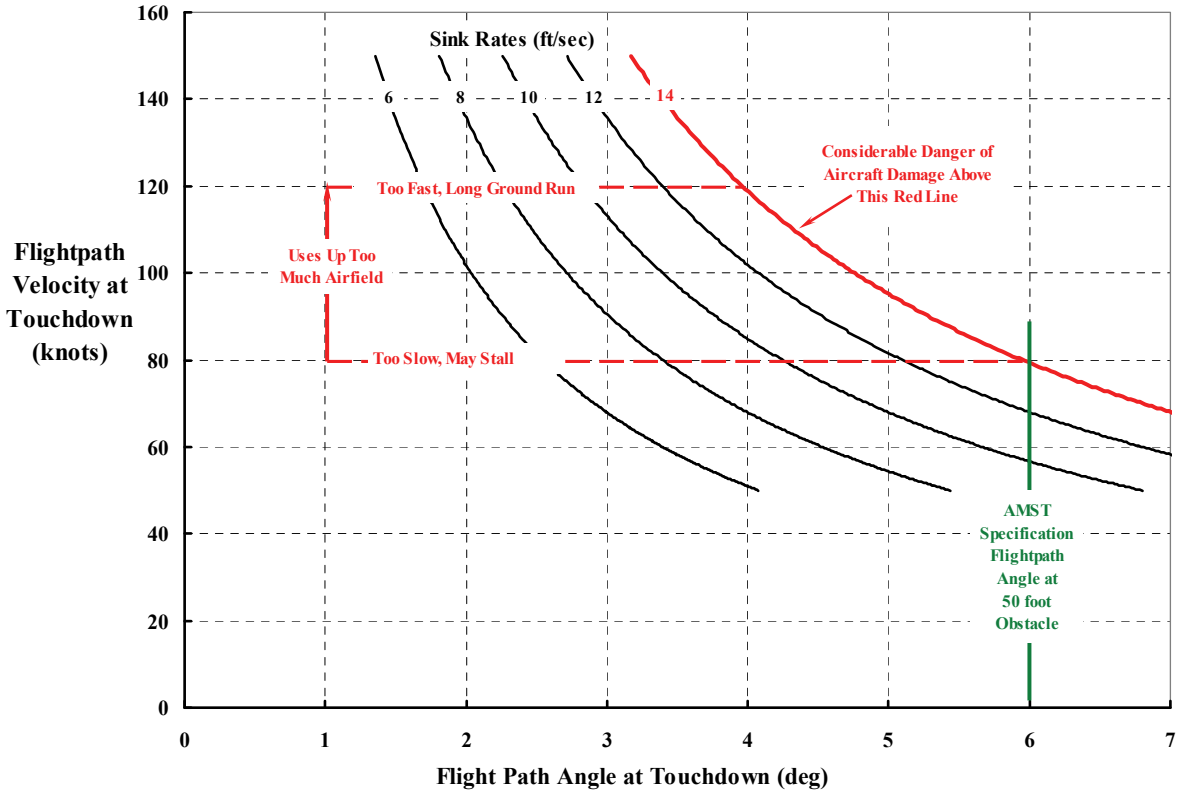

Fig. 3-185. AMST STOL aircraft pilots had to stay within a pretty narrow window to avoid overshooting or undershooting the touchdown point.

This brings me to the landing gear itself. In Jack Wimpress' retelling [400] of the Boeing YC-14 program, he mentioned several key points about the aircraft's gear. He wrote that

> "The landing gear was one of the fundamental features of the airplane that made it a good STOL configuration. As discussed previously, it was desired to make the STOL landings without a flare so that the airplane could be positioned close to the approach end of the runway at touchdown. This requirement led to a very long stroke on the landing gear and to its trailing arm configuration (Fig. 31). The stroke actually was about 3 ft between gear touchdown and gear compressed. The other requirement for the landing gear was the ability to support operations on a field having a CBR of 6. A CBR of 6 is a surface hard enough to drive a car on but one that can be penetrated easily with a shovel. It was required that the airplane be able to make 400 passes on that kind of a field without destroying the surface. The main landing gear consisted of a separate support for each pair of wheels. Each pair of wheels was attached to a trailing arm which, in turn, was fastened to a vertical support member anchored rigidly to the body. An oleo strut connected each trailing arm to a movable support member attached to the fuselage. Gear retraction was done by moving this upper support for the oleo strut, which pulled the trailing arm and wheels into the wheel well directly above their normal operating position.
>
> As the details of the landing gear developed, the pod to enclose them kept getting bigger and bigger. Considerable wind tunnel testing was done to get the drag of this pod as low as possible. It was found that there was a good deal of mutual aerodynamic interaction between the gear pod shape and the aft body shape, so that relatively small changes in the gear pod could have large effects on the drag. Here again, Boeing did not do as much development work as they should have done during this design refinement period and, as a result, the landing-gear pod required modification during flight test."

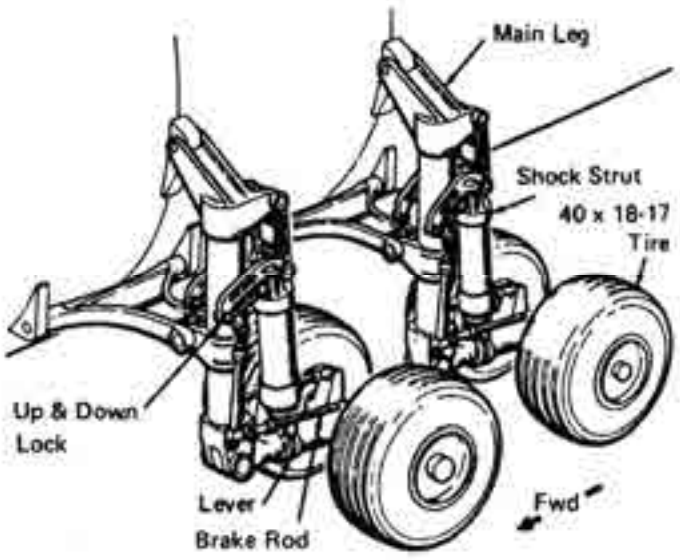

Fig. 3-186. The port-side main landing gear of the Boeing YC-14 weighed 4,461 pounds, and the nose gear weighed 1,855 pounds; the total weight of all the landing gear was 10,717 pounds (or just under 9 percent of the aircraft's weight empty). The parasite drag area (fe = D/q) of the three gears was on the order of 48 square feet. The main landing gear had a stroke of about 36 inches. It could withstand high sink rate landings and roll over 6-inch rocks or curbs without damage [400, 631].

As you have read, the influence of the ground on both advanced STOLs was quite noticeable. Considerable quantitative data about this ground effect was uncovered during the AMST program. The performance data, as you can read in the Air Force evaluation of the McDonnell Douglas YC-15 [617], included theoretical development and its comparison to test results. I found it quite interesting to learn from the YC-15 report that

> "An investigation of the effect of ground proximity on the YC-15's aircraft aerodynamics, called ground effect, was conducted during the program. Doctor E. K. Parks, a Professor of Aeronautical Engineering at the University of Arizona, was contracted by NASA and assigned to the AMST JTF to study the ground effects of the YC-15. The following is a summary of the ground effect work Dr. Parks presented in YC-15 AMST Data Transmittal 086-JTF-36, 17 August 1976. This work applied the theories of Biot-Savart and Blasius to ground effect to develop relationships from which to estimate the change in aircraft aerodynamics while in ground proximity. This work also developed procedures for extracting ground effect data from flight test results so that comparisons between the theoretical estimations and actual test results could be made."

Four figures, such as Fig. 3-187, showing the increments in lift and drag coefficients as a function of wing height (h) divided by wingspan (b) are included in the YC-15 report. A fifth figure shows that ground proximity affected the pilot's airspeed instrument reading by as much as ± 2 knots. Let me point out that with the dangling wheels just touching the top of the 50-foot obstacle, the wing is about 65 feet above the ground. This means that the YC-15, with its 110-foot wingspan, has an h/b ratio of just under 0.6, therefore the aircraft is already experiencing quite measureable—and pilot noticeable—ground effects.

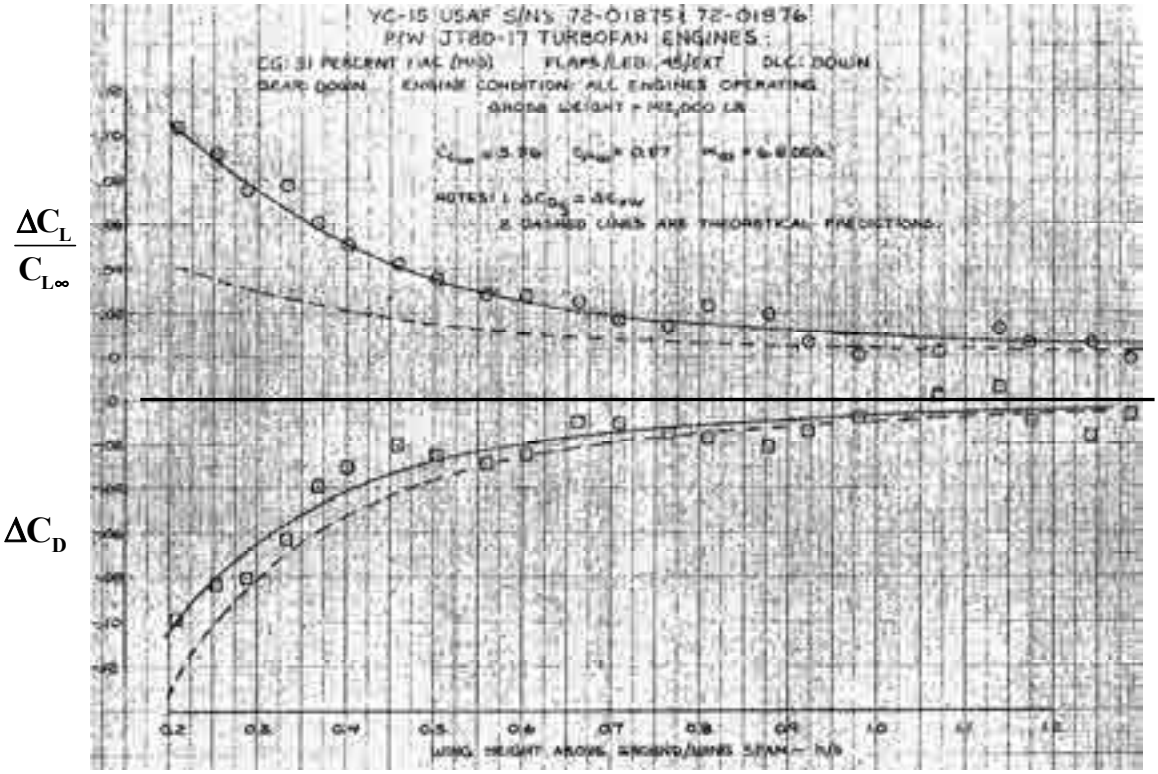

Fig. 3-187. Ground effect analysis of the McDonnell Douglas YC-15's aerodynamics was contributed by Professor Edwin Parks of the University of Arizona [617].

To me, Professor Parks' work is of significant historical interest, so let me include the words directly from the YC-15 report (with only minor condensing). The report states that

> "For most aircraft, ground effect produces a positive lift increment as the aircraft nears the ground, providing a ground cushion during a landing maneuver. However, wind tunnel measurements and analytical predictions indicated that at large values of lift coefficient ground effect may become negative, resulting in a 'suckdown' rather than a cushion during landing. Powered lift STOL configured aircraft, such as the YC-15, have the capability of developing lift coefficients sufficiently large for certain configurations to produce negative ground effect. The effect that the 'suckdown' would have on the ability of the pilot to control the aircraft during landing was an area of concern.
>
> To better understand ground effect, it is advantageous to develop at least a simplified aerodynamic model of the phenomena. One method of simulating a ground plane in the wind tunnel is to place an identical model in an inverted position on the opposite side of the tunnel centerline from the test model (figure 22). Thus, the ground effect produced by flying an airplane close to the ground is the same as that produced by an inverted image model of the airplane flown in free air.
>
> An elementary potential flow representation of a lifting wing in free air is made by using a horseshoe vortex in a uniform flow (figure 23). A simple representation of a lifting wing in ground proximity is made by considering the flow induced by a mirrored horseshoe vortex placed symmetrically below the ground surface.
>
> The lift of the airplane in ground effect is affected by both the trailing vortices and bound vortex (figure 24) of the mirrored image. The image trailing vortices produce upwash at the wing and hence reduce the induced angle of attack of the wing. Figure 22 sketches the ground induced upwash. Reduction of the downwash reduces the angle of attack of the wing required to produce the same out of ground effect (OGE) lift coefficient, CL0, by an amount $\Delta\alpha$. If the same angle of attack is maintained as OGE, then the lift coefficient will be increased by an amount ΔCL (figure 25). This increase in the lift coefficient caused by the effect of the image trailing vortices can be estimated from the following equation:

$$\frac{\Delta C_L}{C_{L\infty}} = \frac{1}{\pi^2 AR\sqrt{1+25.94\left(h/b\right)^2}}\left[\frac{8\left(dC_L/d\alpha\right)_\infty}{\pi\sqrt{1+25.94\left(h/b\right)^2}} - \frac{C_{L\infty}}{2\left(h/b\right)}\right]$$

> This equation indicates that negative ground effect will occur when CLw is large and/or the slope of the lift curve, is small. Negative ground effect will therefore be associated with airplanes of low effective aspect ratio and with high CL capabilities. Powered lift STOL airplanes fall in this category.
>
> Ground effect also affects aircraft drag. Since induced drag is a product of the induced angle of attack and the lift, the reduction in induced angle of attack caused by the image trailing vortices also causes a reduction in induced drag. The image bound vortex reduces the free air velocity in which the airplane is immersed. The skin friction drag is therefore reduced (figure 25). However, the image bound vortex also modifies the longitudinal pressure distribution on the airplane and hence produces a drag modification.
>
> A change in aircraft pitching moment results from ground effect. The image trailing vortex induced upwash modifies the flow field of the airplane wing-body combination and hence causes a change in the pitching moment. The downwash at the tail is reduced by the ground constraint. Up elevator is therefore required to trim the airplane in ground effect."

Perhaps even more interesting is the flight test procedure Professor Parks describes so that data could be obtained for the test-versus-theory example you have with Fig. 3-187. In this regard, he wrote,

> "Ground effect data were collected during both landing approaches and a specialized maneuver designed specifically to investigate ground effect. Several landing approaches were flown 'hands off' with the SCAS in attitude command and at fairly low sink rates. Power changes were not made during these approaches in order to keep C_μ constant. The Attitude Command function of the SCAS served to hold attitude, and hence angle of attack, constant. Except for the conditions stated above, the approaches were flown in the normal profile. In order to obtain a longer time span in which to collect the ground effect data, a specialized maneuver was designed. The aircraft was first stabilized in a very low sink rate descent at about 200 feet above the Rogers Dry Lakebed, and then was allowed to descend to the surface. Power was not altered after the aircraft was stabilized. SCAS was also employed to keep attitude and angle of attack constant."

In my view, Professor Parks' concluding remarks are the most informative. He wrote,

> "The data on figure C46 [Fig. 3-186] were collected at a C_L of 3.36 and Cu_0 of 0.97, numbers very close to the maximum experienced during landing, and as seen, the ground effect is quite positive. In fact, positive ground effect was demonstrated throughout the program. Application of the theoretical equation for $\Delta C_L/C_L$ indicates that the ground effect for the landing configuration is positive throughout the C_L and C_μ range expected for the YC-15 during landing.
>
> The reduction in airplane drag in ground effect is also evident from these figures. This reduction in drag usually led to a slight increase in airspeed while in ground effect.
>
> The change in aircraft pitching moment in ground effect was found to be in the nose down direction for the conditions tested. With the SCAS in Attitude Command, up elevator was always commanded upon entry into ground effect to overcome the ground effect induced change in pitching moment. Sufficient elevator authority was available for the conditions tested to overcome this change in pitching moment.
>
> The results of the investigation into ground effect indicate that relatively good agreement exists between the theoretical predictions of the change in airplane aerodynamics due to ground effect and the actual flight test derived effect. *While it is evident that high C_L can lead to negative ground effect, the YC-15 did not produce C_L's large enough for typical landing conditions to produce a negative ground effect.*"

Professor Parks' analysis followed the most basic aerodynamic theory that was being developed as far back as the early 1920s, both in Germany [632] and the United States [633], however, I have never seen his concise formula in my career. The major shortcoming is, of course, that the wing is assumed to be ideally loaded with an elliptical bound circulation distribution. Powered lift aircraft really do not have elliptical bound circulations at all, as you saw with Fig. 3-20 on page 352. Still, Professor Parks' analysis and simple equation captures the YC-15's measured data trend. And you should remember that the AMST program included flight testing time for a fundamental aerodynamics research topic, which shows—I think—considerable clear thinking by program management.

To conclude this discussion about ground effect, Boeing YC-14 data [618] provided one figure showing that the aircraft incurred ground effects very similar to the YC-15.

The last phase of landing is the ground run. It is here, I think, that the Boeing YC-14 outshone the McDonnell Douglas YC-15, although both excelled when compared to all preceding STOLs. The advantage went to the YC-14 because of several knots slower touchdown speeds and greater reverse thrust-to-weight ratios. You will recall from the preceding discussion of propeller-driven aircraft landings and from Appendix H just how important the touchdown velocity is. After that, the brake system must be overdesigned, and thrust reversal is an absolute must. Both of these very advanced STOLs incorporated these fundamental requirements. In addition, both aircraft had a feature whereby, as soon as the wheels began to spin up, lift spoilers automatically deployed so that more of the aircraft's weight was on the wheels much faster than if the pilot had to accomplish this manually. This feature, among others, was aimed directly at reducing the time necessary to maximize the deceleration force. Keep in mind that at touchdown speeds around 85 to 90 knots, these aircraft were using up runway at the rate of about 150 feet per second. With respect to brakes, both aircraft had equivalent rolling braking coefficients (μ) well above 0.40 at their respective design mid-mission weights.

3.10.2.3 The STOL Aircraft Lift-Drag Polar

The decades leading up to the AMST program saw a continual refinement in the way aerodynamicists created and presented lift-drag polars quantifying low-speed, powered lift performance. Not only did symbology get more or less settled on, but theory and test became more comparable. And, I think, the McDonnell Douglas YC-15 flight test data established the best way to fly a turbofan STOL aircraft so that a performance map of lift and drag could be derived. A year later, YC-14 pilots flew—even more carefully—flight after flight of low-speed climbs and descents, as well as trimmed level flights. When you read the YC-14 flight evaluation report, you will see many graphs of experimental points compiled into very quantitative trends with quite smooth curves drawn through the data. Virtually all of the key configurations such as, first and foremost, engine out, followed by several flap deflection angles in combinations with many power (i.e., thrust) settings, were tested. In my opinion, the Air Force YC-14 report [618] should be used as a textbook for budding aircraft engineers. Therefore, let me include a relatively short discussion of a STOL aircraft's lift-drag polar using the Boeing YC-14 as the example.

I think of the low-speed lift-drag polar as a STOL performance map for low-speed operations. You see such a map here as Fig. 3-188. You will recall that the Boeing YC-14 obtained its maximum STOL performance during the approach phase with the landing gear down and with both GE CF6-50D turbofan engines blowing their jet exhausts over the wing (i.e., upper surface blowing or USB). The flaps were deflected 60 degrees, and the jet thrust was bent both downward (i.e., powered lift) and rearward (i.e., propulsive force). The Air Force report assigned the symbol (C_J) to the jet thrust, which was the nondimensional engine force coefficient calculated as

$$C_J = \frac{T_{eng1} + T_{eng2}}{\left(\frac{1}{2}\rho V_{FP}^2\right) S_W}.$$

As you can see from Fig. 3-188, the propulsive force component easily overcomes the positive drag of the aircraft's frame so that a net negative drag is available for acceleration and/or climbing. Before continuing, take a look at Fig. 3-189. This sketch shows that the angle of attack (α) in flight test is the sum of the aircraft's glide angle (γ) and its pitch attitude (θ). It is also important to remember that while the flap may be deflected 60 degrees trailing edge down (δ_F), it is not at all clear just how much of the engine's jet thrust is actually directed downward and how much is directed aft. That is why you see by my sketch that the resultant jet thrust acts at the aerodynamic angle (δ_J). Lastly, keep in mind that there can be some loss in thrust as the exhaust travels from the engine nozzle rearward and then turns through the aerodynamic angle. These are just some of the major factors acting to reduce the maximum powered lift performance from ideal.

Based on the sketch in Fig. 3-189, you have the fundamental lift-drag polar forces defined as

$$\begin{aligned} \text{Aircraft } C_L &= \text{Airframe } C_L + C_J \sin(\alpha + \delta_J) \\ \text{Aircraft } C_D &= \text{Airframe } C_D - C_J \cos(\alpha + \delta_J) \end{aligned} \quad (3.188)$$

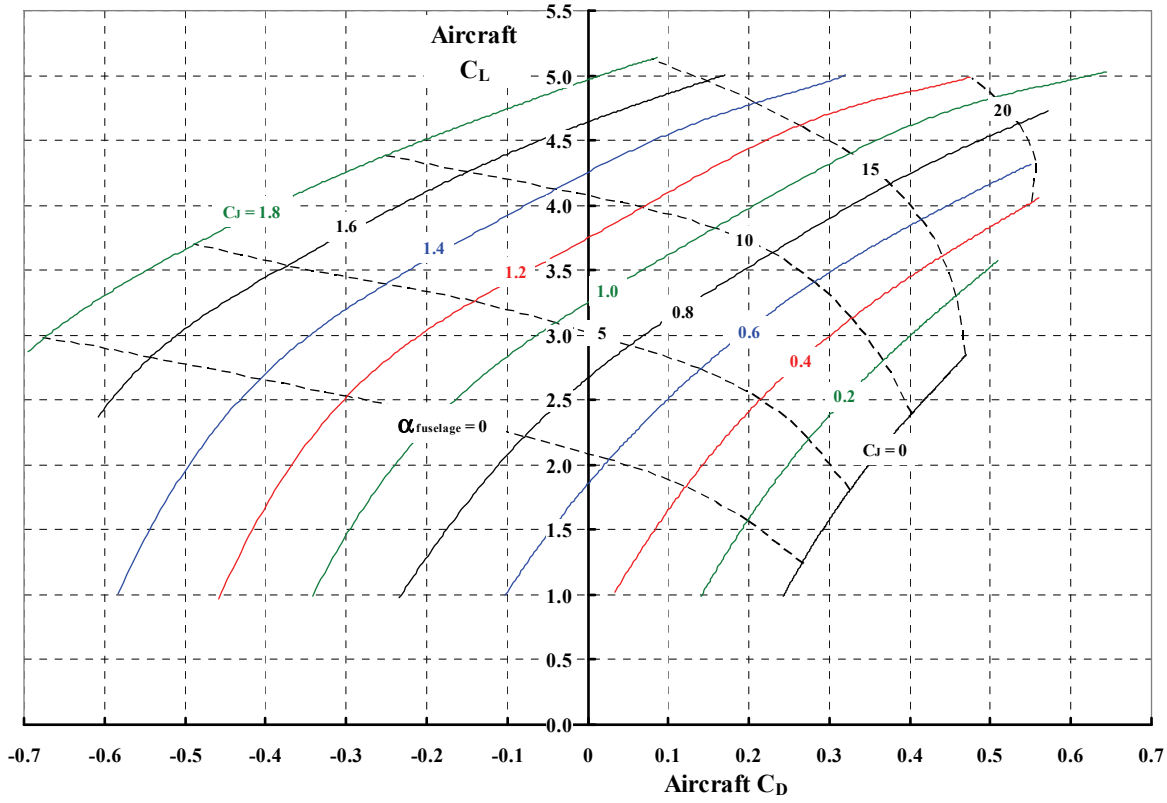

Fig. 3-188. The Boeing YC-14 STOL performance map for low-speed operations; landing gear down and flaps deflected 60 degrees trailing edge down.

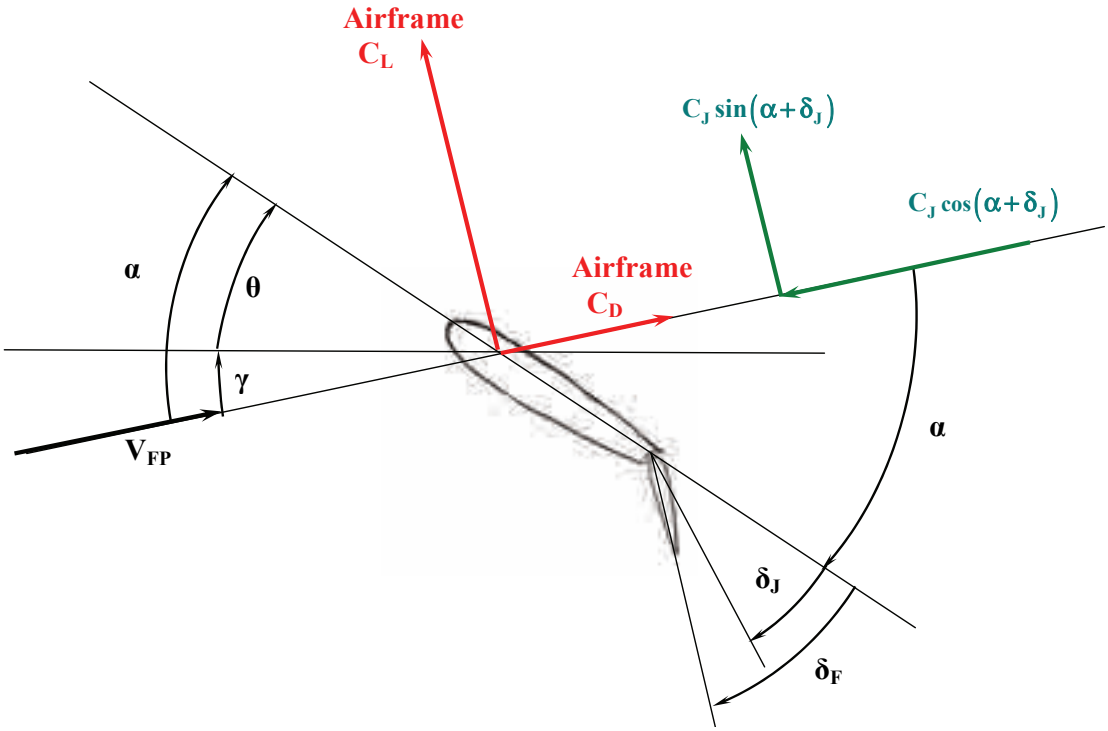

Fig. 3-189. A handy sketch.

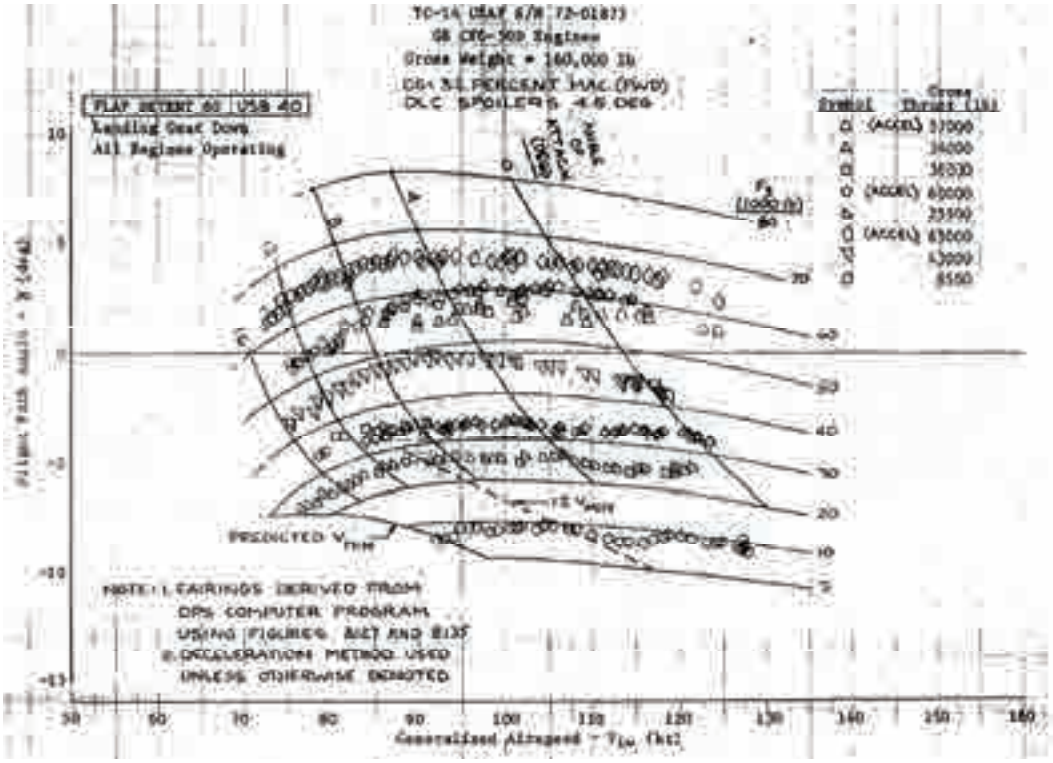

Fig. 3-190. The Boeing YC-14 performance map for low-speed operations.

Perhaps you are curious as to how the performance map in Fig. 3-188 was obtained from flight test data. The answer lies with the "raw data" shown in Fig. 3-190. Here you see that the pilot repeatedly flew a speed range at a constant engine thrust. The aircraft is in steady level flight (i.e., flightpath angle equals zero) at only two speeds and only for a small range in engine thrust. Otherwise, the aircraft is either climbing or descending. Both aircraft pitch angle (θ) and flightpath angle (γ) were quite accurately measured so that the angle of attack (α) could be computed. In fact, the angle of attack was available from several sensors. By using a computer program called DPS, a sort of statistical curve fitting program, the flight test data could be both interpolated and extrapolated. Then the whole data set was nondimensionalized by dynamic pressure and wing area, and the smooth curves of Fig. 3-188 were exposed.

Now let me bring your attention to several things you can learn from the performance map. I have repeated the performance map in Fig. 3-188 here as Fig. 3-191 with several labels removed to avoid clutter. The first thing to notice is that maximum climb performance after a ground run, and very slow speed approach performance prior to touchdown, are points lying along a straight line defined by

$$\gamma = \frac{180}{\pi} \arctan\left(\frac{C_D}{C_L}\right) \quad \text{in degrees}. \tag{3.189}$$

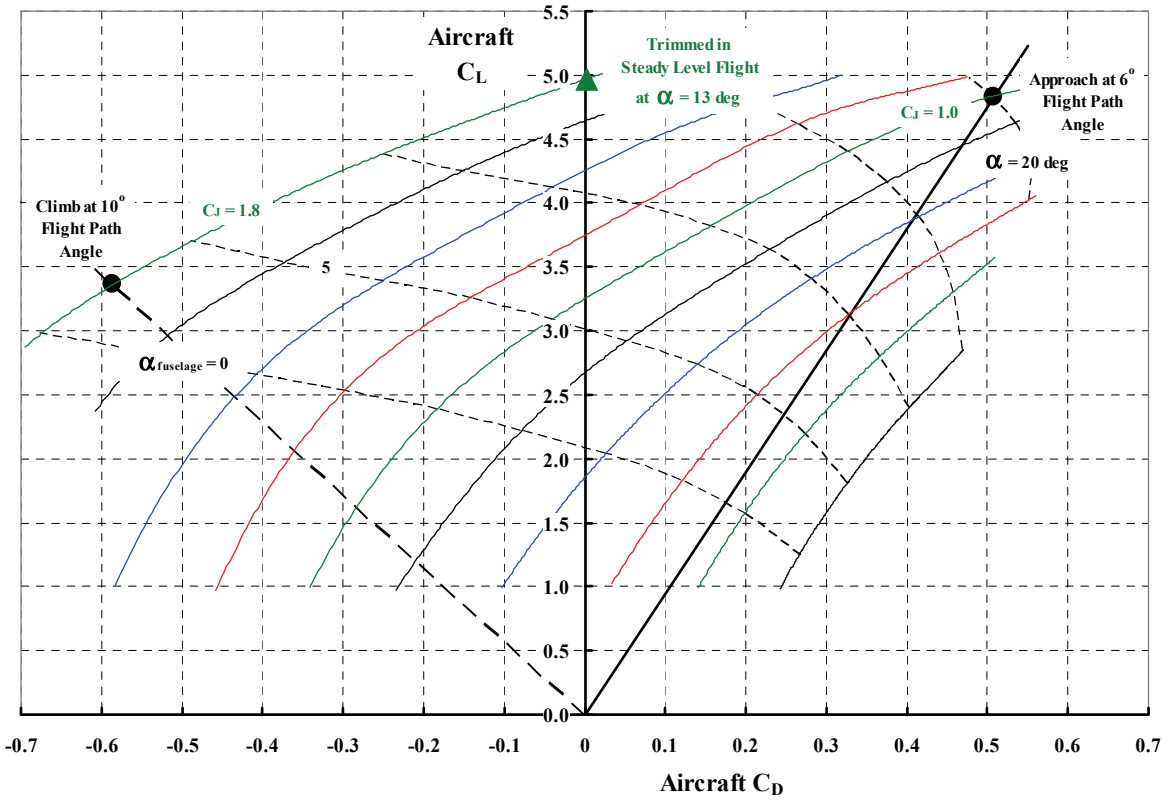

Fig. 3-191. The STOL performance map can be used to quickly identify key operating points during conceptual design.

In the approach phase, for example, the more drag the aircraft has for a given weight, the slower the machine will be flying and the steeper the approach angle can be. Of course, safe slow-speed flying requires excellent flying qualities as well as speed margins for the case when an engine fails. However, the minimum slow speed based solely on performance capability can be calculated quite easily as follows. The Boeing YC-14 was to have a mid-mission gross weight of 160,920 pounds when landing at sea level with the outside air temperature at 103 ^{o}F, which is an air density (ρ) of 0.002191 slugs per cubic foot. The upper limit data point along the 6-degree flightpath angle line shown on Fig. 3-191 is at about an aircraft lift coefficient of 4.8 with an angle of attack (α) of 20 degrees and the engines thrusting at a force coefficient (C_J) of 0.8. Thus, the airspeed is calculated from

$$(3.190)\quad V_{FP} = \frac{1}{1.687}\sqrt{\frac{2W}{\rho S_W C_L}} = \frac{1}{1.687}\sqrt{\frac{2(160,920)}{0.002191(1762.4)(4.8)}} = 78 \text{ knots},$$

which is a dynamic pressure (q) of 19 pounds per square foot. Of course, the actual approach speed that the pilot would be more comfortable flying could be 5, or even 15, knots higher.[151] The total engine thrust available must be at least 26,800 pounds based on

$$(3.191)\quad T_{eng1} + T_{eng2} = [qS_W]C_J = 19 \times 1,762.4 \times 0.8 = 26,788 \text{ pounds},$$

which is a throttling down of the YC-14's engines to about one-half maximum thrust available.

The maximum steady-state climb performance point can be determined rather quickly as well. This point establishes the aircraft's climb capability somewhat beyond the 50-foot obstacle. This point depends on having the most total thrust (T) per pound of weight (W). This means that the ratio of maximum C_J to C_L is equal to T divided by W. Now the maximum total thrust output from the Boeing YC-14's engines on the sea level hot day was on the order of 86,100 pounds. And the performance map states that the maximum C_J is approximately 1.8. Therefore, the lift coefficient for the climb angle beyond the 50-foot obstacle must be

$$(3.192)\quad C_L = \frac{W}{T_{eng1} + T_{eng2}}(\text{Max. } C_J) = \frac{160,920}{86,100}1.8 = 3.36,$$

which has a corresponding aircraft drag coefficient (C_D) of – 0.586. Following Eq. (3.190), the flightpath velocity will be about 93 knots, and from Eq. (3.189), the climb angle will be just under 10 degrees.

From these examples, I think you can see that a performance map offers a quick and direct way to estimate slow-speed performance during the conceptual design phase.

Another thing you can establish from a performance map is the aerodynamic angle (δ_J) that the engine thrust has been bent to by the flap deflection. Again, let me repeat Fig. 3-188 so the picture remains uncluttered. Following Fig. 3-192, you can easily see that

[151] I recall one pilot telling me that he added 5 knots for every child he had. He had four children.

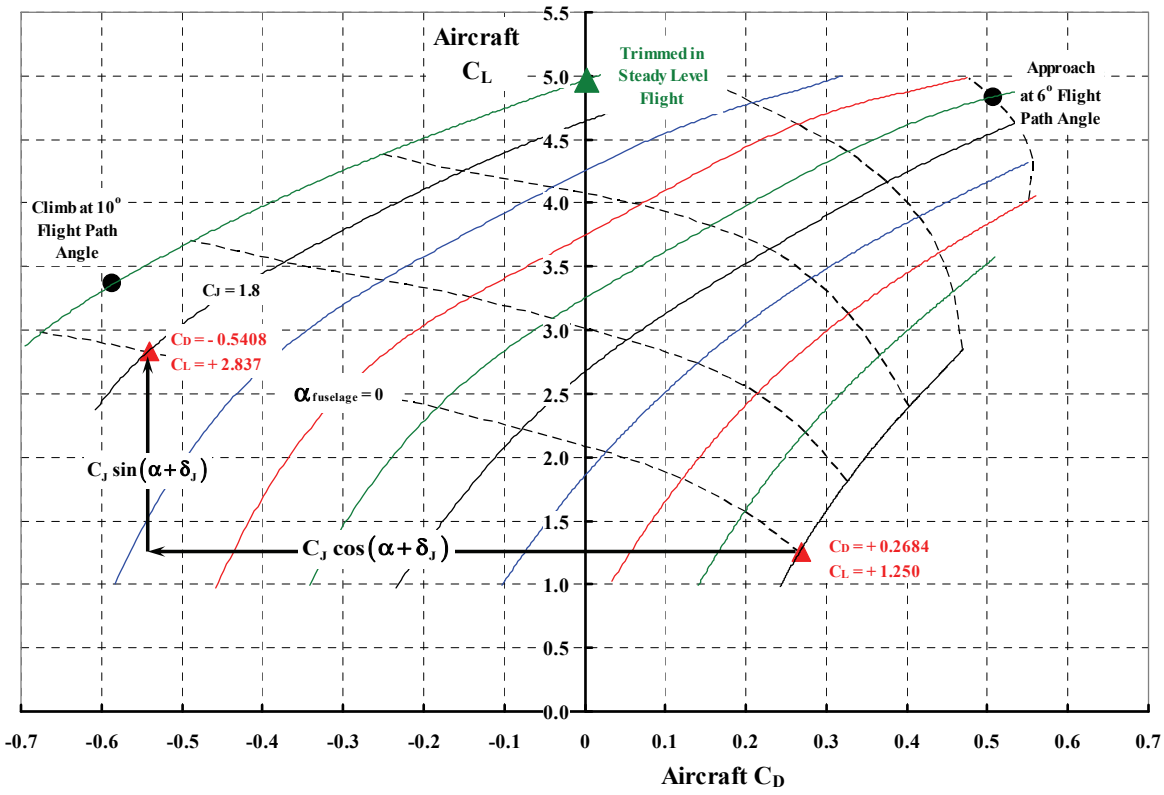

Fig. 3-192. Even though the flap is deflected 60 degrees trailing edge down, the USB system only turns the YC-14 engines' thrust through 36 to 40 degrees.

$$(3.193)\quad \frac{+C_J \sin(\alpha+\delta_J)}{-C_J \cos(\alpha+\delta_J)} = \frac{2.837-1.250}{-(-0.5408-0.2684)} = \frac{0.587}{0.8092} = 0.7254 = \tan(\alpha+\delta_J),$$

and therefore you have

$$(3.194)\quad \alpha+\delta_J = \frac{180}{\pi}\arctan(0.7254) = 36 \text{ degrees}.$$

But the angle of attack is 0 degrees for this numerical example, so you have an aerodynamic angle of 36 degrees. Thus, even though the flap is deflected 60 degrees, trailing edge down, the USB system is only able to turn the engine thrust through 36 degrees. You might notice the boxed note saying "Flap Detent 60 USB 40" on Fig. 3-190.

Lastly, let me address the question, Just how efficient is the Boeing YC-14 with its USB configuration? To answer this question, let me compare the flight test derived lift-drag polar to what I believe is the ideal lift-drag polar. *I believe George Schairer's approach that you read about in section* 3.3.7 *defines the ideal.* Now consider Fig. 3-193, and first study the heavy, dashed red line that begins at zero aircraft lift with an aircraft drag coefficient of +0.2. This is Helmbold's theory, which you learned about in the beginning of this STOL aircraft discussion (section 3.1). Now shift your attention to the solid blue line where the jet blowing

coefficient (C_J) is 1.4. Notice that I have made a *slight* extrapolation of the flight test data down to zero lift with the blue line. This extrapolation yields an aircraft drag coefficient of – 0.61. You can immediately sense that with a jet thrust coefficient of 1.4 overcoming an airframe drag (C_D) of + 0.2, the aircraft drag coefficient should have been more on the order of – 1.2, not the – 0.61 that was measured. On this basis, I think the USB concept demonstrated with the YC-14 was only about 60 percent of ideal. In fact, using Mr. Schairer's theory with a jet thrust coefficient of 0.82 creates a curve quite comparable to the measured data. To emphasize this point about test versus ideal, I found that the experimental data with a jet thrust coefficient of 1.8 can be approximated by Mr. Schairer's ideal theory using a coefficient of 1.16.

Just think about this last point for a moment. Suppose you were in the very early stage of concept design. You could easily create a complete STOL performance map with Mr. Schairer's theory just by assuming that the design will have a 60-percent efficiency. You would only need to define the wing aspect ratio and the aircraft drag coefficient at zero lift, consider selection of the engines, and assume that the landing gear is down and the flaps are set, as in this example, at 60 degrees, trailing edge down for landing. The task then would be to evolve the configuration in more detail.

Now let me go on to the third major AMST requirement, which dealt with ferry range.

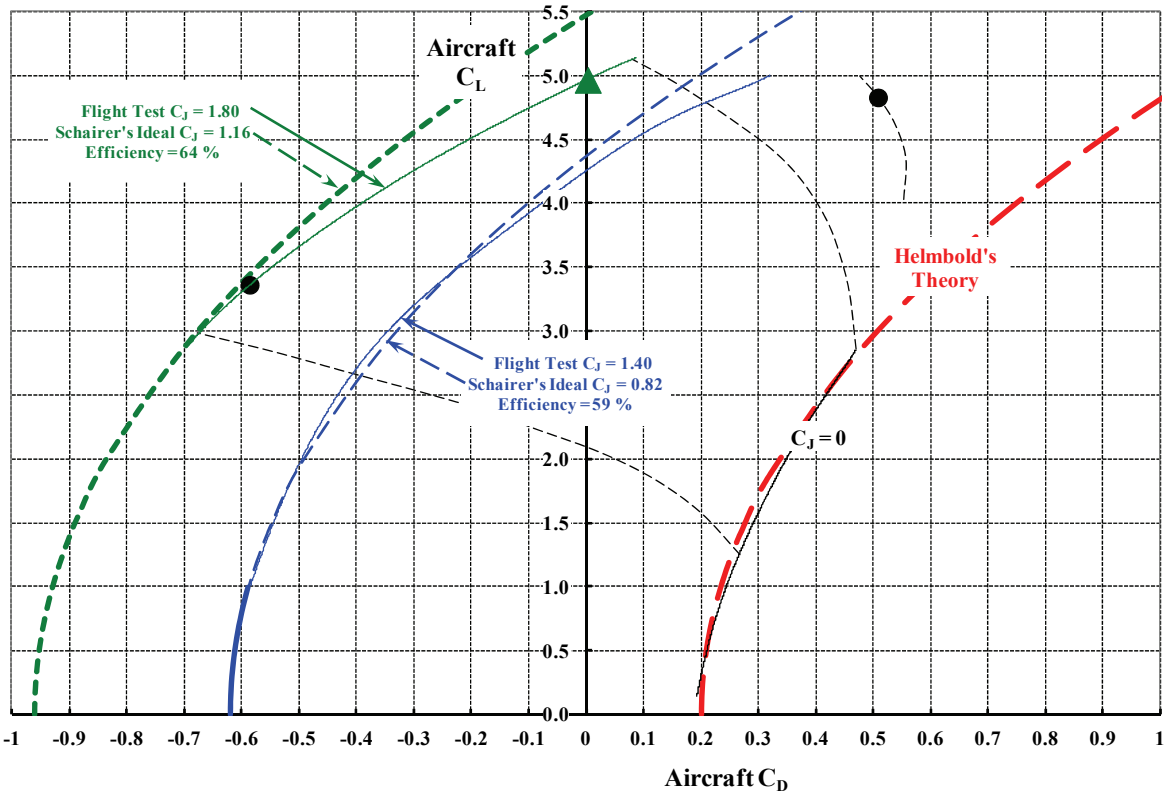

Fig. 3-193. Bending a jet engine's exhaust downward even with a 60-degree deflected flap does not appear very efficient when compared to Mr. Schairer's ideal theory.

3.10.3 Self Deployment Ferry Mission

In addition to exceptional STOL performance, the Air Force demanded nothing less of both Boeing and McDonnell Douglas than an aircraft that could ferry itself worldwide—without in-flight refueling. The requirement read as follows (my italics): "A zero payload, 2,600 nautical mile, self deployment ferry mission without refueling *with fuel contained only in the wings*." Furthermore, they expected high-altitude cruise speeds in the Mach number range above 0.6. As it turned out, the Boeing machine was credited with a ferry range of 2,363 nautical miles, although with drag reduction modifications, the range was estimated by the Air Force evaluators to increase to 2,422 nautical miles. The McDonnell Douglas YC-15 was credited with only 1,760 nautical miles, although with the addition of extra fuel tanks in the fuselage, the range requirement could be nearly met. The YC-15 with a modified wing [624] was predicted to have a ferry range of 2,426 nautical miles. I suspect that the Air Force evaluators were not particularly concerned about these estimated ranges because fixed-wing transport designers are well versed in improving cruise speeds and fuel efficiency above shortfalls found with their X models, their Y models, and even their low-rate production models. You only need reread the Lockheed C-130 story to have a perfect example.

Table 3-18 shows the ferry range mission profile for both of the AMST aircraft. I constructed this very interesting summary from the two Air Force flight evaluation reports. (While I retained the rounding off of the numbers to the nearest pound, I did not have my heart in it because it is clear that the flight test data is hardly good to better than ±1 percent!)

Rotorcraft advocates might be interested in note 2 on Table 3-18. This note states that the long-range cruise phase of the mission was based on flying at a constant ratio of weight (W) to air pressure (δ), and at a constant Mach number. Rotary wing performance engineers work almost exclusively using only air ambient density (ρ) or density ratio ($\sigma = \rho_{am}/\rho_o$), which

Table 3-18. YC-14 and YC-15 Ferry Range Flight Profiles

Bookkeeping Item	YC-14	YC-15
Operating weight empty	123,867	105,378
Mission fuel(1)	62,259	51,961
Engine start gross weight	186,126	157,339
Fuel used for ground operations, takeoff, and acceleration to climb speed	– 2,209	– 2,840
Fuel used to climb to cruise altitude and distance traveled (nm)	– 4,001 57	– 4,742 73
Gross weight at beginning of cruise	176,916	149,757
Fuel used in cruise, at Mach number and altitude range (1,000 ft)(2)	49,823 0.64 35 to 45	39,183 0.65 35 to 42
Gross weight at end of cruise and distance traveled (nm)	127,093 2,306	110,574 1,687
Fuel held in reserve(3)	6,226	5,196
Cruise nautical miles/cruise fuel used (nm/lb)	0.0462	0.0380

Notes: 1. Fuel used includes a 5-percent factor for conservatism.
2. Cruise flown at optimum W/δ and Mach number.
3. Reserve requirement is 10 percent of initial mission fuel.

they calculate from measured pressure and temperature at the flight condition of interest. This is quite reasonable because their aircraft class hardly ever encounters flight speeds that make compressibility a significant factor.[152] In contrast, fixed-wing performance engineers deal continually with cruise flight conditions where compressibility effects can seriously degrade aircraft class performance. This group much prefers to work in the ambient air pressure ratio ($\delta = p_{am}/p_o$) and temperature ratio ($\theta = T_{am}/T_o$). The relationships between pressure altitude, ambient air temperature, and air density can be found in reference [634]. In my wind tunnel days, I generally had barometric pressure altitude in pounds per square foot or inches of mercury and ambient air temperature in degrees Fahrenheit or centigrade. Therefore, I grew up using the following equation:

$$(3.195)\quad \delta = \frac{p_{am}}{p_o} = \frac{p_{am}}{2116.229\ \text{psf}} = \frac{p_{am}}{29.92117\ \text{in. of Hg}}.$$

When the pressure altitude is given in feet as in most flight test reports, I am quick to assume that a correction to a standard day has been made so that

$$(3.196)\quad \delta = \frac{p_{am}}{p_o} = \left[1 - 0.00687558563\left(\frac{\text{H in feet}}{1{,}000}\right)\right]^{5.255876113} \quad \text{for a standard day}.$$

On ground or in the air, you always have the absolute temperature ratio calculated from

$$(3.197)\quad \theta = \frac{T_{am}}{T_o} = \frac{T_{am}\ \text{in °F} + 459.67}{518.67} = \frac{T_{am}\ \text{in °C} + 273.15}{288.15}.$$

Then it follows that the density ratio (σ) is found from

$$(3.198)\quad \sigma = \frac{\rho_{am}}{0.002378\ \text{slug/ft}^3} = \frac{\delta}{\theta}.$$

Mach number (M) depends on true airspeed and the speed of sound (a_S), which is

$$(3.199)\quad a_S = 1{,}116.45\sqrt{\theta}\ \text{ in ft/sec or } 661.48\sqrt{\theta}\ \text{ in knots}.$$

You should be aware that the U.S. military has created several different "days" other than the International Standard Atmosphere (ISA) day. For example, the AMST program dealt with primary STOL performance at sea level on a hot day. The U.S. Army has two design points—4,000 feet on a 95 °F day and 6,000 feet on a 95 °F day.[153] The following table may be of some use:

Design Condition	Pressure Ratio	Temperature Ratio	Density Ratio
Sea Level, 103 °F	1	1.084832	0.921801
4,000 feet, 95 °F	0.863662	1.069408	0.807607
6,000 feet, 95 °F	0.801378	1.069408	0.749366

[152] Please let me skip a discussion of the advancing tip Mach number of edgewise flying rotors as a performance issue.

[153] Wayne Johnson researched the military specified polar, tropical, and hot days. It is a ragged story at best as you can read in his publication *NDARC—NASA Design and Analysis of Rotorcraft* [635].

You will find in the YC-15 flight evaluation report [617] that cruise performance is, of course, based on the aircraft's lift coefficient versus drag coefficient characteristics, which depend on Mach number. But rotary wing curves of "power required" versus speed are not of particular interest to fixed-wing aerodynamicists when estimating cruise performance and range. Rather, the primary data they desire is referred fuel flow, $W_F/\delta\sqrt{\theta}$, versus Mach number for several referred weights (W/δ). This very practical data is illustrated here in Fig. 3-194, and it is the most fundamental performance graph I know of when comparing the cruise efficiency of several different V/STOL production configurations.[154] I have taken a minor liberty in referred fuel flow by using $\sqrt{\theta}$. Engine manufacturers have found that their gas turbine engines do not quite follow ideal gas laws, so you will find several different empirical approximations in place of $\sqrt{\theta}$. This helps bring calculated engine performance into agreement with measured performance. For this introductory discussion, I have ignored this simple fact of life.

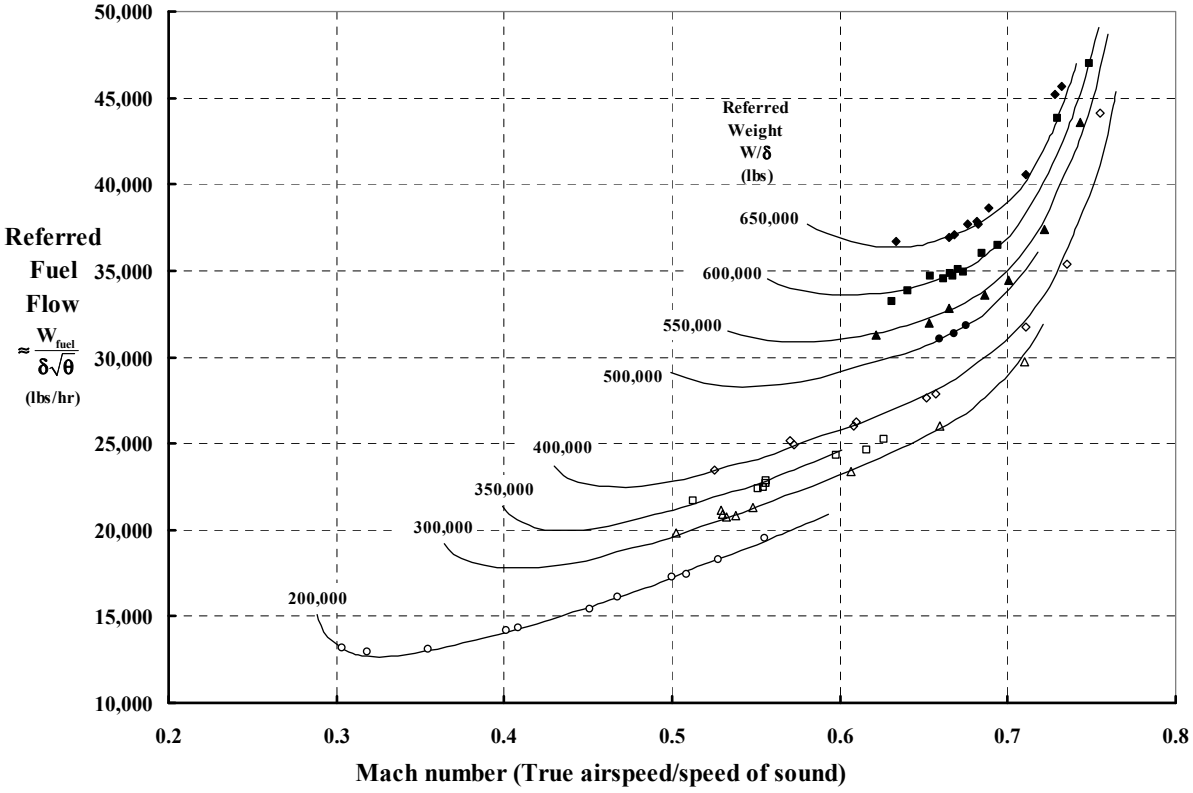

Fig. 3-194. Cruise performance analysis of the two AMST aircraft began with this example graph of referred fuel flow versus Mach number. The Air Force flight test evaluators appear to not have much confidence in calculated engine thrust, choosing instead the measured fuel flows.

[154] To me, power or thrust required versus speed or Mach number does not reflect the combination of V/STOL airframe and engine (be it piston or gas turbine). A very good airframe in combination with a very inefficient fuel-burning engine may well be a very non-competitive choice. Too frequently designers of an experimental machine have had to face this situation. I would say that McDonnell Douglas ran into this problem with the YC-15 as Bill Norton [26] pointed out to you.

Some additional discussion about fixed-wing aerodynamics may be of interest to rotary wing advocates. For example, dynamic pressure can be calculated two ways:

$$q = \tfrac{1}{2}\rho V^2 \text{ or } q = 1{,}481.35\,\delta M^2 .$$

Then lift coefficient becomes

$$C_L = \frac{W}{q S_W} = \frac{W}{\left(\tfrac{1}{2}\rho V^2\right) S_W} = \frac{W}{\left(1{,}481.35\,\delta M^2\right) S_W} = \frac{W/\delta}{\left(1{,}481.35 S_W\right) M^2} .$$

Thus, when the statement is made that the cruise portion of the mission will be calculated at constant W/δ and constant Mach number, it means that the cruise portion is calculated at a constant lift coefficient. Of course, this does not mean that actual true airspeed, altitude, or weight remain constant as fuel is burned off during the mission.

Now let me show you a simple way to approximate the performance the Air Force flight test evaluators arrived at for the YC-15 (Table 3-18). The evaluators state that the aircraft began cruise at 35,000 feet and began descent after flying 1,687 nautical miles and using up 39,183 pounds of fuel. At that point the aircraft's weight was down to 110,574 pounds. As the cruise time went up, the pilots increased altitude, ending up at about 42,000 feet. At a constant Mach number of 0.65 for the mission, the cruise began at a true airspeed of 374 knots. At the end of cruising, the aircraft was higher but traveling at a somewhat slower true airspeed of 363 knots. My objective now is to "ballpark" the 1,687-nautical-mile distance given the fuel burned.

First of all, range is fundamentally calculated from

$$(3.200)\quad R = \int_{t_{final}}^{t_{initial}} V\,dt = \int_{W_{final}}^{W_{initial}} V \frac{dt}{dW} dW = \int_{W_{final}}^{W_{initial}} \frac{V}{dW/dt} dW \approx \int_{W_{final}}^{W_{initial}} \frac{V}{\Delta W/\Delta t} dW$$

where the initial weight (W_i) is the weight after climbing to altitude and starting cruise. Accordingly, this initial weight is 149,757 pounds for the YC-15. At the end of the high-speed, high-altitude cruise phase of the mission profile, the final weight (W_f) is 110,574 pounds. As you know, the rate of fuel consumption ($\Delta W/\Delta t$) has the units of pounds per hour. I chose to express this fuel burn rate by specific fuel consumption (SFC) in pounds per hour per pound of engine thrust *times* engine thrust, which is to say

$$(3.201)\quad \frac{\Delta W}{\Delta t} = (SFC)\left(T_{eng}\right),$$

and in steady cruise flight the engine thrust(s) required is simply the aircraft's drag in pounds. Therefore,

$$(3.202)\quad T_{eng} = D_{a/c} \approx q S_W \left(C_{Do} + \frac{C_L^2}{\pi AR\, e} \right) = q S_W C_{Do} + \frac{W^2}{q \pi b^2 e},$$

which is a very satisfactory approximation as Oswald [636] showed in 1932. I found it interesting that both AMST aircraft had drag polars adequately characterized for this introductory volume by a minimum drag coefficient (C_{Do}) equal to 0.032 and an Oswald efficiency factor (e) equal to 0.85, not including drag due to compressibility.

Given the aircraft's aerodynamic character and a simple representation of the engine's fuel efficiency with specific fuel consumption (SFC), the range equation requires evaluating the following integral

$$(3.203)\quad R = \frac{1}{(SFC)_{avg}} \int_{W_{final}}^{W_{initial}} \left\{ \frac{V}{\left[\left(\tfrac{1}{2}\rho V^2\right) S_W C_{Do} + \frac{W^2}{\left(\tfrac{1}{2}\rho V^2\right)\pi b^2 e} \right]} \right\} dW \text{ in feet.}$$

The engine's SFC is taken outside the integral and replaced with an average SFC because it varies relatively little over the computation range.[155] The integral is easily found by assuming that velocity varies only a few knots over the cruise distance. In that case, you have

$$(3.204)\quad R = \frac{1}{1.687(SFC)_{avg}} \sqrt{\frac{\pi V^2 b^2 e}{S_W C_{Do}}} \arctan\left[\frac{K\left(W_{initial} - W_{final}\right)}{1 + K^2\left(W_{initial} W_{final}\right)} \right] \text{ in nautical miles}$$

$$\text{where } K = \frac{1}{q\sqrt{\pi S_W C_{Do} b^2 e}}.$$

This result makes an interesting point: a high cruise speed is beneficial. Of course, decades of transport aircraft development have repeatedly shown that compressibility will increase the minimum drag coefficient (C_{Do}) when cruise Mach numbers begin to exceed, oh say, 0.6. One estimate of an incremental drag coefficient (ΔC_{Dc}) due to compressibility is provided in reference [638], a very interesting design study completed by Air Force engineers in April 1972. Their conceptual design was very similar to the YC-15. You see the authors' assumption, Fig. 3-195, of just how large—even before Mach 1 is approached—the incremental drag coefficient (ΔC_{Dc}) due to compressibility becomes.

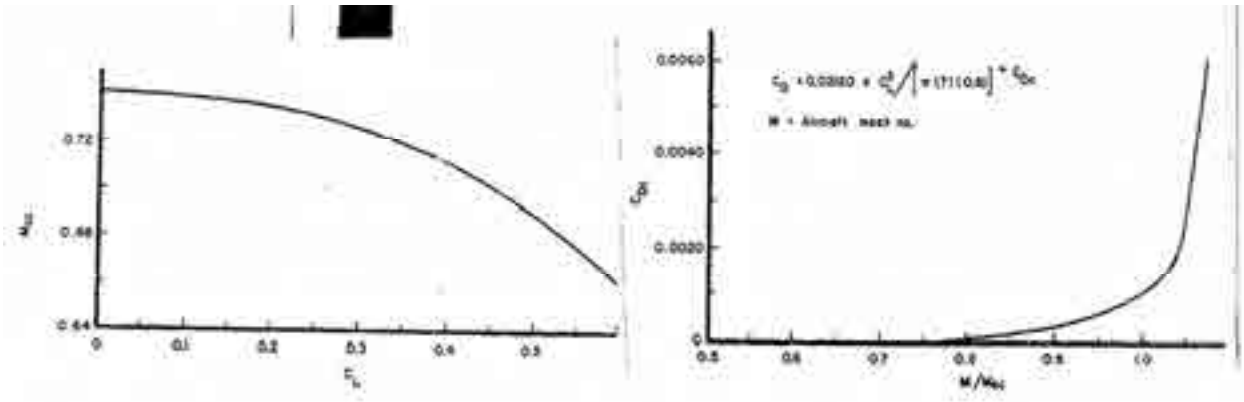

Fig. 3-195. Compressibility increases aircraft minimum drag coefficient [638].

[155] Barney McCormick's book [637] has an excellent discussion in Chapter 6 dealing with Specific Engine Characteristics and Performance. Mike Scully directed me to http://jet-engine.net, a very useful site for data. This site quotes the thrust SFC at 30,000 feet and 0.80 Mach number for the P&W JT8D-17 as 0.814 at a thrust of 5,140 pounds. For the GE CF6-50C at 11,100 pounds thrust at 35,000 feet and 0.80 Mach number, TSFC equals 0.657. Although these data assume the engines are not installed, they do illustrate key performance differences.

Just for the fun of it, I made a simple comparison of the high-altitude cruise performance between the two AMST aircraft using Eq. (3.204). My results are shown in Table 3-19. It appears to me that the Boeing machine had about 25 percent more fuel to burn because of its wing design. Its more modern, higher bypass ratio engines consumed less fuel per pound of thrust and the machine's cruise lift-to-drag ratio was higher.

There is a footnote to this ferry range story that may interest you. The competition between McDonnell Douglas and Boeing for the AMST really came to an end when, in February 1978, Secretary of Defense Harold Brown officially terminated Source Selection. But before that decision was made, one major performance question got answered. The question was this: What would the performance of the YC-15 have been if the aircraft had a larger wing? This question got answered with an extension to the McDonnell Douglas YC-15 contract. This Phase II/III effort allowed modification to—and flight testing of—one YC-15. The modification was a wingtip extension to the aircraft that increased the wingspan to 132.6 feet and area to 2,107 square feet. The results were reported [624] in January of 1978. Based on flight testing, the evaluators were prepared to credit a YC-15 (Mod) with a range of 2,425 nautical miles (i.e., 85 nautical miles for climb) with an engine start weight of 188,391 pounds. The high-altitude cruise phase of the mission profile had the aircraft beginning cruise at 178,949 pounds and then burning off 56,195 pounds while covering about 2,340 nautical miles. At the end of the high-altitude cruise portion of the ferry range mission, the pilots began descent at a gross weight of 122,754 pounds. The cruise lift-to-drag ratio was increased from 12.0 to 13.3.

Table 3-19. Harris' View of YC-14 and YC-15 Ranges; Both Aircraft Began Cruise at 35,000 Feet and at 0.65 Mach Number (370 knots)

Parameter	Symbol	Unit	Boeing YC-14	McDonnell Douglas YC-15
Initial weight	Wi	lb	176,916	149,757
Final weight	Wf	lb	127,093	110,574
Fuel burned	ΔW	lb	49,823	39,183
Wingspan	b	ft	129.0	110.4
Wing area	S_W	ft^2	1,762.4	1740.0
Lift coefficient	C_L	na	0.711	0.610
Minimum drag coefficient	C_{Do}	na	0.031	0.031
Oswald efficiency factor	e	na	0.85	0.85
Cruise lift-to-drag ratio	L/D	na	13.9	12.0
Configuration constant	K	lb^{-1}	4.474×10^{-6}	5.345×10^{-6}
Average specific fuel consumption(1)	SFC_{avg}	lb/hr per lb	0.70	0.76
Range in cruise portion of mission	R	nm	2,300	1,690
Average specific range	SR	nm/lb	0.0462	0.0380

Note 1. SFC_{avg} values selected so calculated range (R) agreed with data on Table 3-18.

3.10.4 Some Cost Aspects

On November 10, 1972, contracts were awarded to Boeing ($96.2 million with a cost plus fixed fee contract, the fee being $6.3 million) and McDonnell Douglas Corporation ($119.4 million with a cost sharing contract with the government's share being $86.1 million and the contractor's share being $33.3 million). The funding profile, as best as I was able to reconstruct it from references [639, 640], was going to total just under $10 billion for 300 aircraft delivered, as you see in Table 3-20.

The AMST prototype program featured a "design-to-cost" goal of $5 million recurring flyaway cost in fiscal year 1972 dollars for the 300th operational aircraft. This goal was equivalent to an average recurring flyaway cost of $7.0 million per aircraft in fiscal year 1972 dollars over a 300-aircraft procurement. Amortizing the cost of tooling—estimated at about $60 million—over the 300-aircraft procurement was expected to increase the average flyaway cost from $7.0 million to $7.2 million, and the 300th unit flyaway cost from $5.0 million to $5.2 million, all in fiscal year 1972 dollars. I suppose by the end of 1981, inflation (about a factor of 2.1) and estimating for success (another 1.5) would have more than doubled the actual program cost for 300 airplanes.

3.10.5 Epilogue

On October 31, 1979, Secretary Brown cancelled the U.S. Air Force Advanced Medium STOL Transport program. This decision now appears to have brought an end to any serious consideration by the U.S. military for a large transport STOL. However, Boeing's upper surface blowing (USB) concept was considered by many to be so promising that the U.S. Navy and NASA continued a major research program begun by NASA with its Quiet Short-Haul Research Aircraft (QSRA), Fig. 3-196, [641-646]. And the Antonov OKB Design Bureau (founded by Oleg Konstantinovich Antonov in 1946 in Kiev, the capital of the Ukraine) began development of the An-72, Fig. 3-197. The history of the AN-72 stretches back to 1977 [647] and is worth a book in its own right. You can, however, capture some of the story by reading *Jane's All the World's Aircraft* starting with the 1978–1979 issue and continuing right up to today because this STOL aircraft is still in production.

Table 3-20. AMST Funding Schedule—Money in 1972 U.S. Dollars (millions)

Item	1973 & Prior	1974	1975	1976	1977	1978	1979	1980	1981	To Complete	Total
Prototypes											
YC-14	14.5	31.2	39.4	10.8	0.3						
YC-15	13.4	32.8	30.3	9.0	0.7						
Gov't	0.1	1.4	6.0	7.7	2.4						
Subtotal	28.0	65.4	75.7	27.5	3.4						
Production					71.1	457.0	997.3	990.7	934.6	5,814.0	9,481.4
Total					74.5	457.0	997.3	990.7	934.6	5,814.0	9,481.4

In my mind, both the YC-14 and YC-15 AMST aircraft required a number of improvements that would have had to be made *before any thought of even low-rate production* could have been contemplated. But so ended the Advanced Medium STOL Transport program—although an issue of aircraft storage did crop up in June of 1980 [648]. By the way, the Lockheed C-130 has been kept in production ever since [649].

Fig. 3-196. NASA's QSRA, a Boeing conversion of a de Havilland Buffalo, first flew July 6, 1978. Operational weight empty was 36,800 pounds; normal takeoff weight was 50,000 pounds. Wingspan was 73.5 feet with an area of 600 square feet. Each Avco YF102 turbofan engine was rated at 7,500 pounds thrust [641-646].

Fig. 3-197. The Antonov Design Bureau An-72 first flew in December 1977. Each Lotarev D-36 turbofan engine is rated at 14,330 pounds thrust. Wingspan is 84.75 feet and area is 969 square feet. At 58,420 pounds takeoff weight, the aircraft takes off in 3,280 feet. Maximum speed is about 410 knots. The aircraft is still in production.

3.11 FINAL THOUGHTS ABOUT STOL AIRPLANES

It seems to me that after nearly half a century of research, development, production, and operation in the field, the practical limits of STOL airplanes have been quite well established. Given that the objective has been to

offer fixed-wing machines that carry more, go faster, fly higher, and yet still takeoff and land within rationally sized airports,

fixed-wing advocates have pursued this objective with metal monoplanes, retractable landing gear, variable-pitch propellers, swept wings, gas turbine engines, high-wing-lift devices such as the Fowler flap, and of course, many forms of powered lift that you have just finished reading about. The conclusion, which seems rather clear to me, is that the "rationally sized airport" for STOL operations is one that contains a 2,000-foot runway. This runway needs 500 feet of obstacle-clear space at either end. If the runway is paved with very high load bearing concrete, so much the better.

The practical limits are threefold. First, takeoffs require very high ratios of static thrust to weight, at and beyond the point of brake release, and this thrust (or power, if you prefer) is very expensive. Second, landings require maximum lift coefficients above 6.0 or even 7.0, plus immediate thrust reversal at touchdown and well designed brakes for repeated, short ground runs. These requirements add mechanical complexity, which is not inexpensive. The adjuncts to these first two limitations are (a) more than sufficient performance following an engine failure, and (b) excellent flying qualities at very slow approach speeds. Without these two features, the average pilot will not have enough confidence to routinely use STOL operations. Third, STOL requirements conflict with cruising efficiently at 35,000 to 45,000 feet at Mach numbers on the order of 0.8 (about 400 knots), which appear to define the optimum, moneymaking commercial *turbojet- or turbofan-powered* airliner. However, I would disagree that the *propeller-driven* military transport should be dismissed out of hand as the U.S. Air Force has done. In the commercial airliner world, it does seem that the traveling public has come to prefer jets to props—at least at equal ticket price.

Let me expand on these summary opinions. I found it very interesting that virtually all of the STOL reports and papers I examined never mentioned takeoff and landing performance at altitude. The preponderance of STOL distance and speed data quoted generally referred to sea level, standard day conditions. Engineering theory was then used to create the Flight Manual curves (Fig. 3-168 and Fig. 3-169) that a pilot needed for day-to-day operations. This made me wonder what competitors for the AMST program would have proposed if the design requirement had been 2,000-foot STOL performance at, oh say, the U.S. Army's VTOL day, which is nominally a 4,000-foot pressure altitude at a temperature of 95 ^{o}F *and with consideration of an engine failure*. After all, this was a key design requirement that Donald Douglas agreed to (Fig. 3-198) with Transcontinental & Western Air, Inc. when he began development of the Douglas Commercial DC-1, Fig. 3-199. You will recall that back then (i.e., late 1920s) the airlines were expanding passenger carrying commercial service using primarily the Ford Trimotor, Fig. 3-200. Because of the high operating cost of these early trimotored aircraft, airlines could not make a profit and government subsidies were

TRANSCONTINENTAL & WESTERN AIR INC

August 1st,
1932

Douglas Aircraft Corporation,
Clover Field,
Santa Monica, California.

Attention: Mr. Donald Douglas

Dear Mr. Douglas:

Transcontinental & Western Air is interested in purchasing ten or more trimotored transport planes. I am attaching our general performance specifications covering this equipment and would appreciate your advising whether your company is interested in this manufacturing job.

If so, approximately how long would it take to turn out the first plane for service tests?

Very truly yours,

Jack Frye
Vice President
in Charge of Operations

JF/GS
Encl.

P.S. Please consider this information confidential and return specifications if you are not interested.

TRANSCONTINENTAL & WESTERN AIR, INC.

General Performance Specifications
Transport Plane

1. Type: All metal trimotored monoplane preferred but
2. Power: Three engines of
3. Weight: Gross (maximum)
4. Weight allowance for radio and wing
5. Weight allowance must also be made for complete instruments,
6. Performance

Top speed sea level (minimum)	mph.
Cruising speed sea level - 75 % top speed	mph. plus
Landing speed not more than	mph.
Rate of climb sea level (minimum)	ft. p.m.
Service ceiling (minimum)	ft.
Service ceiling any two engines	ft.

This plane, fully loaded, must show satisfactory
under good control at any
two engines.

Kansas City, Missouri
August 2nd, 1932

Fig. 3-198. These documents are part of the story that Arthur Pearcy tells in *Douglas Propliners: DC-1 to the DC-7* [650]. His book is absolutely terrific. In my view, a one-page specification for a new aircraft is quite sufficient to get started. A short letter on company stationary (signed by the president) requesting a proposal is rather nice too.

Fig. 3-199. Pearcy's caption to this photo states that on 16 August 1933, "the DC-1 is seen embarking passengers despite still carrying experimental X registration." Its first flight was on Saturday morning, July 1, 1933 [650].

Fig. 3-200. The Ford Trimotor, a 12-passenger airliner, was developed by the Stout Metal Airplane Division of the Ford Motor Company. Its first flight was made on June 11, 1926. It did not, however, earn early airlines a profit. Still, the commercial airline industry expanded thanks to government subsidies.

Fig. 3-201. The Boeing Model 247, a 10-passenger airliner, overcame many of the trimotor's problems so that the airlines could make a profit carrying passengers only. Its first flight was on February 8, 1933.

required. When Boeing developed its Model 247, Fig. 3-201, United Airlines ordered all that Boeing could produce, leaving all the other airlines out in the cold with their unprofitable Fords. This competitive situation caused Jack Frye to write his letter (Fig. 3-198).

The three aircraft that you see here are representative of passenger carrying commercial airliners before the start of World War II. Each of them operated around the United States, and each one could fly in and out of airports with runways—even "unprepared runways"—less than 2,000 feet long. Most importantly, the Boeing Model 247 and the Douglas DC-3 (developed from the DC-1) were moneymakers for the airlines [2]. To me, these two aircraft had STOL capability by today's definitions and therefore represent a key reference point for all future STOL aircraft.

In my view, the key requirement for the DC-1 was the simple, almost parenthetical note that Jack Frye included in the specification:

> "This airplane, fully loaded, must make satisfactory takeoffs under good control at any TWA airport on any combination of two engines."

Clearly, TWA was expecting a three-engine aircraft. What they got was a twin-engine aircraft that met the one-engine-out specification. As Arthur Pearcy [650] tells it, with my additions in brackets:

> "Gross load tests were completed on 24 August 1933. Loaded with sandbags to 17,500 lb, the DC-1 lifted off the runway in 1,000 ft. [At Clover Field, Santa Monica, California, so sea level on a standard or warm day.] Speed tests were conducted over a measured course at different altitudes, the best speed attained being 212 mph. Jack Frye brought over a TWA pilot, Captain Smith, to fly the DC-1. Eddie Rickenbacker, Vice-President of Eastern Air Transport, was another interested visitor. On 4 September 1933, the transport was put through its most difficult test to demonstrate its ability to meet TWA's most stringent requirement—a flight from Winslow, Arizona, to Albuquerque, New Mexico, with one engine shut down from take-off to landing. Personnel on board included Eddie Allen, pilot; 'Tommy' Tomlinson, co-pilot; Frank Collbohm, flight test engineer; 'Doc' Oswald, aerodynamicist [as in Oswald efficiency factor]; Bill Birren, Wright Aeronautical; Ralph Ellinger, TWA factory inspector; and Clarence Young, US Department of Commerce.
>
> The following day, after one of its engines had been switched off during the take-off run, the DC-1 climbed slowly from 4,500 ft to its cruising altitude of 8,000 ft, and, single-engined, successfully flew the 280 miles between the two airports. Winslow had an altitude of 4,878 ft with runway 24/06, a length of 4,752 feet. Douglas had proved, without any doubt, the ability of the new DC-1 to meet all TWA's requirements. On 13 September 1933, the DC-1 became TWA property. The airline placed an initial order for twenty DC-2s, a derivative of the DC-1 with the fuselage length increased by two feet to accommodate an additional row of two seats.
>
> On 15 November 1933 Donald Wills Douglas took his first flight in the DC-1 with Carl Cover and 'Tommy' Tomlinson as pilots on the aircraft's first cross-continental flight from Santa Monica to Newark, New Jersey. Douglas had business with Dick Robbins, President of TWA, to re-negotiate the airframe contract price of $58,000 each to $65,000, due to the United States going off the gold standard. The DC-1 had cost the Douglas Aircraft Company $306,778 to design, build and test. The new airliner was introduced to both the press and the general public on a 'show-and-tell' public relations exercise. Numerous airports were visited during check flights.
>
> The DC-1 was officially handed over to TWA during December 1933, in a ceremony at Los Angeles Municipal Airport when the company handed Donald Douglas a cheque for $125,000."

Think about this timeline: Donald Douglas got a letter dated August 2, 1932, requesting a 12-passenger commercial airliner. TWA took delivery of the first DC-1 on November 15, 1933. Barring world war, things go faster when taxpayer money is not involved.

Perhaps you would be interested to know that the final production model of this first moneymaking airliner, the DC-3, was tested at 1/11 scale [651][156] in the Guggenheim

[156] Thanks to Mike Scully's suggestion, I called Sam Ferguson who also worked at Bell Helicopter during my tenure. Sam had tracked down this report and was kind enough to send me a copy. You may also find references [652-654] of interest.

Aeronautics Laboratory wind tunnel at the California Institute of Technology. Furthermore, Donald Douglas had the honor of giving the 23rd Wilbur Wright Memorial Lecture [655] in November 1935. His paper was titled "*The Developments and Reliability of the Modern Multi-Engine Air Liner*." This is a paper that every student of aviation should read. You should know that the aviation historians who compiled a two-volume collection of very significant papers [656, 657] included Donald Douglas' lecture before the Royal Aeronautical Society. His speech was included because it "stressed the importance of single-engine operation within the demands of long-range operation, an issue that set the American flight environment apart from Europe and that served as a major stimulating factor in U.S. technological development." At that time Donald Douglas was President of the Institute of Aeronautical Sciences, which, as you know, is now the AIAA. Later, in 1967, Douglas merged his company with St. Louis-based McDonnell Aircraft Corporation and became an honorary chairman of McDonnell Douglas. Douglas then retired, but continued to be active in the aerospace sector and received many honors from around the world. He was born on April 6, 1892, and died on February 1, 1981, at the age of 88. He was an active sailor, and his ashes were scattered over the Pacific Ocean.

Now consider STOL takeoff and landing performance from a technical point of view. The governing physics are still the same as they were in early 1935 [658] or later, in mid-1957, [659] because (1) the maneuver profiles are so similar; (2) the reference velocity for liftoff or touchdown is derived from a maximum lift coefficient; (3) the ground run portion is calculated with the same $\Sigma F_X = ma_X$ equation; and (4) the first-order parameters are wing loading (W/S_W), accelerating or decelerating force to weight ratio (F/W), and maximum lift coefficient (C_{Lmax}). Therefore, it is sufficient for these final thoughts to just deal with the takeoff problem, which, as a reminder, begins with

$$\begin{aligned}\sum F_X &= F - D - \mu_{roll}(W - L) = F - \mu_{roll}W - (D - \mu_{roll}L)\\ &= (F - \mu_{roll}W) - \left[(\tfrac{1}{2}\rho S_W)(C_D - \mu_{roll}C_L)_{GR}\right]V_x^2\\ \sum F_X &= A - BV_x^2\end{aligned} \tag{3.205}$$

and therefore, the ground run distance to liftoff ($D_{Liftoff}$) behaves as

$$\begin{aligned}D_{Liftoff} &= \frac{W}{g}\int_0^{V_{Liftoff}} \frac{V}{\sum F_x}dV = \frac{W}{g}\int_0^{V_{Liftoff}} \frac{V}{A - BV^2}dV = \frac{W}{g}\left\{\frac{-1}{2B}\ln\left[1 - \frac{BV_{Liftoff}^2}{A}\right]\right\}\\ &\approx \frac{V_{Liftoff}^2}{4A^2}\left(2A + BV_{Liftoff}^2\right).\end{aligned} \tag{3.206}$$

But the liftoff speed ($V_{Liftoff}$) is approximated based on the aircraft's maximum lift coefficient ($C_{L\,max}$) so you have

$$V_{Liftoff}^2 = \frac{2}{\rho_o}\left(\frac{W/S_W}{\sigma\, C_{L-Liftoff}}\right) \quad \text{or} \quad \approx K\frac{2}{\rho_o}\left(\frac{W/S_W}{\sigma\, C_{L\,max}}\right) \text{ in feet per second squared.} \tag{3.207}$$

The constant (K) is greater than one and reflects the fact that STOL operations are conducted at 1.1 to 1.3 times the stall speed.

Now, after a few algebra steps, you arrive at

$$(3.208)\quad D_{Liftoff} \approx \left(\frac{1}{2g\rho_o}\right)\left(\frac{W/S_W}{\sigma C_{L-Liftoff}}\right)\left(\frac{1}{\frac{F}{W}-\mu_{roll}}\right)\left[2+\frac{(C_D-\mu_{roll}C_L)_{GR}}{\left(\frac{F}{W}-\mu_{roll}\right)C_{L-Liftoff}}\right].$$

This derivation shows you that the primary parameters of interest are

$$\left(\frac{W/S_W}{\sigma}\right) \qquad \left(\frac{F}{W}-\mu_{roll}\right) \qquad (C_D-\mu_{roll}C_L)_{GR} \quad \text{and} \quad C_{L-Liftoff}.$$

What is interesting about this decades-old parameter identification search is that you really need a three-dimensional graph to display the results of Eq. (3.208). For my purposes here, I have chosen to assume values for the second-order parameters (i.e., $\mu_{roll} = 0.025$) and the ground run aircraft drag (i.e., $C_D - \mu_{roll}C_L$) of 0.0875 based on $C_D = 0.1$ and $C_L = 0.5$. To account for the distance after liftoff, I have simply chosen the AMST result you saw in Fig. 3-176 and the equation

$$(3.209)\quad D_{50\,ft}=373+1.112D_{Liftoff}+0.0000523\left(D_{Liftoff}\right)^2.$$

With this approach and assumptions, I was able to correlate calculated versus experiment data for 15 aircraft as you can see in Appendix H and here in Fig. 3-202. I must add that this correlation required acknowledgement that the accelerating force (F) decreases as the ground speed increases. That is, the distance depends on an average accelerating force (F_{avg}). To me, the more meaningful force is the force at brake release

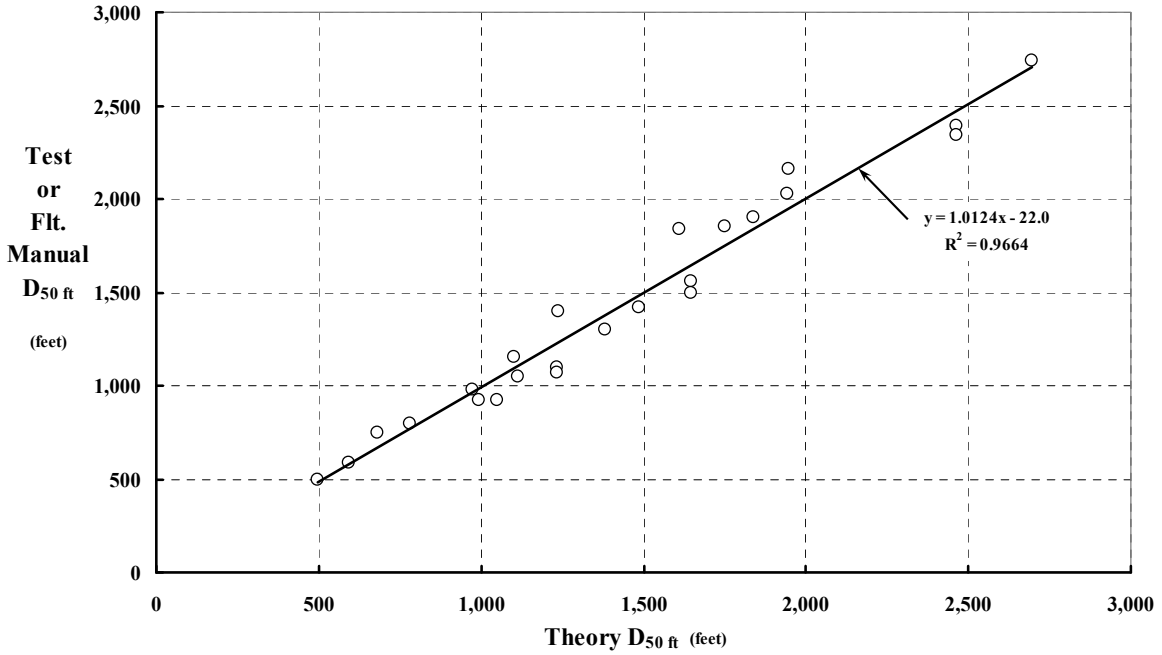

Fig. 3-202. Basic physics plus a little empiricism is adequate to estimate takeoff distance over a 50-foot obstacle during the conceptual design phase.

($F_{brake\ release}$).[157] Therefore, in Eq. (3.208), I let average force equal 0.85 times the force at brake release for propeller-driven aircraft. For the two AMST turbofan-powered STOL aircraft I used a factor of 0.70. Therefore, you have

(3.210) $F_{average} = 0.85\, F_{brake\,release}$ for propeller and $F_{average} = 0.70\, F_{brake\,release}$ for turbojet/turbofan.

The correlation you see with Fig. 3-202 gave me enough confidence to construct a conceptual design graph showing takeoff distance over a 50-foot obstacle (D_{50ft}) versus $F_{brake\ release}/W$ for lines of constant $\frac{W/S_W}{\sigma C_{L-Liftoff}}$. Fig. 3-203 shows my version of a conceptual design chart that you will find in the literature—in one form or another.

This conceptual design chart, Fig. 3-203, immediately shows you that as the wing loading (W/S_W) increases to suit higher speeds at higher altitudes, a STOL requirement demands a much higher lift coefficient at liftoff ($C_{L\text{-}Liftoff}$). Not only that, the ratio of the force at brake release to takeoff gross weight must be on the order of 0.5 or higher. It seems to me that the Boeing YC-14 defines the lower boundary for future designs of large-transport STOL airplanes. If you accept my conclusion, then the STOL design space quickly shrinks to where

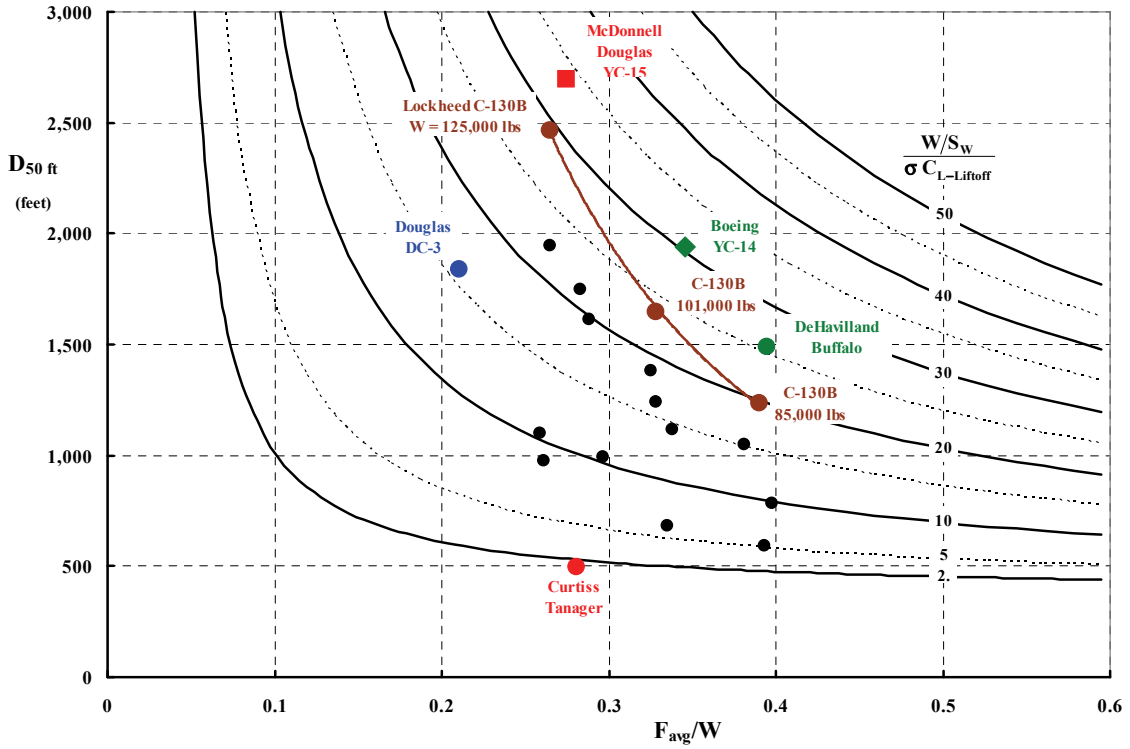

Fig. 3-203. Designing for a STOL takeoff over a 50-foot obstacle from a runway shorter than 2,000 feet becomes more and more expensive as the aircraft grows in weight and the wing area increases. At some point, VTOL must be very seriously considered.

[157] In fact, I would suggest that it would be relatively simple to measure force at brake release, although I have only found one such measurement in my literature search [644].

installed power (i.e., static-thrust-to-weight ratio, if you prefer) forces you to consider directing the propulsive force more downward and with more turning efficiency than is obtained with some horizontal airstream bent around flaps. This ultimately leads to serious consideration of vertical takeoff and landing (VTOL) aircraft.

You will find a prime example summarizing basic research on STOL in NASA Ames flight testing of what they called the Quiet Short-Haul Research Aircraft (QSRA) (Fig. 3-196). This outstanding research program extended over more than a decade as Dennis Riddle, Victor Stevens, and Joseph Eppel point out in their 1987 paper [645]. Those authors were proud to say:

> "The authors wish to acknowledge the contributions of past members of the QSRA Office, government and contractor personnel of the Flight Dynamics and Controls Branch, and personnel of the Ames Research Aircraft Operations Division. Without their efforts, this paper and the accomplishments reported herein would not have been possible. In particular, we wish to dedicate this paper to John Cochrane, past QSRA Program Manager, and to Robert Innis, past Chief, Flight operations Branch. Both gentlemen, now deceased, devoted much of their lives to the development of powered lift aircraft and the QSRA. Their efforts and achievements will not be forgotten."

An earlier paper presented by Dennis Riddle [644] included a graph (figure 23) comparing QSRA takeoff performance to a large group of conventional takeoff and landing (CTOL) commercial jet aircraft. This data collection, when added to Fig. 3-203, provides a clear picture of STOL potential versus CTOL performance as you see below in Fig. 3-204.

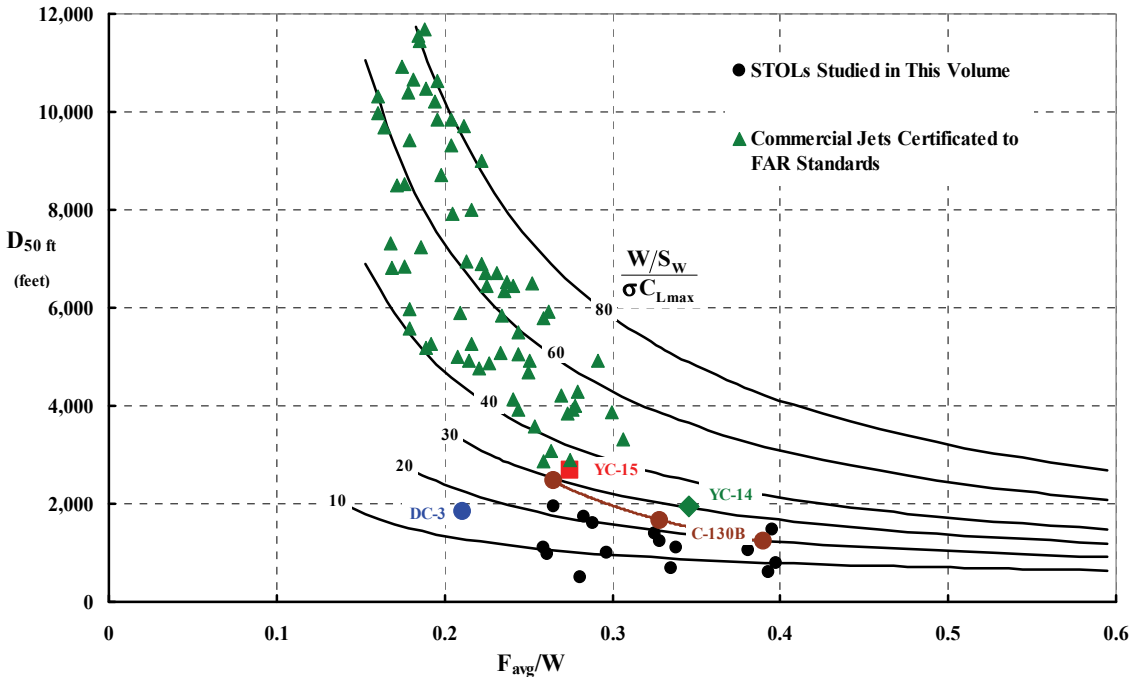

Fig. 3-204. The potential for STOL technology to shorten takeoff distances of aircraft in the commercial aviation world became quite clear by the end of 1981. The commercial aircraft data came primarily from *Jane's All World's Aircraft* for 1979–1980 [644]. I applied the 0.70 factor so data would be based on the average accelerating force.

As I mentioned, aircraft wing loading (W/S_W) increases to suit efficient cruising at higher speeds and higher altitudes. This brings me to the subject of best lift-to-drag ratios of military transport airplanes where the cargo defines the box that is "streamlined" by a fuselage. This is what the AMST specification led to as Fig. 3-173 clearly shows. Boeing and McDonnell Douglas met this specification with STOL aircraft that performed the STOL mission flying at Mach 0.64 to 0.65 at 35,000 to 42,000 feet. In contrast, modern, commercial turbofan-powered airplanes (such as Boeing's 737 on upwards) cruise at about 0.80 Mach number up at 35,000 feet. There is a very interesting conceptual design fact that explains this military cargo airplane versus commercial passenger carrying airplane outcome; an outcome driven by best lift-to-drag ratio.

Let me remind you of results obtained by classical equations. You will recall from Eq. 3.199 *that when compressibility is not a factor*:

$$T_{eng} = D_{a/c} \approx qS_W\left(C_{Do} + \frac{C_L^2}{\pi e\, AR}\right) = qS_W C_{Do} + \frac{W^2}{q\pi b^2 e},$$

and following Eqs. 1.4 to 1.9, you know that

$$(3.211)\quad \left(\frac{L}{D}\right)_{max} = \frac{1}{2}\sqrt{\frac{\pi e\, AR}{C_{Do}}} \qquad \text{at } C_L = \sqrt{\pi e C_{Do} AR}\ .$$

It follows then that the wing loading for high-altitude, high-speed cruising should be on the order of

$$(3.212)\quad \left(\frac{W}{S_W}\right)_{optimum} = q\sqrt{\pi e C_{Do} AR} = 1,481.35\ \delta M^2\sqrt{\pi e C_{Do} AR}\ .$$

In most missions requiring long distances, Flight Manuals recommend that the pilot increase altitude as fuel is used up. This suggestion means the designer wants the pilot to fly at a constant ratio of weight to pressure altitude (δ), which is to say

$$(3.213)\quad \left(\frac{W/\delta}{S_W}\right)_{opt.} = 1,481.35\ M^2\sqrt{\pi e C_{Do} AR}\ .$$

Or, if you are given the wing loading (based, say, on a STOL requirement) and desire efficient, high-altitude cruising, the design Mach number is

$$(3.214)\quad M_{opt} = \left\{\frac{W/S_W}{1,481.35\ \delta\sqrt{\pi e C_{Do} AR}}\right\}^{1/2} = \left\{\frac{W/b_W}{1,481.35\ \delta\sqrt{e f_e}}\right\}^{1/2},$$

where the aircraft aspect ratio (AR) is replaced by (b_W^2/S_W), and equivalent parasite drag area (f_e), in square feet, replaces $S_W C_{Do}$.

Both the Boeing YC-14 [618] and the McDonnell Douglas YC-15 [617] appear to confirm aircraft aerodynamics along the above classical lines. For example, in performing the STOL mission, the YC-14 arrived at the mission midpoint weighing 161,000 pounds, at a pressure altitude of about 42,000 feet (δ = 0.1682), and a Mach number of 0.64. This is a

dynamic pressure of 102 pounds per square foot. The aircraft was operating at a lift coefficient of 0.9 given its wing area of 1,762.4 square feet. The aircraft's drag polar behaved approximately as

$$(3.215)\quad C_D = 0.0302 + \frac{C_L^2}{\pi(9.44)(0.9)} + 0.0127\,C_L^4 \quad \text{for } M = 0.65,$$

which means the aircraft's drag coefficient is 0.069, and therefore the lift-drag ratio is about 13. The *incompressible*, maximum L/D according to Eq. (3.211) is 14.8, and this occurs at a lift coefficient of 0.946 and a lower Mach number of about 0.62. Both AMST aircraft were performing the STOL mission penalized by compressibility drag, which is the last term in Eq. (3.215). A penalty of this magnitude (i.e., $0.0127 \times 0.90^4 = 0.0083$) is not tolerated in commercial aviation because it reduces an aircraft's efficient cruise speed.

You may be interested to know that there is another form of Eq. (3.211). This alternate form is found by referencing the minimum drag (qS_WC_{Do}) to the frontal area of the fuselage, not to the wing area. This alternate form is discussed in Perkins and Hage [269] and Hoerner's invaluable book on drag [660]. Thus you write,

$$(3.216)\quad D_o = qC_{Do}S_W = qC_{D\pi}A_{Frontal} = qC_{D\pi}\left(\tfrac{\pi}{4}d_{body}^2\right).$$

When you solve for best lift-to-drag ratio starting with

$$(3.217)\quad D_{a/c} \approx qC_{D\pi}\left(\tfrac{\pi}{4}d_{body}^2\right) + \frac{W^2}{q\pi b^2 e},$$

you will find that

$$(3.218)\quad \left(\frac{W}{D_{a/c}}\right)_{max} = \sqrt{\frac{e}{C_{D\pi}}}\left(\frac{b_{wing}}{d_{body}}\right) \quad \text{at } W = \frac{\pi}{2}q\,b_{wing}d_{body}\sqrt{eC_{D\pi}}.$$

Aircraft with large, round fuselages with short, stubby wings attached are not recommended (unless, of course, you are designing a fighter).

Now you can see from Eqs. (3.211) and (3.214) that both AMST aircraft had excessive drag (i.e., a C_{Do} of 0.03) compared to modern commercial jets, which have drag coefficients more on the order of 0.02. To achieve cruise Mach numbers of about 0.80, parasite drag must be much lower, and the wing loading should be greater. But then a 2,000-foot STOL runway requirement would mean increasing the lift coefficient at liftoff. This is the design compromise when STOL is balanced with cruising at high speed and high altitude. As always, compressibility, weight empty, cost, and engine selection just complicate finding a design solution.

Before concluding my thoughts about fixed-wing STOL aircraft, let me point out a fact about turbofan engines. Bill Norton mentioned, you will recall, that Boeing chose "two enormous and powerful 51,000-lbf (227-kN) thrust (48,680 lbf installed at sea level, standard day conditions) General Electric F103-GE-100 turbofans (also designated YF-103-F2). More commonly known as the CF6-50D, this was the new commercial "fanjet" with a 4.2:1 bypass ratio." In 1973, this gave the Boeing YC-14 nearly 100,000 pounds of thrust for a maximum

takeoff weight of 225,000 pounds, or the mid-mission weight of 161,000 pounds for the STOL mission. Today, you might seriously consider four General Electric CFM56-5C4 engines (Fig. 3-205), each having a 34,000-pound rated thrust. After all, even more of the wingspan could be covered with jet exhaust as was achieved with NASA's QSRA, and the average accelerating force-to-weight ratio could be significantly increased. But to me—as a rotorcraft advocate—these modern turbofan engines have a latent shaft horsepower that I envy. The CFM56 engine has a thrust-to-uninstalled-weight ratio of roughly 3.8. The 6-foot-diameter ducted fan produces 26,900 pounds of thrust from 26,700 input shaft horsepower. In addition, the engine produces 7,100 pounds of thrust from the engine core. To me, this power available would be better used if the engine was driving a larger-diameter thrust-producing device. Furthermore, for STOL I would suggest that aiming this thrust in the right direction (i.e., more downward) would be quite helpful. All in all, fixed-wing STOL advocates would, I suggest, do better in the future by bending a little on their advocacy of "fixed."

Finally, the preceding 270 odd pages have introduced you to quite a few STOL aircraft and their technology. However, only a few have reached production, and they have all been relatively small, propeller-driven machines. Of these, the de Havilland Buffalo is the best example and, of course, the Bréguet 941 with its interconnected propellers must surely be considered. Only the two Advanced Medium STOL Transport aircraft were "jet" propelled STOLs, and both were well beyond the concept demonstration phase. Of these two, I would say that Boeing's YC-14 was the more promising example.

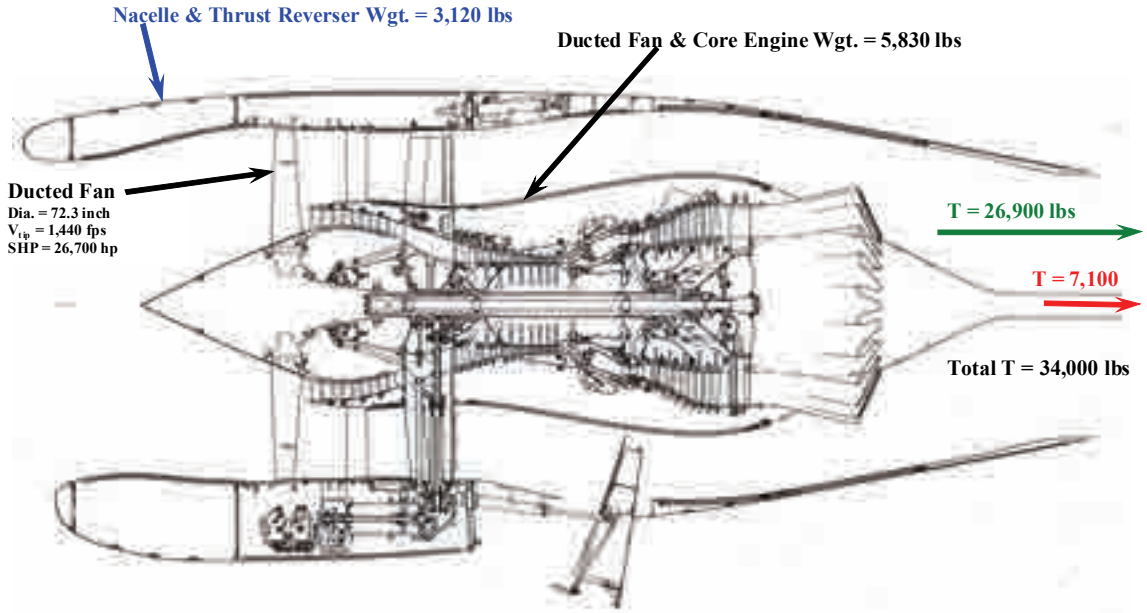

Fig. 3-205. The CFM International SA Model CFM56-5C4 produces 34,000 pounds of thrust at sea level standard day. Note that the thrust reverser is shown open on the lower half and closed on the upper half of drawing[158] (data courtesy of Bob Arnold at GE).

[158] I reached Bob at GE back in September of 2009 when I was preparing a report for Bill Warmbrodt titled *Airplane vs. STOL vs. VTOL* [661]. Bob was very, very helpful and forthright, I might add.

4 CLOSING REMARKS

One key theme tying together this three-volume book about autogyros, helicopters, and other V/STOL aircraft has been Gabrielli and von Karman's October 1950 paper [175]. You will recall the frontispiece for Volume I that you see here again as Fig. 4-1. For years, their paper and this figure have been the first source that I have turned to when any new aircraft type appeared on the scene. In fact, I frequently use Fig. 4-1 to get a first impression of any new machine that is exciting the transportation industry. Now, some six decades later, it is possible to more definitively place several VTOL and STOL aircraft on this quite well known graph. That Gabrielli and von Karman had enough data to postulate an upper bound to speed given a power loading still gives me wonder. They postulated this upper bound as

$$\frac{\text{HP}}{\text{Ton of Gross Weight}} = 0.001V_{\text{mph}}^2 = 0.001324V_{\text{knots}}^2 ,$$

which appears as a straight line when plotted on log-log paper. And now, with decades of operational aviation experience behind us and with aircraft characteristics available from many sources, it is possible to fill in the aviation areas that Gabrielli and von Karman grouped with nearly hand-drawn boundaries. The purpose of my closing remarks is to first expand and

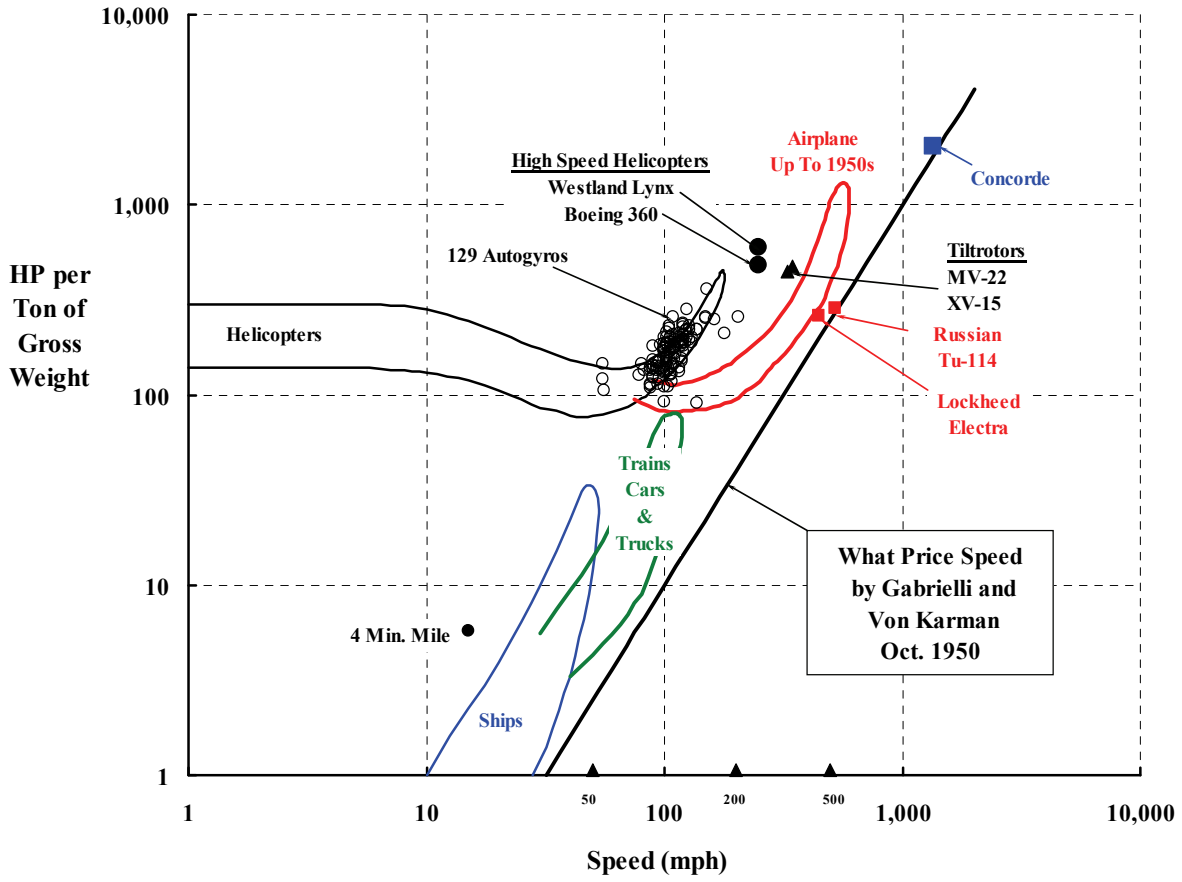

Fig. 4-1. Rotorcraft enjoy a unique position in the transportation industry [175].

update Gabrielli and von Karman's figure, and then to provide several aircraft trends that you may find rather interesting.

Gabrielli and von Karman chose to use a log-log graph and speed in miles per hour to gather up all the data trends they wanted you to see. But because it is only aircraft data that you will see here, I have used conventional linear scales on Fig. 4-2. On the vertical axis I have chosen engine maximum takeoff rated power (uninstalled in the aircraft) at sea level on a standard day, which is the most common data engine manufacturers quote. I have converted jet engine static thrust available to equivalent shaft horsepower (ESHP) with ideal, classical momentum theory, which says

$$(4.1)\quad \mathrm{ESHP} = \frac{T_{static}}{550}\left(\frac{T_{static}}{2\dot{m}}\right).$$

Here the takeoff static thrust is in pounds, and the mass flow ($\dot{m}$) is in slugs per second. This gives a somewhat optimistic ESHP because gas turbine engines are not 100 percent efficient. The gross weight used on the vertical axis in Fig. 4-2 is the maximum takeoff gross weight in tons.

The horizontal axis is speed in nautical miles per hour (1 mph = 1.1508 knots). Precisely establishing the "speed" for a large group of aircraft presents a rather interesting challenge. This is because aircraft manufacturers are quite frequently less than specific when publically quoting (e.g., marketing brochures) cruise speeds. There are, for example, at least two different "cruise" speeds. Engineers prefer to define cruise speed as the speed just slightly above the speed for maximum nautical miles per pound of fuel burned (or if you prefer, miles per gallon). Sometimes this speed is quoted as *economical* cruise speed. It is my experience that the marketing department wants to quote cruise speed as the speed obtained when the aircraft is flown at maximum continuous engine power (i.e., normal rated power). As you saw with Fig. 3-131, the difference in these two speeds can be quite large. Furthermore, just having a cruise Mach number without a cruise pressure altitude and ambient temperature is less than specific. This makes comparing several aircraft rather difficult, to say the least. I might add that a portion of the data point scattering you see on Fig. 4-2 is simply due to a less than specific choice of speed between several references.

Notwithstanding some apples-to-oranges comparison problems, let me first discuss the considerable gap between helicopters and airplanes that Gabrielli and von Karman perceived in 1950. This gap is the difference in cruise speeds at equal power loading for the two aircraft types. Today, this gap can be more clearly defined as Fig. 4-2 shows. I think now you can obviously see just how large the gap has become. First of all, the airplane has always enjoyed a performance advantage over the helicopter. This advantage has come about for two reasons:

1. The rotary wing industry has used power to increase payload carrying capability in hover and paid little attention to fielding low-drag machines, which might subtract from payload at equal gross weight. A perfect example is this group's refusal—with a few exceptions—to use retractable landing gear technology. It is quite correct, however, to note on Fig. 4-2 that the rotary wing industry does know how to design and demonstrate a "high-speed" helicopter. I have shown two examples on the figure. The first is the Boeing Model 360, a tandem rotor demonstrator that

you learned about earlier with Fig. 2-50 in section 2.10 starting on page 100. This helicopter nearly set the world speed record and clearly could cruise at a practical 180 knots. The second helicopter, also discussed in section 2.10, is the Westland G-Lynx (Fig. 2-49). This helicopter is of great importance because it currently holds the world speed record (216.3 knots) in its class. This 8,700-pound helicopter was designed specifically to set the record.

2. The fixed-wing industry has used power to increase payload and speed but paid little attention to short field landing machines, which would subtract from payload. A perfect example is that this side of the industry refuses—with few exceptions—to maximize the use of powered lift technology. Instead, it relies on long stretches of concrete being available. The fixed-wing industry finally produced the Douglas DC-1 (Fig. 3-199) just before the start of World War II. To me this airliner, as the DC-3, set the benchmark for future transport airplanes so I have highlighted it on Fig. 4-2. I have also added the Lockheed Electra (Model 188) because it was the top-of-the-line U.S. propeller-driven commercial airliner before the transition to Boeing's 707. The Russian Tupolev TU-114 was a propeller-driven airliner derived from the TU-95 strategic bomber, which was comparable to the Boeing B-52. The TU-114 holds the world record (470 knots) for a turboprop land airplane.

For at least seven decades now, it has been left to a relatively small group of enthusiasts to advocate for a gap-filling aircraft.

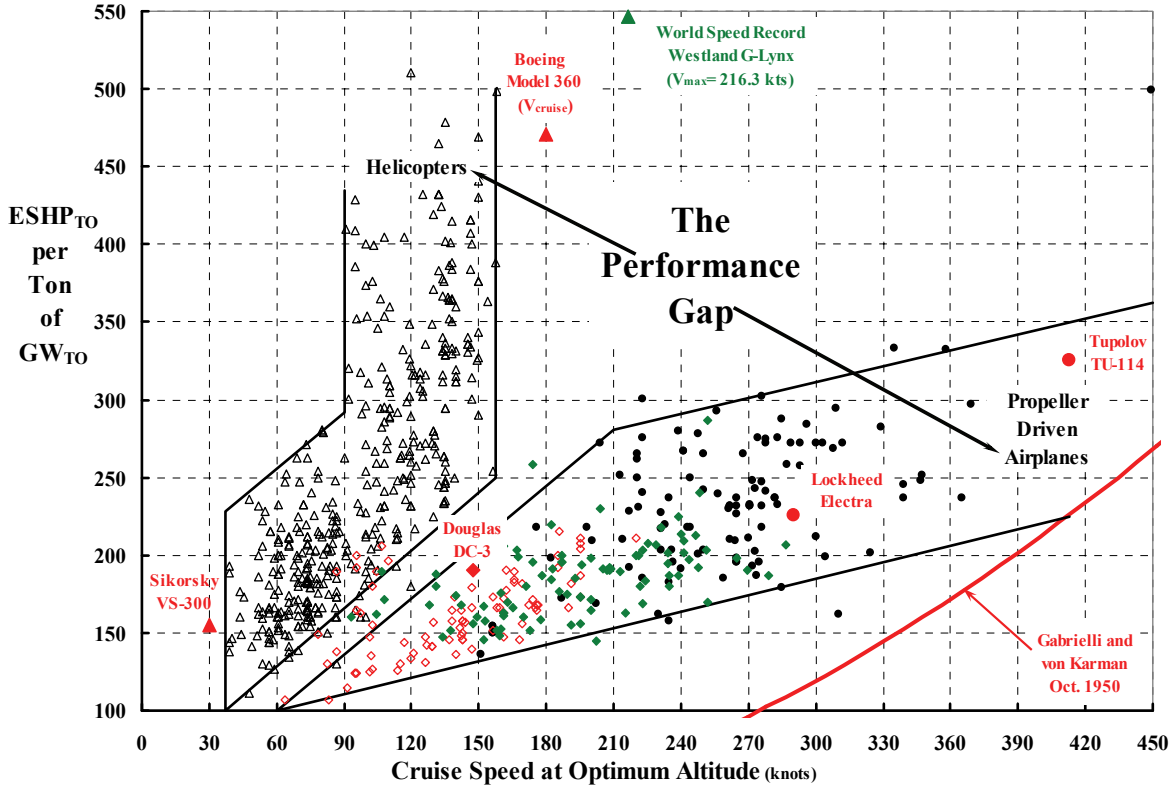

Fig. 4-2. Quite a performance gap exists between helicopters and airplanes (circa 1994).

These gap-filling[159] enthusiasts favoring a rotary wing solution researched helicopters with many combinations of wings and propellers added to their basic machine. They called these machines compound helicopters. These VTOL aircraft duplicate lifting and propulsive devices to overcome the disadvantages of edgewise flying rotors at high speed—but with a discouraging loss in payload at equal design gross weight. As you read in Chapter 2 and will see shortly, the compound helicopter only partially filled the gap. A majority of the gap-filling enthusiasts then turned to tilting the rotor from a hovering position to a propeller position for high-speed flight. They called this propulsive device a proprotor, and had considerable success by tilting both the wing and proprotor as an assembly as the Canadair CL-84 and LTV XC-142 demonstrated. Further effort led to tilting just the proprotor assembly as the Bell XV-15 demonstrated. The payoff came when the U.S. Marines championed the Bell- Boeing MV-22B Tiltrotor.

On the other hand, many of the gap-filling enthusiasts advocate STOL as a sufficient way to overcome the insatiable need of fixed-wing aircraft for long, concrete runways. The aviation industry and the N.A.C.A—and then NASA—have researched the waterfront of configurations (in my opinion) and have shown what powered lift can do to shorten both the takeoff and landing distances of fixed-wing aircraft. Their research of propeller slipstream—and gas turbine exhaust—effects on wings plus deflected flap aerodynamics is really monumental. The payoff of this research came when the U.S. Air Force conducted a competition for an Advanced Medium STOL Transport that would provide tactical support to the U.S. Army. As you have just read, two STOLs were developed and flown, Fig. 3-171 and Fig. 3-172, but neither was chosen for production.

You have become acquainted with quite a few V/STOL aircraft as you thumbed through this Volume III. So now let me pick a *select few* of these aircraft to add onto my version of Gabrielli and von Karman's 1950 figure. The gap-filling aircraft I have selected are listed in Table 4-1. Their position in the world of transportation is shown graphically in Fig. 4-3. Note first that I have uncluttered Fig. 4-2 by removing all the helicopter and airplane points, but I kept the boundary lines so that the gap is still well defined by the solid line boundaries.

My select few are a very short list as you can see. I based my selection first on advanced aircraft that showed V/STOL capability using a 2,000-foot or less runway as the benchmark. Then I whittled the list down further by selecting only those aircraft that were at least preproduction examples. Of course, you may well disagree with my selections.

Let me draw your attention to the green dashed line on Fig. 4-3. This line represents the vertical takeoff and landing state of the art as I see it at the end of 2015. It now appears to me that transport STOLs having 2,000-foot or less runway capability require just as much installed power per ton of gross weight as VTOL aircraft. The real differences in V/STOLs are speed and the never-ending debate about proprotor propulsion versus jet propulsion [662].

[159] I use this adjective with great respect, particularly because I count myself as a member of this group for over six decades. I became fascinated with helicopters right around the time I got my driver's license. All my model airplanes flew okay; all my model helicopters were absolute utter failures. And so I was hooked.

Table 4-1. Sixteen Concrete Examples of V/STOL Aircraft After 65 Years of R&D

Class	Aircraft	Total Takeoff ESHP (hp)	Gross Weight (lb)	Cruise Speed (kts)	ESHP/ (GW/2000) (hp per ton)	Weight Empty (lb)
Rotary Wing						
a. Compound	Fairey Rotodyne	5,600	33,000	161	339	22,000
	Sikorsky X2	1,630	6,100	260 est	534	5,000
	Eurocopter X^3	4,540	11,464	232 est	792	na
	Lockheed AH-56A	4,600	18,300	221	503	12,215
b. Tiltwing	Canadair CL-84	2,800	14,500	249	386	8,417
	LTV XC-142A	12,320	41,500	251	594	25,552
c. Tiltrotor	Bell Boeing MV-22B	12,300	52,600	291	468	33,459
	AgustaWestland 609	3,880	16,800	275	462	10,483
Fixed Wing						
a. Propeller (piston)	de Havilland Caribou	2,900	28,500	158	204	18,260
	Fairchild C-123B	5,000	54,000	166	185	30,900
b. Propeller (turboprop)	de Havilland Buffalo	6,266	49,200	250	255	23,197
	Bréguet 941S	6,000	58,420	260	205	32,400
	Lockheed C-130H	16,200	155,000	300	209	74,000
c. Turbofan	Antonov An-72	21,372	67,240	388	636	42,000
	Boeing YC-14	108,636	225,000	370	966	116,397
	McDonnell YC-15	92,430	216,680	375	853	101,400

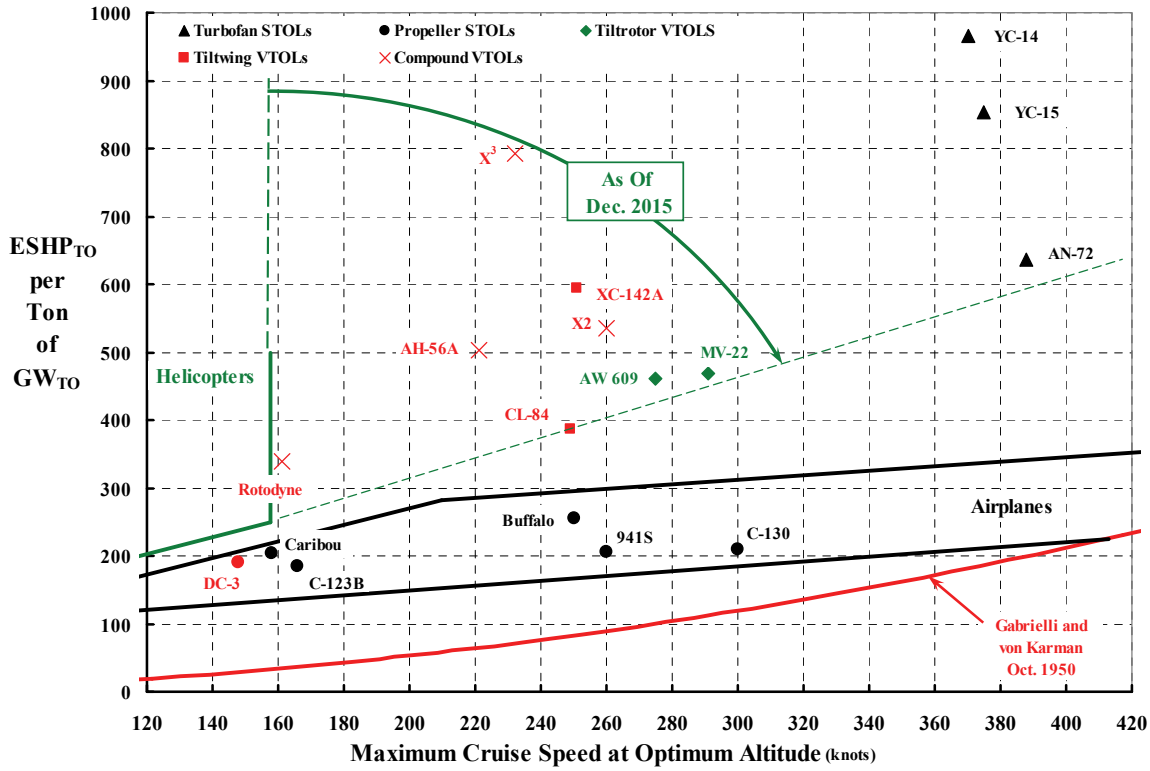

Fig. 4-3. The "gap" is closing after 65 years of R&D, but little production has followed.

Another example of the performance gap is seen when you compare cruise efficiency between helicopters and airplanes. This comparison is shown in Fig. 4-4. Here I have used nautical miles traveled per pound of fuel burned (i.e., specific range (SR)) as the measure of cruise efficiency. This measure could, of course, just as easily have been statute miles per gallon. The horizontal axis is takeoff gross weight when you follow Bréguet's range equation, which can be reduced to

$$(4.2)\quad SR \approx 326\left[\frac{(L/D)_{a/c}}{SFC}\right]_{avg.}\frac{1}{W_{initial}}\left[1+\frac{1}{2}\left(\frac{W_{fuel}}{W_{initial}}\right)\right]\approx\frac{1{,}000\ K_{SR}}{GW_{TO}}.$$

From Fig. 4-4, it appears that even the lower bound of airplane specific range performance is clearly 50 percent better than the highest bound of helicopter cruise efficiency. I would be more inclined to broadly conclude that the average airplane is twice as fuel efficient as the average helicopter—at equal takeoff gross weight. My list of selected V/STOL aircraft appear to use fuel more efficiently than helicopters. However, as of December 2015, none of the V/STOL machines can claim to be competitive with fixed-wing aircraft. This, of course, means that fuel costs for a given range will increase operating costs over those of a comparable airplane, and this will dampen the enthusiasm of potential V/STOL aircraft buyers.

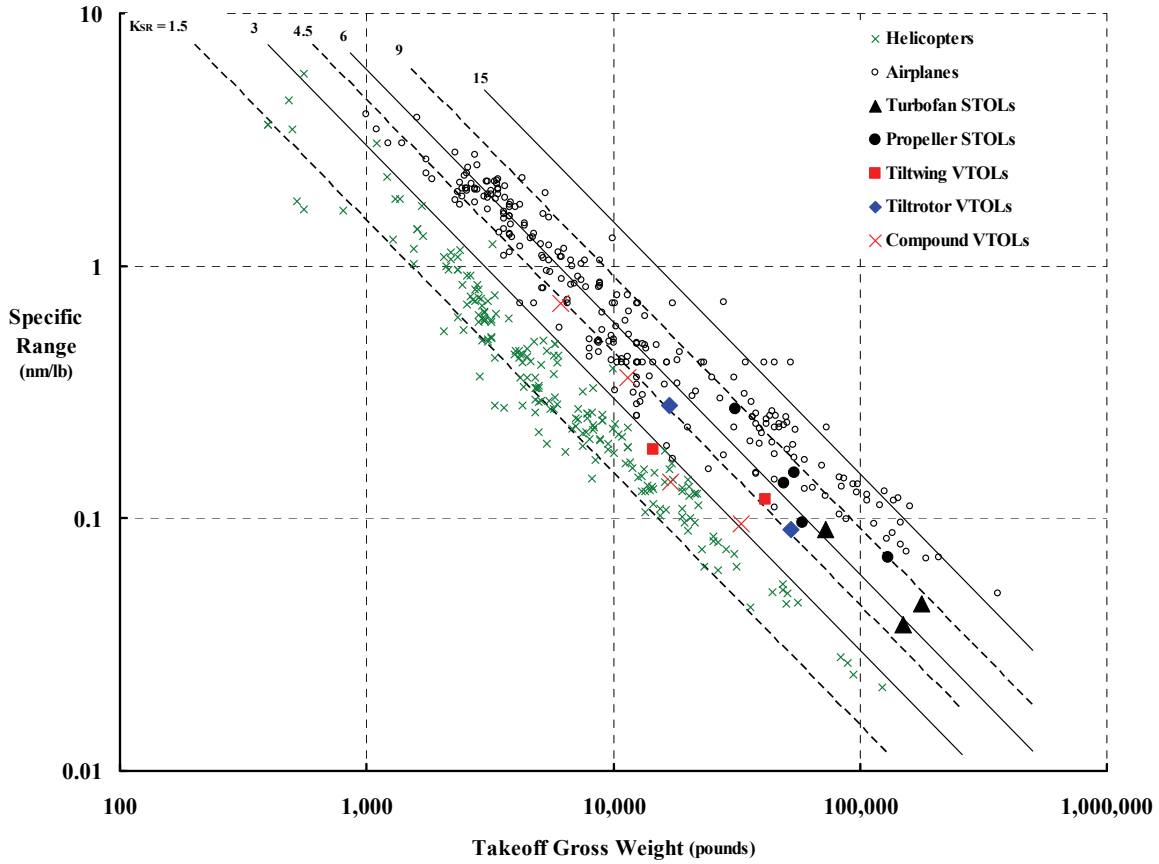

Fig. 4-4. V/STOL aircraft are more efficient than helicopters but, so far, still fall short of being as fuel efficient as airplanes.

Weight empty fraction (i.e., K = WE/GW) is, of course, a key measure of how well V/STOL aircraft compare to other aircraft that the aviation industry has produced over many decades. As you can see from Fig. 4-5, the industry has produced a multitude of helicopters and fixed-wing aircraft. My conclusion is that both aircraft types have successfully operated in service with a weight empty fraction from as low as 0.5 to as high as 0.7. Frankly, this is quite a spread in such an important design characteristic. But I must immediately point out that the selection of several weight empty values quoted[160] for any given machine is hardly consistent. And this, I suggest, accounts for a portion of the wide band in the weight empty fraction that you see on Fig. 4-5.

Fig. 4-5 also shows the 16 aircraft I have chosen as concrete V/STOL aircraft examples. There is little evidence that V/STOL aircraft have a severe penalty in their weight empty fraction. After all, the Bell Boeing MV-22B has a weight empty fraction of 0.636, even with all of its shipboard compatibility features.

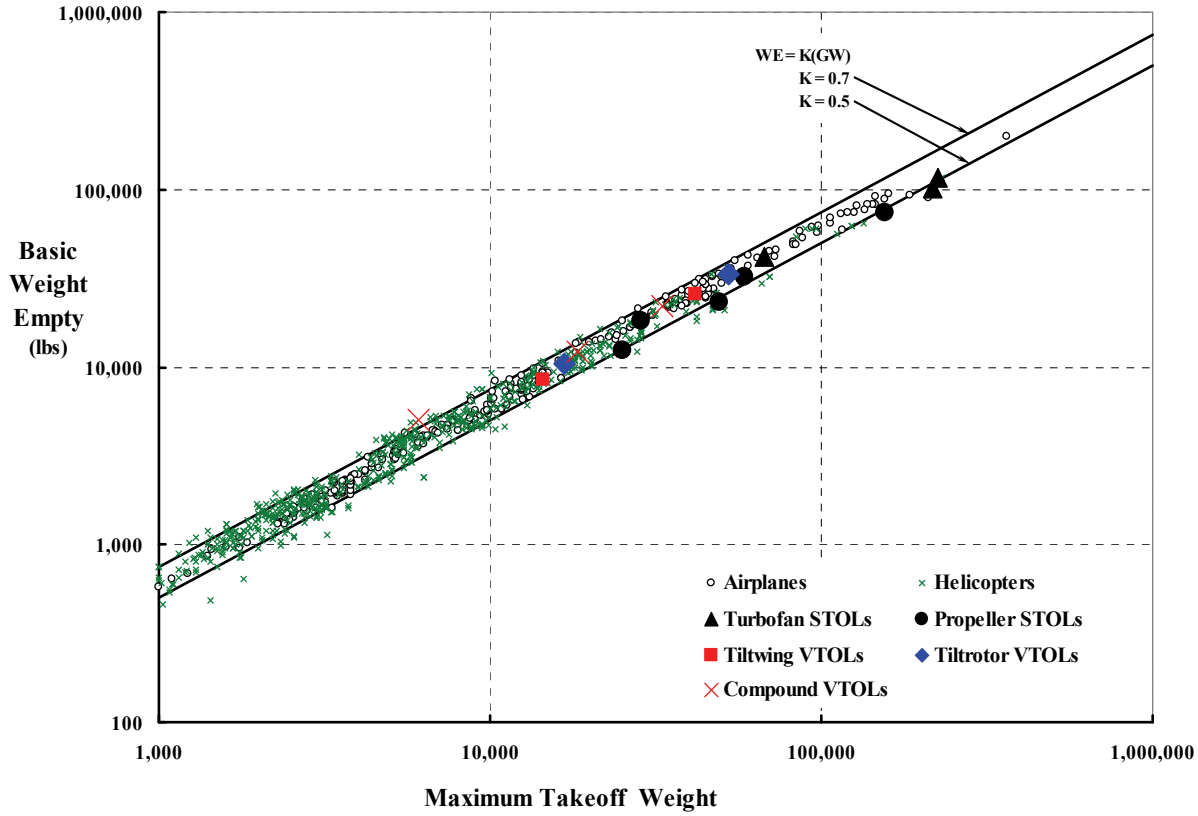

Fig. 4-5. It appears that V/STOL aircraft can have reasonable weight empty fractions when compared to both helicopters and airplanes.

[160] *Jane's All The World's Aircraft* is probably the most referenced source for aircraft characteristics. Unfortunately, it relies on manufacturers' input data, which can be wildly optimistic at times when compared to a pilot's Flight Manual. You will also see this when you read any test and evaluation report from, oh, say, the U.S. Air Force Flight Test Center at Edwards Air Force Base in California. Or you can look up the FAA Type Certificate Data Sheet, which the manufacturer obtains when its commercial aircraft is certificated. Personally, I take data offered in *Jane's* with a grain of salt because it may have been the marketing department that furnished the information.

The selling price (or cost to purchase, if you prefer) of rotary wing aircraft in particular has been a severe impediment to the widespread use of VTOL machines—at least beyond the military [391]. Norm Augustine [351] also drew attention to cost growth over several decades with his statistical trend for Department of Defense helicopters, which you saw earlier as Fig. 2-195 on page 314 in this volume. While you might want to attribute all of the cost growth to inflation, I suggest that inflation only accounts for a factor of 40 between 1942 and 1992. You see my view in Fig. 4-6. Helicopter improvements in higher hover ceilings with greater gross weight (and payload) and with higher cruise speeds just raised this machine's price. For example, the introduction of turboshaft engines increased the selling price by a factor of 1.779, and going from single engine to twin engines raised the price by another 1.352 [391]. Unfortunately, helicopter productivity per "buck" has continually decreased as you saw in Fig. 2-201 on page 324.

Perhaps the most difficult question to answer is, What will one of these V/STOL machines cost? The reason this is so difficult to answer is that the selling price of one machine depends primarily on the cost to make the first one, and then—to the first approximation—on the total quantity purchased, on the production in any given year (i.e., production rate), and on inflation. These factors lead me to the learning curve [663]. You will recall the discussion about learning curves in Volume II, which was part of the discussion about Bell's UH-1 program starting on page 553. There you learned that

$$\text{Cost of Aircraft N} = \text{First Aircraft Cost}_{(N=1)} \left[\text{LCF}\right]^{\left(\frac{\log N}{\log 2}\right)} \tag{4.3}$$

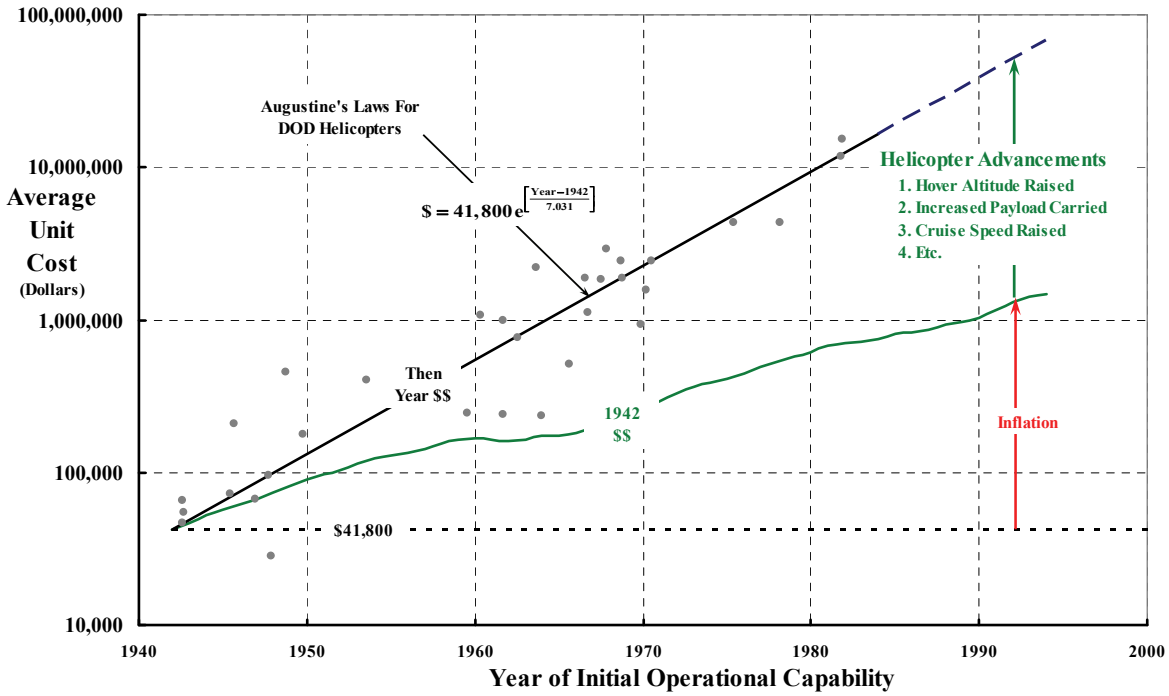

Fig. 4-6. Norm Augustine's law for the growth in unit flyaway cost of DoD helicopters reflects both inflation and advancements in technology.

where the LCF is the learning curve factor and is a number less than 1.0, one hopes. Only a single V/STOL transport aircraft has reached production—the Bell/Boeing MV-22B for the U.S. Marines. However, this single example is sufficient to illustrate several important points about how to answer the question I have posed.

To begin with, you see in Fig. 4-7 the unit flyaway cost of one MV-22B dropping as the number of aircraft built increases. This is the classical learning curve trend originally postulated for aircraft by T. P. Wright in February of 1936 [663] and later confirmed by aircraft production during World War II [664]. I have constructed Fig. 4-7 from data recorded in Table 4-2. Because theoretical learning curves are based on constant dollars (i.e., no inflation), you see the actual cost of one V-22 in then-year cost deflated to constant 1997 dollars, which was approximately the year production of the V-22 series began. Knowing how many aircraft were produced in any given year is important, and you have that data for the V-22 program in the numbers within the circles.

Given the actual unit flyaway cost (after the fact), it is very easy to see that the MV-22 program had, in fact, two distinct learning curves. The way you see this is to change the cost data from linear scales to log-log scales, which I have done in Fig. 4-8. In effect, Eq. (4.3) mathematically now becomes

$$\log(\text{Cost of Aircraft N}) = \log\left\{\text{First Aircraft Cost}_{(N=1)}\,[\text{LCF}]^{\left(\frac{\log N}{\log 2}\right)}\right\} \tag{4.4}$$

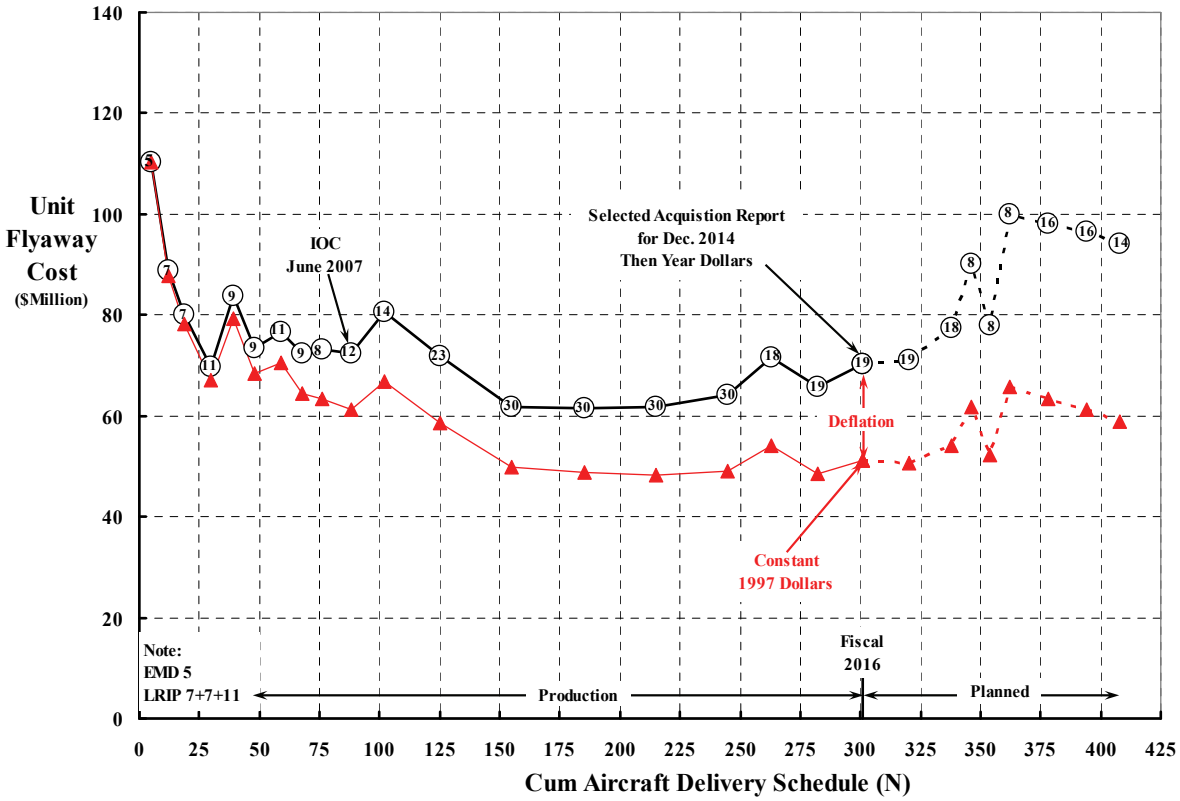

Fig. 4-7. The U.S. Marines' cost for an MV-22B steadily dropped as Bell and Boeing learned how to produce the aircraft more efficiently—at least up to the 150th aircraft.

Equation (4.4) suggests that log N is the primarily variable, and that means the log of an aircraft's cost should be plotted versus log N. When you make this graph as shown in Fig. 4-8, you immediately discover that the V-22 program had two learning phases. As you study Fig. 4-8, you might recall the V-22's development story from Chapter 2. The technical problems overcome and the programmatic chaos endured before the aircraft officially reached its initial operational capability (IOC) in June 2007 [665] now border on legendary in my mind. However, it is well to keep in mind that the V-22's program history is hardly unique as Norm Augustine has recounted [351].

With Fig. 4-8 in hand, you see that the initial V-22 program phase—Engineering & Manufacturing Development (EMD) plus Low Rate Initial Production (LRIP)—is described with a learning curve of

(4.5) $$\text{Cost of Aircraft N} = 172\left[0.830\right]^{\left(\frac{\log N}{\log 2}\right)}.$$

After a great deal of redesign that yielded a truly production-ready product acceptable to the U.S. Marines, you see a second learning curve of

(4.6) $$\text{Cost of Aircraft N} = 172\left[0.855\right]^{\left(\frac{\log N}{\log 2}\right)}.$$

I should note that a log-log graph is a very handy working graph when dealing with certain problems. However, it is generally more helpful to see results in the commonly used linear scale graph form. The results from Eqs (4.5) and (4.6) are shown with linear scales in Fig. 4-9. In this example using the Bell/Boeing V-22 program it is quite clear that, had the

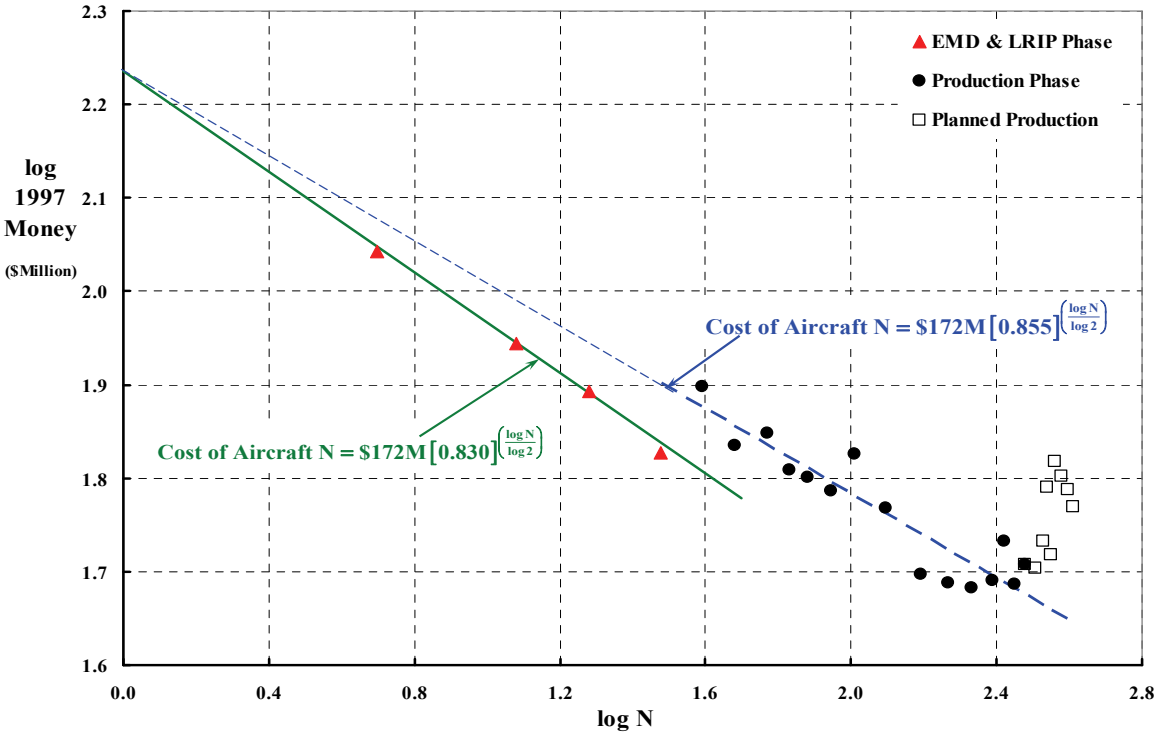

Fig. 4-8. The Bell/Boeing V-22 program experienced two different learning curves.

effort "been done right the first time," as is so often said by *whoever they are*, the 300th production MV-22B would probably have cost about $10 million less in 1997 dollars *or* in then-year dollars.

Now that you have this perspective about unit flyaway cost in hand, and with Fig. 4-9 in front of you, let me ask my original question again: What will one of these V/STOL machines cost? Imagine that the U.S. Secretary of Defense is asking you this question, and he or she is going to Congress later this month to plead for money. Having Fig. 4-9 in mind, you can now see that the answer must be very carefully qualified.

But to go on, accurately estimating just the cost of any one aircraft in some future V/STOL aircraft procurement program cannot be done based solely on some prescribed learning curve factor (LCF). Some speculative thought must be given to inflation. And, just as important, the production rate per year must be set almost in concrete. But what I believe is most important is risk assessment for the next V/STOL aircraft. To sell the V-22 program, decision makers bet that the jump from the XV-15 (i.e., a concept demonstrator) directly to a YV-22 (i.e., preproduction configuration) could be made without an XV-22 intermediate step. That was pretty heady thinking if you ask me, but it has been tried many times in the past—occasionally with success. In today's world, and based on Bell's UH-1 program you read about in Volume II starting on page 553, and now with the V-22 program successfully in the books, it appears to me that *realistic* program cost estimating must:

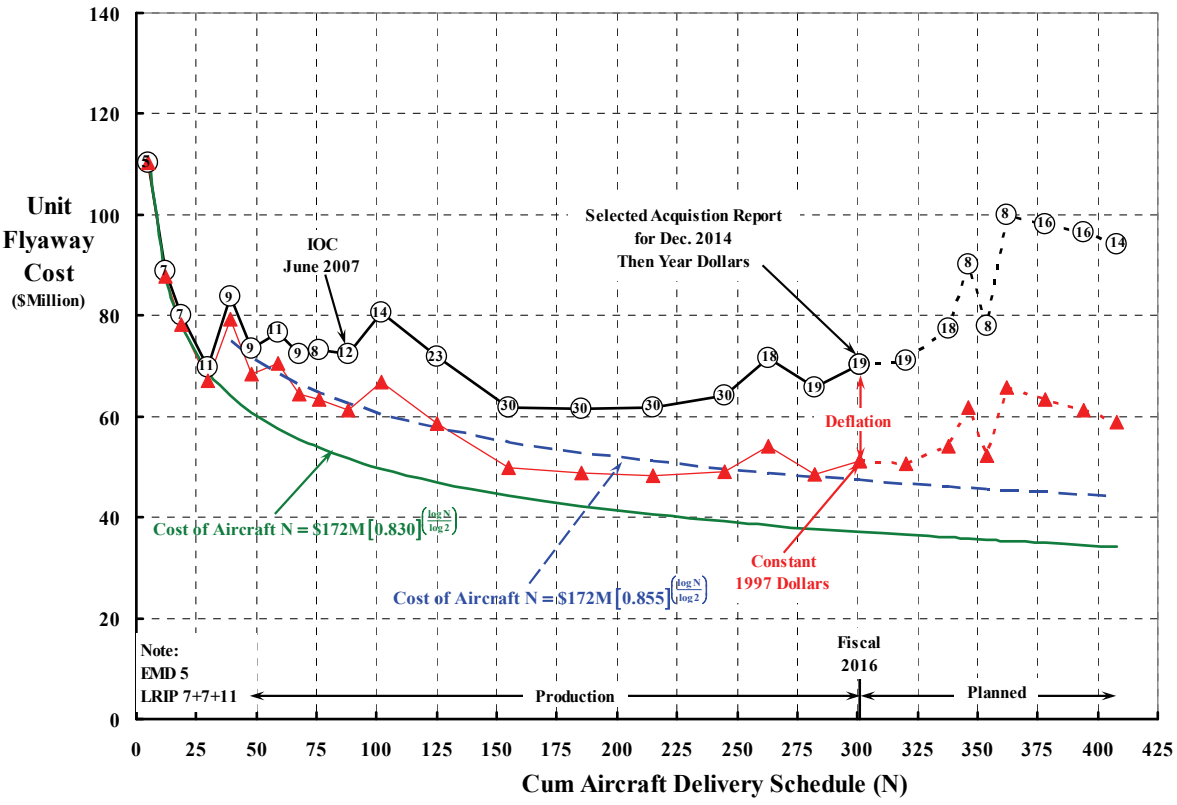

Fig. 4-9. The V-22 program experienced two separate phases with two different learning curves.

1. Have an up-front, carefully agreed upon amount of money over the 10- to 15-year period required to field a new aircraft.
2. Have a firm commitment to the number of aircraft (N) to be procured over the period, and keep production per year constant.
3. Use a base LCF only as the first estimate.
4. And then maybe even double the estimate obtained from step 3.

I suppose that if these suggestions were followed, there would never be another new military aircraft fielded—if for no other reason than that a realistic cost estimate having 95 percent assurance of success appears wildly extravagant when compared to a saleable estimate with only 50 percent assurance of success.

Table 4-2. The Marine/Bell/Boeing V-22 Program Flyaway Cost History [666]

Program Phase	Fiscal Year	Number of Units Bought	Cum of Units	Unit Flyaway, Then-Year $Millions	Cum Flyaway Then-Year $Billions	Deflation Factor [667]	Unit Flyaway, Constant 1997 $Millions	Cum Flyaway Constant 1997 $Billions
EMD	1997	5	5	110.4	0.552	1.000	110.4	0.552
LRIP	1998	7	12	88.9	1.174	1.011	87.9	1.167
LRIP	1999	7	19	80.2	1.736	1.025	78.2	1.715
LRIP	2000	11	30	69.9	2.504	1.041	67.1	2.453
Production	2001	9	39	83.7	3.257	1.057	79.2	3.166
↓	2002	9	48	73.4	3.918	1.075	68.3	3.780
↓	2003	11	59	76.7	4.762	1.089	70.5	4.556
↓	2004	9	68	72.4	5.414	1.125	64.4	5.135
↓	2005	8	76	73.1	5.998	1.155	63.3	5.641
↓	2006	12	88	72.4	6.867	1.182	61.2	6.375
↓	2007	14	102	80.7	7.996	1.206	66.9	7.312
↓	2008	23	125	71.8	9.648	1.225	58.6	8.660
↓	2009	30	155	61.9	11.503	1.242	49.8	10.154
↓	2010	30	185	61.6	13.351	1.263	48.8	11.618
↓	2011	30	215	61.9	15.207	1.284	48.2	13.062
↓	2012	30	245	64.1	17.129	1.306	49.1	14.534
↓	2013	18	263	71.7	18.418	1.328	54.0	15.505
↓	2014	19	282	65.7	19.666	1.351	48.6	16.429
Planned	2015	19	301	70.3	21.003	1.377	51.1	17.399
↓	2016	19	320	71.0	22.351	1.404	50.5	18.360
↓	2017	18	338	77.4	23.744	1.432	54.0	19.332
↓	2018	8	346	90.1	24.465	1.461	61.7	19.825
↓	2019	8	354	77.8	25.087	1.490	52.2	20.243
↓	2020	8	362	100.0	25.887	1.518	65.8	20.770
↓	2021	16	378	98.2	27.458	1.546	63.5	21.786
↓	2022	16	394	96.5	29.001	1.575	61.3	22.766
Production Ends	2023	14	408	94.2	30.320	1.603	58.8	23.589

Now let me discuss the last important factor (in my mind) that lies in the gap between rotary wing and fixed-wing aircraft. This factor is operating costs, one of the major factors in the mind of a potential buyer of a transportation product. In the United States today, for example, an automobile buyer is most certainly concerned about what fuel mileage the car that he (or she) wants is going to get. This concern is the same in the world of rotorcraft and other V/STOL aircraft. But beyond the question of fuel efficiency, a potential V/STOL buyer must also consider total operating costs for each future year.

Total operating cost (TOC) is frequently broken down into fixed costs (e.g., hanger rental for a year) and variable costs, which are costs that are incurred every time the machine is flown. Fig. 4-10 provides a more detailed summary of the cost accounting. You read about TOC in some detail in Volume II starting on page 579 and continuing to page 661. In that introductory discussion about TOC, you will recall that I suggested that

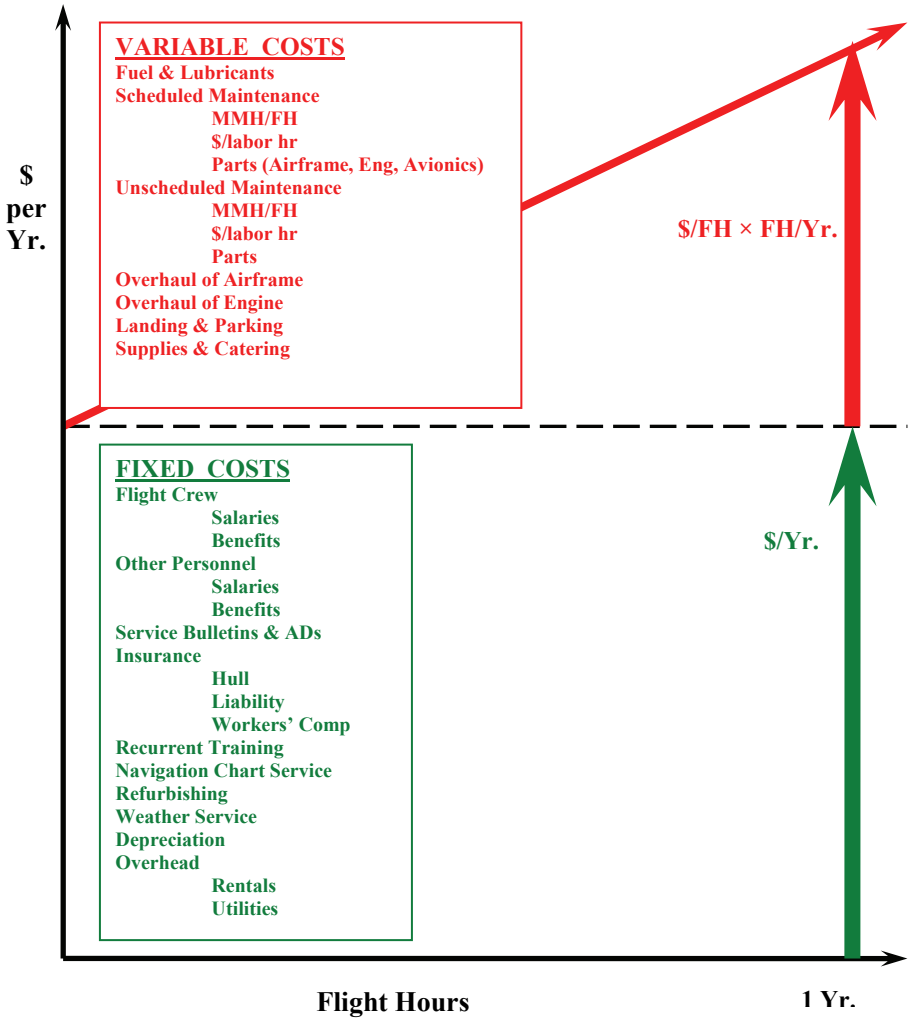

Fig. 4-10. Total operating costs for a year can be divided into two groups: (1) variable (with flight hour), and (2) fixed (typically for a 1-year period) [668].

$$(4.7)\qquad \frac{\text{TOC}}{\text{Year}} = \frac{\text{Fixed Costs}}{\text{Year}} + \left(\frac{\text{Variable Costs}}{\text{Flight Hour}}\right)\left(\frac{\text{Flight Hour}}{\text{Year}}\right),$$

and that total operating costs per year could be roughly estimated—*at least for helicopters*—by

$$(4.8)\qquad \frac{\text{TOC}}{\text{Year}} = \left[175{,}000 + 29.8\left(\frac{\text{Price}}{1{,}000}\right)\right] + \left[8.92\left(\frac{\text{Price}}{1{,}000}\right)^{0.57}\right]\left(\frac{\text{Flight Hour}}{\text{Year}}\right).$$

The price basis in Eq. (4.8) was the list price of the helicopter in 2011 dollars. You see this equation displayed graphically in Fig. 4-11. The reason the total operating costs per flight hour are so dependent on the helicopter's list price is that spare part prices are nearly in direct proportion to the fully assembled helicopter's price.

Let me remind you of one key figure (figure 2-432 on page 641 in Volume II) that I have reproduced here as Fig. 4-12. It is quite true that fuel used inefficiently by current rotary wing aircraft and other V/STOL aircraft is a major operating expense when compared to fixed-wing aircraft. But I believe that the simple fact that rotary wing aircraft require too many spare parts to keep then flying[161] is the root cause of excessive operating costs for that class of aircraft.

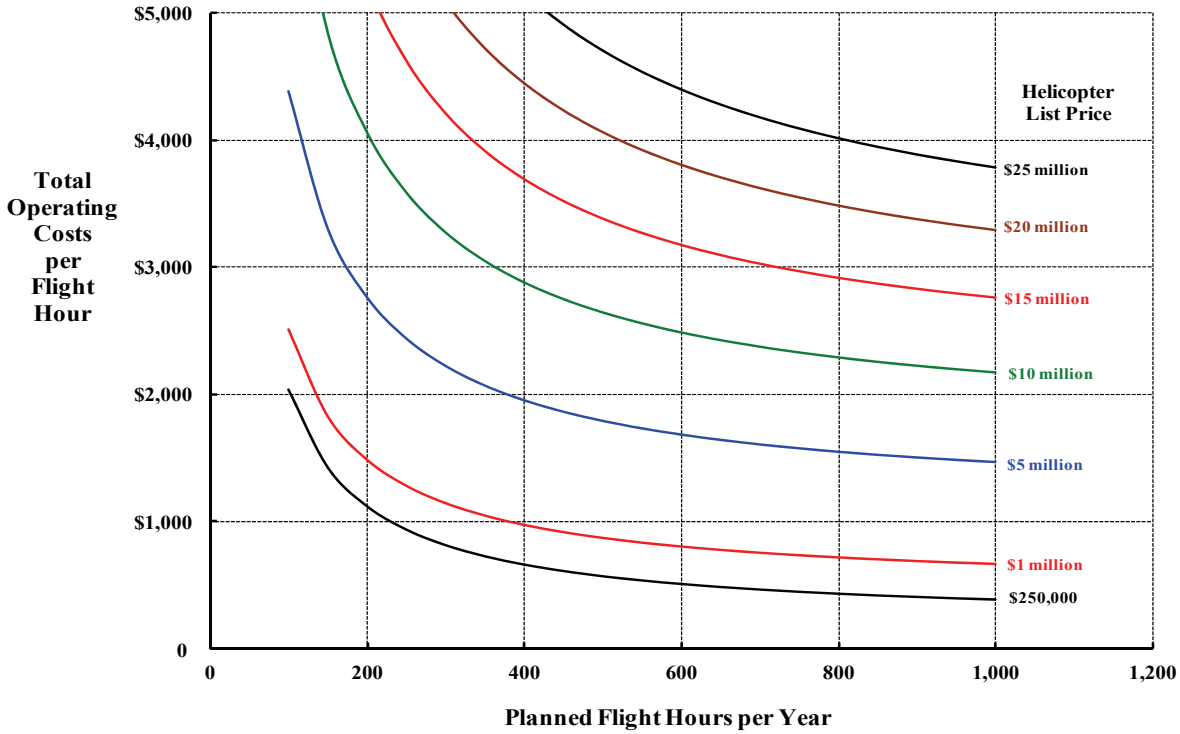

Fig. 4-11. TOC per flight hour for helicopters is quite sensitive to the number of flight hours planned for a year (note: 2011 dollars).

[161] Keep in mind that the sale of spare parts is a significant source of income to helicopter manufacturers. Can you imagine what the cost of a 2015 Cadillac would be if you just ordered all the parts from the dealer's Parts Department and assembled the vehicle yourself?

Using the Robinson R-22 for this example, I would say that a third of the machine (dollar wise) is rebuilt after 2,000 hours of use. You might compare that to a car. A car driven for 100,000 miles at 50 miles per hour will reach 2,000 hours of use. Today's car (in my experience) does not require anything like that amount of reinvestment. It seems to me that the military are satisfied with a very short time interval (i.e., time between overhaul or TBO) before replacement of very expensive components is mandatory. Their satisfaction comes because flight hours per year are much less then those for commercial operators. When you think commercially, turboshaft engine TBOs are on the order 20,000 to 30,000 hours—then it seems to me that helicopter and V/STOL products fall far short. This kind of logic says that operating costs can only be reduced by first concentrating on the top one-third (by price) of spare parts. As an example, I would say that a transmission used in commercial rotary wing VTOL aircraft should be designed for a TBO of 20,000 hours. Maybe it would weigh a little more than if it was designed to a military requirement of 2,000 hours, but the reduction in operating costs would be significant to a potential airline company's buyer. Should you want to study total operating costs for both fixed-wing and rotary wing aircraft in more detail, I suggest you start by purchasing the Conklin & de Decker product called *Aircraft Cost Evaluator* [669]. I used this software (along with several conversations with Bill de Decker, an old friend from my Boeing-Vertol days) to understand the key factors driving helicopter operating costs. A similar investigation could be carried out for the fixed-wing aircraft in their database.

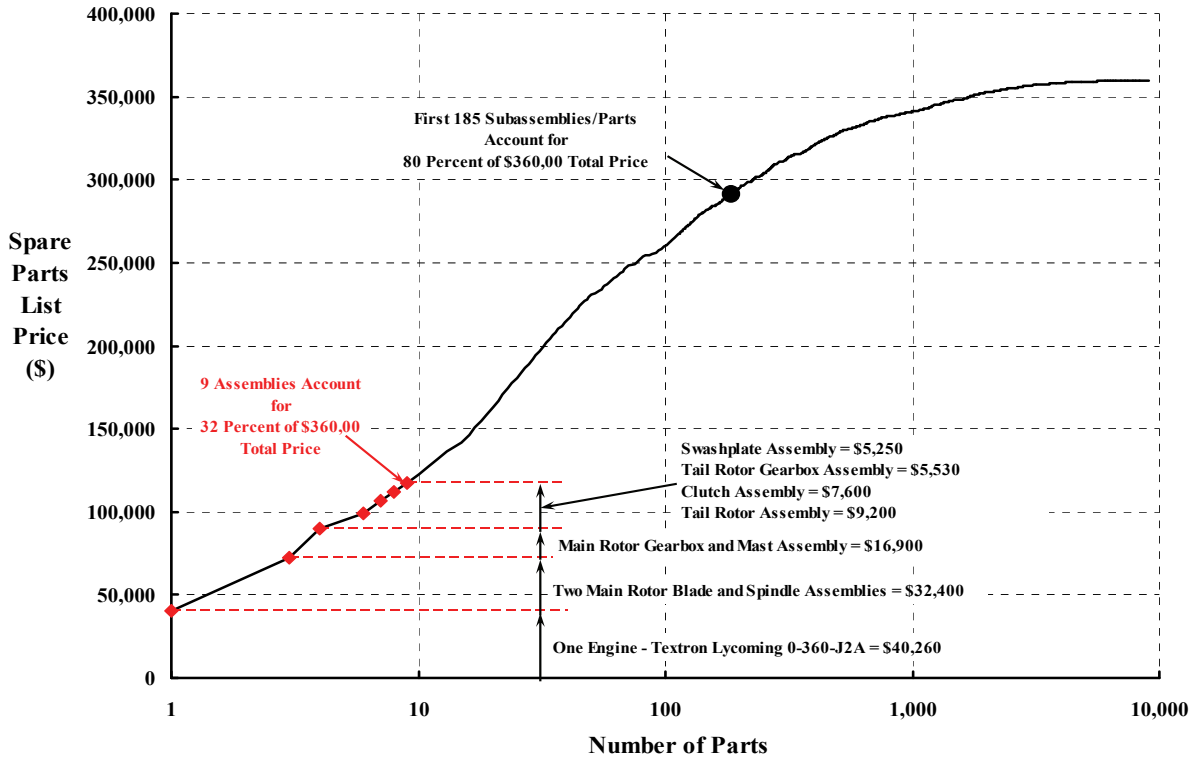

Fig. 4-12. Twenty percent of the assemblies/subassemblies/parts account for 80 percent of the spare parts list price in 2007. Data constructed from Robinson R-22 Spare Parts Manual. See Volume II, Table 2-60, page 639-641.

Now let me conclude this volume—first with a six-decade summary as I see it, then with my views about the need for V/STOL aircraft, and finally with a technical opinion about several V/STOL types.

For nearly six decades now I have wondered if any VTOL aircraft or even some STOL aircraft would be attractive to a commercial airline operator such as Southwest Airlines in the United States. Every once in a while I would run across a paper or report that raised my hopes—only to have that hope again go into hibernation. Let me give you a few examples:

1. The Fairey Rotodyne [70] looked like it was on its way in the early 1950s, but by 1962 "things" and events had conspired to bring the program to a halt. In late 1965, Ling-Temco-Vought was making considerable progress with the XC-142 tiltwing, so much so that an LTV internal study of a commercial version reached my desk [670]. But then U.S. Air Force advocates of this very promising VTOL threw in the towel, and in November 1967 the door closed on the tiltwing—quite prematurely in my mind.

2. However, some momentum did exist in the mid-1970s because requirements for vertiports and air traffic control were being talked about [671, 672]. In 1976, the Massachusetts Institute of Technology (MIT) Flight Transportation Laboratory published an interesting report about the cost of reducing tiltrotor noise in the commercial world [673]. This report suggested that noise would not be a serious threat to a commercial tiltrotor, and I was buoyed up.

3. By the late 1970s, the U.S. Air Force had explored the capability of powered lift (i.e., the two AMST aircraft) to meet their STOL requirements, and then they quit a very promising production program on October 31, 1979. At nearly the same time, the NASA/Army/Bell XV-15 program [37, 331] raised the spirits of every VTOL advocate during the 1980s. And when the V-22 made its first flight on March 19, 1989, I, along with many others [44, 378-380, 674, 675], thought that an attractive civil tiltrotor capable of carrying many passengers was seriously on the horizon. Given that the future of regional transport aircraft was promising [676], one would have thought that a civil tiltrotor could not be far behind.

4. But then the enthusiasm seemed to wane. In fact, the U.S. Congress Office of Technology Assessment published a fascinating report [677] contrasting a tiltrotor aircraft with magnetically levitated vehicles as a solution to transportation woes. That high-speed ground transportation should always be a consideration for crowded corridors was brought home to me again in 1993 [678], and again in 2002—even more forcefully—by R.E.G. Davies [399].

5. In the early 2000s, I began to wonder again just how the U.S. airline industry operated and what their operating costs really were. I learned a lot [679], which gave me a better appreciation of what V/STOL advocates were up against if an airline company like Southwest was going to be sold on a VTOL or STOL machine.

6. In 2007 the Marines MV-22B went to war and clearly demonstrated its value despite a less than satisfactory level of required maintenance [680]. Shortly thereafter, some of NASA's thoughts (as of January 2010) about the next-generation commercial air transportation system were published [681].

7. As of mid-2015, the original Bell 609 small civil tiltrotor that first hovered in March of 2003 has found a home with AgustaWestland. Two AW 609 prototypes have logged over 1,200 hours, and FAA certification is expected *sometime* in 2017 [682]. That amounts to 14 years of gestation to get a civil tiltrotor actually sold.

8. Now the future of V/STOLs appears to rest on the tiltrotor configuration as championed by Bell Helicopter Textron with its entrée to the U.S. Army's Joint Multi-Role program, and Karem Aircraft Inc. with Abe Karem's optimum speed tiltrotor (OSTR) in the United States. In Europe, AgustaWestland is now moving ahead with research very applicable to commercial tiltrotors of any size through the Enhanced Rotorcraft Innovative Concept Achievement (ERICA) and CleanSky programs [388, 389].

In retrospect, it seems that V/STOL advocates have patiently waited for any one of their many configurations to reach production. It appears that the tiltrotor configuration has rewarded all their patience and all the hard work by so many people. As for myself, I am wondering about the encore because I think the shipboard compatible, tiltrotor configuration that now satisfies the U.S. Marines is *most certainly not* the machine to satisfy the civil airline industries of well-developed nations. A direct conversion of the U.S. Marines MV-22B to an airliner makes absolutely no sense to me. That would be just like converting a World War I surplus bomber into a passenger carrying "airliner," which, I will admit, got the airline business started in 1920. But now the world's population has reached about 7 billion, spread across about 200 nations,[162] and their civil transportation needs must be considered.[163] This raises the question of whether the tiltrotor is the only configuration they need. My view is that the answer is an emphatic no, and this leads me to examine the need for V/STOL and to provide some technical opinions about the configurations that can fill that need.

It is relatively easy to see V/STOLs helping to solve city-to-city transportation problems in well-developed countries. But then I wonder about town-to-town transportation in less developed nations. Or what about village-to-village transportation needs in even less developed countries. Thinking this way always leads me to a three-by-three matrix that you see here:

	City	Town	Village
City			
Town			
Village			

Connecting any pair of population centers with some level of transportation service that any given nation can afford leads to quite a few choices. Certainly there is still a need for four-

[162] The United Nations keeps book on these numbers, but how they do it with such accuracy is a mystery to me.

[163] Their military needs are beyond the scope of this closing discussion.

legged animals. Certainly low-speed railroads will always have a place. Automobiles cannot be denied in more prosperous countries. I do not see ferries being displaced by V/STOL. But when transportation by air is under consideration, the V/STOL aircraft choices are now really quite few. I suggest that the six-decade weeding-out process has arrived at:

1. Helicopters
2. Compound VTOLs
   a. Helicopter
   b. Airplane
3. Vectored-thrust VTOLs
   a. Proprotor-driven tiltrotor
   b. Proprotor-driven tiltwing
4. Powered lift STOLs
   a. Propeller driven
   b. Turbofan driven

My rational for this selection relative to the city/town/village matrix is based on travel time and distance. Taking more than 4 hours to travel from one destination to another is my limit. A 200-statute-mile trip to Grammy's for Thanksgiving is my baseline.[164] In the United States, the car will do just fine; a commercial airliner will not, if for no other reason than the Transportation Security Administration (TSA). If I must fly commercial, then the time from when I enter the departure terminal to when I exit the arrival terminal counts as a portion of my 4-hour limit. Today my trip from Oklahoma City Airport to San Jose International Airport in California by Southwest Airlines (about 2,000 statute miles) takes, on average, 7-1/2 hours with the standard one stop to change planes. The airplane (a Boeing 737) flies at 400 to 450 knots (a Mach number around 0.8 at 35,000 feet), but my body feels like it never exceeded 250 to 275 knots. So much for block speed versus flight speed. Of course, if you add traveling time to get to the airport, and then from the final airport to your final destination, your block speed will probably be cut in half. So much for the state of air/ground travel in the United States. At the other extreme, traveling between two villages separated by even 25 miles might be well served by helicopters rather than walking or riding a four-legged animal.[165] But then, who provides the helicopter and does a ticket have to be bought?

Now let me summarize my view of the configurations listed above.[166]

Helicopters—Civil aircraft in this class have been spun off from military requirements in the majority of cases. They are technically well developed but terribly expensive to buy. Operating costs are quite unreasonable because all of the high-price components have too low a time between overhaul or replacement. The helicopter can fill every box in my matrix, but many of the 200 nations cannot afford even one. The majority of future R&D should be directed towards significant price and operating cost reductions. To get started, I suggest that:

---

[164] That is Rose Valley, Pennsylvania, to New Haven, Connecticut, via I-95 by car with two young kids in the back seat.

[165] Covering 25 miles in 7 or 8 hours would be about it for a horse in good condition carrying one rider.

[166] Do not lose sight of the fact that this is just one man's view.

1. Upper management direct the finance departments to share cost data with engineers—to the extent they know it.
2. A survey of civil helicopter flight and maintenance manuals for lists of parts requiring overhaul/replacement in less than 20,000 flight hours be completed.
3. Detail designers be sent out to do maintenance on the helicopters they designed and have them report back with redesign suggestions.
4. A few helicopters be selected and then have detail designers do a redesign—at equal rotor geometry and engine—for selling price and TOC cost reduction. See what the weight empty change is and what requalification cost would be.
5. Engineering students (and not just aero types) not be allowed to graduate without requiring at least an internship in the field.

Compounds—This configuration has suffered from a very inadequate R&D program. The choices made by Fairey with its Rotodyne and McDonnell with its XV-1 in the 1950s only proved that rotor tip drive was unacceptable from noise and fuel consumption points of view *even though* vertical takeoff and landings were of short duration. The many research compounds funded by the U.S. Army in the 1960s established that rotor system aeroelastic stability at high advance ratio and high advancing tip Mach number was technically understood.

Today, *without* a very low drag hub, the compound helicopter is not a candidate for the future. *With* a low-drag hub there are two choices: (1) a low-solidity rotor for hovering plus a wing and propellers (a compound airplane such as the Eurocopter X^3), or (2) a very high solidity rotor with propellers but no wing (a compound helicopter such as the Sikorsky X2). The installed power for either configuration must be based on high cruise speed at or above 25,000 feet.

Bob Ormiston (recently retired from the U.S. Army AFDD at NASA Ames) gave the American Helicopter Society's 2015 Nikolsky Lecture at the 71st Annual Forum [683]. He pointed out how the compound VTOL has been virtually ignored for many decades. He proposed opening the door again, starting with a concentration on hub drag reduction coupled with retractable landing gear. I could not agree more with his views.

I believe the compound need hardly be more complex than a helicopter, and I would expect this machine to have lower fuel costs compared to a helicopter. A compound helicopter, or maybe even better yet, a compound airplane, is a very viable configuration for the city/town blocks in my matrix. The majority of R&D should first be spent on raising this machine's maximum lift-to-drag ratio, starting with hub drag reduction. To get started, I suggest that:

1. The AH-56A hub should be borrowed from the Ft. Rucker museum and wind tunnel tested to measured its drag.
2. Advocates of the compound should read Bob Ormiston's 2015 AHS Nikolsky Lecture.

Vectored thrust—Vectoring a proprotor's thrust from vertical for hovering flight to horizontal for fixed-wing flight is now an accomplished feat. Whether done by tilting a wing plus proprotor assembly (e.g., VZ-2, CL-84, and XC-142) or just the proprotor assemblies alone (e.g., XV-3, XV-15, and MV-22B) seems rather immaterial to me—at least based on flight testing. A primary issue that is frequently raised to influence the choice is disc loading, but both vectored-thrust configurations can be obtained with disc loadings ranging from a low of 20 pounds per square foot to at least 50 or 60 pounds per square foot. I believe the much more important design criteria is to install enough power at sea level so that (1) vertical takeoff and landing can be safely made with full seats and fuel at, or maybe even above, 6,000 feet on a 95 ^{o}F day, and (2) cruising efficiently even at 400 to 450 knots at 35,000 feet is an economical fact.

Rotorcraft advocates continually choose a lower disc loading and only install enough power to hover. In the several vectored-thrust design studies I have reviewed, it seems that high cruise speed has not been given much consideration, although NASA Ames studied what they called a Short Haul Civil Tiltrotor (SHCT) in the late 1990s [684]. Rotorcraft advocates seem to just be elated that their vectored-thrust airplane-like machines go faster than their helicopters. Elation is not good enough.

My view is that tiltrotor and tiltwing aircraft are ideal for the turboprop market operating as regional transportation aircraft. However, the six vectored-thrust machines that have flown should not be used as models for future commercial designs; they were developed to satisfy military requirements. Vectored-thrust configurations easily fill the city/town blocks in my matrix.

The majority of R&D should be spent on raising the maximum lift-to-drag ratios to at least 15 for these aircraft, starting with wingspans better suited to the design gross weight, not to the naval ships currently available as was the case of the V-22, and certainly not to be carried in some military logistic fixed-wing transport. When vectored-thrust aircraft are "cleaned up," then lower installed power will get the speed and range it needs to be competitive. To get started, I suggest that:

1. The 1991 NASA-contracted studies, *Technology Needs for High-Speed Rotorcraft* provided by Boeing [685], Sikorsky [686], and McDonnell Douglas [687], be re-examined and brought up to date.
2. Proprotors providing propulsive efficiency greater than 0.8 (and capable of satisfactory operation) at Mach numbers greater than 0.8 be designed using our most advanced analytical tools and then a select few be tested.

Powered lift STOLs—Reasonably adequate powered STOL aircraft have been demonstrated using either propellers (e.g., the de Havilland Caribou and Buffalo, Bréguet 941, and Lockheed NC-130B) or turbofans (e.g., the NASA QSRA, Antonov An-72, Boeing YC-14, and McDonnell Douglas YC-15). Clearly, the design challenge is to obtain absolutely safe flight control and stability down to at least 60 knots, even at 6,000 feet on a 95 ^{o}F day when the aircraft has full seats and fuel. I believe that the 60-knot takeoff and landing speed,

with consideration of one engine out, will ensure aircraft certification for runways less than 2,000 feet. Frankly, I would forget STOL without absolutely safe flight control and stability down to at least 60 knots at 6,000 feet/95 ^{o}F and with consideration of one engine out.

I very much favor propeller-driven over turbofan-driven aircraft if the Bréguet 941 cross-shaft design philosophy is applied. The Bréguet 941 cross-shaft approach solved the 60-knot design problem as you have learned. Furthermore, propeller designs easily capable of Mach 0.8 with propeller efficiency about 0.8 were developed [688-691] during the mid-1970's oil crises. STOL application of these propellers was studied in 1985 [692]. Therefore, propeller-driven commercial transports in this class can concentrate on at least an objective of 400 knots cruise speed at 35,000 feet, and this might attract commercial airlines to STOL.

As to the turbofan-driven STOL, these configurations need to have their engine thrust vectored more downward for takeoffs and landings before I would become interested. Trying to turn jet engine exhaust downward by flaps is just too inefficient.

Powered lift configurations seem ideal for the town-to-town block and to and from the town-to-city blocks of my matrix. The majority of R&D should first be spent on giving regional turboprop aircraft STOL capability using less than 2,000 feet of concrete or "semi-prepared" earth and much higher cruise speeds than those aircraft currently in operation. To get started, I suggest that:

1. A few aircraft from the current fleet of regional turboprop airliners be selected and a redesign of those few for STOL operation over their current route structure be completed.
2. With knowledge from step 1, a reassessment of whether STOL airliners really have a place in the world of commercial transportation be made.

In closing, let me leave you with these thoughts:

Today, V/STOLs fall in the class of turboprop-driven regional aircraft. Because the commercial airline business does not think about propeller-driven airliners until fuel is expensive, there has been very little interest in "puddle jumping" aircraft carrying relatively few passengers on the shorter routes. Therefore, there has been only a limited need for turboprop aircraft and certainly no crying need voiced for V/STOL aircraft. But V/STOL advocates must be more far-sighted in their thinking. A good example is what McDonnell Douglas did when they demonstrated the Bréguet 941S (as the McDonnell Douglas Model 188) to Eastern Airlines, American Airlines, and others in the late 1960s. Surely, V/STOL advocates can *demonstrate* a few of their other choices.

Wondering how the U.S. Federal Aviation Administration (FAA), for example, would deal with a large fleet of even one of the above commercial V/STOLs is beyond me. But before talking to the FAA, I would start by analyzing the world's airline companies' current route structures and operational economics. Then I would approach the airlines with suggested future routes and ask them if they could make money on these future routes with any of the

configurations presented above. I suspect their responses will center around future passenger markets, expanded route structures to be developed, purchase price, and operating cost. So what will V/STOL advocates say and what will they propose?

My view is that V/STOL aircraft should take off and land—*with seats and tanks full*—from a 2,000-foot runway located at 6,000 feet on a 95 ^{o}F day. Furthermore, their cruise performance goal is shown by the green square on Fig. 4-13. Shooting for this goal means that there is a great deal of work left to do.

I am quite confident that commercial V/STOL aircraft will slowly but surely become part of the world's transportation system—just like the Wright Brothers' invention has and just like our helicopter pioneers envisioned.

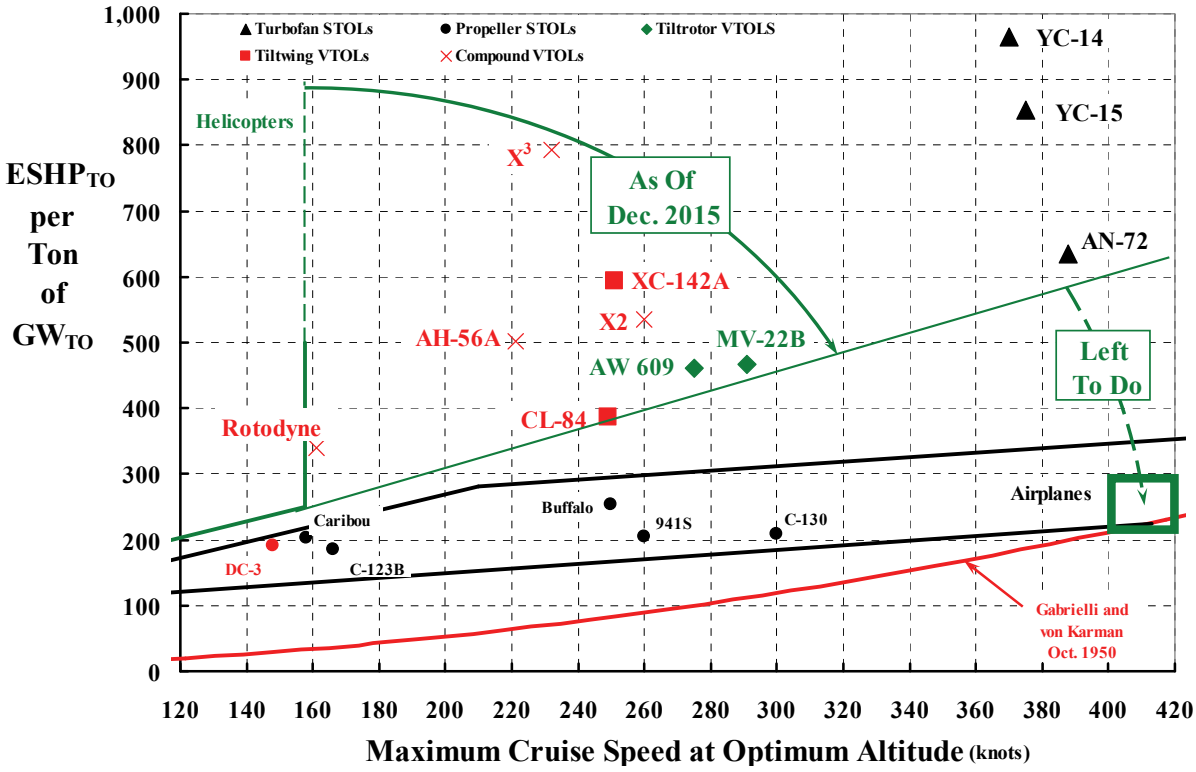

Fig. 4-13. V/STOL advocates have a great deal of work left to do.

5 REFERENCES

1. Loftin, L. K.: Quest for Peformance: The Evolution of Modern Aircraft. NASA SP-468, 1985.
2. Davies, R. E. G.: Airlines of the United States. Washington, D.C.: Smithsonian Institution Press, 1972.
3. Miller, R. E.; and Sawers, D.: The Technical Development of Modern Aviation. New York, N.Y.: Praeger Publications, 1970.
4. Guggenheim, H. F.: Pioneer Educator in the Air Age. New York University, New York, N.Y., 1956.
5. Guggenheim, D.: The Daniel Guggenheim International Safe Aircraft Competition—Final Report. New York, N.Y.: The Daniel Giggenheim Fund, Jan. 31, 1930.
6. Brooks, P. W.: Cierva Autogiros: The Development of Rotary-Wing Flight. Washington, D.C.: Smithsonian Institution Press, 1988.
7. Juptner, J. P.: U.S. Civil Aircraft Series. Blue Ridge Summit, Pa.: TAB Aero, 1993.
8. Prandtl, L.: Applications of Modern Hydrodynamics to Aeronautics. NACA TR 116, 1921.
9. Dearborn, C. H.; and Soulé, H. A.: Full-Scale Wind-Tunnel and Flight Tests of a Fairchild 22 Airplane Equipped With a Fowler Flap. NACA TN 578, Aug. 1936.
10. Juptner, J. P.: U.S. Civil Aircraft: Vol. 5 (ATC 401-ATC 500). Blue Ridge Summit, Pa.: Tab Aero Publishers, 1993.
11. Ransone, R. K.; and Basquez, J. G.: The Report of the Ad Hoc Committee on VSTOL Terminology. AFFTC-SP-67-1001, Air Force Flight Test Center, Edwards Air Force Base, Calif., July 1967.
12. Anon.: Dictionary of Military and Associated Terms, Joint Publication 1-02. U.S. Department of Defense, Washington, D.C., Nov. 8, 2012, p. 281.
13. Dowden, P. R.: Hiller X-18 Research VTOL Aircraft. AHS Newsletter, vol. 4, no. 12, Dec. 1958.
14. Schairer, G. S.: A Summary and Overview of V/STOL Concepts. V/STOL Technology and Planning Conference, Las Vegas, Nev., Sept. 26, 1969.
15. Anon.: Type Certificated Data Sheet No. A45EU. Department of Transportation, Federal Aviation Administration, Washington D.C., Jan. 9, 1979.
16. Schairer, G. S.: Looking Ahead in V/STOL. Eighth Anglo-American Aeronautical Conference, London, England, Dec. 1961.
17. Schairer, G. S.: Some Opportunities for Progress in Aircraft Performance, 27th Wright Brothers' Lecture. AIAA Mtg., New York, N.Y., Jan. 20, 1964.
18. Liberatore, E. K.: Rotary Wing Aircraft Handbooks and History, Volume 13, Convertible Aircraft. Prewitt Aircraft Co., Clifton Heights, Pa., 1954.
19. Crowell, L. C.: Improvement in Aerial Machines. U.S. Patent No. 35,437 Issued June 3, 1862.
20. Anon.: Danish Aviation From Ellehammer to SAS. Royal Danish Aero Club. The Royal Danish Ministry for Foreign Affairs, Copenhagen, Denmark, Sept. 4, 1956.

21. Liberatore, E. K.: Helicopters Before Helicopters. Malabar, Fla.: Krieger Publishing Co., 1998.
22. Lindenbaum, B.: V/STOL Concepts and Developed Aircraft. Volume I—A Historical Report (1940–1986). June 26, 1986.
23. Andrews, H.: Rolling Along—The VSTOL Wheel. AHS Vertiflite, vol. 43, no. 2, Apr. 1997.
24. Campbell, J. P.: Vertical Takeoff and Landing Aircraft. New York, N.Y.: The MacMillan Co., 1962.
25. Rogers, M.: VTOL Military Research Aircraft. New York, N.Y.: Orion Books, Div. of Crown Publishers, Inc., 1989.
26. Norton, B.: STOL Progenitors: The Technology Path to a Large STOL Aircraft and the C-17A. Reston, Va.: American Institute of Aeronautics and Astronautics, Inc., 2002.
27. McCormick, B. W.: Aerodynamics of V/STOL Flight. Orlando, Fla.: Academic Press, Inc., 1967.
28. Anon.: Proc. Experimental V/STOL Aircraft Lessons Learned Sessions. AIAA/AHS/ASEE Aircraft Design, Systems, and Operations Mtg., American Institute of Aeronautics and Astronautics, Dayton, Ohio, Sept. 17–19, 1990.
29. Kruesi, F. E.: Civil Tiltrotor Development Advisory Committee Report to Congress. Volume I: Final Report (see also ADA306654). U.S. Department of Transportation, Washington, D.C., Dec. 1995.
30. Kruesi, F. E.: Civil Tiltrotor Development Advisory Committee Report to Congress. Volume 2: Technical Supplement (see also ADA306655). U.S. Department of Transportation, Washington, D.C., 1995.
31. Kohlman, D. L.: Introduction to V/STOL Airplanes. Iowa City, Iowa: University of Iowa Press, July 30, 1981.
32. Kuhn, R. E.; Margason, R. J.; and Curtis, P.: Jet Induced Effects: The Aerodynamics of Jet- and Fan-Powered V/STOL Aircraft in Hover and Transition, Vol. 217. Reston, Va.: American Institute of Aeronautics and Astronautics, Inc., 2006.
33. Hager, R. D.; and Vrabel, D.: Advanced Turboprop Project: NASA SP-495, 1988.
34. Whittle, R.: The Dream Machine—The Untold History of the Notorious V-22 Osprey. New York, N.Y.: Simon & Schuster, 2010.
35. Gunston, B.: The Osprey Encyclopedia of Russian Aircraft, 1875–1995. London, England: Osprey Aerospace Ltd., 1995.
36. Anon.: V/STOL Special Issue. AHS Vertiflite, vol. 43, no. 2, Mar./Apr. 1997.
37. Maisel, M. D.; Giulianetti, D. J.; and Dugan, D. C.: The History of the XV-15 Tilt Rotor Research Aircraft: From Concept to Flight. NASA SP-2000-4517, 2000.
38. Miller, J.: The X-Planes. Arlington, Tex.: Aerofax, Inc., 1988.
39. Norton, W. J.: Vought/Hiller/Ryan XC-142A Tiltwing VSTOL Transport (Air Force Legends No. 213). Simi Valley, Calif.: Steve Ginter Books, 2006.
40. Norton, W.: Bell Boeing V-22 Osprey (Aerofax Series). Hinckley, England: Midland Publishing, Oct. 1, 2004.

41. Covert, E. E.: Aeronautical Technologies for the Twenty-First Century—Executive Summary. Aeronautics and Space Engineering Board, National Research Council, Washington, D.C., 1992.
42. Covert, E. E.: Aeronautical Technologies for the Twenty-First Century. Aeronautics and Space Engineering Board, National Research Council, Washington, D.C., 1992.
43. Statler, W. H.; and Blay, R. A.: The Role of the Rotary Wing in Future Short-Haul Transportation. Lockheed Horizons Magazine, no. 6, 1968.
44. Anon.: Tiltrotor—A National Transportation Asset. Bell Helicopter Textron, Ft. Worth, Tex., 1999.
45. Thompson, P., et al.: Civil Tiltrotor Missions and Applications, Phase II: The Commercial Passenger Market, Summary Final Report. NASA CR-177576, Jan. 1991.
46. Lightfoot, R. B.: VTOL-1968. AIAA VTOL Systems Committee, 1968.
47. Few, D. D.: A Perspective on 15 Years of Proof-of-Concept Aircraft: Development and Flight Research at Ames-Moffett by the Rotorcraft and Powered-Lift Flight Projects Divisions, 1970–1985. NASA RP-1187, Aug. 1987.
48. Stouffer, V.; Johnson, J.; and Gribko, J.: Civil Tiltrotor Feasibility Study for the New York and Washington Terminal Areas. NASA/CR-2001-210659, Jan. 2001.
49. Anon.: Future Vertical Lift—Report to Congress: A Strategic Plan for United States Department of Defense Vertical Lift Aircraft. Office of the Under Secretary of Defense; Director, Land Warfare and Munitions; Acquisition, Technology & Logistics (AT&L), Aug. 27, 2010.
50. Schairer, G. S.: 27th Wright Brothers Lecture—Some Opportunities for Progress in Aircraft Performance. J. Aircraft, vol. 1, no. 2, Mar.–Apr. 1964.
51. Fradenburgh, E. A.: Overview of Helicopters and V/STOL Aircraft and Basic Aerodynamics for Rotor Performance. Special Course on Aerodynamics of Rotorcraft, AGARD Fluid Dynamics Panel, von Karman Institute, Brussels, Belgium, April 2–5, 1990.
52. Stepniewski, W. Z.; and Tarczynski, T.: Open Airscrew VTOL Concepts. NASA CR-177603, Sept. 1992.
53. Carroll, R. H.; Jants, J. W.; and Milns, P.: STOL Tactical Aircraft Investigation, Volume 1—Configuration Definition: Medium STOL Transport With Vectored Thrust/Mechanical Flaps. Air Force Flight Dynamics Laboratory AFFDL-TR-73-19, May 1973.
54. White, R. P.; and Yeates, J. E.: Volume I—Propellers and Rotor Aerodynamics. Proc. CAL/USAAVLABS Symposium: Aerodynamics Problems Associated With V/STOL Aircraft, Buffalo, N.Y., June 22–24, 1966.
55. White, R. P.; and Yeates, J. E.: Volume II—Propulsion and Interference Aerodynamics. Proc. CAL/USAAVLABS Symposium: Aerodynamics Problems Associated With V/STOL Aircraft, Buffalo, N.Y., June 22–24, 1966.
56. White, R. P.; and Yeates, J. E.: Volume III—Aerodynamic Research on Boundary Layers. Proc. CAL/USAAVLABS Symposium: Aerodynamics Problems Associated With V/STOL Aircraft, Buffalo, N.Y., June 22–24, 1966.
57. Colin, P. E.; and Williams, J.: The Aerodynamics of V/STOL Aircraft. AGARD-VKI Lecture Series, von Karman Institute, Brussels, Belgium, May 1968.

58. Anon.: NASA Conference on V/STOL Aircraft. NASA-TM-X-70202. NASA Langley Research Center, Langley Field, Va., Nov. 17–18, 1960.
59. Anon.: First National V/STOL Aircraft Symposium (AD626360). Wright-Patterson Air Force Base, Dayton, Ohio, Nov. 3–4, 1965.
60. Anon.: Conference on V/STOL and STOL Aircraft. NASA SP-116. NASA Ames Research Center, Moffett Field, Calif., April 4–5, 1966.
61. Anon.: STOL Technology Conference. NASA SP-320. NASA Ames Research Center, Moffett Field, Calif., Oct. 17–19, 1972.
62. Anon.: Powered-Lift Aerodynamics and Acoustics. Conference at Langley Research Center, Hampton, Va., May 24–26, 1976.
63. Nielsen, J. N. (Ed.): Proc. Circulation-Control Workshop 1986. NASA CP-2432. NASA Ames Research Center, Moffett Field, Calif., Feb. 19–21, 1986.
64. Anon.: NASA/Industry High Speed Rotorcraft Mtg. Proc. American Helicopter Society 47th Annual Forum, Phoenix, Ariz., May 8, 1991.
65. Jones, G. S.; and Joslin, R. D.: Proc. 2004 NASA/ONR Circulation Control Workshop. NASA/CP-2005-213509, Parts 1 and 2. Radisson-Hampton, Hampton, Va., Mar. 16–17, 2004.
66. Anon.: Vehicle Technology for Civil Aviation—The Seventies and Beyond. NASA SP-292. Langley Research Center, Hampton, Va., Nov. 2–4, 1971.
67. Hall, T. L.: International Congress on Subsonic Aeronautics. New York, N.Y., Nov. 22, 1968. New York Academy of Sciencies, vol. 154, art. 2, pp. 245–1117.
68. Franklin, J. A.: V/STOL Dynamics, Control, and Flying Qualities. NASA/TP-2000-209591, Oct. 2000.
69. Anon.: A Preliminary Study of V/STOL Transport Aircraft and Bibliography of NASA Research in the VTOL-STOL Field. NASA TN D-624, Jan. 1, 1961.
70. Gibbings, D.: Fairey Rotodyne. Gloucestershire, UK: The History Press, 2009.
71. Olson, W. M.: Aircraft Performance Flight Testing. AFFTC-TIH-99-01, Air Force Flight Test Center, Edwards Air Force Base, Calif., Sept. 2000.
72. Jones, R. T.: Classical Aerodynamic Theory. NASA RP-1050, Dec. 1979.
73. Harris, F. D.: Rotary Wing Aerodynamics—Historical Perspective and Important Issues. Proc. National Specialists' Mtg. on Aerodynamic and Aeroacoustics, American Helicopter Society Southwest Region, Arlington, Tex., 1987.
74. Arcidiacono, P. J.: Aerodynamic Characteristicts of a Model Rotor Operating at Advance Ratios as High as 2.5. United Aircraft Corp. Research Laboratories Report R-0324-1, Dec. 1959.
75. Ewans, J. R.; and Krauss, T. A.: Model Wind Tunnel Tests of a Reverse Velocity Rotor System. Fairchild Report HC144R1070, Fairchild Industries, Inc., Farmingdale, N.Y., Jan. 31, 1973.
76. Jenny, D. S.; Arcidiacono, P. J.; and Smith, A. F.: A Linearized Theory for the Estimation of Helicopter Rotor Characteristics at Advance Ratios Above 1.0. Proc. American Helicopter Society 19th Annual Forum, Washington, D.C., May 1–3, 1963.
77. Ewans, J. R., et al.: Further Model Wind Tunnel Tests of a Reverse Velocity Rotor System. Fairchild Report HC171R1089, Fairchild Industries, Inc., Farmingdale, N.Y., July 18, 1975.

78. Tayor, R. B.: Vibratory Hub Load Data Reduction and Analysis From the Reverse Velocity Rotor Wind Tunnel Test. NASA CR-137780, Jan. 1976.
79. Ashby, D.; Eadie, W.; and Monotoro, G. J.: An Investigation of the Reverse Velocity Rotor Concept and Its Application to High Speed Rotorcraft. 2002 Biennial International Powered Lift Conference and Exhibit, AIAA No. 2002-5991, Williamsburg, Va., Nov. 5–7, 2002.
80. McCloud, J. L.; and Biggers, J. C.: An Investigation of Full-Scale Helicopter Rotors at High Advance Ratios and Advancing Tip Mach Numbers. NASA TN D-4632, July 1968.
81. Charles, B. D.; and Tanner, W. H.: Wind Tunnel Investigation of Semi-Rigid Full-Scale Rotors Operating at High Advance Ratios. USAAVLABS TR 69-2, Jan. 1969.
82. Charles, B. D.: An Experimental/Theoretical Correlation of Model and Full-Scale Rotor Performance at High Advancing-Tip Mach Numbers and High Advance Ratios. USAAVLABS TR 70-69, Jan. 1971.
83. Jenkins, J. L., Jr.: Wind-Tunnel Investigation of a Lifting Rotor Operating at Tip-Speed Ratios From 0.65 to 1.45. NASA TN D-2628, Feb. 1965.
84. Sweet, G. E.; Jenkins, J. L.; and Winston, M. M.: Wind-Tunnel Measurements on a Lifting Rotor at High Thrust Coefficients and High Tip-Speed Ratios. NASA TN D-2462, Sept. 1964.
85. Doetsch, H. K.; and Mark, L.: Wind-Tunnel Investigation to Determine the Critical Advance Ratio of the 8/31-Scale McDonnell Model 82 Convertiplane Rotor. WADC TR 53-125, Wright Air Development Center, Wright-Patterson Air Force Base, Dayton, Ohio, Apr. 1953.
86. Horvay, G.: Rotor Blade Flapping Motion. Quarterly of Applied Mathematics, vol. 5, no. 2, July 1947, pp. 149–167.
87. Hohenemser, K.: A Type of Lifting Rotor With Inherent Stabiliy. Institute of the Aerospace Sciences 18th Annual Mtg., New York City, N.Y., Jan. 23–26, 1950.
88. Hohenemser, K.: Some Aerodynamic and Dynamic Problems of Compound Rotary-Fixed Wing Aircraft. Proc. American Helicopter Society 8th Annual Forum, Washington, D.C., May 15–17, 1952.
89. Head, R. E.; and Hohenemser, K. H.: Aerodynamic Characteristics of a Two-Bladed, Eight-Foot Rotor Model at High Tip-Speed Ratios as Measured in the UWAL Wind Tunnel. McDonnell Aircraft Corp. Report No. 1951, Jan. 1951.
90. Hohenemser, K. H.: Higher Flight Speeds for Rotary Wing Aircraft by Combination With Fixed Wing. First Convertible Aircraft Congress, Philadelphia, Pa., Dec. 1949.
91. Jenkins, J. L., Jr.: Trim Requirements and Static-Stability Derivatives From a Wind-Tunnel Investigation of a Lifting Rotor in Transition. ADA956532. Langley Research Center, Hampton, Va., Feb. 1965.
92. Kisovec, A.: Advanced Rotor System Summary Report Concerning the Twistable Blade Segment and Related Hardware. The Boeing Co., Vertol Div. Report No. R-327, Aug. 23, 1963.
93. Harris, F. D.: Model Segmented Rotor Test—Quick Look at Wind Tunnel Results. Vertol Interoffice Memorandum 8-7440-1-528, from Frank Harris to Phil Sheridan, Apr. 16, 1965.

94. Ekquist, D. G.: Design and Wind Tunnel Test of a Model Helicopter Rotor Having an Independently Movable Inboard Blade Panel. USAAVLABS TR 65-63, Oct. 1965.
95. Zientek, T. A.: Expanding the Flight Envelope With a Segmented Rotor. Proc. American Helicopter Society 57th Annual Forum, Washington, D.C., May 9–11, 2001.
96. McHugh, F. J.; and Harris, F. D.: Have We Overlooked the Full Potential of the Conventional Rotor? Proc. American Helicopter Society 31st Annual National Forum, Washington, D.C., May 13–15, 1975.
97. McHugh, F.; Clark, R.; and Soloman, M.: Wind Tunnel Investigation of Rotor Lift and Propulsive Force at High Speed, Data Analysis. NASA CR-145217-1, Oct. 1977.
98. McHugh, F.; Clark, R.; and Soloman, M.: Wind Tunnel Investigation of Rotor Lift and Propulsive Force at High Speed. Test Data Appendix Part 2. NASA CR-145217-2, Oct. 1977.
99. McHugh, F.; Clark, R.; and Soloman, M.: Wind Tunnel Investigation of Rotor Lift and Propulsive Force at High Speed. Test Data Appendix Part 3. NASA CR-145217-3, Oct. 1977.
100. Sheffler, M.: Analysis and Correlation With Theory of Rotor Lift-Limit Test Data. NASA CR-159139, Nov. 1979.
101. Yeo, H.: Calculation of Rotor Performance and Loads Under Stalled Conditions. Proc. American Helicopter Society 59th Annual Forum, Phoenix, Ariz., May 6–8, 2003.
102. Hall, K. C.; and Hall, S. R.: A Variational Method for Computing the Optimal Aerodynamic Performance of Conventional and Compound Helicopters. J. American Helicopter Society, vol. 55, no. 4, 2010.
103. Johnson, W.: CAMRAD II Comprehensive Analytical Model for Rotorcraft Aerodynamics and Dynamics—Theory Manual. Johnson Aeronautics, Inc., Palo Alto, Calif., 1993.
104. Keennon, M., et al.: Tailless Flapping Wing Propulsion and Control Development for the Nano Hummingbird Micro Air Vehicle. American Helicopter Society Future Vertical Lift Aircraft Design Conference, San Francisco, Calif., Jan. 18–20, 2012.
105. Johnson, W.: Performance and Loads Data From a Wind Tunnel Test of a Full-Scale Rotor With Four Blade Tip Planforms. NASA TM-81229 (see also USAAVRADCOM TR 80-A-9), Sept. 1980.
106. Trenka, A. R.: The Aerodynamic and Aeroelastic Characterics of a Full-Scale Rotor at Very High Advance Ratios and During Start/Stop Operation. USAAVLABS TR 70-60, May 1971.
107. Wheatley, J. B.; and Hood, M. J.: Full-Scale Wind-Tunnel Tests of a PCA-2 Autogiro Rotor. NACA TR 515, 1935.
108. Harris, F. D.: An Overview of Autogyros and the McDonnell XV-1 Convertiplane. NASA/CR-2003-212799, Oct. 2003.
109. Harris, F. D.: Rotor Performance at High Advance Ratio: Theory Versus Test. NASA/CR-2008-215370, Oct. 2008.
110. Harris, F. D.; Tarzanin, F. J.; and Fisher, R. K.: Rotor High Speed Performance, Theory vs. Test. V/STOL Technology and Planning Conference, Las Vegas, Nev., Sept. 23–25, 1969.

111. Quackenbush, T. R., et al.: Next Generation Modeling Technology for High Speed Rotorcraft. Continuum Dynamics, Inc. Report No. 10-13, Aug. 2010.
112. Flores, M. W.; and Johnson, W.: Performance Analysis of the Slowed-Rotor Compound Helicopter Configuration. American Helicopter Society Fourth Decennial Specialists' Conference on Aeromechanics, San Francisco, Calif., Jan. 21–23, 2004.
113. Marks, M. D.: Flight Test Development of XV-1 Convertiplane. American Helicopter Society Third Western Forum, Dallas, Tex., Oct. 8, 1956.
114. Robb, R. L.: Hybrid Helicopters: Compounding the Quest for Speed. AHS Vertiflite, vol. 52, no. 2, Summer 2006.
115. Simon, D.; and White, J. W.: Compound Helicopter Review (Purchase Contract ACP 826 With Boeing-Vertol). CAPCON, Ltd., Sandy, Utah, Aug. 19, 1992.
116. Landis, T.; and Jenkins, D. R.: Lockheed AH-56A Cheyenne. North Branch, Minn.: Specialty Press, 2000.
117. Van Wyckhouse, J. F.; and Cresap, W. L.: Summary Report High-Performance-Helicopter Program Phase I. U.S. Army TRECOM TR 63-42, Sept. 1963.
118. Van Wyckhouse, J. F.; and Cresap, W. L.: Summary Report High-Performance-Helicopter Program Phase II. U.S. Army TRECOM TR 64-41, Oct. 1964.
119. Van Wyckhouse, J. F.: High-Performance UH-1 Compound Helicopter Maneuver Flight Test Program. U.S. Army AVLABS TR 66-17, Feb. 1966.
120. Sonneborn, W. O.: High Mach Number/High Advance Ratio Flight Test Program With the UH-1 Compound Helicopter. U.S. Army AVLABS TR 71-2, 1971.
121. Whitfield, A. A.; and Blackburn, W. E.: UH-2 Helicopter High-Speed Flight Research Program Utilizing Jet Thrust Augmentation—Final Report. U.S. Army TRECOM TR 65-14, Mar. 1965.
122. Blackburn, W. E.; and Whitfield, A. A.: UH-2 Jet-Augmented High-Speed Research Helicopter Maneuverability and Dynamic Stability Evaluation. U.S. Army AVLABS TR 65-23, July 1965.
123. Blackburn, W. E.; and Rita, A. D.: UH-2 Helicopter High-Speed Flight Research With Lift and Thrust Augumentation. U.S. Army AVLABS TR 67-12, Oct. 1967.
124. Blackburn, W. E.; and Rita, A. D.: Flight Research Program to Evaluate Methods of Improving Compound Helicopter Maneuver Capability. U.S. Army AVLABS TR 67-59, Apr. 1968.
125. Foulke, W. K.: Exploration of High-Speed Flight With the XH-51A Rigid Rotor Helicopter. U.S. Army AML TR 65-25, June 1965.
126. Wyrick, D. R.: Extension of the High-Speed Flight Envelope of the XH-51A Compound Helicopter. U.S. Army AVLABS TR 65-71, Nov. 1965.
127. Lentine, F. P.; Groth, W. P.; and Oglesby, T. N.: Research in Maneuverability of the XH-51A Compound Helicopter. U.S. Army AVLABS TR 68-23, June 1968.
128. Cruz, E. S.; Gorenberg, N. B.; and Kerr, A. W.: A Flight Envelope Expansion Study for the XV-51A Compound Helicopter. U.S. Army AVLABS TR 69-78, Oct. 1969.
129. Bartsch, E. A.: In-Flight Measurement and Correlation With Theory of Blade Airloads and Responses on the XH-51A Compound Helicopter, Vol. I. U.S. Army AVLABS TR 68-22A, May 1968.

130. Bartsch, E. A.: In-Flight Measurement and Correlation With Theory of Blade Airloads and Responses on the XH-51A Compound Helicopter, Vol. II. U.S. Army AVLABS TR 68-22B, May 1968.
131. Bartsch, E. A.: In-Flight Measurement and Correlation With Theory of Blade Airloads and Responses on the XH-51A Compound Helicopter, Vol. III. U.S. Army AVLABS TR 68-22C, May 1968.
132. Anon.: Preliminary Flight Test Data, XH-51A Rigid Rotor High Speed Flight Program—Interim Report No. 9. U.S. Army TRECOM (see also DTIC AD 621893), Dec. 1964.
133. Segel, R. M., et al.: Final Report NH-3A (Sikorsky S-61F) Flight Test Program. Sikorsky SER-611344 (see also DTIC AD726764), Mar. 20, 1969.
134. Meyers, D. N.; Tompkins, L. V.; and Goldberg, J. H.: 16H-1A Flight Test Research Program. U.S. Army AVLABS TR 67-58, Aug. 1968.
135. Ruddell, A. J.: Advancing Blade Concept (ABC) Technology Demonstrator. U.S. Army AVRADCOM-TR-81-D-5, Apr. 1981.
136. Paglino, V. M.; and Beno, E. A.: Full-Scale Wind-Tunnel Investigation of the Advancing Blade Concept Rotor System. U.S. Army AMRDL TR 71-25, Aug. 1971.
137. Ruddell, A. J.: XH-59A ABC Technology Demonstratot Altitude Expansion and Operational Tests. U.S. Army AVRADCOM-TR-81-D-35, Dec. 1981.
138. Arents, D. N.: An Assessment of the Hover Performance of the XH-59A Advancing Blade Concept Demonstrator Helicopter. U.S. Army AMRDL TN-25, May 1977.
139. Yamakawa, G. M.: Attack Helicopter Evaluation, Blackhawk S-67 Helicopter. U.S. Army ASTA Project No. 72-09, July 1972.
140. Anon.: Substantiation Technical Data, AH-56A Attack Helicopter—Book 1. Lockheed Report No. 25271, May 31, 1972.
141. Anon.: Substantiation Technical Data, AH-56A Attack Helicopter—Book 2. Lockheed Report No. 25271, May 31, 1972.
142. Johnson, J. N.; Bender, G. L.; and Burden, J. R.: Engineering Evaluation AH-56A Compound Helicopter With Advanced Mechanical Control System. U.S. Army ASTA Project No. 72-44, Mar. 1973.
143. Perry, F. J.: Aerodynamics of the Helicopter World Speed Record. Proc. American Helicopter Society 43rd Annual Forum, St. Louis, Mo., May 18–20, 1987.
144. Mecklin, R.: A Look at the Model 360 Development. Society of Experimental Test Pilots, Oct. 1988.
145. Walsh, D., et al.: High Airspeed Testing of the Sikorsky X2 Technology Demonstrator. Proc. American Helicopter Society 67th Annual Forum, Virginia Beach, Va., May 4, 2011.
146. Scott, M. T.; Sigl, D.; and Strawn, R. C.: Computational and Experimental Evaluation of Helicopter Rotor Tips for High-Speed Flight. AIAA J. Aircraft, vol. 28, no. 6, June 1991.
147. Grina, K. I.: The Model 360 Advanced Composite Helicopter. 30th Annual Conference on Aviation and Astronautics, Israel, Feb. 15–16, 1989.
148. Grina, K. I.: The Boeing Helicopter Model 360 Advanced Technology Helicopter. AHS Vertiflite, vol. 34, no. 1, 1988.

149. Grina, K. I.: Development of Helicopter Design Capability Progress From 1970 to 1973—The 1993 Alexander A. Nikolsky Lecture. J. American Helicopter Society, vol. 39, no. 1, May 1993.
150. Harvey, D.: Boeing Vertol's 360: Form Fitting Function. Rotor & Wing International, Sept. 1987.
151. Anon.: Boeing 360: Helicopter Hi-Tech. Flight International, Apr. 18, 1987.
152. Mecklin, R.: Model 360 Flight Data. Personal Communication to Frank Harris. Jan. 4, 2013.
153. Hartman, L. J.; Mecklin, R.; and Wiesner, R.: Boeing Model 360 Advanced Technology Helicopter—Design Features and Flight Test Update. Proc. American Helicopter Society 44th Annual Forum, Washington, D.C., June 16–18, 1988.
154. McVeigh, M. A.; and McHugh, F. J.: Recent Advances in Rotor Technology at Boeing Vertol. Proc. American Helicopter Society 38th Annual Forum, Anaheim, Calif., May 4–7, 1982.
155. Wisniewski, J. S.: The Boeing Model 360 Advanced Technology Demonstrator Helicopter. 51st Annual Conference of the Society of Allied Weight Engineers, Hartford, Conn., May 18–20, 1992.
156. Zinner, R. A.; Boxwell, D. A.; and Spencer, R. H.: Review and Analysis of the DNW/Model 360 Rotor Acoustic Data Base. NASA TM-102253 (see also USAAVSCOM TM 89-A-002), Nov. 1989.
157. Beaumier, P., et al.: Evaluation of Airload Prediction Methodologies Using BH-360 Test Data. Proc. American Helicopter Society 53rd Annual Forum, Virginia Beach, Va., Apr. 28–May 1, 1997.
158. Dadone, L., et al.: Model 360 Rotor Test at DNW—Review of Peformance and Blade Airload Data. Proc. American Helicopter Society 43rd Annual Forum, St. Louis, Mo., May 18–20, 1987.
159. Bagai, A.: Aerodynamic Design of the X2 Technology Demonstrator Main Rotor Blade. Proc. American Helicopter Society 64th Annual Forum, Montreal, Canada, Apr. 29–May 1, 2008.
160. Walsh, D., et al.: Development Testing of the Sikorsky X2 Technology Demonstrator. Proc. American Helicopter Society 65th Annual Forum, Grapevine, Tex., May 27–29, 2009.
161. Blackwell, R.; and Millott, T.: Dynamics Design Characteristics of the Sikorsky X2 Technology Demonstrator Aircraft. Proc. American Helicopter Society 64th Annual Forum, Montreal, Canada, Apr. 29–May 1, 2008.
162. Wake, B. E., et al.: Assessment of Helicopter Hub Drag Prediction With an Unstructured Flow Solver. Proc. American Helicopter Society 65th Annual Forum, Grapevine, Tex., May 27–29, 2009.
163. Guess: The Eurocopter X3 Hybrid Helicopter Making High Speed Cost Effective. American Helicopter Society Future Vertical Lift Aircraft Design Conference, San Francisco, Calif., Jan. 18–20, 2012.
164. Harris, F. D.: AHIP: The OH-58D From Conception to Production. Proc. American Helicopter Society 42nd Annual Forum, Washington, D.C., June 2–5, 1986.

165. Anon.: News in Brief: Boeing Model 360 Grounded. Flight International, Feb. 2–27, 1990.
166. Daly, K.: Model 360 Eyes Helicopter Speed Record. Flight International, July 18–24, 1990.
167. Johnson, C. L.: Kelly—More Than My Share of It All. Washington, D.C.: Smithsonian Books, 1985.
168. Nelms, D.: Aviation Week Flies Eurocopter's X3. Aviation Week, July 9, 2012.
169. Maisel, M. D.: Tilt Rotor Research Aircraft Familiarization Document. NASA TM-X-62407, Jan. 1975.
170. Scully, M.: Details of the TU-95. Personal communication to Harris, F. D., Feb. 2013.
171. Anon. (Bell Helicopter Co.): Advancement of Proprotor Technology, Task II—Wind-Tunnel Test Results. NASA CR-114363, Sept. 30, 1971.
172. Arrington, W. L.; Kumpel, M.; Marr, R. L.; and McEntire, K. G.: XV-15 Tilt Rotor Research Aircraft Flight Test Data Report, Volume II of V: Peformance and Handling Qualities. NASA CR-177406, Vol. II, June 1985.
173. Arrington, W. L.; Kumpel, M.; Marr, R. L.; and McEntire, K. G.: XV-15 Tilt Rotor Research Aircraft Flight Test Data Report, Volume III of V: Structural and Dynamics. NASA CR-177406, Vol. III, June 1985.
174. Arrington, W. L.; Kumpel, M.; Marr, R. L.; and McEntire, K. G.: XV-15 Tilt Rotor Research Aircraft Flight Test Data Report, Volume I of V: Introduction. NASA CR-177406, Vol. I, June 1985.
175. Gabrielli, G.; and von Karman, T.: What Price Speed. Mechanical Engineering, vol. 72, Oct. 1950.
176. Harris, F. D.: An Analytical Study of Rotor Performance at High Forward Speeds. Proc. American Helicopter Society 17th Annual National Forum, Washington, D.C., May 3, 1961.
177. Ransone, R. K.; and Jones, G. E.: XC-142A V/STOL Transport Tri-Service Limited Category I Evaluation. AFFTC FTC-TR-65-27, Air Force Flight Test Center, Edwards Air Force Base, Calif., Jan. 1966.
178. Hendrickson, C. L.; and Jones, G. E.: XC-142A VSTOL Transport Catgory II Performance Evaluation. AFFTC FTC-TR-68-21, Air Force Flight Test Center, Edwards Air Force Base, Calif., Oct. 1968.
179. Bolesney, J.: Actual Weight and Balance Model XC-142A (Second Airplane). Ling-Temco-Vought (LTV) Report No. 2-53460/4R-950, Sept. 30, 1964.
180. Norton, W.: Bell/Boeing V-22 Osprey (Aerofax Series). Hinckley, England: Midland Publishing, Oct. 1, 2004.
181. Stanzione, K. A.; and Oliver, L. L.: Downwash Design Criteria for VTOL Aircraft. American Helicopter Society 49th Annual Forum, St. Louis, Mo., May 1993.
182. Anon.: Development of the U.S. Army VZ-2 (Boeing Vertol Model 76) Research Aircraft. The Boeing Co., Vertol Div. Report No. R-219 (see also DTIC AD 417836), Aug. 1963.
183. Pegg, R. J.: Summary of Flight-Test Results of the VZ-2 Tilt-Wing Aircraft. NASA TN D-989, Feb. 1962.

184. Reeder, J. P.: Handling Qualities Experience With Several VTOL Research Aircraft. NASA TN D-735, Jan. 1, 1960.
185. Newsom, W. A.; and Tosti, L. P.: Force-Test Investigation of the Stability and Control Characteristics of a 1/4-Scale Model of a Tilt-Wing Vertical-Take-Off-and-Landing Aircraft. NASA Memo 11-3-58L, Jan. 1959.
186. Tosti, L. P.: Flight Investigation of the Stability and Control Characteristics of a 1/4-Scale Model of a Tilt-Wing Vertical-Take-Off-and-Landing Aircraft. NASA Memo 11-4-58L, Jan. 1959.
187. Taylor, R. T.: Wind-Tunnel Investigation of Effect of Ratio of Wing Chord to Propeller Diameter With Addition of Slats on the Aerodynamic Characteristics of Tilt-Wing VTOL Configurations in the Transition Speed Range. NASA TN D-17, Sept. 1959.
188. Kuhn, R. E.: An Investigation to Determine Conditions Under Which Downwash From VTOL Aircraft Will Start Surface Erosion From Various Types of Terrain. NASA TN D-56, Sept. 1959.
189. Thomas, L. P.: A Flight Study of the Conversion Maneuver of a Tilt-Wing VTOL Aircraft. NASA TN D-153, Dec. 1959.
190. Yaggy, P. F.; and Rogallo, V. L.: A Wind-Tunnel Investigation of Three Propellers Through an Angle-of-Attack Range from 0° to 85°. NASA TN D-318, May 1960.
191. Tosti, L. P.: Aerodynamic Characteristics of a 1/4-Scale Model of a Tilt-Wing VTOL Aircraft at High Angles of Wing Incidence. NASA TN D-390, Sept. 1960.
192. Pegg, R. J.: Damage Incurred on a Tilt-Wing Multi-Propeller VTOL/STOL Aircraft Operating Over a Level, Gravel-Covered Surface. NASA TN D-535, Dec. 1960.
193. Ward, J. F.: Structural-Loads Surveys on Two Tilt-Wing VTOL Configurations. NASA TN D-729, Mar. 1961.
194. Tosti, L. P.: Rapid-Transition Tests of a 1/4-Scale Model of the VZ-2 Tilt-Wing Aircraft. NASA TN D-946, Oct. 1961.
195. Pegg, R. J.: Flight-Tested Investigation of Ailerons as a Source of Yaw Control on the VZ-2 Tilt-Wing Aircraft. NASA TN D-1375, July 1962.
196. Tosti, L. P.: Longitudinal Stability and Control of a Tilt-Wing VTOL Aircraft Model With Rigid and Flapping Propeller Blades. NAS TN D-1365, July 1962.
197. Newsom, W. A.; and Tosti, L. P.: Slipstream Flow Around Several Tilt-Wing VTOL Aircraft Models Operating Near the Ground. NASA TN D-1382, Sept. 1962.
198. Mitchell, R. G.: Full-Scale Wind-Tunnel Test of the VZ-2 VTOL Airplane With Particular Reference to the Wing Stall Phenomena. NASA TN D-2013, Dec. 1963.
199. Schade, R. O.; and Kirby, R. H.: Effect of Wing Stalling in Transition on a 1/4-Scale Model of the VZ-2 Aircraft. NASA TN D-2381, Aug. 1964.
200. Kirby, R. H.; Schade, R. O.; and Tosti, L. P.: Force-Test Investigation of a 1/4-Scale Model of the Modified VZ-2 Aircraft. NASA TN D-2382, Aug. 1964.
201. Segner, D. R.: Navy Evaluation of the Vertol Model 76C Tilt Wing Aircraft. Naval Air Test Center Report No. 1, Final Report, Oct. 31, 1960.
202. Stepniewski, W. Z.; and Dancik, P. J.: Flight Testing Experiments With the Tilt-Wing Aircraft. Aero/Space Engineering, Feb. 1959.

203. Loewy, R. G.; and Yntema, R. T.: Some Aeroelastic Problems of Tilt-Wing VTOL Aircraft. J. American Helicopter Society, vol. 3, no. 1, Jan. 1958.
204. Spenser, J. P.: Vertical Challenge, The Hiller Aircraft Story. Seattle, Wash.: University of Washington Press, 1992.
205. Nichols, J. B.: The Hiller X-18 Experimental Aircraft Lessons Learned. Proc. Experimental V/STOL Aircraft Lessons Learned Sessions of the AIAA/AHS/ASEE Aircraft Design, Systems, and Operations Mtg., Dayton, Ohio, Sept. 1990.
206. Tosti, L. P.: Flight Investigation of Stability and Control Characteristics of a 1/8-Scale Model of a Tilt-Wing Vertical-Take-Off-and-Landing (VTOL) Airplane. NASA TN D-45, Mar. 1960.
207. Tosti, L. P.: Force-Test Investigation of the Stability and Control Characteristics of a 1/8-Scale Model of a Tilt-Wing Vertical-Take-Off-and-Landing (VTOL) Airplane. NASA TN D-44, Mar. 1960.
208. Sweeney, R.: X-18 Rollout Accentuates VTOL Research. Aviation Week, Dec. 15, 1958.
209. Pickler, R. A.; and Milberry, L.: Canadair—The First Fifty Years. Toronto, Ontario, Canada: CANAV Books, 1995.
210. Kelley, H. L.; Reeder, J. P.; and Champine, R. A.: Summary of a Flight-Test Evaluation of the CL-84 Tilt-Wing V/STOL Aircraft. NASA TM X-1914, Mar. 1970.
211. Honaker, J. S., et al.: Tri-Service Evaluation of the Canadair CL-84 Tilt-Wing V/STOL Aircraft. USAAVLABS Technical Report 67-84, U.S. Army Aviation Material Laboratories, Ft. Eustis, Va., Nov. 1967.
212. Lindenbaum, B.; and Fraga, D. E.: A Review of the U.S. Tri-Service V/STOL Programs. AGARD Flight Mechanics Panel Symposium on Military Applications of V/STOL Aircraft, NATO Headquarters, Brussels, Belgium, Oct. 23–25, 1972.
213. Anon.: Upwardly Mobile: A VTOL Research Aircraft for the UK. Air Enthusiast, vol. 121, Jan. 1960.
214. Perkins, C. D.: Final Report of the Defense Science Board Task Force on V/STOL Aircraft. DTIC ADA 201049. Office of the Under Secretary of Defense for Research and Engineering, Nov. 1979.
215. Anon.: Utility Flight Manual, USAF Series XC-142A Aircraft, T.O. 1C-142 (X) A-1, Aug. 15, 1964.
216. Down, H. W.; and Jones, G. E.: XC-142A Limited Category II Stability and Control Tests. U.S. Air Force Flight Test Center Report No. FTC-TR-68-9, July 1968.
217. Lucero, F. N.; and Jones, G. E.: XC-142A Operational Suitability Tests. U.S. Air Force Flight Test Center Report No. FTC-TR-67-28, Dec. 1967.
218. Chopin, M. H.: Propeller Static Peformance Tests for V/STOL Aircraft—Part I, Summary Report. ASD-TR-69-15 (see also DTIC AD708501), Jan. 1970.
219. Chopin, M. H.: Propeller Static Peformance Tests for V/STOL Aircraft—Part II, Test Data (Appendix III). ASD-TR-69-15 (see also DTIC AD 708742), Jan. 1970.
220. Herrington, R. W., et al.: Flight Test Engineering Handbook. Air Force Report No. 6273 (see also DTIC AD636392), Jan. 1966.
221. Hemke, P. E.: Elementary Applied Aerodynamics. New York, N.Y.: Prentice-Hall, Inc., 1946.

222. Goodson, K. W.: Comparison of Wind-Tunnel and Flight Results on a Four-Propeller Tilt-Wing Configuration. NASA SP-116. Conference on V/STOL and STOL Aircraft, NASA Ames Research Center, Moffett Field, Calif., Apr. 4–5, 1966, pp. 51–62.
223. Newsom, W. A.; and Kirby, R. H.: Flight Investigation of Stability and Control Characteristics of a 1/9-Scale Model of a Four-Propeller Tilt-Wing V/STOL Transport. NASA TN D-2443, Sept. 1964.
224. Goodson, K. W.: Longitudinal Aerodynamic Characteristics of a Flapped Tilt-Wing Four-Propeller V/STOL Transport Model. NASA TN D-3217, Feb. 1966.
225. Deckert, W. H.; Page, V. R.; and Dickinson, S. O.: Large-Scale Wind-Tunnel Tests of Descent Performance of an Airplane Model With a Tilt Wing and Differential Propeller Thrust. NASA TN D-1857, Oct. 1964.
226. Goodson, K. W.: Effect of Ground Proximity on the Longitudinal, Lateral, and Control Aerodynamic Characteristics of a Tilt-Wing Four-Propeller V/STOL Model. NASA TN D-4237, Dec. 1967.
227. Turner, T. R.: Endless-Belt Technique for Ground Simulation. NASA SP-116. Conference on V/STOL and STOL Aircraft, NASA Ames Research Center, Moffett Field, Calif., Apr. 4–5, 1966, pp. 435–446.
228. Head, A. L.: A Review of the Structural Dynamic Characteristics of the XC-142A Transport (proc. vol. II). CAL/TRECOM Symposium, Buffalo, N.Y., June 26–28, 1963.
229. Head, A. L.; and Smith, W. D.: Dynamic Model Testing of the XC-142A Aircraft. Symposium on Aeroelastic and Dynamic Model Testing Technology, Dayton, Ohio, Sept. 23–25, 1962.
230. Anon.: V/STOL Handling-Qualities Criteria. AGARD Report No. 577, Part II, June 1973.
231. Weitz, P. J.: A Qualitative Discussion of the Stability and Control of VTOL Aircraft During Hover (Out of Ground Effect) and Transition. Naval Postgrauate School Thesis (see also DTIC AD 022205), Oct. 19, 1965.
232. Anderson, S. B.: Considerations for Revision of V/STOL Handling Qualities Criteria. NASA SP-116. Conference on V/STOL and STOL Aircraft, NASA Ames Research Center, Moffett Field, Calif., April 4–5, 1966, pp. 229–248.
233. Black, E. L.; and Booth, G. C.: Correlation of Aerodynamic Stability and Control Derivatives Obtained From Flight Tests and Wind Tunnel Tests on the XC-142A Airplane. Air Force Flight Dynamics Laboratory AFFDL-TR-68-167, Nov. 1968.
234. Schane, W. P.: Effects of Downwash Upon Man. U.S. Army Aeromedical Research Unit Report No. 68-3, Nov. 1967.
235. Dausman, G. E.: The LTV XC-142 Experimental Aircraft—Lessons Learned. AIAA/AHS/ASEE Aircraft Design, Systems, and Operations Mtg., Dayton, Ohio, Sept. 1990.
236. Kolesar, C. E.: Isolated Cyclic Pitch Propeller: Results of Wind Tunnel Test. The Boeing Co., Vertol Div. Report No. D170-10037-1, June 1970.
237. Guerrier, M. A.: Letters to the Editor. AHS Vertiflite, vol. 34, no. 5, Sept./Oct. 1988.
238. Lichten, R. L.: Helicopter Perfromance. J. Aeronautical Sciences, July 1946.

239. Lichten, R. L.: Some Aspects of Convertible Aircraft Design. J. Aeronautical Sciences, Oct. 1949.
240. Gustafson, F. B.: Auto Accident Injuries Fatal to R. L. Lichten. AHS Vertiflite, vol. 17, no. 8, Sept./Oct. 1971.
241. Brown, D. A.: The Bell Helicopter Textron Story—Changinge the Way the World Flies. Hinckley, England: Midland Publishing, July 1995.
242. Cobey, W. E.: Transcendental Aircraft Corporation—Background, Personnel and Facilities. Courtesy of Gordon Fries, Glen Riddle, Pa., 1955.
243. Cobey, W. E.: Transendental Convertiplanes. Newsletter (later AHS Vertiflite), vol. 2, no. 11, Nov. 1956.
244. Norton, B.: Transcendental Aircraft—The Real First Tiltrotors. AHS Vertiflite, vol. 52, no. 2, Summer 2006.
245. Lynn, R. R.: The Rebirth of the Tilt Rotor—The 1992 Alexander A. Nikolsky Lecture. J. American Helicopter Society, vol. 38, no. 1, Jan. 1993.
246. McClarren, R. H. (Ed.). Proc. Rotating Wing Mtg., Franklin Institute, Philadelphia, Pa., Oct. 28–29, 1938.
247. Tapscott, R. J.; and Kelley, H. L.: A Flight Study of the Conversion Manuever of a Tilt-Duct VTOL Aircraft. NASA TN D-372, Nov. 1960.
248. Kelley, H. L.: Transition and Hovering Flight Characterisics of a Tilt-Duct VTOL Research Aircraft. NASA TN D-1491, Nov. 1962.
249. Kelley, H. L.; and Champine, R. A.: Flight Operating Problems and Aerodynamic and Performance Characteristics of a Fixed-Wing, Tilt-Duct, VTOL Research Aircraft. NASA TN D-1802, July 1963.
250. Yaggy, P. F.; and Mort, K. W.: A Wind-Tunnel Investigation of a 4-Foot-Diameter Ducted Fan Mounted on the Tip of a Semispan Wing. NASA TN D-776, Mar. 1961.
251. Yaggy, P. F.; and Goodson, K. W.: Aerodynamics of a Tilting Ducted-Fan Configuration. NASA TN D-785, Mar. 2, 1961.
252. Goodson, K. W.; and Grunwald, K. J.: Aerodynamic Characteristics of a Powered Semispan Tilting-Shrouded-Propeller VTOL Model in Hovering and Transition Flight. NASA TN D-981, Jan. 1962.
253. Mort, K. W.; and Yaggy, P. F.: Aerodynamic Characteristics of a 4-Foot-Diameter Ducted Fan Mounted on the Tip of a Semispan Wing. NASA TN D-1301, Apr. 1962.
254. Mort, K. W.; and Yaggy, P. F.: The Effectiveness of Three Exit Vane Cascade Configurations for Vectoring the Thrust of a Ducted Fan. NASA TN D-1688, Oct. 1964.
255. Mort, K. W.: Performance Characteristics of a 4-Foot-Diameter Ducted Fan at Zero Angle of Attack for Several Fan Blade Angles. NASA TN D-3122, Dec. 1965.
256. Deckert, W. H.; and Ferry, R. C.: Limited Flight Evaluation of the XV-3 Aircraft. AFFTC-TR-60-4, Air Force Flight Test Center, Edwards Air Force Base, Calif., May 1960.
257. Miller, J., et al.: Bell's XV-3. Aerophile, vol. 2, no. 1, June 1979.
258. Miller, J.: World's First Successful Tiltrotor Under Restoration. AHS Vertiflite, vol. 50, no. 4, Winter 2004.

259. Pinero, E.: Bell XV-3 Tiltrotor Restoration Complete. AHS Vertflite, vol. 52, no. 3, Fall 2006.
260. Davis, C. E.: Practical V/STOL—The XV-3 Story. Newsletter (later AHS Vertiflite), vol. 6, no. 6, June 1960.
261. Thomason, T.: The Bell XV-3 and XV-15 Experimental Aircraft. AIAA/ASEE Aircraft Design, Systems and Operating Conference, Dayton, Ohio, Sept. 17–19, 1990.
262. Anon.: The Bell Composite—Practical, Cost-Effective V/STOL. AHS Vertiflite, vol. 13, no. 5, May 1967.
263. Koenig, D. G.; Greif, R. K.; and Kelly, M. W.: Full-Scale Wind-Tunnel Investigation of the Longitudinal Characteristics of a Tilting-Rotor Convertiplane. NASA TN D-35, Dec. 1959.
264. Deckert, W. H.; and Ferry, R. C.: Preliminary Report—AFFTC Flight Evaluation of the XV-3. Air Force Flight Test Center, Edwards Air Force Base, Calif. (see also DTIC AD A951617), July 22, 1959.
265. Anon.: Pilot Evaluation of the Bell Model XV-3 Vertical Takeoff and Landing Aircraft. U.S. Transportation Material Command, Aviation Technology Office TR-62-01, Feb. 1962.
266. Edenborough, H. K.: Investigation of Tilt-Rotor VTOL Aircraft Rotor-Pylon Stability. AIAA J. Aircraft, vol. 5, no. 6, Apr. 1968.
267. Lynn, R. R.: XV-3 Incident Report NASA Ames 40- by 80-Foot Tunnel. Bell Helicopter Company Report No. 599-075-120, June 10, 1966.
268. Quigley, H. C.; and Koenig, D. G.: A Flight Study of the Dynamic Stability of a Tilting-Rotor Convertiplane. NASA TN D-778, Apr. 1961.
269. Perkins, C. D.; and Hage, R. E.: Airplane Peformance, Stability, and Control. New York, N.Y.: John Wiley & Sons, Inc., 1949.
270. Etkin, B.: Dynamics of Atmospheric Flight. New York, N.Y.: John Wiley & Sons, Inc., Dec. 1, 1972.
271. Bisplinghoff, R. L.; Ashley, H.; and Halfman, R. L.: Aeroelasticity. Reading, Mass.: Addison-Wesley Publishing Co., Inc., Nov. 1957.
272. Prouty, R.: Helicopter Performance, Stability, and Control. Boston, Mass.: PWS Publishing Co., 1986.
273. Vaughen, J. F.: Sef-Feathering Rotary Wing. American Helicopter Society Vertical Lift Aircraft Design Conference, San Francisco, Calif., Jan. 1995.
274. Amer, K. B.: Theory of Helicopter Damping in Pitch or Roll and a Comparison With Flight Measurements. NACA TN 2136, Oct. 1950.
275. Lynn, R. R.: Fifty Years of Challenge. Royal Aeronautical Society, 37th Cierva Memorial Lecture, London, England, Oct. 1996.
276. Gaffey, T. M.; Yen, J. G.; and Kvaternik, R. G.: Analysis and Model Tests of the Proprotor Dynamics of a Tilt-Proprotor VTOL Aircraft. Air Force V/STOL Technology and Planning Conference, Las Vegas, Nev., Sept. 1969.
277. Zbrozek, J. K.: The Simple Harmonic Motion of a Helicopter Rotor With Hinged Blades. Aeronautical Research Committee R&M 2813, Apr. 1949.

278. Britland, C. M.; and Fail, R. A.: Preliminary Measurements of the Aerodynamic Damping in Pitch of a 12 ft Diameter Helicopter Rotor. Ministry of Supply, C.P. No. 22, ARC Technical Note Aero 2049, May 1950.
279. Sissingh, G. J.: Comparison of Helicopter Rotor Model Tests of Aerodynamic Damping With Theoretical Estimates. Ministry of Supply, ARC Technical Note Aero 2118, Aug. 1951.
280. Sissingh, G. J.: The Effect of Induced Velocity Variation on Helicopter Rotor Damping in Pitch and Roll. Ministry of Supply, ARC Technical Note Aero 2118, Nov. 1951.
281. Castles, W.; and New, N. C.: A Blade-Element Analysis for Lifting Rotors That is Applicable for Large Inflow and Blade Angles and Any Reasonable Blade Geometry. NACA TN 2656, July 1952.
282. Wheatley, J. B.: An Aerodynamic Analysis of the Autogiro Rotor With a Comparison Between Calculated and Experimental Results. NACA TR 487, 1934.
283. De la Cierva, J.: Engineering Theory of the Autogiro (Original Notes). Bennett, J. A. J. (Ed.). Philadelphia, Pa.: Pitcairn Cierva Autogiro Company of America, 1929.
284. De la Cierva, J. (Ed.): Theory of Stresses on Autogiro Rotor Blades (Original Notes). Philadelphia, Pa.: Pitcairn Cierva Autogiro Company of America, 1934.
285. Hall, W. E.: Prop-Rotor Stability at High Advance Ratios. J. American Helicopter Society, vol. 11, no. 2, Apr. 1966.
286. Johnson, W.: Analytical Modeling Requirements for Tilting Proprotor Aircraft Dynamics. NASA TN D-8013, July 1975.
287. Collar, A. R.: Aeroelasticity—Retrospect and Prospect, the Second Lanchester Memorial Lecture. J. Royal Aeronautical Society, vol. 63, no. 577, Jan. 1959.
288. Collar, A. R.: The First Fifty Years of Aeroelasticity. Aerospace (The Royal Aeronautical Society's Journal), vol. 5, no. 2, Feb. 1978.
289. Garrick, I. E.; and Reed, W. H.: Historical Development of Aircraft Flutter. AIAA J. Aircraft, vol. 18, no. 11, Nov. 1981.
290. Taylor, E. S.; and Browne, K. A.: Vibration Isolation of Aircraft Power Plants. J. Aeronautical Sciences, vol. 6, Dec. 1938, pp. 43–49.
291. Loewy, R. G.: Review of Rotary-Wing V/STOL Dynamic and Aeroelastic Problems. AIAA/AHS VTOL Reserach, Design, and Operations Mtg., AIAA Paper No. 69-202, Atlanta, Ga., Feb. 1969.
292. Ormiston, R. A., et al.: Survey of Army/NASA Rotorcraft Aeroelastic Stability Research. NASA TM-101026 (also USAAVSCOM TR 88-A-005), Oct. 1988.
293. Houbolt, J. C.; and Reed, W. H.: Propeller-Nacelle Whirl Flutter. Institute of the Aerospace Sciences 29th Annual Mtg., Aeroelasticiy Session, New York, N.Y., Jan. 1961.
294. Abbott, F. T.; Kelly, H. N.; and Hampton, K. D.: Investigation of Propeller-Power-Plant Auroprecession Boundaries for a Dynamic-Aeroelastic Model of a Four-Engine Turboprop Transport Airplane. NASA TN D-1806, Aug. 1963.
295. Bland, S. R.; and Bennett, R. M.: Wind-Tunnel Measurement of Propeller Whirl-Flutter Speeds and Static-Stability Derivatives and Comparison With Theory. NASA TN D-1807, Aug. 1963.

296. Reed, W. H., III: Review of Propeller-Rotor Whirl Flutter. NASA TR R-264 (see also NASA TM X-56678), July 1967.
297. Reed, W. H.; and Bennet, R. M.: Propeller Whirl Flutter Considerations for V/STOL Aircraft. Proc. CAL/TRECOM Symposium, Vol. II, June 1963.
298. Young, M. I.; and Lytwyn, R. T.: The Influence of Blade Flapping Restraint on the Dynamic Stability of Low Disc Loading Propeller-Rotors. Proc. American Helicopter Society 23rd Annual National Forum, Washington, D.C., May 10–12, 1967.
299. Magee, J. P.; and Pruyn, R. R.: Prediction of the Stability Derivatives of Large Flexible Prop/Rotors by a Simplified Analysis. Proc. American Helicopter Society 26th Annual National Forum, Washington, D.C., June 16–18, 1970.
300. Edenborough, H. K.; Gaffey, T. M.; and Weiberg, J. A.: Analysis and Tests Confirm Design of Proprotor Aircraft. AIAA 4th Aircraft Design, Flight Test and Operations Mtg., Los Angeles, Calif., Aug. 1975.
301. Johnson, W.: Predicted Dynamic Characteristics of the XV-15 Tilting Proprotor Aircraft in Flight and in the 40- by 80-Ft Wind Tunnel. NASA TM X-73158, June 1976.
302. Johnson, W.: The Influence of Pitch-Lag Coupling on the Predicted Aeroelastic Stability of the XV-15 Tilting Proprotor Aircraft. NASA TM X-73213, Feb. 1977.
303. Nixon, M. W.: Parametric Studies for Tiltrotor Aeroelastic Stability in High-Speed Flight. Proc. 33rd AIAA/ASME/ASCE/AHS Structures, Structural Dynamics, and Materials Conference, Dallas, Tex., Apr. 13–15, 1992.
304. Acree, C. W.; Peyran, R. J.; and Johnson, W.: Rotor Design for Whirl Flutter: An Examination of Options for Improving Tiltrotor Aeroelastic Stability Margins. Proc. American Helicopter Society 55th Annual Forum, Montreal, Canada, May 25–27, 1999.
305. Peyran, R. J.; and Rand, O.: The Effect of Design Requirements on Conceptual Tiltrotor Wing Weight. Proc. American Helicopter Society 55th Annual Forum, Montreal, Canada, May 25–27, 1999.
306. Howard, A. K. T.: The Aeromechanical Stability of Soft-Inplane Tiltrotors. Aerospace Engineering Dept., Pennsylvania State University, University Park, Pa., Aug. 2001.
307. Johnson, S. C.: Design and Testing of a Small, Semi-Span, Prop-Rotor Model for Whirl Flutter Stability. The Pennsylvania State University, University Park, Pa., Dec. 2013.
308. Acree, C. W.: Current Challenges and Future Directions in Rotorcraft Aeromechanics. Fifth Decennial American Helicopter Society Aeromechanics Specialists' Conference, San Francisco, Calif., Jan. 22–24, 2014.
309. Kvaternik, R. G.; and Kohn, J. S.: An Experimental and Analytical Investigation of Proprotor Whirl Flutter. NASA TP-1047, Dec. 1977.
310. Roark, R. J.; and Young, W. C.: Formulas for Stress and Strain (Fifth Ed.). New York, N.Y.: McGraw-Hill Book Co., Inc., 1965.
311. Anon.: Army Orders Design of Advanced Aircraft. Army Research and Development Monthly News Magazine, vol. 8, no. 4, Apr. 1967.
312. Anon.: Stopped-Stowed Rotor Composite Research Aircraft. USAAVLABS TR 68-40, U.S. Army Aviation Material Laboratories, Ft. Eustis, Va., Jan. 1969.

313. Cardinale, S. V.; and Donham, R. E.: Full-Scale Wind Tunnel Testing and Analysis of a Stopped/Folded Rotor. Lockheed-California Company Report LR 21016, June 1968.
314. Donham, R. E.; and Harvick, W. P.: Analysis of Stowed Rotor Aeroelastic Characteristics. J. American Helicopter Society, vol. 12, no. 1, Jan. 1967.
315. Donham, R. E.: Analyses of Stowed Rotor Aerodynamic/Aeroelastic Characteristics. AGARD CP 22, Sept. 1967.
316. Deckert, W. H.; and McCloud, J. L.: Considerations of the Stopped Rotor V/STOL Concept. J. American Helicopter Society, vol. 13, no. 1, Jan. 1968.
317. Donham, R. E.; Watts, G. A.; and Cardinale, S. V.: Dynamics of a Rigid-Rotor Controlled by a High Speed Gyro as it Slows/Stops at High Forward Speed. Proc. American Helicopter Society 25th Annual National Forum, Washington, D.C., May 14–16, 1969.
318. Watts, G. A.; and Biggers, J. C.: Horizontal Stoppable Rotor Conversion. Proc. American Helicopter Society 27th Annual National V/STOL Forum, Washington, D.C., May 19–21, 1971.
319. Smith, C. R.: Hot Cycle Rotor/Wing Composite Research Aircraft. USAAVLABS TR 68-31, U.S. Army Aviation Material Laboratories, Ft. Eustis, Va., Aug. 1968.
320. Cohan, S.; and Hirsh, N. B.: XV-9A Hot Cycle Research Aircraft Program. USAAVLABS Technical Report 66-10, U.S. Army Aviation Material Laboratories, Ft. Eustis, Va., June 1966.
321. Wernicke, K. G.: Tilt-Rotor Composite Research Aircraft. USAAVLABS TR 68-32, U.S. Army Aviation Material Laboratories, Ft. Eustis, Va., Nov. 1968.
322. Wernicke, K. G.: Composite Aircraft Program, Exploratory Definition Phase, Technical Volume—Dynamic Model Tests and Analystical Studies of High-Risk Areas. Bell Helicopter Co. Model 266, Report No. 266-099-212, Nov. 1968.
323. Anon. (Bell Helicopter Co.): V/STOL Tilt-Rotor Study. Task I: Conceptual Design. NASA CR-114441, Mar. 1972.
324. Anon. (The Boeing Co., Vertol Div.): V/STOL Tilt Rotor Aircraft Study. Volume II: Preliminary Design of Research Aircraft. NASA CR-114438, Mar. 1972.
325. Anon. (The Boeing Co., Vertol Div.): V/STOL Tilt Rotor Aircraft Study. Volume III: Overall Research Aircraft Project Plan, Schedules and Estimated Cost. NASA CR-114439, Mar. 1972.
326. Anon. (The Boeing Co., Vertol Div.): V/STOL Tilt Rotor Aircraft Study. Volume IV: Wind Tunnel Investigation Plan for a Full-Scale Tilt-Rotor Research Aircraft. NASA CR-114440, Mar. 1972.
327. Anon. (The Boeing Co., Vertol Div.): V/STOL Tilt Rotor Aircraft Study. Volume I: Conceptual Design of Useful Military and/or Commercial Aircraft. NASA CR-114437, Mar. 1972.
328. Anon. (Bell Helicopter Co.): V/STOL Tilt-Rotor Study. Task II: Research Aircraft Design. NASA CR-114442, Mar. 1972.
329. Anon. (Bell Helicopter Co.): V/STOL Tilt-Rotor Study. Task III: Research Aircraft Project Plan. NASA CR-114443, Mar. 1972.
330. Anon. (Bell Helicopter Co.): V/STOL Tilt-Rotor Study. Task IV: Wind Tunnel Investigation Plan. NASA CR-114444, Mar. 1972.

331. Thomason, T.: Bell XV-15. Aerophile, vol. 2, no. 2, Oct. 1979.
332. Zuk, J.: Budget History—Tilt Rotor Research Aircraft. Personal Communication From John Zuk to Frank Harris. Apr. 28, 1982.
333. Arrington, W. L.; Kumpel, M.; Marr, R. L.; and McEntire, K. G.: XV-15 Tilt Rotor Research Aircraft Flight Test Data Report, Volume IV of V: Appendix A. NASA CR-177406 Vol. IV, June 1985.
334. Arrington, W. L.; Kumpel, M.; Marr, R. L.; and McEntire, K. G.: XV-15 Tilt Rotor Research Aircraft Flight Test Data Report, Volume V of V: Appendix B. NASA CR-177406 Vol. V, June 1985.
335. Conahan, F. C.: DOD Acquistion—Case Study of the Navy V-22 Osprey Joint Vertical Lift Aircraft Program. GAO/NSIAD-86-45S-7, July 31, 1986.
336. Anon.: Technology Assessment of Capability for Advanced Joint Vertical Lift Aircraft. JVX Program Office, St. Louis, Mo., May 1983.
337. Anon.: Joint Services Operational Requirement. JVX Program Office, St. Louis, Mo., Dec. 14, 1982.
338. Anon.: Request for Proposal, Preliminary Design Phase—Attachment 2, Draft System Specification. AV-S-JVX-X10000, JVX Program Office, St. Louis, Mo., 1983.
339. Bedard, P.: Tacoma Loses Navy Business. Defense Week, Feb. 24, 1986.
340. Taft, W. H.: Memorandum for the Secretary of the Navy. Subject: V-22 Osprey Program. May 1, 1986.
341. Tipton, R.: Osprey Rollout Commemorative Issue—Raising the Curtain on a New Dimension in Flight. Bell Helicopter News, June 1988.
342. Anon.: V-22 First Flight Met All NAVAIR Requirements. Bell Helicopter News, Mar. 31, 1989.
343. Terrazas, B.: It Hovers–It Tilts–And Now It Flies Like a Plane. Fort Worth Star-Telegram Newspaper, Ft. Worth, Tex., Sept. 15, 1989.
344. Atwood, D.: Protection of the Public Fiscal Interest in Termination of V-22 Osprey Aircraft Procurement. U.S. Department of Defense, Washington, D.C., Dec. 1, 1989.
345. Bond, D.: Navy Terminates $328.8 Million in V-22 Advance Production Contract. Aviation Week & Space Technology, Dec. 11, 1989.
346. Harvey, D.: The V-22 Crash: Not a Killing Blow. Rotor & Wing International, Aug. 1991.
347. Dailey, J. R.: Memorandum for the Secretary of Defense. Subject: Report of the Panel to Review the V-22 Program. Apr. 30, 2001.
348. McDonald, H.: Tiltrotor Aeromechanics Phenomena: Report From Independent Assessment Panel, NASA Ames Research Center, Moffett Field, Calif. Aug. 2001.
349. Schinasi, K.: Defense Acquisitions: Readiness of the Marine Corps' V-22 Aircraft for Full-Rate Production. U.S. General Accounting Office GAO-01-369R Defense Acquisition, Feb. 20, 2001.
350. Jackson, P.; Munson, K.; and Peacock, L. (Eds.): Jane's All the World's Aircraft 2011–2012. London, England: Jane's Information Group Ltd., May 1, 2011.
351. Augustine, N. R.: Augustine's Laws and Major System Development Programs (Second Ed.). Reston, Va.: American Institute of Aeronautics and Astronautics, Inc., 1984.

352. Masiello, Colonel G.: Selected Acquisition Report for V-22 Osprey Joint Services Advanced Vertical Lift Aircraft. Defense Acquisition Management RCS: DD-A&T (Q&A) 823-212, May 21, 2013.
353. Osborne, A.: AW 609 Begins Certification Flying. Aviation Week, Feb. 25, 2014.
354. McVeigh, M. A.; Grauer, W. K.; and Paisley, D. J.: Rotor/Airframe Interactions on Tiltrotor Aircraft. Proc. American Helicopter Society 44th Annual Forum, Washington, D.C., June 16–18, 1988.
355. Felker, F. F.: Wing Download Results From a Test of a 0.658-Scale V-22 Rotor and Wing. Proc. American Helicopter Society 47th Annual Forum, Phoenix, Ariz., May 6–8, 1991.
356. Felker, F. F.; Maisel, M. D.; and Betzina, M. D.: Full Scale Tilt Rotor Hover Performance. Proc. American Helicopter Society 41th Annual Forum, Ft. Worth, Tex., May 15–17, 1985.
357. Agnihotri, A., et al.: V-22 EMD Design Loads Development Using V-22 FSD Flight Test Data. Proc. American Helicopter Society 50th Annual Forum, Washington, D.C., May 11–13, 1994.
358. Narramore, J. C.; Farrell, M. K.; and Grauer, W. K.: Aerodynamic Evaluation of the V-22 Osprey Wing Section. Proc. American Helicopter Society 50th Annual Forum, Washington, D.C., May 11–13, 1994.
359. Lee, E. W.; Butzloff, P. R.; and Sewell, K. D.: Predictive Manufacturing of V-22 Composite Grips. Proc. American Helicopter Society 50th Annual Forum, Washington, D.C., May 11–13, 1994.
360. Maffatt, A. W.: Reducing Costs of Ownership Through Selective Technology Applications for the V-22 Osprey. Proc. American Helicopter Society 50th Annual Forum, Washington, D.C., May 11–13, 1994.
361. Dadone, L., et al.: Proprotor Design Issues for High Speed Tiltrotors. Proc. American Helicopter Society 50th Annual Forum, Washington, D.C., May 11–13, 1994.
362. Meakin, R.: Unsteady Simulation of the Viscous Flow About a V-22 Rotor and Wing in Hover. AIAA-95-3463-CP. AIAA Atmosheric Flight Mechanics Conference, Baltimore, Md., Aug. 7–10, 1995.
363. Popelka, D., et al.: Results of an Aeroelastic Tailoring Study for a Composite Tiltrotor Wing. Proc. American Helicopter Society 51st Annual Forum, Ft. Worth, Tex., May 9–11, 1995.
364. Bilger, J., et al.: V-22 Empennage Buffet Dynamics. Proc. American Helicopter Society 51st Annual Forum, Ft. Worth, Tex., May 9–11, 1995.
365. McVeigh, M. A.; Liu, J.; and Wood, T.: Aerodynamic Development of a Forebody Strake for the V-22 Osprey. Proc. American Helicopter Society 51st Annual Forum, Ft. Worth, Tex., May 9–11, 1995.
366. Kilmain, C. J.; Murray, R.; and Huffman, C.: V-22 Drive System Description and Design Technologies. Proc. American Helicopter Society 51st Annual Forum, Ft. Worth, Tex., May 9–11, 1995.
367. Brand, A., et al.: The Nature of Vortex Ring State. Proc. American Helicopter Society 63th Annual Forum, Virgina Beach, Va., May 1–3, 2007.

368. Dunford, P. J.; Marr, R. L.; Martin, P.; and Price, B.: V-22 Flight Test Update. 22nd European Rotorcraft Forum, Brighton, UK, Sept. 1996.
369. McVeigh, M. A., et al.: V-22 Osprey Aerodynamic Development—A Progress Review. The Aeronautical Journal, Royal Aeronautical Society Paper No. 2225, June/July 1997.
370. Betzina, M. D.: Tiltrotor Descent Aerodynamics: A Small-Scale Experimental Investigation of Vortex Ring State. Proc. American Helicopter Society 57th Annual Forum, Washington, D.C., May 9–11, 2001.
371. McCluer, M.: Tiltrotor Hover Performance Comparisons. Naval Air System Command Air Vehicle Engineering Conference, La Jolla, Calif., May 2002.
372. Brand, A., et al.: V-22 High Rate of Descent (HROD) Test Procedures and Long Record Analysis. Proc. American Helicopter Society 60th Annual Forum, Baltimore, Md., June 7–10, 2004.
373. Kisor, R., et al.: V-22 Low-Speed/High Rate of Descent (HROD) Test Results. Proc. American Helicopter Society 60th Annual Forum, Baltimore, Md., June 7–10, 2004.
374. Acree, C. W., Jr.: JVX Proprotor Performance Calculations and Comparisons With Hover and Airplane-Mode Test Data. NASA/TM-2009-215380, Apr. 2009.
375. Decker, W. A.: Piloted Simulator Investigations of a Civil Tilt-Rotor Aircraft on Steep Instrument Approaches. Proc. American Helicopter Society 48th Annual Forum, Washinton, D.C., June 3–5, 1992.
376. Decker, W. A., et al.: Evaluation of Two Cockpit Display Concepts for Civil Tiltrotor Instrument Operations on Steep Approaches. American Helicopter Society Conference on Flying Qualities and Human Factors, San Francisco, Calif., Jan. 1993.
377. Hindson, W. S., et al.: Piloting Considerations for Terminal Area Operations of a Civil Tiltwing and Tiltrotor Aircraft. American Helicopter Society Conference on Flying Qualities and Human Factors, San Francisco, Calif., Jan. 1993.
378. Anon.: Civil Tiltrotor Missions and Applications: A Research Study—Summary Final Report. Boeing Commercial Airplane Co., NASA CR-177452, July 1987.
379. Anon.: Civil Tiltrotor Missions and Applications Phase II: The Commercial Passenger Market. Boeing Commercial Airplane Co., NASA CR-177576, Jan. 1991.
380. Gazdag, D.; and Alton, L.: Potential Use of Tiltrotor Aircraft in Canadian Aviation. NASA TM-102245, Dec. 1990.
381. Bolkcom, C.: V-22 Osprey Tilt-Rotor Aircraft. Congressional Research Service (CRS) Order Code RL 31384, The Library of Congress, Washington, D.C., Aug. 23, 2006.
382. Anon.: House Passes Civil Tiltrotor Panel. Bell Helicopter News, Aug. 15, 1992.
383. Van Nimmen, J.; and Bruno, L. C.: NASA Historical Data Book: Vol. I—Nasa Resources 1958–1968. NASA SP-4012, 1976.
384. Anon.: NASA's Fiscal Year Budget Summaries. http://www.nasa.gov/news/budget/index.html#.U44whCj-Yab, 1997 to 2015. Accessed May 2015.
385. Flater, M. E. R.: The 2006 NASA Budget Request and Broken Promises. AHS Vertiflite, vol. 51, no. 1, 2005.
386. Wise, J.: Dawn of the Ultra Copter. Popular Mechanics, vol. 191, no. 6, June 2014.
387. Erwin, S. I.: Bumpy Ride Ahead for Military's Future Helicopter Program. National Defense Magazine, June 4, 2014.

388. Bianco-Mengotti, R.: The Augusta Westland Path to the New Generation Tilt-Rotor. Centro Alti Studi per la Didesa, Rome, Italy, Nov. 22, 2012.
389. Stabellini, A., et al.: First NICETRIP Powered Wind Tunnel Tests Successfully Completed in DNW-LLF. Proc. American Helicopter Society 70th Annual Forum, Montreal, Quebec, Canada, May 20–22, 2014.
390. Harris, F. D.: The Joint Heavy Lift Program. Special Panel at the 46th Annual Forum of the American Helicopter Society, Washington, D.C., Apr. 28, 2008.
391. Harris, F. D.; and Scully, M. P.: Rotorcraft Cost Too Much. J. American Helicopter Society, vol. 43, no. 1, 1998.
392. Jackson, P. A. (Ed.): Jane's All the World's Aircraft 1995–1996. London, England: Jane's Information Group Ltd., Oct. 1995.
393. Chung, W. W., et al.: Modeling High-Speed Civil Tiltrotor Transports in the Next Generation Airspace. NASA CR-2011-215960, Oct. 2011.
394. Chung, W. W., et al.: An Assessment of Civil Tiltrotor Concept of Operations in the Next Generation Air Transportation System. NASA/CR-2012-215999, Jan. 2012.
395. Kojm, C.: Globel Trends 2030: Alternate Worlds. National Intelligence Council NIC 2012-01, Washington, D.C., Dec. 2012.
396. Anon.: European Aviation Safety Agency Type-Certificate Data Sheet No. EASA.A.069. Cologne, Germany, Dec. 16, 2011.
397. Anon.: UK Civil Aviation Authority Propeller Type-Certificate Data Sheet No. 114. Apr. 9, 2001.
398. Anon.: European Aviation Safety Agency Type-Certificate Data Sheet No. IM.E.040. Cologne, Germany, Aug. 29, 2008.
399. Davies, R. E. G.: Air Transport Directions in the 21st Century (The Lessons of History). Jenkins, D. (Ed.), Handbook of Airline Economics (Second Ed.), ISBN 007-982394-7, Aviation Week, Div. of McGraw-Hill Co., Inc., May 17, 2002.
400. Wimpress, J.; and Newberry, C.: The YC-14 STOL Protype: Its Design, Development, and Flight Test. Reston, Va.: American Institute of Aeronautics and Astronautics, Inc., Jan. 1, 1998.
401. Helmbold, H. B.: Limitations of Circulation Lift. J. Aeronautical Sciences, vol. 24, no. 3, Mar. 1957, pp. 237–238.
402. Cone, C. D.: A Theoretical Investigation of Vortex-Sheet Deformation Behind a Highly Loaded Wing and Its Effect on Lift. NASA TN D-657, Apr. 1961.
403. Pope, A.: Basic Wing and Airfoil Theory. New York, N.Y.: McGraw-Hill Book Co., Inc., 1951.
404. Nichols, J. B.: The Limitations of a Wing for Low Speed Flight. Proc. American Helicopter Society 13th Annual National Forum, Washington, D.C., May 8–11, 1957.
405. Smith, A. M. O.: High-Lift Aerodynamics. J. Aircraft, vol. 12, no. 6, June 1975.
406. Cleveland, F. A.: Size Effects in Conventional Aircraft Design. J. Aircraft, vol. 7, no. 6, Nov.–Dec. 1970.
407. Fowler, H. D.: Variable Lift. Western Flying, Nov. 1931.
408. Weick, F. E.; and Platt, R. C.: Wind-Tunnel Tests of the Fowler Variable-Area Wing. NACA TN 419, May 1932.

409. Young, A. D.: The Aerodynamic Characteristics of Flaps. Aeronautical Research Council R&M No. 2622, Feb. 1947.
410. Fink, M. P.; Cocke, B. W.; and Lispon, S.: A Wind-Tunnel Investigation of a 0.4-Scale Model of an Assault-Transport Airplane With Boundary-Layer Control Applied. NACA RM L55G26a, May 7, 1956.
411. Weiberg, J. A.; Griffin, R. N.; and Florman, G. L.: Large-Scale Wind-Tunnel Tests of an Airplane Model With an Unswept, Aspect-Ratio-10 Wing, Two Propellers, and Area-Suction Flaps. N.A.C.A. Technical Note 4365, Sept. 1958.
412. Griffin, R. N.; Holzhauser, C. A.; and Weiberg, J. A.: Large-Scale Wind-Tunnel Tests of an Airplane Model With an Unswept, Aspect-Ratio-10 Wing, Two Propellers, and Blowing Flaps. NASA Memo 12-3-58A, Dec. 1958.
413. Weiberg, J. A.; and Page, V. R.: Large-Scale Wind-Tunnel Tests of an Airplane Model With an Unswept, Aspect-Ratio-10 Wing, Four Propellers, and Blowing Flaps. NASA TN D-25, Sept. 1959.
414. Joslin, R. D.: Aircraft Laminar Flow Control. Annual Review of Fluid Mechanics, vol. 30, 1998, pp. 1–29.
415. Kelly, M. W.; and Tolhurst, W. H.: Full-Scale Wind-Tunnel Tests of a 35° Sweptback Wing Airplane With High-Velocity Blowing Over the Trailing-Edge Flaps. NACA RM A55IO9, Nov. 15, 1955.
416. Wenzinger, C. J.; and Harris, T. A.: Wind-Tunnel Investigation of an N.A.C.A. 23012 Airfoil With Various Arrangements of Slotted Flaps. NACA TR 664, 1939.
417. Smelt, R.; and Davies, H.: Estimation of Increase in Lift Due to Slipstream. Aeronautical Research Committee R&M No. 1788, Feb. 3, 1937.
418. Kuhn, R. E.: Semiempirical Procedure for Estimating Lift and Drag Characteristics of Propeller-Wing-Flap Configurations for Vertical- and Short-Take-Off-and-Landing Airplanes. NASA Memo 1-16-59L, Feb. 1959.
419. Stüper, J.: Effect of Propeller Slipstream on Wing and Tail. NACA TM 874, Aug. 1938.
420. Moens, F.; and Gardarein, P.: Numerical Simulation of the Propeller/Wing Interactions for Transport Aircraft. AIAA-2001-2404. AIAA 19th Applied Aerodynamics Conference, Anaheim, Calif., June 11–14, 2001.
421. Hunsaker, D.; and Snyder, D.: A Lifting Line Approach to Estimating Propeller/Wing Interaction. AIAA 24th Applied Aerodynamics Conference, San Francisco, Calif., June 2006.
422. Gennaretti, M.; Colella, M. M.; and Bernardini, G.: Prediction of Tiltrotor Vibratory Loads With Inclusion of Wing-Propeller Aerodynamic Interaction. AIAA J. of Aircraft, vol. 47, no. 1, 2010.
423. Vigevano, L., et al.: Code-to-Code Comparison of Aircraft-Mode Tilt-Rotor Aerodynamics. 38th European Rotorcraft Forum, Amsterdam, The Netherlands, 2012.
424. Roosenboom, E.; Heider, A.; and Schroder, A.: Propeller Slipstream Development. AIAA 25th Applied Aerodynamics Conference, Miami, Fla., 2007.
425. Anderson, J. D., Jr.: A History of Aerodynamics. Cambridge, England: Cambridge University Press, 1997.

426. Glauert, H.: The Elements of Aerofoil and Airscrew Theory (Second Ed.). New York, N.Y.: Cambridge University Press, 1959.
427. Roberts, J. C.; and Yaggy, P. F.: A Survey of the Flow at the Plane of the Propeller of a Twin-Engine Airplane. NACA TN 2192, Sept. 1950.
428. Yaggy, P. F.: A Method for Predicting the Upwash Angles Induced at the Propeller Plane of a Combination of Bodies With an Unswept Wing. NACA TN 2528, Oct. 1951.
429. Rogallo, V. L.: Effects of Wing Sweep on the Upwash at the Propeller Planes of Multiengine Airplanes. NACA TN 2795, Sept. 1952.
430. Schubauer, G. B.: Jet Propulsion With Special Reference to Thrust Augmentors. NACA TN 442, Jan. 1933.
431. Spence, D. A.: The Lift Coefficient of a Thin, Jet-Flapped Wing. Proc. Royal Society of London, Series A, Mathematical and Physical Sciences, vol. 238, Aug. 1956, pp. 46–68.
432. Lowry, J. G.; and Volger, R. D.: Wind-Tunnel Investigation at Low Speeds to Determine the Effect of Aspect Ratio and End Plates on a Rectangular Wing With Jet Flaps Deflected 85°. NACA TN 3863, Dec. 1956.
433. Lockwood, V. E.; Turner, T. R.; and Riebe, J. M.: Wind-Tunnel Investigation of Jet-Augmented Flaps on a Rectangular Wing to High Momentum Coefficients. NACA TN 3865, Dec. 1956.
434. Helmbold, H. B.: Theory of the Finite-Span Blowing Wing. J. of the Aeronautical Sciences, vol. 24, no. 5, May 1957.
435. Dimmock, N. A.: An Experimental Introduction to the Jet Flap. Aeronatical Research Council Technical Report C.P. No. 344, 1957.
436. Dimmock, N. A.: Some Further Jet Flap Experiments. National Gas Turbine Establishment Report N.G.T.E.: M.255, May 1, 1956.
437. Maskell, E. C.; and Spence, D. A.: A Theory of the Jet Flap in Three Dimensions. Royal Aircraft Establishment, Dec. 1958.
438. Lowry, J. G.; Riebe, J. M.; and Campbell, J. P.: The Jet-Augmented Flap. Institute of the Aerospace Sciences 25th Annual Mtg. (I.A.S. Preprint No. 715), Jan. 1957.
439. Spence, D. A.: Some Simple Results for Two-Dimensional Jet-Flap Aerofoils. Royal Aeronautical Society Aeronautical Quarterly, vol. 5, no. 4, Nov. 1958, pp. 395–406.
440. Williams, J.; Butler, S. F. J.; and Wood, M. N.: The Aerodynamics of Jet Flaps. Aeronautical Research Committee R&M No. 3304, Jan. 1961.
441. Chin, Y.; Aiken, T. N.; and Oates, G. S.: Evaluation of a New Jet Flap Propulsive-Lift System. AIAA J. Aircraft, vol. 12, no. 7, July 1975.
442. Aiken, T. N.; Aoyagi, K.; and Falarski, M. D.: Aerodynamic Characteristics of a Large-Scale Model With a Swept Wing and a Jet Flap Having an Expandable Duct. NASA TM X-62,281, Sept. 1973.
443. Turner, T. R.; Davenport, E. E.; and Riebe, J. M.: Low-Speed Investigation of Blowing From Nacelles Mounted Inboard and on the Upper Surface of a Aspect-Ratio-7.0 35’ Swept Wing With Fuselage and Various Tail Arrangements. NASA Memo 5-1-59L, June 1959.

444. Maglieri, D. J.; and Hubbard, H. H.: Preliminary Measurements of the Noise Characteristics of Some Jet-Augmented-Flap Configurations. NASA Memo 12-4-58L, Jan. 1959.
445. Davenport, E. E.: Wind-Tunnel Investigation of External-Flow Jet-Augmented Double Slotted Flaps on a Rectangular Wing at an Angle of Attack of 0° to High Momentum Coefficients. NACA TN 4079, Sept. 1957.
446. Riebe, J. M.; and Davenport, E. E.: Exploratory Wind-Tunnel Investigation to Determine the Lift Effects of Blowing Over Flaps From Nacelles Mounted Above the Wing. NACA TN 4298, June 1958.
447. Koenig, D. G.; Corsiglia, V. R.; and Morelli, J. P.: Aerodynamic Charateristics of a Large-Scale Model With an Unswept Wing and Augmented Jet Flap. NASA TN D-4610, June 1968.
448. Cook, A. M.; and Aiken, T. N.: Low-Speed Aerodynamic Characteristics of a Large-Scale STOL Transport Model With an Augmented Jet Flap. NASA TM-X-62017, Mar. 1971.
449. Falarski, M. D.; and Koenig, D. G.: Aerodynamic Characteristics of a Large-Scale Model With a Swept Wing and Augmented Jet Flap. NASA TM X-62029, July 1971.
450. Aoyagi, K.; and Hall, L. P.: Wind-Tunnel Investigation of a Large 35° Swept-Wing Jet Transport Model With an External-Flow Jet-Augmented Double-Slotted Flap. NASA TN D-6482, Aug. 1971.
451. Falarski, M. D.; and Koenig, D. G.: Longitudinal and Lateral Stability and Control Characteristics of a Large-Scale Model With a Swept Wing and Augmented Jet Flap. NASA TM X-62,145, Apr. 1972.
452. Aoyagi, K.; Hall, L. P.; and Falarski, M. D.: Wind-Tunnel Investigation of a Large-Scale 35° Swept-Wing Jet Transport Model With an External Blowing Triple-Slotted Flap. NASA TM-X-2600, July 1972.
453. Falarski, M. D.; and Koenig, D. G.: Lomgitudinal Aerodynamic Characteristics of a Large-Scale Model With a Swept Wing and Augmented Jet-Flap in Ground Effect. NASA TM-X-62174, Oct. 1972.
454. Albers, J. A.: Theoretical and Experimental Internal Flow Characteristics of a 1397-Centimeter-Diameter Inlet at STOL Takeoff and Approach Conditions. NASA TN D-7185, Mar. 1973.
455. Parlett, L. P.; Smith, C. C.; and Megrail, J. L.: Wind-Tunnel Investigation of Effects of Variations in Reynolds Number and Leading-Edge Treatment on the Aerodynamic Characteristics of an Externally Blown Jet-Flap Configuration. NASA TN D-7194, Aug. 1973.
456. Aoyagi, K.; Falarski, M. D.; and Koenig, D. G.: Wind Tunnel Investigation of a Large-Scale Upper Surface Blown-Flap Transport Model Having Two Engines. NASA TM-X-62296, Aug. 1973.
457. Aoyagi, K.; Falarski, M. D.; and Koenig, D. G.: Wind-Tunnel Investigation of a Large-Scale 25-Deg Swept-Wing Jet Transport Model With an External Blowing Triple-Slotted Flap. NASA TM-X-62197, Nov. 1973.

458. Parlet, L. P.; Freeman, D. C.; and Smith, C. C.: Wind-Tunnel Investigation of a Jet Transport Airplane Configuration With High Thrust-Weight Ratio and an External-Flow Jet Flap. NASA TN D-6058, Nov. 1970.
459. Parlet, L. P.; Greer, H. D.; Henderson, R. L.; and Carter, C. R.: Wind-Tunnel Investigation of an External-Flow Jet-Flap Transport Configuration Having Full-Span Triple-Slotted Flaps. NASA TN D-6391, Aug. 1971.
460. Butchart, S. P., et al.: Flight Studies of Problems Pertinent to High-Speed Operation of Jet Transports. NASA Memo 3-2-59H, Apr. 1959.
461. Tambor, R.: Flight Investigation of the Lift and Drag Characteristics of a Swept-Wing, Multijet, Transport-Type Airplane. NASA TN D-30, Sept. 1960.
462. Aiken, T. N.; and Cook, A. M.: Results of Full-Scale Wind Tunnel Tests on the H.126 Jet Flap Aircraft. NASA TN D-7252, Apr. 1973.
463. Laub, G. H.: Low Speed Wind Tunnel Tests on a One-Seventh Scale Model of the H.126 Jet Flap Aircraft. NASA TM-X-62433, Apr. 1975.
464. Anon.: ER. 189D Prototype Notes for Hunting H.126. British Ministry of Aviation (CD file bought from www.Flight-Manuals-on-cd.com Ltd.), 1962.
465. Harris, K. D.: The Hunting H.126 Jet-Flap Research Aircraft. AGARD Lecture Series No. 43, AGARD-LS-43-71, von Karman Institute, Belgium, Feb. 1971.
466. Anon.: Jetwing From Colorado. Air International, vol. 14, no. 2, pp. 69–71, Feb. 1978.
467. Solies, U. P.: Flight Measurements of Downwash on the Ball-Bartoe Jetwing Powered Lift Aircraft. AIAA J. Aircraft, vol. 29, no. 5, Oct. 1992, pp. 927–205.
468. Kimberlin, R. D.: A Flight Test Evaluation of the Ball-Bartoe Jetwing Propulsive Lift Concept. UTSI Report 81-1, University of Tennessee Space Institute (see also DTIC AD A103579), July 1, 1981.
469. Kimberlin, R. D.; Solies, U. P.; and Sinha, A. K.: A Flight Test Evaluation and Analytical Study of the Ball-Bartoe Jetwing Propulsive Lift Concept Without Ejector. UTSI Report 82/17 (see also DTIC AD A121733), Oct. 1, 1982.
470. Colucci, F.: NFAC is Back. AHS Vertiflite, vol. 53, no. 3, Fall 2007.
471. Jackson, A. J.: De Havilland Aircraft Since 1909 (Revised and Updated). Annapolis, Md.: Naval Institute Press, 1978.
472. Whittley, D. C.: The Augmentor-Wing: A New Means of Engine Airframe Integration for STOL Aircraft. AIAA Paper No. 64-576, 1964.
473. Whittley, D. C.: The Augmentor-Wing Research Program: Past, Present, and Future. AIAA Paper No. 67-741, Oct. 1967.
474. Sutcliffe, P. L.: Aerodynamic and Propulsion Considerations of Minimum Field Aircraft. Eighth Anglo-American Aeronautical Conference, Sept. 1961.
475. Whittley, D. C.: The Buffalo/Spey Jet-STOL Research Aircraft. AGARD Paper No. CP-126, Apr. 1973.
476. Quigley, H. C.; Innis, R. C.; and Grossmith, S.: A Flight Investigation of the STOL Characteristics of an Augmented Jet Flap STOL Research Aircraft. NASA TM-X-62334, May 1974.
477. Ashleman, R. H.; and Skavdahl, H.: The Development of an Augmentor Wing Jet STOL Research Airplane (Modified C-8A): Volume I—Summary. NASA CR-114503, Aug. 1972.

478. Skavdahl, H.; and Patterson, D. H.: The Development of an Augmentor Wing Jet STOL Research Airplane (Modified C-8A): Volume II—Analysis of Contractor's Flight Test. NASA CR-114504, Aug. 1972.
479. Anon.: Jet-STOL Wing. FLIGHT International, Feb. 24, 1972, pp. 295–297.
480. Anon.: STOL Buffalo Flies. FLIGHT International, May 11, 1972, p. 658.
481. Quigley, H. C., et al.: A Progress Report on the Development of an Augmentor Wing Jet STOL Research Aircraft. SAE Paper 710757. National Aeronautics and Space Engineering and Manufacturing Mtg., Los Angeles, Calif., Sept. 1971.
482. Cumpsty, N.: Jet Propulsion—A Simple Guide to the Aerodynamic and Thermodynamic Design and Performance of Jet Engines (Second Ed.). New York, N.Y.: Cambridge University Press, 2003.
483. Streeter, V. L.: Fluid Mechanics. New York, N.Y.: McGraw-Hill Book Co., Inc., 1951.
484. James, H. A., et al.: Wind-Tunnel and Piloted Flight Simulator Investigation of a Deflected-Slipstream VTOL Airplane, The Ryan VZ-3RY. NASA TN D-89, Nov. 1959.
485. Fink, M. P.: Full-Scale Wind-Tunnel Investigation of the VZ-5 Four-Propeller Deflected-Slipstream VTOL Airplane. NASA TM-SX-805, Feb. 20, 1963.
486. Kuhn, R. E.; and Grunwald, K. J.: Longitudinal Aerodynamic Characteristics of a Four-Propeller Deflected Slipstream VTOL Model Including the Effects of Ground Proximity. NASA TN D-248, Nov. 1960.
487. Kuhn, R. E.; and Grunwald, K. J.: Lateral Stability and Control Characteristics of a Four-Propeller Deflected-Slipstream VTOL Model Including the Effects of Ground Proximity. NASA TN D-444, Jan. 1961.
488. Grunwald, K. J.: Investigation of Longitudinal and Lateral Stability Characteristics of a Six-Propeller Deflected-Slipstream VTOL Model With Boundary-Layer Control Including Effects of Ground Proximity. NASA TN D-445, Jan. 1961.
489. Campbell, J. P.: Status of V/STOL Research and Development in the United States. Ninth Anglo-American Aeronautical Conference, Boston, Mass., Oct. 17–22, 1963.
490. Borchers, P. F.; Franklin, J. A.; and Fletcher, J. W.: 1940–1997 Flight Research at Ames: Fifty-Seven Years of Development and Validation of Aeronautical Technology. NASA/SP-1998-3300, 1998.
491. Weiberg, J. A.; and Holzhauser, C. A.: STOL Characteristics of a Propeller-Driven, Aspect-Ratio-10, Straight-Wing Airplane with Boundary-Layer Control Flaps, as Estimated From Large-Scale Wind-Tunnel Tests. NASA TN D-1032, June 1961.
492. Innis, R. C.; and Quigley, H. C.: A Flight Examination of the Operating Problems of V/STOL Aircraft in STOL-Type Landing and Approach. NASA TN D-862, 1961.
493. Weiberg, J. A.; and Holzhauser, C. A.: Large-Scale Wind-Tunnel Tests of an Airplane Model With an Unswept, Tilt Wing of Aspect Ratio 5.5, and With Four Propellers and Blowing Flaps. NASA TN D-1034, June 1961.
494. Kuhn, R. E.: Take-off and Landing Distance and Power Requirements of Propeller-Driven STOL Airplanes. Preprint No. 690, Institute of the Aerospace Sciences 25th Annual Mtg., New York, N.Y., Jan. 28–31, 1957.

495. Hiscocks, R. D.: A Case Study on the de Havilland Family of STOL Commuter Aircraft. Reston, Va.: American Institute of Aeronautics and Astronautics, 2000.
496. Johns, S. L.; and Campbell, J. K.: Category II Performance and Stability Tests. AFFTC-TR-60-41, Air Force Flight Test Center, Edwards Air Force Base, Calif., Nov. 1960.
497. Anon.: Takeoff and Landing Capabilities of the Caribou CV-2B Aircraft on Unprepared Surfaces. U.S. Army Aviation Test Activity-TR-63-4 (see also USATECOM Project No. 4-4-1142-01), Sept. 1963.
498. Finnestead, R. L.; and Antoniou, M. N.: Final Report of Performance Tests of the CV-2B Airplane. USAATA Project No. 63-74, June 1965.
499. Blaha, J. T.; Mattuller, N. A.; and Wilson, D. R.: Stability and Control and Performance Test (Phase D) of the CV-7A Transport Airplane. USAAVNTA Project No. 65-10, Mar. 1966.
500. Anon.: Chipmunk DHC-1 Operation and Maintenance Manual. De Havilland Aircraft of Canada Ltd., Toronto, Canada, 1952.
501. Anon.: Chipmunk Aircraft—Repair and Recondition Instructions. British Air Ministry Publication 4308, vol. 6, 1952.
502. Taylor, J. W. R.: Jane's All The World's Aircraft 1965–1966. London, England: Sampson Low, Marston & Co., Jan. 1, 1966.
503. Anon.: Beaver DHC-2 Flight Manual. De Havilland Aircraft of Canada Ltd., Downsview, Ontario, Canada, Mar. 31, 1956.
504. Anon.: Otter DHC-3 Flight Manual. De Havilland Aircraft of Canada Ltd., Downsview, Ontario, Canada, May 30, 1957.
505. Anon.: Flight Manual, USAF Series C-7A Aircraft and Performance Data. USAF T.O. 1C-7A-1 and T.O. 1C-7A-1-1, Oct. 1, 1970.
506. Anon.: Canadian Forces Aircraft Operating Instructions—Buffalo (C-115). Canadian Forces EO 05-200A-1, Aug. 15, 1967.
507. Anon.: DHC-6, Twin Otter Series 100 Flight Manual. De Havilland Aircraft of Canada Ltd., Downsview, Ontario, Canada, Dec. 20, 1968.
508. Quigley, H. C.; Innis, R. C.; and Holzhauser, C. A.: A Flight Investigation of the Performance, Handling Qualities, and Operational Characteristics of a Deflected Slipstream STOL Transport Airplane Having Four Interconnected Propellers. NASA TN D-2231, Mar. 1964.
509. Innis, R. C.; Holzhauser, C. A.; and Gallant, R. P.: Flight Tests Under IFR With an STOL Transport Aircraft. NASA TN D-4939, Dec. 1968.
510. Lecomte, P. E.: Recent French Experience in the Field of V/STOL Aircraft. SAE 670B. National Aero-Nautical Mtg., Society of Automotive Engineers, Washington, D.C., Apr. 1963.
511. Ricard, G., et al.: The Bréguet Family of STOL Aircraft. SAE 610100, Oct. 1961.
512. Antoniou, M. N.: Flying Qualities and Performance Evaluation of the Bréguet 941 Turbo-Prop Troop Transport. U.S. Army Aviation Test Activity ATA-TR-63-6, Jan. 1965.
513. Reeder, J. P.: The Impact of V/STOL Aircraft on Instrument Weather Operations. NASA TN D-2702, Feb. 1965.

514. Anon.: A Timeline of Lockheed's Georgia Division. Lockheed-Georgia Co., Div. of Lockheed Aircraft Corp., 1967.
515. Anon.: C-130 Hercules Variant Briefing—Volumes 6, 7, and 8. World Air Power Journal, 1991–1992.
516. Simmons, C. D.; and Ballentine, W. A.: C-130A Phase IV Performance, Stability, and Control. AFFTC-57-32, Air Force Flight Test Center, Edwards Air Force Base, Calif., Feb. 1958.
517. Kroll, C. E.; and Allavie, J. E.: C-130B Category II Performance Test. AFFTC-TR-60-10, Air Force Flight Test Center, Edwards Air Force Base, Calif., Apr. 1960.
518. Davidson, J.; Martin, K. L.; and Loewe, W. R.: C-130E Category II Performance Tests. AFFTC-TDR-63-37, Air Force Flight Test Center, Edwards Air Force Base, Calif. (see also AD 0430223), Jan. 1964.
519. Davidson, J.; Martin, K. L.; and Loewe, W. R.: Appendix III, C-130E Category II Performance Tests. AFFTC-TR-63-37, Air Force Flight Test Center, Edwards Air Force Base, Calif. (see also AD 460501), Mar. 1965.
520. Martin, K. L.; and Cretney, F. D.: C-130E Performance at Emergency-Wartime-Use-Only Gross Weights. AFFTC-YR-64-35, Air Force Flight Test Center, Edwards Air Force Base, Calif. (see also AD 455140), Jan. 1965.
521. Anon.: Flight Manual, C-130B and SC-130B. USAF T.O. 1C-130B-1, Dec. 31, 1962.
522. McDermott, E. P.: Selected Acquisition Report C-130J Hercules Transport Aircraft Defense Acquisition Management RCS: DD-A&T (Q&A) 823-250, May 21, 2013.
523. Anon.: ASL Aviation Group Signs Letter of Intent to Procure Lockheed-Martin LM-100J Freighters. Lockheed Martin Press Release, July 16, 2014.
524. Anon.: Lockheed Martin Files for FAA Type Design Update. Lockheed Martin Press Release, Feb. 3, 2014.
525. Anon.: Type Certificate Data Sheet No. A1SO. Department of Transportation, Federal Aviation Administration, Washington D.C., Jan. 11, 2010.
526. Dickerman, F. N.; and Branson, C. F.: The Lockheed BLC Hercules—A Practical STOL Transport. Metropoltan Section of the Society of Automotive Engineers Preprint S259, Nov. 1, 1960.
527. Dansby, T., et al.: V/STOL Development of the C-130 Hercules. AIAA J. Aircraft, vol. 1, no. 5, Sept.–Oct. 1964.
528. Leonard, J. M.: The Allison Engine Catalog 1915–2007. Indianapolis, Ind.: Rolls-Royce Heritage Trust—Allison Branch, 2008.
529. Quigley, H. C.; and Innis, R. C.: Handling Qualities and Operational Problems of a Large Four-Propeller STOL Transport Airplane. NASA TN D-1647, Jan. 1963.
530. Quigley, H. C.; and Lawson, H. F.: Simulator Study of the Lateral-Directional Handling Qualities of a Large Four-Propellered STOL Transport Airplane. NASA TN D-1773, 1963.
531. Quigley, H. C., et al.: A Flight and Simulator Study of Directional Augumentation Criteria for a Four-Propellered STOL Airplane. NASA TN D-3909, May 1967.
532. Prandtl, L.: Theory of Lifting Surfaces, Part I. NACA TN 9, July 1920.
533. Reid, E. G.: Tests of Rotating Cylinders. NACA TN 209, Dec. 1924.

534. Seewald, F.: Increasing Lift by Releasing Compressed Air on Suction Side of Airfoil. NACA TM 441, Dec. 1927.
535. Reid, E. G.; and Bamber, M. J.: Preliminary Investigation on Boundary Layer Control by Means of Suction and Pressure With the U.S.A. 27 Airfoil. NACA TN 286, May 1928.
536. Wieland, K.: Experiments With a Wing From Which the Boudary Layer is Removed by Pressure or Suction. NACA TM 472, July 1928.
537. Katzmayr, R.: Wings With Nozzle-Shaped Slots. NACA TM 521, July 1929.
538. Schwier, W.: Lift Increase by Blowing Out Air, Tests on Airfoil of 12 Percent Thickness, Using Various Types of Flaps. NACA TM 1148, June 1947.
539. Krull, H. G.; and Steffen, F. W.: Performance Characteristics of One Convergent and Three Convergent-Divergent Nozzles. NACA RM E52H12, Sept. 29, 1952.
540. Fradenburgh, E. A.; Gorton, G. C.; and Beke, A.: Thrust Characteristics of a Series of Convergent-Divergent Exhaust Nozzles at Subsonic and Supersonic Flight Speeds. NACA RM E53L23, Mar. 12, 1954.
541. Cook, W. L.; Griffin, R. N.; and Hickey, D. H.: A Preliminary Investigation of the Use of Circulation Control to Increase the Lift of a 45° Sweptback Wing by Suction Through Trailing-Edge Slots. NACA RM A54I21, Dec. 14, 1954.
542. Riebe, J. M.: A Correlation of Two-Dimensional Data on Lift Coefficient Available With Blowing-, Suction-, Slotted-, and Plain-Flap High-Lift Devices. NACA RM L55D29a, Oct. 3, 1955.
543. Kelly, M. W.; and Tolhurst, W. H.: Full-Scale Wind-Tunnel Tests of a 35° Sweptback Wing Airplane With High-Velocity Blowing Over the Trailling-Edge Flaps. NACA RM A55IO9, Nov. 15, 1955.
544. Dods, J. B.; and Watson, E. C.: The Effects of Blowing Over Various Trailing-Edge Flaps on a NACA 0006 Airfoil Section, Comparisons With Various Types of Flaps on Other Airfoil Sections, and an Analysis of Flow and Power Relationships for Blowing Systems. NACA RM A56C01 (republished as NASA TN D-8293, Aug. 1976), June 12, 1956.
545. Spreemann, K. P.; and Kuhn, R. E.: Investigation of the Effectiveness of Boundary-Layer Control by Blowing Over a Combination of Sliding and Plain Flaps in Deflecting a Propeller Slipstream Downward for Vertical Take-Off. NACA TN 3904, Dec. 1956.
546. Spreemann, K. P.: Effectiveness of Boundary-Layer Control, Obtained by Blowing over a Plain Rear Flap in Combination With a Foreward Slotted Flap, in Deflecting a Slipstream Downward for Vertical Take-off. NACA TN 4200, Feb. 1958.
547. Kelly, M. W.; Anderson, S. B.; and Innis, R. C.: Blowing-Type Boundary-Layer Control as Applied to the Trailing-Edge Flaps of a 35° Swep-Wing Airplane. NACA TR 1369, Jan. 1958.
548. Lockwood, V. E.; and Vogler, R. D.: Exploratory Wind-Tunnel Investigation at High Subsonic and Transonic Speeds of Jet Flaps on Unswept Rectangular Wings. NACA TN 4353, Aug. 1958.
549. Lockwood, V. E.: Lift Generation on a Circular Cylinder by Tangential Blowing From Surface Slots. NASA TN D-244, May 1960.

550. Turner, T. R.: Ground Influence on a Model Airfoil With a Jet-Augmented Flap as Determined by Two Techniques. NASA TN-D-658, Feb. 1961.
551. Lockwood, V. E.: Effect of Groundboard Height on the Aerodynamic Characteristics of a Lifting Circular Cylinder Using Tangential Blowing From Surface Slots for Lift Generation. NASA TN D-969, Oct. 1961.
552. Englar, R. J., et al.: Application of Circulation Control to Advanced Subsonic Transport Aircraft. Part I: Airfoil Development. Part II: Transport Application. AIAA J. Aircraft, vol. 31, no. 5, Sept.–Oct. 1994.
553. Horton, E. A., et al.: Analysis of the Effects of Boundary-Layer Control on the Take-off and Power-off Landing Performance Characteristics of a Liaison Type of Airplane. NACA TR 1057, 1951.
554. Darby, R. A.: STOL Airplanes—A New Approach to Air Transport. Institute of the Aerospace Sciences Conference, New York, N.Y., Dec. 1955.
555. Johnston, G. W.: NATO—Advisory Group for Aeronautical Research and Development Report 81, Aug. 1956.
556. Wagner, F. G.: Design Considerations for BLC STOL Airplanes. Aero/Space Engineering, Oct. 1958.
557. Schwartzberg, M.: Blown Flap System for STOL Performance—Weight Considerations. IAS Aero/Space Engineering, vol. 18, no. 3, Mar. 1959.
558. Kuhn, R. E.: Review of Basic Principals of V/STOL Aerodynamics. NASA TN D-733, 1961.
559. Adamson, A. P.; and Cochran, D.: Some Considerations in Selecting VTOL Propulsion Systems. Eighth Anglo-American Aeronautical Conference, London, England, Sept. 1961.
560. Campbell, J. P.: Ground Proximity Effects Associated With V/STOL Aircraft. Eighth Anglo-American Aeronautical Conference, London, England, 1961.
561. Pearson, H.: Engines for VTOL Aircraft. Eighth Anglo-American Aeronautical Conference, London, England, 1961.
562. Sutcliffe, P. L.; Merrick, V. K.; and Howell, A. R.: Aerodynamic and Propulsion Considerations of Minimum-Field Aircraft. Eighth Anglo-American Aeronautical Conference, London, England, 1961.
563. Deckert, W. H.; and Franklin, J. A.: Powered-Lift Aircraft Technology. NASA SP-501, 1989.
564. Hendrickson, C. L.; and Schiele, J. S.: Project Rough Road Alpha—Takeoff and Landing Capabilities of C-130B, JC-130B, NC-130B (BLC), C-123B, and YC-123H Aircraft on Off-Runway (Unprepared) Surfaces. AFFTC-TDR-63-8, Air Force Flight Test Center, Edwards Air Force Base, Calif. (see also AD 407144), Apr. 1963.
565. Jackson, R.; and Seigler, J.: Phase IV Performance Tests of the C-123B Aircraft USAF S/N 54-552. AFFTC-TR-55-12, Air Force Flight Test Center, Edwards Air Force Base, Calif., June 1955.
566. Fetty, R. L.; and Prahl, V. E.: Phase II Tests of the C-123B Aircraft. AFFTC TR 54-6, Air Force Flight Test Center, Edwards Air Force Base, Calif., Feb. 1954.
567. Anon.: Flight Manual USAF Series C-123B Aircraft. USAF T.O. 1C-123B-1, Sept. 1, 1959.

568. Stroukoff, M.: Substantiating Data C-123B Pilot's Handbook—Takeoff Performance. Report No. 8B-160, Chase Aircraft Co., Inc., Trenton, N.J., Dec. 15, 1952.
569. Stroukoff, M.: Substantiating Data C-123B Pilot's Handbook—Landing Performance. Report No. 8B-161, Chase Aircraft Co., Inc., Trenton, N.J., Dec. 15, 1952.
570. Johns, S. L.; and Campbell, J. K.: YAC-1DH Category II Performance and Stability Tests. AFFTC-TR-60-41, Air Force Flight Test Center, Edwards Air Force Base, Calif., Nov. 1960.
571. Johnson, R. L., et al.: Phase I Project Rough Road—An Evaluation of C-130B Short Field Takeoff and Landing Capabilities on Unprepared Surfaces. AFFTC-TDR-62-25, Air Force Flight Test Center, Edwards Air Force Base, Calif. (see also AD 0294566), Aug. 1962.
572. Johnson, R. L.: Phase II Project Rough Road—An Evaluation of C-130B Short Field Takeoff and Landing Capabilities on Unprepared Surfaces. AFFTC-TDR-62-25, Air Force Flight Test Center, Edwards Air Force Base, Calif. (see also AD 0294565), Aug. 1962.
573. Kidwell, J. C.: Final Report of Engineering Tests of Takeoff and Landing Capabilities of the Caribou CV-2B Aircraft on Unprepared Surfaces. U.S. Army Aviation Test Activity-TE-63-4 (see also AD 0440406), Sept. 1963.
574. Horwood, I.: Interservice Rivalry and Airpower in the Vietnam War. Ft. Leavenworth, Kans.: Combat Studies Institute Press, 2006.
575. Glauert, H.: The Landing of Aeroplanes (Part I and Part II). British Advisory Committee for Aeronautics R&M 666 and 667, 1920.
576. Anon.: Operator's Manual—Army Models 0-1A, 0-1A(1T), T0-1A, 0-1D, 0-1E, T0-1E, 0-1F, and 0-1G Aircraft. Army TM 55-1510-202-10, Dec. 1968.
577. Anon.: Performance Phase Textbook, Vol. I. USAF Test Pilot School USAF-TPS-CUR-86-01, Apr. 1986.
578. Hurt, H. H.: Aerodynamics for Naval Aviators. NAVAIR 00-80T-80, Jan. 1965.
579. Anon.: Flight Test Guide for Certification of Transport Category Airplanes. Advisory Circular (AC) 25-7C, Department of Transportation, Federal Aviation Administration, Washington, D.C., Mar. 29, 2011.
580. Hedrick, W. S.; and Douglass, W. M.: An Experimental Investigation of the Thrust and Torque Produced by Propellers Used as Aerodynamic Brakes. NACA ARR No. 4H26. Aug. 1944.
581. Borst, H. V.: Summary of Propeller Design Procedures and Data. Volume I. Aerodynamic Design and Installation. USAAMRDL TR 73-34A, Nov. 1973.
582. Durand, W. F.; and Lesley, E. P.: Experimental Research on Air Propellers, II. NACA TR 30, 1919.
583. Hartman, E. P.: Negative Thrust and Torque Characteristics of an Adjustable-Pitch Metal Propeller. NACA TR 464, 1933.
584. Hartman, E. P.; and Biermann, D.: The Negative Thrust and Torque of Several Full-Scale Propellers and Their Application to Various Flight Problems. NACA TR 641, 1938.
585. Gray, W. H.; and Gilman, J.: Characteristics of Several Single- and Dual-Rotating Propellers in Negative Thrust. NACA WR-L-634, Mar. 1945.

586. Drees, J.; and Hendal, W. P.: Airflow Patterns in the Neighborhood of Helicopter Rotors. J. Aircraft Engineering, vol. 23, no. 266, Apr. 1951.
587. Reynolds, R. M.: Preliminary Results of an Investigation of the Effects of Spinner Shape on the Characteristics of an NACA D-Type Cowl Behind a Three-Blade Propeller, Including the Characteristics of the Propeller at Negative Thrust. NACA RM A53J02, Nov. 12, 1953.
588. McLemore, H. C.; and Cannon, M. D.: Aerodynamic Investigation of a Four-Blade Propeller Operating Through an Angle-of-Attack Range from 0° to 180°. NACA TN 3228, June 1954.
589. Reynolds, R. M.; Sammonds, R. I.; and Walker, J. H.: An Investigation of Single- and Dual-Rotation Propellers at Positive and Negative Thrust, and in Combination With an NACA 1-Series D-Type Cowling at Mach Numbers up to 0.84. NACA TR 1336, 1957.
590. Yaggy, P. F.; and Mort, K. W.: Wind-Tunnel Tests of Two VTOL Propellers in Descent. NASA TN D-1766, Mar. 1963.
591. Glauert, H.: The Elements of Aerofoil and Airscrew Theory. New York, N.Y.: Cambridge University Press, Apr. 1926.
592. Glauert, H.: Aerodynamic Theory—Volume IV, Section L, Airplane Propellers. Durand, W. F. (Ed.). Gloucester, Mass: Peter Smith Publishers, Inc., 1935.
593. Drees, J.: A Theory of Airflown Through Rotors and Its Application to Some Helicopter Problems. J. Helicopter Association of Great Britain, vol. 3, no. 2, 1949.
594. Gessow, A.; and Myers, G.: Aerodynamics of the Helicopter. New York, N.Y.: Frederick Ungar Publishing Co., 1967.
595. Payne, P. R.: Induced Aerodynamics of Helicopters, Part I. J. Aircraft Engineering, vol. 28, nos. 324 and 327, Feb. 1956.
596. Harris, F. D.: Performance Analysis of Two Early NACA High Speed Propellers With Application to Civil Tiltrotor Configurations. NASA CR-196702, Aug. 1996.
597. Wachpress, D. A.; Quackenbush, T. R.; and Boschitsch, A. H.: First-Principles Free-Vortex Wake Analysis for Helicopters and Tiltrotors. Proc. American Helicopter Society 59th Annual Forum, Phoenix, Ariz., May 6–8, 2003.
598. Johnson, W.: Rotorcraft Aeromechanics. New York, N.Y.: Cambridge University Press, 2013.
599. Johnson, W.: Model for Vortex Ring State Influence on Rotorcraft Flight Dynamics. NASA/TP-2005-213477, Dec. 2005.
600. Stack, J.; Caradonna, F. X.; and Savas, O.: Flow Visualizations and Extended Thrust Time Histories of Rotor Vortex Wakes in Descent. J. American Helicopter Society, vol. 50, no. 3, July 2005.
601. Ahlin, G. A.; and Brown, R. E.: Wake Structure and Kinmatics in the Vortex Ring State. J. American Helicopter Society, vol. 54, no. 3, July 2009.
602. Wright, T. P.: Development of a Safe Airplane—the Curtiss Tanager. SAE International, vol. 25, no. 4, 1930.
603. Osborn, R. R.; and Wright, T. P.: Aircraft. U.S. Patent No. 2,000,666 Issued May 7, 1935.

604. Hotson, F. W.: The de Havilland Canada Story. Toronto, Ontario, Canada: CANAV Books, 1983.
605. Kidwell, J. C.; and Clay, W.: Evaluation of L-19A Equipped With Continental O-470-11C1 Fuel Injected Engine. U.S. Army Aviation Test Office ATO-TR-61-1, Edwards Air Force Base, Calif., 1961.
606. Davidson, J. D.; and Ferry, R. G.: TL-19D Phase IV Performance. AFFTC-TR-57-14, Air Force Flight Test Center, Edwards Air Force Base, Calif., 1957.
607. Anon.: Phase II Flight Test of the Cessna L-19A. WCTSE-WCT-2355, Wright-Patterson Air Force Base, Dayton, Ohio, 1951.
608. Anon.: Description and Maintenance Manual for Heron Hydomatic Propeller Installation. De Havilland Propeller Ltd. Publication 5030, July 1955.
609. Anon.: De Havilland Hyromatic, Three-Bladed, Constant-Speed, Feathering and Braking Propellers. De Havilland Propeller Ltd. Publication A3HFB, Jan. 1953.
610. Anon.: Handbook for the de Havilland Hydromatic Airscrew. Hatfield Aerodrome, Herts, England: De Havilland Aircraft Company Ltd., 1931.
611. Rosen, G.: Thrusting Forward: A History of the Propeller. Hartford, Conn.: Hamilton Standard, 1987.
612. Mortimer, G.: Chasing Icarus—The Seventeen Days in 1910 That Forever Changed American Aviation. New York, N.Y.: Walker & Company, 2009.
613. Ackroyd, J. A. D.; and Riley, N.: Hermann Glauert FRS, FRAeS (1892–1934). J. Aeronautical History, vol. 1, paper no. 2011/2, 2011.
614. Glauert, H.: On the Necessary Size of Aerodromes in Order That a Landing May Be Made if the Engine Fails When Getting Off. Aeronautical Research Committee R&M No. 996, 1926.
615. Ziegler, H.: The Develpment of Short Range Air Transport Through the Use of V/STOL Aircraft. J. Royal Aeronautical Society, vol. 65, no. 605, May 1961.
616. Anon.: USAF Aircraft in Southeast Asia Tested by the Air Force Flight Test Center. AFSC Historical Publication (DTIC ADA 529707), Mar. 1970.
617. Beech, S. H.; Clark, G. W.; and Webb, A. T.: Propulsion System and Peformance Evaluation of the YC-15 Advanced Medium STOL Transport. AFFTC-TR-76-41, Air Force Flight Test Center, Edwards Air Force Base, Calif., Mar. 1977.
618. Trlica, L. G.; Kennington, R. G.; and Springer, R. N.: Performance Evaluation of the YC-14 Advance Medium STOL Transport. AFFTC-TR-77-36, Air Force Flight Test Center, Edwards Air Force Base, Calif., Feb. 1978.
619. Lee, R. E.; Kreitner, G. K.; and Stoddart, S. A.: Flying Qualities Evaluation of the YC-14 Advanced Medium STOL Transport. AFFTC-TR-77-35, Air Force Flight Test Center, Edwards Air Force Base, Calif., Jan. 1978.
620. Hooten, B. R.: The C-17: We Need It Yesterday. Student Essay, U.S. Army War College, Carlisle Barracks, Pa., Apr. 1985.
621. Norton, B.: C-17 Globemaster III in Action. Carrollton, Tex.: Signal Publications Inc., 2013.
622. Kennedy, B. R.: Globemaster III, Acquiring the C-17. Scott Air Force Base, Ill.: Air Mobility Command Office of History, 2004.

623. Wood, R. A.; Hanson, R. O.; and Peterson, S. D.: Flight Control Systems and Flying Qualities Evaluation of the YC-15 Advanced Medium STOL Transport. AFFTC-TR-76-40, Air Force Flight Test Center, Edwards Air Force Base, Calif., Jan. 1977.
624. Clark, G. W.; Sorokowski, P. J.; and Harris, J. A.: Addendum I—Propulsion System and Peformance Evaluation of the YC-15 Advanced Medium STOL Transport—Limited Flight Evaluation of the Modified YC-15 (Phase III). AFFTC-TR-76-41, Air Force Flight Test Center, Edwards Air Force Base, Calif., Jan. 1978.
625. McPherson, R. L.: YC-14 Flight Test Results. AIAA Aircraft Sysems & Technology Mtg., Seattle, Wash., Aug. 1977.
626. Harris, F. D.: The Joint Heavy Lift Program. Proc. American Helicopter Society 64th Annual Forum, Montreal, Canada, Apr. 29–May 1, 2008.
627. Mendenhall, M. R., et al.: Calculation of the Longitudinal Aerodynamic Characteristics of Wing-Flap Configurations With External Blown Flaps. NASA CR-2705, Sept. 1976.
628. Mendenhall, M. R.; and Spangler, S. B.: Calculation of the Longitudinal Aerodynamic Characteristics of Upper-Surface-Blown Wing-Flap Configurations. NASA CR-3004, 1978.
629. Harris, F. D.: Boeing V/STOL Wind Tunnel—1973 Accomplishments. The Boeing Co., Vertol Div., Mar. 4, 1973.
630. LeMaster, D. P.: Airport Performance Estimation for Powered Lift Aircraft. Air University, DTIC ADA 081910, Wright Patterson Air Force Base, Dayton, Ohio, Dec. 1978.
631. Foody, J. J.: The Air Force/Boeing Advanced Medium STOL Transport Prototype. SAE Paper No. 730365, 1973.
632. Wieselsberger, C.: Wing Resistance Near the Ground. NACA TM 77, Apr. 1922.
633. Raymond, A. E.: Ground Influence on Airfoils. NACA TN 67, Dec. 1921.
634. Anon.: U.S. Standard Atmosphere, 1976. NASA TM X-74335, 1976.
635. Johnson, W.: NDARC—NASA Design and Analysis of Rotorcraft. NASA/TP-2015-218751, Apr. 2015.
636. Oswald, W. B.: General Formulas and Charts for the Calculation of Airplane Performance. NACA TR 408, 1932.
637. McCormick, B. W.: Aerodynamics, Aeronautics and Flight Mechanics. New York, N.Y.: John Wiley & Sons, Inc., 1979.
638. Krabal, R. J., et al.: Advanced Propulsion Technology Assessment for an Externally Blown Flap Transport. AFAPL TR-72-17 (DTIC AD 905701), Apr. 1972.
639. Anon.: U.S. General Accounting Office Staff Study—Advanced Medium STOL Transport Program. U.S. General Accounting Office, Mar. 1974.
640. Anon.: Information on the Requirement for Strategic Airlift. Comptroller General of the United States PSAD-76-148, June 8, 1976.
641. Shovlin, M. D.; and Cochrane, J. A.: An Overview of the Quiet Short-Haul Research Aircraft Program. NASA TM-78545, Nov. 1978.
642. Wilcox, D. E.; and Patterakis, P.: Cost and Schedule Management on the Quiet Short-Haul Research Aircraft Project. NASA TM-78547, Jan. 1979.

643. Queen, S.; and Cochrane, J.: Quiet Short-Haul Research Aircraft Joint Navy/NASA Sea Trials. AIAA J. Aircraft, vol. 19, no. 8, Aug. 1982.
644. Riddle, D. W., et al.: Powered-Lift Takeoff Performance Characteristics Determined From Flight Test of the Quiet Short-Haul Research Aircraft (QSRA). AIAA Paper 81-2409. AIAA/SETP/SFTE/ITEA/IEE Flight Testing Conference, Las Vegas, Nev., Nov. 11–13, 1981.
645. Riddle, D. W.; Stevens, V. C.; and Eppel, J. C.: Quiet Short-Haul Research Aircraft—A Summary of Flight Research Since 1981. Society of Automotive Engineers Paper No. 872315, Dec. 12, 1987.
646. Eppel, J. C.: Quiet Short-Haul Research Aircraft Familiarization Document, Rev. 1. NASA TM-81298, Sept. 1981.
647. Anon.: AN-72...Blown Wings From Kiev. Air International, Sept. 1979, pp. 140–142, 151.
648. Stolarow, J. H.: Air Force Justification for Storing its Advanced Medium Short Takeoff and Landing Prototype Aircraft. U.S. General Accounting Office PSAD B-199037, June 16, 1980.
649. Rodrigues, L. J.: Intratheater Airlift—Information on the Air Force's C-130 Aircraft. U.S. General Accounting Office GAO/NSIAD-98-108, Apr. 21, 1998.
650. Pearcy, A.: Douglas Propliners: DC-1 to the DC-7. Shrewsbury, England: Airlife Publishing, Ltd., 1995.
651. Lombard, A. E.: Report on Wind Tunnel Tests on 1/11th Scale Models of the Douglas DC-3 and DC-6 Airplanes. Guggenheim Aeronautical Laboratory, California Institute of Technology GALCIT Report No. 244, Aug. 15, 1939.
652. Becker, J. V.; and Leonard, L. H.: High-Speed Tests of a Model Twin-Engine Low-Wing Transport Airplane. NACA TR 750, 1942.
653. Belsley, S. E.; and Jackson, R. P.: The Effect of Amphibious Floats on the Power-Off Stability and Control Charcteristics of a Twin-Engine Cargo Airplane. NACA WR-A-73, Jan. 1943.
654. Wong, P. Y.: The Effect of the Skies on the Power-Off Stability Characteristics of a Twin-Engine Cargo Airplane. NACA MR-A5F18, June 1945.
655. Douglas, D. W.: The Developments and Reliability of the Modern Multi-Engine Air Liner. Royal Aeronautical Society Aero. 23rd Wilbur Wright Memorial Lecture, vol. 39, Nov. 1935, pp. 1009–1046.
656. Hansen, J. R. (Ed.): The Wind and Beyond: A Documentary Journey Into the History of Aerodynamics in America. Volume I: The Ascent of the Airplane. NASA SP-2003-4409 Vol. I, 2003.
657. Hansen, J. R. (Ed.): The Wind and Beyond: A Documentary Journey into the History of Aerodynamics in America. Volume II: Reinventing the Airplane. NASA SP-2003-4409 Vol. II, 2007.
658. Wetmore, J. W.: Calculated Effect of Various Types of Flap on Take-Off Over Obstacles. NACA TN 568, May 1936.
659. Zeck, H.; and Van Heyningen, V. F.: A Study of the Take-Off and Landing Characteristics of "STOL"-Type Airplanes With Deflected Jet Thrust. Boeing Airplane Co. Document No. D2-3126, Aug. 1957.

660. Hoerner, S. F.: Fluid-Dynamic Drag (Second Ed.). Brick Town, N.J.: Author Published, 1965.
661. Harris, F. D.: Airplane vs. STOL vs. VTOL. NASA/CR–2010-216385, May 2010.
662. Robertson, F. H.: Turboprop vs. Turbojet. Shorts Quarterly Review, vol. 2, no. 15, Dec. 1958, pp. 2–6.
663. Wright, T. P.: Factors Affecting the Cost of Airplanes. J. Aeronautical Sciences, vol. 3, no. 4, Feb. 1936.
664. Anon.: Source Book of World War II Basic Data: Airframe Industry, Vol. I—Direct Manhours—Progress Curves. Army Air Forces, Air Material Command (see also DTIC ADA 800199), 1946.
665. Anon.: Selected Acquisition Report (SAR) for V-22. Department of Defense RCS: DD-A&T (Q&A) 823-212, Washington, D.C., Dec. 31, 2010.
666. Anon.: Selected Acquisition Report (SAR)—V-22 Osprey Joint Services Advanced Vertical Lift Aircraft (V-22). Department of Defense RCS: DD-A&T (Q&A) 823-212, Washington, D.C., Dec. 2014.
667. Anon.: National Defense Budget Estimates for FY 2015. U.S. Department of Defense, Office of the Under Secretary of Defense (Comptroller), Washington, D.C., Apr. 2014.
668. Anon.: Guide for the Presentation of Helicopter Operating Cost Estimates. Economics Committee, Helicopter Association International (HAI), Alexandria, Va., 2010.
669. Conklin, A.; and de Decker, W.: Aircraft Cost Evaluator—Helicopters. Conklin & de Decker, Orleans, Mass., 2011.
670. Pearson, G. B.; and Louthan, J. D.: Direct Operating Costs Commercial Version C-142. Ling-Temco-Vought (LTV) Report 2-55100/5R-50315, Nov. 1, 1965.
671. Eastman, S. E.: Comparitive Costs and Capacity Estimates of Vertiports and Airports, 1975–1985. AIAA/AHS VTOL Research, Design, and Operations Mtg., AIAA Paper No. 69-208, Atlanta, Ga., Feb. 17–19, 1969.
672. Hudock, R. P.; and Leonard, W. D.: Qualitative V/STOL Air Traffic Control Requirements. AIAA/AHS VTOL Research, Design, and Operations Mtg., AIAA Paper No. 69-208, Atlanta, Ga., Feb. 17–19, 1969.
673. Faulkner, H. B.; and Swan, W. M.: The Cost of Noise Reduction for Departure and Arrival Operations of Commercial Tilt Rotor Aircraft. NASA CR-137803, Feb. 1976.
674. Alexander, H. R.; Allen, E. M.; and Bertie, K. M.: Advanced Tiltrotor Transport Technology: Cost/Benefit/Risk Assessment, Phase I Final Report. NASA CDCR-20001, Aug. 1994.
675. Aroesty, J.; Rubenson, D.; and Gosling, G.: Tiltrotors and the Port Authority of New York and New Jersey Airport System. Rand Corp. Report No. R-397-PA, 1991.
676. Harvey, W. D.; and Foreman, B.: Future Regional Tranport Aircraft Market, Constraints, and Technology Stimuli. NASA TM 107669, Oct. 1992.
677. Gibbons, J. H., et al. : NEW WAYS: Tiltrotor Aircraft and Magnetically Levitated Vehicles. U.S. Congress, Office of Technology Assessment OTA-SET-507, Oct. 1991.

678. Mead, K. M.: High Speed Ground Transportation. U.S. General Accounting Office, Testimony Before the Subcommittee on Surface Transportation, GAO/T-RCED-93-45, May 20, 1993.
679. Harris, F. D.: An Economic Model of U.S. Airline Operating Expenses. NASA/CR-2005-213476, Dec. 2005.
680. Whittle, R.: Osprey Proves Its Mettle. AHS Vertiflite, vol. 61, no. 3, May/June 2015, pp. 22–28.
681. Blake, M., et al.: Advanced Vehicle Concepts and Implications for NextGen. NASA/CR-2010-216397, Jan. 2010.
682. Hirschberg, M.: Robust Sales, New Developments Buoy Civil Market. AHS Vertiflite, vol. 61, no. 3, May/June 2015, pp. 10–12.
683. Ormiston, R. A.: Alexander Nikolsky Honorary Lectureship, Revitalizing Research for the Next Generation of Advanced Rotorcraft. Proc. American Helicopter Society 71st Annual Forum, Virginia Beach, Va., May 5–7, 2015.
684. Anon.: Research and Technology, 1995, Ames Research Center. NASA TM-11049, 1995.
685. Wilkerson, J. B., Schneider, J.J. and Bartie, K.M.: Technology Needs for High-Speed Rotorcraft (1). NASA CR 177585, May 1991.
686. Scott, M. W.: Technology Needs for High-Speed Rotorcraft (2). NASA CR 177590, August 1991.
687. Rutherford, J., O'Rourke, M., Martin, C. , Lovenguth, M. and Mitchell, C.: Technology Needs for High-Speed Rotorcraft. NASA CR 177578, April 1991.
688. Jeracki, R. J.; Mikkelson, D. C.; and Blaha, B. J.: Wind Tunnel Performance of Four Energy Efficient Propellers Designed for Mach 0.8. Cruise. NASA TM-79124 (see also SAE Paper 790573), Apr. 1979.
689. Whitlow, J. B.; and Sievers, G. K.: Fuel Savings Potential of the NASA Advanced Turboprop Program. NASA TM-83736, 1984.
690. Rohrbach, C.; Metzger, F. B.; Black, D. M.; and Ladden, R. M.: Evaluation of Wind Tunnel Performance Testing of an Advanced 45° Swept Eight-Bladed Propeller at Mach Numbers From 0.45 to 0.85. NASA CR-3505, 1982.
691. Mikkelson, D. C.; Blaha, B. J.; Mitchell, G. A.; and Wikete, J. E.: Design and Performance of Energy Efficient Propellers for Mach 0.8 Cruise. NASA TM-X-73612, Mar. 1977.
692. Stefko, G. L.; and Jeracki, R. J.: Wind Tunnel Results of Advanced High Speed Propellers at Takeoff, Climb, and Landing Mach Numbers. NASA TM-87030, Aug. 1985.

APPENDIX A

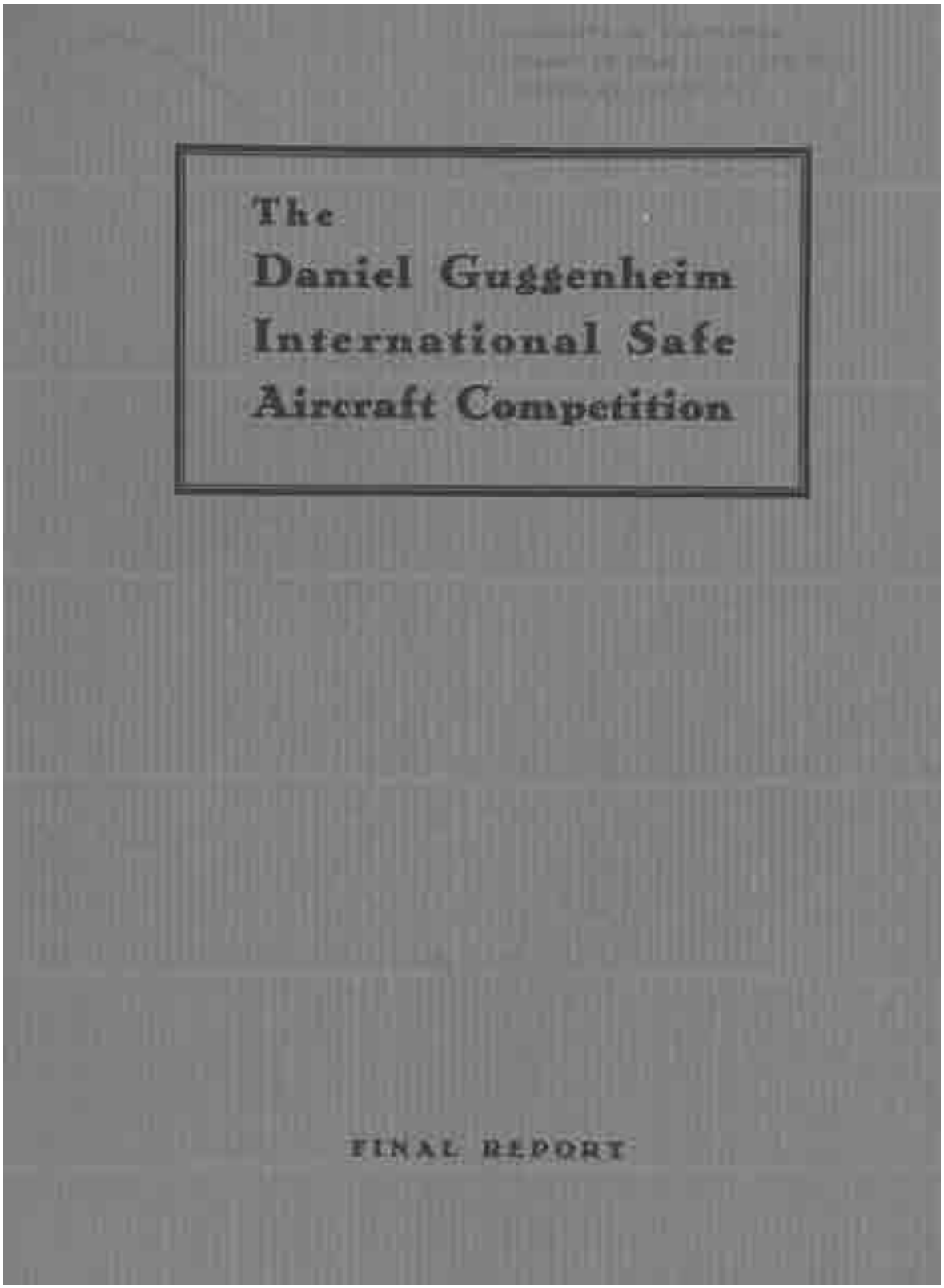
The
Daniel Guggenheim
International Safe
Aircraft Competition
FINAL REPORT

The

DANIEL GUGGENHEIM INTERNATIONAL SAFE AIRCRAFT COMPETITION

FINAL REPORT

JANUARY 31, 1930

THE DANIEL GUGGENHEIM FUND
FOR THE PROMOTION OF AERONAUTICS, *Inc.*
598 MADISON AVENUE · NEW YORK CITY

Safe Aircraft Competition Officials

Standing—Prof. Alexander Klemin, Maj. E. E. Aldrin, Capt. Ernest S. Land, William P. MacCracken, Jr., Milburn Kuppers, Dr. George W. Lewis, Edward P. Warner, Thomas Carroll

Kneeling—Capt. Walter Bender, K. F. Ruppel, F. K. Teichman, Lieut. Stanley Umstead, E. W. Rocker, Prof. William G. Brown

INDEX

Photographs and Figures

Personnel of the Safe Aircraft Competition

Committee of Judges

MR. ORVILLE WRIGHT, *Chairman*

MR. F. TRUBEE DAVISON — MR. EDWARD P. WARNER

MR. WILLIAM P. MACCRACKEN, JR. — ADMIRAL RICHARD E. BYRD

DR. GEORGE W. LEWIS

Technical Advisers

PROF. ALEXANDER KLEMIN, N. Y. U.

MAJOR E. E. ALDRIN, U. S. Army Air Corps (Reserve)

MAJOR R. H. MAYO, O. B. E.

Manager of Information Bureau

MR. MILBURN KUSTERER

Field Manager

CAPTAIN WALTER BENDER, U. S. Army Air Corps

Pilots

MR. E. W. ROUNDS — MR. THOMAS CARROLL

LIEUTENANT STANLEY UMSTEAD, U. S. Army Air Corps

Observers

PROF. WILLIAM G. BROWN, M. I. T.

MR. OTTO LUNDE, N. Y. U. — MR. K. F. RUPERT, N. Y. U.

MR. F. K. TEICHMAN, N. Y. U.

E N T R I E S

Great Britain

De Havilland Aircraft Company, Ltd.
Gloster Aircraft Company, Ltd.
Cierva Autogiro Company
Handley-Page, Ltd.
Vickers, Ltd.

Italy

Societa Italiana Ernesto Breda

United States

Pitcairn-Cierva Autogiro Company of America

Brunner Winkle Aircraft Corporation
Whittelsey Manufacturing Company
J. S. McDonnell, Jr., & Associates
Rocheville Aircraft Corporation
John H. Wiggins Company, Inc.
Cosmic Aircraft Corporation
Gates Aircraft Corporation
Dare Airplane Company
Command-Aire, Inc.
Heraclio Alfaro

Curtiss Aeroplane & Motor Company, Inc.
Cunningham-Hall Aircraft Corporation
Taylor Bros. Aircraft Corporation
Schroeder-Wentworth Company
Bourdon Aircraft Corporation
Ford-Leigh Safety Wing, Inc.
Moth Aircraft Corporation
Charles Ward Hall, Inc.
Fleet Aircraft, Inc.
V. J. Burnelli

Introductory Note

ON April 20, 1927, the Daniel Guggenheim Fund for the Promotion of Aeronautics announced a Safe Aircraft Competition. The object of this competition was "to achieve a real advance in the safety of flying through improvement in the aerodynamic characteristics of heavier-than-air craft, without sacrificing the good, practical qualities of the present-day aircraft."

As an incentive to the development and construction of an aircraft having characteristics which would fulfill the conditions laid down by the Rules for the Daniel Guggenheim Safe Aircraft Competition, the Fund offered a First Prize of $100,000 and five "Safety Prizes" of $10,000 each.

Applications for entry in the Competition were invited on and after September 1, 1927, up to October 31, 1929 as a final date.

It was expected that aircraft entered in the Competition would be presented from time to time during the approximately two year period and it was considered that the object of the Competition might be achieved before the final date, in which case the Fund intended to announce the closing of the Competition. Moreover, if the entries could be presented throughout the life of the Competition, the officials would be able to conduct tests under favorable weather and field conditions. This did not prove to be the case, as the first airplane was not presented until after the middle of August, 1929, and practically all of the competitors presented their entries in the last month of the life of the Competition, that is, in October, 1929. The tests were carried out with meticulous care, but weather conditions and field conditions were not favorable and it was impossible to carry on the Competition expeditiously.

Many of the entries were presented without being thoroughly tried out by the owners. This caused many delays and seriously interfered with carrying out some of the tests as thoroughly as desired. Furthermore, contestants made many requests relative to minor alterations, adjustments, etc., and the Competition officials, with the

approval of the Fund, were very lenient in granting these requests, insofar as it was in any way practicable. To those familiar with aviation flight test work, the difficulties and complications in connection with a competition of this character will be readily appreciated.

From the total of twenty-seven entries in the Competition, only fifteen airplanes appeared at Mitchel Field, where the tests were conducted. Of these fifteen, three withdrew without test, two sustained damages in preliminary flying which prevented their presentation within the time limit, and eight failed to pass all of the Qualifying Requirements.

Only two airplanes, one of which failed to pass a minor Qualifying Requirement, exhibited attributes which warranted completion of the Safety Tests and Demonstrations.

While the entries for the Competition were required to be made previous to midnight of October 31, 1929, certain of the aircraft which were delayed by circumstances, after bona fide attempts to meet the date set, were allowed additional time to appear for test.

Curtiss Plane Is Winner

The tests were finally completed on January 1, 1930. The presentation of the first prize was made to the Curtiss Aeroplane and Motor Company on January 6, 1930.

In presenting the check for the first prize to Mr. C. M. Keys, president of the Curtiss Company, Captain Emory S. Land, vice-president of the Fund, said:

"Congratulations to the Curtiss Aeroplane and Motor Company and particularly those 'down the line' in the organization who had the engineering details to design and construct. The best plane won. All hands agree to that.

"This Competition was designed to obtain the greatest advantages in aerodynamic safety without loss of efficiency. Its object was 'to achieve a real advance in the safety of flying through improvement

in the aerodynamic characteristics of heavier-than-air craft, without sacrificing the good, practical qualities of the present-day aircraft.' This has been accomplished.

"No one in the Fund expected to obtain a 'fool-proof' plane—there isn't any such animal. Moving masses cannot be made 'fool-proof,' but they can be made safe. Old man 'Kinetic Energy' can always do damage to a fool. The Fund's idea was to see a plane developed that the lay pilot could fly with satisfaction, security, efficiency and safety. The fundamental idea of the Fund throughout this Competition is: 'What we want in aviation is progress.'

"Tangible results are before you today. There is nothing revolutionary about the winner, but there are a number of evolutionary ideas transplanted from the design board to the air in a flying competition, in a most efficient manner. These are the ideas that count. They speak for themselves and are the most conclusive proof that can possibly be obtained. American aviation may well be proud of these results.

Great Intangible Results

"Officials of the Fund have always felt that the intangible results of the Safe Aircraft Competition would be far greater than the tangible results. We still feel that way. This Competition has initiated development throughout the aviation world. This will continue for years to come. The seed planted by this Competition will bear fruit for the next decade.

"It is deeply regretted that the Honorable Harry F. Guggenheim, President of the Fund, on account of his Ambassadorial duties in Cuba, cannot be present today, as his intense interest, enthusiasm and zeal are responsible for the accomplishments of the Fund. It is also deeply regretted that the donor of the Fund, on account of a slight indisposition, cannot be present in person, as he is in spirit, to make this presentation. The aviation world owes a debt of gratitude to Mr. Daniel Guggenheim."

The Daniel Guggenheim Fund for the Promotion of Aeronautics was formed in January, 1926, with deeds of gift from Mr. Daniel Guggenheim totalling $2,500,000, of which both interest and principal was to be expended. This sum was increased later by further gifts from Mr. Guggenheim.

The purpose of the Fund was to promote aeronautical education throughout the country, to assist in the extension of aeronautical science and to further the development of commercial aircraft, particularly in its use as a regular means of transportation of both goods and people. The administration of the Fund was placed in the hands of the following Trustees and Officers:

HARRY F. GUGGENHEIM, *President*

EMORY S. LAND, *Vice-President*

H. I. CONE	R. A. MILLIKAN
F. TRUBEE DAVISON	DWIGHT W. MORROW
W. P. DURAND	ELIHU ROOT, JR.
CHARLES A. LINDBERGH	JOHN D. RYAN
A. A. MICHELSON	ORVILLE WRIGHT

Maj. Gen. George W. Goethals, U. S. A., one of the original Trustees, died in 1928. Mr. J. W. Miller served as Secretary of the Fund during its existence. Rear Admiral H. I. Cone, U. S. N., was Vice-President of the Fund until his appointment to the United States Shipping Board. He remained as a Trustee, but was succeeded as Vice-President by Capt. Emory S. Land, U. S. N. (C.C.).

The purposes of the Fund having been accomplished, it liquidated its affairs and ceased to function as of February 1, 1930.

Acknowledgments

THE Fund desires to express its gratitude and appreciation to the following organizations and individuals for their advice, assistance and cooperation in connection with the many phases of the Safe Aircraft Competition:

The Army Air Corps for permission to utilize Mitchel Field, not only for conducting the tests, but also for hangar and office facilities. The Honorable F. Trubee Davison, Assistant Secretary of War, was particularly helpful in connection with this matter.

The commanding officers of Mitchel Field during the life of the Competition.

The Field Manager, who not only carried out his duties as Field Manager in a most satisfactory and efficient manner, but also maintained a splendid cooperative spirit among all the competitors.

The late Lieutenant Moorman carried out advance tests in 1927 in a VE-7, which materially aided all Competition officials in interpreting the rules.

Very valuable test work was carried out by Mr. Thomas Carroll in 1928 in a D.H. Moth. A complete set of interpretations and auxiliary rules was prepared as a result of this test work.

New York University rendered valuable assistance, particularly in connection with instruments and afforded facilities for calibration, test and checking.

The assistance of New York University officials, both in an advisory and consulting capacity, proved most helpful throughout the entire period.

The Bureau of Standards sent their instrument expert to Mitchel Field to check all the instruments used in the flight tests.

Previous acknowledgment has been made to those who assisted in the preparation of the rules. It is a pleasure for the Fund to again acknowledge the very able assistance rendered.

The Judges contributed their services and the Fund is particularly grateful for the assistance rendered.

The technical advisers, pilots and observers devoted their time to the Competition whenever called upon and it is the sincere belief of the Fund that their work could not be improved upon by any other organization in the aviation world.

Curtiss "Tanager"

12

General Summary

ONLY one airplane satisfactorily fulfilled both the Qualifying Requirements and the Safety Tests and Demonstrations. This was the Curtiss "Tanager," designed and built by the Curtiss Aeroplane and Motor Company, of Garden City, Long Island, N. Y. The "Tanager" was designed for the express purpose of meeting the requirements of the Competition, but incorporates features of advantage for commercial flying. It was awarded first prize.

Inasmuch as none of the other contestants successfully completed the Safety Tests and Demonstrations the Curtiss Company was the only entrant eligible for a Safety Prize.

Except for the winner, the only airplane to in any way approach the required conditions was the Handley-Page entry. This airplane, which was the only foreign participant, proved to be an excellent flying machine and with the exception of a few items was about on a par with the Curtiss entry as far as meeting the requirements of the rules was concerned.

Although no new device was developed particularly for the Competition, the entries covered almost the whole field of features which either practically or theoretically are expected to improve the control or speed range of aircraft. These include the following:

1. Variable wing area.
2. Variable wing camber.
3. Trailing edge flaps.
4. Leading edge slots.
5. Slots ahead of trailing edge flaps.
6. Variable incidence wing.
7. Spoiler lateral control.
8. Floating ailerons.
9. Fixed leading edge auxiliary airfoil or slot.

The various features will be discussed later in detail, but certain general conclusions from the results of the Competition tests may be summarized as follows:

1. The advantages, if any, of variable wing area and variable camber could not be determined due to the unsatisfactory flying characteristics of those aircraft using these features.

2. The use of a variable incidence wing appears to have little or no justification from any standpoint.

3. The advantages of slots and flaps in lowering the minimum speed were clearly demonstrated.

4. The airplane equipped with floating ailerons exhibited unusually good controllability at speeds near the minimum either with or without slots and flaps in operation as such.

5. The use of the spoiler device did not provide the desired lateral control on the aircraft using it.

6. With the present type of longitudinal control it is practically impossible to fly an airplane at angles of attack greater than that at which the maximum lift of the airfoil combination is obtained.

7. The fixed leading edge slot proved to be a detriment to high speed and its effect on low speed could not be established on the airplane equipped with it.

In addition to the above the Competition appeared to show that the design and construction of an airplane which will successfully meet a given set of conditions can best be handled by a manufacturer having a well equipped and experienced engineering division.

It is regretted that all of the competitors originally entered did not submit aircraft for demonstration. The absence of the Autogiro was particularly disappointing, since no results of its performance directly comparable with other types of aircraft are available.

In addition to the performance data given above the following was obtained on the Curtiss "Tanager" with different slot and flap combinations:

Minimum Horizontal Speed

Slots open, flaps down	30.6 m.p.h.
Slots open, flaps up	34.8 m.p.h.
Slots closed, flaps down	35.4 m.p.h.
Slots closed, flaps up	41.5 m.p.h.

Minimum Gliding Speed

Slots open, flaps down	37.1 m.p.h.
Slots open, flaps up	42.1 m.p.h.
Slots closed, flaps down	41.5 m.p.h.
Slots closed, flaps up	48.8 m.p.h.

TABLE OF FINAL DATA

	Maximum speed (m.p.h.)	Rate of climb at 1000' (ft./min.)	Minimum horizontal speed (m.p.h.)	Minimum gliding speed (m.p.h.)	Landing run (feet)	Landing over obstruction (feet)	Take off run (feet)	Take off over obstacle (feet)	Flattest glide (degrees)	Steepest glide (degrees)	Empty weight (lbs.)	Useful load (lbs.)	Full load weight (lbs.)	Rated horse power	Wing loading (lbs. per sq. ft.)	Power loading (lbs. per h.p.)
1. Alfaro	108.6										1,100	550	1,650	110	9.7	15.0
2. Bourdon	103.3										1,179	486	1,665	90	7.1	18.5
3. Brunner Winkle	106.0										1,205	451	1,656	90	6.5	18.4
4. Burnelli	Appeared at Field but withdrew															
5. Command-Aire	114.8	900	46.0								1,482	851	2,333	170	9.5	13.7
6. Cunningham-Hall	94.2		44.0	41.0							1,303	470	1,773	90	8.7	19.7
7. Curtiss	111.6	700	30.6	37.1	90	293	295	500	6	13.2	1,979	880	2,859	176	8.6	16.3
8. Fleet	108.6	610									1,100	500	1,600	90	8.1	17.3
9. Ford-Leigh	102.4										1,550	575	2,125	115	7.3	18.5
10. Gates	Appeared at Field but withdrew															
11. Handley-Page	112.4	730	33.4	39.7	82	320	290	440	7.2	12.8	1,378	778	2,156	155.6	7.4	13.9
12. McDonnell	Airplane crashed in demonstration flight															
13. Moth	Appeared at Field but withdrew															
14. Schroeder-Wentworth	Airplane crashed in preliminary flight															
15. Taylor	108.5		45.5	50.4							1,197	470	1,667	90	9.5	18.5

General Comment

As stated in the Rules for the Daniel Guggenheim Safe Aircraft Competition the object of the Competition was "to achieve a real advance in the safety of flying through improvement in the aerodynamic characteristics of heavier-than-air craft, without sacrificing the good, practical qualities of the present-day aircraft."

Whether or not the above object was achieved must be a matter of opinion, but using the conditions as prescribed by the rules as a measure, two airplanes, the Curtiss and Handley-Page, approached very closely to the standard desired.

Certain features of the airplanes competing proved themselves valuable for specific purposes, but no opportunity was had to thoroughly investigate their effect on performance at altitude either in climb or level speed. The use of the features can therefore be recommended only for their most obvious use.

It is believed that the following devices, all of which are to be found on either the Curtiss or Handley-Page entries, are worthy of incorporation on various types of aircraft or of further study:

1. Automatic leading edge slots.
2. Flaps, either automatic or manually controlled.
3. Floating ailerons.
4. Long stroke oleo landing gear with provision for locking in the position assumed under load.
5. Extreme range adjustable stabilizer.
6. Brakes.

Leading edge slots, while used on several entries, were probably best exemplified in the case of the Curtiss and Handley-Page entries. The effect on minimum speed of opening the slots on the Curtiss "Tanager" was measured with the trailing edge flaps on both extreme positions, up and down. Based on the results obtained with the Handley-Page, there seems to be no advantage in having independent slots over the span of the aileron, provided slots extend over the entire span, unless the aileron slots are interconnected with the ailerons.

This is due to the fact that the object of wing slots over the aileron span only was to prevent the wing tip from stalling at as low an angle of attack as the rest of the wing. This is obviously not obtained when the slots over the aileron spans are identical in operation with the slots over the rest of the wing.

Use of Fixed Slot

The use of the fixed slot, which was exemplified by the Ford-Leigh Safety Wing, entailed too great a sacrifice of high speed, and so seriously changed the balance of the airplane that ballast had to be placed as far forward as possible on the engine crankcase.

In view of the peculiar behavior of the Handley-Page airplane under certain conditions, the interconnection of the slot with the trailing edge flap is considered unsatisfactory. This plane when under power could be stalled so that the slots closed and the flaps moved up after the nose dropped below horizontal due to the stall. This made the plane lose considerable altitude and before control was regained the speed had risen appreciably. This characteristic is possibly dangerous in such a case as when trying to pull over an obstruction at the end of a small field.

Trailing edge flaps, either automatic (controlled by slot) or manually operated, were used on several of the entries. In the case of the Curtiss the flaps were used in conjunction with a slot immediately forward of the flap leading edge.

In order to obtain satisfactory balance and control throughout the working ranges of slots and flaps it is necessary to provide an unusually large stabilizer adjustment or to decrease its size and increase the area of the elevators. The former method was used on both Curtiss and Handley-Page entries. The stabilizer of the Handley-Page was generally rectangular in shape, while that of the Curtiss was triangular. It is considered that at high angles of attack the latter type is preferable, as less blanketing of the vertical surfaces and consequently greater directional control is obtained. Lowering of the flaps at any given speed tended to make the airplanes tail-heavy. The flaps were only lowered at low

Wright Curtiss "Pusher"

16

speeds, very large forces being developed at high speeds.

As a means of obtaining satisfactory lateral control at low speeds the Curtiss "Tanager" was equipped with the so-called "floating type" ailerons. These, in addition to being controlled in the usual way by stick movement, were also arranged in such a way that both ailerons could change their angles in the same direction when acted upon by forces other than given by stick movement. The two ailerons being statically balanced while the center of pressure always remained aft of the hinge tended to lie with their chords parallel to the air flow acting upon them. This feature permitted them to act always at an efficient angle of attack and never to approach a stalling angle. Since the ailerons could not be locked to prevent "floating," it was impossible to determine whether the excellent lateral control was entirely due to the type of aileron or whether other features contributed markedly. It is considered that while the "floating" aileron probably assisted greatly, the stability of the airplane and relatively effective directional control at slow speeds were large factors in producing good lateral controllability.

Variable Incidence Wing

Two airplanes were equipped with the "spoiler" type of lateral control. Both of these planes were deficient in lateral control, one of them crashing due to this cause. The advantages of the "spoiler" control were not demonstrated in the Competition.

A device which for some unknown reason has always interested certain designers is the variable incidence wing. The Taylor entry exhibited this feature. At low speed the angle of incidence of the wing, according to the competitor, should be made as great as possible while at high speed it should be placed at the minimum angle. Obviously, the angle of incidence of the wing referred to the airplane has no particular connection with the angle of attack with the exception of the effect of the lift of the portions of the airplane exclusive of the wing. It is probable that lower minimum speed would be obtained with the wing in the assumed position for high speed due to additional lift supplied by the fuselage at high angles of attack. As stated previously in the report, the variable angle of incidence appears to be of little or no value when applied to the main wings of a normal airplane.

Oleo landing gears having unusually long stroke were used on several of the entries. That installed on the Curtiss "Tanager" was of such rugged design that the airplane could be allowed to settle into the ground at nearly its steepest gliding angle. This appeared also to be the case with the McDonnell entry, which unfortunately crashed during its demonstration flights. In addition to the oleo feature, the Curtiss entry was equipped with a latch by means of which the wheels could be held in the position assumed by the gear on the ground. While this was installed in order to shorten the measured run in getaway, it also served to decrease the exposed length of strut while in the air. This possibly decreased the drag of the landing gear.

Brakes were installed on nearly all the entries for the purpose of shortening the landing run and providing control on the ground. With the exception of the Handley-Page plane, the brakes were controlled by foot pedals or levers and could be used to steer the airplane while on the ground. The Handley-Page plane was at times difficult to handle on the ground in a cross wind due to the method of applying both brakes at once and the excessive flexibility of the landing gear when not pumped up to the proper pressure. The brakes on the Handley-Page were operated by a hand lever which was difficult to reach due to the cramped position of the pilot in the unusually small cockpit.

The Burnelli and Alfaro entries incorporated a variable area device intended to increase the speed range of the airplane. Due to the unsatisfactory flying characteristics of these airplanes the effect of the feature mentioned was not determined.

Applications for Entry

Twenty-seven applications for entry in the Safe Aircraft Competition were accepted, all of them having included the information required with the form of application for entry. Several alternative arrangements of power plant or structure were offered in some cases with the request that the decision as to which would be used be left until the first flight tests. In general, the Fund took a lenient view of these requests, although it was realized that changes during tests would be an inconvenience and source of delay.

In the case of several entries which were obviously stock models with no reason for entering

except for the publicity to be gained, the information furnished with the application for entry was only the minimum required for acceptance.

Qualifying Requirements

All of the airplanes which actually appeared at Mitchel Field arrived during the last few months before the closing of the Competition. Many of the entries were put through certain tests by the competitor's pilot and nearly all were demonstrated by the same pilot before being accepted by the Fund for test.

Power Plant — With the exception of the Ford-Leigh entry, all of the aircraft were equipped with an engine of approved type. Some difficulty arose in deciding on the normal horse power and r.p.m. for test purposes, but in no case did this have any material bearing on the performance obtained. All entries used fuel supplied by the Fund except the Curtiss airplane which used a 10 percent benzol mixture. All the entries were equipped with engine starters at the time of their acceptance for test, although several arrived at the Field without this equipment.

Structural Strength — All entries were assumed to have satisfactory structural strength based on one or more of the following points:

1. General inspection.
2. Stress analysis.
3. Approved type certificate.
4. Competitor's demonstration.

Only minor structural weaknesses appeared during the tests. These involved the damage done to landing gears of the Ford-Leigh, Alfaro, Handley-Page and Curtiss entries.

Performance — The maximum speed requirement rather surprisingly proved to be the stumbling block for seven out of the ten planes tested, although this had no direct bearing on the Safety Tests, and any number of stock planes could have met this condition. Those which passed this condition were the Curtiss, Handley-Page and Command-Aire entries. Neither the Command-Aire nor those which failed on the high speed test showed any possibility of being able to pass more than a few of the Safety Tests and Demonstrations.

The rate of climb specified was easily met by those entries tested for this item of performance. The Curtiss, Fleet, Command-Aire and Handley-Page airplanes passed this test.

Useful Load—All aircraft carried the specified useful load of 5 pounds per horse power. On several of the entries it was necessary to increase the useful load above this figure in order to have sufficient fuel available for testing.

Fuel and Oil—The fuel and oil capacity of all entries was adequate.

Instruments—All entries were equipped with the proper instruments.

Accommodation—Only one of the airplanes submitted was considered unsatisfactory as regards accommodation for the pilot and observer. The Handley-Page entry had cockpits so narrow and small that it was impossible to wear a parachute. Moving around after being closed in was very difficult. Due to the interest in the airplane and since it was a foreign entry, this matter of accommodation was not stressed and the Handley-Page entry was put through all the Safety Tests and Demonstrations. The required cabin or cargo space was provided in the Curtiss, Handley-Page and Command-Aire. All entries provided for dual control by pilot and observer.

Vision—This item was considered satisfactory on all airplanes, taking into consideration the type.

Fire Risk — All reasonable precautions against fire risk were taken by the arrangement of the power plant in accordance with standard practice, the provision of a firewall behind the engine and the installation of a hand fire extinguisher.

The two planes which satisfactorily passed all the Qualifying Tests were the Curtiss and Command-Aire.

The Handley-Page entry, on account of its aerodynamic features and the probability that it would approach very closely to the standards set by the rules, was permitted to remain in the Competition in spite of failure to provide adequate accommodation for pilot and observer.

Safety Tests and Demonstrations

Speed Tests—Minimum Flying Speed—Both the Curtiss and Handley Page entries were able to maintain level and controlled flight at air speeds below 35 m.p.h. The Command-Aire entry, the only

other airplane to meet the Qualifying Requirements, failed on this test by 11 m.p.h., a very considerable amount. At the request of the competitors, minimum flying speed was measured on the Cunningham-Hall and Taylor entries. Neither of them fulfilled the requirements, although they performed on this item better than the Command-Aire entry.

MINIMUM GLIDING SPEED — The Curtiss "Tanager" was the only airplane to meet the minimum gliding speed requirement. In addition to the Handley-Page, the minimum gliding speed was measured on the Cunningham-Hall and Taylor, again at the request of the competitors.

TEST OF LANDING RUN—Only the Curtiss and Handley-Page entries were tested. Both airplanes met the requirements, the Handley-Page being superior to the Curtiss in this test, in spite of the fact that the brakes were more readily operated on the Curtiss entry.

TEST OF LANDING IN CONFINED SPACE — The Curtiss and Handley-Page entries were both tested. The Handley-Page failed to meet the requirements while the Curtiss was successful. One reason for the failure of the Handley-Page was the fact that the landing gear was not rugged enough to permit landing from the steepest glide. In addition, the possibility of stalling the airplane with consequent undesirable action of slots and flaps as noted above, made it necessary to glide at a speed higher than the stall.

TEST OF TAKE OFF — Both the Curtiss and Handley-Page entries met the requirements, the Handley-Page being superior to the Curtiss in both take off run and distance to clear the 35-foot obstructions.

TEST OF GLIDING ANGLE — The Curtiss and Handley-Page entries were both successful in meeting the requirement of flattest glide, the Curtiss being slightly superior.

Neither airplane was able to fulfill the requirement of steepest glide, and it was considered by the officials conducting the tests that the requirement was too severe. For this reason the angle specified was modified from 16 to 12 degrees by unanimous approval of all Competition officials.

TEST OF STABILITY IN NORMAL FLIGHT—Both the Curtiss and Handley-Page entries were determined to have reasonably satisfied the conditions of longitudinal stability, although neither airplane was perfect under all conditions.

The Curtiss entry passed the general stability requirements, but the Handley-Page was only satisfactory when trimmed at air speeds of about 60 to 80 m.p.h. At other speeds a slight disturbance would cause the latter airplane to eventually go into a left-hand spiral which gradually steepened with increasing air speed.

TEST OF ABILITY TO RECOVER FROM ABNORMAL CONDITIONS—Both the Curtiss and Handley-Page entries satisfactorily fulfilled the requirements in the tests of ability to maintain control in case of engine failure.

In the tests of ability to recover from violent disturbances both airplanes were satisfactory in recovery from the dive.

In the recovery from abnormal attitudes it was found that recovery could be made from the attitude assumed in the required limit on loss of height when the controls were used. However, with free controls the airplanes could not recover within the required distance. In order to effect recovery both entries then made use of rubber cord on the control stick, which was intended to give the effect of more horizontal tail area. It was found that a relatively slight deviation from the normal attitude was sufficient to make recovery uncertain within the specified limit. For this reason the abnormal condition was reduced in violence until one of the airplanes, which happened to be the Curtiss entry, was considered satisfactory. Although with the modified initial disturbed attitude, the Curtiss plane was assumed to be satisfactory, it was found that the adjustment necessary on the rubber cord, which was used to meet the requirements, was so critical that a slight change would cause the airplane to change from the stable to a definitely unstable condition. The Handley-Page entry never succeeded in obtaining the proper adjustment to give the desired recovery, all maneuvers eventually ending in a steep spiral to the left with increasing air speed.

It is believed that no airplane at the present time can meet the specified limit in recovery with free controls.

TEST OF CONTROLLABILITY—While both Curtiss and Handley-Page entries were assumed to be controllable at all throttle settings and were probably

more so than any other types, neither airplane could be controlled perfectly at the stall. The Curtiss, due to the fact that the flaps were manually operated, was better than the Handley-Page in this respect. When stalled under power the former would drop the nose, pick up about 3-5 m.p.h. and again return to the stall, continuing this cycle apparently indefinitely. Lateral and directional control appeared good at the stall under any slot or flap adjustment.

The Handley-Page under power would, when stalled, do one of two things. If completely stalled so that the nose dropped, the slots would close and the flaps move up, which resulted in the speed rising some 10-15 m.p.h. in a short dive before sufficient control was regained to again stall the airplane. When flown steadily just above stalling speed, a slight disturbance often caused the nose of the plane to swing, usually toward the right. After starting, nothing could stop the turn and resultant falling off until speed was picked up as in the former case by a short dive accompanied by closing of the slot and upward movement of the flaps.

When gliding at minimum speed both airplanes are apt to get into an oscillation which is difficult to stop without increasing speed considerably before again approaching the stalling speed. The Curtiss airplane appears to be much more controllable than the Handley-Page, judging from the steadiness with which it can be flown near the stalling point. The assumption that the tail surfaces of the Curtiss "Tanager" provide better control than those of the Handley-Page has already been discussed. Lateral control is noticeably better, probably due partially to the yawing produced on the Handley-Page at stalling speeds when the ailerons are used.

The effectiveness of the controls appeared to be little affected by gusty air, although the airplanes could not be flown as steadily as in smooth air.

Test of Maneuverability in Restricted Territory—The original interpretation for this test specified that the engine could be switched off at any time and the airplane must then land within a plot 500 feet square, from which it has just taken off. Owing to the getaway characteristics of the airplanes, this test was considered to involve danger in its accomplishment and the conditions were so modified as to allow cutting off the engine after an altitude of 100 feet was reached. Both Curtiss and Handley-Page entries were considered to have satisfactorily met the revised requirements.

Test of Maneuverability on the Ground—Both Curtiss and Handley-Page airplanes were considered to be satisfactorily maneuverable on the ground in a 20 m.p.h. wind. In this respect the Curtiss was superior to the Handley-Page due to steering possibilities of the brakes and more satisfactory landing gear. Under certain conditions the landing gear of the Handley-Page permitted tilting of the plane sideways to an objectionable extent.

Basis for the Award of the Prize

It was expected that more than one airplane would pass the Qualifying and Safety Tests and that the award of the first prize would depend upon points made in comparative tests. Since only one airplane reached the stage for award of points the comparative tests were not conducted and the prize was awarded to the Curtiss "Tanager."

The Handley-Page was a close second to the Curtiss entry all during the Competition. For this reason the points for performances are given for both in the tests passed:

Points Assigned

	Curtiss	Handley-Page
Speed tests:		
(a)	8.8	3.2
(b)	3.6	0.0
(c)	0.0	0.0
Test of landing run	6.7	12.0
Test of landing in confined space	3.5	0.0
Test of take off:		
Length of run	0.3	0.7
Distance to clear obstacle	0.0	6.0
Total points	22.9	21.9

The following features incorporated in the Curtiss "Tanager" are considered to be points of superiority:

1. Manually controlled flaps.
2. Floating ailerons.
3. Design of tail surfaces to eliminate blanketing.
4. Long stroke rugged landing gear with latch
5. Independently operated brakes.
6. Adequate accommodation for occupants.

Notes on Results from an Aerodynamical Standpoint

BECAUSE of the failure of all but two planes to pass the Qualifying Tests and the fact that all planes were presented for test at practically the same time, comparatively little numerical data in the slow speed region were obtained. The following brief notes summarize some of the aerodynamical information secured:

1. MAXIMUM LIFT COEFFICIENTS IN GLIDING FLIGHT

Three planes were tested for slow speed on the glide. In the following table derived from these tests, the net area of the wings, without allowance for possible lift of fuselage or tail surfaces, is taken as the reference area.

From the results of the tests on the Taylor machine, it can be seen that no appreciable error would have been made, for the particular section employed, in calculating the stalling speed from atmospheric tunnel values. Since the center of gravity of this machine was at 29.3 per cent of the mean aerodynamic chord, no appreciable lift would be found on the tail at the stall, and the slight discrepancy between wind tunnel and full scale value of maximum Ky would be readily accounted for by the lift of the fuselage.

The increase in lift obtained with the Curtiss entry indicates that starting with a basic airfoil of medium thickness and high maximum Ky, it is possible to obtain an appreciable increase in lift. The scale effect, as between tunnel and full scale machine, as regards maximum lift with slots open and flaps down, is seen to be negligible:

Airplane	Curtiss "Tanager"	Handley-Page	Taylor
Gross Weight	2859	2156	1667
Net wing area	333 (exclusive of floating ailerons)	293	175
Disposition of lift increasing device	Automatic slots along upper and lower wing. Flaps along trailing edges manually operated. Flaps are slotted.	Interconnected slots and flaps, slot device on aileron	Monoplane wing variable incidence
Minimum speed on glide	37.1 m.p.h. with slots open and flaps down 32 degrees	39.7 with slots open and flaps down	50.4
Maximum Lift Coefficient referred to net wing Area	.00623	.00466	.00374
Basic Airfoil	C-72	R.A.F. 28	
Maximum Ky of basic airfoil from atoms. tunnel	.0035	.00253	.0035 (estimated)
Maximum Ky from tunnel test for basic airfoil with slot open and flap depressed	.00604		
Percent increase in lift over basic airfoil	78%	84%	
Scale Effect. Thickness of airfoil	11.7%	9.82%	

Handley-Page, Ltd.

The comparative tests of the Curtiss entry with slots and flaps in various positions also give a check on their lift increasing properties:

Condition	Minimum Gliding Speed	$Ky = \frac{W \text{ gross}}{AV^2}$
Slots open, flaps down	37.1 m.p.h.	.00623
Slots open, flaps up	42.1 m.p.h.	.00482
Slots closed, flaps down	41.5 m.p.h.	.00498
Slots closed, flaps up	48.8 m.p.h.	.00360

These results are in agreement with the previous table.

In considering the increase in lift obtained by the use of slots and flaps in the Handley-Page entry, data on the R.A.F. 28 were not available.

In the Royal Aeronautical Society Journal for August, 1928, Handley-Page gives the following approximate wind tunnel figures for the R.A.F. 31, a section which is similar to the R.A.F. 28.

Maximum Ky of basic section	.002814
Maximum Ky with front slot open, and rear slotted flap depressed 20 degrees	.006037
Percent increase	114%

In the Handley-Page entry the ailerons on the top wing could not act as lift producing elements. Nevertheless the entry realized so much less of the lift increase indicated by the wind tunnel than did the Curtiss entry that another argument appears in favor of the manually controlled rear flap.

2. Effect of Airscrew on Minimum Speed

The Competition confirms the fact that the speed in horizontal flight with power on can be appreciably lower than the minimum speed on the glide. This does not seem to have been due to difference in control, as control with power off at low speeds was substantially as good as control with power on. Therefore the difference in speeds may be attributed to

1. Slipstream effect on the wings.
2. Helicopter effect of the airscrew when the thrust line is at a large angle to the flight path.

Of these the first is undoubtedly the more important.

British investigations (see R. & M. 1083) indicate that as the V/n D decreases, the lift coefficient with power on bears a larger ratio to the lift coefficient with power off. This is logical since with decrease V/n D the slipstream bears a larger ratio to the forward velocity. The British experiments covered a V/n D range only between 0.6 and 1.3, and at V/n D of 0.6, $\frac{\text{Ky max. in slipstream}}{\text{Ky max}}$ was approximately equal to 1.07.

The table indicates that at still lower values of V/n D the effect of slipstream on the lift becomes even more important, as the increases in maximum Ky are of the order of 25 to 40 percent.

It would seem advisable in making performance calculations to take this effect into account.

This slipstream effect on lift also goes far to explain the extraordinarily low landing speeds which are sometimes achieved by pilots of commercial aircraft. Landing with power on, cutting the engine at the right moment, killing speed and pancaking should give landing speeds far below those of the minimum speed on the glide.

EFFECT OF AIRSCREW ON MINIMUM SPEED

Airplane	Curtiss "Tanager"	Handley-Page	Command-Aire	Taylor
Gross weight	2859	2156	2333	1667
Wing area	333	293	245	175
Minimum speed-power on	30.6 m.p.h.	33.4 m.p.h.	46	45.5
Lift. Coef. Power on	.00915	.0066	.0045	.00460
Basic Section	C-72	R. A. 28	Aeronavine 2A	
Lift coefficient basic section	.0035	.00253	.00352	.0035 (estim.)
Lift coefficient on minimum glide Power off	.00623	.00466		.00374
Percent increase due to slipstream	47%	41½%		23%
V/ND at minimum sped power on	.205	.26		.32

3. Effects of Flaps on Trim

From pilots' reports it appears that the "Fleet" provided with powerful rear flaps became very tail heavy and lost longitudinal control when the flaps were depressed.

This would appear to contradict the usually accepted theory that with rear flaps down, the center of pressure moves to the rear owing to the banking up of the air.

On the other hand with flaps down, the lift coefficient increases and the downwash increases at the same time. The increase in the downwash calculable theoretically from the circulation round the wing and the tip vortices would be quite large. But this theoretical downwash might be still further increased by the extreme variation in the form of the wing, and duration of the air stream above and below the wing in the region of the trailing edge.

If rear flaps are employed it would seem desirable to give the stabilizer far greater upward range than is normally the case.

4. Steep Glide and Horizontal Tail Surfaces

The steepest glide for the Curtiss "Tanager" was 13.2 degrees, for the Handley-Page, 12.8. The corresponding L/Ds are 4.25 and 4.4. From these values of the L/D and from the fact that the steepest glides were made at speeds below the permissible 45 miles per hour, it would appear that the planes could not readily be maintained in attitudes above the stall, in spite of the maximum downward displacement of the stabilizer. Elsewhere in the report it is stated that the aircraft were not completely controllable at the stall. In the following table are given the conventional horizontal tail surface constants. It is seen that neither the Curtiss nor the Handley-Page attempted the use of oversize horizontal tail surfaces, and the above difficulties may be attributed to this.

Aircraft	Area	Horizontal Tail Surface Area	Distance from c. g. to Tail Surface	$K_H = \frac{\text{Horizontal Tail Surface Area} \times \text{Distance from c. g. to Tail Surfaces}}{\text{Wing Area} \times \text{chord}}$
Curtiss "Tanager"	333 sq. ft.	47.6 sq. ft.	17 ft.	.485
Handley-Page	293 sq. ft.	33.4 sq. ft.	17½ ft.	.455
Curtiss "Fledgeling"	293 sq. ft.			.420
Curtiss "Rovin"	293 sq. ft.			.474
Bellanca "Columbia"	293 sq. ft.			.338
Fairchild J-5				.478

5. Efficiency at High Speed

As during the Safe Aircraft Competition a number of commercial planes were tested under exactly the same methods and reliable data on the performance of commercial planes are rare, a brief analysis of the high speed results is of interest.

Warner states that a reliable formula for maximum speed is

$$V_{max} = 127 \left\{ \frac{P}{S} \right\}^{0.39}$$

where P = horse power
S = area of wing in square feet.

For the machines tested in the Competition, the results obtained with the use of this formula are:

Entry	Horse power P	Wing Area S (in sq. ft.)	V max (from test)	P/S	$K = \frac{V\ max}{(P/S)^{0.39}}$
1. Curtiss "Tanager"	176	333	111.6	.528	143.0
2. Handley-Page	155.6	293	112.4	.530	142.0
3. Bourdon "Kitty Hawk"	90.0	233.4	103.3	.387	152.5
4. Fleet	90.0	197.0	108.6	.457	147.5
5. Taylor C-2	90.0	175.0	108.5	.512	140.0
6. Brunner Winkle	90.0	254.0	106.0	.354	159.0
7. Cunningham-Hall	90.0	203.0	94.2	.443	129.0
8. Alfaro	110.0	170.0	108.6	.646	129.0
9. Ford-Leigh	115.0	291.0 (with safety wing)	102.4	.396	147.0
10. Command-Aire	170	245.0	114.8	.666	132.0
			Average		143.2

APPENDIX III

Rules for the Daniel Guggenheim Safe Aircraft Competition

OBJECT OF THE COMPETITION

THE object of the Competition is to achieve a real advance in the safety of flying through improvement in the aerodynamic characteristics of heavier-than-air craft, without sacrificing the good, practical qualities of the present-day aircraft.

PLAN OF COMPETITION

The Competition will be conducted in accordance with the following plan:

1. Conditions for Entrance

Application for entry will be received on and after September 1, 1927. All applications must be made on forms which will be furnished by the Fund upon request. All applications must be forwarded to the Fund at 598 Madison Avenue, New York, N. Y. An entrance guarantee of one hundred dollars ($100.00) must be forwarded with the application and will be returned upon rejection of the entry, or upon the acceptance and presentation of the aircraft for test. Before any aircraft can be tested in the Competition full information as to its design and construction must be supplied to the Fund. The application must be accompanied by a statement giving in so far as possible the information called for under "Information Required with the Form of Application for Entry," in which the applicant is required to produce evidence as to the aerodynamic characteristics of the aircraft and as to its general suitability for entering the Competition having the object given above. The Fund reserves the right to accept or reject any application for entry and to close the list of entries whenever, in its opinion, sufficient entries have been received to give a reasonable prospect that the object of the Competition will be achieved.

Any heavier-than-air craft based on any principle and built in any country shall be eligible for entry for the Daniel Guggenheim Safe Aircraft Competition, provided preliminary evidence satisfactory to the Fund is produced that it will promote the object which the Daniel Guggenheim Safe Aircraft Competition seeks to further. The employment of design features which, in the opinion of the Fund, are copied from the design of another competitor, may render the aircraft ineligible for entry.

2. Qualifying Requirements

Every aircraft whose entry for the Competition has been duly accepted will be called upon to demonstrate that it satisfies all the qualifying requirements which are prescribed under "Qualifying Requirements." In the case of an aircraft which departs radically from conventional practice in securing flight, the Committee of Judges may substitute for those requirements that are impossible of attainment, other tests that will satisfy the object of the Competition.

3. Safety Requirements

On satisfactory demonstration that all the qualifying requirements are satisfied, the aircraft will be eligible to take part in the Competition proper, consisting of the safety tests and demonstrations under "Safety Tests and Demonstrations."

4. Prizes and Grants

The winner of the Competition will receive a prize of $100,000, which amount will include the safety prize if previously received as provided below.

The winner will be the competitor whose aircraft satisfies the qualifying requirements and all the safety requirements and is awarded the highest number of points in the four safety tests enumerated in "Basis for the Award of the Prize." Should more than one aircraft win the same maximum number of points, division of the prize will rest within the discretion of the Committee of Judges.

The first five competitors, in order of presentation of their aircraft for examination and test at the designated field, whose aircraft satisfies all of the safety requirements called for in "Safety Tests and Demonstrations," each will receive a safety prize of $10,000.

The Fund will consider an application for special grants toward the cost of transporting duly accepted entries to the place where the Competition is held, which will be at a flying field in the vicinity of New York City, on the basis of one dollar per mile in excess of 1,000 miles up to a maximum grant of $2,000 for any contestant. This grant will not be made until all the qualifying requirements have been satisfied.

5. General Conduct of the Competition

Notification of the result of their applications will be sent to applicants as soon as possible. The Competition will be held at a suitable field in the vicinity of New York City. The examination of the aircraft and the qualifying and safety tests will be held from time to time as designated by the Fund. The tests will be conducted by a Committee of Judges assisted by a Field Manager and Technical Advisers, selected by the Fund. Decisions of the Committee shall be subject to the approval of the Fund.

The general conditions under which the tests will be carried out are specified under "General Conditions."

6. Closure of Competition

The Competition shall be closed on October 31, 1929, and no aircraft will be accepted for test unless presented for test at the designated field on or before this date.

The Fund may advance the date of the closure if and when in its opinion the object of the Competition has been achieved.

If the date of closure is thus advanced, any contestant whose entry has been duly accepted before the date of the closure thus advanced, will be granted a reasonable extension of time in which to present his aircraft.

7. Proprietary Rights

The award of prizes shall not entail the abandonment of any proprietary rights on the part of the contestant, but the Fund shall have the right to disseminate complete information pertaining to the aircraft in any way it sees fit.

Information Required With the Form of Application for Entry

(Appendix I of Original Rules)

1. The name of designer and constructor.
2. Date when contestant will be ready to undertake tests.
3. Three-view drawing.
4. Brief general technical description of the aircraft.
5. Type of engine or engines used, with particulars as to official type trials of such engines and fuel used.
6. Weight estimates and estimates of useful load and volumetric carrying capacity and the horse power for which same are calculated.
7. Any performance estimates and calculations available.
8. Information and sketches as to power plant installation, seating, vision for the pilot, instruments and controls.
9. Any further information available including in the case of aircraft involving a radical departure from normal practice in aerodynamic form:
   (a) Results of wind tunnel tests or any other data available.
   (b) Statement as to whether a full scale aircraft of similar type has been flown previously.

In cases where it is not possible to supply the whole of the above particulars when application for entry is made, the fullest information possible in regard to the proposed design should be supplied at the time of making application, and the remaining items of information specified above should be forwarded to the Fund as soon afterwards as possible.

If the applicant desires to withhold any of the above information as likely to divulge valuable secrets, he should give his reasons for withholding the information and the Fund will decide whether such reasons may be considered valid.

Qualifying Requirements

(Appendix II of Original Rules)

Every aircraft whose entry for the Competition has been duly accepted must be presented for examination and test at the designated flying field on the date designated by the Fund when the tests will be carried out within a reasonable time. Reasonable delay may be granted by the Fund.

Before an aircraft is presented for test the following additional information to that given under "Information required with the form of application for entry" will be required.

(1) Three-view drawing with principal dimensions of important parts.

(2) Dimensional drawings and particulars required for verification of stress analysis.

(3) Stress analysis in accordance with the methods approved for Civil Aircraft by the U. S. Department of Commerce or by any recognized Government Agency responsible for the issue of Airworthiness Certificates including a statement as to the materials used and the mechanical properties assumed for same. Stress analysis for machines in which sustentation is provided by other means than that of fixed wings shall be required to show a theoretical basis of the strength calculations for the structure as well as the calculations themselves.

(4) Balance diagram.

The following are the qualifying requirements every aircraft must satisfy:

1. Power Plant

The engine or engines used must be of a type which has been submitted to duly authenticated type tests, full particulars of which must be supplied by the entrant. The horse power of the engine will be considered to be the rated normal horse power at full throttle as developed with the same or equivalent accessories used in the type tests, and throughout the tests the r.p.m. of the engines shall be limited accordingly. During the whole of the tests in connection with the Competition, the fuel used shall be the standard fuel supplied by the Fund or fuel of the same quality as was employed during the type tests of the engine. The aircraft must be provided with mechanical or electrical means of starting the engine or engines, or alternatively the engines may be started by hand providing a starting gear is fitted which involves no risk of injury to personnel. Starting by direct pulling over of propellers by hand will not be permitted. Any starting gear used will be considered to be a part of the aircraft and must be carried throughout the Competition.

2. Structural Strength

The structural strength of the aircraft shall be in accordance with the requirements of the U. S. Department of Commerce Air Regulations. Where a designer has reason to deviate from such requirements an explanatory statement should be submitted with his stress analysis. Copies of the U. S. Depart-

ment of Commerce Air Regulations and of the method proposed for stress analysis by the Department of Commerce will be furnished on request.

If the contestant contemplates landings made with considerable vertical velocity, computations for strength of landing gear covering this condition should be submitted.

If an aircraft shows structural weakness during the Competition, test of the aircraft may be discontinued at the discretion of the Fund.

3. Performance

When carrying full load the aircraft shall satisfy the following minimum requirements in regard to performance:

Maximum Speed (corrected to standard air at sea level)—110 m.p.h.

Rate of Climb (at 1,000 ft.)—400 ft. per min.

4. Useful Load

The aircraft shall carry 5 lbs. of useful load per h.p. "Useful load" shall include the following items:

Pilot
Observer
Fuel
Oil

Any special instruments or equipment fitted by the Fund for the purpose of the Competition.

5. Fuel and Oil

The aircraft shall provide tank capacity for fuel and oil for 3 hours at full throttle at the normal r.p.m. as given in the type tests.

6. Instruments

The aircraft shall be provided with all necessary power plant instruments required by the engine installation, and the following flying instruments:

Altimeter
Air Speed Indicator

7. Accommodation

Adequate accommodation and dual control for pilot and observer. For every 10 lbs. of useful load carried in addition to the items specified under (4) above, there shall be provided at least one cubic foot of cabin or cargo space.

8. Vision

Adequate vision must be provided for the pilot.

9. Fire Risks

All reasonable precautions against fire risks shall be provided in the design. At least one fire extinguisher of approved type shall be carried and placed conveniently for the pilot; the weight of this shall not be included in useful load.

Safety Tests and Demonstrations

(Appendix III of Original Rules)

Every aircraft shall be subjected to the following safety tests which shall be carried out in any sequence the Fund may determine.

(Note) The use of devices by which the aerodynamic characteristics of the aircraft can be varied during flight will in general be permitted, subject to the following conditions:

If the device is not automatic and requires operation by the pilot, the operating control must be simple, quick in action and conveniently placed, and must not involve appreciable physical effort by the pilot. If in the opinion of the Fund the safety of the aircraft is prejudiced by dependence on the operation of such device in emergency, the aircraft may be called upon to pass any or all of the safety tests at one fixed setting of the device, in which case the Rate of Climb Test under "Qualifying Requirements" must be passed at the same fixed setting of the device.

1. Speed Tests

Object: To demonstrate the ability of the aircraft to fly and glide at much lower speeds than is possible in the case of present-day commercial aircraft, thus reducing the risk involved in negotiating forced landings, particularly under conditions of bad visibility and when approaching small and confined landing space.

Requirements

(a) Minimum Flying Speed.
The aircraft to maintain level and controlled flight at a speed not in excess of 35 m.p.h.

(b) Minimum Gliding Speed.
The aircraft to be able to glide for a period of 3 minutes with all power switched off, during which time the air speed shall never exceed 38 m.p.h.

The aircraft will not be considered to have passed either of the above tests unless it is clearly demonstrated that each and all of the controls are properly effective at the minimum speed specified.

2. Test of Landing Run

Object: To demonstrate the ability of the aircraft to effect a safe landing in a small field.

Requirements

The aircraft shall land with all power switched off, and after first touching the ground shall come to rest within a distance of 100 ft.

The landing shall be made in a straight line; turning, side slipping or trick flying will not be permitted.

The use of braking devices will be permitted provided that control is fully retained until the aircraft has come completely to rest and provided that no serious injury to the surface of the landing field results.

Such braking devices must not require special equipment which is not carried on the aircraft in flight.

3. Test of Landing in Confined Space

Object: To demonstrate that in case of complete engine failure the aircraft can approach and land in a small confined space surrounded by obstructions, such as trees, buildings, etc.

Requirements

The aircraft shall make a steady glide in over an obstruction 35 ft. high and land in a straight line with all power switched off. After landing, the aircraft shall come to rest within a distance of 300 ft. from the base of obstruction.

The approach to the landing ground shall be straight; turning, side slipping, or trick flying will not be permitted.

The use of braking devices will be permitted under the conditions set out under (2) above.

4. Test of Take Off

Object: To demonstrate that the aircraft can take off from a small field and after taking off can climb at a steep angle so as to clear obstructions, such as trees, buildings, etc.

Requirements

(a) The aircraft shall take off after running not more than 300 ft. from a standing start. The aircraft will not be considered to have passed this test if it touches the ground again after taking off.

(b) After taking off within a distance of 300 ft. from a standing start, the aircraft shall clear an obstruction 35 ft. high at a distance of 500 ft. from rest. The approach to the obstruction shall be straight and trick flying will not be permitted. External assistance in starting the run will not be permitted in either (a) or (b).

5. Test of Gliding Angle

Object: To demonstrate the ability of the aircraft to glide for a reasonable distance in case of engine failure and alternatively to glide at steep angles in order to facilitate the approach to a possible landing ground.

Requirements

(a) Flattest Glide: The aircraft shall be able to glide with all power switched off so that the angle between the flight path and the horizontal is not greater than 8 degrees.

(b) Steepest Glide: The aircraft shall be able to glide with all power switched off so that the angle between the flight path and the horizontal is not less than 16* degrees. During this test the air speed shall not exceed 45 m.p.h. In both cases the aircraft must demonstrate that all the controls are definitely effective throughout the test, and that it can land safely out of this glide from a useful altitude.

* See page 18

6. Test of Stability in Normal Flight

Object: To demonstrate that the aircraft is stable under all normal flying conditions, that is to say that if the attitude of the aircraft is disturbed either by gusts or by the application of the controls, the aircraft shall return to its original attitude of its own accord when the controls are left free.

Requirements

(a) Longitudinal Stability: The aircraft to be provided with means by which it can be trimmed so as to fly with the elevator control free at any speed within the range of 45 m.p.h. to 100 m.p.h. and at any throttle opening of the engine or engines. The test of longitudinal stability shall be as follows:

The elevator control to be moved toward its maximum extent either backwards or forwards sufficiently to give a fair test of stability and then released. In either case the aircraft must return to steady flight in its original attitude within a reasonable time.

(b) General Stability: The aircraft to be capable of flying at any air speed from 45 m.p.h. to 100 m.p.h. and at any throttle opening of the engine or engines with all controls left free for a period of not less than 5 minutes in gusty air.

In the case of a multi-engine aircraft, all the engines may be throttled to the same extent.

During any of these tests, the aircraft must hold a reasonably steady course and if disturbed from its normal attitude, must return to such attitude within a reasonable time and without losing height appreciably.

7. Test of Ability to Recover from Abnormal Conditions

Object: To demonstrate the ability of the aircraft to recover from any attitude into which it may get either because of disturbances in the air or of incorrect application of the controls by the pilot, or of sudden failure under difficult circumstances.

Requirements

(a) Test of Ability to Maintain Control in Case of Engine Failure.

The aircraft must demonstrate that it can be satisfactorily controlled by the pilot in case of sudden engine failure when flying at any attitude. In case of multi-engine aircraft, the pilot must be able to maintain control when any one of the engines or any combination of the engines or all of the engines suddenly fail.

The aircraft will be required to demonstrate that in case of complete engine failure (all power being switched off) it will take up a steady gliding attitude when all controls are left free from the moment of switching off the engine or engines.

The aircraft will further be required to demonstrate that if the elevator control is pulled its toward its maximum extent at the moment of switching off and held in that position, the aircraft will remain under control, not get into any violent or dangerous maneuvers, and descend on a steep glide path at a speed not exceeding 40 m.p.h.

(b) Test of Ability to Recover from Violent Disturbances

1. The aircraft to be dived with all power switched off until air speed reaches 20 percent above maximum level flying speed. At this speed it must answer all the controls correctly and effectively. All controls will then be released and the aircraft must of its own accord return to a steady gliding attitude without serious loss of height.

The aircraft may be required to pass this test when trimmed for any speed from 80 m.p.h. to 110 m.p.h

2. The aircraft to be flown at full throttle at an air speed of 45 m.p.h. trimmed for any speed from 45

m.p.h. to 75 m.p.h. The engine is to be switched off and at the moment of switching off, the pilot is to move any one or any two, or all of the controls in such manner that an abnormal attitude results. Complete recovery is to be made with the aid of the controls and a steady glide to be taken up with a loss of height of not more than 250 ft. from the height at which the abnormal flight attitude was obtained.

The same test is repeated with the exception that when in an abnormal flight attitude, all controls are to be released, and the aircraft must make complete recovery of its own accord and take up a steady gliding attitude with a loss of height of not more than 500 ft.

8. Test of Controllability

Object: To demonstrate that the control system is simple and easy to operate and that under all conditions of flight and gliding, effective control in all senses is maintained. Every aircraft must be equipped with three substantially independent controls corresponding to three axes mutually at right angles and these three controls must continue to be substantially independent and collectively effective in the same direction at any attitude of the aircraft from the attitude at maximum level flying speed to the attitude at the steepest glide and at any throttle opening of the engine or engines. The aircraft must clearly demonstrate that it is not subject to complete loss of control when any particular attitude is reached, such as the loss of control which accompanies the phenomenon of stalling.

Requirements

The aircraft will be required to demonstrate the effectiveness of each and all of the controls at any speed and at any attitude from the attitude at maximum level flying speed to the attitude at the steepest glide and at any throttle opening of the engine or engines. This will be tested by making definite and sharp movements of any particular control or controls, which must result in the aircraft making corresponding definite rotations about the respective axes. The controls must not only be effective in producing disturbances of attitude but also enabling rapid and definite recovery to be made from disturbances.

The effectiveness of any one control or combination of two controls when the other control or controls are left free or held in fixed position must be demonstrated.

The aircraft may be called upon to pass these tests in calm or gusty air.

9. Tests of Maneuverability in Restricted Territory and on the Ground

Object: To demonstrate that the aircraft can be safely and effectively maneuvered when taking off or landing in restricted territory and when taxying on the ground under its own power without external assistance.

Requirements

(a) Maneuverability in Restricted Territory.

A square plot, 500 feet by 500 feet, will be marked off and shall be considered as surrounded by an obstruction 25 feet high along its entire boundary. The pilot shall take off in any manner he judges best, and climb either above the square plot or outside of it, providing he passes above the imaginary boundary construction. The engine may be switched off at any time and the pilot shall land the aircraft within the square plot without passing through the imaginary boundary obstruction.

(b) Maneuverability on the Ground.

The aircraft will be required to demonstrate that it can be taxied under its own power and without external assistance in any direction in a wind whose mean speed at ground level is at least 20 m.p.h.

The aircraft will also be required to demonstrate that it can be easily handled and moved by ground personnel as required of any aircraft operating for commercial purposes.

Basis for the Award of the Prize

(Appendix IV of Original Rules)

Points will be awarded as specified in the four following tests:

	Maximum Number of Points Obtainable
1. SPEED TESTS	
(a) 2 points for every m.p.h. less than 35 m.p.h. at which level controlled flight can be maintained - - - - - - - - - - - - -	10
(b) 4 points for every m.p.h. less than 38 m.p.h. which is not exceeded in a steady controlled glide during a period of 3 minutes - - - -	24
(c) Any aircraft which obtains a combined total of at least 24 points under tests (a) and (b) will be eligible to receive points for high speed in excess of 110 m.p.h. as follows: 1 point for every 2 m.p.h. in excess of 110 m.p.h. at which level flight can be maintained	10
2. TEST OF LANDING RUN	
2 points for every 3 ft. less than 100 ft. in coming to rest after first touching ground - -	40
3. TEST OF LANDING IN CONFINED SPACE	
1 point for every 2 ft. less than 300 ft. from the base of an obstruction 35 ft. high in coming to rest after gliding in over the obstruction - - - - - - - - - - - -	75
4. TEST OF TAKE OFF	
1 point for every 15 ft. less than 300 ft. required to take off from standing start - -	15
1 point for every 10 ft. less than 500 ft. to clear obstruction 35 ft. high from a standing start - - - - - - - - - - - - - - -	26
	200

General Conditions

(Appendix F of Original Rules)

1. Contestants shall comply with the Rules laid down by the Field Manager in regard to all work and conduct on the Field.

2. Aircraft shall be kept at the designated field throughout the Competition unless special authority for its removal is obtained in writing from the Field Manager.

3. Aviation fuel of standard quality will be supplied free of charge, but another fuel may be used provided such fuel was used in the official trials of the engine or engines employed.

4. Prior to any tests made by the Fund, contestants may be required to demonstrate in flight by their own pilot that their machines are airworthy and provided with proper controls.

5. All tests in the Competition will be carried out by pilots supplied by the Fund but contestants shall be given reasonable opportunities for instructing the Fund's pilot in the flying of their aircraft prior to the commencement of the tests.

6. Contestants shall supply their own mechanics and transport, and prepare and maintain their aircraft during the Competition at their own expense.

7. The Fund will accept no liability at any time in connection with any risks involved to the aircraft or to the contestant's personnel, or in connection with any third-party risks involved when the aircraft is being flown by the contestant's pilot.

8. The contestant will not be held liable for injury to flying personnel representing the Fund.

9. The Fund may at any time suspend temporarily or permanently any aircraft from taking further part in the Competition if, in the opinion of the Fund, danger to flying personnel in involved, or the object of the Competition is not likely to be furthered by proceeding with tests of such aircraft.

10. Contestants shall be allowed at least three fair attempts to pass any test.

11. Alterations to the aircraft during the Competition may be approved, but any such alteration may entail requalification in any or all of the tests at the discretion of the Fund. Unauthorized alterations may entail elimination from the Competition.

12. Variations in the form of features of the aircraft which cannot be conveniently and easily effected by the pilot during flight, as, for example, variations in angular settings of supporting surfaces, will be regarded as alterations.

13. The same design of propeller shall be used throughout the trials. In case of propeller breakage or damage a new propeller of identical design may be substituted. Propeller blade settings must be the same throughout the test except that a pitch-varying mechanism may be used if it can be operated from the pilot's cockpit during flight.

APPENDIX B
JUPTNER'S FOREWORDS TO NINE VOLUMES

Foreword, Volume 1. ATC 1-100.

Just a short three or four decades ago, the sound of an airplane overhead as it flew serenely by, would cause heads for a mile around to turn upward; gazing up with shaded eyes to watch and to marvel at the contraption up there that was riding the wind so easily on it's flimsy wings. Or perhaps some would even watch with a little envy and inwardly yearn for a chance to lift themselves up into that vast sea of air and become unshackled, if only for a time, from a bond with the earth. Yes, the wonder and magic of flying was still very new to many, and the sight of an airplane flying overhead was indeed an occasion worthy of a few minutes pause.

Today, airplanes fly by only minutes apart, racing towards distant terminals which will be reached in a matter of hours ... and hardly a head is turned; the wonder of flying is no more new, it is no longer awe-inspiring. New contraptions continually vie for our notice and the airplane is more or less taken for granted. Surely, this was destined to happen, this is what hundreds upon hundreds of good men had dreamed for, strived for, and some even died for, but what is saddening to me at least, is the fact that so little is known and even less is remembered of the years of struggle that took place in the decades just gone by. A struggle in search for answers that often led to the point of heartbreak and catastrophe in order to bring about this vast knowledge and comparative maturity in the air that we now so casually enjoy.

In view of this, I humbly submit a plea that some obligation must be shown and a mark of credit recorded for the untold number of these pioneers in aviation, and the many creations they brought forth. A mark of credit for their boundless dreams that often knew no limit, and even an appreciation for their occasional folly; their every effort no matter even how small was another lesson learned, a point proven, and a valuable contribution added to the science of flight. Like another milestone on the path of evolution towards our modern airplane.

These following pages tho' they may sometimes sound like the nostalgic memories out of one man's past, are meant to be a factual storytelling account of little-known facets of these early formative years, and to exalt for a brief moment at least, the many efforts that contributed to the make-up of our early aircraft industry. I would say that the advent of the "Approved Type Certificate" for the manufacture of civil aircraft was more or less a charter for the beginning. It was at first a challenge that soon made way for opportunity and brought on an era of new dreams and new enthusiasm; it might actually be called the birth of the commercial aircraft industry.

A space of three years saw the aircraft industry emerge from a backyard operation to one of the up-and-coming industries of the country. Of the many and varied offerings presented in the first three year period, the government agency, very tolerant and working

feverishly, saw fit to certificate some 284 “types” of airplanes. This was far, far too many for the market available, to be sure, but many things were learned in the process, things that might have normally taken many more years.

With an intent to present this coverage in it’s proper perspective and in some sort of sequence, we have chosen to list all of the airplane “types” that received the “Approved Type Certificate,” because these were the ones that earned the stamp of approval and the blessings of the Dept. of Commerce to be built for the civil market. This then, for the most part, will present a cross-section of the scope of activity in the aircraft industry thru’ all these years, and it’s pattern of evolution towards the airplane of today.

Joseph P. Juptner

Foreword, Volume 2. ATC 101-200.

We know that aviation was literally dropped with a big flop right after World War I and would have been left to slowly die had it not been for a handfull of adventurous young-bloods who had aviation in their heart and soul: stout-hearted men who could not stand by and see it come to such an ignoble end.

Like ambassadors of goodwill toward aviation, they chose to roam the countryside with their craft, acquainting many thousands of people with their first-hand look of an airplane and spreading the gospel of aviation as ardently as any dedicated evangelist. By the early "twenties" a good deal of progress had already been made towards the preservation of aviation in itself, but there was slowly rising a keen yearning among these men to develop more useful aircraft, more practical craft to replace the tired and worn war-surplus aircraft that had been the backbone of the so-called "commercial aviation" they were trying to sell. By far the easiest and simplest approach to this problem was the modification or modernization of these existing aircraft into somewhat more useful vehicles, but several men of wider and keener vision felt this was surely not the answer; undertaking to design and develop aircraft on entirely new lines and principles. At first, some of these new designs seemed to be only little removed from those they were to replace, but several breakthroughs resulted in the latter half of the "twenties" and a whole new concept of design was beginning to take shape. The immediate success of several of the new designs gave added impetus to the new movement and by the time 1927 rolled around, there was a clamoring evidence that commercial aviation, though yet an infant, would soon be growing into a strapping youngster of capable proportion.

The year 1927, though blessed with fervent bally-hoo for public attention, was quite like a dawning of purpose in commercial aviation, a beginning that was soon to blossom in the next few years from a hobby-like backyard operation into one of the up-and-coming industries of our nation; a happy young giant that had found use for it's services and was attracting world-wide notice. Opportunities, especially for aircraft manufacturers, during the next two years were never better, and new airplanes to fit all the varied services were pouring out of factories both large and small, by the hundreds and the thousands. Along with this phenomenon of aircraft manufacture that mushroomed as the months went by, came a surging wave of sporting people who wanted to fly and to own their own airplanes; so it is recognizable that every facet of commercial aviation, be it airplane manufacturer or dealer, airline or air-service operator, flying-school operator, or be it Joe Propwash who was hopping passengers on weekends for $ 3.00 a ride, all were in clover and were having their hey-day.

Best remembered by me as sort of a symbol of these times, was the happy young pilot that always used to taxi up to the line with a grand flourish, raise up his goggles and flash that big boyish smile that reflected an unfettered joy; people seemed to be so happy in their new-found joy of flying or just any form of participation in aviation for that matter, and to me that flash of boyish smile remains as a symbol that portrayed the general feeling of these times. Aviation was again proving useful, everyone felt a pride in being a part of it, and above all, flying was great fun and each flight like a new adventure.

Joseph P. Juptner

Foreword, Volume 3. ATC 201-300.

Year 1929 as we remember it was quite an exciting and bewildering year in aviation progress; it seemed that each monthly issue of the airplane magazines announced the formation of from 3 to 6 new "airplane factories," there was nearly a 200% increase in licensed pilots, domestic airmail poundage was more than doubled, scheduled airline operations increased from 27,000 to 100,000 miles daily, 166 aircraft "types" had been approved that year by the overworked Dept. of Commerce, 19 new engines received their certificates of approval, more and more people were taking to aviation, and every facet of the aviation trade was riding high, wide, and handsome.

Then, like a sudden storm lashing out of nowhere and without perceptible warning, came circumstances that caused the onset of our great economic depression. Needless to say, everyone was rocked back on their heels in bewilderment, without a full realization of just what had happened; everybody was at first skeptical, somewhat worried, and had no immediate plans on how to cope with this situation. Soon to add to this dilemma came cancellations of airplane orders which in turn forced manufacturers to cancel orders for engines, propellers, and raw materials; indeed, this had a sobering effect on all manufacturers and operators in the business, and they were taking time to think. Now with all the froth and gayety just about gone, the aviation industry was forced to take stock of itself and a good hard look at its predicament; by and large it soon came to realize that it had better become a more sensible and more stable member of the industrial family if it was to survive. This was to take much effort and quite a bit of heartbreak but it was something that was inevitable and had to be done.

Despite the severe blow that had shaken it to its very roots, the year 1929 was a very interesting period in the annals of airplane development. It was also a time when most of the pioneers of aviation, around whom the romance and adventure of early airplane development was woven, were beginning to share the stage with many bright-eyed young men coming up with a new outlook, who perhaps a decade from now would surely be the giants in charge of a vast and comparatively healthy industry. It was a time too when the aura of romance and adventure was binding itself into an era of a sobering industry that was forced to think more carefully and be more practical. There were lean years ahead; many operated on that proverbial shoestring and many were finally forced to close their doors but progress in airplane development pushed forward just the same, if not more so. It has often been said in jest that aviation people are at their best when hungry; the outstanding developments brought forth in the next few years would almost lead one to believe it.

Joseph P. Juptner

Foreword, Volume 4. ATC 301-400.

The "Great American Depression" was less than a year old but already was getting a good toehold in the hip-pockets of the aviation industry. Dazed and unbelieving, many could not realize yet just what had happened; but one by one, like felled warriors, they pulled in the remnants of what they could salvage and made plans to carry on as best they could, if they could. Over-production in 1929 left many inventories at a high level and in some cases were cleared away at bargain-basement prices; others that had no inventory problems were still forced to pinch the budget, and warmed-over old designs were being offered with tongue-in-cheek as something new. Those fortunate enough not to have old inventories to move and had a healthy budget that allowed for some new development, were bringing out interesting airplanes that caused a slight revival in airplane buying.

The glider movement took the country's fancy for a while and then the inexpensive low-powered airplane made its formal debut. This gave thousands a chance to keep flying, who otherwise would have been forced to quit. The cold fact of economics led many to the light, less expensive airplane and for nearly the next decade, the light-plane was to carry on its back the destiny of aviation.

The lush days of 1929 were now gone and there was no great promise on the horizon just yet; but there were now several new avenues for channeling energies and these held some promise of keeping things going. It is thus that we came up through a period of doubt, perhaps even verging on despair, and then slowly and cautiously moved into a period of new confidence that was based on more sober planning. The forlorn outlook worn by most people of the aviation industry, earlier in the year of 1930, had been brightened somewhat by the end of the year and 1931 began to look much better. One of the most outstanding qualities of the aviation pioneer was the almost religious fervor he had for the "aviation game" and his great inner passion to further its development regardless of the privations it imposed upon him.

Joseph P. Juptner

Foreword, Volume 5. ATC 401-500.

Statistics show us that 215 "aircraft companies" had been doing business in 1930 and by the end of 1931 this number had fallen to 110; of those that somehow remained the following year of 1932 was to take an additional toll. Where was it going, and where was it to end? Aircraft manufacturers both big and little were slowly losing out to effects of the national depression, and many earned barely enough to pay the utilities that were necessary to stay open; but, optimists that they were, they hung on grimly by hook or by crook for better or for worse. Some of the grief and the sentiment they harbored within themselves for a way of life they hated to lose is reflected quite poignantly in the following ad: "A factory site and flying field bordering a railroad in southern Ohio, offered free if used for aviation purposes." We can see then that profit was not even considered; they just hated to see aviation give up and go under. At this point it is as if we were on the threshold of another era in aviation, or better to say we were standing on a ledge and viewing the crumpled ruins of a familiar industry down below us. Turning from this view with a heavy heart, we are conscious of seeing a new scene forming before us; we don't know yet if it will be any better, or if we will even like it, but surely it holds some promise—so we enter to find out where we fit.

Throughout the entire industry, what was left of it, everyone was finding it difficult to adjust; but spirits were not dimmed for very long, and morale was holding up. True, everyone was pining for happy days just gone by, but perhaps all was not lost yet. The light flivver-type monoplane just recently introduced was permitting many people to keep flying, and new pilots were even enticed into the fold occasionally. To a greater extent business people were learning that it was a distinct advantage to own an airplane; airline passenger traffic was even increasing despite the decline in surface travel, and air-express shipments took a terrific jump in poundage. Selecting from a much wider variety of "strictly-for-sport" airplanes, the sportsman pilots were now more active than ever, and every day some new job or errand for an airplane was being discovered. The flying-service operators suffered the biggest part of the blow, but many managed to stay in business by ingenuity; and automobile gas at "twelve [cents] for a dollar" allowed many of the weekend pilots to continue flying. By far the most widespread activity of this period was hangar-flying, and groups were mostly indulging in reminiscences of better days; but many future developments in aviation were also discussed and planned at these sessions.

A certain part of this great clan, undimmed by circumstances, still held onto sky-high adventure which lured them off on transoceanic flights, altitude records, endurance records, distance records, or speed records; and then still cast about for something more daring or new to do. Air racing took on a new stature and became the means of harnessing ideas and energies that otherwise would have been dormant; and commercial aircraft development profited considerably from what was learned at the races. It also became a lot harder to recognize and identify the pioneer or the genius because they were all around as one of us; and even though aviation was to sink into still greater depths, everyone felt reasonably confident that soon it surely must be lifted to even greater heights. There was no premium to pay on dreams, so they all dreamed.

Jos. P. Juptner

Foreword, Volume 6. ATC 501-600.

Each year since commercial flying began, there had been steady, or sometimes dramatic improvements in airplanes, but the period of 1934–35 produced greater advancements than in any period since the Wright Brothers first flew in 1903. Here in this volume, as it unfolds, we will find the scientific advancements that nearly doubled the speeds with greater regularity, and provided comfort and security that won the public confidence in traveling by air. Achievement of this phenomenal advancement was a joint effort in refining methods of propulsion, the application of new concepts in aerodynamics, and the introduction of advanced methods in all-metal construction. Oil companies had also developed new fuels that allowed engine manufacturers to design powerplants of fantastic power-to-weight ratios, supercharging had nearly doubled the service ceiling, and the controllable pitch propeller was providing efficient performance from the ground up. Transport airplanes were especially in the limelight, and specifically the "Douglas Commercial" (DC-2) which practically forced all previous airliners into obsolescence. The huge "Clipper Ships" by Sikorsky and Martin blazed new trails in various directions from our shores and opened up the possibility of scheduled transoceanic service. Other transport airplanes came out in the new pattern to fit different loads and schedules, and America's air transport system, as the fastest and the finest, became the envy of the world. While it was the airliners that had shown the greater progress, the so-called private airplane was also taking advantage of new advancements to offer more speed, comfort, and reliability at a reasonable price. The sportsman had a prolific array to choose from, the businessman could find exactly what he needed most, and the choice for the private-pilot was only limited by the cash in his pocket. From the tiny "Cub" to the huge "Clipper" there were designs to fire one's enthusiasm and dreams; many of these airplanes became classics that stood the test of time. Surely, advancements continued as the years went by, that is normal, but weren't they mostly refinements of the principles brought out in this memorable 1934–35 period?

Jos. P. Juptner

Foreword, Volume 7. ATC 601-700.

Taking a quizzical look at this 1936–38 period one would be inclined to guess at first that it would have to be just a tuning-up period, a leveling off to enjoy the many great advancements that were introduced in the two-year period just previous. So much had happened in that time, and so much had been achieved, that one could not even criticize had the aviation industry decided to coast awhile and rest on its past laurels. But, that was not to be. This "game" that everyone called "the aviation industry" was an assemblage of special individuals; some were dedicated individuals, dedicated to aviation's future, some were restless individuals that couldn't leave well-enough alone, and some were individuals who soon brushed aside their latest accomplishments to go on to something else. This was the phenomenon within the industry, and it had always been like this. So, at this particular time the aircraft industry was not exactly percolating, but at least it was squirming within looking for new avenues to progress.

No sir, the aviation industry was not resting on its past laurels. We thought the Douglas DC-2 "Airliner" was simply marvelous, but the new DC-3 was now even better. One could now fly from coast to coast in 15 hours for less than $150.00 while at sleep in the cradle of luxury. Airlines at last were making money with the DC-3, and it was fast becoming the standard equipment of every major airline in the world. Airplane factories, large and small, some new and some old, were humming with production all over the land. Production of civil aircraft in the first quarter of 1936 had increased nearly 35% over the same period in 1935, the first quarter of 1937 showed an increase of 25%, and production continued to increase again in 1938. The most noticeable increase, of course, was in the building of light planes; 100 were built in the first 3 months of 1936, and soon manufacturers were rolling out 75 and even 100 airplanes per month. There were so many new airplanes around to dazzle the airplane buyer at this time that it is hard to understand how he could make a rational choice. Yes sir, the aircraft industry was showing unmistakable signs of improved health and continued growth.

Everyone was enjoying the increased activity. Business was getting better for everybody and many, many businesses were now using airplanes as a matter of course. The airplanes for business had become more comfortable too, more practical, and even faster; we now had several 200 m.p.h. commercial airplanes. Flying schools once again were operating from dawn to dusk, and the weekend flier was flying every weekend and not just once in a great while. The "puddle-jumpers" like those of Taylor, Piper, and Aeronca were dotting the airports all over the country, and boxcar loads were being shipped out almost every day. It was a great feeling to drop in on some little airport to see it lined with dozens of airplanes, and hear the drone of many engines overhead. Maybe this period of 1936–38 did not produce any major advances in aeronautical science, but we did pretty well at that, and we had a whole lot more of everything. As we hastened to our daily chores we tried not to notice as war clouds were forming over Europe; this had nothing to do with us, but there was an excitement of sorts in the air, and yet it was fearful too.

Jos. P. Juptner

Foreword, Volume 8. ATC 701-800.

This volume takes us into one of the most turbulent and frantic periods of aviation history. We had just nicely recovered from a crippling "depression," everything was on the upswing, and the aviation game was once more a satisfying and paying endeavor. And, each day saw aviation rise to new importance. Civil aircraft production by 1940 nearly doubled over 1939, and was reaching an all-time high. Of course, everyone was excited too by the CPTP [Civilian Pilot Training Program] pilot-training program because it meant we could muster a gigantic defense force of aviators, but we did go along in our daily pursuits with an over-the-shoulder apprehension. And why not; trouble was brewing all over the world it seemed, but as the normal civilian viewed this with mixed feelings, we of aviation wondered quietly as to when it would envelope us. On the one hand the "boom" that was caused by our planning for preparedness was like a "bonanza" to many who had before only eked out a passable living in aviation, but on the other hand as the threat of war was becoming a reality the imposed regulations hampered much of our free spirit.

The world-enveloping war, when it finally did touch upon our lives, soon distorted everything and forced aviation way out of its true proportions. The manufacturing and flying of military airplanes naturally overshadowed all normal activities, and airplanes were being built around the clock to satisfy the need; statistics showing the money spent each month for military airplanes was enough to make the head swim. On 8 Dec. 1941 all civilian flying was suspended; by March of 1942 this edict was relaxed somewhat, but there were still enough regulations to hamper the average flyer. By Sept. of 1942 all civil aircraft production was halted, primarily due to a metals shortage; we were using up our resources faster than they could be dug up, and nearly everyone that was able was given contracts for war work. The war was now all-important; these were busy years both at home and abroad.

As the war began to wind down in 1944 the War Production Board tells the aviation industry it could go ahead with post-war planning. This was literally a time of dreaming. Transport airplane builders could already foresee a new era when huge super-transports would span continents and oceans swiftly and surely to bring commerce and travel to even the remotest places. Literally, the whole world would now be our neighbor. The civil airplane manufacturers were busy dreaming too; we saw page upon page in periodicals discussing every reasonable and unreasonable idea for the coming market which loomed on the horizon like a ghostly cloud. As they began to announce their post-war designs there were cheap single-seaters, fancy two-seaters, family sedans, sport amphibians, then there were the two-controllers, the non-spinners, everyman's airplane, the flying autos, the convertible glider, and the helicopter. When the war finally did end via VE day and VJ day, there was a mad scramble by everyone to sell their wares, and many did fairly well. The returning warrior, well exposed to aviation during the war, was a good customer, and literally hundreds of thousands were anxious to fly. But, then the frantic pace leveled off and by a set of unfortunate circumstances we found ourselves in a slump once again which brought many manufacturers to their knees and wiped out several that had been proud names in aviation. It was a period of readjustment that followed and as things began to look normal again, we were confronted with another government-sponsored "boom" caused by the Korean War. By then

the amount of companies manufacturing airplanes had leveled off to perhaps a dozen builders who were the survivors; using even the most optimistic figures it was easy to see there just wouldn't be a civil market big enough for even the surviving companies to share. So it proved again what someone had once said "the building of airplanes is one of man's most complicated and disheartening fields of endeavor." We have learned to know this, but there are always those who are driven to keep trying!

Jos. P. Juptner

Foreword, Volume 9. ATC 801-817.

It is almost with a sigh of relief that I present this final volume of U.S. Civil Aircraft; to continue the series any further would take a younger mind with a fresher outlook on all that was developing in the era after World War II. For a writer who was brought up in the early era of aviation—and who lived it practically every waking hour—it has been a joy to recount the development of the commercial airplane. I did my best to picture the different airplanes with their fascinating shapes and lyrical names such as "Swallow," "American Eagle," "Red Arrow," "Skyrocket," "Flamingo," and others—airplanes that were just as fascinating as their names imply. This was at a time, too, when airplanes had distinct personalities, were colored gaily with every hue of the rainbow, and even had smells that excited the senses. It is doubtful that the airplane was more personal then than it is today; but surely it was time happily spent, when flying was out of the question and we just puttered around the airplane and delved into its intriguing innards.

Of course, the behavior of some of these older airplanes left much to be desired; but at least one felt better with the thought that they were much better than what we had before. Because of the relentless drive in aviation development it is still hard to realize how much aviation changed in the quarter century between 1925 and 1950. The wildest dreamer of 1925 surely could not have predicted what airplanes would be like in the fifties!

This book has now entered the era of the fifties, and what lies ahead in aviation is almost apart from what had taken place in the decades before. The individual drive and enthusiasm for all things aeronautical was all but gone, the "backyard manufacturer" was a thing of the past, every experiment had already been proven or disproven, and the "lone eagle" type of aviator had gone out of style. Airplanes began to take on a sort of sameness, and companies building airplanes for civil use could be counted on less than ten fingers. This is not to say that aviation had relaxed and gone sedate—because progress and development did continue—but it just didn't seem the same old game. An airplane was no longer the vision of one or two men; a single airplane and an enterprising pilot did not a flying service make; and the aviator himself was no longer considered a special kind of man.

Surely, much of what has been written in this series of books are feelings and nostalgic memories out of one man's past fortified by extensive research into the times. But after twenty years of dedication to this project I found myself looking for a likely cutoff point. It presented itself more or less by a whim of the government agency that instituted the "Approved Type Certificate" used until the end of World War II. For more than twenty years until that time all ATC approvals were in numerical order (listed in this volume to #817).

But after the war and down to the present, approvals have been awarded by district. There are now six dispensing districts in the United States, and their approvals are allocated with such legends as 2A1, 5A9, 6A4. Such a system does not lend itself to any sort of recording in chronological sequence, and the end of the numerical sequence was a logical place to end this series.

Joseph P. Juptner

APPENDIX C
GENE LIBERATOR'S SKETCHES OF POSSIBLE V/STOLS

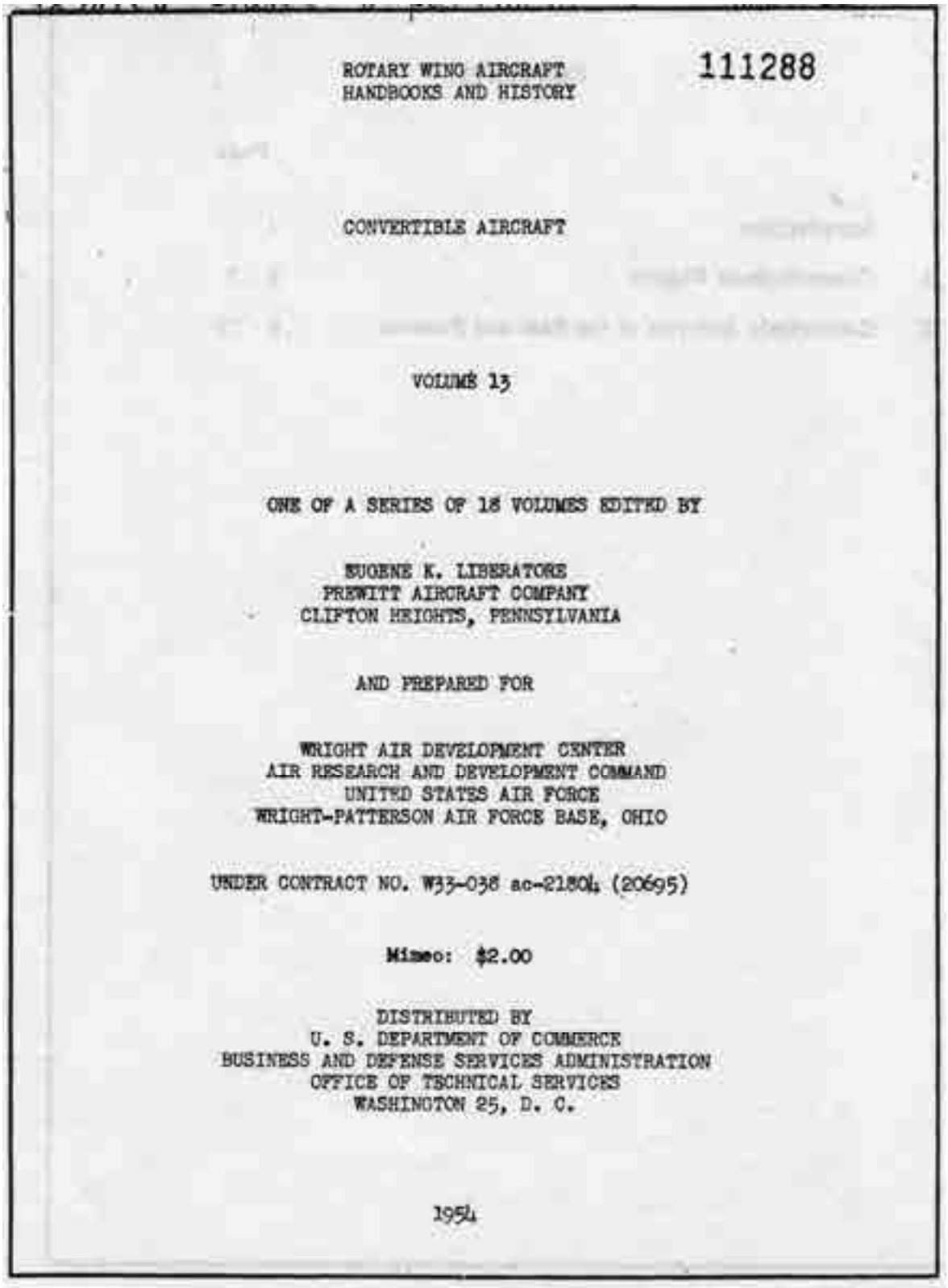

ROTARY WING AIRCRAFT
HANDBOOKS AND HISTORY

111288

CONVERTIBLE AIRCRAFT

VOLUME 13

ONE OF A SERIES OF 18 VOLUMES EDITED BY

EUGENE K. LIBERATORE
PREWITT AIRCRAFT COMPANY
CLIFTON HEIGHTS, PENNSYLVANIA

AND PREPARED FOR

WRIGHT AIR DEVELOPMENT CENTER
AIR RESEARCH AND DEVELOPMENT COMMAND
UNITED STATES AIR FORCE
WRIGHT-PATTERSON AIR FORCE BASE, OHIO

UNDER CONTRACT NO. W33-038 ac-21804 (20695)

Mimeo: $2.00

DISTRIBUTED BY
U. S. DEPARTMENT OF COMMERCE
BUSINESS AND DEFENSE SERVICES ADMINISTRATION
OFFICE OF TECHNICAL SERVICES
WASHINGTON 25, D. C.

1954

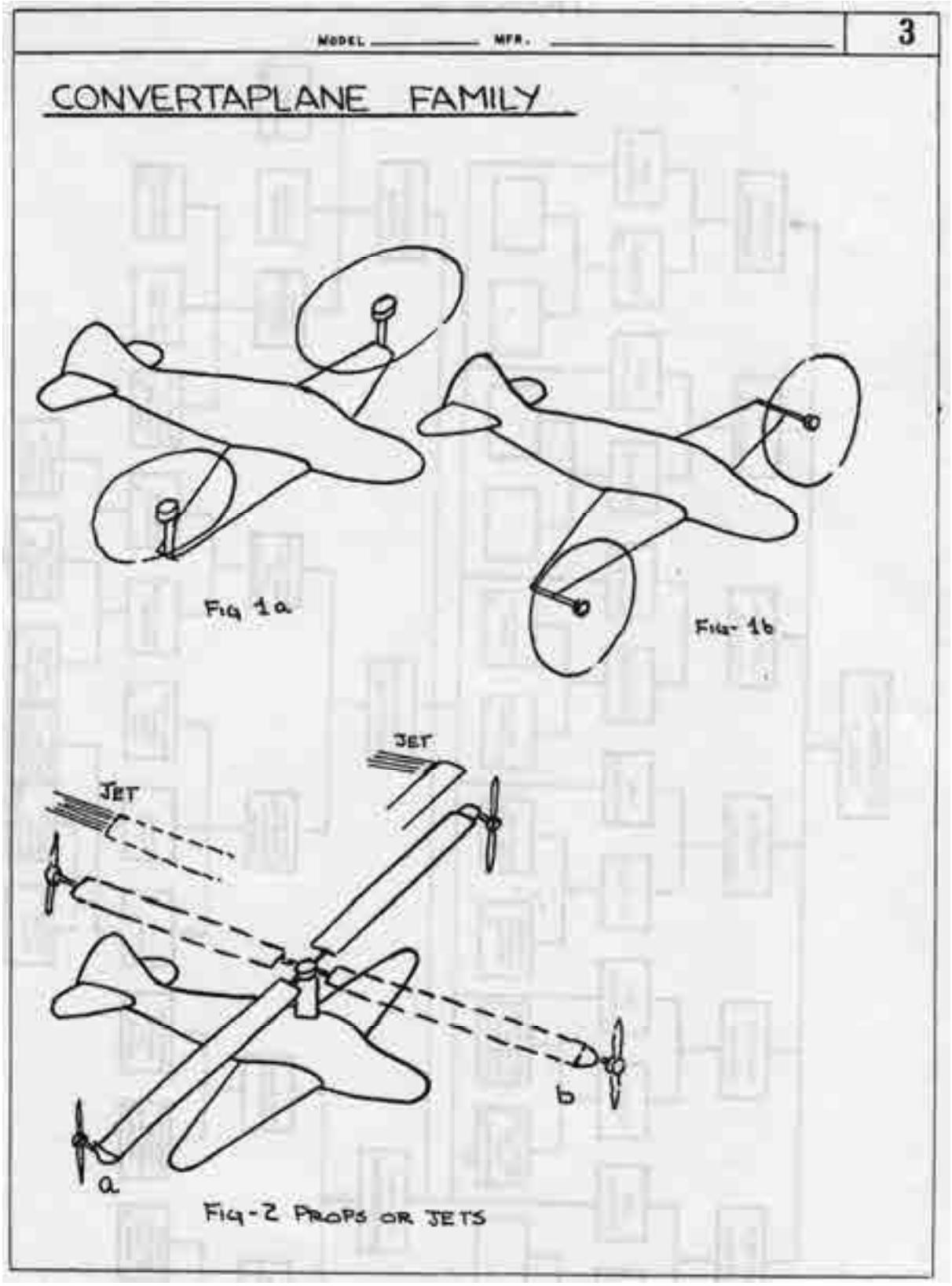
MODEL _____ MFR. _____
3
CONVERTAPLANE FAMILY
Fig 1a
Fig- 1b
JET
JET
b
a
Fig-2 PROPS OR JETS

MODEL _____ MFR. _____ 3

CONVERTAPLANE FAMILY

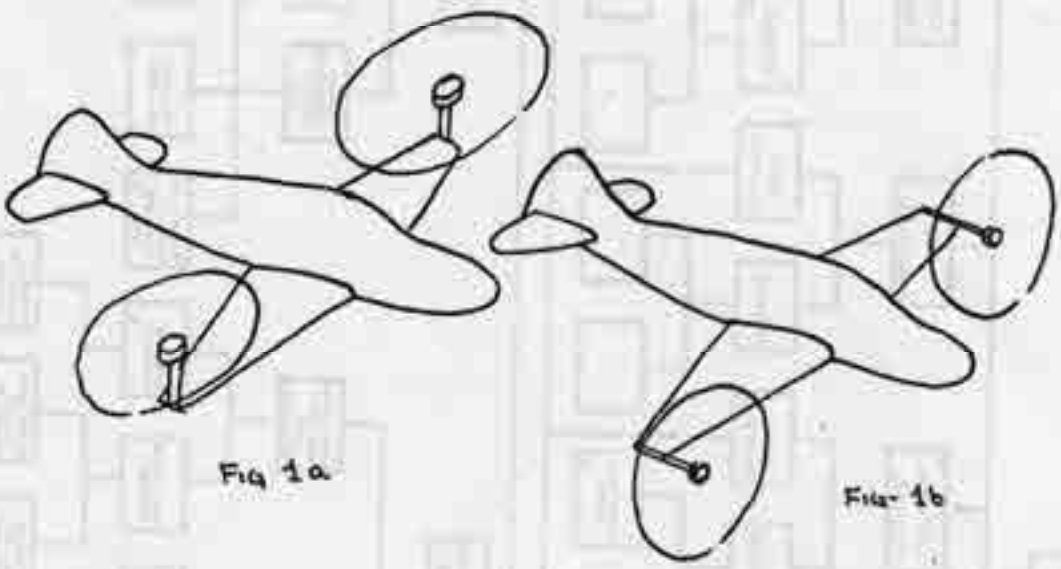

Fig 1a

Fig- 1b

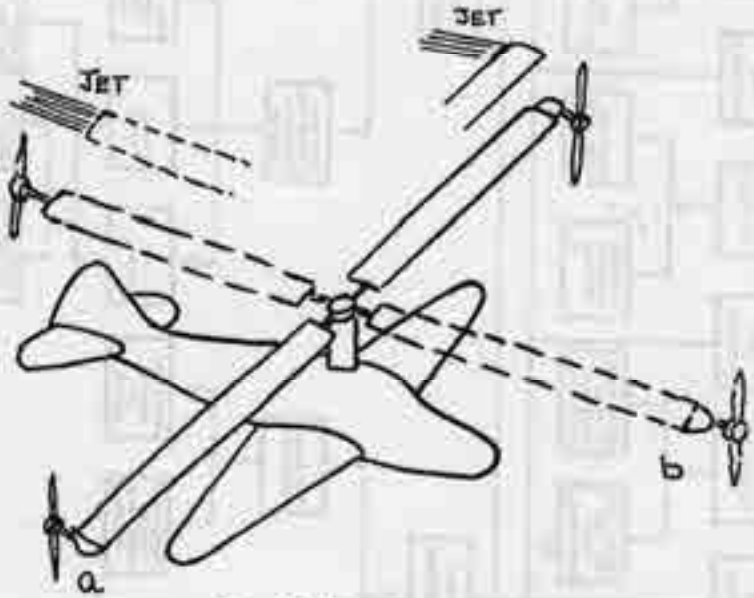

Fig-2 PROPS OR JETS

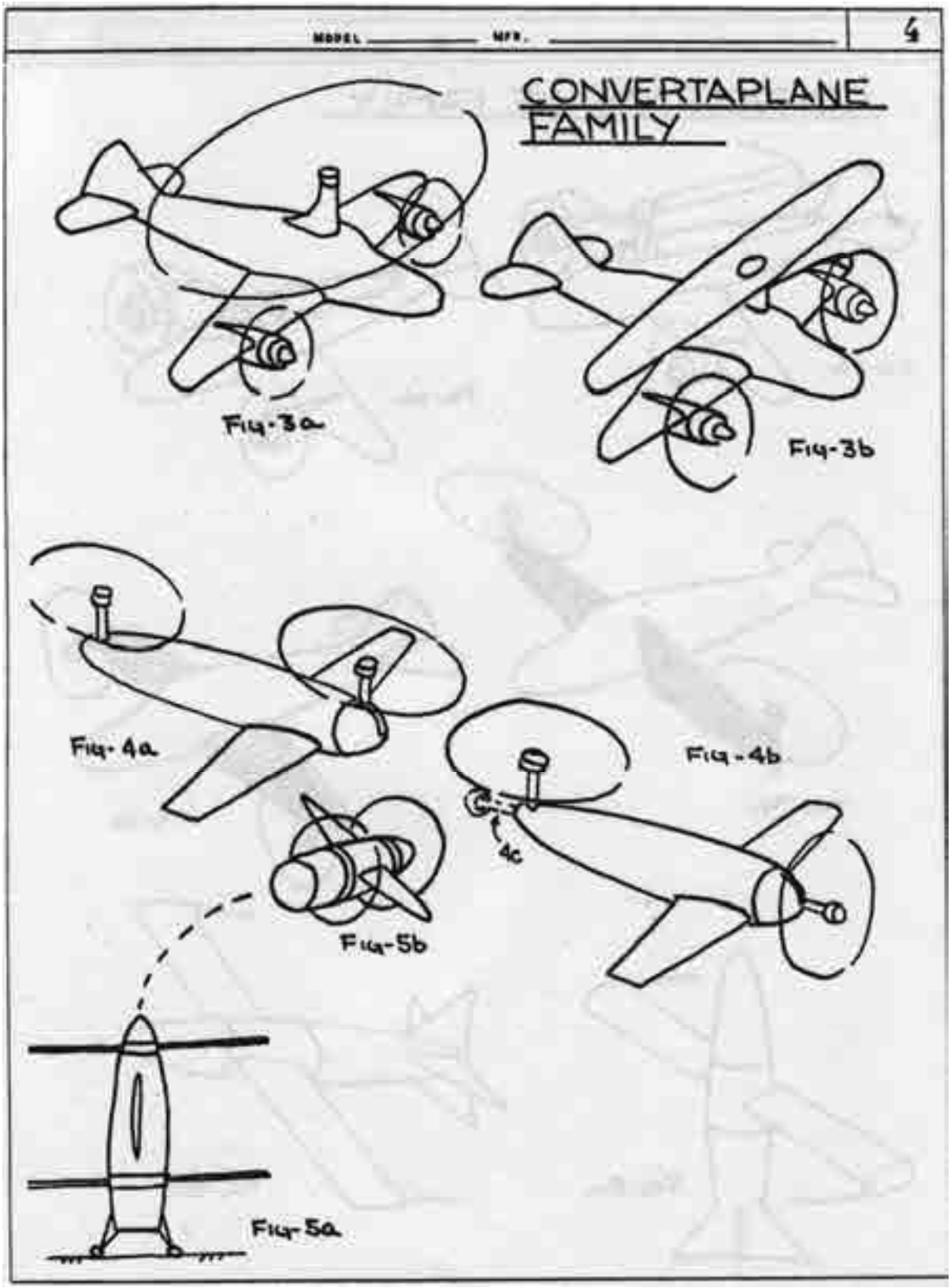
MODEL
MFR.
4
CONVERTAPLANE FAMILY
Fig-3a
Fig-3b
Fig-4a
Fig-4b
4c
Fig-5b
Fig-5a

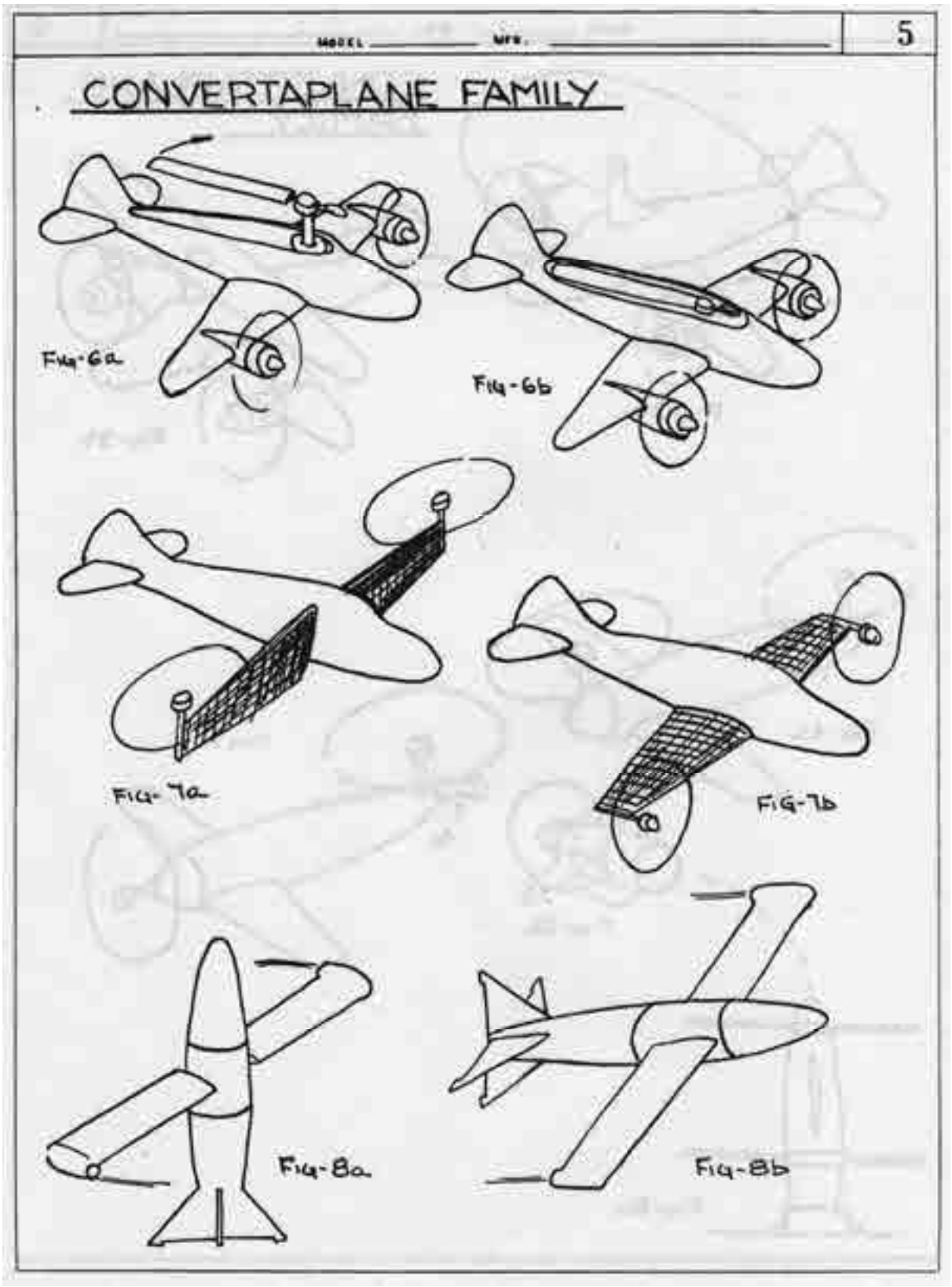
MODEL
MFR.
5
CONVERTAPLANE FAMILY
Fig-6a
Fig-6b
Fig-7a
Fig-7b
Fig-8a
Fig-8b

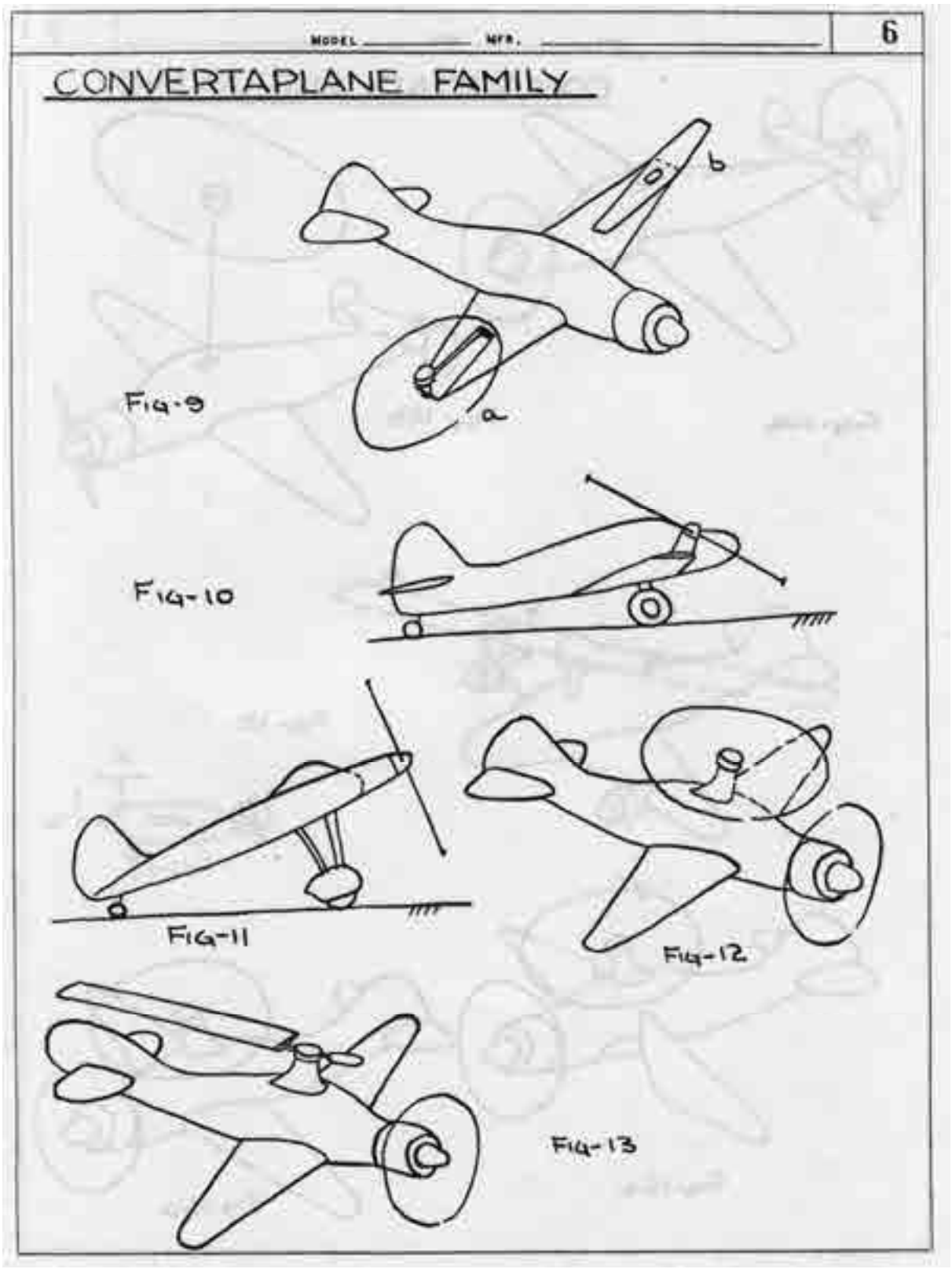
MODEL
MFR.
6
CONVERTAPLANE FAMILY
b
a
Fig-9
Fig-10
Fig-11
Fig-12
Fig-13

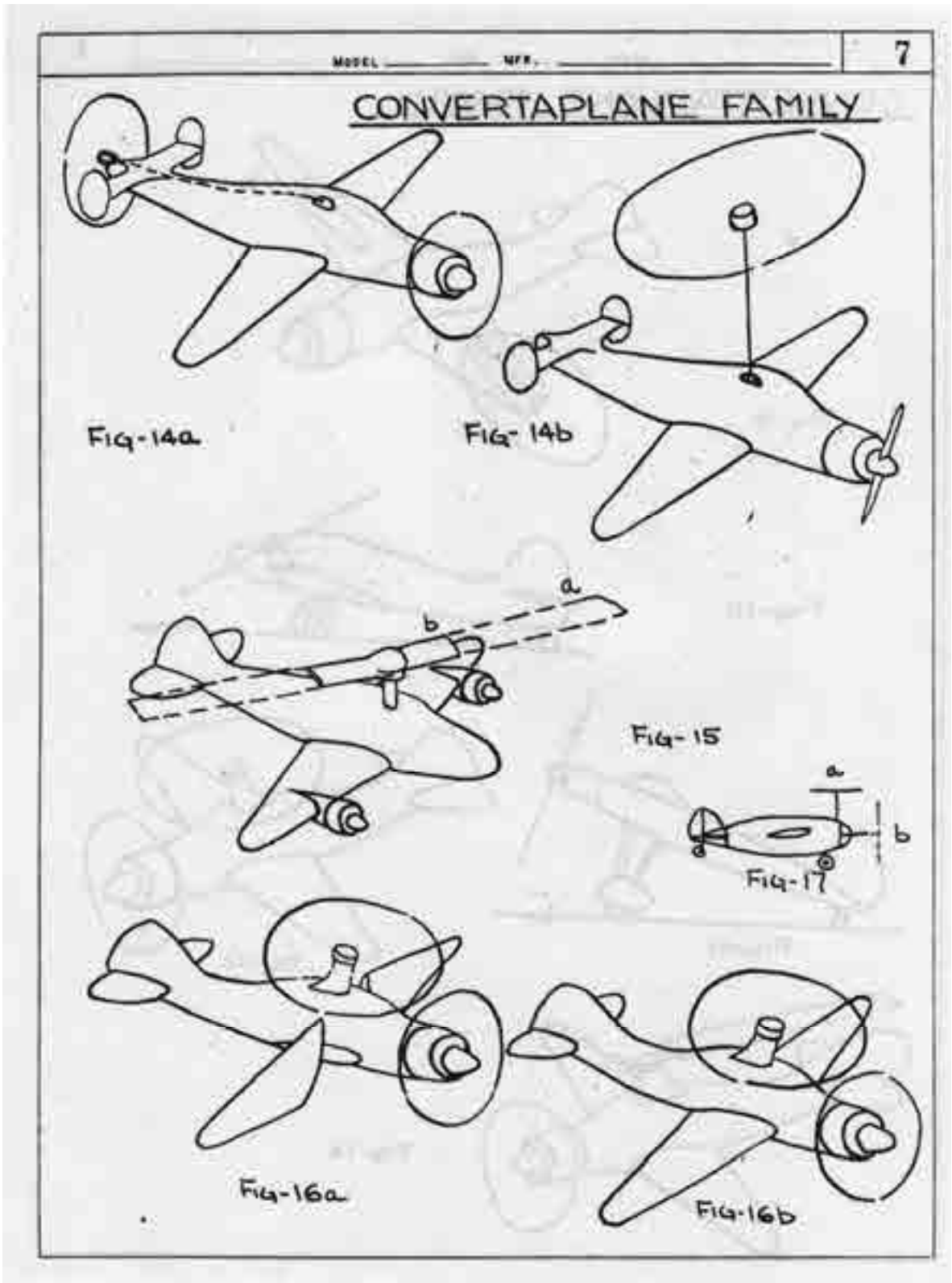
MODEL
MFR.
7
CONVERTAPLANE FAMILY
FIG-14a
FIG-14b
a
b
FIG-15
a
b
FIG-17
FIG-16a
FIG-16b

APPENDIX D
COMPOUND V/STOL AIRCRAFT PERFORMANCE FUNDAMENTALS

The various rotorcraft configurations that use a rotor for vertical or short-field takeoff and landing (i.e., V/STOL) and a propeller in forward flight invariably lead to a calculation of power required to fly. The simple sketch shown in Fig. D-1 helps guide this calculation for compound helicopters and compound airplanes. The installed power plant, say a reciprocating or turboshaft engine, is coupled to a propeller and can be coupled and uncoupled to a rotor. The propeller is directly driven by the engine. The rotor receives its power from a right-angle gear box, which is driven by a separate shaft from the engine. The rotor drivetrain might well have a clutch to manage its portion of the engine power. The basic question raised by Fig. D-1 is, How much power must the engine provide so that the machine will fly?

The answer to this "engine power required to fly" question can be found with a very simple approach using the principle of energy per unit time, which is power. To begin with, the engine power (P_{engine}) must equal—at a minimum—the sum of power required by the propeller (P_{prop}) and power required by the rotor (P_{rotor}).[1] That is

$$P_{engine} = P_{prop} + P_{rotor} . \quad (1)$$

The propeller power required can be calculated in a relatively direct manner as

$$P_{prop} = T_{prop} V + P_{prop\ induced} + P_{prop\ profile} \quad (2)$$

where T_{prop} is the propeller thrust, V is the aircraft flight speed, $P_{prop\ induced}$ is the propeller-induced power to produce thrust, and $P_{prop\ profile}$ is the profile power required to overcome the propeller blade drag.

Fig. D-1. The simple elements of compound aircraft. Tail rotor not shown for clarity. Rendition by Gerardo Nunez from author's sketch.

[1] The engine must, of course, also supply additional power to overcome transmission losses and to run accessories, but these burdens are not included in this discussion.

In a similar manner, the rotor power required can be obtained from

$$(3) \qquad P_{rotor} = X_{rotor} V + P_{rotor\ induced} + P_{rotor\ profile}$$

where X_{rotor} is the propulsive force the rotor can add to the propeller thrust so that there is force equilibrium in the horizontal direction (i.e., $\sum F_X = 0$), $P_{rotor\ induced}$ is the rotor-induced power to produce thrust, and $P_{rotor\ profile}$ is the rotor profile power required to overcome the blade drag.

Consider next the equilibrium of forces in both the horizontal and vertical directions assuming steady level flight. In the vertical direction you have

$$(4) \qquad \sum F_Z = 0 = L_{wing} + L_{rotor} - W$$

and in the horizontal direction

$$(5) \qquad \sum F_X = 0 = T_{prop} + X_{rotor} - D_{wing} - f_e \left(\tfrac{1}{2} \rho V^2 \right)$$

where f_e is the equivalent parasite drag area of the aircraft, and ρ is the density of air.

Now, the propeller thrust depends on the rotor propulsive force, the wing drag (D_{wing}), and the parasite drag. Thus, from Eq. (5)

$$(6) \qquad T_{prop} = -X_{rotor} + D_{wing} + f_e \left(\tfrac{1}{2} \rho V^2 \right).$$

But, from Eq. (3) the rotor propulsive force is simply

$$(7) \qquad X_{rotor} = \frac{P_{rotor} - P_{rotor\,induced} - P_{rotor\,profile}}{V},$$

and therefore the propeller thrust is

$$(8) \qquad T_{prop} = -\left(\frac{P_{rotor} - P_{rotor\,induced} - P_{rotor\,profile}}{V} \right) + D_{wing} + f_e \left(\tfrac{1}{2} \rho V^2 \right).$$

Suppose now that the rotor is autorotating, which means that $P_{rotor} = 0$. The propeller thrust—*in this special case*—then becomes

$$(9) \qquad T_{prop} = \left(\frac{P_{rotor\,induced} + P_{rotor\,profile}}{V} \right) + D_{wing} + f_e \left(\tfrac{1}{2} \rho V^2 \right),$$

and the engine is supplying all of its power to the propeller and none to the rotor. Then after substituting T_{prop} from Eq. (9) into Eq. (2), the engine power required amounts to

$$(10) \qquad P_{engine} = \left[\left(\frac{P_{rotor\,induced} + P_{rotor\,profile}}{V} \right) + D_{wing} + f_e \left(\tfrac{1}{2} \rho V^2 \right) \right] V + P_{prop\ induced} + P_{prop\ profile}.$$

Before addressing the rotor-induced and profile powers, the other powers in Eq. (10) must be discussed. First of all, the wing drag and parasite drag are calculated with any number

of classical airplane aerodynamic approaches. Secondly, the propeller-induced and profile powers have first-order approximations of

$$P_{\text{prop induced}} = T_{\text{prop}} \left\{ \sqrt{\left(\frac{V}{2}\right)^2 + \frac{T_{\text{prop}}}{2\rho A_{\text{prop}}}} - \frac{V}{2} \right\}$$

(11)

$$P_{\text{prop profile}} = \left[\frac{\rho (bcR) V_t^3 C_d}{8} \right]_{\text{prop}} \left\{ \left(1 + \frac{5}{2}\lambda^2\right) \sqrt{1+\lambda^2} + \frac{3}{2}\lambda^4 \ln\left[\frac{1+\sqrt{1+\lambda^2}}{\lambda} \right] \right\}$$

where the propeller advance ratio (λ) equals V/V_t.

For the rotor, equally simple and useful approximations, slightly modified with empirical corrections, are available. For example, the rotor-induced power ($P_{\text{rotor induced}}$) has the first-order approximation of

$$P_{\text{rotor induced}} = K_i \frac{L_{\text{rotor}}^2}{2\rho A_{\text{rotor}} V}$$

(12) where $K_i = 1.075 \operatorname{Cosh}\left(6.76\mu^2\right)$ for $\mu \le 0.5$

and $K_i = 1 - 29.332\mu + 92.439\mu^2 - 51.746\mu^3$ for $0.5 \le \mu \le 1.0$.

The rotor disc area (A_{rotor}) equals πR^2, and R is the radius of a rotor blade. The rotor profile power is frequently estimated for simple rectangular blade geometry as

$$P_{\text{rotor profile}} = \Omega Q_{\text{rotor profile}} + V H_{\text{rotor profile}}$$

(13)

$$= \left[\frac{\rho (bcR) V_t^3 C_d}{8} \right]_{\text{rotor}} \left(1 + 4.65\mu^2 + 4.15\mu^4 - \mu^6\right) \quad \text{for } \mu \le 1.0$$

where b is blade number, c is blade chord, and R is rotor blade radius. The blade airfoil drag coefficient is denoted by C_d and the blade tip speed by V_t.

It is important to remember that a rotor cannot autorotate if rotor lift is zero. When the rotor lift is zero, the engine must supply power ($\Omega Q_{\text{rotor profile}}$) to the rotor, and the propeller must provide a thrust equal to the rotor's H-force ($H_{\text{rotor profile}}$) plus any other aircraft drag. In fact, there is a threshold level for rotor lift (which depends on advance ratio) that must be reached before autorotation begins. This minimum threshold lift is crudely given by

(14) $$\text{Rotor shaft power} = \Omega Q_{\text{rotor profile}} - L_{\text{rotor}} \left(\alpha_S + a_{1S}\right) V = 0$$

where ($\alpha_S + a_{1S}$) is the rotor's tip path plane angle of attack as shown in Fig. D-1. Equation (14) says that the decelerating torque created by blade element drag (which tends to reduce rotor speed) must be offset by an accelerating torque created by blade element lift. From Eq. (14) it follows that in autorotation

(15) $$L_{\text{rotor}} = \frac{\Omega Q_{\text{rotor profile}}}{\left(\alpha_S + a_{1S}\right) V} \quad \text{for autorotation} \quad \text{(Note: very crude, neglects induced drag.)}$$

This approximation to the rotor lift required for autorotation can be put in standard rotor coefficient form by dividing both sides of Eq. (15) by $\rho A_{rotor} V_t^2$, which yields

(16) $$\text{Rotor } C_L = \frac{C_{Q\,\text{rotor profile}}}{(\alpha_S + a_{1S})\mu} \text{ for autorotation.}$$

The minimum rotor profile torque coefficient ($C_{Q\,\text{rotor profile}}$) is on the order of

(17) $$\text{Minimum } C_{Q\,\text{rotor profile}} = \frac{\sigma C_d}{8}\left\{1 + \frac{3}{2}\mu^2 - \frac{\mu^4}{16}\left[5 + 3\ln\left(\frac{2}{\mu}\right)\right] + \frac{7}{64}\mu^6\right\},$$

and therefore the minimum rotor blade loading coefficient (C_L/σ) for autorotation is

(18) $$\text{Minimum } \frac{C_L}{\sigma} = \frac{C_d}{8(\alpha_S + a_{1S})\mu}\left\{1 + \frac{3}{2}\mu^2 - \frac{\mu^4}{16}\left[5 + 3\ln\left(\frac{2}{\mu}\right)\right] + \frac{7}{64}\mu^6\right\} \text{ for autorotation .}$$

The term $\frac{P_{\text{rotor induced}} + P_{\text{rotor profile}}}{V}$ in Eqs. (9) and (10) is frequently referred to as the rotor effective drag (D_E). In the general case, this effective drag follows from Eq. (3) and is written as

(19) $$D_E = \frac{P_{rotor}}{V} - X_{rotor} = \frac{P_{\text{rotor induced}} + P_{\text{rotor profile}}}{V}.$$

Note that the effective drag can be obtained through experiment by dividing measured power by flight velocity and subtracting rotor propulsive force. On the other hand, only theory (so far) can separately calculate induced and profile power. Also note that when the rotor is autorotating (i.e., $P_{rotor} = 0$), the effective drag becomes the actual rotor drag. That is

(20) $$D_E = \frac{0}{V} - X_{rotor} = -X_{rotor} = D_{rotor} = \frac{P_{\text{rotor induced}} + P_{\text{rotor profile}}}{V}.$$

This effective drag can be estimated from rather simple classical theory using empirical corrections. The semiempirical relationship is

(21) $$D_E = K_i \frac{L_{rotor}^2}{2\rho A_{rotor} V^2} + \frac{\rho(bcR)V_t^3}{V}\left(\frac{C_d}{8}\right)\left(1 + 4.65\mu^2 + 4.15\mu^4 - \mu^6\right).$$

The approximation can be put in the airplane form of drag divided by dynamic pressure ($1/2\ \rho V^2$), which is a rotor parasite drag area. Thus,

(22) $$\frac{D_E}{q} = \frac{K_i}{\pi}\left(\frac{L_{rotor}}{2Rq}\right)^2 + \frac{(bcR)C_d}{4}\left(\frac{1 + 4.65\mu^2 + 4.15\mu^4 - \mu^6}{\mu^3}\right).$$

The rotor effective drag can also be put in standard rotor coefficient form by dividing both sides of Eq. (21) by $\rho A_{rotor} V_t^2$

(23) $$C_{D_E} = K_i \frac{C_L^2}{2\mu^2} + \left(\frac{\sigma C_d}{8}\right)\left(\frac{1 + 4.65\mu^2 + 4.15\mu^4 - \mu^6}{\mu}\right).$$

It is quite common to divide Eq. (23) through by rotor solidity (σ) and apply this result universally to any rotor of differing solidity. The result of this step is

$$(24) \qquad \frac{C_{D_E}}{\sigma} = \frac{K_i \sigma}{2\mu^2}\left(\frac{C_L}{\sigma}\right)^2 + \left(\frac{C_d}{8}\right)\left(\frac{1 + 4.65\mu^2 + 4.15\mu^4 - \mu^6}{\mu}\right).$$

While this step gives the familiar blade loading coefficient (C_L/σ) and can be handy for many purposes (e.g., identifying the onset of blade stall), the step can be misleading because more advanced theory that includes a complete model of the rotor wake shows that induced power (or induced drag) does not scale with solidity. This point is emphasized in Fig. D-2, which was obtained with today's advance theory. One way of keeping this point in mind is to write the rotor solidity for a rotor with rectangular blades as

$$(25) \qquad \sigma = \frac{bc}{\pi R} = \left(\frac{b}{\pi}\right)\left(\frac{1}{R/c}\right) = \frac{b}{\pi(\text{Aspect Ratio})}.$$

Of course, when theory is compared to test *at equal solidity* this important point is mute.

Simple theory—such as Eq. (23)—suggests that the rotor effective drag coefficient varies as lift-coefficient squared. Experimental data confirms this dependency as Fig. D-3 shows for the H-34 rotor with untwisted blades (tested in the National Full-Scale Aerodynamics Complex 40- by 80-Foot Wind Tunnel at NASA Ames Research Center). The divergence of the experimental data versus the simple theory occurs when blade stall becomes a factor, in this case approximately at $C_L/\sigma = 0.07$.

An important question can now be raised: How much does the rotor effective drag coefficient vary as the rotor propulsive force varies while the rotor lift coefficient is held constant? When the rotor tip path plane is tilted aft (as shown in Fig. D-1), the rotor can be in or near autorotation. As power is applied and the tip path plane is tilted forward, the rotor propulsive force overcomes its own drag. A further forward tilting accompanied by an increase in power allows the rotor to provide a useable propulsive force. This behavior is illustrated with Fig. D-4 using the full-scale H-34 rotor data tabulated in NASA TN D-4632, Table IV-4 for the untwisted blade set, and Table IV-1 for the –8-degree twisted blade set. Autorotation occurs somewhere along the dashed line defined by Eq. (20). Note that at this advance ratio and lift coefficient both untwisted and twisted blades autorotate with nearly equal drag. However, when required to propel, the twisted blades offer a performance advantage.

There is a considerable advantage in looking at performance in a more direct way using Eq. (3) in coefficient form. By dividing both sides by $\rho A_{rotor} V_t^3$ you have

$$(26) \qquad C_P = C_X \mu + C_{P\,\text{induced}} + C_{P\,\text{profile}}.$$

In this view, $C_X \mu$ is the ideal power to propel, and the induced and profile powers are primarily required to produce lift. Therefore, it makes sense to graph total power (C_P) versus ideal power ($C_X \mu$). This graph is provided in Fig. D-5. Ideal propulsive power is shown on this figure with the dashed line. Suppose now that the power at zero propulsive force is taken

as the reference for the sum of induced and profile power. A further forward tilt of the tip path plane produces propulsive force, and this increases the total power. The increase is slightly greater than ideal propulsive power for the untwisted blade set. That is, the slope of the untwisted blade's total power with ideal propulsive power is nearly parallel with the dashed line in Fig. D-5. The –8-degree twisted blade set presents an entirely different conclusion. From the reference $C_X = 0$ power, this twisted blade set requires less power than ideal with increasing propulsive power (i.e., the slope is *less* than the dashed line). However, in the range of $C_X \mu = 0.0003$ to 0.0004, the slope of power versus ideal power appears parallel to the dashed line. This indicates the advantage twisted blades have over untwisted blades for helicopters, which use the rotor to both lift and propel. Of course, the question as to whether this is the "optimum" twist for this advance ratio, lift, and rotor geometry is not answered by Fig. D-5.

To conclude this discussion of performance fundamentals, consider the special case of autorotation using experimental data obtained with the H–34 untwisted blade set at an advance ratio of 0.304 from NASA TN D-4632, Table IV-4, as an example. The test data was obtained by varying collective pitch, holding shaft angle of attack constant, and adjusting longitudinal and lateral cyclic controls so that first harmonic flapping (a_{1S} and b_{1S}) was zero (or nearly zero). The cyclic control adjustment to zero-out flapping means that the rotor tip path plane angle of attack ($\alpha_S + a_{1S}$) is virtually identical to the shaft angle of attack (α_S). Data analysis is, however, generally clearer by plotting any measured parameter versus shaft angle of attack or versus rotor lift *holding collective pitch constant* as shown in Fig. D-6.

Three key graphs are necessary to fully understand rotor performance in autorotation. The first establishes the rotor lift at which autorotation will occur, and this graph is shown in Fig. D-6. The data points at equal collective pitch are connected with solid lines. The secondary information dealing with the shaft angle of attack is noted by the dashed lines. The variation of power coefficient with lift as the tip path plane angle of attack is increased—holding collective pitch constant—defines the lift coefficient (for each collective pitch) at which autorotation is obtained. Interpolation and some extrapolation are obviously needed.

The second key graph is shown in Fig. D-7. In this figure, the rotor drag when power is zero can be traced out using the rotor lift points defined from Fig. D-6. The heavy blue line on Fig. D-7 shows the rotor drag versus lift at zero power and is, for practical purposes, the rotor's drag polar. This rotor at this advance ratio has its maximum lift-to-drag ratio of 9.80 at the blade loading coefficient of 0.085.

The third key graph is shown in Fig. D-8, and this figure establishes the lift versus angle-of-attack behavior at constant collective pitch. The rotor has a clearly defined lift curve slope just like an airplane wing has. Furthermore, the rotor collective pitch acts just like a wing flap in that the angle of attack for zero lift can be controlled by the amount of collective pitch applied. Finally, the heavy blue line traces out the combinations of angle of attack and collective pitch at which autorotation is obtained.

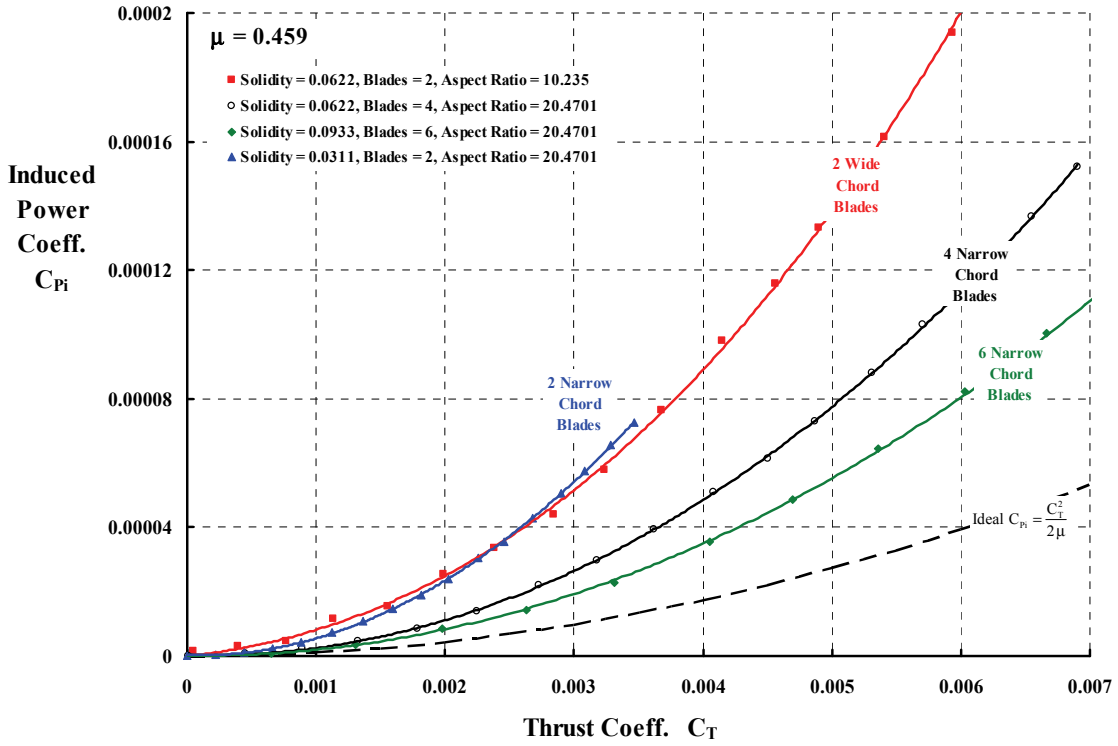

Fig. D-2. The induced power of four narrow-chord blades is less than that of two wide-chord blades, keeping solidity constant. Rectangular, untwisted blades with N.A.C.A. 0012 airfoil. Calculated with CAMRAD II, an advanced rotor theory.

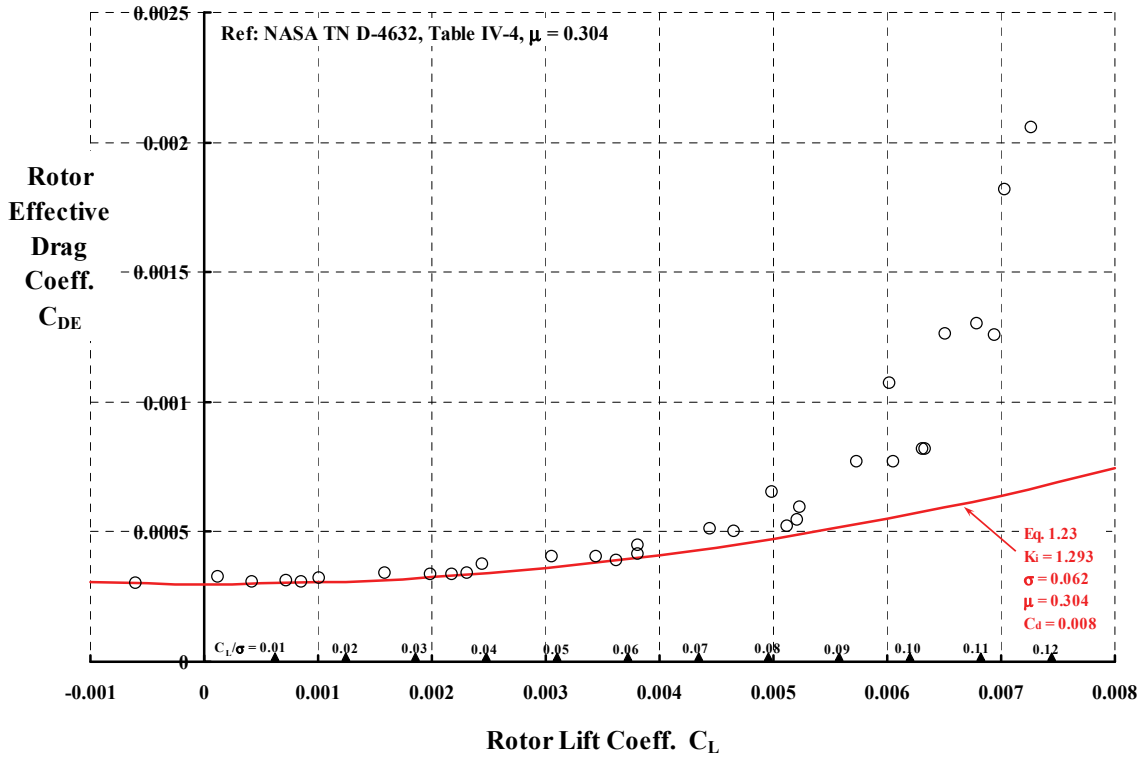

Fig. D-3. Effective drag varies as lift-squared, up to the onset of blade stall.

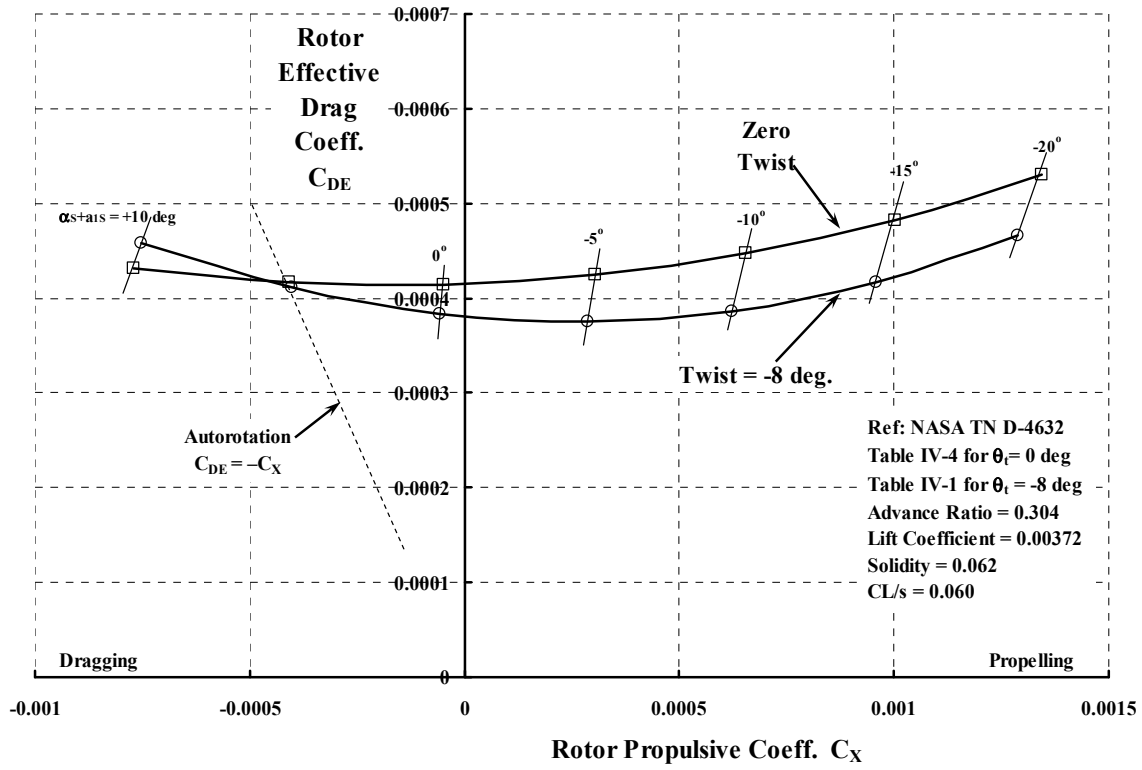

Fig. D-4. The effect of propulsion on rotor effective drag coefficient at constant rotor lift is influenced by blade twist.

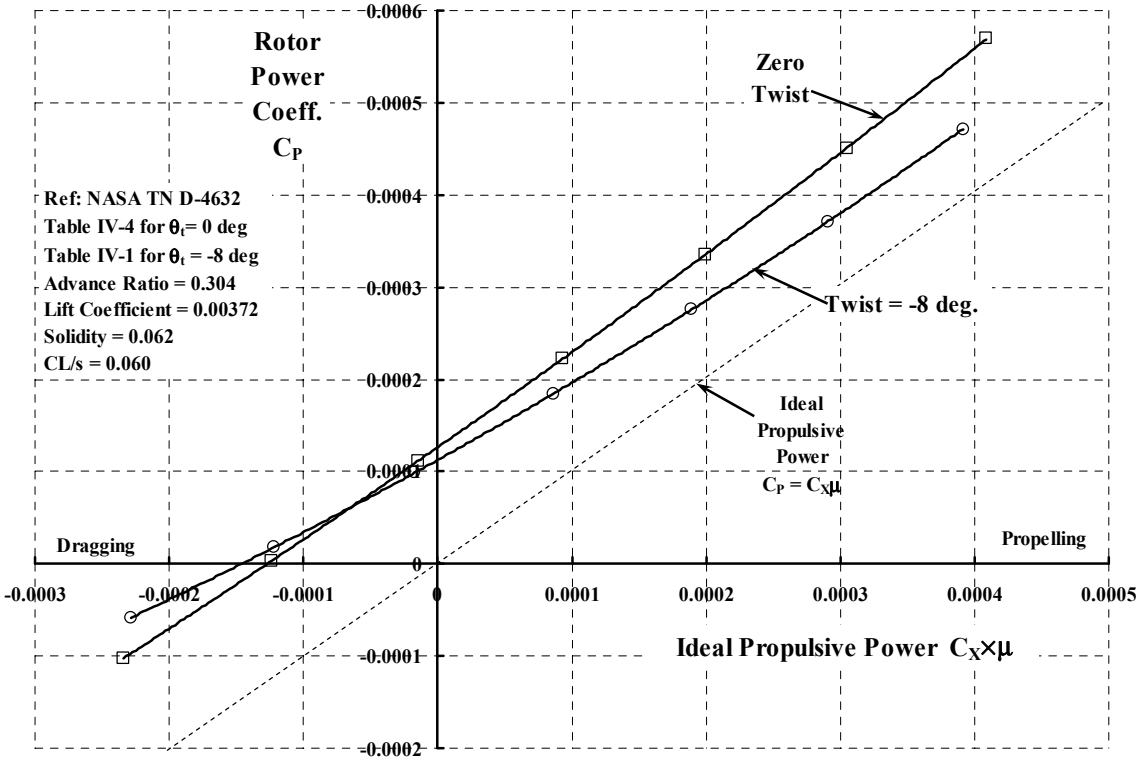

Fig. D-5. The effect of propulsion on rotor total power.

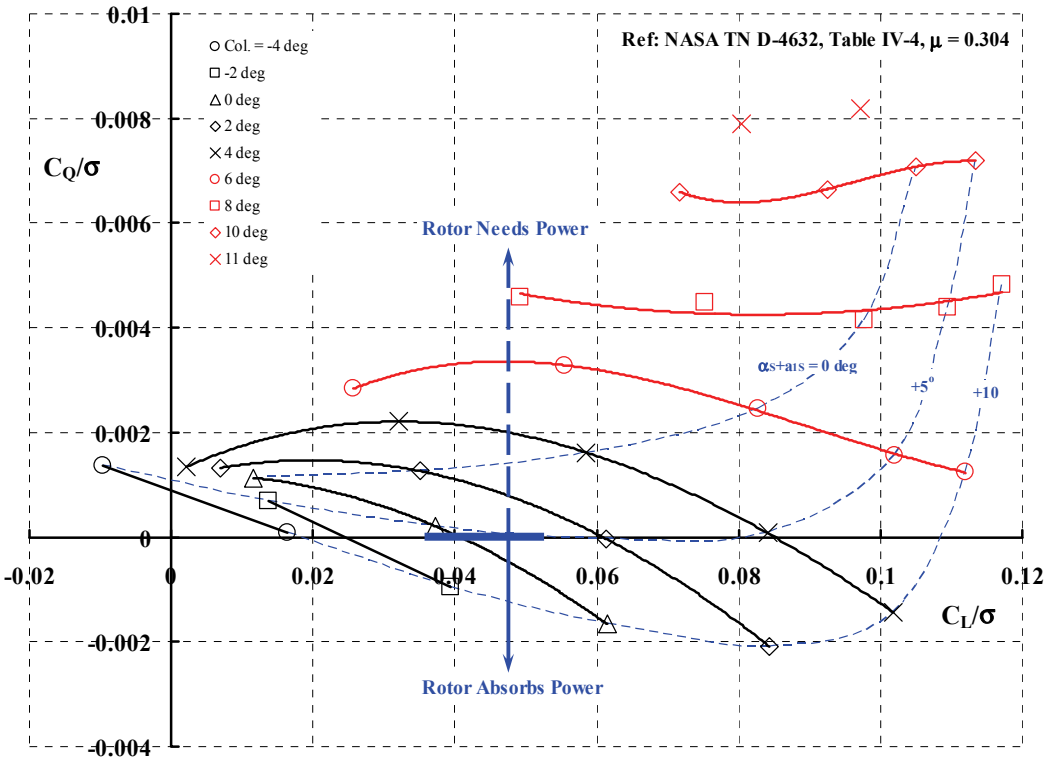

Fig. D-6. The variation of rotor power with rotor lift, holding collective pitch constant and varying shaft angle of attack. Untwisted H–34 blades.

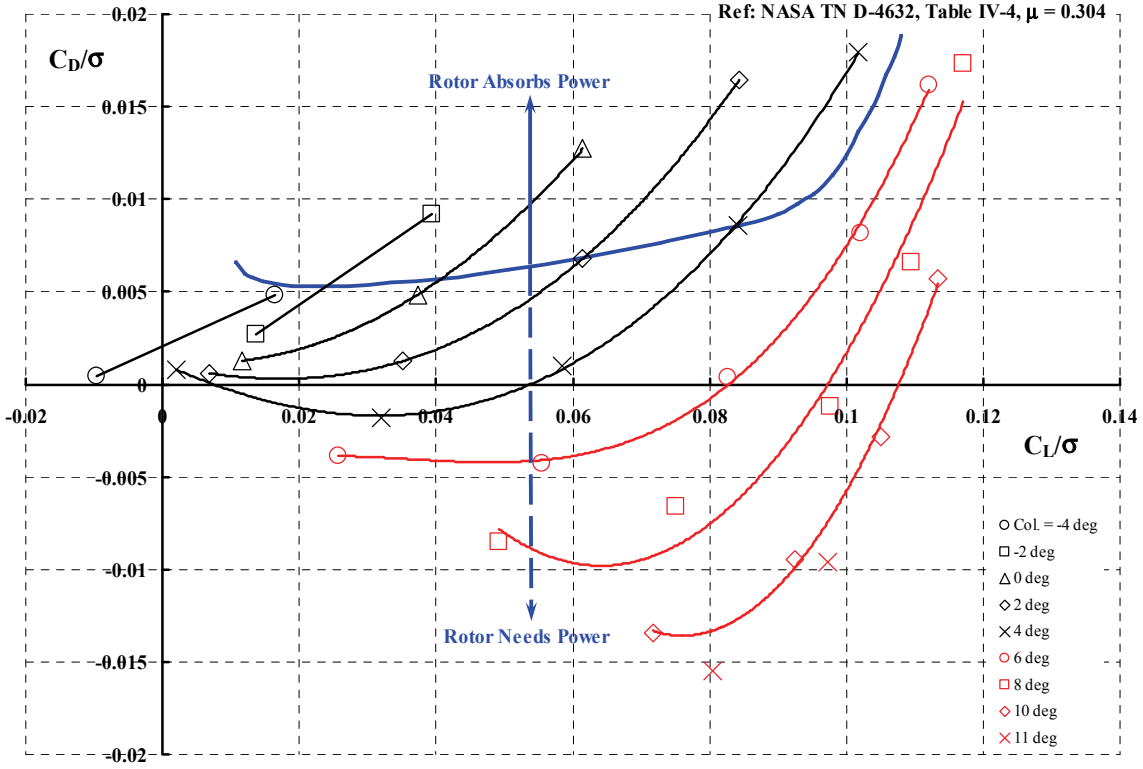

Fig. D-7. The variation of rotor drag with rotor lift, holding collective pitch constant and varying shaft angle of attack. Untwisted H–34 blades.

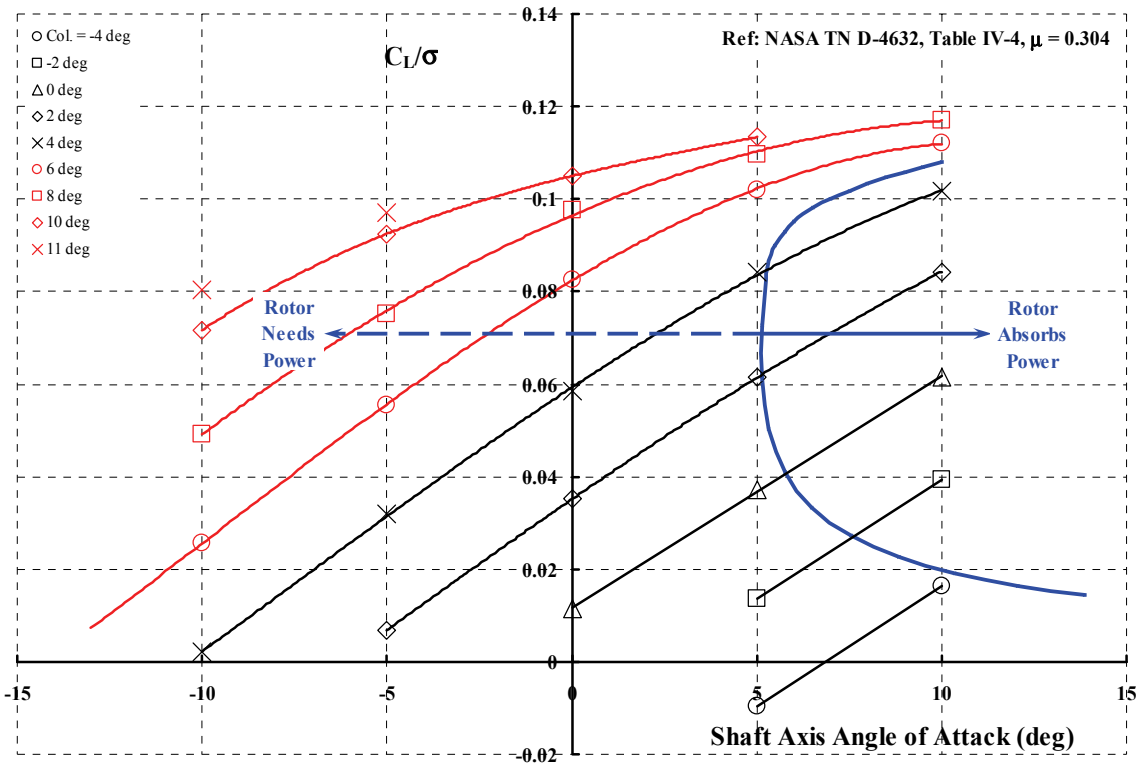

Fig. D-8 The variation of rotor lift with shaft angle of attack, holding collective pitch constant. Untwisted H–34 blades.

APPENDIX E
PROPROTOR THRUST, BLADE FLAPPING MOTION, AND H-FORCE INCLUDING SHAFT MOTION

Understanding how shaft motion affects proprotor forces for either tiltrotor or tiltwing aircraft is absolutely essential to rotorcraft development. The problem I have introduced in this Volume III and with this appendix is, I think, ideally suited to engineering students. Certainly, experiments with a simple model both on the bench and in a wind tunnel are easily done. Reporting on theory-versus-test results for this relatively simple problem has not been done since Zbrozek's, Britland and Fail's, and Sissingh's work in 1949 through 1951. A simple theoretical experiment concludes this appendix.

Blade Element Thrust

Castle and New's NACA TN 2656 used the airfoil lift equation $C_\ell = a \sin\alpha$ rather than $C_\ell = a\alpha$ to derive all the basic rotary wing equations that you saw in Volume I, appendix E. This was (in my opinion) an ingenious way around most of the first-order small angle assumptions then being made before the use of digital computers became commonplace. You see Castle and New's derivation of blade element thrust by following Fig. E-1 and writing

$$(1) \qquad dT_\psi = (dL\cos\phi)\cos\beta = \left\{\left(\tfrac{1}{2}\rho V_t^2\right) c\left(U_T^2 + U_P^2\right)\left[a\sin\left(\theta + \arctan\left(\frac{U_P}{U_T}\right)\right)\right] dr\right\}\left(\frac{U_T}{U}\right)\cos\beta$$

and, with a little trigonometry expansion, you have a very tractable

$$(2) \qquad dT_\psi = dL\cos\phi\cos\beta \approx \left(\tfrac{1}{2}\rho V_t^2\right) ac\left[U_T^2\sin\theta + U_P U_T\cos\theta\right] dr \quad \text{if } \beta \text{ is a small angle.}$$

Keep in mind that blade element lift (dL) acts perpendicular to the blade's span axis. And do not forget that the blade is at a flapping angle (β) so only the component of the blade element lift parallel to the shaft is thrust. For this introductory discussion, I have decided to neglect any contribution of airfoil drag (dD_o) to blade element lift (dL) and thrust (dT). And I have assumed the flapping angle is a small angle so that $\cos\beta = 1$ and $\sin\beta = \beta$.

Of course, you need additional equations for the inplane or tangential velocity (U_T), the inflow or upward velocity (U_P), and the blade pitch angle (θ). Based on Al Gessow's NACA TN 1604, which was generally adhered to in the 1950s, let me suggest the following:

$$(3) \qquad \begin{aligned} U_T &= x + \mu\sin\psi - X_{pr}\frac{d\Theta}{d\psi}\sin\psi \qquad U_P = \lambda - x\frac{d\beta}{d\psi} - \mu\beta\cos\psi + x\frac{d\Theta}{d\psi}\cos\psi \\ \theta &= \theta_0 + x\theta_t - B_{1C}\sin\psi - A_{1C}\cos\psi + \frac{\Delta\theta}{\Delta\beta}\beta. \end{aligned}$$

Both the classical autogyro/helicopter rotor inflow ratio (λ) and advance ratio (μ) can be based on the angle of attack of the proprotor shaft (α_s). To put these ratios in terms of proprotor parameters, you have, following Fig. 2-143 on page 229,

$$(4) \qquad \alpha_s = -90 + \alpha_f + i_{tilt} + \Theta_t.$$

Then the two ratios become

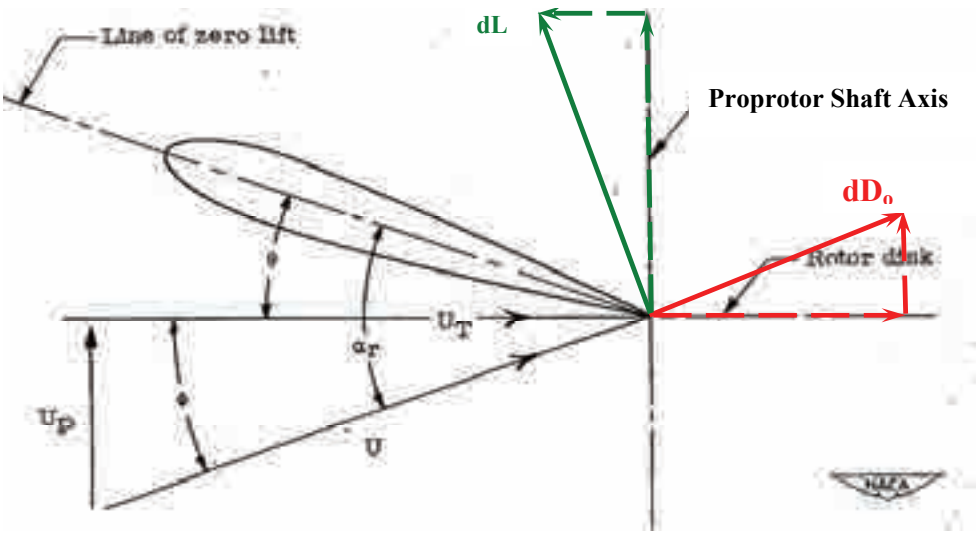

Fig. E-1. This standard convention for rotor blade element analysis was defined by Al Gessow at NACA Langley in June of 1948 with NACA TN 1604. His complete definitions of symbols for helicopters were generally followed by rotorcraft engineers in the industry.

$$(5) \qquad \lambda = \frac{V\sin\alpha_s}{V_t} = -\frac{V\cos\left(\alpha_f + i_{tilt} + \Theta_t\right)}{V_t} \qquad \text{and} \qquad \mu = \frac{V\cos\alpha_s}{V_t} = \frac{V\sin\left(\alpha_f + i_{tilt} + \Theta_t\right)}{V_t}.$$

In my nomenclature, I have set the proprotor's shaft tilt incidence (i_{tilt}) relative to the aircraft's waterline reference system to zero when the aircraft is in airplane mode. In the hover mode, you have (i_{tilt}) equal to +90 degrees. This is in keeping with the flight test definition for the XV-3, although the flight test report refers to (i_{tilt}) as the CVA angle.

The influence of a sinusoidal shaft pitching motion (Θ_t) is included simply as

$$\Theta_t = \frac{d\Theta}{dt}t + \Theta_{amp}\sin\left[(pf)t\right]$$

$$(6) \qquad \text{so} \quad \frac{d\Theta}{dt} = \Theta_{st} + \Theta_{amp}(pf)\cos\left[(pf)t\right] \quad \text{or} \quad \frac{d\Theta}{d\psi} = \bar{\Theta}_{st} + \Theta_{amp}(\nu)\cos\left[(\nu)\psi\right]$$

$$\text{and} \quad \frac{d^2\Theta}{dt^2} = -\Theta_{amp}(pf)^2\sin\left[(pf)t\right] \quad \text{or} \quad \frac{d^2\Theta}{d\psi^2} = -\Theta_{amp}(\nu)^2\sin\left[(\nu)\psi\right].$$

First, notice in Eq. (6) that I have adopted the shorthand notation that a pitch rate in radians per second is defined as ($d\Theta/dt$) in the time domain but becomes ($d\Theta/d\psi$) in the azimuth domain and then has no units. Second, notice that in the azimuth domain, the frequency of the pitching motion (pf) is ratioed to rotor speed (Ω), and I have adopted the Greek letter nu (ν) for (pf/Ω). Incidentally, you will not find the inclusion of shaft motion in many elementary textbooks or reports or papers. But you cannot study proprotor behavior without including this degree of freedom whenever the aircraft is in unsteady flight. Of course, aircraft structural deformation even in steady flight can cause serious problems, even aircraft destruction, because of whirl flutter caused by shaft motion.

Blade Flapping Motion

Now consider the blade motion identified by the *rigid blade* flapping angle (β) and its change with azimuth (dβ/dψ). It is this angle and its first derivative upon which the calculation of rotor forces such as thrust (T) and H-force (H) are so dependent. In simple rotorcraft problems the basic assumption as far back as the autogyro era has been that the blades are hinged to the hub and that only first harmonic flapping occurs. *If there are no aircraft oscillations going on*, rotorcraft engineers convey this assumption symbolically as

$$\beta = \beta_0 - a_{1S}\cos\psi - b_{1S}\sin\psi, \tag{7}$$

and the change of flapping with azimuth (dβ/dψ)—the first derivative—and the second derivative ($d^2\beta/d\psi^2$) are, respectively,

$$\frac{d\beta}{d\psi} = +a_{1S}\sin\psi - b_{1S}\cos\psi \qquad \text{and} \qquad \frac{d^2\beta}{d\psi^2} = a_{1S}\cos\psi + b_{1S}\sin\psi = \beta_0 - \beta. \tag{8}$$

However, w*hen there are aircraft oscillations and structural deformations to be considered*, then a blade's flapping motion is much more difficult to determine because the simplest assumption is that

$$\beta = \beta_0 - \left(a_{1S}\right)_\psi \cos\psi - \left(b_{1S}\right)_\psi \sin\psi, \tag{9}$$

and the change of flapping with azimuth (dβ/dψ) then becomes[1]

$$\frac{d\beta}{d\psi} = -\left[-\left(a_{1S}\right)_\psi \sin\psi + \cos\psi\frac{d\left(a_{1S}\right)_\psi}{d\psi}\right] - \left[\left(b_{1S}\right)_\psi \cos\psi + \sin\psi\frac{d\left(b_{1S}\right)_\psi}{d\psi}\right]. \tag{10}$$

Now let me address what I think are the two keys to understanding the fundamentals of rotor forces as they are influenced by shaft motion. The first key is that the angle of attack at a blade element is very dependent on U_P as seen in Fig. E-1. And from Eq. (3), U_P depends on both flapping angle (β) and the change of flapping with blade azimuth (ψ), or symbolically, dβ/dψ. The second key is that to find the blade motion you must solve a mass (m) – damper (c) – spring (k) type of problem, which you learned about on pages 226 and 227. When shaft motion is included, the equation for flapping motion of a hinged, rigid blade is extended to include gyroscopic terms, and you have

$$I_{flap}\frac{d^2\beta}{dt^2} + I_{flap}\omega^2\beta = \left(M_{aero}\right)_t - 2I_{flap}\Omega\frac{d\Theta}{dt}\sin\psi + I_{flap}\frac{d^2\Theta}{dt^2}\cos\psi\ . \tag{11}$$

Most authors convert this equation in time to a differential equation in blade azimuth, which is done by noting that time (t) equals blade azimuth (ψ) divided by rotor speed (Ω). Thus, you can immediately say that $\frac{1}{t} = \frac{\Omega}{\psi}$, $\frac{1}{dt} = \frac{\Omega}{d\psi}$, and $\frac{1}{dt^2} = \frac{\Omega^2}{d\psi^2}$. With this substitution you have

[1] It is little things like this that cause many members of the rotorcraft industry to say, "Rotorcraft technology is much more complicated than fixed-wing technology and therefore we require more time and money." You might keep in mind that I have assumed the blade to be rigid. But, in fact, the blade has elastic deflections that must be accounted for. Of course, now we are talking real money spent by over a hundred engineers during a couple of decades of time before the rotorcraft industry has adequate tools.

$$(12)\qquad I_{flap}\Omega^2\frac{d^2\beta}{d\psi^2}+I_{flap}\omega^2\beta=\left(M_{aero}\right)_\psi-2I_{flap}\Omega^2\frac{d\Theta}{d\psi}\sin\psi+I_{flap}\Omega^2\frac{d^2\Theta}{d\psi^2}\cos\psi.$$

Of course, the very next step is to divide Eq. (12) through by ($I_{flap}\Omega^2$) giving you

$$(13)\qquad \frac{d^2\beta}{d\psi^2}+\left(\frac{\omega}{\Omega}\right)^2\beta=\frac{1}{I_{flap}\Omega^2}\left(M_{aero}\right)_t-2\frac{d\Theta}{d\psi}\sin\psi+\frac{d^2\Theta}{d\psi^2}\cos\psi.$$

When you assume a simple shaft motion as in Eq. (6), you have a hint of the increasing technical complexity the rotorcraft industry has faced for many, many decades. That is

$$(14)\qquad \frac{d^2\beta}{d\psi^2}+\varpi^2\beta=\frac{1}{I_{flap}\Omega^2}\left(M_{aero}\right)_\psi-2\bar{\Theta}_{st}\sin\psi-2\Theta_{amp}(\nu)\cos\left[(\nu)\psi\right]\sin\psi-\Theta_{amp}(\nu)^2\sin\left[(\nu)\psi\right]\cos\psi$$

where the system's natural frequency (ω), when divided by rotor speed (Ω), is (ϖ).

The last step in solving this problem is to define the aerodynamic moment (M_{aero}) about the hub's flapping hinge. In shorthand, you write

$$(15)\qquad \left(M_{aero}\right)_\psi=\int_0^R r\,dT=\left(\tfrac{1}{2}\rho V_t^2\right)\left(acR^2\right)\int_0^1\left[U_T^2\sin\theta+U_PU_T\cos\theta\right]xdx,$$

and here I have nondimensionalized the blade span location (r) by rotor radius (R) to define the blade element's radial location by (x = r/R). Therefore, you have

$$(16)\qquad \frac{1}{I_{flap}\Omega^2}\left(M_{aero}\right)_\psi=\left[\frac{\left(\tfrac{1}{2}\rho V_t^2\right)\left(acR^2\right)}{I_{flap}\Omega^2}\right]\int_0^1\left[U_T^2\sin\theta+U_PU_T\cos\theta\right]xdx.$$

C. N. H. Lock, a British engineer, defined a number in 1927 that came to be called Lock's number (γ) and was quickly was shortened to just Lock number (γ). That is,

$$(17)\qquad \left[\frac{\left(\tfrac{1}{2}\rho V_t^2\right)\left(acR^2\right)}{I_{flap}\Omega^2}\right]=\frac{\left(\tfrac{1}{2}\rho\Omega^2R^2\right)\left(acR^2\right)}{I_{flap}\Omega^2}=\frac{1}{2}\left(\frac{\rho acR^4}{I_{flap}}\right)=\frac{\gamma}{2}\text{ and therefore }\gamma=\left(\frac{\rho acR^4}{I_{flap}}\right).$$

You should note that Lock number, while unit-less, varies with air density (ρ) and the proprotor's blade geometry of chord (c) and radius (R), and the blade's airfoil, which has a lift curve slope (a). Many rotorcraft engineers calculate and quote Lock number at sea level standard, where the air density equals 0.002378 slugs per cubic foot, and then proceed to neglect the influence of altitude.

The deceptively simple differential equation to be solved is just

$$(18)\qquad \frac{d^2\beta}{d\psi^2}+\varpi^2\beta=\frac{\gamma}{2}\int_0^1\left[U_T^2\sin\theta+U_PU_T\cos\theta\right]xdx$$
$$-2\bar{\Theta}_{st}\sin\psi-2\Theta_{amp}(\nu)\cos\left[(\nu)\psi\right]\sin\psi-\Theta_{amp}(\nu)^2\sin\left[(\nu)\psi\right]\cos\psi.$$

This equation becomes much messier when you substitute Eq. (3)'s expressions for U_T, U_P, and θ. Then you cannot forget to substitute Eq. (5)'s and (6)'s expressions for λ, μ, and Θ. At this point the equation can be written out on several sheets of paper with a few pencils.

General Solution Approach

The most expeditious approach I found to solve for the flapping motion was to program Eq. (18) in Mathcad. Mathcad software includes a differential equation solver. It was quite simple to use Mathcad's Runge-Kutta methodology to perform a time history. It was necessary, however, to perform the radial integration at each time step, and this slowed the process down somewhat. I set the time integration to azimuth (ψ) steps of 1 degree and let the solution end after 40 revolutions. I used 40 revolutions so that flapping behavior with a slowly oscillating shaft motion was accurately captured. One computation took 30 seconds.

I should point out that the radial integration can be performed in closed form for any given azimuth station (ψ_n). You might suspect this by first studying the equation for inflow (U_P), which, from Eq. (3), is $U_P = \lambda - x\frac{d\beta}{d\psi} - \mu\beta\cos\psi + x\frac{d\Theta}{d\psi}\cos\psi$. The two dependent variables ($d\beta/d\psi$) and (β) become immediately apparent, and this suggests that Eq. (18)'s aero moment can be broken into three integrals so that

$$(19) \qquad \frac{1}{I_{flap}\Omega^2}\left(M_{aero}\right)_\psi = \frac{\gamma}{2}\left[K0_\psi + K1_\psi\frac{d\beta}{d\psi} + K2_\psi\beta\right].$$

Secondly, the blade pitch angle (θ) given by Eq. (3) contains a linear twist term ($x\theta_t$), and you can, therefore, regroup the blade pitch angle to read

$$(20) \qquad \begin{aligned}\theta &= \theta_0 + x\theta_t - B_{1C}\sin\psi - A_{1C}\cos\psi + \frac{\Delta\theta}{\Delta\beta}\beta \\ &= \left[\theta_0 - B_{1C}\sin\psi - A_{1C}\cos\psi + \frac{\Delta\theta}{\Delta\beta}\beta\right] + x\theta_t = \theta_b + x\theta_t.\end{aligned}$$

Keep in mind that from trigonometry you have $\sin\theta = \sin\theta_b\cos\left(x\theta_t\right) + \cos\theta_b\sin\left(x\theta_t\right)$ and $\cos\theta = \cos\theta_b\cos\left(x\theta_t\right) - \sin\theta_b\sin\left(x\theta_t\right)$. This step shows that integrals of the form $x^n\sin(x\theta_t)$ and $x^n\cos(x\theta_t)$ are required.

Do not overlook the fact that a portion of the pitch angle is controlled by the pitch-flap coupling term $\left(\frac{\Delta\theta}{\Delta\beta}\beta\right)$. When the time integration is performed, this coupling term leads to products of flap angle times flap angle rate, as well as the square of the flap angle. This means the basic differential equation is nonlinear.

A little algebra shows you that the three time-varying parameters in Eq. (19) are

$$(21) \qquad K0_\psi = \int_0^1\left(U_T^2\sin\theta\right)x\,dx + \int_0^1\left[\left(\lambda + x\frac{d\Theta}{d\psi}\cos\psi\right)U_T - X_{pr}\frac{d\Theta}{d\psi}\sin\psi\right]x\cos\theta\,dx$$

$$K1_\psi = -\int_0^1 U_T x^2\cos\theta\,dx \qquad K2_\psi = -\mu\cos\psi\int_0^1 U_T x\cos\theta\,dx$$

where, to repeat, $U_T = x + \mu\sin\psi - X_{pr}\frac{d\Theta}{d\psi}\sin\psi$.

Calculating Thrust and H-Force

Once the blade flap angle (β) and the flap angle azimuth derivative ($d\beta/d\psi$) are found for many revolutions, then the inflow (U_P), inplane velocity ratio (U_T), and blade pitch angle (θ) are available for any radial station ($x = r/R$) and azimuth angle (ψ). And then the thrust and H-force are relatively easy to calculate.

Following Eq. (2), the thrust of one blade, neglecting blade element profile drag (D_o), is

$$(22) \qquad T_\psi = \left(\tfrac{1}{2}\rho V_t^2\right) acR \int_0^1 \left[U_T^2 \sin\theta + U_P U_T \cos\theta \right] dx \qquad \text{if } \beta \text{ is a small angle.}$$

The calculation of H-force needs a little more discussion because there are two blade element forces involved. H-force acts in a plane normal to the shaft (i.e., the rotor disc plane), so the two blade element forces (dL) and (dD) must be resolved into that plane. Let me start with the force geometry shown in Fig. E-2.

From Fig. E-2, you have the blade element force ($dF_{tangential} = dD_o \cos\phi - dL \sin\phi$). This force projects directly onto the rotor disc plane without regard to the flap angle. Because the flap angle will, most likely, not be zero, there is a component of the blade element force ($dF_{normal} = dL \cos\phi + dD_o \sin\phi$) directed towards the centerline of rotation. The projection of this force onto the rotor disc plane is by the sine of the flap angle. The rotor system's H-force is a little more involved because both forces must be resolved to the H-force axis. Following Fig. E-2, you arrive at a blade element's H-force at radial station (x) varying with azimuth as

$$(23) \qquad dH_\psi = dF_{tangential} \sin\psi - dF_{normal} \sin\beta \cos\psi \approx dF_{tangential} \sin\psi - \beta\left(dF_{normal} \cos\psi\right) \qquad \text{if } \beta \text{ is a small .}$$

All that remains is to integrate from the blade root ($x = 0$) to the tip ($x = 1$) to obtain the contribution of one blade's H-force to the rotor system's total H-force.

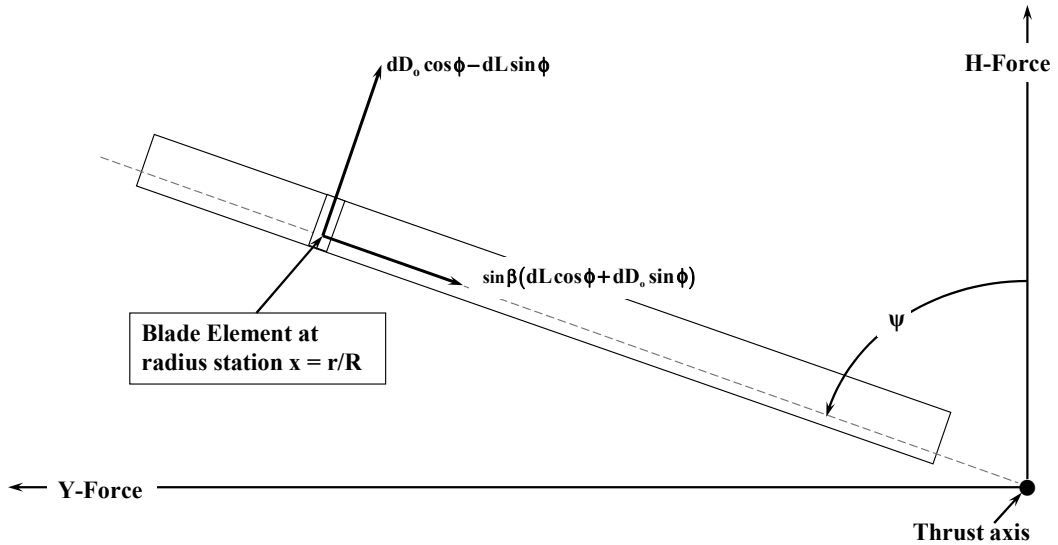

Fig. E-2. The view of the rotor disc plane when looking down the shaft from upstream. Forces shown lie in the rotor disc plane; thrust force is pointing at you.

Calculating Blade Element Profile Drag

As I have mentioned, I have simply ignored blade element profile drag in this introductory material about how shaft motion affects blade flapping, thrust, and H-force. But Castle and New found an interesting way of including blade element profile drag in their NACA TN 2656. They began by discarding the classical assumption that

(24) $\text{Airfoil } C_d = C_{do} + \delta_1\alpha + \delta_2\alpha^2$

and chose instead a Fourier series curve fit assuming

(25) $\text{Airfoil } C_d = \varepsilon_0 + \varepsilon_1 \sin\alpha + \varepsilon_2 \cos\alpha$.

Today, their choice in 1952 that $C_d = 0.8439 - 0.0126\sin\alpha - 0.8349\cos\alpha$ does not look very satisfactory for angles of attack greater than 15 degrees as you can see from Fig. E-3. I would suggest that a more accurate approximation for angles of attack beyond 15 degrees would be

(26) $C_d = 0.01+1.75\ (\sin\alpha)^2$.

The joining of Eqs. (25) and (26) at a 15-degree angle of attack produces a jump in airfoil drag coefficient that roughly approximates blade element stall.

Now in calculating blade element forces ($dF_{tangential}$ and dF_{normal}) you need $dD_o \sin\phi$ and $dD_o \cos\phi$. Therefore, you start with

(27) $dD_o = \left(\tfrac{1}{2}\rho V_t^2\right)\left(U_T^2 + U_P^2\right)(cRdx)C_d$,

which expands to two terms given Eq. (26). That is, you have

$$\begin{aligned} dD_o &= \left(\tfrac{1}{2}\rho V_t^2\right)\left(U_T^2 + U_P^2\right)(cRdx)C_{do} \\ &\quad + \left(\tfrac{1}{2}\rho V_t^2\right)\left(U_T^2 + U_P^2\right)(cRdx)\delta_1 \sin^2(\theta+\phi). \end{aligned} \tag{28}$$

Because the inflow angle (ϕ) is the arc tangent of U_P/U_T, it follows, after a little trigonometry, that

$$\begin{aligned} dD_o \sin\phi &= \left(\tfrac{1}{2}\rho V_t^2\right)(cRdx)C_{do}\left\{U_P\sqrt{U_T^2 + U_P^2}\right\} \\ &\quad + \left(\tfrac{1}{2}\rho V_t^2\right)(cRdx)\delta_2\left\{\frac{U_P}{\sqrt{U_T^2 + U_P^2}}\left[U_P^2\cos^2\theta + U_T U_P \sin(2\theta) + U_T^2\sin^2\theta\right]\right\} \end{aligned} \tag{29}$$

and

$$\begin{aligned} dD_o \cos\phi &= \left(\tfrac{1}{2}\rho V_t^2\right)(cRdx)C_{do}\left\{U_T\sqrt{U_T^2 + U_P^2}\right\} \\ &\quad + \left(\tfrac{1}{2}\rho V_t^2\right)(cRdx)\delta_2\left\{\frac{U_T}{\sqrt{U_T^2 + U_P^2}}\left[U_P^2\cos^2\theta + U_T U_P \sin(2\theta) + U_T^2\sin^2\theta\right]\right\}. \end{aligned} \tag{30}$$

You can now clearly see that including airfoil profile drag in the problem (in the 1950s) was not going to be easy. But today with a digital computer, adding only a few extra lines of code to include accurate airfoil properties is nearly a trivial task.

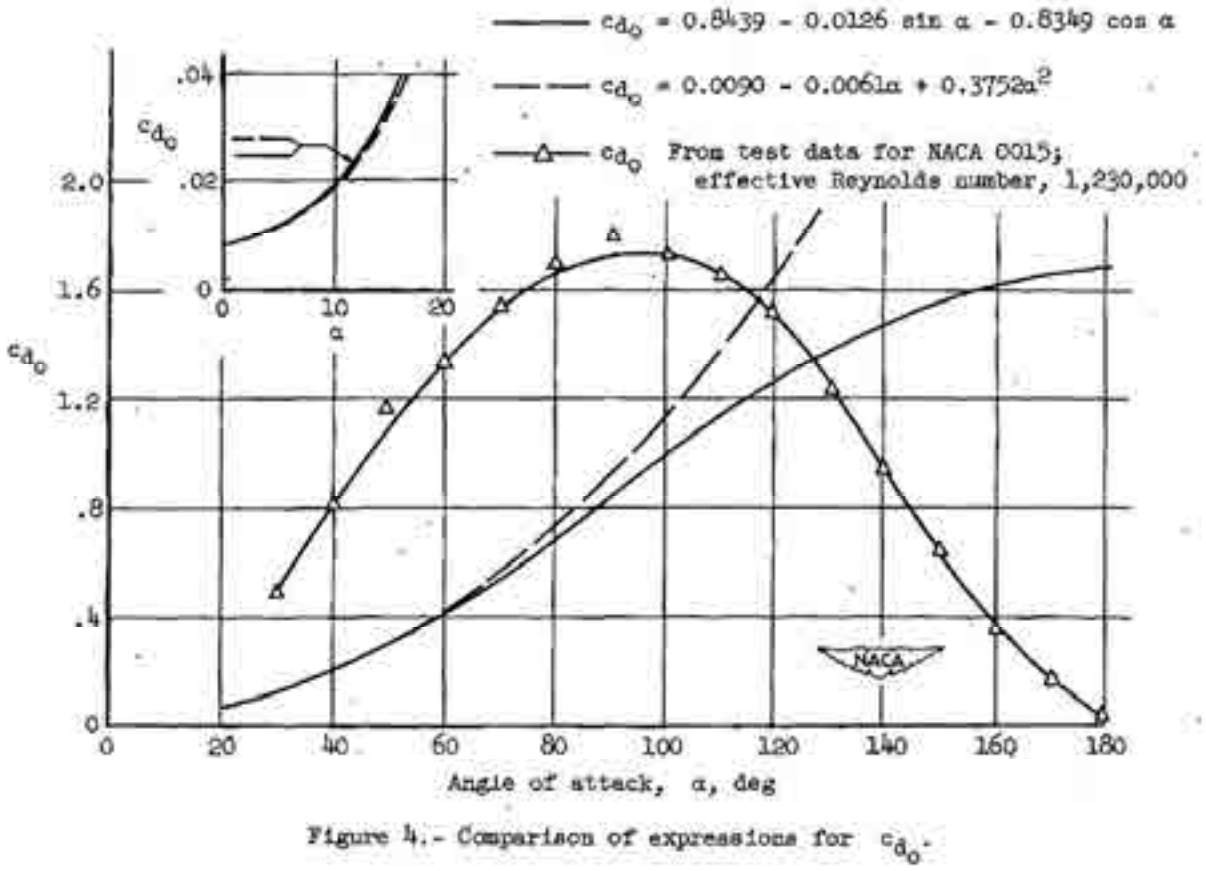

Figure 4.- Comparison of expressions for c_{d_o}.

Fig. E-3. Castle and New's airfoil drag coefficient approximation in 1952 (see NACA TN 2656).

Table E-1. Bell XV-3's Teetering Rotor Properties Used for Shaft Motion Calculations

Item	Symbol	Units	Values	Notes
Diameter	D	ft	23	
Chord	c	ft	0.9167	11/12
Blade twist	θ_t	deg	– 40	washout
Tip speed	V_t	ft/sec	390	RPM = 324, Ω = 33.9292 rad/sec
Airfoil lift curve slope	a	per radian	5.73	
Delta-3	δ_3	deg	+ 20	$\Delta\theta/\Delta\beta$ = – 0.36397
Density altitude	h_D	ft	7,500	ρ = 0.001898 slug/ft^3
Flap inertia	I_F	slug-ft^2	82.7	per blade
Lock number	γ	nd	2.1084	$\gamma = \rho acR^4/I_F$
Hub-to-tilt-axis distance	Xpr	ft	3.76	

A Simple Analytical Experiment

Suppose you have a two-bladed rotor system where each (nearly rigid) blade is attached to the hub with a flapping hinge at or very near the center of rotation. Both blades are as nearly identical as manufacturing can achieve. The properties of the XV-3's blades in Table E-1 are a representative basis for a model rotor system.

This rotor system is mounted at the free end of a shaft that is 3.76 feet long (X_{pr} = 3.76/11.5 = 0.327) as measured from the tilt axis to the hub centerline. The shaft is given a sinusoidal pitching motion by some sort of actuator such that the shaft pitching motion can be described by

$$\Theta_t = \Theta_{amp} \sin\left[(pf)t\right]$$

$$\text{so} \quad \frac{d\Theta}{dt} = \Theta_{amp}(pf)\cos\left[(pf)t\right] \quad \text{or} \quad \frac{d\Theta}{d\psi} = \Theta_{amp}(\nu)\cos\left[(\nu)\psi\right] \tag{31}$$

$$\text{and} \quad \frac{d^2\Theta}{dt^2} = -\Theta_{amp}(pf)^2 \sin\left[(pf)t\right] \quad \text{or} \quad \frac{d^2\Theta}{d\psi^2} = -\Theta_{amp}(\nu)^2 \sin\left[(\nu)\psi\right].$$

The differential equation used to find the flapping motion established from Eqs. (18) and (19) is

$$\frac{d^2\beta}{d\psi^2} + \varpi^2\beta = \frac{\gamma}{2}\left[K0_\psi + K1_\psi \frac{d\beta}{d\psi} + K2_\psi \beta\right] \tag{32}$$
$$-2\Theta_{amp}(\nu)\cos\left[(\nu)\psi\right]\sin\psi - \Theta_{amp}(\nu)^2 \sin\left[(\nu)\psi\right]\cos\psi$$

where, because the experiment is conducted at zero forward speed (i.e., μ and λ are zero), you have from Eq. (3)

$$U_T = x - X_{pr}\frac{d\Theta}{d\psi}\sin\psi \qquad U_P = -x\frac{d\beta}{d\psi} + x\frac{d\Theta}{d\psi}\cos\psi \qquad \theta = \theta_0 = 0, \tag{33}$$

which gives the simplification

$$K0_\psi = \int_0^1 \left[\left(x\frac{d\Theta}{d\psi}\cos\psi\right)U_T - X_{pr}\frac{d\Theta}{d\psi}\sin\psi\right]x\,dx \tag{34}$$

$$K1_\psi = -\int_0^1 U_T x^2\,dx \qquad K2_\psi = 0$$

Creating such a simple problem means that the radial integrals of the time-varying constants can be written out in longhand, and the aerodynamic flapping moment term is

$$\frac{1}{I_{flap}\Omega^2}M_{aero} = \frac{\gamma}{2}\left[\frac{1}{4}\cos\psi\frac{d\Theta}{d\psi}\right] - \frac{\gamma}{2}\left[\frac{X_{pr}}{3}\cos\psi\left(\frac{d\Theta}{d\psi}\right)^2\right] - \frac{\gamma}{2}\left[\frac{1}{4} - \frac{X_{pr}}{3}\sin\psi\frac{d\Theta}{d\psi}\right]\frac{d\beta}{d\psi}. \tag{35}$$

Note that the flap damping is clearly identified. Now when you substitute Eq. (35) into Eq. (13) and move the flap damping term to the left-hand side of this mass-damper-spring problem, the flapping differential equation to be solved is

$$\frac{d^2\beta}{d\psi^2}+\frac{\gamma}{8}\left[1-\frac{4}{3}X_{pr}\sin\psi\frac{d\Theta}{d\psi}\right]\frac{d\beta}{d\psi}+\beta=\frac{\gamma}{2}\left[\frac{1}{4}\cos\psi\frac{d\Theta}{d\psi}\right]-\frac{\gamma}{2}\left[\frac{X_{pr}}{3}\cos\psi\left(\frac{d\Theta}{d\psi}\right)^2\right] \tag{36}$$
$$-2\frac{d\Theta}{d\psi}\sin\psi+\frac{d^2\Theta}{d\psi^2}\cos\psi$$

where $\Theta_\psi=\Theta_{amp}\sin\left[(\nu)\psi\right]$ and $\nu=pf/\Omega$

$$\frac{d\Theta}{d\psi}=\Theta_{amp}(\nu)\cos\left[(\nu)\psi\right] \quad \text{and} \quad \frac{d^2\Theta}{d\psi^2}=-\Theta_{amp}(\nu)^2\sin\left[(\nu)\psi\right].$$

Two approaches to solving Eq. (36) can be taken for this simple problem. The first is to give the problem to Mathcad or some other product such as Wolfram's *Mathematica*. The second approach is to ignore the nonlinear terms created by including the hub-to-tilt-axis distance (Xpr) effect and then solve the force vibration problem with classical mathematics. In this second approach, Eq. (36) is reduced to

$$\frac{d^2\beta}{d\psi^2}+\frac{\gamma}{8}\left[1-\frac{4}{3}X_{pr}\sin\psi\frac{d\Theta}{d\psi}\right]\frac{d\beta}{d\psi}+\beta=\frac{\gamma}{2}\left[\frac{1}{4}\cos\psi\frac{d\Theta}{d\psi}\right]-\frac{\gamma}{2}\left[\frac{X_{pr}}{3}\cos\psi\left(\frac{d\Theta}{d\psi}\right)^2\right] \tag{37}$$
$$-2\frac{d\Theta}{d\psi}\sin\psi+\frac{d^2\Theta}{d\psi^2}\cos\psi.$$

The classical solution to Eq. (37) is somewhat messy, but it can be "programmed" in Microsoft® Excel® with very little effort using the following equations:

$$\beta=A1_S\sin\left[(1-\nu)\psi\right]+A1_C\left[\cos(1-\nu)\psi\right]+A2_S\sin\left[(1+\nu)\psi\right]+A2_C\left[\cos(1+\nu)\psi\right] \tag{38}$$

where

$$A1_S=\frac{Fl_S\left[1-(1-\nu)^2\right]+Fl_C\left[\frac{\gamma}{8}(1-\nu)\right]}{D} \qquad A1_C=\frac{Fl_C\left[1-(1-\nu)^2\right]-Fl_S\left[\frac{\gamma}{8}(1-\nu)\right]}{D} \tag{39}$$
$$Fl_S=-\frac{1}{2}\nu(2-\nu)\Theta_{amp} \qquad Fl_C=\frac{\gamma}{16}\nu\Theta_{amp} \qquad D=\left[1-(1-\nu)^2\right]^2+\left[\frac{\gamma}{8}(1-\nu)\right]^2$$

and

$$A2_S=\frac{F2_S\left[1-(1+\nu)^2\right]+F2_C\left[\frac{\gamma}{8}(1+\nu)\right]}{D} \qquad A2_C=\frac{F2_C\left[1-(1+\nu)^2\right]-F2_S\left[\frac{\gamma}{8}(1+\nu)\right]}{D} \tag{40}$$
$$F2_S=-\frac{1}{2}\nu(2+\nu)\Theta_{amp} \qquad F2_C=\frac{\gamma}{16}\nu\Theta_{amp} \qquad D=\left[1-(1+\nu)^2\right]^2+\left[\frac{\gamma}{8}(1+\nu)\right]^2$$

My comparison of the Mathcad numerically integrated solution, which includes X_{pr} = 0.327, to the closed-form solution given by Eqs. (38), (39), and (40), shows indistinguishable graphical results for the flapping motion. This may not be true for a test in a wind tunnel with the wind on. Of course, in forward flight, the influence of hub distance from the oscillating axis will be very important because the moment produced by H-force will depend on this distance. However, it is not clear that the H-force itself is significantly affected by X_{pr} in forward flight.

Imagine now that a simple test is carried out where a blade's flapping motion in response to the shaft's pitching motion with time is recorded digitally. The model itself can have blades of any convenient size because the controlling parameter is Lock number $\left(\rho acR^4/I_{flap}\right)$. You might also try one counterbalanced blade just for the fun of it. Probably the blade(s), hub, and drive system could come from any one of several electric-powered model helicopters on the market. The motor and its shaft probably need to be oscillated in pitch or yaw with some sort of actuator. A sketch of the model I have in mind is shown in Fig. E-4. Only one blade's flapping motion needs to be measured.

The test variables are the amplitude of the shaft pitching motion (Θ_{amp}) and the pitching frequency (pf) divided by rotor speed (Ω) denoted by (ν), which is unit-less.

Suppose you start the test with model flapping blade(s) having a Lock number of $\gamma = 2$ and select testing at Θ_{amp} = 5 degrees (0.08727 radians to be used in the analysis). Then measure flapping response with pitching frequencies of ν = 0.25, 0.50, 0.75, 1.00, and 1.25. Figs. E-5, -6, -7, -8, and -9 show my theoretical results. I wonder what the test results look like in comparison to the theoretical results you have before you.

To me, the preceding investigation is a very good assignment for any young engineer interested in rotorcraft. He or she might start by confirming my theoretical results. After all, it is not a foregone conclusion that my work is correct.

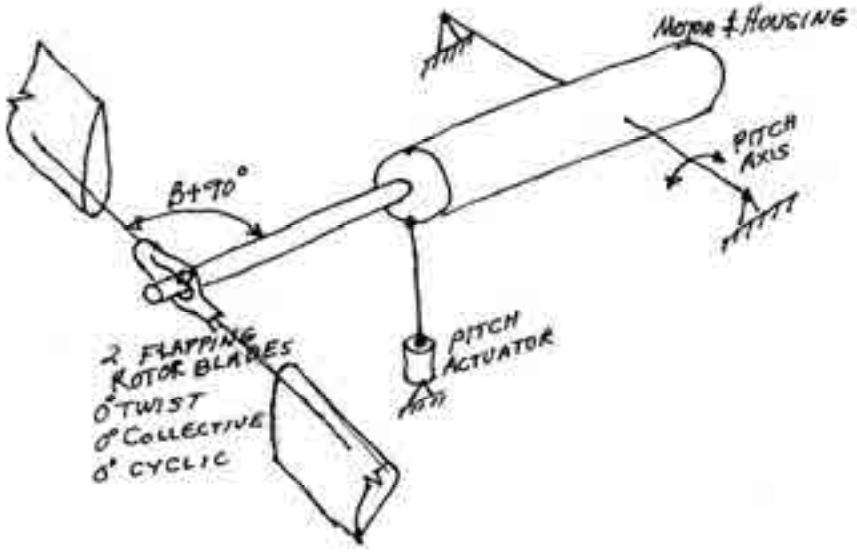

Fig. E-4. Simple oscillating shaft model assembly for experiment.

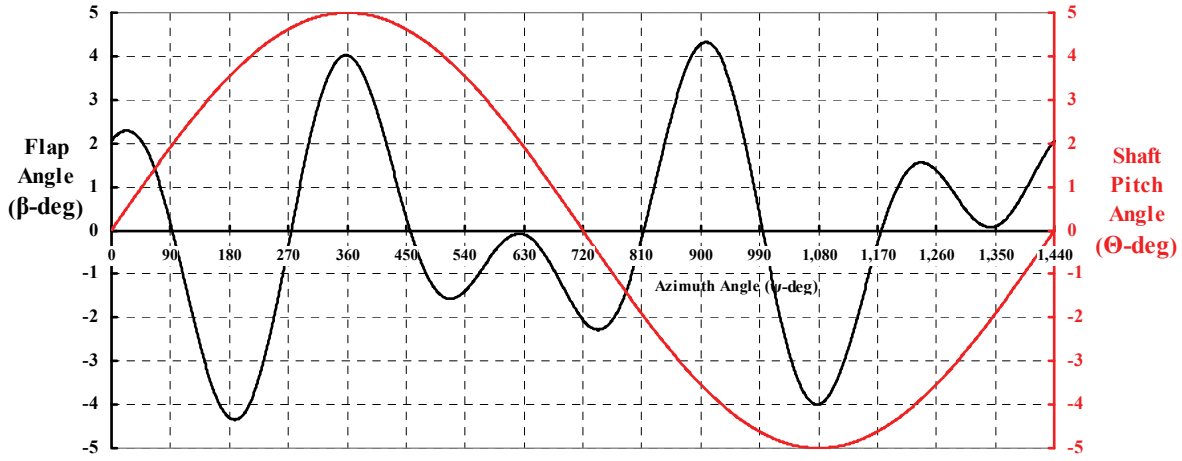

Fig. E-5. Case One: ν = 0.25, Θ_{amp} = 5 deg, X_{pr} = 0.327, Lock number = 2.

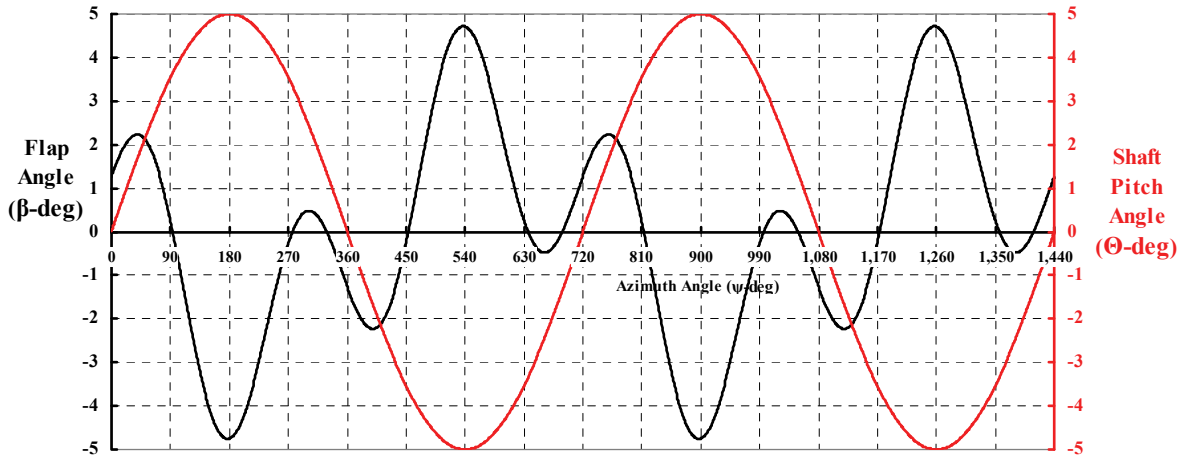

Fig. E-6. Case Two: ν = 0.50, Θ_{amp} = 5 deg, X_{pr} = 0.327, Lock number = 2.

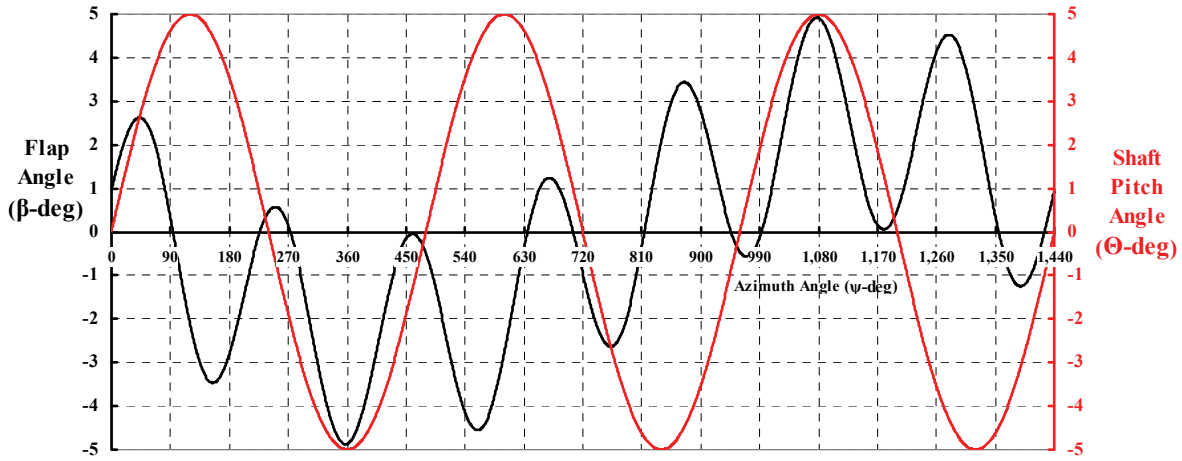

Fig. E-7. Case Three: ν = 0.75, Θ_{amp} = 5 deg, X_{pr} = 0.327, Lock number = 2.

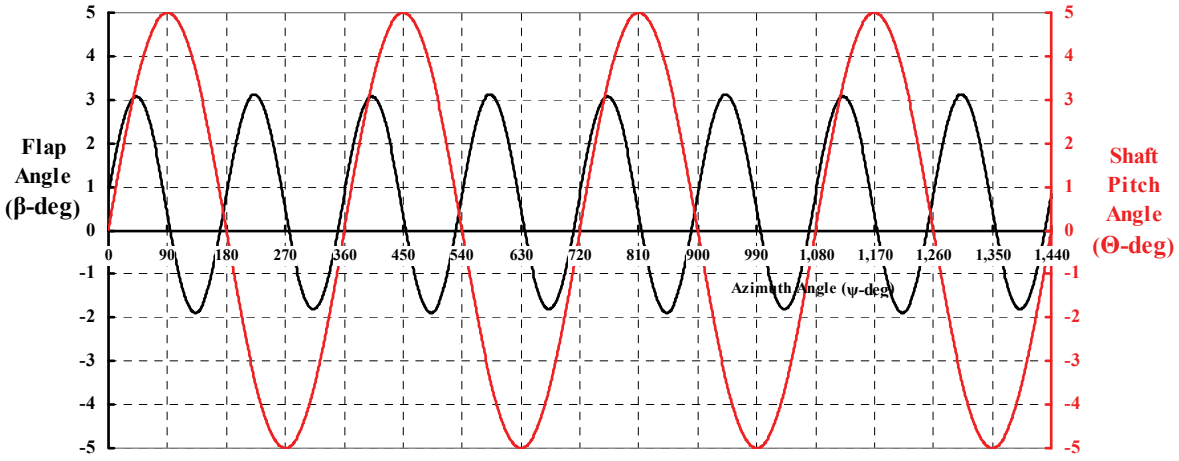

Fig. E-8. Case Four: ν = 1.00, Θ_{amp} = 5 deg, X_{pr} = 0.327, Lock number = 2.

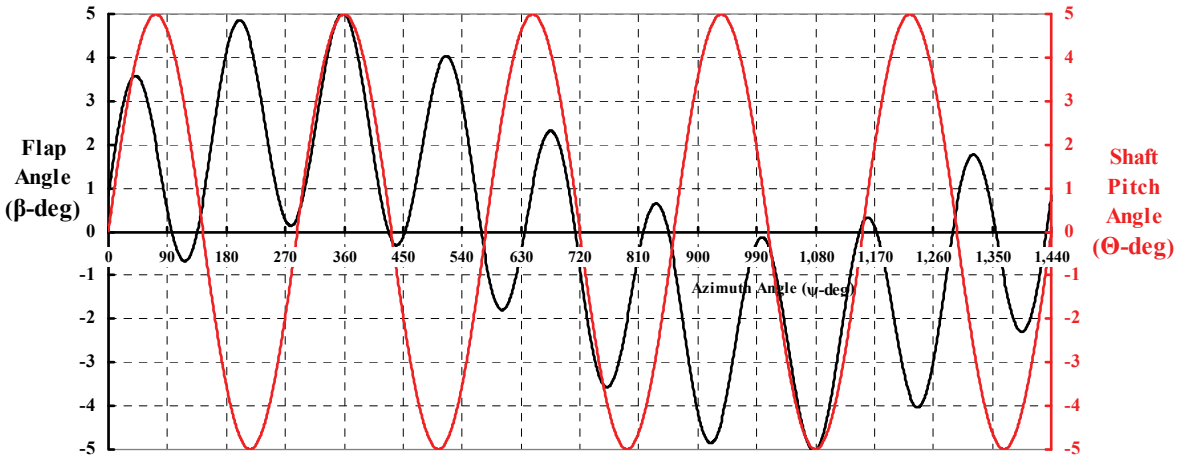

Fig. E-9. Case Five: ν = 1.25, Θ_{amp} = 5 deg, X_{pr} = 0.327, Lock number = 2.

APPENDIX F
KEN WERNICKE'S LETTER ABOUT THE DEVELOPMENT OF THE XV-3

Ken Wernicke gained first-hand experience about tiltrotors early in his career at Bell Helicopter. This was the period when Bob Lichten was the driving force behind the tiltrotor concept. Later, Ken used this experience to guide development of Bell's XV-15. To me, Ken was *the chief engineer* of the XV-15, which—I would say—was one of the most, if not *the* most, successful concept demonstrators the rotorcraft industry has ever seen. Without the XV-15, the U.S. Marines would not be flying their MV-22Bs in combat today.

In early 2014, I had several phone conversations with Ken about parts of my understanding of the XV-3's longitudinal stability (see paragraph 2.13.2.2 starting on page 222). Ken was kind enough to send me his views in a handwritten letter that passed on invaluable historical background and very important technical notes. I received his letter on July 28, 2014. His letter, now in type with some editing by me, reads as follows:

1. Start of the Development of the XV-3 Convertiplane With Three-Bladed Fully Articulated Rotors

Bell's development of the XV-3 convertiplane started with a concentrated effort, much like Transcendental's, to "lick" the problem of mechanical instability.[1] What Bell's engineers actually did at the start and finish of the long ground development program to tame mechanical stability is not known at this time. But even before the roll-out of the first aircraft on February 10, 1955, they were testing a single rotor on a whirl stand. Snubber cables were used to cinch down the pylon when instability was encountered. Prior to flight, the aircraft was mounted on a tie-down test stand, Fig. F-1. This test stand had snubber cables that could cinch down the right- and left-hand pylons in helicopter and airplane pylon positions.

After almost a half of a year of tie-down testing, Floyd Carlson, chief pilot from the first Bell Helicopter until his retirement, made the first hover on August 11, 1955. Floyd noticed a vibration that was thought to be associated with mechanical instability, so the aircraft went back on tie-down for almost a year to tame mechanical instability. Items that could be varied included the elastomeric pylon mounting spring rates in pitch and lateral, the pylon dampers in pitch and lateral, the dampers about the lag hinges, the rotor shaft length, the wing struts, and the blade pitch flap coupling (δ_3) and the blade pitch lag coupling ratios. The blade pitch coupling offered the possibility of providing aerodynamic damping.

[1] Mechanical instability is discussed in Technical Note 1 at the end of Ken's letter.

Fig. F-1. Ground tests to develop a stable rotor-pylon (from Bob Lynn's 1992 Nikolsky Lecture).

Flying started in June 1956 with several more returns to ground tie-down testing. On October 25, 1956, with Dick Stansbury as the test pilot, while in forward flight after tilting the pylons forward 20 degrees at a speed of 80 knots, a mechanical instability commenced and Dick got to the ground as quickly as possible, making a crash landing that destroyed the aircraft (Fig. F-2) and broke his back. Dick was crippled for the rest of his life and worked in engineering until retirement. (A comment made by Bob Lichten was overheard; he said a small change had been made to the blade pitch coupling without retesting on tie-down.) After 2 years, Bell gave up on the development of the three-bladed articulated rotor, but not the convertiplane.

Fig. F-2. October 25, 1956 was a black day in the history of the XV-3 program (from Jay Miller's article in Aerophile, vol. 2, no. 1, June 1979).

2. Development With the Two-Bladed Stiff-Inplane Rotor

The decision was made to terminate the development (to tame mechanical instability) of the articulated rotor and to proceed with the second XV-3 using two-bladed semi-rigid rotors that were free to flap about a see-saw hinge and stiff enough to have the blade chord bending motion (i.e., the lead-lag mode of motion) above rotor speed. With the blade lead-lag mode frequency above 1/rev, mechanical instability is not possible.

Two-bladed rotors had been used on all prior Bell helicopters. (However, operation of a two-bladed stiff-inplane rotor at the RPM of the pylon mounting frequencies can have a self-excited instability if the fore and aft and lateral mounting frequencies are identical.) Even so, much more development was required to achieve stable rotor and pylon dynamics on the XV-3. Twenty months passed from the start of ground whirl tests until the start of uninterrupted flight envelope expansion. In addition to ground and flight tests, two series of tests were made with the XV-3 in the NASA Ames 40- by 80-Foot Full-Scale Wind Tunnel.

A 100-hour ground whirl test with one rotor was started on April 22, 1957 (Fig. F-3). Rotor "weaving" was encountered, and more mass balance weights had to be added to the blades' leading edges to resolve the problem. Weaving was a little-understood problem that had occurred on all Bell helicopters up to the XH-40 (Huey). Weaving is a wobbling of the rotor disc plane (i.e., subharmonic disc tilting that can be rapidly divergent).[2]

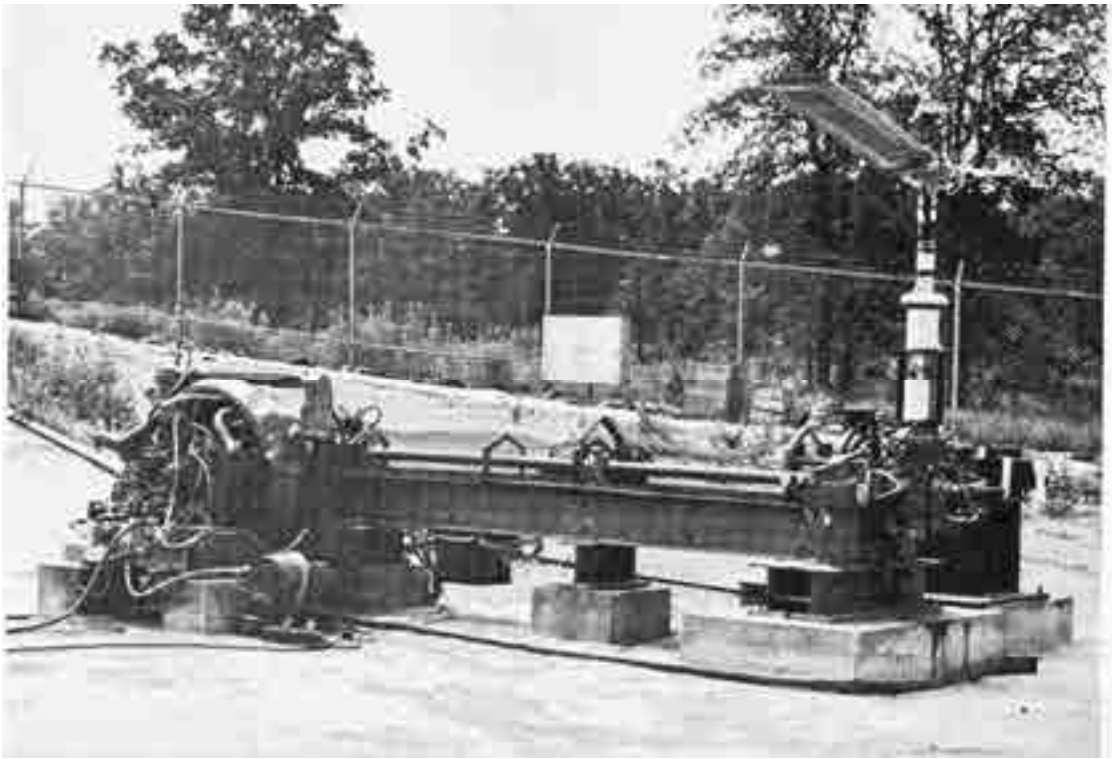

Fig. F-3. XV-3 ground testing of the two-bladed configuration began with testing of just one rotor assembly (from AHS Newsletter, vol. 6, no. 6, June 1960).

[2] A detailed explanation of rotor weaving is given in Technical Note 2 at the end of Ken's letter.

Mark W. Kelly, the NASA Ames Full-Scale Wind Tunnel Branch Chief, was eager to help and was a strong believer in the convertiplane concept. He suggested that they could put the XV-3 in the tunnel and that the tunnel was available. So, to reduce the flight risk, Bell decided to take the opportunity and immediately readied the aircraft and added mount points—a very fortunate decision.

The XV-3 was airlifted to the tunnel and remote controllers installed. Tunnel testing started on September 6, 1957, and continued for 6 weeks (Fig. F-4). The XV-3 was tested up to 100 knots with 10 degrees of forward pylon tilt, but with 60 degrees (30 degrees from airplane) or more tilt, it wasn't possible to go more than 70 knots without encountering low-frequency (1.5 to 2.2 cps) fore and aft motions of the pylons and rotor disk planes. What and why was not known. It was called pylon rock. Now we can surmise that it was what we have come to call proprotor-pylon instability. This is an instability caused by the negative damping (unstable) resulting when the proprotor is pitching at high inflow and producing inplane H-forces. The H-force produces unstable damping moments about the pylon pitching axis.[3]

Not knowing what was causing the oscillations, it was decided to shorten the masts 26 inches, which would increase the pylon longitudinal and lateral frequencies by 60 percent and make the pylon dampers more effective. This was exactly the right thing to do to increase the damping of the proprotor-pylon stability. Not only was increasing the frequency a big help, but shortening the mast 26 inches reduced the moment arm of the destabilizing rotor's H-force by 38 percent. The result was stability at 90-degree pylon (airplane position) to 110 knots where rotor weaving was encountered. The addition of more mass balance to the blades' leading edges resolved this problem, and the XV-3 operated satisfactorily up to the maximum tunnel speed then available of 150 knots. Then the rotor diameter was decreased from 25 to 23 feet to hopefully increase the stability further and increase the propulsive efficiency.

Fig. F-4. The XV-3's first entrée into NASA's 40- by 80-foot wind tunnel started on September 6, 1957 (from AHS Newsletter, vol. 6, no. 6, June 1960).

[3] See Technical Note 3 at the end of Ken's letter.

Now much data was collected throughout the helicopter conversion and airplane modes to measure and define performance and longitudinal control and static stability characteristics (NASA TN D-35). Drag was 25 percent higher than measured in the 1/4-scale-model wind tunnel tests. Propulsive efficiency was as high as 78 percent when using the gearshift to reduce RPM to 62 percent from helicopter RPM.

The XV-3 was shipped back to Bell in Fort Worth, Texas, by C-130 and made the first hover with the two-bladed rotors on January 21, 1958. It was determined that there was "insufficient longitudinal control," and the control system was modified to increase the fore and aft cyclic pitch. As a result, the effective control system stiffness at the rotor head was much reduced. Envelope expansion was started with Bill Quinlan, the test pilot, but was suspended after weaving was encountered on May 6, 1958, at a pylon angle of 60 degrees (30 degrees from airplane). Since this had not occurred in the wind tunnel, it must have been the result of the decrease in control system stiffness. It is now believed that if the blades had been properly mass balanced, control system stiffness would not have mattered. It was decided to do a direct analog computer study of the XV-3 rotor and pylon dynamics system and go back to the full-scale tunnel before flying again. Jim Gean did the analog study at Computer Engineering Associated. Jim found that appreciable damping of weaving could be obtained by 1) increasing control system stiffness, 2) removing the collective-pitch force-reducing counterweights from the blades, 3) increasing hub and blade chordwise stiffness, and 4) moving the blade chordwise center of gravity toward the leading edge (more balance). The XV-3 went back to the wind tunnel, and on October 7, 1958, the test began—this time with Bill Quinlan, the Bell test pilot, operating the XV-3 from inside the cockpit. First the weaving encountered in flight was duplicated in the tunnel, and then the cyclic pitch controls were stiffened. This made the proprotor stable throughout the predicted operating range, and a further increase in damping by removal of the counterweights provided sufficient damping for even higher speeds and allowed operation to the then maximum tunnel speed of 150 knots. Increasing mass balance and blade chordwise stiffness were not evaluated.

Bill Quinlan was then able to gain experience flying in the wind tunnel doing conversions and gear shifts from helicopter to airplane rotor speeds. Air Force pilot Captain Bob Ferry and NASA test pilot Fred Drinkwater also gained experience flying the XV-3 in the tunnel. Testing was completed on October 24, 1958, and the XV-3 returned to Bell via C-130.

On December 18, 1958, the XV-3, with Bill Quinlan flying, made the first complete in-flight conversion—at long last. Vertical fin area was added to provide Dutch roll damping in airplane flight. The unstable yaw damping was coming from the proprotor H-forces, which we discovered later.

On April 24, 1959, Bell's envelope expansion including stalls and rolling takeoffs and landings, with "roller skates" installed on the strut tubes, was completed, and the XV-3 was dismantled for shipment to Edwards Air Force Base in California for start of government flight evaluations.

Technical Note 1.
Explanation of Mechanical Instability and Its Challenge to the Convertiplane

Mechanical instability, commonly called "ground resonance," had been encountered with the fully articulated rotors on autogyros and helicopters in the 1930s and was fully understood and "tamed" by the 1940s.

The possibility of a mechanical instability occurs when the lateral motion of the helicopter, rocking on its landing gear, couples with the blade lead-lag motion in the plane of the rotor. This happens when the natural frequency of these two modes of motion coalesce. For example, a three-bladed rotor has a lag hinge offset of 5 percent of rotor radius, which gives the lead-lag natural frequency of each of the blades as 25 percent of the rotor's RPM at all RPMs. (Greater hinge offsets give a higher lag natural frequency.) If the blades oscillate at their natural frequencies about their lag hinges in an unsymmetrical pattern, a rotating unbalance is produced with a resulting whirling radial force pulling on the hub at a frequency of 25 percent rotor RPM. Say the operating RPM in flight is 240. Then this whirling radial force will be 0.25×240 rpm as viewed in the rotating system. This force felt in the fixed system by the airframe and landing gear will be at a frequency of once per RPM (1/rev) higher [60 + 240 = 300 rpm], or at a frequency of 1/rev lower [60 – 240 = 180 rpm]. Now suppose the lateral rocking frequency on the landing gear is 80 rpm, so there is no coalescence. But as the rotor slows down, after landing, to an RPM of 106.7, with a lag frequency equal to 0.25×106.7 rpm in the rotating system with a radial whirling frequency in the airframe of 26.7 – 106.7 = 80 rpm, there is now a coalescence. This is more than a resonance and can be a disastrous self-excited instability that will diverge (blow up) unless there is sufficient damping in the landing gear shock struts and lag hinge dampers to contain it. This could occur in a vacuum, and that is why it is termed mechanical instability. The presence of air actually produces a small amount of damping via air drag on the blades. The value of damping required in the gear shock struts and lag dampers can be calculated from equations in NACA TR 1351. In spite of this, there have been a number of helicopters destroyed by ground resonance as a result of infrequent or incorrect maintenance of the shock struts and lag dampers.

Why then is mechanical instability a problem for the convertiplane with the thorough theory giving understanding and success when applied to the helicopter?

The challenge for the convertiplane is not ground resonance but the occurrence of mechanical instability in flight when the blade lead-lag motion can couple with an airframe resonant mode of vibration. The possibilities of coalescence are compounded by the range of RPM from helicopter mode to airplane mode (532 rpm/8.87 cps to 324 rpm/54 cps for the XV-3) and the variation of airframe natural frequencies as the pylon and rotor shaft tilt from vertical to horizontal. The pitching frequency of the pylon is determined by the series springs of the twisting of the wing with the pitching of the pylon about its elastomeric mounting to the wingtip, and to a lesser degree, with the wings' chordwise deflection when in helicopter mode (pylon and shaft vertical), and to a greater degree, with the beamwise deflecting wingtip in airplane mode. Similarly, the lateral hub motion (pylon roll in helicopter mode and pylon yaw in airplane mode) is a combination of the lateral elastomeric pylon springs with wing bending

stiffness in helicopters and chordwise bending in airplane mode. There are many more natural frequencies and airframe modes of motion in addition to the primary motion (first mode) of pylon pitching and yawing and rolling. For instance, in the case of pitching in airplane mode, the primary or first mode occurs with the wingtip bending up when the pylon is pitching up about its elastomeric mounting. The second natural mode occurs when the wingtip is bending down when the pylon is pitching up. This second mode has a higher frequency.

Now consider what the designers of the XV-3 were faced with. They had to provide for mechanical stability when passing quickly through each of these frequencies and starting or stopping the rotor and shifting from helicopter high-RPM to airplane low-RPM, as well as the possibility of steady operation at an RPM where the lag frequency minus rotor speed and/or the lag frequency plus rotor speed could be at or near one of the many airframe modes that involved hub translation.

Helicopter experiences had shown that damping in the landing gear (airframe) as well as the rotor lag motion were required to ensure stable mechanical dynamics. Soft-mounting the pylon to the wingtip provided a place to locate dampers as well as a means of isolating rotor vibrations. The shortcomings of this are that the dampers will only dampen the motion across the elastomeric mounts and not across the wing springs and, as the damper setting is increased, the motion across the elastomers and dampers decreases and the motion across the wing increases.

The softness of the elastomers is limited by static deflection requirements as well as frequency placement. The first consideration would be placing the fundamental modes (first modes) of pylon pitching, rolling, and yawing frequencies away from the operating RPMs to isolate vibration due to unbalance.

The pylon-pitch frequency could be set as high as 4.7 cps for pylon pitch giving excellent isolation of 1/rev out of balance at helicopter RPM, 8.87 cps, and acceptable isolation at airplane RPM, 5.4 cps. Placing the lateral pylon frequency the same as the pitch frequency would increase the susceptibility to mechanical instability passing through 4.7 cps when starting and stopping the rotor. Placing the lateral pylon frequency at 6.7 cps would give acceptable 1/rev isolation when operating either helicopter RPM, 8.87 cps, or airplane RPM, 5.4 cps. But this would be a bad situation for mechanical stability for operating continuously in helicopter mode at 532 rpm, 8.87 cps, placing the lag frequency (as viewed in the fixed system) at $0.25 \times 8.87 = 2.22 - 8.87 = 6.65$ cps, exactly at a lateral pylon frequency of 6.76 cps. So it would be better to raise the pylon frequency closer to the 8.87-cps helicopter rotor speed or lower closer to the airplane rotor speed of 5.4 cps.

Technical Note 2.
Rotor Weaving and Its Solution Explained

Rotor weaving had been a plague at Bell with all of its helicopters prior to the Huey. It was not then understood. On the helicopter, it was resolved by increasing the stiffness of the rotating controls and "tweaking" the stabilizer bar damper settings.

Weaving appears as a low-frequency wobbling of the tip path plane, and can be as much as several feet on a large rotor if not quickly arrested by dropping the collective pitch. When it takes place, the blades are flapping at the blade chordwise (i.e., lead-lag) natural frequency. If the chordwise frequency is 1.3 times rotor speed (1.3/rev), it appears to the observer in the nonrotating system as a 0.3/rev wobble of the tip path plane. This instability can occur when the blades are coned or bent up or down so that blade drag is either above or below the blade's feathering axis (i.e., the pitch change axis). As a result, drag will produce a blade pitch change depending on how compliant or stiff the control system is. Now with an incremental pitch change as a result of drag, this change will produce lift and more drag and a blade flapping moment. Hence, there is a feedback loop than can produce an instability showing up in unstable blade flapping at the blade chordwise frequency. However, this can only be unstable if the isolated blade, without a control system to restrain it, is statically unstable. Such a static instability is possible if the blade has its mass balance point aft of the blade quarter chord (more exactly, its aerodynamic center). If the blade as a total is mass balanced at the quarter chord or ahead, it will be statically stable, and a weaving instability is not possible.

Why then was Bell's helicopter plagued with weaving if simply properly mass balancing the blades would have eliminated weaving? Because in the early days, and even today, rotor blade designers thought that it wasn't necessary to balance the inboard blade sections where the airflow was low, and that balancing the outboard blade sections would be sufficient. However, if the outboard blade sections are only balanced to the quarter chord and there are inboard sections that are unbalanced, the blade as a whole is unbalanced and weaving is a possibility. The outboard sections must be overbalanced to account for the underbalanced inboard sections. This is done by weighting the radial stations proportionately to the dynamic pressure of the air flowing over each blade section.

The weighting for the condition in hover is simply $(\Omega r)^2$ or r^2 and also weighting by chord (c) for a tapered blade. Solution for the effective chordwise position, $\overline{c}_{mb}$, of the total blade mass relative to the spanwise line of aerodynamic centers is given by the following formula:

$$(1) \quad \overline{c}_{mb} = \frac{\sum_0^R \left(c_{cg} - c_{ac}\right)\left(\frac{\Delta w}{\Delta r}\right)\left(r^2\right)c\Delta r}{\sum_0^R \left(\frac{\Delta w}{\Delta r}\right)\left(r^2\right)c\Delta r} .$$

The weighting for the condition on the advancing blade in helicopter forward flight is simply $(r + R\mu)^2$. The solution for the effective position of the chordwise balance of the total blade is given by:

$$(2) \quad \overline{c}_{mb} = \frac{\sum_0^R \left(c_{cg} - c_{ac}\right)\left(\frac{\Delta w}{\Delta r}\right)\left(r + R\mu\right)^2 c\Delta r}{\sum_0^R \left(\frac{\Delta w}{\Delta r}\right)\left(r + R\mu\right)^2 c\Delta r} .$$

The weighting for the condition on the blade when acting as a propeller is $r^2 + R^2\lambda^2$. The solution for the effective portion of the chordwise balance of the total blade is then:

$$(3) \quad \overline{c}_{mb} = \frac{\sum_0^R \left(c_{cg} - c_{ac}\right)\left(\frac{\Delta w}{\Delta r}\right)\left(r^2 + R^2\lambda^2\right) c\Delta r}{\sum_0^R \left(\frac{\Delta w}{\Delta r}\right)\left(r^2 + R^2\lambda^2\right) c\Delta r}$$

where,

$\overline{c}_{mb}$ = effective chordwise position of blade mass relative to a spanwise line through the aerodynamic center (plus is aft and negative is forward, i.e., for stability less than or equal to zero inches).

c_{cg} = distance from leading edge (or a line parallel to a spanwise line through the aerodynamic centers of airfoils from the root to the tip for a tapered blade) to the center of gravity of the blade section at radius, r, in inches.

c_{ac} = distance from leading edge (or a line parallel to a spanwise line through the aerodynamic center of airfoils from the root to tip for a tapered blade) to the aerodynamic center of the blade airfoil section at radius, r, in inches.

r = radial distance to center of blade section, in inches.

c = blade chord at radius station, r/R, in inches.

$\Delta w/\Delta r$ = blade weight per unit radial distance at radius, r, in lb/in.

Δr = radial width of blade section at radius, r, in inches.

μ = forward speed of helicopter divided by tip speed = $V/\Omega R$.

λ = forward speed in airplane mode divided by tip speed = $V/\Omega R$.

If blades are mass balanced per the formulas above there will be no weaving, regardless of how soft the control system is or how far the drag of the blades are displaced away from the feathering axis. The more the blades are unbalanced, the stiffer the control system will have to be to prevent weaving depending on how far the blade drag is displaced away from the feathering axis.

As discussed above, mass balance is based on stabilizing a blade in the first flapping mode where beam flapwise bending is not a factor and mass balance can be placed inboard as well as outboard, but of course placing balance weight near the tip requires the least weight. Flutter is another consideration when deciding where to place the balance weight. If the bulk of the mass balance weight is located near the node point of the first bending mode (approximately a frequency of 3/rev) flutter in this mode would be possible. (I have witnessed such a flutter on two different types of two-bladed rotors in ground test.)

Technical Note 3.
Loss of Dutch Roll and Longitudinal Short-Period Damping Explained and Analyzed

Bob Lichten wanted to submit a convertiplane proposal for the Tri-Service VTOL competition in 1961 (won by the LTV-Hiller-Ryan team and resulting in the XC-142 Tiltwing). He came to me and said, "You must figure out the cause and come up with a solution for the longitudinal short-period and Dutch roll low-damping stability problem identified in the government flight tests of the XV-3, to have a credible proposal."

I found that the cause was the negative damping from the proprotor's inplane shear force, the H-force, produced when the rotor plane was pitching (or yawing) in space. This H-force results from the aerodynamic flapping moment that is required to make the rotor plane precess to follow the aircraft's pitching. The higher the blade inertia and the higher the pitch rate, the higher the H-force and negative damping on the aircraft. The magnitude of the H-force and negative damping is proportional to the inflow ratio, $\lambda = V/\Omega R$, and hence becomes progressively worse as airspeed increases in propeller operation. In helicopter autorotation the H-force due to pitch rate produces positive damping on the helicopter, while it produces negative damping in a climb. This was discovered and explained (with equations for its calculation) by Ken Amer in 1950 (NACA TN 2136), and has been called the "Amer Effect." Note that this effect in helicopter flight is relatively small in comparison to the large stable damping produced by the rotor thrust vector, tilt, and hub moments, if any, when the tip path plane is precessing to keep up with the helicopter pitch rate. But in propeller flight, the stable damping from thrust vector tilt (i.e., a small percentage of gross weight) is almost trivial in comparison to the effect of the H-force.

The following figure,[4] F-5, illustrates how the up-thrust on one side of the disc and the down-thrust on the other side of the disc (required for a precessing moment to pitch the tip path plane nose-up) both produce an increment of H-force in the up direction; hence causing a nose-up pitching moment to the aircraft. The H-force and the moment are in the direction, and proportional to the pitch rate, of the disc. This is negative damping. From the vector diagram it is seen that the incremental H-forces are proportional to the tangent of the blade element inflow angle, ϕ_o, thus the Δ H-forces along the blade are all proportional to the forward velocity of the aircraft, V.

This unstable damping moment, M_H, can be estimated simply with the following expression:

$$(4) \quad M_H = \frac{b I_b \left(\dot{a}_1 + \dot{\phi}_X \right) V h}{\bar{R}^2}$$

[4] Taken from *Composite Aircraft Program, Exploratory Definition Phase, Technical Volume—Dynamic Model Tests and Analytical Studies of High-Risk Areas*, Bell Helicopter Company Model 266, Report No. 266-099-212, Label 1228.

where:

b = number of blades.

I_b = blade inertial about flapping axis.

V = aircraft velocity.

h = distance from hinge axis to aircraft center of gravity.

$\bar{R}$ = radius to the mean center of lift (0.75R for rectangular blade).

$\dot{\phi}_X$ = nose-up pitch rate of the rotor shaft.

$\dot{a}_1$ = rate of increase of aft flapping.

$\left(\dot{a}_1 + \dot{\phi}_X\right)$ = total nose-up pitch rate of rotor alone in space .

ϕ_o = inflow angle at mean bade element, $\arctan\left(V/\Omega\bar{R}\right)$.

Recognizing that the total pitch rate, and hence destabilizing H-force, is the sum of the flapping rate, $\dot{a}_1$, as well as the rotor shaft pitch rate, $\dot{\phi}_X$, I included a high value of pitch-flap coupling (δ_3 = 45 degrees) along with a large tail volume as the design solution for Bell's Tri-Service Convertiplane proposal.

Now, over 50 years later, I wondered how well I would have correlated with the XV-3 flight test results using the same equations and hand calculation methodology I used way back then. At that time we only had data reported in Hervey Quigley and Dave Koenig's NASA TN D-778 giving measured short-period damping ratios shown in their figures 5 and 6, which I have included here as Fig. F-6.

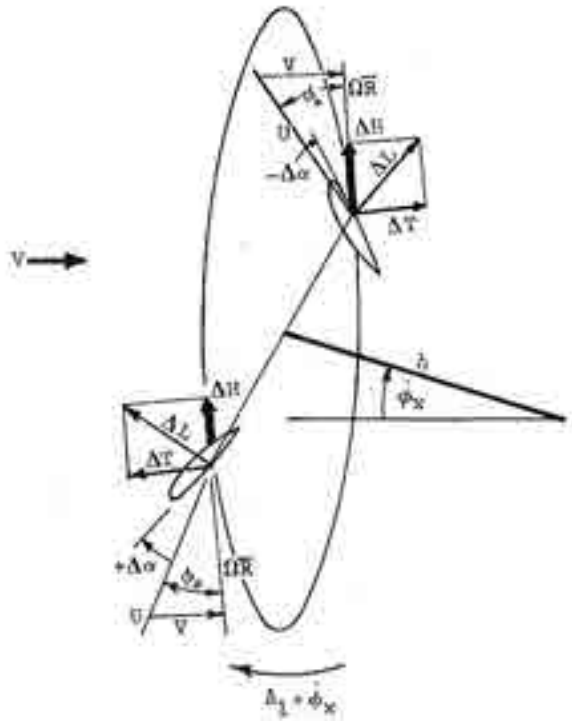

Fig. F-5. Delta thrust on either side of the disc produces H-force in the up direction causing a nose-up pitching moment to the aircraft.

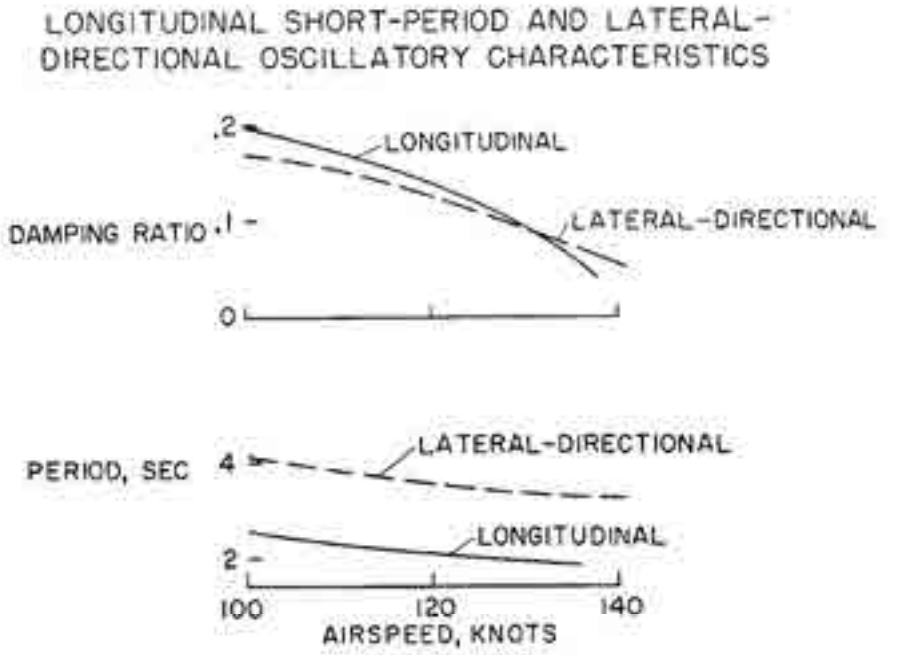

Figure 5

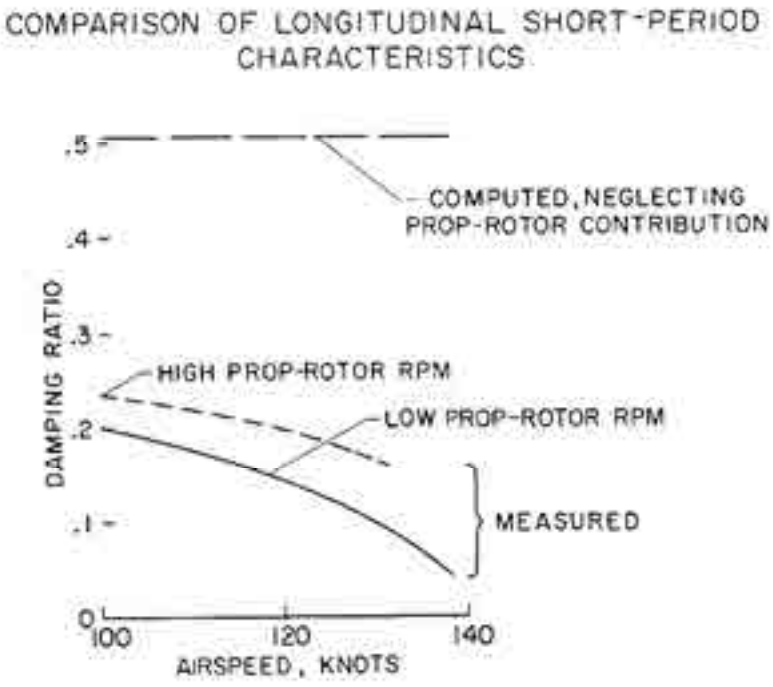

Figure 6

Fig. F-6. Short-period damping ratios from NASA TN D-778.

The equation for the short-period longitudinal mode for an airplane given in Perkins and Hage's[5] equation 10-107 (page 403), assuming no airspeed change (which is legitimate because the frequency is normally so high that there is not enough time for the airspeed to change), is given in nondimensional coefficient form as:

$$(5)\quad \lambda^2 - \left(\frac{1}{h}Cm_{d\theta} - \frac{1}{2}CL_{\alpha} + \frac{1}{h}Cm_{d\alpha}\right)\lambda - \left(\frac{1}{h}Cm_{\alpha} + \frac{CL_{\alpha}}{2h}Cm_{d\alpha}\right) = 0 .$$

The terms in parenthesis for the λ term give the damping of the short period, and the terms in the last parenthesis yield the undamped natural frequency of the short period. Using the aerodynamic parameters for the XV-3 at a mass weight of 4,800 pounds, a density altitude of 7,500 feet, a blade Lock number (γ) = 2.1, and an airframe pitch radius of gyration = 5.0 feet, yields a critical damping ratio (CDR) = 0.433 for the rotors-off case. This meets the then military requirement of a CDR no less than 0.34. At 105 knots true airspeed, the undamped period is 2.89 seconds, and the damped period is 3.21 seconds.

The addition of rotors makes positive changes to the pitch rate damping term, $Cm_{d\theta}$, and moment due to rate of angle-of-attack changes, $Cm_{d\alpha}$, hence negative damping to the short-period mode. This is a result of the H-force produced when the rotor disc is pitching in space as evaluated by Eq. (4) on page 756. If the rotor is producing thrust, a positive damping contribution will result from the fact that the rotor disc lags behind the pitching of the aircraft by the flapping angle, a_1, due to pitch rate as expressed by the following equation:

$$(6)\quad \frac{\partial a_1}{\partial q} = -\frac{\dfrac{16}{\gamma\Omega\cos\phi} - \dfrac{\Delta\theta/\Delta\beta}{\Omega\cos^2\varphi}}{1 + \dfrac{(\Delta\theta/\Delta\beta)^2}{\cos^4\phi}} .$$

Rotor thrust also produces negative angle-of-attack stability as a result of flapping, a_1, as expressed by the following equation:

$$(7)\quad \frac{\partial a_1}{\partial \alpha} = \frac{\tan^2\phi}{1 + \dfrac{(\Delta\theta/\Delta\beta)^2}{\cos^4\phi}} .$$

This equation is also used to determine $Cm_{d\alpha}$ for the rotor's H-force contribution by realizing that in a free oscillation (i.e., sinusoidal) $d\dot{\alpha}/d\dot{\theta}$ equals the ratio $d\alpha/d\theta$.

The rotors-on contributions and the critical damping ratio (CDR) were calculated for two, 23-foot-diameter rotors, with two blades each having a Lock number (γ) = 2.10 at 7,500 feet altitude, a mast length from the flapping axis to the aircraft's center of gravity (c.g.) = 3.5 feet, a pitch-flap coupling ($\Delta\theta/\Delta\beta$) = – 0.36 (i.e., δ_3 = 20 degrees), and a high RPM (helicopter) of 532 and a low RPM (airplane) of 324.

[5] *Airplane Performance, Stability and Control,* Fourth Printing, John Wiley & Sons, 1954.

Fig. F-7 shows the correlation of the predicted CDRs with the measured short-period damping ratios from the flight test in NASA TN D-778. The test data is for a density altitude of 7,500 feet. The calculations were made estimating the thrust at full power because the aircraft had to dive to achieve the airspeeds shown. The trends of decreasing damping with lowering RPM and increasing airspeed are predicted; however the measured, very rapid decrease of damping with airspeed, especially at the low RPM, is not predicted.

Remember, the pylons of the XV-3 were elastically mounted to the wingtips allowing the rotor shafts to pitch relative to the airframe, so it would be expected that the rotor discs would be precessing through larger angles than if the pylons were rigidly attached to an inelastic airframe. Larger H-forces and more negative damping would produce a proportional decrease in the short-period CDR with airspeed but not the very rapid decrease measured at the lower RPM. This rapid decrease was a result of the airspeed approaching the onset of a proprotor-pylon instability. At the time of my analysis in 1961, the problem of proprotor-pylon instability had not yet been discovered. Later in 1962, in the third full-scale wind tunnel test, the problem was encountered. And in 1963, after concentrated wind-tunnel model and analytical research, proprotor-pylon stability was identified and explained. A computer code developed by Earl Hall showed that it was the rotor flapping mode that was going unstable, i.e., the damping of rotor flapping (normally heavily damped) decreased with increased airspeed; hence, the flapping response to short-period longitudinal pitching increased causing a decrease in the CDR measured in the XV-3 flight test.

Fig. F-7 also shows the predicted CDRs when rotor thrust is set to zero. Thrust improves the damping but not significantly, especially as speed increases. Typically, damping of the short-period mode and the various proprotor-pylon modes is calculated with zero thrust to be conservative and to assess the critical condition of glide and low-power diving.

Fig. F-8 shows the benefit of using my proposed design solution of a high value of pitch-flap coupling, $\Delta\theta/\Delta\beta$ (tan δ_3), on the XV-3 at low RPM with zero thrust. The benefit is greater the higher the airspeed because $d\dot{\alpha}/d\dot{\theta} = d\alpha/d\theta$ increases with airspeed, and this is reduced the higher the δ_3. Instability of the short period can be prevented even at 300 knots with a $\delta_3 = 45$ degrees, but the damping remains below the required CDR of 0.34. This is because $\Delta\theta/\Delta\beta$ (tan δ_3) has no effect on the H-force arising from pitch rate, $d\theta/dt$, but only on rate of change of angle of attack with time, $d\alpha/dt$.

It should be pointed out that negative δ_3, (i.e., $+\Delta\theta/\Delta\beta$) also is effective as positive δ_3, (i.e., $-\Delta\theta/\Delta\beta$) in reducing flapping and negative damping. Negative δ_3 is used on all Bell tiltrotor aircraft since the XV-3. This can be done with rotors that have see-saw (two-blade) or gimbaled (three-or-more-blade) hubs. On hubs that have flapping hinges, a negative δ_3 could cause coning stability problems.

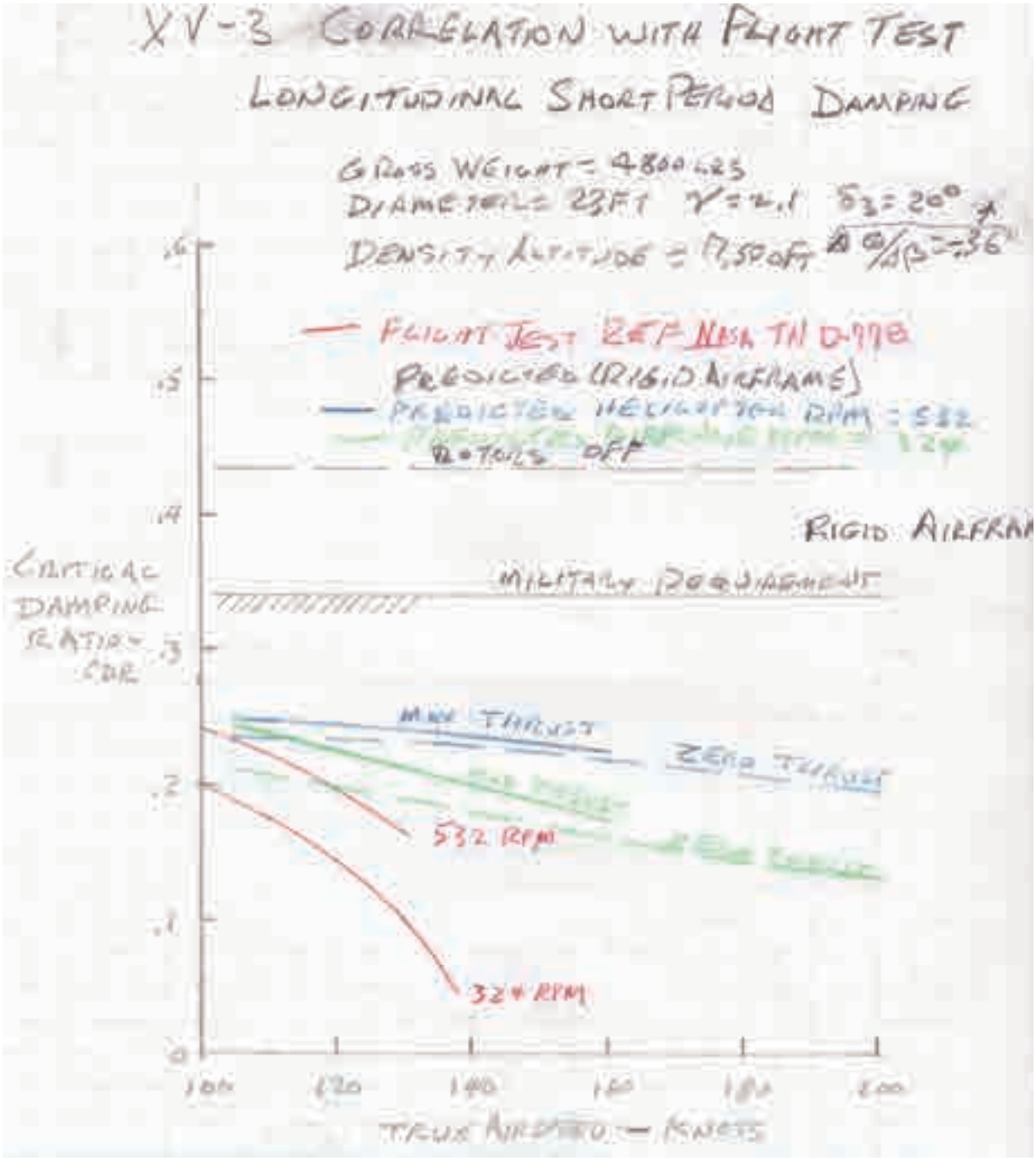

Fig. F-7. Prediction of longitudinal short-period damping.

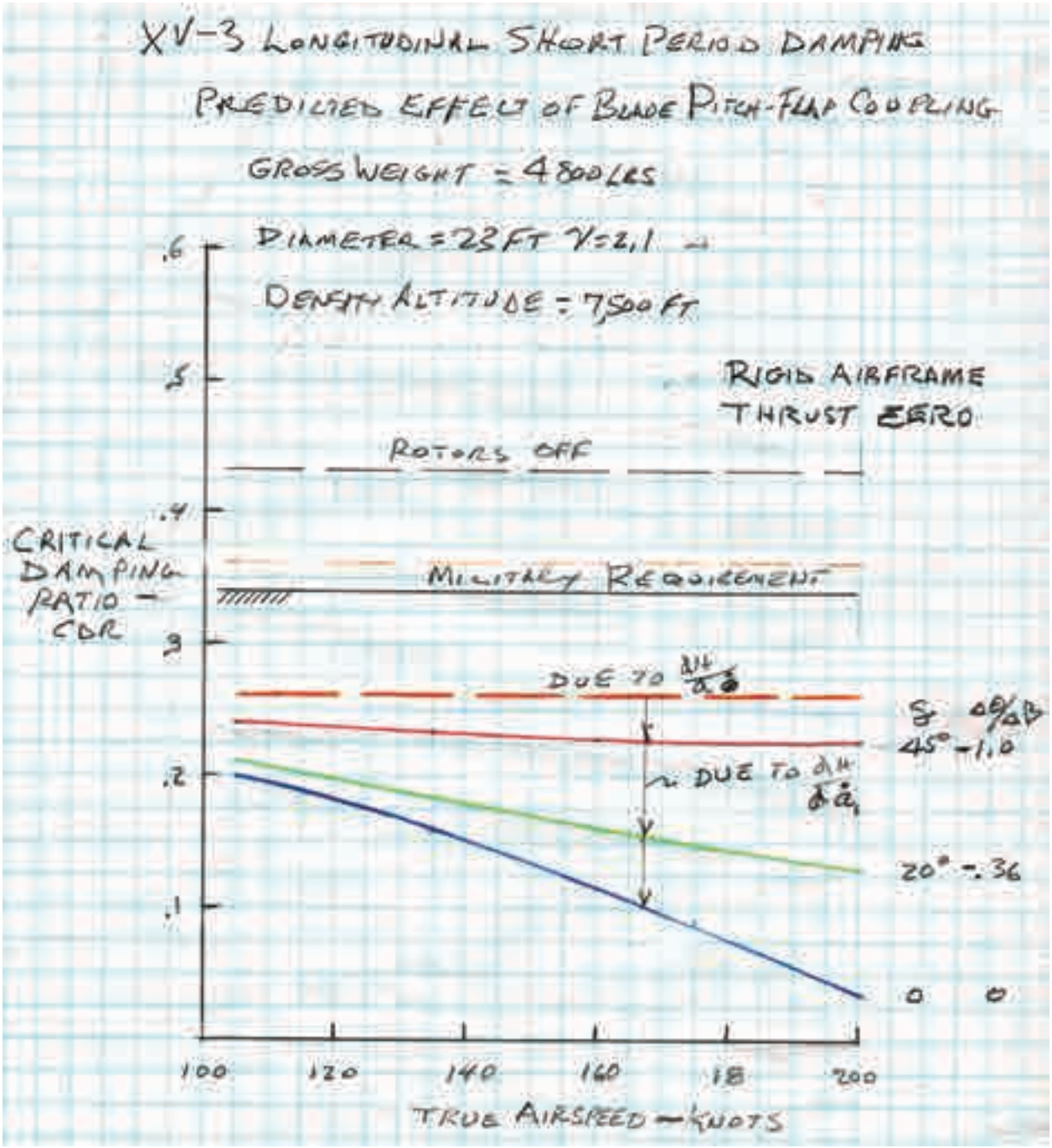

Fig. F-8. Prediction of the effect of blade pitch-flap coupling.

Figure F-9 illustrates my other design solution of increasing the tail volume. In this figure the tail area is held constant, and the tail arm is increased from the XV-3's tail arm of 13.7 feet to 22.4 feet for the XV-15. The XV-15 has 25-foot-diameter rotors, and the XV-3 started out with 25-foot-diameter three-bladed rotors before flying with two-bladed, 23-foot-diameter rotors. Fig. F-9 contrasts the short tail arm of the XV-3 with the longer arm of the XV-15. It is seen in Fig. F-9 that even with the XV-3's δ_3 = 20 degrees, the CDR meets the military requirement of 0.34 to 200 knots and to unlimited speeds with δ_3 = 35 and 45 degrees. These calculations were made using the XV-3's airframe pitch radius of gyration of $\bar{R}$ = = 5.0 feet. Moving the tail aft would increase the radius of gyration decreasing the short-period frequency and lengthening the period that would increase the damping values calculated in Fig. F-9. These calculations are for an inelastic airframe. An elastic airframe, even with pylons stiffly mounted to the wingtips, could have less stability. Because of this aspect, all subsequent Bell tiltrotor aircraft had rigidly mounted pylons to the wingtips.

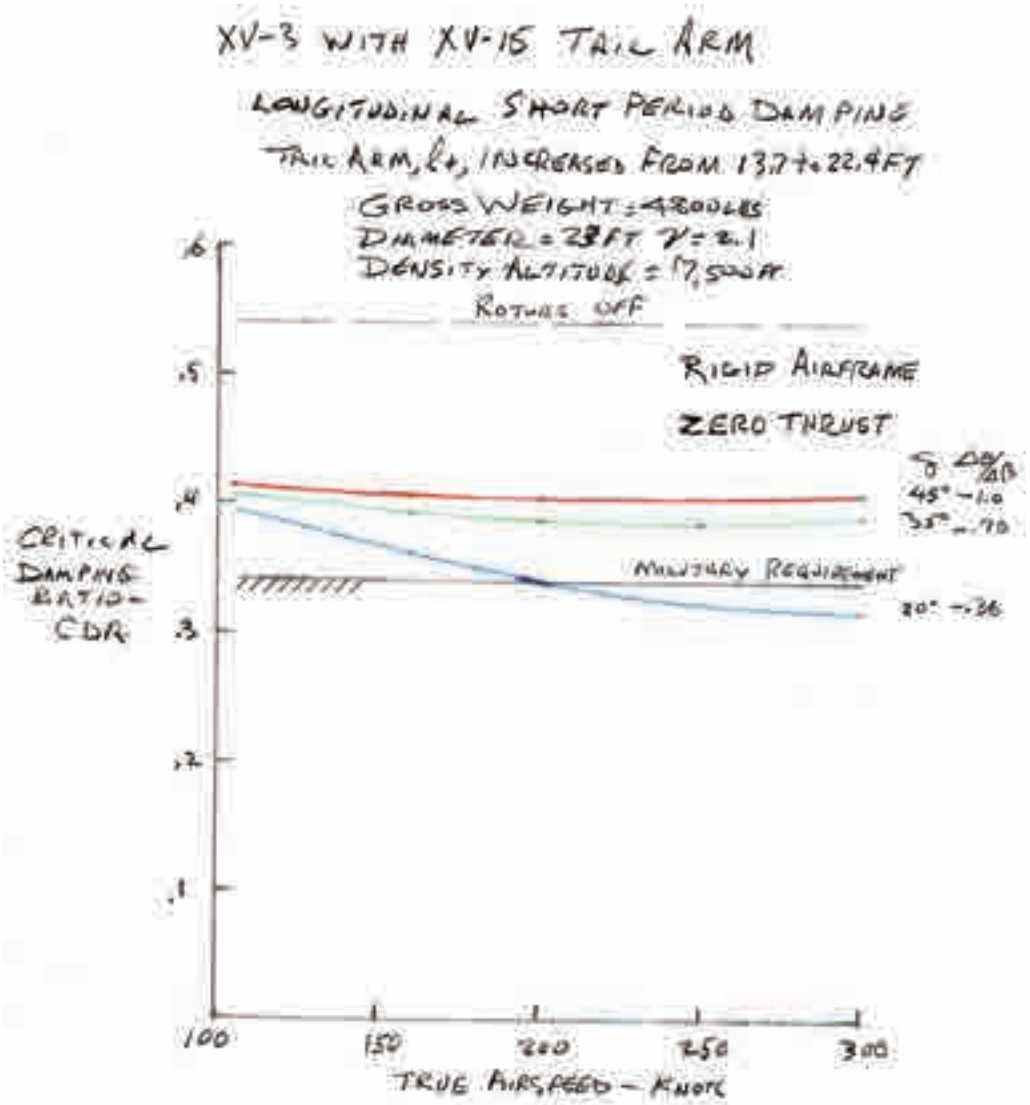

Fig. F-9. Prediction of longer tail arm on longitudinal short-period damping.

Technical Note 4.
The XV-3 Encounters Proprotor-Pylon Instability in the Third Wind Tunnel Test

After losing the Tri-Service VTOL competition, Lichten was still anxious to pursue the development of a convertiplane and thought that flying the XV-3 again with improved damping of the short-period and Dutch roll modes would be the next step. Because increasing the tail arm would be a very expensive change, it was decided that an increase of δ_3 would be enough to show that the claimed solution to the low-damping problem was correct.

The XV-3's delta three of $\Delta\theta/\Delta\beta = -0.36$ ($\delta_3 = +20$ degrees) was increased to $\Delta\theta/\Delta\beta = -0.70$ ($\delta_3 = +35$ degrees). In June/July 1962, the aircraft was installed in the NASA Ames 40- by 80-Foot Full-Scale Wind Tunnel for the third time to ensure that this change in δ_3 would not cause any unforeseen flight hazards. The testing was conducted with Bill Quinlan inside the cockpit. At 130 knots he encountered a low-frequency limit-cycle pylon oscillation that he called rotor "nervousness." It was thought that the XV-3 might be on the verge of a divergent instability, so testing was terminated. At the time, the pylon oscillation was unexplainable. Later it was defined as proprotor-pylon instability caused by the rotor inplane H-forces producing negative damping when the rotor plane was precessing in space.

The XV-3 was never to fly again, but later (in May 1966) there was a fourth and final full-scale wind tunnel test with the XV-3 to prove Bell had solutions in-hand for solving proprotor-pylon instabilities. The confidence established was discussed by Kip Edenborough in an A.I.A.A. Journal of Aircraft paper (vol. 5, no. 6) published in March–April 1968.

APPENDIX G
HARLAN FOWLER'S ARTICLE IN WESTERN FLYING MAGAZINE

In my research about Harlan Fowler and what I grew up learning as the "Fowler flap," I was fascinated to discover that all of his papers and other material now reside at San Jose State University in California in a repository identified as MSS-1995-04. The Online Archive of California (OAC) website has a complete description of what is stored there along with this biography:

Born June 18, 1895, Harlan Davey Fowler grew up in Sacramento, California. Fowler married twice and had two children. He spent his professional life as an aeronautical engineer and inventor. He died on April 27, 1982. The year 1917 marked the beginning of Fowler's lifelong career as an aeronautical engineer and inventor. Fowler worked as an independent consultant and also for a number of aeronautical firms including Fokker, The Glenn L. Martin Co., Convair, Douglas Aircraft Co., Fowler Aircraft Co., the Bureau of Aeronautics, and the U.S. Air Force. He also patented 20 inventions, the most significant of which include: Variable-Area Wing, 1921, patent no. 1392005; Cargo Container for Airplanes, 1948, patent no. 2442459; and Convertible VTOL Aircraft, 1963, patent no. 3093347, and 1967, patent no. 3312426.

His greatest professional achievement was the development of the variable area wing, commonly known as the Fowler flap. The Fowler flap is a high-lift device located on the trailing edge of an airplane wing that increases wing area and lift. During the late 1910s and early 1920s, many engineers experimented with wings, slots, and flaps to improve airplane performance. Fowler developed a flap that slid back from the wing and rotated down, creating a slot. This flap increased the curvature and area of the wing, which tuned it to operate more efficiently at lower speeds occurring during takeoff and landing. The design and testing of the Fowler flap was performed as a private venture, using Fowler's own time and funds. In the summer of 1927, Fowler and airplane mechanic Stanley Crowfoot first tested the Fowler flap. Several years of testing followed, after which the National Advisory Committee for Aeronautics (NACA) concluded that the Fowler flap would reduce landing speed, decrease landing and takeoff runs, and improve climbing ability. In 1937 Lockheed added the flap to the Lockheed 14 twin-engine airliner. Previously the flap had been used on German planes such as the Fieseler Fi 97. Later it was used on Boeing B-29 bombers, some versions of the Lockheed P-38 Lightning, and the Boeing B-17. Today, variations of the Fowler flap are still being used on many commercial aircraft.

In 1949 the Franklin Institute of Philadelphia, Pennsylvania, awarded Fowler the John Price Wetherill Medal for the development of the "Variable Lift Airplane Wing." In 1971 the institute elected him to Life Fellow Membership. Fowler was active in the Society of Automotive Engineers and was elected to the status of Fellow in 1977. Fowler wrote a comprehensive text on flap design, *Fowler Flaps for Airplanes: An Engineering Handbook* (1948). He also published three books outside his field: *Camels to California* (1950), *Three Caravans to Yuma* (1980), and *Behold the Flaming Sword* (1983).

Timeline:

1910	Built man-carrying kites of Cody/Hargrave type.
1917	Signal Corps; Aeronautical Engineer Production.
1919–1920	McCook Field, Dayton, OH. Engineering Division; Assistant Engineer in charge of design.
1921	Mather Field, Sacramento, CA; Assistant Engineer; Aerial Forest Fire Patrol.
1922–1925	G. Elias & Bros., Buffalo, NY; Aeromarine Plane and Motor Co.; Naval Aircraft Factory.
1925–1927	Pitcairn Aviation Co., Philadelphia, PA.
1927	U.S. Army Air Corps; Engineer.
1928	Miller Corp., New Brunswick, NJ; Chief Aeronautical Engineer.
1929–1936	Glenn L. Martin Co., Baltimore, MD; Staff Engineer.
1943	Fowler Aircraft Co., San Diego, CA.
1946	Independent Consulting Aeronautical Engineer, Whittier, CA.
1951	McCook Field, Dayton, OH; Engineering Division.
1956–1957	Independent Consulting Aeronautical Engineer, Longmont, CO.
1962–1974	Independent Consulting Aeronautical Engineer, Burlingame, CA.
1975–1982	Retired, Solvang, CA.

Variable Lift

By Harlan D. Fowler

IN spite of the achievements of the Guggenheim Safe Aircraft Competition, little progress seems to have been made toward the solution of the problem of increasing the lift of wings without sacrificing top speed. The following article is presented with the hope that it will stimulate more thought on the subject. —*The Editors.*

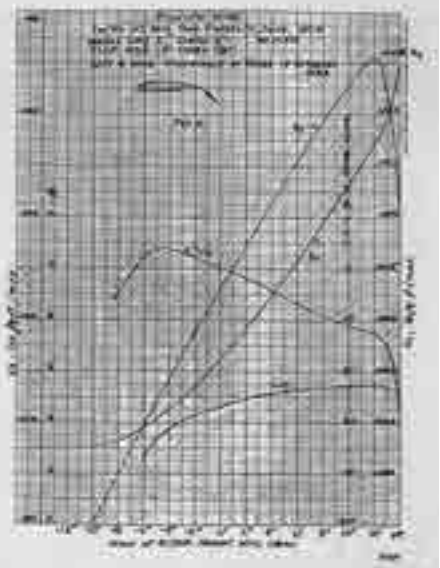

FIG. 1 (below) shows results of wind tunnel test of normal wing with and without recess.

FIG. 2 (right) shows test with wing extended. Max. Ky of .00556 occurs at only 12 deg. angle of attack

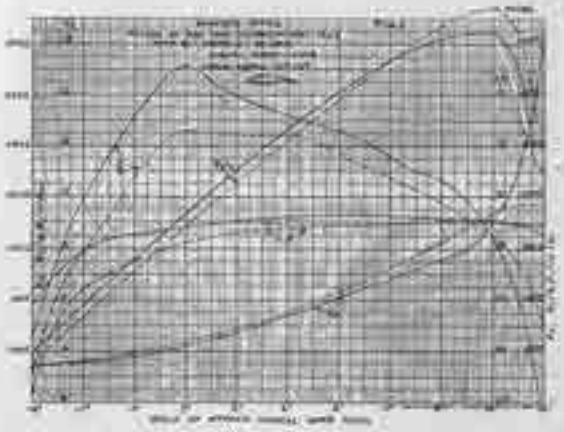

TIME consumed in taking off and landing is a matter of a few minutes, whereas straightaway flying takes hours. Simply because sufficient lift must be available for this landing and take-off, we afflict ourselves with the use of oversized wings. When once in the air, the smallest of wing, consistent with controllability, can be used safely.

Why, then, do we continue to be so far removed from the most important and far reaching development of variable lift wings? As far back as 1910, the subject of utilizing variable lift wings was frequently discussed by engineers. The methods suggested were:

(a) variable camber,
(b) variable area,
(c) variable angle of attack, and later
(d) slotted wings.

Many laboratory experiments have been made on airfoils with the camber adjustable from a streamline section to that of a heavily convexed section, with promises of a wide variation in aerodynamic characteristics. Variable area has presented a mechanical problem of the first order. The variable angle of attack offers the least, if any, improvement, although several airplanes have been tried out using this idea. Perhaps the most successful devices have been the various forms of slotted wings. All four methods have been considered extensively in published articles. However, it is unfortunately true that the benefits obtained from each type alone have not justified its continued development.

The Fowler Wing Principle

It was long recognized by the writer that if the best features of each one could be incorporated into a simultaneous and coordinated alteration of the wing, the fullest advantage would be utilized. This was easier "thought of" than practically solved. Fundamentally and foremost, the basic structure of the wing must not be interfered with.

Hence, the conception of the Fowler Variable Area Wing, which incorporates the following points: (1) A structurally sound basic wing; (2) An increase in area; (3) Variable angle of attack; (4) A variable camber, and (5) The slotted wing.

about 100 per cent by the combined use of these relations. Each feature contributes to the increased lift in the following proportions: Variable camber, 43 per cent; variable area, 28 per cent; recessed camber, 7 per cent; and slots, 22 per cent. And it is all accomplished by the one simple expedient of extending the auxiliary area wing downwardly and rearwardly, which rapidly brings about the simultaneous characteristics of each desirable relationship.

Wind Tunnel Tests

Figures 1 and 2 give the characteristics for the normal and extended area. The tests were conducted at the New York University. The maximum Ky normal is .0036 and extended .00556. The normal area is 63 sq. in. and extended 80 sq. in. Viewed on the assumption that the normal wing characteristics are influenced by these alterations by virtue of being self-contained, it will have the equivalent maximum Ky of

$$.00556 \times \frac{80}{63} = .00705$$

or

$$\frac{.00705}{.0036} - 1 = 0.96 \text{ increase}$$

FIG. 3—Installation of Fowler wing with extension full out. Note slot

Ky of .0073 as referred to the normal area—the highest lift obtained from any airfoil.

This increase in lift was obtained without impairment of aileron effectiveness, only 70 per cent of the wing span being utilized for the auxiliary wing.

Full Flight Tests

Performance tests were made with a Pitcairn PA-3 which was originally a biplane of 338 sq. ft. An OXX-6 engine of 100 h.p. and the same wood propeller was used throughout the trials without alterations or overhauling. The following data were obtained:

	Original PA-3	Fowler Wing No. 1	Fowler Wing No. 2
Low speed, normal, M. P. H.	46.2	58.2	57.0
Low speed, extended, M. P. H.	—	44.5	42.0
High speed, M. P. H.	91.0	103.0	106.0
Cruising speed, M. P. H.	77.0	84.0	87.0
Rate of climb, ft./min.	519	430	529
Take-off time, seconds	10	11	10
Landing time, seconds	9	11	8
Total weight of plane, lbs.	1850	1900	2000
Wing area, normal, sq. ft.	338	130	141
Wing area, extended, sq. ft.	—	166	181
Wt. per sq. ft., normal	5.72	14.61	13.9
Wt. per sq. ft., extended	—	12.00	10.73
Speed range	1.97	2.36	2.42
Design load factor of wing	5.39	6.00	10.58
Weight of wings, complete, lbs.	377	393	409

Performances for the PA-3 and Fowler Wing No. 1 are based on flight tests over a one-mile course and are the averages of several runs.

Wing No. 2 is an entire new design with a special normal airfoil and aspect ratio of 9. It is designed for a gross weight of 2850 pounds with a load factor of 7, which for the 2000-pound plane is equivalent to a load factor of 10.

It will be noted that in spite of using an extended area of less than half that of the biplane, the stall speed was nearly 2 m.p.h. lower.

The stall speed for the normal wing monoplane is 58.2 m.p.h. and represents the typical monoplane. By extending the area, this speed was reduced to 44.5 m.p.h. Thus, the average monoplane can have its stall speed reduced not less than 14 m.p.h.

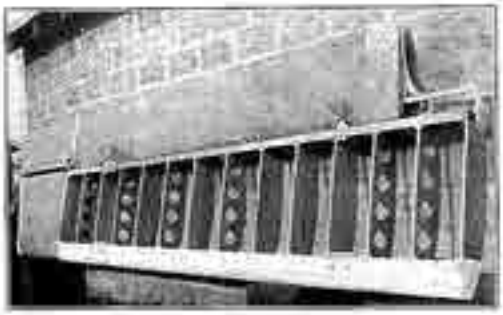

FIG. 4—Showing construction of the Fowler wing in the closed position

The high speed was increased from 91 m.p.h. for the biplane to 101 m.p.h. for the normal area Wing No. 1. For the original biplane to have attained 101 m.p.h., at least 136 horsepower would be necessary, resulting in a heavier engine and increased fuel capacity, or an increase in weight of about 185 pounds, using a water-cooled engine. This in turn would raise the stall speed from 46.2 to 48.7 m.p.h. The most important fact is this—the additional cost of a new engine at about $2,000 far exceeds the cost of a set of variable wings.

Weight Comparison

Wing No. 2 has been designed according to the strength requirements of the Department of Commerce and approved for installation on planes with gross weight up to 2850 pounds and up to 225 h.p. The actual weight of the wing is itemized as follows:

Main wing, with fittings	242.50 lbs.	
Ailerons	17.00 lbs.	
Five gallons gas tank	8.50 lbs.	
Main wing, complete		268.
Extension surface	36.00	
Extension surface rails, etc.	24.00	
Extension surface controls	6.00	
Extension assembly, complete		66.
Fowler Wing No. 2, complete		334.

Struts and wires for installation to plane weigh about 75 pounds, giving a total weight of 409 pounds.

This wing can be designed for a closed cabin without special difficulties.

For comparison with the conventional wings, the following typical data are given:

	Rated H. P.	Gross Weight	Area sq. ft.	Weight Wings	Stall Speed	Load Factor
Fowler Wing	225	2850	141	409	57.0	7.00
"A" Biplane	180	2877	151	422	49.0	7.00
"B" Biplane	150	2702	169	418	54.0	7.00

Note—Even though Wing No. 2 is lighter than the conventional wings, no attempt was made to resort to expensive light-weight detail construction. With such an excess of HP. available, this is unnecessary. However, with design refinement, at least 10 per cent further saving in weight is possible. A and B are well-known airplanes.

Application to Cantilever Wings

As shown before, for the same stall speed, the area may be reduced one-half by using the variable area wing. Since the extension feature can be easily incorporated in a cantilever wing, the span can be reduced 25 per cent for the same aspect ratio. Since the gross weight is about the same, the cantilever bending moment is correspondingly reduced. A stiffer and cheaper structure would result from this reduction in size.

From the standpoint of strength, the determination of structural sizes is simple and straightforward, being governed entirely by conventional design practice. No unusual or tricky supporting members nor articular parts are used in the wing.

For extremely high speed purposes, it is necessary

to go into high landing speeds. The Schneider Cup Race planes land at speeds varying from 100 to 125 m.p.h.

Let us assume that with a high speed airfoil, the wing loading is 30 pounds per sq. ft. Substituting the variable area wing, the extended wing loading would be 60 pounds per sq. ft. at 100 m.p.h. stall speed and normal area is 76 pounds per sq. ft. at 143 m.p.h. stall speed. This is a reduction of 43 m.p.h. It is acknowledged that the wing loadings are very high, but the wing could be of a cantilever type and very small in size. The high speed would be greatly improved.

When landing with the wing extended, the glide is steep and the run on the ground short.

Wing Reduces Need for Increased Power

If increased high speed is desired, it is usually the practice to put in a higher power engine. This will not be necessary if the Fowler wing is used.

Let us consider a pure cantilever monoplane with a 420-h.p. engine, wing area 265 sq. ft. and a gross weight of 4500 pounds. The pay load is 600 pounds without including 150 gallons of fuel. Stall speed is 66 m.p.h.

Installation of a 525-horsepower engine would only increase the high speed of this plane from 200 to 215 m.p.h. It is an unfortunate fact that in changing to higher power, the expected increase in speed is rarely obtained. The average loss is about one-third of the theoretical increase. This is largely attributed to the increase in cylinder number and diameter, overall engine diameter, and loss of propulsive efficiency. Therefore, it is very probable that the high speed of 215 m.p.h. for the 525-h.p. engine may be more like 210 m.p.h. or even less, if available data are trustworthy.

The added cost of the larger engine is about $600. The larger gas tank to receive 30 gallons more fuel, propeller, etc., would add at least $100 more, or a total of $700.

A variable wing would cost about 15 per cent or $375 less than the original wing. The total net initial saving would be $1,075. The operating savings on gas consumption, depreciation of engine, and maintenance would also be considerable.

Climb and Ceiling

Numerous tests with the extension in various locations between all-in and all-out show a very definite gain in the rate-of-climb when set about halfway out. This is, then, the best setting for take-off and climb.

With the fully extended wing, the rate of climb is lower, as is to be expected, in view of the lower L/D. Incidentally, for the same reason, the high speed was found to be about 79 m.p.h. This condition is in reality a decided safety measure in that it would be impossible to manœuver sharply. It thus prevents undue strain on the extended surface and supports.

The planes on which the Fowler wing was used had fixed stabilizers, and these were not readjusted at any time.

The extension can be operated by the pilot while flying and set at any position desired. The position of the control stick is changed forward when extending the wing, but little change of balance is noted for the two conditions of all-in or all-out.

The plane had adequate control at and beyond stalled position.

FIG. 5—Cross-section of Fowler wing. Note recess under trailing surface to receive extension

Design Features

The normal wing, which is of two halves joined at the center, is of conventional construction, although employing materials in a different manner. The spars are of solid spruce. The ribs are of 3/8 and 7/16-inch spruce. The nose is of solid balsa wood. (Fig. 4.) No internal drag bracing is used because the covering is of plywood which is glued and nailed directly to the spars and ribs.

The auxiliary wing has a single spar to which are secured the solid ribs and balsa wood nose piece. The whole is plywood-covered. This small wing fits snugly under the trailing portion of the main wing. (Fig. 4.)

Figure 5 is a drawing of the complete combination, showing the supporting rail, trolley and relation of the large and small airfoils. The four supporting rails, which are 3/16 inch thick by 3½ inches deep, are of steel, but may be of duralumin. These rails are attachable in up or down movements by eccentrics located at the main fitting attachments so as to provide clearance between the auxiliary wing and the under surface of the main wing when it is closed.

Operation of the extension is by means of a continuous cable wrapping around a drum. To this drum is secured the control shaft and handle reaching down to the pilot who can operate it at his convenience. All control cables, including those for the ailerons, are led along the open face of the rear spar. Nothing is concealed.

Commercial Applications

Due to the high lift of the Fowler wing, it can be applied as follows: (1) Light planes, stall speed 25 m.p.h.; (2) cargo planes, actual payload, 7 pounds per h.p.; (3) optional equipment, substitute for conventional wings, and (4) reduced initial cost of planes and better performance.

A Cook Stove *for the* Akron

A COOK stove which has met the requirements for minimum weight and size has been developed for the U.S.S. Akron for installation in the dirigible's galley. The manufacturers who had the contract for the stove, the Toledo Stove Company of Mansfield, Ohio, dp-

110 pounds on which can be prepared meals for the dirigible's personnel of 99 officers and men. In the stove, cast and sheet aluminum predominate. Propane gas, derived from natural gas, will be used as fuel for the stove. The gas will be compressed into liquefied

APPENDIX H
LANDING AND TAKEOFF PERFORMANCE ANALYSES

This introduction to STOL performance of fixed-wing aircraft would be incomplete without some more detailed discussion of how to estimate landing and takeoff distances in the early stages of concept design. There are, of course, a multitude of reports and papers offering all manner of methodologies to calculate these key distances. In fact, there are too many to even reference, most of which I found less than satisfactory. Therefore, I felt it necessary to offer my analysis, which starts with basic physics. Fortunately I had access to flight test data obtained with many fixed-wing aircraft. This data, augmented with several pilot flight manuals for the production aircraft, gave me confidence that a relatively simple analysis would be of use to you.

The Landing Distance Problem

The total distance a fixed-wing aircraft needs before coming to a stop after passing over a 50-foot obstacle at some airspeed can be divided into two parts. The first part is the distance traveled while descending from the 50-foot obstacle to the touchdown. I will call this the air distance (D_{air}). The second part is the ground distance covered in bringing the aircraft to a halt. Let me call this second distance ground run ($D_{Grd\ Run}$). Based on the test data shown in Fig. 3-154 on page 531, I would say that the air distance is on the order of

$$(1) \quad D_{air} = 0.1(V_{FP}\ \text{at}\ 50\ \text{feet})^2$$

or less, where the flight path velocity at the 50-foot obstacle (V_{FP}) is in knots.

Now let me concentrate on calculating the ground distance.

Accurately calculating ground run distance requires application of Newton's law that says F = ma, which is applied in the X direction (i.e., horizontal). To begin with, you write Newton's law as

$$(2) \quad \sum F_X = ma = \frac{W}{g}a = \frac{W}{g}\frac{dV}{dt} = \frac{W}{g}\frac{dV}{dD}\frac{dD}{dt} = \frac{W}{g}\frac{dV}{dD}V .$$

It follows then that the ground run distance ($D_{Ground\ Run}$) *only* requires solving an integral of the form

$$(3) \quad D_{Ground\ Run} = \frac{W}{g}\int_{V_{Touchdown}}^{0} \frac{V}{\sum F_x} dV .$$

You can find the components making up the horizontal force summation (ΣF_x) in any number of textbooks and reports. A classical force diagram is shown in Fig. H-1. I prefer to account for the braking force (F_{Brake}) as a separate force as you see here with Eq. (4)

$$(4) \quad \begin{aligned} \sum F_X &= F_P - D - \mu_{roll}(W - L) - F_{Brake} + T_{jet} \\ &= (F_P - \mu_{roll}W - F_{Brake} + T_{jet}) - (qS_W)(C_D - \mu_{roll}C_L) \end{aligned}$$

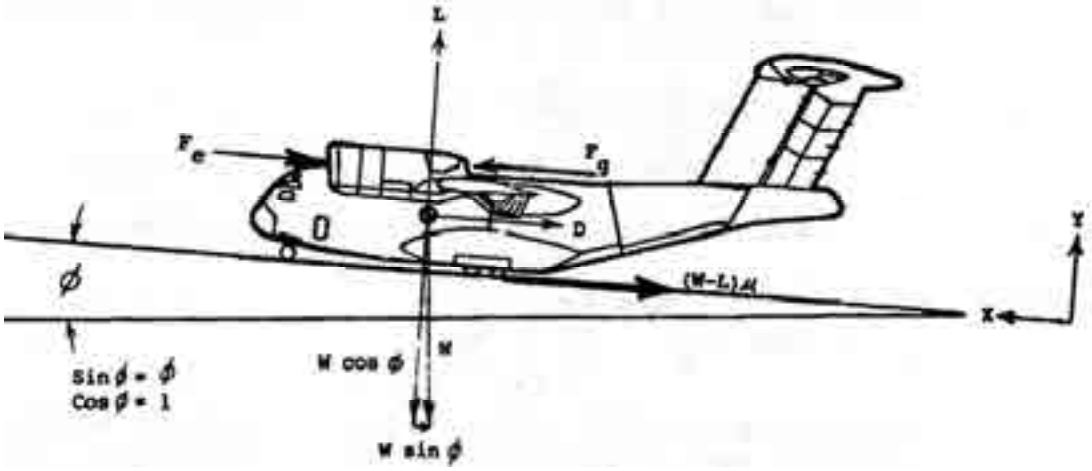

Fig. H-1. Forces to be accounted for in the ground run calculation.

where the thrust of one propulsive force unit (T_P) in pounds is multiplied by the number of units (N) so that F_P equals N times T_P. A propulsive force unit can be a propeller driven by a piston engine or a turboshaft engine, or it can be a pure turbojet/turbofan engine. I have included a force component (T_{jet}) should the calculation require more fidelity. Keep in mind that the thrust (T_P) is generally negative for the ground run calculation. The aircraft's drag (D), lift (L), and weight (W) are in pounds. The aircraft's conventional lift and drag forces can be expressed in coefficient form, which illuminates the dependence of the force summation on dynamic pressure ($q = \frac{1}{2} \rho V^2$). The coefficient of rolling friction (μ_{roll}) on paved surfaces with brakes off is nominally 0.025 to 0.030.

Keep in mind that from an aircraft design point of view, turboshaft engines have a residual jet thrust that comes with the direct shaft horsepower provided to the propeller. Recalling footnote 129 on page 499, the Allison T56-A-7 turboshaft engine had a jet thrust of about 740 pounds while sending 3,755 horsepower to the propeller. This jet thrust (T_{jet}) acts to accelerate the aircraft during the landing ground run, which is not helpful—to say the least.

It is a simple step to substitute Eq. (4) into Eq. (3) and see the integral that must be obtained. Of course, the ground run distance calculation would be incomplete without some consideration of the time it takes for the pilot to reconfigure the machine and the aircraft to transition from flying to beginning the landing. It takes a finite time to apply brakes even in a dead stick (i.e., power off) landing, and it takes even more time to obtain full reverse thrust. Therefore, I suggest that every ground run distance ever quoted or measured includes a distance of

(5) $$D_{Pilot} = V_{touchdown} t_{Pilot} .$$

You can now see that the total ground run distance calculation takes the form

(6) $$\text{Total } D_{GroundRun} = V_{touchdown} t_{Pilot} + \frac{W}{g} \int_{V_{Touchdown}}^{0} \frac{V}{\left(F_P - \mu_{roll} W - F_{Brake} + T_{jet}\right) - \left[\left(\frac{1}{2}\rho S_W\right)\left(C_D - \mu_{roll} C_L\right)\right] V^2} dV.$$

Now consider a simple case where the propulsive force unit is at zero thrust. That is, there is no reverse thrust from a propeller or a turbojet/turbofan engine, and therefore F_P and T_{jet} both equal zero. This would be the case of a dead stick landing. In this case, the integral can be obtained in closed form, and the result is

$$(7) \quad D_{\text{Ground Run}} = V_{\text{touchdown}} t_{\text{Pilot}} + \frac{W}{g}\left[\frac{1}{2(\tfrac{1}{2}\rho S_W)(C_D - \mu_{\text{roll}} C_L)}\right] \ln\left[1 + \frac{(\tfrac{1}{2}\rho S_W)(C_D - \mu_{\text{roll}} C_L)}{\mu_{\text{roll}} W + F_{\text{Brake}}}\right].$$

Including the propulsive force unit from an operating propeller driven by a piston engine immediately introduces complications because the reverse thrust produced by a propeller is a very unique aerodynamic problem. Propeller reverse thrust deserves additional discussion, so let me stop here to give you some background.

I ran across a very interesting article about propeller operation in the reverse thrust regime that was published in March of 1945. The article, written by Mr. Franklin D. Walker, was included in volume 36, number 3 of *Flying* magazine. The lead-in to the article showed an eye-catching figure that you see here as Fig. H-2. While Walker's discussion was rather simple, it did emphasize the value of reverse thrust in significantly reducing ground run distance.

The actual calculation of propeller reverse thrust was possible even as far back as the 1930s using blade element theory. I first learned this theory in my freshman year at R.P.I. in 1956. Our textbook for the beginning of our aeronautical engineering education was Paul Hemke's *Elementary Applied Aerodynamics*, copyrighted in 1946. With only a slide rule,

Fig. H-2. The caption of this artist's rendition reads, "Picture illustrates effect of reverse thrust in reducing landing roll. Churning props throw air forward, brakes plane."

the calculation was very tedious, to say the least, taking several hours to get thrust at one collective pitch and flight condition. Our professor was quick to turn our attention to experimental data such as that provided in NACA Report 464. This report, authored by Edwin P. Hartman,[1] is titled *Negative Thrust and Torque Characteristics of an Adjustable-Pitch Metal Propeller* and was published in 1933. I have re-digitized his experimental data and graphed it in a slightly different form shown here as Fig. H-3.

To give you a sense of the reverse thrust problem, consider Fig. H-4 where you see a propeller's blade element velocity and force diagram at two points in the landing maneuver. As the aircraft is virtually at touchdown the propeller is nominally at zero thrust and the propeller's blade pitch angle at the three-quarter radius station ($\theta_{0.75R}$ or $\beta_{0.75R}$) is at a value equal to the inflow angle ($¾V_t/V_{FP}$), and therefore the blade element angle of attack is nominally zero. Shortly after touchdown, full reverse pitch is applied, which means the collective pitch at the three-quarter radius station is at least zero or perhaps even –15 to –20 degrees. At this reverse thrust blade element angle, you can see that the angle of attack is really negative. Rotorcraft engineers will liken the flight condition to a helicopter in power-on vertical descent. This group would do well, however, not to jump to the conclusion that the propeller in reverse thrust operation will be in the vortex ring state. I say this because the propeller's disc loading is significantly greater than a helicopter's rotor. In fact, the data

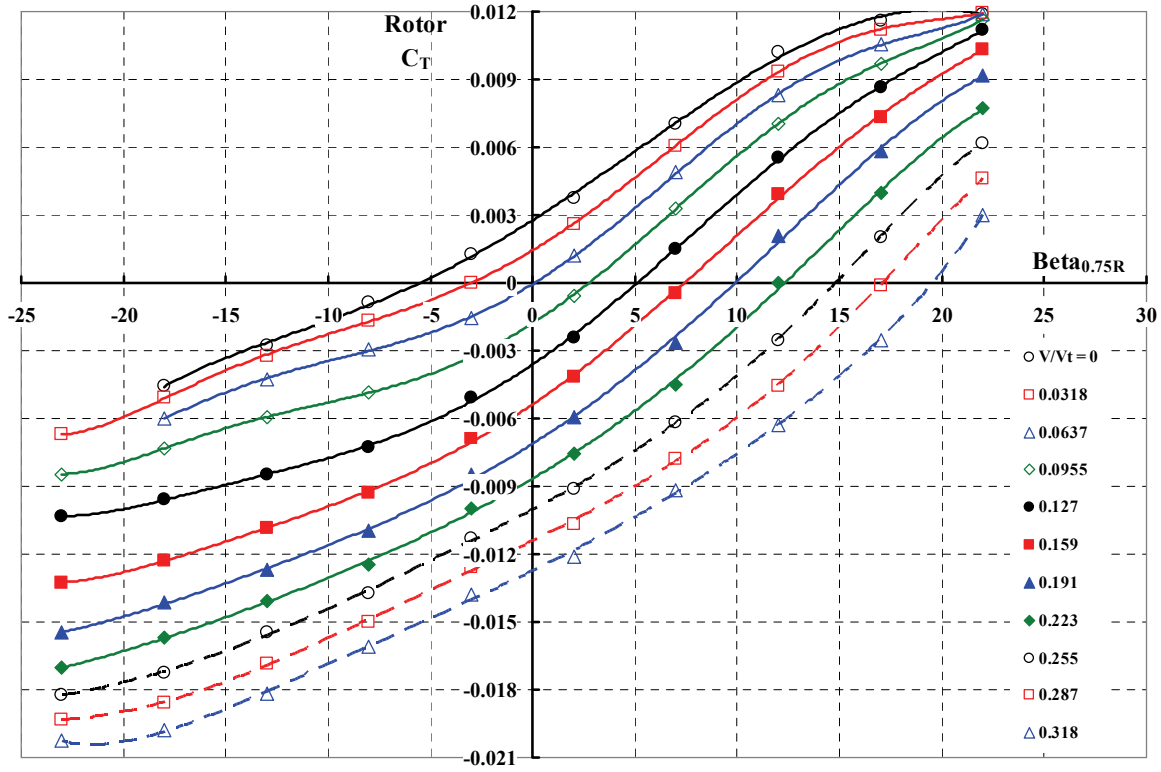

Fig. H-3. Propeller reverse thrust appears, experimentally, quite well behaved.

[1] In my view Edwin Hartman was a giant in the field of propeller development all through the 1930s and 1940s. He enjoyed great respect at the N.A.C.A. and later, NASA.

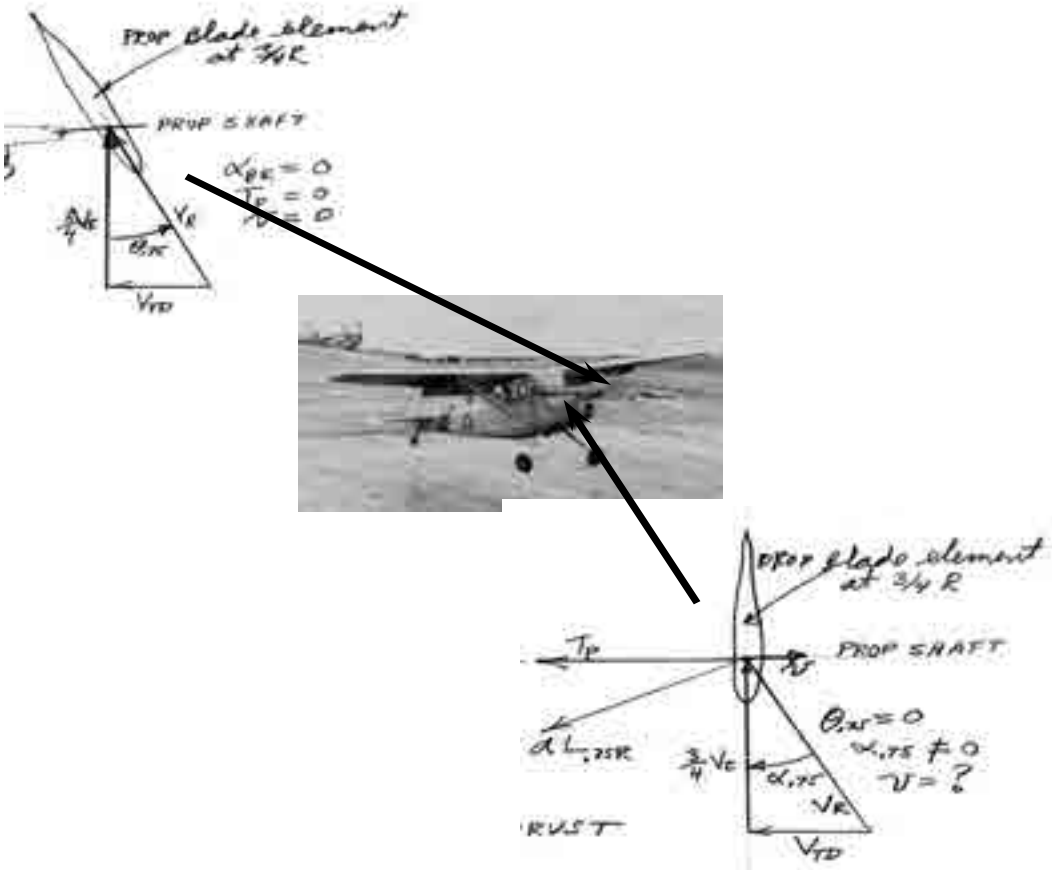

Fig. H-4. A propeller operating in the reverse thrust region can lead to many blade elements stalling.

offered in Fig. H-3 places the propeller in the flow state region where the momentum theory value of hover induced velocity $\left(\text{i.e.}, v_{hover}/V_{tip} = \sqrt{C_T/2}\right)$ is considerably less than the inflow ratio V_{FP}/V_{tip}. For rotorcraft engineers, this state is referred to as the windmill break state.

In early 2015 I prevailed upon Todd Quackenbush at Continuum Dynamics, Inc. to make computations using Continuum's CHARM theory in comparison to Hartman's experimental data shown in Fig. H-3. Before I knew it, Todd had sent me Fig. H-5. His accompanying e-mail (dated February 19, 2015) said,

> "Frank – Here is our first cut at a subset of the Hartman data.
>
> As you can see, the integrated C_T starts to wander off the measurements when you get to largeish negative Beta. We know that our airfoil data for the Clark Y is iffy for angles approaching negative stall, and we are trying to tease apart the role airfoil data plays from anything to do with wake behavior in this region.
>
> We are likely going to go on to other issues for the next week or so, given a deadline we have mid next week, but will look again at this matter after that.
>
> TQ"

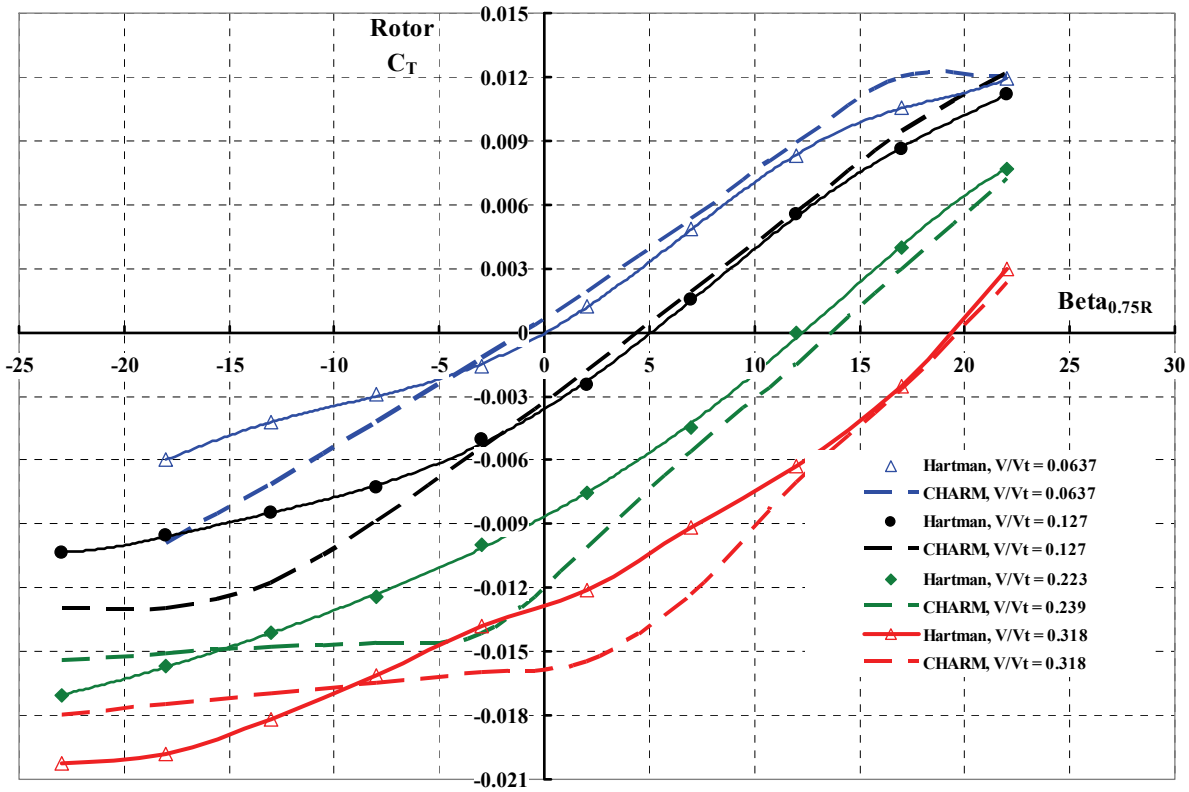

Fig. H-5. A rotorcraft tool suited to predicting propeller reverse thrust really has yet to be developed and proven. However, I am sure propeller manufactures (e.g., Hamilton Standard and McCauley in the United States) are well equipped to make accurate predictions (courtesy of Todd Quackenbush at Continuum Dynamics, Inc.).

Now let me return to the landing problem. For this introductory Volume, I decided to create a generic equation to estimate propeller thrust in the reverse thrust region. This equation, using rotorcraft symbology, is

$$(8) \quad T_P = \left(\rho A_P V_t^2\right)\left(\frac{\sigma_p a_{airfoil}}{2}\right)\left(-0.0321\frac{V}{V_t} - 0.0734\left(\frac{V}{V_t}\right)^2 + 1.3062\left(\frac{V}{V_t}\right)^3 + 0.05658\left(\beta_{0.75R}\right)\right).$$

Perhaps you are beginning to sense that the integral set forth by Eq. (6) has just been complicated because the propulsive unit force (F_P) now depends on the ground run velocity (V) as a cubic function. That is, $F_P = N \times T_P$ and a closed-form solution is rather messy. Therefore, I programmed the integral into Mathcad.

It took about 2 weeks to make comparisons of this semi-empirical theory to the test results for the several aircraft listed in Table 3-15 (page 542). With what I considered rational input provided in Table 3-15, I arrived at what you see in Fig. 3-167 on page 545. This graph shows that a "ballpark" estimate of the ground run distance during landing can be made to within ±15 percent with a *relatively simple* theory given rational input and a digital computer.

The Takeoff Distance Problem

Throughout the many decades of STOL aircraft research, development, and some production, I found several simple methods of estimating the takeoff distance required to clear a 50-foot obstacle. You saw three examples with Fig. 1-15 on page 21, Fig. 3-67 on page 417, and Fig. 3-170 on page 548. Now with nearly nine decades of aircraft data to draw upon, I thought a more complete analysis of the takeoff problem might be of interest. My ultimate goal was to offer a STOL design graph that would help fixed-wing designers evaluate their STOL aircraft early in the concept design phase. You saw this graph as Fig. 3-203 on page 601.

The substantiation for Fig. 3-203 was the correlation provided by Fig. 3-202 on page 600. The following discussion explains how the correlation was obtained.

Assume that the ground run distance portion of the takeoff problem is adequately described by $\Sigma F_X = ma_X$, where the force summation is simply

$$(9)\qquad \begin{aligned}\sum F_X &= F_P - D - \mu_{roll}(W - L) = F_P - \mu_{roll}W - (D - \mu_{roll}L)\\ &= (F_P - \mu_{roll}W) - \left[(\tfrac{1}{2}\rho S_W)(C_D - \mu_{roll}C_L)_{GR}\right]V_x^2.\end{aligned}$$

Here, I chose not to include a detailed variation of the propulsive force (F_P) with speed as was done in the landing problem. Rather, I simply stated that the propulsive force during the ground run is some average force (i.e., $F_P = F_{avg}$). In fact, the more meaningful force—to me—is the force at brake release ($F_{brake\ release}$). Therefore, I let average force equal 0.85 times the force at brake release for propeller-driven aircraft. For the two Advanced Medium STOL Transport (AMST) turbofan-powered STOL aircraft, I used a factor of 0.70. Therefore, you have

$$(10)\qquad F_{avg} = 0.85\,F_{brake\ release} \text{ for propeller and } F_{avg} = 0.70\,F_{brake\ release} \text{ for turbojet/turbofan.}$$

This simplification leads directly to $\sum F_X = A - BV_x^2$, and then the ground run distance to liftoff ($D_{Liftoff}$) behaves as

$$(11)\qquad \begin{aligned}D_{Liftoff} &= \frac{W}{g}\int_0^{V_{Liftoff}} \frac{V}{\sum F_x}dV = \frac{W}{g}\int_0^{V_{Liftoff}} \frac{V}{A - BV^2}dV = \frac{W}{g}\left\{\frac{-1}{2B}\ln\left[1 - \frac{BV_{Liftoff}^2}{A}\right]\right\}\\ &\approx \frac{V_{Liftoff}^2}{4A^2}\left(2A + BV_{Liftoff}^2\right).\end{aligned}$$

Now the liftoff speed ($V_{Liftoff}$) is approximated based on the aircraft's maximum lift coefficient ($C_{L\,max}$), so you have

$$(12)\qquad V_{Liftoff}^2 = \frac{2}{\rho_o}\left(\frac{W/S_W}{\sigma\, C_{L-Liftoff}}\right) \text{ or } \approx K\frac{2}{\rho_o}\left(\frac{W/S_W}{\sigma\, C_{L\,max}}\right) \text{ in feet per second squared.}$$

The constant (K) is greater than one and reflects the fact that STOL operations are conducted at 1.1 to 1.3 times the stall speed.

With just a few mathematical steps, you arrive at

$$(13)\quad D_{Liftoff} \approx \left(\frac{1}{2g\rho_o}\right)\left(\frac{W/S_W}{\sigma C_{L-Liftoff}}\right)\left(\frac{1}{\frac{F_{avg}}{W}-\mu_{roll}}\right)\left[2+\frac{\left(C_D-\mu_{roll}C_L\right)_{GR}}{\left(\frac{F_{avg}}{W}-\mu_{roll}\right)C_{L-Liftoff}}\right].$$

This derivation shows you that the primary parameters of interest are

$$\left(\frac{W/S_W}{\sigma}\right) \qquad \left(\frac{F_{avg}}{W}-\mu_{roll}\right) \quad \left(C_D-\mu_{roll}C_L\right)_{GR} \quad \text{and } C_{L-Liftoff}.$$

It is interesting to note that the term $\left[2+\frac{\left(C_D-\mu_{roll}C_L\right)_{GR}}{\left(\frac{F_{avg}}{W}-\mu_{roll}\right)C_{L-Liftoff}}\right]$ in Eq. (13) is, in fact, just slightly greater than 2. For example, assume $C_{D\text{-}GR} = 0.1$, $C_{L\text{-}GR} = 0$, $C_{L\text{-}Liftoff} = 2.0$, $\mu_{roll} = 0.025$, and $F_{avg}/W = 0.525$, and this shows you that

$$\left[2+\frac{\left(C_D-\mu_{roll}C_L\right)_{GR}}{\left(\frac{F_{avg}}{W}-\mu_{roll}\right)C_{L-Liftoff}}\right] = 2+\frac{0.1}{0.5\times 2} = 2+\frac{1}{10} = 2.1.$$

On this basis, you could say that to the first order

$$(14)\quad D_{Liftoff} \approx \left(\frac{1}{g\rho_o}\right)\left(\frac{W/S_W}{\sigma C_{L-Liftoff}}\right)\left(\frac{1}{\frac{F_{avg}}{W}-\mu_{roll}}\right) \approx 13.1\left(\frac{W/S_W}{\sigma C_{L-Liftoff}}\right)\left(\frac{1}{\frac{F_{avg}}{W}-\mu_{roll}}\right).$$

To account for the distance after liftoff, I have simply chosen the AMST result you saw in Fig. 3-176 on page 559 and the associated equation, which is repeated here for convenience as

$$(15)\quad D_{50\,ft}=373+1.112D_{Liftoff}+0.0000523\left(D_{Liftoff}\right)^2.$$

With this approach and assumptions, I was able to correlate calculated versus 23 experiment data points from 15 aircraft given mostly input data from flight test. This input data is provided here in Table H-1. The correlation result is graphed in Fig. H-6.

Table H-1. Calculated Results for the Takeoff Problem With Comparison to Test Data

Aircraft	Rated BHP or ESHP	F_P at Brake Release (lb)	Weight at Liftoff (lb)	F_{avg}/W	$V_{Liftoff}$ (knots)	$C_{L\text{-}Liftoff}$	$\frac{W/S_W}{\sigma C_{L-Liftoff}}$		Est $D_{Liftoff}$ (ft)	Test $D_{Liftoff}$ (ft)		Est D_{50ft} (ft)	Test D_{50ft} (ft)
Tanager	170	938	2841	0.281	27	3.55	2.40		129	295		497	500
Chipmunk	150	734	1,860	0.335	43	1.68	6.41		293	775		683	750
L-19A	150	971	2,100	0.393	41	2.12	5.70		214	280		593	590
Beaver	450	1,383	4,500	0.261	52	2.00	9.00		544	539		974	980
Turbo Beaver	550	2,385	5,100	0.397	55	2.00	10.20		379	na		782	800
Otter	600	2,435	8,000	0.259	56	2.00	10.67		652	630		1,101	1,155
Twin Otter	620	4,973	12,500	0.338	66	2.00	14.88		664	515		1,115	1,050
Caribou	1,450	9,947	28,500	0.297	57	2.84	11.01		560	550		992	920
Buffalo	3,133	22,856	49,200	0.395	88	2.00	26.03		974	na		1,486	1,420
C-123B	2,500	18,000	47,000	0.326	75	2.02	19.07		889	900		1,383	1,300
C-123B	2,500	18,000	54,000	0.283	80	2.03	21.69		1,189	1,230		1,749	1,850
C-130B	4,050	39,000	125,000	0.265	94	2.39	29.95		1,754	1,690		2,465	2,390
C-130B	4,050	39,000	101,000	0.328	85	2.39	24.20		1,106	1,060		1,647	1,560
C-130B	4,050	39,000	85,000	0.390	78	2.39	20.36		766	700		1,235	1,100
JC-130B	4,050	39,000	125,000	0.265	94	2.39	29.95		1,754	1,640		2,465	2,340
JC-130B	4,050	39,000	101,000	0.328	85	2.39	24.20		1,106	1,000		1,647	1,500
JC-130B	4,050	39,000	85,000	0.390	78	2.39	20.36		766	670		1,235	1,070
NC-130B	4,050	39,000	125,000	0.265	83	3.07	23.35		1,346	1,510		1,945	2,160
NC-130B	4,050	39,000	115,000	0.288	78	3.20	20.62		1,077	1,220		1,612	1,840
NC-130B	4,050	39,000	101,000	0.328	71	3.39	17.09		768	820		1,238	1,400
DC-3	1,050	6,438	26,000	0.210	68	1.68	15.67		1,260	820		1,837	1,900
YC-14	na	79,500	160,920	0.346	101	2.90	31.50		1,344	1,409		1,942	2,030
YC-15	na	58,652	149,300	0.275	105	2.49	34.51		1,932	1,890		2,696	2,740

Notes: (1) F_P calculated for propeller driven aircraft from HP assuming a Figure of Merit of 0.7.

(2) F_P for YC-14 and YC-15 from manufacturer's data.

(3) YC-14 and YC-15 data at sea level, hot day; all other aircraft at sea level, standard day.

(4) $F_{avg} = 0.85\ F_{brake\ release}$ for propeller and $F_{avg} = 0.70\ F_{brake\ release}$ for turbojet/turbofan.

(5) $C_{D\text{-}GR} = 0.1$, $C_{L\text{-}GR} = 0.5$, and $\mu_{roll} = 0.025$ for all data points. Therefore, $(C_D - \mu_{roll}\ C_L)_{GR} = 0.0875$ for all data points.

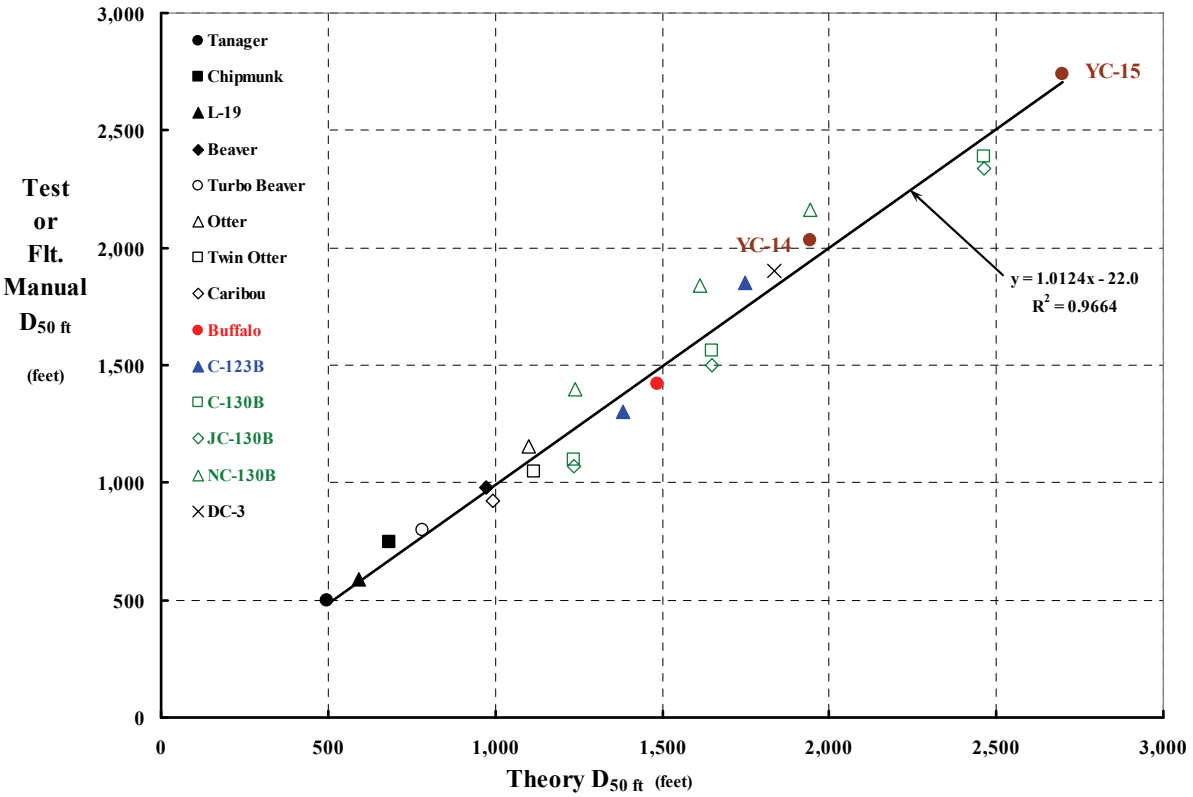

Fig. H-6. Basic physics plus a little empiricism is adequate to estimate takeoff distance over a 50-foot obstacle *during the early stages of conceptual design*.

The correlation you see with Fig. H-6 gave me enough confidence to construct a conceptual design graph showing takeoff distance over a 50-foot obstacle (D_{50ft}) versus F_{avg}/W for lines of constant $\frac{W/S_W}{\sigma C_{L-Liftoff}}$. Fig. H-7 shows my version of a conceptual design chart that you will find in the literature—in one form or another.

This conceptual design chart, Fig. H-7, immediately shows you that as the wing loading (W/S_W) increases to suit fuel efficient, higher speeds at higher altitudes, a STOL requirement demands a much higher lift coefficient at liftoff ($C_{L\text{-}Liftoff}$). Not only that, the ratio of the average propulsive force during takeoff to takeoff gross weight must be on the order of 0.5 or higher. It seems to me that the Boeing YC-14 defines the lower boundary for future designs of large-transport STOL airplanes. If you accept my conclusion, then the STOL design space quickly shrinks to where installed power (i.e., static-thrust-to-weight ratio, if you prefer) forces you to consider directing the propulsive force downward and with more turning efficiency than would be obtained with a horizontal airstream bent around flaps. This ultimately leads to serious consideration of vertical takeoff and landing (VTOL) aircraft.

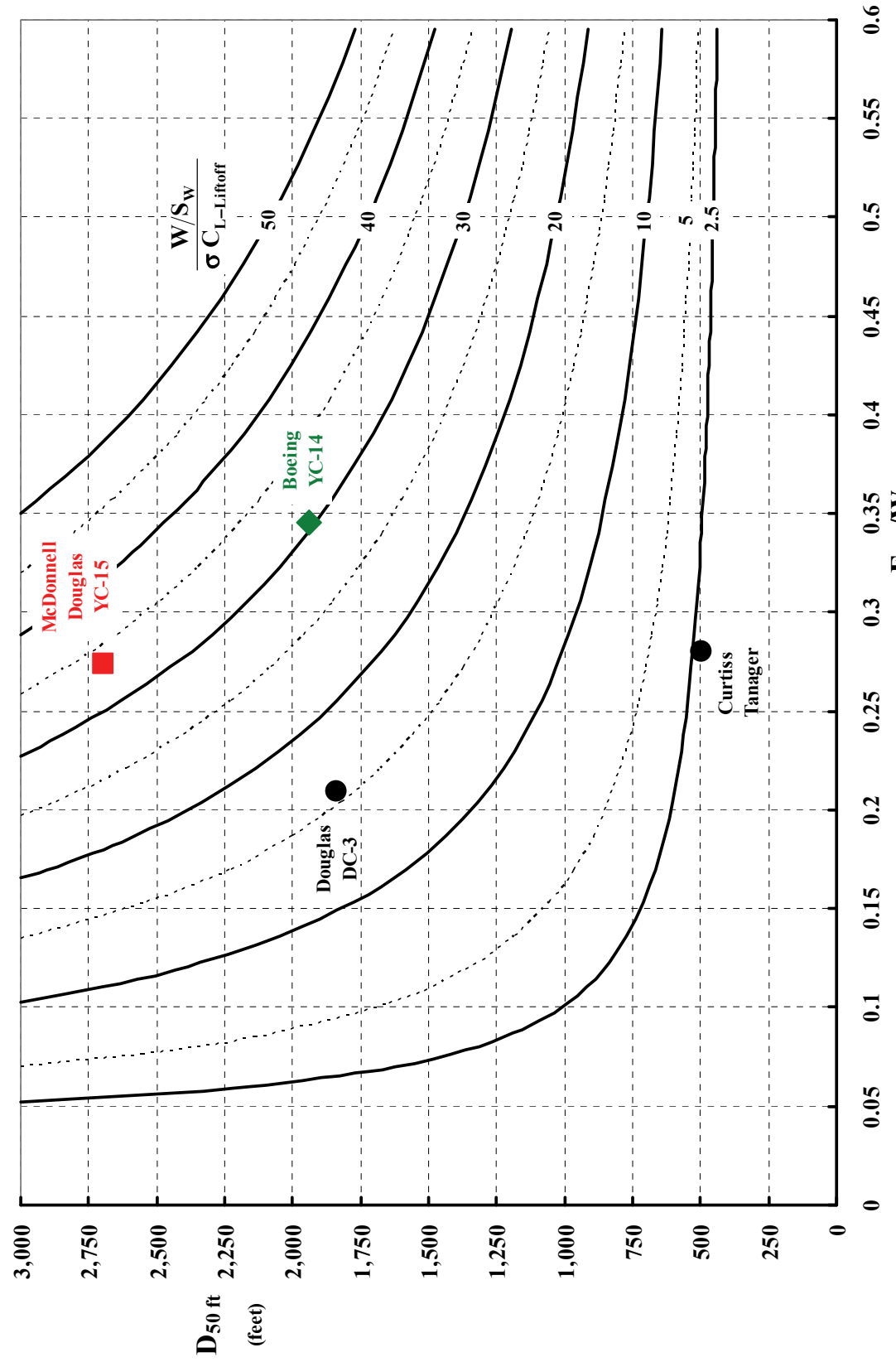

Fig. H-7. Harris' conceptual design chart for STOL takeoffs.

INDIVIDUALS

These men and women, with their thoughts, words, and deeds, helped crystallize my views about V/STOL aircraft.

AIRCRAFT AND ENGINES

AIRCRAFT

Airplanes

Autogyros

Helicopters

STOLs

VTOLs

ENGINES

Piston

Turbine

INDEX